TRANSACTIONS

OF THE

AMERICAN INSTITUTE OF MINING AND METALLURGICAL ENGINEERS

(INCORPORATED)

Volume 172

IRON AND STEEL DIVISION

1947

TECHNICAL PAPERS, DISCUSSIONS AND SYMPOSIA PRESENTED BEFORE THE DIVISION AT MEETINGS HELD AT ATLANTIC CITY, NOVEMBER 18–20, 1946, AND AT NEW YORK, MARCH 19–22, 1947.

PUBLISHED BY THE INSTITUTE
AT THE OFFICE OF THE SECRETARY
29 WEST 39TH STREET
NEW YORK 18, N.Y.

Notice

This volume is the twentieth of a series containing papers and discussions presented before the Iron and Steel Division of the American Institute of Mining and Metallurgical Engineers since its organization in 1928; one volume each year, as follows:

1928, Iron and Steel Technology in 1928 (later listed as Volume 80 of the TRANSACTIONS); 1929 (vol. 84), 1930 (vol. 90), 1931 (vol. 95), 1932 (vol. 100), 1933, 1934, 1935, 1936, 1937, 1938, 1939, 1940, 1941, 1942, 1943, 1944, 1945 and 1946, TRANSACTIONS of the American Institute of Mining and Metallurgical Engineers, Iron and Steel Division.

This volume contains papers and discussions presented at the meetings at Atlantic City, November 18–20, 1946, and at New York, March 19–22, 1947.

Papers on iron and steel subjects published by the Institute prior to 1928 are to be found in many volumes of the TRANSACTIONS of the Institute; in Vols. 37 to 45, inclusive; 47, 50 and 51, 53, 56, 58, 62, 67 to 71, inclusive; 73 and 75. Vol. 67 was devoted exclusively to iron and steel.

Iron and steel papers published in the TRANSACTIONS before the year 1936 may be found by consulting the general indexes to Vols. 1 to 35 (1871–1904), Vols. 36 to 55 (1905–1916), Vols. 56 to 72 (1917–1935), and Vols. 73 to 117 (1926–1935).

COPYRIGHT, 1948, BY THE
AMERICAN INSTITUTE OF MINING AND METALLURGICAL ENGINEERS
(INCORPORATED)

PRINTED IN THE UNITED STATES OF AMERICA

THE MAPLE PRESS COMPANY, YORK, PA.

East Engin.
Print
11-23-48
23043

FOREWORD

THE 1947 Transactions of the Iron and Steel Division is the twentieth volume published since the organization of this group as a division of the AIME. In the course of these two decades the Transactions of this division have reflected the progress that has been made in the ferrous field, and many of the papers during this period represent milestones in metallugical thinking.

The present volume contains thirty papers of this division published in the period from September, 1946 to August, 1947. Included with these is the Howe Memorial Lecture presented by H. W. Graham, entitled "The Factors Which Determine Iron and Steel Making Processes." This is a particularly pertinent paper, as it presents a study of raw materials as related to present and future processing methods.

The technical papers deal with a diversity of subjects and reflect the wide range of interests of the Iron and Steel Division. In the field of steelmaking it is apparent that the role of oxygen is still being given much attention, as four out of five papers are devoted to this subject. Among the excellent papers concerned with the metallurgy of the solid phase, it is interesting to note that many of them deal with stress and fracture studies, and it will be noted that a symposium was held during the year on the subject of Multiaxial Stresses in Metals with the titles of the papers shown which are being published in the Institute of Metals Division Transactions.

T. S. WASHBURN, *Chairman*,
Iron and Steel Division.

CHICAGO, ILLINOIS
October 27, 1947

AIME OFFICERS AND DIRECTORS

For the year ending February 1948

PRESIDENT AND DIRECTOR
CLYDE WILLIAMS, Columbus, Ohio

PAST PRESIDENTS AND DIRECTORS
HARVEY S. MUDD, Los Angeles, Calif.
LOUIS S. CATES, New York, N. Y.

VICE-PRESIDENT AND TREASURER
ANDREW FLETCHER, New York, N. Y.

VICE-PRESIDENTS AND DIRECTORS
H. J. BROWN, Boston, Mass.
ERLE V. DAVELER, New York, N. Y.
D. H. MCLAUGHLIN, New York, N. Y.
LEO F. REINARTZ, Middletown, Ohio
ROBERT W. THOMAS, Ray, Ariz.

DIRECTORS
C. H. BENEDICT, Lake Linden, Mich.
ARTHUR JOHN BLAIR, Birmingham, Ala.
OLIVER BOWLES, Washington, D. C.
W. E. BREWSTER, Chicago, Ill.
A. B. KINZEL, New York, N. Y.
PHILIP KRAFT, New York, N. Y.
WILLIAM W. MEIN, SR., San Francisco, Calif.
C. V. MILLIKAN, Tulsa, Okla.
D. D. MOFFAT, Salt Lake City, Utah
ROBERT H. MORRIS, Ansted, W. Va.
J. C. NICHOLLS, Toronto, Ont., Canada
RUSSELL B. PAUL, New York, N. Y.
W. B. PLANK, Easton, Pa.
EARLE E. SCHUMACHER, Murray Hill, N. J.
JOHN R. SUMAN, Houston, Texas
CLYDE E. WEED, New York, N. Y.
EUGENE A. WHITE, Tacoma, Wash.
W. E. WRATHER, Washington, D. C.

DIVISION CHAIRMEN—Directors Ex-officiis
E. A. ANDERSON (Institute of Metals), Palmerton, Pa.
HOWARD C. PYLE (Petroleum), Glendale, Calif.
THOMAS S. WASHBURN (Iron and Steel), Chicago, Ill.
EVAN EVANS (Coal), Lansford, Pa.
J. R. CUDWORTH (Mineral Industry Education), Tuscaloosa, Ala.
JOSEPH L. GILLSON (Industrial Minerals), Wilmington, Del.

SECRETARY
A. B. PARSONS, New York, N. Y.

STAFF IN NEW YORK

Assistant Secretaries
EDWARD H. ROBIE
E. J. KENNEDY, JR.
ERNEST KIRKENDALL
WILLIAM H. STRANG

Assistant to the Secretary
H. NEWELL APPLETON

Advertising Manager "Mining and Metallurgy"
WHEELER SPACKMAN

Assistant Treasurer
H. A. MALONEY

CONTENTS

PAGE

Foreword, by T. S. Washburn 3
AIME Officers and Directors 4
Iron and Steel Division Officers and Committees 7
R. W. Hunt Award 10
Howe Lectures and Lecturers 11
Photograph of H. W. Graham, Howe Lecturer 1947 14

TECHNICAL PAPERS AND DISCUSSIONS

Howe Lecture

Factors Which Determine Iron and Steel Making Processes. By H. W. GRAHAM. (*Metals Tech.*, Aug. 1947, T.P. 2217) 15

Ore Reduction and Slags

The Rate of Reduction of Geneva Iron Ore. By J. R. LEWIS. (*Metals Tech.*, June 1947, T.P. 2177). With discussion 27
Experimental Laboratory Study on Effect of Pressure on Carbon Deposition and Rate of Reduction of Iron Oxides in the Blast-furnace Process. By L. F. MAREK, A. BOGROW and G. W. KING. (*Metals Tech.*, June 1947, T.P. 2184). With discussion 46
German Iron Ores Yield Vanadium. By R. P. FISCHER. (*Metals Tech.*, Sept. 1946, T.P. 2070). With discussion 71
Production of Low-sulphur Sponge Iron. By R. C. BUEHL, E. P. SHOUB and J. P. RIOTT. (*Metals Tech.*, Oct. 1946, T.P. 2093). With discussion 76
An Electrochemical Study of the Properties of Molten Slags of the System $CaO\text{-}SiO_2$ and $CaO\text{-}Al_2O_3\text{-}SiO_2$. By LO CHING CHANG and G. DERGE. (*Metals Tech.*, Oct. 1946, T.P. 2101). With discussion 90
The Identification of CaO-MgO Orthosilicate Crystals, Including Merwinite $3CaO\cdot MgO\cdot 2SiO_2$, through the Use of Etched Polished Sections. By R. B. SNOW. (*Metals Tech.*, June 1947, T.P. 2167). With discussion 121

Steelmaking

Oxygen in Liquid Open-hearth Steel—Oxygen Content during the Refining Period. By T.E. BROWER and B. M. LARSEN. (*Metals Tech.*, Sept. 1946, T.P. 2035). With discussion . . 137
Oxygen in Liquid Open-hearth Steel—Effect of Special Additions, Stirring Methods and Tapping. By T. E. BROWER and B. M. LARSEN. (*Metals Tech.*, Oct. 1946, T.P. 2076). With discussion 164
The Mechanism of the Carbon-oxygen Reaction in Steelmaking. By C. E. SIMS. (*Metals Tech.*, Jan. 1947, T.P. 2129). With discussion 176
Oxygen in Basic Electric-furnace Baths. By S. F. URBAN and G. DERGE. (*Metals Tech.*, June 1947, T.P. 2185). With discussion 196
Training of Metallurgical Engineers in the Steel Industry. By E. C. WRIGHT. (*Metals Tech.*, Sept. 1946, T.P. 2051) 212

PAGE

Mechanical Properties of Steel

Effect of Alloys in Steel on Resistance to Tempering. By W. CRAFTS and J. L. LAMONT. (*Metals Tech.*, Sept. 1946, T.P. 2036). With discussion . . . 222
Calculation of Tensile Strength and Yield Point from the Chemical Composition and Cooling Rate. By I. R. KRAMER, P. D. GORSUCH and D. L. NEWHOUSE. (*Metals Tech.*, Sept. 1946, T.P. 2067). With discussion . . . 244
Boron in Certain Alloy Steels. By M. C. UDY and P. C. ROSENTHAL. (*Metals Tech.*, Oct. 1946, T.P. 2085). With discussion . . . 273
The Izod Impact Strength of Heat-treated Alloy Steel. By W. CRAFTS and J. L. LAMONT. (*Metals Tech.*, Feb. 1947, T.P. 2134). With discussion . . . 303
Influence of Plastic Deformation, Combined Stresses, and Low Temperatures on the Breaking Stress of Ferritic Steels. By D. J. MCADAM, JR., G. W. GEIL and R. W. MEBS. (*Metals Tech.*, Aug. 1947, T.P. 2220) . . . 323
The Effect of Prior Tensile Strain on Fracture. By EDWARD SAIBEL (*Metals Tech.*, June 1947, T.P. 2186). With discussion . . . 363
Anomalous Changes in Tensile Properties of Quenched Iron-cobalt (35 per cent Co) Alloys. By J. K. STANLEY. (*Metals Tech.*, Aug. 1947, T.P. 2221). With discussion . . . 374
Stress Rupture of Heat-resisting Alloys as a Rate Process. By E. S. MACHLIN and A. S. NOWICK. (*Metals Tech.*, Feb. 1947, T.P. 2137). With discussion . . . 386

Metallographic Methods

Quantitative Metallography by Point-counting and Lineal Analysis. By R. T. HOWARD and M. COHEN. (*Metals Tech.*, Aug. 1947, T.P. 2215). With discussion . . . 413
The Factorial Experiment in Engineering Research. By M. K. BARNETT. (*Metals Tech.*, June 1947, T.P., 2161) . . . 427
A New Method for Making Rapid and Accurate Estimates of Grain Size. By F. C. HULL. (*Metals Tech.*, July 1947, T.P. 2160) . . . 439

Microstructure; Diffusion; Atmospheres

Transformation of Austenite in an Aluminum-chromium-molybdenum Steel. By R. A. GRANGE, W. S. HOLT and E. T. TKAC. (*Metals Tech.*, Dec. 1946, T.P. 2109). With discussion . . . 452
The Effect of Cobalt on the Rate of Nucleation and the Rate of Growth of Pearlite. By M. F. HAWKES and R. F. MEHL. (*Metals Tech.*, Aug. 1947, T.P. 2211) . . . 467
Hot Deformation Structures, Veining and Red-shortness Cracks in Iron and Steel. By A. HULTGREN and B. HERRLANDER. (*Metals Tech.*, Dec. 1946, T.P. 2106) . . . 493
Austenite Grain Size in Cast Steels. By M. F. HAWKES. (*Metals Tech.*, June 1947, T.P. 2170). With discussion . . . 510
The Diffusion Rates for Carbon in Austenite. By F. E. HARRIS. (*Metals Tech.*, Aug. 1947, T.P. 2216). With discussion . . . 531
Controlled Atmospheres from City Gas for the Heat-treatment of Steels. By IVOR JENKINS. (*Metals Tech.*, Jan. 1947, T.P. 2121). With discussion . . . 556

Symposia

Some Questions on Interrelated Processes Going on in the Blast Furnace. By B. M. LARSEN (*Metals Tech.*, Feb. 1947, T.P. 2132). With discussion . . . 621
Effect of Multiaxial Stresses on Metals
See page 663 for contents.
Contents Volume 171, Institute of Metals Division, 1947 . . . 661
Index . . . 665

IRON AND STEEL DIVISION

Established as a Division February 22, 1928

(By-laws printed in the 1939 TRANSACTIONS Volume of the Division)

Officers and Committees for Year ending February 1948

T. S. WASHBURN, *Chairman*, Chicago, Ill.
W. E. BREWSTER, *Past-Chairman*, Chicago, Ill.
JOHN CHIPMAN, *Vice-Chairman*, Cambridge, Mass.
H. W. MCQUAID, *Vice-Chairman*, Cleveland, Ohio
GILBERT SOLER, *Vice-Chairman*, Welland, Ont., Canada.
ERNEST KIRKENDALL, *Secretary*, 29 West 39th Street, New York 18, N. Y.

Past Chairmen

RALPH H. SWEETSER, 1928
G. B. WATERHOUSE, 1929
W. J. MACKENZIE, 1930
F. M. BECKET, 1931
F. N. SPELLER, 1932
JOHN JOHNSTON, 1933
L. F. REINARTZ, 1934
A. B. KINZEL, 1935
C. E. WILLIAMS, 1936
FRANCIS B. FOLEY, 1937
J. T. MACKENZIE, 1938
J. HUNTER NEAD, 1939
FRANK T. SISCO, 1940
C. H. HERTY, JR., 1941
E. C. SMITH, 1942
H. W. GRAHAM, 1943
W. A. HAVEN, 1944
ERLE G. HILL, 1945
E. E. BREWSTER, 1946

Executive Committee

Until 1948
K. L. FETTERS
J. S. MARSH
C. E. SIMS

Until 1949
M. GENSAMER
H. E. PHELPS
H. K. WORK

Until 1950
W. A. STEELE
F. M. WASHBURN
E. C. WRIGHT

Blast Furnace, Coke Oven and Raw Materials

R. A. LINDGREN, *Chairman*
T. L. JOSEPH, *Vice-Chairman*
R. W. CAMPBELL, *Vice-Chairman*
T. F. PLIMPTON, *Secretary*

Program Sub-Committee
C. G. HOGBERG, *Chairman*
FORDYCE COBURN
H. V. LAUER
C. L. WYMAN

Papers Sub-Committee
E. J. GARDNER, *Chairman*
J. E. EBERHARDT
G. W. HEWITT
K. C. MCCUTCHEON

Open Hearth Steel

W. C. KITTO, *Chairman*
E. L. RAMSEY, *Past-Chairman*
C. R. FONDERSMITH, *Vice-Chairman*
ERNEST KIRKENDALL, *Secretary-Treasurer*

CLYDE DENLINGER
J. J. GOLDEN
H. M. GRIFFITH
H. G. GRIM
E. G. HILL
L. A. LAMBING
B. D. MCCARTHY
A. P. MILLER
L. F. REINARTZ
A. E. REINHARD
A. H. SOMMER
A. W. THORNTON
F. L. TOY
D. N. WATKINS
T. T. WATSON
W. H. YECKLEY

Bessemer Steel

H. W. Graham, *Chairman*

H. C. Dunkle, K. L. Fetters, J. D. Gold, E. C. Penrod, A. W. Thornton, F. L. Toy, G. M. Yocum

Electric Furnace Steel

Executive Committee

W. J. Reagan, *Chairman*
C. W. Briggs, *Past-Chairman*
Ernest Kirkendall, *Secretary*

A. L. Feild, S. D. Gladding, John Juppenlatz, G. A. Lillieqvist, T. J. McLoughlin, W. M. Patterson, H. E. Phelps, H. A. Schwartz, Gilbert Soler

Conference Committee

J. B. Caine, *Chairman*
Norman I. Stotz, *Vice-Chairman*

H. V. Beasley, J. A. Bowers, E. J. Chelius, W. M. Farnsworth, R. H. Frank, R. J. Knerr, Charles Locke, H. W. Poole, C. E. Sims, C. C. Spencer, R. H. Stone, A. C. Texter, E. C. Troy, H. F. Walther

Physical Chemistry of Steelmaking

B. M. Larsen, *Chairman*
W. O. Philbrook, *Secretary*

H. R. Belding, M. B. Bever, W. S. Debenham, Gerhard Derge, L. G. Ekholm, H. B. Emerick, G. R. Fitterer, A. G. Forrest, H. J. Forsyth, J. J. Golden, T. L. Joseph, L. A. Lambing, J. S. Marsh, Shadburn Marshall, D. L. McBride, C. E. Sims, C. R. Taylor, Michael Tenenbaum

Membership

Norman F. Tisdale, *Chairman*

H. J. Cutler, Samuel Epstein, J. W. Halley, H. E. Johnson, Vernon Jones, C. L. Labeka, J. C. Murray, Earl Penrod, C. E. Sims, J. M. Stapleton, S. P. Watkins, T. T. Watson

Physical Metallurgy

J. W. Halley, *Chairman*

Samuel Epstein, M. Gensamer, R. A. Grange, M. F. Hawkes, J. H. Hollomon, W. T. Lankford, W. E. Mahin, A. R. Troiano

Mining and Metallurgy

C. G. Hogberg, *Chairman*

M. Gensamer, F. G. Norris

Howe Memorial Lecture

T. S. Washburn, *Chairman*

M. A. Grossmann, C. H. Herty, Jr., J. T. MacKenzie, E. C. Smith

Robert W. Hunt Medal and Prize

T. S. Washburn, *Chairman*

John Chipman, K. C. McCutcheon, H. A. Strain, H. K. Work

J. E. Johnson, Jr. Award

F. M. Rich, *Chairman*

C. F. Hoffman, C. G. Hogberg, L. F. Sattele, J. M. Stapleton

Programs

J. S. MARSH, *Chairman*

R. S. ARCHER
J. B. AUSTIN
JOHN CHIPMAN
I. R. KRAMER
R. K. KULP
W. O. PHILBROOK
B. R. QUENEAU
C. S. SMITH
MICHAEL TENENBAUM
F. L. TOY
F. M. WALTERS, JR.

Publications

F. B. FOLEY, *Chairman*
B. M. LARSEN, *Vice-Chairman*

R. J. ALLEN
JANET Z. BRIGGS
G. R. BROPHY
R. K. KULP
R. H. SCHAEFER

Nominating

W. E. BREWSTER, *Chairman*

H. W. GRAHAM
W. A. HAVEN
E. G. HILL
FRANK T. SISCO

The Howe Memorial Lecture

THE Howe Memorial Lecture was authorized in April 1923, in memory of Henry Marion Howe, as an annual address to be delivered by invitation under the auspices of the Institute by an individual of recognized and outstanding attainment in the science and practice of iron and steel metallurgy or metallography, chosen by the Board of Directors upon recommendation of the Iron and Steel Division.

So far, only American metallurgists have been invited to deliver the Howe lecture. It is believed that this lecture would gain in importance and significance were it possible to include metallurgists from other countries, but the Institute has not yet been able to do this on account of lack of special funds to support this lectureship.

The titles of the lectures and the lecturers are as follows:

1924 What is Steel? By Albert Sauveur.
1925 Austenite and Austenitic Steels. By John A. Mathews.
1926 Twenty-five Years of Metallography. By William Campbell.
1927 Alloy Steels. By Bradley Stoughton.
1928 Significance of the Simple Steel Analysis. By Henry D. Hibbard.
1929 Studies of Hadfield's Manganese Steel with the High-power Microscope. By John Howe Hall.
1930 The Future of the American Iron and Steel Industry. By Zay Jeffries.
1931 On the Art of Metallography. By Francis F. Lucas.
1932 On the Rates of Reactions in Solid Steel. By Edgar C. Bain.
1933 Steelmaking Processes. By George B. Waterhouse.
1934 The Corrosion Problem with Respect to Iron and Steel. By Frank N. Speller.
1935 Problems of Steel Melting. By E. C. Smith.
1936 Correlation between Metallography and Mechanical Testing. By H. F. Moore.
1937 Progress in Improvement of Cast Iron and Use of Alloys in Iron. By Paul D. Merica.
1938 On the Allotropy of Stainless Steels. By Frederick Mark Becket.
1939 Some Things We Don't Know about the Creep of Metals. By H. W. Gillett.
1940 Slag Control. By C. H. Herty, Jr.
1941 Some Complexities of Impact Strength. By Alfred V. de Forest.
1942 Time as a Factor in the Making and Treating of Steel. By John Johnston.
1943 The Development of Research and Quality Control in the Modern Steel Plant. By Leo F. Reinartz.
1944 Gray Iron—Steel Plus Graphite. By J. T. MacKenzie.
1945 Toughness and Fracture of Hardened Steels. By Marcus A. Grossmann.
1946 The Blast-furnace Process and Means of Control. By T. L. Joseph.
1947 Factors which Determine Iron and Steel Making Processes. By H. W. Graham.

Robert W. Hunt Award

THE Robert W. Hunt award was established in 1920 by the partners and employees of the distinguished metallurgist and testing engineer for whom it was named. Recipients are nominated by a continuing committee of four members of the Iron and Steel Division, together with the Chairman of the Division as member ex-officio.

The award is made for the best original paper or papers on iron and steel contributed to the Institute during the year under review and consists of a gold medal, a silver medal, or a money prize, together with a certificate. The only condition attached to the award is that the money prize shall not be given to anyone who was more than 40 years of age when the paper that merited the award was presented.

Awards have been made as follows:

1920 Robert Woolston Hunt: Manufacture of Steel Rails. TRANSACTIONS (1920) **62,** 174.

1926 Charles Lewis Kinney, Jr.: Economic Significance of Metalloids in Basic Pig Iron in Basic Open-hearth Practice. TRANSACTIONS (1924) **70,** 136.

1928 Charles H. Herty, Jr.: Some Factors Affecting the Elimination of Sulphur in the Basic Open-hearth Process. (Co-authors: A. R. Belyea, E. H. Burkart and C. C. Miller.) TRANSACTIONS (1925) **71,** 512. Chemical Equilibrium of Manganese, Carbon and Phosphorus in the Basic Open-hearth Process. TRANSACTIONS (1926) **73,** 1107. Desulphurizing Action of Manganese in Iron. (Co-author: J. M. Gaines, Jr.) TRANSACTIONS (1927) **75,** 434.

1928 John A. Mathews: Austenite and Austenitic Steels. TRANSACTIONS (1925) **71,** 568.

1929 Edgar Collins Bain and William E. Griffiths: An Introduction to the Iron-chromium-nickel Alloys. TRANSACTIONS (1927) **75,** 166.

1930 James Aston: A New Development in Wrought Iron Manufacture. TRANSACTIONS (1929) **84,** 166.

1931 Edmund S. Davenport: Transformation of Austenite at Constant Subcritical Temperatures. (Co-author: E. C. Bain.) TRANSACTIONS (1930) **90,** 117.

1932 Howard Scott: Transformational Characteristics of Iron-manganese Alloys. TRANSACTIONS (1931) **95,** 284.

1933 Clarence E. Sims and Gustaf A. Lillieqvist: Inclusions—Their Effect, Solubility and Control in Cast Steel. TRANSACTIONS (1932) **100,** 154.

1934 Cyril Stanley Smith and Earl W. Palmer: The Precipitation-hardening of Copper Steels. TRANSACTIONS (1933) **105,** 133.

1936 Carl C. Henning: Manufacture and Properties of Bessemer Steel. TRANSACTIONS (1935) **116,** 137.

1937 William F. Holbrook and Thomas L. Joseph: Relative Desulphurizing Powers of Blast-furnace Slags. TRANSACTIONS (1936) **120,** 99.

1938 Thomas S. Washburn and John H. Nead: Structure of Rimmed-steel Ingots. TRANSACTIONS (1937) **125,** 378.

1939 Kenneth Charles McCutcheon and John Chipman: Evolution of Gases from Rimming-steel Ingots. TRANSACTIONS (1938) **131,** 206.

1940 Axel Hultgren and Gösta Phragmén: Solidification of Rimming-steel Ingots. TRANSACTIONS (1939) **135,** 133.

1941 Alden B. Greninger and Alexander R. Troiano: Crystallography of Austenite Decomposition. TRANSACTIONS (1940) **140,** 307.

1941 George E. Steudel: Effect of the Volume and Properties of Bosh and Hearth Slag on Quality of Iron. TRANSACTIONS (1940) **140,** 65.

1942 Harold K. Work: Photocell Control for Bessemer Steelmaking. TRANSACTIONS (1941) **145,** 132.

1943 Marcus A. Grossmann: Hardenability Calculated from Chemical Composition. TRANSACTIONS (1942) **150,** 227.

1944 Clarence David King: The Washing of Pittsburgh Coking Coals and Results Obtained on Blast Furnaces. TRANSACTIONS (1944) **158,** 67.

1945 Edwin Chester Wright: Manufacture and Properties of Killed Bessemer Steel. TRANSACTIONS (1944) **158,** 107.

1947 Harry K. Ihrig: The Effect of Various Elements on the Hot-workability of Steel. TRANSACTIONS (1946) **167,** 749.

TECHNICAL PAPERS
AND
DISCUSSIONS

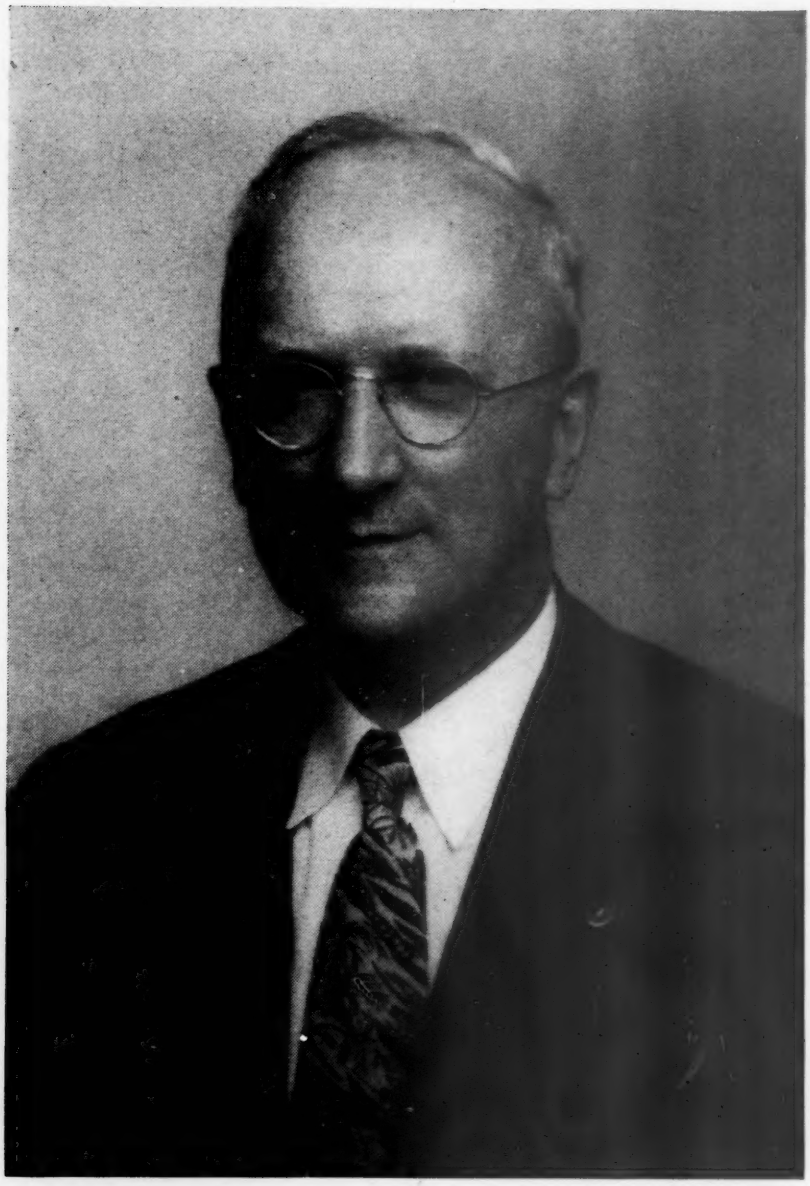

H. W. Graham
Henry Marion Howe Memorial Lecturer, 1947

Factors which Determine Iron and Steel Making Processes

By H. W. Graham*

(Henry Marion Howe Memorial Lecture†)

As these annual occasions in honor of Henry Marion Howe continue through the years, there is progressively less likelihood that the lecturer will have had personal knowledge of Dr. Howe. The present speaker is one of those who unfortunately had no opportunity to come under the inspiring presence of this great metallurgist.

A review of Howe's work shows it to cover a comprehensive range of interests and to evidence an impressive richness of detail. Not only was Howe at home in the laboratory, but he was familiar with the processes of iron and steel making and had a real understanding of them. His writings include much that is descriptive of processes with a wealth of material that is becoming of increasing historical value. He recorded his studies of the theoretical aspects of processes and published at least two process classifications, one in 1890 that was lengthy and somewhat theoretical, and a second in 1906 that was more of a practical listing. Wide as Howe's field of interest was, it is significant of the circumstances of his time that he gave little consideration to raw materials or to their effect on iron and steel making processes.

In 1933, Waterhouse, Howe lecturer for that year, presented a descriptive summary of the major steel making processes, and in 1946 Joseph discussed the blast furnace process. Otherwise Howe lectures have not dealt with processes as major subjects.

In today's lecture, with no effort to describe the mechanical arrangements of iron and steel making facilities, it is proposed to examine the essential technological elements of the processes, to explore the inter-relation of these elements, and particularly to seek recognition and understanding of those factors which determine why certain processes are or are not used. The discussion of this lecture will deal with the major well-known large tonnage processes, with only such attention to processes of minor tonnage and special character as may be warranted for explanation by contrast. Subject to the errors of generalization and the shortcomings of condensation involved in presentation limited to a single hour, it is proposed to examine broadly but intensively those operations which convert raw materials into steel.

It is an innovation for a Howe lecturer to discuss the raw materials of the iron and steel industry, but the changing circumstances of passing years intensify the influence of raw materials on processes and require the metallurgist to be alert for the process adjustments that may become advisable or mandatory. For a half century the metallurgical processing of iron and steel has followed a surprisingly straight path, but this does not necessarily mean that there are no curves in the road ahead.

Ages ago primitive man came to know iron in its metallic form, not only by the

Manuscript received at the office of the Institute March 21, 1947. Issued as T.P. 2217 in Metals Technology, August 1947.

* Director of Metallurgy and Research, Jones and Laughlin Steel Corporation, Pittsburgh, Pennsylvania.

† Presented at the New York Meeting, March 1947. Twenty-fourth Annual Lecture.

few rare meteorites that he found, but also by the fortuitous reduction of lumps of hard iron ore that were mixed with the rocks he used to shield his campfire. From that day on there followed a long list of process developments by which the ferrous industry became what it now is—the greatest aggregation of manufacturing capacity that man has yet achieved.

Simplest Essentials

In its essentials a metallurgical process is an action in which raw materials of given physical and chemical character are brought together under selected conditions of temperature and pressure, resulting in physical changes and chemical reactions that proceed by certain mechanisms at a given rate to produce a given volume and quality of product.

In the operations of the iron and steel industry, an impure iron is made by removing oxygen from an impure iron ore. Some of the impurities of the iron are removed from it by melting, but the iron in melting absorbs some of the impurities of its solid state together with an appreciable content of the reducing agent carbon. The process of steelmaking consists of using iron oxide to reduce the carbon content of the pig iron to the desired level, adjusting other elements, and achieving general refinement. Beyond this oversimplified exposition of iron and steel making there is much detail to merit interest and attention.

Raw Materials

Mineralogy of Iron Ores

The iron ores of the United States are predominately hematite or associated forms, some magnetite, and a very small proportion of carbonate ores. Classification of iron ores as to mineralogy is of little importance in relation to the processes of iron making, since all iron ores are essentially iron oxides. The physical structure of iron ore has a considerable influence on the expense and practicability of beneficiation procedures, and the particle size of iron oxide occurrence has a very basic relation to processes which is well worth extended discussion.

There has always been some proportion of fines in commercial iron ores, but the blast furnace automatically rejects fines by blowing them out of the top of the furnace as flue dust. Prior to the first World War there began the development of sintering methods to salvage the fine flue dust by sintering it into lumps within the size range suitable for blast furnace use. With sintering facilities available, in addition to recovering flue dust, ores that had previously been considered objectionably fine could be transformed into reasonably good blast furnace material. It became possible to beneficiate certain types of ores by crushing, washing off part of the lighter gravity gangue, and sintering the fine product. Likewise, sintering made feasible the use of magnetite concentrates. Magnetite commonly occurs in particles finely disseminated in rocky minerals, and the crushing required for separation of ore and gangue results in a product too fine for blast furnace use without sintering. The operation of sintering burns off much of the sulphur in the ore mix, and considerable tonnages of inadmissibly high sulphur ores are by sintering being brought down to an acceptable level of sulphur content.

Thus it is apparent that sintering serves in a number of useful ways, and the utility of this method has resulted in a great increase in its use. From the first small installation of 1911, the sintering capacity in the United States has increased to over twenty-five million gross tons per year. With a total annual ore consumption in this country of about eighty million tons, the industry is sintering in the neighborhood of 20 pct of its blast furnace ore. Sintering is appropriate to a discussion of processes because it is an

operation imposed upon the industry by the fact that the blast furnace requires coarse lump ores. If a process of ironmaking were available which could deal with ores of fine particle size, then the sintering process could be dispensed with and its cost avoided.

As useful as the sintering method is, its cost is appreciable; and the product has admitted deficiencies of physical quality and strength. Accordingly it is not surprising that there are currently being developed other methods of agglomerizing, nodulizing, and briquetting. Some of these methods give promise of economy with good quality of product but such developments still contribute nothing to a basically desirable solution by which fine materials would be dealt with as such, rather than sustaining an existing system which requires materials in large physical size.

As this nation proceeds inevitably toward extended use of lean ores requiring crushing, grinding, and beneficiation, the tonnage of fine ores will increase in proportion to the total ore consumed, and the cost of sintering or other agglomerizing will constitute an influence increasingly unfavorable to the continued existence of the present day blast furnace. While a radical development that would to any great extent supplant the blast furnace appears remote, yet clear thinking makes it necessary to realize that there is a growing economic need for an ironmaking process which would tolerate ore of fine particle size.

The Chemistry of Iron Ores

The chemistry of iron ores has a definite and determinative influence upon iron and steel making processes, and the essential effects have long been recognized.

Iron Content

While the iron content of ores profoundly affects production, it has little relation to the process used, except insofar as the maintenance of iron content above a given minimum level may require preparatory treatment of lean ores. In United States practice an ore below 45 pct iron is generally considered as requiring beneficiation for blast furnace use.

Phosphorus

Phosphorus is a dominant element in its effect on steelmaking processes. It is only weakly stable in chemical combination, and hence it is completely reduced in the blast furnace and all of the phosphorus in the burden is absorbed into the iron.

Steelmaking operations are divided into two broad types; those processes carried on with acid slags in acid-lined furnaces which do not remove phosphorus, and those processes carried on with basic slags in basic-lined furnaces in which phosphorus is removed.

Acid bessemer steel has come by custom and engineering practice to be considered of suitable analysis when phosphorus is about 0.10 pct. Translated back through blast furnace practice, this results in the maximum upper limit of bessemer iron ore being set at 0.045 pct phosphorus.

Oddly enough, though the acid open-hearth operation removes no phosphorus, trade practice sets a usual maximum phosphorus content for this steel at a level between 0.040 and 0.060 pct. The purchaser has herein taken all of the advantage of the reduction of phosphorus brought about by dilution with low-phosphorus steel scrap. Acid open-hearth iron is a low phosphorus specialty.

Since the basic open hearth easily reduces a considerable amount of phosphorus, down to 0.040 pct or under in its product, it is suitable for iron up to and exceeding 0.5 pct phosphorus; but with over 1 pct phosphorus in the iron, the basic open-hearth process requires such a large volume of relatively refractory

slag that operation becomes slow and expensive.

Where the available ores naturally yield an iron of 2 to 3 pct phosphorus, the basic bessemer process is highly suitable. It is carried on in a basic-lined converter with a basic finishing slag. To avoid undue erosion of the converter lining, the basic bessemer process demands a low silicon iron—in European practice commonly in the range of 0.30 to 0.60 pct. With such iron, much of the heat required for the process must come from the contained phosphorus. It has been found that with a low silicon content, iron for the basic bessemer process must contain a minimum of 1.8 pct phosphorus. Since ores producing this high phosphorus content do not exist in the United States and since increasing phosphorus by such expedients as adding phosphate rock are not economically practicable, the basic bessemer process is not suitable for use in this country.

The gradual depletion of the low phosphorus ores required for acid bessemer steelmaking might appear as a not too distant threat to that process, if it were not for the currently increasing production of New York State magnetites, where concentration is favorable to low phosphorus. These magnetite concentrates yield phosphorus well within existing specification limits.

Silica

That portion of iron ore which is made up of silica, alumina, and other earthy gangue materials is not of primary influence upon ironmaking processes, except as it interferes with direct processes; but the gangue content does affect blast furnace production. A silica content of about 8 or 10 pct is most suitable, for with the appropriate flux charge a proper slag volume is formed for fluxing coke ash and removing sulphur. Over 12 pct gangue results in an excess slag volume, and wastes fuel, flux, and furnace volume that could be utilized for the production of iron.

Manganese

About 75 pct of the manganese in the blast-furnace burden is dissolved into the iron as metallic manganese. Since a manganese-bearing iron is advantageous in the conventional basic iron and scrap open-hearth process for deoxidation and sulphur removal, its presence in ores is welcomed.

For acid open-hearth operation, however, manganese is highly erosive on the sand banks of the furnace bottom and it must be kept to a minimum.

In the acid bessemer, manganese over 0.5 pct in the iron tends to increase the amount of metal ejected from the converter mouth by the force of the air blast. Hence for the acid bessemer, the manganese content of iron ores should preferably not exceed 0.35 pct.

Sulphur

Iron ore of reasonable sulphur content has been and still is available in quantity, but there are large reserves of high sulphur ores which will be economically desirable for use in the future. If the economics of the situation justify sintering, then the sulphur will be reduced to usable limits.

The construction of a sulphur balance sheet for the blast furnace is not an easy task, but data have been prepared that show that the sulphur in the iron ore charged into the blast furnace represents only about 5 pct of the sulphur in the pig iron product. The sulphur in iron ore does, however, make its undesirable contribution to the final steel analysis and it must therefore be considered detrimental.

Titanium

The presence of titanium oxide in appreciable percentages has long been

and still is a largely unsolved problem in blast furnace operation, and titaniferous ores are not today considered satisfactory raw materials. The utilization of this type of ore appears to await either some new technique of mineralogical separation of the oxides of iron and titanium, or a new approach to process reduction and separation.

Even with ores containing only minor quantities of titanium oxide, there are intensifications of the problems of making iron for bessemer operation; but these are not such as to necessitate a change of process.

The process importance of the phosphorus, manganese, and titanium contents of iron ores relate not only to the production of bessemer steel, but is involved in the converter part of the duplex steel process, wherein iron is bessemerized before being dephosphorized in a basic open-hearth furnace.

Fuel and Flux

While such matters as the ash content of coal, its coking properties and sulphur content, the purity of limestone and its relative physical hardness, are all matters which profoundly affect production and costs, they do not directly determine which of present steelmaking processes is or is not usable.

Oxygen

For years there has been interest in the possibility of using pure oxygen to enrich the air blast for the blast furnace or bessemer, or for open hearth combustion or reactions. There has been experimentation in the field and the matter is currently quite active, but such proposals show no prospect of altering the essentials of the involved processes. The blast furnace will still be a blast furnace, even if supplied with a 30 pct oxygen air blast rather than normal air with 200 pct oxygen.

Process Conditions

Temperature

In considering the conditions under which its raw materials are processed, it is a notable fact that iron and steel making is carried on at very high temperatures, higher than those used in any other major manufacture, even in the field of metals. While the initial removal of the oxygen from the iron ore is completed in the solid phase in the range of 1000 to 2000°F, the material is quickly carried up into the molten phase between 2000 and 3000°F and kept in that range until the final ingot is cast.

That the development of iron and steel making did proceed upward in temperature into the molten phase is undoubtedly the most important and far-reaching condition in the processes of today—a condition involving a number of interesting features.

Reasons for a Molten Phase

A century or so ago the industry faced a rapidly growing social need for iron products, and furnaces were being developed of a size and efficiency that were quite creditable for that period. But the ironmasters of that day encountered several conditions that resulted in a largely unrecognized decision on their part.

The removal of oxygen from the iron ore and the production of a sponge iron was an already accomplished fact, but the early ironmakers experienced serious reoxidation in taking the hot sponge iron into the outdoor atmosphere and such efforts as they made toward the design of cooling chambers with controlled atmospheres were not simple and workable enough to be satisfactory.

If the development of furnaces and blowing equipment had proceeded more slowly, or if the temperature required to melt reduced iron had been a few hundred degrees higher, the industry might have been forced to continue to struggle with

the situation in the solid phase. As it was, however, it was found possible to melt the iron and thus to avoid any serious degree of reoxidation.

Difficulties of a Solid Phase

In addition to difficulties with reoxidation, a direct iron process wholly in the solid phase would not eliminate any gangue from the iron ore. Most of the iron ores of the world either contain naturally about 8 to 12 pct gangue or can be beneficiated to such an analysis without too great expense. Even the purest ores available in large tonnages today range upward of 2.50 pct silica and other gangue materials. With no elimination of gangue, the iron product resulting from such materials would be unacceptable under today's standards for all but a very few metallurgical applications.

It is obvious that to yield a sufficiently pure iron or steel product, a direct process that rejected no gangue would require substantially pure iron oxide as a raw material. Mechanical beneficiation has progressed in recent years to a high degree of efficiency and cheapness, but the limiting factor as to the extent to which beneficiation could be carried toward complete purity is to be found in the mineralogical structure of iron ores.

While most of the gangue in iron ores commonly occurs as a rather coarse impurity which can be removed with reasonable effort and expense, the last few percent of gangue occurs in very fine dissemination with the iron oxide. In most iron ore deposits and iron formations the dissemination of iron oxide and the last few percent of silica is so fine in character that complete dissociation could be obtained only by grinding to a degree of fineness beyond existing technology and mechanics.

Thus it is evident that although there are available annually in the United States some fifteen or twenty millions of tons of iron-bearing materials which are already in a fine particle size and therefore particularly suitable for a direct process, yet the purity of these materials is not adequate for a process which would not progress into the molten phase and which therefore would not reject any gangue. The achievement of such a process, which would be desirable in many ways, must therefore await not only the mechanical development of the process itself, but also a higher purity of the ores.

Chemical Methods

The molten phase is avoided in the small scale metallurgy of tantalum and tungsten, where the raw materials are purified by chemical leaching before the metallic compound is reduced to the metal. The facilities required for the chemical purification are quite a large proportion of the total plant. Such a relatively large chemical plant is acceptable in the metallurgy of rare metals, where the quantities involved are measured in ounces or pounds. If the iron and steel industry chose to deal with low-temperature, liquid, chemical solutions rather than high-temperature molten metals, such a process would displace coke ovens, blast furnaces, steelmaking furnaces, and even blooming mills—admittedly large and costly facilities. It would replace them with chemical plants of staggering physical size and financial cost, if production were to be on the scale already existent in the steel industry. Nevertheless, a pilot plant is now being constructed to produce iron powder by this general type of procedure and its functioning will be watched with interest.

There have been and now are those who propose to use direct processes in conjunction with existing liquid iron and steel procedures. The simplest of these suggestions proposes to use a direct method for partial reduction to provide

a higher than natural iron content in the blast furnace burden. Since this method would involve expense in addition to all of the cost of the present process, there appears little reason to expect that the increase of iron production would justify the extra step in processing.

In at least one instance there has been a serious effort to work out the further proposal to use direct reduction on a more or less impure iron ore to yield a product suitable for use as melting stock to replace steel scrap in either open-hearth or electric-furnace operation. So far as this development has progressed to date, the cost of the impure iron product is not yet normally competitive with either scrap or pig iron. Some mechanical details still remain unsolved problems, but even if successfully overcome the contribution does not appear to be basic in character. All in all, a direct process applied to impure ores and yielding a product for later melting has as yet resulted in no development that can be regarded as strongly promising.

For a century, operators and metallurgists and inventors have dreamed of ways of rejecting the gangue and achieving a direct iron product by gaseous reduction, by fluid catalysis, or by electrothermal procedure. The economic pressure is increasing, technology marches toward an ever higher level of capability, and the answer may even now be closer than it appears.

It is a simple but interesting fact that today's large tonnages of iron are made by purifying the iron after reduction from the oxide rather than purifying the iron oxide before reduction.

The present day blast furnace accomplishes the removal of gangue by melting the impure reduced iron and disposing of the gangue as molten slag. This objective is achieved, however, with an accompanying absorption of a considerable content of carbon. This absorption of carbon is an important feature of the industry's processes because it is responsible for much of the later expense and efforts of those procedures which constitute steel making. If the molten product of the blast furnace were a carbon-free iron, the introduction of a desired amount of carbon would appear a simple and inexpensive matter as compared to the present elaborate steps required to reduce an excess of dissolved carbon.

In addition to carbon, molten iron and steel absorb silicon, manganese, phosphorus, sulphur, oxygen, and nitrogen, which are variously desirable or undesirable. In any event, they must be controlled and adjusted to desired precise contents, a task which makes up the major part of steel works metallurgy.

Pressure

Contrasted with temperature, the part played by pressure in iron and steel making appears relatively unimportant. The industry's processes are essentially low pressure ones. Even where an airblast is employed as in the blast furnace or converter, the pressures do not ordinarily exceed 30 psi.

But beyond the generally commonplace picture of pressures in the iron and steel industry, is the recent development attempting to increase blast furnace top pressure from the usual figure of 1½ psi to a positive top pressure of about 10 psi. The mechanical and operating measures required are still under development but this change has features that are pertinent to the present lecture.

In normal blast-furnace practice substantially all very fine particles of the burden are blown out of the furnace as flue dust, but between the sizes of 20-mesh and ¼-in., particles may or may not be ejected depending upon the particular stock line conditions which influence the individual particle.

With a back top pressure of 10 lb, less

flue dust is produced and the decrease is obtained largely by retaining in the furnace a greater proportion of the larger particle sizes. Thus the higher top pressure has definitely increased the capacity of the blast furnace to deal with small particle sizes.

It is interesting to speculate whether top pressures could be increased with consequent decrease of stock line velocity to the point where substantially no flue dust would be produced. Under such conditions the blast furnace might conceivably be able to handle the smallest particles of ore without sintering. Unfortunately it appears that under such conditions the stock column would become so dense that there is serious question if practical operation could be accomplished.

Time Rate

Features which deal with the rate of speed at which iron and steel making processes proceed are rich in metallurgical interest. It requires 10 to 12 hr or more for the stock to pass through a blast furnace and making a heat of steel in an open-hearth furnace requires a similar time. In contrast to these long periods of time it strikes one forcefully that the essential reactions can take place instantaneously under favorable conditions. It may be perceived, therefore, that the time required in iron and steel making is not dependent upon the time required for the essential reactions. The time consumed is the result of operations that are preparatory and it is required by the mechanics of the process and by disposition of the end products of the reactions. Much of the reason for this situation leads again to a consideration of particle size.

The iron and steel industry commonly uses the phrase "assembly of raw materials" to embrace all those operations and expenses which are involved in the physical and mechanical mining of iron ore, coal and limestone with such preparation as may be required, and the transportation of these materials to a common geographical location.

When the physical assembly of raw materials is accomplished, there still remains a metallurgical assembly and preparation of these materials for the final reactions which alter raw materials into product. Iron ore charged into the blast furnace must be heated, dried, and dehydrated; limestone must be calcined; and coke must be burned to produce a reducing gas. Even when all of these preliminary and preparatory steps are complete only surface reactions may occur. For most of the iron ore in a blast furnace, further slow diffusion is required. When a molecule of carbon monoxide penetrates to that molecule of iron oxide which is at the center of a 3-in. lump of iron ore, then only can the final reaction of iron making take place.

In the steel works a similar metallurgical assembly and preparation of materials are required. Assembled scrap must be slowly and clumsily charged into and melted in an open-hearth furnace (admittedly not a rapid or efficient facility for that purpose); fluxes must be charged and melted; and iron must be added, to be melted if cold stock or increased in temperature if hot metal. When preparation is accomplished, surface reactions take place instantly, but final completion of the process necessitates long waiting for the slow migration of compounds throughout large baths of molten metal.

That iron and steel making is surprisingly slow, considering the practically instantaneous character of the reactions, results largely from the fact that the procedure of diffusion is involved, which is in turn imposed by the large lumps or masses that are present. As large lumps decrease in size toward fine particles, the ratio of surface to mass increases tremendously. Hence the ratio of surface reaction to diffusion increases in com-

parable proportion as particle size decreases. At a 20-mesh size, the amount of diffusion required for reduction has become very little as compared to that required for a 3-in. lump, and at 100-mesh sizes diffusion is for practical purposes almost non-existent. Since some 10 to 20 pct of the total iron ore now used by the industry is already less than 20-mesh in particle size, it is rather tantalizing to think about the possibility of carrying on reduction in this small physical size range. There is an indirect parallel in the combustion of powdered coal, wherein coal of fine particle size is burned at a rate which borders on the explosive. Possibly some such analogous procedure may be developed for iron reduction, but up to the present the large blast furnace is the effective facility for its purpose.

Pursuant to those logistics of the iron and steel industry which are referred to as assembly of raw materials, there are operations necessary for the shipment of products and for disposal of waste materials. Likewise pursuant to the metallurgical assembly and preparation of materials for reaction there follows the problem of disposing of the products of reaction.

The reactions of iron and steel making are predominantly those which occur between very thin films of gas to solid, or gas to liquid, or liquid to liquid phase systems. When materials are brought together under suitable conditions the reaction occurs immediately, but further action may be retarded by the spent products of reaction which must be removed before fresh reacting films can be brought together.

Process Mechanisms

The Blast Furnace

Technical literature on the physical chemistry of the blast furnace uniformly states that most of the iron oxide is reduced by carbon monoxide but that the lesser remaining proportion is reduced by solid carbon as an impalpable powder formed by the dissociation of carbon monoxide. Obviously in a solid to solid reaction, a fine particle size for at least one of the two solids appears to be inescapable for it is impossible to conceive how a lump of ore and a lump of coke, both the size of baseballs, could react with each other.

Whether the reducing agent is a solid carbon powder or a film of carbon monoxide in the uprushing column of gas, the initial reaction with a fresh lump of unreduced ore will be immediate. But one of the products of this initial reaction will be solid iron, fortunately rather spongy or porous in character. For further reaction it will be necessary for either carbon or carbon monoxide to diffuse slowly through the iron envelope to reach the still unreduced iron oxide in the center of the lump of iron ore. The necessity for diffusion through the relatively large size of the lumps of ore sets up time limitations for the blast-furnace system. Since the blast furnace process is a slow one, the furnaces must be large for satisfactory volume and economy of production.

The Open Hearth Process

In simplest terms the elements of the open hearth process are a quiescent molten metal bath and a molten slag blanket with a single large interface of contact. In contrast to the blast furnace both the reacting materials and the products of reactions are wholly in the gas or liquid phases, but the relative lack of turbulence restricts the speed of the process.

Turbulence of sufficient intensity to favor any rapidity of interface reactions exists during only a limited part of the heat time, hence diffusion must be relied on to a considerable extent to bring reacting materials into contact and to dispose of the spent products of reaction. Because of the large part played by slow

diffusion, open-hearth furnaces must be of large size for a satisfactory tonnage. Variations of open-hearth practice, whether or not they be so recognized, are mostly toward accelerated diffusion and increased interface action. The use of oxygen or air jets introduced into the metal bath is essentially an effort to approach in the open hearth the turbulence, rapid interface reaction, and high production rate per hour that exists in the bessemer process.

The Bessemer Process

In the bessemer process a blast of atmospheric air creates a violent turbulence in a molten metallic bath. The reactions are entirely in the gas to liquid and liquid to liquid phases. Since all the materials and products are either gases or liquids, they are highly mobile and free to move under the mechanical force and turbulent stirring action of the air blast. The method is entirely an interface process, with ideal conditions for rapid film reaction. The rapid supply of atmospheric oxygen under pressure continually oxidizes iron to iron oxide in quantities adequate for oxidation of silicon, manganese, and carbon. The turbulence caused by the blast brings iron oxide in contact with carbon-containing molten iron with an instantaneous reaction of the films constituting the interfaces. The reaction products are instantly swept aside and new films of fresh materials ready for reaction are brought into contact with each other. Thus with a process mechanism approaching closely to perfection, the productive speed of the bessemer process is quite understandable.

The Side-blown Bessemer Process

In the side-blown bessemer converter an air blast is directed obliquely across the metal bath rather than through the bath as in bottom-blowing. Iron is oxidized at the surface and a pool of iron oxide is created as a slag layer. This iron oxide reacts with the carbon of the bath and turbulence is set up by carbon monoxide as a reaction product. The essential distinction between the bottom-blown and side-blown bessemer processes is that turbulence is set up by an atmospheric air blast in bottom-blowing, while in side-blowing turbulence is effected by carbon monoxide. In the bottom-blowing there is a considerable absorption of nitrogen since the turbulence-producing agency is atmospheric air containing 80 pct nitrogen. In side-blowing the agency producing turbulence is almost wholly carbon monoxide and there is substantially no absorption of nitrogen.

The Talbot Process

Conditions quite like those of the side-blown bessemer were created in the Talbot process without the use of an air blast. Molten pig iron in limited quantities was added to a very hot low carbon steel bath under a highly oxidized slag. The initial liquid to liquid reaction resulted in a gaseous product of reaction which set up turbulence that made the reactions proceed more rapidly. The reaction increased in speed by self-induced turbulence until it reached a violence just short of the explosive.

In the Talbot process the reduction of carbon and metalloids was accomplished in a minute or two, but the restriction that the furnace had to go through the slow task of melting its own slag brought its rate of production per hour below that of good open-hearth furnace practice.

The Perrin Process

The Perrin process is a deoxidation or refining procedure rather than a steel-making process, but the mechanism is quite similar to that of the bessemer and Talbot processes, with the distinctly interesting variant that slags are prepared and melted in a separate furnace provided solely for

that purpose. Steel is decanted into separately prepared slag which has been placed in the bottom of the steel ladle. Turbulence is achieved by the mechanical force of pouring from a height and by the gaseous reaction products. Under these conditions reactions are complete in a minute or so of time.

Any student of processes will sooner or later find his attention engaged by the possibility of providing facilities specially designed and separately operated for melting scrap and melting slags. Such possibilities are at least theoretically attractive. If premelted scrap and separately melted fresh slags were available for use by the open-hearth furnace, the open hearth process would become a very different and a very much more rapid procedure than it now is. But such an arrangement would involve the investment cost of three high temperature units instead of one, with some increase in operating and maintenance expense and with increased metallic losses in handling. The experience of the industry is that process elaborations, which involve combinations of furnaces rather than a single unit, must be considered cautiously and are economically successful only under favorable circumstances.

The Duplex Process

There are various ways in which process units are joined together in multiple arrangements but the combination that is the most important in tonnage is that in which iron is decarburized in a bessemer converter and then dephosphorized in a basic open hearth furnace. Thus a very low phosphorus steel can be produced from relatively high phosphorus iron.

This duplex process contains little that is of distinct metallurgical interest except as relates to the nitrogen absorbed in the converter and carried over into the open hearth. The nitrogen can be largely eliminated or substantially reduced to the level of nitrogen in scrap and metal open hearth steel by stopping the bessemer blow before the carbon is completely eliminated, and by creating conditions to favor rapid carbon removal in the open hearth. These conditions cause carbon monoxide to be evolved rather rapidly and a degree of turbulence is set up which favors the elimination of nitrogen.

Throughout the whole field of iron and steel making processes turbulence stands out impressively as a condition favoring increased speed and economy of production and very frequently an improved quality of product. But the service rendered by turbulence resides not in turbulence itself but in the fact that a turbulent condition favors interface reactions and decreases the proportion of iron and steel making which must be accomplished by the tediously slow mechanism of diffusion.

The Electric Furnace

The electric furnace is the very efficient modern successor to the pot crucible furnace of past generations. Its refining operations contain many features that are of great interest in the physical chemistry of molten steel and molten slags, and the exactitude that has been achieved in its manipulation is highly creditable, as is the quality of the considerable tonnage of steel manufactured by this facility.

Nevertheless, the electric furnace as used in the United States contributes little or nothing to those steps by which the industry converts iron ore into steel. Regardless of the high level of metallurgical technique employed and the high quality of steel produced, the electric furnace is a salvaging facility rather than a steel-making unit.

Conclusion

The serious student of process metallurgy may envision a future in which there may become economically practicable and mechanically feasible on a large tonnage

scale, a direct process wholly in the solid phase with or without chemical preparation. But such a development would not bring an end to the metallurgy of molten steel. So long as the characteristics of steel and the circumstances of its use remain substantially as they are today, there will be a justification for the salvaging of steel scrap, until that time when virgin steel becomes so cheap as to make reclaiming operations economically unjustifiable. From today's point of view that eventuality appears remote indeed.

No situation within the limits of practical envisionment shows any end to the metallurgy of molten steel. Imagination may fancy iron and steel as resulting directly or as a by-product from atomic transmutation, but that future is hidden in the as yet unrolled scroll of years to come.

By constantly building on the ruins of its own best efforts, the iron and steel industry has achieved tremendous accomplishments which warrant justifiable pride. But the industry which has done these great things will not make the mistake of considering its processes perfect or its knowledge thereof complete. Rather will it carry on toward improvement of process and increase of knowledge in that attitude of the industry, which becomes with the passage of the years, more and more a high tradition.

Rate of Reduction of Geneva Iron Ore

By John R. Lewis,* Member AIME

(New York Meeting, March 1947)

During the past few years there has been considerable interest in the sizing and the preparation of the iron ore fed into blast furnaces. Furnacemen know that proper sizing of ore tends to increase the efficiency of the furnace.

It has been shown by Joseph[1] and his associates that there is a direct relationship between the porosity of an ore particle and the time required for its reduction in the blast furnace. This relationship may be stated as follows: *All other factors remaining constant, the time for reduction of a given sample of ore is inversely proportional to its porosity.* As a consequence, large pieces of very porous ore, say 3 or 4 in. in cross section, will be completely reduced by the time they reach the hot zone just above the tuyeres, while large pieces of dense, nonporous ore may reach the hot zone with their centers unreduced. This means that for the latter complete reduction will be accomplished by the so-called "direct method;" i.e., where carbon reacts directly with the ore.

Some recent work by Philbrook[2] seems to contradict this rule. He found that of two unlike ores he studied, the one with the lower porosity reduced more readily. He explained his results as "possibly due to an apparently greater tendency of the 'A' ore (lower porosity) to crack during preliminary dehydration and during reduction." This brings his results in line with the rule stated above.

It is not the author's intention to enter into a discussion of the merits of "direct" versus "indirect" reduction. It is enough to say that, in general, indirect reduction is desirable. For the greatest efficiency, Gruner's theorem[3] requires that all reduction in the blast furnace be indirect. Joseph seems to believe this also, because in his recent article on Some Comparisons between Iron Ore, Sinter and Nodules as Blast Furnace Feed[4] he concludes that: "In general, the carbon in blast-furnace coke is used most efficiently when the largest amount of the carbon charged reaches the tuyeres." However, P. V. Martin,[3] in an excellent paper, has shown that some direct reduction may actually increase the efficiency of the furnace; that is, increase its rate of production while maintaining maximum fuel economy.

For nonporous ores there is more opportunity to have an excess of direct reduction unless the factors that make for indirect reduction are favored; for instance; the proper sizing of the ore particles.

Another factor that has an important bearing on the reduction rate, as it is affected by particle size, is the flow of heat into the particle. The ore particle

This study was first started at the suggestion of Mr. James Stapleton, Superintendent of Blast Furnaces at Geneva. After Mr. Stapleton returned to the East, the work was continued with the cooperation of Mr. J. S. McMahon, who was Mr. Stapleton's successor at Geneva. The author is especially indebted to Dr. Walther Mathesius, President of Geneva Steel Co., for reading this paper and for the valuable suggestions he made. Manuscript received at the office of the Institute Dec. 31, 1947. Issued as T.P. 2177 in Metals Technology, June 1947.

* Head, Department of Metallurgy, University of Utah, Salt Lake City, Utah.

[1] References are at the end of the paper.

is at atmospheric temperature, say 70°F, when it enters the top of the furnace. Immediately it comes in contact with gases at a temperature of 350° to 400°F. Heat will flow into the particle as it descends. The problem is complicated by the fact that the temperature of the contact gases increases continuously as the particle descends. During this time the heat is flowing in toward the center of the particle. Since the gases, flowing up between the ore particles, contain quantities of carbon monoxide, and a little hydrogen, the reduction of the iron oxide begins when a suitable temperature is reached. Naturally, the outside of the particle will be ready for reduction first, since it will be heated first. Reduction inside the particle will take place when the temperature reaches a certain minimum value.

The rate of reduction of the interior of the particle depends, then, on two factors: (1) the rate at which heat flows from the outside to the inside, and (2) the rate at which carbon monoxide (or hydrogen) diffuses into and carbon dioxide (or water) diffuses out of the central portion of the particle. Large particles will have unreduced centers while small particles will be completely reduced. T. P. Colclough[5] has suggested that "the practical limit of carbon monoxide reduction is reached when the carbon monoxide to carbon dioxide ratio is 65 to 35 and the temperature of the reaction between carbon monoxide and iron oxide is 700°C." Colclough also pointed out that (for a large particle) if the temperature outside the particle is over 900°C the carbon dioxide formed in the center reaction will react with carbon as follows:

$$Fe_2O_3 + 3CO \rightarrow 2Fe + 3CO_2 \quad [1]$$

$$3C + 3CO_2 \rightarrow 6CO \quad [2]$$

$$Fe_2O_3 + 3C \rightarrow 2Fe + 3CO \quad [3]$$

Thus it may be said that carbon consumed by this "solution loss" reaction is being used for direct reduction.

If too high a percentage of fine ore (less than ⅜-in.) is charged into a blast furnace, serious operating (mechanical) difficulties may be encountered. The introduction of sintered ore has been beneficial, but here again the character of the sinter—i.e. whether soft, hard, porous—will have an important bearing on the way it reduces in the furnace.*

Recently, fine ores have been converted into pellets and nodules. In these forms, the ore may become rather useful as furnace feed, and may replace part of the sinter now used. It is doubtful, however, whether pellets, nodules or sinter will ever completely replace properly sized ore particles as blast-furnace feed.

The iron ore used in the Geneva blast furnaces is a rather hard, dense hematite or hematite-like material containing magnetite. A microscopic analysis of ore sample A was made by Prof A. L. Crawford, of the Utah Engineering Experiment Station. Chemical analyses of ore samples A and B were made by Mr. C. K. Hanson, Utah Engineering Experiment Station analyst. For comparison, an analysis of a "mixed sample" of Geneva ore is also given. These analyses are tabulated in Table 1.

Experimental Procedure

The ore used in this study came from two typical samples of Geneva ore, sample A and sample B. Of the two, sample B was harder and less porous than sample A.

Ore Cubes.—Following the method used by Joseph,[1] a series of cubes was made. These cubes varied in size from ½ to 1 9/16 inches. All the cubes from ore sample A

* In this paper, the author has neglected the role of coke in the operation of a furnace. Needless to say, the quality of the coke may mean the difference between success and failure of a given furnace.

were made from one lump of the ore. Likewise, one lump furnished the cubes of ore sample B. These cubes were first made by roughing them out with a chisel and then finishing them on a "mud" (polishing) wheel. This method proved to be rather unsatisfactory because it was difficult to make true cubes of specified dimensions. However, a number of fair cubes were made by this method, which subsequently were used in some of the preliminary experiments. The second method, developed by Roscoe Woolley, of the Utah Engineering Experiment Station, gave very satisfactory cubes.* Briefly, the method "rough-shapes" the cube on a heavy-duty machine-shop grinder. The first grinding is done on the side of the lump that presents the most nearly flat surface. After the first side is flat and smooth, the remaining five sides are ground in a similar manner. The feed adjustment is set to give a table movement of about $\frac{1}{16}$ in. per stroke. For the first cuts, the wheel is lowered to give about $\frac{1}{32}$-in. depth of cut. For finishing, this is changed to give a cut about 0.010 in depth. Cubes made in this way are remarkably true to the desired dimensions, with edges and corners preserved. Fig 1 shows some of these cubes before and after reduction in the furnace.

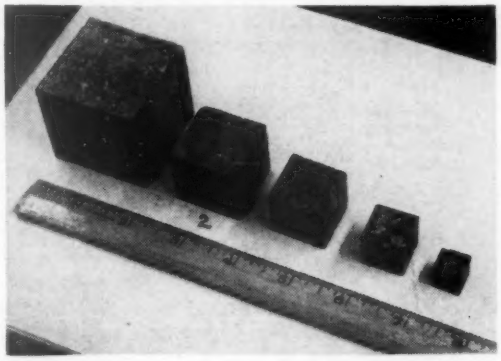

FIG 1—IRON-ORE CUBES. NO. 2 HAS BEEN REDUCED.

TABLE 1—*Mineralogical and Chemical Composition of Geneva Iron Ore*

Mineralogical		Chemical		Chemical		Chemical	
Ore A[a] (Approximate)	Per Cent	Ore A[b]	Per Cent	Ore B[b]	Per Cent	Mixed Ore[c]	Per Cent
Ore Material:							
Magnetite (Fe_3O_4)	35	Iron	57.2	Iron	58.80	Iron	54.3
Martite (Fe_2O_3)	15	SiO_2	5.38	SiO_2	3.75	SiO_2	7.2
Specularite (Fe_2O_3)	5	CaO	4.67	CaO	4.98	CaO	3.0
Goetheite and limonitic matter	5	Al_2O_3	4.37	Al_2O_3	3.26	Al_2O_3	1.75
Gangue Material		MgO	0.75	MgO	0.80	MgO	1.50
Calcite	25	P	0.52	P	0.32	Mn	0.10
Talcose	5	S	0.07	S	0.07	P	0.10
Quartz	5	All others	27.04	All others	28.20	All others	32.05
Feldspathic material	5						
Total	100		100		100		100

[a] Analysis made by Prof. A. L. Crawford, Utah Engineering Experiment Station.
[b] Analysis made by C. K. Hanson, Utah Engineering Experiment Station Analyst.
[c] Analysis supplied by Geneva Steel Company.

second step in the process is the "finish grinding" done on a shaper with a tool post grinder mounted on the ram of the machine. The shaper ram speed is set at about 25 strokes per minute and the

Apparatus.—The reduction apparatus consisted (see Fig 2) of: (1) a flowmeter; (2) an electric combustion furnace B containing a Pyrex glass tube *C* filled with fine, copper turnings; (3) two drying towers *D* and *E*, filled with anhydrous calcium chloride and phosphorus pentoxide, re-

* A detailed description of Mr. Woolley's method for making cubes may be obtained by writing to the Director, Utah Engineering Experiment Station, University of Utah, Salt Lake City, Utah.

spectively; (4) an 18 by 3-in. electric combustion furnace *F* containing a porcelain tube of special design *G*, 42 in. long, 7/8 in. inside diameter on the small end and 2 5/8-in. inside diameter at the large end; (5) a U-tube *H*, containing drying agents; (6) a thermocouple *I*; and (7) a perforated steel boat to hold the ore cube.

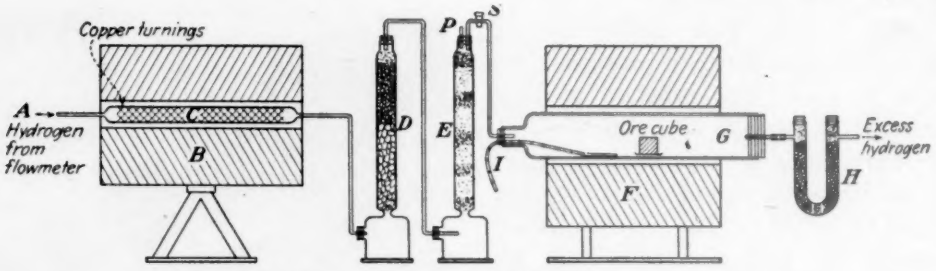

FIG 2—REDUCTION APPARATUS.

A. Flowmeter (not shown).
B. Electric combustion furnace.
C. Pyrex glass tube.
D. Drying tower.
E. Drying tower.
F. Electric combustion furnace.
G. Porcelain tube.
H. U drying tube.
I. Thermocouple.

Procedure in Making a Run.—A dried and weighed ore cube is placed at the proper position in the combustion tube *G* and the large rubber stopper, containing a glass delivery tube, inserted to close the end of the tube. Then the electric current is turned into the cold furnace. Next nitrogen from a cylinder of the compressed gas is passed through the flowmeter and then through the tube of copper turnings, which is maintained at about 600°C by furnace B. This removes any oxygen present in the nitrogen. After removal of oxygen, the gas is passed through the two drying towers where water vapor is removed. Next it passes through the combustion tube *G* containing the ore cube. Nitrogen continues to flow through the system until the temperature of furnace *F* reaches and remains constant at 800°C. At this point a weighed absorption U-tube is attached to the glass tube outlet of tube *G*. Now the stopcock *S* is closed and the plug *P* removed, and hydrogen, from a cylinder or the compressed gas, is turned into the system instead of the nitrogen. Sufficient time, about 3 minutes, is allowed for the hydrogen to replace the nitrogen remaining in drying towers, the tube of copper turnings and connecting tubing. After this has been accomplished, the stopwatch is started just as the stopcock *S* is opened and the plug *P* is inserted. This marks the beginning of the run.

At the end of a definitely known time interval, say 10 minutes, the U-tube is removed and another attached to the apparatus. This is repeated until the reaction is completed. The reaction is considered complete when the U-tubes fail to gain more than 3 mg during a 10-min. period. After the reaction is complete, the hydrogen gas is replaced by nitrogen, which passes through the system while the furnace cools to room temperature.

OTHER EXPERIMENTAL DETAILS

Flow of Hydrogen.—Following Joseph's procedure,[1] the hydrogen was passed through the system at the rate of approximately 800 cc per minute. It was observed that at the beginning of a run, water condensed in the tube leading into the absorption U-tube. Philbrook[2] made a similar observation. He overcame the difficulty by passing the gas through his apparatus at a much higher velocity. In this work, the water condensation was prevented by heating the tube. This was accomplished by placing a 100-watt light bulb in a box having a slit top. The slit paralleled the tube where the water vapor was condensing. By proper adjustment of the slit directly under the glass tube resulted in its effective

heating with the prevention of condensation of water vapor.

Absorption Tubes.—The absorption U-tubes were of large size (6 in. by 0.625-in. i. d.) and were filled in a novel way. The arm of the tube, where the water vapor and excess hydrogen entered, was filled with anhydrous calcium chloride. The other arm was filled with anhydrous magnesium perchlorate (dehydrite). The two anhydrous salts were separated by a glass-wool plug. This arrangement proved very satisfactory. When the calcium chloride showed signs of becoming saturated with water, the arm containing the perchlorate appeared to be unchanged. Consequently, the spent calcium chloride could be replaced by a fresh supply without disturbing the magnesium perchlorate. This arrangement was just as effective as the use of two U-tubes connected in series, and it was more convenient to use.

Temperature Control.—The furnace *F*, a 220-volt a. c. type Hevi-Duty multiple unit, made by the Hevi-Duty Electric Co. of Milwaukee, Wis., was maintained at 800°C by means of an induction-type voltage regulator. The actual temperature was determined by means of a chromel-alumel thermocouple inserted in the reduction tube, next to the iron ore cube but not touching it.

Drying of Cubes.—Before the cubes were placed in the reduction apparatus, they were heated in an electric oven at approximately 450°C for several hours. This removed all moisture. They were stored in a desiccator until used.

Weighings.—All cubes, absorption tubes, and other apparatus were carefully weighed on an analytical balance.

Porosity of Cubes.—In order to determine the porosity of ore cubes, it was necessary to determine the true specific gravity of the ore and also the apparent specific gravity. The apparent specific gravity is obtained by dividing the weight in grams of a cube by its volume in cubic centimeters.

The volume of the ½-in. cube (the smallest used in these experiments), assuming a perfect cube, is 2.048 cc. A rather simple, rapid and reasonably accurate method of determining the volume

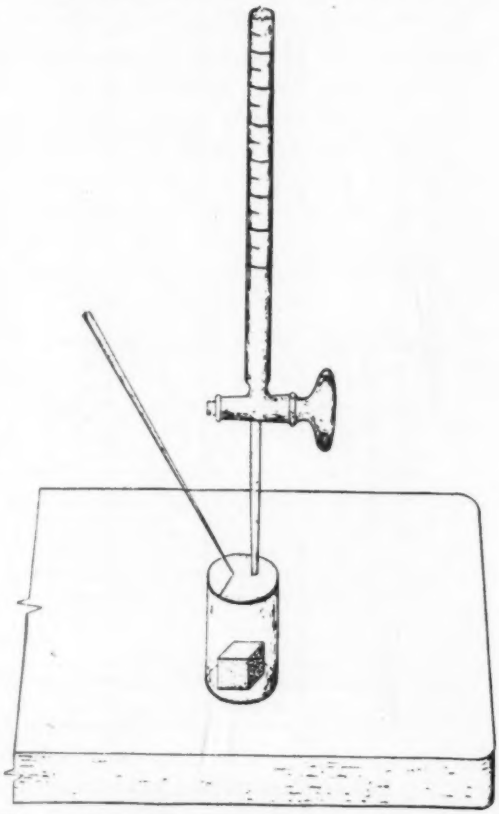

FIG 3—APPARATUS FOR DETERMINING VOLUME OF CUBES.

is as follows: The volume of a glass vial is determined by completely filling it with water at a known temperature. To make sure the vessel is filled to exactly the same height each time, it is placed on the platform of a burette stand in such a position that the tip of a small-diameter metal rod arranged in a nearly perpendicular position (about 20°) is at the same height as the top of the vial. During the filling of the vial from a burette, a reflection of the metal rod is visible in the water. At the instant the vial is filled the reflection of the tip of the rod "touches" the tip of the metal rod.* (See Fig 3).

* This procedure is similar to that used for adjusting the level of the mercury in a weather bureau type of mercury barometer.

After determining the volume of the vial in this manner, an ore cube (just removed from a beaker of water and wiped visibly dry) is placed in the vial and enough water is added from the burette to fill the vial to the same level as that obtained using water only. Typical results using this method are given in Table 2.

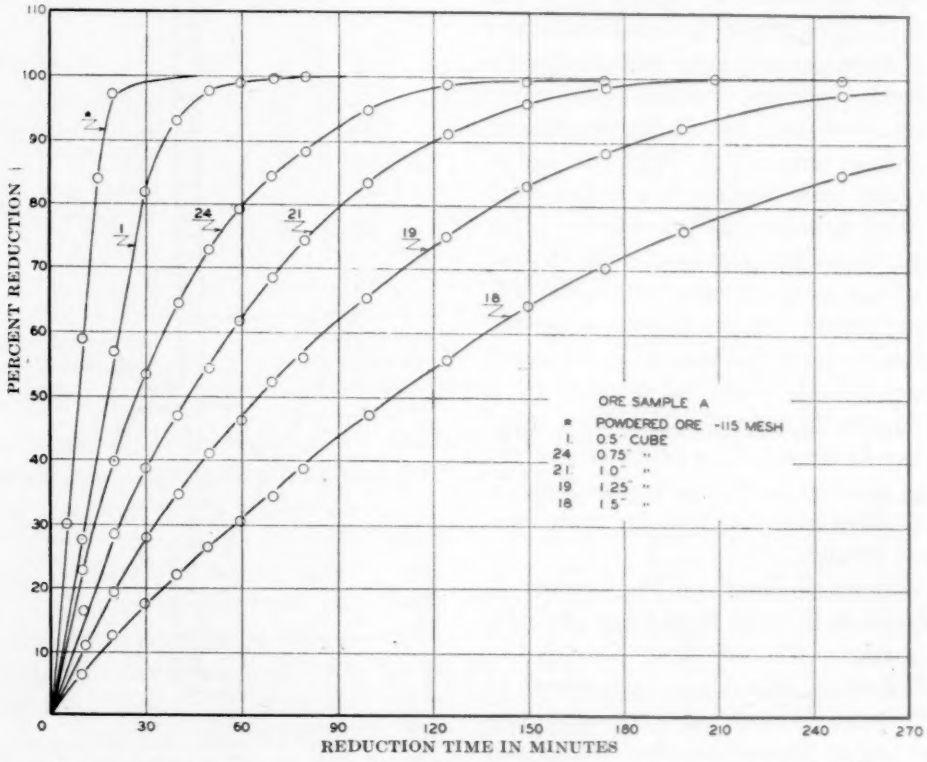

FIG 4—PERCENTAGE REDUCTION OF CUBES AS A FUNCTION OF TIME AT 800°C.

TABLE 2—*Volume of Cubes*

Cube No.	Theoretical Volume, cc	Measured Volume (Average of 5 Determinations), cc
1	2.048	1.99
2	2.048	1.98
3	2.048	2.03

The true specific gravity of the ore is determined by adding a known weight of powdered ore to a specific gravity bottle. To this is added enough distilled water to half fill the bottle. It is then placed on a water bath containing boiling water and allowed to remain for one hour. The bottle is then removed and enough water added to fill it up to the neck, after which it is cooled to room temperature. Next the bottle is completely filled with water and the contents is weighed. The true specific gravity is determined by the following formula:

$$\text{True Specific Gravity} = \frac{W}{W - (W' - P)}$$

where

W = weight in grams of minus 100-mesh dry ore.

W' = weight in grams of the specific gravity bottle and the dry ore and water required to fill it.

P = weight in grams of the bottle and water required to fill it.

EXPERIMENTAL RESULTS

The data obtained are summarized in Tables 3 and 4 and shown graphically in

TABLE 3—*Reduction of Iron-ore Cubes of Sample A at 800°C as a Function of Size*[a]

Cube No.....	1	24	22	21	19	18	
Weight cube, grams	7.6832	24.9676	37.210	55.3304	109.2	186.2	
Volume, cc.....	2.05	6.91	10.98	16.387	32.00	55.306	
Total wt H_2O, grams	2.108	6.4206	10.707	15.347	30.0	51.0	
Grams H_2O / Gram ore	0.2746	0.2572	0.2875	0.2773	0.2740	0.2739	Average 0.2741
Porosity, pct.....	11.0	14.3	19.6	20.0	19.2	20.0	
Percentage Reduction at Various Time Intervals							
Minutes							
10	27.3	22.7	21.05	16.3	11.0	6.	
20	56.5	39.5	36.29	28.1	20.0	12.5	
30	81.5	53.04	49.24	38.4	27.5	17.5	
40	93.1	63.83	61.0	46.3	34.5	21.76	
50	97.55	72.35	70.7	54.2	40.5	26.2	
60	99.3	79.13	77.9	61.4	46.0	30.4	
70	99.5	84.46	84.45	68.3	52.2	34.0	
80		88.0	86.25	74.25	56.0	38.2	
100		94.92	95.61	83.25	65.0	46.25	
125		98.6	98.4	90.7	75.2	55.35	
150		99.4	98.96	95.92	82.8	64.0	
175		99.7	99.3	98.2	88.0	70.4	
200		99.85	99.6	98.94	92.1	76.0	
250				99.5	97.4	85.0	
300					98.52	91.75	
350					98.9	95.75	
400					99.3	97.8	
470						98.6	
650						99.45	

[a] Cubes made from a large piece of ore sample A; true density, 4.22. Average of four determinations.

TABLE 4—*Reduction of Iron Ore Cubes of Sample B at 800°C as a Function of Size*[a]

Cube No.....	50	51	52	17	
Weight cube, grams.....	8.086	26.8642	60.549	244.42	
Volume, cc.....	2.048	6.91	16.387	62.6	
Total wt H_2O, grams.....	2.0765	6.90	15.054	68.663	
Grams H_2O / Gram ore	0.257	0.2568	0.249	0.281	Average 0.261
Porosity, pct.....	9.25	10.35	14.75	9.8	
Percentage Reduction at Various Time Intervals					
Minutes			Min.	Min.	
10	33.6	17.7	(11) 11.5	(10) 2.34	
20	54.25	33.1	(21) 21.7	(30) 6.01	
30	70.90	46.25	(31) 31.3	(50) 7.74	
40	82.50	57.25	(41) 39.7	(80) 12.87	
50	90.20	66.31	(51) 47.4	(120) 17.48	
60	93.75	74.28	(61) 54.4	(140) 20.13	
70	97.36		(71) 60.9	(160) 23.06	
80	98.57	86.36	(81) 67.3	(200) 28.73	
90	99.05		(91) 72.1	(290) 49.13	
100	99.51	93.67		(390) 52.73	
110	99.89		(111) 80.3	(480) 63.81	
120	99.94	97.65		(595) 75.8	
130			(131) 87.1	(640) 79.85	
140		99.42	(172) 95.8	(715) 86.67	
150			(191) 97.6	(805) 91.78	
160		99.94	(221) 99.1	(925) 95.55	
170			(251) 99.74	(1015) 96.6	
180			(276) 99.94	(1075) 96.98	
				(1285) 99.78	

[a] Cubes made from a large piece of sample B; true density, 4.34. Average of four determinations.

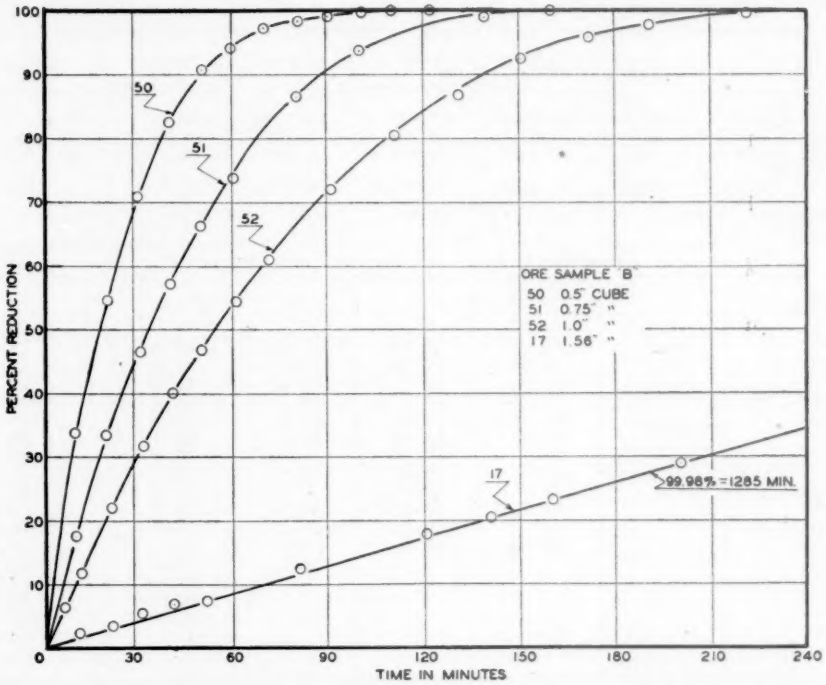

FIG 5—PERCENTAGE REDUCTION OF CUBES AS A FUNCTION OF TIME AT 800°C.

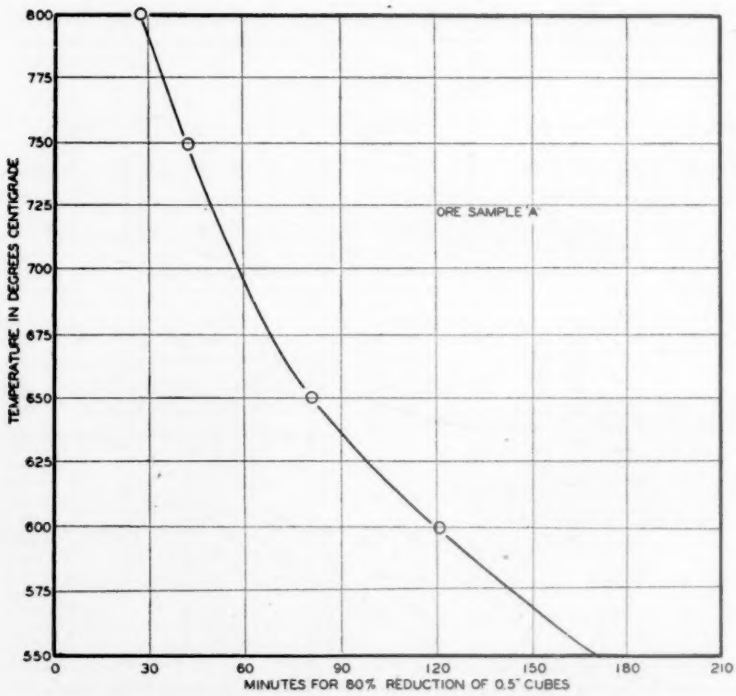

FIG 6—EFFECT OF TEMPERATURE ON TIME REQUIRED FOR 80 PERCENT REDUCTION OF 0.5-INCH CUBES.

TABLE 5—*Data for Cubes*

Cube No.	Ore Sample	Dimensions of Cube, In.	Volume, Cu In (a)	Volume, Cu Cm (b)	Wt Grams (w)	Apparent Density $\left(\frac{w}{b}\right)$	True Density
1	A	0.5	0.125	2.048	7.683	3.75	4.22
24	A	0.75	0.422	6.91	24.967	3.61	4.22
23	A	0.75	0.422	6.91	26.437	3.83	4.22
22	A	0.875	0.669	10.97	37.21	3.39	4.22
21	A	1.0	1.00	16.387	55.33	3.37	4.22
19	A	1.25	1.953	32.00	109.2	3.41	4.22
18	A	1.5	3.375	55.3	186.2	3.37	4.22
50	B	0.5	0.125	2.048	8.086	3.94	4.34
51	B	0.75	0.422	6.91	26.8642	3.89	4.34
52	B	1.0	1.00	16.387	60.549	3.7	4.34
17	B	1.562	3.814	62.6	244.42	3.91	4.34

TABLE 6—*"Reduction Index" Data at* 800°C

Cube No.	Time for 50 Pct Reduction, Min.	$\frac{1 \times 10^3}{\text{Min. 50 Pct Red.}}$	Time for 80 Pct Reduction, Min.	$\frac{1 \times 10^3}{\text{Min. 80 Pct Red.}}$	Time for 90 Pct Reduction, Min.	$\frac{1 \times 10^3}{\text{Min. 90 Pct Red.}}$
Ore Sample *A*						
1	18	55.6	29	34.5	37	27.1
24	28	35.7	62	16.1	85	11.75
22						
21	45	22.2	92	10.9	123	8.13
19	67	14.92	140	7.14	187	5.34
18	110	9.1	223	4.47	286	3.5
Ore Sample B						
50	19	52.7	37	27.1	50	20.0
51	33	30.3	78	12.84	88	11.35
52	55	18.2	110	9.1	142	7.05
17					760	1.315

several figures. Table 3 gives the reduction data for ore sample A while Table 4 gives the same information for ore sample B. Dimensional, volume and density data for the various ore cubes are summarized in Table 5. The times for 50 pct, 80 pct and 90 pct reduction of the various cubes and the reciprocal of these values are shown in Table 6.

Figs 4 and 5 show graphically the relation between the time in minutes and the percentage of total reduction for cubes of ore sample A and of ore sample B, respectively. Fig 6 shows the relation between temperature of reduction in degrees centigrade and the time in minutes necessary for 80 pct reduction of ½-in. cubes of ore sample A.

The effect of cube size on the time for 50 pct, 80 pct and 90 pct reduction at 800°C for ore samples A and B are shown graphically in Figs 7 and 8. The effect of cube size on the "index of reduction" is shown in Fig 9. Plotted on semilog paper, Figs 10 and 11 show, for ore samples A and B, the percentage of cubes of various sizes not reduced at various time intervals.

DISCUSSION OF EXPERIMENTAL RESULTS

The curves plotted in Fig 4 show the "family of curves" obtained from powdered ore and cubes of various sizes made from ore sample A. Although the porosity varies some from cube to cube, these curves show very clearly that the time for any given percentage of reduction varies as the size of the cube. For ore sample A,

the curves are straight lines once the initial "induction" period is passed. See Fig 7. This induction period may be due, in part, to the time necessary for after reduction maintained their original shape.

Curves in Fig 5 show the same general characteristics as those in Fig 4. The

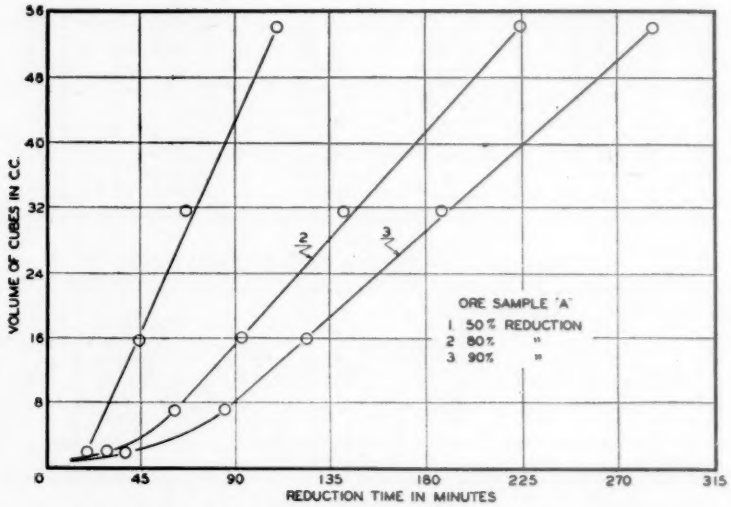

FIG 7—EFFECT OF CUBE SIZE ON TIME FOR REDUCTION AT 800°C.

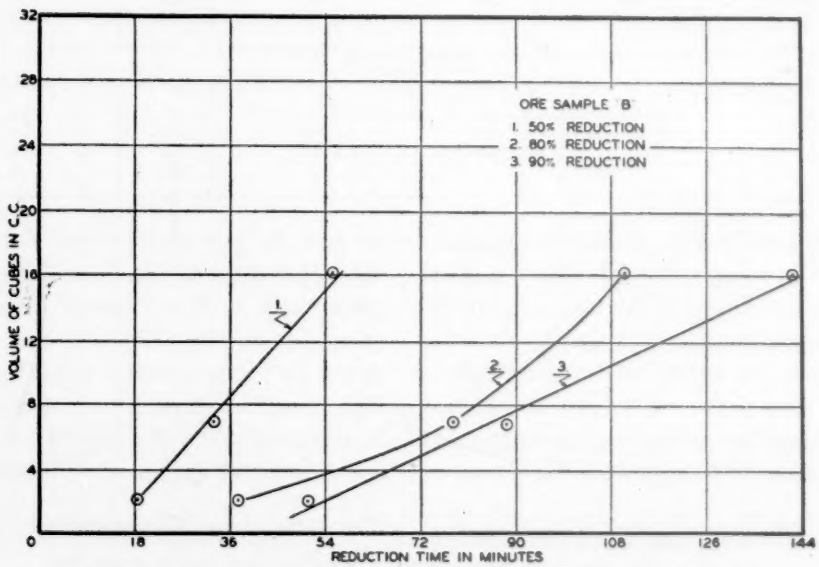

FIG 8—EFFECT OF CUBE SIZE ON TIME FOR REDUCTION AT 800°C.

the water first formed to find its way into the absorption U-tube. These curves indicate that, unlike ore A studied by Philbrook,[2] no appreciable amount of cracking or spalling takes place during reduction. Cubes removed from the furnace

anomalous behavior of cube 17, the largest cube reduced in this study, is only partially explained by pointing out: (1) that the slope of the *porosity*—time *for* 90 *pct reduction* curve is steep for an ore with a porosity less than 10 pct.

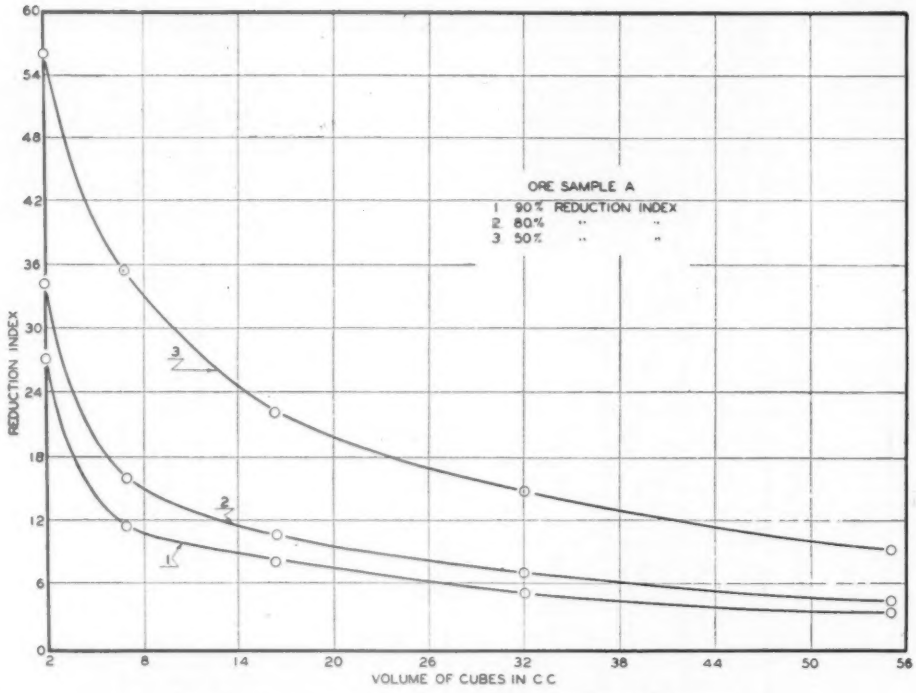

FIG 9—EFFECT OF CUBE SIZE ON "REDUCTION INDEX."

$$\text{Reduction index} = \frac{1}{\text{Minutes for percentage of reduction}}$$

The data obtained showing the relationship between porosity and rate of reduction for these Geneva ores are in line with results obtained by Joseph on Mesabi, Alabama and India ores. Table 10 and Fig 13 show this relationship.

TABLE 7—*Data Showing Values for Various Terms in First Order*

Equation $\left(K = \frac{2.303}{t} \log \frac{a}{a-x}\right)$ $t = 650°C$

$a = 1.969$ x = grams water at time t

1	2	3	4	5
t	$\log \frac{a}{a-x}$	$K \times 10^4$	$\frac{a-x}{a}$	$1 - \frac{a-x}{a}$
10	0.10346	238.3	0.788	0.212
20	0.1897	218.2	0.646	0.354
30	0.2690	206.5	0.538	0.462
40	0.3454	198.9	0.452	0.548
50	0.41075	189.2	0.388	0.612
60	0.49275	189.1	0.321	0.679
70	0.56284	185.2	0.274	0.726
80	0.63857	183.8	0.229	0.771
90	0.7282	186.3	0.187	0.813
100	0.8224	189.4	0.151	0.849
110	0.9199	192.6	0.120	0.880
120	1.0069	193.2	0.098	0.902
130	1.0890	192.9	0.083	0.917
140	1.1870	195.3	0.065	0.935

Both Joseph[1] and Philbrook[2] attempted to find some suitable "reducibility index" for purposes of comparison. Joseph used the reciprocal of the time for 90 pct reduction $\left(\frac{1}{\text{min. for 90 pct reduction}}\right)$. (See Table 6.) Philbrook's "slope index" is obtained by determining the slopes of the reduction curve at the end of 20 minutes (slope A) and 60 minutes (slope B), respectively. The expression is:

$$\text{Slope index} = \log_{10} \frac{\text{(slope A)}}{\text{slope B}}$$

The advantage of the "slope index," according to Philbrook, is that a reduction experiment need not take much longer than one hour to obtain the necessary data for a given sample of ore or sinter.

The experimental reduction curves apparently follow an exponential law. Observation of this fact was the basis for Philbrook's mathematical derivation of his "slope index." Through a similar line of reasoning, the author of this paper applied

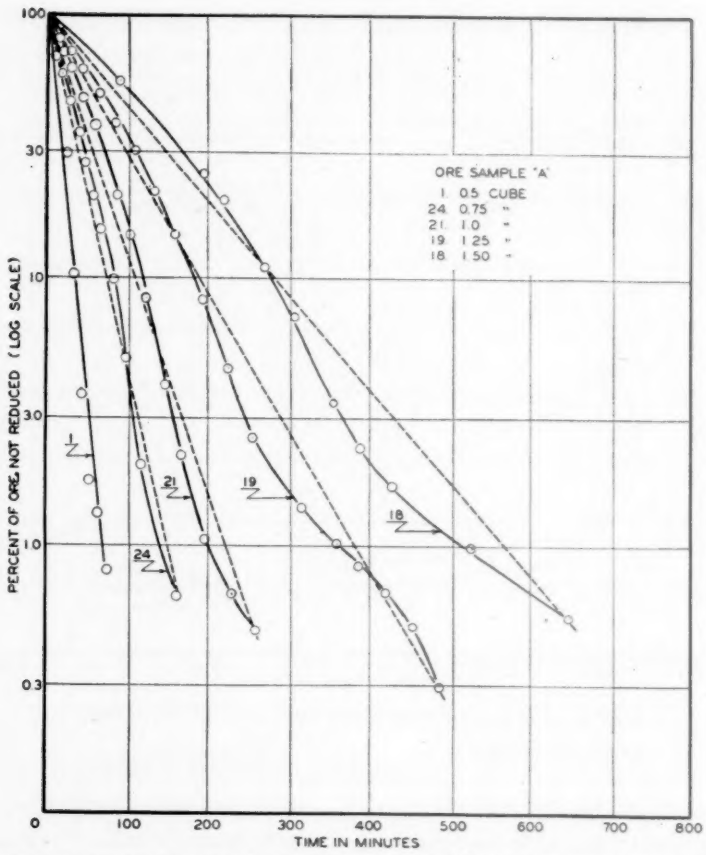

FIG 10—PERCENTAGE OF CUBES NOT REDUCED AT 800°C AT END OF VARIOUS INTERVALS.

TABLE 8—*Data Showing Fraction of Cubes Not Reduced at Various Time Intervals (Minutes) at* 800°C

Cube No.												
Ore Sample A												
1	10 0.727	25 0.296	36 0.103	46 0.037	56 0.018	66 0.013	76 0.008					
24	10 0.773	20 0.605	30 0.469	40 0.361	50 0.276	60 0.208	70 0.158	85 0.094	100 0.051	120 0.020	140 0.011	180 0.003
21	10 0.837	20 0.719	30 0.616	46 0.484	60 0.385	75 0.285	106 0.146	152 0.041	170 0.022	200 0.011	260 0.005	290 0.003
19	8 0.913	19 0.812	31 0.725	45 0.626	66 0.5050	90 0.386	110 0.302	165 0.138	195 0.083	315 0.014	420 0.006	510 0.002
18	15 0.903	35 0.796	65 0.679	95 0.556	125 0.446	155 0.347	220 0.199	280 0.107	350 0.043	430 0.017	650 0.005	770 0.003
Ore Sample B												
50	10 0.664	20 0.457	30 0.291	40 0.175	50 0.098	60 0.063	70 0.026	80 0.014	90 0.009	100 0.005	110 0.001	
51	10 0.823	20 0.669	30 0.537	40 0.427	50 0.337	60 0.257	80 0.136	100 0.063	120 0.024	140 0.005	160 0.003	
52	11 0.885	21 0.783	31 0.687	41 0.603	51 0.526	61 0.456	71 0.391	91 0.279	131 0.129	172 0.042	221 0.009	276 0.001
17	10 0.976	20 0.961	30 0.940	40 0.928	50 0.922	80 0.871	140 0.799	200 0.713	390 0.473	640 0.202	925 0.044	1075 0.031

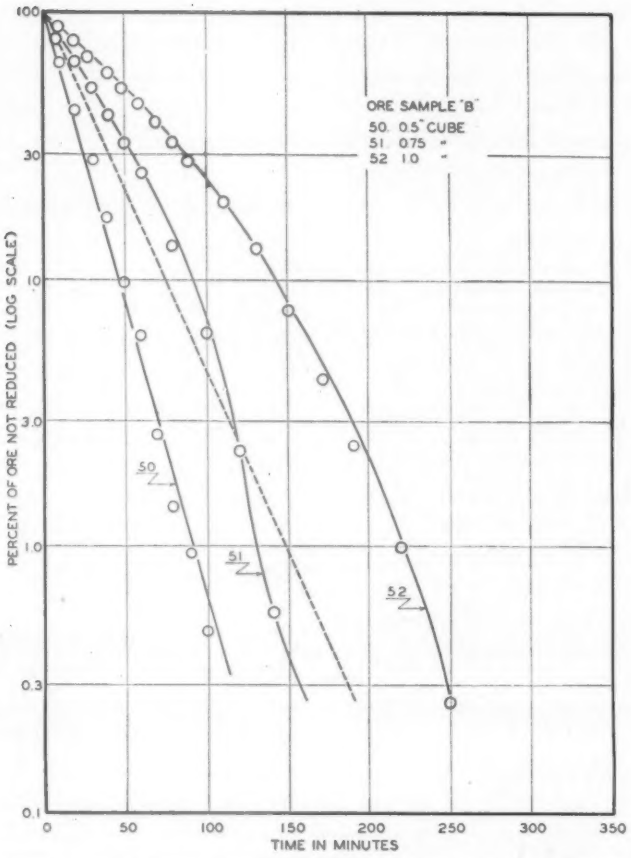

FIG 11—PERCENTAGE OF CUBES NOT REDUCED AT 800°C AT END OF VARIOUS TIME INTERVALS.

the "first order" equation to data for some of the cubes. The results obtained are tabulated in Tables 7 and 8. Likewise, data were plotted on semilog paper as shown in Figs 10 and 11.

TABLE 9—*Reducibility Indexes*

Cube No.	Joseph's 90 Pct Index × 10^3	Philbrook's Slope Index
	Ore Sample A	
1	27.1	1.56
24	11.75	0.382
21	8.13	0.326
19	5.34	0.272
18	3.50	0.230
	Ore Sample B	
50	20.0	0.774
51	11.35	0.298
52	7.04	0.158
17	1.32	0.045

These data and curves show that the small cubes follow the first-order equation much more closely than do the larger cubes. This suggested that the reliability of the "slope index" as a means of measuring the reducibility of an ore will depend on the size of particles used in the reduction tests. Table 9 and Fig 12 point this out very clearly for ore samples A and B.

TABLE 10—*Porosity and Time for 90 Per Cent Reduction of Various Ores at* 800°C

Ore	Porosity	Time for 90 Pct Reduction, Min.
Mesabi No. 3[a]	35.7	29.8
India[a]	31.5	36.1
Geneva ore A	19.6	58.0
Mesabi No. 1[a]	14.6	62.
Geneva ore B	9.8	67.
Alabama[a]	6.9	78.8

[a] Data from Joseph's paper.[1]

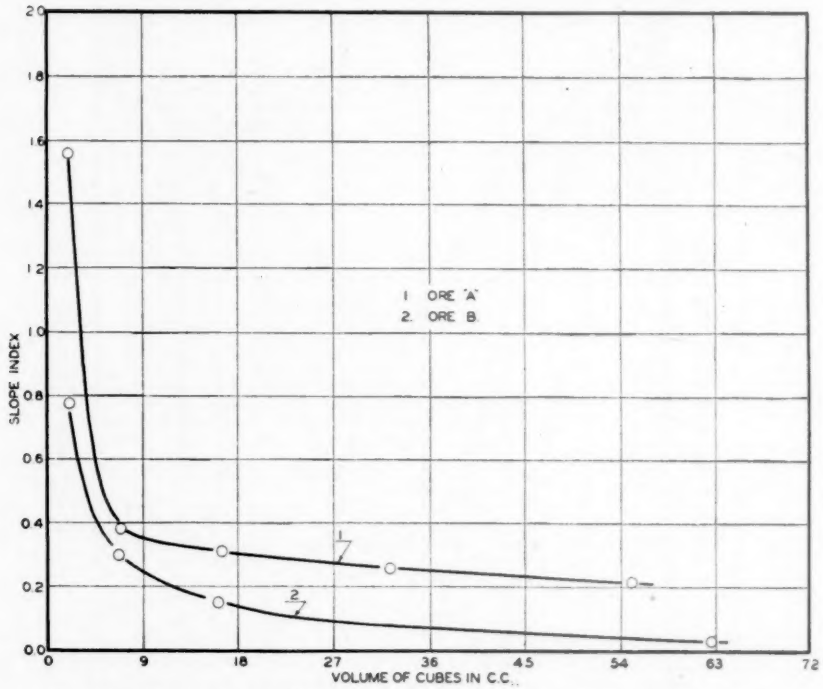

FIG 12—PHILBROOK'S "SLOPE INDEX" FOR CUBES OF VARIOUS SIZES.

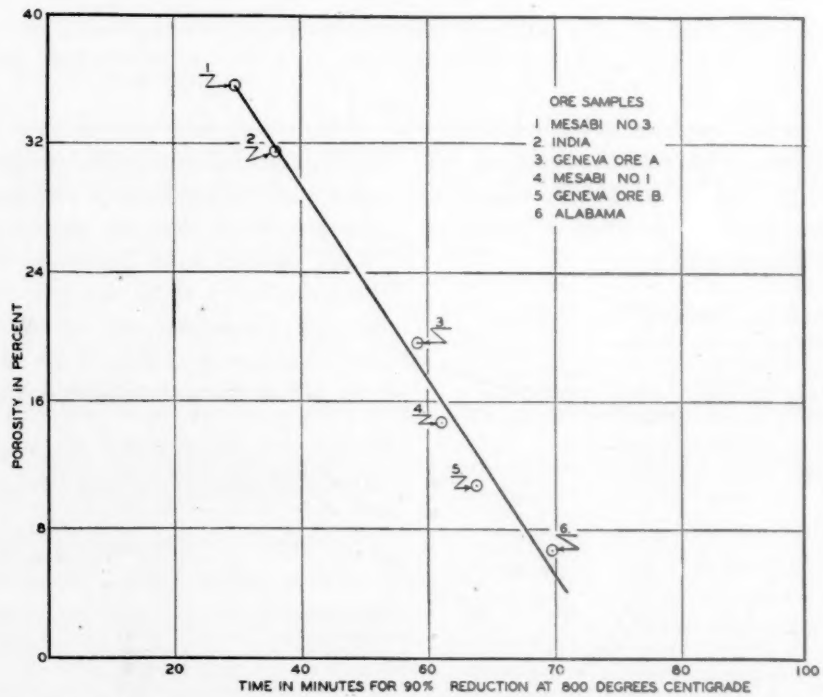

FIG 13—RELATION BETWEEN POROSITY AND TIME FOR 90 PER CENT REDUCTION OF SEVERAL IRON ORES.

Summary and Conclusions

1. An apparatus was built for studying the rate of reduction of Geneva iron ore by the use of hydrogen. This apparatus is suitable for powdered ore, sinter, and cubes of various sizes.

2. The data obtained are tabulated in various tables and shown graphically in figures.

3. For ore sample A, allowing for an induction period, the time of reduction of cubes was directly proportional to their size (volume). For ore sample B, this relationship did not hold as well.

4. The reduction curves are exponential in character. Data for the small cubes (0.5 in.) closely follow the first-order law.

5. The effect of temperature on the rate of reduction of 0.5-in. cubes has been determined. Under the conditions of these experiments the reaction rate increases approximately 1.44 times for each 50°C rise in temperature. This indicates that the limiting factor is the diffusion of the reaction products from the interiors of the cubes.

6. Joseph's "reduction index" is quite satisfactory as a method of expressing the reducibility rate of various ores. However, it does require that each determination be carried to completion, which is time consuming.

7. Philbrook's "slope index" method has the advantage of requiring only 60 minutes for securing the necessary data on which the order of reducibility of various ores can be based; but results will not be sufficiently accurate unless each charge is made up of particles of nearly the same size.

Acknowledgments

The author gratefully acknowledges the financial sponsorship of this study by the University Research Committee. He also wishes to thank Dr. J. H. Hamilton, Director of the Utah Engineering Experiment Station, and Prof. J. W. Johns, of the Department of Metallurgy, for valuable suggestions and for numerous courtesies. Appreciation is due to Leon A. Monson and Arthur Lewis for laboratory assistance and Betty Fowlks and Martin Fassell for making some of the graphs.

References

1. T. L. Joseph: Porosity, Reducibility and Size Preparation of Iron Ores. *Trans.* A.I.M.E. (1936) **120**, 72–89.
2. W. O. Philbrook: A Study of the Reducibility of Ores and Blast Furnace Sinter. *Blast Furnace and Steel Plant* (1943) **31**, 890–897.
3. P. V. Martin: Effect of Solution Loss on Furnace Efficiency. *Trans.* A.I.M.E. (1940) **140**, 31–58.
4. T. L. Joseph and G. Bitsianes: Some Comparisons between Iron Ore, Sinter and Nodules as Blast-Furnace Feed. *Proc.* Blast Furnace and Raw Materials *Conf.*, A.I.M.E. (1944) **4**, 70–91.
5. T. P. Colclough: Blast-furnace Practice. Considerations of Changes Necessary for Fuel Reduction. *Iron and Steel* (1944) 799.

DISCUSSION

(*W. E. Brewster presiding*)

W. O. Philbrook*—I have found this paper quite interesting. The experimental technique seems to be entirely valid. It is of particular interest because it extends our investigations of reducibility to considerably larger cubes than most people have studied, and that was, of course, quite appropriate for the hard lump ores that were dealt with.

Fig 13 is especially valuable and affirms Professor Joseph's observation that the time for reduction is inversely proportional to the porosity of the ore. It gives two additional points from a different type of ore that seem to fit well into the curve of the previous investigation and tends to increase our confidence that this relationship is somewhat universally applicable.

I think Professor Lewis should also be credited with bringing out explicitly the fact that heat penetration is important in reduction in the blast furnace shaft. Too often in laboratory work at constant temperature we have been inclined to forget that point, but in an

* Carnegie Institute of Technology, Pittsburgh, Pa.

actual furnace we must have heat penetration taking place at the same time that reducing gases are diffusing, and that gives a more complicated picture.

the top of page 36: "For ore sample A, the curves are straight lines once the initial induction period is passed." The statement seems to apply to Fig 7. If this is true, since the co-

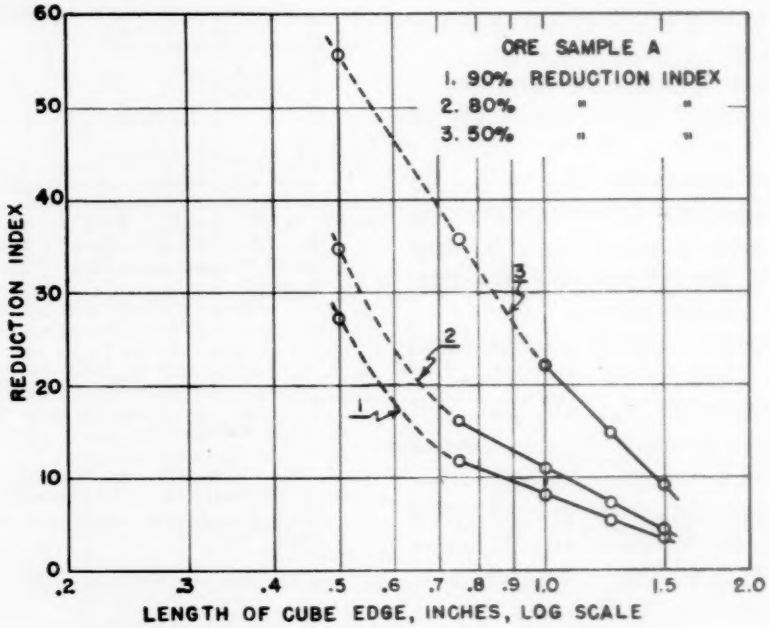

FIG 14—EFFECT OF CUBE SIZE ON "REDUCTION INDEX."

It was of interest to me, of course, that Professor Lewis had studied the shape of the curves and had attempted to apply the slope index. Quite properly he has said only that the curves apparently are exponential in character, and I think that we should limit ourselves to that statement; we should not yet state that it is a true first-order reaction, but only that it appears to follow a pseudo first-order curve.

With reference to the slope index, he found that it appears to be valuable for the smaller cubes that reduce rather readily, and not so useful for the larger cubes. This follows along the same lines as our own observation, namely, that the slope index was fairly useful for ores that reduced readily and not so useful for hard, dense sinters which were difficult to reduce. Apparently we should consider that this index is more useful for fairly small or fairly easily reduced materials. If we are dealing with slower reductions, perhaps the choice of some other times at which to measure the slopes, such as 30 min and 90 min, would increase the utility of that method.

I am not quite clear about the statement at

ordinate here is the time for a substantial completion of reduction, it is not a graphical representation of a rate of reaction, and I think "induction period" is a misnomer. This graph does indicate, however, that the smaller cubes reduce more rapidly than would be predicted from the study of the larger cubes.

Incidentally, if we were to project some of these curves of times for reduction or rate of reduction against size, down to smaller sizes, we would find that the tendency is toward extremely rapid reduction at extremely small particle size, which again indicates that same conclusion that Professor Lewis has drawn: that it probably is not the rate of the chemical reaction which is controlling in this process.

In Fig 9 the author has plotted a reduction index, which in this instance was the reciprocal of time for percentages of reduction stated in the legend, against the volume of the cube and has obtained curves which are convex upwards. As indicated in Fig 14, it appears that if we plot the log of the length of the cube edge in inches (which is the same as $\frac{1}{3}$ log of volume in cu in.) against the reduction index, then for cubes

larger than three-quarters of an inch the points appear to fall on a straight line. Below three-quarters of an inch the curve turns upward abruptly, and again if we project it to a cube of very small size, we would find our reducibility index approaching infinity, meaning very rapid reaction.

I do not want to imply that there is any theoretical reason why that should be a straight line and I am not proposing any mechanism for it. It might be useful as an empirical observation to enable us to predict the reducibility of large cubes more readily. It is easier to extrapolate a straight line than a curve.

Fig 6 shows increasingly greater reducibility, more rapid reduction, with increasing temperature. It shows no tendency for a maximum rate of reduction at approximately 600°. Specht and Zappfe[1] show that the presence of a 600° rate maximum was employed as being true for all types of iron ore, and a mechanism of reduction was developed which would explain that observation. That observation is not valid for hematite ores. At least my interpretation of Joseph's work was that reducibility increased continuously with temperature. My own work had indicated no rate maximum, and apparently this work again verifies it. It appears that hematite ores reduce more readily with increasing temperature on a continuous basis, whereas much of the published data on magnetite ores does show a rate maximum at some intermediate temperature. Apparently the mechanism of reduction is different for magnetites than it is for hematites, perhaps because of differences in crystallographic structure, but I think we should clarify our thinking and perhaps investigate that feature of the reduction of iron ores before we become dogmatic about reaction mechanisms.

B. M. LARSEN*—In reference to the relation between temperature and reduction rate, we observed a maximum in some work at the U.S. Steel Laboratories. The effect observed was in hydrogen reduction tests on a mill scale which would probably be more like magnetite.

From a practical point of view, it seems the obvious development in such laboratory studies of ore reduction would now be to carry them on up to higher temperatures such as would be encountered in the slag-forming zone of the blast furnace.

One feature of this use of iron ore cubes is that if diffusion is a limiting factor in the reduction rate, the situation is analogous to heat flow and I believe the heat flow near the corners in a cube will be different in relation to its dimensions from the flow in from the flat faces.

The ideal shape for reduction tests would therefore be a sphere, although I would hate to have the job of making spheres of this material. In the logarithmic plot showing percentage of the ore unreduced, the reduction goes faster first and then slows down. This probably results from the fact that the diffusion on the corners goes in different directions and the corners are more easily reduced.

It would be interesting to know whether the central zone in the partially reduced cubes toward the end of the reduction period tended toward a spherical shape.

In trying to work out the mechanism of the reaction from plots of that kind where size comes into the picture, a shape factor might be used according to methods worked out on heat flow problems.

T. L. JOSEPH*—My work on the reduction of iron ores was aimed primarily at the problem of determining the size to which the ore should be crushed for use in the blast furnace, and because of that, much attention was paid to the actual time required for substantially complete reduction.

For example, an ore such as one of these samples of about ½-in. diam requires over 1,200 min for 90 pct reduction at 800°C in a stream of hydrogen. From this one gets some appreciation of the fact that that ore should be crushed smaller than an inch and a half if it is desired to attain any degree of completeness of reduction above the bosh of the blast furnace.

The fact that one ore reduces more slowly than another does not necessarily mean that it is a poorer ore. In fact, if I were to select an ore and had a complete choice, I would take a very dense iron ore and crush it to the proper size.

[1] O. George Specht, Jr. and Carl A. Zappfe, The Low-temperature Gaseous Reduction of Magnetite Ore to Sponge Iron, AIME TP 1960, *Metals Tech.* June 1946. *Trans.* (1946) **167**, 237.

* Research Laboratory, U. S. Steel Corp., Kearny, N. J.

* Professor of Metallurgy, Minnesota School of Mines, Minneapolis, Minn.

Such an ore has a large heat capacity in the furnace and would have some definite advantages in the smelting because of its high bulk density. It could be crushed to such a size that there would be ample time for reduction under blast furnace conditions.

When it comes to the reducibility of sinters, Mr. Philbrook was attempting to find the reduction characteristics of sinter so as to make some change presumably in the sintering process. The size of sinter is usually small, and the slope index he proposed fits that type of work very well. It shortens the test and this is important when a large run of them is needed.

In determining whether a new ore compares favorably with tested ores, I think reduction should be carried to completeness, perhaps at higher temperatures than we usually use.

We no longer prepare cubes. Minus three-quarters plus one half inch pieces can be separated out readily and seem to serve about as well as cubes. A more representative sample can be obtained because more pieces are used.

From previous work we can tell how the new ore compares with other ores and what the approximate size of crushing should be: whether it should be crushed to an inch as in the case of Alabama ore or whether a considerably larger size would be satisfactory.

Reducibility tests have less significance when applied to small sizes. The problem then in blast furnace practice is not to get the penetration into the lump but rather to get the gases to the surface of the ore particle. In dealing with fine sizes we should immediately turn to the reduction characteristics of a bed of that material, not the individual piece.

A few small particles may have a tremendously high rate of reduction but when they are reduced en masse, it is difficult to prevent channeling of the gas through a bed or column of such material.

As to the question of an optimum temperature of about 600°C for reduction of natural magnetite, we reduced some seven or eight hematite ores at various temperatures from 600 to 800°C and found, as Professor Philbrook indicated, that as the temperature increased, the rate of reduction increased.

This is not the case with natural magnetite. There is an optimum temperature of about 600° at which ore will reduce more rapidly than at 700, 800 or 900°C. We are doing some work on that problem now, studying the reduced particles or partially reduced particles to see if there is any difference in the mechanism of reduction at, say, 600 and 700°C.

We found one curious thing about the Provo ore and I wonder if Professor Lewis found any indication that at 600°C there is a tendency for more complete reduction than at the lower temperatures.

We had included in some seven or eight ores a sample of Utah ore, and the 20 pct magnetite seemed to have some effect on the reduction characteristics of the Provo ore. It began more slowly at 600°C but was more rapid and complete in the final stages. In Fig 6 Lewis plotted the effect of temperature on time required for 80 pct reduction. I wonder if this same relationship would hold for more complete reduction.

In reducing ore particles at 700 and 800°C, the curves may come up rather sharply up to about 80 pct and then flatten off quite definitely. This is true of natural magnetite. At 600°C however, the curves start off with a flatter slope but in place of leveling off continue to rise until reduction is substantially completed.

J. R. Lewis (author's reply)—We were not primarily interested in the effect of temperature on the rate of reduction of Geneva ore. The results were obtained (Fig 6) from experiments on the more porous sample (ore A). Table 1 shows this ore contained an appreciable quantity of magnetite. If magnetite ores have a reduction rate maximum near 600°C, our results do not show it. However, since the problem is an important one, it should be investigated more systematically.

Mr. Larsen's suggestion that we carry out reduction rate tests at considerably higher temperatures is an interesting one and one that may be of theoretical and practical value to blast furnace operators. We may try this problem in the near future.

By starting with samples of Geneva ore of low porosity, approximately 10 pct, we may be able to prepare some ore spheres. If successful, we could then compare the reduction characteristics of these spheres with cubes of comparable size. The paths of reduction from surface to center of the cubes and spheres could then be followed easily.

Mr. Philbrook's comments and suggestions are important and will add considerably to the value of this paper. An induction period was observed in some of our rate experiments, but Professor Philbrook is correct in pointing out that the term "induction period" as it refers to Fig 7 is a misnomer. Fig 7 shows that small ore cubes (or small pieces of ore) reduce more rapidly, proportionately, than larger ones. This suggests that diffusion is not a limiting factor for small cubes or particles.

Fig 14 as prepared by Professor Philbrook is a re-plot of the data shown in Fig 9. This new plot serves to emphasize what is shown in Fig 7, namely that small cubes reduce much more rapidly than would be predicted from the reduction behavior of larger cubes.

Experimental Laboratory Study on Effect of Pressure on Carbon Deposition and Rate of Reduction of Iron Oxides in the Blast-furnace Process

By L. F. Marek,* A. Bogrow,* and G. W. King*

(New York Meeting, March 1947)

The purpose of this paper is to present the data and some interpretation of the results of a laboratory study of the reduction of iron ore and the deposition of carbon from the reducing gas mixtures in such reductions. One major object of the study was to determine the effect of gas pressures on these chemical processes. Effort was made to approximate the conditions of temperature, gas composition, linear and mass gas velocities, pressure range, and extent of reduction prevailing in commercial blast furnaces.

The results show that the reduction of Fe_2O_3 proceeds by two steps, largely consecutive under the conditions used herein: reduction of Fe_2O_3 to FeO, and reduction of FeO to Fe. Unless the gas has a CO/CO_2 ratio greater than 2.1 only the first step occurs under these conditions (850°C) but the following generalizations apply to either step or to the combination.

The rate of reduction of relatively fine ore particles at any time is proportional to the mass rate of supply of CO (provided some of it is thermodynamically available): the rate therefore is proportional to the linear velocity at constant pressure, or to the pressure at constant linear velocity. Thus, the rate of reduction may be increased without increase in linear velocity of the reducing gas by increasing the mass velocity of the gas and increasing the pressure correspondingly to avoid any increase in the linear velocity. The rate "constants"—i.e., the efficiency of conversion of the "available" CO supplied—is not actually constant but decreases as the reduction proceeds, and is a function only of the state of the ore; i.e., of the amount of reduction already accomplished and hence of the amount of CO passed.

The particle size of ore used in nearly all the experiments was relatively small (8 to 14-mesh). The rate of reduction in run 16 with 3 to 8-mesh ore particles is within experimental error the same as with the finer ore. Although this would indicate an absence of effect due to particle size in this range of ore particles, it is desirable to have more data on other ore sizes and on ore of different densities before arriving at any generalizations on this point.

Although it is possible to extend the analysis of these results to consideration of the more detailed kinetics and mechanism of iron oxide reduction, such extension is beyond the scope of the present paper.

From the experiments on carbon deposition, it was evident that if carbon deposition is increased at all by the application of pressures up to 10 psi ga., such increase appears to be less than the experimental and analytical error. It appears safe to conclude that at top pressures on the order

Manuscript received at the office of the Institute Dec. 23, 1946. Issued as T.P. 2184 in Metals Technology, June 1947.

* Arthur D. Little, Inc., Cambridge, Massachusetts.

of 10 psi ga. no perceptible difficulty with carbon deposition will be encountered.

Pressures on the order of 5 atms. abs greatly increased carbon deposition under the conditions used. When appreciable carbon was deposited at one atmosphere, increasing the pressure to five atmospheres increased the carbon deposition by ten to fifteenfold.

A rather pronounced maximum of carbon deposition occurred at about 489°C (912°F) at 5 atm pressure and 60 min. exposure time. The maximum deposition at the peak was over threefold the deposition at temperatures 50°C higher or lower.

The literature contains several accounts of studies made on iron-ore reduction at different gas pressures, mainly directed to the problem of sponge-iron manufacture. Diepschlag,[1] for example, studied the reduction of finely ground iron ore, contained in a small boat, by carbon monoxide and by hydrogen at pressures of 1, 3, 5, and 7 atms. absolute and temperatures of 400°, 600°, and 800°C for each pressure. He used a large excess of reducing gas, however, and experimental conditions that made interpretation difficult. Also, he did not measure rate of reduction during the course of a test but determined the degree of reduction at the end of a 30-min. period.

Somewhat later Tenenbaum and Joseph[2] studied the reduction of limonitic iron-ore cubes by hydrogen and carbon monoxide under pressure. In the reduction by CO, for example, a gas composition representative of that occurring in a blast furnace was used (CO/CO_2 ratio = 3.45). The published curves for extent of reduction as a function of time have a shape comparable with those obtained in this work, including a change at the FeO point. With certain assumptions regarding Tenenbaum and Joseph's ore sample, rough calculations on the data give results that compare closely with those obtained herein.

In a more recent paper by Specht and Zapffe,[3] there is a good review of the literature on iron-ore reduction.

In 1938, Avery[4] discussed the pressure operation of the pig-iron blast furnace and the problem of solution loss. In concluding that paper, Avery suggested that pressure operation offered a virgin field for development of blast-furnace design and operating technique, and gave promise of a handsome reward for the expense and effort needed for achievement of substantial results.

Since that time, the results from the commercial operation of full-size blast furnaces under top pressure have become available. Without giving any details of these results, it may be said that they fully justify the confidence expressed by the proponents of operation of the blast furnace under high top pressure.

Reduction of Iron Ore

Experimental Method

A commercial hematitic ore was used. The conditions chosen for the preliminary work were those of plane 3 (between zones C and D) where the temperature is 850°C (1560°F) and the gas composition 27.7 pct CO, 11.9 pct CO_2, 60.4 pct N_2 ($CO/CO_2 = 2.328$). Plane 3 is a level about 22 ft below the stockline of a furnace in the Chicago district investigated by the Bureau of Mines.[5] Since these conditions are very close to those of the Fe-FeO equilibrium, we found it advisable to carry out some experiments at a lower temperature, 690°C (1270°F), corresponding to plane 2, and at other gas compositions. The mass velocities, varied fiftyfold from 0.00667 to 0.302 cu ft per min., were, on the basis of the weight of the sample, of the same order as in an average blast furnace, 44,300 cu ft per min. per 700 tons. The linear velocities were varied tenfold and covered the actual linear velocities and hence, time of contact, obtaining in an actual furnace;

[1] References are at the end of the paper.

namely 44,300 cu ft per min. per 20 sq ft and 0.02 sec, respectively. The pressures used varied from 1 to 5 atm and therefore included the actual pressure in plane 3 of 1½ atm as well as extending the study to conditions not yet used in practice.

The particle size of ore used in these experiments was relatively small (8 to 14-mesh) in practically all experiments. Some data were collected with 3 to 8-mesh ore. Limited data were obtained with ore column lengths differing from the chosen standard of 2¼ in.

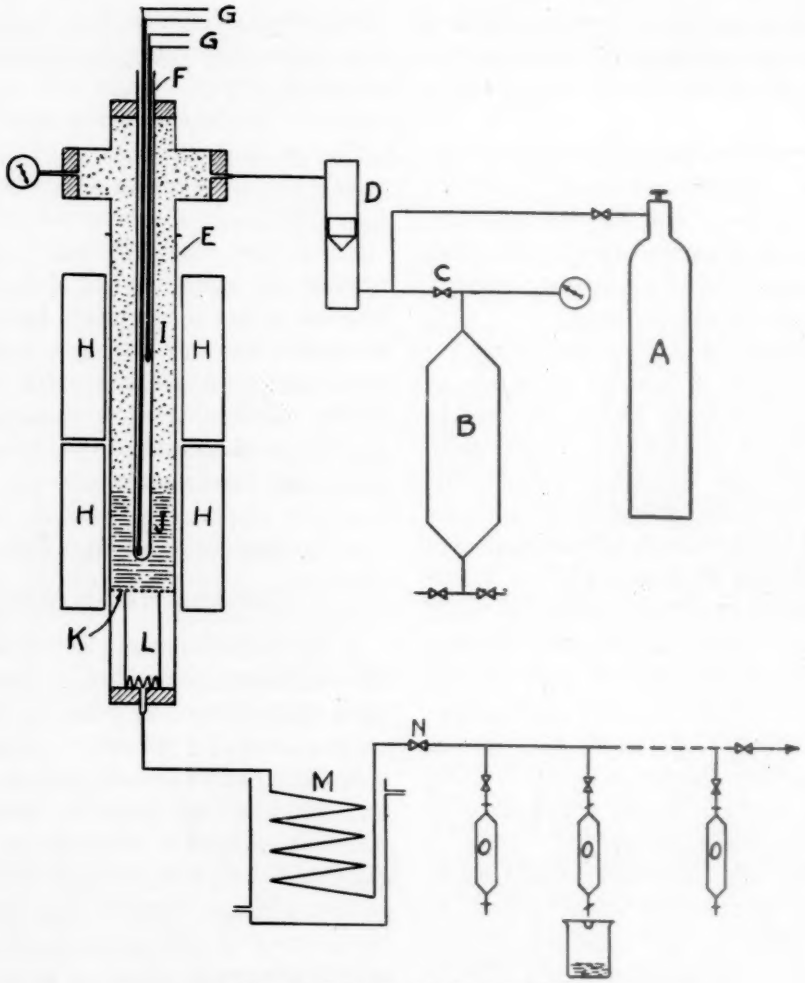

FIG 1—SCHEME OF APPARATUS.

A. Compressed-nitrogen cylinder.
B. Mixing and storage cylinder for reducing gas.
C. Gas-rate control valve.
D. Rotameter.
E. Stainless-steel reduction tube.
F. Stainless-steel thermowell.
G. Thermocouples.
H. Electric furnaces.
I. Quartz packing.
J. Iron ore.
K. Stainless-steel screen.
L. Serrated supporting tube.
M. Cooling coil.
N. Pressure-control valve.
O. Gas-sampling tubes.

Construction of Apparatus

The apparatus is shown in Fig 1. A compressed-nitrogen cylinder *A* and a tank *B* containing the compressed reducing-gas mixture, both provided with fine

reducing valves, were connected by a Y-shaped copper-tubing line to the inlet of a carefully calibrated rotameter *D*, mounted in the upper right-hand corner of a 48 by 40-in. board, which served as a support for all the other parts of the apparatus. The outlet of the rotameter was connected by a copper tube to one branch of a ¾-in. steel cross at the upper end of the reaction tube *E*, the other branch of the cross providing a connection for a 100-lb pressure gauge, and the top of the cross serving as an outlet for a ¼-in. o.d. by ⅛-in. i.d. brazed-in stainless-steel thermowell *F*, which descended axially to within 16 in. from the lower end of the reaction tube.

The bottom of the cross was screwed over the top of the vertical reaction tube *E*, which consisted of a 48-in. length of standard ¾-in. 18-8 stainless-steel seamless pipe, and terminated at the bottom in a ¾-in. coupling, a reducing bushing, a ¼-in. elbow, and a copper-tubing connection. From this connection, a copper-tubing line led to a small copper coil *M* cooled by running water, followed by a fine-pressure-regulating valve *N*, and finally by a rubber and glass-tubing manifold serving to lead the exit gases to drying and CO_2-absorbing cylinders, or to the gas-sampling tubes *O*.

The ¾-in. cross and the upper 30⅞ in. of the reaction tube were, except for the thermowell, completely filled with 3 to 8-mesh broken quartz *I*. Below this, there followed a 2¼-in. column of iron ore *H* (except in run 16, where the height of the ore was 3½ in., and in run 22, where only ⅛ of the usual ore charge was used), supported by a circle *K* of 40-mesh stainless-steel screen, which was held in place by a 14⅞-in. length of ⅜-in. stainless-steel tubing *L* resting on the bottom bushing below the reaction tube. The edges of the ⅜-in. tube *L* were serrated, in order not to impede the uniform penetration by the reducing gas of any portion of the iron ore.

The reaction tube was heated by two combustion-tube furnaces *H* of hinged design, each 13 in. long, placed one immediately above the other, and so arranged with respect to the tube that the column of iron ore corresponded to the hottest portion of the lower furnace. The input of electricity into each furnace was closely controlled by a Variac transformer (not shown in Fig 1) and the temperatures of the ore column and of the hottest point of the preheating section were measured by means of two thermocouples *G* permanently placed in the thermowell.

In this arrangement, the ore sample *J*, in all runs except Nos. 16 and 22, was arranged in the reaction tube in the form of the cylinder of the following dimensions: 20.8 mm o.d., 57.2 mm high (in runs 16 and 22, the height was 88.9 mm and 11.4 mm, respectively). Because of the presence of the thermowell of diameter 6.35 mm, the upper half was a hollow cylinder of area 3.1 sq cm., the lower half a solid cylinder of area 3.4 sq cm.

Raw Materials

The iron ore selected for these experiments was a Lake ore obtained from the Mystic Iron Works, Everett, Mass. This McCook ore from the Mesabi Range is a "washed" hematitic ore, which has lost most of its clayey constituents by natural weathering, so that it has a somewhat sandy character. The analysis is given in Table 2.

In order to obtain a sufficient supply of completely uniform ore for all the experiments, approximately 200 lb of the raw ore was mechanically crushed, sifted to the desired size of 8 to 14-mesh (1.5 to 3.0 mm), except for a small supply of 3 to 8-mesh (3.0 to 8.0-mm) for run 16, dried in an oven at 105°C, and very thoroughly mixed.

In most runs the same weight, 38.41 grams, of ore was used, corresponding

to a volume of ore of 20 ml and a column length of 57.2 mm (except in run 16, where a 3 to 8-mesh ore was used and 38.41 grams corresponded to a volume of 25 ml and a column length of 88.9 mm). In run 22 only 7.68 grams was used, with a column height of 11.4 mm.

The apparent specific gravity of this ore as measured by its displacement of water was 2.955. The actual weight of one cubic centimeter of 8 to 14-mesh ore was 1.92 grams; one gram of ore contains about 104 particles. The porosity was probably about 35 pct.

The reducing agents employed in these experiments were mixtures of commercial compressed carbon monoxide, carbon dioxide, and nitrogen, the compositions of these mixtures simulating gas compositions occurring in various zones of an actual blast furnace.

The desired gas mixture was prepared in a vertical storage and supply tank *B*, 48 in. high and 8 in. in diameter, provided with a pressure gauge and fine needle valves at the top and bottom of the tank. Prior to the first experiment, the tank was completely filled with water, whereupon the compressed-nitrogen cylinder was connected to the top inlet, and the water was displaced by nitrogen pressure, being drained out of the bottom outlet. The nitrogen pressure in the tank having been built up to the partial pressure of N_2 in the desired gas mixture, the nitrogen cylinder was successively replaced by the CO and CO_2 cylinders, and the desired amounts of these gases, as measured by the pressure rise in the tank, were added to the contents of the supply tank. Subsequent gas mixtures were prepared by the addition of the desired amounts of the three gases, as measured by the pressure rise in the tank, to the gas remaining in the tank after previous experiments. In order to obtain a perfectly homogeneous gas mixture, the addition of gases was always followed by application of the Bunsen burner to one side of the storage tank for several hours, to ensure the circulation and complete mixing of the gases.

Each gas mixture was then sampled and carefully analyzed with an Orsat apparatus. Any deviation from the predetermined gas composition was adjusted by the addition of the deficient components to the gas mixture, followed by further thermal stirring and analysis of the new mixture.

Experimental Procedure

Before the beginning of each run, the portion of the reaction tube below the quartz layer was thoroughly cleaned by swabbing with a long-handled test-tube brush, whereupon exactly 38.41 grams of ore (7.68 grams in run 22) was charged into the tube, and the apparatus was assembled. A slow stream of nitrogen was started through the reaction tube, and the latter was heated by means of the tube furnaces. As the required temperature was approached in the column of ore, the stream of nitrogen was increased, and its pressure was controlled by means of the pressure-regulating valve *N*, until the conditions of flow were similar to those intended for the gas in the actual run, whereupon the settings of the Variacs were adjusted to maintain the desired temperature in both the preheating and operating portions of the tube. This procedure was adopted in order that the operating temperature might not be affected by changing the rate of gas flow during the switch from nitrogen to the reducing gas.

The desired temperature having been attained and stabilized, the nitrogen was cut off, the pressure in the tube was rapidly reduced to atmospheric, a current of reducing gas was sent through the apparatus, and the rate and pressure of the gas were adjusted by means of valves *C* and *N* to the desired values. The running

time was measured from the moment of opening the gas-inlet valve, when a stop clock was started ("zero time"). The correct gas rate and pressure usually were attained within 30 sec from zero time.

The conditions of pressure, temperature, and gas rate were thereupon maintained constant throughout the period of the run, and at predetermined intervals samples of the exit gas were taken by displacing a confining solution (5 pct H_2SO_4 saturated with Na_2SO_4) from a 250-ml gas-sampling tube *O*. In all, from six to nine such gas samples were taken during each run, the time interval of each sample being carefully noted. Except in the first two runs, it was found possible to reduce the time required for collecting each sample to between 6 to 20 sec.

Subsequent to the run and (except after run 20) on the same day, the gas samples were subjected to Orsat analysis for CO_2 and CO, the N_2 content being calculated by difference. During several of the runs, an additional check was obtained on the total quantity of CO_2 evolved by passing all of the exit gas (except that sampled) through a drying tube and then through a tower filled with Ascarite or soda lime.

The run was concluded by stopping the flow of gas at the predetermined time, switching off the furnaces, releasing the gas pressure, and introducing a slow current of nitrogen, whereupon the hinged furnaces were opened and the reaction tube was allowed to cool as rapidly as possible to room temperature.

The cooled tube assembly (from the cross above to the copper-tubing connection below, and including the thermocouples) was removed from the apparatus, inverted, opened by unscrewing the bottom coupling, and emptied of the reduced ore, which was weighed and analyzed.

Traces of oxygen in the nitrogen, which was not deoxidized, tended to bring about oxidation of the small proportion of ferrous iron in the ore to the ferric state. This is shown in Table 2, and was necessarily taken into account.

Experimental Results

Nature of Data

The data given in Tables 1 to 3 were obtained in the form of the composition of several outlet gas samples taken in short periods of time (generally 30 sec or less) at intervals during the reduction. Table 4 shows the composition of the original and reduced ore samples for 12 runs.

The amount of reduction at any time *t* is determined by the amount of iron or lower oxide produced or of oxygen removed. Every gram-equivalent of oxygen removed gives rise to the formation of a gram-equivalent or mol of CO_2, or to the removal of a gram-equivalent or mol of CO in the gas. The amount of reduction during a run was measured by the amount of CO_2 produced, or CO converted, corrected if necessary for C deposition, in cubic feet at standard conditions, and the reduced ore was analyzed at the end of the run. The degree of reduction of the ore at any time is obtained by dividing the amount of CO_2 made by the amount of removable oxygen in the ore expressed in the same units (cubic feet of CO_2 at standard conditions).

In all experiments except one the weight of ore sample was 38.41 grams, and the stoichiometric equivalent of removable oxygen in the ore sample was 0.49 cu ft CO_2. In order to eliminate the weight of sample as a variable, all quantities measured in cubic feet may be reduced to an equivalent basis by dividing by 0.49.

For simplicity in the handling and interpretation of the data, the following notations were established:

y = the proportion of total reduction to metallic iron achieved in time t, calculated

TABLE I—*Experimental Data for Lean Mixtures*[a]

		t	Gas Composition, Pct			dy/dx	x
			CO_2	CO	N_2		
Run No.	1						
CO_2, pct	10.8	4.50	36.8	1.3	61.9	0.932	0.0851
CO, pct	27.9	12.00	25.0	13.0	62.0	0.517	0.2268
N_2, pct	61.3	27.25	11.9	26.2	61.9	0.036	0.5155
CO/CO_2	2.583	44.75	11.8	26.5	61.7	0.0309	0.845
Mass rate of flow, cfm	0.0333	59.25	11.8	26.4	61.8	0.0309	1.118
Pressure atm abs	5	74.25	11.4	26.6	62.0	0.0180	1.402
Temperature, deg F	1553						
Duration, min	75						
Wt. loss, grams	3.61						
	2						
CO_2	10.8	1.48	37.7	0.5	61.8	0.964	0.02800
CO	27.9	5.08	37.2	1.0	61.8	0.946	0.09602
N_2	61.3	10.42	32.1	6.0	61.9	0.763	0.197
CO/CO_2	2.583	15.46	22.3	15.7	62.0	0.410	0.292
Rate of flow	0.0333	24.96	13.2	24.9	61.9	0.0827	0.471
Pressure	3	71.42	12.2	25.8	62.0	0.0467	1.350
Temperature	1574						
Duration, min	75						
Wt. loss	3.33						
	3						
CO_2	10.8	1.75	37.2	0.3	62.5	0.947	0.0331
CO	27.9	5.54	36.7	0.8	62.5	0.928	0.1047
N_2	61.3	11.25	30.3	7.1	62.4	0.698	0.2125
CO/CO_2	2.583	15.50	25.7	11.9	62.4	0.532	0.2930
Rate of flow	0.0333	25.50	16.8	20.8	62.4	0.212	0.487
Pressure	1	71.79	12.6	25.0	62.4	0.0611	1.357
Temperature	1565						
Duration, min	75						
Wt. loss	4.07						
	7						
CO_2	12.2	2.27	27.7	10.6	61.7	0.587	0.2034
CO	26.4	5.27	16.3	22.2	61.5	0.1553	0.4725
N_2	61.4	7.72	13.2	25.2	61.6	0.0379	0.6927
CO/CO_2	2.164	11.92	12.5	26.1	61.4	0.01136	1.069
Rate of flow	0.1667	20.00	12.2	26.4	61.4	0	1.796
Pressure	5	37.13	12.2	26.4	61.4	0	3.332
Temperature	1570						
Duration, min	40						
Wt. loss	2.96						
	21A						
CO_2	13.4	2.13	29.2	8.6	62.2	0.637	0.1797
CO	24.8	5.38	17.6	20.4	62.0	0.1693	0.4538
N_2	61.8	8.55	13.8	24.2	62.0	0.01613	0.721
CO/CO_2	1.851	10.83	13.4	24.6	62.0	0	0.913
Rate of flow	0.1667	14.38	13.4	24.8	61.8	0	1.213
Pressure	5	23.92	13.3	24.9	61.8	0	2.020
Temperature	1350						
Duration, min							
Wt. loss, not weighed							
	4						
CO_2	10.8	5.92	37.0	0.3	62.7	0.939	0.02237
CO	27.9	20.79	37.0	0.4	62.6	0.939	0.07848
N_2	61.3	40.46	37.1	0.4	62.5	0.943	0.1529
CO/CO_2	2.583	75.70	21.8	15.8	62.4	0.392	0.2861
Rate of flow	0.00667	121.00	17.0	20.6	62.4	0.219	0.457
Pressure	1	171.08	15.0	22.7	62.3	0.1474	0.647
Temperature	1575						
Duration, min	180						
Wt. loss	3.52						

TABLE I—(*Continued*)

		t	Gas Composition, Pct			dy/dx	x
			CO_2	CO	N_2		
Run No.	5						
CO_2	12.0	2.30	38.6	0.2	61.2	0.974	0.03715
CO	27.3	4.67	38.9	0.1	61.0	0.985	0.0754
N_2	60.7	6.33	38.9	0.1	61.0	0.985	0.1023
CO/CO_2	2.275	11.10	37.1	1.8	61.1	0.920	0.1794
Rate of flow	0.029	19.98	23.3	15.8	60.9	0.414	0.3229
Pressure	5	72.13	13.2	25.8	61.0	0.0374	1.165
Temperature	1567						
Duration, min	75						
Wt. loss	4.01						
	6						
CO_2	12.0	2.50	38.8	0.0	61.2	0.982	0.0716
CO	27.3	4.50	38.5	0.4	61.1	0.971	0.1289
N_2	60.7	6.67	35.6	3.4	61.0	0.865	0.1911
CO/CO_2	2.275	10.43	24.9	14.1	61.0	0.473	0.2987
Rate of flow	0.0514	19.77	14.7	24.5	60.8	0.0989	0.5665
Pressure	5	36.50	13.5	25.7	60.8	0.0549	1.046
Temperature	1582						
Duration, min	40						
Wt. loss	3.81						

• The mass rate of flow is given as cubic feet per minute at standard conditions. The pressure is given in atmospheres absolute; the temperature as degrees F; the duration in minutes. Weights are in grams.

as y = integral of (pct CO_2 made) (rate of flow as cfm) (time in minutes)/0.49 between the limits of 0 and t minutes:

$100y$ = percentage reduction to time t.

x = the proportion of CO supplied up to time t relative to the stoichiometric requirement for complete reduction, calculated as x = (pct CO in feed gas) (rate of flow as cfm)(time in minutes)/0.49. The amount of CO thermodynamically available for reduction will be only a portion of x, as discussed later.

$100x$ = percentage of stoichiometric requirement for CO supplied to time t.

$\frac{dx}{dt}$ = (rate of flow as cfm) (pct CO in feed gas)/0.49 is the rate of supply of CO, held constant during a run.

$\frac{dy}{dt}$ = (rate of flow as cfm) (pct CO_2 made)/0.49 is the rate of reduction, varying during the run from fast at first to slow or zero at the end.

$\frac{dy}{dx}$ = CO_2 made/CO supplied or efficiency of conversion.

Extent of Reduction

Correction for Carbon Loss—At the temperatures and compositions used in these experiments the equilibrium is in favor of deposition of carbon. However, in all samples the total amount of carbon in the exit gases is practically the same as in the incoming gas. The small decrease observed of less than 0.5 pct corresponds to a small amount of carbon deposited. This correction is less than the amount of scattering of the data, and was not applied.

Phase Diagrams—The extent of reduction of Fe_2O_3 is known to be dependent on the oxidation-reduction potential of the gas; i.e. on the relative CO content, as shown in Fig 2.[6,7] For the present discussion, we shall assume the phases mentioned, Fe, FeO, Fe_3O_4, Fe_2O_3 are pure compounds, although in reality some of them are solid solutions. In addition, some phases may contain iron carbide as a solute.

Only metallic iron can be in equilibrium with very high ratios of CO/CO_2. For a

TABLE 2—*Experimental Results for Rich Mixtures*

		t	Gas Composition, Pct			dy/dx	x
			CO_2	CO	N_2		
Run No.	8						
CO_2, pct	7.4	1.93	37.0	0.4	62.6	0.962	0.0404
CO, pct	30.8	5.83	37.3	0.2	62.5	0.972	0.1219
N_2, pct	61.8	10.38	26.5	11.1	62.4	0.620	0.217
CO/CO_2	4.162	15.68	20.3	17.6	62.1	0.419	0.328
Rate of flow, cfm	0.0333	25.47	13.3	24.7	62.0	0.1916	0.533
Pressure	5	72.77	12.6	25.4	62.0	0.1688	1.522
Temperature	1573						
Duration, min	75						
Wt. loss	7.74						
	9						
CO_2	7.4	4.30	37.2	0.3	62.5	0.967	0.0900
CO	30.8	10.42	23.5	14.0	62.5	0.523	0.218
N_2	61.8	15.00	19.4	18.2	62.4	0.389	0.314
CO/CO_2	4.162	24.97	14.4	23.3	62.3	0.227	0.522
Rate of flow	0.0333	71.42	12.9	24.9	62.2	0.1784	1.493
Pressure	5	98.37	12.2	25.7	62.1	0.1558	2.060
Temperature	1573						
Duration, min	150	145.57	10.1	27.7	62.2	0.0877	3.045
Wt. loss	8.96						
	10						
CO_2	7.4	2.33	22.8	14.9	62.3	0.500	0.244
CO	30.8	4.52	15.0	22.8	62.2	0.247	0.474
N_2	61.8	6.60	12.9	25.1	62.0	0.1784	0.692
CO/CO_2	4.162	8.80	11.8	26.1	62.1	0.1428	0.923
Rate of flow	0.1667	11.20	11.7	26.2	62.1	0.1395	1.174
Pressure	5	14.07	11.6	26.3	62.1	0.1363	1.474
Temperature	1566	19.73	11.2	26.7	62.1	0.1233	2.070
Duration, min	40	28.02	10.5	26.6	62.9	0.1006	2.940
Wt. loss	8.70	37.45	9.7	28.2	62.1	0.0747	3.925
	11						
CO_2	7.4	2.40	36.9	0.4	62.7	0.958	0.0502
CO	30.8	4.97	36.3	1.2	62.5	0.939	0.1041
N_2	61.8	10.73	24.2	13.3	62.5	0.546	0.2245
CO/CO_2	4.162	15.28	20.5	17.0	62.5	0.425	0.320
Rate of flow	0.0333	20.50	17.0	20.6	62.4	0.312	0.429
Pressure	1	27.58	14.2	23.4	62.4	0.221	0.577
Temperature	1575	35.53	13.0	24.8	62.2	0.1817	0.744
Duration, min	75	45.45	12.1	25.1	62.8	0.1526	0.952
Wt. loss	5.41	72.18	11.3	26.2	62.5	0.1266	1.511
	12						
CO_2	7.6	2.15	15.9	23.1	61.0	0.267	0.412
CO	31.1	4.57	11.9	27.0	61.1	0.1383	0.876
N_2	61.3	6.97	11.6	27.2	61.2	0.1286	1.335
CO/CO_2	4.092	9.83	11.5	27.3	61.2	0.1253	1.882
Rate of flow	0.302	14.80	11.3	27.5	61.2	0.1190	2.835
Pressure	5	18.12	10.8	28.1	61.1	0.1029	3.470
Temperature	1303						
Duration, min	20						
Wt. loss	8.17						
	13						
CO_2	7.6	2.28	15.2	23.7	61.1	0.244	0.437
CO	31.1	4.00	12.8	26.1	61.1	0.1671	0.767
N_2	61.3	7.18	12.1	26.9	61.0	0.1446	1.375
CO/CO_2	4.092	10.07	12.0	26.9	61.0	0.1413	1.929
Rate of flow, cfm	0.302	14.95	11.6	27.3	61.1	0.1286	2.865
Pressure	5	17.87	10.9	27.9	61.2	0.1060	3.425
Temperature	1236						
Duration, min	20						
Wt. loss	7.14						

TABLE 2—(*Continued*)

		t	Gas Composition, Pct			*dy/dx*	*x*
			CO_2	CO	N_2		
Run No.	14						
CO_2	7.6	1.45	23.9	14.7	61.4	0.524	0.1533
CO	31.1	4.17	15.4	23.3	61.3	0.251	0.441
N_2	61.3	9.50	12.3	26.5	61.2	0.1511	1.004
CO/CO_2	4.092	13.12	11.9	26.9	61.2	0.1382	1.388
Rate of flow	0.1667	17.80	12.1	26.7	61.2	0.1447	1.882
Pressure	5	22.32	11.5	27.2	61.3	0.1253	2.360
Temperature	1261						
Duration, min	25						
Wt. loss		Reduced ore lost by spontaneous combustion					
	15						
CO_2	7.6	1.12	31.3	6.8	61.9	0.759	0.1184
CO	31.1	5.23	14.2	24.5	61.3	0.212	0.553
N_2	61.3	10.12	12.3	26.4	61.3	0.1511	1.071
CO/CO_2	4.092	14.98	11.8	26.9	61.3	0.1350	1.583
Rate of flow	0.1667	20.72	11.6	27.1	61.3	0.1286	2.190
Pressure	1	28.02	11.1	27.6	61.3	0.1125	2.965
Temperature	1574						
Duration, min	30						
Wt. loss		Reduced ore lost by spontaneous combustion					
	16						
CO_2	7.5	2.68	19.8	18.9	61.3	0.394	0.2625
CO	31.2	5.93	13.3	25.4	61.3	0.1859	0.581
N_2	61.3	8.55	12.0	26.7	61.3	0.1442	0.838
CO/CO_2	4.160	11.43	11.6	27.1	61.3	0.1313	1.120
Rate of flow	0.1667	15.87	11.2	27.5	61.3	0.1186	1.554
Pressure	5	21.47	11.0	27.7	61.3	0.1121	2.105
Temperature	1540	27.48	10.7	27.9	61.4	0.1025	2.693
Duration, min	30						
Wt. loss	6.75	3 to 8 mesh ore used in this run					
	17						
CO_2	7.2	19.90	12.0	27.0	61.0	0.1509	2.155
CO	31.8	29.88	11.2	27.7	61.1	0.1257	3.235
N_2	61.0	39.95	9.8	29.2	61.0	0.0817	4.32
CO/CO_2	4.417	49.92	8.5	30.5	61.0	0.0409	5.40
Rate of flow	0.1667	59.88	7.8	31.2	61.0	0.01887	6.48
Pressure	5	69.70	7.5	31.5	61.0	0.00944	7.55
Temperature	1557	79.75	7.4	31.6	61.0	0.00629	8.64
Duration, min	100	89.38	7.2	31.8	61.0	0	9.68
Wt. loss	9.62	98.65	7.2	31.8	61.0	0	10.69
	18						
CO_2	7.2	19.45	12.0	26.8	61.2	0.1513	2.097
CO	31.7	29.57	11.2	27.7	61.1	0.1262	3.185
N_2	61.1	39.75	9.8	29.1	61.1	0.0820	4.29
CO/CO_2	4.403	49.65	8.6	30.3	61.1	0.0442	5.36
Rate of flow	0.1667	59.43	7.7	31.2	61.1	0.01577	6.40
Pressure	3	69.52	7.4	31.5	61.1	0.00631	7.50
Temperature	1553	79.42	7.3	31.6	61.1	0.00316	8.57
Duration, min	100	89.33	7.2	31.7	61.1	0	9.63
Wt. loss	10.00	98.28	7.2	31.7	61.1	0	10.60
	19						
CO_2	7.3	19.58	12.0	27.1	60.9	0.1478	2.120
CO	31.8	29.48	11.2	27.9	60.9	0.1226	3.190
N_2	60.9	39.68	10.0	29.1	60.9	0.0849	4.29
CO/CO_2	4.356	49.67	8.6	30.5	60.9	0.0409	5.38
Rate of flow	0.1667	59.77	7.7	31.4	60.9	0.01257	6.46
Pressure	1	69.52	7.5	31.6	60.9	0.00629	7.52
Temperature	1520	79.67	7.5	31.6	60.9	0.00629	8.62
Duration, min	100	89.43	7.3	31.8	60.9	0	9.67
Wt. loss	9.37	98.37	7.3	31.8	60.9	0	10.63

TABLE 2—(*Continued*)

		t	Gas Composition, Pct			dy/dx	x
			CO_2	CO	N_2		
Run No.	20						
CO_2	7.5	100.33	12.4	26.8	60.8	0.1546	2.160
CO	31.7	150.25	11.6	27.6	60.8	0.1293	3.235
N_2	60.8	200.83	10.3	28.9	60.8	0.0884	4.32
CO/CO_2	4.227	250.42	9.0	30.2	60.8	0.0473	5.40
Rate of flow	0.0333	300.50	8.0	31.2	60.8	0.01577	6.47
Pressure	1	349.50	7.7	31.5	60.8	0.00631	7.53
Temperature	1550	396.67	7.6	31.6	60.8	0.00315	8.55
Duration, min	430	425.00	7.5	31.7	60.8	0	9.15
Wt. loss	10.14						
Reduction of FeO							
Run No. 21-B		2.12	12.2	27.0	60.8	0.1527	0.2315
CO_2	7.3	5.15	12.1	27.1	60.8	0.1495	0.562
CO	32.1	8.02	12.0	27.2	60.8	0.1464	0.875
N_2	60.6	12.08	11.8	27.5	60.7	0.1402	1.319
CO/CO_2	4.397	24.28	11.2	28.1	60.7	0.1214	2.650
Rate of flow	0.1667	32.95	10.6	28.7	60.7	0.1027	3.595
Pressure	5	47.36	9.0	30.3	60.7	0.0530	5.16
Temperature	1553	60.48	8.1	31.2	60.7	0.0249	6.60
Duration, min	75	74.18	7.4	31.9	60.7	0.00312	8.09
Wt. loss	9.67	For 21-A and 21-B Combined					
Run No. 22		1.75	12.0	27.1	60.9	0.1464	0.956
CO_2	7.3	4.25	9.9	29.5	60.6	0.0809	2.320
CO	32.1	7.00	9.3	30.1	60.6	0.0623	3.820
N_2	60.6	11.67	9.4	30.0	60.6	0.0654	6.37
CO/CO_2	4.397	17.63	8.8	30.6	60.6	0.0467	9.63
Rate of flow	0.1667	24.37	8.3	31.1	60.6	0.0311	13.29
Pressure	1	29.33	8.1	31.3	60.6	0.0249	16.01
Temperature	1523	34.60	7.7	31.7	60.6	0.01246	18.88
Duration, min	45	43.25	7.6	31.8	60.6	0.00934	23.62
Wt. loss	2.20[a]						
Run No.	23		Pure CO				
CO_2	1.5	1.60	42.0	57.8	0.2	0.412	0.535
CO	98.3	3.35	28.6	71.2	0.2	0.2755	1.120
N_2	0.2	6.68	25.2	74.6	0.2	0.2410	2.252
CO/CO_2	65.53	11.45	3.6	96.2	0.2	0.02135	3.825
Rate of flow	0.1676	17.85	1.8	98.0	0.2	0.00305	5.97
Pressure	3	23.15	1.5	98.3	0.2	0	7.74
Temperature	1543	28.35	1.5	98.3	0.2	0	9.48
Duration, min	45	34.15	1.5	98.3	0.2	0	11.41
Wt. loss		43.35	1.5	98.3	0.2	0	14.48

[a] Run made with ⅓ usual wt of ore.

given temperature, say 850°C (1560°F), there is a definite ratio of CO/CO_2 (2.1) at which both Fe and FeO are in equilibrium with the gas: below this FeO is the only stable phase, and unless the gas has more CO than this ratio of 2.1, Fe_2O_3 will be reduced no further than to FeO. Of the CO supplied only the excess over the ratio 2.1 is available for reduction to metallic Fe. Neglecting the mixed oxide Fe_3O_4 for the moment, Fig 2 shows that all mixtures with CO/CO_2 ratios below the Fe-FeO value of 2.1 down to the FeO-Fe_2O_3 ratio of 0.01 will reduce Fe_2O_3 to FeO. But mixtures leaner in CO than the FeO-Fe_2O_3 point of 0.01 will cause no reduction at all. The small value of this ratio means that essentially all the CO supplied is available for reduction of Fe_2O_3 to FeO.

If Fe_3O_4 were an intermediate, the CO supplied would be still essentially all available for its formation; but the gases used in these experiments never contained so little CO that the reduction would be halted at the Fe_3O_4-FeO equilibrium.

Extent of Reduction Observed—Runs 1 to 7 and 21A were carried out with gas compositions and temperatures corresponding to plane 3 of a blast furnace, which happens to be very nearly the equilibrium concentration for Fe-FeO (see point marked "lean" in Fig 2); the ratio CO/CO_2 is in the neighborhood of 2.1, giving mixtures that we shall refer to as "lean." In confirmation, the analyses (Table 4, Fig 3) showed that the Fe_2O_3 was essentially reduced only as far as FeO. A small amount of metallic iron was produced when the gas composition was slightly above the equilibrium value. As a further confirmation, the amount of oxygen removed, as measured by the integral of (pct CO_2 made) versus (volume of gas passed) was 0.335 equivalents (nine runs averaged by a method described later) or almost exactly one third, corresponding to reduction only to FeO.

TABLE 3—*Summary of Pressures and Rates of Flow*

Atm Pressure	Rate of Flow, Cfm				
	0.00667	0.029	0.0333	0.0514	0.1667
	Lean Reducing Gas				
1 3 5	Run 4[a]	Run 5	Run 3 Run 2 Run 1	Run 6	Runs 7, 21A[b]
	Rich Reducing Gas				
	0.0333		0.1667		0.302
1 3 5	Runs 11, 20 Runs 8, 9		Runs 15, 19, 22[c] Run 18 Runs 10, 14,[d] 16,[e] 17, 21B		Runs 12,[d] 13[d]

[a] Details given in Tables 1 and 2. Temperatures in neighborhood of 850°C (1570°F) unless otherwise indicated.
[b] Very lean gas, 732°C (1350°F).
[c] One fifth normal sample.
[d] 680°C (1260°F).
[e] Large particles.

Runs 8 to 20 and 21B were made at CO concentrations where only Fe is in equilibrium with the incoming gas; the ratio CO/CO_2 is greater than the limiting value of 2.1, giving what we shall refer to as "rich" mixtures. Complete reduction is possible, and is observed, as shown by analysis (Table 4 and Fig 3) and by the total amount of oxygen removed being 0.906 equivalents (average of 14 runs).

The analyses of the solid residue in terms of ferric, ferrous, and metallic iron (Table 4 and Fig 3) make it clear that in experiments 1 to 7 and 21A, with the lean mixtures, the reduction seems to be directly to FeO; and with richer mixtures, experiments 8 to 20, although the reduction ultimately reaches metallic iron, FeO is a definite intermediate. This is also shown by following the course of reduction during the runs by gas analysis.

The analyses of the reduced ore samples given in Table 4 have been plotted in Fig 3 to show the fraction of the iron present as ferric, ferrous, and metallic iron in each sample as a function of the extent of reduction measured by the fraction of the total original oxide oxygen that has been removed as CO_2.

Iron-oxygen Phases—The solid phase "FeO" referred to in the phase diagram of Fig 2 is not the chemical compound FeO (22.25 pct oxygen by weight), but a solid solution of FeO and Fe_3O_4 (or Fe_2O_3) known as "wüstite." When in equilibrium with Fe(α) this wüstite has a composition corresponding to a formula of $FeO_{1.05}$ (23.2 pct oxygen by weight). In our experiments we find from the analyses of the residual ores, and from the determination of the amount of oxygen removed by the CO, that the intermediate state of reduction has the composition corresponding to wüstite.

Rate of Reduction

The extent of reduction during a run, at constant inlet gas rate, pressure and composition, is represented by the amount of CO_2 made and determined from the difference between inlet and outlet gas compositions. The data for

TABLE 4—*Analyses of Ore Samples*

Description of Sample	Original Ore Dried at 105°C	Original Ore Dried in N_2 at Red Heat	Run No. 1	2	3	4	5	6	7	8	9	10	11	19	21
Total iron, Fe	59.96	64.07	73.23	74.09	72.51	71.67	71.80	70.47	70.15	78.34	84.72	82.18	73.77	89.67	
Ferric iron, Fe^{+++}	59.07	64.01	9.41	1.73	9.14	9.24	4.81	5.73	8.75	0.08	0.76	0.00	0.00	0.85	
Ferrous iron, Fe^{++}	0.89	0.06	56.79	58.30	56.62	55.51	61.36	60.11	60.40	33.74	13.95	7.26	42.14	0.28	
Metallic iron, *Fe*			7.03	14.06	6.75	6.92	5.63	4.63	1.00	44.52	70.01	74.92	31.66	88.54	
Free carbon, C			0.05	0.03	0.04	0.05								0.08	
Phosphorus, P	0.08	0.09	0.08	0.08	0.07	0.08									0.04
Manganese as Mn_3O_4	0.30	0.27	0.23	0.24	0.20	0.23									
Silica, SiO_2	5.97	5.98	6.00	4.76	5.90	5.45									
Alumina, Al_2O_3	0.66	0.86			0.041										
Magnesia, MgO	0.23	0.24	0.25	0.19	0.19	0.22									
Sulphur, S	0.01			0.003	0.001	0.022									
Lime, CaO															
Ignition loss (H_2O)	7.00														
Percentage of total iron:															
Ferric, Fe^{+++}	98.5	99.9	12.8	2.3	12.6	12.9	6.7	8.1	12.5	0.1	0.9	0.0	0.0	0.95	
Ferrous, Fe^{++}	1.5	0.1	77.6	78.7	78.1	77.4	85.5	85.3	86.1	43.1	16.5	8.8	57.0	0.31	
Metallic, *Fe*			9.6	19.0	9.3	9.7	7.8	6.6	1.4	56.8	82.6	91.2	43.0	98.74	
Percentage of total original O removed	0.0	0.0	35.5	45.3	35.4	35.6	36.4	35.1	30.2	71.2	88.2	94.1	62.1	98.8	

percentage of CO_2 made as a function of time in minutes given in Table 1 are sketched in Fig 4. The spread of tenfold in the elapsed times required to reach rates of flow shows that if the mass rate is increased n-fold the time taken to reach any specified degree of reduction is decreased exactly n-fold. This exact

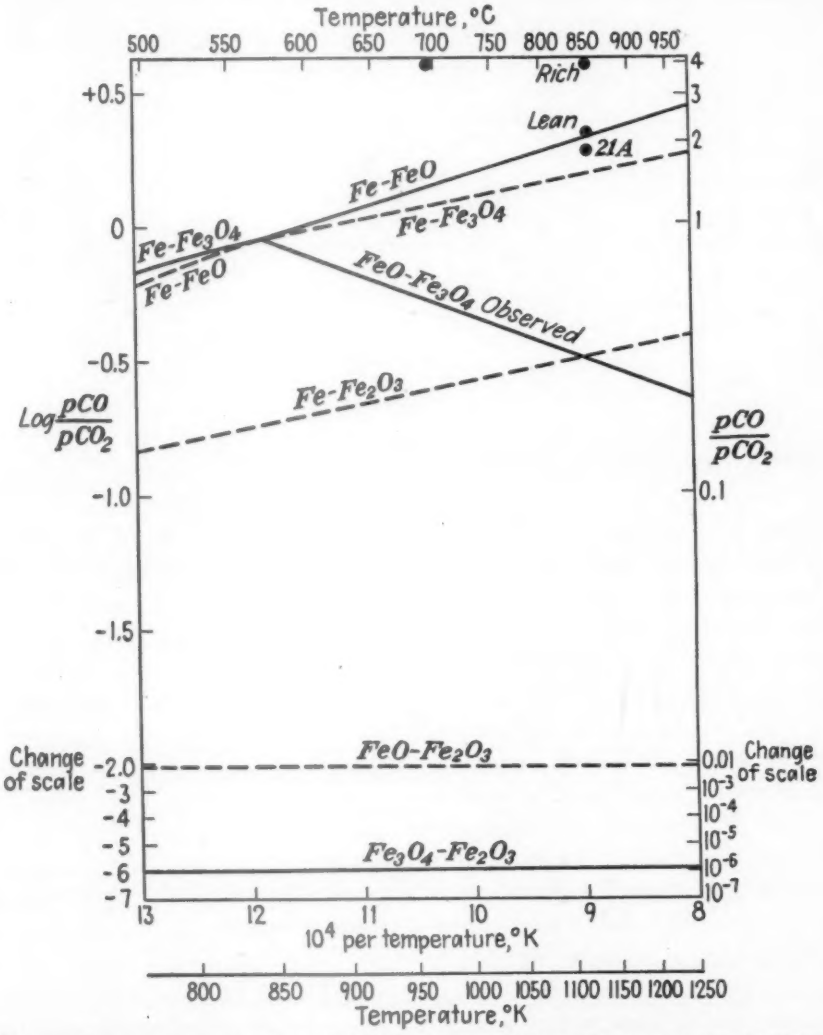

FIG 2—PHASE DIAGRAM OF IRON OXIDES WITH CARBON MONOXIDE AND DIOXIDE. Circles represent roughly the gas compositions and temperatures used.

corresponding states of reduction indicates the wide variations of conditions. Nevertheless, although the linear velocities varied tenfold, and the pressure fivefold, the curves for the same mass rate of flow (dx/dt) were identical, for a given inlet gas composition, irrespective of linear velocity or pressure. Further, a comparison of results for different mass proportionality occurs whether the mass rate of flow is increased by increasing the pressure at constant linear velocity, or by increasing the linear velocity at constant pressure.

The limited results at the lower temperature range of 690°C (1270°F) and those with the larger ore-particle size of 3 to 8-mesh agree, within experimental

error, with the results from the runs at the chosen base conditions of 850°C (1560°F) and 8 to 14-mesh ore size.

Changes in gas composition, however, did give different curves, especially in passing over the Fe-FeO equilibrium CO concentration.

In order to determine the effect of different variables on the rate of reduction of iron ore shown by this mass of data, it was necessary to evolve a method of treatment that would show the true controlling variable or variables.

It is clear that if these proportionalities hold, identical curves should be obtained for a given inlet-gas composition by plotting (pct CO_2 made) against the (amount of CO fed), rather than against elapsed time as in Fig 4. Such a relationship serves to eliminate from the plot the variables of pressure and linear velocity of the gas, and reduces mass velocity and elapsed time to the amount of CO fed up to any given time.

Although the gas compositions did not vary greatly, the relationship obtained for different gas compositions on either side of the equilibrium ratio can be put

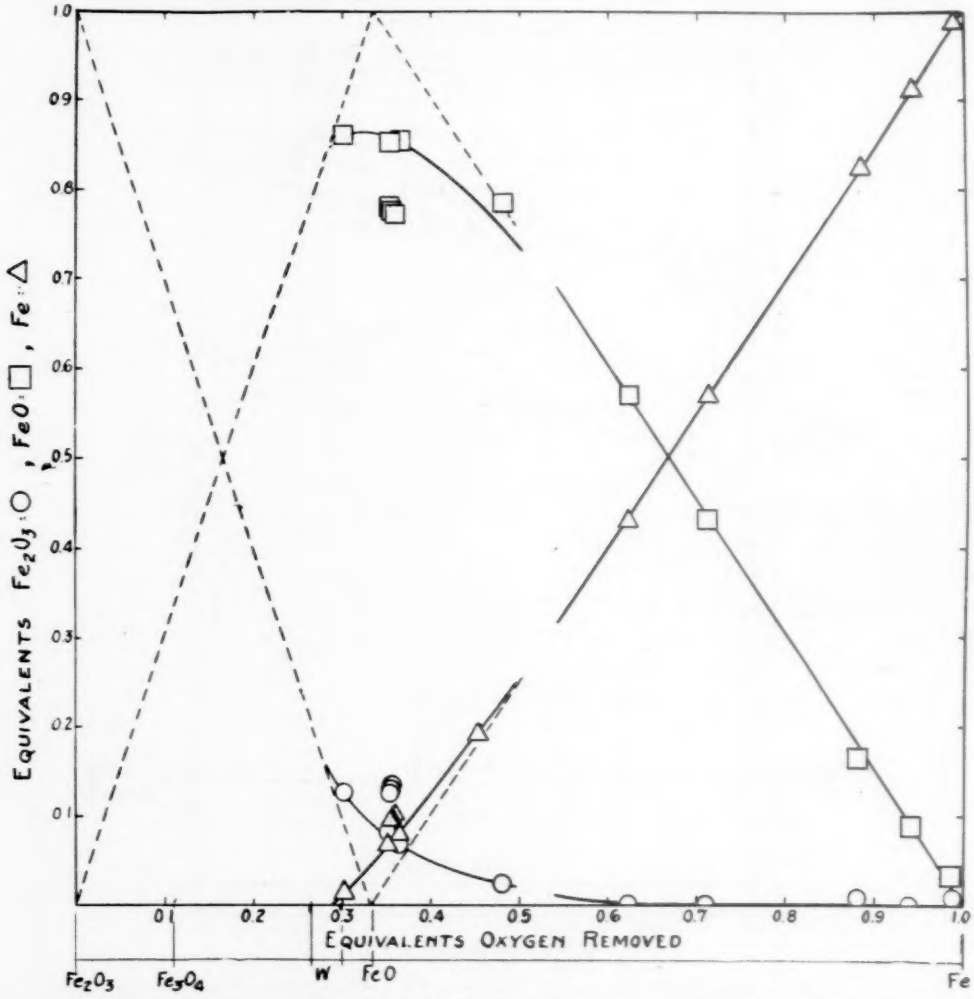

FIG 3—EXTENT OF REDUCTION AS DETERMINED BY ANALYSIS OF RESIDUAL ORE.
All points to right of break in curves (at $y = 0.5$) are for rich mixtures; those to left for lean mixtures. *W* marks the concentration range of wüstite.

on the same basis by dividing the (pct CO_2 made) by the (pct CO in original gas), giving essentially an efficiency of conversion (amount CO_2 made)/(amount CO supplied), or dy/dx at any particular instant in the course of a run. It is now found (provided the composition does not change beyond the equilibrium concentrations) that all the curves of dy/dx vs x are identical. The values of:

dy/dx = (pct CO_2 made)/(pct CO supplied)
and x = (pct CO in feed gas)(time in minutes) (rate of flow in cfm)/0.49

are calculated for each experimental point as shown in Table 1, and all the data are plotted in Fig 5 (lean mixtures) and Fig 6 (rich mixtures). The data plotted in this way show that the points obtained from the samples taken during runs under widely varying conditions map out essentially a single curve for the lean (Fig 5) and another for the rich mixtures (Fig 6). The existence of these unique curves means that the *rate* of reduction depends on the mass rate of flow of available CO and that the *efficiency* of reduction depends only on the amount of CO already passed—i.e., on the amount of reduction or state of the ore—and not at all on the pressure, linear velocity, size of particle, temperature, or composition (within equilibrium limits).

The scattering of the points is attributable to experimental error in determining the time of the sample, a short but finite time being required for gas sampling and zero time for a run being indeterminable to within 20 sec. In particular, the points for runs 8 and 9, 11 and 20, 15 and 19, 12 and 13, in which each member of the pairs was run under identical conditions, indicate the reproducibility. In view of this scattering, there is no justification for identifying any trends with pressure, linear velocity, etc. In any case, any such trends in the dy/dx vs x curves are insignificant compared with the variations obtained in rate of reduction as a function of elapsed time by varying the mass rate of flow of gas by pressure or linear velocity.

The areas under the unique efficiency curves in Figs 5 and 6 are 0.335 and 0.906, respectively, corresponding to the reduction to FeO and to metallic Fe. The former value is a little high, because some metallic iron was produced. In the value for the conditions of complete reduction given above, the 9 pct oxygen not accounted for in the exit gas was

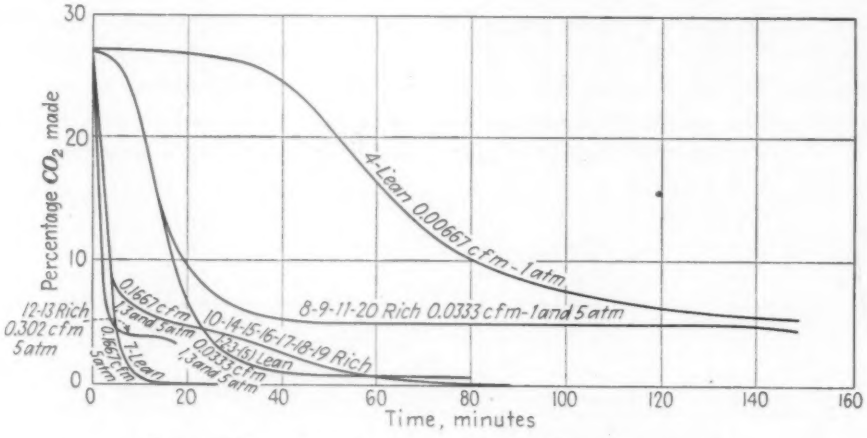
Percentage CO_2 made
Time, minutes
4-Lean 0.00667 cfm-1 atm
8-9-11-20 Rich 0.0333 cfm-1 and 5 atm
10-14-15-16-17-18-19 Rich
12-13 Rich 0.302 cfm 5 atm
0.1667 cfm 1 3 and 5 atm
0.1667 cfm 5 atm
7-Lean
0.0333 cfm 1 3 and 5 atm
123-(5) Lean

FIG 4—SKETCH OF ORIGINAL DATA IN TABLES 1 AND 2.
Numbers refer to runs. The mass rate of flow, not pressure or linear velocity, determines the shape of the curves.

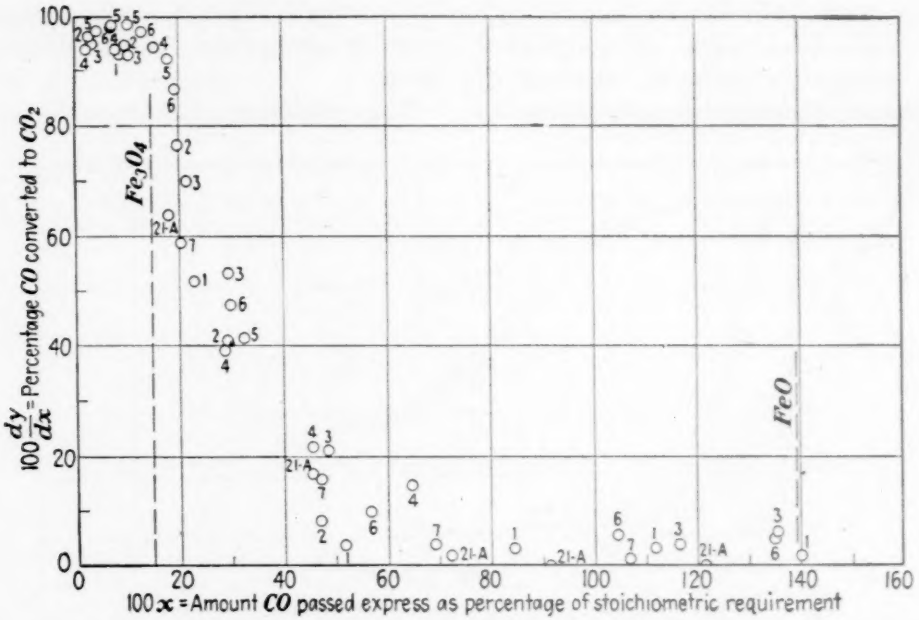
100 dy/dx = Percentage CO converted to CO2
100 x = Amount CO passed express as percentage of stoichiometric requirement
Fe3O4
FeO

FIG 5—TREATED DATA FOR LEAN MIXTURES (RUNS 1 TO 7 AND 21A).
The apparent initial rise may be due to presence of nitrogen that has to be swept out before reduction begins.

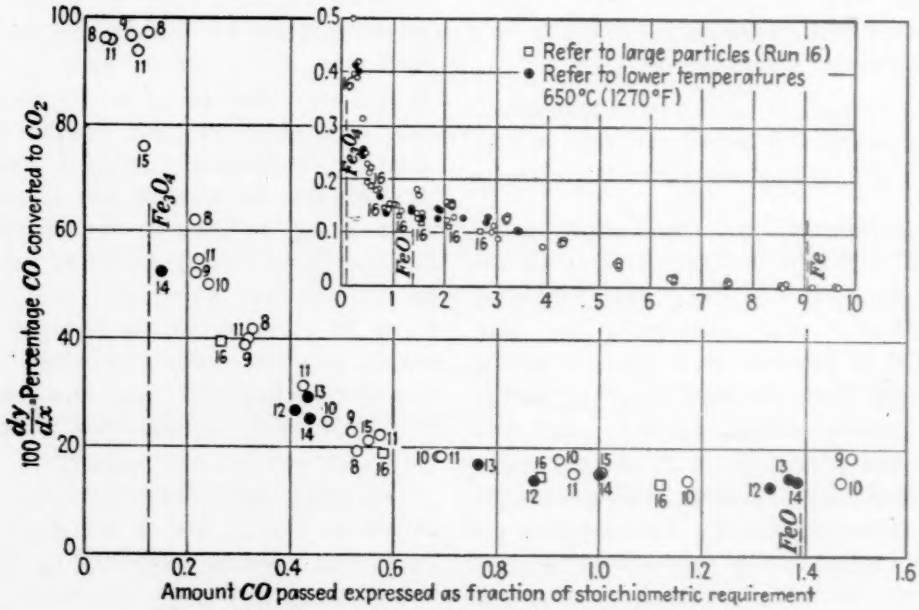
Refer to large particles (Run 16)
Refer to lower temperatures 650°C (1270°F)
100 dy/dx = Percentage CO converted to CO2
Amount CO passed expressed as fraction of stoichiometric requirement
Fe3O4
FeO
Fe

FIG 6—TREATED DATA FOR RICH MIXTURES (RUNS 8–21B).
Open squares refer to large particles (run 16).
Solid circles refer to lower temperatures 650°C (1270°F).

removed from the ore during the change-over from nitrogen to reducing gas at the beginning of the experiments, before the stopwatch was started. In other words, the curves of Figs 5 and 6 should have been extrapolated to negative values of x, dropping down to zero at about $x = -0.1$.

Fig 6 and comparison of Figs 5 and 6 show that the curve for the rich gas is compound, indicating the formation of FeO as an intermediate. The curve for the rich gas shows that Fe_2O_3 is first reduced to FeO with the same rate and efficiency as by the lean gas. This step appears to be essentially complete before any substantial reduction of FeO to Fe occurs. In run 21 the two reduction steps were separated. First, FeO was prepared by reduction with lean gas (21A), then this was reduced to Fe by rich gas (21B). The actual time for complete reduction was as long as that required for other rich gas runs. By plotting the efficiency of conversion of CO "available" above the Fe-FeO equilibrium value as a function of "available" CO supplied for this latter reduction, it is found that the rate for this step is essentially the same as for the reduction of Fe_2O_3 to FeO. The longer time actually required for the second step is due to smaller proportion of thermodynamically "available" CO in the gas mixture.

The rate of reduction depends only on the mass rate of flow of the reducing gas mixture and not on pressure or linear velocity of the gas mixture.

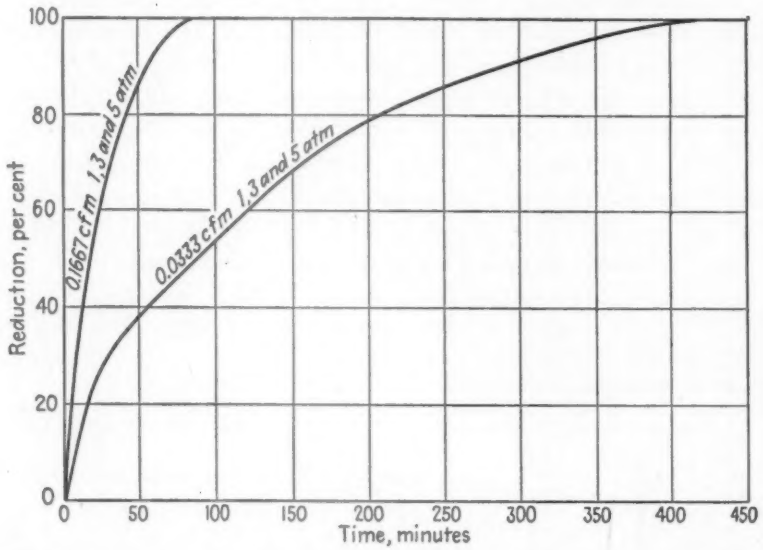

FIG 7—EFFECT OF MASS RATE OF FLOW OF REDUCING GAS ON RATE OF REDUCTION AT SEVERAL PRESSURES.

Effect of pressure at constant mass rate of flow is within experimental error under conditions of experiment.

The times of complete reduction for two rates of flow and two pressures are given in the Table 5. Thus, pressure at constant mass velocity of reducing gas has no effect on the time required for reduction. Pressure does permit the supply of more gas in shorter time without

TABLE 5—*Reduction* Fe_2O_3 *to* Fe
$CO/CO_2 = 4.16$

Gas Rate, Std., Cfm	Pressure, Atm	Velocity, Ft per Min.	Time Required, Min.
0.0333	1	260	430
0.0333	5	57	430
0.1667	1	1260	86
0.1667	5	250	86

TABLE 6—*Carbon Deposition*

Temperature, Deg C	CO/CO_2 Ratio in Inlet Gas	Carbon Deposition, Wt Pct of Reduced Ore, in			Carbon Deposition, Wt Pct of Original Ore, in			Carbon Deposition, Wt Pct of CO in Gas, in			Total Pressure, Atm
		30 Mins.	60 Mins.	120 Mins.	30 Mins.	60 Mins.	120 Mins.	30 Mins.	60 Mins.	120 Mins.	
Pressure, 1 Atm; Gas Rate, 0.1667 Std. cfm											
426	1.29		0.18			0.17			0.17		
433	1.28		0.23			0.19			0.22		
450	0.487		0.06			0.05			0.10		
451	1.16		0.10			0.09			0.11		
450	1.24		0.08			0.07			0.08		
466	1.28		0.20			0.18			0.21		
477	1.24		0.07			0.06			0.07		
482	1.27		0.24			0.22			0.25		
488	1.26		0.13			0.12			0.14		
494	2.29	0.36			0.31			0.64			
497	2.29		1.10			0.95			0.87		
503	1.26		0.12			0.11			0.12		
505	1.28		0.19			0.18			0.18		
515	1.28			0.09			0.08			0.04	
516	1.26		0.04			0.04			0.05		
535	1.26		0.10			0.09			0.10		
547	1.32	0.02			0.02			0.04			
549	1.32		0.03			0.03			0.03		
Pressure Range, 2 to 5 Atm, Gas Rate, 0.1667 Std. cfm											
484	1.34		0.26			0.23			0.25		2
498	1.29		0.44			0.39			0.43		3
433	1.28		0.97			0.83			0.92		5
453	0.487		0.20			0.17			0.32		5
466	1.28		2.30			2.13			2.44		5
474	1.27		2.68			2.55			2.68		5
477	1.21		1.26			1.11			1.33		5
483	1.27		3.64			3.38			3.84		5
491	1.28		3.22			2.94			3.34		5
493	1.28	0.25			0.24			0.48			5
497	2.43		10.62			10.73			9.50		5
499	2.43	4.27			3.36			6.79			5
501	1.28			5.52			5.24			2.68	5
503	1.28		3.33			2.76			3.19		5
503	1.25		2.91			2.68			3.05		5
520	1.25		2.19			1.97			2.26		5
530	1.26		1.06			0.95			1.08		5
542	1.30	0.21			0.18			0.39			
552	1.30		0.04			0.03			0.04		5
Pressure, 1 Atm; Gas Rate, 0.0333 Std. cfm											
498	1.36		150 Min. 0.13			150 Min. 0.12			150 Min. 0.25		

increase in linear velocity and thus permits more rapid reduction. Comparison of the first and last runs in Table 5 shows that at the same linear velocity of gas the time for reduction can be decreased to one fifth by increasing the pressure fivefold (and the mass velocity correspondingly).

SUMMARY

The rate of reduction of a hematitic ore has been investigated under various conditions of mass rate of flow, linear velocity of gases, composition of gas mixture, time of contact, pressure, temperature and particle size of ore, which, except for the latter, are close to those occurring in blast-furnace operation. The reduction proceeds by at least two steps, the reduction to FeO followed by reduction of FeO to Fe. The second step does not occur unless the CO/CO_2 ratio is above a minimum value, but apart from this

thermodynamic availability of the CO, the kinetics of the two steps are identical. The chemical reactions are extremely fast, the rate-determining factor being merely the hydrodynamic problem of bringing thermodynamically available CO in contact with the iron oxides. The rate of reduction at any stage is proportional to the mass rate of supply of CO. Hence, the time taken to bring the ore to any stage of reduction is inversely proportional to mass rate of supply of CO. The efficiency of conversion is a function only of the state of reduction of the ore, and not of the gas composition, linear velocity, pressure, or temperature. Consequently, the rate of reduction can be increased *proportionately* by increasing the mass rate of flow by higher linear velocities or by higher pressures. The time required for reduction will be decreased proportionately.

Carbon Deposition

Samples of a hematitic iron ore were subjected to the action of various mixtures of CO, CO_2, and N_2 under conditions of different pressures, temperatures, and times of exposure, in order to measure the extent of carbon deposition on the partially reduced ore.

Apparatus and Procedure

The apparatus and procedure for contacting the ore with the gas were identical with those described for the experiments on reduction of iron ore. Briefly, a weighed sample of iron ore (38.41 grams = 20 ml) was supported in an externally heated ¾-in. stainless-steel tube, which served as a reaction chamber. The ore was preheated to the desired temperature in a current of nitrogen, whereupon the flow of nitrogen was replaced by a current of the reducing gas at the desired rate, temperature, and pressure. The reduction was continued for the desired period of time, during which samples of the exit gas were taken periodically and analyzed by means of an Orsat apparatus for their content of CO and CO_2. At the end of the run, the gas flow was again replaced by a current of nitrogen at atmospheric pressure, in which the reaction chamber was allowed to cool to room temperature; it was then opened and the ore sample was removed to a tared jar for weighing and analysis. As some of the reduced ore samples proved to be pyrophoric upon contact with air, care was taken during the transfer of the ore sample not to allow the latter to come in contact with the atmosphere. This was accomplished by keeping the space surrounding the reduced ore flooded with nitrogen at all times. Each ore sample was analyzed in its entirety for total carbon, metallic iron, ferrous iron, and ferric iron.

TABLE 7—*Carbon Deposition*
Influence of Pressure up to 10 Pounds per Square Inch Gauge at Constant Temperature

Temperature, Deg C	Pressure, Psi Gauge	CO/CO_2 Ratio in Inlet Gas	(*a*) Wt of Reduced Ore, Pct C	(*b*) Wt of Original Ore, Pct C	(*c*) Conversion of CO to C, Pct
503	0.0	1.26	0.12	0.11	0.12
503	2.5	1.26	0.08	0.07	0.08
503	5.0	1.26	0.13	0.12	0.14
505	7.5	1.26	0.10	0.09	0.11
504	10.0	1.26	0.13	0.12	0.14

Ore—In each experiment, 38.41 grams of 8 to 14-mesh McCook Mesabi hematite of 23.4 pct porosity was used. The ore occupied a gross space of approximately 20 ml.

Rate of Gas Supply—Except in one experiment, the rate of gas flow was 0.1667 std cfm (at standard conditions). In one experiment, the rate was ⅕ of this, or 0.0333 std. cfm.

Pressure—Most of the experiments were done at pressures of one atmosphere and five atmospheres, each set of conditions being usually duplicated at the two pressures. One experiment was conducted

at two atmospheres, and another at three atmospheres. To observe the effect of pressure variations from atmospheric pressure to 10 psi ga., a set of five runs was made at a fixed temperature at closely spaced pressure intervals.

Temperature—The temperature range covered extended from 799° to 1022°F (425° to 550°C).

Composition—The gas composition employed in most of the experiments was similar to that occurring in an efficient blast furnace in the zones corresponding to the temperature range studied. This composition was approximately:

CO_2 = 18 to 17.5 pct
CO = 23 to 22.5 pct
N_2 = 59 to 60.0 pct
ratio CO/CO_2 = 1.28:1.28

To observe the effects of a richer mixture, several experiments were carried out with approximately:

CO_2 = 11 pct
CO = 27 pct
N_2 = 62 pct
ratio CO/CO_2 = 2.45

To observe the effect of a mixture sufficiently lean to prevent reduction to metallic Fe, a gas of approximately the following composition was used in another group of experiments:

CO_2 = 28 pct
CO = 13.5 pct
N_2 = 58.5 pct
ratio CO/CO_2 = 0.487

Duration—All experiments but one were carried out for periods of 30, 60, or 120 min., most runs being conducted for 60 min. A period of 60 min. would materially exceed the time of residence of the ore in the carbon-deposition zone of a commercial blast furnace. One experiment, run at ⅓ of the usual gas rate, was continued for 150 min.

Results

The results of the carbon-deposition experiments are summarized in Tables 6 and 7. The amount of carbon deposited is expressed in three ways: (1) as percentage of carbon on the weight of the reduced ore sample; (2) as percentage of carbon on the weight of the original ore sample; (3) as percentage of the conversion to carbon of the total carbon monoxide passed over the sample, according to the reaction:

$$2CO \rightarrow CO_2 + C$$

Extent of Reduction

Since, in the majority of the experiments made, equal weights (38.41 grams) of the same ore were kept in contact for equal periods of time (60 min.) with gas of substantially the same composition flowing with the same mass velocity (0.1667 std. cfm), and since the temperatures of operation were relatively low and varied over a range of only approximately 100°C (from 433° to 535°C), it was to be expected that the ore in these experiments would be reduced to very nearly the same extent. The analyses of the solid residues actually showed that the extent of reduction was identical in the runs, within experimental and analytical error, and that, under the conditions of these experiments, the reduction of the hematite proceeds only as far as Fe_3O_4. No significant difference in extent of reduction of the iron ore was observed between the experiments made at 1 atm. and those at 5 atm. The calculated formula for the average composition of the residues from the 5 atm. runs was $Fe_3O_{3.97}$; from the 1 atm. runs, $Fe_3O_{4.06}$; mean of all runs, $Fe_3O_{4.03}$.

Effect of Pressure

The application of pressures of the order of 5 atm. greatly increases the extent of carbon deposition. In all cases where an appreciable amount of carbon is deposited at all, increasing the pressure from 1 to 5 atmospheres results in a

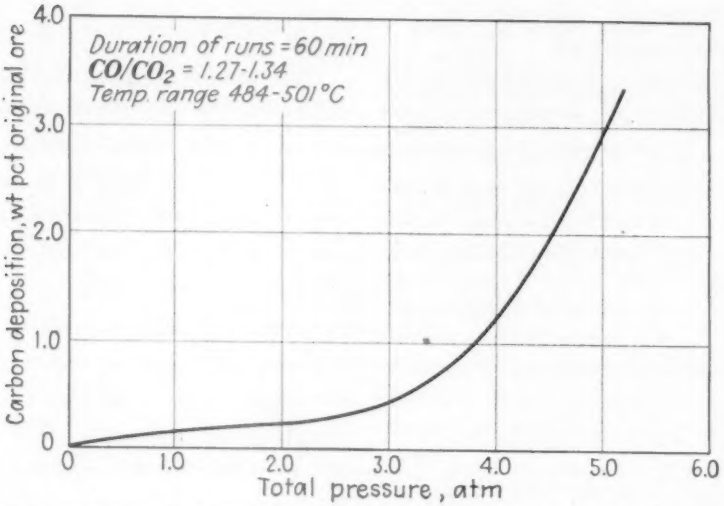

FIG 8—EFFECT OF TOTAL PRESSURE ON DEPOSITION OF CARBON UNDER CONDITIONS SHOWN.

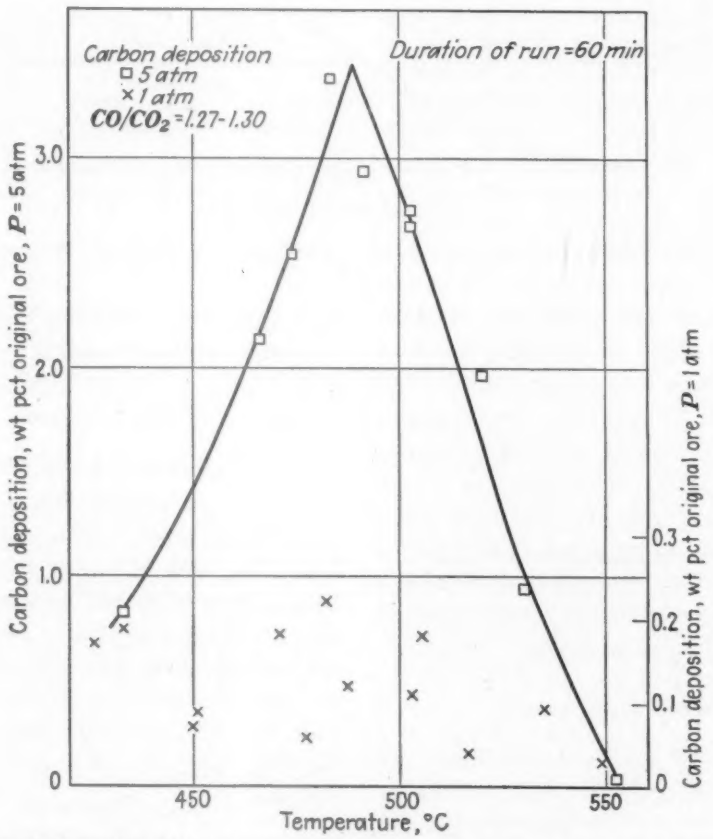

FIG 9—CARBON DEPOSITION AT ONE AND FIVE ATMOSPHERES PRESSURE AS A FUNCTION OF TEMPERATURE.

tenfold to fifteenfold increase in the amount of carbon deposited.

If carbon deposition is increased at all by the application of pressures up to 10 psi ga. under the conditions of these experiments, such an increase appears to be less than the experimental and analytical error. In operating the apparatus at these mild pressures, no visual evidence of increased carbon deposition was noted, and it appears safe to conclude that, in the operation of an actual blast furnace at top pressures on the order of 10 psi ga., no perceptible difficulty with carbon deposition will be encountered.

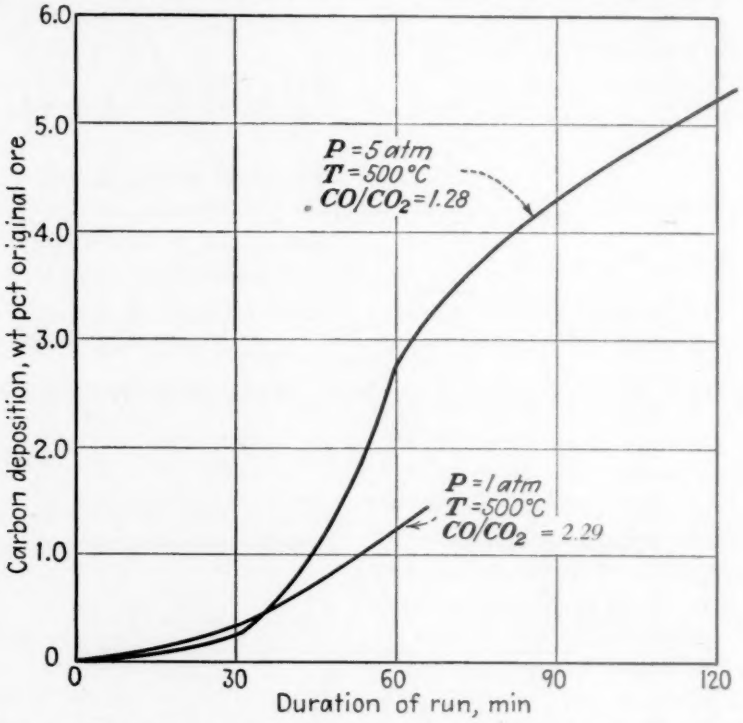

FIG 10—CARBON DEPOSITION UNDER TWO SETS OF CONDITIONS AS A FUNCTION OF DURATION OF RUN.

Effect of Temperature

Fig 9 illustrates the effect of temperature upon carbon deposition, other conditions being equal or practically so. It was found that a smooth curve could be drawn through the experimental points of the series of experiments, which definitely indicated a sharp single maximum at about 489°C.

The carbon deposition in the 1 atm. runs was so low that the experimental and analytical error masked any regular variation with temperature, and no attempt was made to connect the 1 atm. points in Fig 9 by means of a curve.

Effect of Gas Composition

Carbon deposition increases with increasing CO/CO_2 ratio. Decreasing the CO/CO_2 ratio to 0.487 at 450°C practically suppresses carbon deposition, even at 5 atm pressure. It may be worth noting that under these conditions no reduction to metallic iron can occur, possibly indicating the catalytic part played by metallic iron in the carbon-deposition reaction.

Effect of Time

Wherever appreciable carbon is deposited, the amount deposited, as expressed

by all three methods, increases much more than proportionately between 30 and 60 min. This again may indicate the catalytic effect of any metallic iron formed. Although the percentage of carbon in the solid ore increased further when the time of the experiment was further increased to 120 min. (500°C, 5 atmospheres, CO/CO_2 = 1.28), the percentage conversion of total CO to carbon actually decreased, possibly indicating the suppression of the catalytic effect of metallic iron due to complete coating of the surface of the ore particles with carbon.

References

1. Diepschlag: Reduction of Iron Ore Under Increased Pressure. *Archiv Eisenhüttenwesen* (Nov. 1936).
2. Tenenbaum and Joseph: *Trans.* A.I.M.E. (1939) **135,** 59–72; (1940) **140,** 106–123.
3. Specht and Zapffe: Low-temperature Gaseous Reduction of Magnetite Ore to Sponge Iron. *Metals Tech.*, A.I.M.E. (June 1946—T.P. 1960); *Trans.* A.I.M.E. (1946) **167,** 237.
4. Avery: Pressure Operation of the Pig Iron Blast Furnace and the Problem of Solution Loss. *Trans.* A.I.M.E. (1938) **131,** 102.
5. Kinney: The Blast Furnace Stock Column. U. S. Bur. Mines *Tech. Pub.* 442 (1929) 148.
6. Chipman and Murphy: *Ind. and Eng. Chem.* (1933) **25,** 319.
7. Chipman and Marshall: *Jnl.* Amer. Chem. Soc. (1940) **62,** 299.

DISCUSSION

(W. E. Brewster presiding)

M. Tenenbaum*—There are several observations that I would like to make with regard to the nature of the reactions that occur. Some mention was made in the paper of the factors affecting the rate, and it was implied that the linear velocity or the pressure of the reducing gas would naturally be reflected in the reaction rates.

There are several processes occurring during reduction that confuse the picture. The first interfering process was discussed: the overall rate as governed by the diffusion of the reacting products to the reacting inter-phase and diffusion of the products of the reaction.

There is a second effect, however, which was not brought out and that is inherent in the nature of the reaction itself. The reaction of a gas phase with a solid phase is a heterogeneous reaction and the process that controls the reaction is an adsorptive process. First the reacting gas is adsorbed onto the surface of the oxide being reduced and this process is the one that determines, (as Mr. Marek described it), the thermodynamic availability of the reacting gas. It does not necessarily follow that the concentration of the reacting products on the adsorbed film are influenced proportionately by the pressure or the concentration of the gas phase.

Some gases adsorb onto a surface very readily and an increase in pressure of those gases does not necessarily reflect a proportional increase in the rate. This is attributed to the fact that when the proportion of the surface originally occupied is very large, only a small area remains to be affected by changes in concentrations in the gas phase.

However, if a very small proportion of the original surface is covered and then the pressure is increased a more nearly proportional increase in the reaction rate might be expected.

In that respect, in a paper by Dr. Lewis* it is commendable that the reaction was not considered directly as first-order. Under the conditions of the experiment, if it turned out to be a first-order reaction, it would be more or less a coincidence.

B. M. Larsen†—The small size of the ore used in most of the runs and the fact that no indication of any ore size effect was found, would indicate that there was an abundance of surface available as fast as the gas reached it and I wonder if this main conclusion would not be more completely established if a wider range of ore sizes was used.

I doubt that the amount of potential surface covered on absorption is involved; it is probably the rate of diffusion into the reacting zone even with this small size. With larger sized particles, would one then get a different effect of varying pressure?

On the matter of carbon deposition, this

* Inland Steel Co., East Chicago, Ind.

* J. R. Lewis: Rate of Reduction of Geneva Iron Ore. This volume, page 27.

† U. S. Steel Corp., Kearny, N. J.

paper indicates that in a blast furnace carbon deposition would be negligible in the commercial furnace process. He believes this is true in view of the short time the ore takes to pass through this critical temperature zone and the small amount of carbon deposition Mr. Marek found at any probable pressure that will be reached shortly in a blast furnace.

I question whether we ought not to be a little cautious about this conclusion. For one thing, there may be tiny concentrations of molecules in the gas phase in a blast furnace which catalyze the carbon deposition reaction, and which were not present in this experimental work: perhaps cyanides or carbonyls or alkali metal compounds that would speed up carbon deposition much more rapidly without any induction period. That is a possibility that should be considered.

I think the main point of the paper was very well brought out and that it is an important contribution.

German Iron Ores Yield Vanadium

By R. P. Fischer,* Junior Member AIME

(Atlantic City Meeting, November 1946)

A large production of vanadium during the war helped Germany to meet her critical requirements for the ferroalloy metals. Vanadium was needed not only in the ordinary high-speed tool steels, but in other alloy steels as a substitute for chromium, nickel, and molybdenum, which were scarce. Lacking a source of vanadium ore, however, the vanadium was obtained as a by-product of the steel industry—vanadium-bearing pig iron smelted from iron ores containing about 0.1 per cent V was blown in converters to yield vanadium-rich slag, from which vanadium was recovered by chemical treatment. The production capacity obtained was said to be about 6,500,000 lb. of vanadium a year.

Although the general processes of preparing vanadium-rich slags as well as the recovery methods described herein are known, some of the details presented may be of interest to both the American steel industry and the vanadium producers. No adequate data on the cost of the vanadium produced in Germany are known, but it seems likely that the cost exceeds the commonly quoted domestic price of about $1.10 per pound of contained V_2O_5.

Information on the German vanadium production was obtained by a team of geologists from the Geological Survey, United States Department of the Interior, during investigations in May and June 1945 of the German utilization of low-grade raw materials. These investigations were sponsored by the Chief of Engineers, War Department. It is a pleasure to acknowledge the aid obtained from Messrs. H. C. Smith and J. D. Dickerson, investigators assigned to the Army Ordnance section of C.I.O.S., and Mr. C. F. Park, Jr., of the Geological Survey team. The data on vanadium recovery from iron ores were obtained from the Kaiser Wilhelm Institut für Eisenforschung, the Hermann Göring steel plant at Watenstedt, and from notes made by other investigators at other German steel plants.

Published by permission of the Director, U. S. Geological Survey. Manuscript received at the office of the Institute Feb. 21, 1946. Issued as T.P. 2070 in Metals Technology, September 1946.

* U. S. Geological Survey, Washington, D. C.

Preparation of Vanadium-rich Slags

Most German iron ores contain only about 0.1 per cent vanadium, or even less, but some of the Scandinavian iron ores available to the German iron industry in the past contain a little more than 0.1 per cent.

In general German practice of vanadium recovery, nearly all of the vanadium in the ore goes into the pig iron, which is blown in the Thomas converter, yielding a slag containing about 1 per cent V. This slag is resmelted, the vanadium again going with the iron, which is again blown in a converter, yielding a slag that averages about 10 per cent V. This slag is treated at special chemical plants, by the process of a sodadizing roast, water leach, and acid precipitation of vanadium oxide.

The Hermann Göring steel plant at Watenstedt used the low-grade Salzgitter iron ores, the average composition of which is shown in Table 1, column 1. The acid and basic iron produced in the blast furnaces contained about 0.3 per cent V. A Thomas

converter plant was started in 1942, after experimental work on the large-scale production of vanadium-rich slags. The Thomas slag resulting from blowing the pig iron averages about 1.5 per cent V. This slag, along with "dust" or spittings from the converter and some Salzgitter ore, was charged into one blast furnace and resmelted, yielding iron rich in vanadium and phosphorus, the average composition of which is shown in Table 1, column 2. This iron was blown down in a converter having a fire-clay lining and a dolomite bottom, yielding a slag of a dry consistency, the average composition of which is shown in Table 1, column 3.

The production of vanadium-rich slag at the Hermann Göring works (Watenstedt) amounted to 50 to 100 metric tons of contained vanadium per month, a substantial part of the German production of vanadium-rich slags.

The vanadium-rich slag was sent to chemical plants for recovery of the vanadium. The residual iron was sent to blast-furnace works producing Thomas iron without vanadium, and the resultant Thomas slag, containing phosphorus but no appreciable amount of vanadium, was sold as fertilizer slag.

TABLE 1

Element	1 Average Composition of the Salzgitter Iron Ores, Per Cent	2 Average Composition of Iron Produced from Thomas Slag, Per Cent	3 Average Composition of Vanadium rich Slag, Per Cent
Fe	25–30		
SiO_2	25–30		0.02
CaO	2–3		2.0
P	0.5–0.6	9.0	9.5
S	0.04–0.08	0.1	0.1
V	0.1	1.5	14.5
C		1.5	
Mn			0.03

Vanadium-rich slags were obtained at the Röschling works at Völklingen from iron ores said to contain between 0.015 and 0.03 per cent V. The pig iron smelted from these ores contained 0.10 to 0.15 per cent V, 1.9 to 2.0 P, 0.5 maximum Si, 0.5 Mn, 3.5 C, and 0.05 S. Either acid or basic slags were made by blowing this iron, and each slag was charged into a separate blast furnace. The batches of iron made from these slags were blown in either an acid or basic converter, each yielding a slag containing 7 to 8 per cent V, and these slags were sent to the vanadium plants.

Another process at Völklingen used a Frisch trommel to make vanadium-rich slag instead of a double blow in converters. Spittings, containing 0.3 to 0.5 per cent V and 70 to 80 per cent iron, from basic converters were charged into a small blast furnace with a small amount of ore and lime as well as residue from the vanadium-extraction plants. The furnace was run only after sufficient accumulation of spittings. The smelted iron, containing about 0.65 per cent V, was blasted with air in the runner that fed the trommel, and the resultant slag, containing 7 to 8 per cent V, was sent to the vanadium plants.

Recovery of Vanadium from Slags

Although practices differed somewhat in detail in the several chemical plants recovering vanadium, the general practice was the same at all plants. The vanadium-rich slags were ground to about 0.15 mm., roasted at about 800°C. with soda ash (Na_2CO_3) or sodium chloride (NaCl), forming a water-soluble sodium vanadate that was leached with water and precipitated with acid. In spite of the range in composition of the vanadium slags, the results obtained were considered favorable, the average yield being about 80 per cent of the vanadium contained in the slags. When the recovery was not satisfactory, it was improved by adding a little red iron oxide (Rotschlamm) or silica compounds, or by mixing slags to obtain a feed of the desired composition. One difficulty commonly encountered in roasting was the use

of too high a temperature, which caused sintering or melting of the slag.

The vanadium-roasting plants utilized existing sulphur-roasting installations, both of the multiple hearth and kiln type. The basic design of these roasters was not considered theoretically satisfactory, for the heating gases went counter to the ore (slag) through the roasters. Dust losses, however, were negligible, as the slag was heavy.

The vertical, multiple-hearth roasters used are similar to the Skinner roaster used in treating vanadiferous sandstone ores in Colorado and Utah. Many of the roasters have a diameter of 7 meters and consist of seven hearths. The reported capacity was about 10 tons a day; the feed was continuous, and 4 to 5 hr. was required for a particle to pass through the furnace. The three middle hearths were kept hottest, about 800°C., but it was said that occasionally the iron in the slag "burned," raising the temperature sufficiently to agglomerate the ground slag and preventing satisfactory reactions. When this occurred, the leach might yield as little as 30 per cent of the vanadium in the slag, and the roasted slag was then returned to the blast furnace to enrich new slags.

The roasting kilns have a capacity of 20 to 40 tons a day, and they were operated continuously, a particle passing through the kiln in about three hours.

A quick leaching quench when the roast is hot, although shown by experiments to yield the highest recovery, was not considered practicable on a commercial scale. The roasted material, therefore, was allowed to cool, and it was leached with water at about 100°C. Contrary to the practice with roasted sandstone ores in the United States, where a multiple leach is commonly used, in Germany the slag was said to be leached only once. The leach time was from 10 to 20 min. in some plants, 1 to 1½ hr. in others.

Because the leach also dissolves the phosphorus in the roasted slag, calcium-bearing solutions were added to make a calcium-phosphate precipitate, and the vanadium-bearing solution was filtered off. Sodium vanadate was precipitated from this solution by adding either H_2SO_4 or HCl, bringing the pH between 2.8 and 3.2. It was said that the precipitate normally contained 48 to 53 per cent V (85 to 94 per cent V_2O_5) and 4 to 10 per cent Na_2O, plus a trace of phosphorus.

Research on Vanadium Recovery

At the beginning of the war, when it became apparent that German needs for vanadium would be critical, research was started to determine the best practice to recover vanadium from iron-ore slags. The occurrence of vanadium in slags was investigated. Much of the vanadium occurs as an iron-vanadium spinel ($FeO.V_2O_3$),[1] which has a high melting point, but the simple compound is rare, and excess FeO and MnO enter the crystal, forming something like $2FeO.V_2O_3$ or $2MnO.V_2O_3$. Vanadium-rich slags produced from Swedish iron ores are relatively easy to treat, and they yield a high percentage of the contained vanadium, presumably because the iron-vanadium spinel is abundantly present. The German ore slags, in which the manganese-vanadium spinel is commonly present, are more difficult to treat with a satisfactory recovery. It was found that MgO can also be present, replacing FeO or MnO, and similarly Cr_2O_3, Al_2O_3, or Fe_2O_3 can replace V_2O_3. Although the composition of the vanadium-bearing compound can thus vary greatly, apparently it is always present in a spinel-like crystal, embedded in a groundmass of iron and manganese silicates.

The composition of the vanadium-rich slags made in Germany ranges widely

[1] C. H. Mathewson, E. Spire and C. H. Samans: *Trans.* Amer. Soc. Steel Treat. (1932) **20**, 357–384.

(Table 2), owing to preparation methods that differ in detail. Although many factors influence the reactions, it was found that in general a distinction should be made between basic and acid slags. Slags from pig iron made from Thomas slag (basic) were especially rich in vanadium and phosphorus, but relatively free of other impurities such as manganese and silica. Some basic slags yielded best results if they were washed with sulphuric acid before roasting with sodium chloride, and if after water extraction the sodium vanadate solution was boiled with lime to precipitate calcium vanadate. On the other hand, siliceous slags yielded better results if roasted with sodium carbonate before leaching with water and the precipitation of sodium vanadate with acid.

TABLE 2.—*Chemical Composition of the Tested Vanadium-rich Slags*

Slag No.	Analysis, Per Cent							
	V	Fe	Mn	Cr	CaO	MgO	P_2O_5	SiO_2
1	8.7	17.2	28.0	1.5	0		4.8	19.4
4	8.1	15.7	17.3	2.9	6.4		4.0	17.0
7	6.5	23.1	18.6	2.2	8.9	1.9	5.9	11.1
11	16.1	34.4	9.1	2.5	2.1	0.4	9.4	12.2
12	10.9	25.6	7.9	2.1	9.3	4.4	7.3	19.3
19	8.4	24.3	2.0	0.5	0			

The comparative results of the water solubility of vanadium in a roasted slag under conditions of quick and slow cooling are shown in Table 3. Material taken from the furnace at the maximum temperature, quenched and leached quickly, yielded better results, but the practice could not be used when handling large amounts of material, as on a commercial basis.

Experiments with artificial (synthetic) slags are thought not to have given much useful information, as the compounds and reactions obtained in commercial practice are very complex. Clean separations of iron-vanadium spinel were made and the percentage of water-soluble vanadium was determined under different conditions (Table 3).

Table 4 shows the comparative results

TABLE 3.—*Roast Tests*

2 Hours at 750°C., Electrical Muffle Furnace

Addition	Water-soluble Vanadium (Per Cent)	
	Quick Cooling (Quick Quench)	Slow Cooling
Vanadium-rich Slag No. 12		
24 % NaCl	68.1	6.9
24 % Na_2CO_3	90.5	60.0
30 % Na_2CO_3	100.0	94.9
Synthetic Slag $2FeO.V_2O_3$		
36 % Na_2CO_3	82.8	81.3
73 % Na_2CO_3	91.9	92.8
108 % Na_2CO_3	92.1	95.8
40 % NaCl	100.0	100.0
80 % NaCl	97.5	100.0

TABLE 4.—*Influence of Water Vapor in Roasting Slags*

Commercial Slags

Slag No.	NaCl, Per Cent	Air	Water-soluble Vanadium, Per Cent	
			Quick Cooling	Slow Cooling
12	24	Dry	29.1	10.0
12	24	Plus H_2O	89.1	69.4
11	34	Dry		23.0
11	34	Plus H_2O		91.0
19	24	Dry		60.7
19	24	Plus H_2O		94.2
1	24	Dry		33.9
1	24	Plus H_2O		73.7

Synthetic Slags

Slags	Addition	Air	Water-soluble Vanadium, Per Cent
$2FeO.V_2O_3$	40 % NaCl	Dry	40.9
	40 % NaCl	Plus H_2O	95.6
	40 % NaCl plus 100 % SiO_2	Dry	76.0
	40 % NaCl plus 100 % SiO_2	Plus H_2O	97.9
$2MnO.V_2O_3$	40 % NaCl	Dry	14.8
	40 % NaCl	Plus H_2O	26.0
	40 % NaCl plus 100 % SiO_2	Dry	34.6
	40 % NaCl plus 100 % SiO_2	Plus H_2O	99.2

of roasting commercial slags (*technischen schlacken*) with and without water vapor. It was concluded that most or all slags leach better if roasted with water vapor, but that some slags require additional factors to yield satisfactory results.

Other tests on the influence of water vapor on roasting synthetic slags, with and without the addition of SiO_2, were made and the results are shown also in Table 4. The relative solubility of vanadium in the iron-vanadium and manganese-vanadium spinels is also shown by these tests. It was predicted that the presence of other elements, such as chromium, will have a significant influence on the reactions.

The experiments conducted were not considered sufficient to give all of the desired answers, but the following conclusions were made:

1. Oxidation of V_2O_3 to V_2O_5 should take place in the roast process used, except where a large amount of Cr_2O_3 is present.

2. Even though a considerable amount of sodium is used, frequently it is not enough, for other compounds in the slag, such as iron, manganese, aluminum, and chromium oxides, also combine with the sodium. If vanadates are formed that contain less than one molecule of Na_2O to one molecule of V_2O_5, oxygen separates spontaneously on the cooling of the roast,[2] forming a poorly soluble vanadium compound containing V_2O_4. This compound was detected by X-ray in roasts that were poorly soluble.

3. The composition of the groundmass of the slag, especially the lime content, and the grain size of the slag, both of the spinel and groundmass, have an important influence on the reactions during roasting.

[2] G. Canneri: *Gaaz chim.* (1928) **58**, 7.

DISCUSSION

(*F. T. Sisco presiding*)

M. TIGERSCHIÖLD*—This process originally was invented in Sweden by Rutger von Seth, about 1920. It has been worked on regularly for many years, and is still used at the Christiana Spigerverk in Oslo. The electric pig-iron furnace is used where the yield of vanadium is better than in the blast furnace.

It was pointed out that all the vanadium from the ore went into the pig iron. I do not believe that. I have figures that show that about 70 pct of the vanadium goes into the pig iron in an ordinary blast furnace. In an electric pig-iron furnace, the yield is higher. I believe it is something approximating 80 to 90 pct. At the Spigerverk an acid Tropenas converter has been used for more than 20 years to take out vanadium. The bath is blown down to about 2 pct carbon and the slag is taken off. As far as I know, a mill scale is not used for the purpose.

I did not understand from this paper whether any other method used in Germany was mentioned. In Saarbrücken, before the war a first treatment of the pig iron was made with mill scale in a rotating furnace, and a slag quite rich in vanadium resulted. That slag was melted again in blast furnaces and a new pig iron very much richer in vanadium was obtained. This was blown in basic converters, just in the way to which you refer.

F. T. SISCO†—This is a record, apparently, of the method by which the steel men in a country where no alloying elements were available during the war made the best of a bad situation, and it seems to me that the fact that they succeeded in producing about six and a half million pounds of vanadium a year is evidence that they had a rather effective method.

* Director of Research, Jernkontoret, Stockholm, Sweden.

† Metallurgical Director, Alloys of Iron Research, New York, N.Y.

Production of Low-sulphur Sponge Iron

By R. C. Buehl,* Member AIME, E. P. Shoub * and J. P. Riott*

(Atlantic City Meeting, November 1946)

Pilot-plant tests have demonstrated that it is possible to produce low-sulphur sponge iron (0.03 to 0.05 per cent sulphur) as a continuous process in an internally fired rotary kiln from iron ore or mill scale; a solid carbonaceous reducing agent; and dolomite to control the sulphur content. The proportion of dolomite employed is small, so that it does not add materially to the cost of the sponge iron. The entire operation is carried out at temperatures well below the melting point of iron, so that the product is discharged in granular form. Compared with other methods for the production of sponge iron, the rotary-kiln method has the advantage of simplicity and low cost of equipment and, in addition, requires little labor for the operation of the process. The pilot-plant equipment used for this work was sufficiently large to demonstrate that the production of low-sulphur sponge iron in rotary kilns is feasible and that the costs are not excessive for applications in which sponge iron has distinct advantages over competing materials.

This report constitutes a part of a program by the Bureau of Mines under a special Congressional appropriation for studying gaseous and solid fuel reduction of iron ores. Numerous articles on various phases of these investigations have appeared in Bureau of Mines publications or technical journals. Other articles are being prepared and will be published in the near future. The present program, which is under the supervision of Dr. R. S. Dean, Assistant Director of the Bureau of Mines, was initiated in 1942. However, a considerable portion of the work was a continuation of previous research performed by the Bureau.

Previous investigators[1-4] utilizing the rotary kiln for the production of sponge iron did not develop a suitable method for controlling the sulphur content. A review of the literature shows that the sulphur content in the product usually exceeded 0.1 per cent unless reducing agents with very low sulphur contents were employed. This high sulphur value made the product generally undesirable for use as melting stock in electric or open-hearth furnaces.

The production of sponge iron in an internally fired rotary kiln has been described in detail in Bureau of Mines *Bulletin* 270[2]; consequently, this article will be confined mostly to new features of the process—that is, means for controlling the sulphur content of the sponge iron. Suitable raw materials include iron ores or mill scale; coal or coke for reducing them, and sized dolomite (−20+100-mesh) as the sulphur-controlling agent. A mixture of the raw materials in granular form is fed into the elevated end of the kiln, which is fired axially from the lower or discharge end. In the reducing zone, which is approximately one third the length of the kiln measured from the dis-

Published by permission of the Director, Bureau of Mines, U. S. Department of the Interior.

Manuscript received at the office of the Institute Feb. 9, 1946. Issued as T.P. 2093 in Metals Technology, October 1946.

* Senior Metallurgical Engineer and Associate Metallurgists, respectively, Metallurgical Division, Bureau of Mines, Central Experiment Station, Pittsburgh, Pennsylvania.

[1] References are at the end of the paper.

charge end, a temperature of 1800° to 2000°F. is maintained. The reduced material is discharged through a cooling chamber, which is an integral part of the kiln and which prevents the material from being reoxidized by air during cooling. The discharge is then passed through a magnetic separator, which removes the magnetic sponge iron from the nonmagnetic char and dolomite.

The method of using sized dolomite as the desulphurizing agent is the result of a systematic investigation of the form in which sulphur exists in sponge iron and of the factors that influence the transfer of sulphur into the sponge iron when solid reducing agents are employed. Early tests indicate that if no sulphur-controlling agent were employed, sulphur contents as high as 0.25 per cent could be expected. The addition of lime, limestone, or dolomite in powdered form to the feed did not lower the sulphur content sufficiently to make the sponge iron desirable as a melting stock. In contrast to these results, the addition of sized dolomite to the feed reduced the sulphur content to the range 0.02 to 0.05 per cent. Sized lime, while beneficial, was not nearly as effective as sized dolomite, sulphur contents being in the range of 0.04 to 0.07 per cent. The authors attribute this difference in the results to the tendency of the particles of lime to be pulverized by tumbling and the abrasive action of the charge in the kiln. Limestone is converted to lime at the operating temperature and therefore loses its physical strength. In contrast, dolomite retains its physical strength when heated so that the particles do not crumble in the rotating kiln. As a result of the pulverizing action in the rotary kiln, fine particles of basic desulphurizing agent adhere to the surface of the sponge-iron granules, and this surface coating has been found to contain most of the sulphur in the sponge-iron product.

An accurate sulphur balance is difficult to obtain because of sulphur loss in the combustion gases. An approximate sulphur distribution is given below for a charge consisting of equal parts of low sulphur magnetite ore (0.02 per cent S) and coke (0.8 per cent S) with the addition of sized dolomite to the extent of 10 per cent of the weight of the ore. Sponge iron with a sulphur content of 0.03 per cent was produced in an internally fired rotary kiln from these raw materials. In this test, low-sulphur oil (0.3 per cent S) was used to supply the heat for the process. With these raw materials, over 90 per cent of the sulphur in the charge is contained in the reducing agent. About 2.5 per cent of the sulphur in the charge appears in the sponge iron, 60 to 70 per cent of the initial sulphur remains in the unconsumed coal and coal ash rejected by the magnetic separator, 16 per cent is contained in the dolomite, and the remainder passes off to the combustion gases. When no desulphurizing agent is employed, the sponge iron contains from 16 to 20 per cent of the sulphur in the charge.

Experimental evidence to demonstrate the existence of a basic coating containing most of the sulphur in the sponge-iron concentrate is presented in the following paragraphs.

Sulphur-bearing Surface Layer

Recent experimental results have indicated that when ore is reduced by coal or coke in the presence of powdered lime, almost all of the sulphur is contained in a basic slaglike coating on the particles rather than being distributed throughout the iron particles. Evidence to support this conclusion is as follows:

Photographs of Slag Layer

Photographs were taken of the surface layer on sponge-iron particles that were reduced in a rotary kiln from a charge consisting of ore; coke made from a mixture of coal and pulverized limestone;[5,6] and

powdered lime. This sponge iron contained a relatively high sulphur content of 0.1 per cent. Fig. 1 shows a micrograph of a particle of sponge iron embedded in bakelite, partially polished, and photographed at 500 diameters. The continuity of the scratches shows that a layer exists on the surface of the particle and that the darker area surrounding the particle is not a gap between the particle and the mounting material. Visual examination of the particles showed that the portion photographed contained a layer of greater than average thickness.

FIG. 1.—SPONGE-IRON PARTICLE EMBEDDED IN BAKELITE AND PARTLY POLISHED, SHOWING COATING ON SURFACE OF PARTICLE. × 500.

Fig. 2 is a similar micrograph of a particle of the same sponge iron, except that water immersion (similar to oil immersion) was employed using water to which a small amount of methyl orange indicator solution was added. The solution immediately adjacent to the edge of the particle turned orange yellow and when photographed with blue filters appeared as a light boundary surrounding the particle. The specimen when observed under water immersion without methyl orange but with the same blue filter did not show the light boundary, indicating that the effect was due to the indicator qualities of the methyl orange and not to refraction. The color change exhibited when taking this micrograph indicates that the slag layer has a basic reaction to the methyl orange indicator. This indicator is transformed from red to yellow orange by basic slags so that it is reasonable to assume that the surface coating on the particles is either lime or basic slag.

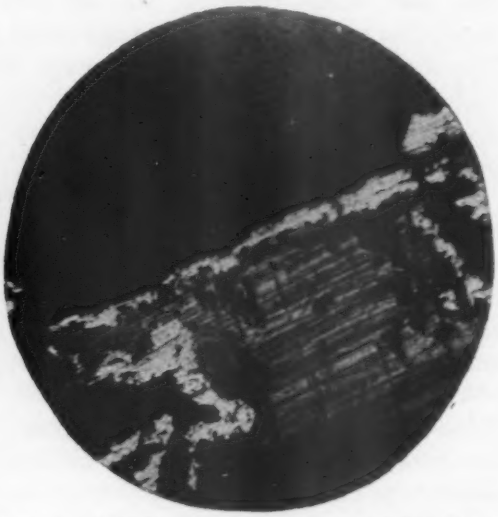

FIG. 2.—SPONGE-IRON PARTICLE, EMBEDDED IN BAKELITE AND PARTLY POLISHED. × 1000.
The basic character of the slaglike coating is demonstrated by treatment with methyl orange indicator solution.

Fig. 3 is an enlarged photograph of a sulphur print with a magnification of about 10 diameters. The two large particles have maximum dimensions of 1.5 mm. or are approximately 10-mesh particles. This print is a further indication that most of the sulphur is contained on the surface of the particles.

Sulphur vs. Particle Size

If a large part of the sulphur in sponge iron is present in a surface layer on particles as indicated by the photograph shown above, then one would expect large particles to have a lower sulphur content than fine particles. Such dependence of sulphur content on particle size occurs as

shown in Figs. 4, 5, and 6, which will be explained in detail later. The variation of sulphur content with particle size, which is to be expected provided the sulphur is largely contained in a surface layer, can be calculated by making reasonable assumptions.

If it is assumed that the sulphur is present as a uniform layer on the surface of particles that are approximately spherical, an equation can be derived to show the variation of sulphur content of a particle with its radius:

$$\text{Weight of sulphur in entire particle} = \frac{\%\text{ sulphur increase}}{100} \times \text{volume} \times \text{density (of sponge-iron particles)} = \frac{\%\ S_p}{100} \times \frac{4\pi R^3 d_p}{3} \quad [1]$$

$$\text{Weight of sulphur in surface layer} = \frac{\%\text{ sulphur in layer}}{100} \times \text{volume} \times \text{density (of layer)} = \frac{\%\ S_L}{100} \times 4\pi R^2 \times T_L \times d_L \quad [2]$$

$\%\ S_p$ = % sulphur increase
R = radius of particle
d_p = density of particle
$\%\ S_L$ = % sulphur in layer
T_L = thickness of layer
d_L = density of layer

Equating Eqs. 1 and 2 and solving for the percentage of sulphur increase gives:

$$\%\ S_p = \frac{3 \times \%S_L \times T_L \times d_L}{R \times d_p} = \frac{K\%S_L T_L}{R}$$

If the percentage of sulphur in the layer ($\%\ S_L$) and the thickness of the layer (T_L) are further assumed to be independent of the particle size, then

$$\%S_p = \frac{K'}{R}$$

that is, the sulphur content of a particle varies inversely as the radius of the particle.

For nonspherical particles of similar shape and proportion, the surface area

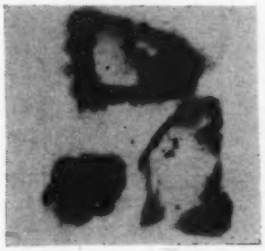

FIG. 3.—SULPHUR PRINT OF SPONGE-IRON PARTICLES. × 10.

is nearly proportional to the square of the largest dimension and the volume to the cube of the largest dimension. Consequently, the form of the relation given above would hold where the largest dimensions were used in place of the radius.

The dependence of both sulphur content and lime increase on particle size was experimentally determined by separating the sponge iron of various tests into sized fractions by sieving. Lime increase is the difference between the lime content of the sponge iron and that of the ore corrected for loss of oxygen. Fig. 4 shows the variation of sulphur content and lime increase with the average reciprocal of the radius for sponge irons made from Chateaugay magnetite ore. This iron was produced in a two-diameter, internally fired, rotary kiln with a reducing section 3 ft. inside diameter, 4½ ft. long, and a preheating section 19 in. inside diameter and 18 ft. long.

The mesh sizes employed are indicated at the top of the curve. The abscissas are located to represent an estimated weighted average of the reciprocal of the radii of the particles in each separated fraction. While the location of the abscissas is not exact, variations within the limits corresponding to the sieve sizes would not greatly influence the shape of the curve or the conclusions drawn.

Curve A (Fig. 4) is for sponge iron reduced from ore by means of coke that contained 0.9 per cent sulphur. This sponge iron as produced has a sulphur content of 0.33 per cent. The increase of sulphur content as particle size decreases is relatively small, so that most of the sulphur is distributed throughout the particles.

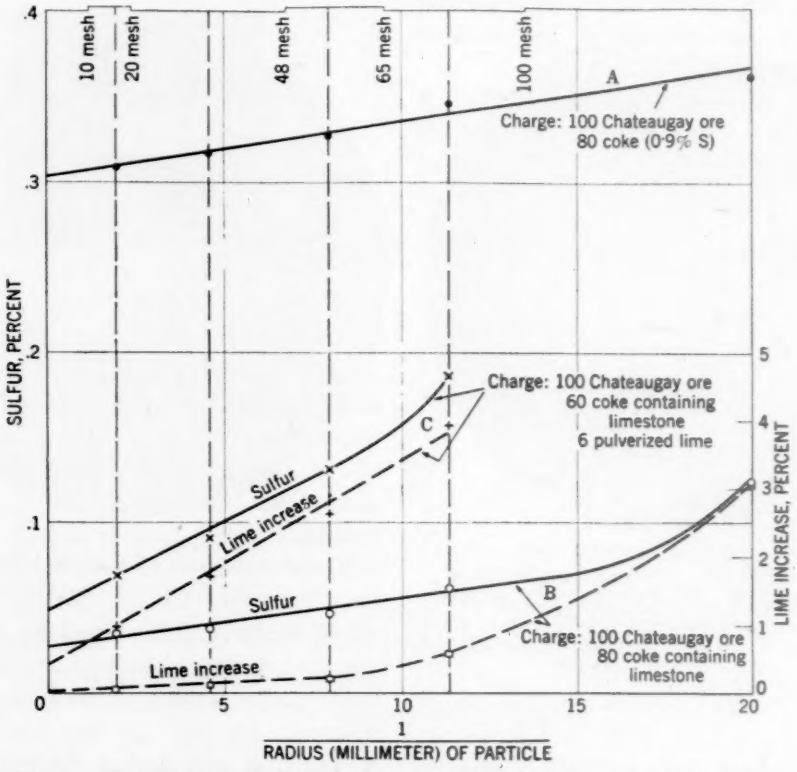

FIG. 4.—VARIATION OF SULPHUR AND LIME CONTENT WITH PARTICLE SIZE.
Sponge iron made from Chateaugay ore (New York magnetite) reduced in an internally fired rotary kiln.

Curves B (Fig. 4) are for sponge iron (average sulphur content 0.045 per cent) reduced with coke made from the same coal used for the coke referred to in curve *A* but to which powdered limestone had been added to the extent of one fifth the weight of the coal before coking.

Curves C (Fig. 4) are for sponge iron prepared in the same manner and from the same raw materials as the product described in curves *B*, except that powdered lime was added to the charge to the extent of one tenth the weight of the lime-bearing coke. This sponge iron contained an average of 0.116 per cent sulphur. The small addition of free lime to the feed causes a considerable increase in the sulphur content. Since both the sulphur and lime increase inversely to the radii of the particles, it appears that a basic layer exists on the surface of the particles that contains most of the sulphur and lime increase in the sponge-iron product.

A comparison of the curves of Fig. 4 leads to certain interesting conclusions. The sulphur content of large particles ($1/\text{Radius} \rightarrow 0$) should approximate the sulphur contained within the particles in contrast with that contained on the surface, which is indicated by the slope of the curves. Because of the porous nature of sponge iron, the sulphur contained within the particles need not be in

solution in the iron but might exist as iron sulphide in the voids. From the curves of Fig. 4, it is evident that addition of lime to the feed reduces the amount of kiln; consequently, sulphur contents, when no desulphurizing agent is employed, are considerably lower in this curve than for curve *A* of Fig. 4.

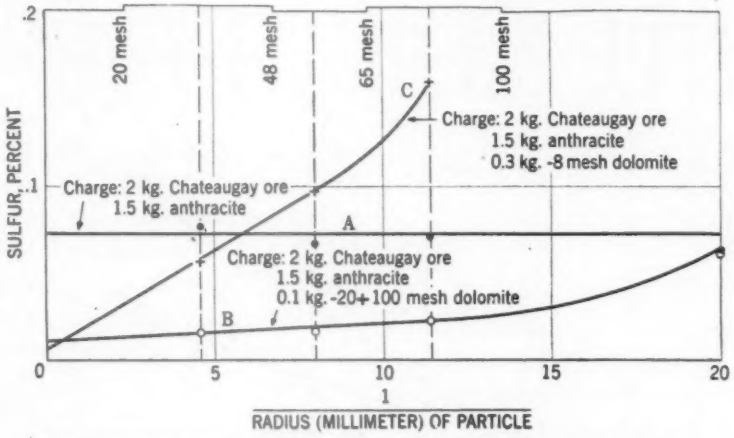

FIG. 5.—VARIATION OF SULPHUR CONTENT WITH PARTICLE SIZE.
Sponge iron made from Chateaugay ore (New York magnetite) reduced in rotating alloy pipe for 80 minutes at 1950°F.

sulphur contained within the particles, but when pulverized lime is present during the reduction it adheres to the surface of the sponge-iron particles; and this lime coating contains a high sulphur content, as indicated by curves *C*. The coating that forms eliminates the use of powdered lime as an effective sulphur-control agent. In lime-coke, curves *B*, most of the lime is prevented from coming into direct contact with the ore and the formation of the surface layer is inhibited.

In Fig. 5, similar data are presented for sponge irons made in an externally heated, horizontally rotating alloy retort 8 in. in diameter and 15 in. long.

Curve A (Fig. 5) refers to sponge iron prepared from a mixture of 2 kg. of Chateaugay ore and 1.5 kg. of No. 4 anthracite (0.7 per cent sulphur) with no desulphurizing agent employed. The sponge iron produced contained 0.07 per cent sulphur before sizing, which appears to be uniformly distributed throughout the particles. Proportionately less coal is consumed when an externally heated retort is used than in an internally heated

Curve B (Fig. 5) is for sponge iron made with a similar charge but with the addition of $-20+100$-mesh dolomite to the extent of one fifteenth the weight of the coal. The addition of the dolomite reduced the sulphur content to 0.019 per cent. It is evident that sized dolomite does not form a surface layer with an appreciable sulphur content on the sponge iron at 1950°F. and is therefore an effective desulphurizing agent.

Curve C (Fig. 5) is for sponge iron also made from the same mixture of ore and coal except that 0.3 kg. of minus 8-mesh dolomite was added as the desulphurizing agent. This dolomite had the normal size distribution that results from grinding, and contained 42 per cent of minus 100-mesh material. The sulphur content of this sponge iron was 0.077 per cent, and is about the same as when no dolomite is employed. It is evident that a surface coating exists, which makes the use of this dolomite ineffective as a desulphurizing agent. From a comparison of the data of curves *B* and *C*, it can be seen that the elimination of the minus 100-mesh fraction

of the dolomite prevents the formation of a surface coating and results in low-sulphur sponge iron. Other tests not herein described have substantiated this choice of the size that should be eliminated to produce low-sulphur sponge iron.

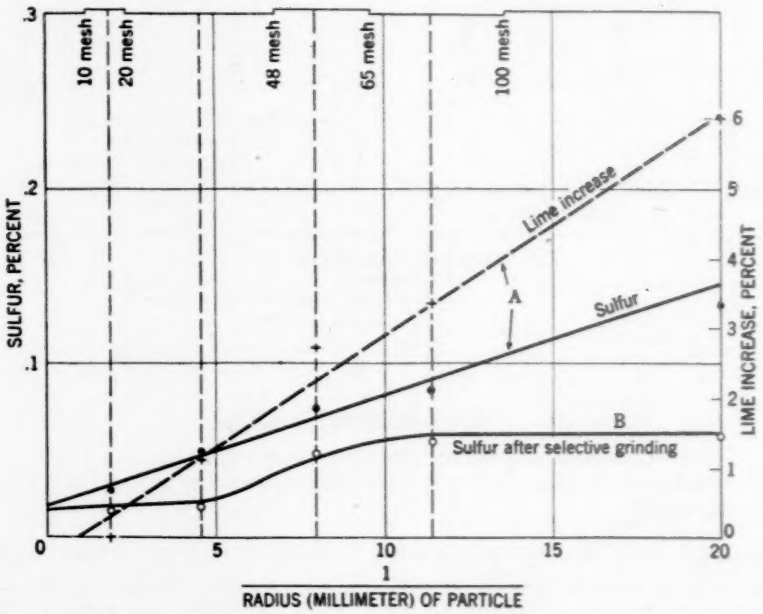

FIG. 6.—VARIATION OF SULPHUR AND LIME CONTENT WITH PARTICLE SIZE.
Sponge iron made from Sunrise ore (Wyoming) reduced with subbituminous coal (Wyoming, 0.4 per cent S) in an internally fired rotary kiln.

SELECTIVE GRINDING

Curves A (Fig. 6) show the variation of sulphur content and lime increase with particle size for sponge iron produced from Sunrise ore (hematite from Wyoming) reduced in an internally fired kiln using a sub-bituminous coal (also from Wyoming) as the reducing agent and ground limestone as the desulphurizing agent. This sponge iron has an average sulphur content of 0.063 per cent as produced and magnetically concentrated.

Curve B (Fig. 6) shows the sulphur distribution in particles of the same sponge iron after partial grinding in a ball mill and then sieving. Because the layer was more brittle than the sponge iron, selective grinding occurred and a large part of the sulphur that existed as a surface coating was removed. By partial grinding and discarding the minus 100-mesh fraction, which constituted 20 per cent of the iron, the sulphur was reduced from 0.063 to 0.033 per cent. From the curve, it appears that only a portion of the coating was removed by the particular grinding procedure and that a more efficient procedure that removed all the layer would reduce the sulphur to about 0.02 per cent.

Factors Affecting the Sulphur Contained within the Particles

When sulphur-control agents such as sized dolomite are employed, which do not form a basic layer on the surface of the sponge-iron particles, the sulphur probably is distributed through the sponge iron as sulphur in solution in the iron or as iron sulphide in the voids at sulphur contents above the solubility limit. Both lime and iron have a strong affinity for sulphur, so the distribution of sulphur between these materials depends on the operating conditions. The sulphur is most likely transferred from the coal to the

sponge iron or desulphurizing agent as H_2S or a carbon sulphur compound such as COS; nevertheless, the reaction giving the end products that determine the distribution of the sulphur between the iron and lime is probably the following:

$$FeS + CaO + CO = Fe + CaS + CO_2$$

Since CaO and CaS are solids at the temperatures employed, probably it is correct to assume that the CaS is a separate phase and not in solution in the CaO. Therefore, the sulphur contained in the sponge iron is not influenced by the amount of lime employed or by the amount of CaS formed; that is, the amount of sulphur introduced with the charge provided that sufficient lime is employed so that all the CaO is not converted to CaS.

The inference that the sulphur content of the sponge iron is not dependent on the amount of lime or dolomite employed is substantiated by the following data on sponge iron produced in the laboratory externally heated rotary pipe furnace mentioned previously, in which the charge consisted of 2 kg. of Chateaugay ore, 1.5 kg. of No. 4 anthracite and varying quantities of dolomite as listed below:

Wt. of Dolomite, Kg.	Sulphur Content of Sponge Iron, Per Cent
0.025	0.10
0.050	0.039
0.10	0.023
0.2	0.033
0.3	0.028

The variation of sulphur content between 0.023 and 0.033 per cent is not considered significant. The coal had a sulphur content of 0.7 per cent, so that theoretically 0.033 kg. of $CaCO_3$ would be required to combine with all the sulphur as CaS. This corresponds to approximately 0.066 kg. of dolomite. Since all the coal is not consumed, a somewhat smaller amount of dolomite should be effective, which is in agreement with the data already given.

The inference that the sulphur content of the sponge iron is not dependent upon the sulphur content of the reducing agent is also verified by experimental data. The sulphur content of sponge iron made in the externally heated rotary retort from ore and limed coke produced from coals of varying sulphur contents are:

Sulphur in Coke, Per Cent	Sulphur in Sponge Iron, Per Cent
1.0	0.046
1.2	0.042
2.2	0.042

In an internally fired kiln, where a surface layer containing sulphur is more likely to be produced, there probably would be some dependence of the sulphur content of the sponge iron on the sulphur content of the reductant.

Since the experimental data indicate that the sulphur content is neither dependent on the amount of lime used nor on the sulphur content of the coal employed, the assumption that the lime and calcium sulphide are present as separate solids rather than as solid solutions appears to be correct, and the activity of these substances can therefore be considered as unity. Also, since the iron is essentially pure, its activity can also be taken as unity without introducing a serious error. For the chemical reaction postulated, the equilibrium constant can then be written

$$K = \frac{1}{\alpha_{FeS}} \times \frac{P_{CO_2}}{P_{CO}}$$

where α denotes activity and P partial pressure. In a solution as dilute as the FeS in the iron, the activity should be proportional to the sulphur content, so the relation first given may be written as

$$\%\,S = \frac{1}{K'} \times \frac{P_{CO_2}}{P_{CO}}$$

In other words, the sulphur content should be proportional to the CO_2:CO ratio.

Analyses of the gases issuing from the bed of charge during reduction in the rotary pipe furnace have shown a CO_2:CO ratio of 0.23 during the early stages of reduction and a ratio of 0.13 after reduction was nearly complete. Consequently, one would expect that the sulphur content of sponge iron produced from low-sulphur ore would increase to a maximum value during the early stages of reduction and be desulphurized as the reduction nears completion and the CO_2:CO ratio decreases. In the rotary kiln process, no consistent dependence of the sulphur content on the degree of reduction could be observed, probably because of the rapid rate of reduction and the occasional presence of a surface coating that contained an appreciable sulphur content. However, in sponge iron produced in clay saggers from columns of ore surrounded by coal-limestone mixtures, a very noticeable dependence of sulphur content on degree of reduction was observed; the sulphur content of the sponge iron was usually around 0.05 per cent for a reduction of 80 per cent and decreased to around 0.02 per cent when the sponge iron was well reduced. This is further illustrated by laboratory tests in which mixtures of Chateaugay magnetite ore and limed coke were charged into crucibles and heated for various lengths of time at 1900°F. as shown below:

Reduction Time, Hr.	Reduction, Per Cent	Sulphur, Per Cent
¾	50.0	0.163
1¼	78.6	0.156
2	91.0	0.117
4	95.4	0.055

In this test, the sponge iron had the unusually high sulphur content of 0.163 per cent in the early stages of reduction but was desulphurized to 0.055 per cent as the reduction progressed. The ore analyzed 0.01 per cent sulphur so that the unusually high sulphur contents were not due to sulphur contained in the ore.

A further indication of the removal of sulphur from sponge iron by the presence of lime in a strongly reducing atmosphere is shown in Table 1. These tests were made by heating in an iron pipe a mixture of high-sulphur sponge iron (0.385 per cent S), −20+60-mesh lime, and wood charcoal in the ratio of 10:1:2.

TABLE 1.—*Desulphurization of Sponge Iron*

Temperature, Deg. F.	Time of Heating, Hr.	Initial S, Per Cent	Final S, Per Cent	Final CaO, Per Cent
1112	1	0.385	0.207	nil
1292	1	0.385	0.068	nil
1472	1	0.385	0.018	nil
1652	1	0.385	0.019	nil
1832	1	0.385	0.019	nil
2012	1	0.385	0.079	1.0

At temperatures of about 1472°F. and above, a high CO:CO_2 ratio exists in equilibrium with charcoal and good desulphurization therefore occurs. Below 1472°F., the CO:CO_2 ratio decreases rapidly with decrease in temperature and, consequently, the desulphurization is less effective. At 2012°F., a basic surface layer must have formed on the sponge iron, as indicated by the high lime content and this accounts for the high sulphur content at this temperature.

Conclusions

1. The existence of a basic layer on the surface of sponge-iron particles produced from a mixture of ore, reducing agent, and lime, limestone, or dolomite in pulverized form has been established. This layer contains all the sulphur in excess of 0.02 to 0.03 per cent.

2. By the use of sized dolomite as the sulphur-control agent, no sulphur-bearing layer is formed and it is therefore possible to produce low-sulphur sponge iron in a rotary kiln using most coals or cokes as the reducing agent. The use of sized dolomite as the sulphur-control agent does not add materially to the cost of the sponge iron.

3. It is also necessary to have strongly reducing conditions—that is, a high ratio of $CO:CO_2$—in order to produce low-sulphur sponge iron. In the rotary kiln process described in this paper, a strongly reducing atmosphere is automatically attained when the operating temperature is sufficiently high for rapid reduction.

References

1. Investigations on the reduction of iron ore in a rotary kiln are too numerous to list; the most successful processes prior to 1927 are summarized in the papers cited in references 2 and 3.
2. C. E. Williams, E. P. Barrett, and B. M. Larsen: Production of Sponge Iron. U. S. Bur. Mines *Bull.* 270 (1927).
3. F. Hodson and O. Smalley: Development in the Low-temperature Reduction of Iron Ore. *Trans.* Amer. Electrochem. Soc. (1927) **51**, 225–245.
4. H. Lehmkühler: Concentration of Low-grade Siliceous Iron Ores by the Krupp Blooming Kiln in the Pilot Plant of the Krupp A.-G. *Stahl und Eisen* (1939) **59** (48), 1281–1288.
5. R. C. Buehl and E. P. Shoub: Production of Low-suphur Sponge Iron. *Min. and Met.* (Dec. 1943) **24**, 550.
6. R. C. Buehl: Production of Low-sulphur Sponge Iron. U. S. Patent 2380406 (1945).

DISCUSSION

(H. W. Graham presiding)

H. W. Graham*—Even though we have a small audience, I am sure there are some here who are interested in sponge iron. It is a large subject, with a lot of economic interest, and one that will continue to grow in importance as the years go by and as the conditions that urge action in that direction increase.

The authors have chosen to deal in this paper with one particular narrow phase of a long program of work by the Bureau of Mines. Before asking for any general discussion, I would myself like to ask Mr. Buehl if he would tell us just a little bit about the mechanism of discharge and the form in which the material was discharged; that is, when dolomite is added, what happens to the dolomite?

R. C. Buehl (author's reply)—You are interested in the equipment that was used?

H. W. Graham—No, just the product.

R. C. Buehl—The product was in granular form, of a shape very similar to that of the ore used. Using minus 10-mesh ore, the product is essentially minus 10-mesh, mixed with the coal and dolomite. It is then passed through a belt type of magnetic separator, which picks up the magnetic iron and allows the dolomite and coal to fall off. If the coal is sufficiently valuable, it can be separated from the dolomite and, provided the coal has a sufficiently low ash content, it can be reused. For instance, if a low-ash reducing agent like petroleum coke is used, it can be reused until all the carbon is consumed.

H. W. Graham—That clears the point for me. I was not quite sure whether the experiment had been carried to any adhesion of the particles. I understand now how that separation is finally effected.

The materials that are applicable to sponge iron are also involved in many sintering processes, where no reduction of iron oxide takes place, but where sulphur is reduced, but here it is shown that the sulphur content can be dealt with in sponge iron.

M. Tigerschiöld*—I feel that the same point applies to Swedish sponge iron. As you might know, the oldest sponge-iron method used is the Höganas, which started in 1911 and has been in industrial production ever since, making about 20,000 tons a year.

Höganas sponge iron is made in fire-clay saggers, and is a fine, high-iron concentrate from the north of Sweden. The ore is packed in layers and between the layers there is a mixture of coke breeze and limestone. The charged saggers are heated for many hours, and, if I remember correctly, the time for heating, reducing, and cooling in that furnace is about 180 hr, and the maximum temperature is approximately 1200°C.

The coke breeze very often contains more than 1 pct sulphur, but in spite of that the sponge iron produced is as low as 0.010 pct in sulphur, or below that.

This very interesting subject is the basic condition for the production of sponge iron according to the Höganas process, and this has been well known in Sweden for many

* Director of Metallurgy and Research, Jones and Laughlin Steel Corp., Pittsburgh, Pennsylvania.

* Director of Research, Jernkontoret, Stockholm, Sweden.

years. In fact, when the process was started at Höganas a high-sulphur, low-grade coal was used instead of coke breeze, and frequently that resulted in too high a content of sulphur in the sponge iron. In such cases, sponge iron cakes were put in saggers together with coke breeze and limestone and reheated, and in that way the sponge-iron cakes were desulphurized to 0.010 pct.

H. W. GRAHAM—Would you tell us something about the purity of the raw materials? I understand you are able to make an exceptionally pure product. I have seen figures for about 0.2 pct of gangue.

M. TIGERSCHIÖLD—The raw material for the Höganas process is the Gellivare concentrates from the north of Sweden. The crude ore runs about 65 to 68 pct of iron, and it is high in phosphorus, about 1 pct. This ore is milled and concentrated and the concentrate comes out with 71.5 pct of iron in the form of magnetite, about 0.008 pct phosphorus and scarcely any sulphur at all. The raw material, consequently, is very pure.

H. W. GRAHAM—At that purity of iron oxide, what would be the analysis of inert materials? What would be the total of silica?

M. TIGERSCHIÖLD—It is difficult to remember the exact figures. The whole content of gangue in this ore is less than 0.9 pct.

In the sponge iron, the content of silica is about 0.4 pct. After a magnetic concentration it can be brought down below 0.2 pct.

We have tried other ores with quite interesting results. We have reduced pyrite cinders with this method, and achieved a sulphur reduction from 0.124 down to 0.03 pct.

H. W. GRAHAM—What was the sulphur in the original concentrate?

R. C. BUEHL—Chateaugay and Scrub Oaks ores, which are very low in sulphur, were used in some tests. We have tried other ores that were considerably higher in sulphur. Ore from the Shasta mine in California for which the sulphur is 0.1 pct after magnetic concentration was used on an experimental scale, and sponge iron was obtained with 0.03 to 0.05 pct sulphur compared with 0.02 to 0.03 pct if low-sulphur ores are used.

I believe that high-sulphur ore usually contains some lime intimately mixed with it and that some of this lime would be present in the sponge iron combined with enough sulphur to interfere with the method described.

I would like to make a few comments in regard to the comparison between the rotary kiln method and the sagger method that was mentioned by Dr. Tigerschiöld. Using the rotary kiln method, with a small experimental unit, one can obtain reduction in as short a time as 15 min. For a large unit, the rate of heat input probably is the limiting factor and reduction may require 80 min. in comparison with 180 hr for the sagger method, which I believe was mentioned by Dr. Tigerschiöld.

M. TIGERSCHIÖLD—Yes, including the heating and cooling period.

R. C. BUEHL—The sulphur problem in the sagger method is certainly different than for the rotary kiln method. In the sagger method there is no movement of the charge or tendency for the lime to come into contact with the ore and form a basic surface layer on the ore particles. Therefore, the problem of the formation of surface layers that was discussed at this meeting does not exist for the sagger method. For this reason, I think people were successful in obtaining low sulphur contents with the sagger method without any control of the particle size of the desulphurizing agent or special methods to keep the lime and ore separated other than merely placing the ore and coke-lime mixture in alternate layers.

The purity of the product that can be produced in this country is pretty close to that made in Sweden by the Höganas method; that is, about 94 pct total iron, gangue elements (silica plus alumina, etc.) below 2 pct, and phosphorus in the order of 0.009 pct. We found that this analysis was very good for electric-furnace operations and that the small amount of gangue did not interfere in the steelmaking process.

It might be of interest to add that some recent publications indicate that they use a much lower grade of ore in Sweden with the Wiberg process than with the Höganas process. I have seen figures showing that the silica, alumina, and other gangue elements exceeded

10 pct, and the reduction was only about 80 pct. Consequently, with the Wiberg process, the sponge iron is probably cheaper but of much lower grade, and the use of this lower grade material would require extra expense in the operation of the electric furnace when steel is produced from the sponge iron.

E. C. SMITH*—In experiments at Republic Steel we found that reduced iron was a powerful desulphurizing material for gases.

R. C. BUEHL—From our experiments, I would say that at high temperatures, and with reducing conditions, lime should be a better desulphurizing agent than reduced iron provided the lime did not sinter, crumble, blow out, or have some other physical disadvantage—that is, if it is not a matter of physical properties, lime should work better than reduced iron.

M. TIGERSCHIÖLD—At Söderfors, where the Wiberg method has been operated during the past five or six years with an ore containing 64 pct of iron as a raw material, a product is made with only 85 pct reduction, containing about 77 pct total iron, and 65 pct metallic iron. There are no ores available that could be concentrated much higher, and it has been found that it is very easy and the cost astonishingly low for melting this poor sponge iron in an electric furnace. It contains approximately 1 pct of carbon, mostly carbon that has been precipitated out of carbon monoxide. It is similar to a fine carbon black. When melting the sponge iron in the electric furnace some extra carbon and some lime are added.

In spite of the fact that the sponge iron contains about 19 pct of gangue, very good results are obtained by melting it in electric furnaces and tapping off the slag during the melting period. At Söderfors, all the quality steel is made with sponge iron as the entire raw material, and the steel is very good.

R. C. BUEHL—This material certainly could be used for powder metallurgical applications. There is a question of whether or not sulphur is particularly harmful. I don't know that it would be in powder-metallurgy application, where we press cold and then sinter the material without any plastic deformation. I rather doubt that sulphur would have too much of a serious influence. As I understand the problem, the main disadvantage of sulphur is the tendency toward hot-shortness.

H. W. GRAHAM—That is correct, and it is an interesting point. On the same basis, it might be true that the manganese that is now needed in rolling would not be necessary.

J. Q. ADAMS*—The great difficulty is impact. Would the sulphur seriously add to that problem?

R. C. BUEHL—It may. From some work we have done, which has not been published, we have found that sulphur has a very low solubility in solid iron, and I rather expect that sulphur would therefore tend to go to the grain boundaries and lower the impact resistance.

On the other hand, as I know powder metallurgy parts, even if a very pure powder is used, such as electrolytic iron, with low sulphur, there is still not a high impact resistance, so that sulphur is not the only thing that influences the impact resistance.

J. Q. ADAMS—Has anything been brought out to indicate that this would offer an economic way of producing a very high-phosphorus steel; say, 0.10 to 0.20 pct phosphorus?

R. C. BUEHL—I would rather expect it might, because if the ores were not high enough in phosphorus, to begin with, some phosphate could be added along with the ore to reduce the phosphate at the same time the ore is being reduced, and quite likely the phosphorus would alloy with the iron; certainly in the melting operation the phosphorus should alloy. There might be a tendency for loss of phosphorus if, during part of the reduction cycle, one of the lower oxides of phosphorus is formed that has a high vapor pressure. I do not know whether any such oxides has a high vapor pressure.

T. L. JOHNSTON†—The statement with data that sized dolomite is superior to lime is

* Chief Metallurgist, Republic Steel Corp., Cleveland, Ohio.

* General Electric Co. Schenectady, N. Y.
† Metallurgist, Bur. of Mines, Laramie, Wyo.

interesting and should be tried on a larger scale.

Screening out of minus 100-mesh dolomite is quite a chore in itself on a large scale. The method of disposing of minus 100-mesh adds another problem.

The statement that high temperature is necessary for high reduction brings in a point that probably is more important than sulphur control in producing sponge iron in a rotary kiln. High temperature is taken as meaning a temperature close to the fusing point of the charge, or about 1000°C. When this temperature is used and there is sufficient CaO present in the charge, there will be a tendency for the CaO to react with FeO and SiO_2 to form a low-melting slag. This slagging or softening of the charge probably would not take place in the absence of lime. When it does take place the result is a stickiness of the charge with subsequent rings of accretions forming on the kiln lining. These rings, unless periodically bored out, amount to one of the main obstacles of successful continuous production of sponge iron in a rotary kiln. Any factor contributing to the formation of rings should be analyzed in that respect. It is claimed that speed dolomite retains its physical strength, but at the temperature used it loses its CO_2, leaving CaO and MgO to react with other elements in the charge, and thus contributes to softening, slagging and ringing.

The experimental work used as a basis for this report is considered by the authors to be on sufficiently large scale to be applicable commercially. This may be true, but large-scale applications of small-scale test results in sponge iron have generally resulted in failure. Small-scale work can be misleading, mostly because of the short duration of the tests. Also, the handling of tons instead of grams of materials magnifies the problems to be solved. It often happens that a small-scale test is terminated before conditions within the kiln are stabilized, making results inconclusive. Rings of accretions form slowly and do not start until the kiln has operated for 24 hr or more, therefore they may not appear in small-scale tests. Once started they are difficult to stop. If allowed to continue, the point will be reached where the whole operation will be forced to stop. If steps are taken for arresting the growth of rings, such as changes in charge composition or temperature changes, stabilized conditions must be reestablished, resulting in irregular operation and production. In other words, the benefit attributed to sized dolomite as a desulphurizing agent may be offset or even surpassed by the detrimental influence of dolomite in contributing to ring formation. This probability should be determined experimentally on a large enough scale and of long enough duration to be conclusive.

R. C. Buehl—Mr. Johnston mentioned the work involved in screening the dolomite and disposing of the minus 100-mesh fraction. In most of the tests, commercial 6/20 size dolomite was used as purchased. This material, which contained about 2 pct of minus 100-mesh particles, was only slightly more expensive than minus 6-mesh unsized dolomite. Usually a dolomite addition to the charge of 5 pct of the ore weight is sufficient, and at Johnstown, Pa., where the tests were conducted, the cost of this proportion of dolomite was less than $0.30 per ton of sponge iron.

Mr. Johnston discussed the very important problem of the formation of accretions on the walls of a rotary kiln and the possible adverse effect of dolomite additions on the formation of such accretions. In our investigations on the use of sized dolomite as a sulphur control agent, only highly concentrated magnetite ores low in silica were reduced. The product showed no evidence of the formation of slag at operating temperatures as high as 1980°F. After magnetic concentration on a belt-type magnetic separator of the cooled discharge from the kiln, the nonmagnetic fraction contained white particles of dolomite of approximately the size range charged while the magnetic portion was nearly free of dolomite. The use of sized dolomite as a sulphur control agent did not appear to have any adverse effect on the formation of accretions. However, it is possible that it might increase the tendency to form accretions when siliceous ores are used, particularly if operating temperatures were high enough to form slag, as mentioned by Mr. Johnston.

Because of a shortage of research funds, tests generally were not continued for more than four or five days, with a production of

about one ton per day in the small kiln. In some tests, no appreciable amount of accretions had formed in such a time, so the next test was started without cleaning the furnace. However, in similar tests, with other reducing agents, accretions of appreciable size formed during several days of operation. The type of reducing agent therefore appears to have an important effect on the formation of accretions.

The authors agree with Mr. Johnston that the method should be tried for longer periods of time and on a larger scale, and hope the opportunity will present itself.

An Electrochemical Study of the Properties of Molten Slags of the Systems CaO-SiO_2 and CaO-Al_2O_3-SiO_2

By Lo Ching Chang,* Junior Member, and Gerhard Derge,† Member AIME

(Atlantic City Meeting, November 1946)

The chemical and physical properties of slag systems are of special interest to metallurgists, for nearly all metals are in contact with molten slags during the primary reduction from their ores and then during the subsequent refining and alloying processes that determine their ultimate use. These processes are carried out at high temperatures and involve such complex chemical systems that fundamental scientific knowledge of the properties and behavior of these slags is inadequate.

Various hypotheses have been proposed to explain known slag characteristics. The commonest of these regard the molten slag as constituted of compounds that are dissociated in varying degrees into their constituent oxides, as illustrated by Schenck[1] and the recent papers of Chipman and co-authors.[2–5] Another proposal is that these compounds dissociate by complete[6] or partial ionization, the evidence for which has been reviewed by Martin and Derge.[7]

Whatever hypothesis is favored, the exact formulation of these compounds is incomplete. It is based on three principal types of information:

1. Studies of solidified slag samples by X ray diffraction, petrography, and similar methods that can be used at room temperature. The correlation of this information with the high-temperature properties of the molten slag is uncertain.

2. Studies of slag-metal equilibria, which have the advantage of providing observations on the molten slag at high temperature. However, even these data present problems of interpretation because they require a complete knowledge of the metal phase.

3. Direct measurements of properties of molten slag at the temperature of greatest metallurgical interest. Viscosity, electrical conductivity, specific heats, and similar properties have been measured, but the data of this type are widely scattered and frequently difficult to interpret. Additional direct measurements of properties of molten slag that can be interpreted in terms of chemical behavior are required, and this paper shows that the standard physical-chemical measurement of reversible electrode potentials, which measure the activity of specific constituents, is a fruitful source of such information.

The purpose of this investigation, therefore, was to find an electrode combination that would yield reversible electromotive force measurements when dipped into the molten slag to be studied. Slags of the systems CaO-SiO_2 and CaO-Al_2O_3-SiO_2 were chosen for study because graphite containers could be used and the data could be correlated with those for viscosity, conductivity, and other proper-

Submitted by L. C. Chang in partial fulfillment of the requirements for D.Sc. in Metallurgy at Carnegie Institute of Technology. Manuscript received at the office of the Institute June 14, 1946. Issued as T.P. 2101 in Metals Technology, October 1946.

* National Resources Commission of China, New York, N. Y.

† Metals Research Laboratory, Carnegie Institute of Technology, Pittsburgh, Pennsylvania.

[1] References are at the end of the paper.

A. Copper lead wires for cell electrodes to a type *K* potentiometer.
B. Copper lead wires for tungsten-molybdenum thermocouple.
C. Copper rods for cell electrode connection.
D. Glass window for observation of centering of electrode and temperature.
E. Gas outlet, atmospheric control unit.
F. Brass top provided with water cooling.
G. Rubber stopper.
H. Zinc silicate cement sealing.
I. Copper coil for water cooling.
J. Copper block, cold junction for electrodes.
K. Thermometer, to register cold-junction temperature of cell electrodes.
L. Flexible copper wire allowing free movement of the cell body.
M. Fused silica protection tube for tungsten-molybdenum thermocouple.
N. Silicon carbide electrode.
O. Graphite rod.
P. Graphite cell body, also serving as the graphite electrode.
Q. Silica tube.
R. Primary induction coil.
S. Alundum sheath.
T. Graphite packing.
U. Transite rods.
V. Transite board.
W. Fused silica tube supporting cell body.
X. Mercury seal.
Y. Gas inlet, from atmospheric control unit.
Z. Adjustable platform to lower or raise the cell body.

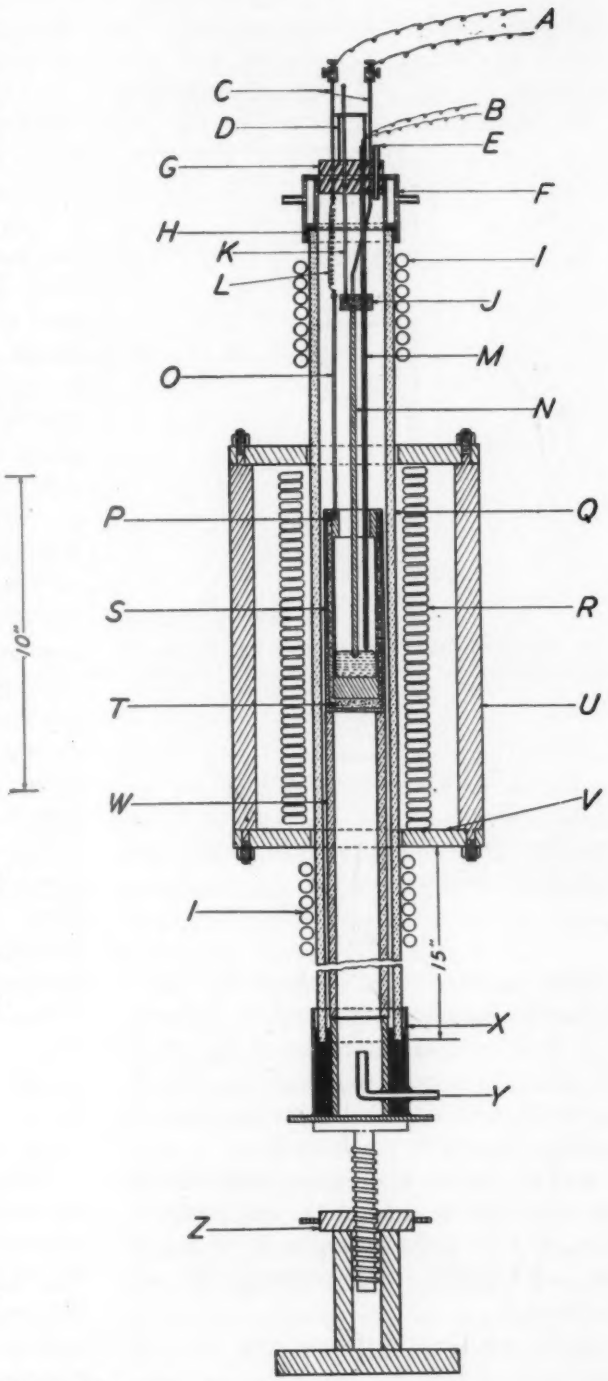

FIG. 1.—APPARATUS.

ties that already have been reported. The effects of chemical composition and temperature on the cell electromotive force were determined to establish the cell reaction and consequently to secure constitutional information.

FIG. 2.—GRAPHITE CELL.

APPARATUS

The apparatus used is shown in Fig. 1. It has the following characteristic features:

1. Free vertical movement of the graphite cell with respect to the silicon carbide electrode, provided by the mercury seal *X* and the adjustable platform *Z*.

2. The use of a tungsten-molybdenum thermocouple to register the cell temperature, and of a thermometer *K* to record the cold-junction temperature of the electrodes.

3. An enclosed system suited for any atmospheric control.

4. The graphite crucible containing the slag also serves as one electrode for the cell.

In high-temperature electromotive-force measurements, it is very difficult to keep both ends of the electrodes at the same temperature level. A thermal electromotive force is always involved. The total electromotive force will then be the algebraic sum of the thermal electromotive force and the electromotive force of the cell reaction.

The graphite cell is 6 in. long and 1½ in. in outside diameter (Fig. 2). With this design the temperature gradient near the bottom part of the cell is small, about 2° to 3° per inch, when the cell is empty. During actual experiments the tungsten-molybdenum thermocouple, which was protected by a fused silica tube closed at the lower end, was held so that the bead of the thermocouple was about ⅛ in. above the slag surface, as it was found unsatisfactory to immerse the thermocouple in the molten slag for long periods of time. A few experiments were made to determine the temperature gradient in the cell under actual experimental conditions. The slag surface was about 9/16 in. above the cell bottom in all experiments. A temperature difference of 9° to 10° was found between a point ⅛ in. above the slag surface and the cell bottom. Thus the average cell temperature was roughly 4° to 5° higher than that indicated by the thermocouple. A temperature correction, however, was not made, as it was not felt that the calibration was good enough to justify this. The thermocouple reading was taken directly as the average temperature of the cell body.

Different electrode pairs were tried in a preliminary investigation. Tungsten-molybdenum, tungsten-graphite and molybdenum-graphite electrode pairs did not yield satisfactory results because the cell readings were small and unsteady. The electromotive force was fairly large for the cell using a platinum-graphite electrode pair, but the platinum electrode soon formed a bead at cell temperatures far below the melting point of platinum. A few experiments were made using a zirconium-graphite electrode pair. The zir-

conium electrode used was a rolled rectangular rod ⅛ in. square. The results with this couple were satisfactory, as shown by a typical example in Fig. 3. difficult to secure a good stable joint at the hot junction. The tungsten-molybdenum thermocouple was found satisfactory. Tungsten and molybdenum wires

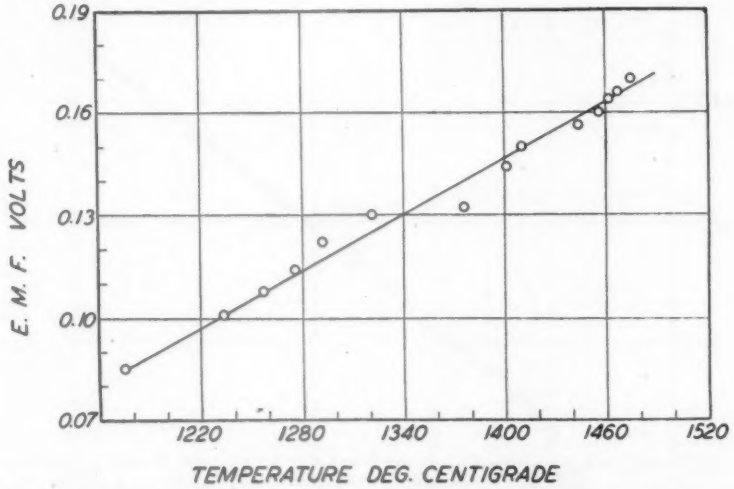

FIG. 3.—TOTAL ELECTROMOTIVE FORCE VS. TEMPERATURE FOR SLAG CONTAINING 15 PER CENT Al_2O_3, 23 PER CENT CaO AND 62 PER CENT SiO_2 BY WEIGHT, USING ZIRCONIUM-GRAPHITE ELECTRODES.

Among all the electrodes tested, the silicon carbide-graphite pair was found to be the most satisfactory. The silicon carbide electrode, 11 in. long and 5/16 in. in diameter, was specially prepared by the Carborundum Company, Niagara Falls, N. Y. It can be reground and reused five or six times. No difference was observed when using new or reground electrodes. As a result of this preliminary investigation the silicon carbide-graphite electrode pair was chosen for study.

TEMPERATURE MEASUREMENT AND CORRECTION FOR THERMAL ELECTROMOTIVE FORCE

Although an optical pyrometer may be used to measure the temperature of hot bodies of known emissivity, it was found unsatisfactory for this research because the slag compositions investigated covered a wide range of compositions of unknown emissivity. The Fitterer[8] thermocouple was also tried and found unsuited for long-time experiments, for it was rather

of 0.025-in. diameter were used to make the thermocouple. With proper annealing the electromotive force of the thermocouple was stable. The couple was frequently calibrated against a standard platinum-platinum rhodium thermocouple. A typical calibration curve is shown in Fig. 4.

As the graphite and silicon carbide electrodes themselves constituted a Fitterer thermocouple and the two ends of the electrodes were not kept at the same temperature level, it was necessary to correct the readings of the cell electromotive force for the thermal electromotive force. A correction curve for the thermal electromotive force was obtained by putting the silicon carbide electrode in direct contact with the bottom of the graphite cell, inserting a platinum-platinum rhodium couple to measure the temperature at the plane of contact, and taking simultaneous readings of the two couples at different temperature levels. A correction curve is shown in Fig. 5. A correction of the total cell electromotive

force is made by measuring the temperature at both ends of the electrodes by means of the tungsten-molybdenum thermocouple and the thermometer and obtaining the thermal electromotive force from the correction curve shown in Fig. 5. The actual cell electromotive force is then the difference between the total cell electromotive force and the thermal electromotive force.

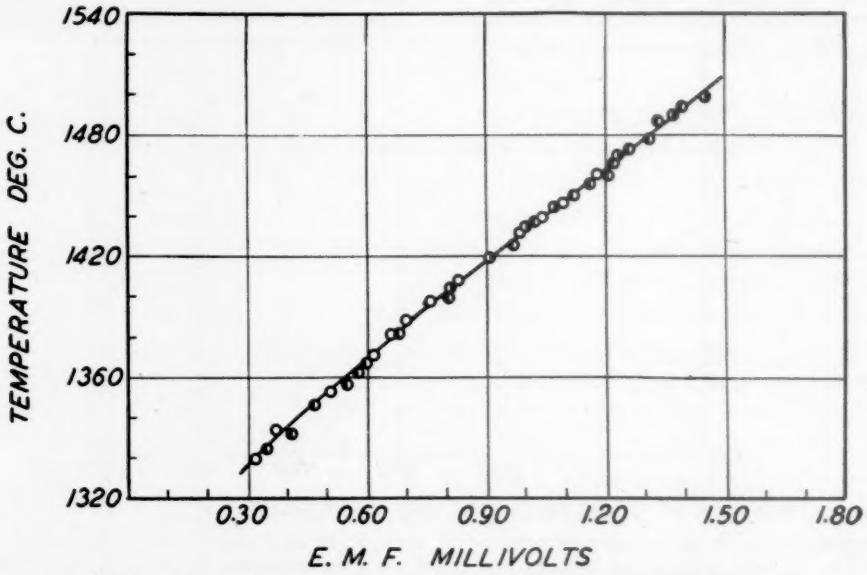

FIG. 4.—CALIBRATION OF TUNGSTEN-MOLYBDENUM THERMOCOUPLE
Showing three calibrations of one thermocouple.

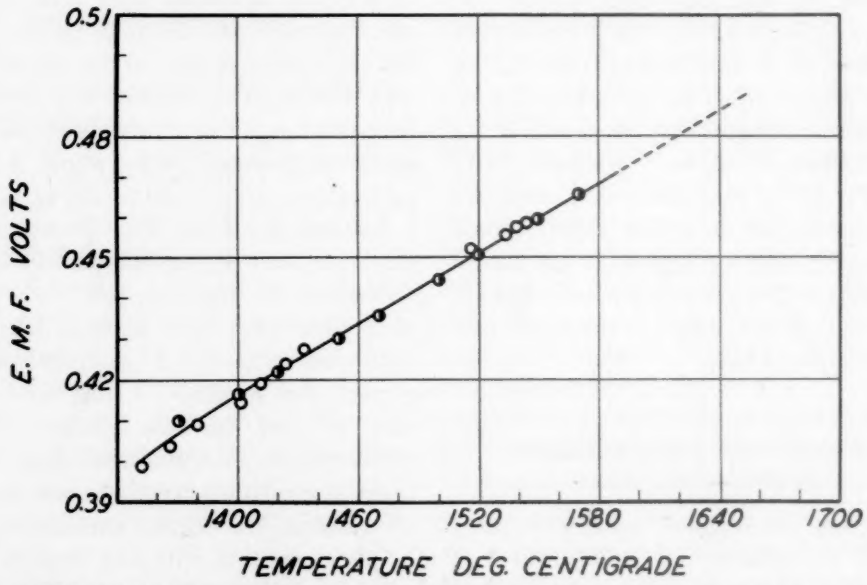

FIG. 5.—CORRECTION CURVE FOR THERMAL ELECTROMOTIVE FORCE OF SILICON CARBIDE-GRAPHITE ELECTRODES.
As converted from Pt-PtRh thermocouple readings.

EXPERIMENTAL PROCEDURE

Synthetic slags were made from chemically pure calcium carbonate, silica and aluminum oxide in amount to give a

depth of about 9/16 in. of molten slag in the cell. The chemicals used all passed a 40-mesh screen. The powdered mixture was weighed out and tumbled in a ball mill for 60 to 72 hr. The mixture was then calcined, transferred to the graphite cell, melted at 1650°C. in the apparatus shown in Fig. 1 under a pure nitrogen atmosphere, held at temperature for 5 min., then cooled down. The pure nitrogen atmosphere was prepared by passing dry tank nitrogen through a calcium chloride drying tube and then a heated copper wire gauze, which frequently was reduced with hydrogen. Necessary electrical connections were made and the cell was again heated up for measurements of the electromotive force. It was found that a change of the depth of immersion of the silicon carbide electrode did not affect the electromotive-force reading, but this depth was kept constant nevertheless at about 3/8 in. in all experiments. A typical curve for time vs. electromotive force at a constant temperature is shown in Fig. 6. When the electromotive-force reading became steady, readings of cell electromotive force, cell temperature (tungsten-molybdenum thermocouple) and cold-junction temperature (thermometer) were taken simultaneously. The cell temperature was lowered slowly and simultaneous readings of cell electromotive force, cell temperature and cold-junction temperature were taken at 5° to 10° intervals.

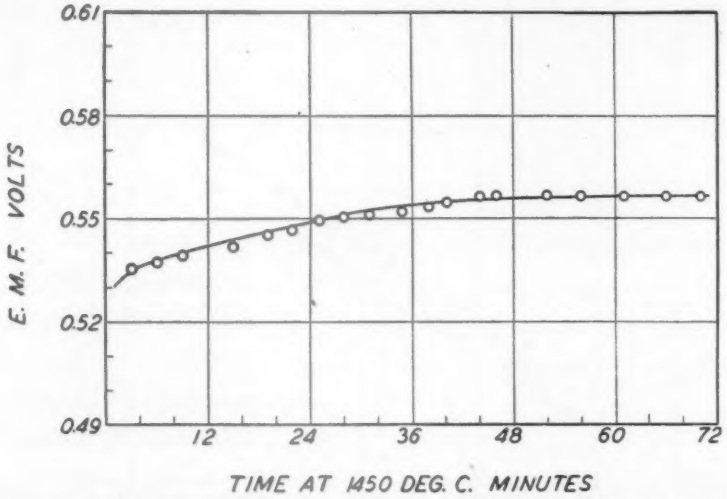

FIG. 6.—TOTAL ELECTROMOTIVE FORCE VS. TIME FOR SLAG CONTAINING 15 PER CENT Al_2O_3, 30 PER CENT CaO AND 55 PER CENT SiO_2 BY WEIGHT.

The composition of the slag was controlled by weighing out the exact amount of each constituent. To ascertain whether this control was satisfactory, a few slags were analyzed after the electromotive-force measurement. The results shown in Table 1 indicate that the control of chemical composition of the slag is satisfactory. The error introduced here is probably within the experimental error of the electromotive-force measurements.

ACCURACY OF THE ELECTROMOTIVE-FORCE MEASUREMENT

In order to test the accuracy of this experimental procedure, four independent sets of measurements were made on slags of the same composition; i.e., the components were weighed separately, mixed separately, fused separately and measured separately. The results (Fig. 7) show that for a given temperature the results are reproducible within about 2 per cent.

To test this point further, two independent sets of measurements were made at 18 different slag compositions and the difference in electromotive force at any given temperature, as measured by half the distance between the two straight-line

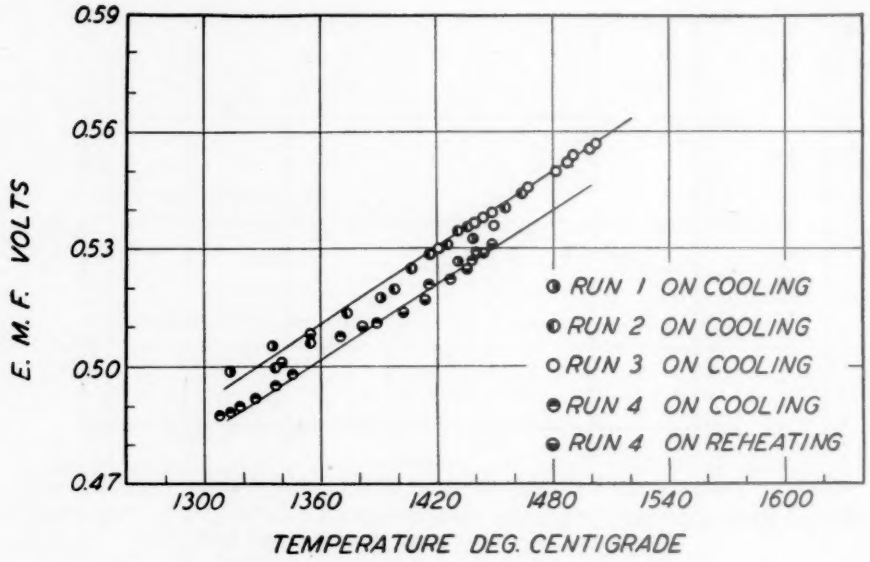

FIG. 7.

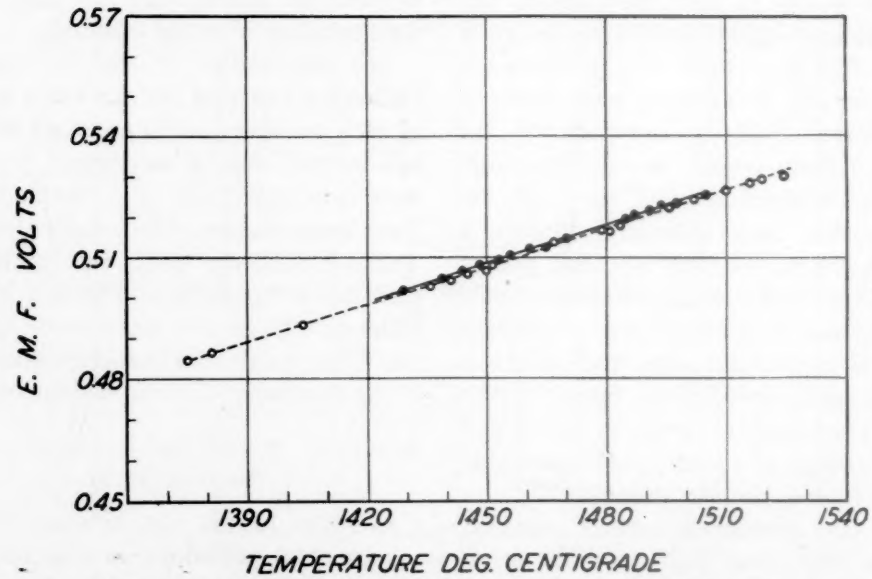

FIG. 8.

FIGS. 7 AND 8.—TOTAL ELECTROMOTIVE FORCE VS. TEMPERATURE.

Fig. 7. Four independent runs of slag composition: 15 per cent Al_2O_3, 40 per cent CaO and 45 per cent SiO_2 by weight.

Fig. 8. Two independent runs of slag composition: 20 per cent Al_2O_3, 25 per cent CaO and 55 per cent SiO_2 by weight. Open circles, run 1; closed circles, run 2.

data were analyzed statistically as follows: The pair of measurements for a single typical slag is shown in Fig. 8. Half the plots measured along the ordinate, is here called the "deviation from the mean" of the two independent runs. The analysis

TABLE 1.—*Comparison of Calculated and Analyzed Slag Composition*

Slag Designation	Calculated Slag Composition, Weight Per Cent			Analyzed Slag Composition, Weight Per Cent					
	CaO	SiO_2	Al_2O_3	CaO	SiO_2	Al_2O_3	Fe	MgO	S
2035A	35.0	45.0	20.0	36.20	44.36	19.40	0.03	0.10	0.022
2035B	35.0	45.0	20.0	36.30	44.34	19.40	0.03	0.10	0.016
2040A	40.0	40.0	20.0	41.34	39.20	18.85	0.02	0.10	0.018
2040B	40.0	40.0	20.0	41.24	39.44	18.80	0.03	0.10	0.016
2045A	45.0	35.0	20.0	45.73	34.64	19.20	0.03	0.08	0.024
2045B	45.0	35.0	20.0	45.93	34.44	19.40	0.03	0.08	0.020

is given in Table 2. The data from Table 2 are plotted in Fig. 9. They show a standard deviation of 4.6 millivolts.

TABLE 2.—*Statistical Analysis*

Slag Designation	Deviation from the Mean, Mv.	Slag Designation	Deviation from the Mean, Mv.
0050	2.0	1540	5.0
0045	6.0	1535	3.3
0040	4.0	1530	3.0
0540	10.0	1525	1.0
0535	5.0	2045	11.0
1035	3.0	2040	1.5
1030	1.6	2035	1.0
1025	0.3	2030	3.0
1545	3.0	2025	0.5

Standard deviation, 4.6 millivolts

In one typical experiment the total electromotive force was 500 mv., of which 400 mv. was provided by the thermal electromotive force of the electrodes. The actual cell electromotive force, after correction for the thermal electromotive force, was 100 mv. The standard deviation of the electromotive-force measurements was 4.6 mv., or 4.6 per cent of the total. Errors introduced in the experiment may be analyzed as follows:

1. Errors introduced in obtaining the thermal electromotive force, which in turn are determined by the errors introduced in measuring the hot-junction and cold-junction temperature of the electrodes.

2. Errors introduced in measuring the cell temperature.

3. Miscellaneous errors caused by electrode condition, pressure variation, presence of impurities in the slag, and other factors.

Range of Compositions Studied

About 150 runs were made, covering 60 slag compositions. The chemical compositions of some of these slags are given in Table 3.

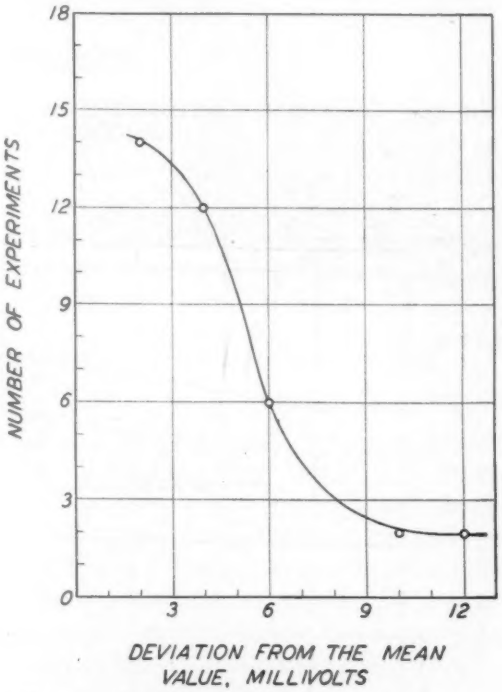

FIG. 9.—STATISTICAL DISTRIBUTION CURVE.

DATA AND RESULTS, SYSTEM CaO-SiO_2

The results for slags of the CaO-SiO_2 system are plotted in Fig. 10 as total cell electromotive force and Fig. 11 as actual cell electromotive force, as corrected for

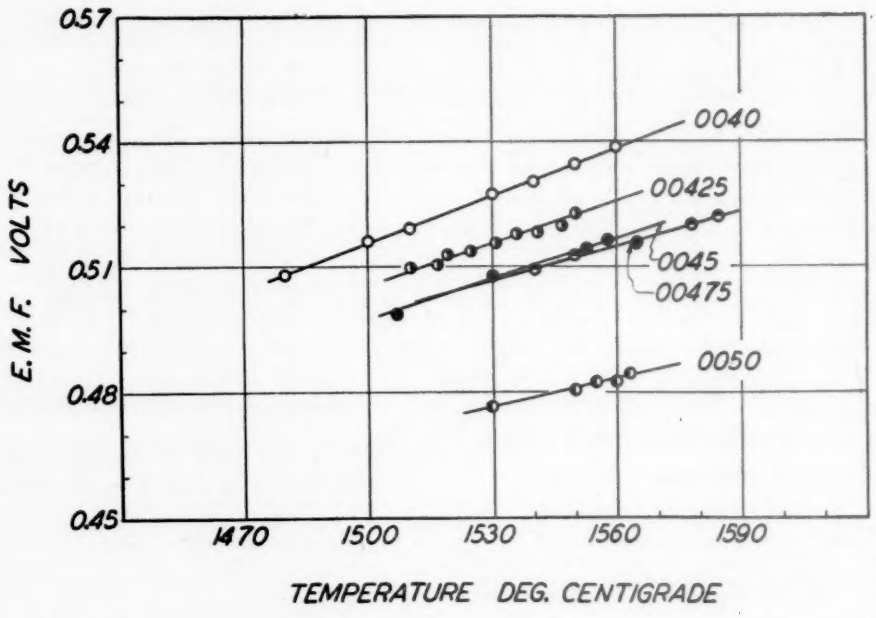

FIG. 10.—TOTAL CELL ELECTROMOTIVE FORCE VS. TEMPERATURE FOR SLAGS OF SYSTEM $CaO\text{-}SiO_2$. See Table 3 for slag compositions.

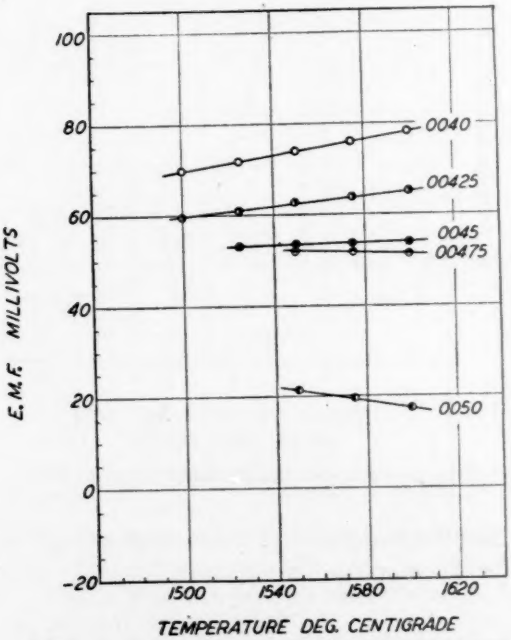

FIG. 11.—ACTUAL CELL ELECTROMOTIVE FORCE (CORRECTED FOR THERMAL ELECTROMOTIVE FORCE) VS. TEMPERATURE FOR SLAGS OF SYSTEM $CaO\text{-}SiO_2$.

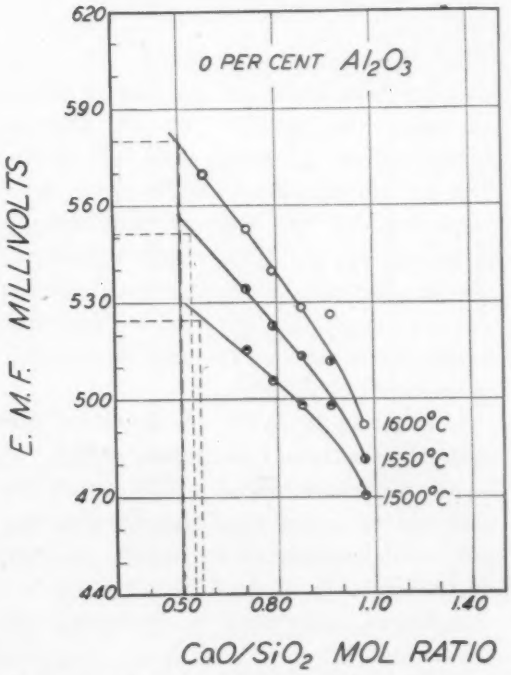

FIG. 12.—TOTAL ELECTROMOTIVE FORCE VS. COMPOSITION FOR SLAGS OF SYSTEM $CaO\text{-}SiO_2$.

TABLE 3.—*Chemical Compositions of Slags*

Slag Designation	Weight Per Cent			Mol Per Cent		
	CaO	SiO_2	Al_2O_3	CaO	SiO_2	Al_2O_3
System CaO-SiO_2						
0050	50.0	50.0		51.7	48.3	
00475	47.5	52.5		49.2	50.8	
0045	45.0	55.0		46.7	53.3	
00425	42.5	57.5		44.2	55.8	
0040	40.0	60.0		41.7	58.3	
0035	35.0	65.0		36.6	63.4	
System CaO-Al_2O_3-SiO_2						
05475	47.5	47.5	5.0	50.2	46.9	2.90
0545	45.0	50.0	5.0	47.7	49.4	2.91
0540	40.0	55.0	5.0	42.5	54.6	2.92
05375	37.5	57.5	5.0	39.9	57.2	2.92
0535	35.0	60.0	5.0	37.3	59.7	2.93
0530	30.0	65.0	5.0	32.1	65.0	2.94
1050	50.0	40.0	10.0	53.9	40.2	5.92
1045	45.0	45.0	10.0	48.6	45.5	5.94
10425	42.5	47.5	10.0	46.0	48.1	5.95
1040	40.0	50.0	10.0	43.4	50.6	5.96
1035	35.0	55.0	10.0	38.1	55.9	5.98
1030	30.0	60.0	10.0	32.8	61.2	6.00
1025	25.0	65.0	10.0	27.4	66.6	6.02
1550	50.0	35.0	15.0	55.0	35.9	9.06
15475	47.5	37.5	15.0	52.3	38.6	9.07
1545	45.0	40.0	15.0	49.7	41.2	9.09
1540	40.0	45.0	15.0	44.3	46.6	9.12
1535	35.0	50.0	15.0	38.9	51.9	9.15
1530	30.0	55.0	15.0	33.5	57.3	9.19
1525	25.0	60.0	15.0	28.0	62.8	9.23
2045	45.0	35.0	20.0	50.7	36.9	12.4
2040	40.0	40.0	20.0	45.3	42.3	12.4
2035	35.0	45.0	20.0	39.8	47.7	12.5
2030	30.0	50.0	20.0	34.2	53.2	12.5
2025	25.0	55.0	20.0	28.6	58.8	12.6
2020	20.0	60.0	20.0	23.0	64.4	12.6
2540	40.0	35.0	25.0	46.3	37.8	15.9
2535	35.0	40.0	25.0	40.7	43.4	15.9
2530	30.0	45.0	25.0	35.0	49.0	16.0

thermal electromotive force. From Figs. 10 and 11, the following things are noted:

1. For any particular slag the electromotive force-temperature relationship within a temperature range of 100° can be represented by a straight line.

2. At a given temperature, the higher the silica content of the slag, the larger is the electromotive force, the greatest change occurring near 50 per cent SiO_2.

3. The slopes of these straight-line plots increase with increasing silica content of the slag. The slopes calculated from Fig. 11 are given in Table 4. This change in dE/dT probably indicates some progressive change of the thermodynamic properties, such as association or dissociation, of the slag as its composition is changed.

TABLE 4.—*dE/dT of Slags of the System* CaO-SiO_2

Slag Designation	Chemical Composition, Per Cent by Weight		dE/dT, Volts per Degree Centigrade
	CaO	SiO_2	
0050	50.0	50.0	-0.68×10^{-4}
00475	47.5	52.5	-0.12×10^{-4}
0045	45.0	55.0	$+0.12 \times 10^{-4}$
00425	42.5	57.5	$+0.55 \times 10^{-4}$
0040	40.0	60.0	$+0.85 \times 10^{-4}$

Table 5 is constructed from Fig. 10, giving the total cell electromotive force of the slags at various temperature levels.

The total electromotive forces given in Table 5 are plotted against the CaO/SiO_2 mol ratio in Fig. 12, from which the following observations can be made:

1. All points, except those of the slag 00475, fall on a smooth curve.

TABLE 5.—*Total Cell Electromotive Force at Different Temperatures of Slags of System* CaO-SiO_2

Slag Designation	CaO/SiO_2 Mol Ratio	Total Cell Electromotive Force, Mv.				
		1600°C.	1575°C.	1550°C.	1525°C.	1500°C.
0050	1.07	492.0	486.8	481.1		
00475	0.97	526.0	519.0	512.0		
0045	0.88	528.6	521.0	513.4	505.9	
00425	0.79	539.8	531.1	522.7	513.9	505.4
0040	0.71	552.9	543.4	534.0	524.8	515.4
0035	0.58	569.2				

2. The electromotive force at a given temperature increases with increasing SiO_2 content, or with decreasing CaO content of the slag.

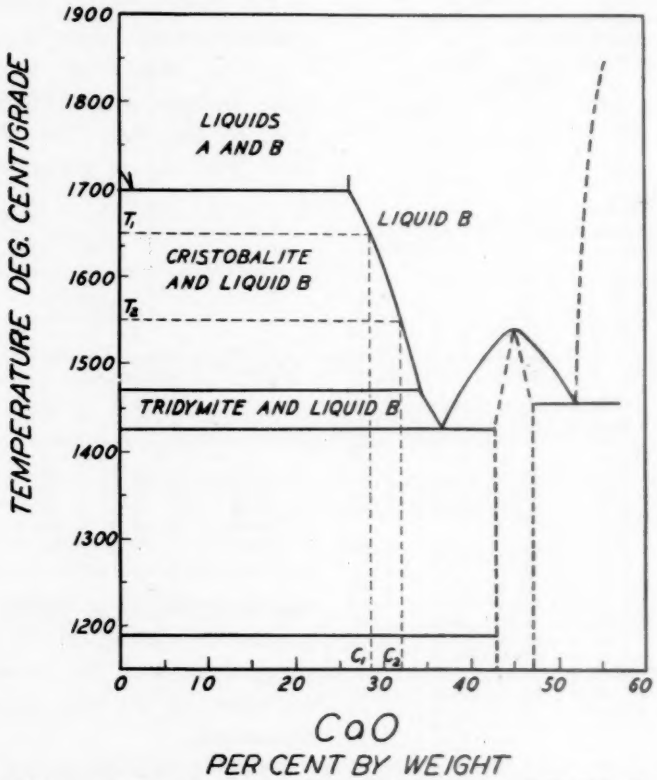

FIG. 13.—CONSTITUTION DIAGRAM FOR SYSTEM $CaO\text{-}SiO_2$.[12]

3. A discontinuity (not shown on the curve) exists near the slag composition 00475, at which the CaO/SiO_2 mol ratio is about unity. Similar discontinuities were observed by Farup[9] in electrical conductivity measurements and by Herty[10] and Rait[11] in viscosity measurements. The interpretation of this irregularity is not apparent, but will be discussed in a later section.

4. It will be noted from Fig. 11 and Table 4 that the dE/dT value for the slag 00475 is less than that of the slag 0045. Thus the discontinuity shown in Fig. 12 near the CaO/SiO_2 mol ratio of unity will be less pronounced the higher the temperature.

From these observations it is apparent that the cell reaction, if reversible, must be such as to reject SiO_2 spontaneously from the molten slag, because the higher the SiO_2 content in the slag the greater is the driving force to reject SiO_2 by means of the cell reaction. The direction of the electromotive force observed is: graphite, cathode; silicon carbide, anode. This indicates that positive ions are moving to the graphite electrode and negative ions to the silicon carbide electrode. In molten slags of the system $CaO\text{-}SiO_2$, the only possible simple ions are Ca^{++}, Si^{4+} and SiO_4^{4-}. From a few manipulations it can be shown that the cell reaction does not involve Ca^{++} ions, because this would require that the observed electromotive force should increase with increase in the CaO content of the slag. Some of the other possibilities will now be considered.

Establishment of the Cell Reaction

The Standard State.—A quantitative treatment of the data requires that some suitable standard state be selected. To do this it will be convenient to refer to the constitution diagram for the two-component system CaO-SiO_2 as shown in Fig. 13.[12] On the SiO_2 side a liquid phase is in equilibrium with beta cristobalite in the temperature range 1470° to 1700°C. Therefore, it is very convenient to choose pure beta cristobalite as the standard state. At a given temperature T_1, the corresponding slag of composition C_1 on the liquidus curve may be chosen as the standard state (see Fig. 13). At a second temperature T_2 the slag of composition C_2 will be the standard state. The actual cell electromotive force of a slag of composition C_1 or C_2 will then be the standard electromotive force, E_o, at the corresponding temperature T_1 or T_2. From Fig. 12 it is possible to read the E_o values for these compositions. The standard states at temperatures of 1600°, 1575°, 1550°, 1525° and 1500°C., as read from Fig. 13, and the corresponding E_o values from Fig. 12 and corrected for thermal e.m.f. are given in Table 6. These values will be used in further consideration of the chemistry of these slags.

TABLE 6.—*Standard Electromotive Forces of the Cell Reactions*

Temperature, Deg. C.	Chemical Composition, Weight, Per Cent		Chemical Composition, Mol, Per Cent		Mol Ratio	
	CaO	SiO_2	CaO	SiO_2	CaO/SiO_2	E_o, Volts
1600	32.0	68.0	33.5	66.5	0.504	0.1054
1575	32.8	67.2	34.3	65.7	0.522	0.0989
1550	33.5	66.5	35.0	65.0	0.538	0.0924
1525	34.0	66.0	35.6	64.4	0.553	0.0857
1500	34.5	65.5	36.1	63.9	0.565	0.0790

Possible Cell Reactions.—A few of the possible cell reactions are suggested as follows:

1. Graphite electrode..... $Si^{4+} + C(gr.) + 4e = SiC(s)$
   SiC electrode..... $SiO_4^{4-} + SiC(s) = 2SiO_2(\beta\text{-crist.}) + C(gr.) + 4e$
   Total cell reaction..... $2SiO_2(soln.) = 2SiO_2(\beta\text{-crist.})$ $n^* = 4$ [1]
2. Graphite electrode..... $Si^{4+} + 2e = Si^{2+}$
   SiC electrode..... $SiC(s) = Si^{2+} + C(gr.) + 2e$
   Total cell reaction..... $SiC(s) + Si^{4+} = 2Si^{2+} + C(gr.)$ $n = 2$ [2]
3. Graphite electrode..... $Si^{4+} + C(gr.) + 4e = SiC(s)$
   SiC electrode..... $2SiC(s) + Si^{4+} = 2Si^{2+} + C(gr.) + 4e$
   Total cell reaction..... $SiC(s) + Si^{4+} = 2Si^{2+} + C(gr.)$ $n = 4$ [3]
4. Graphite electrode..... $Si^{4+} + C(gr.) + 4e = SiC(s)$
   SiC electrode..... $SiO^{4-} + 4SiC(s) = 2(SiC)_2O(s) + SiO_2(\beta-\text{crist.}) + 4e$
   Total cell reaction..... $2SiO_2(soln.) + C(gr.) + SiC(s) = 2(SiC)_2O(s) + SiO_2(\beta\text{-crist.})$ $n = 4$ [4]
5. Graphite electrode..... $3Si^{4+} + 3C(gr.) + 12e = 3SiC_{(s)}$
   SiC electrode..... $3SiO_4^{4-} + 2SiC(s) = 5SiO_2(\beta\text{-crist.}) + 2CO + 12e$
   Total cell reaction..... $6SiO_2(soln.) + 3C(gr.) = SiC(s) + 5SiO_2(\beta\text{-crist.}) + 2CO$ $n = 12$ [5]

These reactions can be examined individually to see whether the theoretical standard free-energy change of any one of them corresponds to the experimentally determined value. Reaction 1 is out of the question because the standard free-energy change would be zero at all temperatures.

* n = number of electrons transferred.

Reactions 2 and 3 are essentially the same, but for the n value, or the number of electrons involved in the cell reaction. These reactions both require the existence of questionable Si^{2+} ions in molten blast-furnace slags. No experimental data are available to evaluate the standard free-energy change of reactions 2 and 3. Reaction 4 is possible, but also requires the existence of an unlikely compound. The compound $(SiC)_2O$ or $(SiC)_xO$ has been reported,[13,14] but a review of more recent literature reveals that the existence of these compounds is doubtful.[15]

This leaves reaction 5 as the most probable cell reaction. If pure beta cristobalite is chosen as the standard state, reaction 5 may be simplified to:

$$SiO_2(\beta\text{-crist.}) + 3C(gr.) = SiC(s) + 2CO \quad [6]$$

The free energies of formation of beta cristobalite, SiC and CO as taken from the literature are.*

$$\beta\text{-cristobalite}^{16}\ldots\ldots \Delta F^\circ_T = -207{,}900 - 7.09T \log T + 0.22 \times 10^{-3}T^2 + 3.042 \times 10^5 T^{-1} + 65.58T \quad [7]$$

$$SiC^{16}\ldots\ldots\ldots\ldots \Delta F^\circ_T = -27{,}050 - 1.11T \log T + 0.16 \times 10^{-3}T^2 + 0.33 \times 10^5 T^{-1} + 5.45T \quad [8]$$

$$CO^{17}\ldots\ldots\ldots\ldots \Delta F^\circ_T = -26{,}089 - 0.966T \log T + 1.028 \times 10^{-3}T^2 - 0.584 \times 10^{+5}T^{-1} + 5.68T^{1/2} - 19.98T \quad [9]$$

From equations 7, 8 and 9, the standard free-energy change of reaction is therefore:

$$\Delta F^\circ_T = +128{,}670 + 4.048T \log T + 1.996 \times 10^{-3}T^2 - 3.88 \times 10^5 T^{-1} + 11.36T^{1/2} - 100.09T \quad [10]$$

The standard free-energy changes of reaction 6 (according to Eq. 10) at different temperatures are given in Table 7. The corresponding experimental standard free-energy changes as calculated from the Eq. $\Delta F^\circ = -nFE_e$ (where $n = 12$, F is Faraday's constant and E_e the experimental standard electromotive force given in Table 6), are also given in Table 7.

* The Lewis-Randall convention will be used for all thermodynamic terms.

TABLE 7.—*Comparison of Theoretical and Experimental Standard Free-energy Changes*

Temperature		ΔF°, Calories		E_e, Volts	
Deg. C.	Deg. K.	Theo.	Expt.	Theo.	Expt.
1600	1873	−27,410	−29,200	0.0990	0.1054
1575	1848	−25,490	−27,400	0.0920	0.0989
1550	1823	−23,530	−25,600	0.0850	0.0924
1525	1798	−21,570	−23,700	0.0778	0.0857
1500	1773	−19,580	−21,800	0.0707	0.0790

The experimentally obtained standard free-energy changes are about 6 to 10 per cent higher than the theoretically calculated ones. It has been pointed out before that the average cell temperature is about 5° higher than that indicated by the tungsten-molybdenum thermocouple. In the foregoing calculations, the cell temperature and the hot-junction temperature (for thermal correction) are both taken as that indicated by the tungsten-molybdenum thermocouple. If a correction is applied to both the cell temperature and the hot-junction temperature, the experimental standard free-energy changes will be decreased by about 3 to 5 per cent. The corrected experimental standard free-energy changes will then be about 5 per cent higher than the theoretical values. The temperature dependence of the experimental values is within 4.6 per cent of that predicted theoretically.

Effect of Pressure Change.—In the previous calculations, the partial pressure of CO is assumed to be one atmosphere. A few experiments were made to determine the effect of cell atmosphere on the electromotive force. Purified nitrogen, dry tank nitrogen and air were tried.

It was found that the cell electromotive force did not respond to the changes in cell atmosphere.* This, however, is explained by the reasoning that it is the partial pressure of CO in the immediate neighborhood of the slag-SiC interface that controls the cell reaction. It may be assumed that the gaseous atmosphere in the immediate neighborhood of the slag-SiC interface is not in equilibrium with the cell atmosphere. Whatever gases are produced at the slag-SiC interface, presumably CO, will accumulate there. But the pressure of the gaseous atmosphere, presumably pure CO, in the immediate neighborhood of the slag-SiC interface will depend on the total pressure of the system, and it should be possible to use this pressure effect as an additional criterion in establishing the proper cell reaction.

TABLE 8.—*Change of Cell Electromotive Force with Change of Total Pressure of System*

Slag Designation	Temperature, Deg. C.	Pressure, Mm. Hg		Δp	ΔE, Mv.
		Original	Final		
1525	1532	735	188	547	+30.7
00425	1560	735	280	455	+26.3
1025	1537	735	318	417	+21.3
1025	1534	735	336	399	+18.5
0540	1478	735	360	375	+19.3
00425	1542	735	548	187	+ 8.0

With this in view, a few experiments were made to determine the effect of change of total pressure of the system on the cell electromotive force. Slags of various composition were used. The cell was first operated at one atmosphere with circulation of purified nitrogen. When the cell electromotive force became steady the pressure of the system was suddenly reduced by means of a mechanical oil pump. The cell electromotive force increased immediately, approaching a constant value in one to two minutes. With alternate pressure increase and decrease, the cell electromotive force decreased or increased correspondingly. The results of six runs are shown in Table 8.

From the proposed cell reaction:

$$6SiO_2(\text{soln.}) + 3C(\text{gr.}) = 5SiO_2(\beta\text{-crist.}) + SiC(s) + 2CO \quad [5]$$

it follows that

$$E - E_o = -\frac{RT}{nF} \ln \frac{P^2_{co}}{(a_{SiO_2})^6} \quad [12]$$

where E = cell electromotive force.

E_o = standard cell electromotive force.

R = gas constant.

T = absolute temperature.

n = number of electrons involved in cell reaction.

F = Faraday's constant.

P_{co} = partial pressure of CO at the slag-SiC interface.

a_{SiO_2} = activity of SiO_2 in slag.

For any given slag at a given temperature, a_{SiO_2} is constant. When P_{co} is changed from P_1 to P_2, the change in cell electromotive force will be:

$$\Delta E = E_2 - E_1 = -\frac{RT}{nF} \ln \frac{P_2^2}{k} + \frac{RT}{nF} \ln \frac{P_1^2}{k}$$

or

$$\Delta E = \frac{2RT}{nF} \ln (P_1/P_2) \quad [13]$$

In Eq. 13, all terms except the number of electrons involved in the cell reaction n are known. Hence the pressure experiment offers a very convenient method for determining the number of electrons involved in the cell reaction. The calculation is given in Table 9. The results given in Table 9 are plotted in Figs. 14 and 15. This pressure experiment not

* In actual experiments the controlling gas sweeps over the outside of the cell body rather than over the slag-metal interface (see Fig. 1).

only establishes reaction 5 as the cell reaction, but also rules out the suggested cell reactions 2 and 3, which should not be subject to pressure variations. It also

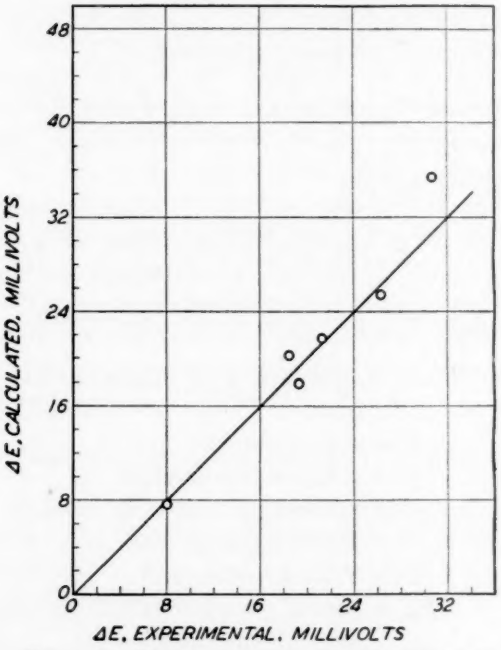

FIG. 14.—PRESSURE EXPERIMENT, SHOWING AGREEMENT BETWEEN THEORETICAL AND EXPERIMENTAL ELECTROMOTIVE FORCE CHANGES.

justifies the assumption made in the previous calculations that the partial pressure of CO is equal to atmospheric pressure.

TABLE 9.—*Calculation of Number of Electrons Involved in Cell Reaction from Pressure Experiment*

Temperature, Deg. K.	Pressure, Mm. Hg		P_1/P_2	E, Volts Observed	n Calculated	E, volts, Calculated Assuming $n = 12$
	P_1	P_2				
1805	735	188	3.91	0.0307	13.8	0.0354
1833	735	280	2.62	0.0263	11.6	0.0254
1810	735	318	2.31	0.0213	12.2	0.0217
1806	735	336	2.19	0.0185	13.0	0.0202
1751	735	360	2.04	0.0193	11.1	0.0179
1815	735	548	1.34	0.0080	11.4	0.0076

Thermodynamic Calculations, CaO-SiO_2 *System*

Activity of SiO_2 *in Molten Slags.*—Since all the electromotive-force determinations

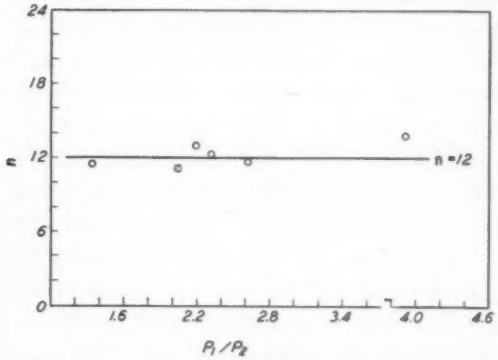

FIG. 15.—PRESSURE EXPERIMENT SHOWING EVALUATION OF n, OR NUMBER OF ELECTRONS INVOLVED IN CELL REACTION.

were carried out under atmospheric pressure, $P_{CO} = 1$ atmosphere. It follows from Eq. 12,

$$E - E_o = -\frac{RT}{12F} \ln \frac{1}{(a_{SiO_2})^6}$$

or

$$E - E_o = \frac{RT}{2F} \ln a_{SiO_2} \qquad [14].$$

where a_{SiO_2} is activity of SiO_2 in slag.

The activities and activity coefficients of SiO_2 in molten slags of the system CaO-SiO_2 calculated according to Eq. 14, using experimental values for E_o, are given in Table 10.

Free-energy Change of Cell Reaction ΔF, *and Partial Molal Free Energy of* SiO_2 $\overline{F}$, *in Molten Slags of System* CaO-SiO_2, *Referred to Pure Beta Cristobalite as the Standard State.*—Equation 6 is obtained from a summation of Eqs. 5 and 15, as follows:

$$\Delta F: 6SiO_2 \text{ (soln.)} + 3C(gr.) = 5SiO_2(\beta\text{-crist.}) + SiC(s) + 2CO \qquad [5]$$
$$6\overline{F}: 6SiO_2(\beta\text{-crist.}) = 6SiO_2(\text{soln.}) \text{ (pure } \beta\text{-crist. as standard state)} \qquad [15]$$
$$\Delta F^\circ: SiO_2(\beta\text{-crist.}) + 3C(gr.) = SiC(s) + 2CO \qquad [6]$$

Hence,

$$\Delta F + 6\bar{F} = \Delta\bar{F}^\circ, \text{ or, } \bar{F} = (\Delta F^\circ - \Delta F)/6 \quad [16]$$

The experimentally determined standard free-energy changes listed in Table 7 are represented by the equation:

$$\Delta F^\circ(\text{experimental}) = 109{,}500 - 74.0T \quad [17]$$

The theoretical standard free-energy changes calculated from free energies of formation and listed in Table 7 are represented by the equation:

$$\Delta F^\circ(\text{theoretical}) = 118{,}600 - 78.0T \quad [18]$$

The experimental free energy of the cell reaction and the partial molal free energy of SiO_2 in molten slags of the system $CaO\text{-}SiO_2$ are given in Table 11.

TABLE 11.—*Free-energy Change of Cell Reaction* ΔF *and Partial Molal Free Energy of* SiO_2, *in Molten Slags of System* $CaO\text{-}SiO_2$

Slag Designation	Mol Fraction of SiO_2 in Slag	ΔF, Cal.	$\bar{F}$, Cal.
0050	0.483	$-40{,}100 + 18.8\,T$	$24{,}900 - 15.5\,T$
00475	0.508	$-20{,}400 + 3.3\,T$	$21{,}600 - 12.9\,T$
0045	0.533	$-8{,}720 - 3.3\,T$	$19{,}700 - 11.8\,T$
00425	0.558	$10{,}500 - 15.2\,T$	$16{,}500 - 9.80\,T$
0040	0.583	$22{,}400 - 23.5\,T$	$14{,}500 - 8.42\,T$

Partial Molal Heat Content of SiO_2 *in Molten Slags of System* $CaO\text{-}SiO_2$.—For any given slag we have:

$$\frac{dlna}{dT} = -\frac{\bar{L}}{RT^2}, \quad \text{or} \quad \frac{dlna}{d(1/T)} = \frac{\bar{L}}{R} \quad [19]$$

where a = activity of SiO_2 in slag.
$\bar{L}$ = partial molal heat content of SiO_2 in slag.
T = absolute temperature.
R = gas constant.

The lna values are plotted against $1/T$ in Fig. 16. The plots are all straight lines. This indicates that the $\bar{L}$ values, which are given directly by the slope of these straight lines, are constant within the temperature range (1500° to 1600°C.) studied. The results are given in Table 12.

TABLE 12.—*Partial Molal Heat Contents of* SiO_2 *in Slags of System* $CaO\text{-}SiO_2$

Slag Designation	Mol Fraction of SiO_2 in Slag	$\bar{L}$, Cal.
0050	0.483	26,100
00475	0.508	22,700
0045	0.533	20,100
00425	0.558	16,670
0040	0.583	14,700

TABLE 10.—*Activities and Activity Coefficients of* SiO_2 *in Molten Slags of System* $CaO\text{-}SiO_2$

Temperature, Deg. C.	Mol Fraction of SiO_2									
	0.483		0.508		0.533		0.558		0.583	
	a[a]	f[a]	a	f	a	f	a	f	a	f
1,600	0.334	0.69	0.509	1.00	0.527	0.99	0.603	1.08	0.710	1.22
1,575	0.366	0.76	0.549	1.08	0.563	1.06	0.639	1.15	0.746	1.28
1,550	0.401	0.83	0.594	1.17	0.605	1.14	0.680	1.22	0.787	1.35
1,525					0.651	1.22	0.722	1.29	0.831	1.42
1,500							0.772	1.38	0.880	1.51

[a] a indicates activity, f indicates activity coefficient, both referred to pure β cristobalite as the standard state.

DATA AND RESULTS, SYSTEM $CaO\text{-}Al_2O_3\text{-}SiO_2$

The total cell electromotive force-temperature relationships and the total cell electromotive force-composition re-

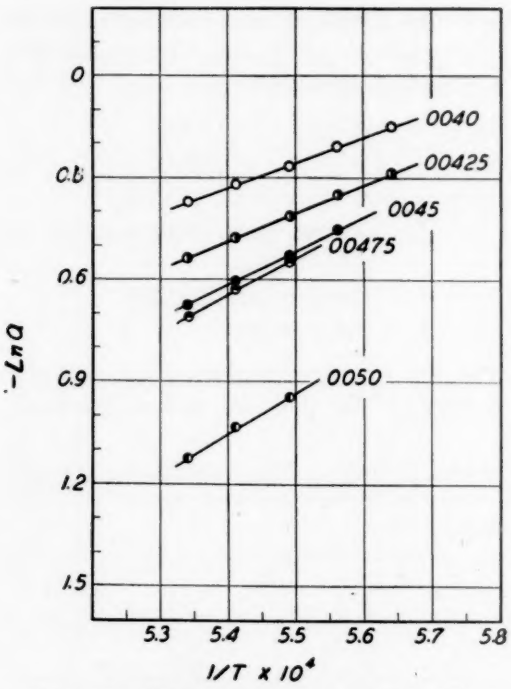

FIG. 16.—EVALUATION OF PARTIAL MOLAL HEAT CONTENTS OF SiO_2 IN MOLTEN SLAGS OF SYSTEM CaO-SiO_2.

lationships for slags of the system CaO-Al_2O_3-SiO_2 are shown in Figs. 17 to 26.

The following points are noted from Figs. 17 to 26:

1. For any single slag, the electromotive force-temperature relationship within the temperature range studied can be represented by a straight line. In other words, the heats of reaction of these slags are constant within the temperature range studied.

2. For a given Al_2O_3 content, the electromotive force increases with increasing SiO_2 content, or with decreasing CaO content of the slag.

3. For a given Al_2O_3 content, the slope of the plot for electromotive force vs. temperature increases with increasing SiO_2 content, or with decreasing CaO content of the slag, indicating a progressive change of some thermodynamic properties of the slag with change of composition.

4. In the plots of electromotive force vs. composition, all experimental points

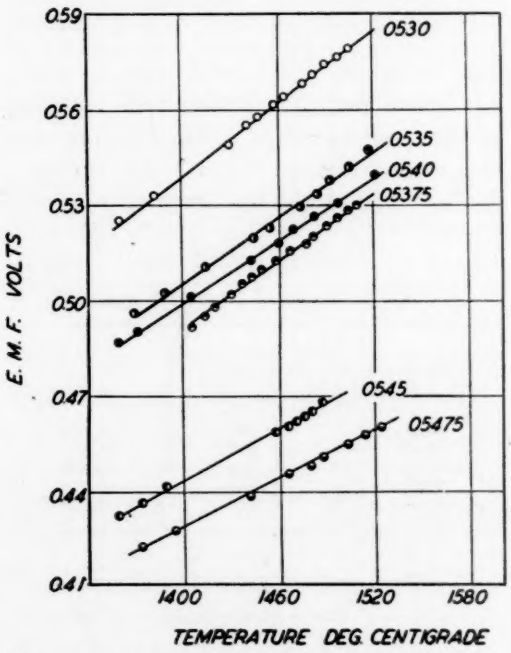

Fig. 17. Slag containing 5 per cent Al_2O_3 by weight.

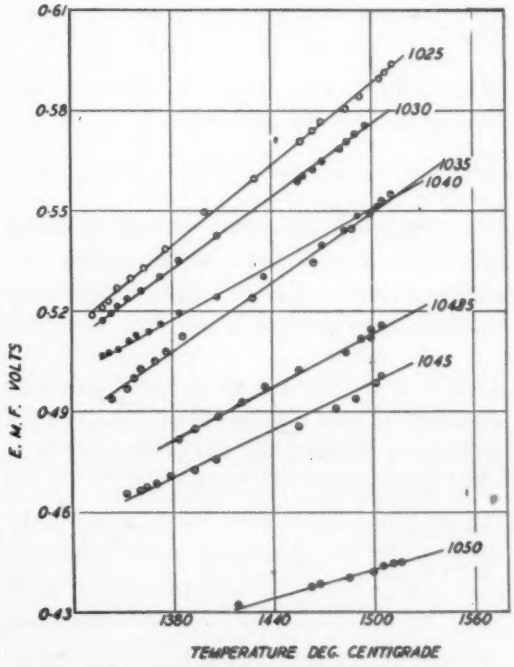

Fig. 18. Slag containing 10 per cent Al_2O_3 by weight.

FIGS. 17–18.—TOTAL ELECTROMOTIVE FORCE VS. TEMPERATURE FOR SLAGS OF SYSTEM CaO-Al_2O_3-SiO_2.

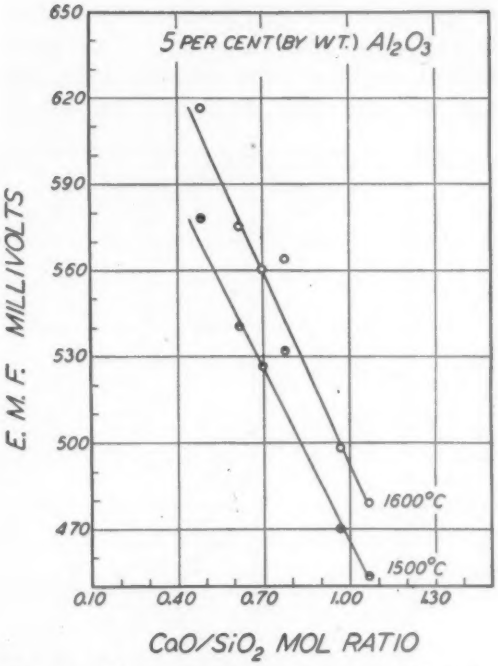

Fig. 19. Slag containing 5 per cent Al_2O_3 by weight.

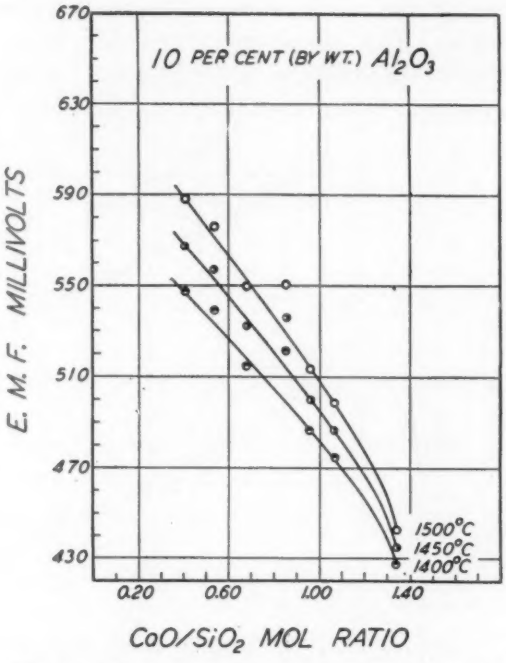

Fig. 20. Slag containing 10 per cent Al_2O_3 by weight.

FIGS. 19–20.—TOTAL ELECTROMOTIVE FORCE VS. COMPOSITION FOR SLAGS OF SYSTEM CaO-Al_2O_3-SiO_2.

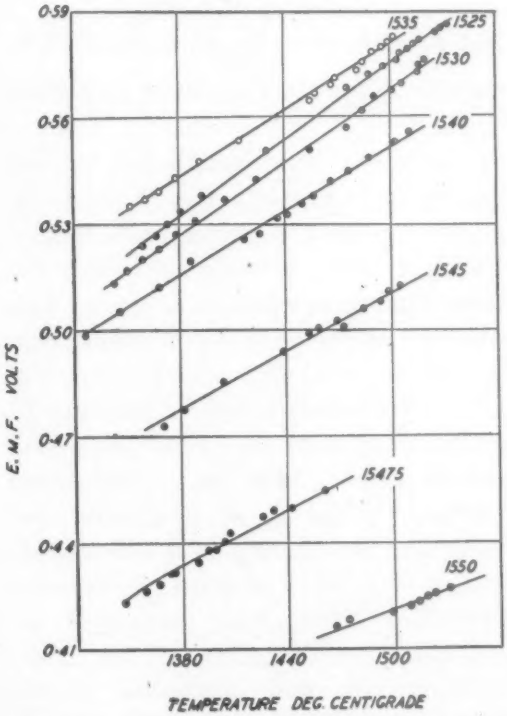

Fig. 21. Slag containing 15 per cent Al_2O_3 by weight.

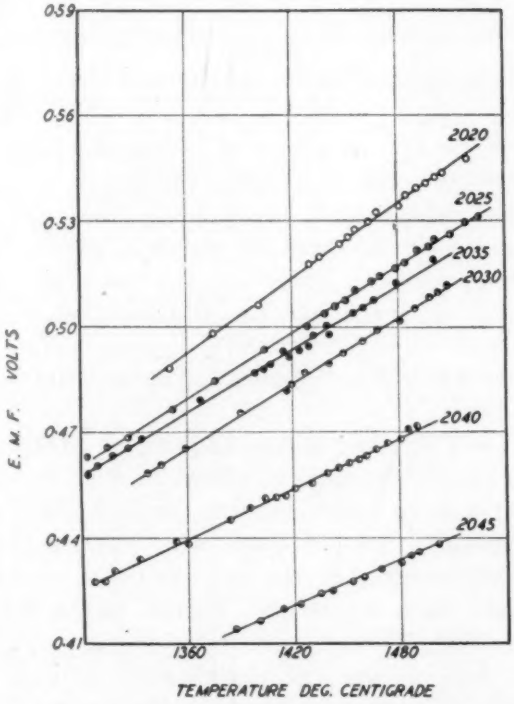

Fig. 22. Slag containing 20 per cent Al_2O_3 by weight.

FIGS. 21–22.—TOTAL ELECTROMOTIVE FORCE VS. TEMPERATURE FOR SLAGS OF SYSTEM CaO-Al_2O_3-SiO_2.

except one in each series fall on a smooth curve. The discontinuity in all these curves occurs at a CaO/SiO_2 mol ratio of 0.70 to 0.80, very likely 0.75 (or CaO/SiO_2 = ¾). Whether this discontinuity reflects some irreversible change in the molten slags or is caused by a change of molecular structure of the slags at the composition indicated is yet uncertain. This is comparable to the discontinuity found in the CaO-SiO_2 system. The problem will be discussed further in a later section.

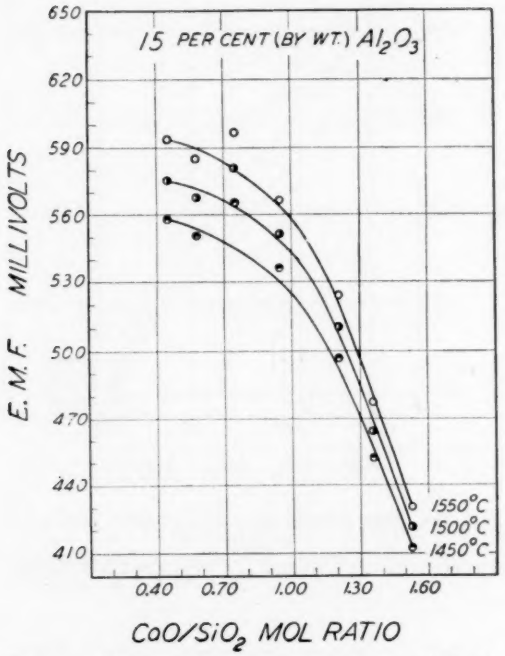

Fig. 23. Slag containing 15 per cent Al_2O_3 by weight.

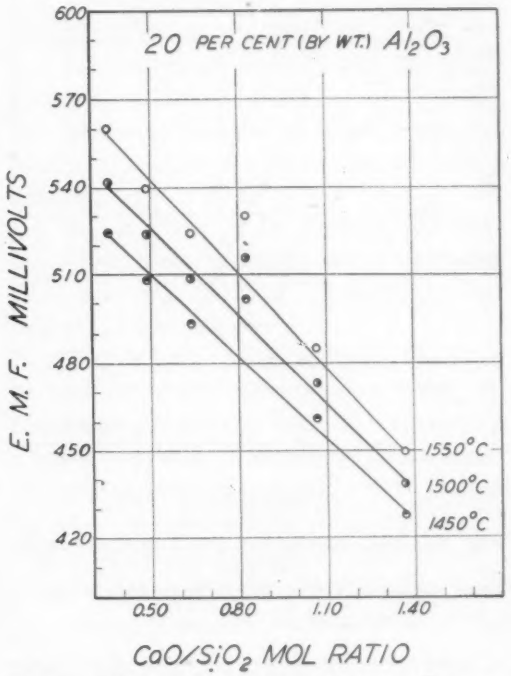

Fig. 24. Slag containing 20 per cent Al_2O_3 by weight.

FIGS. 23–24.—TOTAL ELECTROMOTIVE FORCE VS. COMPOSITION FOR SLAGS OF SYSTEM CaO-Al_2O_3-SiO_2.

5. The effect of the addition of Al_2O_3 to CaO-SiO_2 slags is shown in Fig. 27. At a given CaO/SiO_2 ratio, the cell electromotive force increases with increasing Al_2O_3 content of the slag up to 15 per cent Al_2O_3 by weight. Further increase in Al_2O_3 concentration of the slag causes a drop in the cell electromotive force. This is a very interesting observation. The explanation is not certain, but the following possibility is suggested: Al_2O_3 is amphoteric. It is reasonable to suggest that at very low concentrations Al_2O_3 acts like an acid; the Al atoms replace Si atoms in the SiO_4^{4-} tetrahedra, thereby causing an increase in the SiO_2 activity of the slag. With increasing Al_2O_3 concentration a stage is reached at which the tetrahedral groups become saturated with Al atoms and some of the Al atoms begin to assume octahedral coordination and act as basic components in the slag. In terms of modern structural chemistry, aluminum can have two coordination numbers, 4 and 6, or tetrahedral and octahedral coordination. It is also possible that an equilibrium always exists between these two forms, with tetrahedral coordination predominating at low Al_2O_3 concentrations and octahedral coordination predominating at higher Al_2O_3 concentrations.

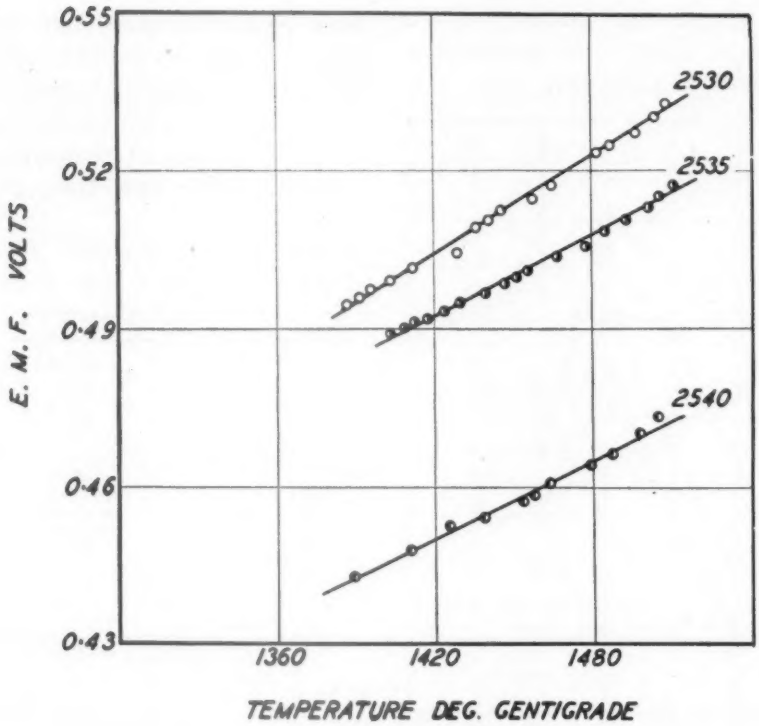

FIG. 25.

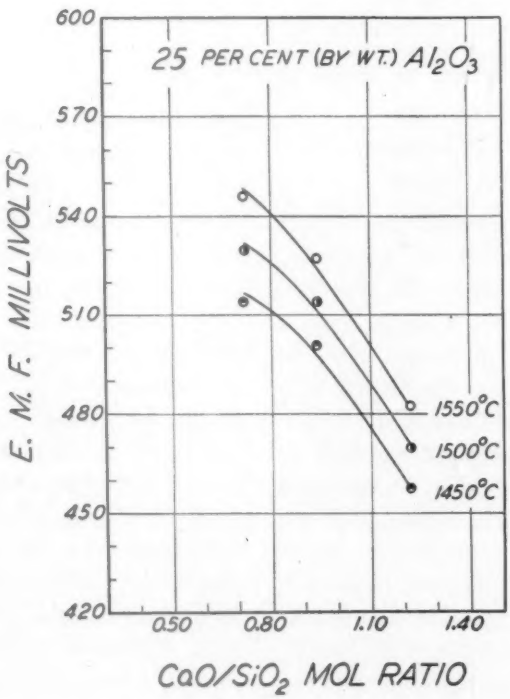

FIG. 26.

FIGS. 25–26.—TOTAL ELECTROMOTIVE FORCE VS. TEMPERATURE (FIG. 25) AND COMPOSITION (FIG. 26) FOR SLAGS OF SYSTEM CaO-Al_2O_3-SiO_2 CONTAINING 25 PER CENT Al_2O_3 BY WEIGHT.

Fig. 28 shows the iso-electromotive force curves at 1600°C. for molten slags of the system CaO-Al_2O_3-SiO_2.

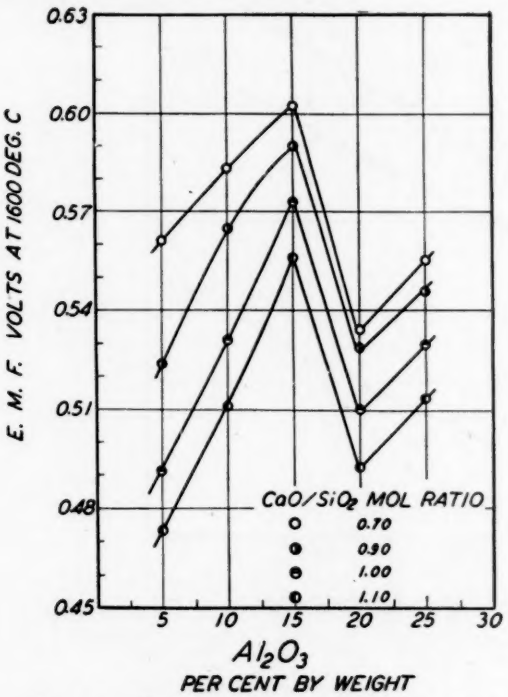

FIG. 27.—TOTAL CELL ELECTROMOTIVE FORCE VS. COMPOSITION FOR SLAGS OF SYSTEM CaO-Al_2O_3-SiO_2, SHOWING EFFECT OF Al_2O_3 AT VARIOUS CaO/SiO_2 RATIOS.

Thermodynamic Calculations, CaO-Al_2O_3-SiO_2 *System*

A ternary-phase diagram for the system CaO-Al_2O_3-SiO_2 is shown in Fig. 29.[18] It is rather difficult to select the standard states for slags of the ternary system CaO-Al_2O_3-SiO_2. The problem can be approached by dividing the slags into a series of constant Al_2O_3 concentrations. Following the same method applied to the binary system CaO-SiO_2, we can find a slag composition on the liquidus curves shown in Fig. 29 for each slag series of constant Al_2O_3 concentration at each temperature. This composition, in equilibrium with beta cristobalite, will be the standard state for the slag series in concern. Unfortunately, there is a limit to the Al_2O_3 concentration above which the molten slag is no longer in equilibrium with beta cristobalite and the choice of beta cristobalite as the standard state becomes impossible beyond this limit. For instance, the limit is about 11 per cent Al_2O_3 by weight at temperature level of 1500°C.; above this Al_2O_3 concentration the slag will come into equilibrium with mullite instead of beta cristobalite. The various standard states, the corresponding slag compositions in equilibrium with these standard states at 1500°C., and the corresponding E_o and $\Delta F°$ values obtained by the same method applied to the binary system CaO-SiO_2, are given in Table 13.

TABLE 13.—E_o and $\Delta F°$ *Values of Cell Reaction at* 1500°C. *for Slags of System* CaO-Al_2O_3-SiO_2

Slag Series, Per Cent Al_2O_3 by Wt.	Standard State	CaO/SiO_2 Mol Ratio, Slag Composition in Equilibrium with the Standard State	E_o, Volts	$\Delta F°$, Cal.
0	Pure β-cristobalite	0.565	0.0790	−21,800
5	β-cristobalite (may contain displaced Al atoms)	0.400	0.138	−38,200
10	Same as 5 per cent Al_2O_3 series	0.197	0.164	−45,400
15	Mullite	0.074	0.131	−36,300
20	Mullite	0.119	0.116	−32,100

At 1500°C. (Table 13) slags containing 5 and 10 per cent by weight of Al_2O_3 can be referred to a beta cristobalite standard state, but the $\Delta F°$ values differ from those for slags containing no Al_2O_3. The $\Delta F°$ values are larger than those for Al_2O_3-free slags by as much as 20,000 cal. Thus it is reasonable to suggest that the solid phase that is in equilibrium with molten slags containing Al_2O_3 may not be pure beta cristobalite, but cristobalite containing some aluminum atoms that displaced the silicon atoms in the tetrahedral network, hence the new $\Delta F°$ value. For slags containing 15 per cent by weight

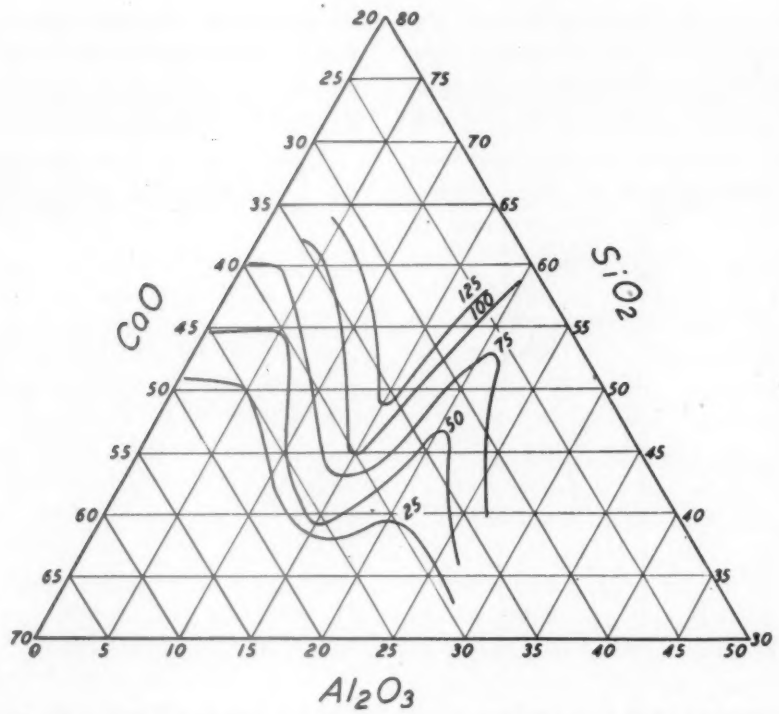

FIG. 28.—ISO-ELECTROMOTIVE FORCE (ACTUAL CELL ELECTROMOTIVE FORCE CORRECTED FOR THERMAL ELECTROMOTIVE FORCE, IN MILLIVOLTS) FOR SLAGS OF SYSTEM CaO-Al_2O_3-SiO_2 AT 1600°C.

Compositions expressed in per cent by weight.

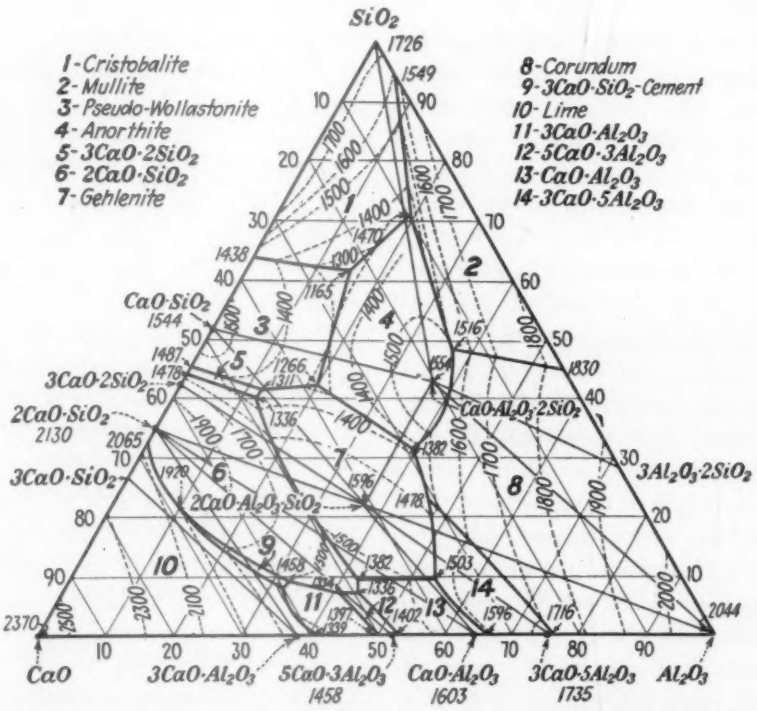

FIG. 29.—CONSTITUTIONAL DIAGRAM OF SYSTEM CaO-Al_2O_3-SiO_2.[18]

of Al_2O_3 or higher, the standard state at 1500°C. will be mullite, hence another new $\Delta F°$ value, as is shown in Table 13.

For the reasons given in the foregoing paragraphs, it is difficult to attempt any thermodynamic calculation of the properties of molten slags of the ternary system CaO-Al_2O_3-SiO_2. The available data are insufficient to warrant such an attempt. A study of the binary system Al_2O_3-SiO_2 is necessary.

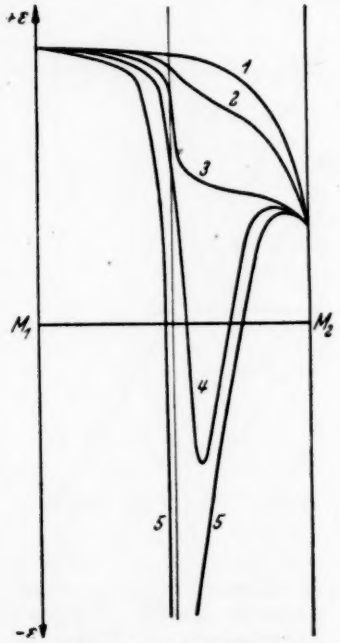

FIG. 30.—POTENTIAL-COMPOSITION CURVES WHEN THERE IS COMPOUND FORMATION IN THE METAL PHASE.[21]

However, for purposes of comparison, we can choose a hypothetical standard state that is always pure beta cristobalite. With this hypothetical state the calculation of the SiO_2 activity in slags of the ternary system CaO-Al_2O_3-SiO_2 is simplified. This treatment is by no means rigorous, yet it offers a convenient way to compare the properties of one slag with another. To avoid confusion, the SiO_2 activity so calculated, by assuming pure beta cristobalite as the hypothetical standard state, will be called the "apparent SiO_2" activity of the slag. The isoactivity lines will be exactly like the iso-electromotive force lines in Fig. 30 and the apparent activities at 1600°C. for the electromotive force contours shown in this figure are as follows:

Actual Cell Electromotive Force at 1600°C., Mv.	Corresponding Apparent Activity of SiO_2 at 1600°C.
25	0.37
50	0.50
75	0.67
100	0.93
125	1.27

It is of interest to compare these activity contours with the other measured properties of these slags. There is a rough reciprocal relation with conductivity data,[7] slags with a low SiO_2 activity have high conductivity. The viscosity contours by McCaffery[23] have an entirely different shape but in general the viscosity decreases with decrease in SiO_2 activity. The desulphurizing contours by Joseph[24] are parallel to these viscosities, a good desulphurizing slag having a low viscosity. It should be remembered that these desulphurizing ratios do not represent either equilibrium or absolute rate measurements, they are simply useful values obtained under a specific set of conditions.

The influence of small additions of MgO, MnO, S, and B_2O_3 on the electromotive force of slags of the CaO-SiO_2-Al_2O_3 system was also investigated. In brief, up to 1 per cent by weight of sulphur had little influence on the electromotive force, up to 4 per cent MgO resulted in a slight increase, up to 7 per cent MnO resulted in a slight decrease, and up to 4 per cent B_2O_3 resulted in a pronounced decrease. These additions may thus be interpreted as having corresponding effects on the activity of SiO_2 in these slags, but a quantitative interpretation of these effects cannot be made because of the difficulty in determining a satisfactory standard state for the high-alumina slags.

DISCUSSION OF RESULTS

It should be noted that in practically all the plots involving composition in this

paper the CaO/SiO_2 mol ratio is chosen as the independent variable. This is arbitrary, although it has been generally felt that there is a fundamental relationship between CaO and SiO_2 in steelmaking slags, which controls the constitution and properties of the slag.[6,19,20]

The present investigation strengthens the belief that molten slags can be treated as solutions of electrolytes. An unexplained observation in this investigation is that discontinuities exist in the plots for electromotive force vs. composition (see Figs. 12, 18, 20, 22, and 24). For slags of the $CaO-SiO_2$ system the discontinuity occurs at a CaO/SiO_2 mol ratio of about unity, while for slags of the ternary $CaO-Al_2O_3-SiO_2$ system the discontinuity occurs at CaO/SiO_2 ratios of 0.6 to 0.8, very likely 0.75. This could be interpreted in two ways:

1. Drossbach[21] made approximate calculations of the electromotive force of a metal phase in equilibrium with a slag phase in a two-component system where there is a compound formed in the metal phase. His theoretical plots are reproduced in Fig. 30, where curve 1 corresponds to complete dissociation, curve 5 to no dissociation and curves 2, 3, and 4 to partial dissociation of the metallic compound. If curve 4 is calculated for a case corresponding to 0.2 per cent dissociation of the compound, curves 1, 2, 3, 4, and 5 will correspond to 100, 25, 5, 0.2, and 0 per cent dissociation of the compound, respectively. Similarly, in the system $CaO-SiO_2$ we could assume the presence of a compound of the formula $(CaO.SiO_2)_n$ in molten slags within the range of compositions studied. For molten slags of the ternary system $CaO-Al_2O_3-SiO_2$ the compound probably is of the form $(3CaO.4SiO_2.xAl_2O_3)_n$, where x and n are integers. The compound dissociates somewhat and the degree of dissociation increases with rising temperature of the slag.

2. The observed discontinuities in the potential-composition plots may be interpreted as a result of change of molecular structure of the molten slag at the composition indicated. According to Preston,[22] molten slag of the system $CaO-SiO_2$ at the composition of $CaO/SiO_2 = 1$ is ideally suited for the ring or chain structure; more SiO_2 will change the ring or chain structure gradually to a sheet structure or three-dimensional network, while more CaO will break up the ring or chain structure to those of smaller sizes. Similar reasoning can be applied to the system $CaO-Al_2O_3-SiO_2$.

In the previous calculations of the SiO_2 activity of molten slags at different temperatures, pure beta cristobalite at the corresponding temperatures is chosen as the standard state; in other words, the activity of pure beta cristobalite is assumed to be unity at all temperatures. Although this treatment is necessary in establishing the cell reaction and in making many thermodynamic calculations, it is not needed in interpreting metallurgical reactions, for which only one reference state is required. Thus, if we arbitrarily choose pure beta cristobalite at 1600°C. as the reference state, the SiO_2 activity of all slags at all temperatures will be referred to unit activity of pure beta cristobalite at 1600°C. We shall here call the activity so obtained the "relative SiO_2 activity." In the following activity equation:

$$E - E_o = -\frac{RT}{2F} \ln A \qquad [14]$$

let E = actual cell electromotive force in volts at a given temperature T.

E_0 = 0.1054 volts, which is the standard electromotive force of the cell reaction at 1600°C. This fixes pure beta cristobalite at 1600°C. as the reference state.

R = gas constant = 1.987.

F = Faraday's constant = 23,066.

then A = relative SiO_2 activity of the slag, referring to unity activity of pure beta cristobalite at 1600°C.

For example, the actual cell electromotive force at 1575°C. for the slag 0045 (45 per cent CaO, 55 per cent SiO_2 by weight) is 0.0537 volts. Substituting the known values of E, E_0, R, T, and F into Eq. 14, we have:

$$0.0537 - 0.1054 = -\frac{1.987 \times 1848}{2 \times 23066} lnA$$

or A = relative SiO_2 activity of slag 0045 at 1575°C. = 0.518. The relative SiO_2 activities of molten slags of the system CaO-SiO_2 at various temperatures are given in Table 14, which shows that with more than 50 per cent SiO_2 the relative SiO_2 activity of a slag increases with rising temperature, and that the rate of increase is larger as the SiO_2 concentration of the slag becomes greater. Thus, with a 100°C. rise in temperature, the relative SiO_2 activity of molten slags of the system CaO-SiO_2 is increased; 2.4 per cent for a slag containing 52.5 per cent SiO_2, 9.6 per cent for a slag containing 60 per cent SiO_2, and 30 per cent for pure beta cristobalite. Although more data are required, it appears that the reverse is true for slags with less than 50 per cent SiO_2.

Similarly, with a 100°C. rise in temperature, the relative SiO_2 activity of molten slags of the system CaO-Al_2O_3-SiO_2 is increased; 1.2 per cent for a slag containing 15 per cent Al_2O_3 and 40 per cent SiO_2, 2.0 per cent for a slag containing 15 per cent Al_2O_3 and 45 per cent SiO_2, and 6.1 per cent for a slag containing the same amount of Al_2O_3 but 55 per cent SiO_2.

Experience has shown that it is necessary to increase the SiO_2 content in the furnace burden and to increase the operating temperature in the blast furnace in order to raise the silicon content of the iron. It can be assumed that the silicon-reduction reaction is:

$$SiO_2 + 2C = Si + 2CO$$

This reaction probably occurs in the hottest reaction zone where the slag is still immature and siliceous. The silicon so obtained, having a high vapor pressure, is immediately taken up by the trickling molten iron. A rise in temperature in this zone increases the relative SiO_2 activity as well as the reaction rate, both contributing to a high silicon content in the molten metal.

On the other hand, the desulphurization process in the blast furnace probably will not occur at an appreciable speed in the silicon-reduction zone until the mass has reached a lower zone where the slag has taken into solution sufficient lime and becomes mature. Assuming the desulphurization reaction to be:

$$CaO + FeS + C = CaS + Fe + CO$$

we see that SiO_2 does not enter the reaction, although it may affect indirectly the CaO activity of the slag. From the previous

TABLE 14.—*Relative* SiO_2 *Activities of Molten Slags of System* CaO-SiO_2, *Referring to Unit Activity of Pure Beta Cristobalite at* 1600°C.

Slag Designation	Relative SiO_2 Activity at					Change of Relative SiO_2 Activity per 100°C. Rise in Temperature
	1600°C.	1575°C.	1550°C.	1525°C.	1500°C.	
0050	0.334	0.337	0.340			Decreases 4 per cent
00475	0.509	0.506	0.503			Increases 2.4 per cent
0045	0.527	0.518	0.513	0.506		Increases 5.5 per cent
00425	0.603	0.590	0.578	0.561	0.545	Increases 9.6 per cent
0040	0.710	0.688	0.667	0.645	0.623	Increases 12 per cent
Pure β-cristobalite	1.000	0.920	0.844	0.770	0.702	Increases 30 per cent

calculation we see that the relative SiO_2 activity of slags in this desulphurization zone changes only very slowly with change of temperature. All these factors lead to the belief that the correlation between the desulphurization in the blast furnace and the relative SiO_2 activity is very poor. The available data, however, do not justify any further interpretation.

The major contribution of this paper is the demonstration of a quantitative method for investigating the properties of molten slags by applying it to a particular cell reaction. It opens a promising future for similar studies of many other metallurgical slags, such as acid and basic open-hearth slags. Since this paper is the first on the electromotive-force measurements of molten slags, it may be considered as an introduction to further investigations. An improvement in the technique of temperature measurement will increase the accuracy of this method of study appreciably. It is hoped that future work will be directed first to similar studies of slags of other binary systems including oxidizing slags. A knowledge of various binary systems is essential to interpretation of the behavior of multicomponent systems such as those used in the basic open hearth.

Summary

A new method of studying the properties of molten slags by means of reversible cell measurements is described. The present study is confined to slags of the systems CaO-SiO_2 and CaO-Al_2O_3-SiO_2. Various electrode pairs have been tried. The silicon carbide-graphite pair seems to yield the best results. Different possible cell reactions are discussed. The suggested cell reaction that has been shown to agree with theoretical calculations is the following:

Graphite electrode.. $3Si^{4+} + 3C\ (gr.) + 12e = 3SiC\ (solid)$
SiC electrode..... $3SiO_4^{4-} + 2SiC\ (solid) = 5SiO_2\ (\beta\text{-crist.}) + 2CO + 12e$
Total cell reaction.. $6SiO_2\ (solution) + 3C\ (gr.) = SiC\ (solid) + 5SiO_2\ (\beta\text{-crist.}) + 2CO.\ n = 12$

The effect of composition and temperature on the cell electromotive force is extensively investigated. The activity of SiO_2 in the molten slag can be evaluated with reference to pure beta cristobalite as the standard state. Some of the thermodynamic properties are also calculated.

Acknowledgments

The authors wish to express their appreciation to the Boardtrust of China and the Carnegie Institute of Technology for the granting of a fellowship to one of them (L. C. Chang). They also wish to acknowledge with thanks the helpful advice of Professors Harry Seltz and Paul Fugassi, of the Department of Chemistry, Carnegie Institute of Technology.

References

1. H. Schenck: Physikalische Chemie der Eisenhuttenprozesse, two volumes. Julius Springer, 1932.
2. K. L. Fetters and J. Chipman: *Trans.* A.I.M.E. (1941) **145**, 95.
3. C. R. Taylor and J. Chipman: *Trans.* A.I.M.E. (1943) **154**, 228.
4. T. B. Winkler and J. Chipman: *Trans.* A.I.M.E. (1946) **167**; also *Metals Tech.* (April 1946—T.P. 1987).
5. N. J. Grant and J. Chipman: *Trans.* A.I.M.E. (1946) **167**; also *Metals Tech.* (April 1946—T.P. 1988).
6. P. Herasymenko: *Ztsch. Elektrochemie* (1941) **47**, 588.
7. A. E. Martin and G. Derge: *Trans.* A.I.M.E. (1943) **154**, 104.
8. G. R. Fitterer: *Trans.* A.I.M.E. (1933) **105**, 290.
9. F. Farup, W. Fleischer and E. Holtan: *Chim. et Ind.* (1924) **12**, 11.
10. C. H. Herty, Jr., and co-workers: *Bull.* Min. and Met. Adv. Boards No. 46 (1930). Pittsburgh, Pa.
11. J. R. Rait, Q. C. McMillan and R. Hay: *Jnl.* Royal Tech. Glasgow (1939) **4** (3), 449.
12. F. P. Hall and H. Insley: *Jnl.* Amer. Ceramic Soc. (1933) **16**, 463; (1938) **21**, 113.
13. R. Brunner: *Ztsch. Elektrochemie* (1932) **38**, 69.
14. E. Weintraub: *Trans.* Amer. Electrochem. Soc. (1915) **27**, 267.
15. A. Eucken and M. Jakob: *Der Chemie-Ingenieur* (1937) **3** (1), 160.
16. K. K. Kelly: Contribution to Data on Theoretical Metallurgy. *Bull.* 407, U. S. Bur. Mines, 1937.

17. M. de K. Thompson: The Total and Free Energy of Formation of the Oxides of Thirty-two Metals. Amer. Electrochem. Soc., 1942.
18. R. B. Sosman and O. Anderson: Ternary Diagram of the System CaO-SiO_2-Al_2O_3, Research Lab., United States Steel Corporation.
19. F. M. Washburn et al.: Basic Open Hearth Steelmaking, 533. A.I.M.E. 1944. Seeley W. Mudd Series.
20. B. Mason: *Blast Furnace and Steel Plant* (1944) **32**, 1328.
21. P. Drossbach: Elektrochemie geschmolzener Salze. Julius Springer, 1938.
22. E. Preston: *Jnl.* Soc. Glass Tech. (1942) **26** (114), 82.
23. R. S. McCaffery: *Trans.* A.I.M.E. (1932) **100**, 64–121.
24. W. F. Holbrook and T. L. Joseph: *Trans.* A.I.M.E. (1936) **120**, 99–120.

DISCUSSION

(*John Chipman presiding*)

L. S. DARKEN*—The authors are to be highly congratulated on this introduction of electrochemical methods to the study of steelmaking problems at this temperature of about 1600°C.

Some years ago, I did a little work on cells at room temperature, and there are difficulties encountered even there. Experimental investigation at 1600°C involves even greater difficulties on account of the high temperature. This work indicates, however, that a start has been made, and I feel that there will be much more work done in this direction now.

There is one question I should like to ask. Could the difficulty of measuring and interpreting a combined thermal and electrochemical emf be eliminated by use of two graphite electrodes, one of which is sheathed with silicon carbide (on the end), so that the only thermal emf would be between the two sides of the silicon carbide sheath? Over that small distance there should be little temperature difference, so it would seem that the electrochemical emf could be measured directly.

I disagree somewhat with the interpretation that has been placed on the results. Any written equation should correspond to experiment. Any symbols written in the equation should have a one-to-one correspondence with the phases and components that actually occur experimentally. It seems to me that that condition, which I would regard as important, has not been exactly fulfilled here. On page 101 of the paper, there are five proposed cell reactions, but as my objections apply nearly equally to all of them, I will consider just Eq 5, which is the one the authors have selected. The reaction occurring at the graphite electrode, as represented there, involves silicon carbide, presumably solid. If solid crystalline silicon carbide is present at the graphite electrode, how did it get there? Certainly, it was not put there. It could get there only by reaction. If it is there, the cell is short-circuited, because silicon carbide is the element for the other electrode. If that is true, the cell is not reversible and does not give a potential that may be directly related to the free energy, as would be true for a reversible cell.

In most of the proposed cell reactions, graphite appears on the silicon carbide electrode, to which I would raise the same objection. The cell is then doubly short-circuited.

In addition, beta cristobalite is represented as being present, and that was not put there either. None of the solutions was saturated with cristobalite. If it is there, equilibrium does not prevail. Yet, it appears in the reaction. Hence either the reaction as written does not correspond to experiment or else the cell was not at equilibrium and should not be treated as though it were.

In the third place, all the reactions involve carbon monoxide; that is, these electrodes are to be pictured as analogous to a hydrogen electrode in that the electrode reactions involve a gas. If that is the way the reaction is written, then surely, if the equation corresponds to experiment, the gas should be present in the vicinity of the electrode, and that gas is CO. However, I believe that purified nitrogen was the gas used. To me, this would be the same as nominally setting up a hydrogen electrode, but actually bubbling nitrogen over it instead. We would therefore anticipate great difficulty in interpreting the results. The author states that nitrogen was only on the outside, that probably there was CO on the inside. Perhaps there was, but, if so, how did it get there? Again, only by the cell reaction proceeding, which again means a short circuit, or that the reaction

* Research Chemist, U. S. Steel Corp., Kearny, N. J.

proceeded in part by a nonelectrochemical mechanism.

In addition to the foregoing objections to the interpretation of the experimental results there is some difficulty in believing the over-all answer. For example, one way of checking the final result would be by means of the iso-emf curves, which appear in Fig 28. If the cell were reversible these would be interpreted also as iso-activity curves. In Fig 29 the isotherms in the beta cristobalite regions are also iso-activity curves—that is, they represent compositions of the solution that are in equilibrium with beta cristobalite. The isotherms of Fig 29 for 1500, 1600, and so on, all slope upward, whereas in Fig 28, the iso-emf curves all slope down. They can not both be right. One of them must be wrong, and it would seem to me that the phase diagram is fairly well established.

Further, in order to interpret the results, the authors have to postulate that alumina has a rather high solid solubility in beta cristobalite. The author does not say how much, but it may be calculated, from the data given, that the activity of beta cristobalite would have to be reduced by a factor of about two, by the presence of whatever alumina is there. As far as I know, there is no other evidence of any sort to indicate that there is solid solution to that extent of alumina in silica, either from phase diagram measurements, petrographic work, or X ray investigation.

I should like to suggest to the authors for consideration the following proposed reactions:

Graphite electrode

$$3C\ (gr.) + 12\epsilon = 3C^{4-}\ (soln.)$$

Silicon carbide electrode

$$3C^{4-}\ (soln.) + SiO_2\ (soln.) = 2CO\ (gas) + SiC\ (solid) + 12\epsilon$$

Cell reaction

$$3C\ (gr.) + SiO_2\ (soln.) = 2CO\ (gas) + SiC\ (solid)\ (n = 12)$$

This postulated cell reaction leads to the relation:

$$\epsilon - \epsilon_0 = \frac{RT}{12\gamma} \ln PCO^2/\epsilon_{SiO_2}$$

and at one atmosphere pressure of CO

$$\epsilon - \epsilon_0 = \frac{RT}{12\gamma} \ln \epsilon_{SiO_2}$$

Comparing this with Eq 14, it is seen that the only difference is that the coefficient 12 appears above where 2 appears in Eq 14. If this proposal is correct, the activity of SiO_2 changes very much more with concentration than is indicated by Table 10. Also the activity coefficient would change more rapidly. This more rapid change would be in considerably better agreement with our present notion of slags; there is a rather large change in the nature of slag on passing from acid to basic and it seems reasonable to expect this to be reflected in a large change of the activity coefficient of silica.

In spite of the criticism offered, I want to emphasize again what I said in the beginning, that I am wholeheartedly in agreement with this method of attack on these problems, and I think it is very promising, and that more work of this nature will be done to great advantage.

A. E. MARTIN*—The authors have done a splendid job of developing a new tool for the study of molten slag systems. The work suggests the possibility that the electromotive forces of a number of individual electrode reactions may some day be measured with reference to some electrode reaction chosen as a standard. If, in addition, the individual reactions can be verified by chemical analysis and other means, great steps toward the understanding of the structure of molten slags will have been taken.

In the theoretical part of their paper, the authors postulated Ca^{++}, Si^{+4} and SiO_4^{-4} as the only possible simple ions present in molten slags of the CaO-SiO_2 system. The cell reactions suggested by them depend upon this hypothetical picture. Thus it is apparent that different conclusions probably would have been obtained from their work if their premise regarding molten slag structure had been different. Therefore, it seems appropriate to mention that one theory of slag structure, of which I am an advocate, differs from that of the authors on one point which seems to me to be of fundamental importance. I refer to the possible presence of Si^{+4} ions in the slag. According to this theory, the presence of Si^{+4} ions as such in molten silicate slags is ruled out because of their relatively high

* Assistant Professor of Metallurgy, University of Minnesota, Minneapolis, Minn.

charges and small diameters. It is assumed that all the silicon ions lose their identity by taking positions within tetrahedral groups of oxygen ions, the simplest group of which is $(SiO_4)^{-4}$. The existence of all the silicon ions within integral anion groups is explained by the assumption that the tetrahedral groups share corners with each other with the formation of $Si_2O_7^{-6}$, $Si_3O_{10}^{-8}$, etc. The average size of these anion groups is dependent primarily upon the $RO:SiO_2$ ratio; i.e., the more acid the slag, the larger the silicate groups. Thus, this theory in a qualitative way accounts for the high viscosity of acid slags as was pointed out by Hellbrüge and Endell.[25] The theory gets additional support from electrical conductance measurements by Wejnarth[26] and from the theory of glass structure of Zacharaisen.[27]

G. DERGE (author's reply)—The discussers of this paper have presented several suggestions that help to emphasize the problems encountered in interpreting high-temperature slag data. We appreciate this constructive interest in the work and will attempt to evaluate the suggestions in the light of the available experimental observations. Some of the questions must remain unanswered until further evidence has been accumulated.

We are in complete agreement with Dr. Martin's views on the fundamental importance of the concept of tetrahedral groups in silicate slags, with oxygen ions at the corners and silicon ions in the centers of the tetrahedra, and with the extent of sharing of the oxygen ions and the size of the groups determined largely by the $RO:SiO_2$ ratio. This may be regarded as a solvation of the silicon ions and, as in aqueous solutions, the solvation can be ignored in writing simple reactions without in any way discounting the value of the theory. Thus, our Eq 5 could be written more elaborately as:

$$3Si^{4+}(SiO_2)_n + 3C_{(gr)} + 12e \rightleftharpoons 3SiC_{(s)} + (SiO_2)_n$$

The elimination of a major part of the thermal emf correction by the change in electrode design suggested by Dr. Darken is quite feasible and we regret that the idea did not occur to us until after a large part of the data had been collected. We did not feel that circumstances justified a repetition of the work because the major objective of demonstrating the applicability of emf measurements to slag studies had been attained.

We cannot agree with the implication that the cell would be short-circuited at both electrodes if the selected cell reaction 5 were correct. An electrode of any substance can function as such when another material is deposited upon it, so long as the electrode surface is not completely covered. In this particular case, SiC must form on the graphite electrode, for it is shown to be a spontaneous reaction under the conditions of the experiment, see Eq 10 and Table 7. However, the experiments show that the cell is reversible, for the results are demonstrated to be reproducible and react as predicted to changes of temperature, composition, and pressure.

Similarly, we believe the results reported in the text demonstrate experimentally that the gas over the slag in the graphite cell is to be regarded as a pressure regulator and a protective atmosphere, preventing excessive oxidation of the graphite parts, rather than as a reactant in the slag. The experiment shown in Table 15 supports this view. The cell atmosphere was changed from as-received dry tank nitrogen to purified nitrogen at the end of the eleventh minute, from purified nitrogen to air at the end of the twenty-sixth minute, and from air back to purified nitrogen at the end of the forty-fourth minute, while no significant change in the cell electromotive force was observed in either case. (Any free oxygen in the cell atmosphere should be converted to carbon monoxide in the presence of graphite at 1500°C.) If the partial pressure of carbon monoxide in the cell atmosphere were controlling the electrode reaction, the change of the cell emf as a result of the change of cell atmosphere would be of the order of 100 to 150 mv. The cell emf changed in response to cell pressure rather than to a change of composition from nitrogen to air. Since the same emf was obtained with any gas, nitrogen was used instead of CO as a matter of convenience.

The fact that the iso-emf curves do not

[25] *Archiv Eisenhuttenw.* (1941) **14**, 307–15.
[26] *Trans.* Amer. Electrochem. Soc. (1934) **65**, 177–187 **66**, 329–343.
[27] *Jnl.* Chem. Physics (1935) **3**, 162–163.

parallel the isotherms of the phase diagram does not concern us because the data represent slag compositions considerably removed from these isotherms, and we know of no evidence to indicate what form the emf contours should take under these conditions.

TABLE 15—*Slag Containing Approximately 20 Pct Al_2O_3, 25 Pct CaO and 55 Pct SiO_2 by Weight*

Time, Min.	Temperature, Deg C	Total emf, Volts	Gaseous Atmosphere
0	1,513	0.528	Dry tank nitrogen (as received) containing about 0.2 pct oxygen by volume, $P_{O_2} \cong$ 1.5 mm Hg
0.5	1,516	0.530	
1	1,510	0.523	
2	1,513	0.521	
3	1,516	0.521	
4	1,517	0.521	
5	1,519	0.521	
7	1,519	0.520	
9	1,519	0.520	
10	1,519	0.520	
11	1,519	0.520	
13	1,523	0.522	Dry tank nitrogen purified over copper gauze at about 400°C, $P_{O_2} \cong 1.5 \times 10^{-7}$ mm Hg
15	1,523	0.521	
17	1,520	0.520	
18	1,520	0.520	
20	1,522	0.521	
21	1,522	0.521	
22	1,523	0.522	
23	1,528	0.523	
24	1,525	0.522	
25	1,525	0.522	
26	1,525	0.522	
29	1,525	0.522	Air, $P_{O_2} \cong$ 150 mm Hg
30	1,525	0.520	
31	1,525	0.517	
32	1,525	0.515	
33	1,525	0.514	
34	1,525	0.513	
36	1,525	0.513	
37	1,525	0.511	
38	1,520	0.510	
40	1,520	0.509	
41	1,520	0.509	
42	1,519	0.507	
44	1,517	0.506	
49	1,517	0.508	Going back to purified tank nitrogen
50	1,517	0.510	
51	1,517	0.512	
52	1,517	0.512	
53	1,517	0.512	
54	1,517	0.512	
55	1,517	0.511	
56	1,517	0.511	

The alternative cell reaction proposed by Dr. Darken, unlike his earlier suggestions, is theoretically possible in that it assigns the observed polarity to the individual electrodes. This mechanism requires the existence of C^{4-} ion in the silicate slag solution, and this seems to us to be extremely unlikely as this is not a common energy state for carbon. Since the evidence required to distinguish between these two possibilities is lacking, we prefer to write the reactions proposed in the text, which involve the more generally recognized solvated Si^{4+} ion. Although the electrode mechanisms are different, Darken's proposal results in the same over-all cell reaction, with the exception that he does not accept the possibility of SiO_2 forming in this system as beta cristobalite. As he points out, this results in a change from 2 to 12 in the activity expression of Eq 14, which results in greater changes in the calculated activities with changes in temperature and composition. Tables 16 and 17 were calculated on this basis and present

TABLE 16—*Activities and Activity Coefficients of SiO_2 in Molten Slags of the System CaO-SiO_2*

Calculated on the assumption that the reaction product is SiO_2 ($_{Soln}$) instead of SiO_2 ($_{\beta\text{-Crist}}$) by the relation $E - E_0 = -\frac{RT}{12F} \ln \frac{1}{a_{SiO_2}}$. To be compared with Table 10 of the text.

Temperature, Deg C.	Mol Fraction of SiO_2					
	0.483		0.533		0.583	
	a	*f*	*a*	*f*	*a*	*f*
1,600	0.0014	0.0029	0.022	0.041	0.130	0.223
1,550	0.0043	0.0089	0.050	0.094	0.242	0.415
1,500					0.478	0.820

TABLE 17—*Relative S_iO_2 Activities of Molten Slags of the System CaO-SiO_2, Referring to Unit Activity of Pure Beta Cristobalite at 1600°C*

Calculated on the assumption that the reaction product is SiO_2($_{Soln}$) instead of SiO_2($_{\beta\text{-Crist}}$) by the relation $E - E_0 = -\frac{RT}{12F} \ln \frac{1}{a_{SiO_2}}$. To be compared with Table 14 of the text.

Slag Designation	Relative SiO_2 Activity at			Change of Relative SiO_2 Activity per 100°C Rise in Temperature
	1600°C	1550°C	1500°C	
0050	0.0014	0.0016		Decreases 22 pct
0045	0.022	0.019		Increases 38 pct
0040	0.130	0.091	0.060	Increases 117 pct

data that can be compared with Tables 10 and 14 of the text.

Further work may provide evidence for a conclusive choice between these possibilities. We considered the suggested form and felt it gave too great a change in activity with both temperature and composition. It must be remembered that the large changes that Darken expects are found in passing over a much wider range of compositions than the reported data include.

In summary, we feel that the discussers have presented interesting alternative interpretations, some of which may be substantiated in the future. The authors' interpretation is in satisfactory agreement with existing experimental data and provides a suitable basis for future work in this field.

Identification of CaO-MgO Orthosilicate Crystals, Including Merwinite ($3CaO \cdot MgO \cdot 2SiO_2$), through the Use of Etched Polished Sections

By R. B. Snow,* Member AIME

(New York Meeting, March 1947)

This paper describes a technique of polishing and etching specimens of open-hearth furnace slags or hearth aggregates for identification of the crystalline constituents—lime (CaO), tricalcium silicate ($3CaO \cdot SiO_2$), dicalcium silicate ($2CaO \cdot SiO_2$), monticellite ($CaO \cdot MgO \cdot SiO_2$), or forsterite ($2MgO \cdot SiO_2$), with especial emphasis on the mineral merwinite ($3CaO \cdot MgO \cdot 2SiO_2$). With proper standardization, this identification does not require the use of the petrographic microscope.

The composition of basic open-hearth slags and furnace bottoms falls, almost without exception, within systems containing CaO, MgO, "FeO," MnO and SiO_2, in which the number of basic molecules so greatly exceeds the orthosilicate ratio (two molecules of base to one of silica) that free basic oxides, and combinations between them such as aluminates or ferrites, are present in cooled specimens. Orthosilicates of (CaO + MgO) are the most common in such specimens, since in nearly all cases, except premelt slags, the molecular ratio of (CaO + MgO) to SiO_2 is more than 2 to 1. When sufficient lime is available it combines with the silica to form dicalcium silicate ($2CaO \cdot SiO_2$), which contains little, if any, MgO, FeO or MnO in solid solution whereas the latter oxides combine to form the oxide solid solution known as periclase. If the lime present is insufficient to form dicalcium silicate ($2CaO \cdot SiO_2$) it combines with MgO to form either merwinite ($3CaO \cdot MgO \cdot 2SiO_2$) or monticellite ($CaO \cdot MgO \cdot SiO_2$); these minerals take little if any FeO or MnO into solid solution and the remaining MgO, FeO and MnO combine as periclase. This generalization seems to be valid for basic slags and furnace bottoms, since minerals such as $CaO \cdot MnO \cdot SiO_2$ and $CaO \cdot FeO \cdot SiO_2$ are found only in slags in which the lime-silica ratio is less than 2 and are not observed in specimens from furnace bottoms.

The identification of crystalline constituents in such materials, especially of fine crystals in the groundmass, is difficult under the petrographic microscope. They are often masked by their neighbors because of their small size in relation to the thickness of the thin section and because of the presence of opaque or colored constituents. The indices of refraction and the optical sign of the mineral are sometimes difficult to determine because of the small size or because of twinning or of inclusions within the crystal. Moreover, the positive identification of merwinite ($3CaO \cdot MgO \cdot 2SiO_2$) from its optical properties is usually difficult in the presence of dicalcium silicate ($2CaO \cdot SiO_2$).

CaO, MgO, $3CaO \cdot SiO_2$ and $2CaO \cdot SiO_2$ in open-hearth slags have been identified for a number of years in the U.S. Steel Corporation Laboratory by the usual

Manuscript received at the office of the Institute Dec. 21, 1946. Issued as T.P. 2167 in Metals Technology, June 1947.

* Research Laboratory, U.S. Steel Corporation, Kearny, New Jersey.

petrographic examination supplemented by examination of polished sections etched in 10 pct aqueous NH_4Cl solution.* The polished surface has the great advantage that each crystal, no matter how small, is revealed as an individual. A further advantage is that it is possible to prepare a polished specimen in 10 to 20 minutes, whereas preparation of a thin section takes much longer.

Method

O. Andersen and M. Baeyertz† developed this means of identification but during the past few years it has been modified and broadened to include merwinite ($3CaO{\cdot}MgO{\cdot}2SiO_2$), monticellite ($CaO{\cdot}MgO{\cdot}SiO_2$) and forsterite ($2MgO{\cdot}SiO_2$). Moreover, by the use of a systematic etching procedure it is now possible to identify crystals in a polished specimen of basic open-hearth slag or furnace bottom without the use of polarized light. This procedure also permits small as well as large crystals of merwinite to be distinguished positively from associated minerals, particularly dicalcium silicate ($2CaO{\cdot}SiO_2$).

This procedure, which has been employed for more than two years, yields such consistent results that the corresponding petrographic examination is often omitted. As identification depends on polishing technique as well as on the nature of the specimen, it is wise to establish standard specimens, which have been checked under the petrographic microscope.

In order to determine the etching characteristics of merwinite ($3CaO{\cdot}MgO{\cdot}2SiO_2$), melts were made having composition in or near the merwinite field; crystals that etched after 30 to 60 sec exposure to the 10 pct NH_4Cl solution were found in each of the compositions that were in equilibrium with merwinite ($3CaO{\cdot}MgO{\cdot}2SiO_2$), either on quenching or after reheating at a temperature where $3CaO{\cdot}MgO{\cdot}2SiO_2$ was in equilibrium with the melt. X-ray data show that $3CaO{\cdot}MgO{\cdot}2SiO_2$ is the constituent in the melts that is attacked by the NH_4Cl solution in the 30 to 60-sec exposure.

More recent work has shown that many specimens are complex and may contain periclase, lime, $3CaO{\cdot}SiO_2$, $2CaO{\cdot}SiO_2$, $3CaO{\cdot}MgO{\cdot}2SiO_2$ and traces of $CaO{\cdot}MgO{\cdot}SiO_2$ as well as one or two constituents that can be recognized but whose composition is unknown. Specimens of this type usually represent material near the interface between partially altered and unaltered material in a rammed bottom. Identification in sections of this type is not clear cut because of increase in the alumina and alkali content of the material. These specimens are in a zone where the last liquid in the system crystallizes out, and for this reason a portion of this paper is devoted to peculiarities that may arise in the course of etching a specimen of this type.

Polishing Technique

Specimens for examination are first mounted in bakelite on a laboratory press, after which the surface for examination is rough-ground (dry) on a belt sander. This is followed successively by the use of 100, 320 and 600 grit *wet-or-dry papers wetted with isopropyl alcohol* on a 9-in. diameter lap having a speed of about 900 rpm, and fitted with a collar-type rim to hold the paper in place. The lap for the final cloth polishing has a speed of between 215 and 400 rpm, depending upon the type of specimen being polished.

The abrasive disks may be used dry but they wear out quickly; experience

---

* Insley has used this solution for differentiating between $2CaO.SiO_2$ and $3CaO.SiO_2$ as shown by a footnote in his article Nature of Glass in Portland Cement Clinker, Jnl. of Research, N.S.B., (1940), **25**, 297.

† O. Andersen was formerly Petrographer, U.S. Steel Corporation Research Laboratory, Kearny, N. J.; M. Baeyertz is Research Metallurgist, South Works, Carnegie-Illinois Steel Corporation, Chicago, Illinois.

has shown that waterproof disks used with plenty of alcohol or water cut more rapidly and last longer than when they are used dry. Either method eliminates the pits in the silicate specimens and leaves fine scratches, which are easily removed on the final cloth. The pits in crystals such as periclase ($MgO + Fe_xO_y$) or chromite $(MgO, FeO)\cdot(Cr_2O_3, Fe_2O_3, Al_2O_3)$ may not be completely removed but they are much smaller and therefore more easily removed than when loose abrasive is used through the cycle. Cloth-backed abrasive disks are superior to paper disks when water or alcohol is used; their longer life and better performance more than compensate for their greater cost. A cloth-backed disk with 600 Carborundum grit (always used wet) did not lose its cutting action after preparation of some 30 specimens, whereas only two or three specimens may be prepared with the paper-backed disks when used wet and only one specimen when used dry.

Final polishing usually is done on a heavy-wool-napped cloth* using levigated alumina, DuPont alumina† or Precisionite.‡ The latter two are dry but can easily be mixed with water or alcohol and after mixing do not agglomerate on standing. The combined polishing time for a silicate or glass specimen amounts to 10 to 15 minutes. If, however, the specimen is to be etched, the surface may not be entirely free of minute scratches, which will show on the etched surface. For specimens of the latter type additional polishing on a second cloth of the same material and provided with the same grade of alumina may help to remove fine scratches.

The double-cloth treatment with suitable alumina and alcohol is our preferred method for polishing $2CaO\cdot SiO_2$, $3CaO\cdot SiO_2$ and CaO in refractories or slags. These minerals decompose in water, but some water usually can be used in polishing specimens of open-hearth slag though the surfaces may show a slight etch. In refractories, on the other hand, these minerals almost always are decomposed on the final polishing cloth when water is used.

As an all-round practice, no water is used when these minerals are suspected. If alcohol is used on the papers as well as in the final polishing even the lime will not be attacked; if the cloth is slightly damp from previous use and alcohol is used CaO will show etching and $3CaO\cdot SiO_2$ and $2CaO\cdot SiO_2$ may also be attacked, especially in a section where the identification is difficult. In such a specimen it is imperative that the best possible polish be given the surface, whereas for general examination this precaution is not imperative. In general, it is advisable to resurface completely an etched surface rather than attempt to remove the etch on the final cloth. When the specimen is removed from the final cloth it is not washed with water but the abrasive and alcohol are wiped from the polished surface with a soft towel or a clean piece of the polishing cloth. This treatment does not cause the scratches suggested above because minerals apparently are not as susceptible to scratching as polished metals.

Etching Technique

The minerals normally present in basic open-hearth slags or furnace bottoms are tabulated in Table 1 according to a systematic etching procedure, using distilled water, a 5 pct (by weight) aqueous solution of NH_4Cl and a 10 pct (by volume) aqueous solution of HCl. A 1 pct nital solution (1 ml HNO_3 solution in 100 ml alcohol) as suggested by Insley[1] can be used instead of the 5 pct NH_4Cl solution for etching $3CaO\cdot SiO_2$ and $2CaO\cdot SiO_2$. Considerable variations from the

* Polishing cloth, finished but undyed, No. 5974; Julius H. Forstmann Co., Passaic, N. J.

† Polishing powder No. P-330, R. and H. Chemical Dept., E. I. DuPont de Nemours and Co., Wilmington, Del.

‡ The Precision Scientific Co., Chicago, Ill.

[1] References are at the end of the paper.

etching time suggested in Table 1 may be found unless distilled water is used at a constant temperature (80°F). If the temperature of the water changes from one time to another the rate of attack on CaO, $3CaO \cdot SiO_2$ and $2CaO \cdot SiO_2$ likewise changes; also, the pH of ordinary tap water is subject to variation. Specimens etched in water are not rewashed in water but are rinsed with isopropyl alcohol and are then dried in a blast of warm air, a type of drying that eliminates most of the staining that may accompany etching. When the NH_4Cl or the HCl solution is used the specimen is washed briefly in cold tap water before rinsing in alcohol and drying.

Etching a crystal causes darkening of its polished surface, the appearance of scratches, evidence of relief (not the result of polishing), appearance of twinning lines, lines related to the crystal structure, cleavage lines, or the appearance of an iridescent surface film.

TABLE 1—*Etching Time for Minerals Found in Furnace-bottom and Slag Specimens*

Mineral	Composition	Rate of Attack by Etchants		
		Distilled H_2O	5 Pct NH_4Cl[a]	10 Pct HCl[b]
Lime	CaO	3–5 sec	very rapid	very rapid
Tricalcium silicate	$3CaO \cdot SiO_2$	10–40 sec	3 sec	very rapid
Dicalcium silicate	$2CaO \cdot SiO_2$	10–60 sec	3 sec	very rapid
Intermediate etching constituent		?	4–6 sec	very varid
Merwinite	$3CaO \cdot MgO \cdot 2SiO_2$		15–60 sec	rapid
Monticellite	$CaO \cdot MgO \cdot SiO_2$		tr	3–6 sec
Forsterite	$2MgO \cdot SiO_2$			tr
Glaucochroite	$CaO \cdot MnO \cdot SiO_2$		tr	3–6 sec
Periclase	$(MgO + Fe_xO_y)$		attack[c]	attack
Monocalcium ferrite	$CaO \cdot Fe_2O_3$			attack
Dicalcium ferrite	$2CaO \cdot Fe_2O_3$			attack
Brownmillerite	$4CaO \cdot Al_2O_3 \cdot Fe_2O_3$			attack
Isotropic dark gray nonetching constituent, index 1.615	?	darkens		attack
Isotropic constituent	(glass)			attack

[a] Weight per cent in distilled water.
[b] Volume per cent in distilled water.
[c] Crystals containing large amounts of FeO and Fe_2O_3.

IDENTIFICATION

On a polished surface individual crystals appear as a shade of gray that is a relative measure of the mean refractive index of the crystal, but the observer's eye is not capable of differentiating between crystals of nearly equal index except by noting grain boundaries. Crystals having refractive indices between 1.50 and 1.65 would be termed "dark gray" but the exact shade depends on the index of the mineral. Crystals having refractive indices between 1.65 and 1.80 are "medium gray" and crystals having indices above 1.80 are "light gray" but become more highly reflecting as the index of refraction increases. In a polished section it is almost impossible to distinguish between $3CaO \cdot SiO_2$, $2CaO \cdot SiO_2$, $3CaO \cdot MgO \cdot 2SiO_2$ $CaO \cdot MgO \cdot SiO_2$ and $2MgO \cdot SiO_2$ by their color in reflected light, although the latter two should be slightly darker gray than the others. $2MgO \cdot SiO_2$ has slightly greater relief than the other minerals in the series. The structures as viewed under the ore microscope seem to be more easily distinguished when a daylight filter is used, although the micrographs in Figs 1 to 10 were taken on a metallographic microscope using a yellow-green filter.

Fig 1 represents an unetched section of a furnace-bottom specimen showing four different shades of gray. After 5 sec in distilled water (Fig 2) the next to

darkest gray constituent has been etched with the formation of an iridescent film, which shows relief and is identified as lime. After 15 sec (total) in distilled water a portion of the darkest gray constituent (Fig 3) has darkened and previously unobserved scratches are noted; this portion of the original darkest gray material is $3CaO \cdot SiO_2$ while the lime has a similar appearance in the photograph but visually it has an iridescent surface.

A further treatment of 3 sec in 5 pct NH_4Cl solution of the same specimen (Fig 4) causes the lime to be largely etched out. The $3CaO \cdot SiO_2$ now has an iridescent surface film while twinning lines show the remainder of the darkest gray constituent to be $2CaO \cdot SiO_2$. The rounded crystals that showed relief in Fig 1 are periclase and the lightest gray material, which we shall call an oxide constituent, probably has a composition between brownmillerite ($4CaO \cdot Al_2O_3 \cdot Fe_2O_3$) and dicalcium ferrite ($2CaO \cdot Fe_2O_3$).

Fig 5 shows a section through a melt made in the merwinite field after etching for 45 sec in a 10 pct NH_4Cl solution (5 pct solution would have given a slightly lighter etch). The rounded crystals showing herringbone twinning are $3CaO \cdot MgO \cdot 2SiO_2$ the groundmass is $CaO \cdot MgO \cdot SiO_2$ and $3CaO \cdot MgO \cdot 2SiO_2$.

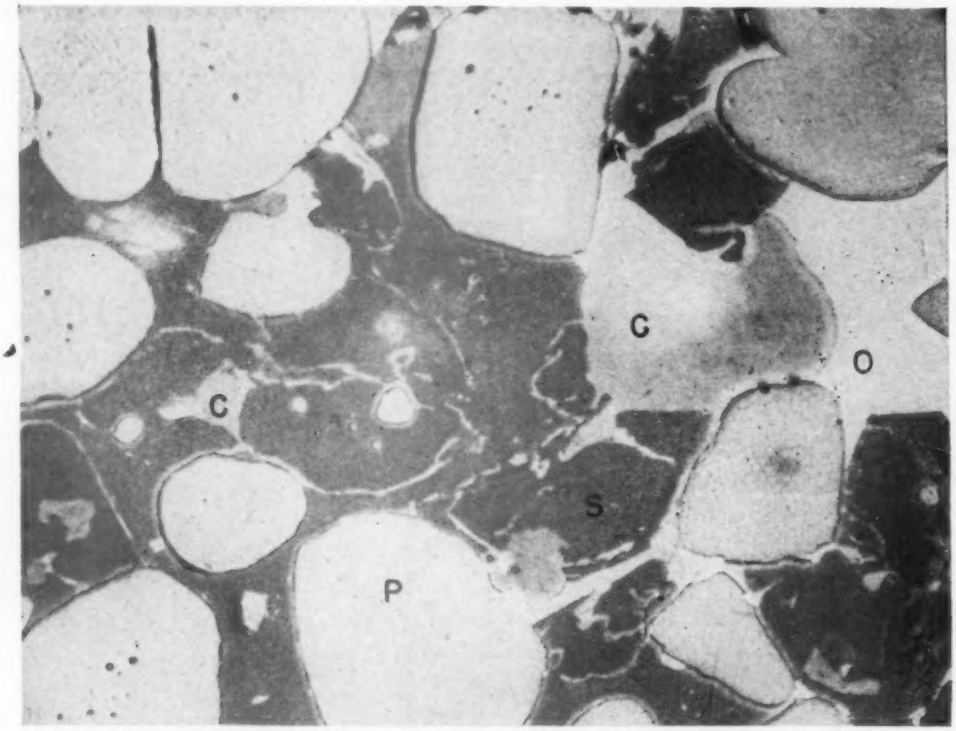

FIG 1—SPECIMEN OF A FURNACE BOTTOM. POLISHED SECTION, UNETCHED. × 500.
Periclase *P*, oxide constituent *O*, and silicate *S*, which contains lighter gray inclusions of lime *C*.
Original magnification given; reduced one fourth in reproduction.

Monticellite ($CaO \cdot MgO \cdot SiO_2$) is never more than barely etched by a 5 pct NH_4Cl solution but is attacked by a 3 to 6-sec exposure to a 10 pct HCl solution; $2MgO \cdot SiO_2$ is not attacked by this treatment.

DETAILED OBSERVATIONS

Periclase ($MgO + Fe_xO_y$ in solid solution) usually is present as rounded crystals, which have the highest relief in the

polished section (Fig 1) unless the section contains chromite (MgO, FeO)·(Cr_2O_3, Al_2O_3, Fe_2O_3). Periclase in furnace bottoms contains both FeO and Fe_2O_3 in solid solution; the crystals are medium gray when pure but become more highly reflecting the larger the amount of iron oxide present. Many periclase crystals contain minute acicular inclusions of a highly reflecting constituent. This is thought to be magnesium ferrite, MgO·Fe_2O_3, that has crystallized out along crystallographic planes from the solid solution during cooling. Where MgO has recrystallized along an interface the crystals may occur as small octahedrons rather than rounded crystals. In some specimens almost the entire mass is composed of the MgO-Fe_xO_y solid solution. This is believed to be mainly an MgO + FeO solid solution because in all furnace-bottom specimens except those from the hearth surface the amount of FeO greatly exceeds the amount of Fe_2O_3 present.

Periclase crystals that contain up to approximately 40 pct of FeO and Fe_2O_3 in solid solution usually do not show attack after 6 sec in the 10 pct HCl solution; crystals containing larger amounts of FeO and Fe_2O_3 in solid solution may etch in the 5 pct NH_4Cl solution.

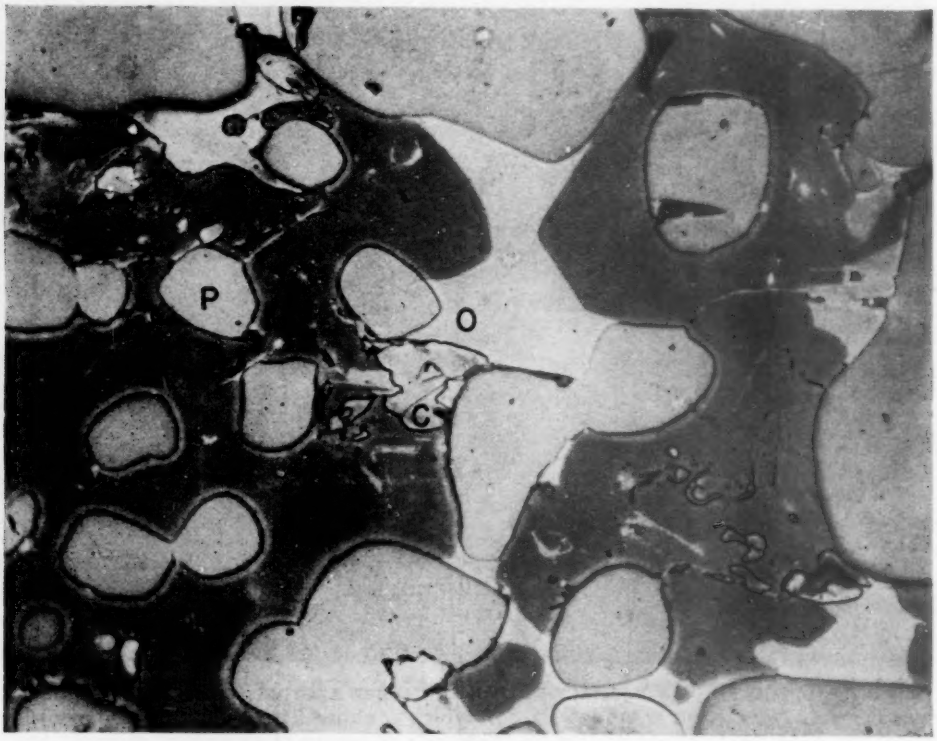

FIG 2—FURNACE BOTTOM. POLISHED SECTION. ETCHING 5 SECONDS DISTILLED WATER. × 500. Lime *C* etched and iridescent, oxide constituent *O*, periclase *P* and silicate *S* unchanged. Original magnification given; reduced one fourth in reproduction.

The Oxide Constituent in the furnace bottoms, which usually has the highest reflectivity of the crystals present, may vary in amount from a few scattered crystals to the entire groundmass or very large rectangular crystals that surround other constituents. It is usually present in larger amounts where the Al_2O_3 content is highest, and under this condition is believed to have a composition near that of brownmillerite $4CaO·Al_2O_3$·-

Fe_2O_3, as judged from the indices of refraction of the crystals. In open-hearth slags the indices of refraction of these crystals are higher than in furnace bottoms but are appreciably lower than those for either monocalcium or dicalcium ferrite

Tricalcium Silicate ($3CaO \cdot SiO_2$) is a medium gray mineral, which after 10 to 40 sec in distilled water (80°F) becomes light brown, with a surface that may or may not be roughened (Fig 3). Almost always $3CaO \cdot SiO_2$ becomes iridescent after

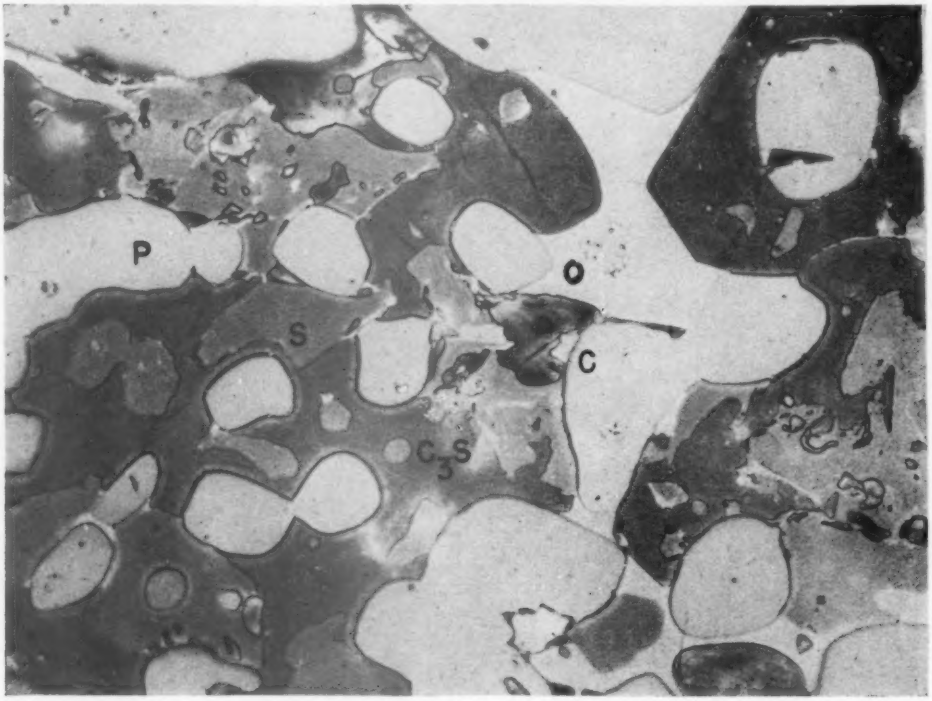

FIG 3—SAME FIELD AS IN FIGURE 2. ETCHING 15 SECONDS DISTILLED WATER. × 500.
Additional darkened areas indicate $3CaO \cdot SiO_2$ while the remainder of the silicate has not been attacked.

($CaO \cdot Fe_2O_3$ or $2CaO \cdot Fe_2O_3$). These oxide constituents are not etched by water or by the 5 pct NH_4Cl solution but may be etched after treatment in 10 pct HCl solution.

Lime (CaO) is rather light gray in polished sections and may occur as inclusions in dicalcium silicate or as single crystals (Fig 1). It stands out in relief and has an iridescent surface (etched) after a 3 to 5-sec exposure to distilled water at 80°F (Fig 2). It is rapidly etched out by 5 pct NH_4Cl solution and is completely removed by a short exposure to 10 pct HCl solution. However, CaO may etch out during polishing if water has been used in the cycle.

40 to 60 sec in water, whereas this treatment never causes the surface of $2CaO \cdot SiO_2$ crystals to show iridescence, and this difference seems to be a guide when distinguishing $2CaO \cdot SiO_2$ from $3CaO \cdot SiO_2$ in a difficult specimen. The $3CaO \cdot SiO_2$ is readily attacked, with the formation of a smooth iridescent surface, by the 5 pct NH_4Cl solution, but the separation between $3CaO \cdot SiO_2$ and $2CaO \cdot SiO_2$ is not as distinct as when water is used; a 10 pct HCl solution decomposes it to such an extent that only holes remain. Near the surface of a furnace bottom $3CaO \cdot SiO_2$ may etch with a pebbled surface (this type gives a pebbled iridescent surface with 5 pct NH_4Cl) or it may show a smooth

surface with parallel lines in one, two, or three directions (Fig 6). In a few sections, crystals that were believed to be $3CaO{\cdot}SiO_2$ did not etch until the surface distilled water causes the crystals to become brownish but usually there is no difference in appearance of the twins and in contrast to $3CaO{\cdot}SiO_2$ the crystals

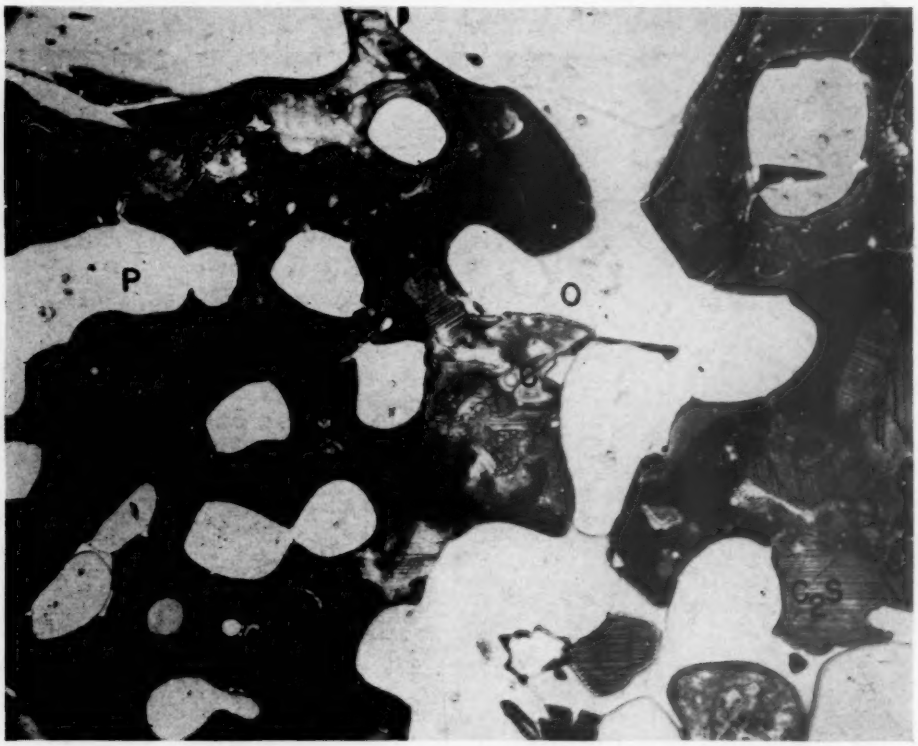

FIG 4—SAME AS IN FIGURES 2 AND 3. ETCHING 3 SECONDS 5 PER CENT NH_4Cl SOLUTION (AFTER 15 SECONDS DISTILLED WATER). × 500.
$2CaO{\cdot}SiO_2(C_2S)$ areas now etched to show parallel twinned structure, with $3CaO{\cdot}SiO_2(C_3S)$ darkened further and iridescent and lime (C) largely etched out.

of the $2CaO{\cdot}SiO_2$ crystals had changed from gray to brown (after 30 to 50 sec exposure to the distilled water). The reason for the latter type of etching may be lack of solid solution in the $3CaO{\cdot}SiO_2$ or the result of a temperature change while in the furnace bottom.

Dicalcium Silicate ($2CaO{\cdot}SiO_2$) is slowly attacked by distilled water at 80°F but if the exposure is less than about 40 sec the material may or may not show a brown coloration. Faint twinning lines may appear if the specimen has been properly polished but scratches will be discernible if the latter have not been completely removed. Longer exposure to usually do not become iridescent when etched in water. On the other hand, a 2 to 3-sec exposure to 5 pct NH_4Cl solution seems to cause attack at the boundary between the parallel twins (after the water etch) so that they stand out in contrast to the rest of the grain (Fig 4). In addition, $3CaO{\cdot}SiO_2$ always turns iridescent in 5 pct NH_4Cl solution after the water etch whereas $2CaO{\cdot}SiO_2$ usually retains its brown color with this short exposure to the etchant. The 5 pct solution seems to permit a better separation between the $2CaO{\cdot}SiO_2$ and $3CaO{\cdot}SiO_2$ than the 10 pct solution as initially used, and, in addition, the stronger

solution almost always overetches the $2CaO \cdot SiO_2$ in the specimen, and for some specimens a 2 pct NH_4Cl etchant might give better results; overetching of the Al_2O_3 is unknown). This constituent does not become iridescent with longer exposure to water whereas CaO and $3CaO \cdot SiO_2$ always, or almost always,

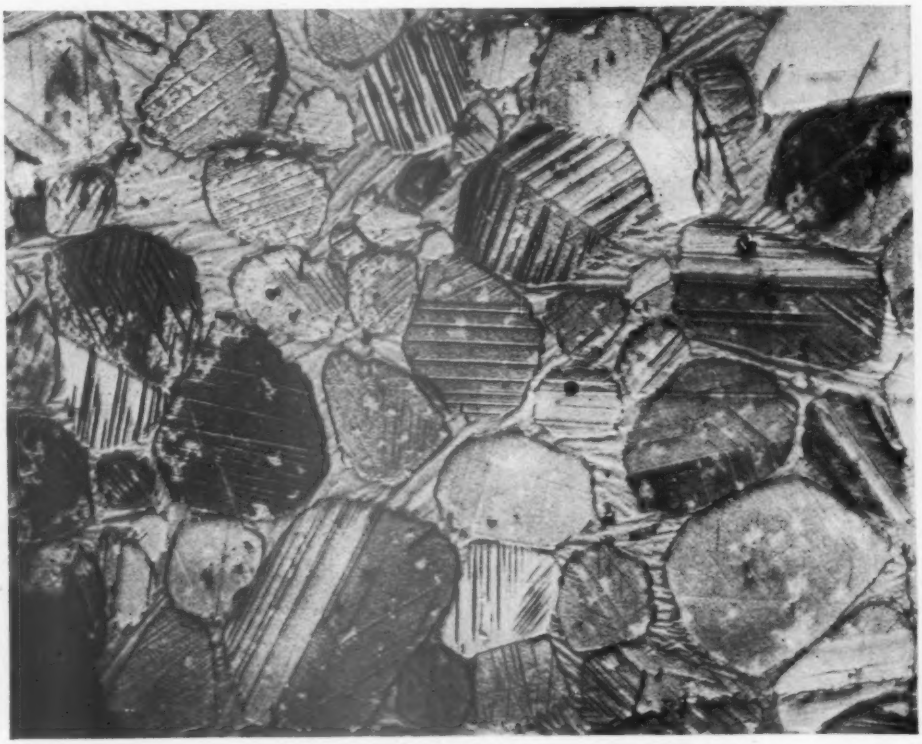

FIG 5—MELT IN MERWINITE ($3CaO \cdot MgO \cdot 2SiO_2$) FIELD OF $CaO\text{-}MgO\text{-}SiO_2$ SYSTEM. POLISHED SECTION. ETCHING 45 SECONDS 10 PER CENT NH_4Cl SOLUTION. × 500.
Complexly twinned crystals of merwinite ($3CaO \cdot MgO \cdot 2SiO_2$) in groundmass of $3CaO \cdot MgO \cdot 2SiO_2$ and monticellite ($CaO \cdot MgO \cdot SiO_2$).

causes the surface to have a somewhat mottled, iridescent appearance. Usually $2CaO \cdot SiO_2$ is completely decomposed by exposure of more than about 8 sec to the 5 pct NH_4Cl solution and the crystals usually decompose so rapidly in the 10 pct NH_4Cl solution that holes appear after only a short exposure.

A constituent having the same color as $2CaO \cdot SiO_2$, but which etches in distilled water in 3 to 5 sec, had been found in the partially altered zone of a rammed bottom. Chemical analyses showed that this zone contained both Na_2O and Al_2O_3 (Na_2O is added because it causes the material to cold-set after ramming but the source become iridescent; but this constituent is slightly darker gray than CaO. After 10 sec in water the crystals may have a slightly brownish color and occasionally one is twinned. In addition, $2CaO \cdot SiO_2$, which accompanies this rapidly etching constituent, may show faint twinning lines after 10 sec exposure to water. This type of material usually is discernible only when the specimen has been given the best possible polish and alcohol is used throughout the cycle.

A comparison between the behavior of this rapidly etching constituent and the results obtained by Green[2] and Green and Bogue,[3] on melts containing CaO

and SiO_2 with Al_2O_3, Na_2O and Fe_2O_3, indicates that the crystals may be $2CaO \cdot SiO_2$ with both Al_2O_3 and Na_2O in solid solution, or may represent the products of exsolution when alpha $2CaO \cdot SiO_2$ transformed to the beta phase (the furnace-bottom specimens were slowly cooled with the furnace after the fuel was shut off). In several instances, the rapidly etching constituent appeared as a groundmass for lath-shaped crystals, which etch in the NH_4Cl solution as if they were $2CaO \cdot SiO_2$; a similar type of structure was reported by Green.[2]

Crystals that etch simultaneously with the polysynthetically twinned $2CaO \cdot SiO_2$ but that show no internal structure are believed to be $2CaO \cdot SiO_2$; the lack of twinning may be related to solid solution. The large polysynthetically twinned $2CaO \cdot SiO_2$ crystals are not observed near the surface of the furnace bottom nor in the furnace slags and therefore represent crystals that were not heated to steelmaking temperatures or that transformed through very slow cooling. The more complexly twinned type found near the surface of the furnace bottom and in slags (Fig 6) probably represents the material that transformed rapidly to the beta type during cooling.

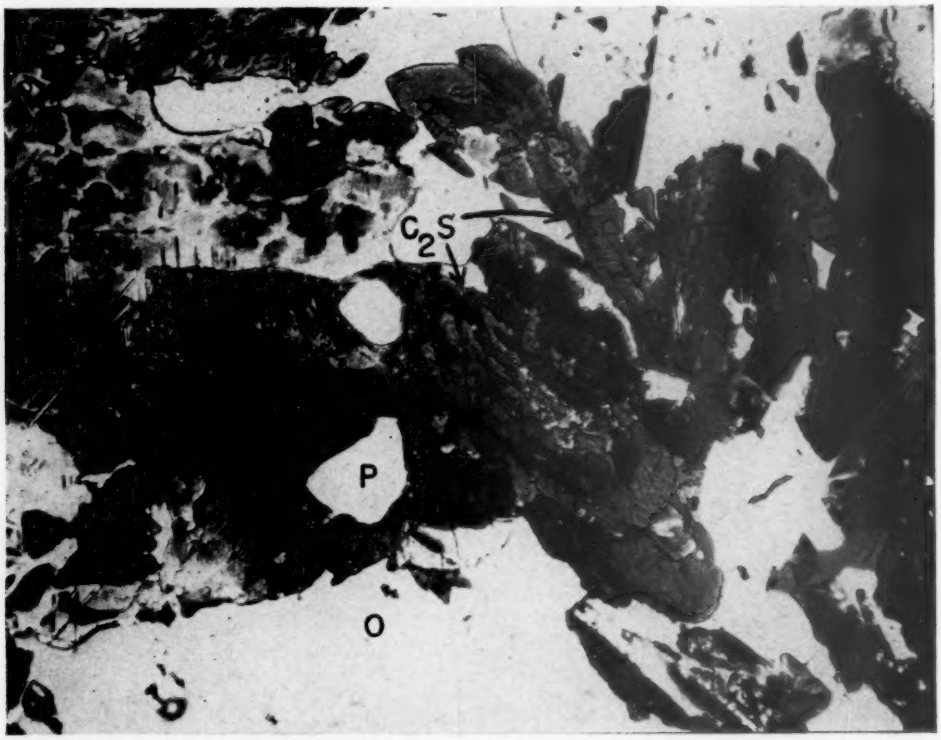

FIG 6—FURNACE BOTTOM. POLISHED SECTION. ETCHING 25 SECONDS DISTILLED H_2O + 2 SECONDS 5 PER CENT NH_4Cl SOLUTION. × 500.

Periclase *P*, oxide constituent *O*, $3CaO \cdot SiO_2$ (C_3S) with lines in three directions, and $2CaO \cdot SiO_2$ (C_2S) with complex twinning.

Original magnification given; reduced one fourth in reproduction.

In many instances $2CaO \cdot SiO_2$ contains CaO either as pointlike inclusions (in rapidly cooled material) or as stringers as large as those shown in Figs 2 and 3, and usually is associated with $3CaO \cdot SiO_2$ or may have the outline of crystals of that mineral. This type of $2CaO \cdot SiO_2$ undoubtedly has been formed through the decomposition of $3CaO \cdot SiO_2$ and probably resulted from lowering of the

temperature by change in the position of the material in the bottom through patching or during the final cooling of the bottom. It is possible that a slow transformation might permit the CaO to form as relatively large crystals (Fig 7).

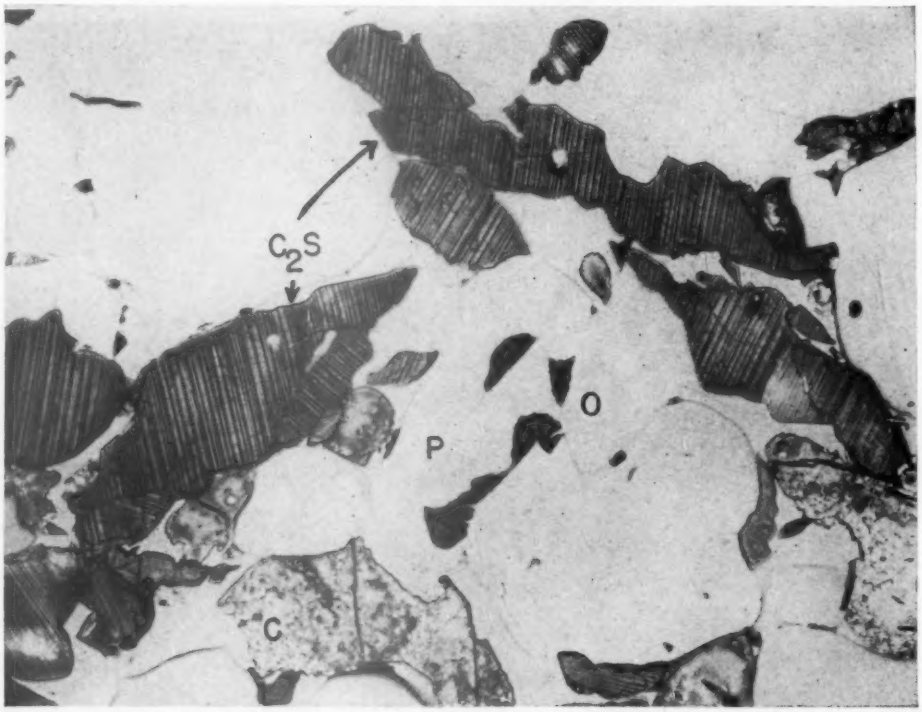

FIG 7—FURNACE BOTTOM. POLISHED SECTION. ETCHING 15 SECONDS DISTILLED H_2O + 3 SECONDS 5 PER CENT NH_4Cl SOLUTION. × 500.
Periclase *P*, oxide constituent *O*, lime *C* and twinned $2CaO \cdot SiO_2$ (C_2S); $3CaO \cdot SiO_2$ not observed in this specimen.
Original magnification given; reduced one fourth in reproduction.

Intermediate Etching Constituent.—Specimens from a new furnace bottom after a few months service have shown alteration downward to a certain level. Above this line of demarcation CaO, $3CaO \cdot SiO_2$, $2CaO \cdot SiO_2$ and $4CaO \cdot Al_2O_3 \cdot Fe_2O_3$ (or related constituents) are present but below this level only minor amounts of the oxide constituent are encountered and $2CaO \cdot SiO_2$ may or may not be present, depending on the initial composition of the bottom material. In furnace bottoms where $2CaO \cdot SiO_2$ was not an original constituent, the interface between material containing $2CaO \cdot SiO_2$ and the underlying unaltered material contains three or four unusual constituents.

Bordering the $2CaO \cdot SiO_2$ is a very thin band of crystals that are only faintly etched after 3 sec in 5 pct NH_4Cl solution (following etching in water) and that are fairly well etched after 4 to 6 sec exposure to the etchant (Fig 8). This constituent is not overetched until 8 to 15 sec in the NH_4Cl solution while the $2CaO \cdot SiO_2$ is occasionally overetched with even 3 sec exposure to this solution. This constituent has been designated as the intermediate type of etching constituent in Table 1 because these crystals usually separate $2CaO \cdot SiO_2$ from $3CaO \cdot MgO \cdot 2SiO_2$. The chemical composition is unknown, but it may belong to the $2CaO \cdot SiO_2$ or a $3CaO \cdot MgO \cdot 2SiO_2$ series of solid solutions possibly with P_2O_5.[4]

Merwinite ($3CaO \cdot MgO \cdot 2SiO_2$) usually

is found adjacent to this intermediate etching constituent in furnace-bottom specimens, and if properly polished may show faint attack after 6 to 10 sec exposure to the 5 pct NH_4Cl solution. No attack was noted visually in the section shown in Fig 8 until after about 10 to 15 sec exposure but scratches that were not observed visually after 4 sec exposure were recorded on the film. After 45 sec exposure to the NH_4Cl solution this constituent is well etched (Fig 9) and shows its twinned structure. The $3CaO{\cdot}MgO{\cdot}2SiO_2$ found in melts prepared in or near the merwinite field in the CaO-MgO-SiO_2 system is shown in Figs 5 and 10. The $3CaO{\cdot}MgO{\cdot}2SiO_2$ is not attacked by water and may be polished without the aid of alcohol. In two or three cases twinning lines etched with much higher contrast after the specimen had been treated with boiling water for 2 sec before the 5 pct NH_4Cl etch; visually the $3CaO{\cdot}MgO{\cdot}2SiO_2$ showed no change after the treatment in boiling water. Initially a 10 pct NH_4Cl solution was used for the identification of $3CaO{\cdot}MgO{\cdot}2SiO_2$ but the 5 pct solution gives almost identical results.

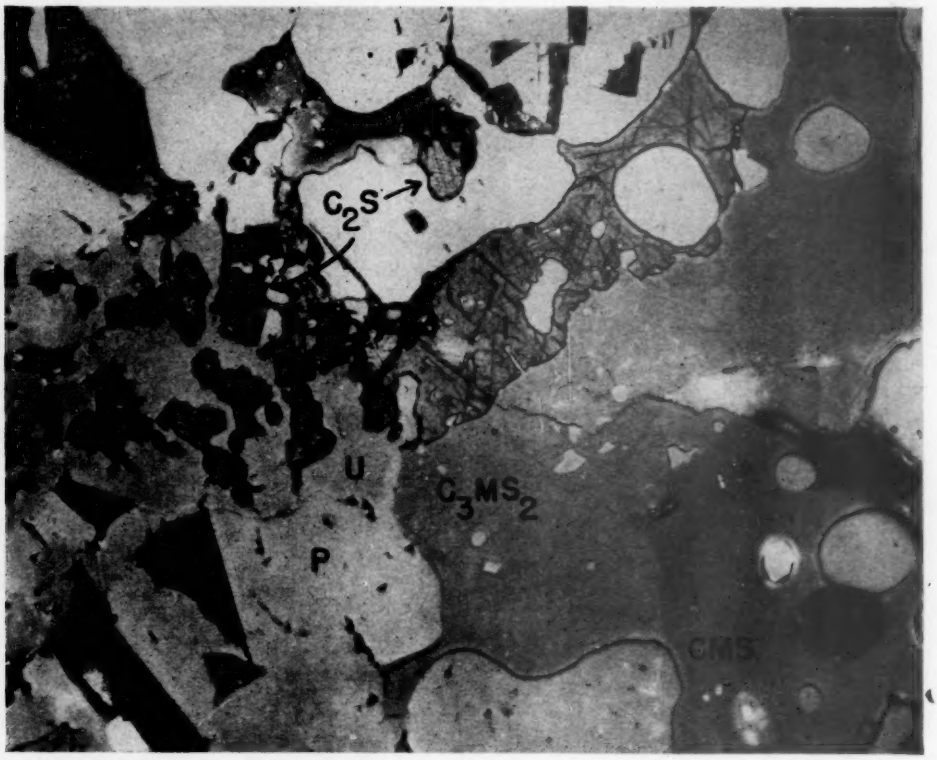

FIG 8—FURNACE BOTTOM. POLISHED SECTION. ETCHING 4 SECONDS 5 PER CENT NH_4Cl SOLUTION. × 500.

Periclase *P*, intermediate etching constituent *I*, unidentified light gray constituent *U*, $3CaO{\cdot}MgO{\cdot}2SiO_2$ (C_3MS_2) and $CaO{\cdot}MgO{\cdot}SiO_2$ (CMS).

Original magnification given; reduced one fourth in reproduction.

Monticellite ($CaO{\cdot}MgO{\cdot}SiO_2$) is never more than barely etched by a 5 pct NH_4Cl solution even after 4 minutes exposure; the surface, however, is roughened, and surface scratches become clearly visible after a 3 to 6-sec exposure to 10 pct HCl solution. On the other hand, $3CaO{\cdot}SiO_2$, $2CaO{\cdot}SiO_2$ and $3CaO{\cdot}MgO{\cdot}2SiO_2$ are usually so completely decomposed by the

latter reagent that only holes show the positions of the crystals.

Forsterite ($2MgO \cdot SiO_2$) is distinguished from $CaO \cdot MgO \cdot SiO_2$ by the fact that a possible unit-cell dimension of 11.98 Å, but no lines of the impurities were observed. This constituent has not been synthesized in pure enough form to determine its composition, but it is largely CaO and Al_2O_3 with some Na_2O. It darkens slightly during etching but is never

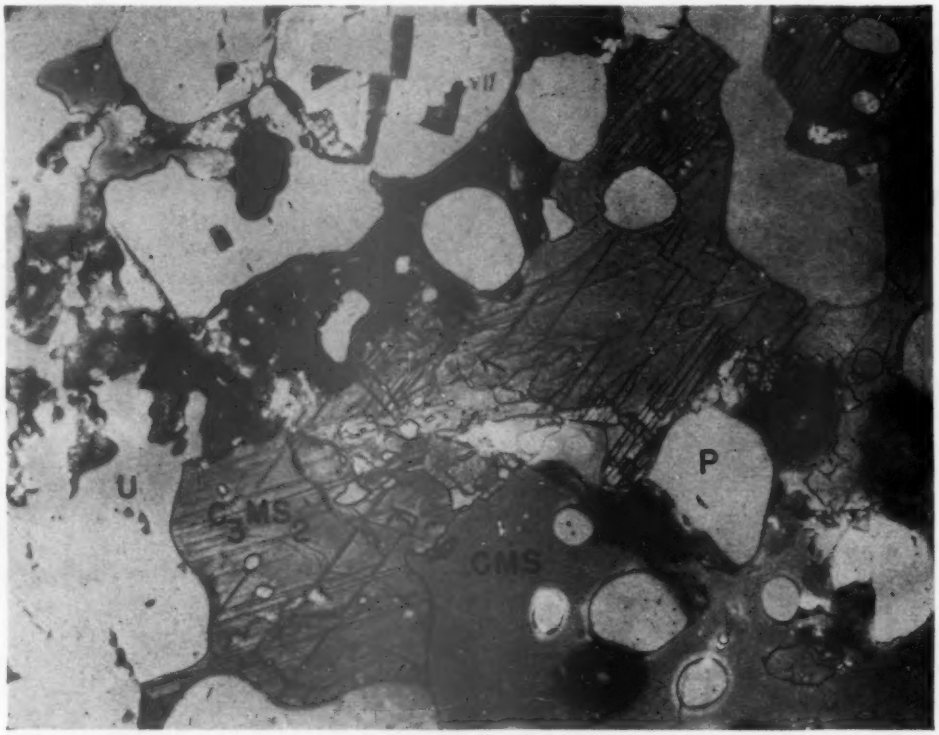

FIG 9—SAME FIELD AS IN FIGURE 8. ETCHING 45 SECONDS 5 PER CENT NH_4Cl SOLUTION. × 500. $2CaO \cdot SiO_2$ and intermediate etching constituent now dissolved, $3CaO \cdot MgO \cdot 2SiO_2$ (C_3MS_2) well etched, other constituents unetched.

6-sec attack by 10 pct HCl solution does not roughen the surface nor bring out the scratches that usually are present on the crystal surface. In addition, $2MgO \cdot SiO_2$ has greater relief than any of the other silicate constituents discussed.

Dark Gray Constituents.—In the furnace bottoms there are two types of dark gray material. One is isotropic with variable index and probably is a frozen liquid or glass, while the other is also isotropic with a constant index of about 1.615 and usually occurs in large masses with regularly oriented inclusions. A pocket of the latter material with $2CaO \cdot SiO_2$ and probably $4CaO \cdot Al_2O_3 \cdot Fe_2O_3$ as impurities gave the X-ray pattern of Table 2 with a

TABLE 2—*Interplaner Spacings for the Dark Gray Nonetching Constituent*

I^a	d/n	Index	Lattice Constant, Å
S	4.881	211	11.956
W	3.204	321	11.988
M	3.003	400	12.012
W	2.754	331	12.005
S	2.680	420	11.985
W	2.552	332	11.969
S	2.444	422	11.946
M	2.188	521	11.983
S	2.122	440	12.004
S	1.944	611	11.984
W	1.662	640	11.985
M	1.604	642	12.003
			11.985 avg.

[a] S, strong; W, weak; M, medium.

definitely attacked except by 10 pct HCl solution. It is unusual because it often occurs with periclase ($2CaO \cdot SiO_2$, $4CaO \cdot Al_2O_3 \cdot Fe_2O_3$), possibly CaO or $3CaO \cdot SiO_2$ and chromite.

having a lime-silica ratio of 1.7 to 1.9 etches after 30 to 60 sec attack by the 5 pct NH_4Cl solution. It usually shows the twinning lines of $3CaO \cdot MgO \cdot 2SiO_2$ and may represent $3CaO \cdot MgO \cdot 2SiO_2$ with

FIG 10—POLISHED SECTION OF MELT MADE IN EDGE OF PERICLASE FIELD BUT NEAR DICALCIUM SILICATE AND MERWINITE FIELDS IN $CaO-MgO-SiO_2$ SYSTEM. ETCHING 45 SECONDS 10 PER CENT NH_4Cl SOLUTION. × 500.

This melt was reheated so as to form $3CaO \cdot MgO \cdot 2SiO_2$ (twinned) and periclase. Untransformed $2CaO \cdot SiO_2$ etched out and is represented by black voids. Cooling was so slow that some $CaO \cdot MgO \cdot SiO_2$ is found between the $3CaO \cdot MgO \cdot 2SiO_2$ crystals.

Other Constituents.—If much P_2O_5 is in solid solution $2CaO \cdot SiO_2$ seems to etch slowly. Quenched as well as normally cooled slags with high P_2O_5 content contain constituents that are not attacked after a 4-minute exposure to the 5 pct NH_4Cl solution.

The lighter gray nonetching constituent in Fig 9 has not been identified but it is occasionally found in areas where a large amount of liquid accumulated and from which small crystals separated out during cooling.

A constituent in open-hearth slags

either FeO or MnO or P_2O_5 in solid solution.

Another constituent that etches after a 20 to 50-sec exposure to 5 pct NH_4Cl solution in a manner similar to that shown for $3CaO \cdot MgO \cdot 2SiO_2$ has been found in the nonmetallic matter associated with high-carbon ferromanganese (the material is thought to be furnace slag that was not separated from the metal before shipment). X-ray data do not positively identify this constituent as $3CaO \cdot MgO \cdot 2SiO_2$ because the other constituents present are solid solutions

and X-ray standards are not available for identifying the interplaner spacings of the various constituents present.

Crystals such as $FeO{\cdot}CaO{\cdot}SiO_2$ or glaucochroite ($CaO{\cdot}MnO{\cdot}SiO_2$) may be distinguished from $CaO{\cdot}MgO{\cdot}SiO_2$ on the basis of chemical composition. Glaucochroite in the premelt open-hearth slags is in the form of needle-like crystals, which etch very rapidly in the 10 pct HCl solution and which may be very faintly etched after 4 minutes exposure to 5 pct NH_4Cl solution; these slags contain 15 to 30 pct of $MnO + FeO$ while $CaO{\cdot}MgO{\cdot}SiO_2$ would not be expected to be present because the MgO content is low. The details on the etching of $CaO{\cdot}FeO{\cdot}SiO_2$ or other solid solutions in these orthosilicates are not known.

Conclusions

A procedure has been developed by means of which the principal crystalline constituents in basic open-hearth slags and furnace bottoms may be identified through the examination of etched polished sections without the use of a petrographic microscope.

This method is especially recommended for distinguishing the mineral merwinite ($3CaO{\cdot}MgO{\cdot}2SiO_2$) from associated constituents.

One new constituent is reported but its composition has not been determined by synthesis although its X-ray pattern is given.

A few notes on related lime-bearing orthosilicates are included.

In any other relatively closed system the minerals present could possibly be identified by etching polished sections. This type of identification should be useful, especially in the field of chrome-bearing refractories, where the crystal constituents are small and are masked by the highly colored or nearly opaque chromite crystals $(FeO, MgO){\cdot}(Cr_2O_3, Al_2O_3, Fe_2O_3)$.

Acknowledgment

The assistance given by John V. Kelly, during part of this investigation was appreciated and is acknowledged with thanks.

References

1. H. Insley: Nat. Bur. Stds. *Jnl. of Res.* (1936) **17**, 353–361.
2. K. T. Green: Nat. Bur. Stds. *Jnl. of Res.* (1944) **32**, 1.
3. K. T. Green and R. H. Bogue: Nat. Bur. Stds. *Jnl. of Res.* (1946) **36**, 185.
4. K. Balajiva, A. Quarrell and P. Vajragupta: A Laboratory Investigation of the Phosphorus Reaction in the Basic Steel Making Process. Iron and Steel Inst., Advance Copy (April 1946) 27.

DISCUSSION

(B. M. Larsen presiding)

R. B. Sosman*—The part of the ternary diagram in which the eruptive rock petrologists are most interested is the more siliceous half, particularly toward the MgO-SiO_2 side. The pyroxenes and the orthosilicate minerals forsterite and monticellite are minerals familiar to the petrologists, while larnite ($2CaO.SiO_2$) and merwinite are relatively very rare. Iron oxide, formally stated as FeO, is an almost universal constituent of the pyroxenes and of the magnesian orthosilicates, forming with the latter the crystalline solution called "olivine." Tricalcium silicate ($3CaO.SiO_2$) is unknown under natural conditions. Why the rocks and minerals high in CaO are so uncommon is not known, unless it be that they are so much more susceptible to hydrolysis than the magnesian series.

A special problem in the pyroxenite and peridotite (orthosilicate) rocks is their surprisingly low temperature of intrusion. Peridotite, particularly, fusible only at a temperature in the vicinity of 1600–1800°C, has been intruded into sedimentary rocks when at a temperature hardly more than 500°C, as I was able to show by a study of inclusions of coal in a peridotite dike.† When we find what natural conditions were responsible for this low temperature of intrusion, we may hope to build a refractory furnace bottom by the same process.

B. M. Larsen—This method has been found useful in unravelling the complexities in the

* U. S. Steel Corp., Kearny, N. J.
† *Amer. Jnl. Science* (5) (1938) **35**-A, 535-539.

slag-soaked layers of open hearth bottoms. Probably the method is so new in some respects, at least among the steelmaking fraternity, that it will require some testing and experimentation before being certain of it.

R. B. SNOW (author's reply)—The initial identification of these minerals, is made through the use of thin sections and powdered specimens examined under the petrographic microscope.

X-ray diffraction patterns are helpful in checking the identification if solid solution has not caused a shift in the lines or if the constituents do not have similar diffraction patterns and if a sufficient amount of the constituent is present in the specimen to give a positive identification.

Oxygen in Liquid Open-hearth Steel—Oxygen Content during the Refining Period

By T. E. Brower* and B. M. Larsen* Member AIME

(Atlantic City Meeting, November 1946)

In an earlier paper[1] we discussed a simple, rapid method of taking samples of liquid steel and analyzing them for oxygen, which, though possibly not absolutely accurate (as is likewise true of all other methods), certainly yields results that are satisfactorily consistent. Accordingly, samples from hundreds of heats in different shops were analyzed for oxygen, with results sufficient in number to be handled statistically and permit estimation of some general trends. Measurements were made in acid as well as in basic open hearths, throughout the refining period, to learn how stirring, blocking, adding ore or lime or sand, affects the oxygen content of the bath; we also followed the changes brought about by tapping, teeming, and deoxidizing. Some of these results, discussed in an earlier paper,[2] bring out the dominant role of the carbon-oxygen reaction in regulating degree of oxidation both of metal and of slag, also the marked variability of concentration of dissolved oxygen [O] in excess of that which would be in equilibrium with carbon and with carbon monoxide at a partial pressure of one atmosphere.

As a logical beginning on this complex problem, we take up in the present paper the variability of this excess oxygen, Δ[O], when other factors are as constant as they ever are in open-hearth operation; namely, toward the end of the refining period, when the bath may be regarded as in the comparatively steady state it approaches in absence of disturbing factors. This condition was chosen because by that time the significant reactions, except carbon oxidation, between slag and metal have come to substantial equilibrium; this facilitates interpretation of the complex situation and thus permits more definite conclusions to be drawn. This excess concentration of oxygen, Δ[O], in the metal is needed, of course, to make the steelmaking process go at a reasonable rate; alternatively it may be regarded as a measure of the virtual pressure increment above one atmosphere, or of the degree of supersaturation, of carbon monoxide in the metal.

According to our measurements, the excess concentration Δ[O] in liquid steel varies from about 0.009 to 0.035 per cent oxygen by weight. It is quite sensitive to change of conditions, being altered temporarily by operations such as stirring with green poles, additions of ore, lime, or sand; but as the disturbance works itself out, it resumes a level within the intermediate range characteristic of the steady state. The conditions most common in average furnace practice are covered by the following:

Conditions	Δ[O] Usual Per Cent Oxygen by Weight
1. Vigorous lime boil	0.009–0.015
2. Steady state	0.015–0.025
3. Working of ore	0.023–0.035

Thus when the bath can be regarded as in a reasonably steady state—that is, when it is boiling normally, is at proper temperature with a well-shaped slag, and has been free from disturbing effects during the preceding half hour—Δ[O] returns from

Manuscript received at the office of the Institute May 14, 1946. Issued as T.P. 2035 in Metals Tech., Sept. 1946; *Proc.* Open Hearth Conf. (1946) **29**, 162.

* Research Laboratory, United States Steel Corporation of Delaware, Kearny, N. J.

[1] References are at the end of the paper.

either direction to, and remains within, the range 0.015 to 0.025 per cent. In this steady state, Δ[O] is substantially the same in acid as in basic furnaces, and in the latter is unaffected by the basicity ratio of the slag over the range 1.7 to 5.5. Studying the possible causes of this variability in the steady state, we find no correlation of Δ[O] with temperature, slag viscosity, or manganese content of either slag or metal, and only a small, probably secondary, effect of iron oxide content of slag after correcting for basicity. Rate of carbon drop not only shows no correlation, but it may vary at least fivefold for a given level of Δ[O].

This entire lack of correlation of Δ[O] with rate of carbon drop makes it certain that some other factor is determining the rate of the carbon-oxygen reaction. This implies that the actual rate depends less on the concentrations of the reactants than on the rate of elimination of the product of reaction from the metal; for if carbon monoxide remains in solution, the reaction ceases. General experience[2] leads us to the view that the dominant factor in this rate is the ease of formation of bubbles of carbon monoxide at the surface of contact between hearth and metal, at which we believe most bubbles start. The validity of this view was confirmed by repeated observations that the measured Δ[O] was lower on a new clean bottom than on one covered with lime-slag accumulations from previous heats. Thus, these observations point distinctly to greater ease of bubble formation on a clean, rough, solid refractory than on a smooth surface covered with a glazed coating; as, indeed, is to be expected from the analogous behavior of many solutions at ordinary temperatures. Therefore, by attending to proper draining, patching and resurfacing of the hearth and by ensuring a close approach to a steady state prior to tap, it would seem possible to keep Δ[O] within the limits 0.015 to 0.022 per cent, an excess that seems to be required for a normal boil, and to that extent to improve the uniformity of product from the subsequent deoxidation.

With respect to the make-up of liquid slag, the following tentative inferences are drawn from our data:

1. The total number (N_s) of molecular units in a given weight of slag increases with basicity ratio b because of the increasing number of "free" molecules of CaO, MgO and MnO, all the MnO present being substantially free when $b = 2.4$.

2. For a given carbon level in the steel, increase of basicity ratio causes an increase of iron oxide content of slag, but this does not represent an increase in its mol fraction or effective concentration in the slag; on the contrary, the latter remains about the same, the iron oxide content changing only to keep pace with the change in N_s.

3. FeO and Fe_2O_3 seem to be present almost entirely as such or in readily dissociable complexes over the range $b = 1.7$ to 5.5; only when b is still lower is an appreciable amount of FeO present as silicate. Complexes such as $CaO.Fe_2O_3$ may be present at the upper surface but are inappreciable at the slag-metal interface.

Some Conclusions Relating to Control of the Open-Hearth Process

It is increasingly evident that during the refining period the temperature of the bath should be at a level high enough to ensure rapid working out of ore feeds and to keep up a steady boil and a regular approach to a steady state prior to tap. Slag viscosity and rate of carbon drop are secondary factors not useful for control purposes, as is the iron oxide content (FeO) of the slag, a quantity that correlates so poorly with [O], the oxygen content of the metal, that it is of little use as an indicator of what should be done to get the desired result.

The fact that slag basicity is without effect on [O] helps to simplify the problem

of control. In the basic furnace, recovery of both manganese and iron is best when the slag basicity ratio is about 2.2 to 2.4, and this range need be exceeded only as required to bring phosphorus and sulphur within the range specified. The main problem is always to get a heat ready to tap at a predetermined, accurately known carbon content; the other essential factors affecting uniformity of oxygen content seem to be: a clean, well-drained, properly repaired bottom; proper temperature; steady boiling without disturbing effects during the last ½ to ¾ hr. before tap.

In the acid furnace the problem is even simpler because temperature and carbon content are the only independent variables to be controlled. The amount of manganese charged can be varied, but since its recovery is low and again dependent on temperature and carbon content, there is no clear justification for charging more than the minimum of manganese that in the available materials accompanies the minimum of carbon needed for proper melting and refining.

In qualification of the foregoing statements, it should be added that in the grades in which quality or cleanliness is a major requirement other considerations may enter the problem of control of the basic furnace process during the period preceding tap; for there is reasonably convincing evidence indicating cleaner steel from heats melted high in carbon, boiled for a long time, finished with high residual manganese and tapped at a rather high temperature. But our data indicate that none of these factors appreciably influences the final oxygen content at tap. Consequently their influence on cleanliness, if real, must depend on some more subtle factor, not yet measured. A possible explanation is that the liquid metal in the bath holds in suspension extremely fine insoluble particles, which somehow affect the precipitation of larger inclusions when deoxidizing agents are added and the steel later cools and solidifies. The removal of these suspended particles by coagulation or solution, which may well be quite slow and difficult, would tend to be quickened by all the factors mentioned above.

Steady State in the Open-hearth Bath

In the open-hearth furnace, oxygen passes from the furnace gases through the slag into the metal and leaves the metal in the form of CO and CO_2; when the rate of inflow and outflow are approximately equal, the bath may be regarded as in a steady state with the carbon-oxygen reaction proceeding at a reasonably steady rate. The main conditions for attainment of such a steady state apparently are: (1) that the metal be at a temperature well above its freezing range, and be boiling normally; (2) that the slag be "shaped up"; and (3) especially that the bath be left undisturbed by addition of anything over a period of 20 to 50 min. This last point is emphasized, because often the furnace operator keeps doing something or other so that there is no close approach to a steady state, sometimes even near the time for blocking or tapping the heat. This is illustrated by the carbon-drop curve in Fig. 1*a*. In the case recorded here, additions of ore and of lime were made until within an hour of tap time, and there was a temperature rise of 120°F. during the last hour. The steady state may have been approached at tap time, but this is doubtful. In the heat illustrated in Fig. 1*b*, in which the last ore was added 75 min. before tap, with small additions of spar as the only other disturbance, a steady state during the last half hour before tap may safely be assumed.

Indeed, a period of steady state may be defined as one in which slag and metal have attained mutual equilibrium with respect to all elements other than carbon and oxygen; and this statement immediately suggests the inference that the carbon-oxygen reaction is exceptional because its

product is gaseous and must somehow leave the system if the reaction is to go on, and consequently that the significant factors are probably only those that affect the formation of bubbles in the steel.

in (FeO) caused by increase of (SiO_2), was also largely completed in the same period.

With the bath in the steady state, the oxygen content of the steel in excess of

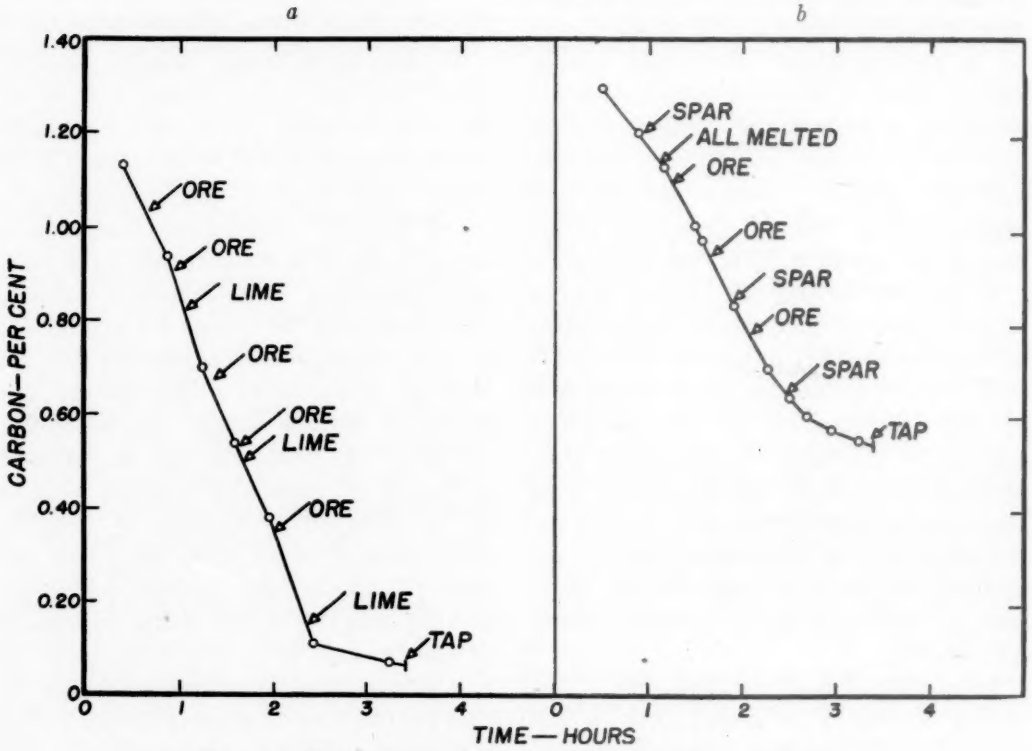

FIG. 1.—CARBON-DROP CURVES THROUGH REFINING PERIOD.
a. Steady state possibly not approached closely even near tap time.
b. Bath probably at steady state during last half hour before tap.

The usual rate of carbon drop in the steady state is from 0.10 to 0.20 per cent an hour, but this can be raised, by the urge toward high production rate, as high as 0.50 to 0.60 per cent by large heat input and heavy ore feeds. Fortunately, however, the measurements indicate that if the bath is hot and boiling well readjustment to a steady state is rapid. This is illustrated by the curve of carbon drop (Fig. 2) during addition of sand to a heat whose temperature was nearly constant over the period, with a well-shaped slag throughout, and no other disturbing factors. The rate of carbon drop increased temporarily, but regained its original value in about 20 min.; the change in slag composition, a decrease

that corresponding to equilibrium with one atmosphere of carbon monoxide is, as indicated in an earlier paper,[2] nearly always within the range 0.015 to 0.025 per cent* and independent of carbon content over

* In the previous paper oxygen content of the metal was expressed in terms of [FeO] as percentage by weight; we now express it, following the more recent convention, as [O] and use the symbol Δ[O] for the excess just defined. The C-O equilibrium probably changes with carbon content and temperature, but not to a large extent.[3] Consequently, for the present purpose we feel justified in considering the product [C] × [O] to be constant and equal to 0.00222, when the pressure of CO is one atmosphere. For example, if [O] was found to be 0.026 per cent by weight and [C] was 0.32 per cent, $\Delta[O] = 0.026 - \frac{0.00222}{0.32} = 0.026 - 0.007 = 0.019$ per cent.

the range 0.08 to 1.20 per cent. Observations on a large number of heats in many shops indicate that Δ[O] just after ore has been added is usually between 0.024 and 0.036 per cent, but drops to the usual range within ½ hr. of completion of the ore reaction; also, that during a lime boil, Δ[O] is usually from 0.009 to 0.015 per cent but soon rises back into the steady-state range after evolution of CO_2 ceases, provided the boil is fairly good and the slag does not contain much undissolved lime.

All our results on this natural readjustment toward a steady state strengthen the view that a regular carbon boil plays the dominant role in controlling the process, consequently that the making of open-hearth steel is essentially nothing but proper control of carbon content and of temperature. In the basic furnace, there is the additional factor of variable slag basicity; and it is necessary to know how this factor affects the dissolved oxygen in the metal, its influence on recovery of manganese and iron and elimination of phosphorus and sulphur being already well established.

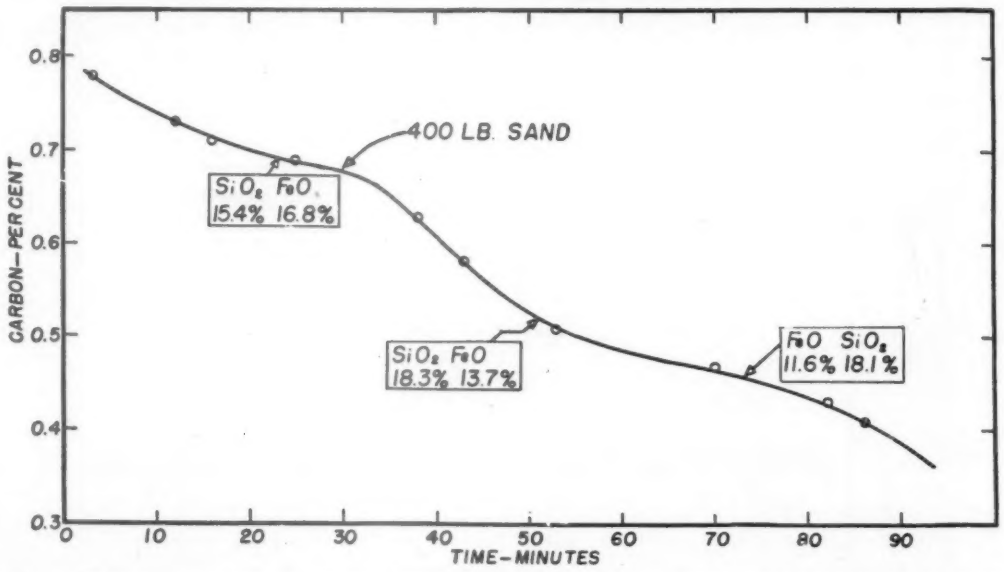

FIG. 2.—CARBON-DROP CURVE DURING ADDITION OF SAND TO SLAG, WITH CORRESPONDING CHANGES IN SLAG COMPOSITION.

SLAG COMPOSITION AND OXYGEN CONTENT OF THE BATH

To determine the extent of the influence of slag-basicity ratio b* upon oxygen content of the liquid steel, we selected, from the results in the several shops, all the pairs of slag-metal samples taken when there was a reasonably close approach to a steady state. These were divided into groups covering one of a number of ranges of [C]; namely, 0.05–0.06, 0.07–0.09, 0.10–0.14, 0.15–0.24, 0.25–0.49, 0.50–1.10 per cent so that in each group the effect of difference in [C] upon the observed [O] would be smaller than the scatter from other factors, known or unknown. Plots of [O] and of $(Fe)_t$ (the total iron content of the slag,) against b were made; those for the carbon range 0.25 to 0.50 per cent, which are typical of all, are shown in Fig. 3.

The moderate upward trend of $(Fe)_t$ (Fig. 3*a*) and the lack of any trend of [O]

* The basicity ratio used here is $b = \frac{(CaO) - 4(P_2O_5)}{(SiO_2)}$ where each quantity in parentheses is expressed in terms of mols per 100 grams (or pounds) of slag.

(Fig. 3*a*) with increase of *b* in the basic slags was duplicated almost exactly for each carbon range. The points to the left of the break in the scale are from two acid furnaces, with 4 per cent or less lime in the slags; $(Fe)_t$ is higher than in the basic slags, but there is no difference in the range of [O] (a conclusion substantiated by a discussion of acid operation in a later section). The restriction of results to periods of steady state and to a small carbon range leaves barely enough points for a convincing conclusion with respect to the trend of [O] with basicity; Fig. 4 combines all the data from the various carbon ranges by using the deviation from the average value of [O] and $(Fe)_t$ in each carbon range to plot against basicity ratio. The upward trend of $(Fe)_t$ with increasing basicity is quite definite here, but the absence of any

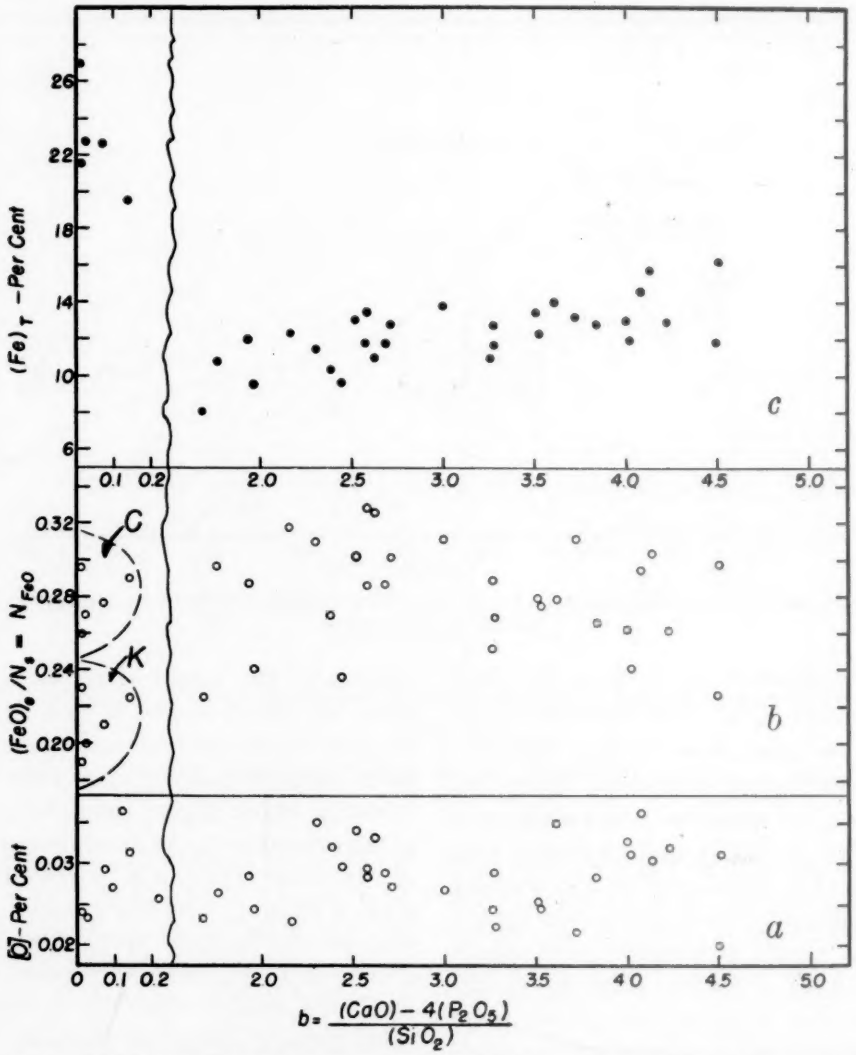

FIG. 3.—SLAG-METAL DATA FROM BATHS AT STEADY STATE WITH [C] BETWEEN 0.50 AND 1.00 PER CENT.

Basically ratio *b* of slag plotted against:

a. Observed oxygen in metal [O].
b. Calculated mol fraction of iron oxide in slag, N_{FeO}.
c. Total iron in slag $(Fe)_T$.

trend in [O] while b changes from 1.7 to 5.6 is evident from Fig. 4*a*. In other words, over the whole range of basicity and composition in both acid and basic furnaces, the composition of the slag, aside from its iron content, has nothing to do with the concentration of oxygen dissolved in the liquid metal, at least under conditions of approach to a steady state.

In order to learn how [O] or Δ[O] correlates with $(Fe)_t$, we divided the data into two groups by drawing an average curve for $(Fe)_t$ through the band of individual points in Fig. 4*c*, and made a statistical comparison of Δ[O] between these groups (with $(Fe)_t$ high or low for given levels of carbon content and of slag basicity). This brought out a small difference, Δ[O]

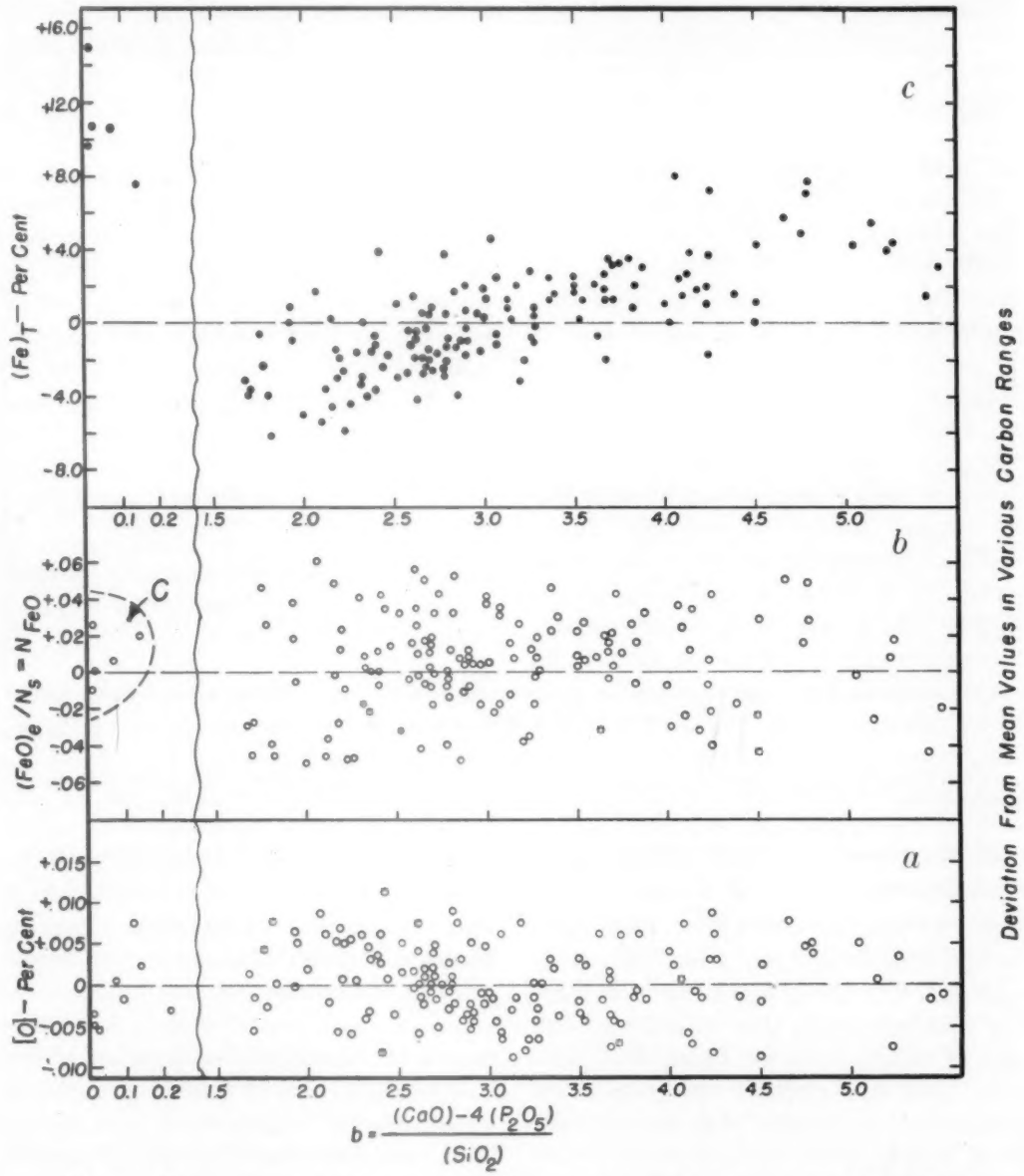

FIG. 4.—COMBINED PLOT OF DATA AS IN FIGURE 3 BUT OVER A WIDER CARBON RANGE. Carbon ranges 0.05–0.06, 0.07–0.09, 0.10–0.14, 0.25–0.49, and 0.50–1.10 per cent are combined by plotting as ordinate the deviation from the mean in each carbon range.

averaging about 0.0015 per cent higher when $(Fe)_t$ is above the mean; but this, being only 10 to 15 per cent of the normal spread of Δ[O], is only a secondary source of difference.

of the differences in Δ[O] (from 0.015 to 0.025 per cent); and this same range of variability was observed in different shops with different designs of furnace and different operating conditions.

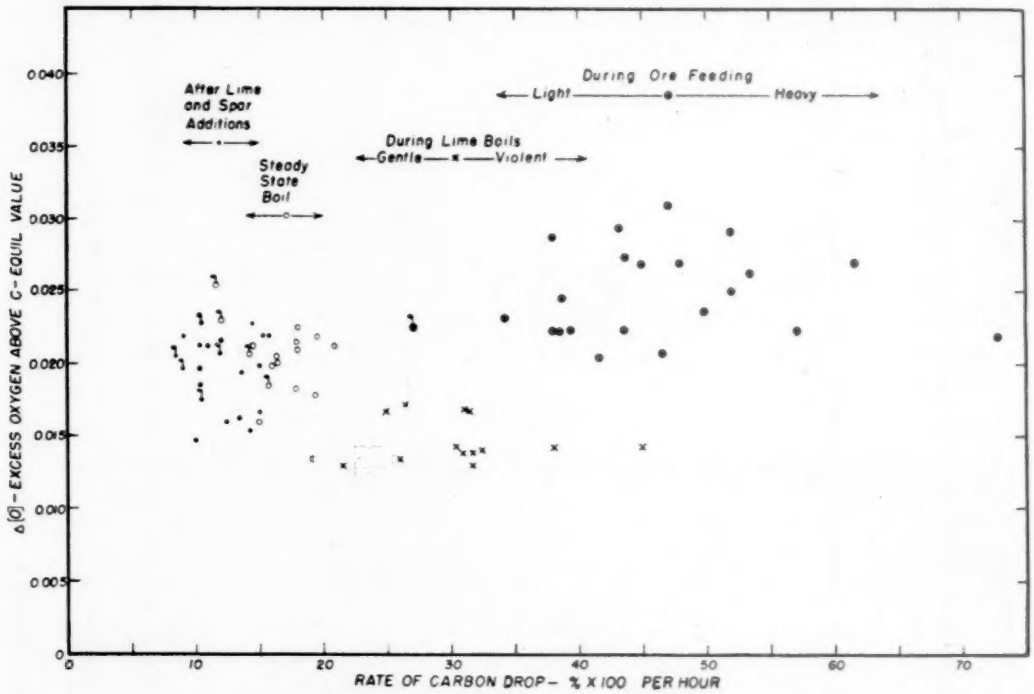

FIG. 5.—RATE OF CARBON DROP VS. Δ[O].
Concentration of oxygen in excess of equilibrium with carbon, and carbon monoxide at one atmosphere.

Measurements of bath temperature, made in only a few of all the heats examined, showed no correlation with Δ[O], though temperature may affect the rate of approach to a steady state. Nor was there any correlation with slag viscosity or with rate of carbon drop, provided that sufficient time had elapsed after the latest addition of ore to permit the reattainment of a steady state. Moreover, repeated checking and re-sampling made it clear that no appreciable part of the spread can be ascribed to errors of sampling or analysis.

To summarize, we were unable to find within the two-liquid system slag-metal in a steady state any measurable factor that would account for more than a fraction

Δ[O] *in Relation to Rate of Carbon Drop*

One would expect some correlation of Δ[O] with rate of carbon drop. There is, however, evidence that the carbon-oxygen reaction occurs mainly at the interface metal-gas, and therefore that its rate is limited by the supply of bubbles. If few bubbles form, the carbon drop would be slower despite increased potential supply of oxygen, as measured by [O]; if bubbles form readily, a rapid carbon drop would result although [O] is smaller. Thus, the expected correlation of carbon drop with [O] may be hidden because of differences in rate of formation of bubbles; and just this situation is indicated by the data.

In Fig. 5 rate of carbon drop for a number of cases where all conditions were

well known is plotted against Δ[O]. The division into groups is obvious, but in any one group there is no direct correlation; indeed, Δ[O] appears to decrease somewhat with increase in rate of carbon drop. While ore is being fed, both Δ[O] and rate of carbon drop (0.35 to 0.60 per cent per hour) are highest, as is to be expected; bubble formation may not keep pace with oxygen supply in such cases. On the other hand, during an active lime boil, the rate is high (0.35 to 0.45 per cent per hour) yet Δ[O] is at its lowest; undoubtedly because carbon dioxide evolved from the limestone is not only a source of oxygen but provides a plentiful supply of bubbles, hence a large surface for the reaction. During periods of normal boils, the rate of carbon drop (0.15 to 0.25 per cent per hour) did not correlate with Δ[O].

Oxygen Content of Bath in Steady State and Condition of Furnace Bottom

This lack of correlation of Δ[O] with anything measurable within the furnace led us to consider other possible sources, and in particular the condition of the surface of the furnace bottom as reflected in the relative ease of formation of gas bubbles there; for bubbles of carbon monoxide seem mainly to start at this surface and consequently its texture might well modify what happens, as it is known to do in analogous cases.

The character of the hearth surface is difficult to assess; a clue to this as a probable factor came from the observation that Δ[O] was higher in the heats that were made immediately after a high-carbon heat than in those preceded by a low-carbon heat. In one shop where many measurements were made, most heats were made to be either above 0.40 or below 0.15 per cent carbon; the bottoms were old, and on the higher-carbon heats, in order to avoid delays, were usually not cleaned up of all lime or other accumulations, which, therefore, during tap, became coated with slag and, in a sense, glazed. On low-carbon heats the higher final temperature and longer refining period would normally clean up the bottom, the slag would drain out more completely, and the surface for the next heat would be more refractory and less glazed.

This clue led us to take all heats on which we had good steady-state measurements of [O] and to divide them in accordance with what may be called their "ancestry," depending on the final level of bath carbon in the three immediately preceding heats. Those preceded by two or three high-carbon (above 0.20 per cent) heats, or by an intermediate followed by one or two high-carbon heats, were put in "high-carbon ancestry"; those preceded by at least two low-carbon heats were designated "low-carbon ancestry," a few heats "intermediate in ancestry" being omitted from both groups. A plot of Δ[O] for both groups is Fig. 6, where a pair of dashed lines include nearly all steady-state data from several shops. The degree of separation of the two groups is remarkable considering that the division according to ancestry is arbitrary and probably does not correlate too well with whatever difference in character of the bottom surface is responsible. The degree of separation is more obvious in the frequency curves of Δ[O] for these same groups (in Fig. 7*a*). Subsequent studies on steel quality based on different yardsticks in two shops showed appreciable differences in favor of the low-carbon ancestry groups.

In a later study of [O] in acid furnaces we happened to get a group of data from the end of the campaign of an old bottom and another group near the beginning of the campaign of a new, rebuilt bottom; the Δ[O] values are shown as frequency curves in Fig. 7*b*. Incidentally, Fig. 7 shows clearly that [O] tends at steady state to be substantially the same in the acid as in the

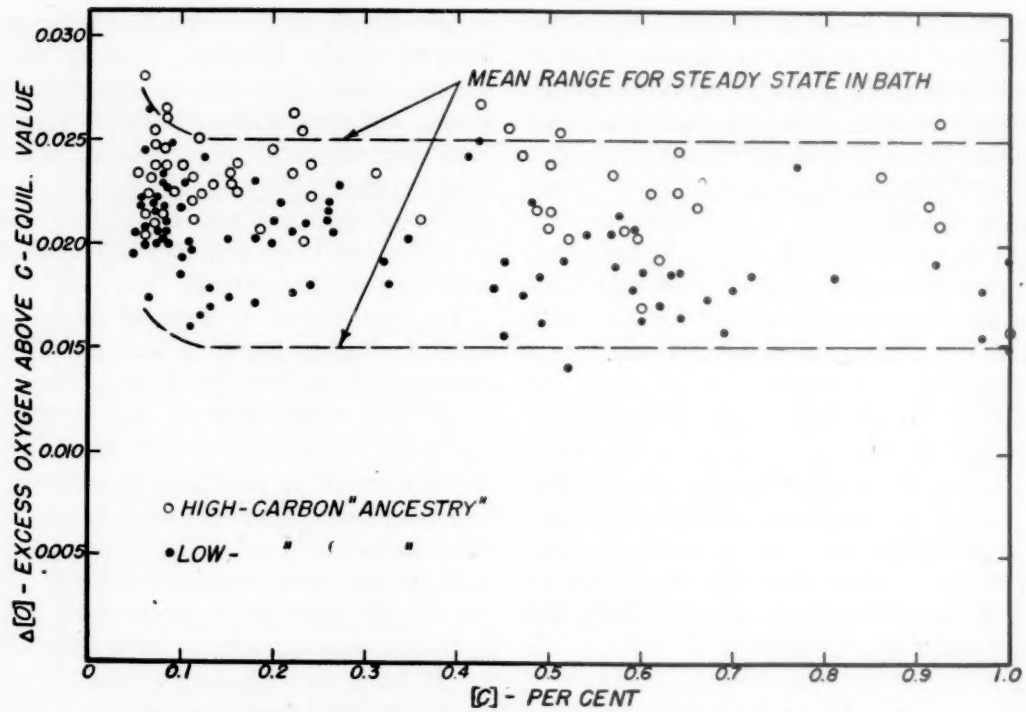

FIG. 6.—Δ[O] AT STEADY STATE DIVIDED WITH RESPECT TO "ANCESTRY."
That is, to the final carbon content of the two or three heats in the same furnace immediately preceding the one being tested.

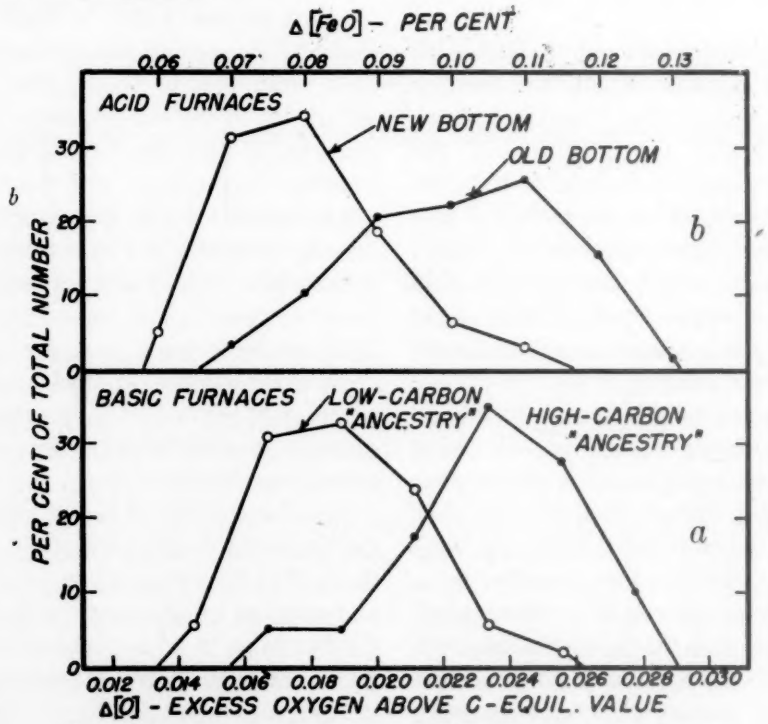

FIG. 7.—FREQUENCY CURVES OF Δ[O] IN COMPARATIVE GROUPS.
a. Separated according to "ancestry" as in Fig. 6.
b. One group on an old bottom, one on a new bottom, in acid open-hearth furnace.

basic furnace, both being essentially controlled by the carbon-oxygen reaction.

The parallelism between *7a* and *7b* strongly suggests a difference in character of bottom surface common to both. The old sand bottom after many years service would probably be saturated with slag and its surface more glazed than the new bottom. Whatever the mechanism, it appears that some variation in surface is responsible for a large part of the variability of Δ[O] in the steady state, and other evidence on conditions affecting bubble formation[2] leads us to believe that some variation in physical character or texture of the surface touching the liquid metal is responsible. If the top layer of the hearth is mostly solid refractory material, its surface will be somewhat porous and rough, and either rough edges or tiny holes not entirely filled with steel should favor easier starting of gas bubbles at such contacts with the metal. On the other hand, on an old slag-soaked surface or on one largely coated with a lime-slag mixture, much of the contact with metal would be at a smooth liquid glaze, which is unfavorable to initiation of bubbles.

Again, though most points in Fig. 5 happen to be of low-carbon ancestry, a few (marked with a tiny flag) were preceded by high-carbon heats; and for these Δ[O] tends to be higher but the rate of carbon drop lower.

The general behavior all suggests that the carbon-oxygen reaction takes place readily only at a surface, and particularly at a metal-gas surface such as that of a bubble rising upward through the metal. Just how this bubble is started in absence of any other gas (such as CO_2 from limestone) must for the present remain uncertain; but there is little question that this reaction is identical with other bubble-forming processes in that all go faster as soon as a tiny bubble appears and that bubbles appear more readily at a rough than at a smooth solid surface. On this view, the rate of carbon drop would depend more on ease of bubble formation than on the driving force as measured by Δ[O], in line with the experimental results adduced above.

TABLE 1.—*Data on Two Heats Before and After Addition of Sand*

Data	Heat A		Heat B	
	Before	20 Min. After	Before	30 Min. After
Slag analysis, wt. per cent:				
CaO	49.6	50.6	45.2	43.5
SiO_2	15.4	18.3	19.8	23.0
FeO	12.9	9.1	10.5	9.9
Fe_2O_3	4.2	5.1	2.8	2.3
MnO	6.0	5.9	8.3	8.2
P_2O_5	2.0	2.0	2.7	2.3
MgO	4.6	5.3	5.4	6.9
Al_2O_3	2.6	2.2	2.9	2.4
Mols per 100 grams:				
$(CaO)_t$	0.885	0.903	0.807	0.776
$4(P_2O_5)$	0.056	0.056	0.076	0.064
(CaO)	0.829	0.847	0.731	0.712
Constituents of liquid slag: (Mols per 100 grams:				
(FeO)	0.179	0.127	0.146	0.138
$3(Fe_2O_3)$	0.079	0.096	0.053	0.043
Equivalent FeO				
$(FeO)_e$	0.258	0.223	0.199	0.181
(MnO)	0.085	0.083	0.106	0.071
(Phosphate)(P_2O_5)	0.014	0.014	0.019	0.016
(Silicates) (SiO_2)	0.257	0.305	0.330	0.383
(Free lime) $(CaO)_f$	0.214	0.135	0.032	
(Al_2O_3)	0.026	0.022	0.029	0.024
(Estimated in solution)(MgO)	0.050	0.040	0.030	
Total mols per 100 grams, N_s	0.904	0.822	0.745	0.675
Basicity ratio b	3.22	2.77	2.21	1.86
Mol fraction equiv. FeO/N_{Fe}	0.285	0.271	0.267	0.268
Bath temperature, deg. F	2850	2860	2910	2910
Carbon in steel, per cent [C]	0.69	0.51	0.25	0.14
Manganese in steel, per cent [Mn]	0.13	0.16	0.24	0.19
Manganese in steel, calculated	0.14	0.16	0.25	0.21

Activity of Oxygen in Open-hearth Slags

In a previous section it was stated that concentration of oxygen in steel trends upward only slightly with increase in total iron $(Fe)_t$ in the slag, and does not seem to correlate with slag composition as a whole. This situation leads us to consider how the

oxygen content of the steel is related to the activity of oxygen in slags, particularly since the percentage of FeO in a slag has been largely used as a measure of the degree of oxidation of the steel that was in contact with that slag.

During the steady state, as defined above, there is a near approach to equilibrium of metal with slag in respect to all the elements except carbon and oxygen; that these should not be in equilibrium is necessary if the reaction is to progress at a reasonable rate. Moreover, oxygen is continuously flowing in from the furnace atmosphere through the slag to the metal, with diminishing activity as it descends. This gradient is altered by anything that affects rate of movement of oxygen through the slag or across the gas-slag or the slag-metal interface, and therefore does not depend uniquely on composition or temperature. It is of interest to see how the average level of oxygen activity in the slag, which seems to lie closer to that of the metal than to that of the atmosphere and hence to be under the dominant control of the carbon reaction, correlates with slag composition.

The activity of oxygen in a slag is determined by its temperature (which is here left out of account because of lack of sufficient data and because its actual variability is, for the present purpose, of secondary importance) and by the mol fraction of iron oxides, as derived from the slag composition on the basis of the general picture, discussed in a previous paper, of the molecular species present in liquid slag. As is set forth in that paper, when both FeO and Fe_2O_3 are present, the use of what may be called the "equivalent" concentration of FeO—namely,

$$(FeO)_e = (FeO) + 3(Fe_2O_3)$$

all expressed in terms of mols per 100 grams slag—works well in calculations of the equilibrium distribution of manganese and sulphur between slag and metal. The mol fraction N_{FeO}, which is a direct measure of the oxygen activity of the slag, may be defined as $N_{FeO} = (FeO)_e/N_s$, where N_s is the total number of mols or molecular units present in 100 grams slag. N_{FeO} as thus derived may be inaccurate owing to: (1) uncertainty of sampling, since composition of the slag layer may vary with depth, (2) error in N_s because of error in assigning slag constitution—for instance, part of the Fe_2O_3 may be present as $CaO.Fe_2O_3$ complexes, or part of the FeO as a silicate such as $CaO.FeO.SiO_2$.

We had data sufficient for such calculations on a pair of heats in which all conditions were uniform except that sand was added, which, as noted before, speeded carbon oxidation. Details of the calculations are in Table 1, according to which addition of sand lowered $(FeO)_e$ but also lowered N_s so that N_{FeO} was changed but little. In making these calculations we made the identical assumptions as in the previous paper[4] except that the MgO dissolved as such was assumed to increase regularly with basicity ratio b and $(FeO)_e$, from a minimum of about 1.5 per cent by weight up to the total calculated from the chemical analysis. MnO was assumed to be all dissolved as such (heat A) above b values of 2.4, but below $b = 2.4$ (heat B) to be present in part as complex silicates in accordance with the average difference between observed and calculated values of [Mn] when b is less than 2.4;[4] the [Mn] as thus calculated again agrees with the result of analysis of the steel. This agreement indicates that in the slag layer in contact with the metal little of the Fe_2O_3 or FeO is present as complexes, though such complexes may be present near the upper slag surface. It may also be noted that, although the carbon content of the steel in heat B was much less than in heat A, N_{FeO} was nearly the same in both, and thus was more effective in B, presumably because of the higher temperature.

It may seem confusing to talk of equilibrium in a system that as a whole is in a steady state of change and therefore not in true equilibrium. Yet it certainly aids in slag composition and temperature are usually slow enough to permit close adjustment to equilibrium of all significant reactions except the carbon-oxygen reac-

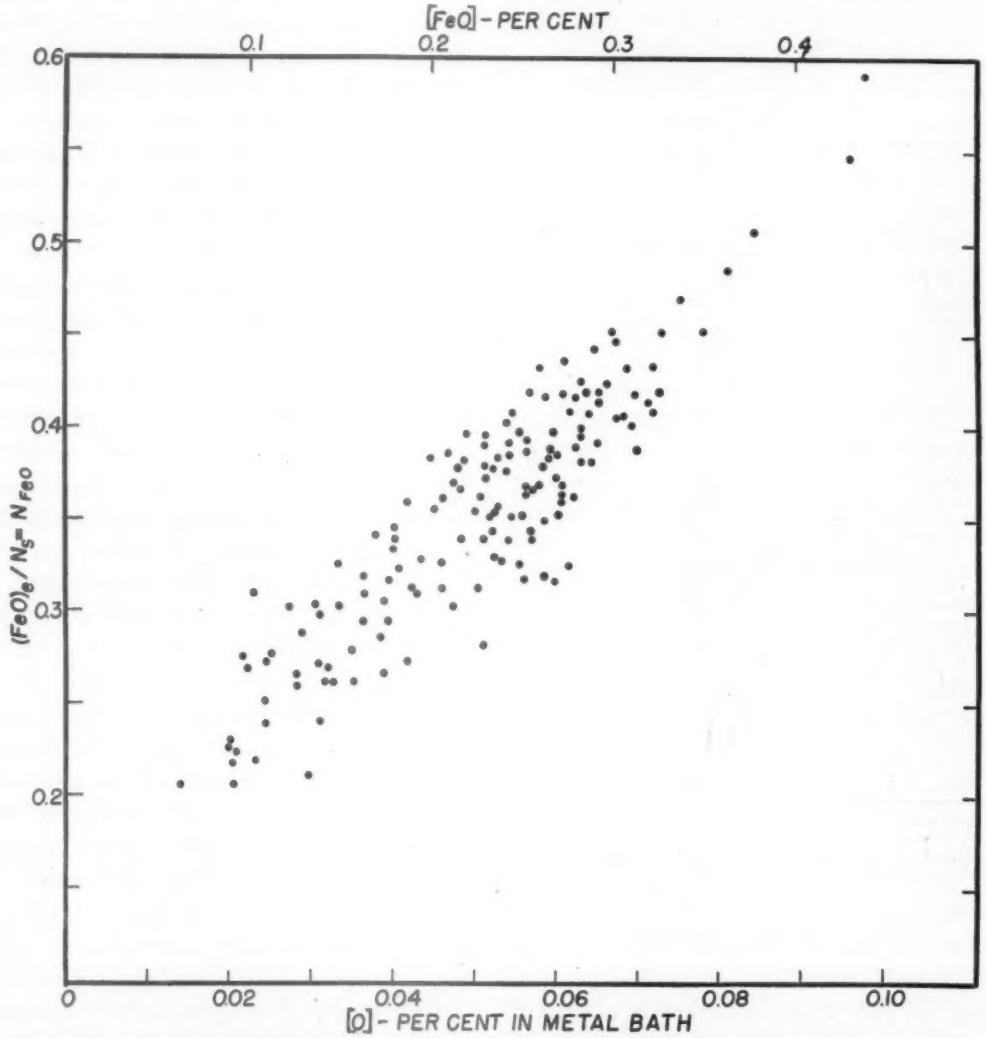

FIG. 8.—[O] FROM BASIC-FURNACE BATHS PROBABLY CLOSE TO STEADY STATE VS. CALCULATED N_{FeO}. Carbon content from 0.02 to 1.2 per cent, b from 1.7 to 5.5 included.

in interpreting the refining process and its products to consider (as was brought out in a previous paper[4] that the distribution of manganese, phosphorus, sulphur, between slag and metal does come close to that calculated on the basis that equilibrium in these reactions is in fact substantially attained. In other words, toward the end of the refining period, the changes tion, which, in our view, thus controls the whole process.

Influence of Slag Basicity on Oxygen Activity N_{FeO}

The observed constancy of Δ[O] over a wide range of basicity, as shown in Figs. 3 and 4, when interpreted on the basis of activity of oxygen in slag, as outlined

above, indicates that the increase of total iron $(Fe)_t$ with basicity is merely a readjustment to keep N_{FeO} at an average level appropriate to the carbon range, and that

TABLE 2.—*Calculations from Slag-metal Data on Three High-carbon Heats Selected to Cover a Wide Range of Basicity*

Data	A	B	C
Slag analysis, wt. per cent:			
CaO	43.0	50.9	51.7
SiO_2	24.1	14.8	11.0
FeO	7.5	8.0	11.9
Fe_2O_3	2.3	5.2	3.7
MnO	9.7	9.5	8.6
P_2O_5	2.8	3.3	1.9
MgO	6.4	5.0	7.0
Al_2O_3	2.7	2.2	2.4
Total Fe $(Fe)_t$	7.4	9.8	11.2
Mols per 100 grams:			
$(CaO)_t$	0.768	0.908	0.923
$4(P_2O_5)$	0.079	0.093	0.053
(CaO)	0.689	0.815	0.870
Constituents of liquid slag: (Mols per 100 grams):			
(FeO)	0.104	0.111	0.166
$3(Fe_2O_3)$	0.042	0.098	0.070
Equivalent FeO $(FeO)_e$	0.146	0.209	0.236
(MnO)	0.086	0.134	0.121
(Phosphate) (P_2O_5)	0.020	0.023	0.013
(Silicates) (SiO_2)	0.401	0.247	0.183
(Free Lime) $(CaO)_f$		0.225	0.500
(Al_2O_3)	0.027	0.022	0.024
(Estimated in solution) (MgO)		0.040	0.060
Total mols per 100 grams, N_s	0.680	0.900	1.137
Basicity ratio b	1.72	3.30	4.75
Mol fraction equiv. FeO (N_{FeO})	0.22	0.23	0.21
Carbon in steel, per cent [C]	0.69	0.88	0.60
Oxygen in steel, per cent [O]	0.0205	0.0194	0.0200

N_{FeO} would show no trend within a limited range of [O]. This deduction is confirmed by Figs. 3*b* and 4*b*, the latter showing that, though there is considerable scatter, there is no trend in N_{FeO}, as the basicity ratio b changes from 1.7 to 5.5. This lack of correlation is also brought out by Table 2, which gives details of calculations on three selected cases that differed widely in total iron $(Fe)_t$ and basicity b; yet the increase in N_s compensates for increase in $(FeO)_e$, and N_{FeO} and [O] are nearly constant.

Fig. 8 is a plot of N_{FeO} against [O] as measured in all heats considered to be at steady state for which we had the requisite slag-metal data; they comprise a range of 0.02 to 1.2 per cent carbon and of basicity ratio from 1.7 to 5.6. There is obviously a considerable scatter of the points, as is to be expected because of the admitted uncertainties of sampling of the slag and in the interpretation of its constitution as well as that arising from differences in temperature; yet we regard it as showing a definite correlation of oxygen activity of slag (but not its content of iron oxide) with oxygen content of metal.

In acid slags the method of calculation used above for basic slags is inapplicable because, being usually saturated with SiO_2 and being comprised in a system with a wide immiscibility gap, they cannot be considered as even nearly ideal solutions. We therefore resorted to the data of Körber and Ölsen[5] on slag-metal melts in a silica crucible, some of which were so close in composition and temperature to our acid slags that from their curves we could read off corresponding values of [O] at equilibrium in absence of carbon. These values, each divided by the concentration of oxygen in iron at 2910°F. in contact with a slag of pure iron oxide—this saturation concentration being 0.32 per cent according to Körber and Ölsen,[7] but 0.23 per cent according to Chipman[6]—yield an approximate measure of N_{FeO} the oxygen activity, the points being marked *K* and *C* respectively in Figs. 3 and 4. The activity so derived is of the same order of magnitude as the values of mol fraction of $(FeO)_e$ in the basic slag, again corroborating the view that it is largely regulated by the carbon-oxygen reaction in the bath and independent of the degree of basicity of the slag. Consequently, the latter can be changed at will in accordance with considerations of slag volume or manganese recovery, or elimination of phosphorus or sulphur, without concern over the amount of residual oxygen to be removed by deoxidation.

Summary

A study has been made of oxygen content of a large number of liquid steels in the furnace and of activity of oxygen in the slag, when a steady state is approached, this being usually near the end of the refining period. Oxygen content of the metal is independent of slag composition over the range commonly used in both acid and basic furnaces; its normal variability in excess of the amount corresponding to equilibrium with carbon and carbon monoxide at atmospheric pressure is largely independent of any of the measured quantities such as rate of carbon drop, or iron oxide content or viscosity of slag. This variability seems to be due mainly to differences in condition of the hearth surface, which affect the ease of bubble formation at the lower surface of the metal.

References

1. T. E. Brower and B. M. Larsen: The Occurrence of Oxygen in Liquid Open-hearth Steel—Sampling Methods. *Trans.* A.I.M.E. (1945) **162**, 712; Summary, *Proc.* Open Hearth conference (1945) **28**, 341.
2. B. M. Larsen: Controlling Reactions in the Open-hearth Process. *Trans.* A.I.M.E. (1941) **145**, 67–83.
3. Basic Open Hearth Steelmaking, 485–488, A.I.M.E., 1944.
4. L. S. Darken and B. M. Larsen: Distribution of Manganese and of Sulphur between Slag and Metal in the Open-hearth Furnace. *Trans.* A.I.M.E. (1942) **150**, 87–112.
5. F. Körber and W. Ölsen: The Fundamentals of Deoxidation with Manganese and Silicon. *Mitt.* K-W-I. Eisenforschung (1933) **15**, 271–309.
6. J. Chipman: Basic Open Hearth Steelmaking, 471, Fig. 125. A.I.M.E., 1944.
7. F. Körber and W. Ölsen: *Mitt.* K-W-I. Eisenforschung (1932) **14**, 181–204.

DISCUSSION

(*M. Tenenbaum presiding*)

C. T. Stott*—Mr. Larsen's recent paper on oxygen in liquid open-hearth steel is another phase in his very excellent study of reactions in the open-hearth furnace. His fresh views and logical presentation of data make a distinct contribution to the study of open-hearth reactions. In the present paper, which deals with the variability of excess oxygen, we were particularly interested in the relation between excess oxygen Δ[o] and the condition of furnace bottoms. The data presented in Fig 7*a* indicate that Δ[o] has a lower value for heats with "low-carbon ancestry" as compared with heats with "high-carbon ancestry." The difference is attributed to the character of the surface of the bottom. The low-carbon bottom, having a rough surface, is more conducive to bubble formation, which in turn is an important factor in the elimination of carbon monoxide. It would be interesting to know whether or not the rate of carbon drop was higher for the heats with "low-carbon ancestry" than for the heats with "high-carbon ancestry."

The thought occurs to us that it might be possible to develop a deoxidation system based on the oxygen in equilibrium with the carbon at tap, which is well known, plus a correction for Δ[o] in the steady state. If the mean value of Δ[o] in the steady state (0.02 pct) were added to the equilibrium oxygen at the particular tapping carbon, could not the aluminum addition be calculated with equal accuracy to an addition based on the FeO content of the slag? Obviously, the tapping carbon would have to be known fairly accurately.

C. E. Sims*—I had occasion to look over these data this past summer while writing a paper that was prepared in an attempt to expound the mechanism of the carbon-oxygen reaction in steel. From the first, the concept of delta oxygen appeared to be a complete anomaly. The idea of a homogeneous reaction like that of carbon and oxygen in molten steel being far out of equilibrium (with as much as 10 times the equilibrium content of oxygen) seemed incongruous. There must be a better explanation.

Using the data of Marshall and Chipman,[8] in which they subjected small melts of iron to various external pressures of CO, up to nearly 20 atm, and, working backward,

---

* Assistant Engineer of Tests, Bethlehem Steel Co., Sparrows Point, Maryland.

* Battelle Memorial Institute, Columbus, Ohio.

[8] S. Marshall and J. Chipman: The Carbon-oxygen Reaction in Liquid Iron. *Trans.* Amer. Soc. for Metals (1942) **30**, 695–745.

results were obtained with which it seemed the concept of delta oxygen could be resolved. This led to the conclusion that equilibrium at any point within the liquid steel is quickly attained. Instead of being in equilibrium with one atmosphere of gaseous CO, however, the carbon and oxygen come to equilibrium with varying amounts of dissolved CO, representing escaping pressures up to 9 atm. Because of inherent difficulties of bubble formation, dissolved CO cannot always escape at 1 atm, and the contact with bubbles of CO formed during the boil is too transient to allow equilibrium with the dissolved CO. This lack of equilibrium in a heterogeneous reaction is considered more plausible.

This paper is scheduled for presentation before the coming session of the Electric Furnace Conference, but there are a few points which appear to be significant in respect to the present paper.

In the data presented by Mr. Larsen, there is no correlation between delta oxygen and carbon content and, likewise, no correlation between delta oxygen and the rate of carbon drop.

Using the mean value for delta oxygen in the steady state, however, and CO pressure calculated from the data of Marshall and Chipman, a very good correlation was found between carbon content and CO pressure. These pressures ranged from 2.0 atm at 0.2 pct C to 7.5 atm at 0.9 pct C. A plot of pct C vs. CO pressure gave a curve that appeared to be a parabola, and when CO pressure was plotted against the square root of carbon content, a straight line was obtained. Extrapolation of this line indicated zero CO pressure at a carbon content of 0.007 to 0.008 pct.

Marsh, in a paper published about two years ago, showed a very good relation between carbon content and rate of carbon drop. When the latter was plotted against the log of carbon, a satisfactorily straight line was obtained.

Putting these two observations together, it is concluded that the chief bottleneck in carbon elimination is the evolution of CO gas. Other conditions, such as hearth surface, being constant, the rate of CO evolution is controlled by its pressure. The chief controlling factor in the pressure is carbon content, because it was shown that, during the steady state "delta oxygen" remains fairly constant. The reason it remains constant is because a faster boil, which eliminates CO at a greater rate, also causes a more rapid transfer of oxygen from slag to metal by the greater turbulence. These two factors tend to come into balance.

Using the formula for the curve obtained by plotting CO pressures vs. $\sqrt{\%\ C}$ the CO pressures may be calculated and a correction made for the relation

$$\%\ C \times \%\ O = m$$

which then becomes

$$\%\ C \times \%\ O = m \times P_{CO} = 0.0193\ (\sqrt{\%\ C} - 0.09)$$

Oxygen values calculated from carbon contents, by this formula, will closely approximate those observed for the steady state.

M. TENENBAUM*—Are there any other comments? If not, I would like to compare some data that we have obtained in our own plant with those of Brower and Larsen. There is an apparent discrepancy between our data and those presented in this paper. This is probably an actual difference, rather than a discrepancy.

In taking samples throughout the carbon range, we found that our delta oxygen is usually definitely lower than the values presented in Mr. Larsen's paper. However, our samples were taken by means of the standard bomb test, and the steel sample was taken just above bottom; that is, the bomb actually rested on the bottom while it was being filled. The difference in the delta oxygen values was not so great in low-carbon steels. However, in the range between 0.25 and 1.0 pct carbon Δo averaged about 0.005 pct lower than the values given by Brower and Larsen.

I think this merely verifies the concept given in an earlier paper by Mr. Larsen, which points out that the reaction actually takes place at the bottom. Since oxygen is being consumed at the bottom, it would be expected to be somewhat lower at that point.

---

* Metallurgist, Inland Steel Co., East Chicago, Indiana.

W. O. PHILBROOK*—I understand that Mr. Larsen's main purpose in presenting this paper was not to give a final answer, but to stimulate discussion to help elucidate this problem. I think he has achieved remarkable success along those lines. I know of no recent paper that has occasioned more discussion than this one has at this meeting and at the last Open Hearth Conference. I would like to offer a few comments in the same vein, of just talking around the subject to try to stimulate further discussion.

I was interested in Mr. Sims' remarks, because it seems to me they appear a little more probable than Mr. Larsen's conception. Let us compare them this way: Larsen's conception is that the carbon and oxygen react directly to form a CO bubble at a nucleus. Mr. Sims' conception is that carbon and oxygen dissolved in steel react to form CO dissolved in steel; that this reaction can go to a limited extent if the CO pressure builds up. The dissolved CO is released only at a nucleus. Therefore, the reaction occurs as a homogeneous reaction, but it occurs only up to a certain point, and the continuance of that reaction is dependent upon the escape of CO. This hypothesis separates the reaction into two different steps. That, to me, is a more conceivable mechanism. I think it sounds more reasonable, but it certainly is a matter for argument.

I do not recall who it was that first suggested that we should calculate the carbon-oxygen equilibrium in the open hearth on the basis of one atmosphere of CO, but that idea has been accepted in more recent work. But let us consider that the bubble does form at the hearth or, a bubble having once formed, that more CO enters it. In order for that bubble to grow, it must push aside liquid steel, and it must push that steel aside against the pressure at that point in the furnace. Now, if we have a bath of 30 in. of steel, which is roughly equivalent to 15 in. of mercury, or half an atmosphere, and have in addition the atmospheric pressure on the surface of the steel bath, that bubble must grow against a pressure of 1½ atm, rather than 1 atm. We must consider in this nonequilibrium reaction the total atmospheric pressure, not the partial pressure of CO.

If this reaction were simply $C + O \rightarrow CO$, the effect of pressure should be that 1½ atm would make a change of 50 pct in the [C][O] product, as against that calculated for an assumed pressure of 1 atm. From the results of Marshall and Chipman,[8] it appears that that correction of 50 pct is too high; it may be closer to 30 or 40 pct. At any rate, it would indicate that Brower and Larsen calculated Δ[O] higher than it should be; that the actual CO pressure that should be considered is not 1 atm but 1.3 or 1.5 atm. If the true Δ[O] is not what they calculated, that would, of course, change qualitatively their conclusions.

This also brings up another consideration. If our CO bubbles all form at the furnace bottom, we should be talking about carbon contents, oxygen contents, and CO pressures at the bottom. Then we should take our sample for oxygen off the bottom, as Mr. Tenenbaum brings out. If the oxygen sample is taken up near the slag-metal interface, there is in addition some diffusion head or convection head, which may or may not be important, added to the effective oxygen concentration at the bottom.

The question of sampling, therefore, enters this whole paper. I do not know how many of these precautions were observed. I am merely suggesting these alternatives as things that should be cleared up to give a more rounded and complete picture of the carbon-oxygen reaction.

There are a few other questions regarding the significance of the data. In the table on the first page of the paper are given the values reproduced in the second column below. There is, however, a fringe of uncertainty on either side of each range, owing to experimental errors inherent in any measurement. As I recall, Brower and Larsen's first paper[9] of this series, the standard deviation involved in the sampling and determination of oxygen would be something of the order of 0.002 pct oxygen. This would indicate an uncertainty of about ±0.004 pct oxygen. We can see the same thing graphically if we refer back to Fig 4 of an earlier paper by Larsen,[10] which apparently

* Carnegie Institute of Technology, Pittsburgh, Pennsylvania.

[9] *Trans.* AIME (1945) **162,** 712.
[10] *Trans.* AIME (1941) **145,** 67.

contains the experimental points upon which these ranges were based, and in which we see that the ranges overlap. If we read off the ranges indicated by the experimental points in Fig 5 of this paper, we obtain the bands given in the third column of Table 3. All of this indicates that these bands or ranges of "excess oxygen" for the different bath conditions overlap to some extent and that the significant portion of these bands is not as wide as implied. I am trying to bring out that perhaps this difference in Δ[O] is not as significant as claimed.

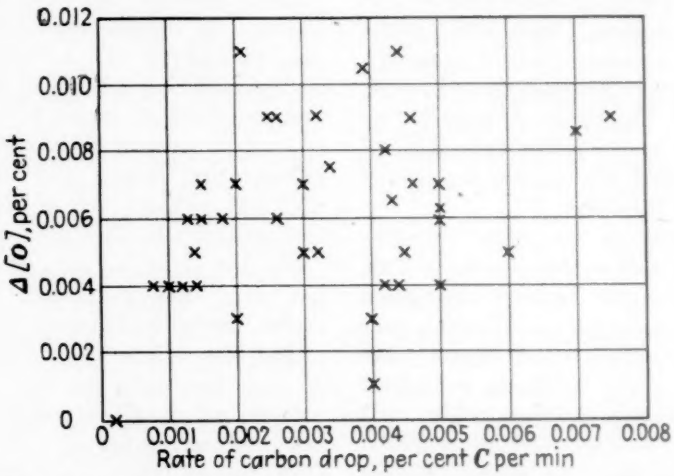

FIG 9—RESULTS WITH ANALYTICAL METHOD SIMILAR TO AUTHORS.

TABLE 3—*Excess Oxygen Ranges*

Conditions	From Paper	From Fig 5
	Δ[O] Usual Percentage of Oxygen by Weight	Δ[O] Bands Estimated from Experimental Points in Fig 5 Only
Vigorous lime oil.....	0.009–0.015	0.013–0.017
Steady state.....	0.015–0.025	0.015–0.025
Working of ore.....	0.023–0.035	0.020–0.032

There is another question concerning the frequency curves shown in Fig 7, which have considerable overlap. Now, whether or not these are significant, whether there is a real difference between those two, is a question that is amenable to a statistical attack. It will depend upon the number of observations in each group. And I think that the number of observations is sufficient so that these differences between old and new furnace bottoms really mean something, but it would be, to me, a little more satisfying if the authors would use a statistical test for significance and tell us whether that apparent difference really means something or whether it is just accident. The fact that it occurs in both acid and basic practices makes it sound quite plausible, but it can be stated, I think, more specifically.

This whole picture, in my opinion, sums up to the fact that you can fool an open-hearth furnace a little bit, maybe, but you cannot fool it much. I think the situation is this: We have gone through a process of complications, we have been confused and groping, and we have tried to adopt complicated slag-control procedures. It seems to me that the trend now is toward simplifying the whole problem, toward a realization that we were reading into slag control and bath reactions a good deal more than we needed to. And the trend now, perhaps, is to let the furnace have its head and give it a chance to work the carbon down rapidly. We should control phosphorus and sulphur, but forget some of these other things we have been worrying out, because when it all comes out in the wash, there really is not so much variation within the steel bath, from heat to heat, as we have imagined.

There is only one other point, which applies to slag control to some extent: if the bath is controlled by carbon in the high-carbon range, as seems evident from Brower and Larsen's

work, there must be some point of low carbon content where we have a change in mechanism, because in a carbon-free bath the oxygen in the bath appears to be related to the oxygen independent of both carbon content and rate of carbon drop. This result can be predicted from the theory of reaction rates which Schenck and other investigators have shown

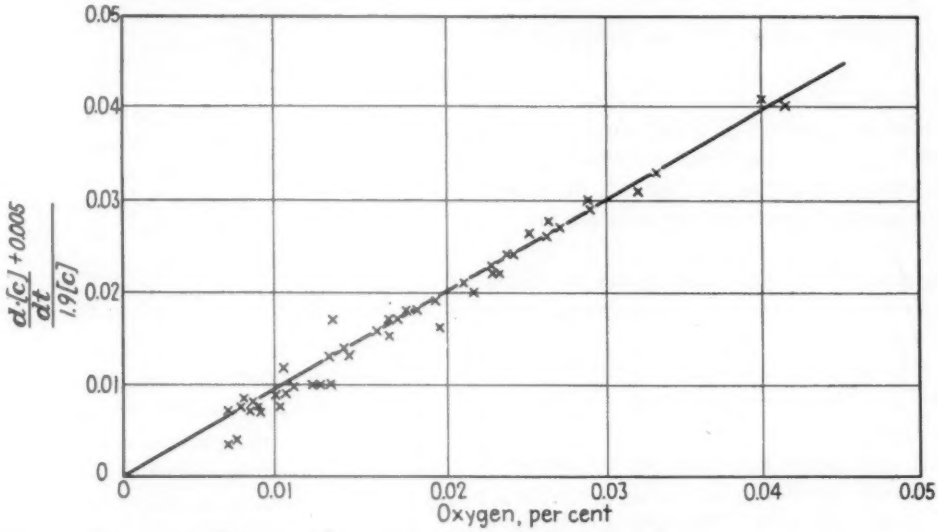

FIG 10—FUNCTION VS. PERCENTAGE OF OXYGEN.
Reproduced from paper on Rapid Determination of Reactive Oxygen in Open Hearth Steel, by one of the writers, Iron and Steel Inst., December 1946.

activity in the slag.[11] At some low carbon content, there must be a transition from control of bath oxygen by carbon to control of bath oxygen by slag oxygen. That is perhaps the reason for the upturn, in Fig 6, of the horizontal band of Δ[O] content, which turns up slightly at the low-carbon end, below 0.1 pct carbon. That may indicate a transition from carbon control to slag control. Perhaps that is the field where we should direct our attention now, to the low-carbon part of the system.

I. M. MACKENZIE* AND T. URIE*—While the application of statistical methods to the study of the function of oxygen in steelmaking is a valuable contribution to work in this field it is an approach that must be employed with care. It is unfortunate that the authors have ignored the considerable body of published work on the carbon-oxygen reaction.

The authors find the oxygen in excess of that in equilibrium with the carbon to be to be applicable to this reaction. The relationship between oxygen, carbon and rate of carbon drop is of the form

$$[O] = \frac{\frac{d[c]}{dt} + k_2 p_{CO}}{[c]k_1}$$

where $k_2 p_{CO}$ and k_1 are constants and $\frac{d[c]}{dt}$ is the rate of carbon drop.

The excess oxygen is a function of both carbon content and rate of carbon drop and cannot be expected to correlate closely with either one of them. This is illustrated in Table 4, which shows the excess oxygen Δ[O] for various carbon contents and rates of boil calculated from the foregoing equation, taking $k_2 p_{CO} = 0.005$ and $k_1 = 1.9$, $\frac{d[c]}{dt}$ being expressed as carbon loss percentage per minute.

As the authors claim (page 138), Δ[O] may vary fivefold for one rate of carbon drop, but this is due to the variation in carbon content.

Fig 9 shows a plot of results obtained using an analytical method very similar to that employed by the authors exhibiting a similar lack of correlation between excess oxygen

[11] C. R. Taylor and J. Chipman: *Trans.* AIME (1943) **154**, 228–245.

* Research Metallurgists, Colvilles Ltd., Dalzell Works, Motherwell, Scotland.

and rate of carbon drop during a steady boil. For the same data values of the function

$$\frac{\frac{d[c]}{dt} + 0.005}{1.9[c]}$$

were plotted against [O] as shown in Fig 10.

It would be interesting to know whether the authors' results would also show that the oxygen content of the metal correlated with a function of carbon content and rate of carbon drop when the bath is boiling steadily.

The hypothesis that the rate of bubble formation is the controlling factor in determining the excess oxygen would appear to be improbable, for two reasons:

1. The amount of oxygen stored in the metal is inadequate to maintain the boil for more than about a minute and the continuance of the boil depends on the steady influx of oxygen from the slag.

2. There will always be small gas pockets present in interstices in the hearth, which will provide nuclei for bubble growth. When the bubbles reach a critical size they will neck off from the gas pocket and rise to the surface of the bath, leaving the gas pocket to nucleate further bubbles. Although a variation in the number of interstices may account for a small variation in the excess oxygen between different casts it cannot account for progressive variations during the working of one cast, or for the widely different values for rates of boil and oxygen content often found for consecutive casts. It would appear more probable that the rate of boil is determined by the rate at which oxygen crosses the slag-metal boundary and diffuses to the hearth.

There does not seem to be any good reason for employing the excess of oxygen above equilibrium rather than the total oxygen content. The authors make no claim that their method of analysis gives absolute values for the oxygen content, yet they subtract from their experimental values a figure calculated from carbon-oxygen equilibrium determinations in which the oxygen has been estimated by a different method. The surprising conclusion that a bath that has gone off the boil may contain about 0.01 pct of oxygen in excess of the equilibrium concentration may be due to the authors' analytical method giving systematically higher results than that used for the equilibrium determinations.

TABLE 4—*Values of Oxygen in Excess of that Required for Equilibrium with Carbon* Δ[O]
WEIGHT PER CENT

$\frac{d[c]}{dt}$ ([c] pct per/min)	Carbon Content [c], Pct			
	0.1	0.2	0.4	0.6
0	0	0	0	0
0.001	0.005	0.003	0.0015	0.0010
0.002	0.011	0.005	0.0025	0.0015
0.003	0.016	0.008	0.0040	0.0025
0.004	0.021	0.011	0.0060	0.0040

ALBERT DE SY*—I have just read very carefully the two very interesting papers by Messrs. Brower and Larsen on the content of oxygen in liquid open-hearth steel. I congratulate the authors on their work.

The study represents a considerable amount of work. It was pursued in an orderly manner and the results obtained, by their regularity and their great number, represent the best contribution we have for the physicochemical study of refining on the hearth.

For about two years I have used the symbol Δ[O] with the same meaning the authors attach to it, and I call it: the potential of decarbonization, thus disclosing that there exists a correlation between the rate of decarbonization and Δ[O], even though the authors say: "Rate of carbon drop not only shows no correlation, but it may vary at least fivefold for a given level of Δ[O]."†

We do not contest (and could not, moreover) the authors' results that have proved a fact; from the theoretical point of view there must be a relation between the speed of the decarbonization v and the potential of Δ[O] and if the experimental results do not show it one is forced to conclude, as the authors do, that the relation between v and Δ[O] is obscured by a purely physical phenomenon in the occurrence of the elimination of the product of the reaction; that is, the vaporization of CO.

---

* Professor, University of Ghent, Belgium. Discussion translated from the French.

† This volume, page 138.

According to the old adage, "A good theory is always the best practice," it is of the greatest importance to try to explain the phenomena ascertained on the basis of our physicochemical knowledge.

The progress of modern technique is intimately connected with science; only science can guide our research work and save us long and useless experiments.

In the following exposition, we shall endeavor to explain on a scientific basis certain facts, which we believe will very soon be held as established. We hope that the following will interest our confreres across the Atlantic.

The decarbonization reaction $FeO + C \rightleftarrows Fe + CO$ in continuous process comprises three phases:

1. The reaction in the homogeneous medium between FeO dissolved and C dissolved with formation of CO, which is dissolved in the metallic bath up to saturation.

2. The vaporization of the dissolved CO:

$$[CO] \rightarrow \{CO\}$$
dissolved gas

3. The transfer of the O by diffusion or migration from the slag to the metal bath.

The rate of carbon drop evidently will be governed by the one of the three phases mentioned that is the slowest. Phase 1, the reaction in the homogeneous medium, is certainly more rapid than the two others, which correspond to the exchanges between two phases.

A. If we consider phase 1 as reaction in a homogeneous medium,

$$[FeO] + [C] \rightleftarrows [Fe] + [CO] \qquad [1]$$

we can write, calling v the rate of reaction from left to right and v_2 the rate of the reaction from right to left,

$$v_1 = \lambda_1'[FeO][C] = \lambda_1[O][C]$$

and $$v_2 = \lambda_2'[Fe][CO] = \lambda_2''[CO]$$

But, by Henry's law, $\frac{p_{CO}}{[CO]} = L = \text{constant}$

Hence $$v_2 = \lambda_2'' \frac{p_{CO}}{L} = \lambda_2 p_{CO}$$

The speed of reaction from left to right, therefore, will be

$$v = v_1 - v_2 = \lambda_1[O][C] - \lambda_2 p_{CO} \qquad [a]$$

Consider the equilibrium of reaction a for p_{CO} = one atmosphere, which would correspond to the contact of the metal bath with one atmosphere of CO at the pressure of one atmosphere; the corresponding concentration [CO] amounts to saturation. We have, therefore,

$$v = v_1 - v_2 = 0$$

i.e., $$\lambda_1[O][C] = \lambda_2 p_{CO} (p_{CO} = 1 \text{ atm})$$

Call $[O]_{ec}$ the oxygen concentration in equilibrium with the carbon for p_{CO} = 1 atm, and $[O]_r$ the actual concentration at a given time,

Hence $$\lambda_1[O]_{ec}[C] = \lambda_2 p_{CO}$$

By substitution in Eq a we obtain:

$$v = \lambda_1[O]_r[C] - \lambda_1[O]_{ec}[C]$$
$$= \lambda_1[C]([O]_r - [O]_{ec})$$

or $$v = \lambda_1[C]\Delta[O]$$

B. Let us consider now phases 1 and 2 together for the carbon drop:

$$\left.\begin{array}{c} [FeO] + [C] \rightleftarrows [FeO] + [CO] \\ [CO] \rightarrow \{CO\} \\ \text{dissolved gas} \end{array}\right\} \qquad [b]$$

The vaporization of CO cannot take place[12] except in places where the bath is in contact with a gaseous phase of which the partial pressure p_{CO} is less than the vapor tension of the dissolved CO. These places of vaporization are indicated by pores, little cavities and fissures of the lining that the melted metal, because of the surface tension, cannot fill.

If the lining is covered by a viscous or vitrified film, the openings mentioned do not occur; the metal bath is in complete contact with the surface of the lining and the layer of vaporization is almost nonexistent.[12] (Think of the use of pieces of porous rock in distillation or other manipulations of chemistry where solutions are made to boil.)

On the other hand, Körber and Oelsen[13] have shown that it is possible to prevent boiling when the wall of an acid crucible is covered by a vitrified film and the bath itself is covered

[12] It does not seem that the bubbles of CO can form spontaneously in the bath; the rising bubble is under too great capillary pressure from the molten metal.

[13] Körber and Oelsen: *Mitt.* K-W-I Eisenforschung (1935) **17**, 39–61.

by a very fluid slag of iron and manganese silicates.

The possibility or the facility of vaporization of dissolved CO depends then on the surface of vaporization S; that is, the whole surface of the gaseous bubbles in contact with the metallic bath.

The combined rate of phases 1 and 2 may be represented by:

$$v = (\lambda_1[O]_r[C] - \lambda_2 p_{CO})f(S)$$

($f(S)$ being a function of the surface of vaporization S)

or $$v = \lambda_1[C]\Delta[O]f(S) \qquad [b]$$

C. For the rate of phases 1, 2 and 3, let us consider now the results found by Brower and Larsen. These authors have proved the following values of $\Delta[O]$ and v.

	$\Delta[O]$, Pct	v, Pct C per Hour
Lime boil	0.009–0.015	0.35–0.45
Steady state	0.015–0.025	0.15–0.25
Working of ore	0.023–0.035	0.35–0.60

These values agree very well with the great majority of values calculated from data on the content of O in a liquid bath given in technical literature.

Brower and Larsen conclude, on the other hand, that there is no correlation between $\Delta[O]$ and carbon (0.08 to 1.2 pct); between $\Delta[O]$ and v, or between $\Delta[O]$ and b (1.7 to 5.5). $\Delta[O]$ increases almost imperceptibly with the content of Fe in the slag. In short, there exists a clear connection between $[O]_r$ and the molar fraction of FeO free from slag.

Given: $[O]_{ec}$ the concentration of O in equilibrium with C in the metal bath; $[O]_{es}$ the concentration of o in the bath in equilibrium with the slag:

we have:

$$\text{or} \quad \left.\begin{array}{l} [O]_{ec} \leq [O]_r \leq [O]_{es} \\ O \leq \Delta[O] \leq \Delta[O]_{es} \end{array}\right\} \text{during boiling}$$

Assuming $f(S) = O$

$$v = O$$

and $$\Delta[O] = \Delta[O]_{es}$$

that is to say, the concentration $[O]_r$ is maximum and equal to $[O]_{es}$.

That proves that a metallic bath that does not boil under an oxidizing slag may nevertheless contain the maximum O.

Preventing boiling or making it more difficult by physical means results therefore in increasing the content of oxygen in the bath. On the contrary, increasing v and also increasing $f(S)$ (for example, by poling) tends to lessen $\Delta[O]$ and consequently $[O]_r$.

Maintenance of boiling, said to be constant, necessitates the migration from the slag to the bath of a quantity of oxygen equal to that which leaves the bath in the form of CO. This indicates that the rate of carbon drop (that is to say, the rate of the phenomena 1, 2 and 3) is determined by the rate of diffusion of FeO from the slag to the metal bath, while the value of the potential $\Delta[O]$ and consequently of $[O]_r$ is governed by that of $f(S)$.

Let us consider the contact established between the bath Fe-C without o and a good oxidizing slag. We establish the diffusion of the FeO leaving the slag for the metal bath and the content of o of the bath tends toward $[O]_{es}$; that is, toward the concentration of the equilibrium with the slag:

$$[O]_{es} = \frac{1}{4.5}[FeO]_{es} = \frac{1}{4.5}(FeO)L_{FeO}$$

The oxygen content of the bath then attains the value $[O]_{ec}$; that is, the concentration of the equilibrium with carbon, and soon exceeds that value. From that time a certain value exists for $\Delta[O]$; that is, there exists a potential of decarbonization. For a certain value of $\Delta[O]$, a value that we call the breakdown potential, active decarbonization is initiated.

The bubbles of CO rising principally from the hearth traverse the bath and increase the surface of vaporization S, causing thus an increase of $f(S)$ and consequently of v. Continuing this reasoning, we can say that the increase of v causes a renewed increase of $f(S)$, and so on.

However, the rate v does not increase indefinitely in practice; the increase is limited by the transfer of oxygen from the slag. That is, a carbon drop rate of v pct C per hour corresponds to an elimination of $4/3v$ pct o per hour; if the slag does not furnish enough of it, the result is a decrease in $\Delta[O]$ and consequently in v.

We see then that under a controlled slag a

system of decarbonization is established that is conditional upon the rate of diffusion of FeO leaving the slag for the bath (from there the great influence of temperature).

$$4/3v \text{ pct O/h} = v \text{ pct C/h} = \lambda_1[C]\Delta[O]f(S)$$

As $\Delta[O]$ is inversely proportional to $f(S)$, it is important therefore to increase $f(S)$ while increasing the roughness of the hearth (influence of a new hearth). Thus it may be concluded that the rate of decarbonization is determined by the activity of the slag, which may be represented by the degree of lack of equilibrium with the bath; that is, by $[O]_{es} - [O]_r$, the temperature, the viscosity of the slag, the mixing, and other factors.

It is not possible to evaluate these variables; we must be content with the determinations of Brower and Larsen for normal boiling (steady state): $\Delta[O]$, 0.015 to 0.025 pct; v, 0.15 to 0.25 pct C per hour and 0.20 to 0.33 pct O per hour.

Consider now the effect of an ore addition. This addition leads to the increase of free FeO in the slag, hence $[O]_{es}$ increases and consequently $[O]_{es} - [O]_r$. The activity of the slag increases and at the same time the slag liberates more oxygen to the metal bath.

Primary consequence is that $\Delta[O]$ and v increase; secondary consequence is that $f(S)$ and v increase. This continues up to the establishment of a new order of things:

$$v = \lambda_1[C]\Delta[O]f(S)$$

The increase in v leads to: (1) increase of $\Delta[o]$, (2) increase of $f(S)$. v must now increase appreciably more, so that it may not prevent the increase in $\Delta[o]$.

Brower and Larsen fully confirm this point of view by the results of their experiments. After addition of ore, they find: $\Delta[o]$, 0.023 to 0.035 pct; v, 0.35 to 0.60 pct C per hour and 0.47 to 0.80 pct O per hour.

Consider now the lime boil. How can we explain that the lowest values of $\Delta[o]$ give relatively high values of v? Brower and Larsen obtain: $\Delta[o]$, 0.009 to 0.015 pct; v, 0.35 to 0.45 pct C per hour. We reply that the $\Delta[o]$ of Brower and Larsen is not the true $\Delta[o]$. This $\Delta[o]$ is fictitious because it is measured by the relation to $[o]_{ec}$ for $p_{CO} = 1$ atm and that in the period of the lime boil the value of p_{CO} is less than that of the two other periods considered in the foregoing pages. If, therefore, we allow $p_{CO} = 1$ atm for the two first, we must allow $p_{CO} < 1$ atm for the period of the lime boil.

During the lime boil, dissociation of $CaCO_3$ must be taken into account, with formation of bubbles of CO_2, which are more or less in contact with the metal bath and which can dissolve CO; we have therefore also bubbles of $CO + CO_2$ mixed (perhaps side by side with bubbles of pure CO and bubbles of pure CO_2).

We can therefore write for the lime boil:

$$P = 1 \text{ atm} = p_{CO_2} + p_{CO}$$

or

$$p_{CO} < 1 \text{ atm}$$

so that no appreciable dilution can be considered for the ore boil and normal ($p_{CO} = P = 1$ atm).

The $\Delta[o]$ of Brower and Larsen is given by

$$\Delta[O] = [O]_r - [O]_{ec} = [O]_r - \frac{0.00222\ p_{CO}(= 1 \text{ atm})}{[C]}$$

We shall consider this value as fictitious, the true value being:

$$\Delta[O] = [O]_r - [O]_{ec} = [O]_r - \frac{0.00222\ p_{CO}(< 1 \text{ atm})}{[C]}$$

As the values of v for the lime boil lie between those for the normal boil and those for the ore boil, it is probable that the same is true of $\Delta[o]$, which does not make it impossible that the true concentrations of oxygen, $[o]_r$, may be lower during the lime boil than during the two others that we have considered in this discussion.

Conclusion

The function $v = \lambda_1[C]\Delta[o]f(S)$, which we take as the expression of the speed of phenomena 1 and 2, gives the expression for the speed of decarbonization imposed by the activity of the slag.

During decarbonization the slag gives up oxygen to the metal bath at a known rate (for example, x pct O per hour). This O is consumed at a rate that is perceptibly the same and that corresponds to a speed of decarbonization: v pct C/h = 3/4 × pct O/h

(for example, 0.15 pct C per hour = 0.20 pct o per hour.)

The rate of carbon drop so imposed is therefore connected with the amounts Δ[o] and $f(S)$ by the relation: $v = \lambda_1[C]\Delta[o]f(S)$. The result is that Δ[o] will be the greater as $f(S)$ becomes smaller, and vice versa.

An important point remains to be elucidated; i.e., the influence of [C]. For fixed values of v and $f(S)$, from the foregoing formula it is evident that Δ[o] must vary inversely with [C]; but the work of Brower and Larsen (and that of Schenck also, although in a less radical way) nullifies this conclusion. Hence [C] has always a constant value, or at least is less variable than is the concentration of carbon in the metal bath.

To explain this, is it not possible to invoke the different states of solution of carbon (atomic, Fe C, Mn_3C . . .) and review the possibility of the existence of an active fraction relatively constant in the domain of the usual concentrations of this element?

B. M. LARSEN (author's reply)—A partial answer to Mr. Stott's first question is given in the paper; referring to Fig 5, it is noted that a few points marked with a tiny flag, to denote "high-carbon ancestry," indicate a greater sluggishness in the bath, having in general lower rates of carbon drop with somewhat higher values of Δ[o] in most cases. More data would be desirable on this point, especially a better means of measuring the bottom surface effect, which we indicate here indirectly by the "ancestry." This effect does not seem to slow up carbon elimination by ore feeds, however, at least to any important extent.

Our experience has indicated that a deoxidation control based on tap carbon is the best approximation for practical purposes. It is just as well to realize that this can be only an approximation, however, if the indications of Fig 7 in the second paper (page 164) are representative of conditions in general in various shops.

It would be interesting to have more published data on [o] values near the hearth by bomb samples such as those briefly indicated by Mr. Tenenbaum. The figures he mentions, however, would seem to confirm the [o] gradient through the bath indicated by our data in an earlier paper on sampling methods.[9] Table 2 in that paper shows an average 0.005 pct lower [o] in deep samples taken by spoon near the hearth surface, as would also be indicated by Mr. Tenenbaum's remarks. Both indications, however, would seem to agree on a definite supersaturation even near the bottom and thus to disagree with certain published data giving values down very near the carbon equilibrium in the metal near the hearth surface.

Mr. Philbrook indicates the desirability of sampling near the bottom where the bubbles start and where the pressure is some 30 to 40 pct higher. Our sampling was in general some 3 to 6 in. below the upper metal surface, and since the bubbles leave the metal at about this level it seemed most logical to assume 1 atm pressure for the oxygen at equilibrium. If we take the higher pressure of 1.5 atm, and also the apparent average decrease of about 0.005 pct [o] from top to bottom, the apparent Δ[o] value required to maintain a boil is much lower. Instead of about 0.013 to 0.015 pct, it becomes about 0.005 to 0.007 pct, but is again nearly constant within this small range for the carbon range of 0.10 to 1.00 pct. Again we have an indication of a small but constant amount of excess oxygen near the hearth surface required to maintain a steady boil, this excess being lowered to a negligible value by a very vigorous lime boil, and the concept of the system as presented in these papers remains essentially unchanged.

Mr. Philbrook comments on the ranges of Δ[o] given for lime boil, steady state, and ore-working periods as being somewhat different from those shown in Fig 5. This plot shows only a small portion of all the values obtained; the ranges of 0.009–0.015, 0.015–0.025, and 0.023–0.035 cover about 90 pct of all values in the respective furnace conditions. There is some overlapping of these ranges, however.

From 50 to 90 individual values are included in each of the frequency curves of Fig 7 in the first paper. Groups of this size are normally large enough to be significant and any other statistical correlation method is less direct and understandable than the simple frequency curves. Such spreads as are shown here are not usually obtained unless one factor is very predominant over other variables. Of course, this evidence is all very

indirect and a mere beginning toward a clear understanding of the effect of the bottom surface on the bath reaction; it is thus not surprising that there is considerable overlapping of the curves.

In the 0.06 to 0.14 pct carbon range, our experience tends to indicate that the refining-slag composition still has little effect on [o] values in the furnace, the biggest problem being the variability in [o] in the stream off the runner as indicated in Fig 7 of the second paper. Lime feeds near tap to lower the oxygen activity and increase the viscosity of the slag combined with some stirring method may have some value here, as indicated by Mr. Sims. In the 0.02 to 0.05 pct carbon range, however, it is quite possible that slag control can be used to minimize [o] values even before tap.

Regarding Mr. Mackenzie's comment on the method of analysis for oxygen, our method was essentially the same as reported in the recent paper by Mr. Mackenzie. We used spoon sampling rather than the bomb method but the details of fine aluminum wire in mold and estimation of Al_2O_3 by turbidity in solution are very much the same. We have used this method since about 1935 and consider that it gives the total content of *dissolved oxygen* in the liquid steel. This conclusion is also confirmed by more recent data given by Swinden and Stevenson.[14] Such values for total dissolved oxygen should, therefore, yield the true excess above any assumed value for the amount at equilibrium with the carbon *in the metal as it arrives in the sampling mold*, at least. The main uncertainty is in the sampling operation. Even rapid dipping and pouring in air with a slagged spoon may increase the oxygen by some 0.002 to 0.004 pct above what it was in the bath; on the other hand, the melting through of a thin steel cap incident to the bomb-mold technique may decrease the oxygen by as much or more below what it was in the bath. We suspect that Mackenzie's [O] values are somewhat low even for deeper layers in the bath, but are quite willing to concede that our values may be slightly higher than even the upper layers. However, it is interesting to note that about 80 pct of the Mackenzie data[15] give Δ[o] values within a range of 0.005 pct over the carbon range from 0.07 to 0.77 pct, though at a lower level (0.005 to 0.010 pct) than indicated by our data.

We do not entirely understand Mr. Mackenzie's objections to bubble surface area as a limiting factor in the reaction. It is quite true, as he says, that "the continuance of the boil depends on the steady influx of oxygen from the slag," but it should be remembered that this steady influx depends very largely on the stirring action of the bubbles themselves, since pure diffusion in a quiet bath should be, relatively, very much slower. This means that oxygen supply rate very probably slows down or speeds up with the rate of bubble formation. The idea that there will always be an abundance of interstices in the hearth surface to provide nuclei for bubble growth may be true, but it remains an opinion rather than a fact established by direct measurement or observation. Also, if bubble starting is largely limited to such nuclei, there may never be enough to eliminate them entirely as a limiting factor in the reaction rate. An actual open-hearth bottom after even a short period of service never has a clean, rough refractory surface unless it is resurfaced after almost every heat, being always soaked up with mainly lime and iron oxide fluxes, and nearly always either eroding away or building up with lime-slag-dolomite accumulations.

An adequate reply to the remarks of Messrs. Sims, Philbrook, Mackenzie and De Sy anent the mechanism of the carbon reaction would require more space than seems reasonable in this discussion; we will touch briefly on a few points:

In all these remarks there is the general tendency toward the assumption of the carbon oxidation as being a homogeneous reaction. It seems fair to point out that there is absolutely no direct proof of this assumed mechanism; it is purely an assumption, which has value only in proportion as it serves to explain all the observed effects. Mr. Mackenzie adheres to the simple conventional viewpoint as applied to this reaction by Schenk in

[14] T. Swinden and W. W. Stevenson: *Jnl.* Iron and Steel Inst. (1943) **148**, 397–407.

[15] I. M. Mackenzie: Iron and Steel Inst. (Dec. 1946).

Germany and by Feild and Jette[16] in this country; understandably so, because it appears to fit his own data. It may be significant, however, that in this Mackenzie data the factors [C], [C] × [O], and d[C]/dt are all rather closely related to each other, thus making it uncertain as to which relationship is fundamental. In our data we find no appreciable correlation between either

$$[C] \times [o] \text{ and } d[C]/dt$$

or

$$[C] \text{ and } d[C]/dt$$

The factors

$$[C] \text{ and } [C] \times [o]$$

correlate, if anything, even more closely in our data than in the data by Mackenzie, however. Thus, on this point and on the relative constancy of Δ[o] with variable [C] we are in good agreement; but it is just these points that seem most difficult to explain on the assumption of a homogeneous reaction mechanism.

A few data from the bessemer converter process indicate a reaction rate that in most cases is practically constant over the [C] range from 1.5 to 2.0 pct down to around 0.1 pct or below, but averages some 50 to 100 times faster than the rates in the open-hearth process. Δ[o] and [C] × [O] values are perhaps more variable but average somewhat lower than in the open hearth, with [C] × [O] again showing a tendency to increase with [C].

Mr. Sims arrives at the concept of effective CO pressure increasing with carbon content, which seems to us equally difficult to explain. If the reaction rate increased fairly regularly (which is not true in our data) with this apparent pressure, one might explain it by assuming that oxygen is stirred in more rapidly as the reaction speeds up, with CO pressure as the fundamental control variable. But in the bessemer vessel, where the reaction is extremely fast, the apparent pressure is lowest, and in the open hearth we find that either [C] or d[C]/dt may vary as much as five to eight times with the other factor constant.

In general, it seems to us that all these difficulties can be eliminated simply by the assumption that *the reaction is heterogeneous*, with the actual combination of C and O units (to form either CO or CO_2) occurring mainly or only at the metal-gas interface. The reaction rate can then be determined by (1) the relative area of this interface on the one hand and (2) by the rate of supply of either oxygen or carbon to this surface reaction zone on the other. The high reaction rate in the bessemer is now reasonable simply because we are increasing both oxygen supply and reaction surface area in about the same proportion. The relative constancy of Δ[O] in the open hearth over a wide carbon range with other conditions about constant (as in the so-called steady-state condition) can then be explained simply by the rather reasonable assumption that O units reach the reaction zone more slowly than C units (over the usual C range) and the amount of excess oxygen above equilibrium becomes the limiting factor, with the increase of [C] × [O] with [C] simply the secondary result or consequence of the rather constant Δ[O] values. On the other hand, the variability of Δ[O] in the bessemer (even after allowing for a possibly variable CO back pressure) and its variability in the open hearth between lime boil and ore-feeding periods, and perhaps with variable bubble nucleation conditions on the hearth surface, all these become more understandable simply because the excess oxygen is simply the resultant effect of two only partially interrelated factors; (*a*) the rate of oxygen supply to the related reaction surface and (*b*) the rate of bubble formation or the area of reaction surface. Thus, if by any means we can increase (*b*) faster than (*a*), Δ[O] will tend to decrease; if (*a*) increases relative to (*b*), Δ[O] will tend to rise.

We are especially appreciative of the rather detailed comments from both Mr. Mackenzie and Professor De Sy as coming from friends across the Atlantic. The mathematical expressions for the rate factors by De Sy seem very rational to us and we would feel that they come closer to expressing the true situation than any others now in the literature. Even here, however, there is the assumption of a homogeneous reaction mechanism (phase 1 of his three steps in the process) which leads eventually to the expression

$$d[C]/dt = K[C]\Delta[o]f(S)$$

[16] E. R. Jette: *Trans.* AIME (1931) **95**, 80–123.

indicating again that the factor [C] should be important to the rate, which is definitely not indicated by our data, as mentioned above.

De Sy's explanation of lower Δ[O] in lime-boil periods as caused by the dilution effect of CO_2 in the bubbles, and consequent lower back pressure, may be valid but we doubt that this is the main effect, at least. The diluting effect of CO_2 here is complicated by: (1) its oxidizing effect, which would seem to have the opposite effect on Δ[O], and (2) the probable very rapid change of CO_2 to CO by reaction with the [C] so that the bubbles should very rapidly change to nearly pure CO near the gas-metal surface. We would be inclined to explain the lime-boil effects as being mainly caused by (1) the oxidizing effect of the CO_2 as the accelerator of reaction speed, and (2) the large increase in bubble-surface area (the (S) factor of De Sy) as the factor tending to lower the Δ[O] values. In the bessemer process, the nitrogen probably is more nearly a true diluent lowering P_{CO}, but the high reaction rate there is not due to this effect but to the combination of rapid oxygen supply and proportionate increase in reaction surface or gas-bubble area where this (in our opinion) heterogeneous reaction takes place.

The discussion of these papers has been most interesting and stimulating and the authors would like to thank all those who have contributed so generously.

Oxygen in Liquid Open-hearth Steel—Effect of Special Additions, Stirring Methods and Tapping

By T. E. Brower* and B. M. Larsen,* Member AIME

(Atlantic City Meeting, November 1946)

In two previous papers[1,2] dealing with the carbon-oxygen reaction, and the simultaneous content of each, in liquid steel in the furnace, we have made use of the quantity Δ[O], defined as the excess oxygen beyond what would be in equilibrium with carbon then present if the pressure of carbon monoxide were 1 atm.; that is, if [C] × [O] is taken as 0.00222, Δ[O] = [O] − 0.00222/[C] where [O] is the percentage of oxygen by weight as measured by the method described earlier.[3] This quantity Δ[O] proves to be substantially independent of carbon content over the range 0.08 to 1.2 per cent, as well as of the basicity of the slag, and is nearly always within the limits 0.015 to 0.025 per cent when the bath is boiling normally and is in what we have termed a steady state. Apparently it must be at least about 0.014 per cent before boiling occurs; but this threshold value seems to depend upon the ease of bubble formation at the metal-hearth interface, hence upon the condition of the surface of the hearth. In any case, Δ[O], on the average, changes considerably following any disturbance of the bath, as by addition of ore. The present paper deals with the average changes in Δ[O] level following addition of spiegel or crop ends, or after procedures to promote stirring, or by tapping of the steel from the furnace. The observations were made on a large number of commercial heats, and consequently are subject to the influence of various disturbing factors; the results have the compensating merit of showing the consistency obtainable under the limitations imposed by practical operation.

Manuscript received at the office of the Institute May 14, 1946. Issued as T.P. 2076 in Metals Technology, October 1946.

* United States Steel Corporation, Research Laboratory, Kearny, New Jersey.

[1] References are at the end of the paper.

Variability of Excess Oxygen in Normal Open-hearth Operation

The preceding general statements refer to the average value of Δ[O] particularly in heats that are boiling actively; on individual heats, which are less active, there may be a variable time lag between the disturbance and its effect, which complicates the interpretation of what is going on. For instance, if in the normal refining process boiling is sluggish, the slag usually is gaining oxygen from the gas phase above it, or from added ore, faster than it is losing oxygen to the metal; yet when the bath starts to boil vigorously, the opposite condition may prevail for some time. The consequence of this lag is a variation of Δ[O], the interpretation of which in a single heat may not be immediately obvious. This condition is illustrated in Figs. 1 and 2.

In Fig. 1, Δ[O] at the beginning of the test period was near the lower limit of its usual range (dashed lines) in the steady state as a consequence of the lime boil, which had ended about as indicated. The bath is now cold, carbon drop is slow, and the first small ore feed causes only a small rise in Δ[O]; as the temperature rises and as lime dissolves in the slag, and the bath becomes more active, the

second small ore feed increases Δ[O] markedly. This increase, which is as great as usually would be expected after a large ore feed, is to be ascribed to lower limit of the normal boil range. In the final sample, taken at the end of the runner and marked "stream," Δ[O] was—contrary to its usual course—some-

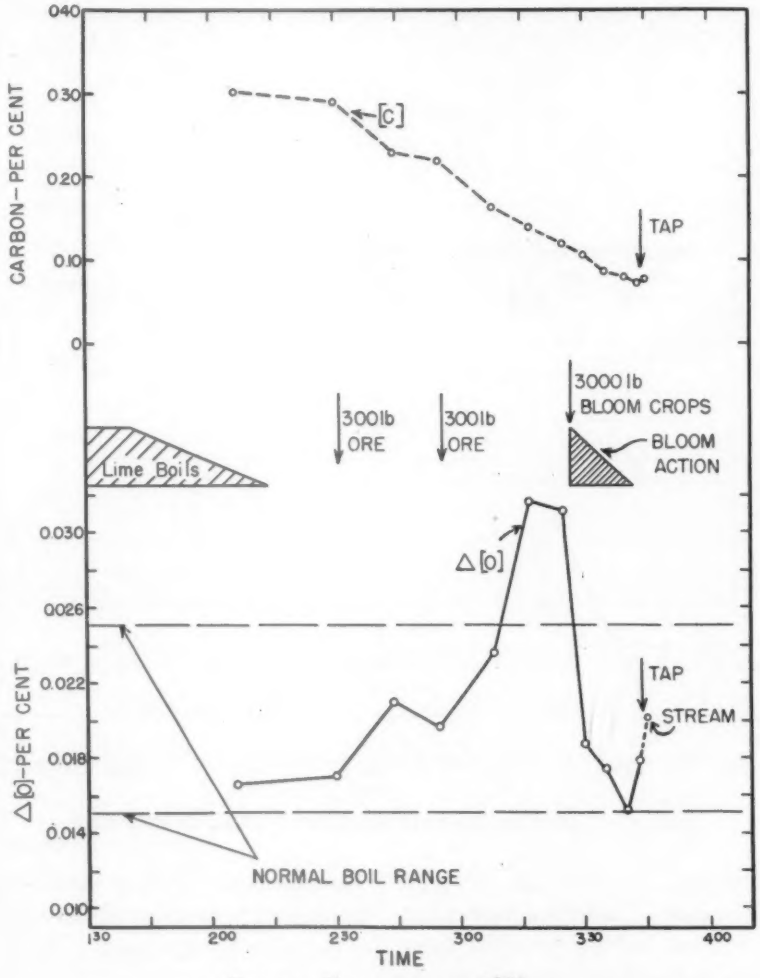

FIG. 1.—VARIATION OF Δ[O].

Example of variation, through the refining period of the heat, of carbon content [C] of metal and of the quantity Δ[O], the measured concentration of dissolved oxygen in excess of that in equilibrium with [C] and with 1 atm. CO, on the basis that for this equilibrium [C] × [O] = 0.00222.

utilization of the excess stored up in the slag. Δ[O], now above 0.030 per cent, would tend to decrease gradually if the bath were let alone; addition of 3000 lb. of heavy bloom crops lowers it quickly to about 0.015 per cent, by promoting a vigorous boil for some 15 min. As these crops dissolve, boiling becomes sluggish, and Δ[O] begins to rise again, as is usual after any lowering of Δ[O] to around the what larger than in the bath just before tap, presumably because it was on its way up at this time.

In Fig. 2, the rise of Δ[O] after each of the first two ore feeds, and the intermediate drop after addition of lime, all follow the expected pattern; but after the third ore feed Δ[O] drops sharply. During the first two, oxygen is being supplied to the metal faster than it is being elimi-

nated as carbon monoxide; but as active boiling develops, this condition is reversed in spite of the third small ore feed, and Δ[O] is again brought into its normal range.

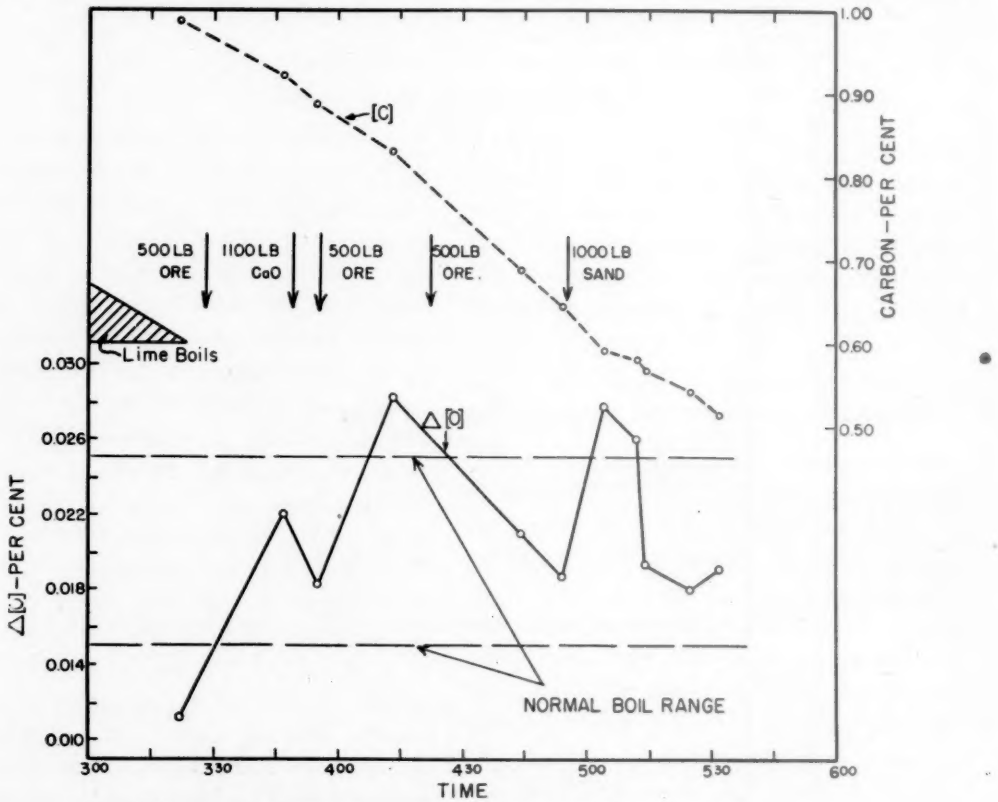

FIG. 2.—ANOTHER EXAMPLE SIMILAR TO THAT OF FIGURE 1.

After the addition of sand at 4:55, it follows the usual pattern, increasing temporarily but, as boiling becomes more vigorous, again diminishing into the normal range in about 20 min. after the sand was added.

That Δ[O] should change as illustrated by these two examples is not surprising in view of the attendant circumstances. The gas phase over the slag is so oxidizing that it builds up the oxidizing power of the slag unless this is kept down by steady reaction with the metal, as indicated by boiling. On the other hand, the boil is to some extent self-stimulating, in that, since the zone of most active reaction seems to be the metal-gas interface, its rate increases with the total surface of the bubbles, whose stirring effect, moreover, helps to increase the amount of oxygen available for reaction. The net result is that the variations in operating technique from heat to heat, as usually made, produce differences in the course of Δ[O] through the refining period.

Because of these differences, which are unavoidable under present operating conditions in the open-hearth furnace, we have resorted to curves made by averaging data from groups comprising from 6 to 12 separate heats, and by this means infer how the excess oxygen in the liquid steel is affected, on the average, by specific operating procedures. The five here considered are, in order: addition of silica or of lime with spar to the slag; artificial stirring; blocking; tapping.

Addition of Silica

The curve in Fig. 3 represents the average course of Δ[O] in 13 separate 90-ton heats when either 2000 lb. ground brick bats, or 1000 lb. sand, was added. It is evident that Δ[O] regains its normal level for the steady state in about 20 min. after the addition. The general course is much the same as when ore is fed to a heat in which the slag is shaped up and hot enough to dissolve the ore rapidly. Addition of silica by lowering the total number of mols present in the slag, as indicated in a previous paper,[2] tends to raise the mol fraction of iron oxides (N_{FeO}), or oxygen potential of the slag,

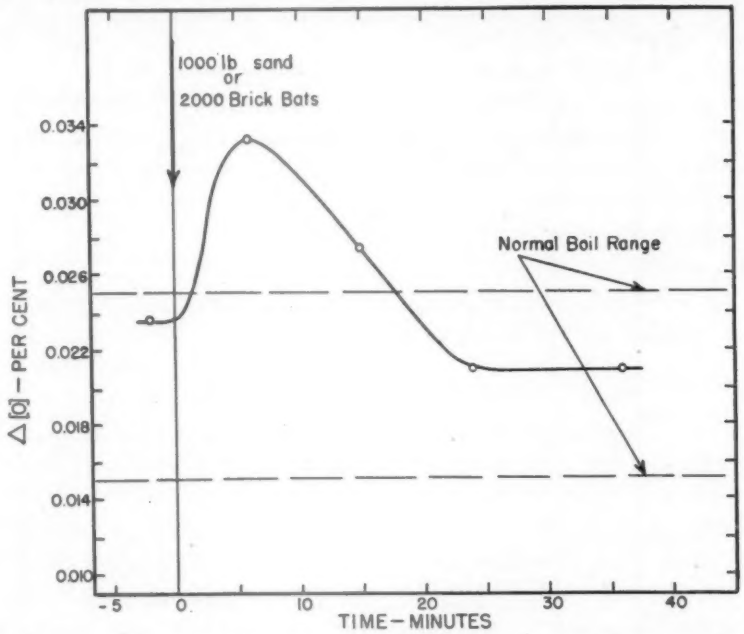

FIG. 3.—EFFECT OF ADDITION OF SAND OR SILICA BRICKBATS TO THE SLAG ON Δ[O]; AVERAGE OF 13 HEATS.

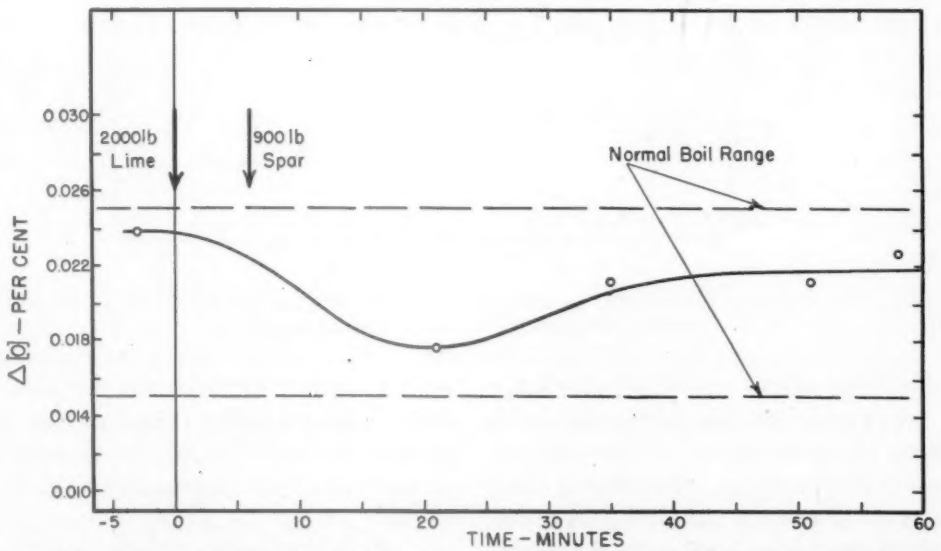

FIG. 4.—EFFECT OF ADDITION OF LIME AND FLUORSPAR TO THE SLAG ON Δ[O]; AVERAGE OF SIX HEATS.

and is thus equivalent in effect to an ore feed. In any case, the net result is merely a temporary alteration of level of oxygen in the metal.

or even increase slightly because of the lowered iron oxide content of the slag.

These observations lead us to express the view that there is no advantage in

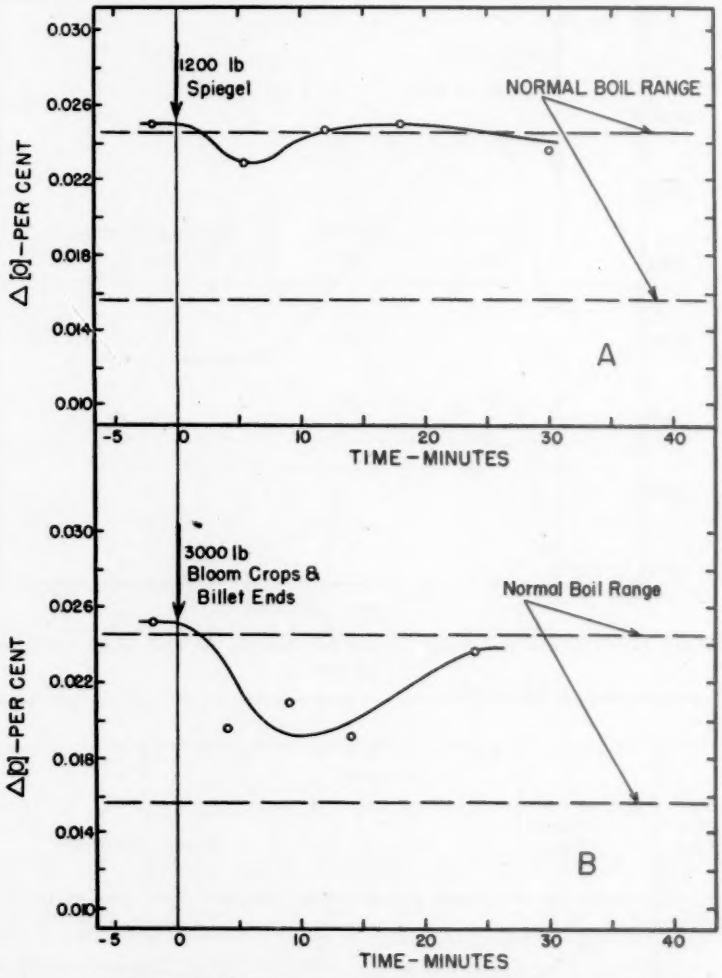

FIG. 5.—COURSE OF Δ[O] DURING (*A*) SPIEGEL REBOIL; (*B*) STIRRING PRODUCED BY BLOOM CROPS OR BILLET ENDS; BOTH AVERAGE OF EIGHT HEATS.

Addition of silica helps to dissolve lime, but we could see no advantage over addition of spar, scale, or fine ore; it has the disadvantage of lowering slag basicity and thereby hindering removal of phosphorus and sulphur from the metal. In these tests, residual manganese decreased 0.01 or 0.02 per cent, as is likely to occur when the basicity ratio b is 2.6 or less; when b is about 3 or higher, the residual manganese may remain unaltered adding silica instead of ore but, on the other hand, a slight disadvantage with respect to recovery of manganese and elimination of phosphorus and sulphur.

Addition of Lime and Fluorspar

The curve in Fig. 4 is the average result of adding 2000 lb. burnt lime and 900 lb. fluorspar to each of six 90-ton heats. While this lime is dissolving (which takes longer than for silica) and for some

time afterward, the rate of carbon drop usually decreases somewhat because of the temporary decrease of N_{FeO} (the mol fraction of iron oxide in the slag) and the consequent lowered rate of supply of oxygen to the metal, until the slag again carries more oxygen by absorption from the furnace gases. This small temporary decrease in Δ[O] would hardly seem to justify addition of lime close to tap in view of the resulting increase of 20 to 30 min. in charge-to-tap time.

Artificial Stirring

The upper curve in Fig. 5 is the average result of eight tests in which 1200 lb. of spiegel was added to a 90-ton heat. The stirring effect is mild, with some stimulation of boiling; but the oxygen level of the metal is practically unaffected.

The lower curve refers to eight heats to which from 2000 to 5000 lb. heavy crop ends were added. This creates a vigorous boil and seems to stir the bath all over; yet it causes only a small lowering of Δ[O], which is erratic from one heat to another and in any case disappears when vigorous boiling ceases. The result of stirring by use of three to six rods was similar in that Δ[O] was again lowered temporarily by a small and varying amount. Likewise, the use of green poles, forced well down into the metal to produce lively stirring, did not substantially alter Δ[O].

The greatest lowering of oxygen level produced by any of these methods of stirring is that shown in Fig. 1; but this lowering never persisted for more than about 15 min. after stirring ceased. There is no doubt that vigorous agitation can lower Δ[O] somewhat below its range during normal boiling, for such a lowering is consistently brought about by an active limestone boil. However, effective agitation of a pool of metal requires much energy and is difficult to maintain by artificial methods; furthermore, a normal carbon boil, with its apparent tendency to evolve bubbles under the metal on the hearth surface, is relatively effective for this purpose.

In general, therefore, it seems that these methods of artificial stirring have little, if any, useful effect on the oxygen content of the steel. Stirring does promote absorption of heat by the steel, as shown on occasion by a rise of temperature during a lime boil on a sharp working furnace, in spite of the heat absorbed by the reactions. How far such stirring promotes the washing out of suspended nonmetallics remains an unanswered question, on which there is as yet no clear evidence.

Effect of Blocking Additions of Ferrosilicon

Each one of the pair of curves in Fig. 6 represents the average of 10 heats, the lower when there was no bottom boil, the upper when there was at least one definite bottom boil. Boiling ceases when Δ[O] is depressed somewhat below 0.015 per cent and begins again around the edges of the bath as Δ[O] rises past about 0.013 to 0.015 per cent. Comparison of the two curves shows that the bath "comes back to a boil" faster in presence of a bottom boil, which speeds diffusion of oxygen from slag to metal.

Effect of Tapping

The evolution of gas from the tapping stream may be observed in nearly all heats tapped without prior blocking, though the amount evolved appears to be somewhat variable from heat to heat. Sometimes there is a blowtorch type of flame over the metal issuing from the taphole; more commonly this is less noticeable, but flaming gas comes off the metal as it flows down the runner. In view of the evidence that in normal boiling the bubbles form on the hearth surface under the bath, it is reasonable to expect that, in tapping, the surface of the tapping hole, over which the metal is forced to flow in a

narrow stream, would stimulate bubble formation and thereby produce gas evolution.

In a previous paper[3] a description was given of the method used for sampling the tapping stream by impinging a block-shaped mold into the side of the stream just off the end of the runner. Fig. 4*B* in that paper indicates agreement to within 0.002 per cent oxygen, on three fourths of all heats, between groups of two or three samples from the stream at various times between beginning and end of tap. Somewhat larger differences observed on some heats may represent real differences. In general, this sampling method gives consistent results. Fig. 7 in the paper just cited[3] shows that the loss of carbon between bath and tapping stream either is equivalent to the loss of oxygen as CO or is larger, probably because of a compensating absorption of oxygen from slag or air. The observations all agree in indicating that the carbon-oxygen reaction tends to accelerate markedly on tapping, so some change would be expected in Δ[O] as between samples from the bath just before tap and those from the stream entering the ladle.

Fig. 7 is a plot of Δ[O] against carbon content for all tapping-stream samples from the heats in which the bath was at steady state before tap and had had no furnace block or other deoxidation. In all these heats Δ[O] in the bath just before tap was within the normal range (dashed lines), so that, as Fig. 7 shows, there is a decided tendency for excess oxygen to decrease during tapping. Although the [C] level (above about 0.08 per cent) seems to have no effect on Δ[O] in the bath, the lowering from bath to stream increases with carbon content and becomes more uniform. Above 0.50 to 0.60 per cent C, Δ[O] is nearly zero in the stream; that is, it decreases nearly to its value at equilibrium with carbon at 1 atm. CO pressure by the time the metal reaches the end of the runner. Thus, in such high-carbon heats, the "shake-out effect" of tapping enables the carbon reaction to deoxidize the steel effectively, with residual oxygen mainly between 0.002 and 0.009 per cent

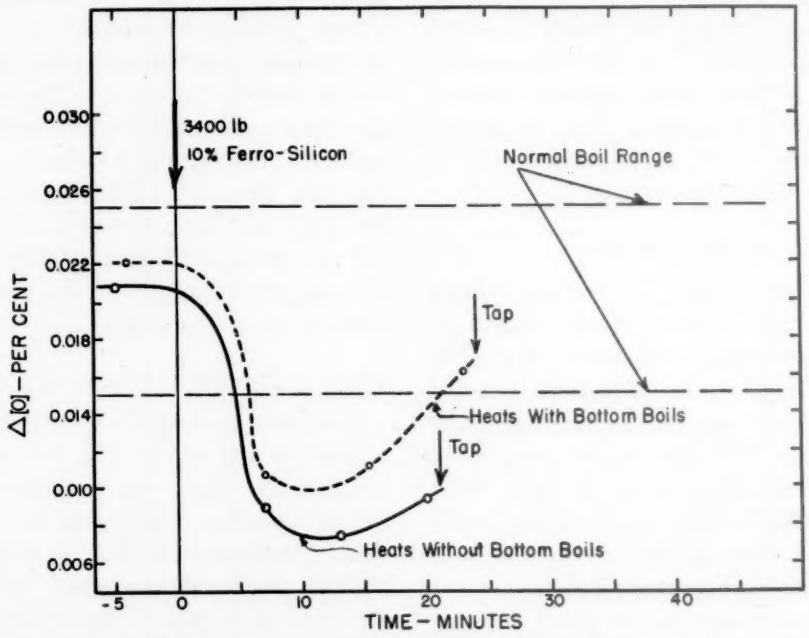

FIG. 6.—COURSE OF Δ[O] FOLLOWING BLOCK WITH FERROSILICON IN PRESENCE AND IN ABSENCE OF BOTTOM BOILS; AVERAGE OF 10 HEATS IN EACH.

in the steel entering the ladle. We have been unable to find any definite clue as to the reason for the wide variability of Δ[O] in stream samples of lower carbon steels; being presumably important to bath after block there is little movement and, as oxygen is diffusing back into the upper layer of metal, Δ[O] in samples from the upper layer tends to be higher than the average for the bath as a whole.

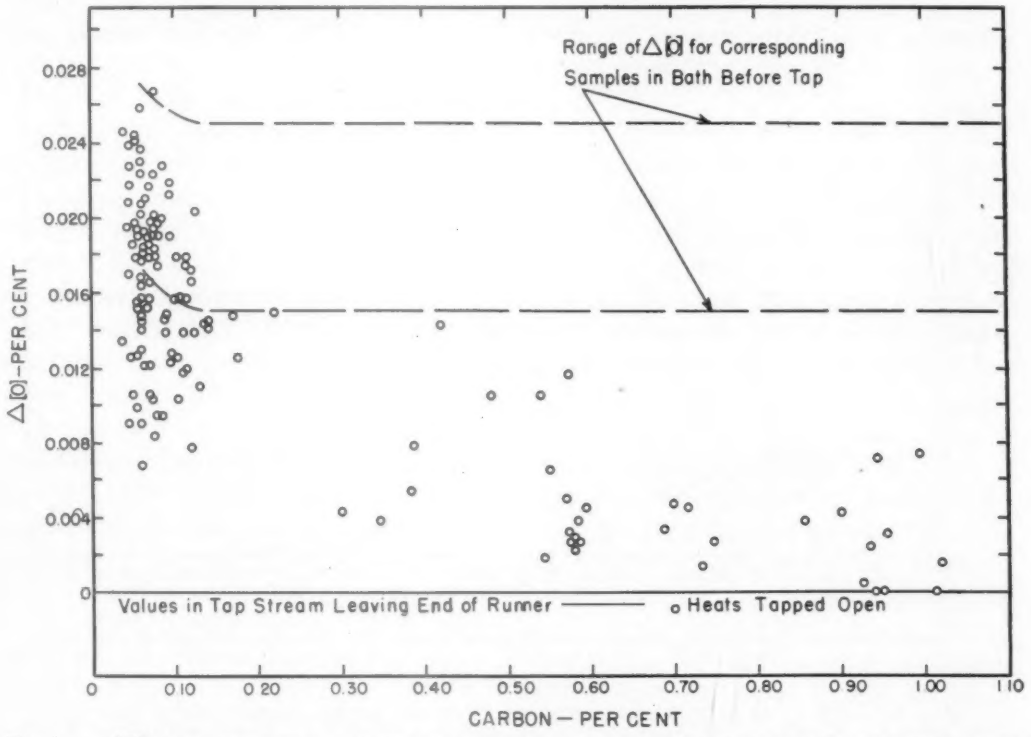

FIG. 7.—Δ[O] AS MEASURED IN TAP STREAM ENTERING LADLE, FROM OPEN HEATS THAT HAD BOILED NORMALLY AND HAD NOT BEEN DEOXIDIZED.

proper control of the final deoxidation process, it is deserving of further study.

The situation is rather different in blocked heats. In such heats the added silicon has lowered Δ[O] well below its normal range, and there is little driving force for bubble formation even when all physical conditions are favorable; nor is there any noticeable gas evolution from the tapping stream. Comparison of Δ[O] before and after tap shows that it is the same or lower in the stream in most cases but higher in some, this lack of apparent uniformity being due probably to the difficulty of sampling blocked heats. In a normally boiling bath the metal is well mixed, and a single sample usually is close to the average; but in a dead

The following figures are the averages from two groups, each of 33 heats, ranging from 0.20 to 1.00 per cent C at tap, one group blocked and the other tapped open on a rapid carbon analysis:

Group	Average Δ[O] for 33 Heats, Per Cent	
	Bath Just before Tap	Tap Stream
Blocked	0.0089	0.0058
Tapped open	0.0205	0.0054

These blocked heats were essentially free from violent bottom boils; those tapped "open" had a ferromanganese addition 5 to 10 min. before tap, but this

was found to have no appreciable general effect on oxygen content.

The distribution of Δ[O] in tapping-stream samples from these blocked heats is shown by Fig. 8, in which the dashed lines include the range of points for the unblocked heats (Fig. 7). From this it appears that there is little to choose between open or blocked heats with respect to the content of dissolved oxygen in the steel entering the ladle. Addition of silicon to the bath causes a sudden lowering (Fig. 6) of [O] by about 0.012 per cent, and presumably precipitates in the

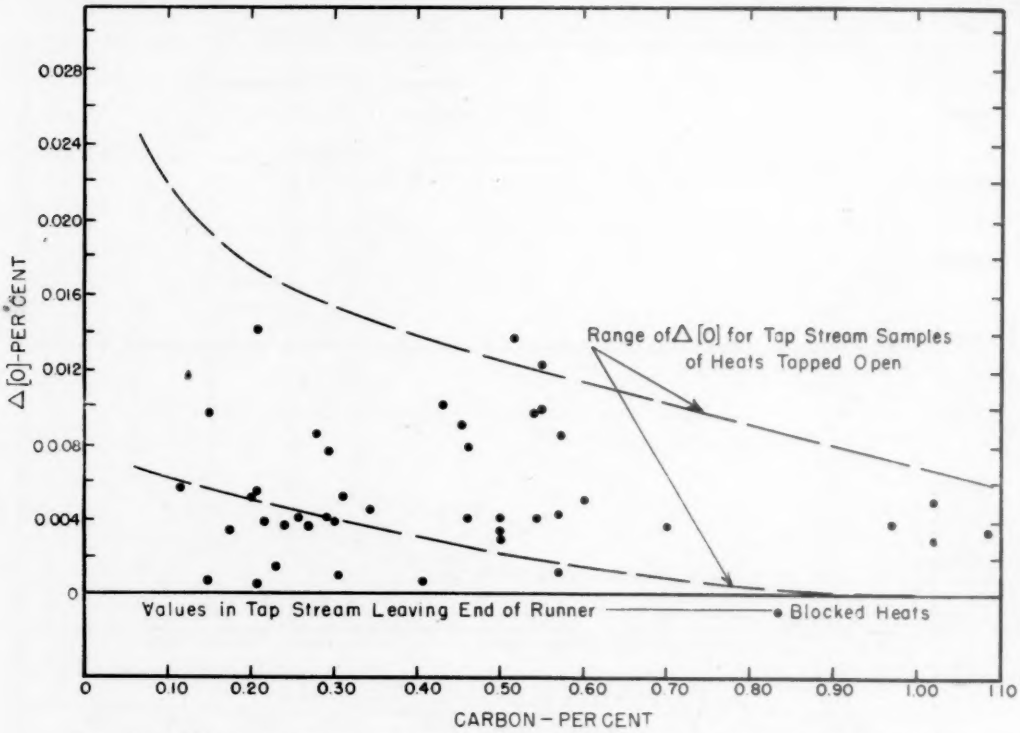

FIG. 8.—Δ[O] AS MEASURED IN TAP STREAM ENTERING LADLE, FROM BLOCKED HEATS.

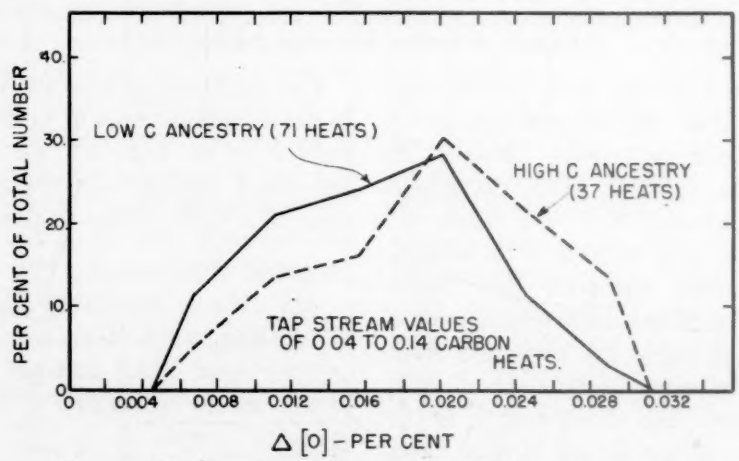

FIG. 9.—FREQUENCY DISTRIBUTION OF Δ[O] IN TAP STREAM.
From heats all ranging from 0.04 to 0.14 per cent carbon at tap, which had been preceded by one or more heats that finished with (*A*) more than 0.3 per cent carbon ("high-carbon ancestry"), (*B*) with 0.12 per cent carbon or less ("low-carbon ancestry").

metal an equivalent amount of silica-rich inclusions, some of which probably remain in the metal leaving the furnace. Since the tap stream from blocked heats carries as much residual *dissolved* oxygen as that from open heats, but presumably more suspended oxides, blocking would seem to offer no advantage with respect to loss of ladle deoxidizers and quite possibly some disadvantage with respect to steel cleanliness. A furnace block tends to increase charge-to-tap time as well as the reversion of phosphorus from slag to metal. Silicomanganese alloys as blocking agents apparently give somewhat cleaner steel than silicon-iron alloys. There are a few grades of alloy steel in which blocking aids in minimizing losses on large alloy additions in the furnace. On a large majority of all steels produced, however, with present rapid methods of carbon analysis, slag control and furnace operation in general, it would seem that blocking serves no useful purpose, even on so-called quality grades. This view has been confirmed by practical experience in several shops.

In a previous paper,[2] evidence was presented that Δ[O] at tap on heats that follow low-carbon heats ("low-carbon ancestry"), and therefore presumably made on a cleaner bottom, is lower than on heats preceded by high-carbon heats, made, presumably, on a more glazed hearth. Since this difference might be largely eliminated by a larger decrease in Δ[O] during tap when Δ[O] is higher in the bath, it is interesting to compare results in tapping-stream samples with respect to "ancestry." Such a comparison is made in the frequency curves (Fig. 9) on data for heats between 0.05 and 0.14 per cent carbon; higher carbon heats show a similar difference at a lower average level of Δ[O]. The difference between these two curves is definitely less than that[2] for samples before tap, presumably because of a tendency toward a greater drop in oxygen content on tapping when Δ[O] is higher in the bath just before tap. In spite of this tendency, however, the condition of the surface of the bottom still affects Δ[O] as measured in the metal stream entering the ladle; this has been confirmed by correlated studies of quality of final product in a few grades of steel.

General Conclusions

When an open-hearth furnace is operated by methods commonly regarded as good standard practice, which comprise maintenance of a clean refractory hearth and of a normal boil and close control of carbon at tap, as well as absence of disturbing effects during the last hour before tap, the content of dissolved oxygen toward the end of the refining period is lowest and most uniform from heat to heat. Although it should be lowered somewhat by vigorous stirring and by extra gas evolution, measurements described herein show that the excess oxygen in the metal is not materially altered, except temporarily, by the methods commonly used to induce stirring; namely, additions of sand or silica brickbats, of lime with fluorspar, of crop ends, ferromanganese or spiegel, or by use of rods or green poles. Accordingly, these procedures, though they may occasionally serve some other purpose, appear to be of no special value as a means of control of final oxygen content of the steel.

When the heat is blocked, Δ[O] is lowered from its usual range (0.015 to 0.025 per cent) during a normal boil to 0.008 to 0.012 per cent; but oxygen soon begins to diffuse from slag to metal and in about 25 to 40 min. it has again risen to the threshold (Δ[O] = about 0.014 per cent) at which the reboil can begin, this effect being speeded up by the presence of bottom boils.

During tapping, Δ[O] tends to decrease with a simultaneous decrease in carbon content; this decrease apparently is brought

about by the formation of bubbles stimulated by the movement of the metal over the refractory surface about the taphole. In steels with more than about 0.40 per cent carbon, in which Δ[O] is a large fraction of total [O], the metal entering the ladle has by this means been so effectively deoxidized that the total oxygen content is less, and often decidedly less, than 0.01 per cent, and for a given carbon content is reasonably uniform from heat to heat. This is an ideal mode of deoxidation because nothing is precipitated in the steel. Since [O] in the stream in blocked heats is no lower on the average, at least with [C] values above about 0.2 per cent, it would appear that furnace block serves no useful purpose as far as oxygen content is concerned.

In steels with less than about 0.15 per cent carbon Δ[O] is a smaller fraction of total oxygen content and is more variable, because it seems to be lowered less uniformly while the steel is being tapped. For instance, total oxygen in the tapping stream of a number of heats, all with 0.10 per cent carbon at tap, varied from 0.029 to 0.046 per cent even when they had been finished in the furnace under uniform and favorable conditions. Further information on the source (or sources) of this variability is highly desirable, since this variability would seem to be one main obstacle in the way of a closer control of degree of final deoxidation and cleanliness of low-carbon steels.

References

1. B. M. Larsen: Controlling Reactions in the Open-hearth Furnace. *Trans.* A.I.M.E. (1941) **145**, 67–83.
2. T. E. Brower and B. M. Larsen: Oxygen in Liquid Open-hearth Steel—Oxygen Content during the Refining Period. This volume, page 137.
3. T. E. Brower and B. M. Larsen: The Occurrence of Oxygen in Liquid Open-hearth Steel—Sampling Methods. *Trans.* A.I.M.E. (1945) **162**, 712–722.

DISCUSSION

(M. Tenenbaum presiding)

G. Derge*—I should like to ask the authors if they found any connection between a high oxygen in the furnace before tap and a high oxygen in the ladle. If the heat was high in the furnace, was it also high in the ladle?

C. E. Sims†—The observations of this paper are not only interesting and potentially useful but very logical as well. They can be explained very nicely on the principles of bubble formation in liquid steel and the concept of dissolved CO gas under pressure.

During the lime boil, for example, the CO_2 from the limestone provides surface for the ready precipitation of CO, and thus a rapid lowering of oxygen content. During this period, the slag is not very oxidizing, and the oxygen is not replaced as fast as it is used.

Bloom butts, while they still have solid steel in contact with the liquid bath, make excellent surfaces for the nucleation of CO bubbles. Until they melt, therefore, dissolved CO will be given off at a very rapid rate.

New linings are used in the spout for each heat, and this rough unglazed surface is almost ideal for bubble formation, again leading to rapid elimination of CO.

In all these reactions, there seem to be two opposing effects regulating the oxygen content. One is the rate of nucleation of bubbles and precipitation of CO, but as this speeds up, the boil becomes more violent. This, in turn, produces more intimate contact with the slag and a faster transfer of oxygen to the bath. These two effects tend to come into balance but can temporarily get out of balance. Thus, after an addition of ore or sand, the oxygen content goes up for a short spurt, while the lime boil or bloom butts cause a decrease, which is short lived. In the steady state, a balance is attained which accounts for the constancy of the oxygen during this period and the self-regulating feature of open-hearth heats.

---

* Carnegie Institute of Technology, Pittsburgh, Pennsylvania.
† Battelle Memorial Institute, Columbus, Ohio.

If there is a desire to bring the bath oxygen to a low value, it appears that this could best be done by making a substantial addition of lime to the slag to lower its oxidizing power and then add bloom butts to the bath. This would give a rapid evolution of CO without the offsetting addition of oxygen from the slag.

J. CHIPMAN*—This paper gives the answers to some questions that many of us have been wondering about for a long time, and I believe the key to those answers lies in the oxygen analysis of samples taken from the tapping stream. I wonder if the author would describe for us the technic of taking those samples.

MEMBER—How did you take your samples during the refining period?

T. E. BROWER (author's reply)—In reply to Dr. Derge's question, there was a tendency for a greater drop in oxygen content on tapping when Δ[O]was higher in the bath just before tap. However, this is not always true, as illustrated by the ancestry plots before and after tap.† In this comparison, the ancestry, or bottom effect that was fairly large before tap is considerably less after tap; nevertheless it is still present and affects the Δ[O] of the metal entering the ladle.

Mr. Sims' remarks regarding the use of lime and bloom butts, just prior to tap, in order to lower the oxygen content to a low value, are in line with some of the experimental work we did. Such a procedure should perhaps be used only on low-carbon heats, since the higher carbon heats tend naturally toward low oxygen values after tapping. With this procedure the heat should be tapped within five to eight minutes after the addition of the bloom butts in order to take advantage of the minimum FeO point of the bloom boil.

In reply to the questions on the oxygen sampling technique: The sampling procedure for the furnace tests consisted in taking fine aluminum wire and rolling it into a ball and placing it within an open-top mold. Then a large well-shaped spoon was carefully slagged and filled with steel. The spoonful of metal was quickly removed from the furnace and a stream of metal was immediately started outside of the mold to be sure the stream was free of slag. Then the stream was moved over to the mold and the mold was quickly filled. Careful observation was made to be sure none of the slag entered the mold and no boiling occurred in the spoon. In such cases the test was rejected.

In the case of the samples obtained from the tapping stream falling from the end of the runner, the procedure was modified. Here a heavier block-type mold was used, to the side of which was fastened a ¾-in. pipe of the desired length. The fine aluminum wire ball was firmly wedged by hand into the inner corners of the mold. Using the railing at the rear of the furnace as a fulcrum point, the mold was edged or plunged into the stream, depending on the type of stream, and the mold was completely filled in one operation. The mold must be removed as quickly as possible, otherwise the edges of the mold will be melted. We have obtained as many as three to five samples from the tapping stream on one heat.

---

* Massachusetts Institute of Technology, Cambridge, Massachusetts.

† Fig. 7*a* page 146 and Fig 9 page 172, respectively.

The Mechanism of the Carbon-oxygen Reaction in Steelmaking

By C. E. Sims,* Member AIME

(New York Meeting, March 1947)

The carbon-oxygen reaction without doubt is the basic reaction in steelmaking. It is important on several counts: In the first place, carbon is the element that distinguishes steel from iron. It is the principal element controlling properties, and its control is of prime concern. Although the principal objective of the carbon-oxygen reaction is to oxidize excess carbon, the accompanying boil should not be underrated. The mechanical agitation, stirring, and mixing resulting from the boil are so useful in the distribution of heat and in promoting uniformity of composition in the bath that, were it not a natural accompaniment of the carbon-oxygen reaction, it is probable that something would have to be invented to replace it. The open-hearth operation, for example, with the bath heated from above by radiation, would be impracticable without the carbon boil. The electric-arc furnace is somewhat less dependent on it, but every melter knows how much easier it is to gain temperature with minimum damage to refractories during the boil than with a dead bath. The motor action of the induced current of the induction furnace makes the carbon boil unnecessary but even there a severe oxidation has been found useful in giving greater freedom from porosity in certain steels.

The quantitative aspects of the carbon-oxygen reaction have been given considerable attention by a large number of investigators, and the principles of physical chemistry have played an important part in these studies. Physical chemistry is the science of the mechanics and mathematics of chemical reactions. It is possible to study the mechanisms of reactions in a qualitative manner without reference to mathematics and thus obtain valuable concepts as to the manner in which the wheels go around.

When it is desired to express quantitative relations in these reactions, however, resort to mathematics is not only convenient but necessary. Mathematics may also be regarded as the shorthand language of physical chemistry. A basic relation whose description requires numerous words may be expressed very simply by a mathematical formula or equation. A good example of this is the equilibrium constant for a chemical reaction. Expressed verbally, it is: *When a chemical reaction has reached a condition of equilibrium, the product of the concentration of the reacting substances on one side of the equation, divided by the product of the concentration of the reacting substances on the other side, gives a quotient that is a constant at constant temperature.* For the carbon-oxygen reaction

$$C + O \rightleftharpoons CO$$

this is expressed simply as

$$\frac{\%\,C \times \%\,O}{\%\,CO} = K$$

where K (from the German *Konstant*) is the equilibrium constant for the reaction.

Although mathematics is such a necessary and useful tool, it is also a potential pitfall. Mathematics in itself is an abstract science, which is not inhibited by consideration of mechanisms or materials.

Manuscript received at the office of the Institute Sept. 18, 1946. Presented at Electric Furnace Steel Conference, Dec. 5, 1946. Issued as T.P. 2129 in Metals Technology, Jan. 1947; printed in Electric Furnace Steel Proceedings, 1946 and Open Hearth Proceedings, 1947.

* Supervising Metallurgist, Battelle Memorial Institute, Columbus, Ohio.

It soars into the realms of the fourth or fifth dimension as readily as our mechanistic minds can visualize three-dimensional space. Thus, it is possible to attain a mathematical concept that is perfectly sound by all the laws of mathematics but for which we are unable to visualize any physical counterpart. A more likely possibility, however, is the mathematical derivation of a concept that is not too difficult to visualize as a mechanism but that does not actually occur.

There is another danger, and it is the one against which the greatest protest has been voiced. By unduly stressing the mathematical derivations of the concepts of physical chemistry without a balanced study and exposition of the mechanisms involved, the physical chemist isolates himself in an atmosphere that is not readily penetrated by the average engineer or metallurgist. This leads to confusion and a woefully inadequate application of many of the well-established principles.

In the present paper, an attempt is made to discuss the physical chemistry of the carbon-oxygen reaction, with the major emphasis on the mechanisms involved, and to relate these mechanisms to the data that have been presented in recent papers on the subject. It is recognized and admitted that much of the mechanics of high-temperature reactions is imperfectly understood or even unknown. The reason for the dearth of such information, of course, is the great technical difficulties involved in making intimate studies at steelmaking temperatures.

Considerable is known or believed about the mechanisms of steelmaking reactions, however, and, while much of this knowledge has been obtained by direct observation, the application of the laws of physical chemistry, and particularly of thermodynamics, has been invaluable in gaining a lucid picture. The method by which such laws may be applied to steel was expounded in a practical manner 13 years ago by Chipman.[1] In general, it may be said that when a proposed mechanism apparently fits all the known data and conforms to the fundamental laws, it is accepted as fact until some new data necessitate the design of a more accurate mechanism. Saying it obeys the fundamental laws is like saying it fits the majority pattern or is orthodox in its behavior.

The Heterogeneous System in the Furnace

A conventional section of an electric furnace is shown in Fig 1. It diagrams the heterogeneous three-phase system of atmosphere, slag, and metal that is typical of electric-furnace practice and shows the principal reactions taking place.

The oxygen to maintain the carbon-oxygen reaction is obtained from two principal sources; namely, the furnace atmosphere and additions of iron ore. In normal operation, the atmosphere of the electric furnace is oxidizing. Neither the doors nor electrode rings are tight, and the thermal drafts cause the insweep of large amounts of air. There are times, however, when a high positive pressure of gases produced inside the furnace prevents any ingress, and during those periods the atmosphere is neutral or possibly reducing.

The manner in which atmospheric oxygen is transferred through the slag to the metal bath has been given scant consideration, but there seems to be but one simple mechanism that fits the conditions. The physical solubility of oxygen in slags is probably too low to account for observed phenomena, and it must enter by chemical solution; that is, by combining with some constituent of the slag. Such oxides as CaO, MgO, SiO_2, and Al_2O_3, of course, cannot take on any more oxygen,

[1] References are at the end of the paper.

and this leaves only FeO, which is oxidized to Fe_2O_3 (MnO, of course, is analogous). This takes place at the atmosphere-slag interface.

in which it was necessary to account for 1634 lb of FeO by atmospheric oxidation in about two hours. Inasmuch as the average Fe_2O_3 content of the slag during this period was only 0.25 per cent, it was calculated that the Fe_2O_3 would need to take 116 round trips to carry the necessary oxygen from the slag-atmosphere interface to the slag-metal interface, and it was considered unlikely that this could happen.

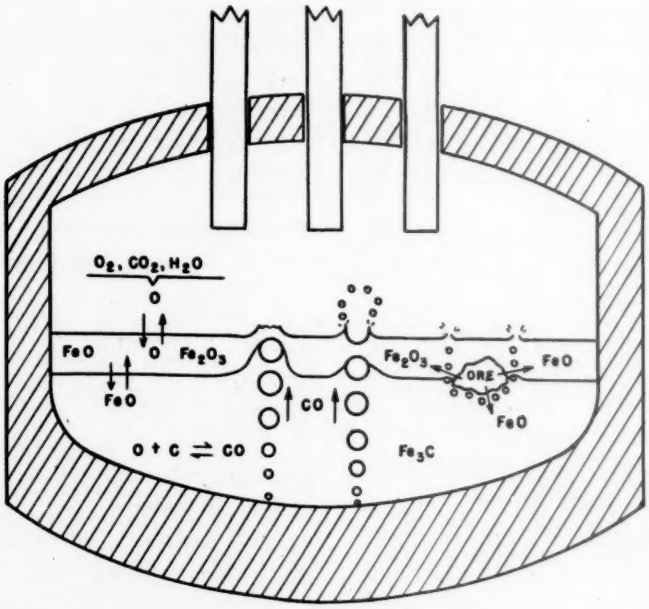

FIG 1—CONVENTIONAL SECTION THROUGH ELECTRIC FURNACE DIAGRAMING CARBON-OXYGEN REACTION.
Oxygen enters bath from atmosphere by way of slag, or from iron ore directly and by way of bath. CO formed by reaction is precipitated at hearth first and then on bubbles as they rise.

The Fe_2O_3 migrates, by diffusion, convection, or turbulence, to the slag-metal interface where it contacts and reacts with Fe:

$$Fe_2O_3 + Fe \rightleftharpoons 3\,FeO$$

The FeO formed is free to go in both directions, back into the slag or into the metal bath, according to the departure from equilibrium conditions. Normally, two molecules must re-enter the slag to replace those that are being oxidized at the upper surface, and one goes into the bath to replace that reduced by carbon.

Some doubts regarding the adequacy of this mechanism have been expressed by Fitterer,[2] who discussed the possibility of oxygen transfer by metal shot that are exposed directly to the gas phase by the action of the boil. He cites as evidence a 40-ton acid open-hearth heat

The mechanism actually does not require a round trip for Fe_2O_3, for this material goes only in one direction; namely, to the slag-metal interface, where it is converted to FeO. During the refining period, the average FeO content of the slag was 22 per cent or 88 times the Fe_2O_3, which means that an ample supply was always available at the upper surface for oxidation by the atmosphere. The average concentration of Fe_2O_3 gives no insight on the rate of transfer. As a matter of fact, the rate was not very high.

The 1634 lb of FeO needed would be supplied by the transfer of 3630 lb of Fe_2O_3, and if it is assumed that the hearth area was about 300 sq ft, that would mean 12 lb per sq ft in 2 hr or 0.1 lb per sq ft per min. The oxygen transfer would be at the rate of 0.01 lb per sq ft per min, which does not seem excessive.

During the working period of this heat, the slag was found to contain approximately one per cent of metal shot, which was about 0.07 per cent of the bath weight. Analysis gave a consistently lower carbon content for the shot, the average content of the bath being 0.78 per cent and of the shot 0.72 per cent. It might be suspected, however, that this slight difference would be accounted for by the extreme difficulty of getting the shot entirely clean of slag. This close similarity in carbon content of shot and bath may seem surprising when the shot is known to be completely surrounded by oxidizing slag, and yet it is a logical expectation in view of the fact, as will be discussed later, that the shot has no mechanism by which it can lose carbon. These shot undoubtedly contain a higher FeO content than the bath and probably are useful in increasing the effective area of the slag-metal interface, but it is not believed that they can carry an important quantity of oxygen directly from the gas or lower the carbon content of the bath appreciably by dilution.

When lump iron ore is used for oxidation, it sinks through the slag, because of its greater density, and contacts the bath directly. Here it reacts with the iron to produce FeO, which dissolves in both slag and metal. Some of the Fe_2O_3 dissolves directly into the slag.

The only interest of the present paper with slag is that it serves as a reservoir of oxygen that is fed to the bath to maintain the carbon-oxygen reaction. The rate at which the oxygen is transferred to the bath is controlled by a number of factors, such as the concentration in the slag and the chemical freedom of the FeO and Fe_2O_3. The interface itself constitutes a considerable resistance to transfer. Some realization of this may be seen in the different rate of oxidation with lump ore, which contacts the bath directly, and with fine ore, which must first dissolve in the slag.

As the carbon reaction depletes the bath of oxygen, however, more and more can flow from the slag. Thus, it is inevitable that a rough relation between the oxygen of the slag and the carbon of the bath should be approached. At equilibrium, there should be a partition of oxygen between slag and bath that is a function of the carbon content of the latter. Oxygen equilibrium between slag and bath seems never to be reached during the working period of a heat, however, and attempts at establishing a quantitative relationship have been disappointing.

Nature of Chemical Equilibrium

Equilibrium is defined as a state of balance between opposing forces, and in the physical sense this usually denotes a static condition. There is a temptation to think of chemical equilibrium as also being a state of complete inactivity, which is far from the truth. "When a system contains molecular species which are reacting chemically with one another to produce other molecular species, which, in turn, are similarly constantly reacting with one another to reproduce the first ones again, so that the rates of reaction in the two directions are equal and, hence, the relative amounts of the different molecular species concerned remain constant, a *chemical equilibrium* is said to exist within the system."

While the net change is zero, at steelmaking temperatures the kinetic energy of molecules and atoms is so great that there is fierce reactivity even after equilibrium is reached. It is like being on a

merry-go-round—one may be traveling fast and yet getting nowhere.

What difference does it make whether equilibrium is considered as a static or an active state? For one thing, the continued high rate of intermolecular reactions as equilibrium is approached explains why equilibrium can be attained so rapidly at steelmaking temperatures. There is not the same slowing down as would occur when approaching a cessation of activity. Also, when equilibrium is departed from, there is no lag or inertia in getting the reaction going.

Activity

In making thermodynamic calculations, it is often possible and sometimes convenient to ignore the exact mechanisms of the reactions concerned and also the constitution or form of the reacting substances. The reverse, however, is not true, and in dealing with mechanisms and rates of reaction, the thermodynamic laws and other fundamental laws must always be considered.

The mass law or law of mass action (which is synonymous with the definition of equilibrium constant given earlier) states that: At a constant temperature, the product of the active masses on one side of a chemical equation when divided by the product of the active masses on the other side of the equation is a constant, regardless of the amounts of each substance present at the beginning of the action.

The law specifically mentions active masses rather than just masses, inferring that not all of a substance present may be active. This actually is found to be true in some cases. Raoult's law states that: In an *ideal* solution, the activity of each component at any concentration is equal to its mol fraction.

Many solutions, however, are not ideal in this sense, and the *activity* of some components is not equal to the mol fraction at all concentrations. In other words, the activity does not vary proportionally with the concentration. The term "activity" seems to have been an unfortunate choice to express this variation from ideal behavior, because activity usually denotes movement or, more specifically, velocity of movement. Undoubtedly it was selected because early investigators thought that the active masses of the reacting substances controlled the rate of chemical reaction, but this, emphatically, is not true, and the activity referred to in the mass law concerns only equilibrium conditions.

If the concentration of a dissolved substance is doubled from any arbitrary starting point, and it *acts* as though there were only 1½ times as much present, it is said that the *activity* is not proportional to the concentration and a correction factor is needed. The ratio of how it acts to how it ought to act under ideal conditions, which in this case is 1.5:2.0, or 0.75, is called the activity coefficient. This is a correction factor by which the analyzed amount of a substance must be multiplied to obtain the active or effective amount, for use in mass-action calculations.

It should be observed also that activities are only relative values and refer to some standard state, usually taken either as the pure material or the material in unit concentrations.

Composition in the System Fe-C-O

The convention to express carbon and oxygen dissolved in liquid iron or in a steel bath is to use [C] to represent the analytical concentration of dissolved carbon and [O] for the concentration of dissolved oxygen. These values include all forms of the dissolved elements. This is both convenient and adequate for some thermodynamic calculations but for the present purpose a better insight into the actual state of occurrence is highly desirable.

Considerable evidence was given by Yap Chu-Phay[3] that carbon exists in liquid steel as a carbide, and Chipman's[1] calculations indicate that the most likely form of carbide at steel-melting temperatures is Fe_3C. Chipman[1] has also given convincing evidence that oxygen dissolved in an otherwise pure iron will exist as an oxide molecule containing but one atom of oxygen. Whether there is more than one atom of iron could not be determined but, inasmuch as oxygen always occurs in rather low concentrations, it does not matter greatly, and it is most convenient to regard it as FeO.

The solubility of CO in steel has been regarded pretty generally as negligibly small. In a liquid steel containing both carbon and oxygen, however, the mass law demands the presence of some CO under equilibrium conditions. It is impossible, of course, to distinguish by chemical analysis between carbon present as carbide and as CO, or of oxygen present as FeO and CO, and only the totals can be determined. Indirect computations by Marshall and Chipman,[8] however, indicate that a convenient average solubility for CO in steel at 2800°F (1540°C) and for one atmosphere pressure is 0.0028 per cent, corresponding to 0.0012 per cent C and 0.0016 per cent O.

It may confidently be assumed then that the system Fe-C-O contains Fe, Fe_3C, FeO, and CO. To complete the picture, however, and to make chemical reaction possible, the presence of dissociation products must also be conceded. Although equations usually are written as though molecules react with one another, the chemist recognizes that only ions or dissociated products of molecules normally can react in a rapid manner. For example, a mixture of H_2 and O_2 will not react until heated to a temperature at which there is appreciable dissociation of the two gases, at least locally.

It is not necessary for Fe to dissociate because metals seem always to be monatomic. There is rather general agreement that the dissociation value for Fe_3C is small, and there are no data known for

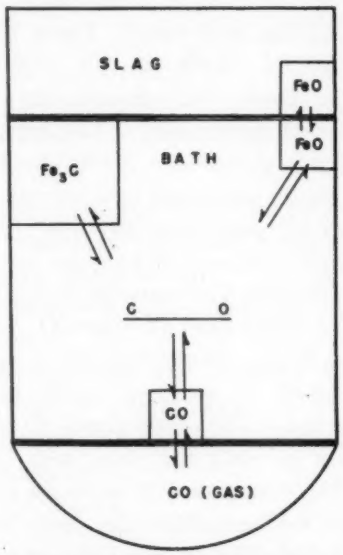

FIG 2—SCHEMATIC REPRESENTATION OF SLAG-BATH AND BATH-GAS SYSTEM TO SHOW INTERRELATIONSHIP BETWEEN SLAG, METAL AND GAS PHASES.

FeO and CO. The dissociation products of these substances will be:

$$Fe_3C \rightleftharpoons 3\,Fe + C$$
$$FeO \rightleftharpoons Fe + O$$
$$CO \rightleftharpoons C + O$$

For constant temperatures and concentrations, the degree of dissociation is a constant. Some of these dissociation products undoubtedly carry electrical charges and can be considered as ions, but, since the bath is a good electrical conductor, the ionization of the dissociation products will not have appreciable influence on subsequent reactions.

THE CARBON-OYXGEN REACTION

A schematic diagram of the carbon-oxygen reaction in a steel bath is shown in Fig 2. Here the steel bath is depicted by a large square with smaller squares representing contents of dissolved Fe_3C, FeO, and CO, respectively. The rectangle above represents slag containing dis-

solved FeO. The gas phase is represented below because the only atmosphere that the bath normally contacts is that of the CO bubbles that are formed at the hearth.

Arrows indicate an interchange of FeO between slag and metal. There need be, and usually there is, no equilibrium between these two phases, for reasons previously mentioned. The slag-metal interface is shown as a heavy line because it represents somewhat of a barrier.

The Fe_3C dissociates to form 3 Fe + C, with which it must always be in equilibrium. Likewise, FeO must be in equilibrium with the dissociated O. The CO, however, also partially dissociates to C and O, with which it in turn must maintain equilibrium. The dissociated C becomes common to both the Fe_3C and the CO, while the dissociated O becomes common to both FeO and CO. The dissociated Fe fades unidentifiably into the great background of Fe atoms. Thus, it is readily seen that at any local point in the steel bath, where the sample is taken for instance, this three-way equilibrium $Fe_3C + FeO \leftrightharpoons (4\ Fe) + CO$ must be attained almost instantly.

Bubble Formation

At the bottom of Fig 2, an interchange of CO between bath and atmosphere is shown. It must cross an interface, which again is shown as a heavy line because it is a partial barrier. Furthermore, the interface is remote from much of the bath and, worse still, it does not always exist.

Bubbles do not form readily within the body of a liquid but only on a surface, preferably a surface in contact with a solid. Beer or champagne poured into a perfectly clean and highly polished glass does not effervesce unless there is violent agitation as by swirling.[10]

The reason for this resistance to bubble formation in a liquid is not difficult to analyze. The solubility of a gas in a liquid varies with the pressure of that gas on the liquid. In the case of CO in steel, the CO does not need to dissociate previous to solution, and the solubility is directly proportional to the CO pressure. Steel, like all liquids, has a property known as surface tension. Any liquid surface has a tensile force tending to restrict the area of that surface, similar to that in the wall of an inflated rubber balloon.

A bubble, starting from scratch, theoretically must start almost infinitely small. While it is infinitely small, the surface tension would exert an infinitely large pressure on it, thus forcing the gas back into solution. Effectively, it prevents the start of a bubble. Once a bubble reaches an appreciable size, of course, the surface tension will be negligibly small, and the pressure of the gas will approximate one atmosphere plus the ferrostatic head of steel. It is then in a position to grow by precipitation of dissolved gas.

This relation can be demonstrated mathematically as follows: The pressure on a bubble exerted by tension in the surface will be

$$\text{Pressure} = \frac{\text{circumference} \times \text{unit surface tension}}{\text{cross-sectional area}}$$

or

$$P = \frac{2\pi r \times T}{\pi r^2} = \frac{2T}{r}$$

From this it can be seen that each time the diameter is halved the pressure will be doubled. Using a value of 1500 dynes per centimeter[11] for the surface tension of molten steel, it may be calculated that the pressure exerted by this force on a bubble 1 mm in diameter would be approximately 0.06 atmospheres which is a negligible figure, whereas the pressure on a bubble of 0.001-mm (1 micron) diameter would be 60 atmospheres, which is a prohibitive figure. At 10 Å units diameter, which is about 3 atom diameters, the pressure would be 60,000 atmospheres.

G. Ranque[4] has calculated an evolution pressure to start bubbles of CO in liquid

steel to be 811 psi, or about 55 atmospheres. Actually, CO does form bubbles, and at considerably lower pressure, but as Larsen[5,6] has emphasized, these bubbles form on a surface, which usually is the solid hearth below the bath. He has shown that not all surfaces are equivalent in this respect.

The types of surface on which bubbles form most readily are those which lead one to suspect that they have adsorbed gas films or contain gas-filled crevices too small for the steel to penetrate. In other words, they provide an atmosphere into which the CO can diffuse with much less resistance than bubbles can start from nothing. As the bubbles grow, portions become detached and rise to the surface. In transit, they contact steel charged with CO under pressure. This CO diffuses rapidly into the bubbles, causing them to grow, but the time of contact obviously is too short for equilibrium to be reached.

A liquid-liquid surface, such as the slag-metal interface, is not conducive to bubble formation. Lump ore does provide a good surface and so does a steel bar. The fact that gas does not form on a slag-metal interface explains why the metal shot, discussed earlier, have a carbon content very near that of the bath. The only mechanisms by which they could lose carbon would be by bubble formation, which is out, or by direct diffusion into the atmosphere above the slag. The latter would require an appreciable time and direct contact with the atmosphere.

Concept of Δ[O]

Brower and Larsen[6] presented evidence to show that an open-hearth bath contains oxygen in excess of the theoretical equilibrium value at one atmosphere throughout the heat. This differential between the equilibrium amount and the amount found was termed delta oxygen, or Δ[O]. The excess was found to vary throughout the heat and with various conditions of the furnace bottom. The conditions found most often in average furnace practice are covered by the following:

Conditions	Δ[O], Usual Percentage Oxygen by Weight
1. Vigorous lime boil	0.009–0.015
2. Steady state	0.015–0.025
3. Working of ore	0.023–0.035

In view of the argument that equilibrium always exists in the steel bath, this requires an explanation. The theoretical equilibrium that was used was obtained as follows:

Assuming that the activity of each component is proportional to the concentration, the full expression of the equilibrium is:

$$\frac{[Fe_3C] \times [FeO]}{Fe^4 \times [CO]} = K$$

where the brackets are a convention representing concentration in the steel bath.

On the premise that the Fe of the reaction is indistinguishable from the solvent Fe of the bath, it may be simplified to:

$$\frac{[C] \times [O]}{[CO]} = K$$

During the boil, the bath is in almost continuous contact with bubbles that are composed almost entirely of CO, although they always contain some CO_2 and very small amounts of H_2 and N_2. The bubbles are always under a total pressure of one atmosphere plus the ferrostatic head at any position. If, from this, it is assumed that the bubbles are practically at one atmosphere and the CO of the bath is in equilibrium with them, the [CO] of the equation is a constant and will cancel out. This further simplifies the equation to:

$$[C] \times [O] = m$$

where m is a constant replacing K for this special condition.

However convenient, this seems to be a case of oversimplification, because the components apparently do not have constant activity coefficients,[7] and the CO of the bath seldom is in equilibrium with one atmosphere of CO.

Marshall and Chipman[8] have furnished some data with which it is believed the concept of Δ[O] may be resolved. They obtained equilibrium values for carbon and oxygen in steel under imposed pressures of CO gas up to almost 20 atmospheres. From their work, the chart of Fig 3 is reproduced.

The original data of the paper by Brower and Larsen were given in an earlier paper,[5] and Fig 4 is reproduced from that paper. Excess oxygen is given as FeO but is readily calculated to Δ[O]. Arbitrarily selecting two carbon levels, 0.80 and 0.20 per cent, respectively, and taking corresponding values of excess FeO from Fig 4 for the high and low side of the range for each condition, the Δ[O] and total [O] values were calculated as follows:

For a carbon content of 0.80 per cent

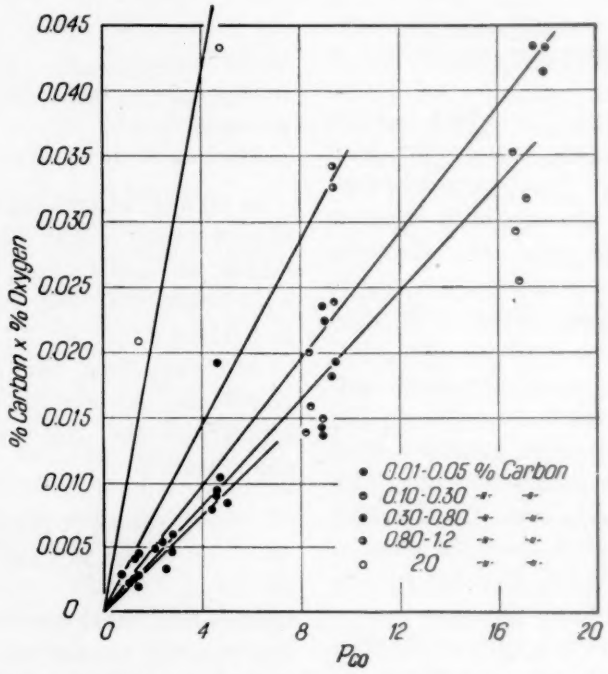

FIG 3—EFFECT OF CARBON MONOXIDE PRESSURES ON PRODUCT, PERCENTAGE OF CARBON TIMES PERCENTAGE OF OXYGEN, AT 2800°F (1540°C[8]).

and excess FeO of 0.04 per cent, and using Larsen's value of $m = 0.00222$ at one atmosphere,

$$\%O = \frac{m}{\%C} = \frac{0.00222}{0.80} = 0.002655$$

Δ[O] = excess FeO × 0.222 or

$$0.04 \times 0.222 = 0.00888$$

total [O] $= 0.01153\%$

These values are shown in the upper part of Table 1. Using them in the chart of Fig 3, the CO pressures at the various stages may be estimated. In the lower part of Table 1, average pressures for the steady state in the carbon range 0.1 to 0.9 per cent have been estimated.

From Table 1, it may be seen that, during the working of ore, while the availability of oxygen is very great, the CO pressure may vary from 3 to 9 atmospheres,

while at all other periods, it seldom exceeds five atmospheres and goes as low as two atmospheres. As to the reasonableness of these figures, it is certain first of all that the pressure must be more than one atmosphere. With the gas liberated at the hearth, the pressure must exceed one atmosphere plus the ferrostatic head of the steel. For a bath 52 in. deep, this would be two atmospheres.

Added to this is the inherent resistance to bubble formation and the effect of much of the bath being remote from the hearth.

TABLE 1—*Pressures for* CO *under Various Conditions Taken from Larsen's Values for* Δ[O] *and Marshall and Chipman's Data in Fig* 3[a]

Condition	Carbon, Per Cent	Δ[O]	Total [O]	Pressure of CO in Atmospheres
Vigorous lime boil..	0.80	0.009	0.0116	3.5
	0.80	0.015	0.0176	5.0
	0.20	0.009	0.0101	2.0
	0.20	0.015	0.0265	3.0
Working of ore.....	0.80	0.022	0.0246	7.0
	0.80	0.031	0.0336	9.0
	0.20	0.022	0.0331	3.0
	0.20	0.031	0.0421	4.5
Steady state.....	0.80	0.015	0.0176	5.0
	0.80	0.024	0.0266	7.0
	0.20	0.015	0.0265	3.0
	0.20	0.024	0.0351	3.5
	0.1	0.020	0.0422	2.0
	0.2	0.020	0.0311	3.25
	0.3	0.020	0.0274	4.0
	0.4	0.020	0.0255	4.75
	0.5	0.020	0.0245	5.5
	0.6	0.020	0.0237	6.0
	0.7	0.020	0.0232	6.5
	0.8	0.020	0.0228	7.0
	0.9	0.020	0.0225	7.5

[a] The upper part of the table gives minimum and maximum values at the various states, for two carbon levels, while the lower part of the table gives average values in the steady state in the carbon range 0.1 to 0.9 per cent.

In the upper layers of the bath, near the source of oxygen, pressures can build up that are unrelieved except for momentary contact with CO bubbles or by diffusion to the hearth. It is significant that the lowest pressures are found during the lime boil when bubbles of CO_2 furnish a flushing action to help liberate dissolved CO. From these standpoints, the pressures appear to be a logical expectation.

It will be observed in Fig 4 that the "excess" oxygen does not vary with carbon content but does seem to vary with such conditions as the available supply of oxygen; i.e., highest after ore additions and lowest during lime boil. On the theory that [C] and [O] are not in equilibrium, one would expect a faster reaction rate at the higher carbon content. Marsh[9] has shown that the reaction rate—that is, the rate of carbon drop—actually is faster at higher carbon contents.

There is one discrepancy, however. It is that Marsh shows the reaction rate to vary, not directly with the [C] as would be expected in a homogeneous reaction, but as a function of the logarithm of the [C]. Obviously then, it is not the carbon concentration that controls the rate. Inasmuch as the only mechanism by which the bath can lose carbon is CO evolution, the heterogeneous reaction $[CO] \leftrightharpoons CO\uparrow$ is apparently the bottleneck.

At the bottom of Table 1, the CO pressures for the average value of Δ[O] are listed for carbon contents from 0.1 to 0.9 per cent. These values were obtained from Fig 3 as accurately as possible but must be conceded some degree of error. They do, however, show steadily increasing CO pressures with increasing carbon. The pressure of CO in solution is a measure of its escaping tendency, and although none of the pressures is high enough to nucleate bubble formation, they do determine the rate at which the CO will escape into a bubble after it is formed.

If the values for CO pressures listed at the bottom of Table 1 are plotted against the square root of carbon, they fall on a straight line, which passes through zero CO pressure at 0.09 or 0.008 per cent C. This means that the CO pressure varies directly as the square root of the carbon content.

The close parallelism between the rate

of carbon drop and the CO pressure now becomes apparent. The fact that one is a logarithmic function of carbon and the other a square root function of carbon means that the CO pressure rises a little faster than the rate of carbon drop, according to the available data. For the present paper, however, it is the purpose only to point out that the rate of carbon drop apparently is controlled by the CO pressure.

Another contribution of the work of Marshall and Chipman[8] may throw additional light on the relationship just described. It is the evidence that the product %C × %O at equilibrium is not a constant even at constant CO pressure but increases with increasing carbon content. This relationship is shown in Fig 5. Those authors interpreted this to mean that the activity coefficients of both carbon and oxygen in steel were lowered in the presence of each other. This is a perfectly valid and satisfactory assumption for the purpose of thermodynamic calculations.

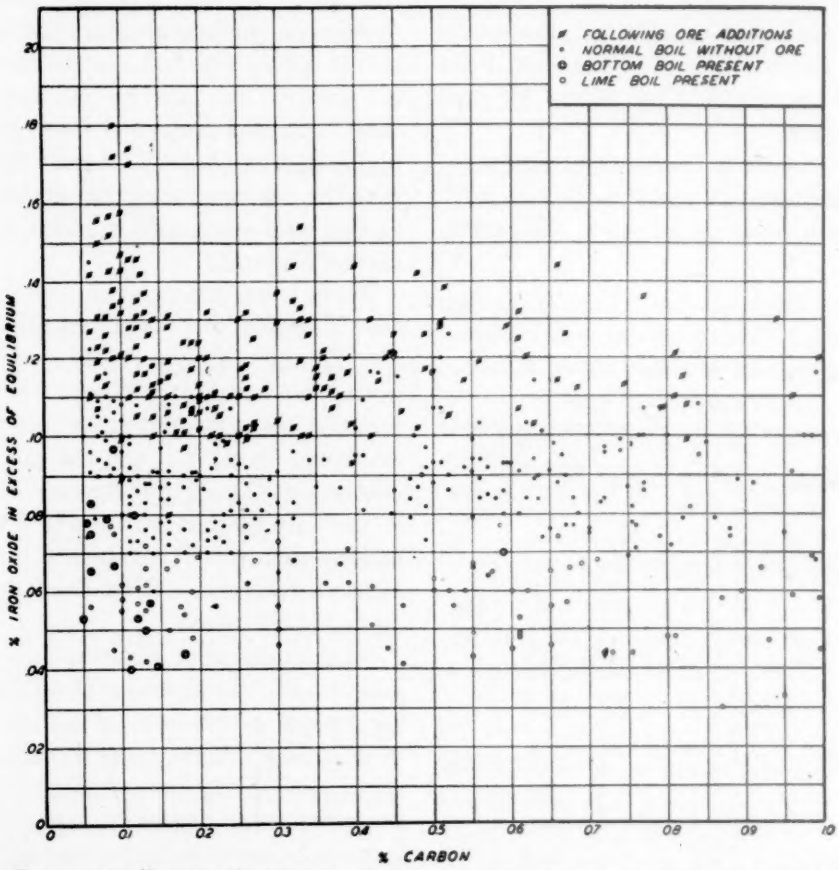

FIG 4—DATA FOR "EXCESS" OXYGEN IN VARIOUS CONDITIONS AS REPORTED BY LARSEN.[5]

It seems fundamentally unlikely that carbon as Fe_3C could depress the activity of oxygen present as FeO or vice versa, and the effect can be explained[8] by accounting for part of the total carbon and oxygen as CO. This gives an expression for the equilibrium constant, based on total carbon and oxygen as follows:

$$K = \frac{(\%\,C - 0.0012\,P_{CO})\,(\%\,O - 0.0016\,P_{CO})}{P_{CO}}$$

This takes into consideration the variation in the solubility of CO with pressure

but does not seem to account entirely for the variation of the product %C × %O with carbon at constant pressure, as shown in Fig 5. A slight variation of the solubility of CO with carbon content,

% C	CO, % AT 1 ATM.
0.2	0.0028 (assumed)
0.5	0.0030
1.0	0.0032
1.5	0.0033
2.0	0.0034

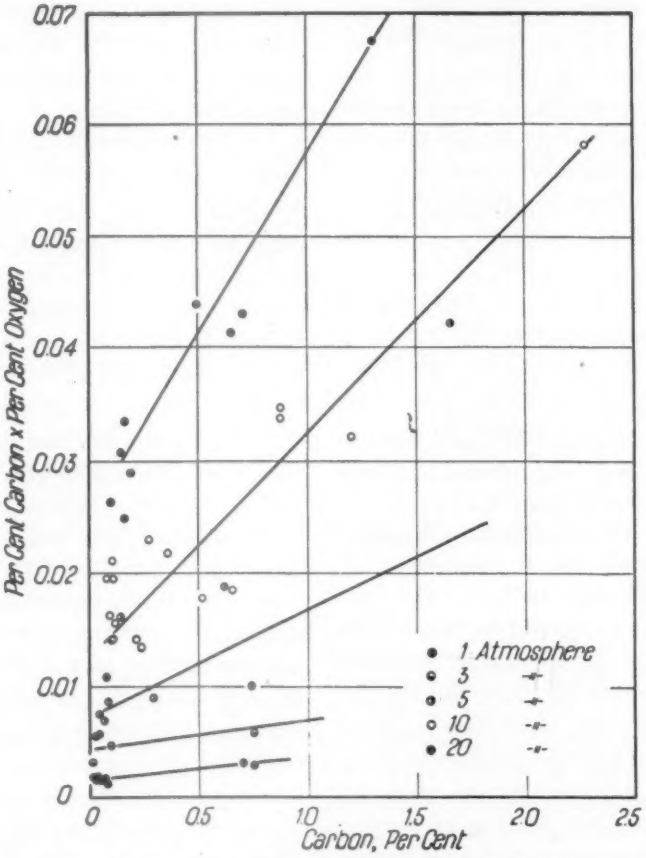

FIG 5—EFFECT OF CARBON ON PRODUCT, PERCENTAGE OF CARBON TIMES PERCENTAGE OF OXYGEN, AT 2800°F (1540°C[8]).

however, seems to account very well for this increase of %C × %O with increasing carbon. The assumption of increasing solubility for CO with increasing carbon does not appear too unreasonable when it is considered that a solution of Fe_3C in Fe is a different environment than Fe alone or FeO in Fe.

Rough calculation from the data of Marshall and Chipman indicates that, in order to keep K of this equation a constant, the solubility of CO would have to vary about as follows:

This solubility of CO furnishes a logical and straightforward mechanism to account for the observed effects. Instead of the activity of FeO being lowered by the presence of carbon, some of the oxygen is on the opposite side of the equation (as CO) and is pressing in the other direction.

In regard to the variation of the product %C × %O with carbon content, it may be assumed that it is the activity coefficient of the CO only that changes. The activity of the CO, by definition, is its pressure,

and if the solubility changes with carbon, pressure exerted by a given amount will be less, which is equivalent to saying that its activity coefficient is lower.

Discussion of Results

It might be asked at this time what relation all this has to practical steelmaking. The foregoing argument is primarily aimed at establishing the probable mechanisms of the carbon-oxygen reaction and how and why they occur. An important aspect of this is considered to be an acceptance of the solubility of CO in steel.

The solubility of CO in steel was denied for a long time, but more recently mounting evidence has led to tentative though sometimes apologetic acceptance. The fact of its solubility cannot readily be proved or disproved by direct evidence, and reliance must be made on indirect evidence. The assumption of solubility seems warranted on the basis that it clarifies much more than it confuses.

For example, it prevents one from getting into such an untenable position as stating in one breath that, during the boil, the very fact that there is a reaction going on is proof that equilibrium does not exist in the bath and that oxygen must be present in excess of the equilibrium value: and in the next breath, that there is ample evidence that the carbon-oxygen reaction is virtually instantaneous.

The reaction can be virtually instantaneous and result in building up a pressure of CO, which gets out of the steel when it can: i.e., at the hearth or by diffusion into a rising bubble. The variable solubility of CO with pressure furnishes a reservoir for CO and gives the reaction a fortunate flexibility. It is when CO is liberated that the equilibrium is upset and the reaction $C + O \rightleftarrows CO$ must then move from left to right to supply the deficiency there.

Every electric-furnace melter has experienced difficulty in getting some heats to start boiling even when he is piling in iron ore and has every reason to believe strong oxidizing conditions exist. Then suddenly it begins to boil with such violence that the furnace can scarcely hold it. This can be ascribed to conditions at least temporarily unfavorable to bubble formation and the building up of a supersaturation of CO.

Or, the boil may taper off to a quiescent state in which reaction seems to be at a standstill, but a steel bar thrust into the bath will start a violent local evolution of gas. This often has been explained on the basis of local chilling of the bath and thus changing the equilibrium constant. Such a bar, however, has a very low heat capacity and could do little effective chilling. A better explanation seems to be that solid steel furnishes the right kind of surface for the evolution of dissolved CO. In a similar manner, CO is liberated at the frozen shell of a rimming ingot.

As has been shown by Larsen[5,6] and others, the carbon-oxygen reaction rates above all other factors in establishing the relative quantities of carbon and oxygen that can be present in a steel bath up to the time of deoxidation. In other words, if the quantity of either carbon or oxygen is known, the amount of the other may be estimated closely. For purposes of more accurate calculation, however, a correction must be made for the pressure of CO. This would take the form:

$$\%C \times \%O = m \times P_{CO}$$

Using Larsen's value of $m = 0.00222$ and the relationship between P_{CO} and %C obtained by plotting the values in Table 1 for the steady state, the following expression is obtained:

$$\%C \times \%O = 0.00222 \times 8.7(\sqrt{\%C} - 0.09)$$

or

$$\%C \times \%O = 0.0193(\sqrt{\%C} - 0.09)$$

This gives a close approximation to the actual oxygen found by analysis of samples taken during the steady state. For greater accuracy, the equation suggested by Marshall and Chipman (see p. 11) should be used, but it is probable that more accurate data are also needed.

Marsh[9] has shown that, during the oxidizing periods, the carbon-oxygen reaction is the same for both open-hearth and electric furnace, and what is true for one is equally valid for the other. Under a finishing slag in the electric furnace, however, the product %C × %O tends to approximate the theoretical equilibrium constant for one atmosphere.

The latter represents quite a different condition, because finishing slags are made and kept purposely low in available FeO. For this reason, the flow of FeO is reversed, and it diffuses from the bath to the slag. The equilibrium in the bath is upset and CO decomposes to produce more FeO. The pressure of CO is thus reduced and the boil stops. This actually constitutes a mild deoxidation, and it would be expected that the product %C × %O would sometimes be even less than the equilibrium value for one atmosphere.

Acknowledgment

Grateful acknowledgment is expressed to Dr. G. A. Moore and Dr. Fred Dunkerley for their helpful counsel in the preparation of this paper.

References

1. J. Chipman: Application of Thermodynamics to the Deoxidation of Liquid Steel. *Trans.* Amer. Soc. Steel Treat. (1934) **22**, 385–446.
2. G. R. Fitterer: Some Fundamental Problems in the Manufacture of Steel by the Acid Open Hearth Process. *Trans.* Amer. Soc. for Metals (1945) **34**, 41–70.
3. Yap Chu-Phay: *Trans.* Faraday Soc. (1931) **27**, 777.
4. G. Ranque: *Rev. de Mét.* (1942) **39**, 331–344, 368–369.
5. B. M. Larsen: Controlling Reactions in the Open-hearth Process. *Trans.* A.I.M.E. (1941) **145**, 67–83.
6. T. E. Brower and B. M. Larsen: Oxygen in Liquid Open-Hearth Steel—Oxygen Content during the Refining Period. *Proc.* Open Hearth Conf. (1946) **29**. A.I.M.E., 1946; also *Metals Tech.* (Sept. 1946—T.P. 2035). See p. 137 this volume.
7. J. Chipman: Physical Chemistry of Liquid Steel. Basic Open Hearth Steelmaking, Chap. XVI, 479. A.I.M.E., 1944.
8. S. Marshall and J. Chipman: The Carbon-Oxygen Equilibrium in Liquid Iron. *Trans.* Amer. Soc. for Metals (1942) **30**, 695–745.
9. J. S. Marsh: Slag-metal-oxygen Relationships in the Basic Open-hearth and Electric Processes. *Proc.* Elec. Furnace Steel Conf. (1944) **2**, 126–136. A.I.M.E., 1945.
10. R. B. Dean: The Formation of Bubbles. *Jnl. Applied Physics* (1944) **15**, 446–451.
11. Bircumshaw: The Surface Tension of Liquid Metals. *Phil. Mag.* (1934) **17**, 181.

DISCUSSION

(B. M. Larsen presiding)

I. M. Mackenzie and T. Urie*—Recent American papers on the mechanism of the carbon-oxygen reaction have broken away from the older conceptions, which were largely due to Schenck, and have replaced them by others of doubtful validity. In view of his reference to chemical equilibrium as a dynamic state it is surprising to find the author defending the concept of excess oxygen, introduced by Brower and Larsen.

If the oxygen in excess of that required for equilibrium with carbon is employed in quantitative work the implication is made that part of the oxygen can be differentiated from the remainder. The accepted approach to chemical equilibria and reaction rates is the law of mass action which deals with the total active concentration of each component. The carbon-oxygen reaction proceeds because the rate of interaction of one set of components exceeds the rate of the reverse action. If the excess oxygen is employed it must be considered in relation to the concentration of carbon with which it interacts. Thus a function of $\Delta[O]$ and $[C]$ must be used. Surely it would be simpler to employ $[O]$ since this is equivalent to the function $\Delta[O] + \frac{m}{[C]}$. In addition to there being no theoretical justification for the use of $\Delta[O]$ it cannot be determined as accurately as the total dissolved oxygen.

* Research Metallurgists, Colvilles Ltd., Dalzell Works, Motherwell, Scotland.

The mechanism described in this paper would necessitate some correlation between the rate of carbon drop and a function of carbon and oxygen. If the reaction rate is limited by bubble formation at the hearth its rate at a given surface will depend on the concentration of carbon and oxygen in the metal and on the temperature since these determine the driving force of the reaction. This will be true whether the reaction proceeds by direct combination of carbon and oxygen atoms at the gas/metal interface or by evolution of dissolved CO since the CO pressure in the metal must depend on the value of a function of the type

$$\frac{[O] \times [C]}{m} = P_{CO}$$

It seems improbable that any analytical method employing killing with aluminum could differentiate between dissolved oxygen and that present as CO. The assumption of solubility of CO is an attractive hypothesis, but is of secondary importance to the melter who is concerned with the concentration of oxygen with which he has to deal at tapping. It appears certain that carbon will be eliminated more rapidly from a highly oxidized bath than from one in which the oxygen content is low and that the rate of boil is little influenced by the nature of the furnace hearth.

L. S. DARKEN*—Mr. Sims has given a very interesting discussion of a problem that has been with us for a long time. There have been several new ideas suggested with some of which I agree, and with others I disagree slightly.

The discussion of formation of bubbles from carbon and oxygen in solution was particularly valuable. It was made quite clear that if a bubble is going to form in the middle of a steel bath, it would have to start with a radius of about $^{2}/_{10}$ mm. As this is a patent absurdity, we see that we are forced to discard this notion. The remaining possibilities are that dissolved carbon and oxygen are eliminated by growth of bubbles already formed or else from bubbles by some other entirely independent mechanism. The most likely process for the formation of bubbles is that they are formed at the bottom of the furnace through some periods undoubtedly from the limestone, and at other periods possibly from porous materials in the bottom which contain gases; and that the bubbles grow on those gas nuclei already present at the bottom.

With the ideas expressed on the molecular structure of liquids in general, and of liquid steel in particular, I disagree. The current concept of the structure of liquid metals is that they are very similar to solid metals. There is some distortion but much of the crystalline structure of the solid is preserved in the liquid. In fact considerable headway has been made in the problem of the behavior of liquids by considering that the liquid phase is very similar to the solid phase with the same structure except that the coordination number is 11 rather than 12. That is, that every atom instead of having 12 nearest neighbors as it does in the close-packed solid has 11 nearest neighbors. In other words, a liquid is like a solid with holes in it.

If we accept that picture, and there is considerable evidence in favor of it, then we would naturally be led to believe that the solution of carbon in liquid iron, would be somewhat similar to the solution of carbon in solid iron, austenite. It is generally accepted that austenite is an interstitial solid solution and that to talk about iron-carbon molecules in austenite is meaningless. I am inclined to believe that the same is true of liquid iron.

The activity measurements discussed do not seem open to serious question but the interpretation is. The activity of carbon is unquestionably a function of the nature of the atoms in the vicinity of the carbon atoms but this fact is not necessarily to be interpreted as evidence of any compound formation.

As to the overall picture of the fundamental process taking place in the steelmaking furnace, it seems to me that the way to deal with the rate problem involved would be the same as for any other rate problem. The usual method of attack is to find out what the slowest step is, and then to determine the factors that control this slowest step. The overall rate is governed by the rate of the slowest step because the process on the whole can go no faster than the slowest part of it can go. In the open hearth steelmaking process, it seems reasonable to postulate that this slowest step involves the transfer of oxygen from the slag through the

* U.S. Steel Corp., Research Laboratory, Kearny, N. J.

metal and into the gas bubbles by which it escapes. This seems reasonable because of the very small amount of oxygen (as compared to carbon) that is present in the metal at any given time; further, if more oxygen is added in any way (as in the bessemer process) the reaction speeds up accordingly.

The author regards the transition of carbon monoxide from the dissolved to the gaseous form as "the bottleneck." Clearly this is not the only slow step since, if it were, the oxygen of the metal would be in equilibrium with that of the slag. Since such is not the case, it would seem that either: (1) two slow steps must be considered—i.e. transfer of oxygen from slag to metal and transfer from metal to gas or (2) the single slow step is involved in the diffusion and convection of oxygen through the liquid metal, or (3) all three steps need be considered. Possibility number two may be tentatively discounted in view of the experimental finding that the oxygen content of the metal shows no excessively large variation from top to bottom of the bath. The first possibility seems the most promising. If two slow steps are involved in a process, then a steady state is usually found in the step or steps between the slow ones. This is indeed the case in the open hearth where the oxygen content of the bath manifests a strong tendency toward steady state when properly controlled.

The usual method of handling such a steady state problem is to equate the input rate to the output rate. If the output rate (of oxygen) is set proportional to $\Delta[O]$ and the input rate assumed approximately constant, under given conditions, then $\Delta[O]$ is found to be constant under these given conditions and to be a function of these conditions, (lime boil, one addition, etc.). This was found experimentally by Larsen and Brower—that $\Delta[O]$ was independent of carbon content. On the other hand if the output rate is set proportional to p_{CO} as suggested by Sims, and the input rate again assumed approximately constant then p_{CO} is found to be constant which, as seen from Table 1, is not in accord with observation. Hence, it seems to me reasonable to suppose that $\Delta[O]$ is more fundamental to this process than p_{CO}.

M. L. Dapogny*—Is the CO formation trearded where larger heats are made than was intended in a furnace of a given size? Would the pressure of an increased bath depth make much difference?

C. E. Sims (author's reply)—Whether it is the slowing or the deeper baths is problematical. I do not think it makes a very great deal of difference.

The amount of pressure that would be built up because of a bath depth is rather a small percentage of the whole. In other words, in order to obtain one additional atmosphere about 52 in. of steel are necessary. Whereas the back pressures of the CO may run all the way from 2 up to as high as 5 atmospheres, and theoretically it should slow it up to some extent.

B. M. Larsen—We have made a few measurements recently on bath depths and a 30-in. bath is a fairly deep bath.

R. B. Sosman*—Mr. Sims spoke about the effect of lump ore in encouraging this reaction, as contrasted with fines. Here is a point that might be worth further consideration. A lump of ore is denser than the slag and tends to sink, while the fines are subject to flotation by the rising gases. The low spot in the iron-oxygen system is only 1371°C (exactly 2500°F). Hence the lump is likely to give off oxygen and melt. In many cases we may have, between the slag and the steel, little lenses or lakes of liquid iron oxide, and the most active reaction will be between the steel and this lake, rather than between the steel and oxide dissolved in the slag itself. This process would be consistent with the observation by steel makers that the ore seems to go through and disappear, leaving a slag of unchanged composition.

B. M. Larsen—We have solved the apparent inconsistencies in our data simply by assuming that it was not a homogeneous reaction but actually was a heterogeneous reaction, with the reaction itself occurring mainly at the gas-metal interface.

M. Tenenbaum†—I wish to compliment Dr. Sims on an excellent presentation on some of the finer details involved in the carbon-oxygen reaction. It would be interesting if we could obtain more concrete information on the exact

* Lehigh Foundries, Inc., Easton, Pa.

* School of Ceramics, Rutgers Univ., New Brunswick, N. J.

† Inland Steel Co., East Chicago, Ind.

surface characteristics that are required to stimulate the carbon-oxygen reaction.

There are a few aspects of the interrelationship between CO pressure, carbon content and reaction rates that still appear a little confused; and they are especially confusing when considered in the light of the observations made during the refining period of certain basic open hearth heats. I think some further discussion of these aspects might be merited.

First, the acceptance of the logarithmic relationship between the carbon drop rate and carbon content in all open hearth heats appears, from general observations, to be an over simplification of a very complex process. It seems that in such a logarithmic relationship, sufficient recognition is not given either to the slag condition or to the more or less unpredictable whims of the furnace operator. The latter factor influences the oreing rate which, by the very nature of the process, must affect the rate of carbon elimination. Thus in the higher carbon ranges where the rate of oreing is greatest we would expect to get the fastest rate of carbon elimination.

Following such ore additions, one naturally gets a rapid rate of oxygen transfer to the bath, and samples taken at that time would, by the method used in this paper, naturally indicate higher CO pressures.

Following ore additions, however, as well as during the steady state, consideration should also be given to the position of sampling before calculating the CO pressures. This feature, by the way, was also stressed by Marsh in his paper. The use of data from samples taken high in the bath (as were the samples of Brower and Larsen) to determine pressures existing at the point of gas formation at the furnace bottom does not seem entirely justified.

The variations in physical conditions of the slag should be considered in any discussion of the effect of pressure on carbon elimination. Any experienced open hearth operator knows that the rate of carbon drop can be effectively retarded simply by cutting the fuel off of the furnace and converting the slag into a chilled viscous cap over the bath. This practice is very common, in fact, in assisting the blocking action during the bath deoxidation. There is some question then as to whether this practice of chilling the bath retards the oxygen transfer or whether it actually suppresses the carbon-oxygen reaction by building up the CO pressure. Available samples indicate that under the chilled slag there is practically no change in oxygen content of the bath. In fact, sometimes there is even a slight increase under the chilled slag while the carbon content changes very slowly. It might be concluded then that there is, if anything, a slight increase in CO pressure under this chilled slag. Since the bottom condition does not change, we have a situation that would not be anticipated if it is accepted that the rate of carbon drop is controlled by the CO pressure.

At the end of the lime boil period in many open hearth heats, slags are relatively acid and fluid and contain numerous lumps of partly calcined limestone. Following ore additions this lime dissolves fairly rapidly and the slag becomes characteristically heavy and mushy. In the absence of any immediate ore boils, the gas coming from the bottom rises slowly through such intermediate slags and a foamy condition results. In the absence of the effect of an ore addition the rate of carbon drop under such slags is fairly slow regardless of the carbon content. As the slag shapes up and becomes more fluid, and this condition is often noted between about 0.15 and 0.35 pct carbon, the bath becomes more active and a vigorous rate of carbon elimination is obtained. This increased rate is often supplemented by the reaction with any ore that is left from additions that were made at a higher carbon.

Finally, at the lower carbon the reaction is again slowed down by stoichiometric limitations in the amounts of the elements present. Again, in these changes of reaction rates there might be some question as to what is the exact role of the CO pressure.

C. E. Sims (author's reply)—Before replying to this most interesting discussion, I wish to state again the purpose of the paper. It was an attempt to take the data on the carbon-oxygen reaction available in the literature and explain them to an audience, many of whom had no training in physical chemistry, in a simple, mechanistic manner. There being no concrete, clear-cut exposition of such a mechanism to use as a precedent, one had to be developed. Such a mechanism, of course, must not only conform to the basic laws and to observed facts but must also be able to predict conditions on

which data are not available. It was thought and hoped that it would be rigorously questioned in order that fallacies would be exposed and corrections made.

Dr. Darken objects to what he terms the molecular structure of liquid steel, a concept not intentionally inferred by the paper. It was intended, however, to convey the idea that liquid steel contains compounds in solution as molecules, partially dissociated.

Considerable evidence has been presented to show the existence of so-called liquid crystals in molten metals, but it is believed that these are confined to a range only a few degrees above the melting point and not in the range of superheat usually employed in working steel.

It is generally agreed that the liquid state has properties intermediate between those of the solid and the gas. The liquid has degrees of freedom greater than the solid but less than the gas. This is shown by the latent heats of fusion and of vaporization. The coordination number of 11 for the liquid state (which apparently is on a statistical basis only) as against 12 for the solid is additional evidence of the greater freedom in the liquid.

In most crystalline inorganic solids, it seems an absurdity to talk of molecules (this is not true of certain crystalline organic materials). In the orderly space lattice of a sodium chloride crystal, who could say where a molecule begins or ends? Likewise in solid metals, the structure is obviously an arrangement of atoms. Solid solutions consist of a replacement of some of the solvent atoms by solute atoms or, in the case of very small solute atoms, of atoms in an interstitial position in the strained lattice of the solvent. The so-called compounds such as iron carbide, Fe_3C, are merely repeating patterns of iron and carbon atoms in a definite proportion

At the other extreme, however, gases or vapors do contain definite molecules. This is true for elements such as O_2, N_2, and H_2 or for compounds such as H_2O, CO, CO_2, and SO_2. Metal vapors, on the other hand, seem always to be monatomic. With iron vapor monatomic and solid iron a space lattice arrangement of atoms, there is no reason to regard liquid iron as occurring in units larger than atoms even though a statistical distribution is indicated. It is not believed that this picture precludes the possibility or probability of dissolved molecules in the molten iron or steel. Thermodynamic data do support strongly the evidence for solute molecules.

Dr. Darken agrees that the presence of oxygen changes the activity of carbon in liquid steel and that carbon has the same effect on the activity of oxygen but does not agree that it is for the reason given in the paper. He says "The activity of carbon is unquestionably a function of the nature of the atoms in the vicinity of the carbon atoms." While this is undoubtedly true for heavy concentrations of the interfering atoms, it is not to be interpreted as being the only mechanism or that large changes in activity could be thus accounted for by minute concentrations as in the case of oxygen in steel. With a content of 0.03 pct O such as might occur with 0.2 pct C, there would be roughly one oxygen atom for each 1000 iron atoms and one carbon atom for each 200 iron atoms. Such a small change in the composition of the solvent could hardly be expected to have an important effect on the activity of dissolved carbon.

How much more logical and simple is the explanation that some of the total carbon and oxygen react to form CO, which reduces the amount not thus combined and which goes over on the other side of the equation. This is a mechanism readily understood and the simpler method is preferred until found untenable.

In discussing the rate problem, it is necessary to ignore Δ[O], which is regarded as a fictitious figure for reasons already given. If it is considered that total [O] (from FeO and CO) varies in its relation to [C] for different conditions with resultant variations in CO pressure, then the rate problem becomes straightforward and uncomplicated.

The evolution of CO from the dissolved to the gaseous state is certainly one of the chief bottlenecks because of the special conditions required for the evolution of CO, but it is not always the controlling factor in rate of carbon drop. It is obvious, of course, that the rate of CO evolution and the rate of carbon drop are synonymous. For a given CO pressure, the rate of evolution will vary with such things as the condition of the hearth surface, but for a given hearth condition, the rate will vary with the CO pressure in the steel. This follows because the CO pressure is a measure of its escaping tendency.

It has already been pointed out that the

total [O] is low during the lime boil. At this time the slag is not very oxidizing and the CO_2 from the limestone aids the escape of CO from the bath. At this time, the bottleneck is apparently the availability of oxygen from the slag. Marsh has shown[9] and is confirmed currently by Urban and Derge that under non-oxidizing finishing slags in the electric furnace, the [O] drops until it is in equilibrium with [C] at one atmosphere pressure of CO. Stated more succinctly, the CO continues to evolve until it is in equilibrium with the bubbles it forms. There it has to stop.

After a heavy ore addition, the total [O] goes up to a high value (high Δ[O] according to Larsen). This builds up a high CO pressure and the immediate result is a vigorous boil that quickly reduces the oxygen back to the steady state value. During this period of high availability for oxygen, the CO evolution is definitely the bottleneck controlling the rate of carbon drop.

If we were dependent on diffusion to carry oxygen from the slag-metal interface to the hearth, carbon elimination would be hopelessly slow, and this step would indeed control the rate. During a lively boil, diffusion rates are of no consequence, and the turbulence created precludes any chance of an appreciable oxygen gradient in bath.

The steady state apparently represents a balanced cycle of interdependent actions. Oxygen entering the bath increases the CO pressure, the increased pressure speeds up the evolution, while the increased turbulence thus produced speeds up the transfer of oxygen from slag to bath. The inverse is also true. When these steps come into balance, the steady state is reached, and it is self-perpetuating as long as carbon remains in the steel and oxygen is available from the slag.

The bessemer represents a special case. Here the availability of oxygen is very high, while the resistance to bubble formation is almost absent because of the ever-present gas phase. Carbon drop can, therefore, progress with great rapidity. Because of the aid to evolution given by the blast, it can be predicted that bessemer blown metal should have lower [O] for any given [C] than open hearth steel. The same thing would be true where oxygen is blown through an open hearth bath.

Thus, there is no fixed bottleneck that always controls the rate of carbon drop. The steps are flexible, changeable, and interdependent. Without regard to bottlenecks, however, the rate of carbon drop is directly a function of CO pressure. During the steady state, as described in the paper, the pressure will vary as a function of the carbon content and, therefore, the rate of drop should be a function of the carbon content during this condition. Data obtained by Marsh indicate that this is true.

Reference is made to the foregoing argument in partial reply to Mr. Tenenbaum. There seems to be no real conflict of opinion or interpretation of observations. The logarithmic relation between carbon content and rate of carbon drop is not a deduction by the present author but is the result of experimental data reported by Marsh.[9] The heats from which the data were obtained must have been in the steady state most of the time. An attempt was made to explain this relation on the basis of CO solubility.

It seems that heavy ore additions must inevitably speed up the boil. A chilled and viscous slag, however, would yield oxygen slowly and would tend to retard a boil. Mr. Tenenbaum cites some apparent discrepancies which need more study for full evaluation. There is no thought that a perfect mechanism has been proposed, and there are apparently conditions which allow a rather high CO pressure to be built up without much evolution.

Dr. Sosman surmised that lump ore would promptly melt and form a liquid layer. Observation shows that this does not occur and that the lump can be seen floating around for quite a while accompanied by a vigorous local boil. The gas formed apparently insulates it and prevents rapid heating.

Mr. Larsen prefers to consider the carbon-oxygen reaction a heterogeneous reaction occurring only at the metal-gas interface of the bubble rather than a homogeneous reaction within the bath. There seem to be serious objections to such a viewpoint. In the first place, it would have to be a second-order reaction, that is, an atom of carbon and an atom of oxygen would have to collide at the surface with sufficient energy to unite and escape simultaneously. In view of the high dilution of both these atoms the frequency of such collisions would be small indeed. Since the question of absolute rates has been raised, it

would be interesting to know whether Mr. Larsen has attempted to calculate such a reaction.

The reaction behaves like a first-order reaction but to achieve this by Larsen's mechanism would require that the surface of the bubble be lined solidly with carbon atoms or with oxygen atoms. Reaction at the surface only, would mean that CO would have to dissociate as it dissolves, and solubility would then vary as the square root of the pressure. The data of Marshall and Chipman,[8] however, indicate that it varies directly with the pressure, i.e., dissolves without much dissociation.

In replying to Messrs. Mackenzie and Urie, it must be obvious from the foregoing argument, if not from the paper, itself, that the author does not defend the concept of oxygen in excess of the equilibrium but strives to prove it untenable, while offering a more plausible mechanism.

There seems to be no analytical method capable of distinguishing among the various forms of oxygen in liquid steel, and the solubility of CO can be determined only by some indirect method such as used by Marshall and Chipman.[8]

The correlation of rate of drop with carbon and oxygen concentration was discussed in the reply to Dr. Darken. A difference in rate of boil as an effect of bottom condition has been observed and reported by Brower and Larsen,[6] and the phenomenon of the bottom boil has been cited above. Messrs. Mackenzie and Urie are probably justified in saying that the rate of boil is little influenced by the nature of the furnace hearth because the normal variation is not very great.

In closing, the thought is again expressed that, although thermodynamic calculations can be made while ignoring mechanisms, any conclusions thus reached are acceptable only when they offer at least one tenable mechanism.

This opportunity is taken to thank those who have contributed this stimulating discussion.

Oxygen in Basic Electric-furnace Baths

By S. F. Urban* and G. Derge†

(New York Meeting, March 1947)

At the time this investigation was initiated variations were observed in the quality of different heats of basic electric-furnace steels, although they had been made under purportedly similar conditions. This indicated that these variations were related to normally unobserved variations in the character of the bath, especially during the "refining" period. Although the slags used for this operation are commonly referred to as "reducing" slags, and are regarded as having a "deoxidizing" action on the bath, no reliable measurements of this action were available. It was decided, therefore, to study the behavior of oxygen in the metal for a large enough number of heats to learn its normal variations and to relate these variations to regularly observed conditions of operation.

The most important general conclusion reached was that the time a heat is held under a reducing slag should be reduced to a minimum, which was about an hour and a half under the conditions studied. Beyond this time no observable beneficial effects are obtained from the reducing slags, insofar as oxygen and sulphur content of the bath are concerned. It is likely that added time may increase hydrogen content as well as heat costs. The oxygen content of the bath is never reduced below the amount in equilibrium with the carbon. Concurrently with this work, J. S. Marsh[1] presented data that supplement and support many of the results of this paper.

Manuscript received at the office of the Institute Dec. 7, 1946. Issued as T.P. 2185 in Metals Technology, June 1947; printed also in Electric Furnace Steel Proceedings, 1946.

*Assistant to Chief Metallurgist, Carnegie-Illinois Steel Corporation, South Works, Chicago, Ill. when paper was written. Now with Titanium Alloy Manufacturing Co., Niagara Falls, New York.

†Metals Research Laboratory, Carnegie Institute of Technology, Pittsburgh, Pennsylvania.

Procedure

The work was done in two different electric-furnace shops of the same plant. The selection of heats was made primarily with regard to the convenience of heat schedules. Companion slag and metal samples were taken just prior to slag-off and throughout the refining period for an initial set of 17 heats, and before slag-off and near tap for an additional 13 heats. Slag sampling presented no particular problem; a spoonful of slag was poured onto a metal plate and when sufficiently cool was sealed in an airtight container. Sampling the metal for oxygen presented a more complex problem. Because of the lack of previous experience in sampling electric-furnace baths, a number of methods were compared.

Chilled Wedge Samples[2]

An unkilled metal sample is removed from the furnace in a well-slagged carbometer spoon and poured immediately into a heavy copper mold designed to provide rapid freezing. Three different types of molds were used to determine the optimum for electric-furnace heats.

The Big Wedge Mold (*a*) was a 4 by 4 by 4-in. split copper mold, yielding a wedge-shaped casting 1 in. wide, 1½ in. long, and ¼ in. maximum thickness, and was finally adopted as the most satisfactory design.

[1] References are at the end of the paper.

The Long Wedge Mold (*b*) was a 2 by 2 by 5¼-in. split copper mold, yielding a wedge-shaped casting 1 in. wide, 2¾ in. long, and ¼ in. maximum thickness.

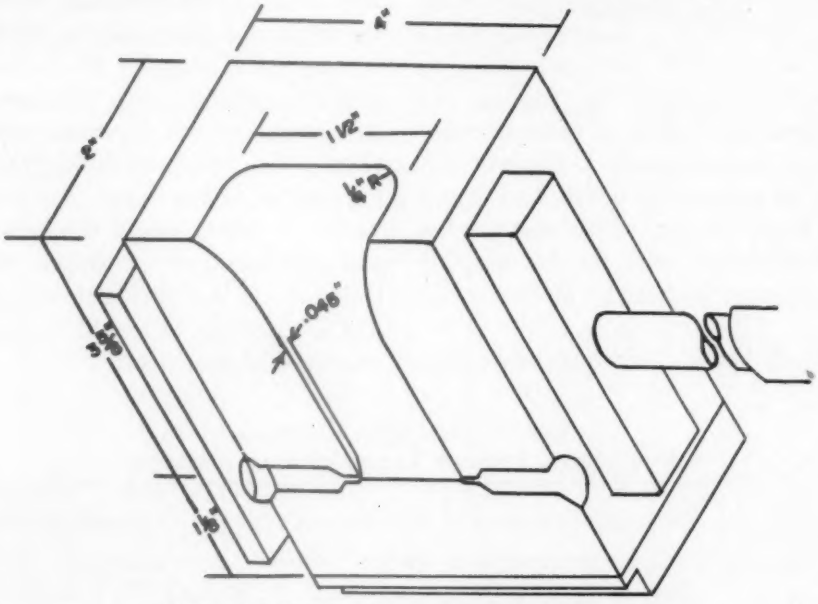

FIG 1—COPPER MOLD FOR CHILLED SAMPLE.

The Small Wedge Mold (*c*) was 2 by 2 by 4-in. split copper mold, yielding a wedge-shaped casting 1 in. wide, 1½ in. long, and ¼ in. maximum thickness.

With the long and small molds, it was difficult to obtain samples free of temper color along the lower section of the wedge, the section that is used for vacuum-fusion analysis. On the other hand, the big wedge mold consistently produced samples that were free of temper colors on the usable lower section, and, in addition, was much easier to manipulate than the other molds. In order to obtain more weight in the usable portion of the sample, this design has since been modified slightly to give a straight-sided casting 1 in. wide, 1½ in. long, 0.09 in. thick. This model (Fig 1) has given equal satisfaction in basic and acid open hearth and electric furnaces.

Only one difficulty was encountered with this type of sampling; namely, keeping the metal in the spoon properly covered when the slag was unusually thin. Subsequent experience has demonstrated that this can be largely overcome by using a smaller spoon, about 3-in. diameter bowl, with only a single pouring lip.

Chilled Spoon Samples

In taking chilled spoon samples the unkilled sample was taken from the furnace in a slagged spoon, which was exactly the same as that used for the chilled wedge samples. However, in order to avoid oxidation while pouring through the air, the metal was frozen by thrusting a 1-in. diameter copper bar into the spoon. This method was not developed to a satisfactory state because of the following difficulties:

1. Thin slags did not keep the metal covered and thick slags stuck to the copper bar and prevented good contact with the metal.

2. Chilling was erratic and inadequate when compared with the chilled wedge method.

3. The sample obtained was irregular in shape and had a poor surface, so that preparing satisfactory sections for analysis was a most difficult cutting problem. In this respect it should be pointed out that cutting a sample adjacent to the depression

formed by the copper rod is difficult because of shape factors, and frequently because of hardness.

Bomb Samples

Bomb samples were taken according to open-hearth procedure[3] by forcing the slagged bomb into the metal bath, allowing the molten steel to melt a tinplate cap covering the neck of the bomb, and to run into the bomb proper, which contained a wad of aluminum wire in the amount of one per cent by weight of the entire sample.

The bomb has a theoretical advantage over any type of poured sample in that there is no opportunity for oxidation by the air. Although it has been demonstrated, particularly by the British,[4] that satisfactory bomb techniques can be developed, the method is inherently cumbersome and cutting small samples from the bomb is difficult, especially with high-carbon steels. The sampling was uncertain with viscous slags. It has also been shown[2] that some of the oxygen in the metal may not be converted to Al_2O_3 before the bomb freezes, and this unconverted oxygen will not be included in the gravimetric analysis for Al_2O_3, although it would be found in a vacuum-fusion analysis.

TABLE I—*Experimental Data*

A—ELECTRIC-FURNACE BATH AND SLAG ANALYSES

Heat No.	Time, Minutes		Vacuum-fusion Analyses			Bath Analyses, Pct			Slag Analyses, Pct				
	From Slag-off	Before Tap	Chill Spoon Spec. % FeO	Long Mold Spec. % FeO	Short Mold Spec. %FeO	S	Si	App. C[c]	FeO	CaO	SiO_2	S	CaC_2
1	[a]	[a]	0.032			0.016	0.025	0.12	25.28	54.44	8.50	0.14	0.10
	40	106	0.042			0.007	0.021	0.31	1.90	56.63	25.80	0.07	0.08
	80	66	0.035	0.067	0.126	0.007	0.023	0.31	1.62	62.11	24.84	0.39	0.78
	110	36	0.027	0.077	0.072	0.007	0.016	0.31	0.66	60.35	23.60	0.30	1.06
	142	4	0.030	0.036	0.036	0.012	0.050	0.41	0.50	66.12	18.24	0.24	0.84
2	[a]	[a]	0.037	0.086	0.112	0.014	0.010	0.80	9.41	44.30	15.16	0.07	0.09
	63	102	0.025			0.019	0.022	0.83	0.66	64.30	26.62	0.18	0.28
	91	74	0.012	0.035	0.054	0.013	0.022	0.83	0.66	63.38	25.98	0.26	0.93
	121	44	0.023	0.027	0.043	0.013	0.016	0.83	0.62	64.49	26.24	0.28	1.34
	136	29	0.015	0.041	0.027	0.012	0.038	0.97	0.46	64.92	24.98	0.32	0.61
	151	14	0.0077	0.059		0.016	0.08	0.97	0.54	66.07	25.20	0.29	0.21
3	47	131	0.135	0.158		0.015	0.05	0.09	9.48	49.37	22.90	0.02	0.21
	67	111	0.086	0.059	0.086	0.012	0.05	0.09	6.15	47.05	28.84	0.03	0.31
	91	87		0.068	0.117	0.016	0.037	0.09	1.85	61.04	28.48	0.10	0.08
	117	61	0.089	0.099	0.135	0.015	0.017	0.09	1.70	57.19	24.60	0.14	0.16
	157	21	0.087	0.117	0.090	0.014	0.040	0.09	2.01	59.95	27.00	0.02	0.53
	165	13	0.072	0.063	0.033	0.014	0.39	0.09	2.17	67.95	16.20	0.13	0.10
4	5	198	0.130		0.135	0.019	0.05	0.06	27.09	25.45	17.56	0.03	0.12
	45	158	0.176		0.153	0.021	0.10	0.13	5.28	40.47	42.90	0.03	0.15
	70	133		0.063	0.090	0.017	0.10	0.13	1.16	50.29	38.66	0.10	0.06
	97	106	0.097	0.072		0.019	0.18	0.13	0.43	58.41	31.48	0.12	0.21
	128	75	0.045	0.063	0.068	0.011	0.13	0.13	0.54	62.63	29.62	0.19	0.43
	165	38	0.059		0.068	0.014	0.06	0.17	0.62	60.41	28.84	0.23	Nil
	195	8	0.064 Ingot No. 3[b]	0.086 Ingot No. 1[b] 0.018	0.099	0.016	0.043	0.17	1.54	57.08	27.98	0.12	0.05

[a] Immediately before slag-off.
[b] Determined on the long-mold specimens.
[c] Bath C was estimated from the chemically determined C reported for the regular test sample taken nearest the oxygen sample.

The slag samples described were analyzed in the chemical laboratory along with the conventional metal tests. The special metal samples were analyzed by conventional vacuum-fusion procedure for oxygen, nitrogen, and hydrogen, but it is believed that no particular significance can be attached to the hydrogen and nitrogen values; consequently, they are not reported in this paper. This is principally because the problem of sampling molten steel for these elements has not been solved satisfactorily.

TABLE I—(*Continued*)

B—SAMPLES OBTAINED BY USING LONG WEDGE-TYPE MOLD

Heat No.	Time, Minutes		Bath Analyses, Pct							Slag Analyses, Pct					
	From Slag-off	Before Tap	Spec. No. 1			Spec. No. 2			App. C[c]	FeO	CaO	MgO	SiO_2	S	CaC_2
			FeO	S	Si	FeO	S	Si							
5	[a]	[a]								13.54	24.11	4.32	16.54	0.05	0.21
	[a]	[a]								14.25	29.61	3.90	10.24	0.09	0.16
	32		0.106						0.19	5.59	56.73	4.64	18.30	0.13	0.21
	95		0.019						0.20	2.65	56.06	12.79	19.48	0.29	0.18
	196									1.58	54.35	10.15	19.86	0.30	0.21
6	[a]	[a]								0.58	65.59	5.83	22.18	0.62	0.85
	95	92				0.056			0.32	0.65	68.56	2.52	23.06	0.57	0.21
	150	37	0.068			0.056			0.39	0.80	67.10	4.96	22.40	0.80	1.24
	173	14	0.014			0.015			0.39	0.77	66.50	5.20	22.18	0.79	0.40
7	101	99	0.135			0.050			0.29	0.65	68.46	2.80	22.30	0.59	1.52
	130	70				0.0315			0.30	1.23	66.98	5.40	20.18	0.67	0.26
	193	7	0.039						0.37	1.08	62.16	10.94	18.90	0.60	0.24
	198	2	0.040						0.37						
8	[a]	[a]	0.054	0.016	0.025	0.135	0.018	0.016	0.27	7.27	36.25	8.57	23.12	0.05	0.08
	73	67	0.090	0.017	0.05	0.090	0.017	0.014	0.31	0.85	66.37	2.55	25.66	0.17	1.22
	122	18	0.054	0.016	0.010	0.049	0.016	0.010	0.34	1.08	66.42	2.55	21.48	0.28	0.13
9	22	152	0.054	0.017	0.016		0.016	0.014	0.36	3.05	51.59	5.76	30.46	0.03	Nil
	159	15	0.058	0.016	0.045	0.022	0.016	0.05	0.36	0.46	63.52	4.47	27.38	0.24	0.29
10	[a]	[a]	0.081	0.019	0.06	0.108	0.018	0.06	0.34	3.94	45.86	9.68	22.92	0.09	0.09
	[b]	[b]	0.040	0.023		0.067	0.024	0.043	0.34	5.26	42.84	11.11	22.48	0.09	Nil
	36	78	0.067	0.019	0.038	0.058	0.026	0.038	0.34	2.14	51.17	5.35	29.66	0.05	Nil
	77	37	0.072	0.021	0.036	0.067	0.018	0.037	0.35	0.39	64.47	4.50	26.46	0.11	0.42
	103	11	0.031	0.027	1.00	0.017	0.024	0.59	0.35	0.43	63.69	4.39	27.06	0.10	0.69
	111	3	0.015	0.019	0.34	0.031	0.018	0.73	0.35	0.62	59.47	4.54	26.30	0.13	0.50
11	36	97	0.072	0.019	0.011	0.153	0.018	0.024	0.27	4.99	46.24	5.98	27.76	0.01	0.05
	121	12	0.036	0.015	0.009	0.067	0.018	0.011	0.29	0.94	60.90	8.64	25.10	0.20	0.08
12	47	83	0.22	0.014	0.010	0.175	0.015	0.007	0.05	3.05	52.85	4.22	25.86	0.05	0.08
	109	21		0.013	0.010				0.05	1.35	58.25	6.73	24.64	0.10	0.08
	122	8	0.103	0.015	0.083				0.05	1.98	54.81	7.70	26.94	0.12	0.12
	127	3	0.085	0.013	0.19				0.05	3.24	50.05	7.81	23.28	0.12	0.08
13	[a]	[a]		0.024	0.018	0.139	0.019	0.005	0.25	6.80	29.19	10.41	24.46	0.03	Nil
	29	89	0.081	0.017	0.008				0.30	1.00	64.82	3.27	23.30	0.10	Nil
	97	20	0.045	0.017	0.030	0.065	0.021	0.040	0.30	0.60	63.14	5.00	28.04	0.26	0.37
14	[a]	[a]		0.035	0.030	0.108	0.030	0.043	0.30	9.85	27.72	8.64	21.46	0.03	0.02
	92	6	0.027	0.021	0.14	0.067	0.022	0.15	0.31	1.00	53.90	8.24	30.58	0.15	0.02
15	[a]	[a]	0.117	0.022	0.023	0.117	0.019	0.026	0.33	5.75	44.66	7.24	24.54	0.03	0.02
	70	34	0.027	0.013	0.010	0.063	0.015		0.33	0.65	63.56	4.53	27.14	0.18	0.14
	92	12	0.065	0.017	0.33	0.075	0.012	0.31	0.35	0.67	63.00	4.75	28.16	0.26	0.08
16	25	117	0.099	0.019	0.004	0.184	0.023	0.008	0.11	5.85	46.69	2.34	29.68	0.04	Nil
	68	74	0.153	0.022	0.010	0.139	0.019	0.004	0.11	0.75	63.00	2.17	28.14	0.18	0.08
	116	26	0.242	0.017	0.008	0.139	0.017	0.024	0.12	1.00	66.15	2.22	27.24	0.26	0.19
	129	13	0.097	0.015		0.094	0.017	0.14	0.12	1.00	65.30	3.42	27.96	0.28	0.58
	152	0	0.076	0.017	0.20	0.094	0.013	0.17	0.12	0.55	64.75	3.31	25.76	0.31	Nil
17	[a]	[a]	0.220					0.013	0.08	24.08	28.56	4.93	13.16	0.05	0.02
	80	81	0.142	0.011	0.021	0.139	0.011	0.011	0.08	1.00	64.25	1.18	28.06	0.18	0.04
	139	22	0.144	0.014	0.021	0.099	0.014	0.025	0.08	2.50	48.31	1.23	25.58	0.21	0.01

[a] Before slag-off.
[b] Finish slag-off.
[c] See footnote *c*, part A.

Experimental Results and Discussion

The experimental data for these heats, including ladle analyses, are given in Table I. Thirty heats are included and the carbons range from 0.03 to 0.95 pct at the time of sampling. The data for some heats are not as complete as for others because of defective specimens and other circumstances beyond control, or because additional data were not required for these phases of the investigation. The heats in Table I are divided into three groups for convenience in discussion. Part A contains four heats, in which no bomb tests were taken, but a comparison of the chilled spoon with wedge molds *b* and *c* can be made. Ladle tests for oxygen are included for one of these. These chilled tests from the ladle were obtained by a slight variation of normal procedure because it was obvious that the sample could not be poured from a slagged spoon. The copper mold assembly was clamped into a long iron rod and thrust directly into the pouring stream at a convenient time when the nozzle was partly closed. Part B shows 13 heats from which oxygen samples were taken by the type *b* chilled-wedge method

TABLE I—(*Continued*)
C—COMPARISON OF SAMPLES FROM *a* AND *b* MOLDS

Heat No.	Time in Minutes		Vacuum-fusion Analyses, Pct					Bath Analyses, Pct	
			Big Mold		Long Mold		Bomb		
	From Slagoff	Before Tap	Spec. No. 1 FeO	Spec. No. 2 FeO	Spec. No. 1 FeO	Spec. No. 2 FeO	Spec., FeO	Si	App. C[c]
18	[a]	[a]	0.154	0.143				0.01[b]	0.25
	63	28	0.057	0.034	0.050	0.076	0.028	0.036	0.36
19	[a]	[a]	0.318	0.418	0.393	0.358	0.244	0.01[b]	0.04
	97	18	0.071	0.116	0.076	0.075	0.022	0.010	0.24
20	73	49	0.106	0.099	0.114		0.073	0.013	0.18
21	[a]	[a]	0.117	0.136			0.024	0.01[b]	0.31
	32	59	0.054	0.052	0.046	0.043	0.042	0.07	0.37
22	133	82			0.113		0.112	0.01[b]	0.08
	197	18	0.025	0.096			0.094	0.024	0.09
23	[a]	[a]	0.495	0.482			0.393	0.007	0.05
	138	121	0.154	0.156			0.136	0.036	0.05
24	55	98	0.056	0.068	0.073	0.072	0.043	0.019	0.25
	141	12	0.086	0.071	0.077	0.066	0.027	0.028	0.36
25	86	31	0.047		0.048	0.064	0.021	0.07	0.36
26	[a]	[a]	0.105	0.065	0.105	0.098	0.043	0.01[b]	0.26
	101	25	0.050	0.059	0.062	0.056	0.034	0.01[b]	0.37
27	[a]	[a]	0.338	0.336			0.145	0.01[b]	0.03
	234	23	0.061	0.031	0.039	0.054		0.14	0.08
28	[a]	[a]					0.070	0.046	0.32
	122	32	0.055	0.044			0.019	0.30	0.38
29	[a]	[a]	0.137	0.098		0.128		0.008	0.26
	56	108	0.077	0.073		0.080	0.051	0.008	0.26
	233	31	0.056	0.069		0.098	0.036	0.036	0.35
30	[a]	[a]					0.144	0.018	0.26
	95	55	0.019				0.027	0.06	0.38

[a] Immediately after slagoff.
[b] From bath conditions silicon estimated at 0.01 pct; other values given are analytical results.
[c] See footnote *c*, part A.

only. Duplicate samples were taken from most of these heats. Part C includes 13 heats that afford a comparison of duplicate samples taken with the type *a* mold, with

because it does not involve exposure of the metal to the air. The bomb samples average lower in oxygen than the poured tests, but this may be due to levigation of Al_2O_3 dur-

TABLE I—(*Continued*)
D—LADLE ANALYSES, PER CENT

Heat No.	C	Mn	P	S	Si	Ni	Cr	Mo	V
1	0.41	0.68	0.022	0.011	0.29	1.80	0.84	0.22	
2	0.98	0.40	0.009	0.015	0.29	0.12	1.38	0.01	
3	0.10	0.47	0.010	0.010	0.29	3.45	1.43	0.01	
4	0.18	0.51	0.014	0.011	0.32	0.14	2.97	0.03	
5	No Ladle Analysis—Heat transferred to another furnace								
6	0.40	0.81	0.014	0.009	0.31	0.50	0.47	0.24	
7	0.38	0.71	0.015	0.009	0.29	1.83	0.80	0.24	
8	0.38	0.71	0.017	0.016	0.33	1.92	0.80	0.24	
9	0.39	0.85	0.019	0.010	0.37	0.16	1.03	0.22	
10	0.38	0.78	0.022	0.019	0.34	0.18	0.93	0.23	
11	0.34	0.69	0.011	0.015	0.24	1.73	0.78	0.32	0.17
12	0.08	0.52	0.022	0.008	0.25	3.50	1.66	0.05	
13	0.37	0.71	0.019	0.014	0.31	1.74	0.80	0.23	
14	0.33	0.69	0.012	0.012	0.24	1.72	0.77	0.32	0.17
15	0.36	0.73	0.015	0.015	0.30	0.29	0.94	0.22	
16	0.14	0.74	0.016	0.012	0.31	0.63	0.51	0.20	
17	0.10	0.55	0.010	0.011	0.35	3.40	1.54	0.03	
18	0.38	0.75	0.011	0.012	0.27	1.75	0.74	0.24	
19	0.26	0.66	0.010	0.012	0.24	0.20	0.12	0.48	
20	0.20	0.83	0.012	0.015	0.23	0.08	0.06	0.04	
21	0.38	0.72	0.020	0.015	0.30	0.25	0.92	0.52	
22	0.10	0.46	0.010	0.010	0.20	3.40	1.65	0.04	
23	0.09	0.50	0.010	0.011	0.24	3.42	1.60	0.10	
24	0.36	0.72	0.018	0.016	0.26	1.80	0.92	0.24	
25	0.39	0.86	0.015	0.015	0.32	0.68	0.57	0.26	
26	0.39	0.87	0.012	0.022	0.28	0.65	0.51	0.26	
27	0.08	0.57	0.013	0.010	0.45	3.47	1.45	0.02	
28	0.39	0.74	0.014	0.019	0.32	1.78	0.80	0.24	
29	0.35	0.73	0.012	0.017	0.25	1.70	0.95	0.24	
30	0.39	0.74	0.018	0.018	0.30	1.75	0.80	0.24	

duplicates taken with the type *b* mold and with bomb tests. The ladle analyses of all heats are shown in part D. Several general remarks should be made at this point.

The chilled-spoon method of sampling was abandoned at an early date for the reasons already given. No one observing these difficulties could feel any confidence in these samples or be at all anxious to adopt them for general practice. Although Table 1*A* shows that these samples are generally lower in FeO than the poured test, there are exceptions to this and it is felt that this can best be explained by their slow freezing.

The comparison of the chilled samples with bomb samples in part C is of greater interest, as the bomb has generally been accepted as the most reliable sampling method, and it is of special interest here

ing freezing, and it must be admitted that some of the bomb results appear quite unreasonable. In heat 21 the bomb sample taken before slagoff gave only 0.024 pct FeO compared with an average of 0.127 pct for the chilled samples. The carbon at this time was 0.31 pct and the carbon-oxygen equilibrium (to be discussed later, see Fig 3) calls for at least 0.04 pct FeO. It is general experience that metal under such basic, oxidizing slags will be supersaturated with regard to FeO.[1,2] The same remarks apply to the bomb sample taken before slagoff for heat 27; therefore one questions the significance of the lower results obtained with the bomb. The data presented by Brower[5] and Larsen show in another way that the oxidation of liquid steel during the pouring of a test does not give rise to a serious error. The present authors also wish to point out

that the lower FeO values found in bomb tests may be due to an action on the bomb similar to a rod boil. In any event, from a practical or operating point of view, it will be shown that the data obtained by either of these sampling methods show the same general trends and indicate the same characteristics of furnace operation.

Duplicate bomb samples were not taken, so no estimate of their reproducibility or comparative precision can be made from these data. Because the results from the chilled wedge samples were used more extensively in interpreting the data, the reproducibility was calculated for the duplicate samples listed in Table 1*C*. It was found that for the "big mold" samples the standard deviation of error σ was 0.024 pct FeO, and for the "long mold" samples the σ was 0.011 pct FeO. This may raise the question as to why the long mold was not adopted for regular use. The reason is that it was more difficult to obtain satisfactory samples with the long mold, and many of these were discarded. As a basis of comparison, it may be stated that in a well-established open-hearth program a σ value of 0.014 pct FeO was found for the big wedge type of mold.

All operators recognize that each heat of steel has characteristics of its own, and this has been kept in mind in the following discussion. However, statistical study of the data in Table 1, parts *A*, *B*, and *C*, leads to some general conclusions. To clarify the discussion, three heats have been selected that illustrate the conclusions that follow. The records from these heats are shown graphically in Figs 2 to 4, which show the variations in FeO in the steel with the other regularly observed chemistry of the heat. These conclusions are:

1. A variation in the CaC_2 content of the slag had little effect on the FeO content of the bath.

2. The FeO in the bath and slag reached a minimum at approximately the same time, but the minimum amount of FeO in the bath was dependent upon the C in the bath, rather than on the FeO in the slag. This will be considered further.

3. The FeO in the bath reached a minimum 40 to 80 min. after slagoff.

4. A variation of the lime-silica ratio between 2 and 4 in the reducing slag had no influence on sulphur removal.

5. The addition of coke to the slag did not increase the sulphur in the bath.

6. The oxygen in the bath never drops appreciably below the value determined by the carbon-oxygen equilibrium, no matter how long it is left under a reducing slag.

From an operating point of view, these observations have considerable importance. The use of large coke additions to develop a highly carbidic slag, and prolonged treatment with such a slag to produce a low oxygen level in the bath, do not appear to be justified. The bath oxygen is dependent upon the carbon-oxygen equilibrium, and this is generally attained within 80 min. of slagoff. It is evident from the data of Table 1 and the graphs of Figs 2 to 4 that no useful purpose was accomplished by the reducing slag beyond the first 80 min.; both bath oxygen and sulphur have been reduced to a minimum, and final alloy additions could have been made at that time. This would not only save considerable heat time, but the shorter time under a quiet bath should result in a lower hydrogen content and better steel quality.[6]

The relationships between carbon and oxygen in the bath are of special metallurgical importance and will be considered in greater detail. The equilibrium has been established by Chipman and Samarin,[7] and the conditions prevalent in the open hearth have been shown by Herty[8] and a number of others.[9] In the open hearth the bath contains more oxygen than the equilibrium amount. Marsh[1] showed that during the oxidizing period of an electric-furnace heat conditions are very much the same as in the open hearth and pointed out that the extent of deviation from equilibrium might

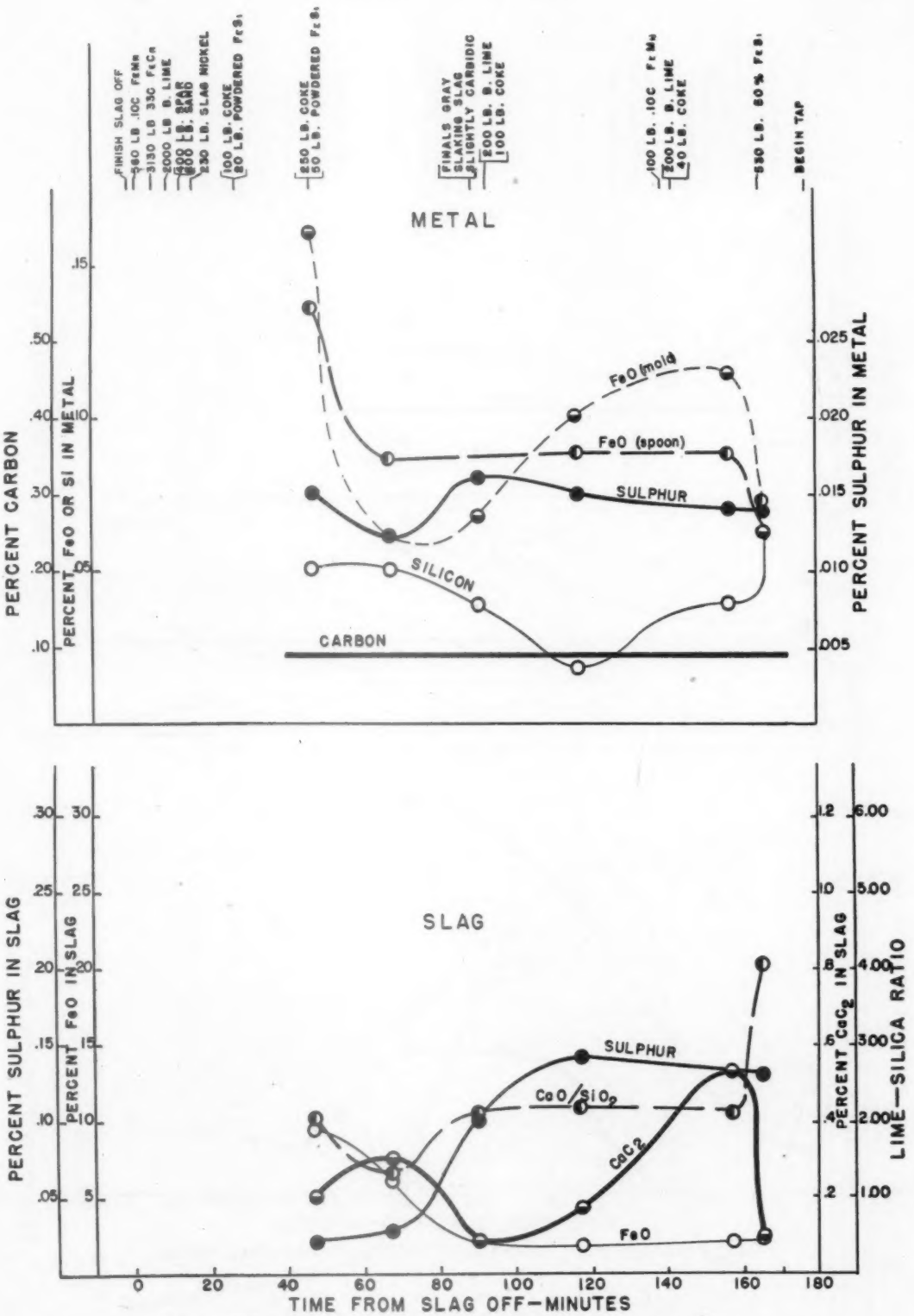

FIG 2—HEAT RECORD DURING REFINING PERIOD FOR HEAT NO. 3.

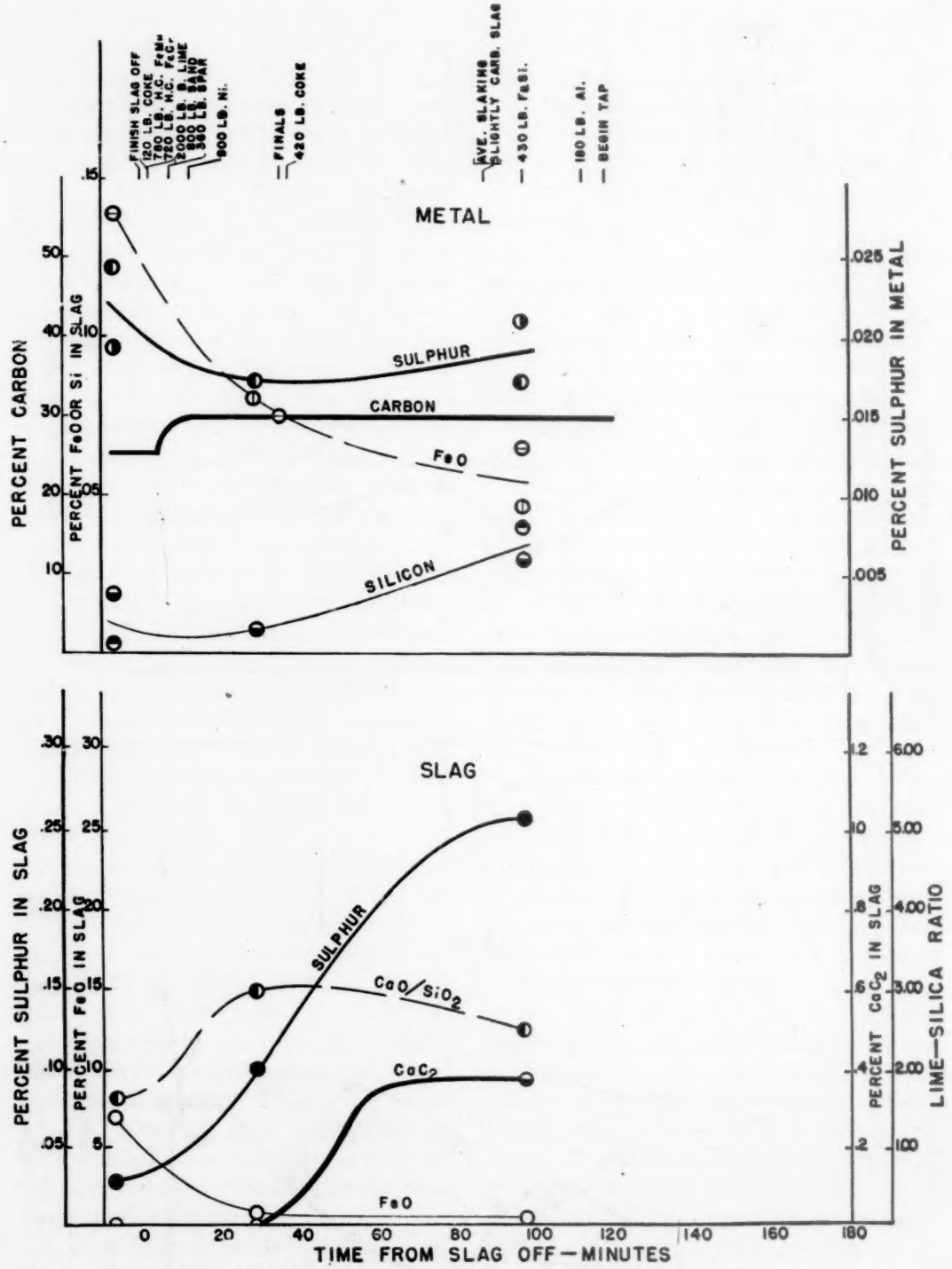

FIG 3—HEAT RECORD DURING REFINING PERIOD FOR HEAT NO. 13.

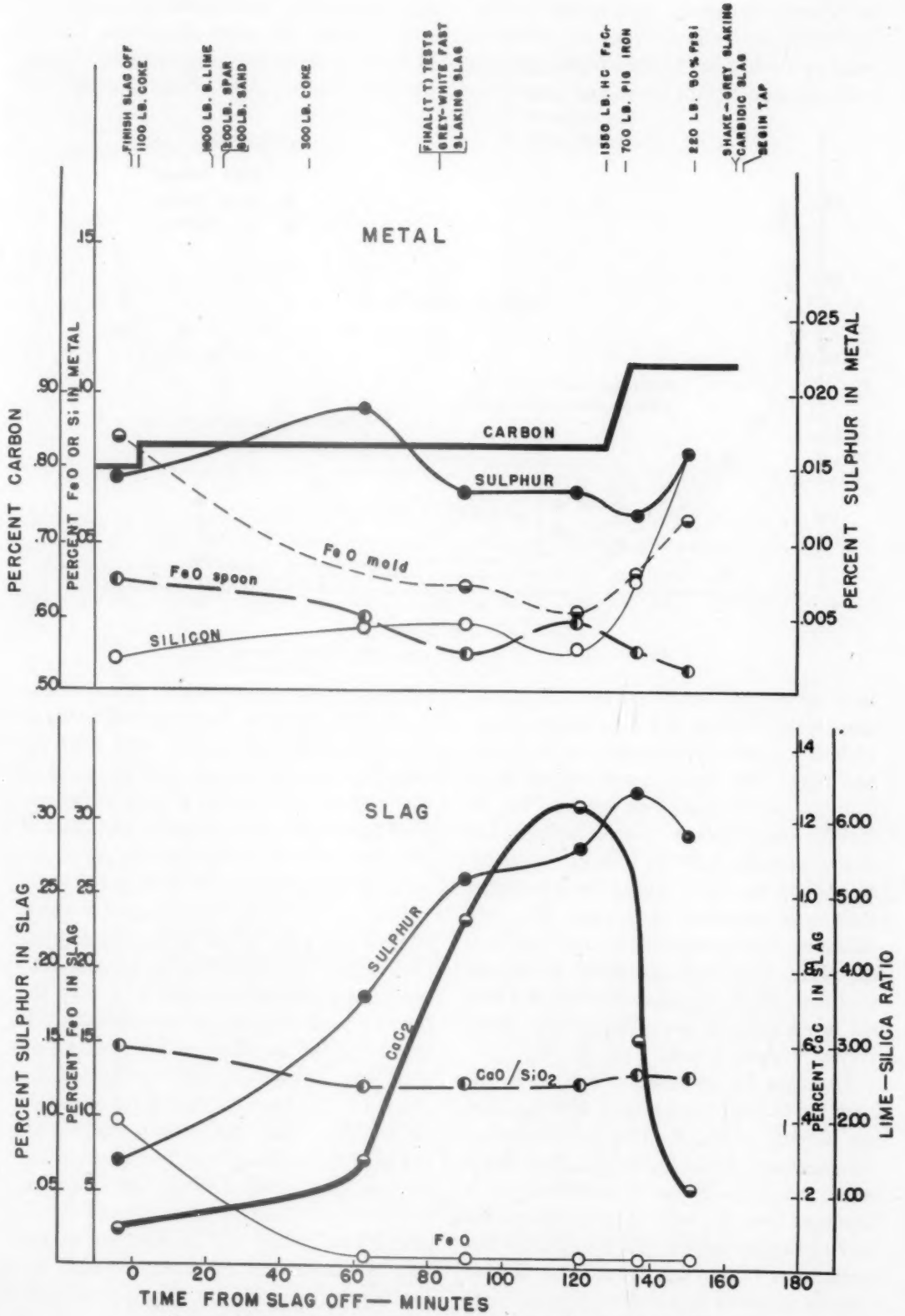

FIG 4—HEAT RECORD DURING REFINING PERIOD FOR HEAT NO. 2.

be expected to depend upon specific operating conditions. The data for the oxidizing slags in Table 1 are plotted in Fig 5, along with the equilibrium curve and previously established open-hearth curves. In general, these data confirm Marsh's earlier observations and extend the data to a lower carbon range. The bomb tests average quite close to equilibrium but are too few to justify quantitative consideration. The chilled samples indicate that in this particular shop the bath oxygen level is higher than in an open-hearth furnace. This indication may be in part due to the method of sampling, but there is reason to believe that more likely it is related to the fact that all heats studied were essentially dead-melted without a boil.

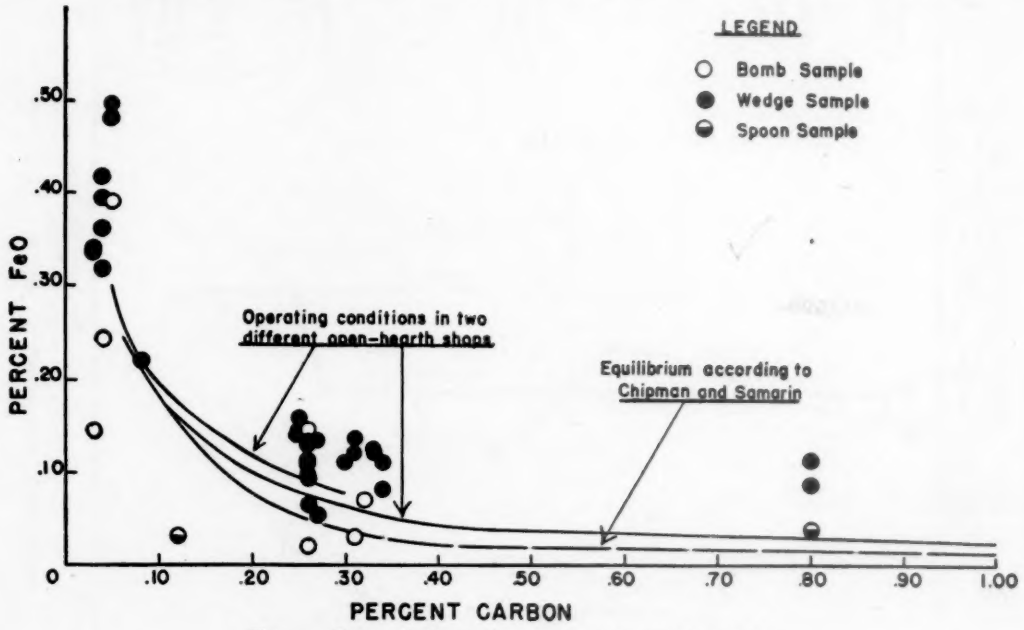

FIG 5—BATH FeO VS C DURING OXIDIZING PERIOD.

The data for carbon and oxygen in the bath for the refining period (reducing slag) are plotted in Fig 6. The points plotted represent samples 40 to 80 min. after slagoff when the oxygen was a minimum. It is apparent that the bath oxygen approaches that of the carbon-oxygen equilibrium but never goes below this level. The limited number of points obtained with bomb tests fall directly on the theoretical equilibrium curves, and the more numerous chilled samples average only slightly above equilibrium. These observations are also in agreement with the work of Marsh,[1] and extend his data to lower carbon values. Thus, independent studies with different sampling and analytical techniques show that the oxygen content of electric-furnace steel cannot be reduced below the value of the carbon-oxygen equilibrium, even by prolonged treatment with a reducing slag.

It appears that the bath sulphur does not reach a minimum at the same time as bath oxygen; namely, 40 to 80 min. after slagoff, but remains essentially constant during the refining period under the conditions studied. This will be considered in connection with the nature of the desulphurizing process in the basic electric furnace and in conjunction with the recent studies by Grant and Chipman[10] on desulphurization in the basic open hearth. The data in Table 1 were used to calculate the desulphurization ratios and excess base in the slag for these electric-furnace heats, according to the method of Grant and Chip-

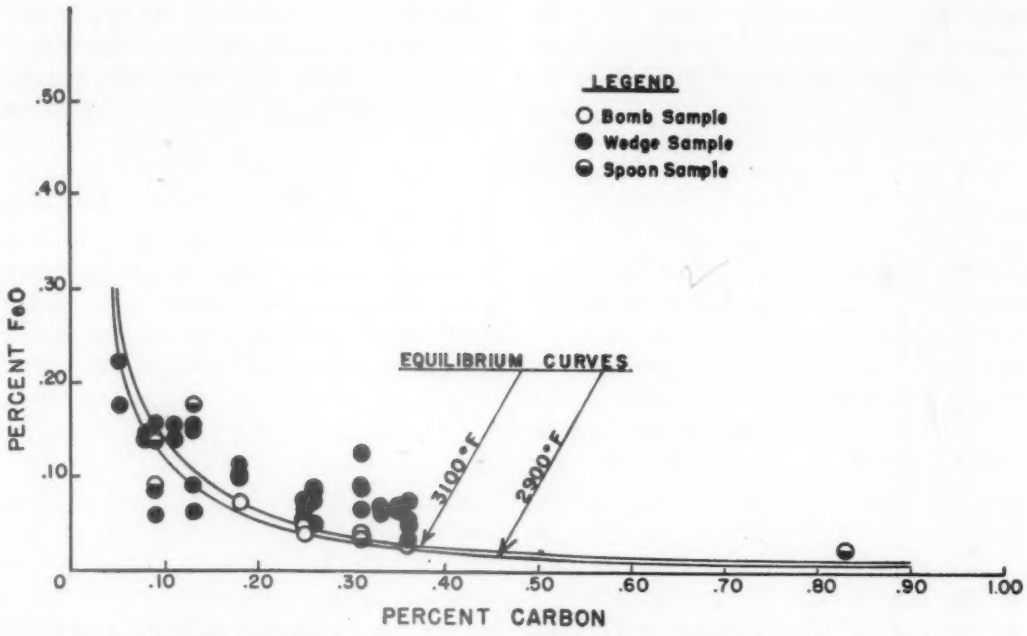

FIG 6—BATH FeO VS C DURING REDUCING PERIOD, 40 TO 80 MINUTES AFTER SLAGOFF.

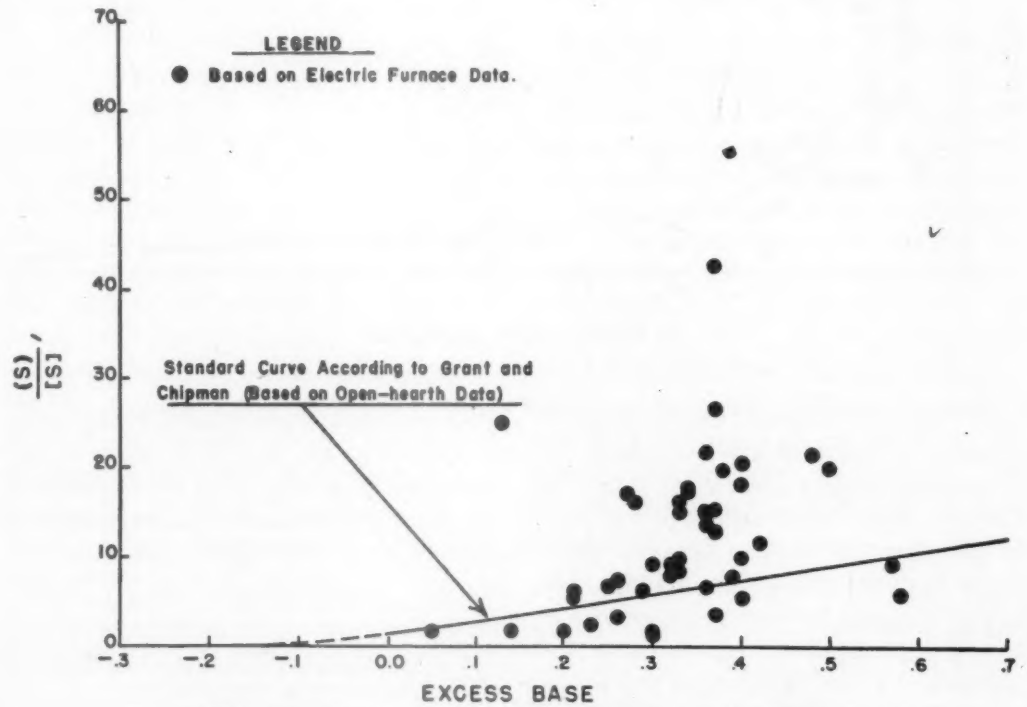

FIG 7—DESULPHURIZATION RATIOS VS EXCESS BASE FOR REDUCING SLAGS.

man,* and plotted in Fig 7 along with the master curve established by these authors for open-hearth operations. These data do not conform well with the open-hearth curve, but this standard curve seems to represent an approximate lower limit for the electric-furnace data. In order to determine what factors might be responsible for these differences between open-hearth and electric-furnace practice, the data in the range between an excess base of 0.3 and 0.4, where the departures are the greatest and where most data are available, were considered further. If the desulphurization ratio is plotted against percentage of FeO in the metal, there is no obvious relation, and the same lack of correlation is obtained when the desulphurization ratio is plotted against the mol fraction of FeO in the slag. However, when the slag alone is considered for all heats and percentage of sulphur is plotted against percentage of

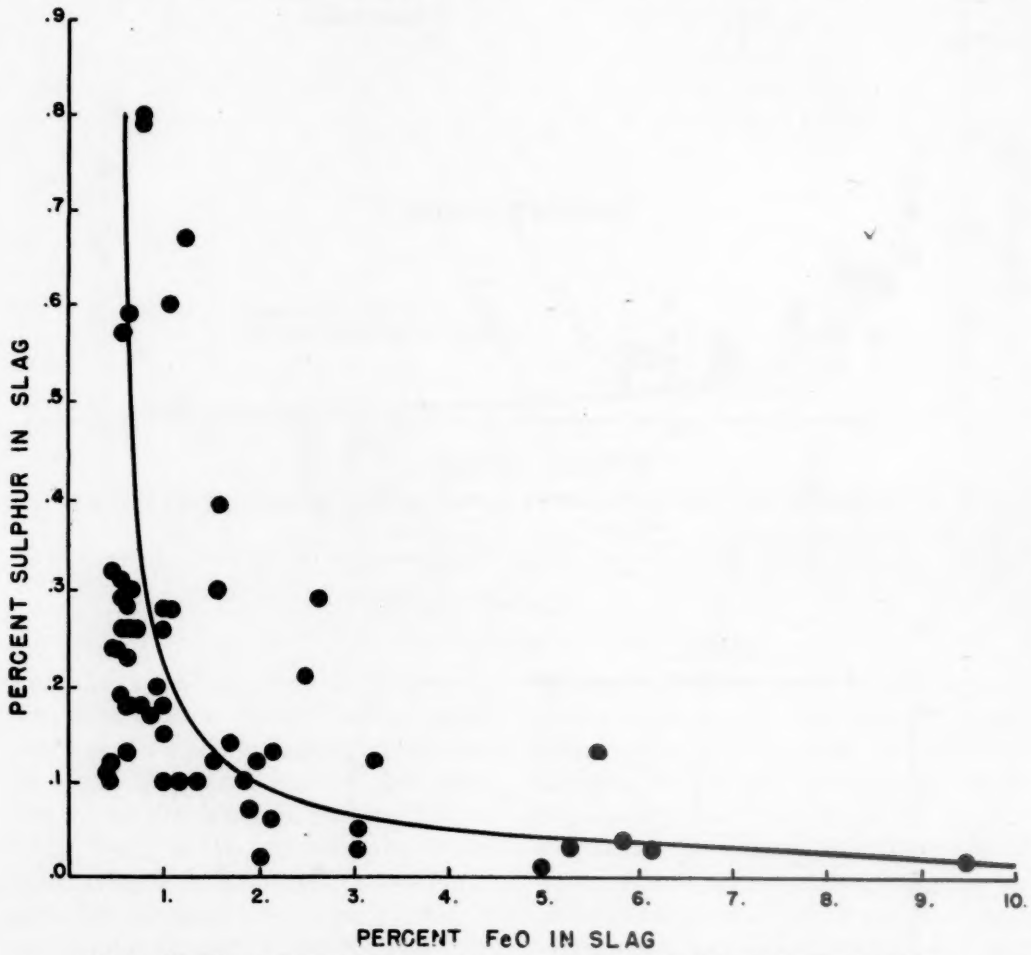

FIG 8—PERCENTAGE SULPHUR IN SLAG VS PERCENTAGE FeO FOR REDUCING SLAGS.

* Desulphurization ratio $= \frac{(S)}{[S]} = \frac{\text{W \% sulphur in slag}}{\text{W \% sulphur in metal}}$

"Excess base" is calculated by converting the slag analysis in weight per cent to mol fractions per 100 grams of slag and determining the amount of base required to neutralize the acid on the following molar basis:

2 base: 1 SiO_2
4 base: 1 P_2O_5
2 base: 1 Al_2O_3
1 base: 1 Fe_2O_3

FeO and CaF_2 are neutral; CaO, MgO, MnO are bases of equal value.

FeO as in Fig 8, it is evident that an inverse relation exists between these quantities, and that slags with large amounts of FeO do not contain large amounts of sulphur. Conversely, a slag that is high in sulphur will be low in FeO. Thus, if low sulphur is to be obtained in an electric-furnace heat, one must consider both slag volume and slag composition, and the most practical course is to use a small volume of completely reduced slag. It would appear that within the range of basicities ordinarily used, the state of oxidation of the slag is far more important than its basicity.

The data recorded in Table 1 and illustrated in Figs 2 to 4, show, with few exceptions, only minor variations in the sulphur content of the bath after slagoff, but an appreciable increase in the sulphur content of the reducing slag. This, coupled with the discussion of the preceding paragraph, can be interpreted as showing that the reducing slag does not act as a desulphurizer toward the metal bath, but rather serves to protect the bath from whatever sulphur may be added to the system in the form of coke and other raw materials. That is why large additions of coke do not increase the sulphur content of the metal. This is analogous to the protecting role of the slag in regard to oxygen. This view of the slag as a blanket over the metal, which excludes both oxygen and sulphur but does not remove these elements from the bath, seems reasonable when the lack of bath action is recalled, and lends weight to the desirability of tapping the heat as soon as the minimum oxygen value is attained.

Summary

Heat records, which include oxygen analyses in addition to the regular slag and metal analyses, have been assembled and examined for 30 electric-furnace heats. The available methods of sampling for oxygen are compared. Based upon observations made during the investigation, as well as upon the data presented, the following conclusions appear to be warranted:

1. Although bomb tests give slightly lower oxygen values than chilled wedge samples, there is insufficient evidence to accept either one as the absolute value. Both methods of sampling the steel bath for oxygen give the same indications of oxygen behavior and are equally useful. The chilled sample seems more convenient.

2. The metal bath reaches a minimum oxygen value after 40 to 80 min. under the reducing slag. Prolonged holding is thus a waste of furnace time.

3. The minimum oxygen value is dependent upon the carbon in the bath and the carbon-oxygen equilibrium, rather than upon the time of holding under the slag.

4. The amount of sulphur held with a given slag is determined by its state of reduction rather than its basicity, in the range of basic compositions studied.

Acknowledgments

This paper is based upon the results of a project sponsored by the Carnegie-Illinois Steel Corporation, dealing with a study of certain aspects of steelmaking. The work involved a number of the personnel of the Operating and Research Departments of that Corporation and of the Metals Research Laboratory of the Carnegie Institute of Technology. The authors wish to acknowledge the efforts of the representatives of both organizations, especially the contributions of Messrs. William Grundman and R. F. Grafmiller, of the South Works, Carnegie-Illinois Steel Corporation, and Mr. W. O. Peifer, of the Metals Research Laboratory.

References

1. J. S. Marsh: Slag-metal-oxygen Relationships in the Basic Open-hearth and Electric Processes. *Trans.* A.I.M.E. (1945) **162**, 672–684.
2. G. Derge: Rapid Analysis of Oxygen in Molten Steel. *Trans.* A.I.M.E. (1943) **154**, 248–256.
3. K. C. McCutcheon and L. J. Rautio: Oxygen Samples from Open-hearth

Bath. *Trans.* A.I.M.E. (1940) **140**, 133–135.
4. T. Swinden and W. W. Stevenson: The Determination of Oxygen in Liquid Steel. 4th Report of the Oxygen Subcommittee of the Committee on the Heterogeniety of Steel Ingots, Iron and Steel Inst., (July 1943) 167.
5. T. E. Brower and B. M. Larsen: The Occurrence of Oxygen in Liquid Open-hearth Steel—Sampling Methods. *Trans.* A.I.M.E. (1945) **162**, 712–722.
6. Symposium on Determination of Hydrogen in Steel. *Trans.* A.I.M.E. (1945) **162**, 353–404.
7. J. Chipman and A. M. Samarin: Effect of Temperature on Interaction of Gases with Liquid Steel. *Trans.* A.I.M.E. (1937) **125**, 331.
8. C. H. Herty, Jr., and associates: The Physical Chemistry of Steelmaking. Carnegie Inst. of Tech. *Coop. Bull.* 68 and 69.
9. Basic Open-hearth Steelmaking, chap. 16, 466 ff. New York, 1944. A.I.M.E.
10. N. J. Grant and J. Chipman: Sulphur Equilibria between Liquid Iron and Slags. *Metals Tech.*, A.I.M.E. (April 1946—T.P. 1988); *Trans.* A.I.M.E. (1946) **167**, 134.

DISCUSSION

(B. M. Larsen and T. B. Winkler presiding)

T. B. WINKLER—I am sure that Dr. Derge's findings have proved of interest to everybody, particularly his significant finding that it is impossible to reduce the oxygen content below that dictated by carbon. Therefore it appears the carbon is the controlling factor in all of these oxygen contents in steel baths. His discussion of methods of sampling of the bath for oxygen determinations was enlightening.

C. E. SIMS*—One of the outstanding points in this paper is that while there were correlations between slag and metal composition that simulated equilibrium, there was apparently no real equilibrium condition reached between these two phases.

One would expect that a slag and metal bath after being in contact for 1 to 2 hrs while the former is kept in a reduced state should, at least, closely approach equilibrium. In other words, the so-called deoxidation period of a basic electric furnace seems to be the most favorable period of all for attaining equilibrium, and yet the evidence indicates that in the heats reported no equilibrium was reached.

One indication of this is the static condition of the sulphur in the bath and its failure to vary with time or condition of the slag. Another is the indirect relation of oxygen content of the slag to that of the metal.

There was a certain correlation between (O) and [O], but it was not an equilibrium type of correlation. It appears that this can best be explained by considering the slag as a reservoir of oxygen which is continuously fed into the bath during the oxidizing period. The bath oxygen is eliminated as CO gas, but during this period, the pressure of dissolved CO builds up to several atmospheres. When the reducing or deoxidizing period is reached, the available oxygen in the slag is lowered, and it simply ceases to supply oxygen to the bath.

The bath, bereft of its source of oxygen, continues to evolve CO, at a greatly reduced rate, until a pressure of 1 atm is approached. There appears to be no other mechanism by which the bath can lose oxygen and carbon and, therefore, the contents can go no lower than the amount in equilibrium with one atm of CO. One must conclude that, under the circumstances, there was no transfer by diffusion of oxygen from bath to slag during the "reducing" period.

Dr. Derge disclaimed any correlation between the sulphur content and basicity of the slag but showed a rather good correlation between the FeO content and sulphur content of the slag. In examining Fig 7, however, it appears that, except for 3 points, there is almost as good a relation, with a similar shaped curve, as there is in Fig 8. Regardless of this argument, the salient point is that the slag failed completely to act as a desulphurizer of the bath and any desulphurization that was accomplished was done under the oxidizing slag.

This indicates there was no exchange between the reduced slag and bath and that for practical results, they might as well have been in different furnaces. They were "dead" in more ways than one. At the immediate slag-metal interface, of course, there must have been some approach to equilibrium. This is a serious deficiency in the present electric arc furnace.

There is a definite inference that inducing an artificial boil, as with some cold steel or by bubbling through an inert gas, would have brought about a minimum oxygen content in a very few minutes instead of 40 to 80 min. and would also have resulted in efficient desulphurization.

* Battelle Memorial Institute, Columbus, Ohio.

B. M. LARSEN—Possibly some of the points that depart from the general trend are more significant than the main group of points. I think the data as a whole, as Mr. Sims pointed out, indicate the tendency to the metal phase to settle back toward the carbon equilibrium because that is a reaction that can occur right down in the metal and does not require necessarily any reaction between the slag and the metal.

I cannot see any theoretical reason why a very low sulphur activity slag should not absorb sulphur from the metal bath if there is enough contact in stirring in this bath. The paper indicates particularly that there was not.

There is no reason why there should not be a surface zone reaction (a heterogeneous reaction occurring at the plane of contact between the slag and metal) if there were enough stirring. Then the contact and the amount of reaction that would occur simply by straight diffusion would be very slow. If that were the only mechanism you would get just what you usually get in this instance.

But if there were stirring, it would be expected that both the sulphur and the oxygen would go lower, because it would appear from other indications that the activity of oxygen in some of these slags was very low. The fact that some of the sulphur ratios do go very much higher than Grant and Chipman's curve indicates that Grant and Chipman's concepts do not take into account all of the chemistry involved. In other words, iron oxide does play a part. There were a few points in the plot of oxygen which are definitely the carbon equilibrium. That may indicate that if there were stirring it would be definitely very much below the carbon equilibrium conditions. This assumes again that the slag was maintained at reducing conditions and that the atmosphere above the slag was kept at reducing conditions.

G. DERGE (author's reply)—In order to avoid any misconception I would like to make it clear that I agree with both of the discussers that these data probably do not represent an equilibrium condition, and I think that is a correct interpretation. The departures from expected behavior which we have here definitely represent a departure from equilibrium, and if we had some way of stirring the slag and metal together, as during the active period of open-hearth operations or during the oxidizing period in the electric furnace, we would find a different result.

I wish also to avoid any misunderstanding on the sulphur question. I feel very strongly that there must be a relationship between basicity and desulphurizing action, but in these reducing slags there must be some additional effect over and above that of basicity.

Dr. Sims has pointed out that our data actually show some influence of basicity on sulphur removal and we do not wish to dispute this statement. However, it is equally clear that basicity is not the only important factor in these "reducing" slags. Referring again to Fig 7, consider the group of slags with essentially constant basicity, i.e. in the narrow range between 0.3 and 0.4 "excess base." The slags in this group which have a high percentage of sulphur in the slag are low in iron oxide and the slags which contain little sulphur are high in oxide. Thus, when the effects of basicity are eliminated and only state of oxidation is considered, one finds that in these "reducing" slags the ones which are lowest in iron oxide are the ones capable of absorbing the largest amount of sulphur. Therefore, over and above the basicity effect, there is this oxygen effect, and this is not in conflict with the ideas which have been presented by Chipman and Grant because their study and interpretation did not include reducing slags. This is additional to the observations which they made on open hearth practice.

Training of Metallurgical Engineers in the Steel Industry

By E. C. Wright,* Member AIME

Chicago Meeting, February 1946

The following article is based on observation of college graduates entering the steel industry in technical work made during the past 25 years, the first five of which were spent as a college instructor in two engineering schools, and the last 20 in the employ of a large steel company that has hired hundreds of engineering graduates for steel-mill operations.

The college graduates encountered during this period have come from many colleges representing schools in Eastern States, Midwestern Universities, many Southern colleges, and many smaller colleges and normal training schools mostly in western Pennsylvania and Ohio. The college training of these students for engineering work naturally has varied widely and the educational qualifications of the entrants have been in many ways different.

It was found at an early date that graduates of standard engineering colleges were much more adaptable than graduates in science from nontechnical schools. The engineering students seemed to be more suited to actual work in steel plants and in general were better able to grasp a knowledge of the operations they observed. However, although the graduates of engineering schools have had somewhat better training in physics, mathematics, and engineering, it has been a general and continual observation that most of the students employed have had inadequate training in the fundamental sciences.

Manuscript received at the office of the Institute March 14, 1946. Issued as T.P. 2051 in Metals Technology, September 1946.

* National Tube Co., Subsidiary U. S. Steel Corporation, Pittsburgh, Pennsylvania.

Since this discussion relates entirely to metallurgical engineers it should be emphasized that students taking metallurgical engineering courses in college seem to be poorly trained in organic chemistry-physics, physical chemistry, thermodynamics, and any higher form of mathematics than simple calculus. It has been noted frequently that young engineers faced with problems in a mill that involve some mathematics generally flounder badly, and that they have little conception of physical chemistry.

Another common deficiency lies in the young graduate's lack of knowledge of where to look for the more detailed literature on any subject. He reverts instinctively to some college textbook whose coverage is usually very elementary. It is recommended that such textbooks contain a bibliography of the source literature, and that students be taught to use the original data.

Many of the students had had previous courses in college dealing with metallurgical work such as steel melting, metallography, etc., but it was found that their grasp of these subjects was extremely sketchy. It was soon realized that an ordinary engineering graduate could be taught more about steel melting and manufacturing processes in a few weeks in a plant than he could learn in a college course on such subjects. A similar statement may be made regarding the ability of students to conduct laboratory work. Their lack of technique and skill in handling equipment and setting up experiments was soon apparent. It became neces-

sary to give metallurgical engineering students courses in routine laboratory work in order to impart to them the manual skill necessary for successful experimental and research work.

General Courses not Desirable

Naturally, a college course in metallurgical engineering cannot be so organized as to apply only to those students who intend to enter a steel mill. Many graduates may go into the copper or aluminum industries, or several of the metallurgical engineering plants where steelmaking or steel applications are not important. As a consequence, the applied metallurgical courses taught in the colleges attempt to give the student a smattering knowledge of all metal smelting and fabrication from gold milling to magnesium reduction. Moreover, too many of these industrial courses are taught by instructors who have had no industrial experience. As a result of our experience, the value of such general courses is seriously questioned. It is felt that a greater stress in college on fundamental courses such as mathematics, physical chemistry, and thermodynamics would much better prepare the metallurgical engineering graduate to enter into any branch in the metallurgical field. An engineer with a sound foundation in basic science can readily adapt himself to any metallurgical industry by means of a few months' study of its literature while working in the industry.

Attitude of Older Employees toward College Graduates

The approach of a college graduate to a steel mill 25 years ago was very different from his entry today. At that time the steel industry was still in its infancy from the technical standpoint. Very few alloy steels were being manufactured, and 95 per cent of the steel tonnage produced was made of plain low-carbon steel for such constructional articles as plates, sheets, beams, pipe, and wire. The executive operating forces in the mills at that time were to a great extent practical steelmen who had grown up in the steel industry from boyhood. Many of these men were not educated beyond the eighth grade and their idea of making steel was to follow the rule-of-thumb procedures set down by the men under whom they had served their apprenticeship. The roller who usually directed the rolling mills was a practical man with ability to lead a crew, who could get out the greatest tonnage of a given item. The heater who operated the furnaces was a king unto himself, who dictated the temperature to be used and the rate of heating to best suit his own experience. The only technical force in the steel mill aside from the mechanical engineer was that in the chemical laboratory under the jurisdiction of the Chief Chemist. In that period this force was mainly interested in the intricacies of analytical chemistry, developing new methods of analyzing steel, and improving the accuracy of their work. The laboratory generally made only routine chemical and physical tests and had little control over operations. In reality there was no Metallurgical Department.

The entry of a technically trained employee into such a group was not at all appreciated and was accepted often with ridicule. From this psychology developed the method of training engineers by the sweat and hard-knock method. A superintendent who had started to work as a laborer while still in his teens naturally assumed that young engineers should have to work their way through similar channels A young graduate in the open-hearth plant was placed in the cinder pit or given some other form of arduous and menial labor. The only thing he was taught about steelmaking was that offered by the melters and foremen in the shop, who filled the neophyte with their opinions and ideas, many of which have since been

proved to be wrong. As a result, the lot of the college graduate between 1920 and 1930 was not at all pleasant and many of the engineering apprentices left the industry or stayed in unimportant positions.

After 1930 the considerable increase in demand for alloy and special steels presented problems with which the old practical steelmakers could not cope, and the necessity for using some technical control over the operations became evident. Those who witnessed the early rollings of stainless steels can testify to this fact! During this period metallurgical staffs were also being organized in the consuming industries, and from this activity resulted a great interest in technical employees. As a result there was a sudden expansion of the acceptance of young engineers into the steel industry. The previous experience had also indicated that these young men should receive some form of training different from that of the hard-knock school, which would allow them to progress more rapidly into an understanding of the processes involved in the plant in which they were working. About the same time the increase in complexity in the steel business required the expansion and building up of metallurgical departments, and the training of metallurgical engineering apprentices from that time became largely a function of the metallurgical departments themselves. In this atmosphere the metallurgical engineering apprentice was usually under the direction of technical men who had originated the metallurgical department, and it was possible to organize the training of engineering graduates for metallurgical work in a more orderly manner. Even under these improved conditions, however, experience has shown that it takes from 5 to 7 years to make an able metallurgical engineer in a steel plant. The truth of this statement may be readily established by a survey of the younger engineers in any plant. Very few with less than 5 years experience will be found in important positions.

Mill Training of Technical Graduates

After 25 years, the training of technical graduates has more or less crystallized into a routine, and more satisfactory results are now being obtained in developing such men. It has been found that the finished metallurgical engineer needs a thorough understanding of routine analytical chemical work, routine physical testing procedure, a good knowledge of statistics, ability to handle men, a thorough knowledge of all the processes and operations in the plant in which he works, and, finally, ability to analyze difficulties and conduct research work.

Chemical Analysis

It has been found to be very beneficial to place metallurgical engineering graduates in a routine analytical chemical laboratory for a period of 3 to 6 months, depending upon their manual aptitude. The skill that these men develop in repeated daily operations in analytical chemistry makes a very sure foundation for any future laboratory work they may encounter. The skill and accuracy of analytical chemists in routine mill laboratories have amazed the writer many times, and the quickness with which the new men acquire the technique is also surprising. Statistical records kept in several mill laboratories have shown that routine chemists analyzing for all the elements in steel will average about five determinations per man-hour worked. For example, it is not unusual for an analyst to complete 60 manganese determinations a day (8 hr.), or 50 chromium determinations. It has been generally found that if a student has had good theoretical chemical training previously, within three months on a variety of determinations he can achieve an output that approaches that of the older chemists. The skill and

manipulative ability thus acquired seem to stick with the students for many years.

The other value of the analytical chemical work is that it gives the student a very thorough grounding in chemical and metallurgical calculations. The daily use of factors, the setting up of standard solutions and other standards enable the trained chemist to handle chemical calculations as readily as ordinary arithmetic. This training has been found to be invaluable later for the metallurgical engineer in conducting calculations involving smelting and processing, which are of prime importance in blast-furnace and steel-melting operations. The metallurgical engineer needs a good course in quantitative analysis in college to supplement this work.

Physical Testing Procedure

It has been found also that a period of from 3 to 6 months on routine physical testing work is very necessary. Here the student receives routine and thorough training in tensile testing, hardness and impact testing, testing of metals at high and low temperatures, and many special forms of physical tests. In addition, statistical summaries of physical test results on materials made in large volume, usually assembled in the physical testing laboratory, teach the student engineer an early familiarity with statistics that have been found to be of great value in studying mill problems of a metallurgical nature. The control of chemistry of the steel, finishing temperatures, annealing treatment, and many other metallurgical processes are most readily reached by making a statistical study of the factors involved. The work in the physical testing laboratory gives the young engineer a real concept of the properties of steel, and an understanding of Hooke's law, elastic limit, and other properties that are the basis of engineering design. The college courses in engineering mechanics begin to have a definite meaning and should be reviewed by the student engineer while working in the testing laboratory.

Metallurgical Laboratory Work

The next step in the student metallurgical engineer's training is in the metallurgical laboratory. A period of several months is also desirable in this field. Here the student is taught the use of the microscope and given routine training in preparation of metal surfaces and in photographic work. Incidental to the routine work occur observations of steel in many of its structural forms; supervision of carburizing, heat-treating, grain-size control, inclusion ratings, the effect of cold-work, finishing temperatures, and many of the other factors that change the structure of steel.

Work on Specifications

A final important part of a metallurgical engineer's training is that of being familiar with the specifications for the steel products being manufactured. Through the years the number of steel specifications has multiplied, and familiarity with the requirements and manufacturing processes necessary to meet these specifications has become an important function of the metallurgical engineer. The young engineer becomes familiar with the chemical and physical test requirements of specifications from his routine work in the testing laboratory. Additional training in this field is now given to the metallurgical engineer by having him pass on inquiries and also on the clearing of orders before placing them for manufacture. This checking of inquiries and orders requires a detailed review of each specification involved, and a few months' work in this field usually gives the engineer a good understanding of the specifications for the products being made.

Mill Control

At the end of this laboratory training period the student has a good background

for testing and has also had about a year and a half in the mill laboratory, with frequent trips through the mill collecting samples or observing some special work, which gives him a fair acquaintance with the mill operations. He is now ready for mill-control work. Metallurgical departments in large steel mills have had to organize a large number of trained engineers for this mill-control work and they are usually designated as "observers." Nearly every producing department has one or more observers conducting such work as temperature control and collecting data on test work being run in the department in which they are working. It has been found that the best policy is to rotate the student engineers as observers through the various important departments of the mill, from melting to finishing. Usually two months observing work will give an intelligent student a fair cross section of the operations and processes in any one department. Since difficulties are continually developing, however, each department is faced with problems in which these observers participate to overcome the difficulty. This association with the problem forces all the men, including the observers, to make a detailed study of all the factors involved, and this has been found to be excellent training, because the young engineers rarely forget the means employed to overcome the difficulty.

The necessary adjunct of mill control and observation work is to become familiar with control instruments such as pyrometers, pressure instruments, combustion controls, speed controls. Most large steel mills make up their own thermocouples and check them for accuracy before they are placed in use. Moreover, the recording instruments are generally under the care of either the mechanical or metallurgical department, and students are taught to regulate and repair these instruments.

Research and Development

A student engineer who has been in observing work for one or two years, which approximates a total of three years in the plant in question, has reached the stage where it is possible to assign more responsibility to him and allow him more initiative in studying problems. At this point the student engineer passes to research and development work, where he is assigned one or more problems with the assistance of other laboratory men for the study. In this work the student engineer is given the responsibility, with all the assistance of the department, in attacking the problem. Student engineers at this stage rapidly show their ability and true quality. Those who cannot take responsibility or who are timid in their approach to a difficulty, soon exhibit these tendencies and have to be removed from special work and assigned to routine duties. Others, who are willing to assume responsibility and show imagination and initiative in working on research problems, rapidly progress. The men supervising the young engineers at this stage of their development have a very important responsibility, as the main object should be to instill confidence in the apprentice. If a young engineer fails on an investigation, and such a failure should cause the loss of valuable material, the supervisor should protect the young engineer from ridicule or censure, whereas if the young engineer brings an investigation to a satisfactory result he should be praised for his efforts and accomplishment. Many young engineers have been set back, unfortunately, either by too severe censure for a mistake or by being pushed along too rapidly during this period. At this stage it is easy to determine whether the student engineer can handle several men in research work and whether he can be assigned responsibility for the work. The student engineers who show the most aptitude for research work have also been frequently transferred

from mill metallurgical departments to the main research laboratory, where they have generally spent one year under the direction of the more highly trained research workers. This part of the training program has been very beneficial to the men of better quality and also supplies to the research laboratory organization a continuing group of younger men who are familiar with manufacturing operations in the company's plants.

Writing Reports

During this period of the student's development the question of writing reports on work completed also arises, and for many metallurgical engineers this becomes very difficult. In the beginning this seems to be largely because of the young engineer's obsession with his own research work and an assumption on his part that the report need cover only the briefest details on the results. The student engineer seems to have no realization of who will later read the report and generally he fails to state clearly the problem itself, the methods of overcoming the problem, and definite conclusions as to the results. It has been shown that it takes from one to two years of continual report writing to demonstrate to the young engineer what is required in a finished report. Naturally, it should be as brief as possible, but it should be understandable and clear not only to his immediate superior, who may be familiar with all the details, but also to the general manager of the plant or some vice president who may later have to read the report. A well written report has often attracted the attention of a higher executive to a young student, and many times has hastened promotion to a better position.

Sales Training

The metallurgical engineer who has spent about five years in a steel mill should be thoroughly familiar with the plant's products and the specifications for all the materials produced He is then ready to meet consumers and to discuss with them metallurgical factors relating to the use of the product in the consumer's plant. It is important that the representatives of the steel mill who visit customers should be very thoroughly grounded in the characteristics of the product being discussed, in order that all questions raised by the customer may be thoroughly and accurately answered. These men should not only know the metallurgical properties of their products but also must be familiar with tolerances, range of sizes, finishes, and any other particular details of the materials being discussed. Experience of this nature is also desirable to the engineer, as it gives him a realization of customers' problems and he returns with the aim of improving the product being made to meet, as far as possible, the deires of the purchaser. The necessity for a large staff of metallurgical engineers circulating among customers has become more and more apparent, and the metallurgical engineer must be trained in this field as much as in the field of manufacture in his own company's plant. The metallurgical engineer who exhibits sales and business ability will be the steel salesman of the future.

Conclusion of Mill Training

The student engineer who has concluded the mill training outlined herein is generally ready to assume executive positions in the plant, or he may be qualified for sales engineering work. Men who have successfully concluded the mill training are generally outstanding and achieve fairly rapid promotion because of their thorough knowledge of the company's manufacturing procedures. A certain proportion of the apprentices become dissatisfied, or are found to be unsuited for engineering work, while others have personal qualifications or limitations in ability that prevent their

promotion to more responsible work. In this latter category fall many of the good, reliable men who are satisfied to stay on some routine metallurgical job. These men often become very proficient in certain lines of work, such as physical testing, order checking, and mill-control work.

Cooperation of College and Industry

The fact that it takes four years for a college to train an engineer in the elementary courses required to prepare him for his profession, and that at least five additional years are necessary to develop a college graduate into a good operating engineer, makes it evident that the college and industry have much in common in this activity. In the writer's experience there has been too little cooperation between colleges and industry in this field. This is not meant to criticize the present curricula of engineering courses in the better colleges. Aside from the criticism given earlier—that more stress might be given to fundamental scientific courses in the college, with less emphasis on industrial engineering courses—it is believed that the courses now taught in the four-year course in engineering are about as well selected as can be grouped in this period, and certainly as much as the ordinary high-school graduate can undertake in the time allotted. One way in which greater cooperation between industry and colleges might be accomplished is through the hiring of undergraduates for summer work. During this 25-year period considerable experience along this line has been accumulated, and results obtained seem to be of definite value. For example, many high-school graduates have worked in our routine chemical and physical testing laboratory during summers while going through the regular college course. It has been shown that men who have done this routine analytical work can complete their general chemical courses, especially quantitative analysis, with much greater ease in college because of the skillful laboratory technique developed in the mill laboratory. Moreover, men who have worked in the physical testing laboratory have approached their courses in engineering mechanics with much greater interest and understanding, and those who have done metallographic work in mill laboratories become outstanding students in this subject in their college course.

It would seem feasible under present conditions that more of industry could hire a certain number of young men who have completed the first year college course to spend two or three months in the summer in an analytical laboratory. Following the second year's college work the student could spend a summer in the physical testing laboratory. After the third year's work the student could spend a summer in the metallographic or metallurgical laboratory. By this arrangement the student would have completed almost one year of his necessary mill training work and certainly get much more from the courses he would be taking in college. The other important advantage of this proposal is that the student soon learns whether he is interested in metallurgical work and either intensifies his efforts or turns to other subjects. At the end of his college course a student so trained could return to the mill where he had spent his summers and more rapidly pass through the metallurgical training course described in the foregoing pages. It is believed that, if such an arrangement could be achieved, a finished experienced metallurgical engineer could be developed within a seven-year cycle beginning with his entrance in college. One other advantage of this method rests in the fact that many college graduates resent working on routine jobs even for a few months or a year, as they believe they are fitted for much better positions as soon as they receive their

diplomas. This natural attitude represents a psychic handicap to young engineers entering industry, and could largely be overcome if much of the routine mill training could be accomplished at a time coincidental with the college work.

These proposals are in no way intended to represent a cooperative course that has been tried many times with varying success. It is felt, however, that any plant requires a continual flow of young engineers to maintain its technical position in industry. The quota of young engineers needed every year can be determined without too much difficulty. Under present conditions, where most employees receive at least two weeks vacation with pay, the hiring of a few college students every summer to substitute for the men on vacation could be readily fitted into the plant force. For example, a chemical laboratory with 20 men on the staff would experience 40 weeks of vacation, which would enable the employment of four college men for 10 weeks each, without increasing the size of the laboratory force. The improvement in the company's supervisory staff is just as important as the maintenance and modernization of equipment. A definite program for recruiting a predetermined number of young technical men each year should be established and maintained at all times, regardless of business activity. Such a policy will make possible constructive cooperation with a selected number of colleges, whose students receive the best training, for the placement of a definite number of undergraduates and graduates each year.

Rates of Payment

An important factor in a successful engineering training course relates to rates paid to these men under training in comparison with the rates paid to older employees in similar occupations. Under the existing labor laws and collective bargaining requirements, the simplest way of approaching this problem is by setting up standard apprentice courses with fixed rates of pay. This situation has been very clearly established by means of a laboratory apprentice course lasting two years, for men who are high-school graduates but not graduates of engineering colleges. Thus undergraduate students working in the summertime could be employed on the laboratory apprentice basis. College graduates in the plant are placed on an engineering apprentice course, which allows higher rates of pay competitive with rates offered by other industries for college graduates. An important feature of both apprentice-rate systems is that the men in training must receive an increase in pay at periods of at least three months, or possibly six months, depending on whether the rates are on an hourly or a monthly salary basis. The men on these apprentice courses must be guaranteed these increases regardless of operating conditions, and also steady work during the period of apprenticeship. With this system it has been found that there is little friction between older employees and the young apprentices regarding the matter of rates. The apprentice work can be made so attractive that many of the regular workmen in the plant will attempt to get placed on the apprentice courses either by taking night courses to make up educational requirements or by exhibiting high ability. Many good men have developed from this source. Apprentice courses described have been conducted for at least 20 years at one plant, with considerable success. It should be emphasized that the increasing scale of rates is a most desirable feature, as men being trained are moved so frequently from one department to another that they have no opportunity to increase their rate in any one department through high efficiency.

Aptitude Tests

At various times during the past 20 years, attempts have been made to classify college graduates by means of standard intelligence tests or aptitude tests, but the results have been usually unreliable as an index of the qualifications of the applicants. It is believed that this was largely because of the inexperience of the examiners in giving such tests and in interpreting the results. Quite probably the colleges could perform this function in a much better manner, and aptitude tests made on college students should be of value not only as an indication of the type of course a student should take but also as a guide to the kind of work a graduate should follow upon leaving college. During the war, the Army and Navy used these methods of selecting men for a multitude of special skills and claimed great success with these procedures. It is believed that such tests have very definite value when properly given and interpreted, and that the intelligent use of aptitude tests would be a further tool in improving the training of young engineers in industry.

Demand for Trained Personnel

Undoubtedly the demand for metallurgical engineers in the steel industry will continue to increase. Many companies have announced plans for new or enlarged research facilities, and the amount of money appropriated for this work in industry after the war will be greatly increased. The report of Dr. Vannevar Bush, of the Office of Scientific Research and Development, recommends federal research work of $33,000,000 for the first year, rising to $122,500,000 a year at the end of 5 years, this expenditure to be in addition to the regular federal expenditures at the peacetime level. More technical men will be needed for fundamental research; more trained engineers for controlling operations and introducing new products for manufacture; and more sales engineers for sales and service work among consumers. In addition, engineering colleges have produced very few graduates during the past three years. The deficiency during the war period is estimated to be 150,000 in the report of the Office of Scientific Research and Development. Any method that will shorten the time to properly train these technical workers will be of the greatest importance in the immediate future. The cooperation proposed between colleges and industry should save at least 2 years in this training period, at least for metallurgical engineers, and should also be applicable to the other branches of technology.

Program for Training

A summary of the experience of the past 25 years in the development of metallurgical engineers in steel plants points to certain pertinent facts, which should be emphasized by any company that wishes seriously to undertake a program for the improvement and expansion of its technical personnel:

1. A definite program covering at least 10 years for the recruiting of a fixed number of undergraduates and graduates each year should be established.

2. Standard apprentice courses should be organized, with definite rates, a standard number of hours worked, embodying a training program that best fits each industry.

3. For metallurgical engineers the training program should include at least one to one and a half years of routine laboratory work followed by observation and development work in plant operations.

4. Engineering apprentices should be under the direct supervision of the technical personnel throughout their training period.

5. Cooperative arrangements should be made with selected colleges to ensure

that apprentices will be obtained from a number of different schools, and every effort should be made to recruit undergraduates for summer and vacation work as early as possible in their college courses.

6. The college course in metallurgical engineering for undergraduate students who are employed should be arranged as far as possible to fit the requirements of the steel industry.

7. More emphasis should be given to fundamental scientific courses, with some reduction of applied industrial engineering courses.

Effect of Alloys in Steel on Resistance to Tempering

By Walter Crafts,* Member AIME and John L. Lamont*

(Atlantic City Meeting, November 1946)

Studies of the effect of composition of steel on hardenability by Grossmann,[1] and as-quenched hardness by Field[2] and by the authors,[3] have made it possible to predict the results of quenching when the composition and cooling rate are known. In order to extend the application of the hardenability calculation to the quenched and tempered condition in which steel is finally used, a survey has been made of the hardness changes caused by tempering. From this study a method has been developed for the prediction of hardness and tensile strength of steel in the tempered condition.

The method of calculation was developed from Rockwell C hardness tests on quenched and tempered Jominy specimens and is expressed in Rockwell C hardness units. It is of an additive type in which the degree of softening from as-quenched hardness is estimated. Tempered properties may be calculated within about plus or minus 5 Rockwell C hardness or plus or minus 15,000 lb. per sq. in. tensile strength. This degree of accuracy is less than that necessary for the control of heat-treatment, but is adequate for the comparative evaluation and selection of alloy steels.

The formula indicates that tempered hardness is primarily dependent on as-quenched hardness and, as in the hardening reaction, the progress of tempering is controlled mainly by the carbon content. Alloys tend to retard softening by a secondary hardening mechanism in which the alloy appears to migrate from ferrite to the carbide phase. The factors for the effects of alloys in tempering vary so much from the effects of alloys in hardening that different steels of equivalent hardenability may, after like heat-treatment, differ considerably in tensile strength.

Procedure

In developing the method for calculating tempered Rockwell C hardness, simple and complex steels were tested over a range from 0.08 to 0.65 per cent carbon and up to 2.68 per cent manganese, 2.18 silicon, 3.50 chromium, 4.94 nickel, and 1.06 molybdenum. The steels were made as small induction-furnace heats at the Union Carbide and Carbon Research Laboratories, Inc. The accuracy of the method was finally checked on a variety of carbon, low-alloy and high-alloy types of heat-treating steels produced under commercial conditions. The method was based on a study of tempered Jominy bars, and its validity was tested by correlation with the center hardness and tensile strength of oil-quenched and tempered bars from ½ to 4 in. in diameter.

The method of calculation was derived from the differences in Rockwell C hardness between as-quenched and quenched and tempered Jominy specimens. Prenormalized Jominy hardenability specimens quenched from a normal temperature for austenitization were used to obtain a range of as-quenched Rockwell C

Manuscript received at the office of the Institute Jan. 7, 1946. Issued as T.P. 2036 in Metals Technology, September 1946.

* Research Metallurgist, Union Carbide and Carbon Research Laboratories, Inc., Niagara Falls, N. Y.

[1] References are at the end of the paper.

hardness. These specimens were then tempered for 2 hr. at 400°, 600°, and 800°F. Hardness surveys were made and the same specimens were retempered at 1000°, 1100°, and 1200°F., respectively. This procedure was necessary because of the small amount of material available from small induction-furnace heats. Hardness values at six points ($\frac{2}{16}$, $\frac{4}{16}$, $\frac{8}{16}$, $\frac{16}{16}$, $\frac{24}{16}$ and $\frac{32}{16}$ in.) from the water-quenched end of the Jominy specimen, were used for calculating the tempering factors.

The pattern and factors for the calculation were developed by graphically comparing the initial as-quenched Rockwell C Jominy hardness with the hardness obtained after tempering the specimens at different temperatures At first, similar simple steels with graduated carbon contents were studied, the basic pattern was outlined, and rough factors for the effects of carbon and temperature were estimated. Manganese and silicon steels were then processed, using the rough carbon and temperature factors. Employing these approximate manganese and silicon factors, the effects of carbon and tempering temperature were then redetermined. Other simple alloy steels and finally complex alloy steels were introduced with recycling of the data until no significant changes were indicated. The data are too numerous to present here.

Method of Calculation

The basic mechanism of softening during tempering appears to be rather simple, although the detailed calculation is somewhat tedious. Hardness and tensile strength are dependent on the average size of the carbide particles[7] and softening reflects the effect of reheating on the growth of the carbides. The average particle appears to grow rapidly until it approaches a size that is typical for a given tempering temperature. Thus, carbides formed at elevated temperatures during quenching, in the form of pearlite or bainite, do not appear to grow readily and the steel is not softened much until the temperature at which they were formed is approached on reheating. Fine carbides formed from martensite appear to grow in a continuous manner as the tempering temperature is raised, provided growth is not impeded. However, in alloy steels the alloying element, which presumably was distributed uniformly in the martensite, tends to be concentrated in the carbides when the temperature permits diffusion of the alloying element. This results in either a retarded growth or more probably a reprecipitation of carbide particles with a corresponding tendency toward secondary hardening. After the migration of the alloy has been completed the increment of hardness gained by the discontinuity in carbide particle growth is retained at higher tempering temperatures. In other respects the alloy steel softens in the same way as a "pure" carbon steel.

The general outline of the method may be visualized from Fig. 1, which represents the calculation of Rockwell C hardness after tempering at one temperature. The untempered hardness is the same as the as-quenched hardness (R_Q) and is represented by the 45° line starting at the origin. After tempering, the steel is softened so that the tempered hardness (R_T) drops below the as-quenched hardness line. When the as-quenched hardness is low (below B), the amount of softening (D) during tempering is independent of composition and varies only with tempering temperature. The tempered hardness in this relatively soft or "unhardened" range is represented by $R_Q - D$. However, if the as-quenched hardness of a "pure" iron-carbon alloy is greater than a certain critical hardness B, the amount of softening is greater than the decrement D for unhardened steel. In the "hardened" range the tempered hardness is represented by the line drawn from B at an angle of less

than 45°, and is represented by the expression $(R_Q - D - B)f + B$. Both the critical hardness B and the factor for disproportionate softening (f) are dependent on carbon content and tempering temperature. It should be noted that the terms: "unhardened" and "hardened" as used in this discussion of tempered hardness do not signify a specific as-quenched condition, but refer to the manner of tempering as influenced by the initial as-quenched hardness.

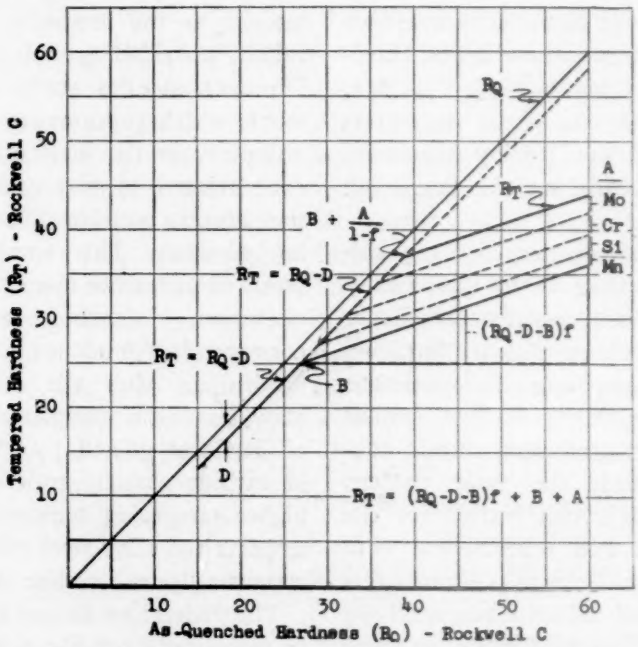

FIG. 1.—SCHEMATIC DIAGRAM FOR TEMPERED HARDNESS CALCULATION.

Alloys retard softening by amounts that vary with the specific alloy and the tempering temperature. The sum of the increments conferred by all of the alloying elements (A) is added to the tempered hardness calculated for a "pure" steel of the same carbon content in order to obtain the tempered hardness of the "alloy" steel. However, $R_Q - D$ is never exceeded, so that up to $B + \frac{A}{1-f}$ the tempered hardness of an alloy steel is represented by $R_Q - D$. At higher levels of as-quenched hardness the tempered hardness of the alloy steel is represented by the upper branch of R_T, which is parallel to the line representing the disproportionate softening in "pure" carbon steel.

Some minor trends were disregarded in order to develop a simple method of calculation. The most noticeable discrepancies were observed after tempering at 400° and 600°F. Wholly martensitic structures of maximum as-quenched hardness softened to a greater degree near the water-quenched end of the Jominy specimen than at less rapidly cooled locations. The difference persisted after tempering at elevated temperatures. Partially martensitic structures at and just below the "shoulder" of the Jominy hardness gradient curve tended to increase in hardness after tempering at low temperatures. This appeared to be due to transformation of austenite retained in conjunction with the formation of ferritic and bainitic structures during quenching. The effect was more noticeable in lower carbon steels and did not persist after tempering at

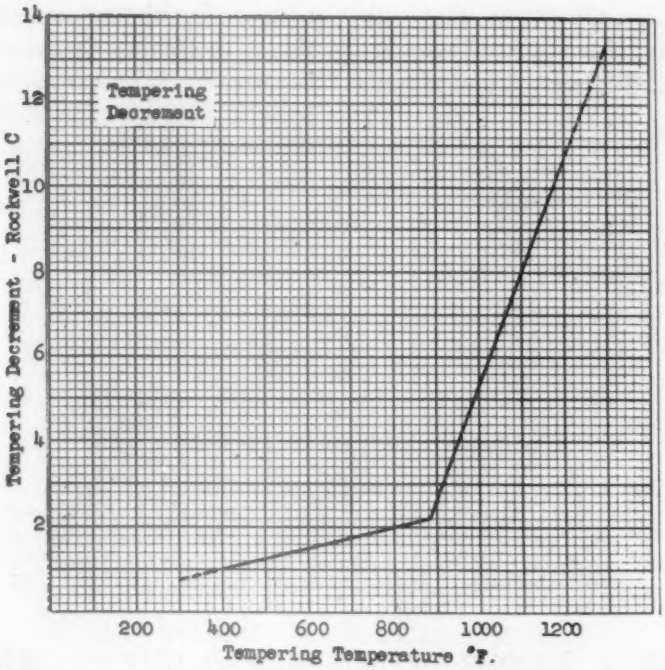

FIG. 2.—HARDNESS DECREMENT *D* FOR "UNHARDENED" STEEL.

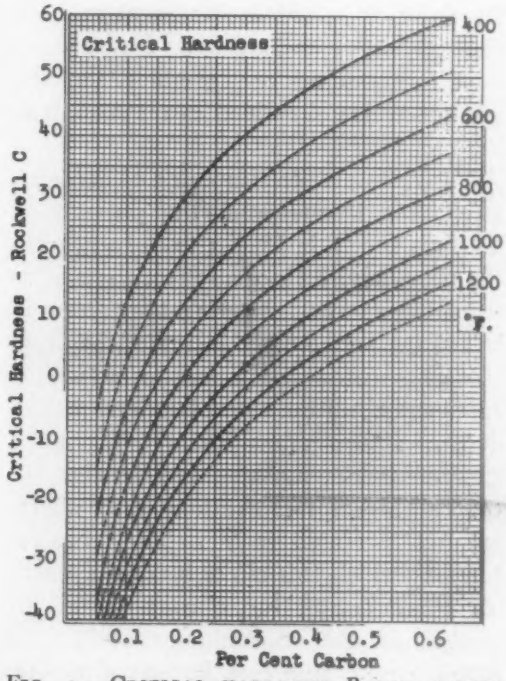

FIG. 3.—CRITICAL HARDNESS *B* FOR ALLOY-FREE STEEL.

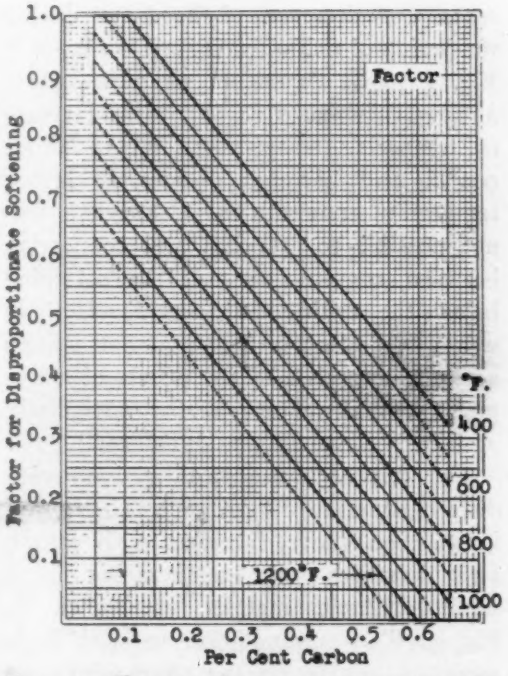

FIG. 4.—FACTOR *f* FOR DISPROPORTIONATE SOFTENING IN "HARDENED" STEEL.

high temperatures. Although these discrepancies amounted to about 5 Rockwell C in extreme cases, they were usually small.

representing the amount of the disproportionate softening, is shown in Fig. 4. It becomes lower as carbon and temperature

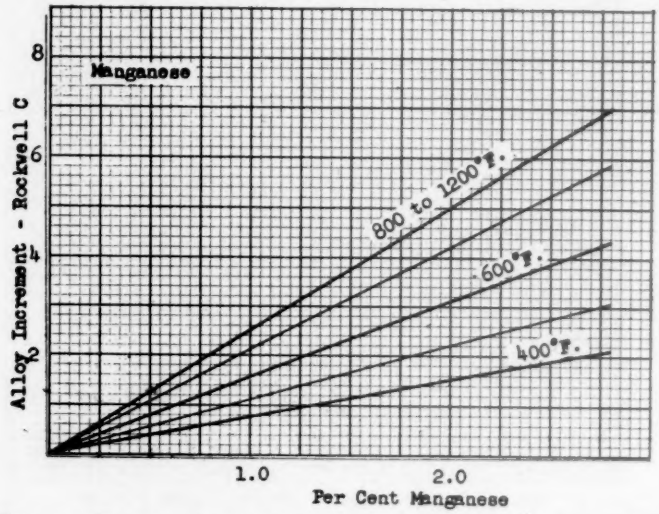

FIG. 5.—EFFECT OF MANGANESE ON RESISTANCE TO SOFTENING.

FACTORS

The decrement of hardness *D* that represents the decrease of hardness during tempering of unhardened steel is shown in Fig. 2 to be dependent on temperature alone. It increases slightly with increase of tempering temperature up to about 900°F. and becomes greater at higher tempering temperatures. Although it was not possible to establish any connection between composition and the softening below the critical hardness level, there was a suggestion in the data that a more accurate appraisal of the effects of alloys might reveal minor effects, particularly with carbon, vanadium, and silicon.

The critical hardness *B*, above which disproportionate softening occurs in "pure" iron-carbon alloys, increases with carbon and decreases with temperature in a semilogarithmic manner as shown in Fig. 3. The extrapolation to 1300°F. is useful in evaluating the effect of longer tempering times by the method of Hollomon and Jaffe,[4] but it was not established by testing above 1200°F. The factor *f*,

are increased. Presumably the disproportionate softening reflects the relatively rapid tempering of hardened structures. In order to avoid laborious calculation, the carbon-dependent and temperature-dependent factors are combined in Fig. 10 to provide a simplified means of estimating tempered hardness.

The resistance to tempering of hardened steel that results from the presence of alloys is shown in Figs. 5 to 9. In general, the alloys have little or no effect on resisting softening at low tempering temperatures, but as the temperature increases they contribute greater resistance to softening. Manganese, silicon, chromium, and molybdenum attain a maximum effect at a characteristic tempering temperature, so that at higher temperatures their effects are not increased further. The temperatures at which this effect reaches a maximum are 600°F. for silicon, 800°F. for manganese and chromium, 1000°F. for molybdenum, and 1100°F. for vanadium. The factor for vanadium was found to be related to carbon and was not determined accurately. The factors for 0.20 per

cent vanadium after tempering at 1100° and 1200°F. are approximately 10 R_C at 0.20 per cent carbon, 7 R_C at 0.30 per cent carbon, 4 R_C at 0.40 per cent carbon, and 2 R_C at 0.50 per cent carbon. Nickel has an increasing effect above 1000°F. that becomes relatively large between 1100° and 1200°F. It is considered probable that this abrupt increase is due to the formation of subcritical austenite and it sometimes appeared that nickel had less than the indicated effect in steels with high critical temperature (Ac_1) ranges. Boron, aluminum, phosphorus, and sulphur in the commonly used amounts and grain size between A.S.T.M. No. 3 and 9½ were found to have no appreciable effect during tempering.

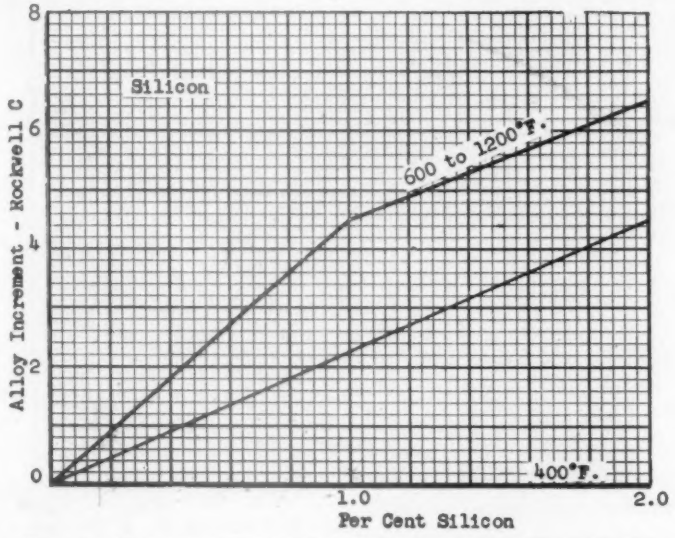

FIG. 6.—EFFECT OF SILICON ON RESISTANCE TO SOFTENING.

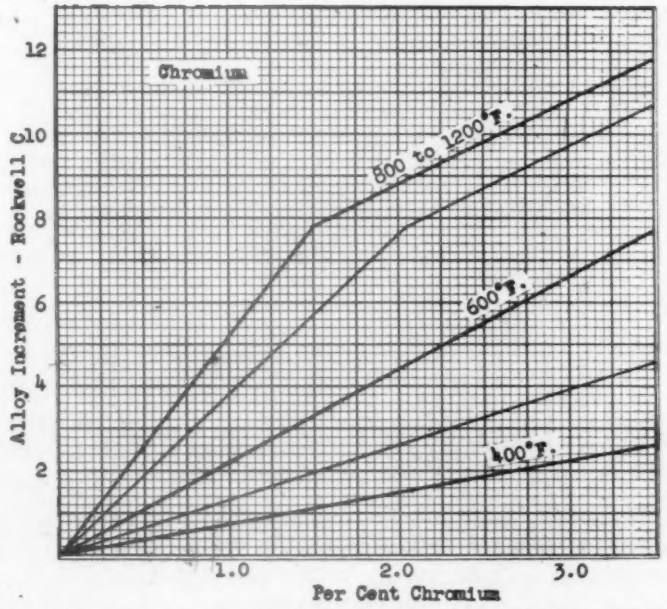

FIG. 7.—EFFECT OF CHROMIUM ON RESISTANCE TO SOFTENING.

The effects of alloys are shown in Table 1 in terms of the percentage of alloy required to retard softening by 1 Rockwell C after tempering for 2 hours.

hardness after a given tempering treatment. Between two simple low-alloy steels, this difference in tempered tensile strength may be of the order of 25,000 lb.

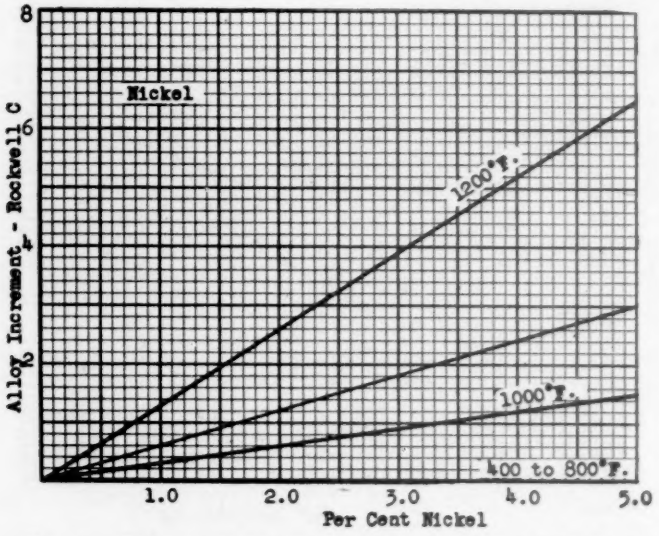

FIG. 8.—EFFECT OF NICKEL ON RESISTANCE TO SOFTENING.

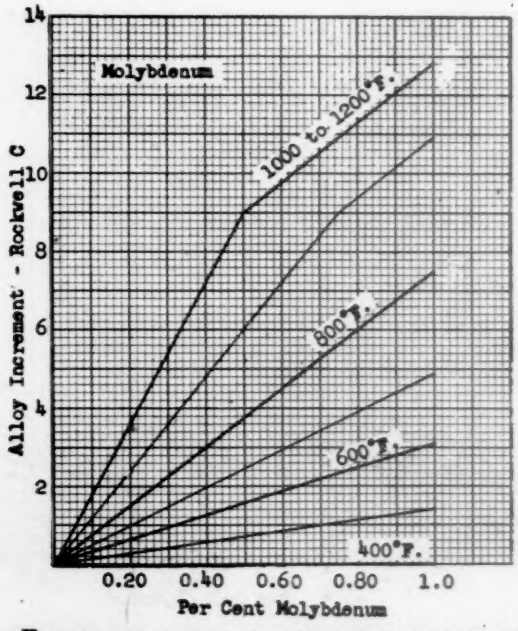

FIG. 9.—EFFECT OF MOLYBDENUM ON RESISTANCE TO SOFTENING.

It is notable that the relative effects of alloys on tempering and on hardening are quite different, so that different alloy steels of the same hardenability and hardness as-quenched do not exhibit the same

per sq. in. The ratio of tempering resistance to hardening power increases in the following order: boron, carbon, manganese, nickel, chromium, molybdenum, silicon, and vanadium. Steels deriving a major

part of their hardenability from alloys in the last half of this list may be expected to retain a relatively higher tempered strength than those dependent for their hardenability on alloys in the first part of the series.

The computation of the carbon-dependent and temperature-dependent expression $(R_Q - D - B)f + B$ is somewhat laborious, and in order to avoid this part of the calculation, a nomographic chart is presented in Fig. 10. In using the chart a straight edge is placed between the as-quenched hardness R_Q at the left, and the intersection of the carbon content and tempering temperature curves in the center. The tempered hardness of the "pure" iron-carbon alloy or the value for the expression $(R_Q - D - B)f + B$ is read at the right. To this value, the total alloy increment A is added to obtain the tempered hardness R_T of the alloy steel. If the calculated tempered hardness R_T is greater than the value of $R_Q - D$, it indicates that the value of $B + \frac{A}{1-f}$ is greater than that of $R_Q - D$ so that $R_Q - D$ is taken as the tempered hardness R_T.

TABLE 1.—*Effects of Alloys*

Element	Tempering Temperature, Deg. F.					
	400	600	800	1000	1100	1200
Manganese	1.33	0.65	0.40	0.40	0.40	0.40
Silicon		0.22	0.22	0.22	0.22	0.22 (up to 1.0 per cent silicon)
Chromium	1.33	0.45	0.19	0.19	0.19	0.19 (up to 1.5 per cent chromium)
Nickel				3.33	1.67	0.77
Molybdenum		0.32	0.13	0.06	0.06	0.06 (up to 0.5 per cent molybdenum)
Vanadium			0.13	0.04	0.03	0.03 (0.30 per cent carbon steel)

Calculation of Tempered Hardness

In calculating tempered Rockwell C hardness, the following equations are used:

$$R_T \left(\text{up to } B + \frac{A}{1-f}\right) = R_Q - D$$

$$R_T \left(\text{above } B + \frac{A}{1-f}\right) = (R_Q - D - B)f + B + A$$

where R_Q = as-quenched Rockwell C hardness
R_T = tempered Rockwell C hardness
D = temperature decrement, Rockwell C
B = critical Rockwell C hardness of Fe-C alloy
f = factor for disproportionate softening
A = sum of alloy factors, Rockwell C

As an illustration of the method, the tempered Rockwell C hardness at a depth of ¼ in. from the water-quenched end of the Jominy specimen is calculated below for a chromium-nickel-molybdenum steel. The as-quenched Rockwell C hardness was 50.4 at this point on the Jominy specimen; the tempering time was 2 hours.

Correlation of Calculated with Actual Tempered Hardness

Correlation charts are shown in order to demonstrate the degree of accuracy of the calculation of tempered Jominy hardness. The center hardness and tensile strength exhibited by bars of the commercial steels heat-treated in ½-in. to 4-in. diameter bars were also compared with calculated tempered values. The tempered hardness of these steels was estimated both from the as-quenched

Tempered Hardness (Rockwell C) Minus Tempered Alloy Increments
$R_T - (\Delta Mn + \Delta Si + \Delta Cr + etc.)$
-40 -30 -20 -10 0 10 20 30 40 50 60
Tempering Temperature °F.
Per cent Carbon
0.10 0.20 0.30 0.40 0.50 0.60
1200 1100 1000 900 800 700 600 500 400
As Quenched Hardness - Rockwell C (R_Q)
60 50 40 30 20 10 0 -10 -20 -30 -40

FIG. 10.—NOMOGRAPHIC SOLUTION FOR $(R_Q - D - Bf + B$ AFTER TEMPERING FOR 2 HOURS.

hardness of actual Jominy specimens and from the estimated as-quenched hardness calculated from composition.[3]

show trends that suggested interrelation between alloys or between alloys and carbon.

TABLE 2.—*Calculation of Alloy Increment and Tempered Hardness*

Calculation of Alloy Increment

Element	Per Cent	Fig.	Tempering Temperature, Deg. F.					
			400	600	800	1000	1100	1200
Carbon	0.32							
Manganese	0.53	5	0.4	0.8	1.3	1.3	1.3	1.3
Silicon	0.37	6	0.0	1.7	1.7	1.7	1.7	1.7
Chromium	1.14	7	0.9	2.5	5.9	5.9	5.9	5.9
Nickel	1.54	8	0.0	0.0	0.0	0.5	0.9	2.0
Molybdenum	0.29	9	0.0	0.9	2.2	5.2	5.2	5.2
Total alloy increment		A	1.3	5.9	11.1	14.6	15.0	16.1

Calculation of Tempered Hardness

		Fig.	Tempering Temperature, Deg. F.					
			400	600	800	1000	1100	1200
Quenched Hardness R_Q			50.4	50.4	50.4	50.4	50.4	50.4
	Subtract D	2	1.0	1.5	2.0	5.3	8.0	10.7
$R_Q - D$			49.4	48.9	48.4	45.1	42.4	39.7
	Subtract B	3	42.2	25.1	13.2	4.0	0.3	−3.1
$R_Q - D - B$			7.2	23.8	35.2	41.1	42.1	42.8
	Multiply by f	4	0.73	0.64	0.54	0.44	0.39	0.34
$(R_Q - D - B)f$			5.3	15.2	19.0	18.1	16.4	14.5
	Add B	3	42.2	25.1	13.2	4.0	0.3	−3.1
$(R_Q - D - B)f + B$			47.5	40.3	32.2	22.1	16.7	11.4
	Add A		1.3	5.9	11.1	14.6	15.0	16.1
$(R_Q - D - B)f + B + A$			48.8	46.2	43.3	36.7	31.7	27.5
Calculated R_T			48.8	46.2	43.3	36.7	31.7	27.5
Actual R_T			50.2	47.7	43.9	36.4	30.1	25.2

The comparison of calculated and observed tempered Jominy hardness of 0.30 per cent carbon induction-furnace steels is shown in Figs. 11 to 16. The charts include four Jominy positions, $\frac{2}{16}$, $\frac{8}{16}$, $\frac{16}{16}$, and $\frac{32}{16}$ in. from the water-cooled end, and three tempering temperatures, 600°, 1000°, and 1200°F. Since it was not possible to include all of the data, this selection was made to show the character of the results obtained on the small heats. In general, the agreement is of the order of plus or minus $4R_C$ in the simple steels and slightly more in the complex steels. The complex steels did not

The effect of treatment with a boron-bearing nonvanadium complex addition agent is illustrated in Fig. 17. The data were determined on Jominy specimens of boron-treated commercial NE-type steels and tempered hardness was calculated from as-quenched hardness without any allowance for a possible effect of boron. The comparison shows the same degree of correlation as the untreated steels, so that, although boron increases hardenability and, therefore, as-quenched hardness, it has no true alloy effect on tempering; that is, an untreated steel, necessarily quenched in a smaller section or at a

faster rate to give the same as-quenched hardness as a similar boron-treated steel, may be expected to have the same hardness

diameter. After normalizing, these bars were heated to suitable temperatures, quenched in oil at room temperature

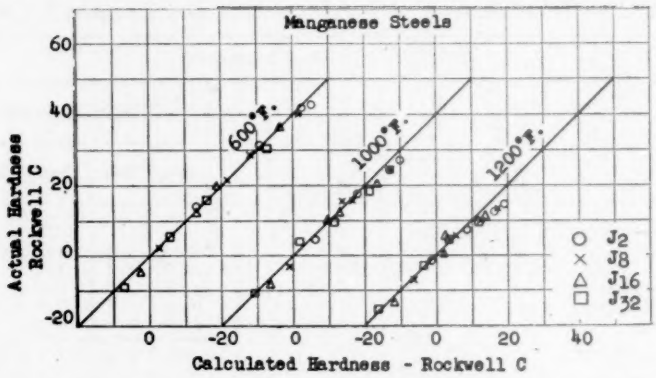

FIG. 11.—JOMINY HARDNESS OF TEMPERED 0.30 PER CENT CARBON-MANGANESE STEELS.

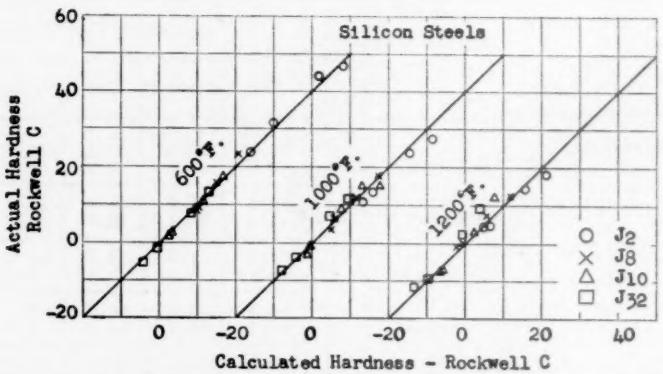

FIG. 12.—JOMINY HARDNESS OF TEMPERED 0.30 PER CENT CARBON-SILICON STEELS.

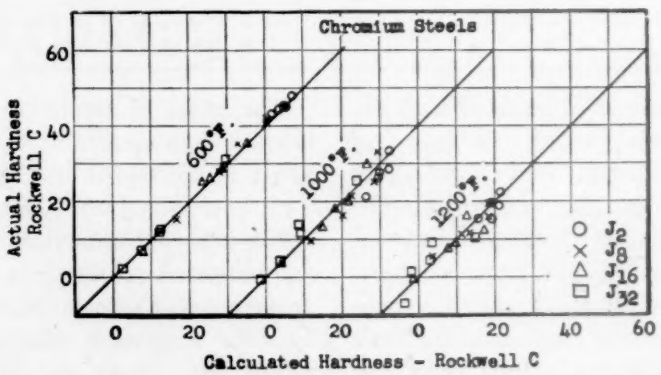

FIG. 13.—JOMINY HARDNESS OF TEMPERED 0.30 PER CENT CARBON-CHROMIUM STEELS.

as the boron steel after being given the same tempering treatment.

Bars of commercial steels at least 4 in. in diameter were forged to suitable sizes to obtain bars ½, 1, 1⅝, 2½ and 4 in. in (H = 0.35 approximately), tempered at 1000°, 1100°, and 1200°F. in the full section and air-cooled. Tensile and impact test specimens were prepared from the centers of the bars and Rockwell C hard-

ness was taken on the impact specimens. Jominy specimens were taken from bars forged to somewhat over 1-in. diameter, machined to 1-in. diameter, normalized, quenched, and tempered for 2 hr. The compositions included carbon steel, SAE and NE types of alloy steel, and several higher alloy steels.

The correlation between calculated and observed tempered Jominy hardness of the commercial steels is shown in Figs. 18 and 19. The points represent Jominy positions ($\frac{2}{16}$, $\frac{6}{16}$, $\frac{10}{16}$, $\frac{15}{16}$, $\frac{29}{16}$ in.) corresponding to the center of oil-quenched bars of the sizes used in testing these steels. Most of the points fall within plus or

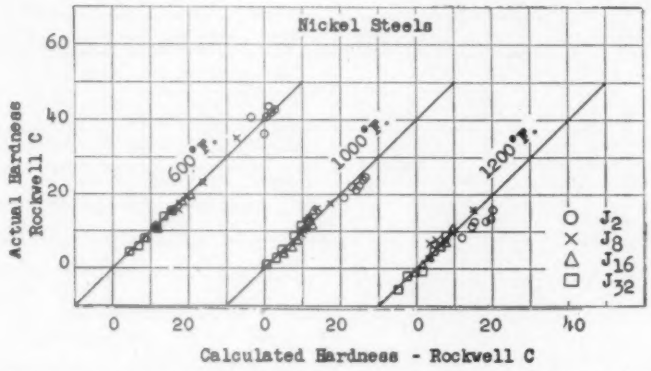

FIG. 14.—JOMINY HARDNESS OF TEMPERED 0.30 PER CENT CARBON-NICKEL STEELS.

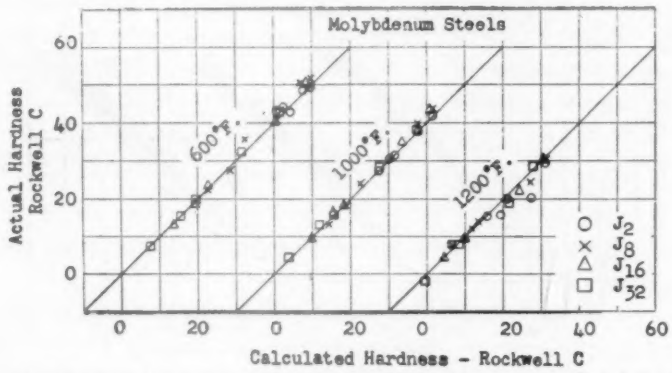

FIG. 15.—JOMINY HARDNESS OF TEMPERED 0.30 PER CENT CARBON-MOLYBDENUM STEELS.

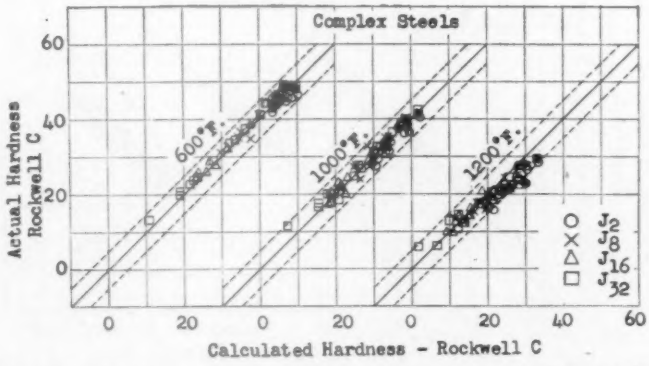

FIG. 16.—JOMINY HARDNESS OF TEMPERED 0.30 PER CENT CARBON COMPLEX STEELS.

minus $5R_C$. This degree of accuracy is approximately the same as that found in the complex experimental steels. It would appear that different manufacturing practices did not have an appreciable influence on the tempering characteristics. Since the chemical analyses were made on the bars themselves, differences due to ingot segregation were not involved in this comparison.

Calculation of hardness and tensile strength of bars involves some additional factors, such as estimated as-quenched hardness and different tempering times. Since it is difficult to determine the as-quenched center hardness of heavy sec-

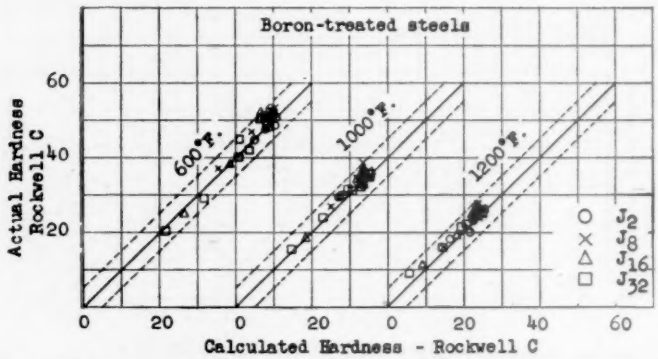

FIG. 17.—JOMINY HARDNESS OF TEMPERED BORON-TREATED STEELS.

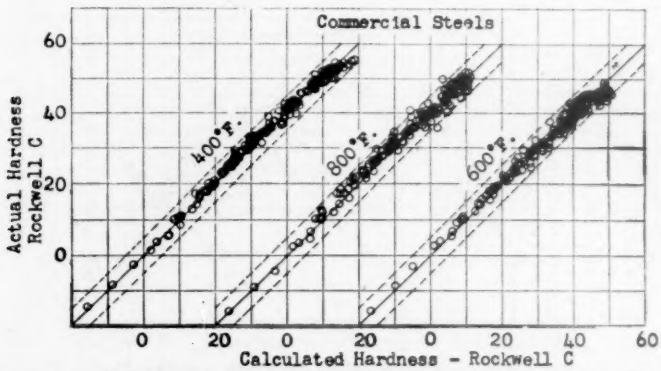

FIG. 18.—JOMINY HARDNESS OF TEMPERED COMMERCIAL STEELS.

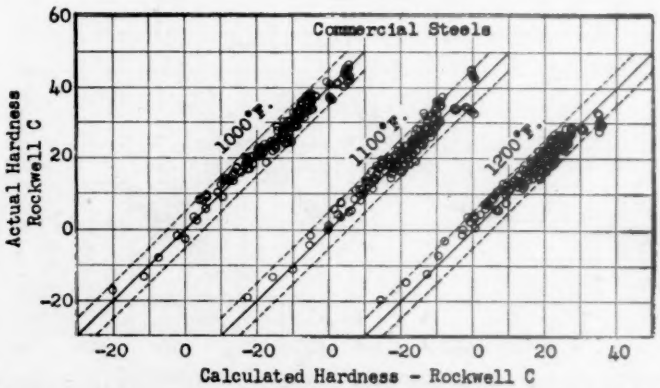

FIG. 19.—JOMINY HARDNESS OF TEMPERED COMMERCIAL STEELS.

tions, it was necessary to estimate it[5] using an H-value of 0.35 that had been found to most closely represent the oil-quenching conditions under which the steels were quenched. The bars were held at the tempering temperature for periods ranging from one hour for the ½-in. bars to about 6 hr. for some of the 4-in. bars, and it was necessary to take the effect of tempering time into consideration. The nature of the calculation of tempered hardness indicated that the time factor would be complex, and efforts to devise a simple hardness correction for time were unsatisfactory. The best correlation resulted from conversion of time to equivalent temperature by the method of Hollomon and Jaffe,[4] who found that the hardness after tempering is a function of the quantity:

$$T(C + \log t)$$

where T = absolute tempering temperature,
C = 19.5 for carbon and low-alloy steels,
t = time in hours.

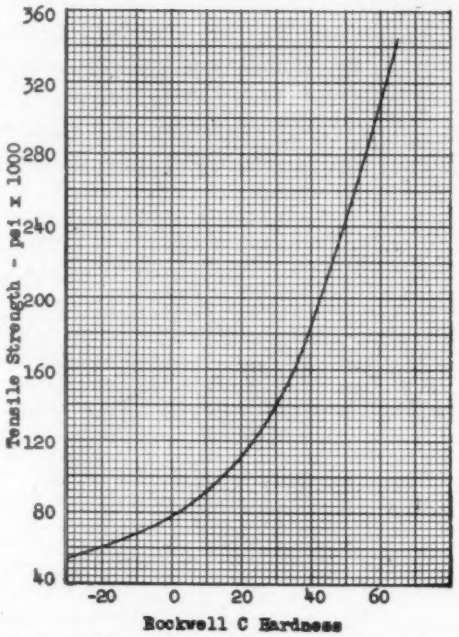

FIG. 20.—CHART FOR CONVERSION OF ROCKWELL C HARDNESS AND TENSILE STRENGTH.

$$T_2 = \frac{(T_1 + 459)(19.5 + \log t_1)}{19.801} - 459$$

where T_1 = actual tempering temperature,
t_1 = actual tempering time,
T_2 = equivalent temperature for a 2-hr. tempering period,
19.801 = 19.5 + log 2 hr.

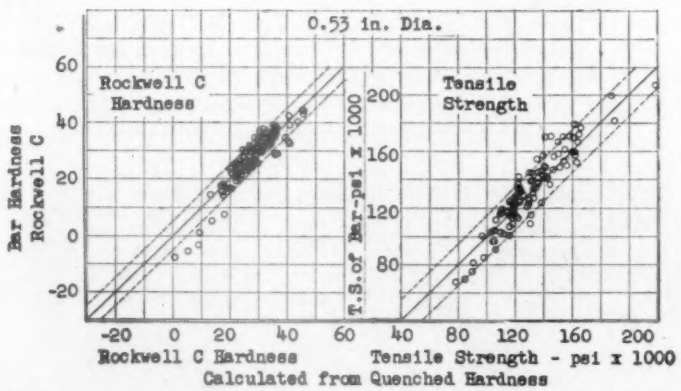

FIG. 21.—HARDNESS AND TENSILE STRENGTH OF 0.53-IN. DIAMETER BARS OF COMMERCIAL STEELS ESTIMATED FROM AS-QUENCHED JOMINY HARDNESS.

To convert the actual tempering time to the equivalent temperature for the 2-hr. tempering period upon which the factors are based, the following expression is used:

The correlation between the actual hardness and tensile strength at the center of the bars and the values calculated from the as-quenched Jominy hardness at the

appropriate locations, and with tempering time converted to 2 hr. is shown in Figs. 21 to 25 for the commercial steels tempered at 1000°, 1100°, and 1200°F. The correlation is relatively poor in the 0.530-in. diameter section and in certain high-chromium-nickel-molybdenum steels in the heavier sections, but the error in hardness is generally within plus or minus $5R_C$. This indicates that the translation from Jominy hardness to bar hardness did not greatly affect the accuracy of the estimate

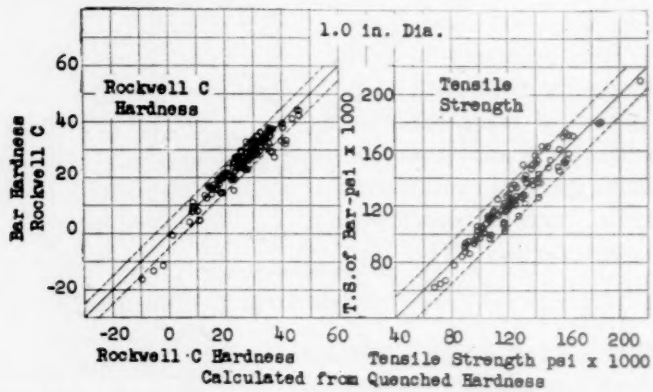

FIG. 22.—HARDNESS AND TENSILE STRENGTH OF 1.0-IN. DIAMETER BARS OF COMMERCIAL STEELS ESTIMATED FROM AS-QUENCHED JOMINY HARDNESS.

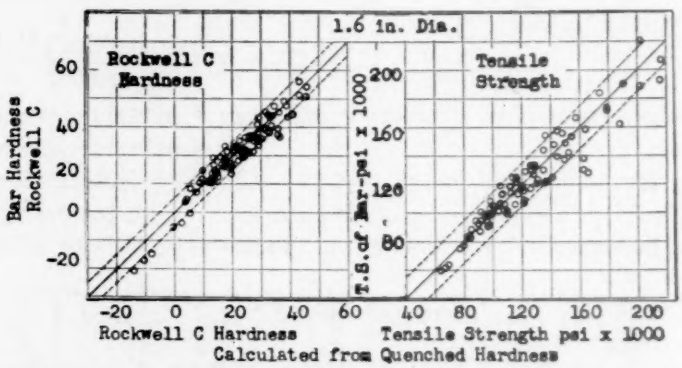

FIG. 23.—HARDNESS AND TENSILE STRENGTH OF 1.6-IN. DIAMETER BARS OF COMMERCIAL STEELS ESTIMATED FROM AS-QUENCHED JOMINY HARDNESS.

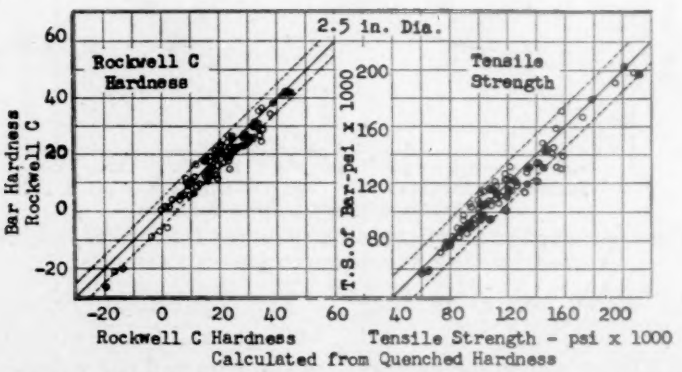

FIG. 24.—HARDNESS AND TENSILE STRENGTH OF 2.5-IN. DIAMETER BARS OF COMMERCIAL STEELS ESTIMATED FROM AS-QUENCHED JOMINY HARDNESS.

of tempered hardness. In the correlation with tensile strength the calculated hardness values, shown graphically in Fig. 20, were converted by means of the table in the 1939 A.S.M. Handbook.[6] The majority of the points are within a range of plus or minus 15,000 lb. per sq. inch.

In order to estimate how accurately the tempered hardness and strength could be predicted directly from the composition and cooling rate, the tempered hardness was also estimated by using the composition to calculate the as-quenched hardness according to the addition method

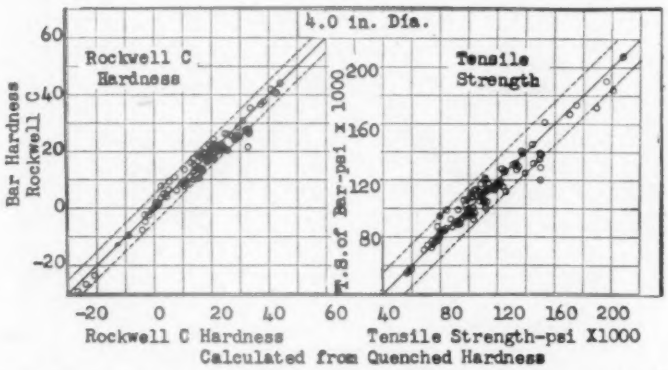

FIG. 25.—HARDNESS AND TENSILE STRENGTH OF 4.0-IN. DIAMETER BARS OF COMMERCIAL STEELS ESTIMATED FROM AS-QUENCHED JOMINY HARDNESS.

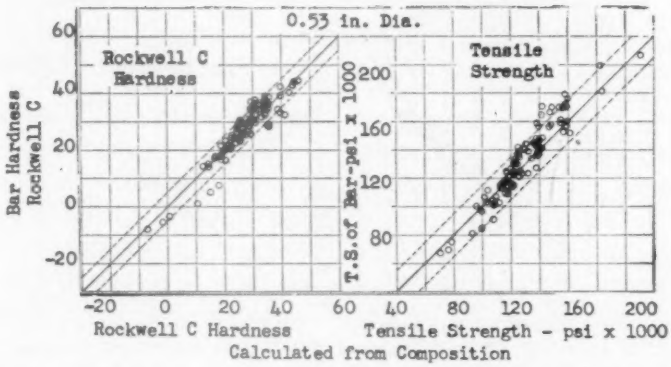

FIG. 26.—HARDNESS AND TENSILE STRENGTH OF 0.53-IN. DIAMETER BARS OF COMMERCIAL STEELS ESTIMATED FROM COMPOSITION.

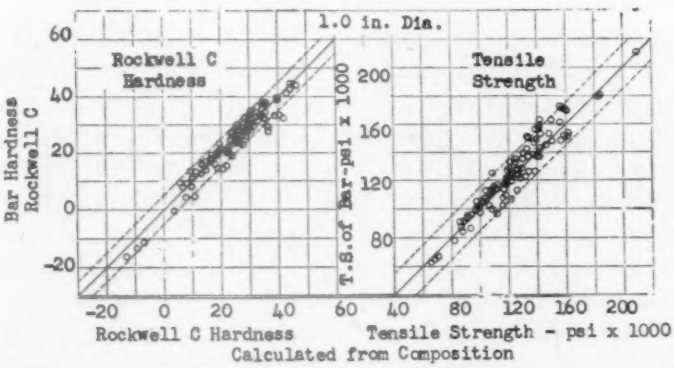

FIG. 27.—HARDNESS AND TENSILE STRENGTH OF 1.0-IN. DIAMETER BARS OF COMMERCIAL STEELS ESTIMATED FROM COMPOSITION.

proposed by the authors.[3] This correlation, which is shown in Figs. 26 to 30, is strikingly similar to that based on actual measured as-quenched Jominy hardness, and indicates that a calculated as-quenched hardness may be used without increasing the degree of error.

It is evident that the hardness and tensile strength of quenched and tempered bars of engineering alloy steel can be calculated from composition with an accuracy of about plus or minus 5 Rockwell C or plus or minus 15,000 lb. per sq. in. tensile strength. While such a spread

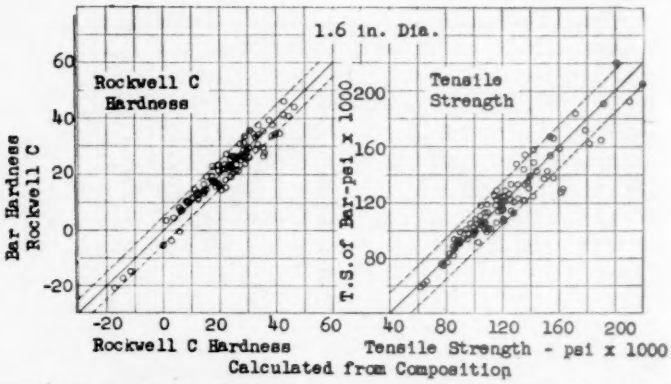

FIG. 28.—HARDNESS AND TENSILE STRENGTH OF 1.6-IN. DIAMETER BARS OF COMMERCIAL STEELS ESTIMATED FROM COMPOSITION.

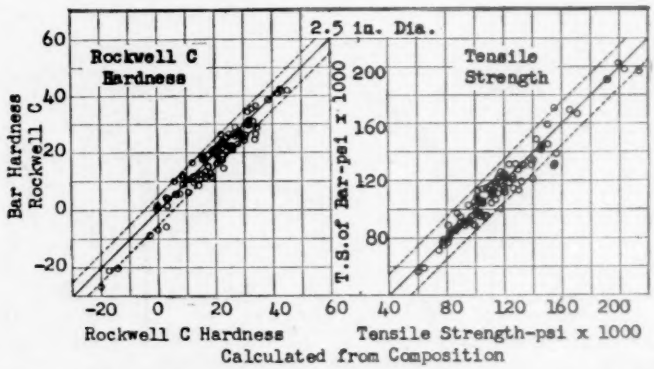

FIG. 29.—HARDNESS AND TENSILE STRENGTH OF 2.5-IN. DIAMETER BARS OF COMMERCIAL STEELS ESTIMATED FROM COMPOSITION.

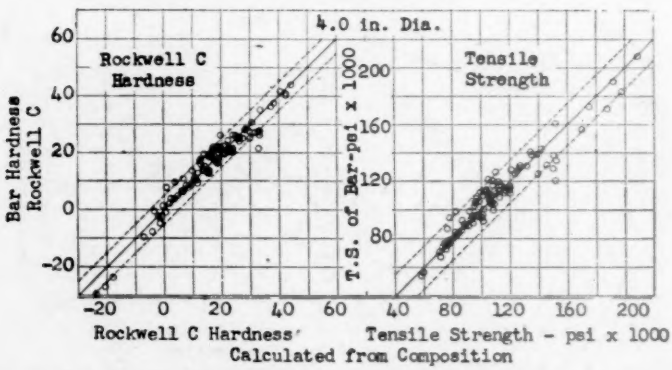

FIG. 30.—HARDNESS AND TENSILE STRENGTH OF 4.0-IN. DIAMETER BARS OF COMMERCIAL STEELS ESTIMATED FROM COMPOSITION.

in estimated tensile strength may seem quite large, the calculation of tempered hardness is no more inaccurate than the present methods of predicting hardenability and as-quenched hardness. It extends further the utility of the hardenability calculation as it is applicable directly to the tempered condition in which steel is used. The calculation of tempered hardness and tensile strength, therefore, should be useful in the relative evaluation of alloy steels and the selection of a steel for a specific purpose.

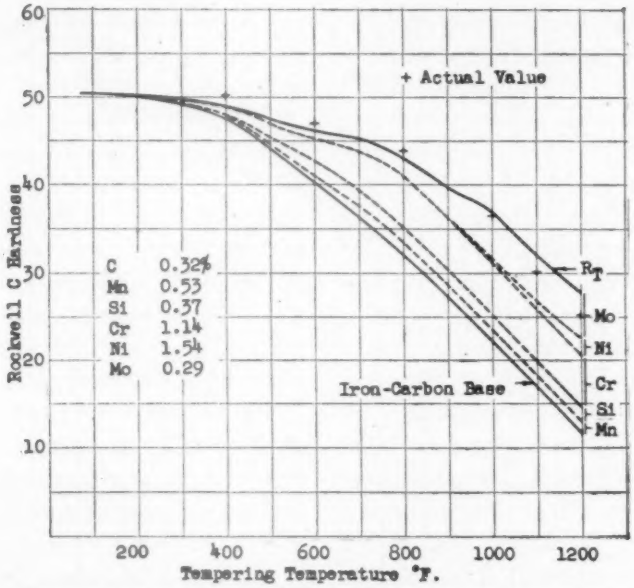

FIG. 31.—SECONDARY HARDENING IN CHROMIUM-NICKEL-MOLYBDENUM STEEL.

DISCUSSION OF THE TEMPERING MECHANISM

The method that has been described for the calculation of tempered hardness is a rather arbitrary approximation of observed data based on a limited range of compositions. Consideration of the behavior of higher alloy steels suggests that a more rational formula might be developed, but even in their present form the factors are suggestive of the mechanism by which alloys influence tempering behavior.

The carbon-dependent factors are continuous over the whole range from 400° to 1200°F. As Gensamer, Pearsall, Pellini and Low[7] have shown that hardness is dependent on "mean ferrite path," a continuous growth of carbide particles with increasing tempering temperature is implied for "pure" iron-carbon alloys. As the decomposition of martensite and eventual formation of a cementite-ferrite aggregate does not appear to be a simple process,[8] it is possible that the carbon-dependent factors for calculation of hardness may be oversimplified. The decrement of hardness loss in the unhardened range seems to be dependent only on tempering temperature and is difficult to rationalize. Its independence of the effects of carbon and alloys may be an illusion resulting from the nature of Rockwell C hardness, degree of error, and mathematical expedients used for calculation.

The alloys, except nickel, resist tempering by amounts that increase with tempering temperature up to a maximum effect at a characteristic temperature. This maximum effect is then maintained up to at least 1200°F. Since the alloys are relatively ineffective in the low-tempera-

ture range, the result, as illustrated by the example in Fig. 31, is to produce a retardation of softening and to give rise to the phenomenon known as secondary hardening. Vanadium, molybdenum, high-chromium and other alloy steels containing strong carbide-forming elements are generally known to develop secondary hardening, and it is evident that the manganese, silicon, and low-chromium steels behave similarly, although the secondary hardening is less apparent.

Since the hardness of low-alloy steel is primarily dependent on the number and size of carbide particles, it must be presumed that retarded softening or secondary hardening results from a modification of the continuous coalescence indicated in alloy-free steel. Since alloy in solution in the ferrite cannot be expected to affect significantly the coalescence of carbides, and if austenite and martensite are essentially homogeneous, the alloy must enter into the carbides in order to affect their number and size. Moreover, after the tempering temperature exceeds the characteristic level above which the effect of the alloy is constant, the rate of softening of alloy steel at higher tempering temperatures is the same as that of "pure" carbon steel, so that a constant difference in hardness is maintained. It would, therefore, appear that the change in the carbides and the development of secondary hardening takes place in the range just below the characteristic tempering temperature where the effect of the alloy is increasing rapidly. Thus, secondary hardening does not appear to result from the presence of alloy in the carbide, but from the entry of alloy into the carbide.

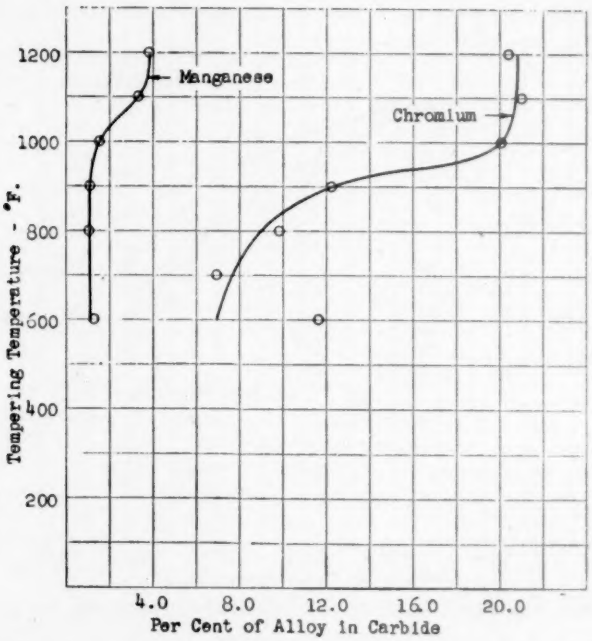

FIG. 32.—ALLOY CONTENT OF ELECTROLYTICALLY EXTRACTED CARBIDES.

That a change in alloy content of the carbide actually takes place has been indicated by the analysis of carbides extracted electrolytically by C. M. Offenhauer from quenched and tempered 0.40 per cent carbon 1.75 per cent manganese and 0.40 per cent carbon, 1.5 per cent chromium steels in the manner described by Crafts and Offenhauer[9] and is shown in Fig. 32. Owing to errors inherent in the extraction method, the actual alloy con-

tents and the temperatures of the transition to higher alloy contents in the carbides are believed to be questionable, but the abrupt increase in alloy content is demonstrated qualitatively. The change in alloy content of the carbides may also be inferred from the fact that alloys have a significant effect on softening only when the as-quenched hardness is relatively high. At low hardness levels, representing structures formed at elevated temperatures where the rate of cooling is slow enough so that the alloy can freely migrate to the carbide, alloys have little or no influence on softening in tempering.

The steels used in this investigation and the formula representing their tempered hardness indicated that the maximum secondary hardening effect is little more than retarded softening. The present observations of secondary hardening might be explained by a simple arrest of carbide growth during the period of migration of alloy from ferrite to carbide. However, steels of higher alloy content have been reported to be susceptible of rehardening to approximately the as-quenched hardness, and a hypothesis involving reprecipitation of alloy carbides has been advanced by Houdremont, Bennek, and Schrader[10] and Bain.[11] In this regard, the electrolytic extraction probably does not recover very small carbide particles, so that the lag in temperature indicated in Fig. 32 for transition of alloy from ferrite to carbide tends to confirm the formation of very fine carbide particles by reprecipitation.

It is obvious that the mechanism of tempering is not as simple as the formula would indicate. In fact, it would appear that a much closer approximation of tempered hardness might require a calculation of such complexity as to be of little practical value. However, even in its oversimplified form the method of calculation clarifies some phases of tempering behavior and provides in a usable form a means for estimating tempered hardness with a degree of accuracy comparable to that of the calculation of as-quenched hardness.

Conclusions

1. An empirical method has been developed for calculating the hardness and tensile strength of quenched and tempered engineering alloy steels. The calculation is accurate within about 5 Rockwell C hardness, or 15,000 lb. per sq. in. tensile strength, and is suitable as a guide in the prediction of hardness and strength for relative evaluation and selection of alloy steels.

2. Tempered hardness is primarily dependent on as-quenched hardness, both on account of the effect of initial hardness itself and because alloys exert their full resistance to softening only in steels hardened above a critical level. With increasing tempering temperature, the degree of softening of hardened steel depends on carbon, except for the effect of nickel and except as softening is arrested in characteristic temperature ranges by the secondary hardening effects of silicon, manganese, chromium, molybdenum, and vanadium. Secondary hardening appears to be associated with the transition of the alloying element from ferrite to carbide.

3. The amounts of alloy that retard softening by one Rockwell C unit after 2 hr. at the higher tempering temperatures are: 0.40 per cent manganese, 0.22 silicon, 0.19 chromium, 0.77 nickel, 0.06 molybdenum, and 0.03 vanadium (0.30 per cent carbon steel).

4. The relative effects of alloys in resisting softening are materially different from their relative effects on hardenability, so that after the same heat-treatment steels of equivalent hardenability but different composition may vary considerably in tempered hardness and tensile strength. The ratio of softening resistance to hardening power of alloying elements increases in the following order: boron,

carbon, manganese, nickel, chromium, molybdenum, silicon, and vanadium.

References

1. M. A. Grossmann: *Trans.* A.I.M.E. (1942) **150**, 227–255.
2. J. Field: *Metal Progress* (March 1943) 402–405.
3. W. Crafts and J. L. Lamont: *Trans.* AIME (1946) **167**, 698; *Metals Tech.* (Oct. 1945—T.P. 1928).
4. J. H. Hollomon and L. D. Jaffe: *Trans.* AIME (1945) **162**, 223. *Metals Tech.* (Sept. 1945—T.P. 1831).
5. J. L. Lamont: *Iron Age* (Oct. 14, 1943) **152**, 16, 64–70.
7. Metals Handbook, Amer. Soc. for Metals (1939) 127–128.
7. M. Gensamer, E. B. Pearsall, W. S. Pellini, and J. R. Low, Jr.: *Trans.* Amer. Soc. for Metals (1942) **30**, 983–1019.
8. D. P. Antia, S. G. Fletcher, and M. Cohen: *Trans.* Amer. Soc. for Metals (1944) **32**, 290–322.
9. W. Crafts and C. M. Offenhauer: *Trans.* A.I.M.E. (1942) **150**, 275–282.
10. E. Houdremont, H. Bennek, and H. Shrader: *Archiv Eisenhüttenwesen* (1932–1933) **6**, 24–32.
11. E. C. Bain: Functions of the Alloying Elements in Steel, 1939. Amer. Soc. for Metals.

DISCUSSION

(R. S. Archer, presiding)

J. H. Hollomon*—I have two comments I would like to make concerning the effects of alloys on tempering and the statement Mr. Crafts made concerning the properties of steels of the same hardness. The latter statement concerns the problem of whether or not the properties are widely different if the treatments are different but the hardnesses are the same.

If a steel contains pearlite before tempering, or bainite, instead of martensite, and they are tempered to the same hardness, it is well known that the properties are quite different. Also, one would expect that if the hardnesses are the same, and one specimen of the same steel was temper-embrittled and the other not, the properties would be quite different. However, experiments have been performed which indicate that if the steel is fully martensite before tempering, a difference in tempering time that produces a given hardness does not affect the tensile or impact properties or any other mechanical properties of the material.

These experiments were performed on a series of steels of different compositions, ranging from low-alloy steels to high-alloyability steels. The range of time to produce the same hardness was from about 3 min. to about 5000 min. After these treatments, the properties were the same, indicating that from a practical point of view, once a given tempered hardness is obtained, it does not make any difference what the tempering cycle is as long as the structure is simply tempered martensitic.

The second point I would like to raise is one that bothers me considerably; it concerns the data that Bain presented on the effect of alloying elements on tempering. Upon analyzing these data, it is found that if molybdenum is added to a chromium steel that exhibits secondary hardening, the secondary hardenability due to chromium disappears.

If, on the other hand, chromium is added to a molybdenum steel that exhibits secondary hardening, there is no effect. How then can the effects of chromium and molybdenum be additive when chromium has no effect when molybdenum is present and does have an effect when molybdenum is not present?

W. Crafts (author's reply)—We agree with Mr. Hollomon that the properties of steel aside from hardness are different, depending on the structure. We have done a little more work along that line and on our own as well as what has been published and I do not think there is any room for argument on that account.

I did not mention in the presentation that in our work we based our study on two-hour tempering time, and in correlation with the larger bars used the Hollomon and Jaffe method for evaluating the effect of time and found it very satisfactory.

Dr. Hollomon's observations with respect to the effects of tempering time on the similarity of mechanical properties of tempered martensitic steels are of considerable interest. It is felt, however, that Janitzky's relationships should be accepted with some caution or with a fairly large allowance for error until they have been studied more fully. For example, the ratio of yield strength

* General Electric Co., Schenectady, N. Y.

to tensile strength seems to be quite sensitive to composition and the relation between reduction of area and tensile strength increases disproportionately as the tempering temperature is raised. In addition, the tests on tempered Jominy specimens indicated that the "martensitic" condition includes structures that, presumably on account of retained austenite, react differently to tempering and it would be surprising if there were not differences in properties other than hardness. Broadly, it is felt that these differences are somewhat academic in character and that the principle of similarity of properties in tempered martensitic steels can be utilized to advantage.

The suggestion that secondary hardening in steels containing more than one carbide-forming element is not additive but is governed by the predominating element is attractive for several reasons. More understanding of secondary hardening is needed to provide a definitive explanation, but it is believed that the available data tend to discourage acceptance of the hypothesis. The present study has indicated that the effects of alloys are additive and that they contribute no more than a retardation of softening. Review of other studies of the tempering of steels that show pronounced rehardening usually indicates that such rehardening is developed when there is an appreciable amount of residual austenite or a tendency toward precipitation of an intermetallic compound. The cause of positive rehardening cannot be answered at present but evidently it is caused by a reaction not found in the steels of the present study. It is also quite possible that alloy contents above an amount dependent on the carbon content might be less effective, but this was not observed in the steels investigated. The effects of alloys on the tempered hardness might be modified somewhat by the presence of retained austenite and by carbides that were not dissolved in the austenite. The compositions of some of Bain's chromium-molybdenum steels suggest that in the quenched condition they probably were not entirely martensitic, and if carbides were present, the associated carbon and alloy would not be effective in the tempering reactions. Thus, although these steels may reflect a mechanism of the type suggested by Dr. Hollomon, it is doubted whether they are suitable examples on which to build a hypothesis. The tempering reactions appear to be very complex and require much more study to gain a better understanding of the subject.

Calculation of Tensile Strength and Yield Point from the Chemical Composition and Cooling Rate

By Irvin R. Kramer,* Member, P. D. Gorsuch* and D. L. Newhouse,* Junior Members AIME

(Atlantic City Meeting, November 1946)

Although many methods have been suggested for the calculation of tensile strength and yield point from chemical composition, their usefulness has been limited to a particular cooling rate or section size. Further limitations have been imposed by failure to take into account many of the alloying elements that exert a considerable influence on the tensile strength or yield point. These systems, nevertheless, have filled an important need in many instances.

The value of a system for the calculation of the tensile properties from the chemical composition and cooling rate is that it permits the prediction of the effect of alloying elements and heat-treatment on the mechanical properties, so that more efficient use of alloying elements may be made. Furthermore, it aids in the choice of steel for a given application and tends to decrease the number of steels that otherwise would have to be tested.

It is the purpose of this work to present a method of calculating tensile strength and yield point from the chemical composition and to suggest a method of correlating the tensile-strength and yield-point factors and cooling rate.

Steelmakers have been interested for many years in the calculation of the tensile strength of hot-rolled steels. Quest and Washburn[1] summarize several of the attempts that have been made to devise formulas. They show the inadequacy of each of these formulas and present one of their own. It is apparent from their work that a simple additive equation of the type $TS = A + BX + Cy + DZ + \cdots$, where A, B, C, D, etc. are experimentally determined constants and x, y, z, etc., are the percentages of alloying elements present in the steel, is not adequate to analyze fully the situation encountered in the calculation of tensile strength. For example, it was found that the difference between the calculated and observed values became progressively greater as the carbon and manganese contents were increased. Therefore, the effect of manganese was given as a function of the carbon content.

Grossmann,[2] in his work on the hardenability of quenched steels, and Walters,[3] in his method of calculation of tensile strength of normalized steels, present two cases in which multiplying factors were successfully used to express the combined effect of alloying elements. The factors in both cases were obtained from the fractional increase in hardenability or tensile strength with increase of alloy content.

Yield point often is more important in design than tensile strength. For quenched and tempered steels a linear correlation exists between yield and tensile strength.[4] This is not true, however, for normalized

The statements or opinions expressed in this article are those of the authors and do not necessarily express the view of the Navy Department. Manuscript received at the office of the Institute March 20, 1946. Issued as T.P. 2067 in Metals Technology, September 1946. Published by permission of the Navy Department.

* Division of Physical Metallurgy, Naval Research Laboratory of the Office of Research and Inventions, Washington, D. C.

[1] References are at the end of the paper.

steels, as is shown by the large scatter of points in the plot of yield points against tensile strength for a number of normalized 5/8-in. plates (Fig. 1). Lacking such a correlation, the development of a separate set of factors for the calculation of yield point at various cooling rates was necessary.

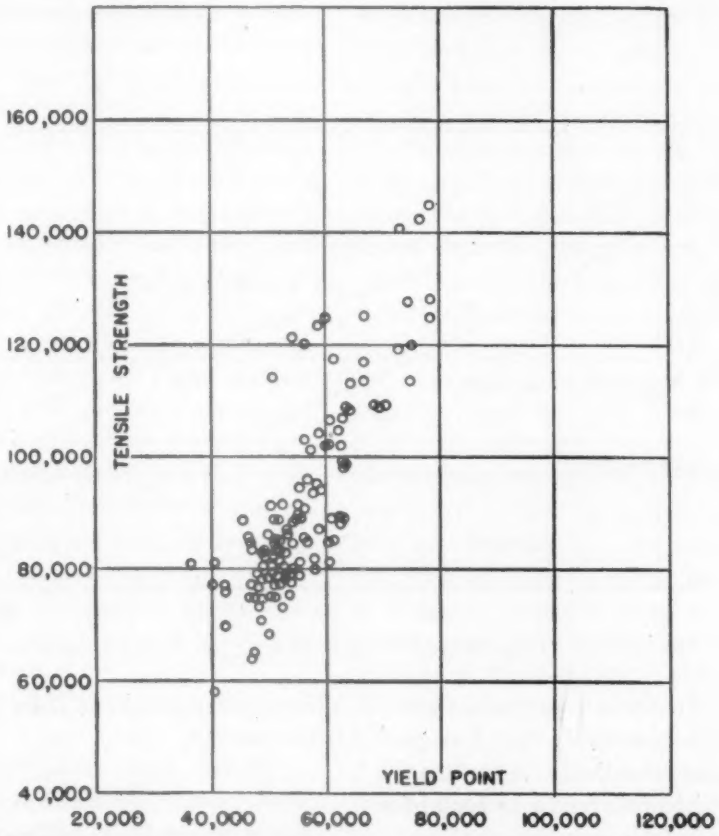

FIG. 1.—RELATION BETWEEN YIELD POINT AND TENSILE STRENGTH, NO. 1 COOLING RATE.

The most important effect of alloying elements on the tensile properties of steel is upon the rate of reaction in the formation of ferrite and pearlite, the fineness and the amount of pearlite. The degree to which they affect the tensile strength or yield point of a steel is influenced by the distribution of the alloying elements among the various phases. Elements such as aluminum, copper, nickel and phosphorus are preferentially soluble in the ferrite and strengthen it to varying degrees. Elements such as chromium, molybdenum, titanium, and vanadium form stable carbides, and their effect on the tensile properties is greatly influenced by the time and temperature of austenitizing.

The tensile strength of an isothermally transformed eutectoid steel has been shown to be a linear function of the interlamellar spacing of the pearlite.[5] As the reaction temperature is lowered, the spacing decreases and the tensile strength and yield strength are increased. This effect should persist in hypoeutectoid steels.

Austenitic grain size is affected by alloying elements such as aluminum, vanadium, titanium, and by the time and temperature of austenitizing. Variations in austenitic grain size affect the tensile properties of steels in two ways, which tend to be mutually compensating. A fine-grained steel should have somewhat higher tensile

properties than a similar steel of coarse grain, owing to increased interference to slip. However, since the S-curve for the fine-grained steel, is displaced to the left of the S-curve for the coarse-grained steel, higher-temperature-transformation products, and correspondingly lower tensile strength and yield point, will be found for the fine-grained steel.

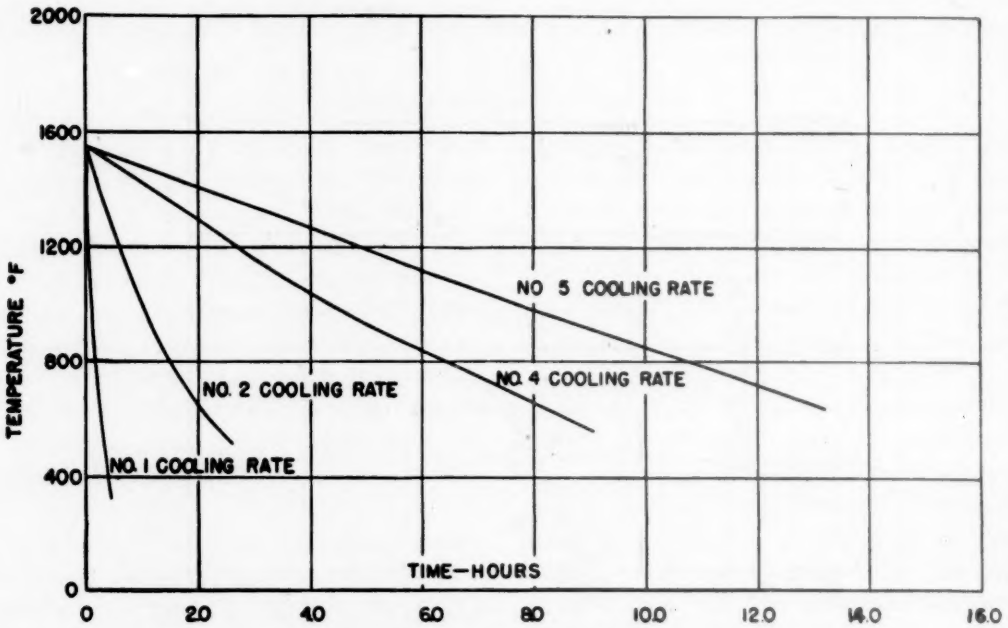

FIG. 2.—COOLING CURVES FOR THE FOUR MAJOR COOLING RATES.

The effect on tensile strength and yield point of the elements that form stable carbides depends upon the austenitizing treatment, which determines how completely such elements are in solution. Thus, the effect of these elements would be greater if they were held at a sufficiently high temperature for a time long enough for the carbides to go into solution. In the case of incomplete solution, the tensile strength or yield point may be decreased because the alloying element has combined with carbon and prevented it from producing its full effect, or because the undissolved carbides act as nuclei to start the transformation reaction at temperatures higher than that expected from the alloy content. Comstock[6] found that high-temperature normalizing (2000°F.) for low-alloy titanium steels caused a marked increase in yield and tensile strength as compared with steels normalized from temperatures below 1800°F.

METHODS

The steels used in this investigation were melted in a 300-lb. basic high-frequency induction furnace. The heats usually were split into five parts and the appropriate alloying additions were made in the furnace before the steel was poured into a cast-iron ingot mold. Some heats were deoxidized with aluminum but in general the heats were silicon-killed. After soaking for 10 hr. at 2300°F., the ingots were rolled into plates ¾-in. thick. For the ⅝-in. plates, parts of the ¾-in. plates were further reduced by forging to plates 6 by 6 by ⅝ inches.

Before heat-treating, tensile-bar blanks were cut from the ¾-in. plate, which were machined after heat-treating. The tensile bars of the ⅝-in. plate were taken from the

center section after the heat-treatment of the plate. The tensile specimen blanks were taken parallel to the direction of rolling.

After the specimens were austenitized for 2 hr. at 1550°F., they were cooled at various rates. The four cooling rates (Fig. 2) used for the calculation of the factors roughly approximate the cooling rates at the centers of air-cooled ⅝-in. 4¾-in. 18-in. and 28-in. plates. For convenience, these cooling rates will be referred to as cooling rates 1, 2, 4, and 5, respectively. For the No. 1 cooling rate, the ⅝-in. plates were cooled in still air from the austenitizing temperature. The No. 2 cooling rate was obtained by austenitizing tensile specimen blanks in a box filled with sand and then cooling the box and specimens in air.

Cooling rates 4 and 5 were obtained in a program-controlled furnace in which cooling of the specimens was made to follow a predetermined cooling curve. Throughout this paper, the number following the steel designation is the cooling rate; for example, PLA-2 refers to steel PLA cooled at the No. 2 cooling rate.

The specimen blanks were then machined into standard 0.505 tensile specimens, except for those taken from the ⅝-in. plates. These were made into special 0.505 specimens with ⅝-in. diameter threaded ends.

The stress-strain curve was recorded by a Baldwin-Southwark recorder until the yield point was passed. The headspeed of the Southwark-Emery 60,000 tensile machine was 0.07 in. per min. before the yield point was reached and 0.14 in. per min. for the remainder of the test. All tensile tests were made in duplicate.

The yield points were determined by the halt of the load indicator and by the stress-strain curve drawn by the automatic recorder. For steels that showed no definite yield point, the yield strength at 0.01 per cent offset was used.

Grain sizes were determined from counts made on photographs taken at appropriate positions along specimens end-quenched from the austenitizing temperature.

The steel used in the determination of the effect of austenitic grain size (PDW) was given special austenitizing treatments in order to develop a range of grain sizes. The specimens were austenitized at various temperatures from 1550° to 2100°F. for 2 hr., then rapidly transferred to a furnace at 1550°F. and cooled at the No. 3 cooling rate from that temperature. A steel free from strong carbide-forming elements was selected for the grain-size experiments, in order to avoid the possibility of indeterminate results because of changes in solubility of the carbides.

There are essentially two methods that may be used for the determination of tensile-strength and yield-point factors. If the chemical composition of the steels is controlled so that the percentage of each alloying element is constant except for the alloying element under consideration, it is only necessary to plot the tensile strength or yield point against the percentage of the alloy and divide each point on the curve by the value for tensile strength or yield point at the intercept for 0 per cent alloy. Since it is extremely difficult to prepare a series of steels in which all of the alloying elements are held constant, it is convenient to resort to other methods for the calculation of the factors. The factors may be determined by solving the equation

$$TS = f_c \times f_{Mn} \times f_{Si} \times \cdots$$

for each of the steels under consideration. This method makes it possible to use data that could not otherwise be used; but the mathematical manipulations for the solution of a large number of such equations become rather cumbersome. However, a series of successive approximations may be employed to solve the equations for all the data available.

In the derivation of the factor curves of yield point and tensile strength, curves of

percentage of alloying element versus tensile strength and yield point were plotted for each alloying element except carbon. A set of approximate multiplying factors was obtained by dividing the tensile strength or yield point at any percentage of alloying element by the tensile strength or yield point at 0 per cent alloying element. These approximate factors were used to determine the first carbon curve. This was done by dividing the tensile strength or yield point of the steel by the product of the factors for all of the alloying elements present. In order to avoid difficulties that may be caused by an extrapolation of the tensile-strength and yield-point curves for carbon to obtain the tensile strength and yield points of "pure" iron,* the factor curves for carbon were derived in terms of tensile strength and yield point based upon the carbon content. The first carbon curve and the approximate silicon-factor curve were used to obtain a manganese-factor curve. Since the carbon, silicon, and other contents of the steels used for the determination of the factors varied, the tensile strengths and yield points were corrected to an average composition; for example, for the manganese-factor curve, a steel containing 0.40 per cent carbon and 0.50 per cent silicon would be corrected to 0.50 per cent carbon and 0.30 per cent silicon by the following equation:

$$TS'' = TS \times \frac{TS'(0.50c) \times f_{0.30_{Si}}}{TS'(0.40c) \times f_{0.50_{Si}}}$$

where TS represents observed tensile strength; TS'', corrected tensile strength; TS', base tensile strength for carbon. The corrected strengths and yield points were plotted against the percentage of manganese and the multiplying factor was obtained by dividing through by the tensile strength and yield point at 0 per cent manganese. This procedure was repeated for silicon and the whole process was repeated by correcting each factor curve in terms of the other until a complete balance was reached between carbon, manganese and silicon factors; that is, until there was no further change in any of the curves upon subsequent correction. At this point, the balanced factor curves for carbon, manganese, and silicon were used to determine the factors for the elements nickel, copper, chromium, molybdenum, and other elements. These newly determined factor curves were then utilized to recalculate the carbon, manganese, and silicon curves, and the procedure was repeated until a completely balanced system was again obtained.

For linear curves, the points were usually averaged by the method of least squares; otherwise, the curve was drawn through the best group averages of the points.

Multiplying factors for the calculation of the tensile strength and yield point from chemical composition have been developed for four different cooling rates. These factor curves represent the effects of the individual elements upon the tensile properties of steel. The usefulness of these factor curves is limited to the four cooling rates employed in their determination. In order to use these multiplying factors for cooling rates other than those from which they were determined, it was necessary to find a correlation between the effects of the various alloying elements on tensile strength and yield point, and cooling rate. The most useful parameter of cooling rate for this purpose was found to be half-temperature time; that is, the time to cool from 1550° to 800°F. The use of the half-temperature time as a parameter for correlating cooling rates and multiplying factors was chosen entirely on an empirical, not on a theoretical basis. No doubt other parameters would serve equally well, but it was found that more consistent results could

* Inasmuch as the corrections for alloying elements did not include nitrogen, oxygen and other elements in small quantities, the effect of these elements is included in the factor for carbon.

be obtained through the use of half-temperature time. The half-temperature times for the various cooling conditions used throughout this study are listed in Table 4.*

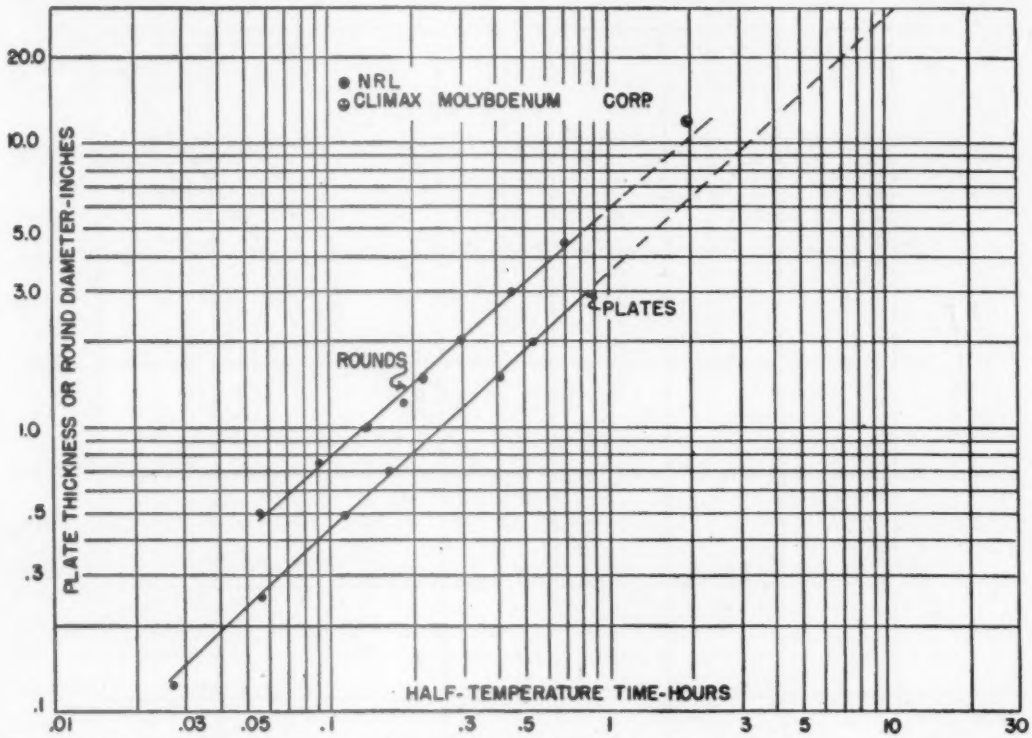

FIG. 3.—HALF-TEMPERATURE TIME (TIME TO COOL FROM 1550°F. TO 800°F.) AT THE CENTERS OF AIR-COOLED PLATES AND ROUNDS.

In order to correlate the cooling data used in the determination of the various multiplying factors with the size of plates and rounds having similar cooling characteristics, the cooling rates at the centers of several air-cooled plates and rounds of varying dimensions were measured (Fig. 3). For this purpose, a thermocouple was flash-welded to the bottom of a hole drilled to the geometric center of the specimen. The specimens were held at temperature for one hour after the center had reached temperature, and then were allowed to cool in still air. The dimensions of all the test pieces were made at least eight times the diameter or thickness, to ensure cooling conditions that simulated those of an infinite round or plate. The cooling rates of 1-in., 1¼-in., 1½-in., 2-in., 3-in. and 4½-in. rounds and 0.7-in. and 2-in. plates were measured with a Leeds and Northrup Micromax recorder. The cooling rates of the ½-in. and ¾-in. rounds and ⅛-in., ¼-in., and ½-in. plates were measured with a Speedomax recorder. Unfortunately, data were not available for cooling rates at the center of a plate thicker than 2 in. For convenience, therefore, the straight line drawn through the experimentally determined points was extrapolated to obtain the half-temperature time for larger plates (Fig. 3). This extrapolation is justified to some extent on the

* All tables (1–7) and Figs. 4, 5, 9, 10, 12, 16–23 and 25–30 have been deposited with the American Documentation Institute. To obtain them, write to American Documentation Institute, Bibliofilm Service, 1719 N St., N. W., Washington 6, D. C., asking for Document No. 2318 and enclosing 50 cents for microfilm (images 1 in. high on standard 35-mm. motion-picture film) or $3.90 for photocopies (6 by 8 in.).

basis that for a constant coefficient of surface transfer H and diffusivity D the relationship between half-temperature time and plate or round size when plotted logarithmically is linear. Further, as will be seen later, the multiplying factors for the alloying elements change but little with rather large changes in cooling rate when the half-temperature time is greater than about 5 hr. Thus, even if the upper portion of the curve of Fig. 3 were not correct, the error would not greatly influence the calculation of the yield point or tensile strength. The authors are indebted to the Climax Molybdenum Co. for the cooling data for the 12-in. round.

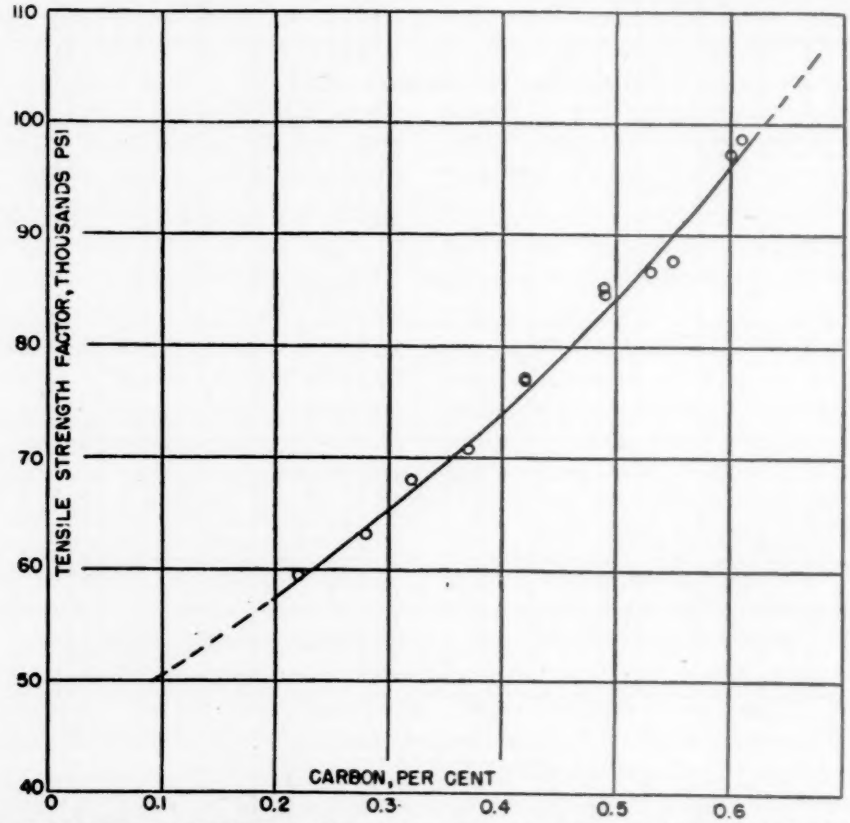

FIG. 6.—EFFECT OF CARBON ON THE TENSILE STRENGTH OF IRON, NO. 1 COOLING RATE.

RESULTS

The chemical compositions of the steels used are given in Table 1* and the corresponding tensile properties are listed in Table 2.* Figs. 6 to 30* show the factor curves for the No. 1 cooling rate and Figs. 31 to 42 the correlation between half-temperature time and multiplying factor.

Since the factor curves for the various cooling rates are very similar, only the factor curves for the No. 1 cooling rate have been given. However, the factor curves for other cooling rates may be constructed from the curves, giving the relation between multiplying factor and half-temperature.

Tensile-strength Factors

The factor curves for carbon were derived from steels at two different manganese levels, 0.4 and 0.7 per cent (Fig. 6). In general, carbon exerted by far the greatest influence on the tensile

* See footnote on page 249.

strength; but with faster cooling rates its effect was greater than with slower rates.

Unlike the carbon-factor curves, the manganese-factor curves were curvilinear for cooling rates 1 (Fig. 7) and 2, and tended to become linear as the cooling rate decreased. As indicated in Fig. 32, in which the manganese factor is given as a function of the half-temperature time, the relative effect of manganese increased as the cooling rate was decreased.

The factor curves for silicon were derived through the use of two series of steels. In one series, carbon varied between 0.32 and 0.26 per cent and manganese between 0.42 and 0.44 per cent; in the other,

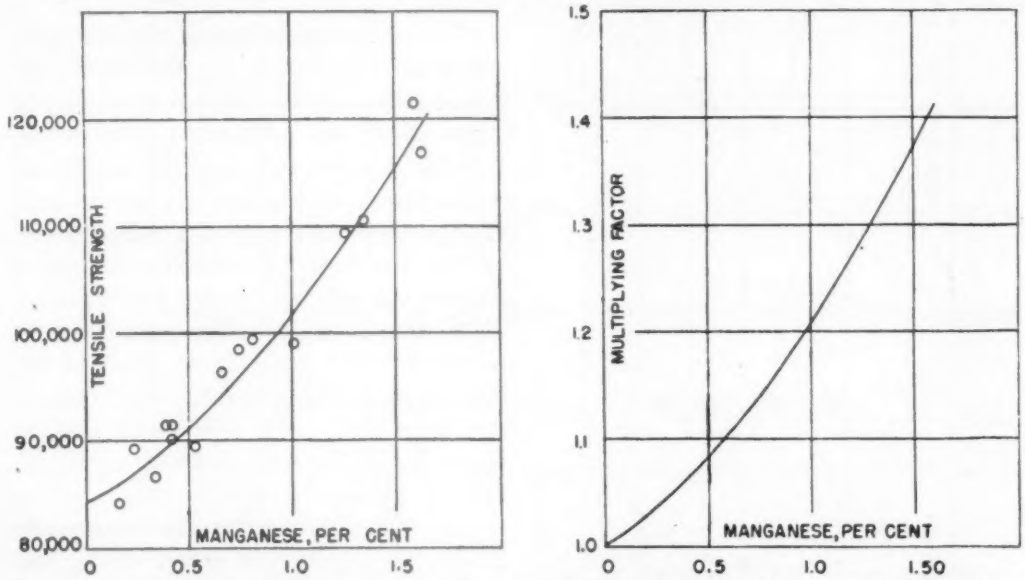

FIG. 7.—(*a*) EFFECT OF MANGANESE ON TENSILE STRENGTH Corrected to 0.40 per cent C, 0.75 per cent Si, AND (*b*) TENSILE STRENGTH FACTOR FOR MANGANESE, NO. 1 COOLING RATE.

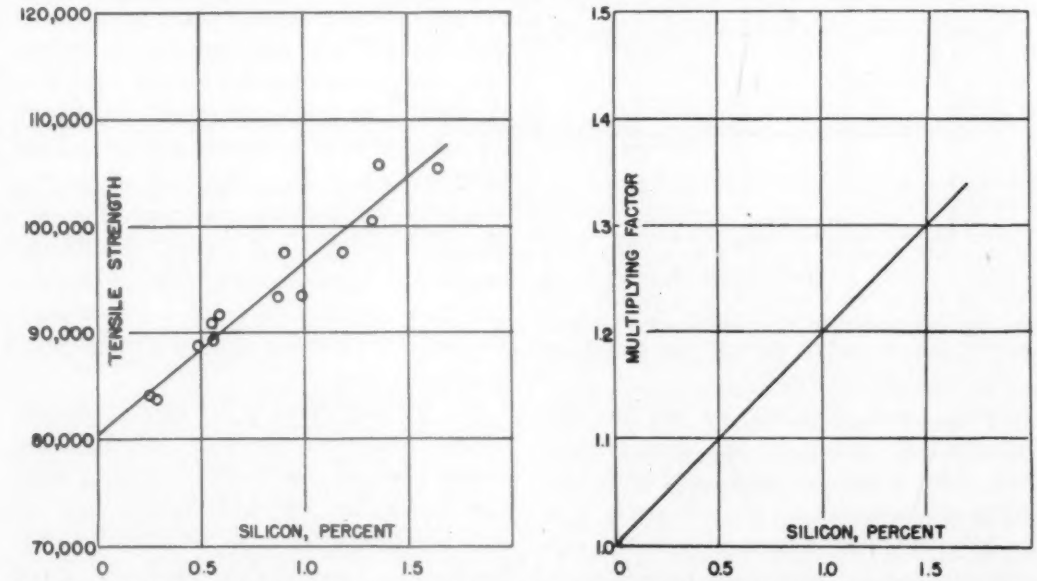

FIG. 8.—(*a*) EFFECT OF SILICON ON TENSILE STRENGTH Corrected to 0.40 per cent C, 0.54 per cent Mn, AND (*b*) TENSILE-STRENGTH FACTOR FOR SILICON, NO. 1 COOLING RATE.

carbon varied between 0.49 and 0.45 per cent and manganese between 0.66 and 0.68 per cent. The individual points on the silicon-factor curve (Fig. 8), although

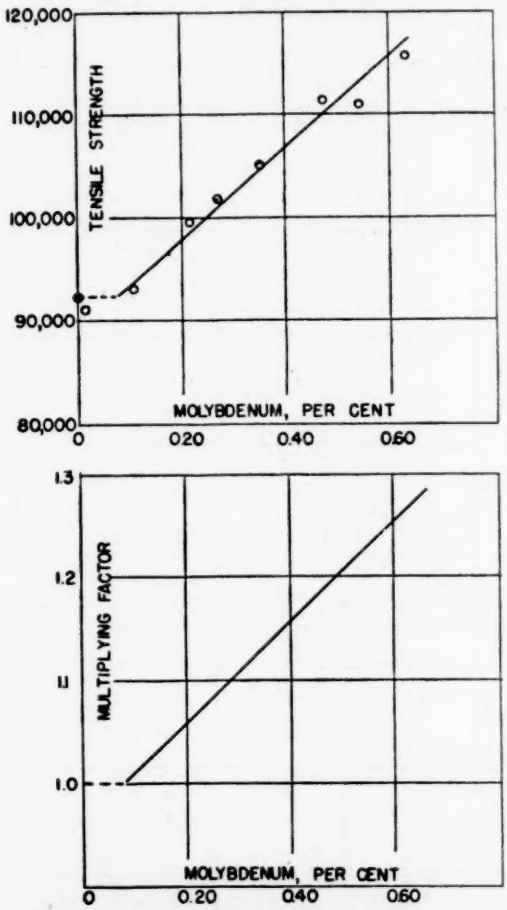

FIG. 11.—(*a*) EFFECT OF MOLYBDENUM ON TENSILE STRENGTH Corrected to 0.38 per cent C, 0.63 per cent Mn, 0.75 per cent Si, AND (*b*) TENSILE-STRENGTH FACTOR FOR MOLYBDENUM, NO. 1 COOLING RATE.

showing some tendency to scatter, did not tend to group in any definite pattern that could be associated with the chemical composition of the steel. The factor curves for silicon were linear and little affected by change of cooling rate. There was a slight tendency for the factors to increase when the half-temperature time exceeded 2 hr. (Fig. 32). A given percentage of silicon has about the same effect on tensile strength as a similar percentage of manganese. In fact, silicon has a slightly higher factor than manganese when present in quantities smaller than 0.50 per cent. At higher percentages the factors for manganese were greater than those for silicon.

Two sets of steels comprising nine compositions were used to determine the nickel-factor curves. The silicon content of these steels was adjusted to two levels, 0.30 and 0.50 per cent, and the carbon and manganese contents were in the vicinity of 0.35 and 0.45 per cent, respectively. Within the expected accuracy the points showed that only one curve could be drawn; although there was a tendency for the steels at the 0.3 per cent silicon level to fall slightly below the curve. The factor curves for nickel (Fig. 9*) were linear and, as shown by Fig. 33, were not affected by the rate of cooling.

The factor curves for chromium were found through the use of five steels, containing 0.37 to 0.38 per cent carbon, 0.36 to 0.43 per cent manganese and 0.35 to 0.45 per cent silicon. For the No. 1 cooling rate the factor curve was slightly curvilinear (Fig. 10*); however, the curves tended to straighten as the cooling rate decreased. As seen in Fig. 33, where the chromium factor is given as a function of cooling rate, the factors for chromium for percentages below 0.50 were practically unaffected by the cooling rate. When the chromium content exceeded 0.75 per cent, the factors decreased rapidly with decreasing cooling rate.

For cooling rates 1, 2, and 4, molybdenum below 0.2 per cent decreased the tensile strength; for the No. 5 cooling rate, the factor at the low percentages of molybdenum seemed to be above unity. For the No. 1 cooling rate, the lower part of the factor curve was drawn with a dashed line because of the uncertainty of the actual course of the curve (Fig. 11). That the factor for molybdenum was strongly

* See footnote on page 249.

affected by the cooling rate can be seen in Fig. 34. The multiplying factors for 0.1 per cent molybdenum remained rather constant with cooling rate, but above 0.2 per cent the factors decreased rapidly as the cooling rate decreased.

The behavior of the copper factor (Fig. 35) as a function of percentage and cooling rate is of interest, since steels containing more than one per cent copper are known to be precipitation-hardening. Up to about 0.75 per cent copper, the multiplying factors were changed only slightly by the cooling rate. However, with 1.0 per cent copper, there was a sharp rise in the curve when the half-temperature time exceeded ½ hr., indicating that precipitation occurred during the cooling. For copper contents greater than 1.0 per cent, precipitation seemed to occur with even faster cooling rates. The factor curve for the No. 1 cooling rate is shown in Fig. 12.*

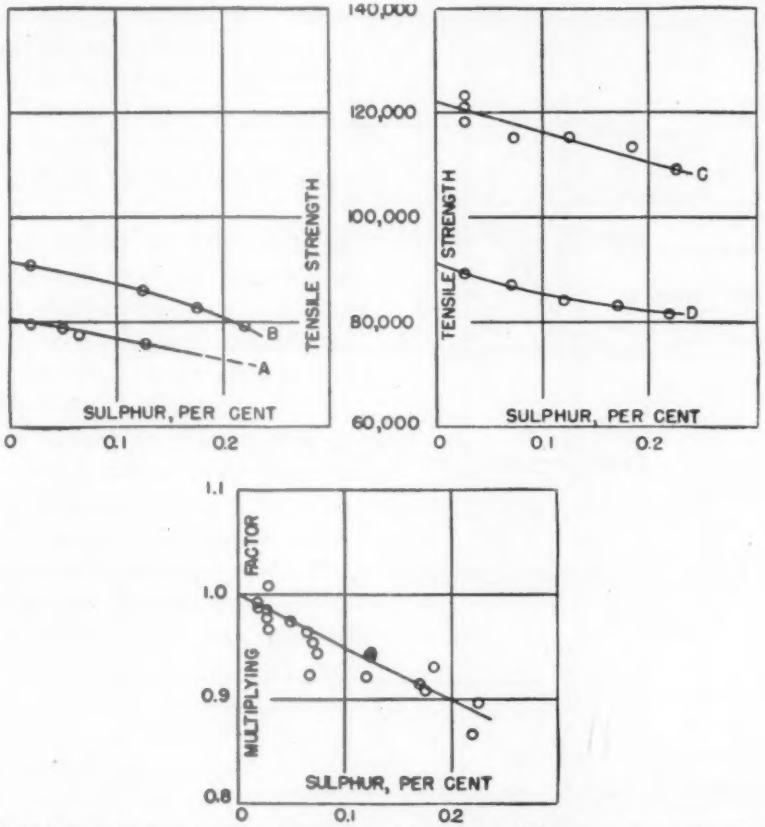

FIG. 13.—(*a*) EFFECT OF SULPHUR ON TENSILE STRENGTH; (*b*) TENSILE-STRENGTH FACTOR FOR SULPHUR, NO. 1 COOLING RATE.

Series A is corrected to 0.37 per cent C, 0.45 per cent Mn, 0.34 per cent Si; series B to 0.29 per cent C, 1.39 per cent Mn, 0.28 per cent Si; series C to 0.47 per cent C, 1.49 per cent Mn, 0.51 per cent Si; series D to 0.39 per cent C, 0.98 per cent Mn and 0.23 per cent Si.

In the experimental work on sulphur, the effect of sulphur was studied in four series of steels in which the manganese and carbon levels were varied. These steels afforded an opportunity to test the principle of multiplying factors and to determine whether the factors for sulphur were entirely independent of the manganese and carbon contents. The results of the No. 1 cooling rate, which are typical of the other cooling rates, were plotted as tensile strength against sulphur content (Fig. 13). Four curves, one for each series of steels,

* See footnote on page 249.

were drawn to show the relationship between sulphur content and tensile strength of each steel in a series by the tensile strength against sulphur content (Fig. 13). When the multiplying-factor curve for each of the series of steels was obtained by dividing the tensile strength of each steel in a series by the tensile strength at 0 per cent sulphur, each series of steels gave, within the expected experimental error, the same sulphur-factor curve. The results for the other cooling rates (Fig. 36) show that in general the multiplying factor of sulphur remained practically constant with changes in cooling rate.

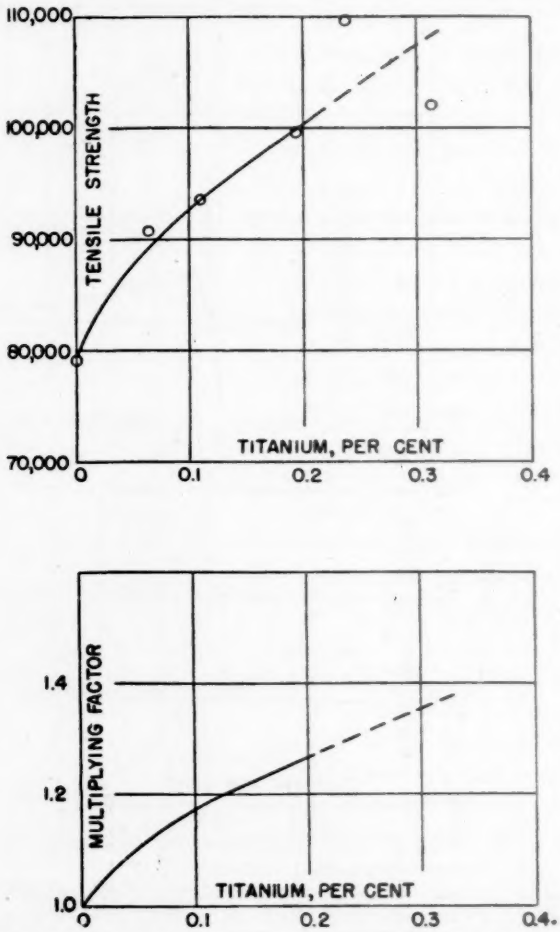

FIG. 14.—(*a*) EFFECT OF TITANIUM ON TENSILE STRENGTH—AS FORGED, Corrected to 0.37 per cent C, 0.44 per cent Mn, 0.53 per cent Si, AND (*b*) TENSILE-STRENGTH FACTOR FOR TITANIUM AS FORGED, NO. 1 COOLING RATE.

The factor curves showing the effect of titanium on the tensile strength were obtained from two conditions of heat-treatment; namely, the "as rolled or forged" and "as normalized." The as-forged plates were obtained by forging at 2200°F. slabs 5 by 5 by 1 in. into plates ⅝ in. thick, which were allowed to air-cool after forging; this cooling rate was comparable to the No. 1 cooling rate. As can be readily seen from Figs. 14 and 15, the factors for the as-forged or as-rolled steels are much higher than those for the as-normalized steels. Further, it appears, from a comparison of Comstock's data for ½-in. plate and the authors' data for ⅝-in.

plate of the as-rolled steels, that the titanium factors are markedly affected by the cooling rate. The factors for the ⅝-in. plate are roughly 40 per cent of those of the ½-in. plate. Incomplete data are available to indicate that the tensile-strength factors for titanium may approach those of the as-normalized steel at a cooling rate comparable to that of an air-cooled 1-in. plate. More work should be done to substantiate this point.

In a manner similar to that used for titanium, the tensile-strength factors for vanadium were derived from steels in the as-forged and as-normalized conditions. As may be expected, vanadium has an effect on tensile strength similar to that of titanium. The factors for the as-forged steels are very much higher than those of the as-normalized steels (Fig. 16*). For the as-normalized condition the factors were only slightly affected by changes in the cooling rate (Fig. 34). No data were available at this time for determining the manner in which as-forged steels change with the cooling rate; however, as the cooling rate decreases, there is some evidence that the factors approach those of the as-normalized condition.

The factor curves for phosphorus (Fig. 17) were determined by the use of five steels having a base composition of 0.35 to 0.36 per cent carbon, 0.20 to 0.29 per cent silicon, and 0.39 to 0.45 per cent manganese. Phosphorus was found to increase the tensile strength to the same degree as carbon. Approximately 0.1 per cent phosphorus increases the tensile strength 10 per cent. The factors for phosphorus are practically unaffected by changes in the cooling rate (Fig. 35).

The base composition of the steels used for the determination of the aluminum-factor curves was similar to that used for vanadium. Aluminum decreased the tensile strength (Fig. 18) and its factor was only slightly affected by the cooling rate (Fig. 36).

Since available data were insufficient for the determination of factors at low per-

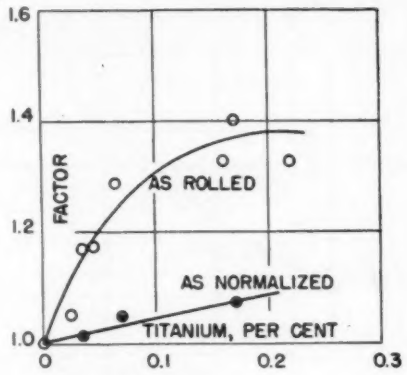

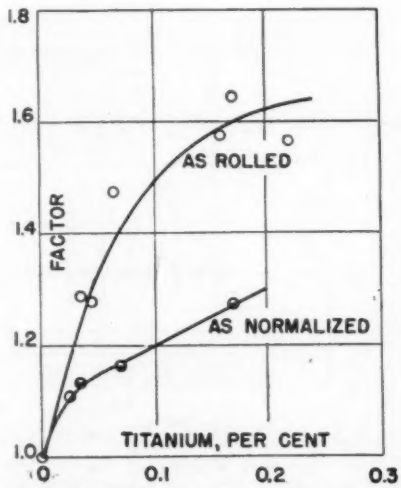

FIG. 15.—(*a*) EFFECT OF TITANIUM ON TENSILE STRENGTH (FROM COMSTOCK[7]), NO. 9 COOLING RATE, AND (*b*) EFFECT OF TITANIUM ON YIELD POINT (FROM COMSTOCK[7]), NO. 9 COOLING RATE.

centages of carbon and at cooling rates faster than that of a normalized ⅝-in. plate, data for the tensile strengths of a series of normalized ½-in. plate were obtained by extrapolating the half-temperature-time curve from 0.147 hr. to 0.118 hr. The value of 0.118 hr., the half-temperature time for the normalized ½-in. plate, was obtained from Fig. 3. The factors for the carbon were then derived by dividing the tensile strength by the

* See footnote on page 249.

product of the factors of all the alloying elements present in the steel (Fig. 5). These points were found to fall on the extrapolated portions of the composite carbon-factor curves (Fig. 31).

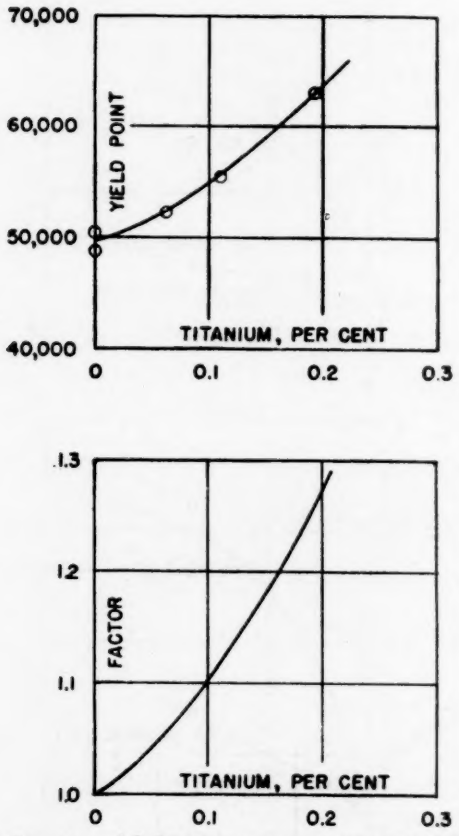

FIG. 24.—(*a*) EFFECT OF TITANIUM ON YIELD POINT—AS FORGED, Corrected to 0.37 per cent C, 0.44 per cent Mn, 0.53 per cent Si, AND (*b*) YIELD-POINT FACTOR FOR TITANIUM—AS FORGED, NO. 1*a* COOLING RATE.

Yield-point Factors

Because of the dispersion of points on the curves for yield-point factor, a greater number of steels was required to establish the carbon, manganese, and silicon-factor curves than the tensile-strength factor curves. Therefore, in addition to the steels used for the tensile-strength factors, 21 steels were added for the determination of curves for the yield-point factor. These steels consisted of low, medium, and high percentages of carbon, manganese, and silicon, and as a result of the wide ranges of composition, these 21 steels were suitable for the determination of all three factor curves. In general, steel used for the determination of the curves for yield-point factor were the same as those used for the curves representing tensile-strength factor.

The curves of yield-point factor for carbon show that it affects the yield point markedly (Fig. 19), but the slope of the factor curves decreases quite rapidly with decreasing cooling rate (Fig. 37). In fact, when the half-temperature time exceeded 10 hr., the factors at various carbon levels were practically equivalent. For example, at a half-temperature time of 0.147 hr., an increase of carbon from 0.1 to 0.6 increased the yield point 36 per cent, whereas for a half-temperature time of 10.76 hr. the increase was only 9 per cent.

The factor curve for manganese for the No. 1 cooling rate (Fig. 20) shows that manganese affects the yield point in about the same magnitude as silicon (Fig. 21); however, the factors for silicon and manganese do not change in the same manner when the cooling rate is decreased. Up to about a half-temperature time of one hour, the manganese factors remained practically constant (Fig. 37) and the factors for silicon increased in a linear manner as the half-temperature time increased (Fig. 38).

The yield-point factors for copper exhibited the same general characteristics as those for the tensile-strength copper-factor curves (Fig. 22). As in the case of the tensile strength, the cooling rate had little or no effect on the copper factors for percentages lower than 0.75 (Fig. 39). At 1.0 per cent the copper factor increased very rapidly when the half-temperature time exceeded one hour. Thus the precipitation-hardening effect evidenced by the tensile-strength factor was also apparent in its effect on the yield point.

The factor curves for nickel (Fig. 23) were, in general, linear, but at the slower

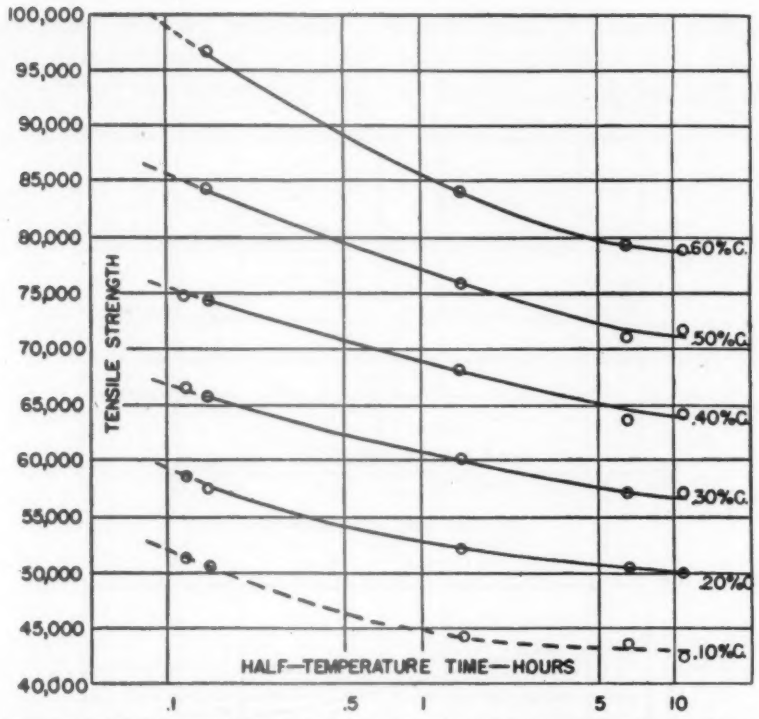

FIG. 31.—CORRELATION OF TENSILE-STRENGTH FACTOR FOR CARBON WITH HALF-TEMPERATURE TIME (TIME TO COOL FROM 1550°F. TO 800°F.

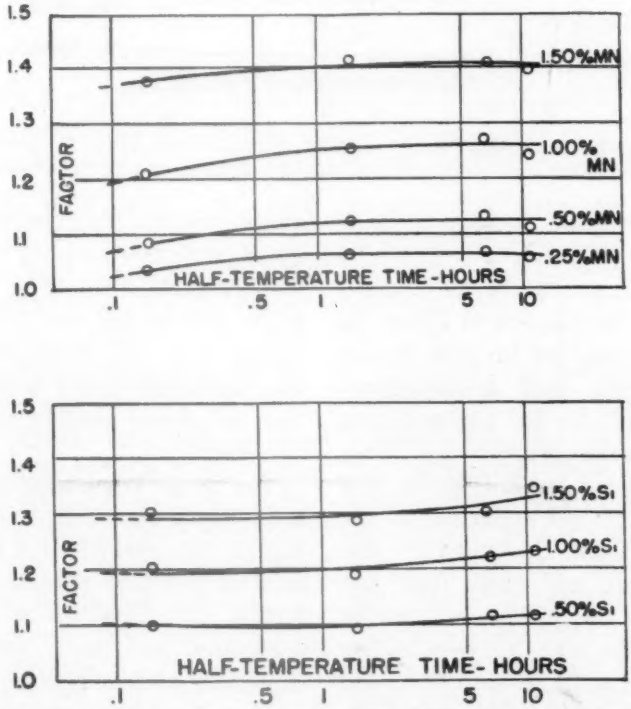

FIG. 32.—(*a*) EFFECT OF COOLING RATE ON THE TENSILE-STRENGTH FACTOR FOR MANGANESE, AND (*b*) EFFECT OF COOLING RATE ON THE TENSILE-STRENGTH FACTOR FOR SILICON.

cooling rates they tended to curve downward when the nickel content exceeded 2.5 per cent. The factors were inclined to increase slightly with increasing half-temperature time (Fig. 38).

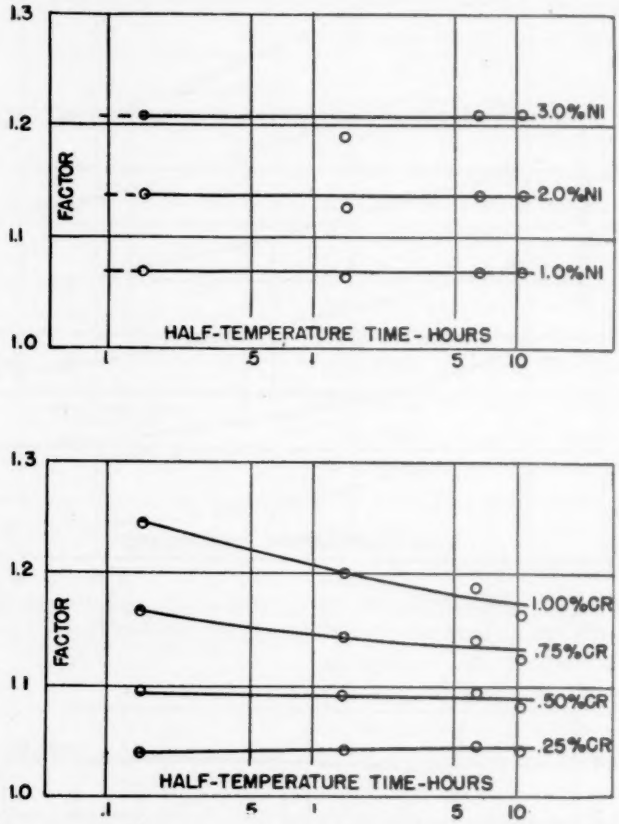

FIG. 33.—(*a*) EFFECT OF COOLING RATE ON THE TENSILE-STRENGTH FACTOR FOR NICKEL, AND (*b*) EFFECT OF COOLING RATE ON THE TENSILE-STRENGTH FACTOR FOR CHROMIUM.

As in the determination of tensile-strength factors, the yield-point factor for titanium was determined in both as the as-rolled or forged and as-normalized conditions. The factors for the as-forged steels were very much greater than those for the as-normalized steels (Fig. 24 and 15). It appears from a comparison of the factors derived from Comstock's[6] data on the ½-in. plate and those from the ⅝-in. plate that the yield-point factors were strongly influenced by the cooling rates. For example, at 0.1 per cent titanium, the factor for the ½-in. plate was 1.49, while that for the ⅝-in. plate was 1.10.

The yield point of vanadium steel was affected by austenitizing treatment in the same manner as was the yield point of titanium steel. The factors for the as-forged steels were much higher than those of the as-normalized steel (Fig. 25*). The yield-point factors for the as-normalized condition (Fig. 40) increased somewhat as the half-temperature increased to 2 hr., but for slower cooling rates the factors decreased.

The factor curves for chromium for all rates, with the exception of the No. 1 cooling rate, exhibited a maximum factor at 0.60 per cent chromium; that is, the factors increased up to 0.60 per cent chromium and then decreased as the chromium content increased. For the No. 1

* See footnote on page 249.

cooling rate (Fig. 26) the factors increased for all of the percentages investigated. The composite curve for chromium (Fig. 41), similar to those for molybdenum and vanadium, showed that below 0.5 per cent chromium the factors increased until the half-temperature time exceeded 2 hr.; for cooling rates slower than this, the factors decreased. For 0.75 and 1.0 per cent chromium the factors decreased as the cooling rate decreased.

The factor curves for molybdenum (Fig. 27) were similar to those of chromium except that they did not decrease as did the chromium factors when the percentages exceeded 0.60. The composite curve (Fig. 41) showed that the factors increased as the half-temperature time increased to 2 hr. and then decreased with the slower cooling rates.

Three series of steels at various carbon and manganese levels were used in the determination of yield-point-factor curves for sulphur. Yield-point curves were drawn for each series and, from these, factor curves were developed. Within the limits of experimental error, each series gave the same factor curve (Fig. 28). As in tensile strength, sulphur lowered the yield point and was affected only slightly by changes in cooling rate (Fig. 40).

In a manner similar to its effect on tensile strength, phosphorus markedly increased the yield point. In fact, owing to the decreasing effect of carbon as the cooling rate decreased, the factors for phosphorus were greater than those for carbon when the half-temperature time exceeded 0.15 hr. The factors for phosphorus continuously increased with decreasing cooling rate (Fig. 39); however, there was a tendency for the factor for 0.25 per cent phosphorus to remain constant for half-temperature times greater than

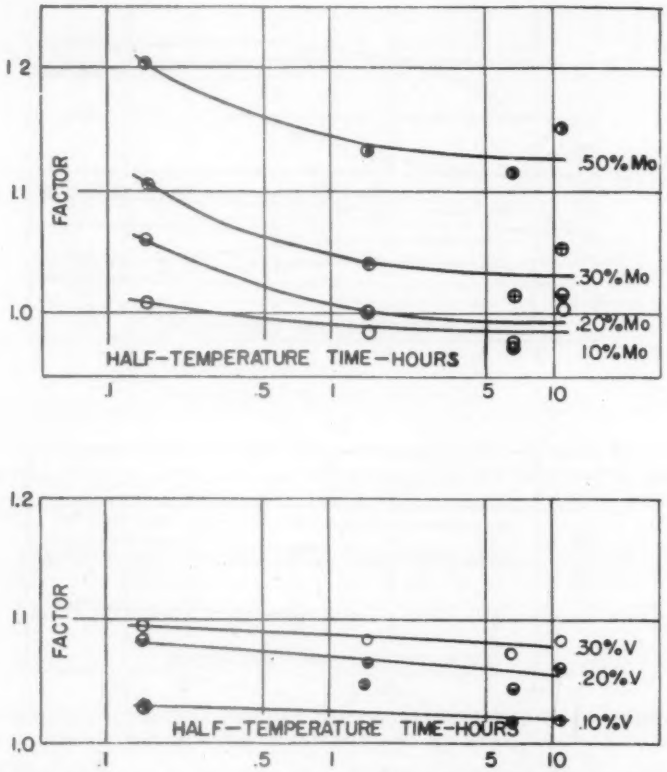

FIG. 34.—(*a*) EFFECT OF COOLING RATE ON THE TENSILE-STRENGTH FACTOR FOR MOLYBDENUM, AND (*b*) EFFECT OF COOLING RATE ON THE TENSILE-STRENGTH FACTOR FOR VANADIUM.

6 hr. The factor curve for phosphorus for the No. 1 cooling rate is given in Fig. 29.

Unlike its effect on tensile strength, aluminum increased the yield point. Although no complete explanation can be given at this time, it may be that aluminum per se decreases the yield point in a manner similar to its effect on the tensile strength. This effect, however, may be masked by the decrease in grain size due to the addition of aluminum; the decrease in turn increases the yield point (Fig. 4). The factor curve passed through a maximum at 0.01 per cent aluminum and then fell rapidly, so that at percentages in excess of 0.03 the factors approached unity (Fig. 30). In general, the factors for aluminum increased with half-temperature time (Fig. 42).

The effect of austenitic grain size on the tensile strength and yield point is shown graphically in Fig. 4*, for an A.S.T.M. grain-size range of 6.0 to 3.0. Within the experimental accuracy, the tensile strength did not change with grain size, but an increase in A.S.T.M. grain-size number from 3.0 to 6.0 caused an increase in yield point of 13 per cent. Grain-size measurements were made on 30 silicon-killed steels of various compositions in order to determine the variation that could be expected in steels used throughout this study. It was found that the grain size varied from 3.5 to 8.0, but that 70 per cent were between 5.5 and 6.5. Thus the normal variations of grain size within the steels used for calculating and testing of the yield-point curves could account for at least 3 to 4 per cent of the average deviation.

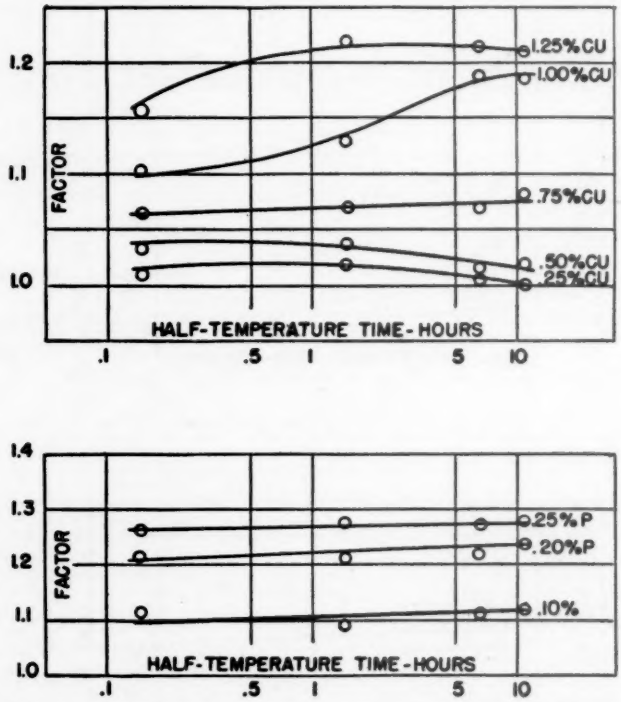

FIG. 35.—(*a*) EFFECT OF COOLING RATE ON THE TENSILE-STRENGTH FACTOR FOR COPPER, AND (*b*) EFFECT OF COOLING RATE ON THE TENSILE-STRENGTH FACTOR FOR PHOSPHORUS.

DISCUSSION OF RESULTS

The magnitude of the effect of alloying elements on tensile strength was different from their effect on yield point. Thus by proper selection of alloying elements the

* See footnote on page 249.

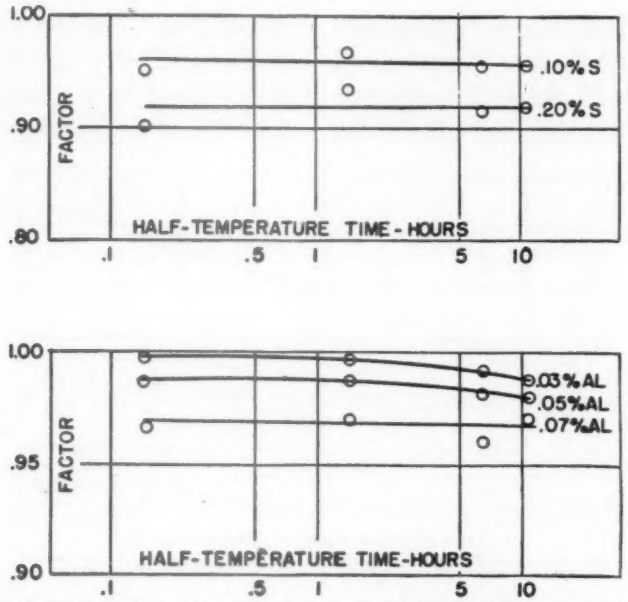

FIG. 36.—(*a*) EFFECT OF COOLING RATE ON THE TENSILE-STRENGTH FACTOR FOR SULPHUR, AND (*b*) EFFECT OF COOLING RATE ON THE TENSILE-STRENGTH FACTOR FOR ALUMINUM.

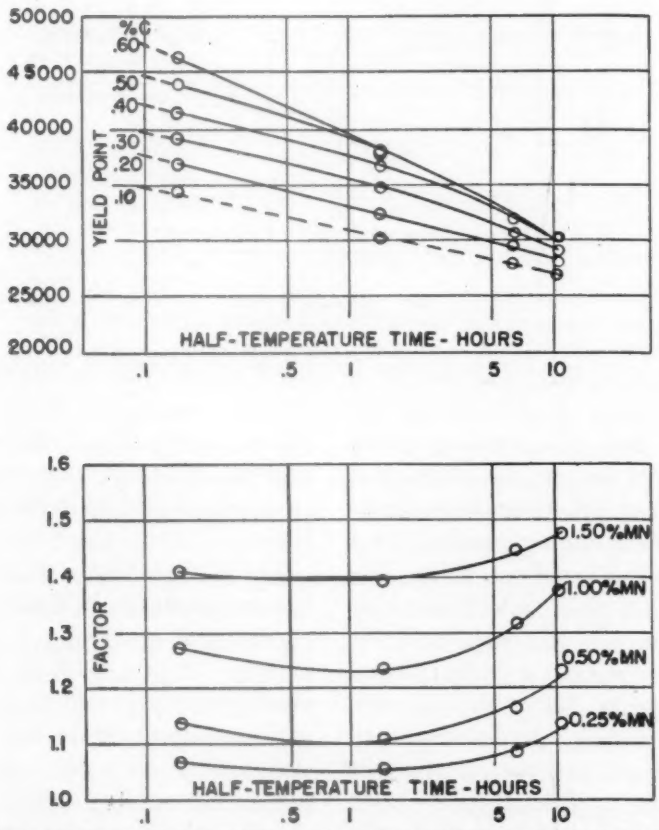

FIG. 37.—(*a*) CORRELATION OF YIELD-POINT FACTOR FOR CARBON WITH HALF-TEMPERATURE TIME, AND (*b*) EFFECT OF COOLING RATE ON THE YIELD-POINT FACTOR FOR MANGANESE.

yield ratio of a steel can be varied considerably. In general, the highest yield ratio on the basis of the carbon alone is obtained with low percentages of carbon and fast cooling rates. High percentages of carbon are especially detrimental to the yield ratio in the slow cooling rates. Manganese, nickel, copper, vanadium, and aluminum increase the yield ratio in all proportions and for all the cooling rates that were studied. In general, silicon has little effect on the yield ratio below 0.75 per cent; above this the yield ratio is increased. The yield ratio is little affected by chromium for the No. 1 cooling rate; however, as the cooling rate decreases, the yield ratio increases when the chromium is below 0.50 per cent, whereas percentages above this cause it to decrease. Molybdenum and phosphorus in the No. 1 cooling rate decrease the yield ratio, but with slower cooling rates they increase the yield ratio slightly. The elements in the order of their effectiveness in increasing the yield ratio are: aluminum, titanium, vanadium, copper, manganese, nickel, silicon, chromium, phosphorus, molybdenum, and sulphur. This order is approximate and may be changed slightly with varying cooling rates.

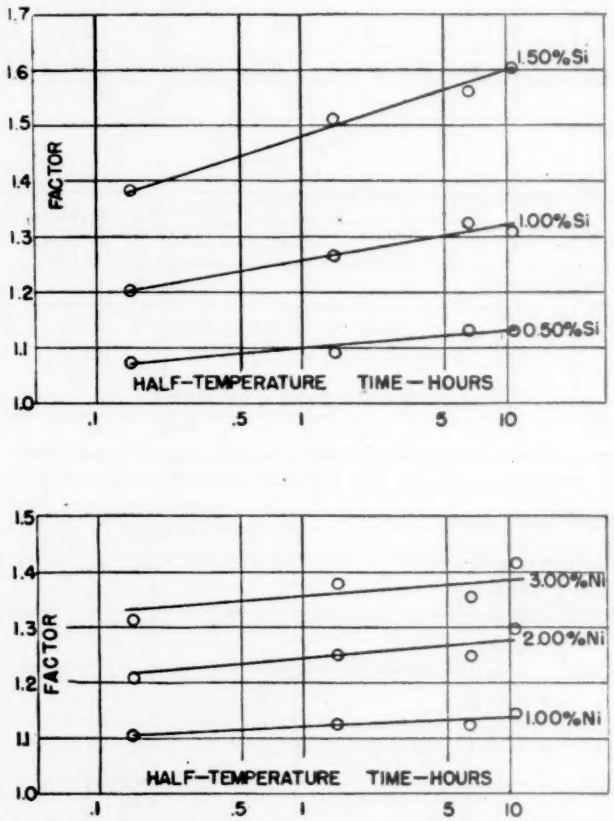

FIG. 38.—(*a*) EFFECT OF COOLING RATE ON THE YIELD-POINT FACTOR FOR SILICON, AND (*b*) EFFECT OF COOLING RATE ON THE YIELD-POINT FACTOR FOR NICKEL.

The data used for testing the multiplying factors are shown in Table 5 and Figs. 44, 45, 46, and 47. Table 5 shows the comparison between calculated and observed tensile strengths and yield points for the various cooling rates. The average deviation obtainable with the multiplying factors for tensile strength in this paper is approximately ± 3 per cent with about 90 per cent of the steels within ± 7 per

cent. The expected accuracy when two or more alloying elements that form stable carbides are present is ±8 per cent. It is suspected that large positive deviations may occur when these alloying elements are present in such quantity that carbides remain undissolved during the austenitizing treatment. These undissolved carbides not only act as nuclei to start the transformation of austenite at a higher temperature than that expected, but also the austenite is lower in both carbon and alloy content. On the other hand, since the curves were derived from pearlitic steels, negative deviations are to be expected when the alloy content is sufficiently high to cause the formation of low-temperature transformation products such as bainite or martensite. The average deviation for the calculation of the yield point is ±5 per cent and approximately 90 per cent of the steels are within ±10 per cent. A contributing factor to the deviation in the yield-point calculations might be the variations of austenitic grain size of the steel. The accuracy when two or more strong carbide-forming elements are present is somewhat less than mentioned above.

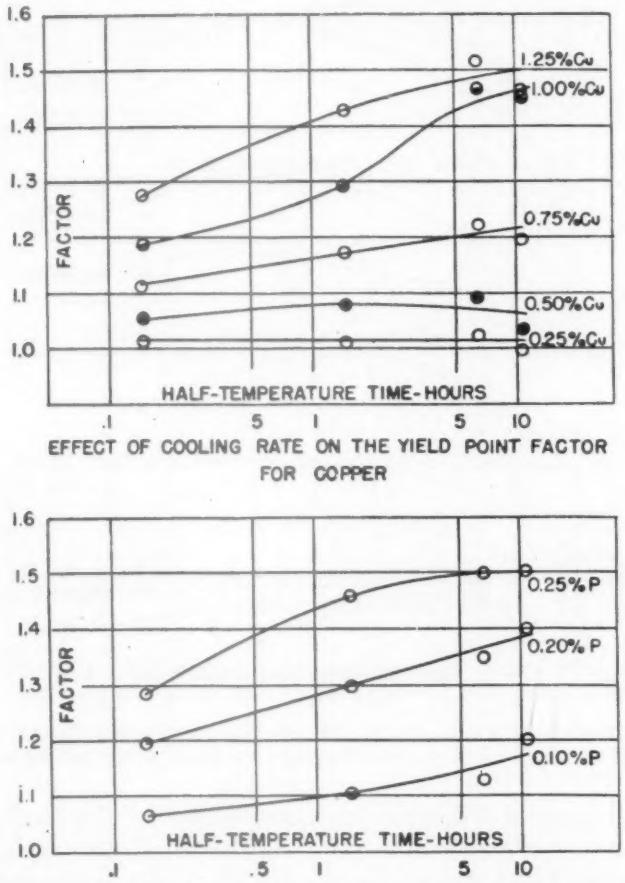

FIG. 39.—(*a*) EFFECT OF COOLING RATE ON THE YIELD-POINT FACTOR FOR COPPER, AND (*b*) EFFECT OF COOLING RATE ON THE YIELD-POINT FACTOR FOR PHOSPHORUS.

For steels that did not have a definite yield point (marked by asterisks in Tables 2 and 5) the yield strengths at approximately 0.01 per cent offset were used. This method worked fairly well when the tensile strength could also be calculated with a reasonable degree of accuracy, but for the steels that had a high tensile or

yield strength the calculated values were about 20 per cent lower than the observed values. In general, when the amount of alloying elements present was great enough to produce low-temperature decomposition products of austenite, the tensile strength could not be calculated and neither could the yield point; however, if the tensile strength of the steel could be calculated, the yield point also could be calculated. For example, in the steel PHW (SAE-4340) in Table 5, the cooling rates 1, 2 and 4 were not sufficiently slow to prevent the formation of low-temperature decomposition products, therefore the calculated values for tensile and yield strength were much lower than the observed value; for the No. 5 cooling rate the tensile strength and yield point agreed very well with the observed values. There are other steels in the test data that show this to varying degrees, especially in the faster cooling rates.

In agreement with the data reported by Comstock,[6] the austenitizing treatment greatly influenced the tensile strength and yield point of steels containing titanium.

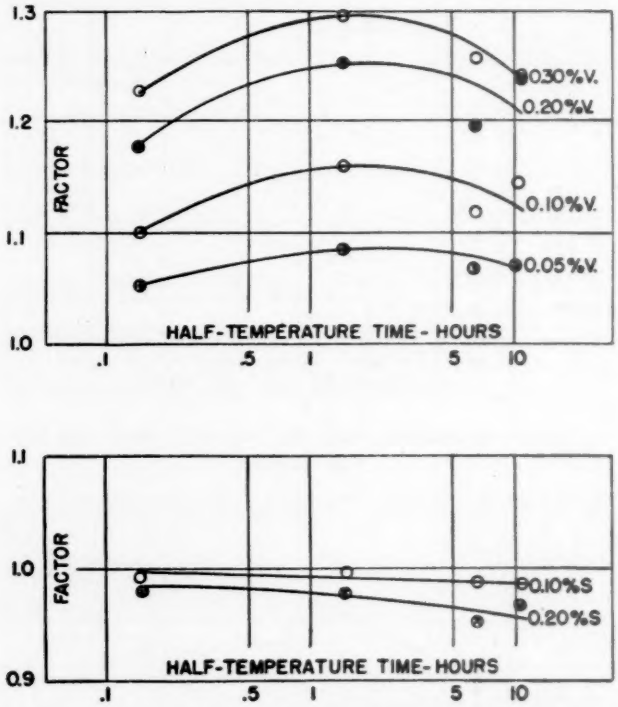

FIG. 40.—EFFECT OF COOLING RATE ON THE YIELD-POINT FACTOR FOR VANADIUM, AND (*b*) EFFECT OF COOLING RATE ON THE YIELD-POINT FACTOR FOR SULPHUR.

According to Comstock,[6] titanium carbide is relatively insoluble in steel and can be caused to dissolve in the austenite only when high austenitizing temperatures are employed. A similar situation may be assumed for vanadium in steel. When titanium or vanadium is dissolved in the austenite, steels are strengthened in much the same way as by other carbide-forming elements. This strengthening effect will be realized when the cooling rates are used that prevent precipitation of the carbides from the austenite before the austenite transformation begins. For the data presented by Comstock for ½-in. plates, it appears that all, or at least a large part of the titanium was held in solution. However, since the titanium factors decreased rapidly as the half-temperature time increased,

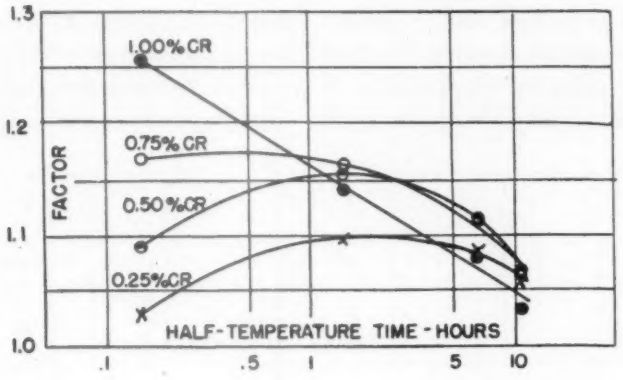

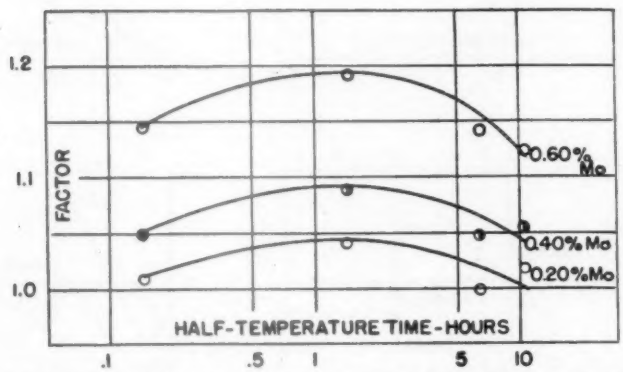

FIG. 41.—(*a*) EFFECT OF COOLING RATE ON THE YIELD-POINT FACTOR FOR CHROMIUM, AND (*b*) EFFECT OF COOLING RATE ON THE YIELD-POINT FACTOR FOR MOLYBDENUM.

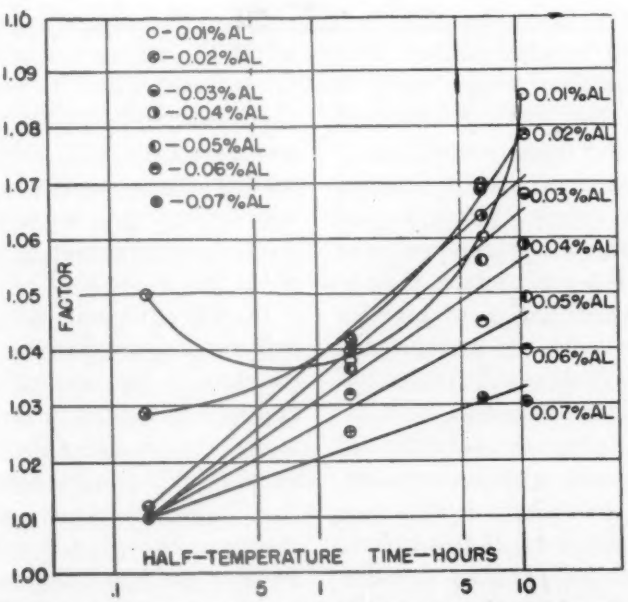

FIG. 42.—EFFECT OF COOLING RATE ON THE YIELD-POINT FACTOR FOR ALUMINUM.

it is reasonable to assume that titanium carbides were precipitated, when the steel was cooled in accordance with the No. 1-A cooling rate (5/8-in. plate). From the large

react as though the carbides had never been in solution. This would cause the tensile strength and yield point to be lower than expected.

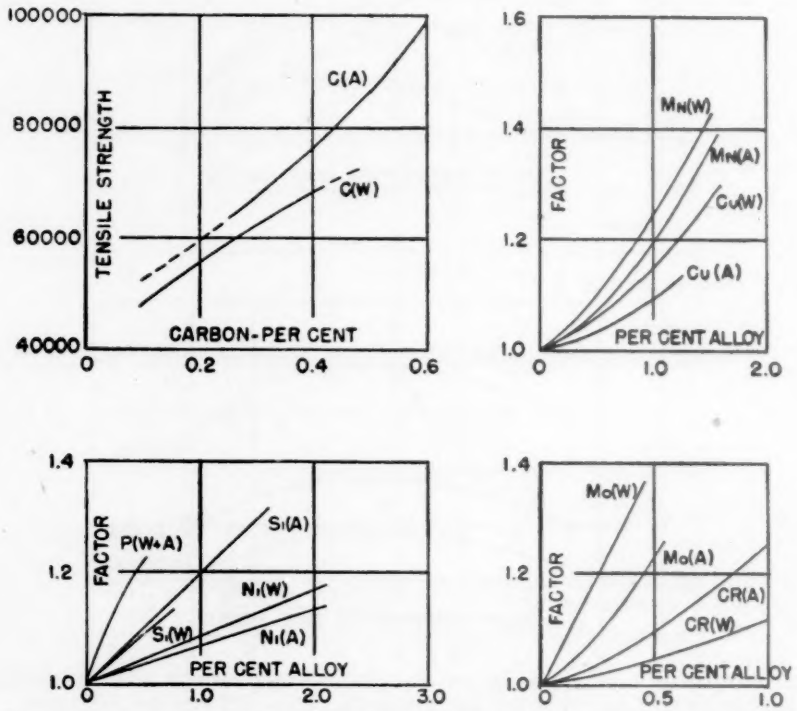

FIG. 43.—COMPARISON OF THE AUTHORS' TENSILE-STRENGTH FACTOR CURVES FOR 3/4-INCH ROUNDS (H. T. T. = 0.091 HOURS) WITH THOSE OF WALTERS.[3]

change in factor with cooling rate, it is expected that the benefits derived from titanium or vanadium might vary in accordance with the method employed in cooling steels after forging or rolling.

In a similar manner, it may be that the decrease in the tensile strength and yield-point factors for chromium and molybdenum at slow cooling rates may be explained by a precipitation of carbides from the austenite. At the austenitizing temperatures employed (1550°F.) the alloying carbides may be dissolved to some extent. However, since the solubility of the carbides decreases with temperature, the carbides can precipitate if the time allowed is sufficiently long. If this occurs, the austenite will be depleted in both alloying elements and carbon and will

Since the austenitizing treatment will affect the amount of carbide in solution in the austenite, it may very well be that successful calculation of the tensile strengths and yield points of steels containing strong carbide-forming elements may depend upon austenitizing at or near the temperatures used in the determination of the factor curves.

In order to test the validity of the half-temperature time as a parameter for correlating the cooling rate with the multiplying factors, a series of steels was cooled at rates other than those for which the multiplying-factor curves were derived. The half-temperature times for these cooling rates (3, 6, 7, 8, and 9) are given in Table 4 and the calculated and observed tensile strengths and yield points in

Table 5. That the half-temperature time serves as an adequate criterion for the correlation of the multiplying factors may be judged from the fact that of approximately 120 steels tested in this manner, the average deviation for the calculation of the tensile strength was ±3 per cent and the average deviation for the calculation of yield point was ±6 per cent.

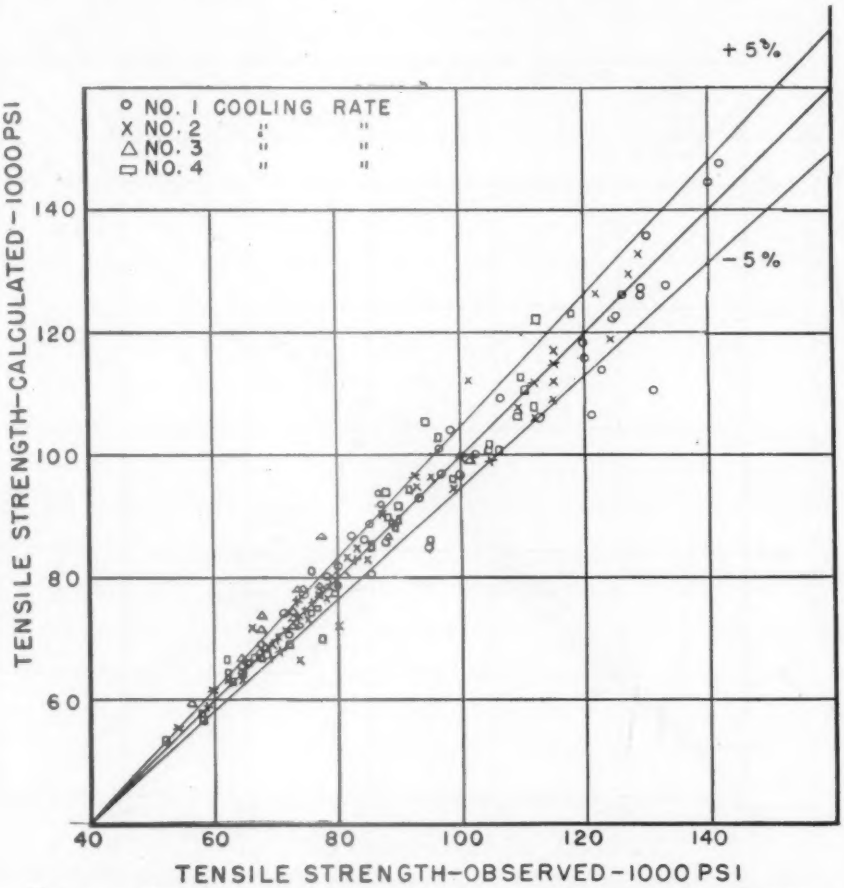

FIG. 44.—COMPARISON OF CALCULATED AND OBSERVED TENSILE STRENGTH.

To test the accuracy of the factors for low percentages of carbon and the usefulness of Fig. 3, which gives the half-temperature time as a function of bar size, tensile-strength data for 1-in. rounds reported by Crafts[10] were utilized. The factor curves were drawn from the curves giving the tensile-strength factors as a function of half-temperature time. The results listed in Table 6 show that the predicted tensile strengths agreed very well with the reported data.

Although only five cast steels were tested (Table 7), the results indicated that these factors may be applicable to the calculation of the tensile strength and yield point of normalized cast steels.

The importance of obtaining a complete chemical analysis must be stressed. For example, in the slow cooling rates a residual of 0.01 per cent acid-soluble aluminum increases the yield point 8 per cent. In general, the usual residual alloying elements account for 4 to 6 per cent of the tensile strength and yield point of commercial steels.

Even though the factor curves were derived at cooling rates similar to those encountered at the center of air-cooled

plates or rounds, these factors may also be used to calculate the tensile strength and yield point for other positions in the test piece, since the cooling rate is the determining factor. If it is desired to calculate the tensile strength or yield point for a particular location, it is necessary to know the half-temperature time, so that the appropriate factor curves may be obtained. To obtain the tensile strength or yield point at the centers of plates or rounds, the half-temperature time may be obtained from Fig. 3 and the factor curves may be drawn from the charts giving the correlation between the factors and the half-temperature time. Suppose it is desired to calculate the tensile strength at the center of an air-cooled bar 1 in. in diameter, the chemical composition of which is given below. For a half-temperature time of 0.137 hr., obtained from Fig. 3, the tensile-strength factors were as follows:

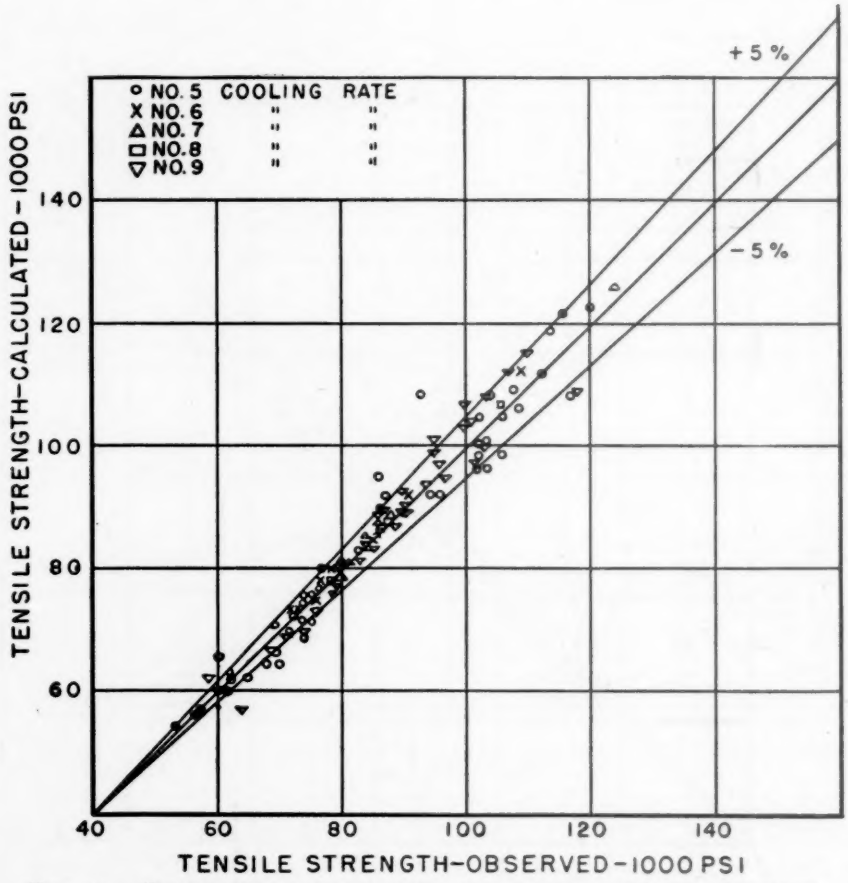

FIG. 45.—COMPARISON OF CALCULATED AND OBSERVED TENSILE STRENGTH.

Constituent	Per Cent	Factor
C	0.08	49,200
Mn	0.96	1.20
Si	0.83	1.16
S	0.018	0.991
P	0.077	1.09
V	0.012	1.003
Cu	0.36	1.02
	Product	75,600

The observed tensile strength was 76,000 lb. per sq. inch.

A comparison between the tensile-strength factors obtained by Walters[3]

for normalized ¾-in. rounds and those of the authors is given in Fig. 43. Since the authors did not determine the tensile-strength factors for ¾-in. rounds, their data were obtained by extrapolating the composite curves for the alloying elements to a half-temperature time of 0.091 hr. The value of 0.091 hr. was the time obtained from Fig. 3 for a normalized ¾-in. round. In general, the factor curves for silicon, nickel and phosphorus agree rather well; however, the authors' curve for carbon is above and the manganese curve below those obtained by Walters. There is also a rather large difference between the authors' curves and those of Walters for chromium, molybdenum and copper. The discrepancy between the two chromium curves and the two molybdenum curves might possibly be due to effects of different austenitizing temperatures and different carbon levels.

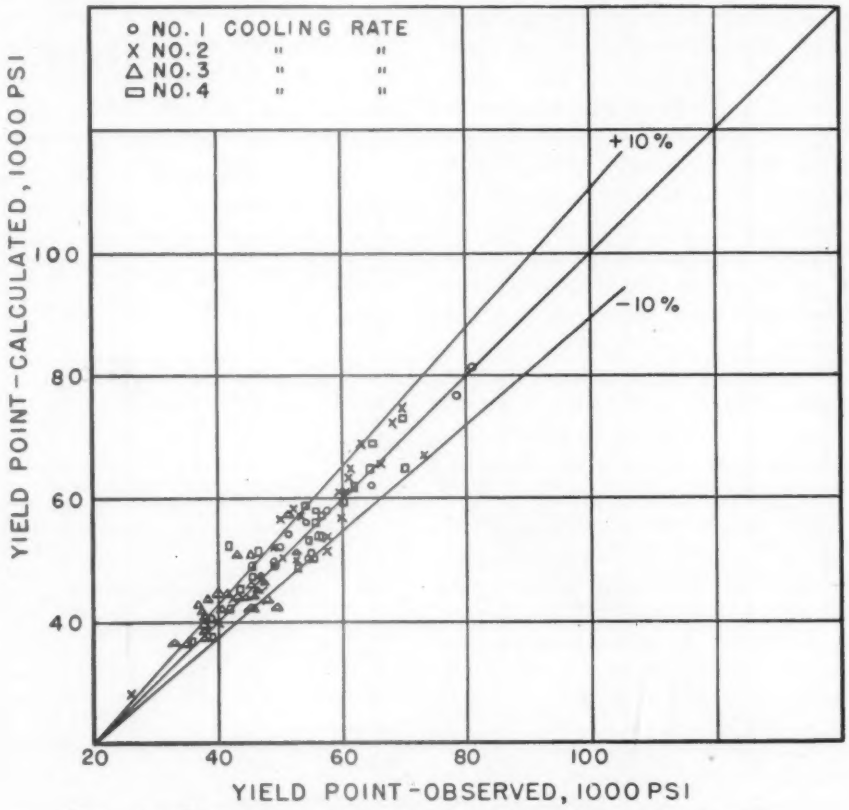

FIG. 46.—COMPARISON OF CALCULATED AND OBSERVED YIELD POINT.

SUMMARY

By means of these factor curves it is possible to calculate, with reasonable accuracy, the tensile strength and yield point of steels cooled at rates between those at the center of a ½-in. plate and those at the center of a 16-in. plate. If the half-temperature time is known, the tensile strength and yield point at any position in the test piece may be calculated.

The most effective combination of alloying elements for a desired tensile strength and yield point may be obtained by examining the individual factor curves for the particular cooling rate involved. Inasmuch as some of the alloying elements do not influence the tensile strength in the same manner as the yield point, a judicious choice of alloying elements must be made in order to achieve a definite yield-tensile ratio in the most economical manner.

When fairly large amounts of low-temperature transformation products of austenite are formed during cooling, multiplying factors developed here are not adaptable for the calculation of tensile strength or yield point. Generally, the yield strength at 0.01 per cent offset of steels that do not have a definite yield point cannot be calculated with any reasonable degree of accuracy unless the corresponding tensile strength can also be calculated.

Best results can be assured with these factors only when complete chemical analysis and cooling rate are known.

The results of the calculations of tensile strengths of five steels indicate that these factors may be used for normalized cast steels.

To make more efficient use of alloying elements in steel, the multiplying-factor curves should be closely examined with respect to their shape as well as their magnitude. Many of the alloying elements—for example, phosphorus, titanium, and vanadium—contribute markedly to both tensile strength and yield point at low percentages, whereas small percentages of molybdenum and copper increase it only slightly, but in larger amounts have a large effect.

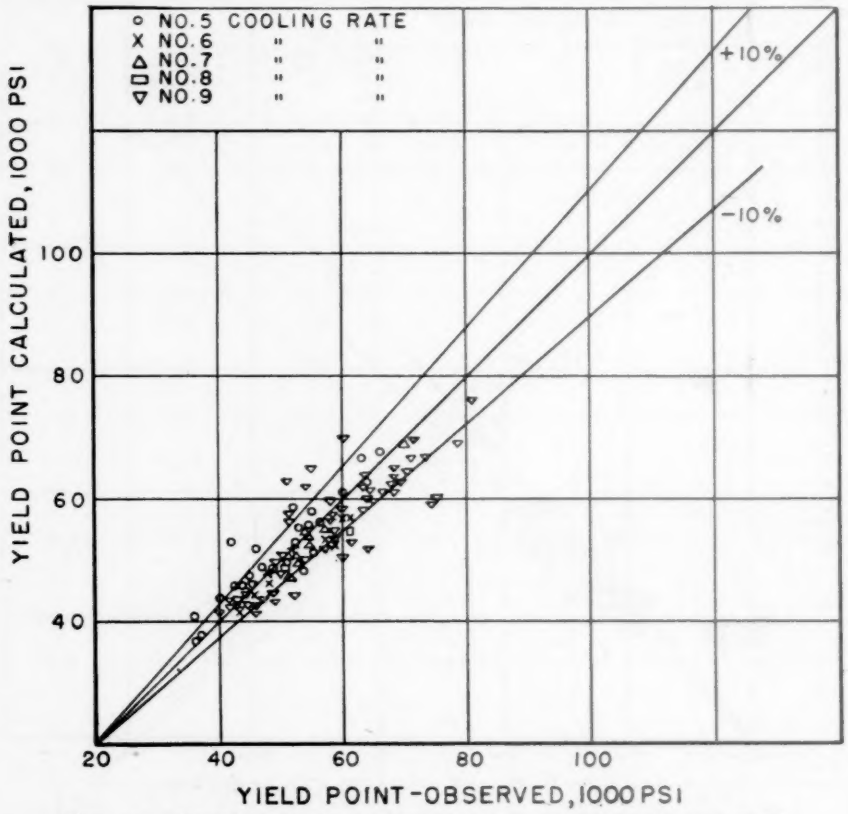

FIG. 47.—COMPARISON OF CALCULATED AND OBSERVED YIELD POINT.

In work of this sort, covering as it does such a large number of variables, a great many more steels than have been used here may be necessary to determine the exact factor curves. This is especially true with regard to yield point where the effects of grain size and perhaps other variables were not considered in the determination of the factors. Since only a limited range of carbon content was used in the calculation of the factor curves for the elements that form stable carbides (chromium, molybde-

num vanadium, titanium, and others), their factors for other levels of carbon might differ from those shown here.

Acknowledgments

The authors wish to express their appreciation of the many helpful suggestions of Dr. F. M. Walters, Jr., Superintendent of the Division of Physical Metallurgy, Naval Research Laboratory, and to thank the Analytical and Metallography Sections of this Laboratory for their work of analyzing and preparing the specimens used in this paper.

References

1. Quest and Washburn: Tensile Strength and Composition of Hot-rolled Plain Carbon Steels. *Trans.* A.I.M.E. (1940) **140**, 489–496.
2. M. A. Grossmann: Hardenability Calculated from Chemical Composition. *Trans.* A.I.M.E. (1942) **150**, 227–259.
3. F. M. Walters, Jr.: Calculation of Tensile Strength of Normalized Steels from Chemical Composition. *Trans.* A.I.M.E. (1943) **154**, 407–412.
4. Janitsky and Boeyertz: The Marked Similarity in Tensile Properties of Several Heat Treated SAE Steels. Metals Handbook, 1939 Ed., 515–518. Amer. Soc. for Metals.
5. M. Gensamer, E. B. Pearsall, W. S. Pellini and J. R. Low, Jr.: The Tensile Properties of Pearlite, Bainite, and Spheroidite. *Trans.* Amer. Soc. for Metals (1942) **30**, 983–999.
6. G. F. Comstock: Some Effects of Heat Treatment on Low Alloy Titanium Steels. *Trans.* Amer. Soc. for Metals (1944) **32**, 324.
7. Jackson, Luther, and Pugacz: Weldability Tests of Silicon-Manganese Steels. *Welding Jnl.* (Oct. 1942) **21** (10), 447S–484S.
8. Jackson, Luther, and Fritz: Weldability Tests of Silicon-Manganese Steels. *Welding Jnl.* (1944) **23** (1) 33S–43S.
9. Jackson and Luther: Weldability Tests of Nickel Steels. *Welding Jnl.* (1941) **20** (10), 437S–452S.
10. W. Crafts: Chromium in Structural Steels. *Trans.* A.I.M.E. (1939) **135**.

DISCUSSION

(R. K. Kulp presiding)

G. F. Comstock*—This paper seems to offer a worth-while refinement over previously offered methods for calculating the strength of steels of known composition. It should be of considerable value for comparing the useful strength of different kinds of steel when actual test data cannot readily be secured.

The writer was especially interested in the comments on the strengthening effect of titanium, which is shown to be less on ⅝ in. plate than on ½ in. plate. The author's suggestion that in plates 1 in. thick the strength of titanium steels might be the same whether as-rolled or normalized is supported by some data recently obtained in the laboratory of the Titanium Alloy Mfg. Co. on plates 1.5 in. thick of the same type of steel from which Fig 15 of this paper was derived. The titanium content of the 1.5-in. plate was 0.034 pct, and the test specimens were heat-treated after cutting to about 6 by 1 by 1.5 in., and tested after machining to ½ in. round with a gauge length of 2 in. Thus the data obtained refer only to the middle third of the 1.5-in. thickness. Averages of transverse tests are reported in Table 1. Lengthwise tests showed about the same relations, with higher ductility, but the corresponding comparable series was less complete. The yield-point data may not be strictly comparable because the normalized specimens were tested with an automatic stress-strain recorder, while the other yield points were determined with dividers.

Table 8—*Transverse Tensile Tests of* 1.5 *Inch Low-alloy Titanium Steel Plates Tested in* 0.5*-Inch Round Section*

Test	As Rolled	Tempered 4 Hr at 1115°F	Normalized 2 Hr at 1650°F
Yield point, psi.....	44,700	49,750	50,850
Tensile strength, psi...	67,550	68,350	68,050
Elongation in 2 in. pct	28.5	31.5	32.5
Reduction of Area, pct	51.5	52.3	55.4

This 1.5-in. plate as rolled is seen to be definitely inferior in both strength and ductility to the heat-treated samples, supporting the author's suggestion that in titanium-steel plates of over 1 in. thickness the strength may not be any higher as rolled than after normalizing. This relation is certainly quite different from the relation between the different conditions of ½-in. plates of titanium steel, where about 0.03 pct titanium would give very appreciably higher strength in the as-rolled condition than after normalizing. A possible

* Chief, Physical Metallurgy, The Titanium Alloy Mfg. Co., Niagara Falls, New York.

explanation is that the thicker plate is finished hotter and cools much more slowly than the thinner plate, so that the steel remains at temperatures between 2000° and 1600°F much longer. This allows the strengthening form of titanium, presumably the carbide in solid solution, to change to the ineffective (precipitated?) form in the as-rolled thicker plate, in the same way as is accomplished by normalizing of the thinner plate. The coarse grain size in the interior of the thicker as-rolled plate could no doubt be refined by suitable heat-treatment, and this may account for the improved properties reported above for the normalized samples. The higher strength of the tempered specimens however must be due to some other cause such as temper-hardening.

The authors should be complimented for suggesting that the strength of low-titanium alloy steel, when rolled to plates 1 in. thick or thicker, may not be greater in the as-rolled condition than after normalizing. The influence of plate thickness on this effect of titanium does not seem to have been generally appreciated previously, and if sufficiently confirmed by future data may indicate the advisability of normalizing all thick plates of this type of steel before use.

Boron in Certain Alloy Steels

By M. C. Udy* and P. C. Rosenthal,† Members AIME

(Atlantic City Meeting, November 1946)

The use of minute boron additions to steel has been given considerable attention in recent years. Comparisons made between boron-free and boron-containing heats of otherwise identical analysis have indicated, beyond a doubt, the potent effect of boron for increasing hardenability. The actual hardenability increase has been expressed as a multiplying factor, or in terms of the percentage of other alloying elements boron might replace.

The present study presents the results of a systematic survey of the use of boron as an addition to two types of alloyed steels and as a replacement for various percentages of molybdenum in these steels. Both cast and wrought steels of the two basic compositions were prepared. Molybdenum, because of its scarcity at the time the investigation was started, was selected as the element to be replaced by boron. Attention was also given to the effects of boron on other properties of the steels, particularly their notched-bar toughness, to investigate other advantages or limitations of this element as an alloy addition.

Experimental Work

Steels Investigated

The two basic compositions used in this survey of boron as a replacement for molybdenum are given in Table 1. The cast steels were higher than the wrought steels in silicon content to improve the casting quality.

Table 1.—*Nominal Composition of the Two Base Alloy Steels*

Alloy Steel	Type	Composition, Per Cent[a]				
		C	Mn	Si	Ni	Cr
Ni-Cr-Mo	Wrought	0.28–0.32	0.70–0.90	0.15–0.25	0.45–0.55	0.45–0.55
	Cast	0.28–0.32	0.70–0.90	0.35–0.45	0.45–0.55	0.45–0.55
Mn-Mo	Wrought	0.28–0.32	1.50–1.70	0.15–0.25		
	Cast	0.28–0.32	1.40–1.70	0.35–0.45		

[a] Sulphur was 0.040 per cent maximum and phosphorus 0.030 per cent maximum.

Each of these base steels, both cast and wrought, was made with molybdenum contents of 0, 0.10, 0.20, 0.30, or 0.40 per cent, the total comprising 20 steels. In addition, each of these 20 compositions was prepared with boron additions in amounts of 0.0015, 0.003, and 0.006 per cent as ferroboron; and in amounts of 0.002 and 0.005 per cent as two commercial intensifier alloys, designated alloys A and B. The boron-treated steels totaled 100, and the entire series 120.

Test Procedure

Each steel was melted as an individual heat in a 50-lb., magnesia-lined induction furnace. Ingot iron scrap or mixtures of ingot iron and steel scrap were used for melting stock. Deoxidation was carried out in the furnace with 0.10 per cent aluminum. The aluminum addition was

This paper is based on work done for the Office of Scientific Research and Development under Contract OEMsr-450 with Battelle Memorial Institute. Manuscript received at the office of the Institute March 8, 1946. Issued as T.P. 2085 in Metals Technology, October 1946.

* Research Engineer, Battelle Memorirl Institute, Columbus, Ohio.

† Formerly Assistant Supervisor, Battelle Memorial Institute; now Associate Professor, Dept. of Mining and Metallurgy, University of Wisconsin, Madison, Wisconsin.

TABLE 2.—*Chemical Analyses of Steels Treated with Various Amounts of Ferroboron or with Alloy A or Alloy B*

Heat No.	Addition Agent	Composition, Per Cent						
		C	Mn	Si	Ni	Cr	Mo	Added B
WROUGHT NICKEL-CHROMIUM-MOLYBDENUM STEELS								
8729		0.30	0.71	0.20	0.51	0.51	0	0
8749	Ferroboron	0.30	0.84	0.21	0.52	0.52	0	0.0015
8769	Ferroboron	0.32	0.84	0.22	0.53	0.52	0	0.003
8789	Ferroboron	0.30	0.81	0.20	0.54	0.54	0.007	0.006
9192	Alloy A	0.29	0.82	0.18	0.53	0.54	0	0.002
9234	Alloy B	0.29	0.89	0.24	0.52	0.53	0	0.005
8730		0.29	0.69	0.16	0.50	0.52	0.10	0
8750	Ferroboron	0.31	0.77	0.17	0.53	0.53	0.10	0.0015
8770	Ferroboron	0.32	0.86	0.23	0.52	0.52	0.10	0.003
8790	Ferroboron	0.29	0.76	0.19	0.54	0.53	0.10	0.006
9193	Alloy A	0.28	0.83	0.19	0.53	0.54	0.10	0.002
9235	Alloy B	0.30	0.87	0.23	0.52	0.53	0.11	0.005
8882		0.32	0.86	0.24	0.54	0.53	0.20	0
8751	Ferroboron	0.31	0.79	0.18	0.53	0.53	0.21	0.0015
8771	Ferroboron	0.31	0.82	0.22	0.52	0.50	0.21	0.003
8791	Ferroboron	0.30	0.76	0.18	0.52	0.52	0.21	0.006
9194	Alloy A	0.29	0.81	0.21	0.53	0.54	0.20	0.002
9236	Alloy B	0.29	0.85	0.23	0.53	0.53	0.20	0.005
8732		0.30	0.72	0.20	0.52	0.52	0.29	0
8752	Ferroboron	0.31	0.84	0.23	0.53	0.52	0.32	0.0015
8772	Ferroboron	0.32	0.82	0.21	0.52	0.51	0.31	0.003
8792	Ferroboron	0.31	0.81	0.20	0.52	0.51	0.30	0.006
9195	Alloy A	0.29	0.86	0.21	0.53	0.53	0.29	0.002
9237	Alloy B	0.28	0.76	0.20	0.51	0.52	0.31	0.005
8733		0.30	0.73	0.20	0.48	0.51	0.39	0
8753	Ferroboron	0.31	0.83	0.21	0.53	0.52	0.42	0.0015
8773	Ferroboron	0.32	0.83	0.22	0.52	0.51	0.41	0.003
8793	Ferroboron	0.32	0.82	0.20	0.52	0.52	0.39	0.006
9196	Alloy A	0.31	0.83	0.20	0.53	0.54	0.40	0.002
9238	Alloy B	0.29	0.86	0.25	0.51	0.52	0.38	0.005
WROUGHT MANGANESE-MOLYBDENUM STEELS								
8883		0.30	1.61	0.23			0	0
8754	Ferroboron	0.32	1.60	0.26			0	0.0015
8774	Ferroboron	0.32	1.60	0.23			0	0.003
8794	Ferroboron	0.30	1.55	0.24			0	0.006
8997	Alloy A	0.29	1.61	0.16			0.02	0.002
9260	Alloy B	0.30	1.63	0.25			0	0.005
8884		0.29	1.62	0.24			0.12	0
8755	Ferroboron	0.32	1.64	0.26			0.10	0.0015
8775	Ferroboron	0.32	1.58	0.22			0.12	0.003
8795	Ferroboron	0.30	1.54	0.23			0.10	0.006
8998	Alloy A	0.31	1.61	0.18			0.11	0.002
9261	Alloy B	0.29	1.64	0.25			0.11	0.005
8736		0.29	1.52	0.19			0.19	0
8756	Ferroboron	0.31	1.58	0.26			0.20	0.0015
8776	Ferroboron	0.30	1.57	0.21			0.21	0.003
8796	Ferroboron	0.30	1.56	0.24			0.20	0.006
8999	Alloy A	0.29	1.59	0.19			0.21	0.002
9262	Alloy B	0.29	1.65	0.26			0.21	0.005
8737		0.29	1.50	0.20			0.30	0
8757	Ferroboron	0.31	1.60	0.27			0.30	0.0015
8777	Ferroboron	0.31	1.55	0.23			0.32	0.003
8797	Ferroboron	0.30	1.56	0.25			0.31	0.006
9287	Alloy A	0.30	1.70	0.27			0.32	0.002
9263	Alloy B	0.30	1.62	0.25			0.31	0.005
8738		0.30	1.53	0.22			0.38	0
9067	Ferroboron	0.29	1.56	0.21			0.40	0.0015
8778	Ferroboron	0.30	1.60	0.24			0.42	0.003
8798	Ferroboron	0.30	1.56	0.21			0.42	0.006
9288	Alloy A	0.31	1.76	0.28			0.42	0.002
9264	Alloy B	0.30	1.57	0.24			0.40	0.005

TABLE 2.—(*Continued*)

Heat No.	Addition Agent	Composition, Per Cent						
		C	Mn	Si	Ni	Cr	Mo	Added B
CAST NICKEL-CHROMIUM-MOLYBDENUM STEELS								
8739		0.29	0.73	0.38	0.54	0.51	0	0
8759	Ferroboron	0.30	0.80	0.35	0.53	0.53	0	0.0015
8779	Ferroboron	0.29	0.83	0.38	0.52	0.51	0	0.003
8799	Ferroboron	0.30	0.79	0.37	0.52	0.51	0	0.006
9275	Alloy A	0.31	0.85	0.42	0.52	0.51	0	0.002
9265	Alloy B	0.31	0.91	0.46	0.47	0.52	0	0.005
8740		0.29	0.72	0.36	0.53	0.52	0.10	0
8760	Ferroboron	0.31	0.79	0.34	0.52	0.61	0.09	0.0015
8780	Ferroboron	0.30	0.78	0.34	0.51	0.51	0.10	0.003
8800	Ferroboron	0.31	0.84	0.38	0.53	0.42	0.11	0.006
9276	Alloy A	0.32	0.86	0.45	0.52	0.51	0.07	0.002
9266	Alloy B	0.32	0.88	0.46	0.48	0.52	0.12	0.005
8741		0.27	0.75	0.35	0.52	0.51	0.19	0
8761	Ferroboron	0.30	0.68	0.37	0.54	0.52	0.19	0.0015
8781	Ferroboron	0.30	0.82	0.36	0.52	0.52	0.21	0.003
8801	Ferroboron	0.30	0.87	0.41	0.53	0.51	0.21	0.006
9277	Alloy A	0.31	0.85	0.45	0.77	0.55	0.20	0.002
9267	Alloy B	0.31	0.89	0.46	0.49	0.52	0.22	0.005
8879		0.30	0.86	0.40	0.53	0.52	0.30	0
8762	Ferroboron	0.30	0.87	0.38	0.53	0.50	0.29	0.0015
8782	Ferroboron	0.30	0.84	0.39	0.52	0.51	0.30	0.003
8802	Ferroboron	0.30	0.82	0.38	0.53	0.51	0.32	0.006
9278	Alloy A	0.32	0.83	0.48	0.53	0.52	0.31	0.002
9268	Alloy B	0.32	0.88	0.45	0.49	0.53	0.32	0.005
8743		0.27	0.74	0.39	0.52	0.51	0.42	0
8763	Ferroboron	0.28	0.78	0.37	0.54	0.52	0.41	0.0015
8783	Ferroboron	0.30	0.81	0.36	0.53	0.52	0.41	0.003
8803	Ferroboron	0.29	0.84	0.39	0.52	0.51	0.41	0.006
9279	Alloy A	0.31	0.87	0.49	0.53	0.51	0.40	0.002
9269	Alloy B	0.32	0.87	0.44	0.49	0.53	0.43	0.005
CAST MANGANESE-MOLYBDENUM STEELS								
8744		0.28	1.40	0.36			0	0
8764	Ferroboron	0.29	1.60	0.42			0	0.0015
8784	Ferroboron	0.30	1.57	0.44			0	0.003
8804	Ferroboron	0.29	1.56	0.36			0	0.006
9182	Alloy A	0.31	1.60	0.40			0	0.002
9270	Alloy B	0.33	1.66	0.46			0	0.005
8745		0.27	1.39	0.37			0.10	0
8765	Ferroboron	0.32	1.62	0.42			0.10	0.0015
8785	Ferroboron	0.27	1.54	0.44			0.10	0.003
8805	Ferroboron	0.31	1.59	0.44			0.11	0.006
9183	Alloy A	0.28	1.54	0.39			0.10	0.002
9271	Alloy B	0.32	1.68	0.46			0.11	0.005
8880		0.32	1.61	0.39			0.21	0
8766	Ferroboron	0.29	1.62	0.44			0.21	0.0015
8786	Ferroboron	0.30	1.58	0.42			0.20	0.003
8806	Ferroboron	0.30	1.59	0.42			0.21	0.006
9184	Alloy A	0.29	1.56	0.40			0.20	0.002
9272	Alloy B	0.30	1.65	0.46			0.21	0.005
8881		0.29	1.62	0.40			0.30	0
8767	Ferroboron	0.30	1.60	0.39			0.31	0.0015
8787	Ferroboron	0.25	1.53	0.40			0.31	0.003
8807	Ferroboron	0.31	1.62	0.46			0.31	0.006
9185	Alloy A	0.29	1.55	0.39			0.29	0.002
9273	Alloy B	0.31	1.66	0.48			0.32	0.005
8748		0.27	1.43	0.36			0.40	0
9068	Ferroboron	0.32	1.62	0.43			0.41	0.0015
8788	Ferroboron	0.29	1.54	0.40			0.42	0.003
8808	Ferroboron	0.30	1.56	0.40			0.42	0.006
9186	Alloy A	0.29	1.57	0.38			0.39	0.002
9274	Alloy B	0.31	1.63	0.48			0.40	0.005

timed at one minute before pouring, and additions of ferroboron, alloy A, or alloy B, if required, were made ½ min. later. The amount and the time for the addition of the other alloys were standardized as much as possible.

The wrought steels were cast into 50-lb. ingot molds and forged and rolled to size; the cast steels were poured into oil-sand core molds of double-legged keel blocks commonly used for cast-steel test-bar stock. The keels measured 1¼ by 1⅛ by 15 inches.

Hardenability specimens for the wrought steels were machined from 1⅛-in. forgings, while notched-bar specimens were cut from 9/16-in. square bar stock that had been rolled down from the forged bars. For some of the tests, hardenability specimens for the cast steels were cut out of the head of the keel blocks. Later in the melting program, an enlarged section was provided on one end of one keel of the keel block so that the end-quench test bar could be machined from this enlarged section without resorting to the use of metal from the head of the keel-block casting. Notched-bar specimens for the cast steels were taken from the portion of the keel remaining after removal of the end-quench specimens.

The cast steels were homogenized at 1900°F. for 2½ hr. and the wrought steels were normalized at 1700°F. for 1 hr. before machining and final heat-treatment. Austenitizing for 20 min. at 1575° or 1600°F., depending on whether the steel was of the nickel-chromium-molybdenum type or of the manganese-molybdenum type, preceded water quenching of the hardenability specimens and of the rough-machined notched-bar specimens. Standard procedures were used for the end-quench tests.

V-notch Charpy impact specimens from cast steels were tempered to a range of 270 to 290 Brinell, and those from the wrought steels were tempered to 350 to 370 Brinell. Tempering was done in a stepwise manner with the temperature gradually raised until the desired hardness was obtained. Specimens were water-quenched from the tempering temperatures. Notches were machined and specimens ground after the final heat-treatments. Notched-bar tests were made at temperatures of +75° to −80°F.; at least two specimens were broken at each testing temperature.

Chemical Analyses

Samples for analysis were drilled from the keel-block heads and from the ingot hot tops, and occasional check samples were taken from used test specimens. The chemical analyses of the various steels are given in Table 2. Only in a few cases are the deviations in composition within each series sufficient to have a noticeable effect on hardenability. This makes it very convenient to compare the effects of the various types of boron additions.

The analyses of the boron alloys are given in Table 3. All three grades were obtained from commercial producers.

TABLE 3.—*Analysis of Boron Alloys*[a]
PER CENT

Constituent	Ferro-boron[b]	Alloy A	Alloy B
Silicon		3.4	37.66
Calcium			9.76
Zirconium		3.6	3.88
Titanium		19.6	9.39
Aluminum		13.0	7.16
Boron	11.2	0.54	1.38
Manganese		7.5	
Copper		1.7	
Carbon		0.05	
Iron	Balance	Balance	Balance

[a] These analyses are of one particular lot of each alloy. Other lots undoubtedly will deviate slightly from the percentages given.

[b] No analyses for other elements in the ferroboron were made, but carbon, silicon, and aluminum may be present in minor quantities as impurities.

DISCUSSION OF RESULTS

Boron Recovery

A number of the heats were analyzed for boron, using the quinalizarin method

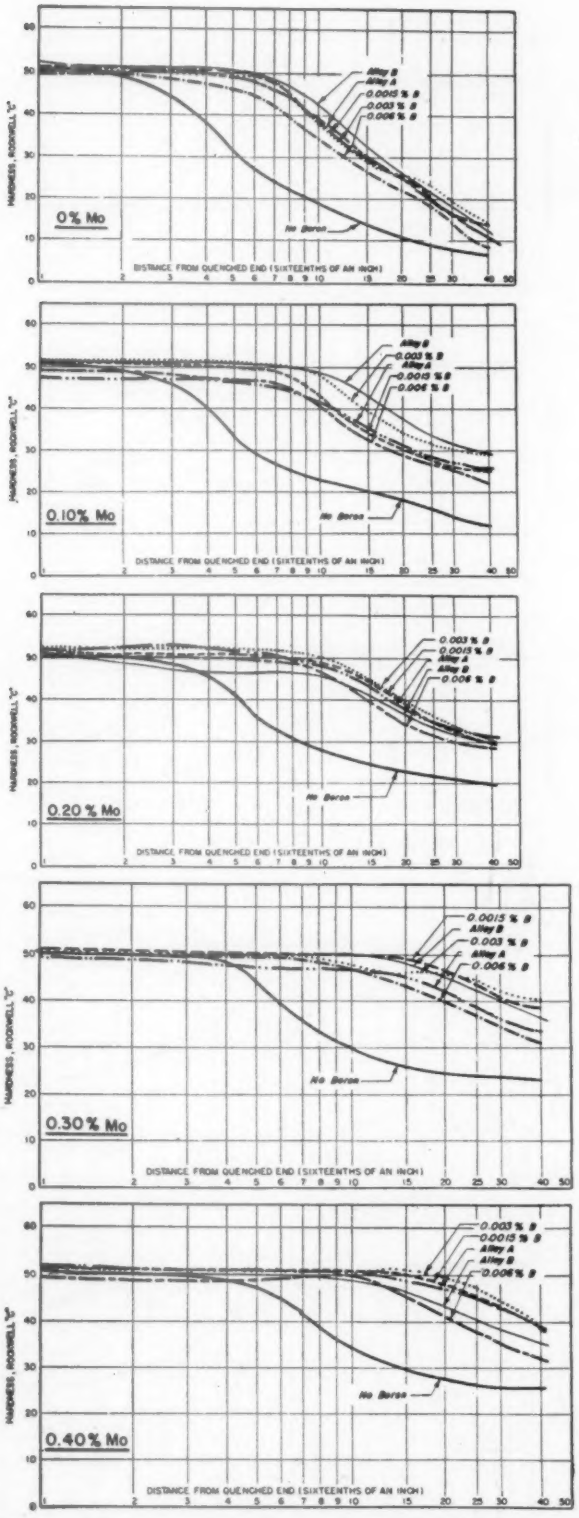

FIG. 1.—END-QUENCH HARDENABILITY CURVES FOR WROUGHT NICKEL-CHROMIUM-MOLYBDENUM STEELS GROUPED ACCORDING TO MOLYBDENUM CONTENTS.

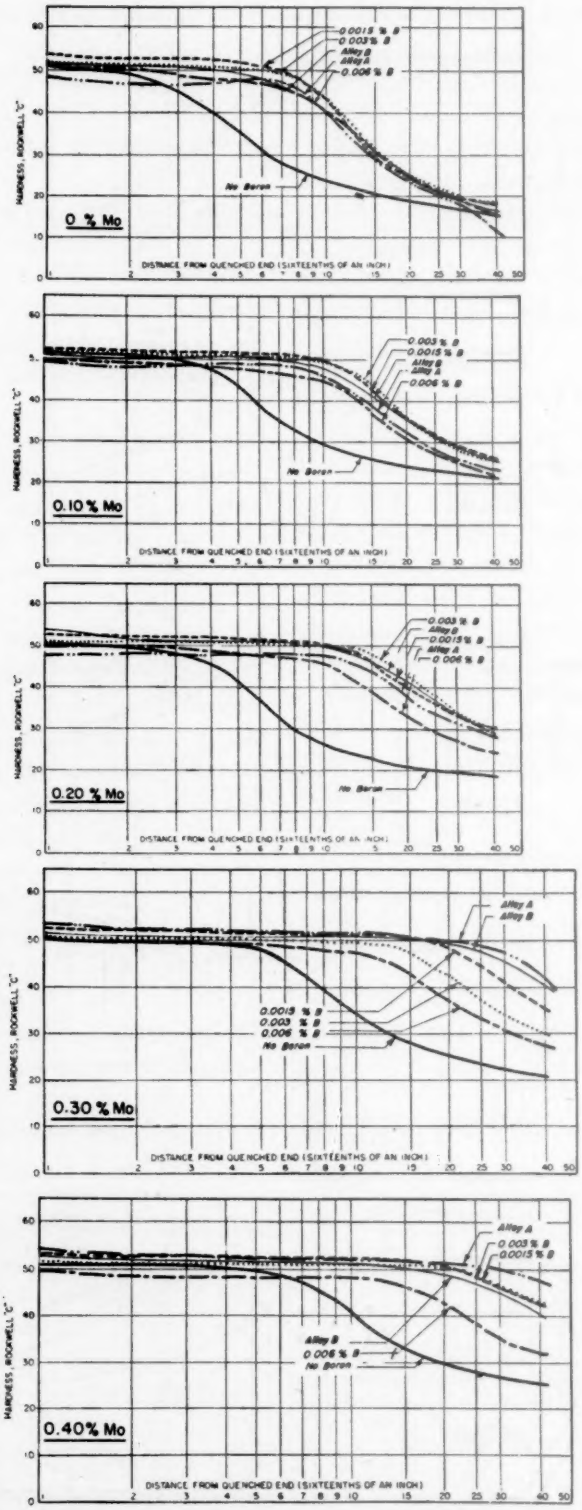

FIG. 2.—END-QUENCH HARDENABILITY CURVES FOR WROUGHT MANGANESE-MOLYBDENUM TYPE STEELS GROUPED ACCORDING TO MOLYBDENUM CONTENTS.

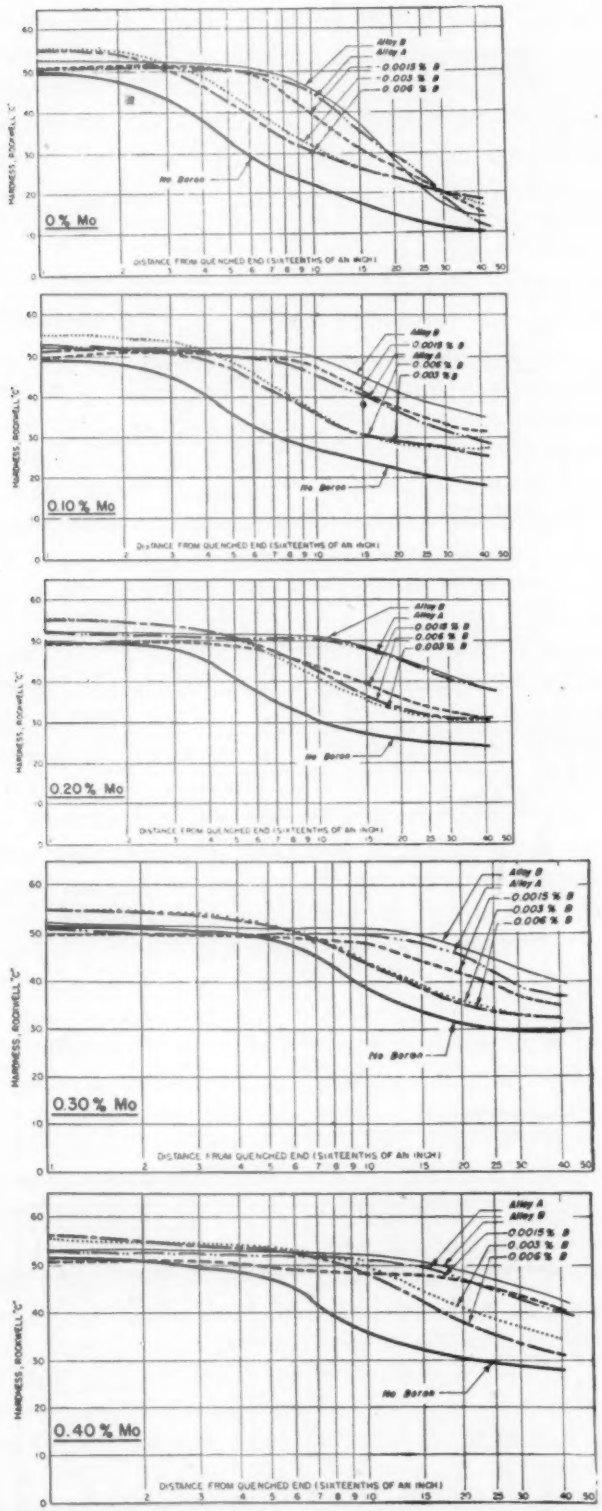

FIG. 3.—END-QUENCH HARDENABILITY CURVES FOR CAST NICKEL-CHROMIUM-MOLYBDENUM STEELS GROUPED ACCORDING TO MOLYBDENUM CONTENTS.

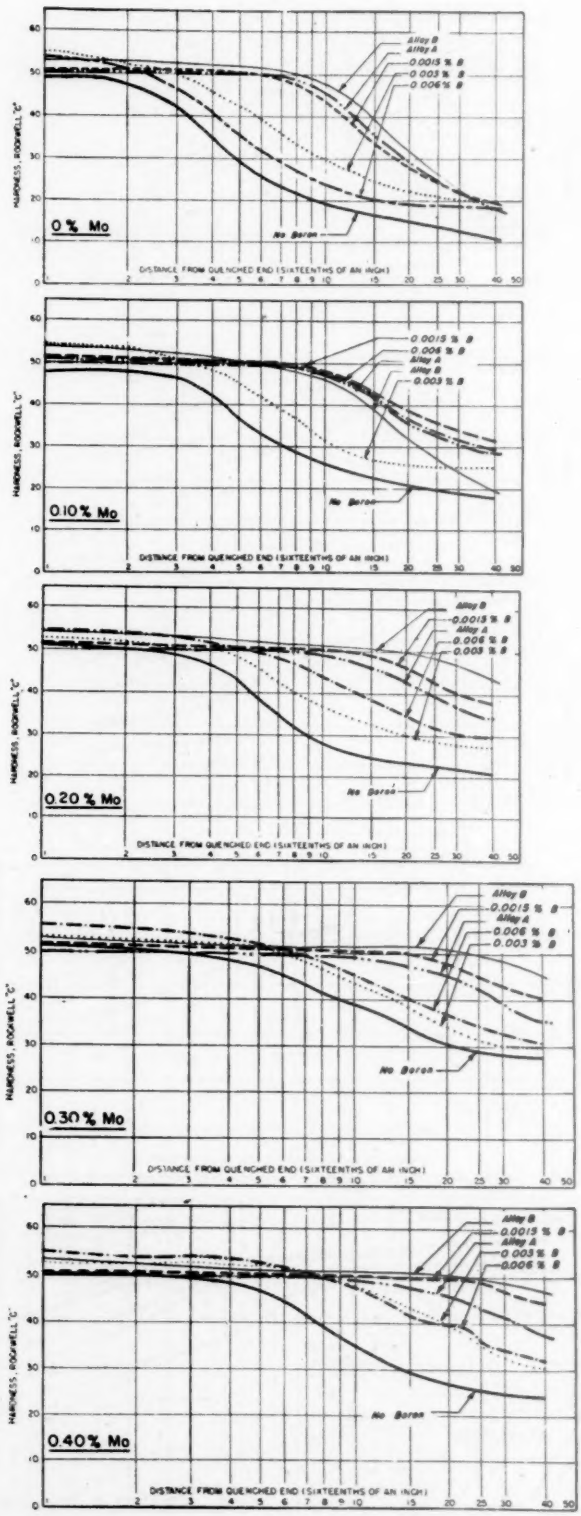

FIG. 4.—END-QUENCH HARDENABILITY CURVES FOR CAST MANGANESE-MOLYBDENUM STEELS GROUPED ACCORDING TO MOLYBDENUM CONTENTS.

of analysis. Generally, good boron recoveries were obtained. However, because it is possible that the boron analysis may be incorrect by a considerable percentage, only the percentage of boron added to the heat has been considered in comparing the effects of boron on hardenability and other properties.

Hardenability

Figs. 1 through 4 show end-quench hardenability curves, and Table 4 gives data for estimating the boron hardenability factor of the experimental steels. The estimated ideal critical diameter (column 6) involves two assumptions: (1) a hardness of 38 Rockwell C on the end-quench bar corresponds to a 50 per cent martensite structure;[1] (2) the relationship, developed by Grossmann,[1] between the 50 per cent martensite point and the ideal critical diameter is valid.

The first assumption is necessary in order that results may be compared with data available for hardenability factors for other alloy elements. However, the limitations of this criterion of hardenability for alloy steels must be recognized and will be discussed later in connection with metallographic examinations. The fact that the base alloys used in this investigation have similar depth-hardening characteristics (compare curves for boron-free steels in Figs. 1 to 4) indicates that a reasonably good comparison of hardenability would be obtained where a point of inflection is found on the curve, regardless of what hardness drop was taken as a measure of hardenability. Further, since the ratios of estimated ideal critical diameter are used, any constant error in the estimated ideal critical diameter largely cancels out.

The second assumption; namely, that the curve relating estimated ideal critical diameters and distance in the end-quench bar to a 50 per cent martensite structure is valid, seems a safe one to make in view of the experiences of others, particularly with regard to steels having ideal critical diameters exceeding about 2.0 inches.*

To compensate for the slight variations in other alloying elements from heat to heat, the estimated ideal critical diameters of the wrought and cast steels of each type were corrected (using Grossmann's factors) to a base analysis that was approximately representative of the series.

No corrections were made if the carbon, manganese, and chromium differed from the base analyses by 0.01 per cent, if the silicon and molybdenum contents deviated by 0.02 per cent or less, and if the nickel content deviated by 0.03 per cent or less. The corrected, estimated ideal critical diameters are listed in column 7 of Table 4. By correcting the ideal critical diameter in the manner described rather than by calculating the hardenability for each composition, the calculations were simplified, and the ratios of the D_I values for the boron-containing heats to those of the boron-free heats of like composition give the various boron factors directly.

When the boron factors were calculated by dividing the estimated ideal critical diameters of the various boron-containing heats by the estimated ideal critical diameter of the comparable boron-free heat, it was found that very large boron factors were obtained for some steels, particularly for most of the steels containing about 0.20 per cent molybdenum. This situation suggested that some of the estimated ideal critical diameters for the boron-free steels erred on the low side to account for the abnormally high boron factors.

To check this, the estimated ideal critical diameters of the boron-free steels, corrected to a base composition were plotted against the molybdenum con-

[1] References are at the end of the paper.

* See discussion and Fig. 22 of Reference 3.

TABLE 4.—*Determination of Boron Factors*

Heat No.	Addition Agent	Added Boron, Per Cent	Fracture Grain Size[a]	Distance on End-quench Bar to 38 R_c, 16ths[b]	Estimated Ideal Critical Diameter D_I, In.[c]	Estimated D_I Corrected to Base Analysis, In.[d]	Ratio, D_I of Boron Heats to D_I of Base Compositions Derived from Fig. 5[e]
Wrought Steels, Ni-Cr-Mo Type							
Base Analysis: 0.30 C, 0.85 Mn, 0.20 Si, 0.52 Ni, 0.52 Cr, 0 Mo, D_I = 2.05 inches							
8729		0		3.75	1.80	2.05	
8749	FeB	0.0015	7	10.50	3.42	3.42	1.67
8769	FeB	0.003	7	10.0	3.32	3.18	1.55
8789	FeB	0.006	7	8.75	3.07	3.11	1.52
9192	A	0.002	7	10.75	3.47	3.51	1.71
9234	B	0.005	7	12.0	3.70	3.53	1.72
Base Analysis: 0.30 C, 0.85 Mn, 0.20 Si, 0.52 Ni, 0.52 Cr, 0.10 Mo, D_I = 2.50 inches							
8730		0		4.5	2.07	2.49	
8750	FeB	0.0015	7	12.5	3.80	4.18	1.67
8770	FeB	0.003	7	16.0	4.45	4.20	1.68
8790	FeB	0.006	7	11.0	3.50	3.76	1.50
9193	A	0.002	7	13.0	3.90	4.04	1.61
9235	B	0.005	7	20.0	5.06	4.84	1.93
Base Analysis: 0.30 C, 0.85 Mn, 0.20 Si, 0.52 Ni, 0.52 Cr, 0.20 Mo, D_I = 2.90 inches							
8882		0	7–8	5.75	2.40	2.23	
8751	FeB	0.0015	7	21.5	5.28	5.65	1.95
8771	FeB	0.003	7–8	23.0	5.50	5.69	1.96
8791	FeB	0.006	7	16.5	4.53	4.99	1.72
9194	A	0.002	7	21.0	5.20	5.28	1.82
9236	B	0.005	7	18.5	4.84	4.72	1.63
Base Analysis: 0.30 C, 0.85 Mn, 0.20 Si, 0.52 Ni, 0.52 Cr, 0.30 Mo, D_I = 3.30 inches							
8732		0		6.5	2.58	2.91	
8752	FeB	0.0015	7	40.0+	7.55+	7.55+	2.28+
8772	FeB	0.003	7	40.0+	7.55+	7.55+	2.28+
8792	FeB	0.006	6–7	23.5	5.56	5.77	1.74
9195	A	0.002		27.0	6.00	6.00	1.81
9237	B	0.005	7–8	36.0	7.10	8.00	2.42
Base Analysis: 0.30 C, 0.85 Mn, 0.20 Si, 0.52 Ni, 0.52 Cr, 0.40 Mo, D_I = 3.75 inches							
8733		0	7	8.5	3.0	3.40	
8753	FeB	0.0015		40.0+	7.55+	7.55+	2.01+
8773	FeB	0.003	7	40.0	7.55	7.31	1.94
8793	FeB	0.006	7	25.0	5.75	5.73	1.53
9196	A	0.002	7	40.0+	7.55+	7.55+	2.01+
9238	B	0.005	7	32.0	6.63	6.57	1.75
Wrought Steels, Mn-Mo Type							
Base Analysis: 0.30 C, 1.60 Mn, 0.24 Si, 0Mo, D_I = 2.05 inches							
8883		0	7	4.5	2.07	2.07	
8754	FeB	0.0015	7–8	11.75	3.65	3.55	1.73
8774	FeB	0.003	7	12.0	3.72	3.72	1.81
8794	FeB	0.006	6–7	11.5	3.56	3.66	1.78
8997	A	0.002	7	11.0	3.50	3.68	1.79
9260	B	0.005	7	11.0	3.50	3.42	1.67

[a] Obtained by comparing fractured ends of end-quench bar with Shepherd's standard fractures.
[b] The approximate hardness corresponding to a 50 per cent martensitic structure in steels of 0.28 to 0.32 per cent C. (See Ref. 1.)
[c] Relationship between end-quench-bar distance and "estimated ideal critical diameter" obtained from paper of Ref. 2.
[d] Factors given by Grossmann were used to correct to the stated base analysis.
[e] This column gives the boron factors.

TABLE 4.—(*Continued*)

Heat No.	Addition Agent	Added Boron, Per Cent	Fracture Grain Size[a]	Distance on End-quench Bar to 38 R_c, 16ths[b]	Estimated Ideal Critical Diameter D_I, In.[c]	Estimated D_I Corrected to Base Analysis, In.[d]	Ratio, D_I of Boron Heats to D_I of Base Compositions Derived from Fig. 5[e]
Base Analysis: 0.30 C, 1.60 Mn, 0.24 Si, 0.11 Mo, D_I = 2.50 inches							
8884		0	7	6.25	2.52	2.48	
8755	FeB	0.0015	7	18.5	4.83	4.49	1.79
8775	FeB	0.003	7	19.0	4.92	4.88	1.95
8795	FeB	0.006	7	15.0	4.27	4.40	1.76
8998	A	0.002	7	16.0	4.45	4.62	1.84
9261	B	0.005	7	18.0	4.76	4.67	1.87
Base Analysis: 0.30 C, 1.60 Mn, 0.24 Si, 0.20 Mo, D_I = 2.90 inches							
8730		0		5.75	2.40	2.60	
8756	FeB	0.0015	7	22.5	5.43	5.41	1.86
8776	FeB	0.003	7	25.0	5.75	5.98	2.06
8796	FeB	0.006	7	16.0	4.45	4.54	1.56
8999	A	0.002	7	20.0	5.06	5.25	1.81
9262	B	0.005	7–8	24.0	5.63	5.40	1.86
Base Analysis: 0.30 C, 1.60 Mn, 0.24 Si, 0.31 Mo, D_I = 3.30 inches							
8737		0		8.75	3.07	3.33	
8757	FeB	0.0015	7	36.0	7.10	6.97	2.11
8777	FeB	0.003	7	25.0	5.75	5.92	1.79
8797	FeB	0.006	6–7	19.5	4.98	5.09	1.54
9287	A	0.002	7	40.0+	7.55+	7.55+	2.28+
9263	B	0.005	7	40.0+	7.55+	7.55+	2.28+
Base Analysis: 0.30 C, 1.60 Mn, 0.24 Si, 0.40 Mo, D_I = 3.75 inches							
8738		0		11.0	3.50	3.78	
9067	FeB	0.0015		40.0+	7.55+	7.55+	2.01+
8778	FeB	0.003	7	40.0+	7.55+	7.55+	2.01+
8798	FeB	0.006	6–7	26.0	5.88	5.96	1.58
9288	A	0.002	7	40.0+	7.55+	7.55+	2.01+
9264	B	0.005	7	40.0+	7.55+	7.55+	2.01+
Cast Steels, Ni-Cr-Mo Type							
Base Analysis: 0.30 C, 0.85 Mn, 0.38 Si, 0.52 Ni, 0.51 Cr, 0Mo, D_I = 2.05 inches							
8739		0	7	4.0	1.93	2.14	
8759	FeB	0.0015	7	11.0	3.50	3.67	1.79
8779	FeB	0.003	7	7.0	2.69	2.74	1.33
8799	FeB	0.006	6–7	6.5	2.58	2.73	1.33
9275	A	0.002		13.0	3.90	3.82	1.86
9265	B	0.005	7	14.5	4.17	3.88	1.89
Base Analysis: 0.30 C, 0.85 Mn, 0.38 Si, 0.52 Ni, 0.51 Cr, 0.10 Mo, D_I = 2.50 inches							
8740		0	7	4.5	2.07	2.38	
8760	FeB	0.0015	7	20.0	5.06	4.98	1.99
8780	FeB	0.003	7	9.5	3.23	3.55	1.42
8800	FeB	0.006		9.0	3.12	3.44	1.38
9276	A	0.002	7	19.0	4.92	4.96	1.98
9266	B	0.005	7	30.0	6.38	5.78	2.31
Base Analysis: 0.30 C, 0.85 Mn, 0.38 Si, 0.52 Ni, 0.51 Cr, 0.20 Mo, D_I = 2.90 inches							
8741		0	7	6.0	2.46	2.90	
8761	FeB	0.0015	7	17.0	4.60	5.36	1.85
8781	FeB	0.003	7	12.5	3.81	3.99	1.37
8801	FeB	0.006		14.0	4.10	3.97	1.36
9277	A	0.002	7	40.0+	7.55+	7.55+(?)	2.60+(?)
9267	B	0.005	7	40.0+	7.55+	7.55+	2.60+

TABLE 4.—(*Continued*)

Heat No.	Addition Agent	Added Boron, Per Cent	Fracture Grain Size[a]	Distance on End-quench Bar to 38 R_c, 16ths[b]	Estimated Ideal Critical Diameter D_I, In.[c]	Estimated D_I Corrected to Base Analysis, In.[d]	Ratio, D_I of Boron Heats to D_I of Base Compositions Derived from Fig. 5[e]
Base Analysis: 0.30 C, 0.85 Mn, 0.38 Si, 0.52 Ni, 0.51 Cr, 0.30 Mo, D_I = 3.30 inches							
8879		0	7	11.0	3.50	3.47	
8762	FeB	0.0015	7	28.0	6.13	6.02	1.82
8782	FeB	0.003	7	16.5	4.53	4.53	1.37
8802	FeB	0.006	6–7	16.0	4.45	4.39	1.33
9278	A	0.002	7	36.0	7.10	6.65	2.01
9268	B	0.005	7	40.0+	7.55+	7.55+(?)	2.28+(?)
Base Analysis: 0.30 C, 0.85 Mn, 0.38 Si, 0.52 Ni, 0.51 Cr, 0.41 Mo, D_I = 3.75 inches							
8743		0	7	8.75	3.07	3.59	
8763	FeB	0.0015	7	40.0+	7.55+	7.55+	2.01+
8783	FeB	0.003	7	27.0	6.00	6.32	1.68
8803	FeB	0.006	6–7	20.0	5.06	5.06	1.34
9279	A	0.002	7	40.0+	7.55+	7.55+	2.01+
9269	B	0.005	7	40.0+	7.55+	7.55+	2.01+
Cast Steels, Mn-Mo Type							
Base Analysis: 0.30 C, 1.60 Mn, 0.40 Si, 0Mo, D_I = 2.05 inches							
8744		0	7	3.5	1.79	2.13	
8764	FeB	0.0015	7	13.0	3.90	3.86	1.88
8784	FeB	0.003	7	6.5	2.58	2.56	1.24
8804	FeB	0.006	7	4.5	2.07	2.17	1.06
9182	A	0.002	7	14.0	4.10	4.10	1.99
9270	B	0.005	7	16.0	4.45	4.00	1.95
Base Analysis: 0.30 C, 1.60 Mn, 0.40 Si, 0.10 Mo, D_I = 2.50 inches							
8745		0	7	4.75	2.13	2.56	
8765	FeB	0.0015	7	22.0	5.35	5.07	2.02
8785	FeB	0.003	7	7.75	2.86	3.05	1.22
8805	FeB	0.006	7	19.0	4.92	4.82	1.93
9183	A	0.002	7	18.0	4.76	5.11	2.04
9271	B	0.005	7	16.0	4.45	4.01	1.60
Base Analysis: 0.30 C, 1.60 Mn, 0.40 Si, 0.20 Mo, D_I = 2.90 inches							
8880		0	7	6.25	2.52	2.46	
8766	FeB	0.0015	7	40.0	7.55	7.31	2.51
8786	FeB	0.003	7	9.5	3.23	3.23	1.29
8806	FeB	0.006	7	16.0	4.45	4.41	1.52
9184	A	0.002	7	29.0	6.26	6.41	2.21
9272	B	0.005	7	40.0+	7.55+	7.55+	2.60+
Base Analysis: 0.30 C, 1.62 Mn, 0.40 Si, 0.30 Mo, D_I = 3.30 inches							
8881		0	7	11.25	3.55	3.55	
8767	FeB	0.0015	7	40.0+	7.55+	7.55+	2.28+
8787	FeB	0.003	7	16.0	4.45	5.92	1.79
8807	FeB	0.006	7	18.0	4.76	4.63	1.40
9185	A	0.002	6–7	33.0	6.75	7.02	2.12
9273	B	0.005	7	40.0+	7.55+	7.55+(?)	2.28+(?)
Base Analysis: 0.30 C, 1.62 Mn, 0.40 Si, 0.41 Mo, D_I = 3.75 inches							
8748		0	7	8.75	3.07	3.70	
9068	FeB	0.0015	7	40.0+	7.55+	7.55+	2.01+
8788	FeB	0.003	6–7	22.0	5.35	5.58	1.48
8808	FeB	0.006	6–7	24.0	5.63	5.82	1.55
9186	A	0.002	7	40.0+	7.55+	7.55+	2.01+
9274	B	0.005	7	40.0+	7.55+	7.55+	2.01+

tents. These results, Fig. 5, verify the previous indication that the estimated ideal critical diameters for most of the boron-free steels containing 0.20 per

1. The reactions of the two types of alloy steels (Ni-Cr-Mo and Mn-Mo) to boron additions were similar. Additions of 0.0015 or 0.003 per cent boron as

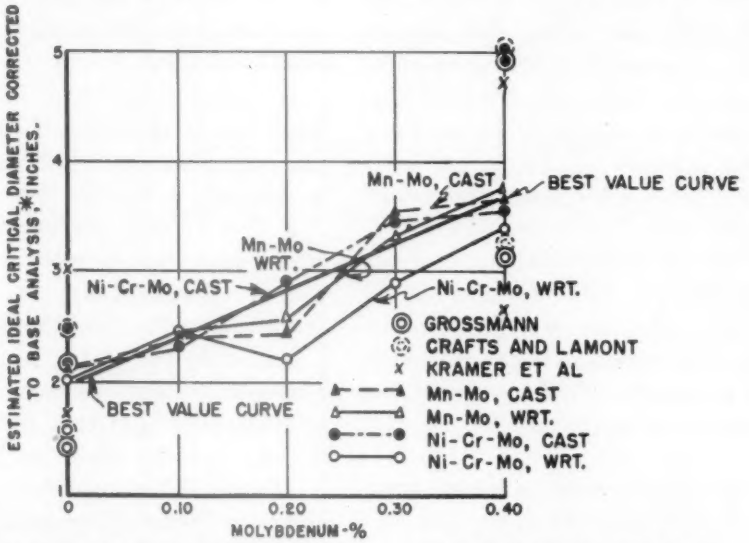

* NICKEL-CHROMIUM—MOLYBDENUM

	WROUGHT	CAST
C	0.30	0.30
Mn	0.85	0.85
Si	0.20	0.38
Ni	0.52	0.52
Cr	0.52	0.51

MANGANESE—MOLYBDENUM

WROUGHT	CAST
0.30	0.30
1.60	1.60
0.24	0.40
——	——
——	——

FIG. 5.—RELATIONSHIP BETWEEN THE IDEAL CRITICAL DIAMETER (ESTIMATED FROM THE END QUENCH CURVE AND CORRECTED TO THE BASE ANALYSES GIVEN BELOW) AND THE MOLYBDENUM CONTENT.

cent molybdenum were low compared with those of steels having higher or lower molybdenum contents. If it is assumed that the low values depicted in Fig. 5 actually are in error, a reasonable approximation of the true ideal critical diameters can be obtained by drawing a curve through what appears to be the best values. This curve is shown in Fig. 5, and the estimated ideal critical diameters it gives for each molybdenum content were used to calculate the boron factors given in column 8 of Table 4.

By comparison of Figs. 1 through 4, the following general observations on the influence of boron on hardenability are noted:

ferroboron, additions of 0.002 per cent boron as alloy A or of 0.005 per cent boron as alloy B were about equally effective in increasing the depth of hardness of these steels. Variations in the effect of these four additions occurred, but these variations were not consistently in one direction.

2. In steels ranging from 0 to 0.40 per cent molybdenum, a 0.006 per cent boron addition gave slightly less hardenability than smaller additions. This and the observation that a 0.0015 per cent boron addition was about as good as one of 0.003 per cent, substantiates the findings of others[1,2] that the increase in hardenability contributed by boron is not a

direct function of the quantity of boron added, and that beyond a certain point, hardenability actually decreases.

3. If the hardenability increases obtained from a fixed boron addition are compared, it is found that the increase is not constant in steels of different molybdenum contents. Thus, the hardenability increase that is developed by a 0.0015 per cent boron addition to the 0 per cent molybdenum steel of the nickel-chromium-molybdenum type is not so great as for the same type of steel containing 0.30 per cent molybdenum. This example would seem to indicate that molybdenum increases the effectiveness of boron. Although this trend is apparent in the wrought steels, it is not definitely established for the cast steels.

4. An unexpected reaction of the cast steels to ferroboron treatment was encountered. With one exception (a manganese-molybdenum steel containing 0.11 per cent molybdenum and treated with 0.006 per cent boron), all additions of ferroboron equivalent to 0.003 or 0.006 per cent boron resulted in a decrease in the depth of hardness penetration, and an increase in the hardness at the quenched end of the test bar. This is clearly seen from the end-quench curves in Figs. 3 and 4. The frequency of this occurrence in the present series, and the fact that it was also found in cast silicon-deoxidized steels treated with alloy A made for another test, (see later discussion on Importance of Deoxidation), suggest a metallurgical cause. Except for this effect, there was little difference in hardenability of wrought and cast steel of similar analysis and boron content.

The boron hardenability factors, obtained from Table 4, as previously described, are plotted against added boron percentages in Fig. 6. From this figure the following conclusions are drawn:

1. A wide scatter in boron factors results from each type of boron addition that was made, the maximum scatter occurring when the boron addition exceeds about 0.002 per cent.

2. Boron additions of 0.0015 per cent as ferroboron, 0.002 per cent as alloy A, and 0.005 per cent as alloy B, were about equally effective.

3. A decreasing trend in boron factors results from additions of 0.003 and 0.006 per cent boron as ferroboron. This trend is especially noticeable in the cast steels.

4. The average maximum boron factor occurs at 0.0015 to 0.002 per cent boron and is approximately 2.0. This is high compared with Grossmann's value of 1.5 at about 0.003 per cent boron,[1] and Crafts and Lamont's value of about 1.7 at about 0.001 per cent boron.[4] If carbon content has the effect upon the increase in hardenability obtained from boron additions indicated by Grange and Garvey,[5] these discrepancies are explainable. The present value of 2.0 for the boron factor falls close to an extrapolation to 0.30 carbon of the shaded range indicated in their Fig. 3, which is replotted here as Fig. 7. The other boron factors mentioned also fall fairly close to this range when plotted against carbon content. As indicated in point 3, there is an optimum boron addition for maximum hardenability. Larger additions have the effect of producing lower than the optimum value. Inasmuch as Grange and Garvey's points for 0.63 and 0.75 per cent carbon were obtained with relatively large boron additions, it is possible that they are lower than the optimum possible hardenability increase; therefore, the curve may not drop off as rapidly as indicated for the higher carbon contents.

Fig. 5 provides supplementary data on the molybdenum hardenability factor. From the slope of the best value curve in this figure, the molybdenum factor is calculated to be $1 + (2.07)(\%\ \text{Mo})$. For comparison with the data plotted, ideal critical diameters are shown for the base

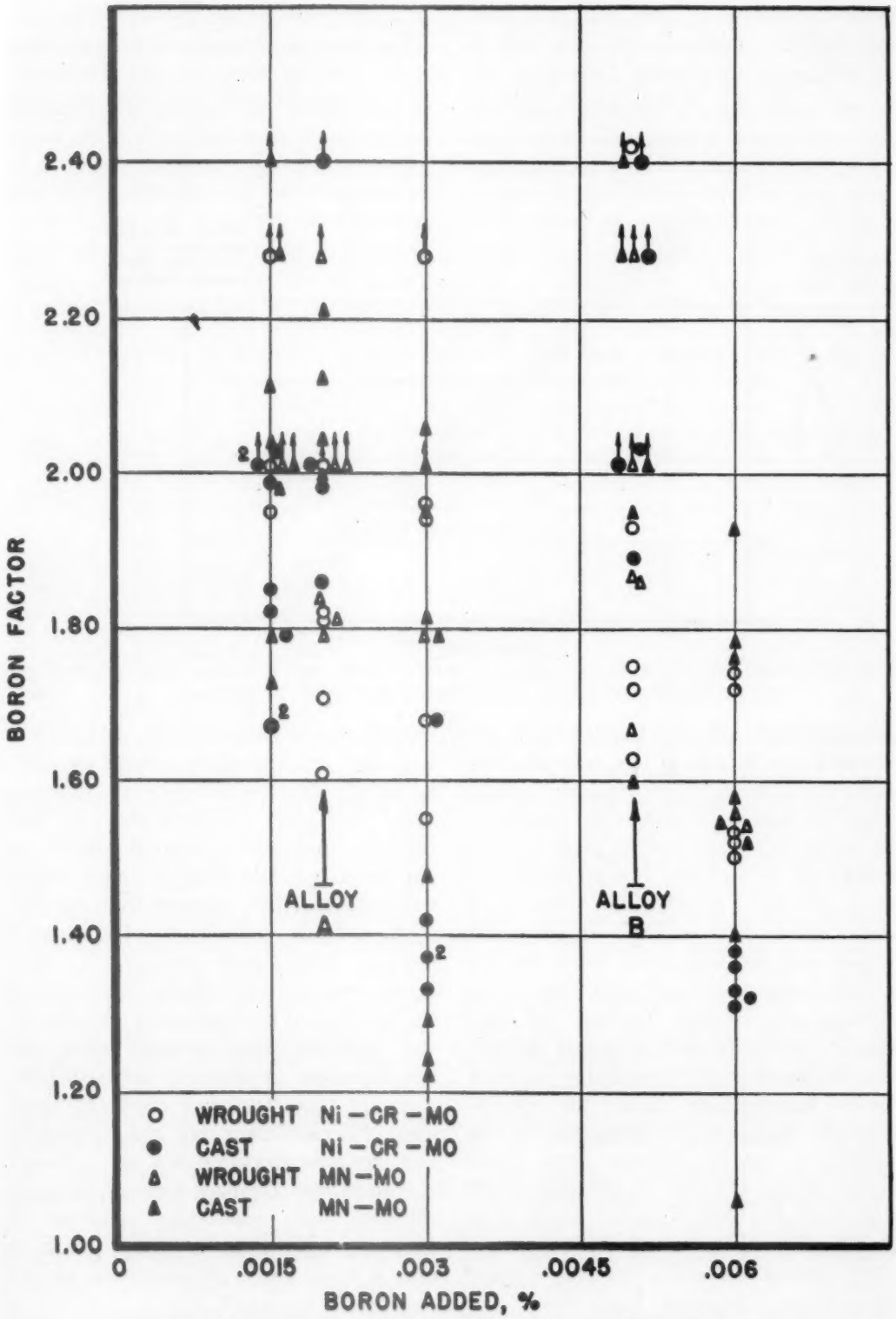

FIG. 6.—BORON FACTORS PLOTTED AGAINST BORON ADDITION.

steels containing 0 and 0.40 per cent molybdenum calculated by the use of Grossmann's,[1] Craft's and Lamont's[4] and Kramer et al.[3] hardenability factors.

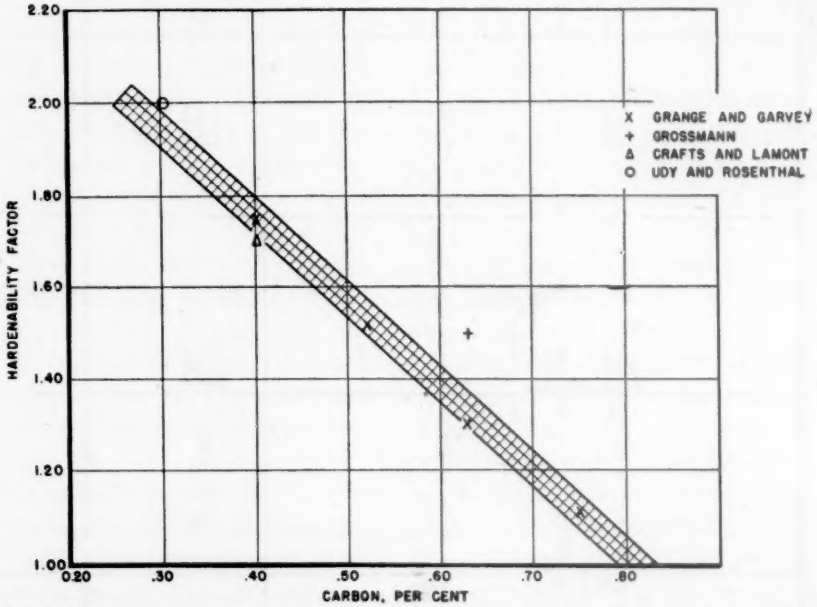

FIG. 7.—APPROXIMATE EFFECT OF CARBON CONTENT UPON THE INCREASE IN HARDENABILITY OBTAINABLE FROM THE ADDITION OF BORON TO STEEL.

Kramer's data show a scatter band for molybdenum factors at molybdenum contents exceeding 0.20 per cent. The points, based on Kramer's data, were calculated by using the boron factors given by the lower edge of this band. It is apparent that at 0 per cent molybdenum there is a close check between the experimental values and the calculated value for the nickel-chromium-molybdenum steel using Grossmann's factors. Despite the fact that the published data on factors indicate the manganese-molybdenum steel to be of lower hardenability than the nickel-chromium-molybdenum type, this is not verified by the experimental data, which show almost identical hardenability. At 0.40 per cent molybdenum, there is a considerable deviation of the calculated ideal critical diameters for the nickel-chromium-molybdenum steel from the estimated ideal critical diameters obtained experimentally.

Hardenability vs. Microstructure

The end-quench hardenability test is a useful tool for depicting the hardnesses that can be obtained for a wide range of cooling rates. Unless the end-quench test bar is examined microscopically, however, there is no way of knowing what structure is represented by the hardness indicated. This limitation is particularly outstanding in alloy steels when the structure changes from 100 per cent martensite to mixtures of martensite and low-temperature bainite. In such cases, there are only slight differences in the hardness of the martensite and bainite, and hardness measurements alone are not adequate in defining the structure. Although there are many instances where such differentiations are not necessary, and hardness measurements are sufficient for comparison, there are some applications where a fully martensitic structure is essential, and it is in these instances that a more exact determination of the structure is required.[6]

To ascertain how the hardness measurements compared with the actual micro-

structure of the bars, a number of wrought steels, representing the extremes in hardenability encountered in these steels, were polished and etched for metallographic examination. The results of the examination were expressed as the distance from the quenched end of the hardenability bar to a structure of 99, 90, or 50 per cent martensite. These data are given in Table 5. Also included are the hardnesses at each of the determined distances.

TABLE 5.—*Results of Examination of End-quench Bars from a Representative Group of Wrought Steels*

Heat No.	Added Boron, Per Cent	Mo, Per Cent	End Hardness, R_c	Distance to 99% M,		Distance to 90% M,		Distance to 50% M,	
				16ths	R_c	16ths	R_c	16ths	R_c
Nickel-chromium-molybdenum									
8733	0	0.39	50.5	4.0	49	5.5	46	9.5	35
8753	0.0015	0.42	51.0	16.5	49.5				
Manganese-molybdenum									
8883	0	0	51.0	2.5	47.5	3.5	46.5	5.0	35
8738	0	0.38	51.0	6.0	49.0	8.0	45.5	11.5	38
8798	0.006	0.42	50.0	16.5	45.0				

It was not difficult to estimate the distance to 99 per cent martensite, but it was much more of a problem to rate the 90 and 50 per cent martensite structures because of banding in the bars and difficulty in judging the approximate percentage of each transformation product in a particular field. The transformation product first to be distinguished from martensite was ferrite, high-temperature bainite, or both. Structures identifiable as pearlite did not appear until an appreciable amount of other transformation products were present.

If low-temperature bainite appeared, it was not always possible to separate it from the martensite. It is suspected that in the deeper hardening steels, such as 8733 and 8798, considerable percentages of low-temperature bainite were present in conjunction with the high-temperature variety that was rated. In these steels, there was a gradual transition along the length of the bar from a definitely martensitic structure to a bainite form, and in 8733 a high-temperature bainite was also intermingled with this background material. Obviously then, a microscopic rating, even to a 99 per cent martensite structure, is subject to considerable error. If hardness may be taken as a criterion, this error is indicated by the lower hardness at 99 per cent martensite for steel 8798. In this steel, the transition from martensite to bainite was particularly gradual and obscure, and the distance given for 99 per cent martensite is only an approximation.

The data in Table 5 give some indication of the marked increase in hardenability conferred by boron, but it must be concluded that because of the inherent difficulties of present-day methods of rating hardenability, an exact evaluation of the boron effect is impossible.

Notched-bar Toughness

The beneficial effects of boron are best utilized in a steel that has been quenched and tempered. It is known that steels with sufficient hardenability to harden through the cross section when quenched will have similar tensile properties if tempered to the same Brinell hardness

value.[7] In this investigation the notched-bar impact toughness of the two cast and wrought alloy-steel types, with various boron contents, was determined with specimens fully hardened by quenching and subsequently tempered at suitable temperatures.

Figs. 8 and 9 show the notched-bar impact test results for the wrought and cast steels, respectively, at testing tem-

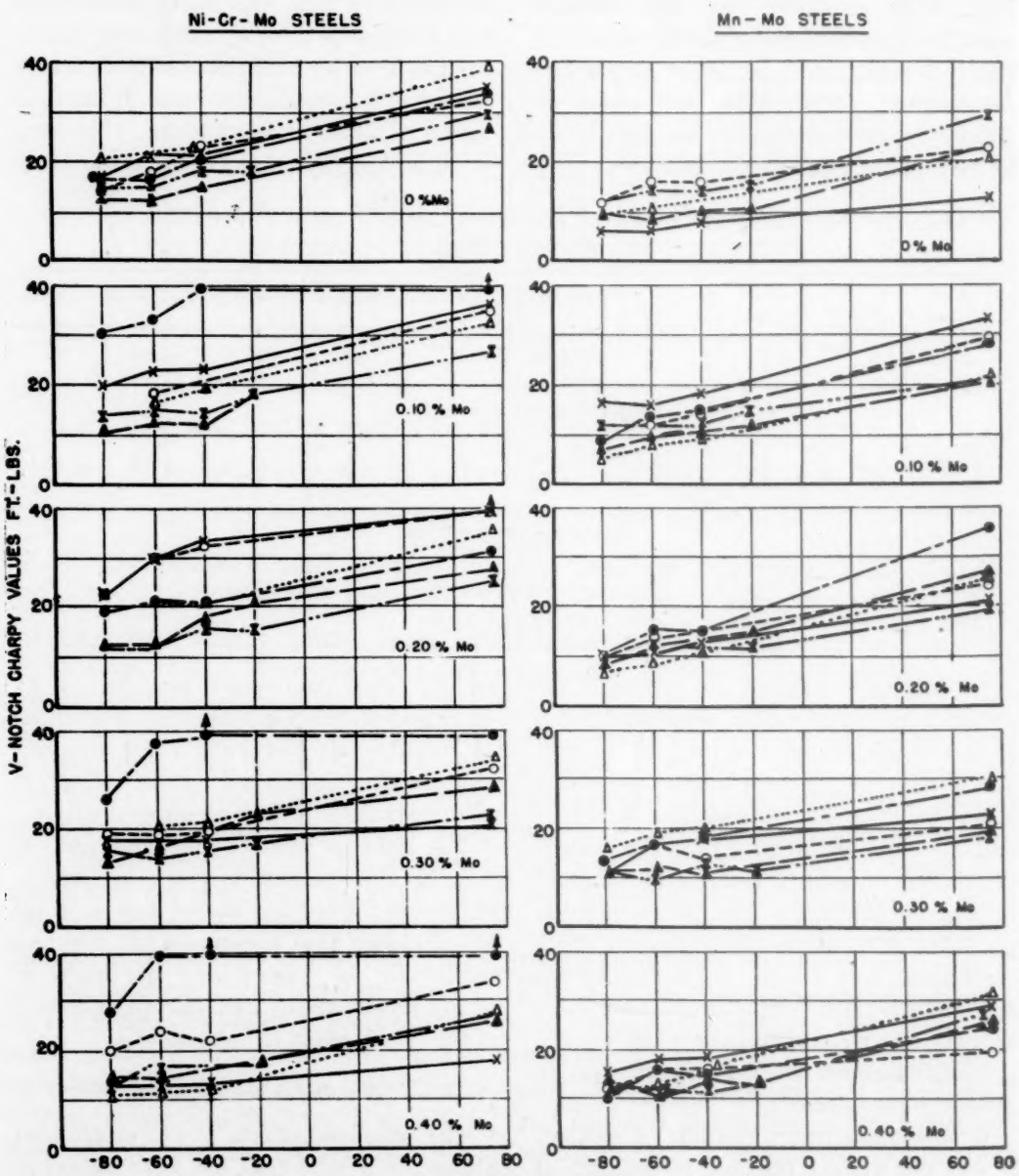

EFFECT, OF TEMPERATURE ON THE NOTCHED BAR TOUGHNESS OF WROUGHT NICKEL-CHROMIUM-MOLYBDENUM AND MANGANESE-MOLYBDENUM TYPE STEELS TREATED WITH VARIOUS AMOUNTS OF FERROBORON OR WITH 0.375 % ALLOY A OR ALLOY B

FIG. 8.

peratures of +75° to −80°F. No evidence that boron reduced the toughness of wrought steels was found. The absence of molybdenum did not appear to have an adverse effect on the notched-bar strength of the nickel-chromium-molybdenum steel even at low testing temperatures. The manganese-molybdenum type of steel, on the whole, was inferior in notch toughness to the nickel-chromium-molybdenum

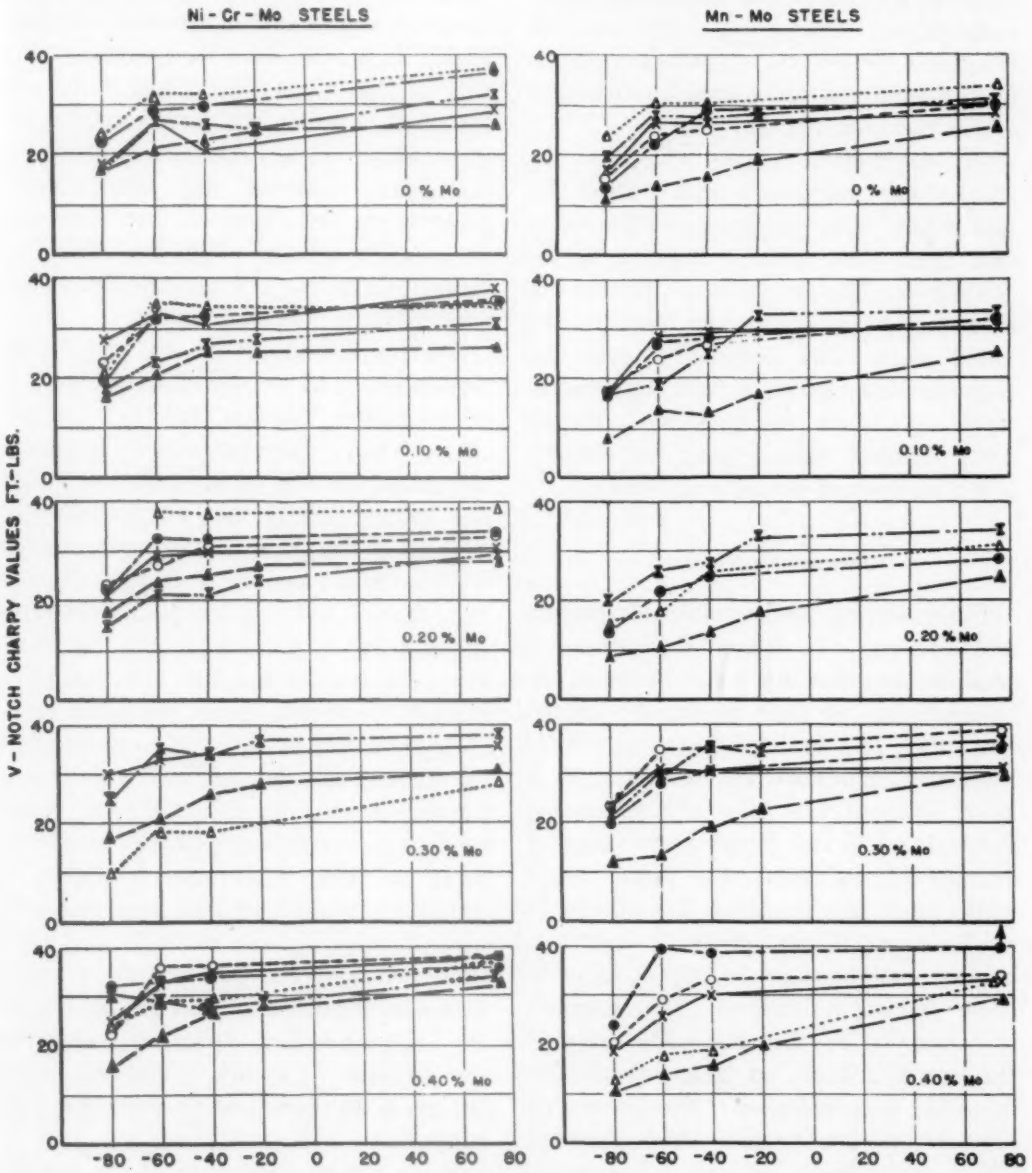

EFFECT OF TEMPERATURE ON THE NOTCHED BAR TOUGHNESS OF CAST NICKEL-CHROMIUM-MOLYBDENUM AND MANGANESE-MOLYBDENUM TYPE STEELS TREATED WITH VARIOUS AMOUNTS OF FERROBORON OR WITH 0.375 % ALLOY A OR ALLOY B

FIG. 9.

type. This was particularly true with steels of zero or low molybdenum content. The toughness was improved somewhat when the molybdenum was raised, but the values were still generally poorer than those obtained with the nickel-chromium-molybdenum type. The difference in toughness of the two types of steels is readily observed by comparing adjacent sets of curves in Fig. 8.

No detrimental effects of boron on notched-bar toughness were noted for cast steels. The manganese-molybdenum cast steels were generally inferior to the nickel-chromium-molybdenum, but the difference was less noticeable than in the rolled steels. One peculiarity that distinguished the cast steels from the wrought steels was their tendency to maintain fairly uniform values down to −60°F., and then drop off abruptly at −80°F.

Temper Brittleness

In considering the possibility of replacing molybdenum with boron, it is desirable to know the effect of such a change on the susceptibility of steel to temper brittleness; i.e., the embrittlement or loss of toughness resulting from tempering in a range of about 750° to 1100°F. or cooling slowly through this temperature range. A number of variables were present that might affect this property. The change in molybdenum content certainly was one, because molybdenum is known to overcome temper brittleness. The presence of boron was another possibility, because the action of boron on temper brittleness in steels was unknown. The tempering temperature used was a third variable, which undoubtedly had an influence on the degree of brittleness produced. A fourth variable was the testing temperature used to reveal temper brittleness. Only the first two variables were investigated; the effect of testing temperature was determined in a general way by testing at room temperature and at −60°F.

Temper-brittleness specimens were prepared by water-quenching two sets of V-notch Charpy bars and tempering them one hour at 1200°F. One set was then water-quenched and the other furnace-cooled from the draw temperature at a rate of 100°F. per hour and both sets tested at −60°F. The former heat-treatment should repress appearance of temper brittleness, whereas the latter should promote its development. The difference in notch toughness after the two heat-treatments is thus a rough measure of the susceptibility to embrittlement.

Certain limitations of the test should be recognized to avoid a mistaken concept of the results. The fact that both furnace-cooled and water-quenched specimens are subject to the usual scatter in notch-bar values implies that occasionally the differences in these values may deviate substantially from the ordinary. There is the chance that other heat-treatments might result in a much greater manifestation of embrittlement. The tests had to be carried out below room temperature to exaggerate the evidence of susceptibility. Obviously, this denotes that, under the conditions imposed by the test, these steels were not so susceptible to embrittlement as those that show evidence of brittleness when tested at room temperature. Finally, the two methods of cooling from the tempering temperature resulted in a somewhat softer steel in the case of the furnace-cooled specimen, so that comparisons of notch toughness were not made on specimens of quite the same hardness.

Table 6 gives the results of the temper-brittleness tests for wrought and cast steels, respectively. No effect of boron on this phenomenon is apparent.

From the data on wrought nickel-chromium-molybdenum steels, it is evident that temper-brittleness susceptibility largely

TABLE 6.—*Temper-brittleness Susceptibility Data*

All steels deoxidized with 0.10 per cent Al before boron addition. Average results obtained at −60°F. on duplicate bars after tempering fully quenched, V-notch Charpy bars at 1200°F., and cooling as indicated in the table.

Heat No.	Addition Agent	Chemistry, Per Cent		Water Quench		Furnace Cool		Difference W. Q. Minus F. C., Ft-lb.
		Mo	Added B	Brinell	Notch Strength, Ft-lb.	Brinell	Notch Strength, Ft-lb.	
WROUGHT STEELS								
Nickel-chromium-molybdenum Type[a]								
Base Analysis: 0.28–0.32 C, 0.70–0.90 Mn, 0.15–0.25 Si, 0.45–0.55 Ni, 0.45–0.55 Cr								
8729	Ferroboron	0	0	219	105+	191	116+	−11.0
8749	Ferroboron	0	0.0015	214	105+	206	27.5	77.5
8769	Ferroboron	0	0.003	220	105+	206	33.0	72.0
8789	Ferroboron	0.01	0.006	217	105+	198	24.0	81.0
9192	Alloy A	0	0.002	219	105+	204	21.5	83.5
9234	Alloy B	0	0.005	214	88.5	205	105.0	−17.5
8730	Ferroboron	0.10	0	238	99.0	216	116.0	−17.0
8750	Ferroboron	0.10	0.0015	229	105+	217	105.0	0
8770	Ferroboron	0.10	0.003	235	99.0	214	105.0	−6.0
8790	Ferroboron	0.10	0.006	229	94.0	214	98.0	−4.0
9193	Alloy A	0.10	0.002	230	93.5	209	33.0	60.5
9235	Alloy B	0.11	0.005	235	83.5	222	95.0	−11.5
8882	Ferroboron	0.20	0	250	100.0	235	105+	−5.0
8751	Ferroboron	0.21	0.0015	241	105+	224	93.0	12.0
8771	Ferroboron	0.21	0.003	241	86.0	228	84.0[b]	2.0
8791	Ferroboron	0.21	0.006	241	60.5	222	40.0	20.5
9194	Alloy A	0.20	0.002	246	83.0	233	99.0	−16.0
9236	Alloy B	0.20	0.005	245	80.5	229	83.5	−3.5
8732	Ferroboron	0.29	0	269	89.5	238	96.5	−7.0
8752	Ferroboron	0.32	0.0015	251	105+	229	96.5	8.5
8772	Ferroboron	0.31	0.003	255	98.0	232	97.0	1.0
8792	Ferroboron	0.30	0.006	255	58.0	230	33.5	24.5
9195	Alloy A	0.29	0.002	268	55.5	235	49.5	6.0
9237	Alloy B	0.31	0.005	243	78.0	230	76.5	1.5
8733	Ferroboron	0.39	0	255	96.5	249	105.0	−8.5
8753	Ferroboron	0.42	0.0015	261	82.0	234	96.5	−14.5
8773	Ferroboron	0.41	0.003	265	86.0	242	88.5	−2.5
8793	Ferroboron	0.39	0.006	259	37.0	241	24.5	12.5
9196	Alloy A	0.40	0.002	268	50.0	253	48.5	1.5
9238	Alloy B	0.38	0.005	255	93.5	244	67.5	26.0
Manganese-molybdenum Type[a]								
Base Analysis: 0.28–0.32 C, 1.50–1.70 Mn, 0.15–0.25 Si								
8883	Ferroboron	0	0	197	105+	185	18.0	87.0
8754	Ferroboron	0	0.0015	200	105+	184	19.5	85.5
8774	Ferroboron	0	0.003	217	105+	193	24.5	80.5
8794	Ferroboron	0	0.006	198	105.0	175	18.5	86.5
8997	Alloy A	0.02	0.002	211	72.0	191	9.5	62.5
9260	Alloy B	0	0.005	202	94.5	181	29.5	65.0
8884	Ferroboron	0.12	0	210	105+	191	100.0	5.0
8755	Ferroboron	0.10	0.0015	222	105+	191	76.0	29.0
8775	Ferroboron	0.12	0.003	213	105+	196	84 5	20.5
8795	Ferroboron	0.10	0.006	223	93.5	192	42.0	51.5
8998	Alloy A	0.11	0.002	219	99.5	213	18.0	81.5
9261	Alloy B	0.11	0.005	217	73.5	197	54.0	19.5
8736	Ferroboron	0.19	0	217	105.0	198	105.0	0
8756	Ferroboron	0.20	0.0015	226	105.0	207	105.0	0
8776	Ferroboron	0.21	0.003	227	105.0	215	105.0	0
8796	Ferroboron	0.20	0.006	220	99.0	209	49.5	49.5
8999	Alloy A	0.21	0.002	224	105+	202	105.0	0
9262	Alloy B	0.21	0.005	226	70.5	208	47.5	23.0
8737	Ferroboron	0.30	0	242	110+	229	95.5	14.5
8757	Ferroboron	0.30	0.0015	231	105.0	225	86.5	18.5
8777	Ferroboron	0.32	0.003	233	95.0	213	92.0	3.0
8797	Ferroboron	0.31	0.006	242	70.5	222	68.0	2.5
9287	Alloy A	0.32	0.002	252	97.5	228	95.5	2.0
9263	Alloy B	0.31	0.005	241	73.5	223	72.0	1.5
8738	Ferroboron	0.38	0	239	105+	224	104.5	0.5
9067	Ferroboron	0.40	0.0015	221	72.5	208	33.0	39.5
8778	Ferroboron	0.42	0.003	249	102.0	225	89.5	12.5
8798	Ferroboron	0.42	0.006	243	87.0	222	84.5	2.5
9288	Alloy A	0.42	0.002	268	77.5	241	69.5	8.0
9264	Alloy B	0.40	0.005	248	58.5	220	29.5	29.0

[a] See Table 2 for complete analyses.

[b] Single value.

TABLE 6.—(*Continued*)

Heat No.	Addition Agent	Chemistry, Per Cent		Water Quench		Furnace Cool		Difference W. Q. Minus F. C., Ft-lb.
		Mo	Added B	Brinell	Notch Strength, Ft-lb.	Brinell	Notch Strength, Ft-lb.	
CAST STEELS								
Nickel-chromium-molybdenum Type[a]								
Base Analysis: 0.28–0.32 C, 0.70–0.90 Mn, 0.35–0.45 Si, 0.45–0.55 Ni, 0.45–0.55 Cr								
8739	Ferroboron	0	0	214	36.0	210	10.5	25.5
8759	Ferroboron	0	0.0015	226	40.0	208	14.0	26.0
8779	Ferroboron	0	0.003	226	43.5	213	12.5	31.0
8799	Ferroboron	0	0.006	229	38.5	208	10.0	28.5
9275	Alloy A	0	0.002	229	28.0	208	12.0	16.0
9265	Alloy B	0	0.005	224	35.5	211	14.0	21.5
8740	Ferroboron	0.10	0	240	34.0	224	33.0	1.0
8760	Ferroboron	0.09	0.0015	250	45.5	235	25.5	20.0
8780	Ferroboron	0.10	0.003	246	44.0	222	26.5	17.5
8800	Ferroboron	0.11	0.006	239	38.5	229	30.0	8.5
9276	Alloy A	0.07	0.002	241	23.0	221	19.0	4.0
9266	Alloy B	0.12	0.005	238	36.0	222	24.5	11.5
8741	Ferroboron	0.19	0	247	39.5	218	41.5	−2.0
8761	Ferroboron	0.19	0.0015	252	40.5	229	41.5	−1.0
8781	Ferroboron	0.21	0.003	244	38.0	232	25.5	12.5
8801	Ferroboron	0.21	0.006	254	28.5	236	20.0	8.5
9277	Alloy A	0.20	0.002	258	31.0	251	23.0	8.0
9267	Alloy B	0.22	0.005	260	30.5	237	21.0	9.5
8879	Ferroboron	0.30	0	268	28.5	249	39.5	−1.0
8762	Ferroboron	0.29	0.0015	269	36.0	244	37.5	−1.5
8782	Ferroboron	0.30	0.003	260	33.5	248	35.5	−2.0
8802	Ferroboron	0.32	0.006	269	19.5	258	20.5	−1.0
9278	Alloy A	0.31	0.002	273	20.5	254	20.0	0.5
9268	Alloy B	0.32	0.005	261	33.5	245	26.5	7.0
8743	Ferroboron	0.42	0	274	33.5	248	44.5	−11.0
8763	Ferroboron	0.41	0.0015	280	29.0	255	31.0	−2.0
8783	Ferroboron	0.41	0.003	283	41.5	263	40.0	1.5
8803	Ferroboron	0.41	0.006	274	44.5	262	31.0	13.5
9279	Alloy A	0.40	0.002	273	22.5	249	21.5[b]	1.0
9269	Alloy B	0.43	0.005	268	38.0	255	23.5	14.5
Manganese-molybdenum Type[a]								
Base Analysis: 0.28–0.32 C, 1.40–1.70 Mn, 0.35–0.45 Si								
8744	Ferroboron	0	0	230	39.0	186	13.0	26.0
8764	Ferroboron	0	0.0015	220	34.5	197	8.0	26.0
8784	Ferroboron	0	0.003	208	40.5	192	13.0	27.5
8804	Ferroboron	0	0.006	205	40.5	184	13.0	27.5
9182	Alloy A	0	0.002	214	18.0	187	4.0[b]	14.0
9270	Alloy B	0	0.005	212	38.0	200	11.5	26.5
8745	Ferroboron	0.10	0	212	49.0	190	26.0	23.0
8765	Ferroboron	0.10	0.0015	225	37.0	209	13.5	23.5
8785	Ferroboron	0.10	0.003	237	39.5	200	21.0	18.5
8805	Ferroboron	0.11	0.006	218	46.5	208	24.0	22.5
9183	Alloy A	0.10	0.002	232	16.5	211	5.0	11.5
9271	Alloy B	0.11	0.005	222	35.0	196	18.5	16.5
8880	Ferroboron	0.21	0	245	39.0	220	31.5	7.5
8766	Ferroboron	0.21	0.0015	230	37.0	216	21.0	16.0
8786	Ferroboron	0.20	0.003	229	45.0	207	26.5	18.5
8806	Ferroboron	0.21	0.006	239	25.0	221	17.0	8.0
9184	Alloy A	0.20	0.002	241	19.0	226	12.0	7.0
9272	Alloy B	0.21	0.005	243	29.0	216	20.5	9.5
8881	Ferroboron	0.30	0	259	37.5	241	37.5	0
8767	Ferroboron	0.31	0.0015	262	39.5	240	25.5	14.0
8787	Ferroboron	0.31	0.003	251	39.5	226	28.0	11.5
8807	Ferroboron	0.31	0.006	258	20.5	239	16.5	4.0
9185	Alloy A	0.29	0.002	253	19.5	230	12.5	7.0
9273	Alloy B	0.32	0.005	248	37.0	231	25.0	12.0
8748	Ferroboron	0.40	0	251	36.5	227	31.0	5.5
9068	Ferroboron	0.41	0.0015	255	38.0	246	17.0	21.0
8788	Ferroboron	0.42	0.003	255	34.0	233	19.5	14.5
8808	Ferroboron	0.42	0.006	251	21.0	241	14.0	7.0
9186	Alloy A	0.39	0.002	267	16.0	242	11.0	5.0
9274	Alloy B	0.40	0.005	252	44.5	238	34.0	10.5

disappears with the addition of 0.10 per cent molybdenum to the steel. With the wrought manganese-molybdenum steels, however, 0.20 per cent molybdenum is necessary to eliminate evidence of temper brittleness. Occasional high difference values occur above the molybdenum values given. It is believed that these are mainly the result of scatter in the test results.

In the cast nickel-chromium-molybdenum steels, it appears that approximately 0.20 per cent molybdenum is necessary to remove all signs of temper brittleness. A similar condition exists for the cast manganese-molybdenum steels, but positive difference values exist throughout the molybdenum range in this type of steel. The generally lower values for the furnace-cooled specimens may mean that steels of this base composition are more susceptible to temper brittleness than are the nickel-chromium-molybdenum type.

Replacement of Molybdenum with Boron

The results discussed in the preceding pages give the impression that a replacement of molybdenum with boron is entirely possible. A more exacting survey of this substitution is worth while. For this purpose, the properties of the base steels containing 0.40 per cent molybdenum and no boron will be used for reference. These compositions are represented by wrought heats 8733 and 8738 and by cast heats 8743 and 8748.

Considering hardenability first, it is obvious that boron additions show up to the least advantage in the cast steels, where additions of 0.003 per cent or greater usually increase the maximum hardness values, but decrease the depth of hardness penetration. If it is assumed that this condition will generally prevail, cast steels treated with 0.003 per cent boron must contain 0.20 per cent molybdenum to have a hardenability equivalent to that of the base analysis. If the boron additions are held down to 0.0015 per cent, a 0.20 per cent molybdenum steel has even a better hardenability than the base steel. These comparisons are illustrated in Fig. 10. With the wrought steels, a steel containing 0.20 per cent molybdenum and treated with either 0.0015 or 0.003 per cent boron has a greater hardenability than the base steel; in fact, this indicates that boron additions could be used to replace all of the molybdenum if hardenability were the only factor to be considered. Fig. 11 contains hardenability curves showing this comparison.

There is no suggestion from the low-temperature notched-bar data that boron cannot be used to replace molybdenum, but the temper-brittleness test results disclose a susceptibility to embrittlement in these steels if the molybdenum drops below 0.20 per cent. This is particularly true for the manganese-molybdenum type steels.

Therefore, from the standpoint of the tests employed on these steels, the use of 0.20 per cent molybdenum with a boron addition of 0.0015 or 0.003 per cent produces a steel that is in no way inferior to an untreated steel containing 0.40 per cent molybdenum. There is every reason to believe that this comparison would hold if other physical properties were considered.

Despite the similarity in the properties compared in these tests, the data also give ample evidence that there is at least one instance where the steels are quite dissimilar. This was apparent in the temper-brittleness data, which revealed that molybdenum raised the tempering temperature required to develop a certain hardness whereas boron had no influence on the hardness resulting from the tempering operation. Hence, fully quenched boron-treated steels of 0.20 per cent molybdenum must be tempered at a lower tempereture to achieve the same hardness obtained

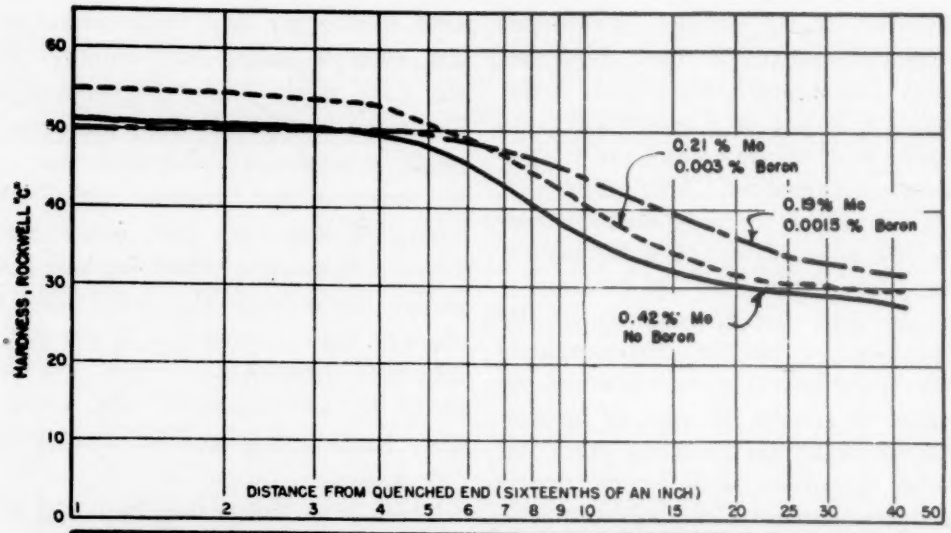

Key	Heat No.	Steel Type	C	Mn	Si	S	P	Cr	Ni	Mo	Al	B	B Added	Quench Temp.	Grain Size	Remarks
———	8743	CAST	.27	.74	.39			.51	.52	.42	.10		—	1575	7	
- - -	8761	"	.30	.82	.36			.52	.52	.21	Ad-		.003	"	7	FERROBORON
———	8761	"	.30	.68	.37			.52	.54	.19	ded		.0015	"	7	FERROBORON

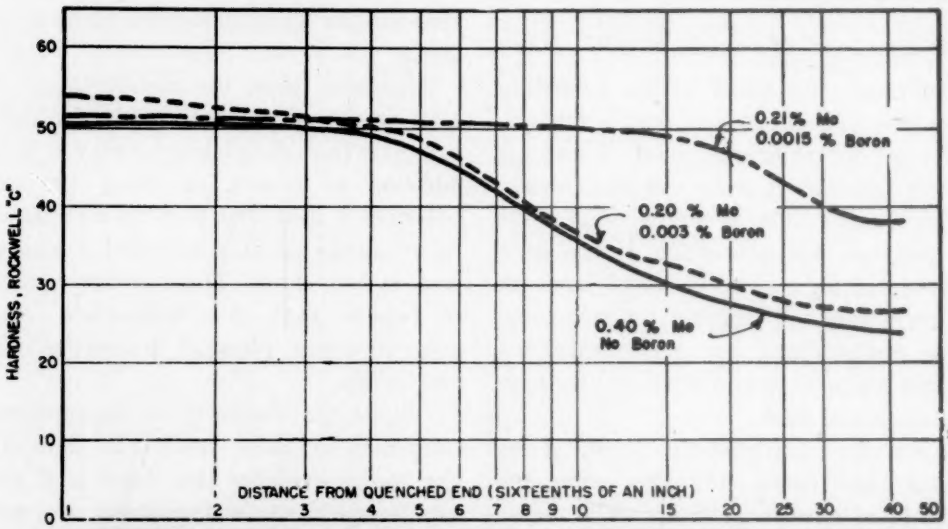

Key	Heat No.	Steel Type	C	Mn	Si	S	P	Cr	Ni	Mo	Al	B	B Added	Quench Temp.	Grain Size	Remarks
———	8745	CAST	.27	1.43	.36			—	—	.40	.10		—	1600	7	
- - -	8766	"	.30	1.58	.42			—	—	.20	Ad-		.003	"	7	FERROBORON
———	8766	"	.29	1.62	.44			—	—	.21	ded		.0015	"	7	FERROBORON

FIG. 10.—END-QUENCH HARDENABILITY CURVES FOR CAST STEELS SHOWING COMPARATIVE EFFECTS OF BORON AND MOLYBDENUM.

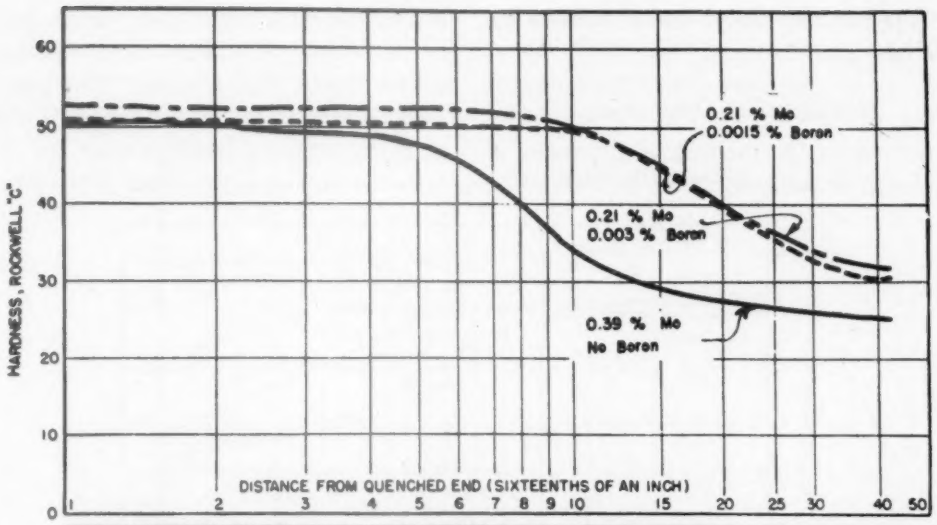

Key	Heat No.	Steel Type	C	Mn	Si	S	P	Cr	Ni	Mo	Al	B	B Added	Quench Temp	Grain Size	Remarks
———	8753	WRT.	.30	.73	.20			.51	.48	.39	.10	—	0	1575	7	
- - -	8751	"	.31	.79	.18			.53	.53	.21	Ad-	—	0015	"	7	FERROBORON
———	8771	"	.31	.82	.22			.50	.52	.21	ded	0029	.003	"	7-8	FERROBORON

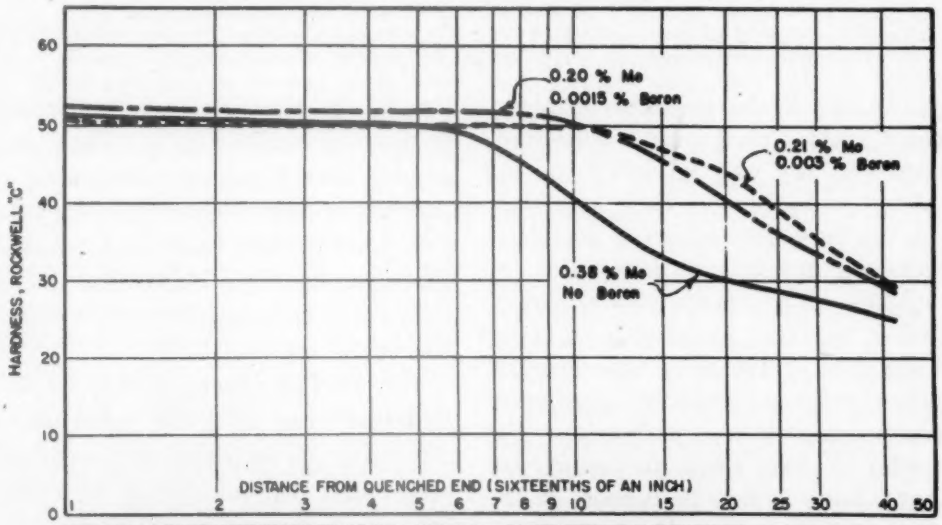

Key	Heat No.	Steel Type	C	Mn	Si	S	P	Cr	Ni	Mo	Al	B	B Added	Quench Temp.	Grain Size	Remarks
———	8738	WRT.	.30	1.53	.22			—	—	.38	.10	—	0	1600	—	
- - -	8776	"	.30	1.57	.21			—	—	.21	Ad-	.002	.003	"	7	FERROBORON
———	8756	"	.31	1.58	.26			—	—	.20	ded	—	0015	"	7	FERROBORON

FIG. 11.—END-QUENCH HARDENABILITY CURVES FOR WROUGHT STEELS SHOWING COMPARATIVE EFFECTS OF BORON AND MOLYBDENUM.

in a 0.40 per cent molybdenum steel of the same base analysis.

Importance of Deoxidation

Previous to the melting of the series of aluminum-deoxidized steels treated with boron addition were also demonstrated by a series of manganese-molybdenum steels, made for another investigation. These steels were deoxidized with aluminum, low-carbon ferrotitanium, or high-carbon ferrotitanium. Their analyses and

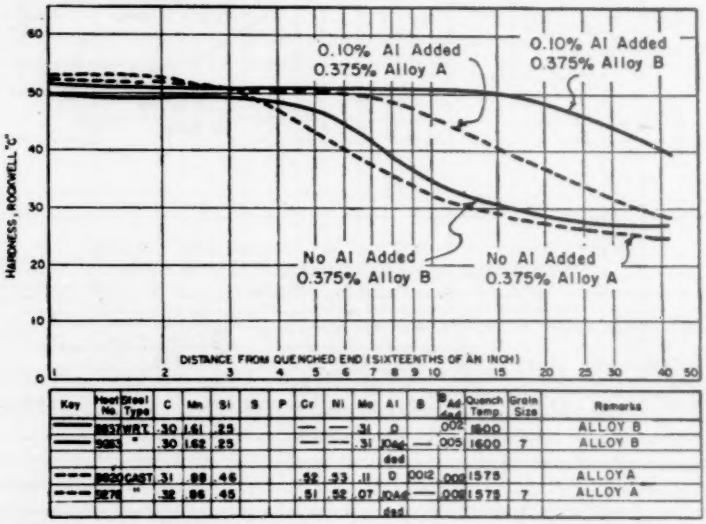

Key	Heat No	Steel Type	C	Mn	Si	S	P	Cr	Ni	Mo	Al	B	B_{Aq}	Quench Temp.	Grain Size	Remarks
———	8837	WAT.	.30	1.61	.25			—	—	.31	0		.002	1600		ALLOY B
———	9085	"	.30	1.62	.25			—	—	.31	.006 dad	—	.005	1600	7	ALLOY B
- - - -	8820	CAST	.31	.88	.46			.52	.33	.11	0	.0012	.002	1575		ALLOY A
- - - -	8878	"	.32	.86	.45			.51	.52	.07	.006 dad	—	.005	1575	7	ALLOY A

FIG. 12.—END-QUENCH HARDENABILITY CURVES FOR WROUGHT AND CAST STEELS SHOWING THE EFFECTS OF DEOXIDATION WITH ALUMINUM BEFORE ADDING BORON ALLOYS.

alloy A or alloy B, the same series had been prepared without aluminum deoxidation.* Examples of the way in which the incomplete deoxidation of these steels affected the hardenability curve are given in Fig. 12. Insufficient deoxidation of wrought alloy B steels resulted in a marked reduction of the hardenability below that for steel of the same base analysis deoxidized with 0.1 per cent aluminum. Hardenability was also reduced in the cast alloy A steel when aluminum was not used, but a noticeable increase in the maximum hardness, not observed in the alloy B steel, occurred.

The effects of deoxidation practice on the hardenability gained from ferro- the results of end-quench hardenability tests are given in Fig. 13. These results suggest that aluminum deoxidation contributes to the realization of the maximum hardenability from a boron addition. Likewise, there is evidence that the ferrotitanium in the amounts used is not effective in this regard.

The adverse effects of incomplete deoxidation when using the boron may not necessarily be restricted to hardenability properties. An interesting example of this was uncovered in an examination of two groups of cast steels, which had been treated with the alloy B, made in an early stage of the work. The steels in these two groups were comparable in every way with regard to melting practice and processing, except that in one case (8400 series in Fig. 14) the heats were made with ingot iron punchings for the melting stock, while the steels in the

* Alloy B containing 0.54 per cent boron was used for heats prepared without aluminum deoxidation. After completion of the experimental work, it was found that the aluminum-deoxidized alloy B heats had inadvertently been made with a lot of alloy B shipped as 0.50 per cent boron but found to contain 1.38 per cent boron. This resulted in the addition of 0.005 instead of 0.002 per cent boron.

other group were made with sheared ingot iron scrap.

Despite the close similarity of these two series, the data in Fig. 14 reveal that scale and is more susceptible to oxidation in the furnace. The greater quantity of oxygen introduced into the melts made with sheared scrap as compared with those

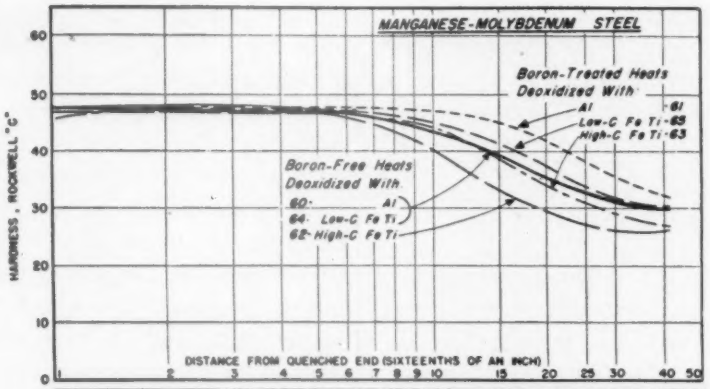

Key	Heat No.	C	Mn	P	Si	Ni	Cr	S	Mo	N	B Added	Al Added	Ti Added	Quench Temp.	Grain Size
———	A 1060	.30	1.76	.007	.42	-	-	.019	.27	.008	-	.10	-	1650°F.	8
- - - -	A 1061	.31	1.75	.009	.44	-	-	.020	.32	.003	.003	.10	-	1650°F.	8
———	A 1062	.28	1.78	.004	.41	-	-	.021	.27	.008	-	-	.06	1650°F.	6
———	A 1063	.29	1.73	.004	.44	-	-	.020	.28	.006	.003	-	.06	1650°F.	6-1/2
———	A 1064	.30	1.78	.005	.44	-	-	.021	.30	.0068	-	-	.06	1650°F.	7
— — —	A 1065	.29	1.80	.009	.41	-	-	.021	.31	.010	.003	-	.06	1650°F.	7

FIG. 13.—INFLUENCE OF THE DEOXIDIZING AGENT ON THE HARDENABILITY OF BORON CONTAINING MANGANESE-MOLYBDENUM STEELS.

there was a decided difference in the notched-bar strength of the cast specimens that were water-quenched and drawn to a definite hardness range. Since subsequent tests proved that temper brittleness was not a factor, recourse was made to metallographic comparisons of these steels.

The micrographs of Fig. 14 demonstrate why the 8500 series cast steels had lower notched-bar toughness values than those in the 8400 series. The grain-boundary, network-type inclusion in cast steels 8591 and 8595 undoubtedly accounted for their inferior impact properties.[8] Inasmuch as the two series were alike in every respect except in the type of melting stock used, the change from ingot iron punchings to sheared ingot iron scrap was the most logical explanation for the difference in inclusion distribution of the two series. Ingot iron punchings have much of their scale removed by the punching operation and oxidize less in the furnace, whereas the sheared scrap, since it is in larger pieces, retains more of its made with punchings apparently was sufficient to oxidize more of the aluminum contained in the intensifier alloy, thereby converting the type of inclusion in the cast steels from the desirable random arrangement to the undesirable grain-boundary network, which gives low impact and ductility properties. Inasmuch as an aluminum treatment before addition of alloy B would have prevented the formation of the network-type inclusion as well as allowed the boron in this alloy to exert its full effect, the danger of considering the intensifier alloys as furnishing adequate deoxidation in themselves is demonstrated.

CONCLUSIONS

1. From the standpoint of hardenability, boron added as ferroboron or as an intensifier alloy replaced at least 0.20 per cent molybdenum in cast or wrought nickel-chromium-molybdenum or manganese-molybdenum type steels originally containing 0.40 per cent molybdenum. The reaction

of boron when added as ferroboron to aluminum-killed steels was not quite the same in the cast steels as in the wrought steels when the boron addition exceeded 0.0015 per cent. With an addition of 0.003 per cent or more boron to the cast steels, their end-quench curves assumed a higher end-hardness, but dropped off more rapidly than the curves for any of the boron additions to the wrought steels or with the 0.0015 per cent boron addition to the cast steels. The best results from boron were obtained with additions of 0.0015 to 0.002 per cent.

2. Boron additions had no apparent adverse effect on notched-bar toughness

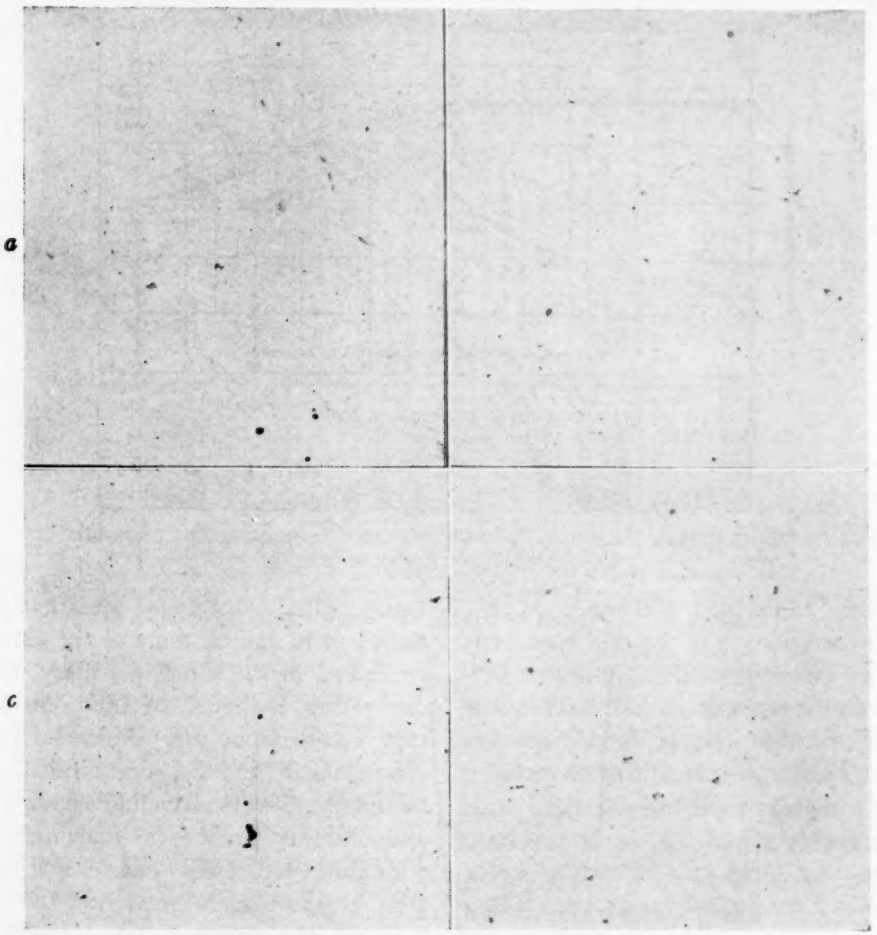

FIG. 14.—THE EFFECT OF MELTING STOCK ON THE TYPE OF INCLUSIONS PRODUCED IN CAST LOW-ALLOY STEELS TREATED WITH AN INTENSIFIER ALLOY. × 100.

Heat No.	Chemistry[a] per cent						Inclusion Type	B.H.N.	Izod Ft.-Lb.	Melting stock
	C	Mn	Si	Ni	Cr	Mo				
A-8450	0.24	0.81	0.46	0.53	0.58	0.36	III	286	46.0	Ingot iron punchings
B-8591	0.30	0.80	0.40	0.54	0.54	0.35	II	288	31.5	Sheared ingot iron
C-8452	0.29	1.40	0.44			0.33	III	287	43.5	Ingot iron punchings
D-8595	0.31	1.52	0.39			0.35	II	282	27.5	Sheared ingot iron

[a] All steels treated with 0.375 per cent alloy B.

at temperatures down to −80°F., whether added to steels of high or low molybdenum contents. The manganese-molybdenum steels proved to be slightly inferior to the nickel-chromium-molybdenum type. This was particularly evident in the wrought steels.

3. No direct effect of boron content on susceptibility to temper brittleness was evident. At least 0.10 per cent molybdenum was necessary in the wrought nickel-chromium-molybdenum steel to overcome temper brittleness; whereas at least 0.20 per cent was required in the wrought manganese-molybdenum type and in the cast steels of both base analyses.

4. As molybdenum increased, the tempering temperature required to reach a fixed hardness also increased. This effect was not found with increasing boron additions.

5. On the basis of the test results discussed in this report, a boron addition of 0.0015 or 0.003 per cent can be used to replace half of the molybdenum in aluminum-killed steels of the following average base compositions: (1) 0.30 per cent C, 0.85 Mn, 0.50 Ni, 0.50 Cr, 0.40 Mo; and (2) 0.30 per cent C, 1.60 Mn, 0.40 Mo.

6. Full deoxidation of the melt was found to be necessary to avoid inconsistent hardenability results from the boron addition. This was just as true for the intensifier alloys used to add the boron as for the ferroboron. In cast steels, deoxidation with aluminum prior to a boron addition also prevented an unfavorable distribution of the sulphide inclusions.

Acknowledgment

This investigation of the replacement value of boron for molybdenum constituted part of a research program sponsored by the National Defense Research Committee of the Office of Scientific Research and Development under the classification, N.D.R.C. Research Project NRC-14. Grateful acknowledgment is made to the Office of Scientific Research and Development for its support and its permission to publish this information, to the War Metallurgy Division of N.D.R.C. and the War Metallurgy Committee for supervising and directing the research, to Dr. C. H. Lorig for his guidance and direction, and to other members of the Battelle staff for their helpful contributions.

References

1. M. A. Grossmann: Hardenability Calculated from Chemical Composition. *Trans.* A.I.M.E. (1942) **150,** 227.
2. R. B. Corbett and A. J. Williams: Effects of Boron in Steel. U. S. Bur. Mines *R. I.* 3816.
3. I. R. Kramer, R. H. Hafner, and S. L. Toleman: Effect of Sixteen Alloying Elements on Hardenability of Steel. *Trans.* A.I.M.E. (1944) **158,** 138–148.
4. W. Crafts and J. L. Lamont: Effect of Some Elements on Hardenability. *Trans.* A.I.M.E. (1944) **158,** 157–167.
5. R. A. Grange and T. M. Garvey: Factors Affecting the Hardenability of Boron-treated Steels. 1945 Preprint, American Society for Metals.
6. J. M. Hodge and M. A. Orehoski: Relationship between Hardenability and Percentage of Martensite in Some Low-alloy Steels. *Trans.* A.I.M.E. (1946).
7. W. G. Patton: Mechanical Properties of NE, SAE and other Hardened Steels. *Metal Progress* (May 1943) **43,** 725 to 733.
8. C. E. Sims and F. B. Dahle: Effect of Aluminum on Properties of Medium Carbon Cast Steel. *Trans.* Amer. Foundrymen's Assn., (Sept. 1938) **46,** 65–131.

DISCUSSION

(Robert S. Archer presiding)

J. R. Zadra*—Have you found that the homogenizing treatment had a marked effect on boron? Did you have any experience with that during your tests?

M. C. Udy (author's reply)—We did not go into that phase of the problem.

W. Crafts†—Udy and Rosenthal's results are quite consistent with ours and we have no criticism to make of the paper.

I should like to add that our results on

* Plant Metallurgist, Colorado Fuel and Iron Co., Pueblo, Colorado.

† Union Carbide and Carbon Research Laboratories, Niagara Falls, New York.

steels that were not martensitic after quenching indicated that boron would not be a substitute for molybdenum in incompletely hardened steel, because of low impact strength.

R. H. ABORN*—Mr. Crafts' last remark warrants some additional comments. If boron is to be effectively used without detrimental effect on the mechanical properties, it is necessary that the steel be fully martensitic as quenched. I do not recall that Dr. Udy spoke of that, but I assume that his specimens were quenched entirely to martensite before tempering.

The second point to be emphasized is that, since the effectiveness of boron is so sensitive to the degree of deoxidation and to the history of the heat before deoxidation, some caution should be used in applying conclusions from experimental laboratory heats to commercial heats, at least until the range of expectancy in production heats is determined.

MAX BOLOTSKY†—From the viewpoint of temper embrittlement one must be cautious in substituting boron for molybdenum. While the results would indicate that based on furnace cool versus water quench no deleterious results were obtained, nevertheless in many cases you will wish to temper within the embrittling range itself (approximately between 600° and 1100°F). In this case you will want the steel to resist temper embrittlement to the maximum, therefore it is not advisable to reduce the molybdenum content. That is a very important point, since the impact properties in many cases will be poor because of temper embrittlement rather than inadequate hardenability. In many cases the temper embrittlement is very much worse than the hardenability in that respect.

O. O. MILLER*—The authors have presented many valuable data using "energy absorbed" in breaking notched impact specimens as a criterion for evaluating the steels. It would be interesting to know whether they made a parallel evaluation of the steels using "type of fracture" on the impact specimens as the criterion; that is, the amount of tough, fibrous fracture and the amount of brittle, cleavage fracture. Interest centers in the type of fracture on impact specimens because recent work indicates that type of fracture may be, for some applications, at least as significant as energy absorbed.

M. C. UDY—I am in accord with almost everything that has been said. It is a well-known fact that to get the maximum effect of boron, the steel must be in fully quenched and tempered condition.

We noted the appearance of the notched-bar fractures, but made no attempt to correlate the appearance of the fracture with the amount of energy absorbed in breaking the bars.

S. EPSTEIN†—It has been observed of the boron steels that when heated to a high forging temperature—that is, after so-called "overheating"—they are more liable to show a very coarse crystalline fracture. The excessive grain coarsening may not always happen but it is more liable to happen than in a similar steel without boron.

---

* Assistant Director of Research, United States Steel Corp., Kearny, New Jersey.

† Metallurgist, Aberdeen Proving Ground, Maryland.

* U.S. Steel Corp. Research Laboratory, Kearny, New Jersey.

† Bethlehem Steel Co., Bethlehem, Pennsylvania.

The Izod Impact Strength of Heat-treated Alloy Steel

By Walter Crafts,* Member AIME, and John L. Lamont*

(New York Meeting, March 1947)

Selection of an alloy steel for a heat-treated article has been facilitated by methods for the calculation of hardenability,[1] as-quenched hardness,[2,3] and tempered tensile strength.[4] Ductility and toughness may also be estimated if the steel is completely hardened on quenching,[5,6] and the present study was carried out in order to develop a basis for estimating the Izod impact strength of partially hardened steel.

The investigation was directed toward the prediction of Izod impact strength in steels of normal commercial quality without consideration of special compositions or heat-treatments that might produce abnormal brittleness. It was found that Izod impact strength of alloy steel is controlled by hardness, degree of hardening on quenching, and grain size. In fine-grained steels the impact strength for any given degree of hardening is inversely proportional to the tempered Rockwell C hardness, and the relation of impact strength to hardness is lowered by incomplete hardening.

Calculation of the tensile strength and impact strength of heat-treating steels has shown that, except at very high strengths, tensile strength is raised by alloys without loss of impact strength whereas the tensile strength gained by higher carbon contents tends to be accompanied by a disproportionate loss of toughness. Plain carbon steels give relatively low and unpredictable impact strength. The calculation is sufficiently accurate to be helpful in the selection of alloy steel, and common grades of alloy steel have been evaluated with respect to combinations of tensile strength and impact strength attainable after heat-treatment in sections from 1 to 4 in. in diameter.

Procedure

The study of the relation of hardness to impact strength was based on test data derived from 24 heats from four producers. The steels included the following SAE and AISI compositions: 1020, 1030, 1040, 1340, 3310, 3316, 4320, 4330, 4340, 8620, 8630, 8640, 8720, 8730, 8740, 9310, 9317, 9440, 9917 and three high-alloy chromium-nickel-molybdenum steels. As far as is known, the steels tested were of normal commercial quality. They were supplied in 4-in. sections, which were forged to smaller sizes, prenormalized, and machined to final dimensions.

Heat-treatment was carried out by heating to the usual austenitizing temperature for the grade of steel, holding for one hour per inch of thickness and quenching in still oil at room temperature. Previous work had indicated that this quenching treatment approximates a severity of $H = 0.35$. The bars were tempered as follows: ½ in., 1 in., and 1⅝ in., 2 hr; 2½ in., 3 hr; 4 in., 5 hr. All bars were air-cooled from the tempering tem-

Manuscript received at the office of the Institute Nov. 15, 1946. Issued as T.P. 2134 in Metals Technology, February 1947.

* Chief Metallurgist and Research Metallurgist, respectively, Union Carbide and Carbon Research Laboratories, Inc., Niagara Falls, N. Y.

[1] References are at the end of the paper.

perature. Tempering was carried out on ½-in. and 1-in. bars at 400°, 600°, 800°, 1000°, 1100°, and 1200°F, and the larger bars were tempered at 1000°, 1100°, and 1200°F. Izod impact specimens were machined from the centers of the bars and were tested at room temperature. Rockwell C hardness was determined on the impact specimens.

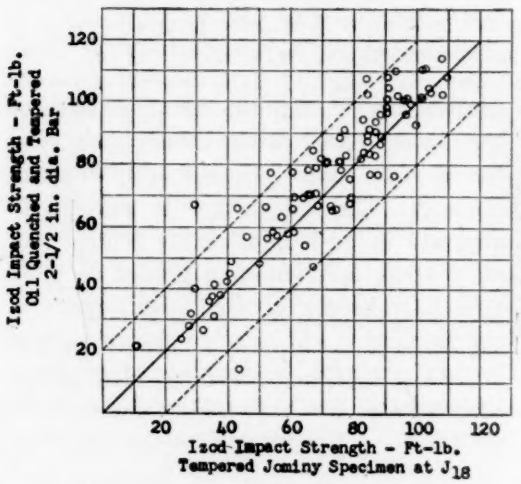

Fig 1

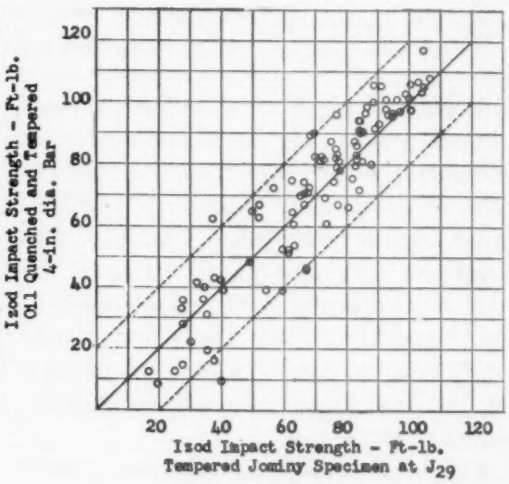

Fig 2

FIGS 1 AND 2—CORRELATION OF JOMINY IZOD IMPACT STRENGTH AND IZOD IMPACT STRENGTH AT CENTER OF OIL-QUENCHED AND TEMPERED BARS.

COMPARISON OF IZOD IMPACT STRENGTHS OF UNIFORMLY QUENCHED BARS AND JOMINY BARS

Izod tests were made from Jominy specimens in order to determine whether the impact strength of large bars could be estimated experimentally from the 1-in. diameter Jominy section in much the same way as the hardenability of bars is predicted from the Jominy test. If this could be done, the impact properties of a steel could be approximated by test over the range of larger sections for which the Jominy specimen is useful. Because the Izod notch cannot be placed nearer to the water-quenched end, the Jominy-Izod test would be applicable only to sections of more than 2½-in. diameter. The impact strength of smaller sections could be estimated by interpolation if a ½-in. or 1-in. uniformly quenched bar were also tested.

The Jominy specimens were end-quenched in the usual way, and tempered at 1000°, 1100°, and 1200°F for 2 hr with air-cooling. The Jominy-Izod specimen was cut with notches at $^{18}/_{16}$ and $^{29}/_{16}$ in. from the water-quenched end to correspond approximately with the cooling rates at the centers of oil-quenched 2½ and 4-in. diameter bars. The 1⅛-in. notch location was necessary because of the dimensions of the Izod impact specimen, but should have been $^{15}/_{16}$ in. for comparison with the 2½-in. diameter bar. The tempering times were also different, so that the data are not exactly comparable. Impact tests were made on duplicate bars so that each value represented the average of two breaks.

As shown in Figs 1 and 2, which include data from other alloy steels as well as those listed above, the Izod values obtained from uniformly quenched bars and Jominy specimens tend to fall within a band of plus and minus 20 ft-lb around the line of perfect correlation. No significant tendencies toward consistent error are

noticeable. Differences in hardness between specimens of these steels[4] are sufficient to explain a part of the error, but it is probable that the errors inherent to the notched-bar test[7] are also represented. The accuracy of plus or minus 20 ft-lb found in the Izod test on Jominy specimens is no better than can be estimated by the calculation described in the following paragraphs.

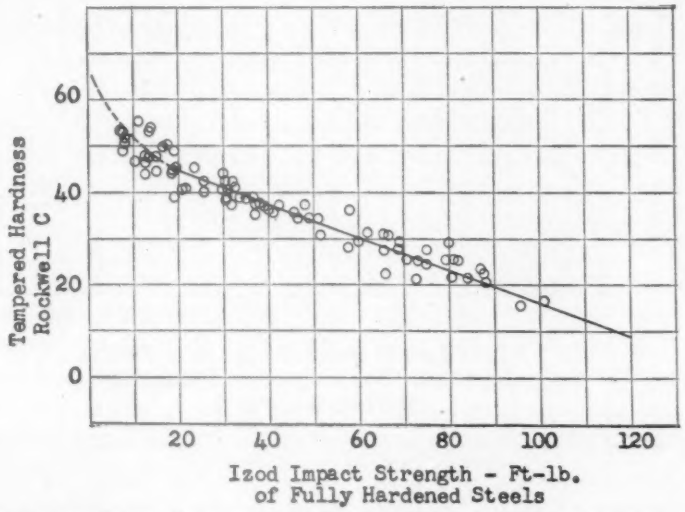

FIG 3—TEMPERED HARDNESS, IZOD IMPACT STRENGTH RELATION FOR FULLY HARDENED FINE-GRAINED STEELS.

CALCULATION OF IZOD IMPACT STRENGTH

In order to evaluate the factors affecting impact strength, the data were classified with respect to the degree of hardening on quenching. The test results of the oil-quenched and tempered bars that were indicated by the Jominy test to have attained maximum hardness are shown in Fig 3. The trend line curves upward above 45 Rockwell C, and below 45 Rockwell C is a straight line represented by the formula

$$I = 2.8(51.7 - R_T)$$

in which R_T is the tempered hardness. These results are in close agreement with the curve shown by Patton.[6] Fig 3 shows that the R_C-Izod relation for fully hardened steels is accurate to about plus or minus 15 ft-lb.

The impact strengths of the partially hardened steels tended to be lower for a given hardness than those for the fully hardened steels shown in Fig 3. The impact strength obtained in each incompletely hardened specimen was compared with the impact strength for fully hardened steel at the same tempered hardness level, and the difference was plotted in Fig 4 against a factor for incomplete hardening. After many trials it was found that incomplete hardening could be represented most accurately by the difference between the maximum attainable hardness for the carbon content of the steel[3] and the estimated as-quenched hardness. As shown in Fig 4, the effect of incomplete hardening on impact strength becomes greater as the degree of hardening becomes less, according to the following relation:

$$I_D = \frac{(R_M - R_Q)^{2.35}}{100}$$

where I_D = difference between actual Izod and base line of Fig 3.
R_M = maximum R_C hardness for carbon content.
R_Q = quenched R_C hardness.

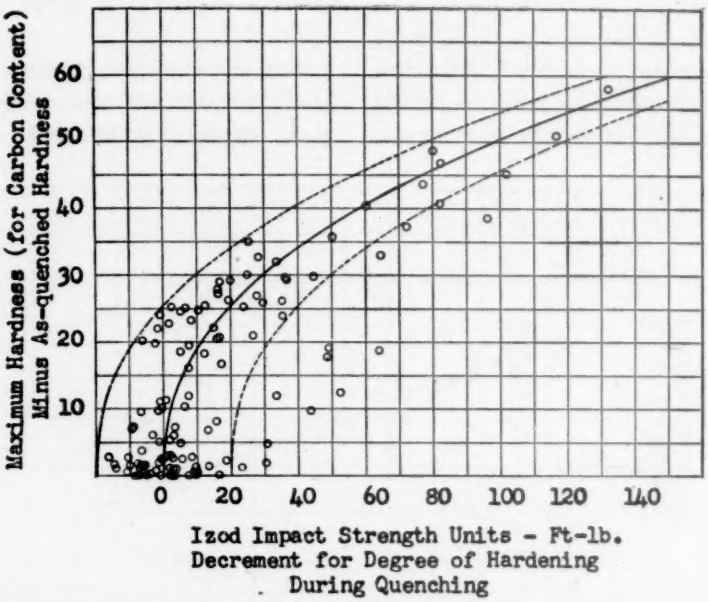

FIG 4—LOSS OF IZOD IMPACT STRENGTH RESULTING FROM INCOMPLETE HARDENING OF FINE-GRAINED STEELS TEMPERED AT 1000°F.

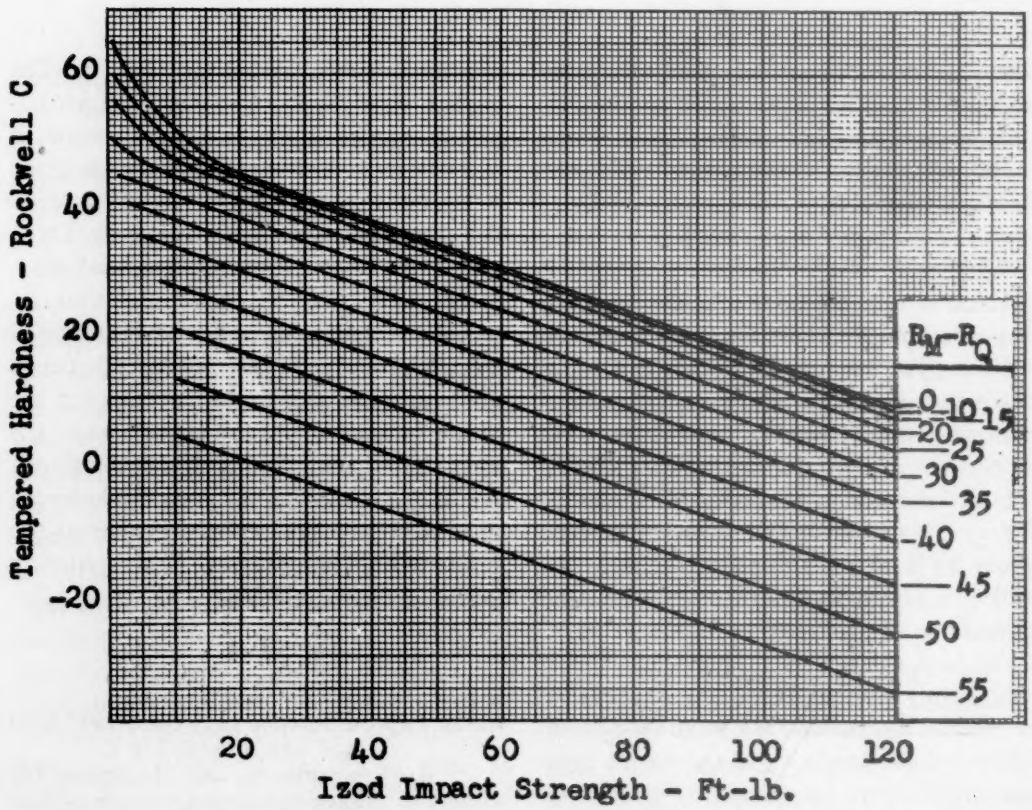

FIG 5—TEMPERED HARDNESS, IZOD IMPACT-STRENGTH RELATION OF FINE-GRAINED STEELS FOR VARIOUS DEGREES OF HARDENING ON QUENCHING.

The expression for calculating Izod impact strength of fine-grained steel is given in the following equation:

$$I \text{ (below 45 } R_C) = 2.8(51.7 = R_T) - \frac{(R_M - R_Q)^{2.35}}{100}$$

$$I \text{ (above 45 } R_C) = \text{(base line of Fig 3)} - \frac{(R_M - R_Q)^{2.35}}{100}$$

The effect of incomplete hardening is also shown in Fig 5, which permits the graphic determination of Izod impact strength if the degree of hardening in quenching and the tempered hardness are known. The Izod impact strengths calculated from this relation are compared with the values obtained by testing in Figs 6 to 12.

Except for plain carbon steels and a few specimens of alloy steel, the relation is accurate within about plus or minus 20 ft-lb. Considerable effort was made to reduce the degree of error by evaluating the specific effects of alloying elements and introducing functions dependent on tempering temperature as well as by the use of different criteria for degree of hardening. Alloying elements such as boron, nitrogen, and phosphorus are known to have harmful effects. It is possible that some other alloys are beneficial, but in this group of steels it was not possible to identify the effects of individual alloying elements, therefore alloys could not be considered to have significantly specific effects with respect to impact strength except for their influence on hardness and degree of hardening. This observation is somewhat surprising, and it should be emphasized that it might not be true for other alloys, such as titanium, vanadium, and zirconium, that combine strongly with nonmetallics and refine the grain size. It also might not be true for other conditions of heat-treatment, for properties other than impact strength or for any specific effects of alloys that might be hidden by the error of plus or minus 20 ft-lb.

Although individual alloying elements were found not to have specific effects, the plain carbon steels were quite erratic and gave many abnormally low values, as shown in Fig 6. On the other hand, results on the alloy steels were quite consistent and, as shown in Fig 7, the values were generally within the normal error. After tempering at 600° and 800°F the alloy steels reflected tempering brittleness with lower than average values. The cause of the disproportionately low impact-strength values found in the carbon steels was not determined. Microscopic examination was not conclusive but indicated that nonuniform response to quenching might have had a considerable influence. In view of the consistent behavior of the alloy steels, it would appear that there is a qualitative difference between carbon steels and alloy steels and that the Izod impact strength of carbon steels cannot be estimated satisfactorily. Since such unknown factors are involved, it is also quite possible that alloy steels under some conditions might exhibit abnormal behavior, but it is considered on the basis of these tests that alloy steels will react in a predictable manner with respect to the calculation of Izod impact strength.

Calculation Restricted to Fine-grained Steels

The restriction of the calculation to fine-grained steels cannot be emphasized too strongly. All of the steels described in this investigation appeared to have been treated with aluminum and approached a No. 8 grain size. The data available to the authors on the effect of coarser and finer grain size are somewhat questionable and meager, so that the grain-size relation could not be studied quantitatively. The toughening effect of fine grain size is well known, and for 15 years grain refinement has been virtually standard practice in the manufacture of American heat-treating alloy steels. It is considered quite plausible that the beneficial effect

of special deoxidizers noted by Patton[6] resulted, at least to a large degree, from more effective grain refinement. The available data indicate that in coarse-grained steels the loss of impact strength may be more pronounced if the steel is incompletely hardened, and in partially hardened coarse-grained steels the Izod values may be more than 30 ft-lb less than comparable values calculated for fine-grained steels. The loss of impact strength due to coarse grain size appears to be comparable to the effect of incomplete hardening. Since these two factors, grain size and degree of hardening, were found to be of much greater importance than any other factors except hardness, the harmful effects of overheating and slack quenching are obvious.

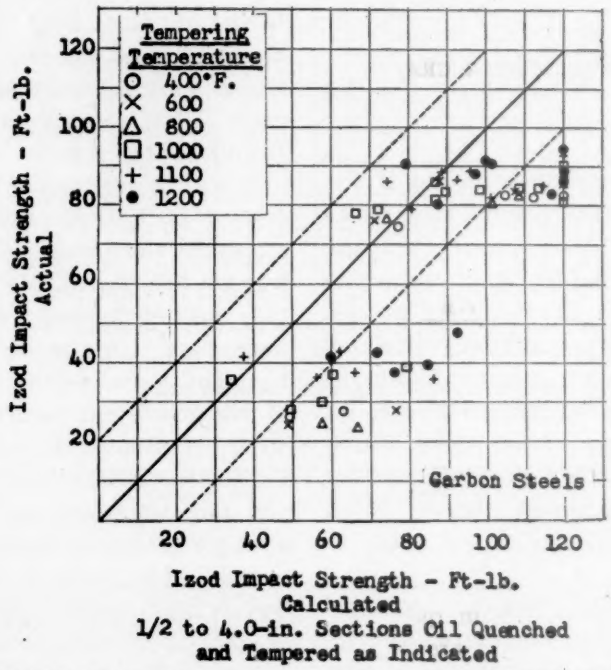

FIG 6—CORRELATION OF ACTUAL AND CALCULATED IMPACT STRENGTH OF CARBON STEELS.

SIGNIFICANCE OF IMPACT STRENGTH IN SELECTION OF STEEL

In order to determine the degree to which impact strength might influence the selection of a steel, the effects of composition, section, and tempering temperature on tensile strength and Izod impact strength were calculated for a number of types of fine-grained 0.20 to 0.50 pct carbon steels. The lower third of the specified range of alloy content was used for SAE and AISI steels with No. 8 grain size and residuals of 0.07 pct Cr, 0.08 Ni, and 0.02 Mo. Also included are steels designated as 2CrOO (0.75 pct Mn, 0.25 Si, 1.50 Cr), 3 CrOO (0.50 pct Mn, 0.25 Si, 3.00 Cr, 0.50 Mo) and *X*9100. Because of inadequate information on the effect of zirconium on as-quenched hardness, the values given for *X*9100 were calculated from actual Jominy curves.[8] Vanadium was assumed to have no effect on as-quenched hardness and vanadium steels may have been calculated to have less than the actual attainable strength. The calculations were based on a quenching severity of $H = 0.35$ for oil and $H = 1.0$ for water at the centers of rounds. Tempering time was assumed to be one hour per inch of thickness. As-quenched hardness

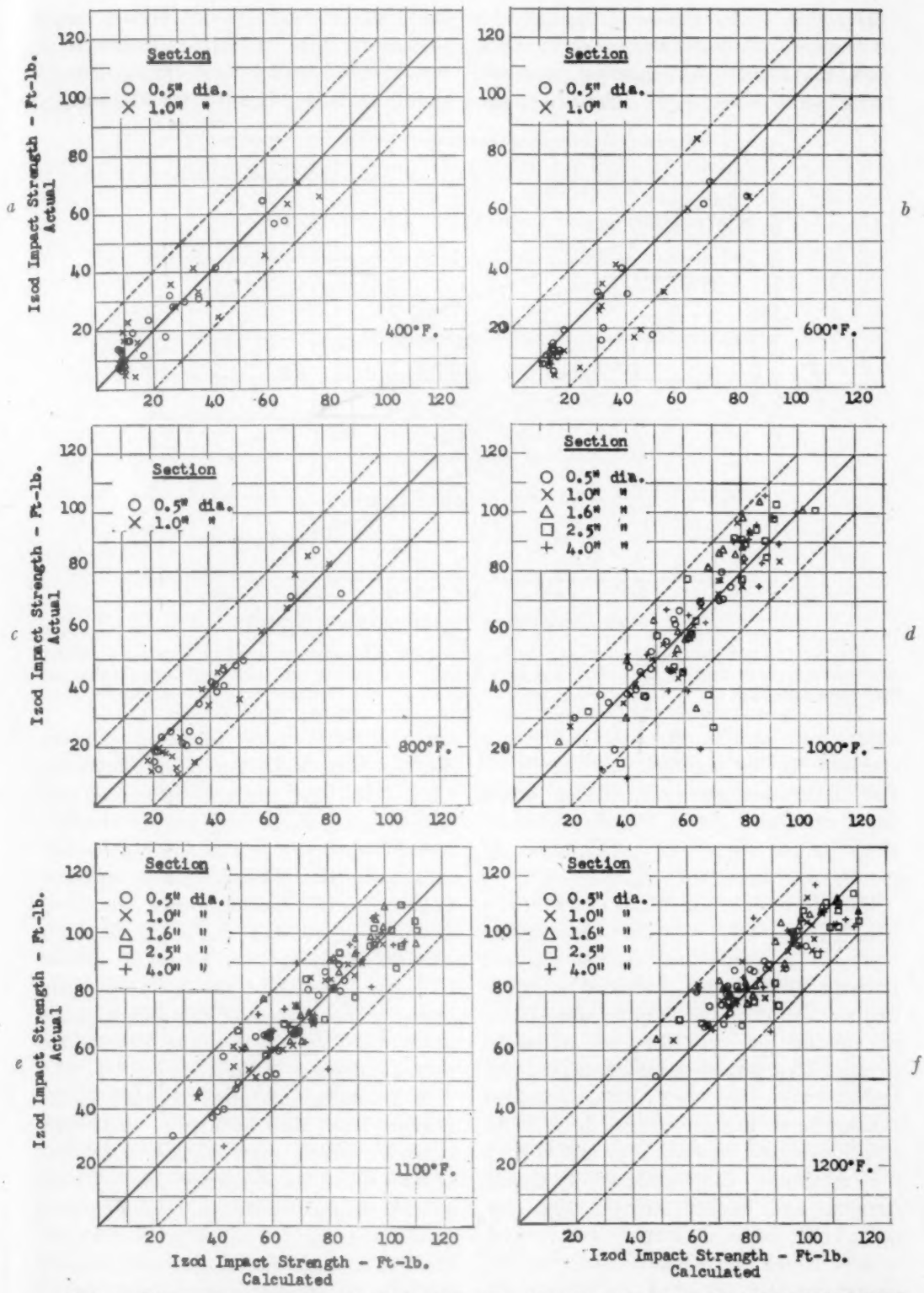

FIG 7—CORRELATION OF ACTUAL AND CALCULATED IMPACT STRENGTH OF ALLOY-STEEL BARS OIL-QUENCHED AND TEMPERED AT TEMPERATURES INDICATED AT LOWER RIGHT CORNER OF EACH FIGURE.

was estimated by the addition method,[3] and tempered hardness and tensile strength were calculated[4] for tempering temperatures from 800° to 1200°F. These hardness values were used to estimate Izod impact strength by the method just described. For illustration purposes, carbon steels were calculated in a similar manner, although the values are not suitable for prediction of impact strength.

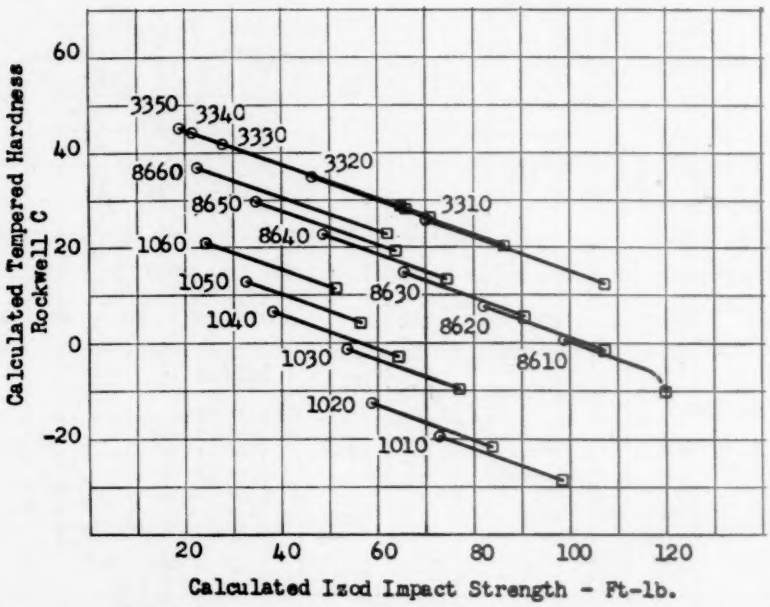

FIG 8—EFFECT OF CARBON ON RELATION BETWEEN TEMPERED HARDNESS AND IZOD IMPACT STRENGTH CALCULATED FOR 4-INCH DIAMETER BARS OIL-QUENCHED AND TEMPERED BETWEEN 800° AND 1200°F.

One of the most significant observations (Fig 5) is that for any hardness number there is a maximum average impact strength that is not exceeded in fully hardened steel of No. 8 grain size. Thus, at 190,000 psi (41 R_C) the maximum average Izod impact strength is 30 ft-lb, and at 155,000 psi (34 R_C) the maximum average Izod impact strength is 50 ft-lb. It is considered reasonable to expect that the maximum combinations of tensile strength and impact strength that are typical for steels of ordinary commercial quality might be increased somewhat by special treatments.

The general effects of carbon and alloy content are indicated in Fig 8, which represents the calculated Rockwell C hardness and average Izod impact strength that might be obtained in oil-quenched 4-in. diameter bars tempered between 800° and 1200°F. In the carbon steel series (SAE-1000) the hardness increases with carbon content and the impact strength becomes critically low in the high-carbon ranges. In the NE-8600 series, as compared with the carbon steels, the additional alloy content raises the hardness without affecting the range of impact strength. The SAE-3300 steels are fully hardened at all carbon contents and the hardness-impact combination is at the maximum shown in Fig 5.

It is notable that although both higher carbon and alloy contents raise the hardness, alloys may increase hardness, at least up to the maximum line, without sacrifice of impact strength. Higher carbon, on the other hand, tends to produce higher hardness at a sacrifice of attainable impact strength. It would appear that carbon raises the level of hardness to a greater

degree than it increases hardenability, so that the impact strength is affected disproportionately. Alloys raise the hardness only through their effect on hardenability, and highest hardness levels the effect of higher alloy contents is to increase the hardness without materially changing impact strength. In smaller sections more

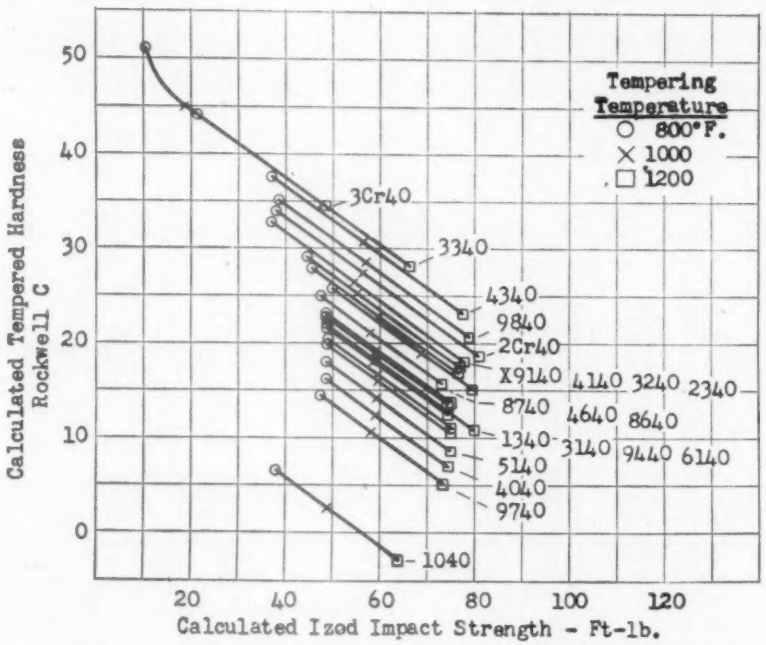

FIG 9—RELATION OF TEMPERED HARDNESS TO IZOD IMPACT STRENGTH CALCULATED FOR 0.40 PER CENT CARBON STEELS OIL-QUENCHED AND TEMPERED IN 4-INCH DIAMETER BARS.

so that hardness is benefited without loss of impact strength.

The hardness-impact-strength relation calculated for 0.40 pct carbon steels oil-quenched in 4-in. diameter bars is shown in Fig 9. The impact strength is fairly high, and would not normally be considered to be critical in any except the fully hardened steels tempered at low temperatures. Between plain carbon and the lowest alloy steels, it is apparent that there is an improvement of both hardness and impact strength. As the alloy content is raised further, the hardness is increased without much change of impact strength until the maximum line is approached. At the maximum the steels are full hardening and the carbon is high enough to produce at low tempering temperatures the very high hardness associated with low impact strength. Except at the lowest of these steels would be hardened to a greater degree on quenching and would reach the higher strength levels where relatively high tempering temperatures are required to develop high toughness.

Tables 1, 2 and 3 were prepared to illustrate in more detail the interrelation of impact strength, tensile strength, and section calculated for different steels. The bracket of tensile strength in which each steel was grouped was determined by the requirements that the maximum strength of the bracket and the indicated minimum Izod impact strength could be obtained by tempering at 800°F or higher. A tempering temperature of 800°F was assumed to be the minimum for a reliable and consistent tempering treatment and, as the tensile strengths shown approximate the maximum strengths attainable, the tables must be viewed with some reserva-

tion. The range of tensile strength in each bracket was chosen so that at tensile strengths over 140,000 psi each bracket would correspond to a change of 10 ft-lb in the Izod impact strength. Because the impact strength is less critical below 140,000 psi tensile strength, the range of 15,000 psi in each of the lower strength brackets was selected for convenience. The Izod levels of 30 ft-lb average (10 ft-lb minimum) in Table 1, 40 ft-lb average (20 ft-lb minimum) in Table 2 and 50 ft-lb average (30 ft-lb minimum) in Table 3 were selected for illustration because they appeared to be of the greatest interest. Tensile strengths at other levels of impact strength may be obtained by calculation.

TABLE 1—*Calculated Tensile Strength of Fine-grained Quenched and Tempered (800°F Minimum) Steels with 30 Ft-lb Average (10 Ft-lb Minimum) Izod Impact Strength*

H = 0.35 (Still Oil).....	1-in Diameter			2-in. Diameter			3-in. Diameter			4-in. Diameter		
H = 1.0 (Still Water)...	1½-in. Diameter			3-in. Diameter			4-in. Diameter			5-in. Diameter		
170,000 to 190,000 psi	3Cr20 3330 4330 3Cr30 3240 3340 4140 4340 X9140	9840 2Cr40 3Cr40 1350 3150 3250 3350 4150	4350 4650 8650 8750 X9150 9450 9850 2Cr50 3Cr50	3Cr20 3330 3Cr30 3340	4340 3Cr40 3350	4350 9850 2Cr50 3Cr50	3Cr20 3330 3Cr30	3340 3Cr40	3350 4350 3Cr50	3Cr20 3330	3Cr30 3340 3Cr40	3350 3Cr50
155,000 to 170,000 psi	3320 9320 X9130 9830	2Cr30 2340 8640	8740 2350 5150 6150	3320 4330 4140 X9140	9840 2Cr40 3150 3250 4150	8650 8750 X9150 9450	3320 4340 9840	2Cr40 3250 4150	X9150 9850 2Cr50		4340 4350 9850 2Cr50	
140,000 to 155,000 psi	3230 1340 3140	4640 5140 6140	9440 4050 9750	9320 9830 2Cr30	3240 8740 1350	2350 4650 6150	4140 X9140 3150		8650 8750 9450	3320 9840	2Cr40	X9150 4150
125,000 to 140,000 psi	9820 2Cr20	4130	8730 4040	X9130 1340 2340	3140	4640 8640 5150	9320 4330 X9130	9830 3240 8740	1350 2350 4650	4330 4140 X9140	2350 3150	3250 8750 9450
110,000 to 125,000 psi	2520 3220 4320 4820 X9120	1330 2330 3130 4630	5130 6130 8630 9430 9740	3230 6140	9440	4050 9750	2Cr30 2340 4640	8640	4050 5150 6150	9320 X9130 9830	2Cr30 2340 3240 1350	4650 6150 8650
95,000 to 110,000 psi	1320 4120 8620		8720 9920 4030	2520 4320 4820 X9120 9820	2Cr20 1330 2330 3130 4130 4630	8630 8730 4040 5140 9740	9820 2330 3230	1340 3140 5140	6140 9440 9750	3230 1340 3140 4640	6140 8640 8740	9440 4050 5150 9750
80,000 to 95,000 psi	2320 3120	4620 5120 6120	9420 9730	1320 2320 3120 3220 4120	4620 8620 8720 9920	4030 5130 6130 9430 9730	2520 3220 4120 4320 4820 8720 X9120	9920 2Cr20 1330 3130 4130 4630	5130 6130 8630 8730 9430 4040 9740	2520 3220 4320 4820 X9120 9820 2Cr20	1330 2330 3130 4130 4630 5130	6130 8630 8730 9430 4040 5140 9740
65,000 to 80,000 psi		4020 9720		4020 5120	6120	9420 9720	1320 2320 3120 4020	4620 5120 6120 8620	9420 9720 4030 9730	1320 2320 3120 4120	4620 5120 6120 8620 8720	9420 9920 4030 9730
50,000 to 65,000 psi										4020	9720	

The steels shown in the top group of each table were all limited by impact strength and were calculated to be tempered at temperatures higher than 800°F in order to lower the strength to a level consistent with the impact strength. All the steels shown below the heavy line

running diagonally through each table had more than the indicated impact strength after tempering at 800°F, so that the tensile strength shown is the maximum attainable with an 800°F minimum tempering temperature. Similarly, in the intermediate groups the strengths of some of the steels were lowered for the sake of impact strength while others required no adjustment. The steels shown in the highest group represent types that are essentially martensitic after quenching, which in all probability will have the anticipated impact strength. The steels in the lower groups below the heavy line in Table 1 are not completely hardened during quenching and the possibility of less than anticipated toughness is greater. Although this qualification is not indicated by the test data, general experience has indicated that incompletely hardened steels may be abnormally erratic

TABLE 2—*Calculated Tensile Strength of Fine-grained Quenched and Tempered (800°F Minimum) Steels with 40 Ft-lb Average (20 Ft-lb Minimum) Izod Impact Strength*

H = 0.35 (Still Oil).....	1-in Diameter	2-in. Diameter	3-in. Diameter	4-in. Diameter
H = 1.0 (Still Water)...	1½-in. Diameter	3-in. Diameter	4-in. Diameter	5-in. Diameter
155,000 to 170,000 psi	3320 4150 9320 X9140 4350 3Cr20 9840 4650 3330 2Cr40 8650 4330 3Cr40 8750 3Cr30 1350 X9150 3240 2350 9450 3340 3250 9850 4140 3250 2Cr50 4340 3350 3Cr50	3320 3Cr40 3Cr20 3350 3330 4350 3Cr30 9850 3340 2Cr50 4340 3Cr50	3Cr20 3Cr40 3330 3350 3Cr30 4350 3340 3Cr50	3Cr20 3Cr40 3330 3340 3350 3Cr30 3Cr50
140,000 to 155,000 psi	3230 2340 8740 X9130 3140 9440 9830 4640 4050 2Cr30 5140 5150 1340 6140 6150 8640	9320 3250 4330 X9140 4150 9830 9840 4650 2Cr30 2Cr40 8650 3240 1350 8750 4140 2350 X9150 8740 3150 9450	3320 4150 4340 X9150 9840 9450 2Cr40 9850 3250 2Cr50	3320 4350 4340 2Cr40 9850 9840 2Cr50
125,000 to 140,000 psi	9820 4130 4040 2Cr20 8730 9750	X9130 2340 8640 1340 3140 6150 4640	9320 3240 3150 4330 4140 4650 X9130 X9140 8650 9830 2350 8750	4330 4150 2350 X9150
110,000 to 125,000 psi	2520 1330 5130 3220 2330 6130 4320 3130 8630 4820 4630 9430 X9120 9740	3230 4050 6140 5150 9440 9750	2Cr30 8740 2340 1350 4640 5150 8640 6150	9320 3240 4650 X9130 4140 6150 9830 X9140 8650 2Cr30 1350 8750 2340 3150 9450 3250
95,000 to 110,000 psi	1320 8720 4120 9920 8620 4030	2Cr20 2520 1330 8630 4320 2330 8730 4820 3130 4040 X9120 4130 5140 9820 4630 9740	9820 5140 2330 6140 3230 9440 1340 4050 3140 9750	3230 6140 9440 1340 8640 4050 3140 8740 5150 4640 9750
80,000 to 95,000 psi	2320 4620 9420 3120 5120 9730 6120	1320 4620 4030 2320 8620 5130 3120 8720 6130 3220 9920 9430 4120 9730	2520 9920 5130 3220 2Cr20 6130 4120 1330 8630 4320 3130 8730 4820 4130 9430 8720 4630 4040 X9120 9740	2520 1330 6130 3220 2330 8630 4320 3130 8730 4820 4130 9430 X9120 4630 4040 9820 5130 5140 2Cr20 9740
65,000 to 80,000 psi	4020 9720	4020 6120 9420 5120 9720	1320 4620 9420 2320 5120 9720 3120 6120 4030 4020 8620 9730	1320 4620 9420 2320 5120 9920 3120 6120 4030 4120 8620 9730 8720
50,000 to 65,000 psi				4020 9720

and predictions of impact strength for steels below the heavy line should be applied with special precautions.

The general pattern is controlled primarily by hardenability, with some sections. With increase of carbon and alloy contents the attainable strength rises rapidly in the small sections, but most of the steels tend to have low strengths in the heavier sections. As the alloy content is raised, the strength of the heavier sections increases, until at high alloy contents the same high strength is obtainable in all sections without sacrifice of impact strength. The increased Izod requirements in Tables 2 and 3 lower the maximum

TABLE 3—*Calculated Tensile Strength of Fine-grained Quenched and Tempered (800°F Minimum) Steels with 50 Ft-lb Average (30-Ft-lb Minimum) Izod Impact Strength*

H = 0.35 (Still Oil).....	1-in Diameter			2-in. Diameter			3-in. Diameter			4-in. Diameter		
H = 1.0 (Still Water)...	1½-in. Diameter			3-in. Diameter			4-in. Diameter			5-in. Diameter		
140,000 to 155,000 psi	3320 9320 3Cr20 3330 4330 3Cr30 3240 3340 4140 4340	X9140 9840 2Cr40 3Cr40 1350 2350 3150 3250 3350	4150 4350 4650 8650 8750 X9150 9450 9850 2Cr50 3Cr50	3320 3Cr20 3330 3Cr30 3340 4340	3Cr40 3350 4350 9850 2Cr50 3Cr50		3Cr20 3330 3Cr30 3340	3Cr40 3350 4350 3Cr50		3Cr20 3330 3Cr30	3340	3Cr40 3350 3Cr50
125,000 to 140,000 psi	9820 2Cr20 3230 4130 8730 X9130 9830	2Cr30 1340 2340 3140 4040 4640 5140	6140 8640 8740 9440 4050 5150 6150	9320 4330 X9130 9830 2Cr30 2340 3240	4140 8740 X9140 9840 2Cr40 1350 2350 3150	3250 4150 4650 8650 8750 X9150 9450	3320 9320 4330 X9130 9830 4140	4340 X9140 9840 2Cr40 2350	3250 4150 X9150 9450 9850 2Cr50	3320 4330 4340	9840 2Cr40 4350	X9150 9850 2Cr50
110,000 to 125,000 psi	2520 3220 4320 4820 X9120	1330 2330 3130 4630 5130	6130 8630 9430 9740 9750	3230 1340 3140	4640 6140 8640	9440 5150 6150	2Cr30 2340 3240	8740 1350 3150	4650 8650 8750	9320 X9130 9830 2Cr30	2340 3240 4140 X9140 2350	3250 4150 8750 9450
95,000 to 110,000 psi	1320 4120 8620		8720 9920 4030	2520 4320 4820 X9120 9820 2Cr20	1330 2330 3130 4130 4630 8630	8730 4040 5140 9740 4050 9750	9820 2330 3230 1340 3140	4640 5140 6140 8640	9440 4050 5150 6150 9750	1340 3140 8640 8740	9440 1350 3150	4650 5150 6150 8650
80,000 to 95,000 psi	2320 3120	4620 5120 6120	9420 9730	1320 2320 3120 3220 4120	4620 8620 8720 9920	4030 5130 6130 9430 9730	2520 3220 4120 4320 4820 8720 X9120	9920 2Cr20 1330 3130 4130 4630	5130 6130 8630 8730 9430 4040 9740	2520 3220 4320 4820 X9120 9820 2Cr20 1330	2330 3130 3230 4130 4630 5130 6130 8630 8730	9430 4040 4640 5140 6140 9740 4050 9750
65,000 to 80,000 psi		4020 9720		4020 5120	6120	9420 9720	1320 2320 3120 4020	4620 5120 6120 8620	9420 9720 4030 9730	1320 2320 3120 4120	4620 5120 6120 8620 8720	9420 9920 4030 9730
50,000 to 65,000 psi										4020	9720	

modification due to the specific effects of individual alloying elements on the resistance to tempering. At very low tensile strengths the low-carbon, low-alloy steels tend to lie horizontally across the tables with little change of strength in different

tensile strength and also restrict the less deeply hardenable types to lower strengths in the heavier sections.

The selection of steel on the basis of impact strength and tensile strength is relatively easy, but the estimation of adequate impact strength is a less tangible problem. Impact strength is seldom critical at low tensile-strength levels, but at very high strengths it is not possible to obtain high impact strength. Obviously, since steels are used successfully at high strengths, it is evident that they are applied in such a way that the impact-strength requirement is not great. It would appear reasonable, therefore, that the impact-strength requirement may be lowered as the strength is raised. Such a sliding scale, ranging from 40 ft-lb minimum Izod at 123,200 psi to 25 ft-lb minimum Izod at 201,600 psi tensile strength, is recognized in Great Britain.[9] The increase in tensile strength that may be obtained by lowering impact strength may be visualized by comparison of Tables 1, 2 and 3.

In the selection of steels to meet certain requirements of tensile and impact strength, it is possible to estimate by methods described in the foregoing pages whether a given steel of known composition will be suitable. However, to determine the composition of a steel that will meet the requirements is not as straightforward unless reference is made to data sheets comparable with Tables 1, 2 and 3. If such tables are not adequate, a rough estimate of a suitable composition may be obtained by reference to Fig 5, in which the relation of tempered hardness to Izod impact strength for fine-grained steel is shown. By locating the desired combination of tempered hardness (tensile strength) and Izod impact strength in the diagram, it is possible to estimate the minimum degree of hardening in quenching ($R_M - R_Q$) that is needed to obtain the required properties. By inspecting Jominy curves for steels of various types, a steel composition can be selected that has the minimum $R_M - R_Q$ value at the proper Jominy depth. When this steel is quenched and tempered its hardness and impact strength should parallel the selected $R_M - R_Q$ line in Fig 5, but the tempering temperature for the desired hardness must be obtained by calculation of the relation of hardness to tempering temperature.[4] If the indicated tempering temperature for the desired hardness is below the toughening range, the use of a steel of somewhat higher carbon or alloy content would be indicated. For this purpose the fine-grained alloy steel types have been classified in Table 4 at graduated levels in approximately equivalent groups with respect to tensile and impact strength. Obviously, this grouping does not take into consideration factors such as abnormal composition, sensitivity to temper brittleness, tendency toward segregation, directional effects, inclusions and abnormal structures, difficulty of holding fine grain size, and incomplete austenitization.

TABLE 4—*Relative Classification of Steels with Respect to Tensile and Impact Strength*

GROUP	TYPE OF STEEL
1	3Cr00
2	3300
3	4300 (except 4320), 9320
4	9800, 2Cr00
5	4100 (except 4120, 4130), X9100
6	2520, 3200, 4320, 4820
7	2300, 4120, 4130, 8700, 9450, 9920
8	1300, 3100, 4600, 8600
9	5100, 6100, 9400 (except 9450)
10	4000, 9700

As a result of contributions from many workers during recent years, it is relatively easy to predict with some degree of accuracy the hardenability and tensile strength as well as impact strength of a steel. These, and closely related properties

such as yield strength and fatigue strength, are primary factors in determining the serviceability of quenched and toughened steels. Since the calculations have indicated that the effects of alloying elements are nonspecific, it may be inferred that, in general, alloys may be used interchangeably without sacrifice of serviceability. This assumption has been confirmed by the successful substitutions made when the demand for certain alloys exceeded the supply. Other properties, such as machinability, quench-cracking, response to heat-treatment, or reliability, which are important in processing a steel through the manufacturing operations, probably are affected to a much greater degree by the type of alloy composition. Thus, after determination of the group of steels that will give the desired tensile and impact strength, the selection of a specific steel from within the group depends largely on the most economical combination of processing factors required to manufacture a consistently serviceable product.

Conclusions

In drawing conclusions from this investigation of impact strength, it cannot be emphasized too strongly that the observations apply only to longitudinal room-temperature Izod impact tests of ordinary commercial alloy-steel bars submitted to a simple quench and draw. The study has not been intended to include special compositions or heat-treatments that might develop abnormal brittleness. Carbon steels were lower in impact strength than could be accounted for by the behavior of the alloy steels. In view of this behavior, and on account of different heat-treating and testing conditions, the observations should be applied conservatively. With limitations of this character, it is concluded that:

1. The Izod impact strength of quenched sections from 2½ to 5 in. in diameter may be estimated by Izod tests cut from end-quenched and tempered Jominy specimens with an accuracy of plus or minus 20 ft-lb.

2. The Izod impact strength of quenched and tempered bars of fine-grained alloy steel up to 4 or 5 in. in diameter may be calculated with an accuracy of plus or minus 20 ft-lb.

3. The Izod impact strength of fully hardened fine-grained alloy steel is inversely proportional to the Rockwell C hardness and is adversely affected by incomplete hardening on quenching. Grain size has an influence of the same order as that of the degree of hardening. In the alloy steels investigated, individual alloying elements did not exert an appreciable amount of specific control over impact strength. Maximum combinations of impact strength and tensile strength require that the steel be made fine-grained and be fully hardened in quenching.

4. Carbon and alloy contents affect impact strength indirectly by their effects on hardness in quenching and tempering. Both higher carbon and alloy contents tend to be beneficial by promoting a closer approach to full hardening. However, because carbon raises hardness to a greater degree than it increases hardenability, the higher carbon steels tend to develop relatively lower values of impact strength. Increase of alloy content in the lower carbon steels raises the tensile strength without sacrifice of impact strength.

5. By the use of methods for evaluating quenching rates, hardenability, tempered hardness, and Izod impact strength, it is possible to predict strength and toughness for the final heat-treated condition in which steel is put into service. The principles for the selection of steel have been outlined with respect to tensile and impact strength and the relative merit of com-

monly produced heat-treating types has been estimated.

References

1. M. A. Grossmann: *Trans.* A.I.M.E. (1942) **150**, 227–255.
2. J. Field: *Metal Progress* (March 1943) 402–405.
3. W. Crafts and J. L. Lamont: *Trans.* A.I.M.E. (1946) **167**.
4. W. Crafts and J. L. Lamont: *Metals Tech.*, A.I.M.E. (Sept. 1946—T.P. 2036). Page 222, this volume.
5. E. J. Janitzky and M. Baeyertz: Metals Handbook Amer. Soc. for Metals (1939) 515–518.
6. W. G. Patton: *Metal Progress* (May 1943) 726–733.
7. C. E. Jackson, M. A. Pugatz, and F. S. McKenna: *Trans.* A.I.M.E. (1944) **158**, 263–279.
8. Properties and Characteristics of N-A-X 9100 Series. Great Lakes Steel Corporation, 1941.
9. Wrought Steels (Carbon and Alloy Steels). B. S. 970–971, British Standards Inst., London, 1941.

DISCUSSION

(H. S. Avery presiding)

J. M. Hodge*—This paper represents a start on the problem of choosing alloy steels for a given application on the basis of toughness as indicated by the room temperature notched bar impact value at the desired hardness level, and as such, is very useful. I believe, however, that the authors will agree that it is only a start on this problem.

The authors state that neglecting temper brittleness or other possible effects of the tempering temperature level, the impact values at a given grain size level will be determined principally by the hardenability. This is, of course, true inasmuch as the hardenability determines the microstructure, but it serves to emphasize the broad field that hardenability now covers, since this study apparently includes microstructures ranging from full martensite to coarse pearlite. Furthermore, the + or − 20 ft-lb spread in the correlation with hardenability, which certainly limits the usefulness of these results for many applications, indubitably reflects the wide range of microstructures corresponding to a given value of hardenability in terms of the difference between full martensite and as-quenched hardness.

For example, in many alloy steels, microstructures ranging from full martensite to 50 pct martensite, correspond to as-quenched hardness values ranging from 0 to 15 Rockwell below full martensite hardness. Since Fig 5 indicates an average drop of only 5 ft-lb for as-quenched hardness values 15 Rockwell below full martensite hardness, and since this 5 ft-lb drop is not only low but also insignificant in comparison with the plus or minus 20 ft-lb accuracy of the correlation, the paper implies that corresponding changes in as-quenched microstructures of from full martensite to 50 pct martensite are likewise insignificant. Furthermore, all the compositions in the top hardness range of Tables 1, 2 and 3 fall within this category and this would seem to imply that microstructural differences, ranging from full martensite to 50 pct martensite, are insignificant for high strength applications. I believe that such an implication is dangerous until we learn more about the relationship between microstructure and properties.

Applications of hardenability values ranging over hardness differences of from 20 to 60 Rockwell C, with which the paper is principally concerned, correspond to microstructures ranging from 50 pct tempered martensite to full pearlite. Furthermore, in the mixtures of tempered martensite and non-martensitic products, these products will range from bainite to pearlite. In this connection, what little work we have done on the effect of non-martensitic products on the impact values of tempered martensite, has indicated that for a given microstructure in terms of the percentage of martensite or even for a given hardness level, pearlite is much more harmful than upper bainite in this respect. The wide range of impact values for a given hardness difference is probably largely a function of the characteristics of these non-martensitic products, and the particularly low values of the plain carbon steels might well result from the preponderance of pearlitic products in such partially hardened steels.

This paper assumes, however, that these microstructural differences, corresponding to a given hardness difference, are insignificant and, therefore, Tables 1, 2 and 3 offer a wide choice of compositions for the lower hardness levels. With this wide range available, the final choice would probably be dictated by cost and this

* Carnegie-Illinois Steel Corp. Carnegie Building, Pittsburgh, Pa.

would lead to the use of low alloy or plain carbon steels whose microstructures would be the most unfavorable. Although this would be justified by the impact value alone, it likewise seems dangerous until more is known about the relationships with other properties.

Thus, although this paper does furnish a useful general guide to the application of alloy steels to meet impact requirements, the method used has many limitations and it should be emphasized that many factors, beyond those involved in these calculations, must be considered in arriving at a final choice of an alloy or plain carbon steel for a given application.

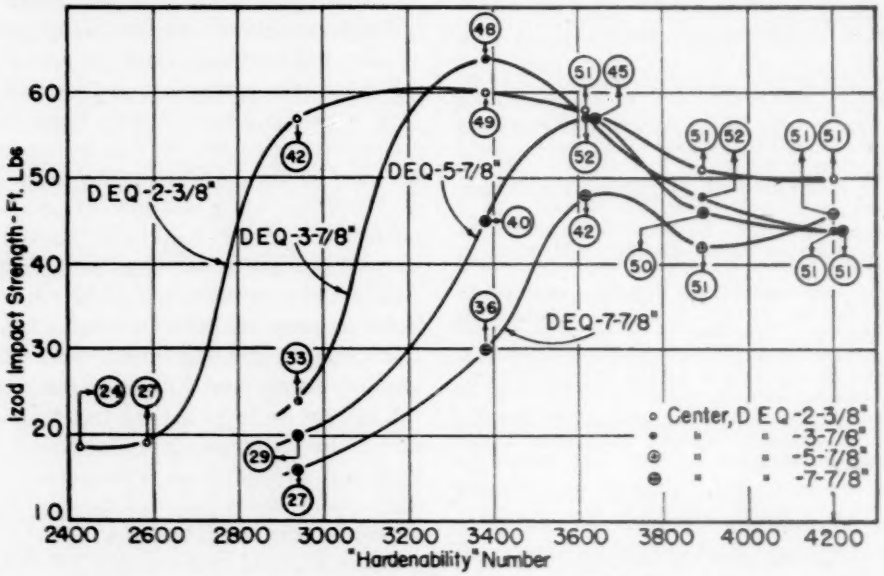

FIG 10—COMPARISON OF IZOD IMPACT STRENGTH AT 23 RC (CONV. BRINELL 240) AT THE CENTER OF QUENCHED AND TEMPERED D.E.Q. 2⅜, 5⅞ AND 7⅞ BY 2-INCH DIAMETER SPECIMENS WITH "HARDENABILITY" NUMBER FOR 0.30 PER CENT CARBON CAST MN-CR-MO STEELS.

H. S. AVERY*—This discussion has highlighted the point that in most cases, in a selection of steel, we wish to avoid mixed structures. I think that that is, by and large, the objective of an engineer who picks a material. We do not ordinarily slack-quench, but usually try to get full martensitic structures.

B. L. JOHNSON, JR.†—Since all of these tests were run at room temperature, I wonder to what extent the results are affected by the difference in spread that is likely to exist in impact values, depending on how near the testing temperature happens to be to the transition temperature of the material. In other words, room temperature being an arbitrary line on the complete energy-temperature plot, for the particular notch condition and strain rate that are involved in the type of sample and test method chosen, the results at room temperature may be nearer or further away from the transition temperature depending on the nature of the steel. The nearer the tests are to the transition temperature the more spread in impact values one may expect.

H. S. AVERY—I might contribute a bit on the relationship of this paper to cast steels, by first referring to Fig 10. This work has been confined to fine grain wrought material, if I understand correctly. A somewhat similar research* on cast materials has used double-end quench Jominy type specimens, enlarged and quenched on both ends to permit obtaining the properties corresponding to slowly cooled thick plates.

The four curves which you see correspond to 2-in., 4-in., 6-in. and 8-in. thick plates with

* Research Metallurgist, American Brake Shoe Co., Mahwah, N. J.

† Mack Manufacturing Co., Plainfield, N. J.

* Wilks, Avery and Cook: "Relation of Quenching Rate and Hardenability to the Mechanical Properties of Several Heat Treated and Alloy Steels." *A.S.M.* 1946 Preprint No. 28.

properties determined, however, on laboratory specimens whose center cooling curves matched those of the quenched plates. The impact strength on the left of the scale falls off sharply as the hardenability of the material is lowered. This is especially true with the heavier sections, because they are not able to fully harden in the center of the section.

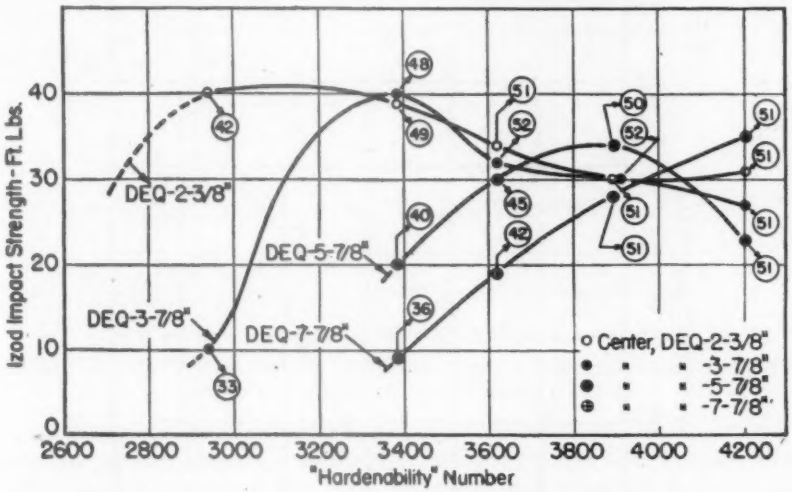

FIG 11—COMPARISON OF IZOD IMPACT STRENGTH AT 32 RC (CONV. BRINELL 300) AT THE CENTER OF QUENCHED AND TEMPERED D.E.Q. $2\frac{3}{8}$, $3\frac{7}{8}$, $5\frac{7}{8}$ AND $7\frac{7}{8}$ BY 2-INCH DIAMETER SPECIMENS WITH "HARDENABILITY" NUMBER FOR 0.30 PER CENT CARBON CAST MN-CR-MO STEELS.

On those representing the Izod values at Rockwell 23°C in the fully hardened end, they cluster about + or − 10—about 52 Izod—falling off as insufficient hardenability or the slow cooling begins to bring in mixed structures.

In comparison with the values that the authors have presented, these will range about 52 + or − 10; whereas the authors, by using their chart, would get values of about 80 + or − 20, as they have stated. However, for the small amount of data that is compared here, the authors' values would be about + or − 10 from their charts, indicating about 30 ft-lb difference between longitudinal wrought specimens and the more equiaxed cast specimens.

In Fig 11 you can see a comparison at Rockwell 32—somewhat harder. Here we again have the same four curves, representing different cooling rates. It is obvious that there is a falling off of properties as the hardenability of the material is not sufficient to obtain maximum hardness as quenched.

These values of about 30 ft-lb + or − 10 compare with approximately 56 ft-lb + or − 10 or 20 that the authors presented for the wrought materials.

In Fig 12 there is a somewhat different way of indicating the loss in Izod impact strength, as the materials are tested at a given hardness but have had different initial hardnesses. The slack-quenching is indicated by the trend of the curves to the left. The point on the right-hand end represents full hardening, and at the two hardnesses—23 Rockwell or 32 Rockwell—there is the definite falling off of Izod impact strength at a given hardness as a result of the incomplete hardening in the quench.

C. WELLS*—When you fully quenched-out specimens from a given material at different hardness levels, did you observe that the spread that you got was fairly constant or did it vary? In fully quenched-out materials our results have indicated that when the average impact value is high, the spread is high and when the average impact value is low, the spread is low.

At a level of 70 or 80 ft-lb, the spread, according to our data, may be of the order of + or − 10 ft-lb. At a level of 20 ft-lb, the spread is only of the order of 3 or 4 ft-lb. These spreads are roughly the three sigma limits. Out of a thousand specimens, on the average, there should not be more than three or four, which would be outside of the limits stated.

* Metals Research Laboratory, Carnegie Institute of Technology, Pittsburgh, Pa.

I. R. KRAMER*—I would like to ask whether the authors observed the type of fracture on the impact specimens. The nature of the fracture is very important in determining the amount of scatter in the impact data. For this work, the testing was done at room temperature and it is not possible to determine the relation of this temperature to the transition temperature range. However, since for some of the steels reported, the impact energies were as low as 20 ft-lb while others were as high as 40 ft-lb there is no doubt that the specimens were at temperatures both above and in the transition zone. For those specimens broken in the transition zone the impact values may wells how a scatter of 30 to 40 ft-lb. For those specimens tested above the transition zone the spread of the energy values may be only 3–5 ft-lb. This, I believe, should have a very definite bearing on the results for the calculation of the impact energies.

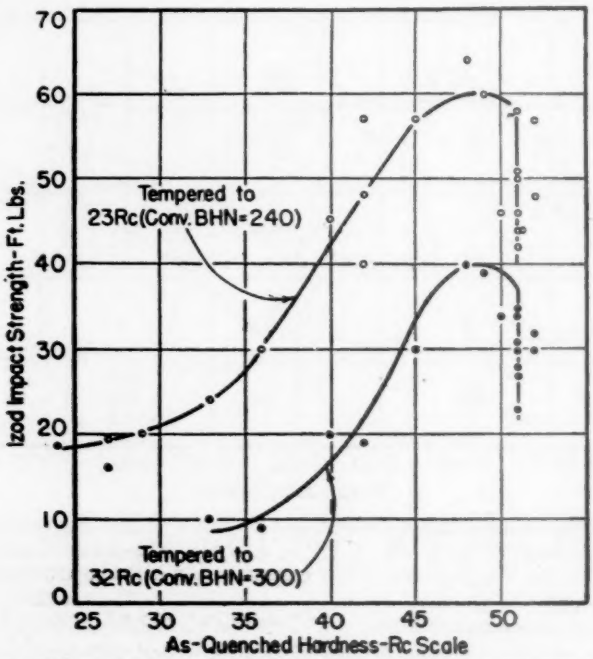

FIG 12—COMPARISON OF IZOD IMPACT STRENGTH OF DOUBLE END-QUENCHED AND TEMPERED 0.30 PER CENT CARBON CAST MN-CR-MO STEELS WITH AS-QUENCHED HARDNESS.

G. DE VRIES†—The authors state that alloying elements such as boron, nitrogen and phosphorus are known to have harmful effects on the impact strength of steel. When comparatively large amounts of boron are added to steel this statement may be true. However, in examining over 300 heats of steel containing varying amounts of boron I have found no instance of impaired impact strength when the amount of boron added to steel is less than 0.002 pct. Did the authors intend to have their statement as to the harmful effects of boron apply when the amount added is less than 0.002?

W. CRAFTS (author's reply)—The authors are grateful to Mr. Hodge for emphasizing the limitations of the impact strength calculation and agree with most of his comments.

Although the effects of non-martensitic microstructures were not studied, it is quite probable that the impact strength is affected more seriously by pearlitic than by bainitic structures so that carbon steels are more sensitive to slight deficiencies in hardening. The alloy steels as a class tend to form bainite more readily than pearlite and the relation in the paper has been further confirmed by analogous tests on about thirty additional simple and complex alloy steels. Therefore the calculations shown in Tables 1, 2, and 3 are fairly reliable above the heavy line. Below the line the steels

* Office of Naval Research, Washington, D. C.

† Metallurgist U. S. Proving Ground, Dahlgren, Virginia.

are not effectively hardened in quenching and we welcome the emphasis given by Mr. Hodge and reiterate the cautionary remarks in the paper. On the other hand, the top brackets in the tables represent fully hardened steel and should have the impact strength shown in Fig 3.

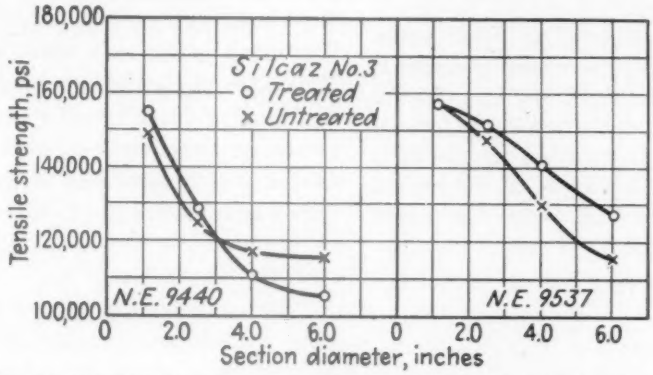

FIG 13—EFFECT OF SECTION ON TENSILE STRENGTH FOR AN IZOD IMPACT STRENGTH OF 40 FOOT POUND IN QUENCHED AND TEMPERED STEELS.

Unquestionably, the formula represents only a first approximation for calculating impact strength and some part of the error of + or − 20 ft-lb is the result of unevaluated factors. However, where the calculation is not involved, as in the comparison of Jominy and uniformly quenched bars, and in the fully martensitic steels, the error is of a comparable order and seems to be an inherent characteristic of the test. Other measures of capacity for deformation, such as reduction of area, may be more reproducible but reflect many additional quality factors that cannot be analyzed readily. Impact strength is also quite sensitive to differences of tensile strength so that in spite of its limitations it seems to be more suitable as a criterion of capacity for deformation. Some measure of ductility is essential in order to evaluate the minimum degree of hardenability and the maximum tensile strength which are consistent with the requirements of serviceability. For this purpose, impact strength seems to provide a more generally applicable basis of comparison, but, as Mr. Hodge points out, under other conditions than those present in this investigation, the impact strength may be quite different. Therefore it is considered that the hardenability-tensile strength-impact strength relation is a comparative guide and that it should be utilized only with allowance for its limitations.

Mr. Johnson has suggested that the error found in the impact test results might be associated with the spread of values found in the transition temperature range. Dr. Wells also stated that in his work the spread of values was found to be more or less proportional to the mean impact strength. Our experience has been similar to that of Dr. Wells with respect to tests on a single steel but has not been found true when the data from several heats have been generalized. The close checks of tests of one steel tend to deny the effect of transition temperature on the error. Quenched and tempered steels, except for consideration of temper brittleness, tend to have transition temperatures well below room temperature and there was no indication that the steels tested were significantly affected by temper brittleness. In reply to Mr. Kramer, it is regretted that the character of the fracture was not examined.

The authors appreciate Mr. Avery's comparison with heat-treated steel castings. Although he has shown a general trend with respect to hardenability, his data from cast steels reveal qualitative differences as well as a translation of the level of impact strength. It is believed that both types of difference are to be expected as our tests were made on longitudinal specimens from rolled and forged bars. A major difference in impact strength would be expected if tests had also been made in the transverse direction and, similarly, castings should also be affected by their lesser degree of orientation. In addition, the impact strength of steel castings is affected to a large degree by nonmetallic inclusions. It is well known that sulphur content and type of deoxidation treatment have

effects that may overshadow hardenability considerations. Therefore it is felt that application of the impact strength relation to castings should be of a qualitative rather than a quantitative character.

Mr. DeVries' statement that boron below 0.002 pct is not harmful to impact strength is true in the case of hardened steels in which a substantial amount of martensite is formed during quenching. In fact when the boron is added as a complex addition agent the impact strength of hardened steel is usually higher than in plain aluminum-treated steels, as stated in the paper. However, if boron-treated steel is not substantially martensitic after quenching, the impact strength is lower than in a comparable untreated steel. This is illustrated by Fig 13 in which Silcaz 3-treated N.E. 9440 steel is shown to develop a relatively low product of tensile strength and impact strength in large sections, whereas a similarly treated deeper hardening N.E. 9537 steel, is improved by Silcaz 3 even in large sections.

Influence of Plastic Deformation, Combined Stresses, and Low Temperatures on the Breaking Stress of Ferritic Steels

By D. J. McAdam, Jr., Member AIME, G. W. Geil, and R. W. Mebs*

(New York Meeting, March 1947)

As shown in previous papers by the authors[9–17]† the resistance of a metal to fracture, like its resistance to plastic deformation, is a function of all three principal stresses.‡ A technical cohesion limit is the technically determined resistance to fracture under a specific stress system. The technical cohesive strength thus comprises an infinite number of technical cohesion limits corresponding to the infinite number of possible combinations of the principal stresses. The technical cohesive strength, therefore, may be represented by a surface in a diagram with the three principal stresses as coordinates. As shown in previous papers,[9–18] the technical cohesive strength increases with plastic deformation, with decrease in temperature, and with increase in the strain rate. The technical cohesion limit, therefore, is affected by the same factors that affect the flow stress,§ namely, the stress system, plastic deformation, temperature, and the strain rate. Moreover, the influence of each of these factors on the technical cohesion limit has been shown to be qualitatively similar to the influence of the same factor on the flow stress.[9–18]

Advance of knowledge about the conditions determining fracture of metals has been retarded by the reluctance of some investigators to abandon preconceived ideas about how metals "should" behave. The incorrect idea is still prevalent that the conditions determining resistance to fracture are very different from those determining the flow stress. Attempts are still being made to express resistance to fracture in terms of a single parameter, such as a limiting value of the greatest principal stress, the maximum shearing stress, or the volume stress (one-third the algebraic sum of the three principal stresses). In these attempts, a sharp distinction is sometimes made between a ductile or "plastic fracture" and a "brittle fracture." In making this distinction, however, the meaning attached to the term "brittle fracture" sometimes is not made clear. The term could mean fracture after very little plastic deformation or it could be used to designate the type of fracture. An ordinary fracture of a ductile metal at room temperature starts as a cleavage, generally transverse to the direction of the greatest principal stress, but eventually changes to a shearing fracture. In some conditions, however, the metal fractures entirely by cleavage, with no evidence of plastic deformation during the fracture; the surface of such a fracture may have a

Manuscript received at the office of the Institute Feb. 24, 1947. Issued as T.P. 2220 in Metals Technology, August 1947.

* Chief of Section on Thermal Metallurgy and Metallurgists, respectively, National Bureau of Standards, Washington, D.C.

† References are at the end of the paper.

‡ Any stress system may be resolved into three principal stresses normal to three mutually perpendicular planes, known as the principal planes, on which there is no shearing stress. Tensile stresses are viewed as positive and compressive stresses as negative. In this paper as in the previous papers, the algebraically greatest principal stress will be designated S_1, the least principal stress will be designated S_3, and the intermediate principal stress will be designated S_2.

§ "Flow stress" is here used in its generally accepted significance to designate the greatest principal stress during flow.

crystalline appearance. Although a fracture of this type sometimes is termed a "brittle" fracture, it may occur after much plastic deformation, and thus does not necessarily indicate that the metal is brittle. To avoid confusion in future discussion, therefore, fracture of this type will be designated "cleavage fracture."

A prevalent idea is that, even if the stress at ordinary fracture is affected by various factors, the stress at cleavage fracture can be represented by a single parameter, such as a limiting value of the greatest principal stress. The idea has even been presented that the stress at cleavage fracture is a physical property and thus is not sensitive to differences of structure. Fürth[5] has attempted to connect resistance to fracture with the latent heat of melting. The evidence presented in support of this view, however, is generally invalid. More recently, Saibel[23,24] has adopted the same idea and has presented evidence purporting to show that resistance to fracture can be expressed in terms of the energy absorbed in deformation to fracture. In adopting this theory, however, he ignores the evidence that the technical cohesive strength of a metal varies with the heat treatment and with plastic deformation. Resistance to fracture increases continuously with the energy absorbed during plastic deformation, and thus cannot be expressed in terms of the total energy absorbed in a single test or in terms of the latent heat of melting.

One of the greatest obstacles to advance of knowledge of the conditions involved in fracture of metals is the prevalent belief, or at least the tacit assumption, that plastic deformation does not affect the technical cohesive strength. In most investigations of the influence of the stress system on resistance to fracture, the possible influence of the widely varying ductility has been ignored in arriving at conclusions. An extreme example of this kind is found in reported investigations by Bridgman.[1,2,3] The test of each specimen started with the stress system in the field of triaxial compression, but the stress system changed gradually during the test and at fracture a transverse radial compressive stress was combined with an axial tensile stress. The effects thus were practically the same as if the specimens had been subjected to plastic deformation in widely varying amounts under the original stress systems and then tested to fracture under the final stress systems. Although the range of plastic deformation in these experiments was enormous, and thus was the dominant influence on resistance to fracture, this influence was ignored. The criterion for fracture over a wide range of conditions was said to be a limiting value of the volume stress.[1,2,3]

In his Campbell Memorial Lecture[6] Gensamer says that "Up to that time (instant of fracture), the metal is flowing because the resistance to flow is less than the resistance to fracture. And up to that time, we cannot know where the fracture curve lies." However, he shows a sketch that seems to indicate some qualitative knowledge of where the curve lies and of its form. This sketch shows a relationship similar to that represented in the previous papers by the authors;[9–17] the curve of fracture and the curve of flow both rise at a decreasing rate with plastic deformation, and intersect at a small angle at the point representing fracture. The basis for the sketch is not mentioned. In the present paper, much attention is given to the influence of plastic deformation and the stress system on the stress at fracture, especially the stress at "cleavage" fracture.

Method of Investigation, Specimens and Materials

Attention is confined to stress combinations with S_2 equal to S_3, that is, combinations that are produced by tension tests of notched or unnotched cylindrical specimens. The paper presents results of

tension tests of specimens with various deep notches, at several temperatures between room temperature and −188°C. Chief attention, however, is given to experiments in which the specimen is first given a chosen amount of plastic deformation at room temperature and then tested to fracture at −188°C. By this means a study has been made of the influence of plastic deformation and of the stress system on the stress at cleavage fracture.

When a notched cylindrical specimen is subjected to longitudinal tension, the minimum section is under transverse radial tension, but the radial stress is not uniform. The longitudinal stress, moreover, is initially highest at the periphery of the minimum section. Even slight plastic deformation, however, greatly diminishes the concentration of longitudinal stress. The tangential and radial stresses after plastic deformation probably are nearly equal at any point in the minimum section, except near the periphery where the radial stress remains zero. By the use of properly notched specimens, therefore, the influence of stress concentration is minimized and the influence of the radial stress ratio (S_3/S_1) is revealed.[11–17]

In the investigation to be described, deep notches were used for this purpose. The notches were nearly all of about the same depth (k = about 0.16),* but the notch angle varied between 170 and 45° and the root radius varied from 0.01 to 0.08 in. Most of the notched specimens were about 5.5-in. long; those having large notch angles were necessarily somewhat longer. The ends of the specimens were threaded to ¾ in. in diameter. Between the threaded ends, the specimen was machined to a selected uniform diameter, generally ¾ in., and a circumferential V-notch was machined at the mid-section. The notch was carefully machined to the selected angle, and so that the conical sides of the notch were tangent to the arc at the root. Care was also taken to minimize heating, bending, or appreciable cold work during the machining.

Before testing, each specimen was carefully measured as follows: The diameter of the maximum uniform section was measured with micrometer calipers; the diameter of the minimum section, at five or more positions uniformly spaced circumferentially, was determined by means of a measuring microscope. The root radius was measured by means of a graduated set of wires of slightly differing diameters and the notch angle was measured on a contour-measuring projector.

Descriptions of the apparatus and method of test,[11] and of the methods of testing at low temperatures,[12] are available. The tensile load was increased or decreased much more slowly than is usual in a tension test, especially during the tests in liquid air. In the approach to a cleavage fracture, the stress generally did not change more than 1000 psi in 30 to 60 sec. Determination of the load at fracture, generally, was quite accurate.

The materials used in the investigation were ingot iron, 0.12 pct carbon steel, annealed 0.42 pct carbon steel, and quenched-and-tempered 0.46 pct carbon steel. In some of the illustrations, results previously obtained with other carbon steels are assembled for comparison. The ingot iron and the 0.12 pct carbon steel were used in both annealed and cold-worked conditions. Although the ingot iron was received in severely cold-drawn condition, additional cold work was applied by extending long rods in a horizontal testing machine until they began to contract locally; this additional extension was about 5 pct. Other rods of the

* Notch depth is expressed in terms of the relative area ($k = b^2/B^2$) of the minimum cross section, where b and B represent the minimum and maximum radii of the section, respectively. Thus, the greater the notch depth, the smaller is the value of k.

original material were annealed and used in that condition. The 0.12 pct carbon steel was received in the hot-rolled condition. Some rods were extended by tension until they began to contract locally, and were then cold drawn to about 9 pct additional extension; the total extension was about 35 pct. Other rods were annealed and used in that condition. The 0.46 pct carbon steel was water-quenched and

TABLE 1—*Description of Metals*

Metal	Designation	Mechanical Treatment	Original Rod Diameter Inches	Chemical Composition, Pct					
				Carbon	Manganese	Iron	Phosphorus	Sulfur	Silicon
Ingot iron	A	Cold-drawn	0.75	0.015	0.05	Diff.	0.003	0.025	<0.01
Ingot iron	Q, QB[a]	Cold-drawn	0.937	0.015	0.04	Diff.	0.003	0.03	<0.01
Ingot iron	DE	Cold-drawn	0.875	0.02	0.04	Diff.	0.004	0.015	<0.01
Ingot iron	DFM[b]	Cold-drawn	0.875	0.02	0.04	Diff.	0.005	0.021	<0.01
0.11 pct carbon steel	CA	Cold-rolled	1.000	0.11	0.84	Diff.			0.05
0.12 pct carbon steel	CBM[c]	Cold-worked	1.000	0.12	0.82	Diff.	0.11	0.22	0.06
0.12 pct carbon steel	AG	Hot-rolled	1.125	0.12	0.44	Diff.	0.020	0.021	0.25
0.42 pct carbon steel	CE	Hot-rolled	1.125	0.42	0.60	Diff.	0.033	0.050	0.20
0.46 pct carbon steel	CH	Hot-rolled	1.000	0.46	0.55	Diff.	0.040	0.039	0.20

[a] Material QB was cold-drawn to a total of 49 pct reduction of area.
[b] This material was cold-worked by extension in addition to the cold-drawing received in manufacture, see text.
[c] This material was cold-worked by extension, followed by cold-drawing, see text.

TABLE 2—*Heat Treatment*

Material	Designation	Rod,[a] Diameter, Inches	Temperature Deg F	Time Held, Hr	Cooled in
Ingot iron	A-17.5	0.750	1750	1	Furnace
Ingot iron	Q-17.5	0.811	1750	1	Furnace
Ingot Iron	DE-17.5	0.875	1750	1	Furnace
0.11 pct carbon steel	CA-16.5	1.000	1650	1	Furnace
0.12 pct carbon steel	AG-17	1.125	1700	1	Furnace
0.42 pct carbon steel	CE-15.5	1.125	1550	1	Furnace
0.46 pct carbon steel	CH-W-10	0.770	1600	1	Air
			1475	1	Water
			1000	1	Air

[a] Rod diameter as heat treated.

tempered. The chemical composition of each of these metals is given in Table 1, and details of heat treatment are given in Table 2.

Influence of Plastic Deformation of Unnotched Specimens of Ferritic Steels on the Stress at Cleavage Fracture

The influence of plastic deformation on the technical cohesive strength of metals can be demonstrated without producing cleavage fractures. Although fracture of a ductile metal generally begins as transverse cleavage, it may eventually change to a shear fracture. By means of tension tests of notched specimens of previously cold-worked ductile metals the authors have shown that plastic deformation causes continuous increase in the technical cohesive strength.[11–16] However, the authors have also presented much evidence that plastic deformation increases the stress required for fracture entirely by cleavage.[12,17] This evidence is based on tests of ferritic steels at the temperature of liquid air (−188°C). Some of the steels were in the annealed condition, others had been plastically deformed at room temperature. Comparison of the breaking stresses of the cold-worked steels with those of the annealed steels revealed the

influence of plastic deformation on the stress at cleavage fracture.

Ferritic steels at −188°C generally fracture entirely by transverse plane cleavage. At this temperature, annealed carbon steels fracture after very little plastic deformation, but steels that have been quenched and tempered generally exhibit considerable ductility. Suitable alloying also generally increases the ductility of ferritic steels at −188°C. Even when the composition and heat treatment are such as to impart much ductility at −188°C, however, ferritic steels generally fracture entirely by transverse cleavage, but a few of the most ductile of such steels fracture with a thin oblique rim around the transverse plane. Crystalline fractures are obtained with annealed low-carbon steels. Prior plastic deformation increases the fineness of the crystalline fracture; after severe prior deformation the fracture appears dull. Dull plane cleavage fractures at −188°C are obtained with annealed steels of higher carbon content and with steels that have been quenched and tempered.

The range of temperature within which ferritic steels fracture by plane cleavage extends at least 60°C above the temperature of liquid air. At −128°C, these steels generally fracture entirely by transverse cleavage, and crystalline fractures are obtained with ingot iron. Dull plane cleavage fractures at −128°C, however, have been obtained with all other ferritic steels.

The influence of plastic deformation on the stress necessary for cleavage fracture, therefore, can be studied by comparing the breaking stresses of cold-worked ferritic steels at −128°C to −188°C with those of annealed steels. Information obtained in this way has been collected from previous papers by the authors and assembled in Figs 1 to 4,* together with additional data not previously published. These diagrams are of a new type, in which comparison is made between stress-strain curves obtained at temperatures ranging from +100°C to −188°C. Plastic deformation is expressed in terms of A_0/A, in which A_0 and A represent the initial and current areas of cross section. As values of A_0/A are represented on a logarithmic scale, abscissas in Figs 1 to 4 represent true strains. The ascending curves thus represent the variation of the mean flow stress with the true strain between yield and fracture. Through the points representing fracture of the same metal at different temperatures a curve (L) is drawn to represent the influence of temperature on the breaking stress and ductility. For a discussion of the form of such curves, reference may be made to a previous paper.[17] In Fig 4, the relatively steep slope of the curve obtained at 100°C is due to strain aging.

In the study of Figs 1 to 4, consideration will be given chiefly to the influence of prior plastic deformation on the stress at cleavage fracture of unnotched specimens, and attention will be given first to data assembled from previous papers. In Fig 1 a comparison is made between results obtained with annealed and with cold-drawn ingot iron.* At −188°C the breaking stress of the cold-drawn iron (QB) was 25 pct greater than that of the annealed iron (Q-17.5) and the surfaces of fracture of both metals had a crystalline appearance.[12] As both metals at −188°C fractured without local contraction, the stress at fracture was practically unidirectional. The difference between the breaking stresses of the cold-drawn and annealed iron, therefore, can be attributed only to the influence of the plastic de-

* All figures are at the end of the paper.

* The chemical analysis that led to the original report[11] that this was a 0.04 pct carbon steel was later found to be incorrect; new analyses showed that the carbon content was only 0.015 pct.

formation. This difference would have been somewhat greater if the plastic extension during the test of the annealed iron at −188°C had not been so much greater than that of the cold-drawn iron (Fig 1). At −118°C, the breaking stress of the cold-drawn ingot iron (QB) was 30 pct greater than that of the annealed iron after the same plastic deformation at −128°C. As both metals at the temperatures ranging from −118°C to −188°C fractured by transverse plane cleavage, the evidence in Fig 1 shows conclusively that plastic deformation increases the stress required for cleavage fracture.

Since publication of these results, Hollomon and Zener[7] reported results of experiments in which pearlitic steels were cold worked various amounts at room temperature and then tested to fracture at −190°C. Their results showed that the breaking stress at −190°C increased continuously with the prior plastic deformation at room temperature. They report, however, that steels with microstructure consisting of tempered martensite showed no evidence of increase of "fracture strength" with prior plastic deformation. Their conclusion was that "the anomalous effect of deformation upon the fracture strength of a pearlitic structure may be interpreted as due to a reorientation of the carbide lamellae." That this interpretation is not valid, however, is indicated by the evidence previously presented by the authors,[11] assembled in Fig 1, that plastic deformation increases the technical cohesive strength of ingot iron, which is practically free from carbide particles. Additional evidence of the great effect of plastic deformation on the technical cohesive strength of ingot iron will be discussed later in connection with Figs 8 and 9.

In Fig 2 a comparison is made between the breaking stresses of cold-drawn and annealed low-carbon steels.[17] The two steels were of nearly the same composition (Table 1). At −188°C, the breaking stress of the cold-drawn steel was about 45 pct greater than that of the annealed steel. The ductility of the steels at this temperature was negligible, and the fractures were crystalline. At −128°C, the breaking stress of the cold-drawn steel was 18 pct greater than that of the annealed steel, in spite of the greater ductility of the annealed steel. The evidence in Fig 2 thus confirms the conclusion that plastic deformation increases the stress necessary for cleavage fracture.

In the previous discussion of Figs 1 and 2 attention has been confined almost entirely to the influence of the plastic deformation induced by cold-drawing. The diagrams for annealed steels (Figs 2, 3 and 4), however, contain evidence that resistance to cleavage fracture is increased by tensile extension. Both the breaking stress and ductility of each of these steels are much higher at −128°C than at −188°C. Even at the maximum load on the 0.42 pct carbon steel at −128°C, the true stress is higher than the breaking stress at −188°C. The higher breaking stress at −128°C can be attributed only to the greater ductility. In order to escape this conclusion, it would be necessary to assert that the cohesive strength of annealed steel is higher at −128°C than at −188°C.

Figs 1, 3 and 4, however, contain new evidence that tensile extension increases the technical cohesive strength. This evidence is based on two-stage tension tests. In the first stage, the unnotched specimen was extended a predetermined amount at room temperature; in the second stage, the specimen was fractured in liquid air. The first test was made in March, 1943, with annealed ingot iron Q-17.5. A specimen was extended at room temperature until the cross sectional area was reduced about 50 pct ($A_0/A = 1.97$), and several days later was tested to fracture in liquid air. The breaking stress of this

specimen was about 47 pct higher than that obtained by a test entirely in liquid air (Fig 1). The increase in the breaking stress caused by the prior tensile extension at room temperature, therefore, was much greater than the increase caused by the cold drawing to about the same reduction in cross section (QB). This discrepancy results partly from the difference between the stress systems at fracture. In the two-stage tension test, the specimen contracted locally during the first stage, and the notch thus formed induced considerable transverse radial tensile stress in the test at −188°C. As the specimen tested completely in liquid air did not contract locally, the stress at fracture was unidirectional. It is possible also that the plastic deformation near the axis of the cold-drawn rod was less than is indicated by the mean 49 pct reduction of cross section.

Between the tension tests of the specimen of ingot iron at room temperature and at −188°C (Fig 1) there was an interval of several days, and during this interval the specimen did not remain in the testing machine. In the subsequent two-stage tests, now to be considered, the specimen remained in the machine during the interval of about one hour between the first and second stages, and was kept under a load of about 500 lb. This procedure was adopted in order to avoid the possibility of slight eccentricity of loading due to re-insertion of the specimen and reloading after embrittlement of the metal on cooling to −188°C. In the first stage (at room temperature), the specimen was surrounded by the metal container that was to be filled later with liquid air for the second stage (−188°C). The amount of plastic deformation during the first stage was determined by means of several calipers, the distance between the caliper points being measured by use of a traveling microscope. This method of measurement was tested thoroughly before use, and evidence for its accuracy will be found in Figs 5 to 11, to be described later.

Results of such two-stage tests are shown in Figs 3 and 4. For each of these tests, a plotted point indicates the amount of plastic deformation during the first stage and the flow stress at the end of this stage. A vertical dash-and-dot line extending from this point indicates the increase of the stress during the reloading to the yield stress in liquid air. The point representing the yield stress in liquid air is the origin of a broken curve showing the increase of the flow stress between yield and cleavage fracture. Curve *P* in each figure represents the influence of plastic deformation at room temperature on the breaking stress at −188°C. This curve, however, does not connect the results obtained in the two-stage tests with the results obtained entirely at −188°C. Curve *P* falls below the upper yield point obtained in a test entirely at −188°C. Since the initial technical cohesion limit is higher than the upper yield stress, the abrupt drop in stress at yield evidently indicates an abrupt decrease in both the flow stress and technical cohesion limit. Curve *P*, if prolonged without reversal, possibly would fall below the lower yield point obtained in a test entirely at −188°C. Such a relationship appears possible because of the non-uniformity of the plastic deformation during yield of low carbon steels. During the successive local extensions, local flow stresses may fall below the minimum value of the mean flow stress (lower yield stress), and the local cohesion limit may fall nearly as low. With further plastic deformation both these local stresses rise again. Fracture, however, does not occur until the flow stress becomes equal to the cohesion limit. At room temperature, therefore, the minimum value of the cohesion limit is not revealed. In a second-stage test made after slight deformation in the first stage, however, the observed fracture

stress probably is determined by the low local cohesion limit, and might be lower than the lower yield stress obtained in a test entirely at −188°C. Because the drop in stress between the upper and lower yield points is relatively less at −188°C than at room temperature, the plastic deformation during yield probably is more nearly uniform in a test at −188°C than in a test at room temperature. It is possible thus to account for the fact that the fracture stress is higher in a test entirely at −188°C than in a second-stage test after the same total plastic deformation.

The ductility of annealed carbon steels at −188°C (Figs 3 and 4) evidently is increased by slight plastic deformation at room temperature. After further plastic deformation, however, the second-stage ductility reaches a maximum, and thereafter changes little over a wide range of plastic deformation; eventually the ductility decreases rapidly (Fig 6 discussed later in the paper). Possible reasons for the increase in ductility will be discussed later.

The flow-stress curves obtained in the second stage of a two-stage test are much steeper than those obtained in the first stage, and are steeper than the curves obtained in tests entirely at −188°C (Figs 3 and 4). Even when the load has passed a maximum at room temperature, it generally traverses a second maximum at −188°C. If the plastic deformation required to reach the second maximum were not so great, this maximum might be viewed as a yield. Any plastic deformation during the second stage increases the technical cohesive strength and thus causes the breaking stress to be higher than if the specimen had no ductility at −188°C. Curve *P* thus represents the variation of the breaking stress under the combined influences of the plastic deformations at room temperature and at −188°C. A curve to represent the influence of the plastic deformation at room temperature alone on the breaking stress at −188°C would be similar in form to curve *P*. It would be below curve *P*, but above the experimental points representing yield at −188°C. Curve *T* has been so drawn to represent approximately the influence of plastic deformation at room temperature on the *initial* technical cohesion limit at −188°C.

A variable other than plastic deformation, however, affects curves *P* and *T*, just as it affects the curve of variation of the flow stress at room temperature. The straight portion of the curve of flow stress represents the variation of the flow stress during the local contraction of the specimen. The combined influences of the increasing radial stress ratio (S_3/S_1), resulting from local contraction, and the increasing plastic deformation cause the flow stress to increase nearly linearly with the true strain. If the radial stress ratio did not increase, the flow-stress curve would not be straight between the points representing maximum load and fracture. Since the corresponding portions of curves *P* and *T* also are straight, the evidence indicates that the increase in the radial stress ratio increases not only the mean flow stress, but also the mean stress at cleavage fracture. Similar evidence that the cleavage stress increases with increase in the radial stress ratio is furnished by other curves for unnotched specimens in Figs 7 to 10.

Flow and Fracture of Notched Specimens of Ferritic Steels at Room Temperature

In this and the following sections consideration will be given to the combined influences of plastic deformation and the stress system on the flow and fracture of ferritic steels. In previous papers the authors have shown that increase in the radial stress ratio (S_3/S_1) tends to cause an increase in the breaking stress of these steels at −188°C. The evidence is

based on tension tests of notched specimens entirely at −188°C. Some results thus obtained have been assembled in Figs 2 and 3 for comparison with the results obtained with unnotched specimens. With decrease in the notch angle, the breaking stress tends to increase because of the increasing radial stress ratio. This effect, however, is opposed by the depressing effect of the increasing stress concentration. With decrease in the notch angle below about 120°, the influence of the increasing stress concentration becomes dominant and the breaking stress decreases (Fig 3). The ductility of ferritic steels at −188°C is enough to relieve most of the slight stress concentration in a specimen with a large notch angle, but is not enough to relieve the high stress concentration in a specimen with a smaller notch angle.

With decrease in temperature, ferritic steels become less adaptable for relief of stress concentration by plastic deformation. This decrease in adaptability is not due entirely to the decrease in ductility. Ductility that would be sufficient for nearly complete relief of stress concentration at room temperature permits little relief at −188°C.[17] When a steel has only slight ductility at −188°C, little relief of stress concentration is possible in tension tests of notched specimens at that temperature (Fig 5). In order to investigate the influence of a wide range of the radial stress ratio (S_3/S_1) on the breaking stress at −188°C, therefore, two-stage tension tests have been made with both notched and unnotched specimens. In the first stage, each specimen was plastically deformed by a predetermined amount at room temperature; in the second stage, the specimen while still in place in the testing machine was cooled to −188°C and tested to fracture. Details of this procedure have been given previously. Since the plastic deformation at room temperature removed much of the stress concentration in the notched specimens, the tests at −188°C generally have revealed more prominently the influence of the radial stress ratio. Moreover, by varying the amount of plastic deformation at room temperature, a study has been made of the influence of plastic deformation on the breaking stress of notched specimens at −188°C. Results thus obtained are shown in Figs 5, 6, 8, 9, and 11.

Each of these figures contains not only results of two-stage tests, but also results of tests to fracture at room temperature and of tests entirely at −188°C. In each diagram representing tests at room temperature, every symbol that is not on the locus of fractures (L or L_T) represents either the end of the first stage of a two-stage test or the results of a measurement of the specimen during a test. When a symbol represents the end of the first stage, another symbol far above it represents either yield or fracture at −188°C.

The primary object is to show the combined influence of plastic deformation and the stress system on the breaking stress at −188°C. However, the results obtained at room temperature are of sufficient importance to receive detailed consideration, especially since a comparison is to be made later between the diagrams representing these results and the corresponding diagrams representing results obtained at −188°C. We will consider first the results obtained at room temperature.

MacGregor has shown that the true stress-strain curve obtained with an unnotched specimen generally is nearly straight between the points representing maximum load and fracture.[19,20] Subsequent investigations by others have shown that this conclusion is correct for most metals. As shown in a previous paper by the authors, however, the flow-stress curve obtained with an unnotched specimen of aluminum has no straight portion.[15] During the local contraction of this relatively soft metal the increase in the

radial stress ratio evidently is not rapid enough to straighten the flow-stress line. MacGregor has also investigated the form of the flow-stress curve for notched specimens, and has drawn straight lines to represent the variation of the flow stress between maximum load and fracture.[20] The evidence on which these lines are based, however, does not appear conclusive. Moreover, the authors have obtained continuously curved flow-stress lines in experiments with notched specimens of aluminum and nickel.[15]

Consideration will now be given to the flow-stress curves obtained at room temperature with ferritic steels, and attention will be given first to the curves obtained with annealed 0.12 pct carbon steel (Fig 5), annealed ingot iron (Fig 7), and 0.46 pct carbon steel (Fig 10). With unnotched specimens nearly straight lines were obtained between the points representing maximum load and fracture. Continuously curved lines, however, were obtained with notched specimens. The curvature is slight for large notch angles but increases with decrease in the angle. The curves of each group thus converge after initial divergence.

With a notched specimen a straight line between the points representing maximum load and fracture cannot be obtained unless the radial stress ratio increases as rapidly as it does during the local contraction of an unnotched specimen. If the radial stress ratio remained constant during plastic deformation, the slope of each flow-stress line would decrease continuously owing to the continuous decrease in the rate of work hardening. The curves of each group, however, would diverge continuously. The convergence of each group of curves in Figs 5, 7, and 10, therefore, indicates that the radial stress ratio induced by each notch eventually decreased.

Variations in the radial stress ratio during plastic deformation are caused by variations in the notch characteristics. During the local contraction of an unnotched specimen the notch thus formed becomes deeper, and the effective notch angle and notch radius decrease. Each of these changes tends to increase the radial stress ratio. During the extension of a notched specimen the notch deepens and the notch angle decreases, but the notch radius increases. The increase in the notch radius tends to decrease the radial stress ratio, and thus opposes the effect of the other two changes. The decrease in the notch angle is slight unless the angle is 150° or more, and the change does not extend far from the root of the notch. The chief effects on the radial stress ratio, therefore, are those due to the increase in the notch depth and the notch radius.

When the notch depth exceeds a certain value, which depends on the notch radius, the variation of the radial stress ratio depends chiefly on the variation of the ratio of the minimum diameter $2b$ of the specimen to the notch radius (r).* The decrease in $2b/r$ during plastic extension of a notched specimen tends to cause a continuous decrease in the radial stress ratio. This effect probably becomes dominant when $2b/r$ becomes less than about 10.[22] For the specimens with the 0.03 in. radius, the initial value of $2b/r$ was about 10, and the value decreased rapidly with plastic deformation. After fracture of the specimens used in obtaining the curves in Figs 5 and 7, the notch radius was found to be much larger than it was before the plastic deformation. The increase, which varied little with the notch angle, was about 30 pct for the 0.12 pct carbon steel and 50 pct for the ingot iron. The value of $2b/r$ at fracture averaged about 4.5 for the 0.12 pct carbon

* The effects of varying the notch radius and notch depth have been investigated by Sachs and co-workers.[22]

steel and 4.2 for the ingot iron; it thus was less than half the initial value.

The change in the form of the steel specimens during extension evidently caused a decrease in the radial stress ratio, at least after considerable plastic deformation. The decrease was most rapid for the initially high radial stress ratios induced by small notch angles. To this cause may be attributed the convergence of the flow-stress curves toward the curve obtained with unnotched specimens (Figs 5, 7 and 10). This convergence suggests that severe plastic deformation may cause the contour near the root of the notch to approach the contour in the neck of an initially unnotched specimen.

No determination has been made of the exact course of the flow-stress curves for notched specimens of the cold-worked 0.12 pct carbon steel (Fig 6) and cold-worked ingot iron (Fig 9). The evidence in Fig 9, however, suggests that the curvature between the points representing maximum load and fracture is less for these steels than for the annealed steels and for the quenched-and-tempered steel (Figs 5, 7, and 10). Since the increase in the notch radius probably is most rapid between yield and maximum load, the total increase in the radius during plastic deformation probably is less for previously cold-worked metals than for metals that have not been cold worked before the machining of the notch. The curvature of the flow-stress lines probably depends also on the notch radius. The notch radii used in the experiments represented in Figs 5 to 11 were chosen primarily for the purpose of investigating the breaking stresses at −188°C.

In Figs 5, 7 and 10, nearly all the flow-stress curves obtained at room temperature have been established by numerous observations of tensile loads and strains.* These determinations were continued almost to the beginning of fracture. The very small decrease of the load between the last load-strain determination and the abrupt fracture was no more than the decrease between the last two load-strain determinations. The point representing the beginning of fracture, therefore, is very near the intersection of a flow-stress curve with the straight sloping line extending upward to the point representing the breaking stress based on the area of cross section after fracture. The area of cross section of each of these specimens after fracture was found to be smaller than that corresponding to the beginning of fracture. This decrease in the area of cross section during fracture is due to the "rim effect," which has been discussed repeatedly by the authors.[11,13] The metal near the rim of the cross section evidently continued to extend while the fracture was progressing from the axis to the periphery, and thus caused continued contraction of the minimum section. The rim effect is most prominent with soft metals such as oxygen-free copper[11,12] and aluminum,[15] but has also been observed in experiments with steels.[13]

The observed breaking load was the load at the beginning of fracture; it corresponded with the sharp change in direction of the automatic load-extension curve. As this load was used in calculating both the uncorrected breaking stress and the actual breaking stress, the ratio of these two stresses is equal to the ratio of the areas of cross section at the beginning and end of fracture. This relationship has been used in constructing the steeply sloping lines extending downward from the points representing the uncorrected breaking stresses. The slope of each of these lines is such that the percentage decrease of the breaking stress is equal to the percentage decrease of A_0/A. These lines are not quite straight because of the difference between the scales of abscissas and ordinates. The intersection of each

* Flow-stress curves established in Figs 7 and 10 have been reproduced in Figs 8 and 11.

of these lines with the corresponding flow-stress curve represents the beginning of fracture.

Curve L in Figs 5, 7 and 10 represents the locus of fractures as determined in the usual way; curve L_T represents the true locus of fractures. In Fig 9, although the true locus of fractures was not determined directly, it would probably differ little from curve L_T as drawn. It intersects the flow-stress curve for unnotched specimens at a point representing the end of the first stage of a two-stage test. In the second stage, this specimen showed greatly reduced strength, thus indicating that fracture had begun at the end of the first stage. Moreover, the two notched specimens used in determining the course of curve L_T in this figure had only 0.01 in. notch radius, and thus showed very little rim effect.

The effect of the notch radius on the course of the uncorrected locus of fractures is illustrated by numerous diagrams in previous papers by the authors.[11,13,17] The notch radius would be expected to have a similar effect on the corrected locus of fractures. The difference in position between the two curves depends on the magnitude of the rim effect. As shown in a previous paper,[13] the rim effect tends to decrease with decrease in the notch radius. Moreover, the rim effect generally is greater for annealed steels (Figs 5 and 7) than for steels that have been quenched and tempered (Fig 10), or for cold-worked steels. For the purposes of the previous papers, a knowledge of the course of the corrected locus of fractures or of the exact form of the flow-stress curves was not important. For the purposes of the present paper, it was necessary to establish the exact course of the flow-stress curves.

With unnotched specimens of the cold-worked 0.12 pct carbon steel (Fig 6), cold-worked ingot iron (Fig 9), and quenched-and-tempered 0.46 pct carbon steel (Fig 10), the rim effect was slight. With unnotched specimens of the annealed ingot iron (Fig 7), however, the rim effect was so prominent that the breaking stress at room temperature could not be determined even approximately from the area of cross section after fracture. As illustrated in Fig 8, the breaking stress was determined by means of a two-stage test.

Influence of Plastic Deformation and Combined Stresses on the Breaking Stress at −188°C.

The results obtained in the second stage of the two-stage tests are shown in the upper areas of Figs 5, 6, 8, 9 and 11. In all these tests, even if considerable plastic deformation occurred at −188°C, the specimens failed by plane cleavage fracture.

In Fig 5 curves P and T, and the plotted points on which they are based, are the same as in Fig 4. The significance of these curves has been discussed. Above curve P in Fig 5 are shown the results of second-stage tests of notched specimens. As the notched specimens of this steel showed no appreciable ductility at −188°C, each symbol representing fracture in the second stage is exactly above a symbol representing the end of the first stage. For each of the five different notch angles a curve has been drawn to represent the influence of plastic deformation in the first stage on the breaking stress in the second stage. The course of each curve depends on the prior plastic deformation at room temperature, and on the variation of the radial stress ratio. In evaluating the influence of notches on the breaking stress at −188°C, therefore, the second-stage curves obtained with notched specimens should not be compared with curve P, which is affected by considerable plastic deformation at −188°C. They should be compared with curve T, which represents approximately the influence of plastic deformation of unnotched specimens at room tempera-

ture on the *initial* technical cohesion limit at −188°C. Curve *T* thus is included in the group of second-stage curves that is to be compared with the group of curves obtained at room temperature.

Each of these second-stage curves is similar in form to the corresponding flow-stress curve. Whether the specimen is notched or unnotched, plastic deformation increases the cleavage-fracture stress in the same way and nearly as much as it increases the first-stage flow stress. With decrease in the notch angle, both the fracture stress and the flow stress increase because of the increase in the radial stress ratio. The entire group of second-stage curves is similar in form to the group of flow-stress curves obtained at room temperature; the curves in each group first diverge and then converge. The variations in the radial stress ratio caused by variations in the notch characteristics evidently sffect the breaking stress at −188°C in the same way that they affect the flow stress at room temperature.

The greatest elevation of the breaking stress above that corresponding to a point on curve *T* was obtained with the 50° notch, and was about 36 pct. This percentage is about twice that obtained with another annealed low-carbon steel in tests entirely at −188°C (Fig 2). Relief of stress concentration in the first stage, therefore, has made it possible to reveal more prominently the influence of the radial stress ratio on the cleavage fracture stress.

If the second-stage curves were extended further to the left, the entire group apparently would fall below the points representing the upper yield, and possibly below the points representing the lower yield, of unnotched specimens tested entirely at −188°C.

Fig 6 shows results obtained with specimens taken from a bar of the same steel after it had been extended by tension and then cold drawn. The total reduction of the cross section of the bar was about 26 pct. The ductility of unnotched specimens at −188°C was considerably greater than that of the specimens that had been extended the same amount (35 pct) entirely by tension (Fig 5). With additional extension at room temperature (Fig 6), however, the ductility at −188°C decreased rapidly. When the plastic deformation in the first stage was nearly enough to cause fracture at room temperature, the specimen showed practically no ductility at −188°C. The evidence in Figs 5 and 6, therefore, indicates that plastic deformation of this steel at room temperature increases the second-stage ductility to a value that changes little over a wide range of plastic deformation, but that the ductility eventually decreases rapidly and disappears. During the eventual rapid decrease in the second-stage ductility the breaking stress decreases from a maximum value, as indicated by curve *P* in Fig 6. The initial decrease from the maximum results entirely from the decrease in the second-stage ductility. The specimen that showed no ductility at −188°C, however, probably had begun to fracture near the end of the first stage.

Curve *P* of Fig 6 has been so drawn that the ordinate at the origin is equal to the ordinate of curve *P* of Fig 5 at abscissa 1.35, which represents the cold work applied prior to the tests represented in Fig 6. The evidence indicates that curve *P* should be practically straight to the point where the rapid decrease in second-stage ductility begins. For reasons given in discussion of curve *T* in Figs 3 and 4, curve *T* in Fig 6 has been drawn to represent approximately the influence of plastic deformation at room temperature on the *initial* technical cohesion limit at −188°C. The flow-stress curve for the unnotched specimens tested entirely at −188°C (Fig 6) is considerably steeper than curves *P* and *T*. Curve *T'*, with the same

origin as curve *T*, represents approximately the increase in the technical cohesion limit during a test of an unnotched specimen entirely at −188°C.*

A specimen with 165° notch showed some ductility when tested entirely at −188°C (Fig 6). The probable variation of the ductility with decrease in the notch angle is indicated by curve *L*. Above this curve are shown the results of two-stage tests of notched specimens.† These results give additional evidence that the breaking stress at −188°C increases with the prior plastic deformation and with the radial stress ratio. As these notched specimens fractured with almost no ductility in the second stage, the results obtained with the notched specimens should be compared with corresponding positions on curve *T*, not on curve *P*. The comparison shows that the greatest elevation of the breaking stress above that of an unnotched specimen was about 37 pct.

Figs 8 and 9 show results of second-stage tests of annealed ingot iron (*DE*) and of cold-worked ingot iron (*DFM*). In these diagrams, as in the diagrams for the 0.12 pct carbon steel (Figs 5 and 6), curves cannot be drawn to connect the results of second-stage tests with the results of tests entirely at −188°C. Results of second-stage tests of unnotched specimens are represented by curves *P*. At the left end, each of these curves falls below the points representing fracture in tests entirely at −188°C. The curve obtained with annealed ingot iron, if extended far enough, possibly would fall below the lower yield point. In this respect, the annealed ingot iron is similar to the annealed 0.12 pct carbon steel (Fig 5). The abrupt drop in the flow stress at yield of these steels evidently is accompanied by an abrupt drop in the technical cohesive strength. With additional plastic deformation, however, the technical cohesive strength increases as indicated by curves *P* in Figs 5 and 8.

The effect of rest after plastic deformation of ingot iron is illustrated by the two points designated by *A* in Fig 8. These points represent the breaking stresses at −188°C of two specimens that had been remachined after the indicated amounts of plastic deformation at room temperature. The breaking stresses of these specimens were considerably higher than if the second-stage had been completed without the delay for re-machining. Since ingot iron specimens become considerably roughened during extension, it seemed possible that the roughening might lower the breaking stress at −188°C. However, the elevation of the breaking stresses of the re-machined specimens probably was not due to the re-machining. Age hardening of ingot iron at room temperature is rapid enough[4,8] to account for the elevation of the breaking stresses during the interval of several days between the tests at room temperature and at −188°C. The effect of plastic deformation of age-hardened ingot iron is illustrated in Fig 9. Curve *P*, as it extends to the left, falls considerably below the three points representing the breaking stresses of unnotched specimens in tests entirely at −188°C. Slight plastic deformation of this cold-worked iron evidently caused an abrupt drop in the technical cohesive strength. With additional plastic deformation, the technical cohesive strength increased as indicated by curve *P*.

During rest, after plastic deformation, the steel hardens and reverts to the same

---

* The slope of the nearly straight portion of a flow stress line is generally considered to be an index of the rate of work hardening. Comparison of slopes at different temperatures, however, is not a comparison of actual rates of work hardening. Comparison must be made between ***relative*** variations of ordinates.

† The arrows attached to some of these symbols indicate that the fracture was not quite at the minimum section. Such fractures obtained in the second stage are due to the combined influences of the deformation gradient and the stress gradient. At the minimum section the breaking stress would be higher than that indicated.

condition of instability that annealed pearlitic steels reveal by slight plastic deformation. This kind of instability appears to be the rest condition of ferritic steels and even of some nonferrous metals. Hardening *after* plastic deformation, therefore, is an approach to the rest condition corresponding to the amount of prior plastic deformation.

Curves *P* in Figs 8 and 9 are similar in form to the corresponding curves of flow stress of unnotched specimens at room temperature. Each curve is nearly straight between the points representing maximum load and fracture. The second-stage fracture stress and the first-stage flow stress evidently are affected similarly by the increasing radial stress ratio during the local contraction of an unnotched specimen.

In the tests entirely at −188°C, the annealed ingot iron showed some ductility (Fig 8). In the second-stage tests the two re-machined specimens (designated by *A*) showed very slight ductility; no other specimens however, showed appreciable ductility (Figs 8 and 9). Since the second-stage ductility of the ingot iron did not increase with plastic deformation at room temperature, the increase in the second-stage ductility of the 0.42 pct carbon steel (Fig 3) and the 0.12 pct carbon steel (Fig 5) can hardly be explained in terms of the previously mentioned views of Holloman and Zener.[7] If the increase in the ductility of these steels resulted from reorientation of cementite particles, the ferrite itself should be quite ductile. Nevertheless, ingot iron, which has practically no cementite particles, is much less ductile at −188°C than cold-worked low-carbon steel (Fig 6).

With notched specimens of annealed ingot iron the elevation of the cleavage-fracture stress above that of an unnotched specimen was no greater in the second-stage tests than in the tests entirely at −188°C (Fig 8). In the tests entirely at −188°C, some elevation of the fracture stress was obtained when the notch angle was 150° or more, but the influence of unrelieved stress concentration predominated when the angle was less than 150°. In the second-stage tests, however, practically no elevation of the breaking stress was obtained when the notch angle was less than 165°. Although plastic deformation had relieved much of the stress concentration during the first stage, the ingot iron did not have enough second-stage ductility to relieve the additional stress concentration induced by the higher stresses required for fracture at −188°C. The ratios of these higher stresses to the stresses at the end of the first stage are generally larger for annealed ingot iron than for the annealed low-carbon steel (Fig 5). The two-stage tests of annealed ingot iron, however, have given additional evidence that plastic deformation of notched specimens at room temperature increases the second-stage fracture stress nearly as much as it increases the first-stage flow stress.

With cold-worked ingot iron (Fig 9) a much wider spread of second-stage fracture stresses was obtained than with annealed iron. The curve of fracture stresses is elevated with decrease of the notch angle to 120°; with further decrease of the angle, the influence of the increasing stress concentration predominated. The greatest elevation of the breaking stress above that of an unnotched specimen was about 25 pct. This elevation is more than twice that obtainable in tests entirely at −188°C. In this respect therefore, two-stage tests are much more effective with cold-worked than with annealed ingot iron. The greater effectiveness may be attributed partly to the smaller ratios of the second-stage fracture stresses to the first-stage flow stresses. After relief of stress concentration during the first stage, the additional stress concentration induced during the increase of the stress to fracture at −188°C is less for previously cold

worked than for annealed ingot iron. Moreover, stress concentration generally is relieved more readily in metals cold worked before notching than in annealed metals.

Fig 11 shows results obtained with a steel that is much more ductile at −188°C than the steels previously discussed. The greater ductility was produced by quenching and tempering as indicated in Table 2. In the lower half of Fig 11 results obtained at room temperature are represented; in the upper half results obtained at −188°C are shown. If the diagram representing results obtained at room temperature were not placed in a separate division of the figure, it would overlap much of the other two diagrams; the first-stage flow stresses are high in relation to the second-stage fracture stresses. (As previously shown, such a relationship is advantageous.) Because of the greater ductility of the steel at −188°C, the diagram representing the results of tests entirely at −188°C covers a much larger area in this figure than in the previously discussed figures; it thus overlaps much of the diagram representing the results of second-stage tests. Consequently, although points representing second-stage yield can be inside the diagram representing results of tests entirely at −188°C, all points representing second-stage fracture must be outside this diagram.

As shown by the experiments with unnotched specimens (Fig 11), the second-stage ductility of this steel decreased with prior plastic deformation at room temperature. When a specimen was extended nearly enough to cause fracture in the first stage, it showed practically no ductility in the second stage. Curve P thus is affected by a variable amount of plastic deformation at −188°C. The final descent of this curve is due to the rapid decrease in ductility, not to damage caused by the plastic deformation. A curve to represent the influence of plastic deformation entirely at room temperature on the *initial* technical cohesive strength at −188°C must be between the points representing second-stage yield and fracture. Such a relationship is represented approximately by curve T. Curve T' represents approximately the increase in the technical cohesion limit during a test of an unnotched specimen entirely at −188°C.

The second-stage ductility of notched specimens of this steel decreases with increase in the prior plastic deformation at room temperature. Moreover, some evidence, not shown, indicates that notched specimens extended nearly to fracture in the first stage have practically no ductility in the second stage. If the curves of second-stage fracture of notched specimens (Fig 11) were extended far enough, therefore, they would traverse a maximum and turn downward. These curves, like curve P, are affected by variable plastic deformation at −188°C. For each notch angle, therefore, a curve to represent the influence of plastic deformation entirely at room temperature on the *initial* technical cohesion limit at −188°C would be between the points representing second-stage yield and fracture. Since the accuracy of such a curve increases with decrease in the second-stage ductility, the accuracy would be least for the curves representing large notch angles, but would increase greatly with decrease in the angle. As these curves would represent *initial* technical cohesion limits, they could be extended across the diagram representing results of tests entirely at −188°C. They would be similar in form to the second-stage fracture curves obtained with annealed 0.12 pct carbon steel (Fig 5). To avoid confusion, these curves have not been included in Fig 11.

The second-stage fracture curves obtained with notch angles 165° and 150° do not extend to the left of the points representing fracture of corresponding specimens in tests entirely at −188°C.

In this respect, these curves are similar to curve *P*. With decrease in the notch angle below about 150°, however, the upper boundary (*L*) of the diagram representing results of tests entirely at −188°C descends abruptly because of an abrupt increase in the stress concentration. Although curve *L* rises again with decrease in the notch angle below about 135°, the whole portion to the left of the point obtained with notch angle 150° is depressed because of the increase in stress concentration with decrease in the notch angle.* Consequently, because more relief of stress concentration was obtained in the two-stage tests, the second-stage fracture curves obtained with notch angles smaller than 150° pass considerably above the corresponding points on the boundary *L*.

The entire group of second-stage fracture curves in Fig 11 is qualitatively similar to the group of flow-stress curves obtained at room temperature. The results of the two-stage tests with this steel, therefore, confirm the previously discussed evidence that the influences of plastic deformation and the stress system on the cleavage-fracture stress are similar to their influences on the flow stress. The influence of the radial stress ratio on the cleavage-fracture stress, however, is more prominently revealed in Fig 11 than in the preceding figures. With the 50° notch angle, the elevation of the fracture stress above that corresponding to a point on curve *T* was about 50 pct.

The evidence, that the variations of the fracture stress with plastic deformation and the stress system are qualitatively similar to the variations of the flow stress, confirms the conclusion expressed in a previous paper[16] that fracture is determined by a limiting value of a shearing stress, either the maximum shearing stress or the octahedral shearing stress. The limiting value of the shearing stress, however, is not constant, but decreases with increase in the volume stress.

* A similar unusual form of the locus of fracture, obtained with a cold-worked 0.57 pct carbon steel at room temperature, is shown in Fig 8 of a previous paper.[17]

Influence of Plastic Deformation on the Technical Cohesive Strength at Room Temperature

The previously discussed variations of second-stage fracture stresses with prior plastic deformation must be attributed to qualitatively similar variations of the technical cohesive strength during plastic deformation at room temperature. In the previous papers,[12–17] the variation of the cohesive strength of a metal with plastic deformation has been represented by a curve a little above the corresponding flow-stress curve; both curves rise and intersect at a small angle at the point representing fracture. Because only one point on such a cohesion curve represents actual fracture, the course of the curve generally can be indicated only approximately. However, by a comparison of cohesion curves obtained in the second-stage tests with the corresponding curves obtained at room temperature, it is now possible to establish definitely the relation between flow stress and cohesion limit during the plastic deformation of ferritic steels at room temperature.

In making such a comparison, the curves obtained at −188°C must be converted into equivalent curves representing the variation of cohesive strength with plastic deformation at room temperature. Such conversion can be made by proper reduction of the ordinates of the curves obtained at −188°C. The principle involved in the proper reduction of the ordinates may be illustrated by a comparison of the flow-stress curves in Fig 3. By multiplying the ordinates of any one of the low-temperature curves by a fraction, which is constant for that curve, the curve may be made to coincide closely with the room-temperature

curve. Such equivalence between curves obtained at different temperatures exists only when the rate of actual work-hardening changes little throughout that range of temperature. By the use of this principle, a second-stage fracture curve may be converted into an equivalent curve to represent the influence of plastic deformation on the cohesive strength at room temperature.

Converted curves thus obtained are assembled in Fig 12 together with the corresponding flow-stress curves. The cohesion curves thus converted are those representing the influence of plastic deformation on the *initial* technical cohesion limit at −188°C (curves *T* in Figs 3, 5, 6, and 11, and curves *P* in Figs 8 and 9). These curves are free from the influence of any variation of plastic deformation at −188°C. The conversion factor has been chosen so that each converted curve of cohesion touches the flow-stress curve at the point representing actual fracture at room temperature.

The pairs of curves assembled in Fig 12 show definitely how the technical cohesive strength of these steels varies during plastic deformation at room temperature. The evidence confirms the conclusion expressed by the authors in previous papers[11–17] and illustrated by numerous pairs of curves of flow stress and cohesion. Because the curves of each pair meet at such a small angle, any variable that has even a slight differential effect on the flow stress and cohesion limit may have a great effect on the ductility. An increase in the radial stress ratio increases the flow stress more than it increases the cohesion limit and thus decreases the ductility. The curves obtained with annealed 0.12 pct carbon steel AG-17 illustrate the effect of the radial stress induced by notches. The same conversion factor was used in deriving the cohesion curves for both the notched and unnotched specimens from the corresponding second-stage curves (Fig 5). The evidence thus indicates that the influence of the radial stress ratio is no less at −188°C than at room temperature. A complete three-dimensional diagram representing the influence of the stress system on the technical cohesion limit probably would have about the same form at both temperatures.

Attention has been invited previously to the relation between curves *T′* and *T* in Fig 11. Consideration will now be given to the position that curve *T′* would occupy if it were converted to an equivalent curve and placed in proper relation to curve *T* for the same steel in Fig 12. If the flow-stress curve corresponding to curve *T′* in Fig 11 were converted to an equivalent curve coinciding with curve *F* for this steel in Fig 12, the equivalent of curve *T′* would be between curves *F* and *T*. The difference between the flow stress and cohesion limit, therefore, evidently is less at −188°C than at room temperature. This relationship accounts for the decrease in the ductility with decrease in temperature.

The curves obtained with unnotched specimens (Fig 12) are affected by the increase in the radial stress ratio during the local contraction of the specimen. The curves obtained with notched specimens are affected by a *decrease* in the radial stress ratio. In Fig 13, the curves are assumed to represent approximately the results that would be obtained in experiments with constant combinations of uniform axial and radial stresses. The empirical method of derivation is described in previous papers.[11,12] The influence of plastic deformation on the technical cohesive strength of a metal cannot be represented completely by a single cohesion curve, but may be represented by a series of curves, each showing the variation of the cohesion limit for a specific radial stress ratio. Such a series, for radial stress ratios ranging from zero to 1.0, is shown in each of the diagrams of Fig 13.

The flow-stress curves corresponding to some of the cohesion curves, however, have been omitted.

Influence of the Notch Angle and of Plastic Deformation at Room Temperature on the Breaking Stress at −188°C.

The qualitative influence of the notch angle on the breaking stress at −188°C is revealed by a comparison of the second-stage fracture curves obtained with different notch angles (Figs 5, 6, 8, 9 and 11). The quantitative influence of the notch angle may be revealed by the use of diagrams of the type shown in Figs 14 and 15. These diagrams show the influence of the notch angle on the yield stresses, ultimate stresses, and breaking stresses obtained in tests to fracture at room temperature, and in tests entirely at −188°C. They also show results of two-stage tests. Attention will be confined to the curves showing the variation of the second-stage fracture stress with the notch angle. Each of these curves shows this variation for the indicated constant amount of plastic deformation (A_0/A). These curves have been derived by obvious procedure from the second-stage fracture curves in diagrams of the type shown in Fig 5. Some of the derived curves pass through corresponding points representing fracture in tests entirely at −188°C. Because of the variable second-stage ductility of the 0.46 pct carbon steel (Fig 11) the second-stage fracture curves in Fig 15 are based partly on estimation of the approximate positions that curves of *initial* technical cohesion limits would occupy in Fig 11.

All the second-stage curves (Figs 14 and 15) except the curve for annealed ingot iron (Fig 14A) rise continuously with decrease in the notch angle. As each of these curves was obtained with constant plastic deformation, the rise of the curves results entirely from the increase in the radial stress ratio with decrease in the notch angle. The descent of the curve obtained with annealed ingot iron (Fig 14A) is the result of the dominant influence of increasing stress concentration (Fig 8).

As the radial stress ratios obtained in the tests of notched specimens are not known, the influence of the radial stress ratio on the breaking stress cannot be represented quantitatively. Fig 16, however, shows qualitatively the variation of the axial stress with the radial stress in cylindrical specimens. Both these stresses are assumed to be uniform. Constant values of the radial stress ratio are represented by the radiating broken lines. The empirical method used in deriving the curves in this figure is described in previous papers.[11,12] Diagrams of this type must be in proper relation to corresponding diagrams of the type shown in Fig 13.

Attention will be confined to the curves representing variations of the cohesion limit for the indicated constant values of prior plastic deformation. Curve T in each diagram of Fig 16 represents the variation of the initial technical cohesion limit, that is, the cohesion limit prior to plastic deformation. In Fig 16A, curve T' represents the variation of the cohesion limit of metal that has been deformed about as much as in a tension test of an unnotched specimen at fracture. In Fig 16B, curves T' represent the variations of the second-stage fracture stress corresponding to the indicated constant amounts of prior plastic deformation at room temperature. Curves T and T' are similar in form to the second-stage fracture curves in Figs 14 and 15.

The Variation of the Breaking Stress with Temperature

Consideration will now be given to the variation of the breaking stress with temperature, when the total plastic deformation is constant. When single-stage

tests are made to determine the breaking stress of a ferritic steel at various temperatures, the variation of the breaking stress with temperature is influenced greatly by the variation of the ductility. This influence of the ductility is illustrated in Figs 1 to 4. It is also illustrated in diagrams of a different type in Figs 17, 18 and 19. In these figures, the temperature scale is the same that has been used in previous papers by the authors.[12–17] Temperatures in degrees Kelvin are plotted on a logarithmic scale. As abscissas are proportional to the logarithm of the degrees Kelvin, the scale is the same in principle as Kelvin's original thermodynamic scale. This scale has been used because it gives a linear relationship between temperature and the strength indices for various metals, except when structural changes occur at certain temperatures.

As shown in Figs 17, 18 and 19 the effect of the variable ductility is conspicuous in the fracture-curves (R) obtained with the annealed steels. The steep descent of these curves with decrease of the temperature from about −128°C to −188°C results from the abrupt decrease in the ductility. The lines made up of very short dashes show approximately the influence of temperature on the breaking stress when the total plastic deformation is held constant. These lines are derived from Figs 1 to 9, and 11. In deriving the lines for unnotched specimens in Figs 17B and 19A, the fracture stress values for −78°C and −128°C have been obtained by extrapolation, using the corresponding flow-stress curves in Figs 4 and 3, respectively. As shown in Figs 17B and 19A, the results indicate that the relationship is nearly linear when the total plastic deformation is held at the indicated constant values. As shown in Fig 19B, the relationship probably is nearly linear for this steel also. In this respect, therefore, these steels are similar to copper, monel metal, and many other nonferrous metals.[12,15] In the absence of complete evidence a similar linear relationship is assumed in Figs 17C and 18B. The evidence in all three figures indicates that, when the total plastic deformation is held constant, the breaking stress increases continuously with decrease from room temperature to −188°C.

Acknowledgments

The authors acknowledge the assistance given by L. R. Sweetman of the Engineering Mechanics Section of the National Bureau of Standards in the tensile extension of the long steel rods of ingot iron and 0.12 pct carbon steel, from which specimens were then obtained for this investigation. Acknowledgment is also due to Miss Frances J. Cromwell for assistance in the experiments and in making the drawings for the illustrations, and to Mr. W. D. Jenkins for general assistance in the investigation.

References

1. P. W. Bridgman: Fracture and Flow in Metals, *Trans.* AIME (1945) **162**, 569.
2. P. W. Bridgman: Effects of High Hydrostatic Pressure on the Plastic Properties of Metals. Rev. of Modern Physics (1945) **17**, No. 1, 3.
3. P. W. Bridgman: The Tensile Properties of Several Special Steels and Certain Other Materials under Pressure. *Jnl.* App. Phys. (1946) **17**, 201.
4. E. S. Davenport and E. C. Bain: The Aging of Steel. *Trans.* Am. Soc. for Metals. (1935) **23**, 1047.
5. R. Fürth: A Thermodynamical Theory of the Tensile Strength of Isotropic Bodies. Roy. Soc. *Proc.* (1940) **177**, p. 217.
6. M. Gensamer: Strength and Ductility. *Trans.* Am. Soc. for Metals. (1946) **36**, 30.
7. J. H. Hollomon and C. Zener: Conditions of Fracture of Steel. *Trans.* AIME (1944) **158**, 283.
8. R. L. Kenyon and R. S. Burns: Aging in Iron and Steel, *Symposium* Age Hardening of Metals. Am. Soc. for Metals (1939), Chicago, 262.
9. D. J. McAdam, Jr.: The Technical Cohesive Strength of Metals, *Trans.* Amer. Soc. Mech. Engrs. (1941) **63**,
10. D. J. McAdam, Jr.: The Technical Cohesive Strength and Yield Strength of Metals, *Trans.* AIME (1942) **150**, 311.
11. D. J. McAdam, Jr. and R. W. Mebs: An Investigation of the Technical Co-

hesive Strength of Metals, *Trans.* AIME (1945) **162**, 474.

12. D. J. McAdam, Jr. and R. W. Mebs: The Technical Cohesive Strength and Other Mechanical Properties of Metals at Low Temperatures. *Proc.* Am. Soc. Test. Mat. (1943) **43**, 661.
13. D. J. McAdam, Jr., R. W. Mebs and G. W. Geil: The Technical Cohesive Strength of Some Steels and Light Alloys at Low Temperatures. *Proc.* Am. Soc. Test. Mat. (1944) **44**, 593.
14. D. J. McAdam, Jr., The Technical Cohesive Strength of Metals in Terms of the Principal Stresses. *Trans.* AIME (1945) **162**, 542.
15. D. J. McAdam, Jr., G. W. Geil and R. W. Mebs: Effects of Combined Stresses and Low Temperatures on the Mechanical Properties of Some Non-ferrous Metals. *Trans.* Amer. Soc. for Metals (1946) **37**, 497.
16. D. J. McAdam, Jr.: Fracture of Metals under Combined Stresses, *Trans.* Amer. Soc. for Metals (1946) **37**, 538.
17. D. J. McAdam, Jr., G. W. Geil and R. W. Mebs: The Effect of Combined Stresses on the Mechanical Properties of Steels Between Room Temperature and −188° Cent., *Proc.* Amer. Soc. for Testing Mat. (1945) **45**, 448.
18. D. J. McAdam, Jr., G. W. Geil, and D. H. Woodard: Influence of Strain Rate and Temperature on the Mechanical Properties of Copper, presented at the annual meeting of the American Society for Testing Materials, Buffalo, N. Y., June 27, 1946. *Proc.* Amer. Soc. for Testing Mat. **46.**
19. C. W. MacGregor: Relations between Stress and Reduction in Area for Tensile Tests of Metals, *Trans.* AIME (1937) **124**, 208.
20. C. W. MacGregor: The Plastic Flow of Metals, *Trans.* AIME (1939) **133**, 302.
21. C. W. MacGregor and L. E. Welch: True Stress-Strain Relations at High Temperatures by the Two-Load Method. *Trans.* AIME (1943) **154**, 423.
22. G. Sachs, J. D. Lubahn and L. J. Ebert: The Effects of Notches of Varying Depth on the Strength of Heat-Treated Low Alloy Steels. *Trans.* Amer. Soc. for Metals (1945) **34**, 517.
23. Edward Saibel: A Thermodynamic Criterion for the Fracture of Metals, Physical Review. (1946) **69**, 667.
24. Edward Saibel: A Thermodynamic Theory of the Fracture of Metals. *Trans.* AIME (1947) **171**, 639. *Metals Tech.* (Feb. 1947—T.P. 2131).

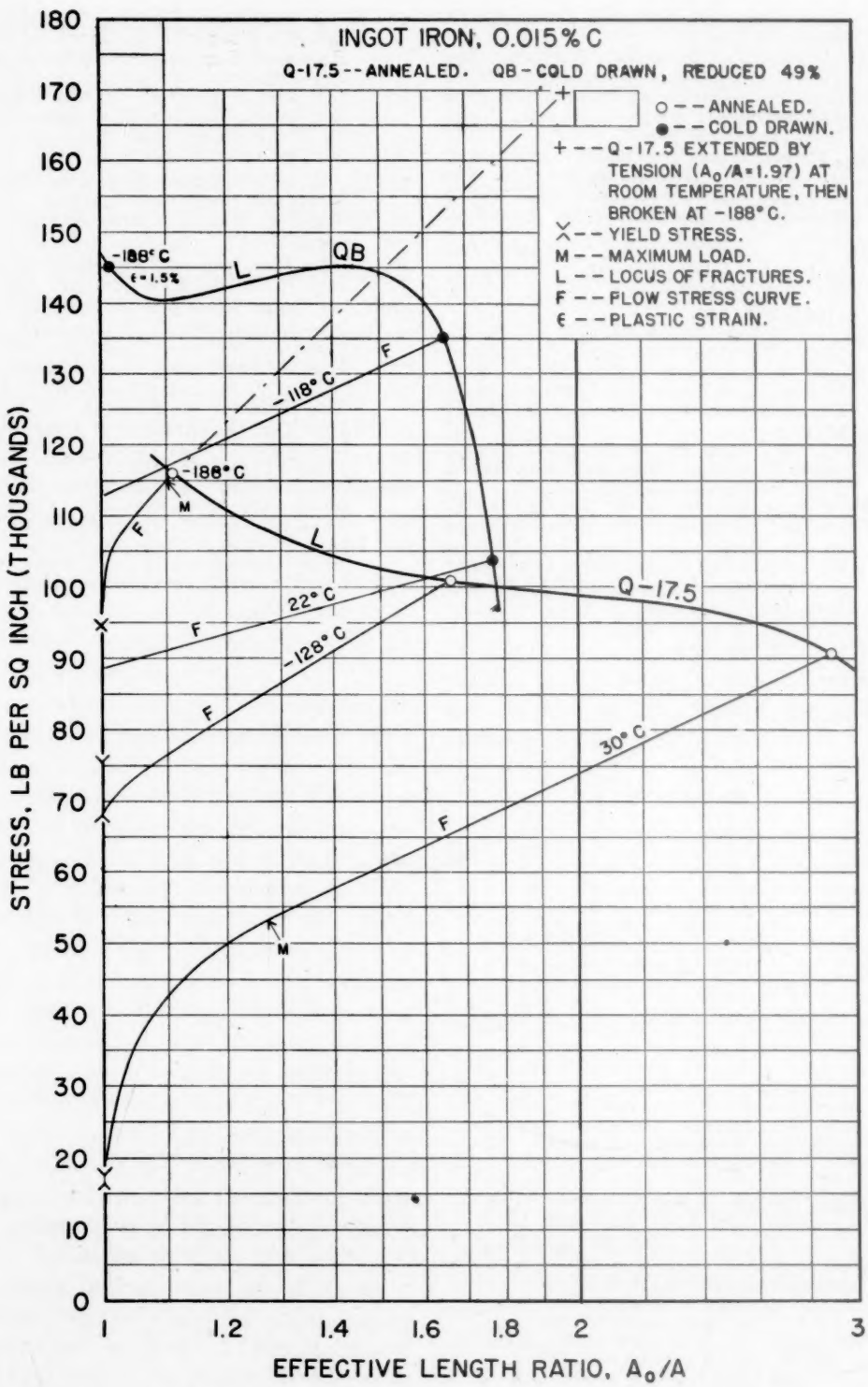

FIG 1—COMPARISON OF BREAKING STRESSES OF ANNEALED AND COLD-WORKED INGOT IRON AT VARIOUS TEMPERATURES.

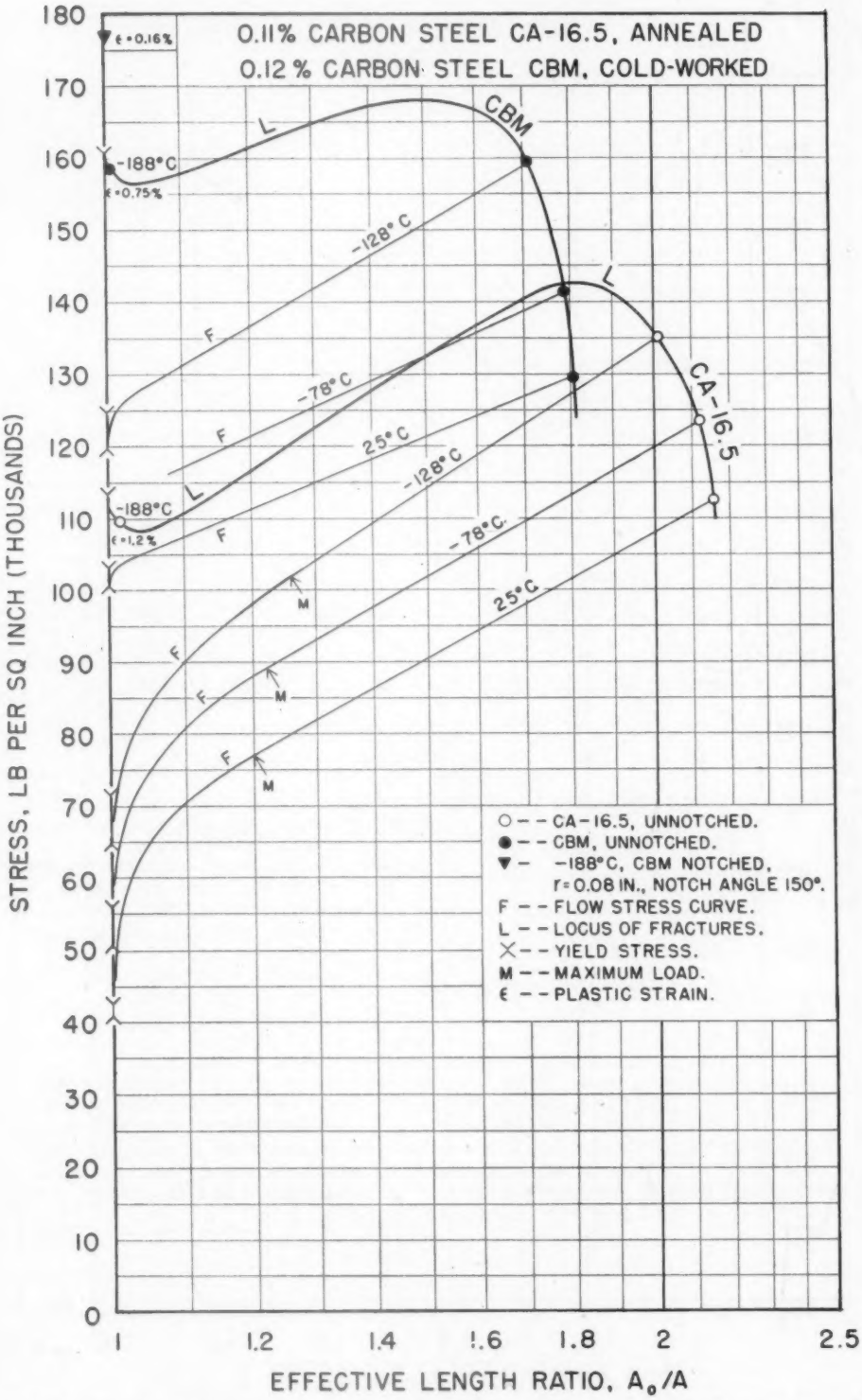

FIG 2—COMPARISON OF BREAKING STRESSES OF ANNEALED AND COLD-WORKED LOW CARBON STEEL AT VARIOUS TEMPERATURES.

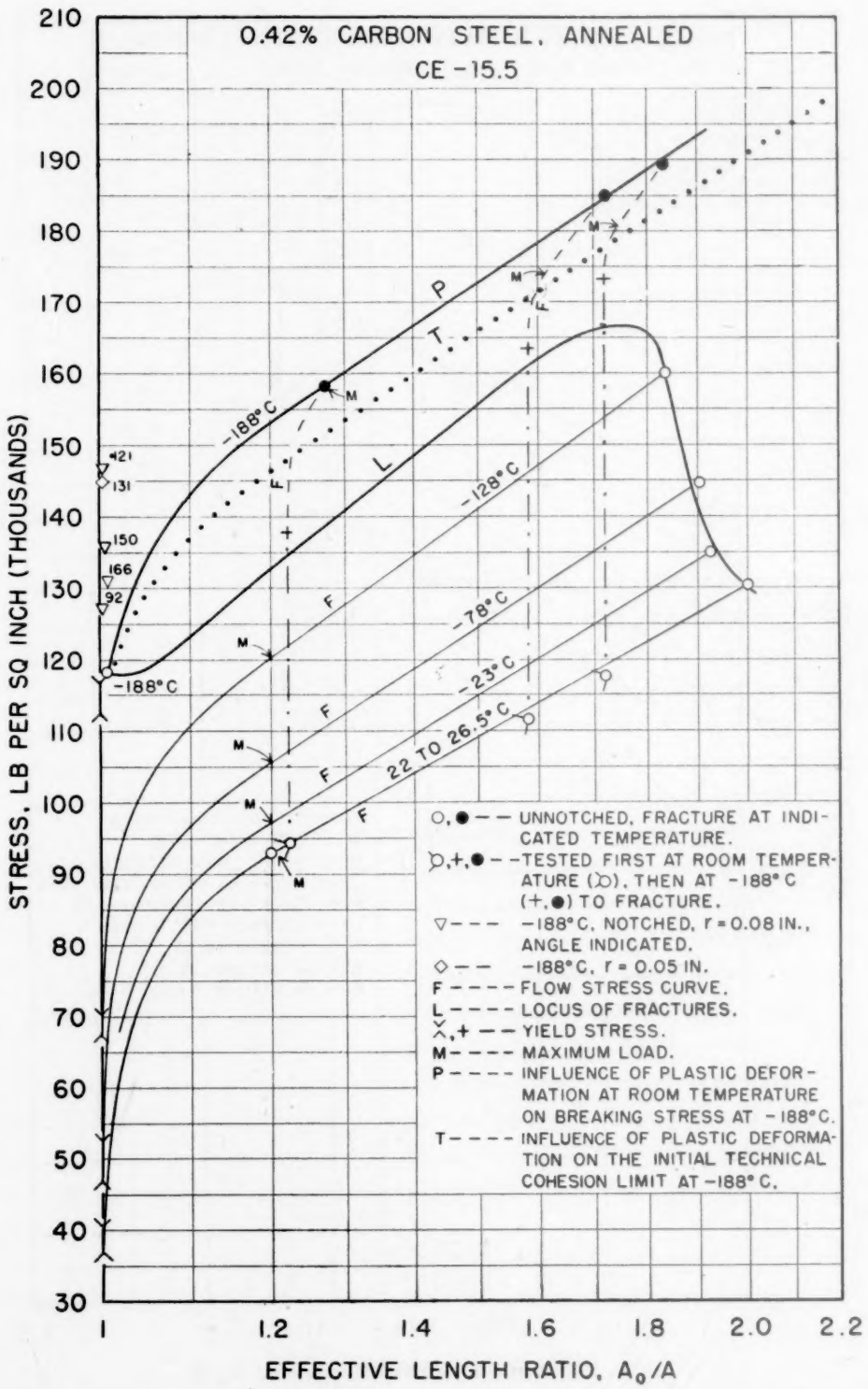

FIG 3—INFLUENCE OF TENSILE EXTENSION OF UNNOTCHED SPECIMENS AT ROOM TEMPERATURE ON THE BREAKING STRESS OF ANNEALED 0.42 PCT CARBON STEEL AT −188°C.

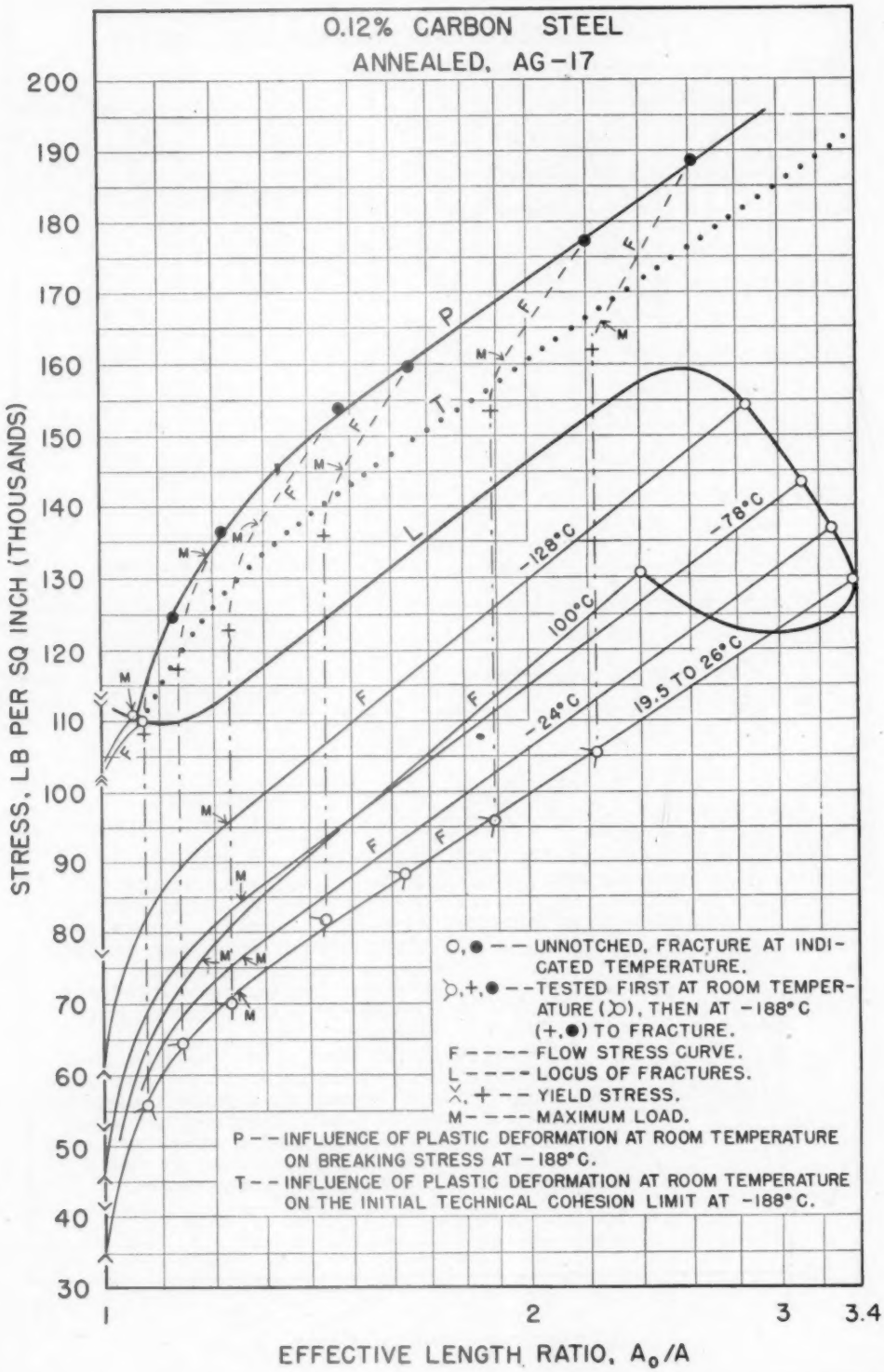

FIG 4—INFLUENCE OF TENSILE EXTENSION OF UNNOTCHED SPECIMENS AT ROOM TEMPERATURE ON THE BREAKING STRESS OF ANNEALED 0.12 PCT CARBON STEEL AT −188°C.

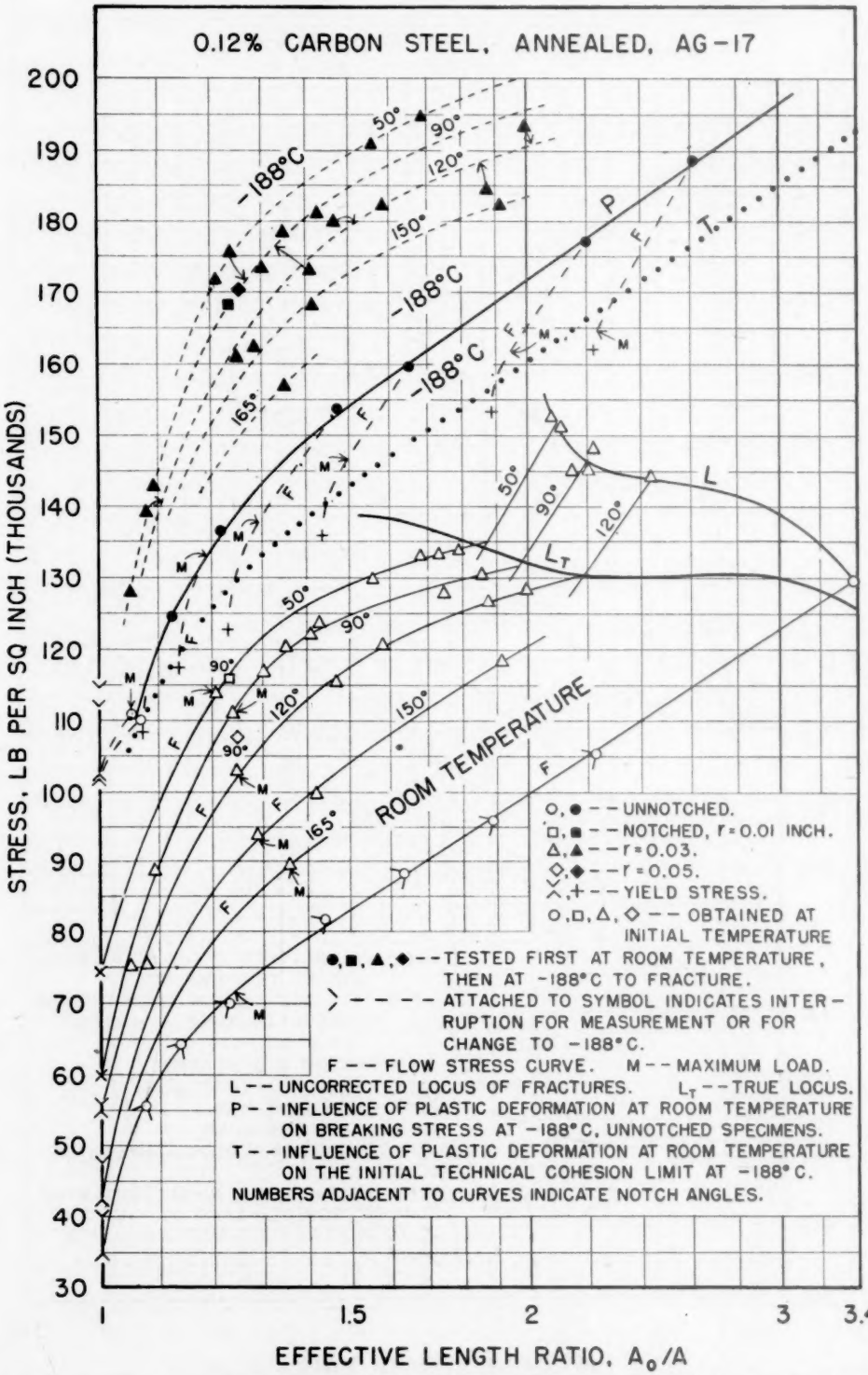

FIG 5—INFLUENCE OF PLASTIC DEFORMATION OF NOTCHED AND UNNOTCHED SPECIMENS AT ROOM TEMPERATURE ON THE BREAKING STRESS OF ANNEALED LOW-CARBON STEEL AT −188°C.

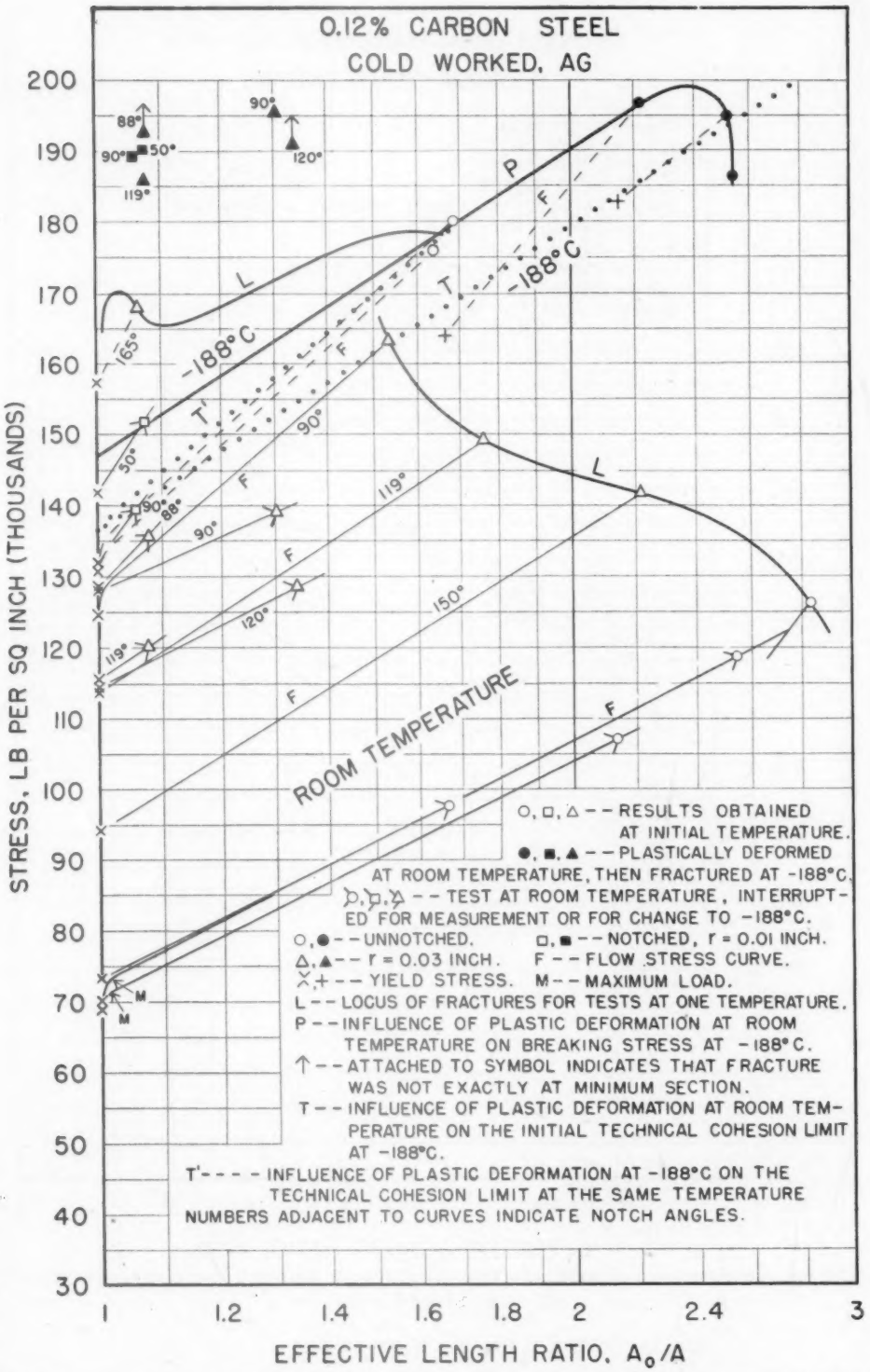
0.12% CARBON STEEL
COLD WORKED, AG
STRESS, LB PER SQ INCH (THOUSANDS)
EFFECTIVE LENGTH RATIO, A_0/A
ROOM TEMPERATURE
-188°C
P
L
T
T'
F
M
○, □, △ -- RESULTS OBTAINED AT INITIAL TEMPERATURE.
●, ■, ▲ -- PLASTICALLY DEFORMED AT ROOM TEMPERATURE, THEN FRACTURED AT -188°C.
◐, ◨, ◭ -- TEST AT ROOM TEMPERATURE, INTERRUPTED FOR MEASUREMENT OR FOR CHANGE TO -188°C.
○, ● -- UNNOTCHED. □, ■ -- NOTCHED, r = 0.01 INCH.
△, ▲ -- r = 0.03 INCH. F -- FLOW STRESS CURVE.
× , + -- YIELD STRESS. M -- MAXIMUM LOAD.
L -- LOCUS OF FRACTURES FOR TESTS AT ONE TEMPERATURE.
P -- INFLUENCE OF PLASTIC DEFORMATION AT ROOM TEMPERATURE ON BREAKING STRESS AT -188°C.
↑ -- ATTACHED TO SYMBOL INDICATES THAT FRACTURE WAS NOT EXACTLY AT MINIMUM SECTION.
T -- INFLUENCE OF PLASTIC DEFORMATION AT ROOM TEMPERATURE ON THE INITIAL TECHNICAL COHESION LIMIT AT -188°C.
T'- - - - INFLUENCE OF PLASTIC DEFORMATION AT -188°C ON THE TECHNICAL COHESION LIMIT AT THE SAME TEMPERATURE
NUMBERS ADJACENT TO CURVES INDICATE NOTCH ANGLES.

FIG 6—INFLUENCE OF PLASTIC DEFORMATION OF NOTCHED AND UNNOTCHED SPECIMENS AT ROOM TEMPERATURE ON THE BREAKING STRESS OF COLD-WORKED LOW-CARBON STEEL AT −188°C.

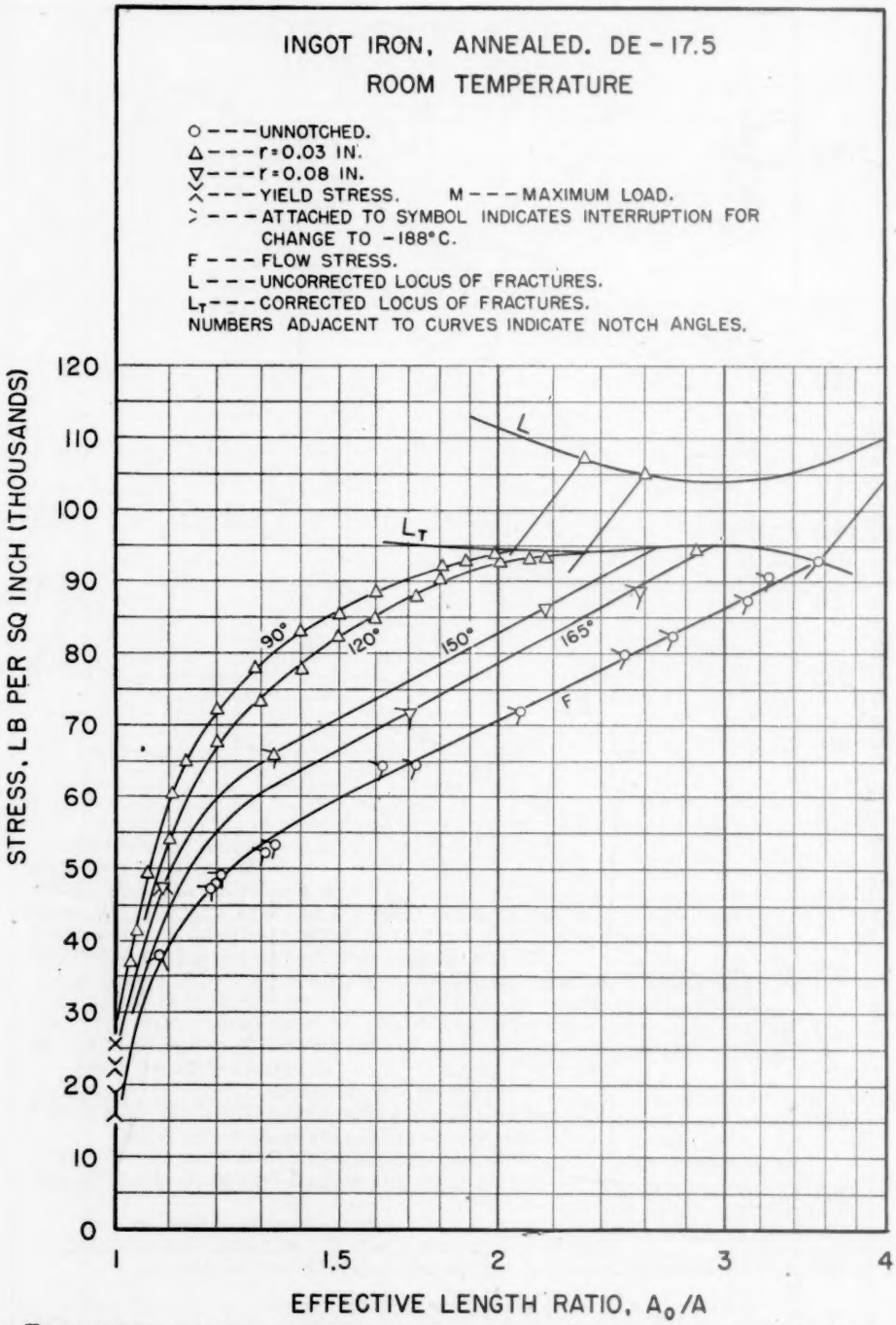

FIG 7—FLOW AND FRACTURE OF NOTCHED AND UNNOTCHED SPECIMENS OF ANNEALED INGOT IRON AT ROOM TEMPERATURE.

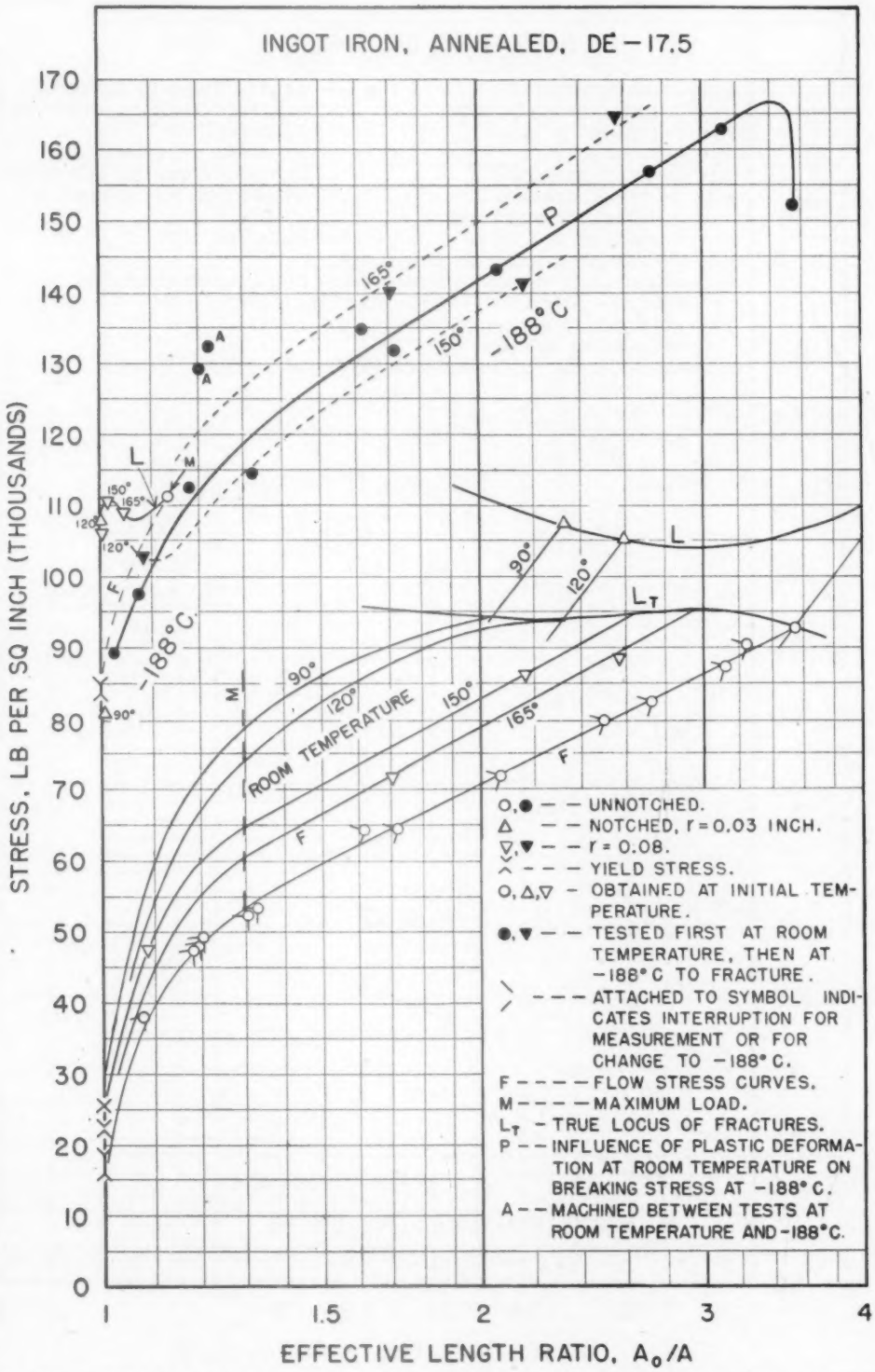
INGOT IRON, ANNEALED, DE – 17.5
STRESS, LB PER SQ INCH (THOUSANDS)
EFFECTIVE LENGTH RATIO, A_0/A
P
L
L_T
F
M
A
165°
150°
120°
90°
-188°C
ROOM TEMPERATURE
O,● – – UNNOTCHED.
△ – – NOTCHED, r = 0.03 INCH.
▽,▼ – – r = 0.08.
^ – – – YIELD STRESS.
O, △, ▽ – OBTAINED AT INITIAL TEMPERATURE.
●, ▼ – – TESTED FIRST AT ROOM TEMPERATURE, THEN AT –188°C TO FRACTURE.
– – – ATTACHED TO SYMBOL INDICATES INTERRUPTION FOR MEASUREMENT OR FOR CHANGE TO –188°C.
F – – – – FLOW STRESS CURVES.
M – – – – MAXIMUM LOAD.
L_T – TRUE LOCUS OF FRACTURES.
P – – INFLUENCE OF PLASTIC DEFORMATION AT ROOM TEMPERATURE ON BREAKING STRESS AT –188°C.
A – – MACHINED BETWEEN TESTS AT ROOM TEMPERATURE AND –188°C.

FIG 8—INFLUENCE OF PLASTIC DEFORMATION OF NOTCHED AND UNNOTCHED SPECIMENS AT ROOM TEMPERATURE ON THE BREAKING STRESS OF ANNEALED INGOT IRON AT –188°C.

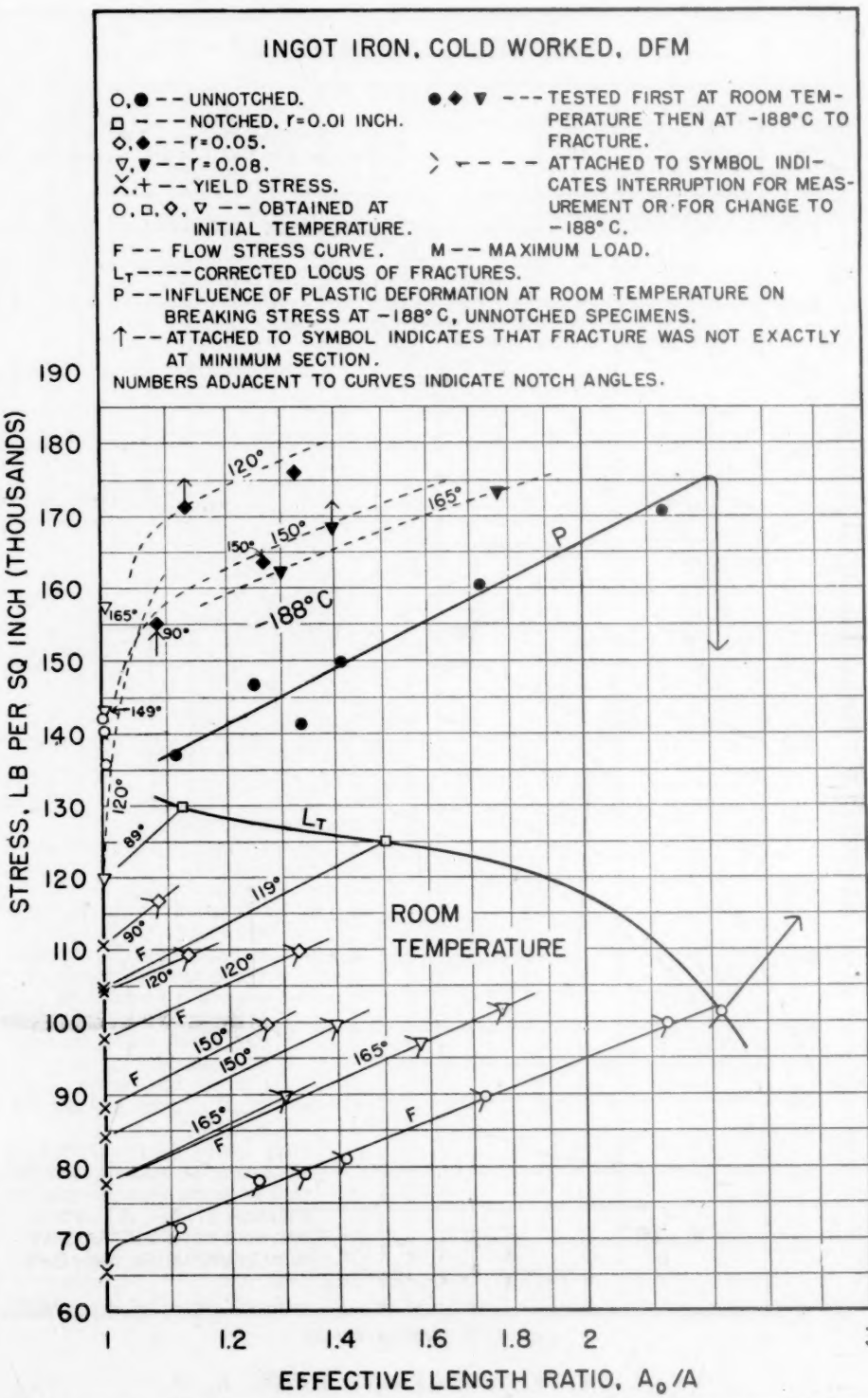

FIG 9—INFLUENCE OF PLASTIC DEFORMATION OF NOTCHED AND UNNOTCHED SPECIMENS AT ROOM TEMPERATURE ON THE BREAKING STRESS OF COLD-WORKED INGOT IRON AT −188°C.

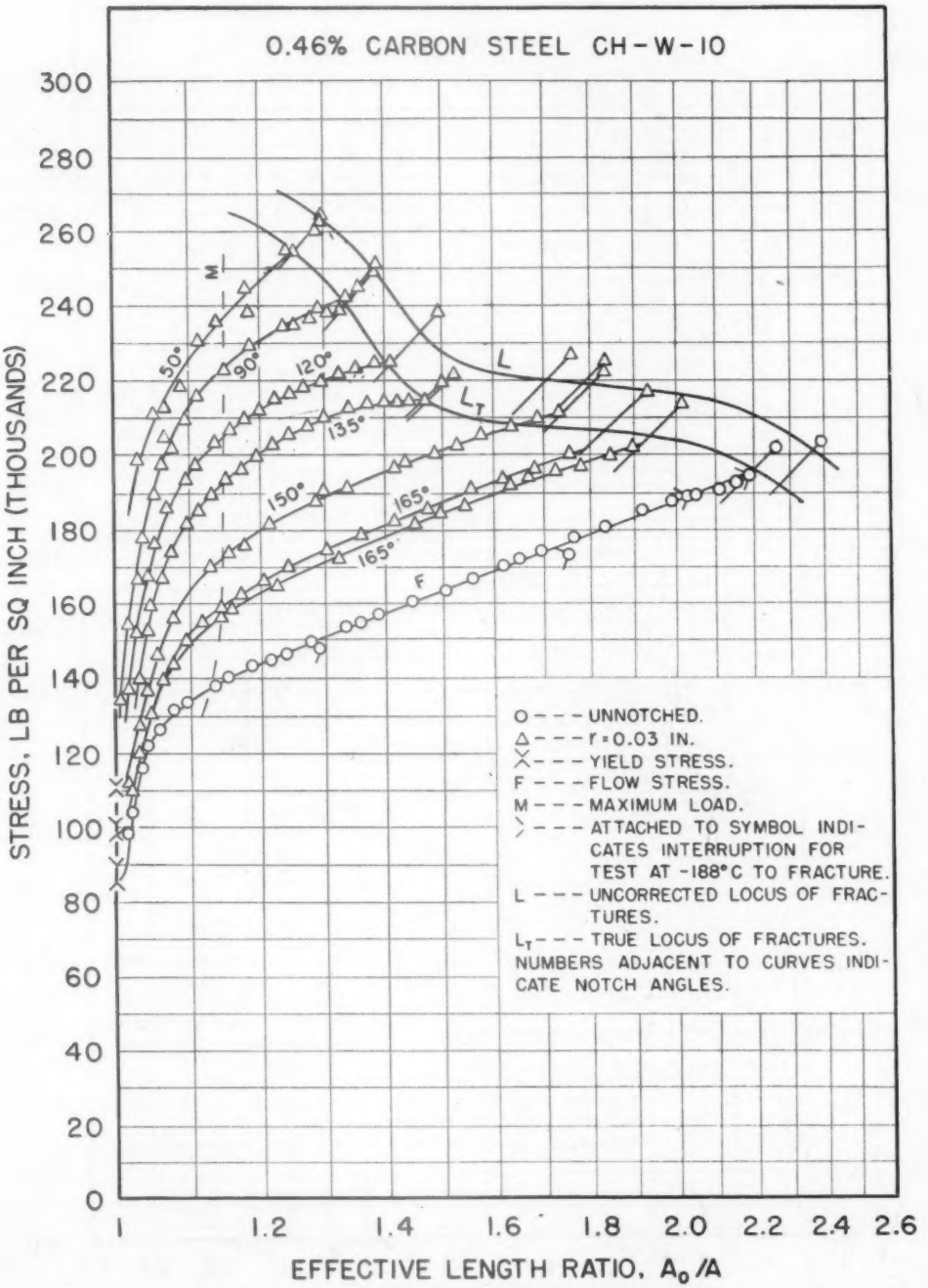

FIG 10—FLOW AND FRACTURE OF NOTCHED AND UNNOTCHED SPECIMENS OF 0.46 PCT CARBON STEEL AT ROOM TEMPERATURE.

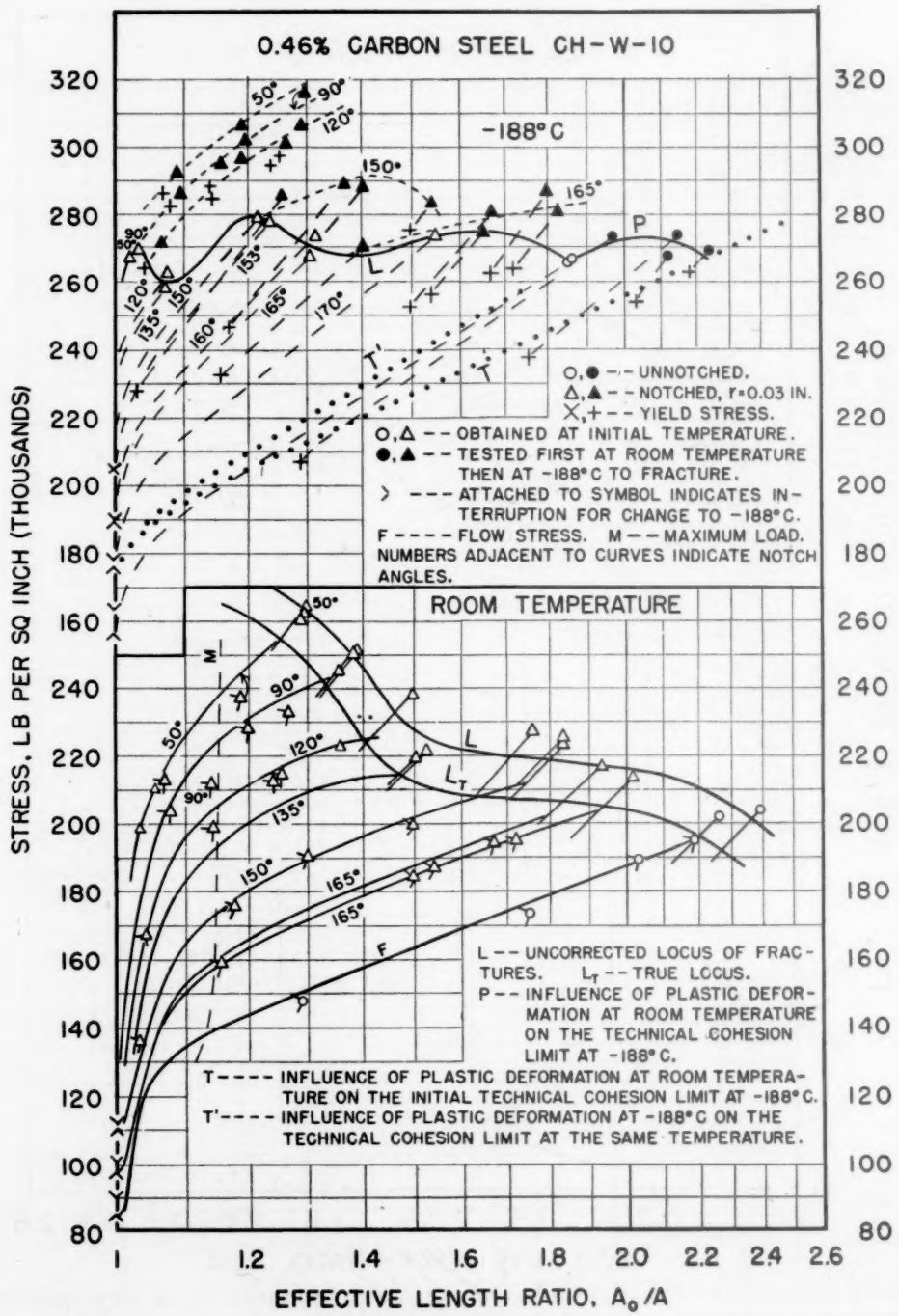
0.46% CARBON STEEL CH-W-10
-188°C
ROOM TEMPERATURE
STRESS, LB PER SQ INCH (THOUSANDS)
EFFECTIVE LENGTH RATIO, A_0/A
O,● -- UNNOTCHED.
Δ,▲ -- NOTCHED, r=0.03 IN.
X,+ -- YIELD STRESS.
O,Δ -- OBTAINED AT INITIAL TEMPERATURE.
●,▲ -- TESTED FIRST AT ROOM TEMPERATURE THEN AT -188°C TO FRACTURE.
> --- ATTACHED TO SYMBOL INDICATES INTERRUPTION FOR CHANGE TO -188°C.
F ---- FLOW STRESS. M -- MAXIMUM LOAD.
NUMBERS ADJACENT TO CURVES INDICATE NOTCH ANGLES.
L -- UNCORRECTED LOCUS OF FRACTURES. L_T -- TRUE LOCUS.
P -- INFLUENCE OF PLASTIC DEFORMATION AT ROOM TEMPERATURE ON THE TECHNICAL COHESION LIMIT AT -188°C.
T ---- INFLUENCE OF PLASTIC DEFORMATION AT ROOM TEMPERATURE ON THE INITIAL TECHNICAL COHESION LIMIT AT -188°C.
T' ---- INFLUENCE OF PLASTIC DEFORMATION AT -188°C ON THE TECHNICAL COHESION LIMIT AT THE SAME TEMPERATURE.

FIG 11—INFLUENCE OF PLASTIC DEFORMATION OF NOTCHED AND UNNOTCHED SPECIMENS AT ROOM TEMPERATURE ON THE BREAKING STRESS OF 0.46 PCT CARBON STEEL AT —188°C.

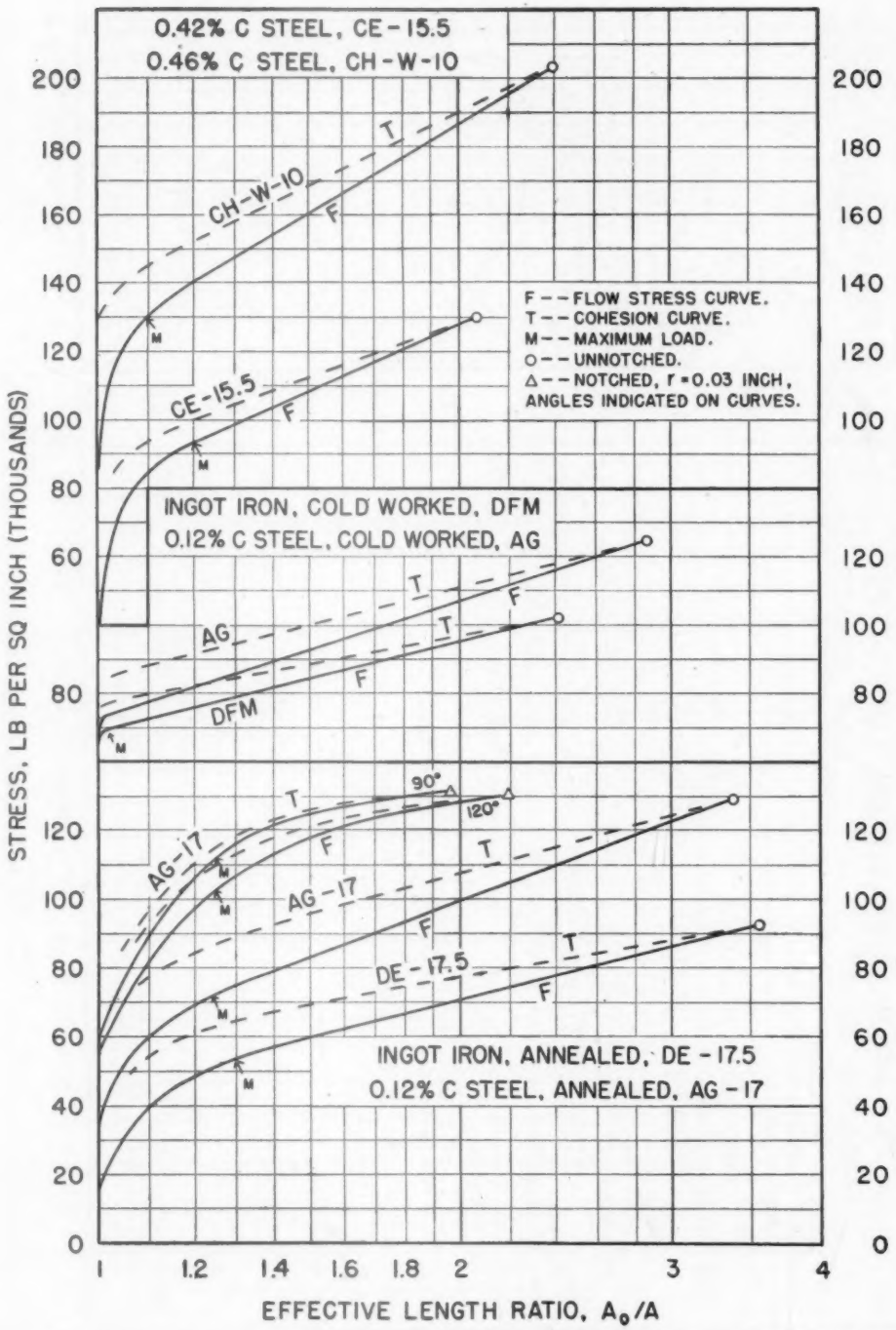

FIG 12—INFLUENCE OF PLASTIC DEFORMATION AT ROOM TEMPERATURE ON THE TECHNICAL COHESIVE STRENGTH AT THE SAME TEMPERATURE.

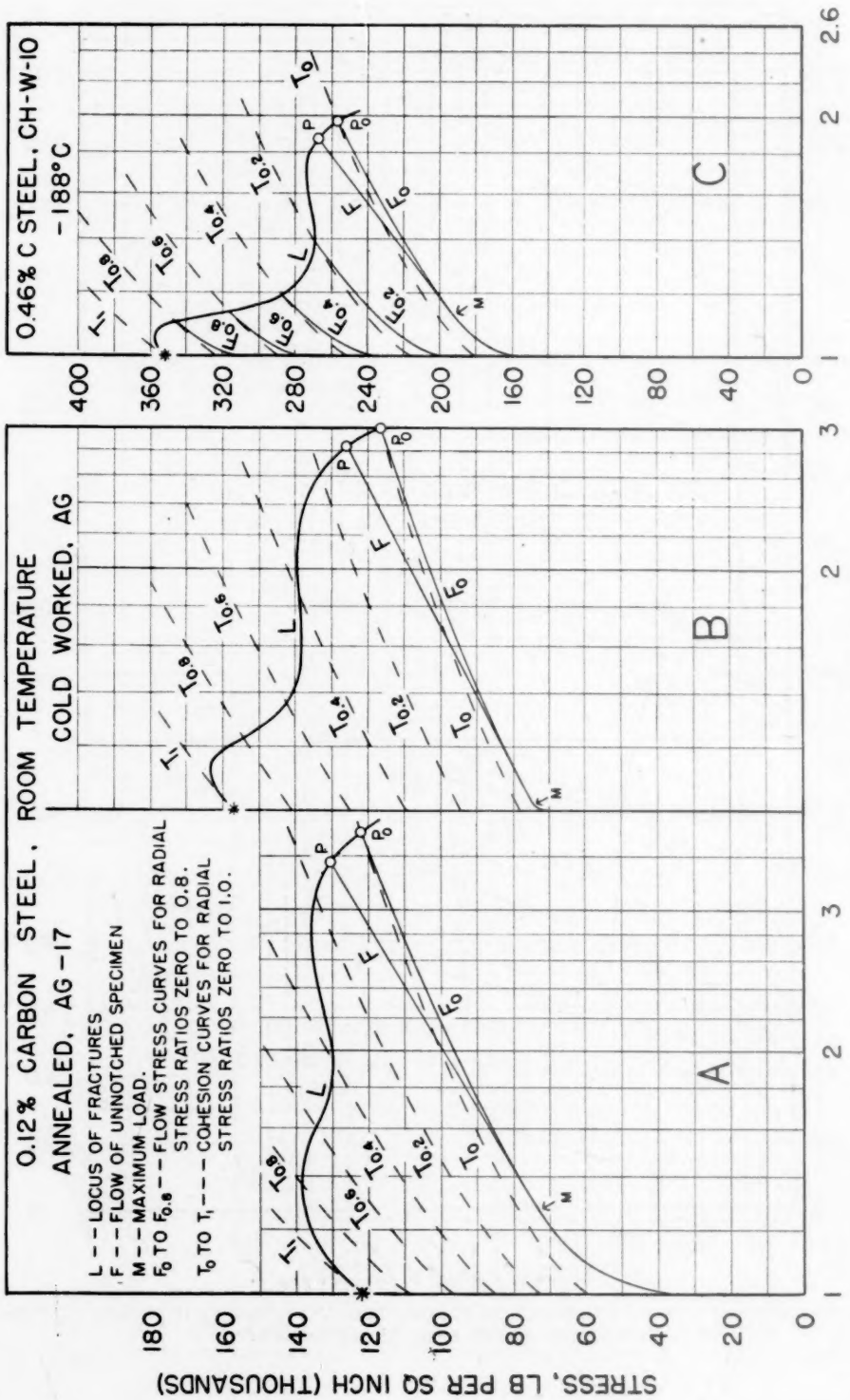
0.12% CARBON STEEL. ROOM TEMPERATURE
ANNEALED. AG-17
COLD WORKED. AG
0.46% C STEEL. CH-W-10
-188°C
L - - LOCUS OF FRACTURES
F - - FLOW OF UNNOTCHED SPECIMEN
M - - MAXIMUM LOAD.
F_0 TO $F_{0.8}$ - - FLOW STRESS CURVES FOR RADIAL STRESS RATIOS ZERO TO 0.8.
T_0 TO T_1 - - - COHESION CURVES FOR RADIAL STRESS RATIOS ZERO TO 1.0.
STRESS, LB PER SQ INCH (THOUSANDS)
EFFECTIVE LENGTH RATIO, A_e/A
A
B
C

FIG 13—INFLUENCE OF PLASTIC DEFORMATION AND THE RADIAL STRESS RATIO OF FLOW STRESS AND TECHNICAL COHESION LIMIT.

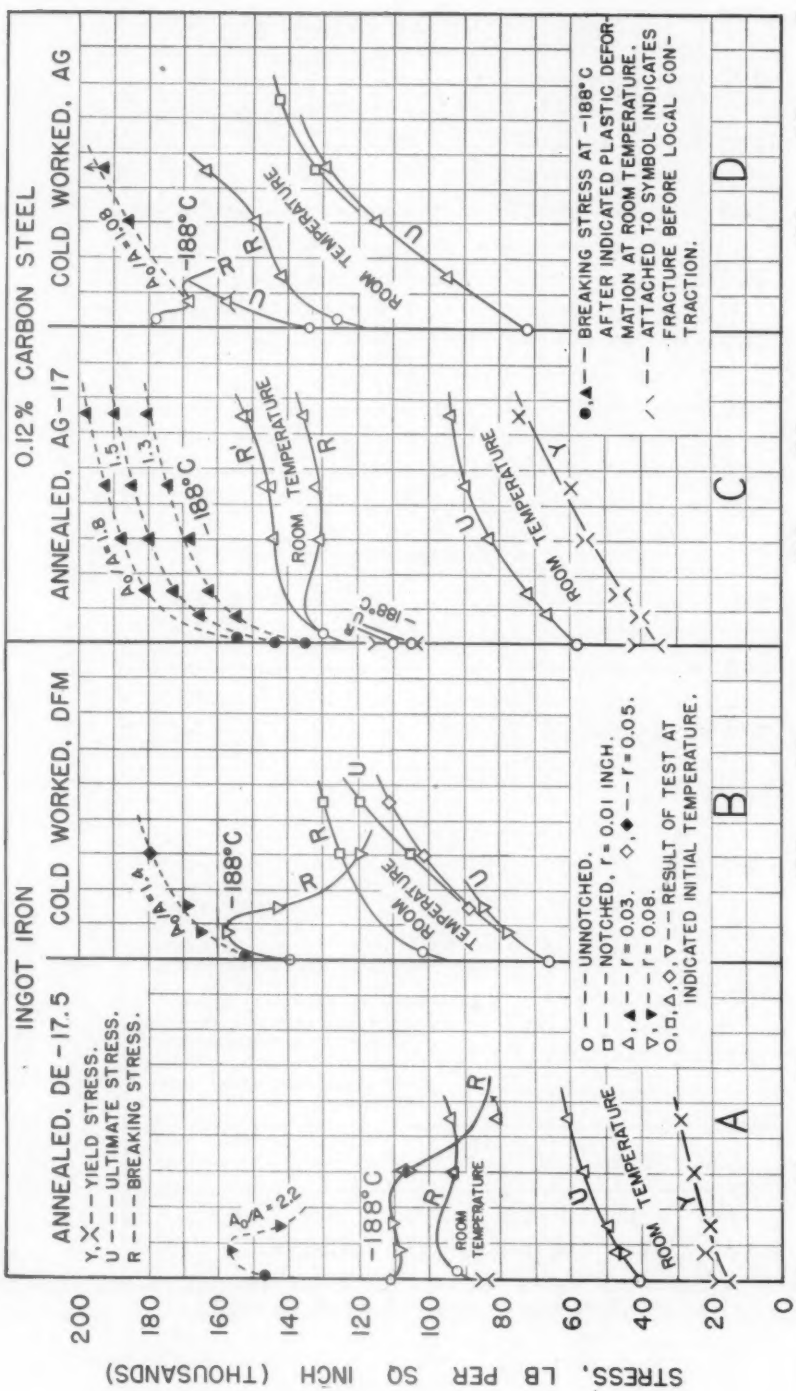
INGOT IRON
ANNEALED, DE-17.5
Y, X-- YIELD STRESS.
U - - - ULTIMATE STRESS.
R - - - BREAKING STRESS.
COLD WORKED, DFM
0.12% CARBON STEEL
ANNEALED, AG-17
COLD WORKED, AG
-188°C
ROOM TEMPERATURE
STRESS, LB PER SQ INCH (THOUSANDS)
NOTCH ANGLE, DEGREES
A
B
C
D
o - - - UNNOTCHED.
□ - - - NOTCHED, r = 0.01 INCH.
Δ, ▲ - - r = 0.03. ◇, ◆ - - r = 0.05.
▽, ▼ - - r = 0.08.
O, □, Δ, ◇, ▽ -- RESULT OF TEST AT INDICATED INITIAL TEMPERATURE.
●, ▲ -- BREAKING STRESS AT -188°C AFTER INDICATED PLASTIC DEFORMATION AT ROOM TEMPERATURE.
/ \ - - - ATTACHED TO SYMBOL INDICATES FRACTURE BEFORE LOCAL CONTRACTION.

FIG 14—INFLUENCE OF THE NOTCH ANGLE AND OF PLASTIC DEFORMATION ON THE FLOW STRESS AND BREAKING STRESS OF INGOT IRON AND LOW-CARBON STEEL.

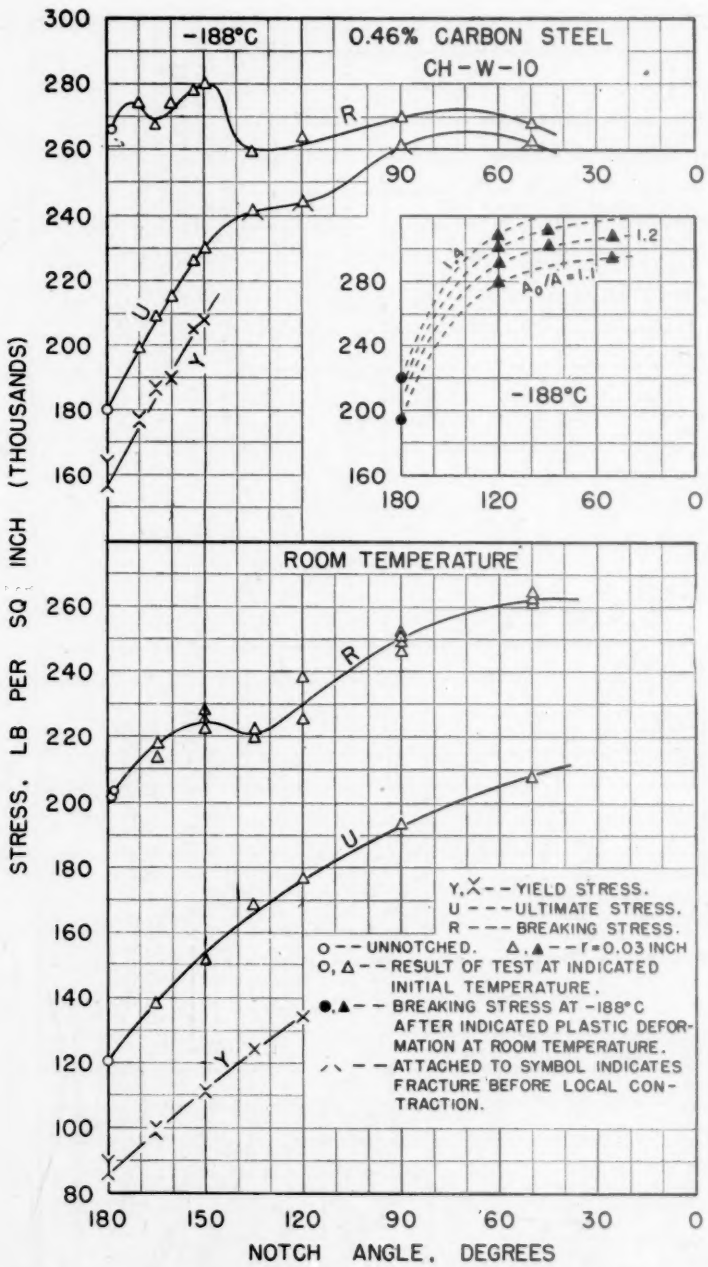

FIG 15—INFLUENCE OF THE NOTCH ANGLE AND OF PLASTIC DEFORMATION ON THE FLOW STRESS AND BREAKING STRESS OF 0.46 PCT CARBON STEEL.

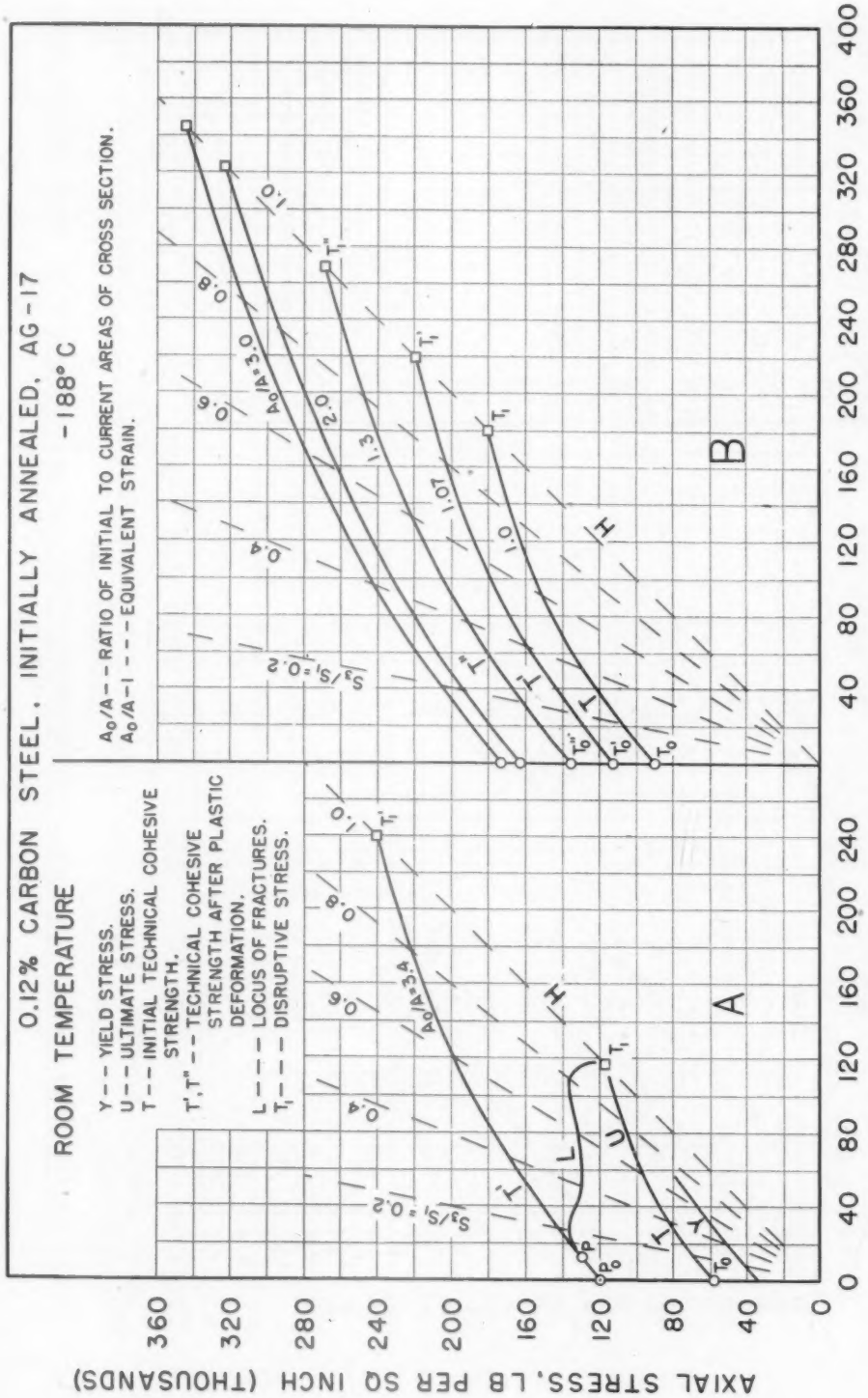
0.12% CARBON STEEL, INITIALLY ANNEALED, AG-17
ROOM TEMPERATURE
-188° C
Y - - YIELD STRESS.
U - - ULTIMATE STRESS.
T - - INITIAL TECHNICAL COHESIVE STRENGTH.
T', T" - - TECHNICAL COHESIVE STRENGTH AFTER PLASTIC DEFORMATION.
L - - - - LOCUS OF FRACTURES.
T1 - - - DISRUPTIVE STRESS.
A0/A - - RATIO OF INITIAL TO CURRENT AREAS OF CROSS SECTION.
A0/A-1 - - - EQUIVALENT STRAIN.
AXIAL STRESS, LB PER SQ INCH (THOUSANDS)
RADIAL STRESS, LB PER SQ INCH (THOUSANDS)
A
B

FIG 16—INFLUENCE OF TRANSVERSE RADIAL STRESS AND OF PLASTIC DEFORMATION ON THE BREAKING STRESS OF ANNEALED LOW-CARBON STEEL.

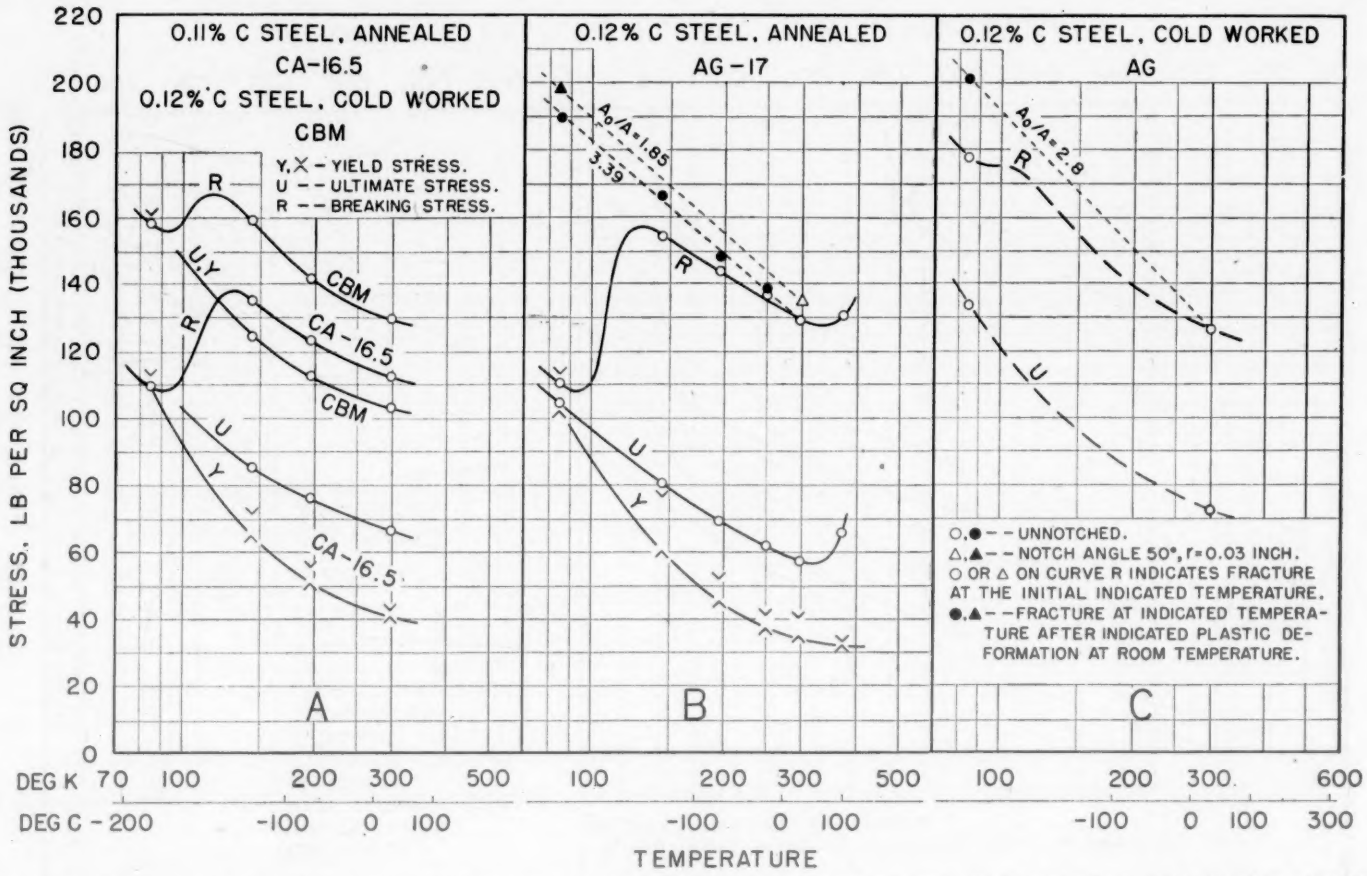

FIG 17—INFLUENCE OF TEMPERATURE AND PLASTIC DEFORMATION ON THE FLOW STRESS AND BREAKING STRESS OF LOW-CARBON STEELS.

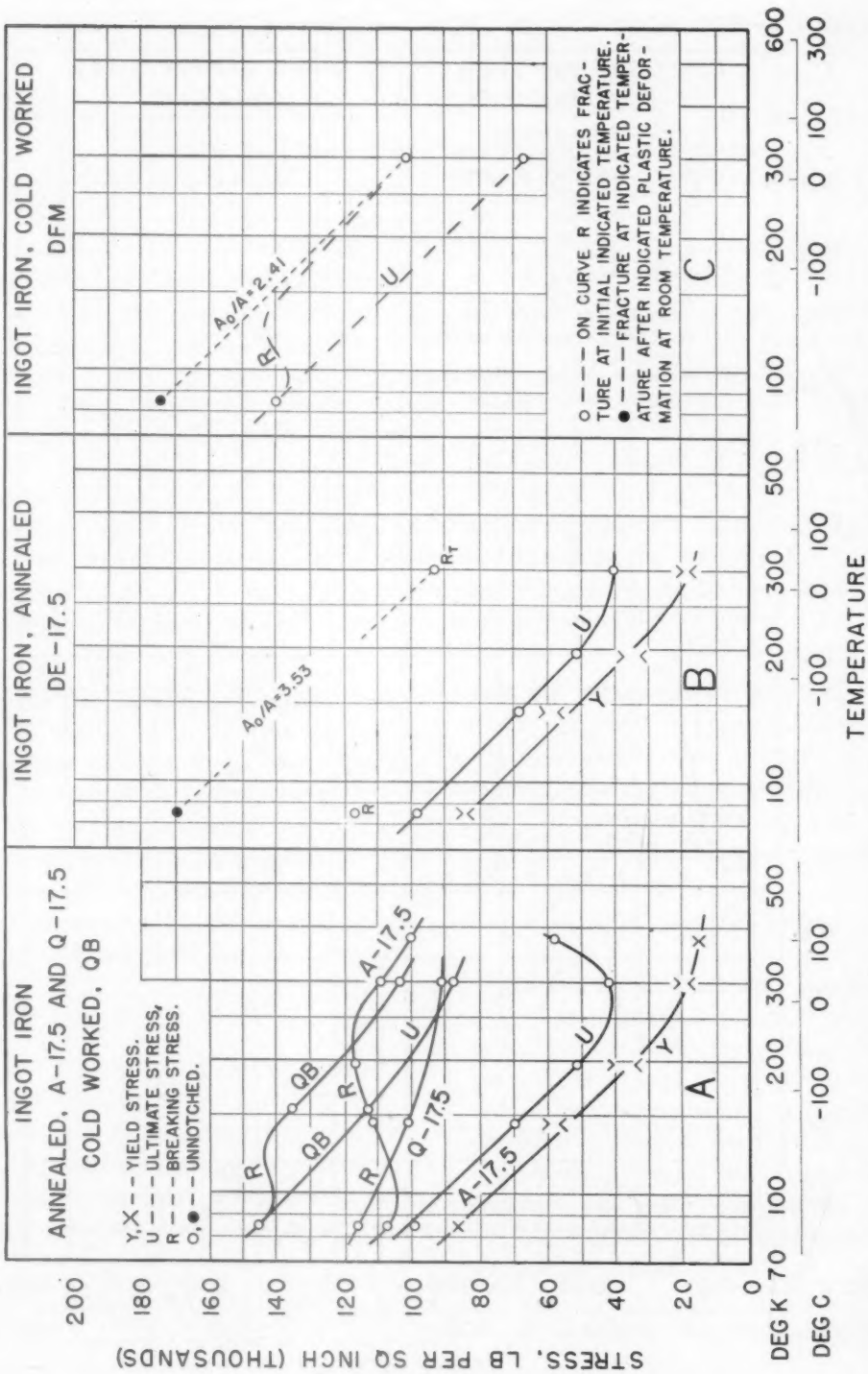
INGOT IRON
ANNEALED, A-17.5 AND Q-17.5
COLD WORKED, QB
INGOT IRON, ANNEALED
DE-17.5
INGOT IRON, COLD WORKED
DFM
Y, X - - YIELD STRESS.
U — — ULTIMATE STRESS,
R — — BREAKING STRESS.
O, ● — — UNNOTCHED.
O — — — ON CURVE R INDICATES FRACTURE AT INITIAL INDICATED TEMPERATURE.
● — — — FRACTURE AT INDICATED TEMPERATURE AFTER INDICATED PLASTIC DEFORMATION AT ROOM TEMPERATURE.
A
B
C
STRESS, LB PER SQ INCH (THOUSANDS)
TEMPERATURE
DEG K
DEG C

FIG 18—INFLUENCE OF TEMPERATURE AND PLASTIC DEFORMATION ON THE FLOW STRESS AND BREAKING STRESS OF INGOT IRON.

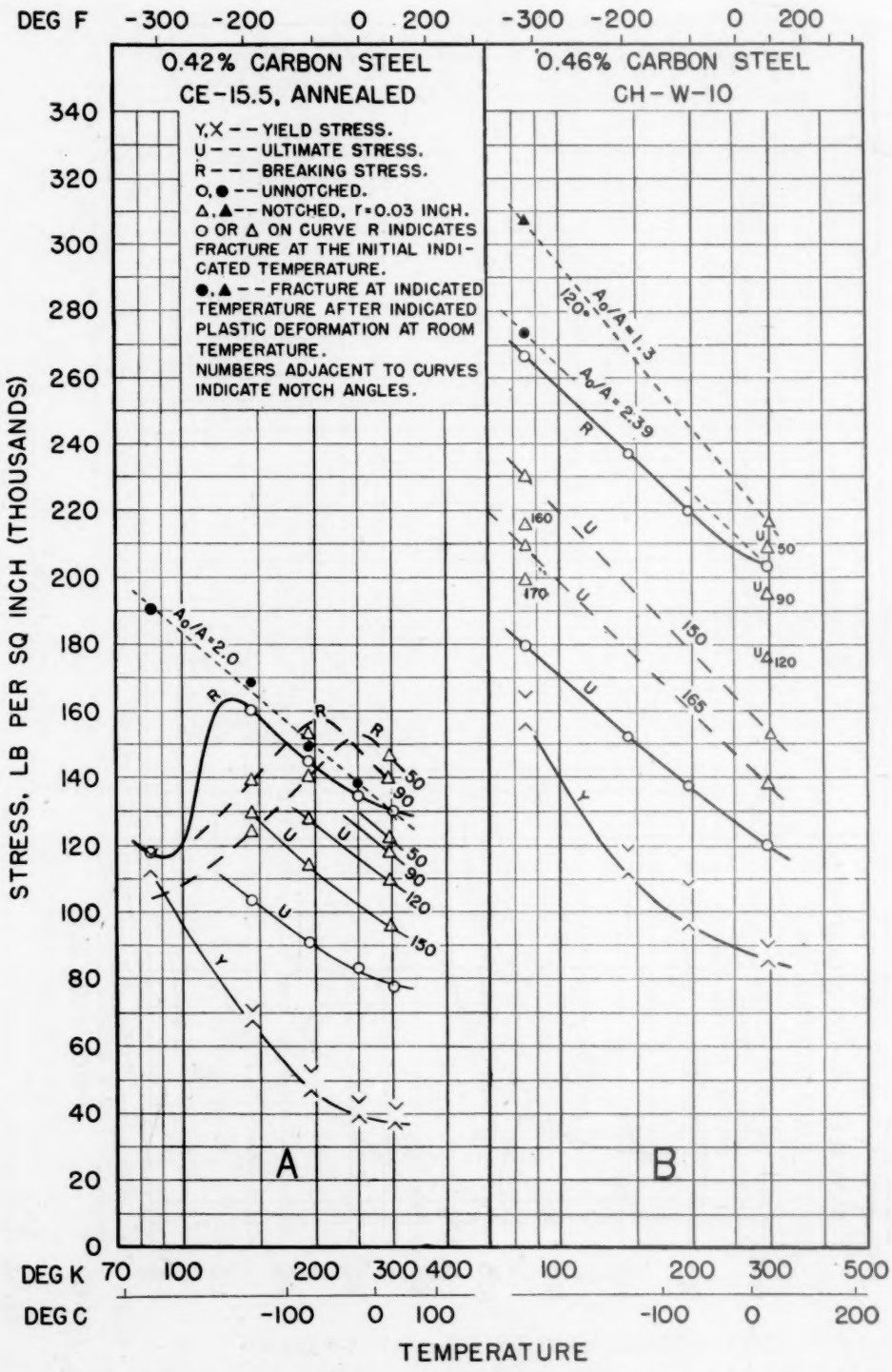

FIG 19—INFLUENCE OF TEMPERATURE AND PLASTIC DEFORMATION ON THE FLOW STRESS AND BREAKING STRESS OF 0.46 PCT CARBON STEEL.

Effect of Prior Tensile Strain on Fracture

By Edward Saibel*

(New York Meeting, March 1947)

The object of this study is to investigate the effect of prior tensile strain on the fracture stress of a metal. This is done in a theoretical manner starting from the point of view developed by the author in his thermodynamic theory of the fracture of metals. The results are compared with experimental findings and a rational interpretation is given to work that shows the variation of fracture stress with prior tensile strain.

Theory of Fracture

In the thermodynamic theory of the fracture of metals developed earlier,[1] it was shown that a critical strain energy per unit volume exists. This is characteristic of the material and may be calculated from basic thermodynamic data. When the area under the flow curve reaches this characteristic value, fracture occurs. The general criterion for fracture is expressed in the form

$$u \pm u_o = JL_m\Delta V/V \qquad [1]$$

where L_m is the latent heat of melting of the unit volume, $\Delta V/V$ is the ratio of the change in volume of the unit volume to the original unit volume on passing from the solid to the liquid state, u_o is an initial energy density, and J is a conversion factor, which changes energy from heat to mechanical units. As a first approximation, it will be assumed that the stress-strain curve is the straight line that extends from the point of maximum load onward, extrapolated back to the axis of zero strain, for example, line AC of Fig. 1. If the point of intersection of the straight line with the axis of zero strain is represented by σ_o, and the slope of the straight line is p, the analytic form of the flow curve is

$$\sigma = \sigma_o + p\delta \qquad [2]$$

and the strain energy per unit volume evaluated from $\int\sigma d\delta$ becomes $(\sigma_o\delta + p\delta^2/2)$. When this latter term reaches the critical value $JL_m\Delta V/V$ (designated hereafter by M), it is assumed that fracture occurs. This leads to the following expression for the fracture stress:

$$\sigma_f = \sqrt{\sigma_o^2 + 2Mp} \qquad [3]$$

The strain at fracture may be calculated from Eqs 2 and 3. It is assumed in this paper that the initial energy density is either zero or that it may be neglected. Furthermore, the complicated states of stress and of strain existing in the necked region of the tensile specimen after "necking" has occurred will also be neglected for the present, so that average conditions will be assumed to prevail.

Flow and Fracture Curves

Ludwig[2] attributed to materials two fundamental properties: (1) a resistance to flow and (2) a resistance to fracture. He reasoned that at each instant the

This work was done in connection with a contract between the David Taylor Model Basin, Navy Department, Washington, D. C., and the Carnegie Institute of Technology. Manuscript received at the office of the Institute Nov. 29 1946. Issued as T.P. 2186 in Metals Technology, June, 1947.

* Associate Professor of Mechanics, Department of Mathematics, Carnegie Institute of Technology, Pittsburgh, Pennsylvania.

[1] References are at the end of the paper.

material is in a certain state that can be described if one knows the variables involved, and being subject to certain stresses, will either flow or fracture. Thus the history of the state of the material during flow can be represented by a hypersurface in a space of many dimensions. This hypersurface may be referred to as a flow surface. On the other hand, he envisaged a surface called the fracture surface, which simply is the locus of the variables for which fracture occurs.

This idea that a material possesses the two characteristic properties, a resistance to flow and a resistance to fracture, has greatly influenced the study of the mechanical behavior of materials. In recent times, considerable research has been directed toward the establishment of the variables upon which the flow and fracture characteristics of metals depend and upon the quantitative effects of these variables.

In its most general form, the problem is extremely complicated because of the large number of variables involved. It is thought that stress system, state of strain, strain rate, temperature, and past history are the important variables in terms of which both resistance to flow and resistance to fracture may be explicitly formulated. In addition to these variables, metallurgical structure also enters, but just how it may be introduced analytically is not clear at the present time.

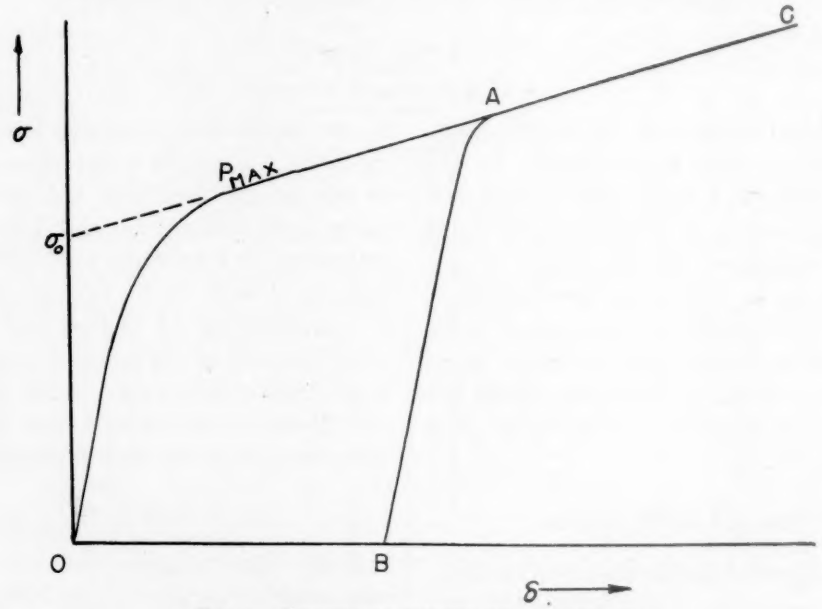

FIG 1—SCHEMATIC STRESS-STRAIN CURVE.

The problem has been greatly simplified by holding constant all of the dependent variables but one. Thus, instead of having to deal with hypersurfaces in a multidimensional space, the representation of flow and fracture resistances may be shown by means of plane curves. Furthermore, assuming the validity of the relationship between significant stress and significant strain, complex states of stress and strain may be represented by a single point in a two-dimensional diagram. It will be recalled that significant stress $\bar{\sigma}$, and significant strain $\bar{\delta}$, are defined as follows:

$$\bar{\sigma} = \frac{1}{\sqrt{2}} [(\sigma_1 - \sigma_2)^2 + (\sigma_2 - \sigma_3)^2 + (\sigma_3 - \sigma_1)^2]^{1/2}$$

$$\bar{\delta} = \sqrt{2/3}\, [\delta_1^2 + \delta_2^2 + \delta_3^2]^{1/2} \qquad [4]$$

where σ indicates the principal stresses and

δ the principal strains. These quantities are seen to be related to the invariants of stress and strain. In the case of the flow curve, little difficulty is experienced in showing the effects of the variables. However, in the case of the fracture-stress curve, only one point can be found directly; that is, the actual point of fracture. Consequently, the fracture-stress curve must be found by some indirect method.

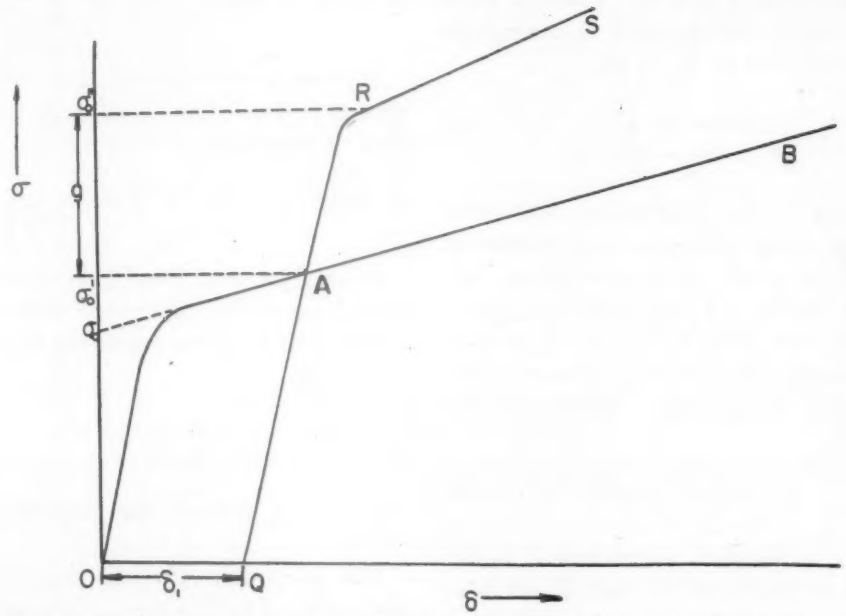

FIG 2—SCHEMATIC STRESS-STRAIN CURVE SHOWING EFFECTS OF PRIOR STRAIN AND LOWERING OF TEMPERATURE.

EFFECT OF PRIOR TENSILE STRAIN ON FRACTURE STRESS

One of the proposed methods for determining the variation of the fracture curve with prior strain has been to strain the specimen at room temperature various preassigned amounts, then lower the temperature and pull to fracture. If the material shows almost no further strain, the method is deemed useful. This may be done for varying amounts of prior strain. It is then possible to plot the stress at fracture against the initial amount of strain. The resulting curve, because of the different temperature of testing, will not intersect the flow curve at the point of fracture that occurs for room temperature testing. This has led Davidenkov and Wittman, followed by Hollomon and Zener,[3] to postulate a shift of the curve, obtained as outlined above, downward parallel to itself until the fracture and flow curves do intersect at the one point that can be obtained experimentally.

The procedure just outlined will now be analyzed on the basis of the fracture theory previously developed. The steps involved are as follows: (1) the metal is prestrained a given amount at room temperature, (2) the temperature is lowered, (3) the specimen is pulled to fracture. This corresponds to the path *OAQARS* in Fig 2.

Assume that the stress-strain curve may be expressed in the form

$$\sigma = \sigma_o + p\delta \qquad [2]$$

and let the amount of prestrain at room temperature be δ_1. Then let the load be removed from the specimen. The path followed on the stress-strain diagram (Fig 1) is *OAB* and the area *OAB* is the

energy per unit volume stored in the specimen.

If the specimen is now loaded again at room temperature, the path taken on the stress-strain curve is BAC. Treating B as the new origin, the equation of the stress-strain curve may be taken as

$$\sigma = \sigma_o' + p\delta \qquad [5]$$

where $\sigma_o' = \sigma_o + p\delta_1$

However, if the temperature is lowered after the initial prestrain and release of load, σ_o' is raised to a new value, say $(\sigma_o' + g)$, see Fig 2. It is possible to approximate this new value $\sigma_o'' = (\sigma_o' + g)$ from the quasi-empirical relation between yield stress and temperature developed by Orowan:[4]

$$\sigma_y = A - B\sqrt{T} \qquad [6]$$

where σ_y is the yield stress and T is the absolute temperature. A and B are constants characteristic of the material. Although this relation was developed for the single crystal, it may be used with a fair degree of approximation for a polycrystalline substance.

In the third and final stage of the process, the specimen is pulled to fracture at the lowered temperature. From Eq 3, the fracture stress is given by

$$\sigma_f = \sqrt{\sigma_o''^2 + 2M''p''} \qquad [7]$$

where (see Fig 2):

σ_o'' is the intercept of the straight-line portion of the stress-strain curve after prior deformation and lowering of the temperature, p'' is the slope of the stress-strain curve under the above conditions, and

$$M'' = M - \sigma_o\delta_1 - \frac{p\delta_1^2}{2}$$

since an amount of mechanical work equal to $(\sigma_o\delta_1 + p\delta_1^2/2)$ has already been done on the system.

Now, $\sigma_o'' = \sigma_o' + g$

and $\sigma_o' = \sigma_o + p\delta_1$

therefore Eq 7 may be written

$$\sigma_f = [(\sigma_o + p\delta_1 + g)^2 + 2p''(M - \sigma_o\delta_1 - p\delta_1^2/2)]^{1/2} \qquad [8]$$

Suppose for the present that there is no change in slope, that is, $p'' = p$. Eq 8 may then be simplified, leading to

$$\sigma_f = [(\sigma_o^2 + 2Mp) + 2pg\delta_1 + 2g\sigma_o + g^2]^{1/2} \qquad [9]$$

It may be seen from Eq 9 that if the second part of the tensile test is carried out at the same temperature as the first part, g is zero, and

$$\sigma_f = [\sigma_o^2 + 2Mp]^{1/2} \qquad [10]$$

or $$\sigma_f = \delta_{f\,\text{orig}} \qquad [11]$$

where $\sigma_{f\,\text{orig}}$ denotes the original fracture stress.

The assumption that the slope p has not been affected by the change in temperature is not quite correct. It is known that for some materials, p is increased and that for others it may be decreased under these conditions. This change in p will be discussed later.

Now, let Eq 9 be expressed in the form

$$\sigma_f = \sqrt{A + B} \qquad [12]$$

where $A = \sigma_o^2 + 2Mp$

and $B = 2pg\delta_1 + 2g\sigma_o + g^2$

In most cases, A will be considerably larger than B, so that Eq 12 may be expanded by the binomial theorem in the form

$$\sigma_f = A^{1/2} + \tfrac{1}{2}A^{-1/2}B - \tfrac{1}{8}A^{-3/2}B^2 + \cdots \qquad [13]$$

$$\text{or } \sigma_f = \sigma_{f\,\text{orig}} + \frac{1}{2}\frac{2pg\delta_1 + 2g\sigma_o + g^2}{\sigma_{f\,\text{orig}}} - \frac{1}{8}\frac{[2pg\delta_1 + 2g\sigma_o + g^2]^2}{\sigma_{f\,\text{orig}}^3} + \cdots \qquad [14]$$

If the data are of such a nature that only the first two terms need be considered, Eq 14 may be written in the approximate

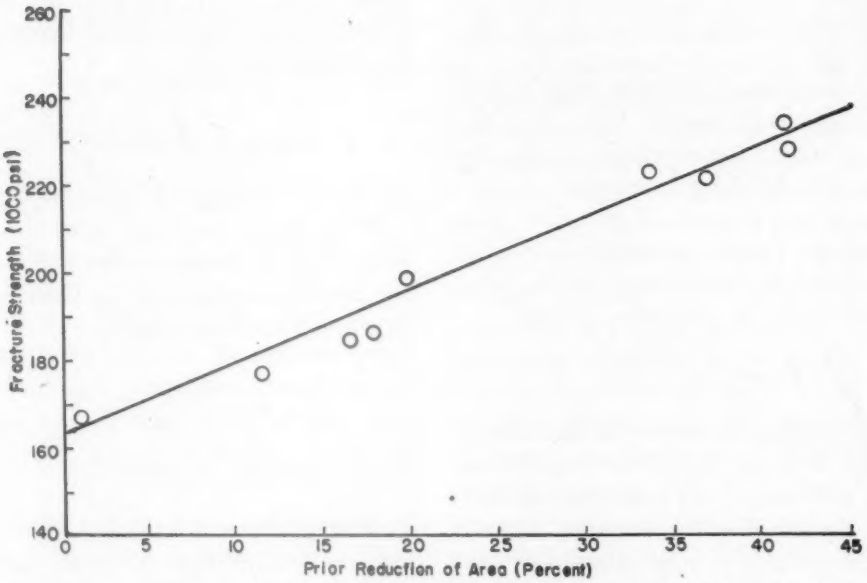

FIG 3—EFFECT OF PRIOR DEFORMATION ON FRACTURE STRESS AT MINUS 190°C, AIR-COOLED STEEL. (*J. H. Hollomon and C. Zener.*[3])

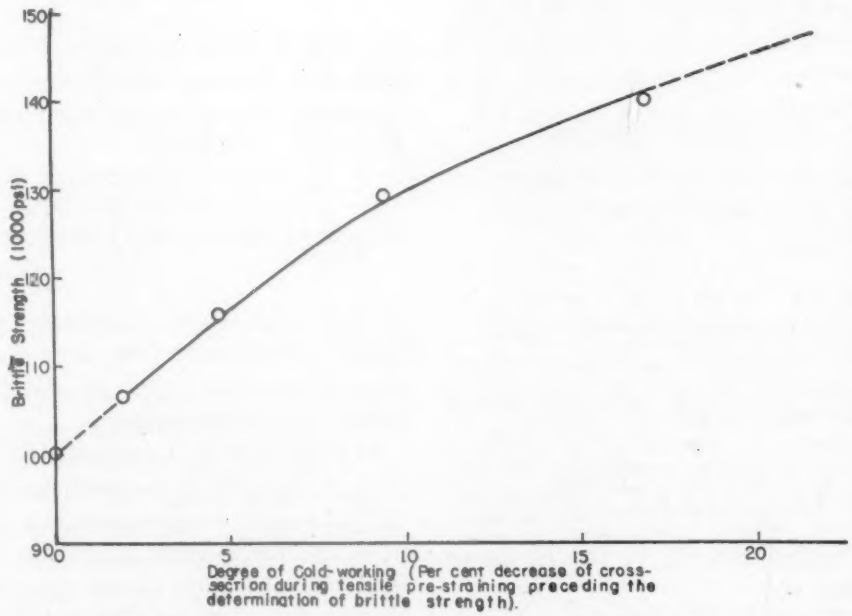

FIG 4—DEPENDENCE OF BRITTLE STRENGTH ON AMOUNT OF PRECEDING PLASTIC DEFORMATION IN TENSION. (*Sakharov.*)[6]

form

$$\sigma_f = \sigma_{f\,\text{orig}} + d + c\delta_1 \qquad [15]$$

where c and d are constants, since g, p, σ_o, and $\sigma_{f\,\text{orig}}$ are constants. Thus, as a first approximation, the fracture stress rises linearly with δ_1, the prior strain.

On the other hand, if the first three terms of Eq 14 are necessary in order to obtain a good approximation, the variation of σ with δ_1 will be parabolic; namely,

$$\sigma_f = \sigma_{f\,\text{orig}} + d + c\delta_1 + a\delta_1^2 \qquad [16]$$

where a, c, and d are constants that may be evaluated in terms of the known quantities: g, p, σ_o, and $\sigma_{f\,\text{orig}}$. This is substantiated by the graphs showing the variation of fracture stress with prior strain that have been advanced by Hollomon and Zener,[5] and Sakharov,[6] whose curves are respectively linear and parabolic to a first approximation. These are reproduced in Figs 3 and 4, respectively. It is evident that in Eqs 15 and 16, d represents the increase in fracture stress due to the lowering of the temperature.

Analysis of Strains

The strains may also be analyzed on the basis of the assumptions made above. In the final stage,

$$\sigma = \sigma_o'' + p\delta$$

or

$$\delta_f = \frac{\sigma_f - \sigma_o''}{p} = \frac{\sigma_f - \sigma_o' - g}{p}$$

Using the value for σ_o',

$$\delta_f = \frac{\sigma_f - \sigma_o - p\delta_1 - g}{p} \qquad [17]$$

Substituting into Eq 17 the results of Eq 15 leads to

$$\delta_f = \frac{\sigma_{f\,\text{orig}} + c\delta_1 + d - \sigma_o - p\delta_1 - g}{p} \qquad [18]$$

However,

$$\delta_{f\,\text{orig}} = \frac{\sigma_{f\,\text{orig}} - \sigma_o}{p}$$

where $\delta_{f\,\text{orig}}$ is the value of the strain at fracture under the original loading. Now Eq 18 may be written

$$\delta_f = \delta_{f\,\text{orig}} + \frac{c\delta_1 + d - p\delta_1 - g}{p} \qquad [19]$$

When there has been prior strain, but no change in temperature, g is equal to zero, and σ_f is equal to $\sigma_{f\,\text{orig}}$. Consequently, as may be seen from Eq 17,

$$\delta_f = \frac{\sigma_f - \sigma_o}{p} - \delta_1$$

or

$$\delta_f = \delta_{f\,\text{orig}} - \delta_1 \qquad [20]$$

This simply means that, in a static tensile test, unloading the specimen and then reloading leads to fracture at the same strain relative to the virgin specimen.

It is interesting to note from Eq 19 that if

$$(c\delta_1 + d) > (p\delta_1 + g) \qquad [21]$$

the series of operations outlined leads to an increase in ductility. Introducing the values for c and d in terms of the known quantities, Eq 21 may be written

$$\frac{g}{\sigma_{f\,\text{orig}}}\left(p\delta_1 + \sigma_o + \frac{g}{2}\right) > p\delta_1 + g \qquad [22]$$

as the condition for increased ductility (strain to fracture). This, after the operations of prestrain by an amount δ_1 and a lowering of the temperature.

In the foregoing, it was assumed that the slope of the straight line taken to represent the stress-strain curve remained constant when the temperature was lowered. Consider how the more general case where p changes to a value $p'' = p + \Delta p_T$, Δp_T being the change in p, positive or negative as the case may be, due to the change in temperature.

The value of σ_o' is still equal to $(\sigma_o + p\delta_1)$. Now, however,

$$\sigma_f = \left[(\sigma_o + p\delta_1 + g)^2 + 2(p + \Delta p_T) \left(M - \sigma_o\delta_1 - \frac{p\delta_1^2}{2} \right) \right]^{1/2} \quad [23]$$

Eq 23 may be written in the form

$$\sigma_f = \left[(\sigma_o^2 + 2Mp) + (2pg\delta_1 + 2g\sigma_o + g^2) + 2\Delta p_T \left(M - \sigma_o\delta_1 - \frac{p\delta_1^2}{2} \right) \right]^{1/2} \quad [24]$$

The first two terms in the bracket on the right-hand side of Eq 24 are positive and the sign of the third term depends upon the sign of Δp_T. M is greater than $\left(\sigma_o\delta_1 + \frac{p\delta_1^2}{2}\right)$. Otherwise, fracture would occur during the first stage of the set of operations that are being applied. Thus if Δp_T is positive, the effect of prior strain is to increase the fracture stress. Suppose that, on the other hand, Δp_T is negative. Consider the value of the term $\left(M - \sigma_o\delta_1 - \frac{p\delta_1^2}{2}\right)$ in the following extreme cases: first, δ_1 large enough to be almost equal to $\delta_{f\,\text{orig.}}$. In this case, $M - \sigma_o\delta_1 - \frac{p\delta_1^2}{2}$ is almost zero and obviously $\sigma_f > \sigma_{f\,\text{orig.}}$. Secondly, consider δ_1 so small that it may be neglected in comparison with other terms. Now, Eq 24 may be written:

$$\sigma_f = [(\sigma_o^2 + 2Mp) + (2g\sigma_o + g^2) + 2M\Delta p_T]^{1/2} \quad [25]$$

and, from a knowledge of the data, it may be determined whether σ_f is greater or less than $\sigma_{f\,\text{orig.}}$. All of the data familiar to the author exhibit either zero or positive values for Δp_T with decrease in temperature. Whether or not there exists the possibility of a decrease in σ_f, in actuality is not known to him. However, there does exist the possibility that the technical cohesive strength may exhibit a minimum.

It is thus seen that an energy theory of fracture will explain the phenomena observed as a result of prior strain. The variation of σ_o with change in initial strain and with change in temperature may be put on a rational basis. However, the change in the slope of the straight-line portion of the stress-strain curve with temperature remains to be worked out theoretically.

Recent work by Mehringer and MacGregor[7] may be used as a partial experimental check of the theory. They have investigated the effect of cold-work on the properties of a low-carbon steel. The test that comes closest to satisfying the conditions postulated in this paper is the one on the effect of cold-working by tensile pull on the true stress-strain curve. They find that prior strain does not affect the stress at fracture to a marked degree when no temperature change is made. This confirms the theory as shown in Eq 11. The strains at fracture should satisfy the condition

$$\delta_f = \delta_{f\,\text{orig.}} - \delta_1 \quad [20]$$

However, it must be remembered that this was derived for an isotropic substance and that prior strain induced by tensile pulling or by cold-rolling makes for a state of anisotropy in the body.

If x is taken as the percentage reduction in area, the natural strain δ may be calculated from

$$\delta = \log \frac{1}{1 - \frac{x}{100}} \quad [21]$$

Table 1 shows a comparison of fracture strains reported by Mehringer and MacGregor[7] with those calculated theoretically.

TABLE 1—*Comparison of Fracture Strains*

Percentage Reduction in Area by Tensile Pull	Prior Strain δ_1	Calculated Fracture Strain	Observed Fracture Strain[7]
5	0.049	0.81	0.74
10	0.104	0.76	0.70
15	0.166	0.69	0.64

CONCLUSION

The point of view adopted in the present paper furnishes a rational explanation of

the variation of fracture strength with prior tensile strain. The theoretical results are substantiated by what meager experimental findings are available. At the same time, further corroboration of the energy theory of fracture is furnished through its success in explaining the additional phenomena treated. Further work, both theoretical and experimental, along these lines would be highly desirable.

Acknowledgment

The author wishes to acknowledge the interest in this work and the support given him by the Navy Department, through the David Taylor Model Basin.

References

1. Saibel: A Thermodynamic Theory of the Fracture of Metals. *Trans.* AIME (1947) **171**, 639. *Metals Tech.* (Feb. 1947—T.P. 2131).
2. Ludwig: Elemente der Technologischen Mechanik, Berlin, 1909.
3. Hollomon and Zener: *Jnl. Appl. Phys.* (1946) **17**, 83.
4. Orowan: *Ztsch. physik* (1934) **89**, 612.
5. Hollomon and Zener: *Trans.* AIME (1944) **158**, 289.
6. Symposium on Cohesive Strength. *Trans.* AIME (1945) **162**, 582.
7. Mehringer and MacGregor: *Trans.* AIME (1945) **162**, 291.

DISCUSSION

(I. R. Kramer presiding)

E. F. Poncelet*—Professor Saibel's paper refers to a "criterion of rupture" perfected by himself, in which he uses the term "criterion of fracture" and brings into his paper the ideas of Ludwig on fracture and flow, that were remarkable when they were written in 1909.

I would like to point out that since that date, new, more precise ideas have superseded the Ludwig conceptions, and that rupture and fracture are no longer interchangeable synonyms.

Fracture of a specimen implies that rupture has been brought about by the propagation of cracks or fractures across the specimen. The mechanism of this phenomenon is today well known and well understood: Two particles of the solid, that were bonded together, are pulled apart, and become each bonded to particles of the surrounding medium, the atmosphere. These particles of the solid then become part of the newly created surface of the solid, absorbing particles of the surrounding atmosphere in the process. This phenomenon propagates at a finite but steeply increasing rate from bond to bond across the solid, leaving characteristic fracture-surfaces as permanent records of the process. The rate of this phenomenon is controlled solely by the tensile stress at the crack-tip, the nature of the solid, the nature of the surrounding medium and the temperature. This crack-tip stress is of course dependent on the configuration of the surface of the solid, and keeps increasing as the crack-depth increases.*

Other phenomena than fracture may also lead to rupture. When mild steel is drawn, it necks down considerably before fracturing. Some specially viscous materials as hot glass neck right down to zero cross-section, bringing about rupture without any fracturing at all. The mechanism of this phenomenon called "flow" is also well understood today. Two particles of the solid that were bonded together are pulled apart, and become bonded to other particles of the same solid sufficiently mobile to come within range. The rate of this phenomenon taking place throughout the solid, is controlled exclusively by the "shape-changing" stresses, the nature of the solid and the temperature.†

It may be recalled that if we call σ_x, σ_y, and σ_z the principal stresses, $\sigma_x + \sigma_y + \sigma_z = 3\sigma$ is called the "volume changing" stress, and $(\sigma_x - \sigma)$, $(\sigma_y - \sigma)$, $(\sigma_z - \sigma)$ is called the "shape changing" stress, the shear stress being a special case of the latter stress.‡

It is clear that the "criterion of rupture" referred to by the author has nothing to do with either of the phenomena discussed so far, the latter having no criteria. We must consequently look for a third process of rupture. Suppose we swing a pipe full of water, closed at the near end with a cap, and at the far

* Research Fellow, Owens Illinois Glass Co., Toledo, Ohio.

* See E. F. Poncelet, Fracture and Comminution of Brittle Solids, AIME *Trans.* (1946) **169**, 39; *Min. Tech.*, Jan. 1946.

† See Nature of Strength and Failure in Brittle Solids, Colloid Chemistry, 1946.

‡ See Brandenberger, Schw. Arch. ang. Wiss. Tech. 1941.

end with a rubber bag. We may pull the water column apart by centrifugal force and thus rupture same. It cannot rupture by fracturing as water does not support propagation of a fracture. It cannot rupture by flow because the pipe prevents the water column from necking down. Water evaporated and the vapor separated the two water-column sections. This spontaneous phenomenon of cavitation is presumably controlled by the "volume-changing" stress (sometimes called hydrostatic stress), the temperature and the nature of the material being broken. It is presumably the type of rupture referred to by the author, the only type for which a criterion can exist.

Examination of most fractured specimens show evidence that both fracture and flow proceeded simultaneously, the former finally outstripping the latter, but no trace attributable to the phenomenon of cavitation has ever been described.

It has been suggested by the author that this spontaneous rupture applies with its criterion to the initial crack only, which subsequently propagates as a fracture. This very clever interpretation of the facts, not only explains most satisfactorily the absence of any trace of cavitation in rupture specimens, but at the same time gives a very original explanation for the genesis of these initial submicroscopic cracks, the existence of which we are compelled to admit from experimental evidence on delayed fracture, but which have eluded the most determined attempts to observe them directly.

In the above light, the complex phenomenon of rupture may be visualized as follows: below the Saibel criterion, the only possible kind of rupture of a solid is viscous, as without an initial crack a fracture would require geological epochs to set in.

Above the Saibel criterion "fracture nuclei," as the initial cracks are sometimes called, would be spontaneously generated in the solid, propagating as fractures at very steeply rising rates, while simultaneously viscous flow would take place at a constant rate. The phenomenon is complicated by a secondary flow sometimes called "elastic flow" (because it is reversible upon release of the stress) taking place at a decreasing rate, and because of this decreasing rate giving rise to the phenomenon usually referred to as "stress-hardening."*

This phase of the rupture process is sometimes called "creep." Eventually the fractures have sufficiently reduced the unbroken cross section of the specimen to cause a general increase of the rates of the various phenomena, bringing about the rupture by fracture.

I believe the author should be congratulated not only for having been able to provide such a neat explanation of the genesis of the fracture nuclei, but also for having succeeded in showing that his criterion changes with the amount of flow.

D. J. McAdam, Jr.†—In previous papers the author gave the impression that he was proposing as a criterion for fracture the total energy applied during plastic deformation to fracture. In the present paper, however, the author admits that plastic extension itself increases the resistance of a metal to fracture. This means that the total energy required for fracture is increased by applying mechanical energy. As shown in a recent AIME paper by D. J. McAdam, Jr., G. W. Geil and R. W. Mebs the energy applied to the same metal before fracture may be varied more than a hundred fold, and that this causes a corresponding variation in the fracture stress. It seems to me that the author's acceptance of this evidence constitutes an abandonment of the ideas expressed in two previous papers.

E. V. Crane‡—To the mass-production industries which depend so largely upon the plastic flow properties of metals in the wide range beyond the elastic limit, a simplification of the approximations which Mr. Saibel derives seems likely to prove of real value. At the constantly increasing speeds of commercial metal working, heat generation assumes proportions which frequently affect work hardening rates and limits to a marked degree. Thus in "cold" or unheated operations in which cumulative elongation may rise to 1000 or even 5000 pct, the resultant structure without intermediate annealing may be substantially that of an annealed metal. Examples

---

* Colloid Chemistry, op. cit.

† National Bureau of Standards, Washington, D. C.

‡ Sam Tour and Co., Inc., New York, N. Y.

of this may be cited in rolling, extruding and drawing of brass, copper, aluminum and steel.

From the rankly utilitarian engineering viewpoint, may we propose, to cover this situation, a chart such as that in Fig 5. In

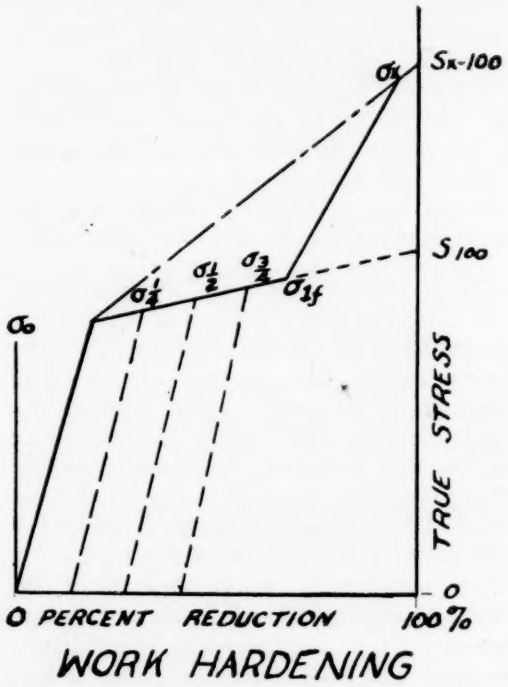

FIG 5—DIAGRAM SHOWING WORK HARDENING CHARACTERISTICS.

this chart the point which Mr. Saibel designates as σ_0 would, in engineering terms, be the theoretical yield point in the commercially annealed state. His point σ_{1f} again represents the normal point of rupture in tests run at sufficiently low speeds to dissipate heat. The intermediate points, $\sigma_{1/4}$, $\sigma_{1/2}$, $\sigma_{3/4}$ represent true stress yield points of quarter hard, half hard and three quarter hard work tempers.

By extrapolating the straight portion of the true stress curve to its interception with the 100 pct reduction line, all of the curves for different degrees of working and different grain sizes in annealing, appear to fall into a common pattern, within engineering limits, and to terminate at a common σ_{1f} point. The extrapolated point of intersection, S_{100}, which we have called the modulus of Strain Hardening in a prior engineering work* becomes a useful value for the comparison of the plastic range properties of the metals used by the mass production industries.

The point of normal rupture, σ_{1f}, appears to be the upper limit for the normal plastic range. It has also been described, by Templin, if we recall correctly, as the point at which favorably oriented slip planes have been exhausted.

Above it there appears to be a further plastic range which admits of reductions going into the nineties and elongations pyramiding as noted, into thousands of percent. It may be utilizing the less favorably oriented slip planes, but in any case the greater mobility would seem to be of thermodynamic origin.

Work hardening effects are ordinarily retained unless the useful conception of $u - u_0$ becomes so high that stress relief occurs, as it does in the drawing of some brasses. In such low carbon steels as that in Table 3, for which Mr. Saibel shows σ_{1f} = 126,000, the limiting tensile values, denoted by σ_x in Fig 5, with favorable (thermodynamic?) conditions, may reach twice that value as in low carbon music wire.

Perhaps confusion has crept into Fig 5, in endeavoring to combine the dissipated heat condition σ_0 to σ_{1f} with the optimum thermodynamic working condition represented by σ_x. Perhaps we should show a series of lines representing increasing rates of work hardening with reductions of thermal losses, up to some optimum condition represented by a line thru σ_0, σ_x to a modulus S_x 100.

I wish to ask also if there has been found a latent heat point at the stress relief point like those at fusion and vaporization.

E. SAIBEL (author's reply)—The author has shown that the relation between fracture strength and prior tensile strain is a natural and logical consequence of the energy criterion of fracture which he developed in a previous paper. So, rather than constituting an "abandonment of the ideas expressed in two previous papers" as thought by Dr. McAdam, Jr., this paper corroborates and strengthens the preceding ones.

The interesting discussion of Dr. Poncelet is more closely related to a previous paper of the author,* in which use was made of the

* E. V. Crane: Plastic Working of Metals and Non-Metallic Materials, John Wiley & Sons.

* A Thermodynamic Theory of the Fracture of Metals. *Trans.* AIME **171**, 639, *Met. Tech.* Feb. 1947—T.P. 2131.

Ludwik concept of stress, as well as of a generalization of the Ludwik flow curve. This concept of stress goes back to 1909. The generalization of the flow curve has been done from different points of view by various persons. Whether it be thought of as a plot of octahedral shear strain versus octahedral shear stress, or as a plot of a stress invariant versus a strain invariant makes no difference for this purpose. The point is that there have been no subsequent improvements in either of these concepts. However, as may be seen from the present paper, the ideas of the author on fracture are very much opposed to those of Ludwik, who thought in terms of the flow curve and of the fracture curve, the latter being purely hypothetical in character, since only by indirect means is it possible to obtain any points on it other than the final one. The sequence of operations for finding these points, namely: a prior strain followed by a lowering of the temperature and then pulling to fracture with little additional plastic strain, is analyzed in the present paper and shown to yield the type of relationship found experimentally. The distinction between fracture and rupture made by Dr. Poncelet is not clear to the writer. In one place it seems that he is using rupture as synonymous with plastic flow, stating that the rate at which this phenomenon takes place is controlled exclusively by the "shape changing" stresses, (evidently the stress deviator), the nature of the solid, and the temperature. However, a paragraph later he states that this has no criterion. There are criteria for this sort of flow, such as maximum shear stress or maximum distortion energy theories. However, what the present author has in mind is the complete separation of surfaces without the re-forming of bonds. The criterion proposed is valid not only for the initiation of the fracture cracks, but also for their propagation. This is possible since the criterion involves the state of stress. Once a crack is formed, the state of stress in the immediate neighborhood changes. This new state of stress must be used in the criterion which then shows whether or not the crack will be propagated.

The comments of Mr. Crane are interesting, and he raises points which require further study. The author would like to point out that the form of the curves and the relationships expressed depend upon the sort of coordinates chosen. For example, instead of plotting, as does Mr. Crane, percentage reduction of area as abscissa, natural strain might well be used, in which case different relationships pertain.

Anomalous Changes in Tensile Properties of Quenched Iron-cobalt (35 Pct Co) Alloys

By James K. Stanley,* Member AIME

(New York Meeting, March 1947)

Iron-cobalt alloys in the range of 35-50 pct cobalt are of interest in the electrical industry because they possess the highest magnetic saturation of any magnetic material known.[1,2] The magnetic saturation induction of the 35 pct alloy is 24,200 gausses, compared to 21,600 for pure iron (Fig 1). This difference is significant in electrical apparatus, where weight or space is at a premium. Saturation values higher than that for iron can be attained up to about 70 pct Co but economics restrict the use to as low a cobalt content as possible without sacrifice of saturation. Fig 2 shows the iron-cobalt equilibrium diagram.

Up to the present time, two factors have retarded the use of iron-cobalt alloys in the electrical industry for magnetic purposes.† One is the high cost of cobalt ($1.50 per pound) and the other is the inherent brittleness of the binary iron-cobalt alloys.

Straight iron-cobalt alloys up to 25 pct cobalt are ductile and easy to process to thin sheet or strip by conventional methods of hot and cold rolling, but the alloys containing higher percentages of cobalt, including those for which the saturation magnetization is a maximum (35 to 40 pct), are increasingly brittle with increasing cobalt, at least up to 50 pct, and are consequently difficult to process, either hot or cold.

Work by White and Wahl[3] indicated that iron-cobalt alloys could be made ductile by alloying with vanadium, and after quenching the alloys (vanadium up to about 4 pct) were found to be cold rollable to very thin gauges.

With this as a background, we resumed our work on these alloys with the objective of developing methods for economical commercial production of wide strip. For this purpose we have concentrated on the 35 pct alloy in order to obtain the highest possible saturation value.

Experiments were carried out on many alloy additions to the iron-cobalt alloys and on the response of these compositions to heat treatments. This work finally culminated in a commercially producible iron-cobalt alloy which has been named Hiperco.*

Materials Studied and Procedure

Binary alloys of iron and cobalt in the range of 35 pct cobalt are difficult to hot work (by forging or rolling) without such additions as C, Mn, Si, V, Cr, Mo, W or perhaps others. Another beneficial effect of such additions is that they increase to a greater or less extent the strangely low electrical resistivity of these alloys (about 10 microohms per cm³

Manuscript received at the office of the Institute Feb. 10, 1947; revised March 21, 1947. Issued as T.P. 2221 in Metals Technology, August 1947.

* Research Metallurgist, Westinghouse Electric Corporation, East Pittsburgh, Pennsylvania.

[1] References are at the end of the paper.

† The iron-cobalt alloys referred to here are of the "soft" magnetic type with low coercive force; they are free of carbon and consequently non-hardenable. There is the other type of cobalt alloy, properly called cobalt steel, which contains considerable carbon and is hardenable; such materials are "hard" or permanent magnet materials.

* "Hiperco" is an alloy containing about ⅓ cobalt and ⅔ iron with addition elements to increase the electrical resistivity and make the alloy workable. The trademark "Hiperco" has been registered with the U. S. patent office.

for 35 pct cobalt iron) thus decreasing the eddy current losses for alternating current applications.

Fourteen compositions were studied.* See Table 1.† These materials were prepared by high frequency heating in air from electrolytic iron, commercial cobalt 2 in. by 2 in. by 10 in. ingots (about 10 lb). The ingots were forged at 1000–1100°C to ½ in. by 1½ in. and were then hot rolled (900–1000°C) in several passes and reheatings to 0.050 in. at which gauge the strip was black. Blanks for tensile specimens were cut to 9-in. lengths with cutoff

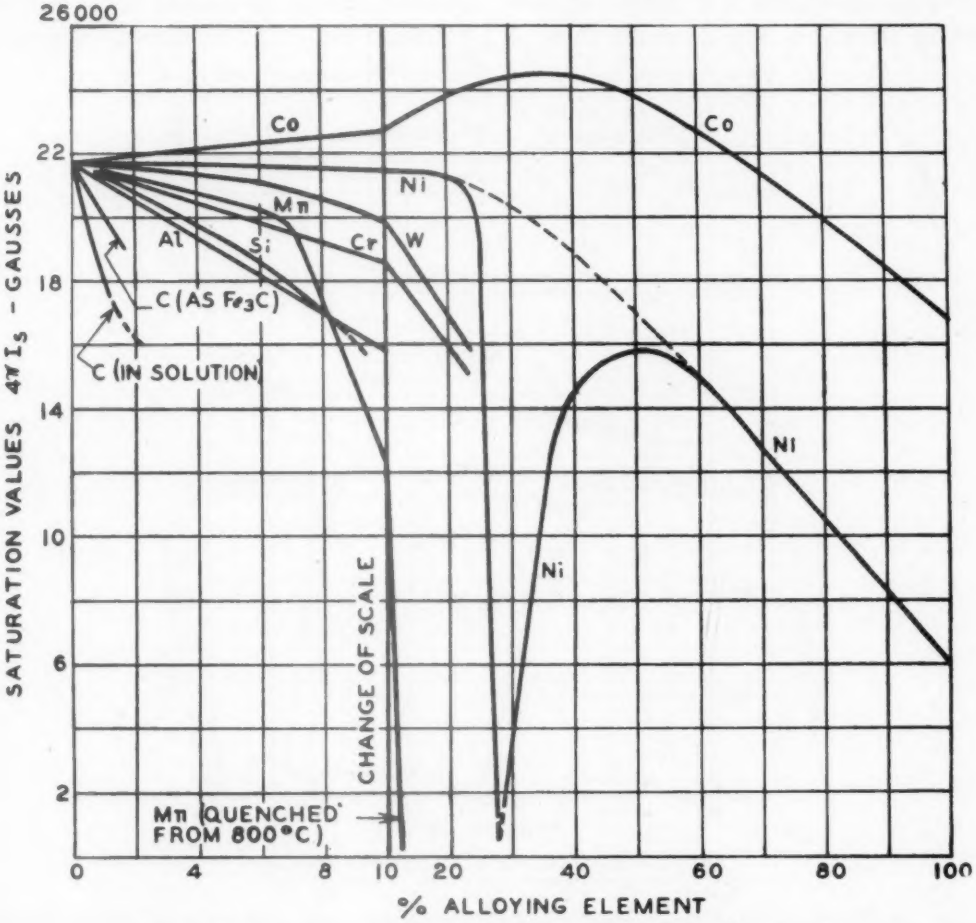

FIG 1—EFFECT OF ELEMENTS ON THE SATURATION VALUES OF IRON.

rondels, and commercial ferroalloys. The metal was deoxidized with calcium silicon and was cast in ceramic molds to make wheels rather than by shearing as the hot rolled material is generally glass-brittle. Standard A.S.T.M. flat tensile specimens[4] were machined without difficulty.

Hardness tests were made on the hot rolled material using the Vickers pyramid hardness tester in order to obtain representative values for the hot rolled material. The oxide surface was ground off and three impressions were made and averaged.

* All the alloys contain about 35 pct cobalt with vanadium or chromium additions and some minor additions such as Mo, Ti, Si or C. Nickel occurs in all the alloys to about 0.1 pct and manganese to about 0.03 pct.

† The chromium contents in the alloys are approximately 0.5 pct while the vanadium contents approximate 1 pct. In order to get the resistivities of the materials equal at about 20 microohms per cm³, primarily for magnetic ac measurements (not reported here), more vanadium than chromium had to be added.

The tensile specimens were sorted into sets of two or three, depending upon the amount of material available. The sets of various materials were grouped, heated to certain temperatures and quenched. For quenching the tensile strips were placed in an expanded-metal basket and were suspended in a vertical electric furnace having a 2½ in.-diam tube. A heavy (0.065 in.) chromel-alumel thermocouple was placed in the center of the basket to get accurate temperature measurements of the samples. Dry nitrogen was continuously passed through the furnace to minimize oxidation. When the charge was at temperature, the basket was released, allowed to fall into a tank containing ice and water (0°C), and was agitated to obtain rapid cooling. The tensile specimens were quenched from temperatures ranging from 300° to 1000°C.

After quenching the shoulders of the samples were lightly ground on a carborundum wheel and hardness determinations were made. After the hardness tests, the specimens were broken in a tensile machine. The tensile strength and elongation were determined on all materials and in some cases yield point determinations were made at 0.2 pct permanent set. To eliminate difficulties resulting from the use of punch marks to measure elongation scratch marks were used on the alloys; this reduced localized stress concentrations. The iron-cobalt alloys have smooth stress-strain curves similar to nonferrous metals.

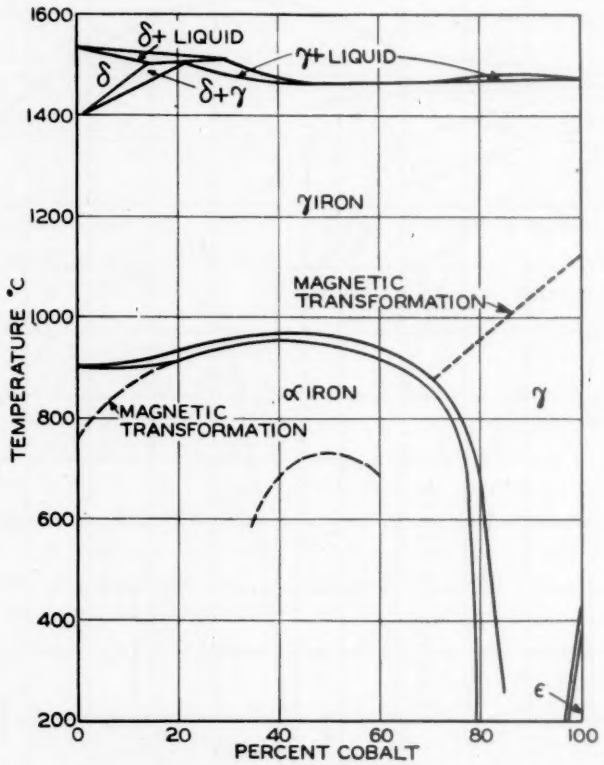

FIG 2—EQUILIBRIUM DIAGRAM FOR FE-CO.

RESULTS

The hardness and tensile data for the 14 alloys investigated are given in Table 1.

An examination of the data seems to warrant the following statements:

1. There is generally a decrease in strength on quenching from increasing temperatures.

2. There is a marked increase in elongation on quenching from above 600°C reaching a maximum around 850 to 900°C and then decreasing with increasing quenching temperatures up to 1,000°C. The maximum average elongation is slightly over 16 pct.

3. There appears to be a slight increase in hardness for quenching temperatures to about 600°C, and then there is a marked decrease for temperatures up to about 800°C, beyond which the hardness remains practically the same.

The change in hardness, tensile strength, and elongation for 14 alloys is shown in Fig 3.

Some of the highest elongation values (over 20 pct) were obtained with both the Fe-Co-Cr (Fig 4) and Fe-Co-V alloys (Fig 5). The behavior of both alloys is practically identical in regard to hardness and elongation.

A further examination of Fig 3 shows that good elongation is obtainable over a fairly wide range of quenching temperatures; i.e., over 10 pct elongation for quenching temperatures between 700 and 1,000°C irrespective of the alloys studied here.

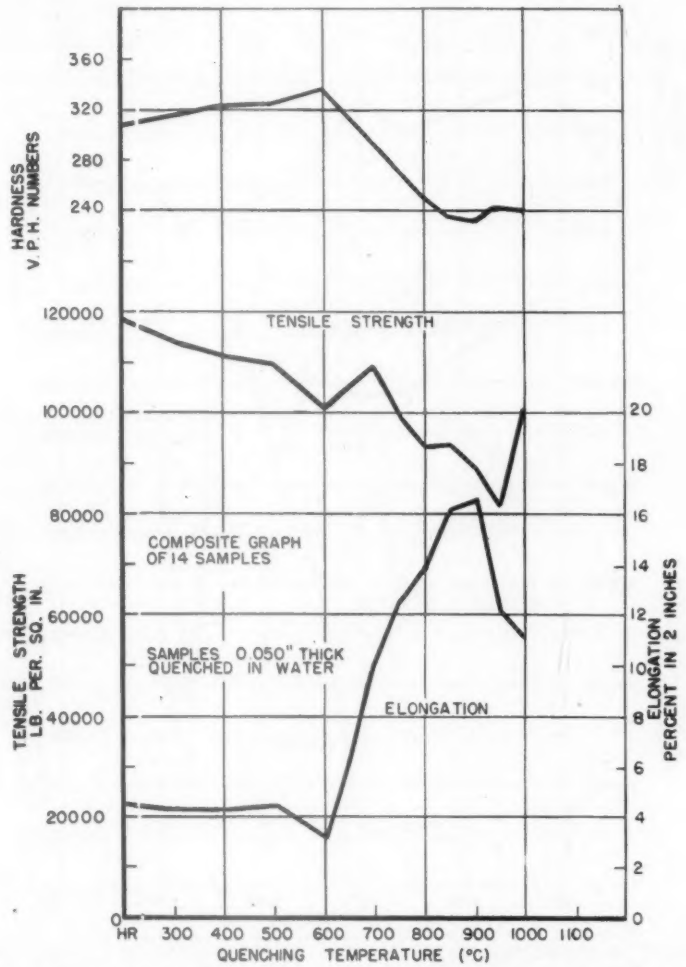

FIG 3—EFFECT OF QUENCHING TEMPERATURE ON 14 IRON-COBALT ALLOYS.

4. The yield strength for 0.2 pct permanent set for some of the alloys is shown in Fig 6. The yield strength shows a rapid decrease for temperatures above 650°C reaching an average figure of 58,000 lb per sq in. for temperatures between 800 and 950°C.

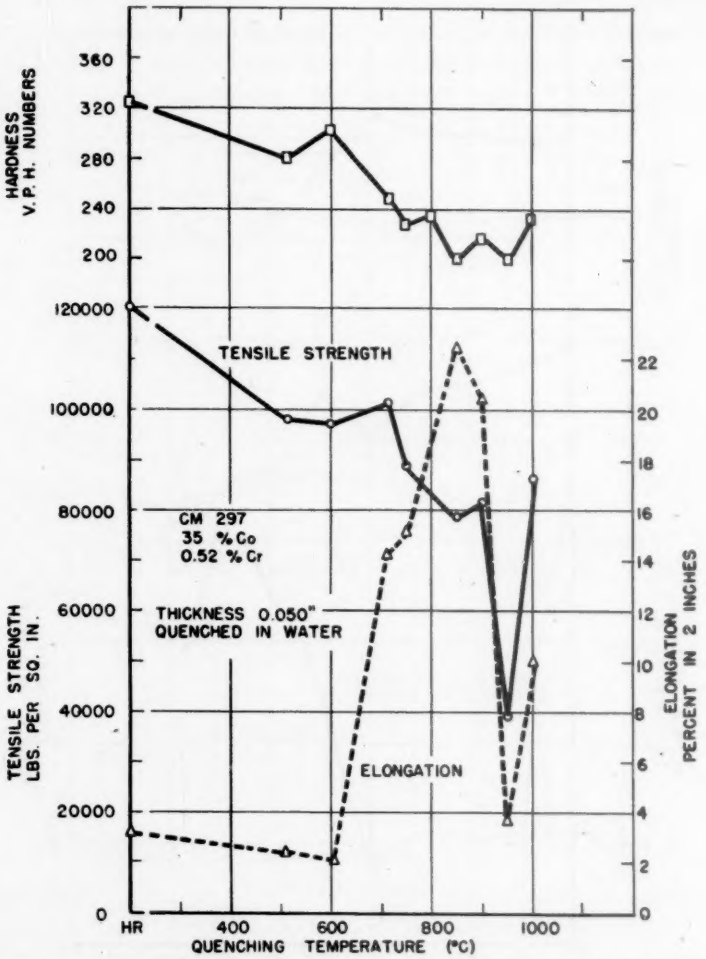

FIG 4—EFFECT OF QUENCHING TEMPERATURE ON PROPERTIES OF CM 297 (FE-CO-CR).

DISCUSSION

In an attempt to learn something concerning the anomalous behavior of these iron-cobalt alloys the following tests, in addition to chemical analysis, were performed: (1) metallographic examination, (2) lattice constant determination, (3) aging.

Metallographic Examination

Examination of several alloys under the microscope gave no clues as to why the ductility is improved by quenching. The microstructure of the hot rolled material shows the grains to be severely broken up and elongated. The material starts to recrystallize at about 750°C. Those samples quenched from 1000°C show evidences of grain refinement resulting from quenching through the α-γ transformation which occurs around 950°C in these alloys; see Fig 2. When recrystallized, the grain size varied from A.S.T.M. 5.5 to 8.5.

Lattice Constant Measurements

All the 35 pct cobalt alloys belong to body centered cubic system. No change in crystal structure was observed.

Four of the samples studied were examined for variation in lattice parameter before and after quenching, to see if differences could be noted, using an 8-in. Wyland focusing camera. One of the alloys was examined in the hot rolled, annealed (10 hr 900°C), and quenched (900°C) conditions; while others were analysed after quenching from 600,770, 850 and 900°C. The determinations showed no variations in lattice constants larger than the usual experimental errors. Parameters were calculated on the K lines of the (110), (200), (211) and (220) planes of each sample and no variations could be detected. The average lattice parameters were found to be 2.857Å. Differences, however, in line intensities were observed, but these observations did not correlate with variations in ductility.

Aging

Aging tests were made both before and after quenching using test specimens

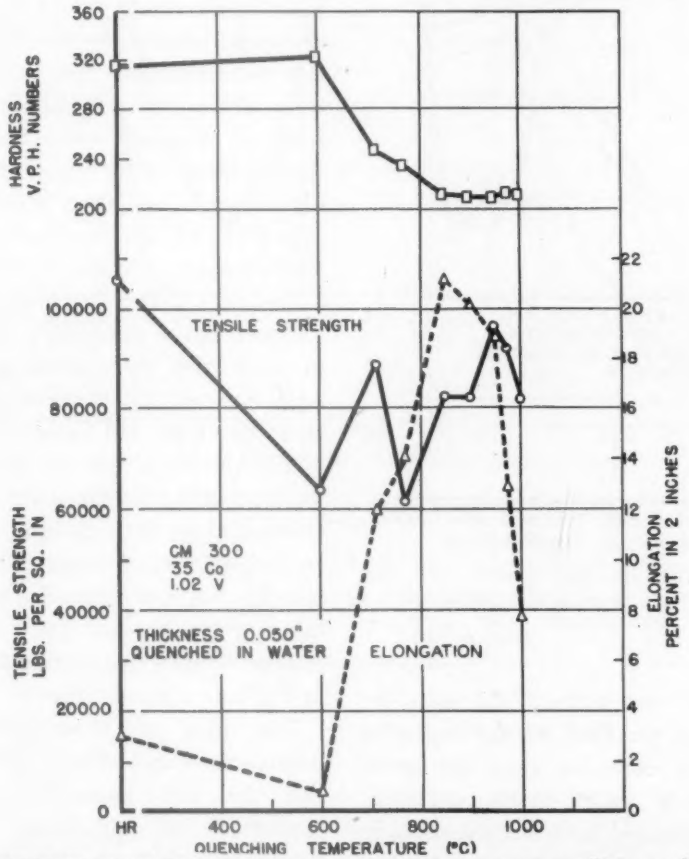

FIG 5—EFFECT OF QUENCHING TEMPERATURE ON PROPERTIES OF CM 300 (Fe-Co-V).

0.05 in. by ½ in. by 3 in. Hardness variations were used to follow the aging.

The pieces were first aged at room temperature for 12 days. No changes were detected. The same strips were then aged at 300°C for 25, 100 and 144 hr with no detectable changes in hardness. The same strips were finally aged at 500°, and now definite changes in hardness were found after 25 hr and further changes

were found after 50 hr, as shown in Fig 7, for both the hot rolled and the quenched samples.

The aged samples were also examined under the microscope. No evidence of

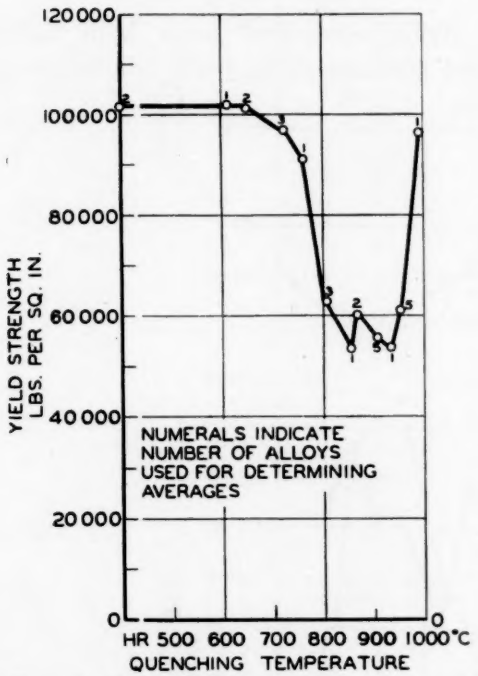

FIG 6—EFFECT OF QUENCHING ON THE YIELD STRENGTH OF 35 PERCENT IRON-COBALT ALLOYS.

any precipitate was noted. The only observed variation was that the aged samples were easier to etch in, that the grain boundaries were more easily outlined, which may be caused by a submicroscopic impurity or impurities migrating to the grain boundaries and making the boundaries more susceptible to attack by the etchant.

Aging is generally ascribed to the decomposition of a supersaturated solution resulting in the formation of a precipitate. Carbon might be ordinarily suspected but the disconcerting thing is that two samples one with 0.048 pct C and the other with 0.002 pct show about the same amount of aging (Fig 8). Based on the above results, carbon is therefore eliminated as the cause of aging in this case.

To explain the fact that the quenched alloys show a decided age-hardening characteristic when heated to 500°C, it may be assumed that there is some constituent precipitating from solution at this temperature. The fact that the aging takes place in alloys containing 0.002 pct C shows that carbon probably is not responsible for the aging. The hot rolled material also ages although this may mean that the conditions of hot rolling were such as to retain the hardening factor. Elements such as nitrogen (less than 0.003 pct) and sulphur (less than 0.02 pct) and phosphorus (less than 0.003 pct) do not appear to be the cause of aging. Oxygen varies from 0.01 to 0.03 pct but it is removed from solution as SiO_2 by deoxidation.

There is the possibility that the change in properties on quenching results from order-disorder phenomena. A super-lattice at 40 to 65 pct cobalt has been reported,[5] and at the Westinghouse Research Laboratories, Mr. R. K. McGeary has shown, by thermal analysis using equipment described by Smith,[6] that some internal change, possibly an order-disorder transformation, takes place around 590° in 35 pct Co alloys. This transformation is shown in Fig 2 as a broken line.

The idea of super-lattice formation is attractive and offers a possible explanation for the variation in mechanical properties on quenching. It may be postulated that a disordered state is preserved by quenching from 600°C and above, varying in degree of disorder with the quenching temperature and that slow cooling of the alloy from above 600° results in ordering which is responsible for the brittle nature of the alloy.

Response of a Quenched Alloy to Cold Rolling

After the iron-cobalt alloys are quenched from an optimum temperature, the ductility is sufficient for the alloy to be cold

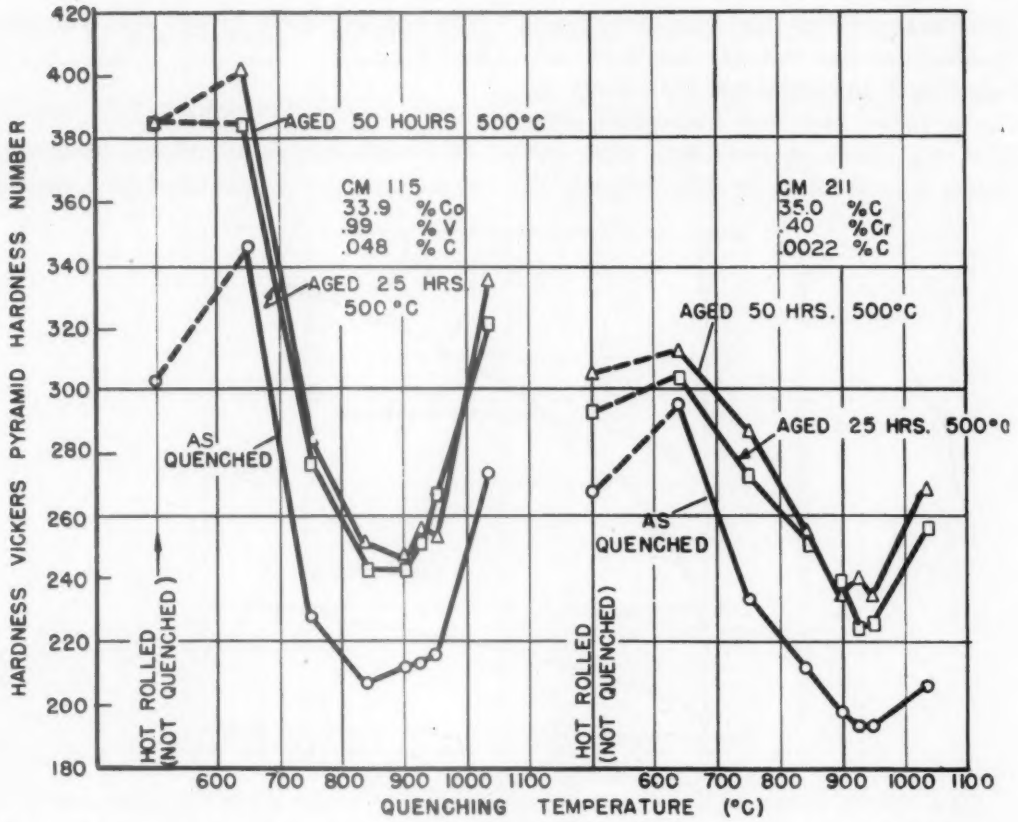

FIG 7—EFFECT OF QUENCHING TEMPERATURE AND AGING TIME ON THE HARDNESS OF CM 115 AND 211.

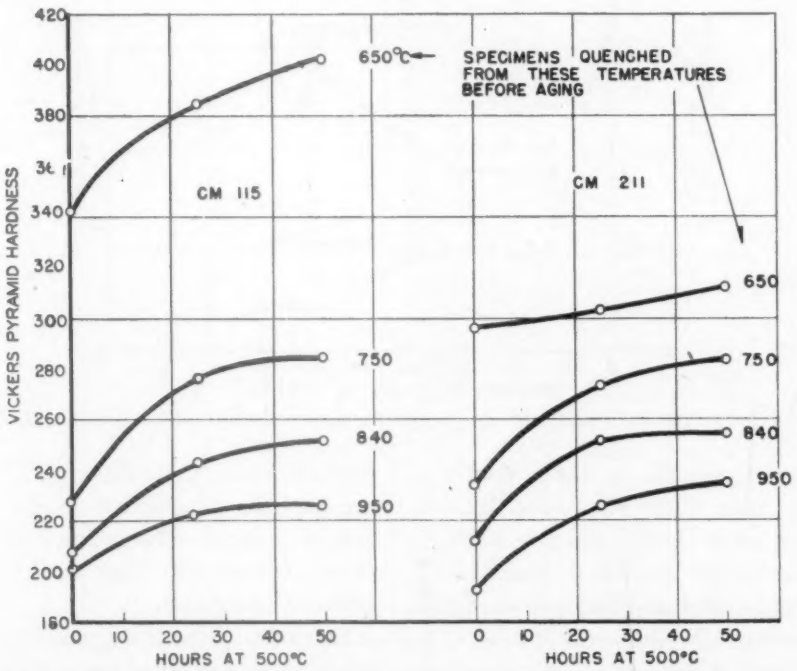

FIG 8—EFFECT OF TIME ON THE HARDNESS OF QUENCHED CM 115 AND 211.

rolled to any desired thickness; for instance, in one case the material has been cold rolled to a thickness less than 0.001 in. Fig 9 shows how the iron-cobalt alloy (CM-279), 18-8 type stainless steel and Armco iron compare in their response to cold rolling. It should be noted that the iron-cobalt alloy does not work harden appreciably after about 35 pct reduction. Fig 10 shows the expected increase in tensile strength and decrease in elongation on cold rolling the iron-cobalt alloy. A tensile strength of 170,000 psi was obtained with approximately 72 pct cold reduction by rolling.

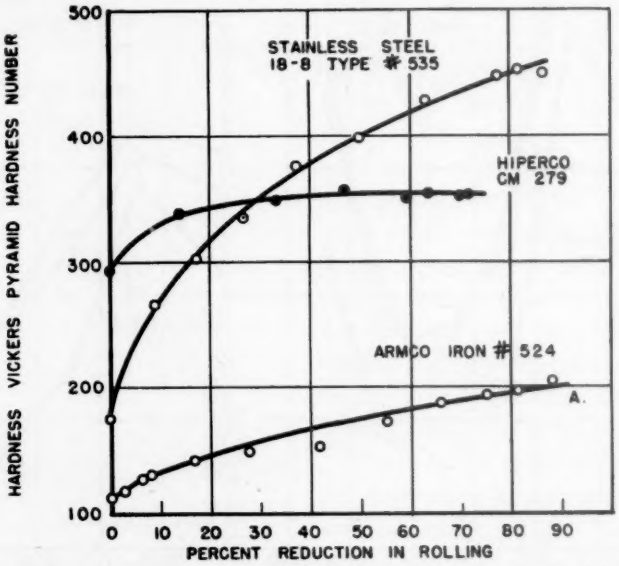

FIG 9—WORK HARDENING OF HIPERCO IN RELATION TO STAINLESS STEEL AND ARMCO IRON.

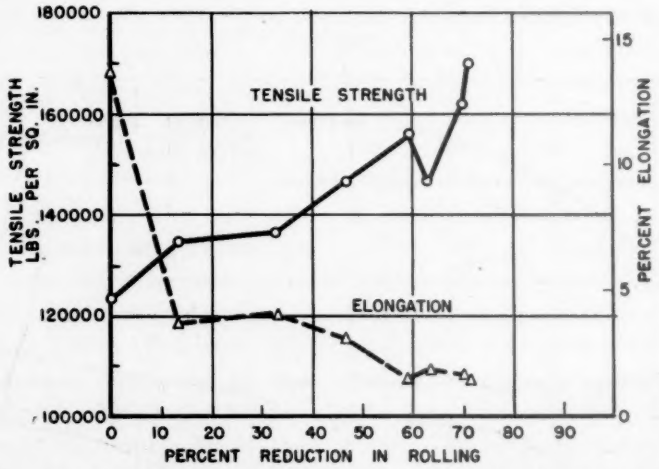

FIG 10—EFFECT OF COLD ROLLING ON STRENGTH AND ELONGATION OF QUENCHED CM 279.

SUMMARY

Fourteen iron-cobalt alloys, containing 35 pct cobalt, were quenched from various temperatures in water at 0°C and their mechanical properties (yield strength, tensile strength, elongation and hardness) were determined. The results are summarized as follows:

Hardness tests show a softening of the alloys when quenched from above 600°C.

TABLE I—*Analysis and Mechanical Properties of the Iron-cobalt Alloys*

Number	Pct Co	Pct V	Pct Cr	Others	Treatment	Yield Point, per Psi	Tensile Strength, Psi	Elongation Pct in 2 In.	Hardness VPN
1 CM115	33.9	0.99		0.048 C	HR	114500	117400	5.8	305
					Q640	114500	122250	5.4	345
					Q750	90400	101600	9.3	255
					Q840	54300	86800	16.7	220
					Q900	53800	85300	17.1	221
					Q925	53000	83900	19.6	222
					Q940	61600	86000	6.2	222
					Q1000	97800	117750	10.6	255
2 CM253	35.0		0.70	0.12 Mo	HR		131000	7.1	283
					Q718	90000	115000	13.0	
					Q734				264
					Q806	57600	84900	13.3	208
					Q850	62700	96200	13.6	
					Q904	47600	82200	13.3	228
					Q955	59200	89100	9.5	293
3 CM254	35.0		0.45	0.36 Mo	HR		135400	3.1	305
					Q602		97500	1.9	359
					Q714		119650	9.8	305
					Q800		108800	12.1	287
					Q900		93200	17.8	227
					Q950		92000	12.7	217
					Q1000		106000	10.6	240
4 CM256	35.0		0.78	0.28 Mo	HR		112300	1.5	316
					Q510		124900	3.9	330
					Q618	114500	116000	4.5	340
					Q718	94900	113600	9.6	287
					Q770		103400	11.5	267
					Q806	64350	94600	11.7	224
					Q850		94650	16.1	248
					Q904	61200	89800	14.0	256
					Q925		122750	13.7	231
					Q955	59150	90350	12.9	300
					Q975		96800	8.3	246
					Q1000		107800	17.6	248
5 CM259	35.0		0.52	0.06 Mo	HR		101000	0.3	310
					Q618		68500	0.2	347
					Q718	105750	118250	6.7	296
					Q806	63700	96250	15.2	229
					Q904	60400	91900	11.5	285
					Q955	63500	94250	13.5	297
6 CM279	35.0		0.54		HR	88500	126500	12.0	294
					Q650	91250	112000	6.9	289
					Q734	73400	102250	13.9	268
					Q806	64250	89450	13.8	248
					Q850	57850	90650	15.9	
					Q904	57550	87700	17.7	212
					Q955	60900	90800	14.2	291
7 CM296	35.0		0.51	.05 Ti	HR				
					Q510		127500	7.7	339
					Q600		117900	5.8	357
					Q714		122300	12.3	300
					Q750		112700	12.4	288
					Q800		114700	12.2	287
					Q900		93800	15.4	233
					Q950		47900	16.4	215
8 CM297	35.0		0.52	.04 Si	HR		120450	3.2	325
					Q510		98100	3.3	280
					Q602		97700	3.1	304
					Q714		101700	14.1	269
					Q750		88500	15.1	246
					Q800				257
					Q850		78550	22.5	197
					Q900		81700	20.9	209
					Q950		39000	3.8	198
					Q1000		86450	10.0	226
9 CM298	35.1		0.51	.16 C	HR		122900	4.3	308
					Q400				331
					Q510		139720	10.2	322
					Q602		109670	2.9	348
					Q714		121500	11.8	310
					Q750		120500	12.2	304
					Q800		106700	12.2	294
					Q900		101100	13.6	237
					Q950		67300	10.6	225
					Q1000		112250	12.1	257

TABLE I—(*Continued*)

Number	Pct Co	Pct V	Pct Cr	Others	Treatment	Tensile Strength, Psi	Elongation Pct in 2 In.	Hardness VPN
10 CM299	35.3		0.51	.10 C	HR	124500	5.3	313
					Q510	128000	6.2	320
					Q602	118900	4.2	330
					Q714	112200	10.3	292
					Q750	110300	13.1	287
					Q800	109700	12.5	282
					Q850	84600	16.6	206
					Q900	96090	16.9	238
					Q950	59400	7.9	216
					Q1000	107000	13.2	256
11 CM300	35.3	1.02			HR	105300	3.0	315
					Q602	64400	0.7	321
					Q714	88900	12.0	245
					Q770	60400	14.2	238
					Q850	82500	21.1	211
					Q900	82300	20.1	208
					Q950	96850	18.9	209
					Q975	92000	12.9	213
					Q1000	82400	7.8	215
12 CM301	35.0	0.97		.06 Si	HR			
					Q600	93800	1.8	351
					Q714	97150	10.2	262
					Q770	65960	12.9	265
					Q850	88570	19.6	224
					Q900	90600	19.0	211
13 CM302	35.1	1.04		.12 C	HR	124950	5.7	337
					Q602	98000	0.8	367
					Q714	114750	12.5	309
					Q770	80400	12.1	300
					Q850	102300	12.8	254
					Q900	47610	13.1	246
					Q975	107000	7.7	252
14 CM303	35.1	1.02		.05 Ti	HR	103500	2.5	308
					Q602	87190	1.8	342
					Q714	100500	10.2	275
					Q770	63000	14.8	238
					Q850	86170	19.2	221
					Q900	84080	20.4	220
					Q950	100500	15.4	215

Tensile strength and yield strength decrease on quenching with increasing temperature up to the transformation range above which they increase.

Elongation shows a marked increase on quenching from above 600°C which reaches a maximum elongation of over 16 pct for quenching from between 850 to 900°C, followed by a decrease with increasing quenching temperature.

Metallographic examination discloses that the grain size is refined by quenching from above the critical temperature. No precipitates were noted in the samples after quenching and aging. It was noted that the aged samples have more sharply defined grain boundaries than before aging.

Lattice constant measurements were carried out with an 8-in. focussing camera but no significant differences were found between the annealed and quenched samples.

The quenched iron-cobalt alloys are readily cold rolled. The alloy does not work-harden rapidly, after about 35 pct cold reduction the hardness remains virtually constant.

REFERENCES

1. P. Weiss, *Compt. rend.* (1913) **156**, 1970.
2. T. D. Yensen, Gen. Elect. Rev. (1915) **18**, 881.
3. U. S. Patent 1,862,559 (1932). J. H. White and C. V. Wahl.
4. A. S. T. M. Standards (1942) I, 898. E-8-42 Standard Methods of Tensions Testing of Metallic Materials.
5. W. C. Ellis and E. G. Greiner: Amer. Soc. Metals (1941) **29**, 415.
6. C. S. Smith, *Trans.* AIME (1940) **37**, 236.

DISCUSSION

(H. S. Avery presiding)

H. S. AVERY—Just what percentage of improvement in generator performance was obtained by substituting this material?

J. K. STANLEY (author's reply)—I am really not at liberty to say, but it was over 10 pct.

H. S. AVERY—Roughly equivalent to the difference in saturation?

J. K. STANLEY—Roughly, yes.

J. H. BACH*—I should like to ask the author whether he made any tests at all on the change of magnetic properties. I have been working on 18 pct cobalt and a 36 pct cobalt steel, which is generally on the market now, and we have had some very peculiar results caused by cold rolling and other treatments; many of them showed change of the magnetic properties.

I have not been able to draw any general conclusions as to how that material will behave. It seems that by heat treatment, which will yet have to be determined, you can raise and lower certain magnetic properties to a marked degree.

We have been working on that steadily for the last eight or nine months, more or less at intervals, and I just cannot get anywhere. I can raise the H_c or lower the H_c, and the B_r values will vary considerably. I wonder whether you have made any tests that will show it.

J. K. STANLEY (author's reply)—Are you referring to cobalt steels of the martensitic type, or are you referring to soft magnetic material?

J. H. BACH—I have tried it on both. I have tried the 36 pct.

J. K. STANLEY—Is that essentially carbon-free?

J. H. BACH—Very little carbon.

J. K. STANLEY—Well, it is true that there are magnetic property changes in both hard and soft cobalt-containing materials that are difficult to explain. Generally, however, we found that at least in the carbon-free material the H_c can be controlled by controlling the carbon content.

J. H. BACH—We do not make the steel; we merely buy a cobalt steel on the market and it is very difficult to vary the carbon content, once you buy the steel.

J. K. STANLEY—What do you use—quenching and then aging—for heat treatment?

J. H. BACH—Yes, quenching and aging. And lately I have been running a series of tests on giving the oil-quench first, the way many factories usually recommend it, and then just heating it and trying to get rid of as much austenite, or produce as much gamma iron as is considered necessary to get the right H_r.

J. K. STANLEY—Our experience has been limited on these cobalt steels. We do know, however, that the temperature from which these are quenched is critical. It is very important in one type with which I am familiar to quench the steel from exactly 950°C in oil. Variations could be caused by probable changes in carbon content, or by something going wrong with the heat treatment.

J. H. BACH—I have not finished the investigations by any means.

J. K. STANLEY—It is a complicated system and I am not too familiar with the steels, because we work with soft cobalt-containing materials which are essentially carbon-free.

B. L. JOHNSON*—I noticed that the author compared this material with Hipersil and similar types of alloys. I would like to ask whether they have developed any preferred orientation in the high cobalt materials.

J. K. STANLEY—We have looked into that. There is a very slight tendency to get preferred orientation. In the 42 pct cobalt alloy, the anisotropy is zero, and there is no preferred orientation. By cold rolling or annealing, one may obtain approximately the 35 pct range.

---

* Sperry Gyroscope Co., Great Neck, Long Island, N. Y.

* Mack Manufacturing Co., Plainfield, New Jersey.

Stress Rupture of Heat-resisting Alloys as a Rate Process

By E. S. Machlin* and A. S. Nowick*

(New York Meeting, March 1947)

One of the main criteria used to rate the heat-resisting properties of alloys is stress rupture.[1] During a stress-rupture test a tensile specimen is held under a constant load at a constant temperature until it fractures. The chief measurement made during this test is the time required for rupture at the specific test stress and temperature. It was found empirically from a series of stress-rupture tests at a constant temperature that when the logarithm of the time for rupture is plotted against the logarithm of stress a straight line is obtained within experimental error.[2,3] This method of showing stress-rupture data has been adopted by many investigators and the NACA.[4] By interpolation and extrapolation from these plots, values of the stresses required to rupture the specimens (the rupture strengths) in 10, 100, and 1000 hr are obtained for specific temperatures. Alloys are then rated for a particular application on the basis of their rupture strengths at the rupture life that most nearly represents the application.

Inasmuch as stress rupture is an important criterion in rating heat-resisting alloys, it would be advantageous to know the quantitative dependence of the time for rupture on stress, temperature, composition, and structure. In order to obtain this information, an investigation was made at the NACA Cleveland laboratory during the spring of 1945. The theory of rate processes was used because it has been found to apply to certain processes such as chemical reactions, viscous flow, and creep that occur at a definite rate for given conditions. It was thought that stress rupture was such a process. An equation was derived that gives, for a given composition and structure, the dependence of the time for rupture on stress and temperature. The investigation is part of a general program to provide information that will lead ultimately to the development of better alloys in order that the efficiency and power output of gas turbines used in aircraft propulsion can be increased.

Reprint of NACA Technical Note No. 1126. Manuscript received at the office of the Institute Sept. 12, 1946. Issued as T.P. 2137 in Metals Technology, February 1947.

* National Advisory Committee for Aeronautics, Aircraft Engine Research Laboratory, Cleveland Airport, Cleveland, Ohio.

[1] References are on page 398.

Theory

The theory of rate processes will first be discussed as a general theory. It will then be shown that if stress rupture of heat-resisting alloys can be treated as a rate process, certain equations must be satisfied. Later sections will then show that these equations are satisfied.

General Theory of Rate Processes

The theory of rate processes[5] developed by Eyring and others has been applied to chemical reactions as well as to other processes such as viscosity of liquids and diffusion. In every case in which rate-process theory can be applied, there is a small subdivision, so that the macroscopic process is the net effect of all the small processes. This smallest subdivision is called the "unit process." For example, in a chemical reaction the unit process is

the reaction between the atoms reacting in numbers given by the stoichiometric chemical equation. Rate-process theory can be applied to any process provided that the corresponding unit process involves a molecule or group of molecules that, in passing from the initial to the final state, must first attain a certain minimum thermal energy. This energy is often considerably greater than the ordinary thermal energy of molecules; therefore the molecule or group of molecules participating in the unit process is said to be "activated" or to have formed an "activated complex" when the minimum energy is attained. The unit process is best illustrated by the potential-energy curve for the reaction (Fig 1). The height of the barrier, which is the minimum energy required for passage into the final state, is called the heat of activation ΔH_a. This energy bears no relation to the heat of the reaction ΔH, the energy difference between the initial and final states also shown. By the "reaction coordinate" is meant the most favorable reaction path on the polydimensional potential-energy surface.

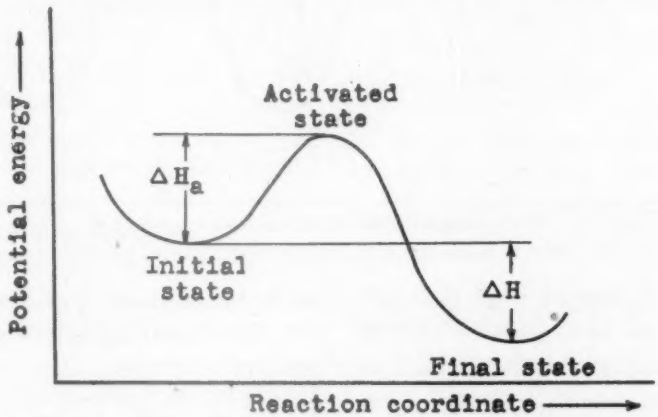

FIG 1—SCHEMATIC REPRESENTATION OF POTENTIAL BARRIER.

The basic assumption of rate-process theory is that the initial reactants and activated complexes are always in equilibrium. Statistical mechanical considerations then give[5] for the rate of the process (number of unit process taking place per unit time) the equation

$$r = (kT/h)\, exp\, [-\Delta F_a/kT] \qquad [1]$$

where

k = Boltzmann's constant, 1.38×10^{-16} ergs per molecule per deg K.
T = absolute temperature, deg K.
h = Planck's constant, 6.62×10^{-27} erg-seconds.
ΔF_a = free energy of activation per molecule.

The term kT/h can be regarded as the effective frequency at which activated complexes cross over the barrier. In the calculation of ΔF_a, the contribution due to the translational degree of freedom along the reaction coordinate has been disregarded because it is included in the factor kT/h. The factor ΔF_a is interpreted as an ordinary free-energy term and can be expressed as

$$\Delta F_a = \Delta H_a - T\Delta S_a \qquad [2]$$

where

ΔS_a = entropy of activation per molecule.

The entropy of activation has the usual physical significance. It is related to the relative probability of the initial and activated states excluding the energy difference, or what may be called the relative freedoms of the two states. A negative value of ΔS_a means therefore that the activated state involves greater

restrictions on the degrees of freedom of the molecules than the initial state, in addition to the energy difference between the two states.

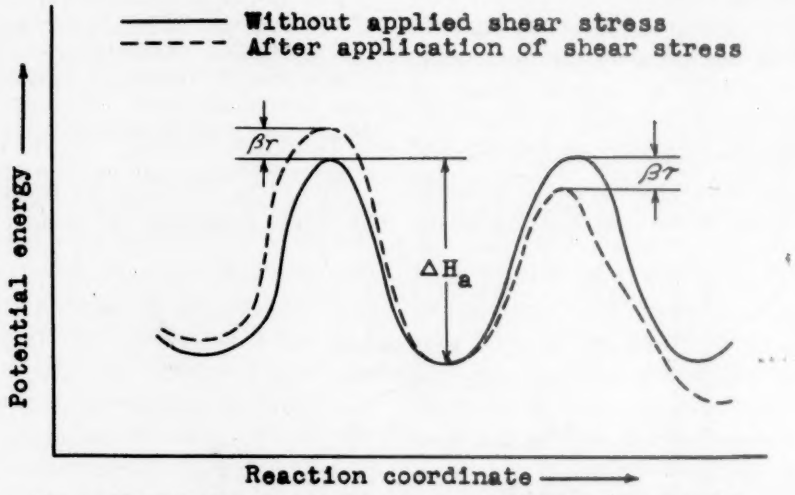

FIG 2—POTENTIAL BARRIER FOR STRESS-DEPENDENT RATE PROCESS.

A process will be termed a "rate process" if Eqs. 1 and 2 can be applied to it; that is, if the unit process can be treated as involving the passing of activated complexes over a potential-energy barrier.

Stress-dependent Rate Processes

In some rate processes the height of the potential-energy barrier is a function of the applied shear stress. The unit processes in these cases may generally take place in either of two opposite directions involving the same energy barrier, as shown by the solid curve of Fig 2, thus the net rate is zero. If the shear stress τ is applied, it may lower the barrier in one direction and raise it in the opposite direction, as shown by the dashed curve of Fig 2. The activation energies for the two directions are no longer equal and the process takes place with a definite net rate. The direction to the right in Fig 2 is designated as positive.

Examples of such a process are the flow of viscous liquids[5] where the unit process is the jump of one molecule past another and the creep of metals[6] where the generation of a dislocation is the unit process. In both these processes, the energy by which the barrier is lowered in the positive and raised in the negative direction was shown to be approximately proportional to the shear stress. The heat of activation for the stress-dependent process in the positive direction (the height of the barrier in the positive direction) is therefore $\Delta H_a - \beta\tau$ and in the negative direction is $\Delta H_a + \beta\tau$. The free energy of activation in the positive direction is $\Delta H_a - \beta\tau - T\Delta S_a$ and in the negative direction $\Delta H_a + \beta\tau - T\Delta S_a$. Inasmuch as $\Delta F_a = \Delta H_a - T\Delta S_a$ the rate of occurrence of unit processes in the positive direction is therefore

$$r^+ = (kT/h)\ exp\ [-(\Delta F_a - \beta\tau)/kT]$$

and in the negative direction

$$r^- = (kT/h)\ exp\ [-(\Delta F_a + \beta\tau)/kT]$$

The net rate in the positive direction is therefore

$$r' = r^+ - r^- = (2kT/h)\ exp\ [-\Delta F_a/kT]\ \sinh(\beta\tau/kT) \quad [3]$$

The factor β, in general is a function of temperature.

Application of Rate-process Theory to Stress Rupture

The supposition is made that stress rupture of heat-resisting alloys is a rate process in the sense of the definition presented in this report. When the unit process is considered in an abstract sense, it is possible to determine only the temperature and stress dependence of the rate r. A definite physical unit process such as the generation of a dislocation[6] would enable the prediction of the dependence of the rate r on the physical structure and properties of materials. This report, however, considers the unit process only in the abstract sense and therefore the contribution that will be expected is a knowledge of the temperature and stress dependence of the time for rupture for a constant composition and structure.

If stress rupture is a rate process, the time for rupture t_r is to be expected to be inversely proportional to a rate r_f or

$$t_r = c/r_f \qquad [4]$$

The unit process is expected to be stress dependent. If the effect of stress is similar to other stress-dependent rate processes—that is, if the amount by which the barrier is lowered or raised by shear stress is approximately proportional to the shear stress—r_f would be given by Eq. 3. If, as in the theory of creep,[6] the grains are taken to be oriented so that the unit process occurs under maximum shear stress, where $\tau = \sigma/2$, this equation becomes in logarithmic form

$$\log_e r_f = \log_e (2kT/h) - (\Delta F_a/kT) + \log_e \sinh(\beta\sigma/2kT) \qquad [5]$$

The factor β may include a stress concentration factor if the unit process takes place at stress raisers.

Inasmuch as $\sinh x = \frac{e^x - e^{-x}}{2}$, where x becomes large, e^{-x} rapidly approaches zero and $\sinh x$ then is given to a good approximation by $\frac{1}{2}e^x$. Thus for sufficiently high values of applied stress

$$\sinh(\beta\sigma/2kT) = \tfrac{1}{2}\, exp\,[\beta\sigma/2kT] \qquad [6]$$

If Eq. 6 is substituted in Eq. 5 and combined with Eq. 4, the equation for the time for rupture is

$$\log_e t_r = \log_e (h/kT) + (\Delta F_a'/kT) - (\beta\sigma/2kT) \qquad [7]$$

where

$$\Delta F_a' = \Delta F_a - CT = \Delta H_a - T(\Delta S_a + C) \qquad [8]$$
$$C \equiv -k \log_e c$$

The term $\Delta S_a + C$ is therefore the apparent entropy of activation.

For the purpose of checking the validity of Eq. 7, common logarithms are most convenient. Eq. 7 can be written

$$\log t_r = \log (h/kT) + (\Delta F_a'/2.3kT) - (\beta\sigma/4.6kT) \qquad [9]$$

A plot of $\log t_r$ against σ for a fixed temperature should then be a straight line of negative slope $\beta/4.6kT$ and intercept

$$\log t_i = \log (h/kT) + (\Delta F_a'/2.3kT) \qquad [10]$$

From Eq. 10, $\Delta F_a'$ can be obtained for each temperature. The heat of activation per molecule ΔH_a usually is either constant or expressible to a good approximation as a linear function of T according to

$$\Delta H_a = \Delta H_{a0} + \Delta H_a' T \qquad [11]$$

Thus a linear plot of $\Delta F_a'$ against T should be a straight line

$$\Delta F_a' = \Delta H_{a0} - T\Delta S_a' \qquad [12]$$

where $\Delta S_a'$ is given by

$$\Delta S_a' = \Delta S_a - \Delta H_a' + C \qquad [13]$$

If stress rupture is given by Eq. 9, practical use of this equation can be made by letting $\log (h/kT)$ equal a constant. The approximation that $\log T$ is constant relative to the term in T will involve no detectable error over a large range of temperature. This approximation was made for Eq. 14.

Sources and Precision of Data

Stress-rupture data were obtained from reference 4, from the Allegheny-Ludlum Steel Corporation, and from the University of Michigan for three different alloys: S816 cast, S816 forged, and low-carbon N155 hot-worked. These alloys were chosen because enough stress-rupture data were available for them in the literature at different temperatures and stresses.

An examination of the data, in general, revealed that a particular rupture life might vary by as much as 100 pct. Approximate experimental errors for the factors β, ΔH_{a0}, and $\Delta S_a'$ are ± 30 pct, $\pm 5 \times 10^{-13}$ ergs, and $\pm 5 \times 10^{-16}$ ergs per deg K, respectively, but the errors in ΔH_{a0} and $\Delta S_a'$ will generally be in opposite directions and therefore tend to compensate. Reference 7 gives an approximate value of the reproducibility of stress-rupture data obtained from duplicate tests on specimens from the same heat. This value is ± 25 pct for two thirds of the tests conducted. For one third of the tests the variation was much larger than ± 25 pct.

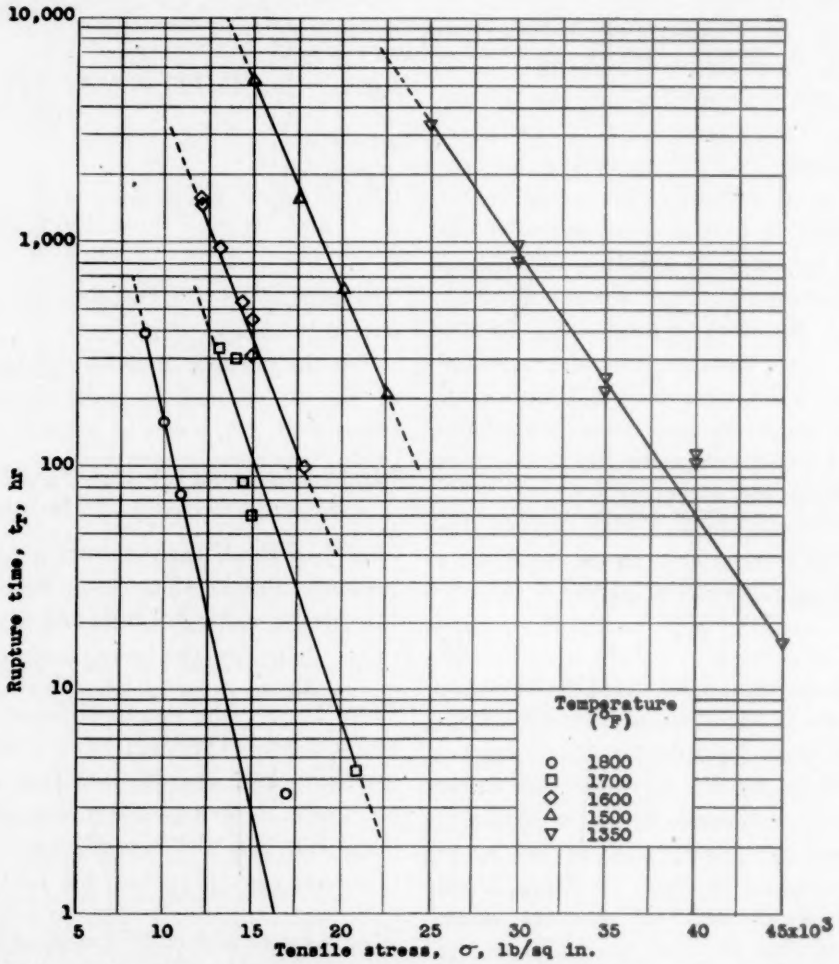

FIG 3—VARIATION OF RUPTURE TIME WITH TENSILE STRESS σ FOR CAST S816.

Discussion of Results

Stress Dependence of log t_r

Equation 9 states that at constant temperature a plot of log t_r against stress at high stresses will yield a straight line

having the negative slope $\beta/4.6kT$. The primary data for S816 cast, S816 forged, and low-carbon N155 hot-worked showed that the plots of log t_r against stress for these alloys were straight lines whose slopes varied with the temperature (Figs 3, 4 and 5). The literature, however, shows straight-line plots of log t_r against log σ for these same alloys. Inasmuch as both plots are not mathematically consistent, only one plot is correct. It will be indicated that stress rupture may be a rate process and therefore the semilog plot should be investigated for use. The magnitude of the experimental error explains why the two plots can be simultaneously obtained. Previous investigators have noticed also that straight-line plots could be obtained by plotting log t_r against σ (discussion of ref. 3). Inasmuch as no basis for choosing between the plots had been available, stress-rupture data were standardized on plots of log t_r against log σ.

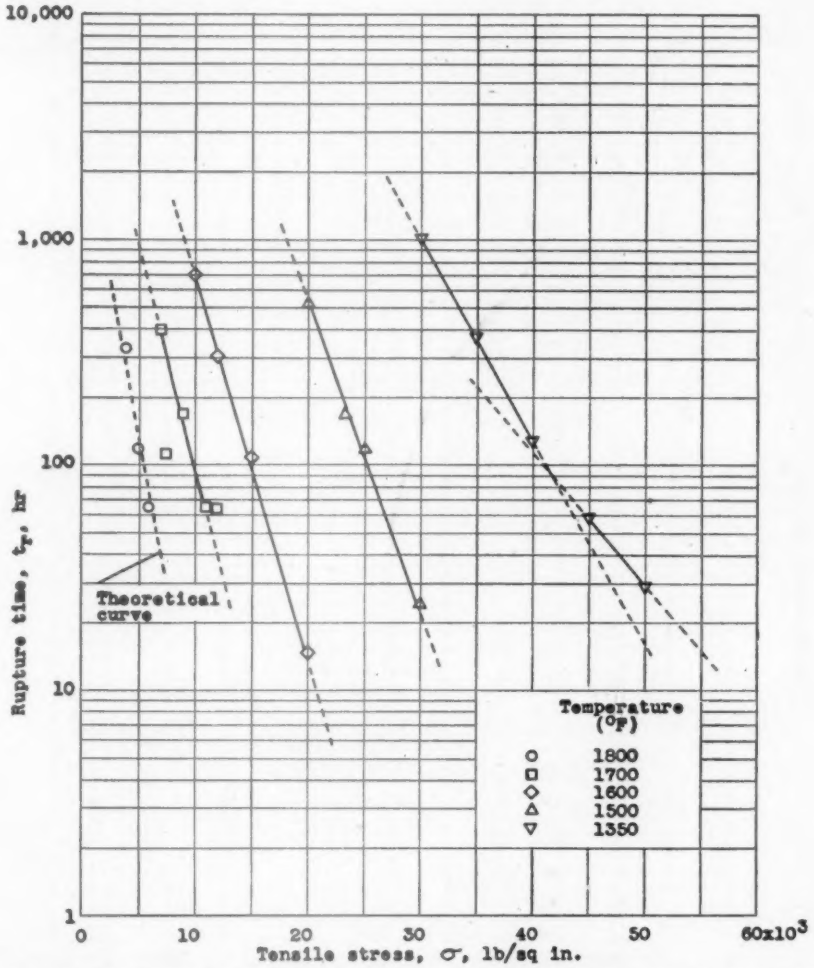

FIG 4—VARIATION OF RUPTURE TIME WITH TENSILE STRESS σ FOR FORGED S816.

The change in slope that occurs because of oxidation on the log-log plots of rupture time against stress[3] also occurs on the semilog plot at approximately the same rupture time and stress. At the same temperature, transcrystalline-type failures will occur at higher stresses than intercrystalline-type failures. No correlation exists, however, between the change in slope and

the transition between transcrystalline and intercrystalline regions of failure. A number of the lines shown in Fig 3 and 4 show changes in slope that cannot be explained by either intercrystalline oxidation or the hyperbolic sine dependence of stress. The change in slope is opposite in sign to that expected for intercrystalline oxidation and also is much sharper than that expected for a hyperbolic sine dependence of stress. It is believed that the change in slope is due to a change of structure as a result of the effect of stress. Harrington,[8] for example, has shown that stress at high temperatures can induce an age-hardening reaction.

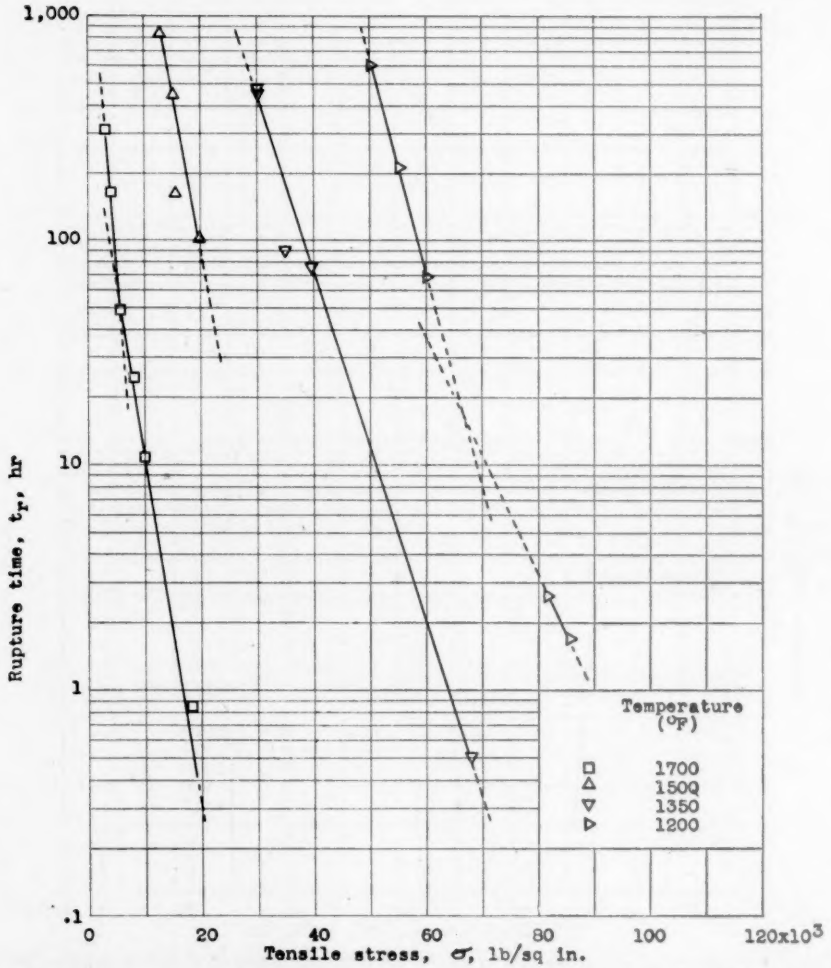

FIG 5—VARIATION OF RUPTURE TIME WITH TENSILE STRESS σ FOR LOW-CARBON N155 HOT-WORKED.

Temperature Dependence of Slope Factor β

In an earlier investigation,[6] it was empirically found that the temperature dependence of the beta factor for creep could be described by the following relation:

$$\beta = Pe^{QT}$$

The data for stress rupture were investigated to show whether a similar relation existed for stress rupture. A plot of log β against T, which gives straight lines within experimental error for the three alloys studied, is shown in Fig 6. The beta values of Fig 6 are of the same order of magnitude as those obtained for creep of iron.[6]

Temperature Dependence of Apparent Free Energy of Activation $\Delta F_a'$

Equation 12 predicts that the quantity $\Delta F_a'$, the apparent free energy of activation, will be linearly dependent on temperature.

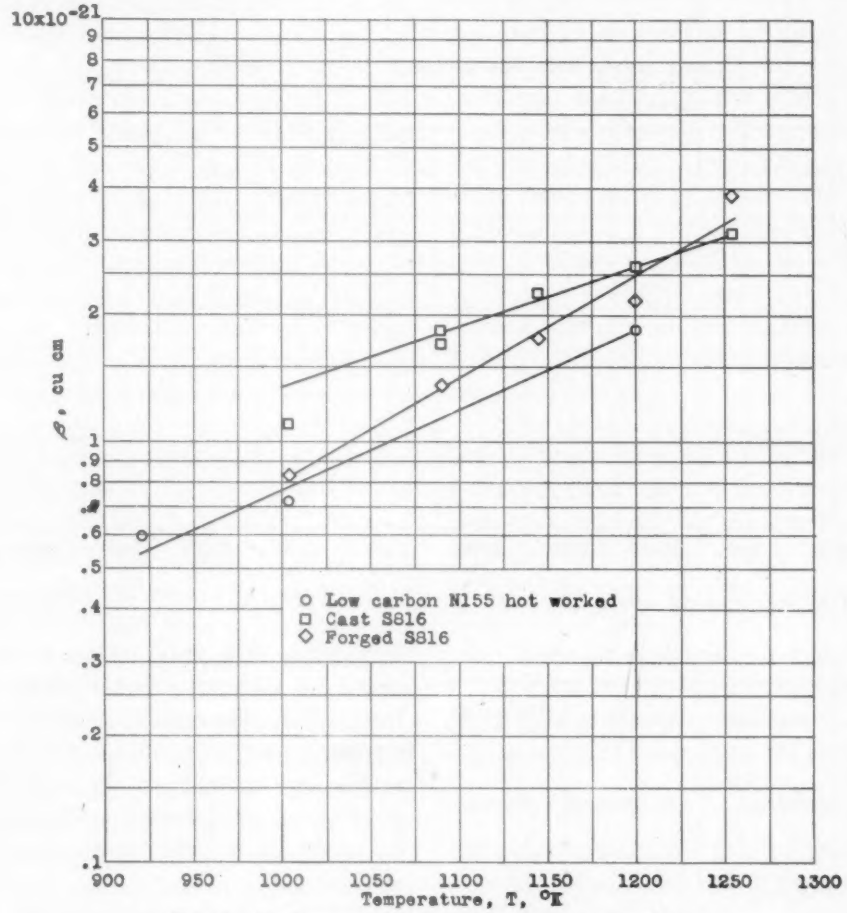

FIG 6—DEPENDENCE OF β ON TEMPERATURE T.

Values of $\Delta F_a'$ were computed from data substituted in Eq. 10 and were plotted against temperature for S816 cast, S816 forged, and low-carbon N155 hot-worked. The results are shown in Fig 7, which substantiates the prediction made by the theory of rate processes that $\Delta F_a'$ would be linearly dependent on temperature.

Values of ΔH_{a0} and $\Delta S_a'$ for stress rupture, the intercepts and slopes, respectively, of the lines in Fig 7, are given in Table 1. The values of similar parameters for creep obtained from reference 6 are given for comparison. The parameters ΔH_{a0} and $\Delta S_a'$ for the creep process are approximately the energy of activation and the entropy of activation, respectively, involved in the generation of a dislocation and are A and B, respectively, in the notation of reference 6.

The table shows that ΔH_{a0} and $\Delta S_a'$ are of the same order of magnitude for the stress-rupture rate process as for the creep rate process, respectively. It therefore appears that the entropy of activation ΔS_a for the stress-rupture rate process is probably a large negative value of the same order of magnitude as the entropy of activation for the generation of a dis-

location and that the parameter C is small compared with ΔS_a (see Eq. 13).

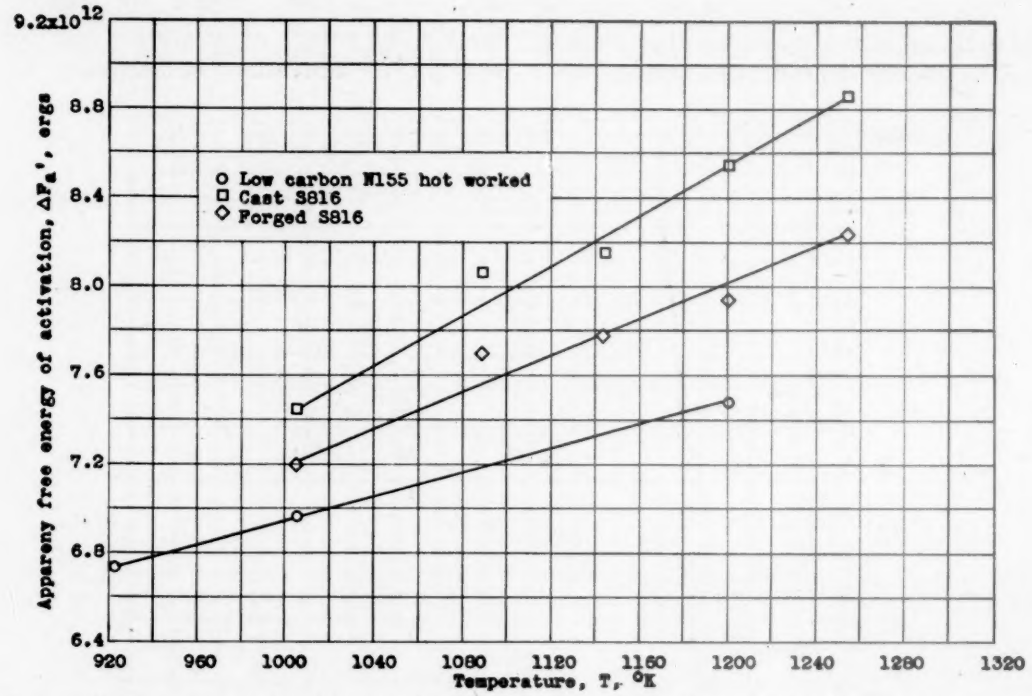

FIG 7—DEPENDENCE OF APPARENT FREE ENERGY OF ACTIVATION $\Delta F_a'$ ON TEMPERATURE T.

TABLE 1—*Data from Figure 7*

Type of Test	Material[a]	ΔH_{a0}, Ergs	$\Delta S_a'$, Ergs per Deg K
Stress rupture....	S816 cast	1.71×10^{-12}	5.7×10^{-15}
Stress rupture....	S816 forged	2.98	4.2
Stress rupture	N155 low-carbon hot-worked	4.19	2.75
Creep.....	Iron	2.10	4.0
Creep.....	Nickel	2.67	4.0

[a] No creep data were available for cobalt but the values of its constants would be expected to approximate closely those for iron and nickel.

EVALUATION OF RESULTS

The theory of rate processes has predicted the temperature dependence of the time for rupture, and this prediction has been substantiated by the data for three heat-resisting alloys. This successful prediction is the justification for applying the theory of rate processes to stress rupture. Because it is indicated that stress rupture is a rate process, plots of the log time for rupture against stress should be investigated for use instead of the log-log plots now used. Not only is the semilog plot based on theory; it is also the only plot from which data can be obtained to predict stress-rupture data at additional temperatures. An example of the accuracy with which data at different temperatures can be predicted is given in the next section of this paper.

The data have revealed that a given material may have three different sets of constants dependent on the stress and temperature to which the specimen is subjected. Two sets of these parameters hold for the unchanged material (stable structure) and for the material in the range of intercrystalline oxidation, respectively. The third set, which describes the region of highest stress, is best explained on the basis of a change induced in the original structure by shear stress. Whether this explanation is correct could be determined by means of an X ray analysis of the crystal

structures in two different regions having different sets of material parameters.

On a log-log plot of rupture time against stress, the line that represents the region of intercrystalline failure in the absence of oxidation is an extension of the line of the region of transcrystalline failure.[3] In the plot of log rupture time against stress for the same data, the line obtained is also unbroken. In terms of the theoretical equation 9, the $\Delta F_a'$ and β values for transcrystalline failure are exactly equal to the $\Delta F_a'$ and β values for intercrystalline failure in the absence of oxidation. It therefore appears that the rate-process mechanism responsible for the transcrystalline failure is the same rate-process mechanism responsible for the intercrystalline failure. This fact leads to the belief that a correlation may exist between creep and stress rupture. From reference 9 it can be implied that during the transcrystalline mode of failure, a relatively large amount of creep takes place. If transcrystalline failure finally results from a shearing of the individual grains, creep may be the controlling factor. Further evidence of a correlation between creep and stress rupture was the agreement of the order of magnitudes and temperature dependence of similar terms in the equations for creep and stress rupture. Further tests, however, are necessary in order to prove whether such a correlation exists.

The practical application of the stress-rupture theory to engineering problems is extensively described in the next section.

Practical Application of Stress-rupture Equations

The equation

$$\log t_r = \frac{A + BT - D\sigma}{T} \qquad [14]$$

where

t_r = time for rupture, hours,
T = absolute temperature, deg R,
σ = applied tensile stress, psi,
A, B = constants of structure and composition,

and

$$\log D = E + FT \qquad [15]$$

where

E, F = constants of structure and composition,

was derived in the theory section of this report from the theory of rate processes as developed by Eyring and others.[5] Eq. 15 was found empirically. The predictions of Eq. 14, especially in regard to the temperature dependence of stress rupture, were investigated and verified for a number of heat-resisting alloys. Eq. 14 is therefore valid and could be used to obtain the dependence of time for rupture on stress and temperature for a given structure and composition.

In order to obtain an evaluation of the constants A, B, E, and F, it is necessary to determine at each of three or four temperatures the time for rupture for at least four different stresses. The results will be found to be more reliable if at each stress a number of tests are run to determine a mean time for rupture.

The constants E and F are evaluated by plotting log mean t_r against σ at a constant temperature. The slope of the straight line obtained is equal to $-\frac{D}{T}$. When values of log D so obtained are plotted against temperature, a straight line is obtained. The slope of the straight line is equal to F and the intercept (at $T = 0$) is equal to E.

The constants A and B are evaluated by obtaining values of the intercept ($\sigma = 0$) of the plot of log t_r against stress. From Eq. 14 this intercept, log t_i, will satisfy the relation

$$T \log t_i = A + BT \qquad [16]$$

When values of T log t_i are plotted against T, a straight line is obtained. The slope of this line is equal to B and the intercept ($T = 0$) is equal to A.

It should be understood that the parameters A, B, E, and F will be constant

only for a given composition and structure and in the absence of intercrystalline oxidation. If a heat-resisting alloy has different structures, as sometimes happens, the values of the parameters for one structure would not apply to predicting stress-rupture data for the other structure. For example, the break in the stress-rupture curve at 1350°F in Fig 4 indicates that the structure in the high-stress range differs from that in the low-stress range because the values of the structure parameters A, B, E, and F for both ranges are not the same. If intercrystalline oxidation takes place, the set of parameters will no longer be valid. These limitations, however, are not severe for the data presented in this report.

In order to illustrate the use of the equations in predicting data, the primary data for forged S816 given in Fig 4 for 1350°, 1500°, 1600°, and 1700°F will be used to compute values of A, B, E, and F. Then these values will be used to obtain a stress-rupture curve for 1800°F, which will then be compared to the experimental stress-rupture curve for 1800°F.

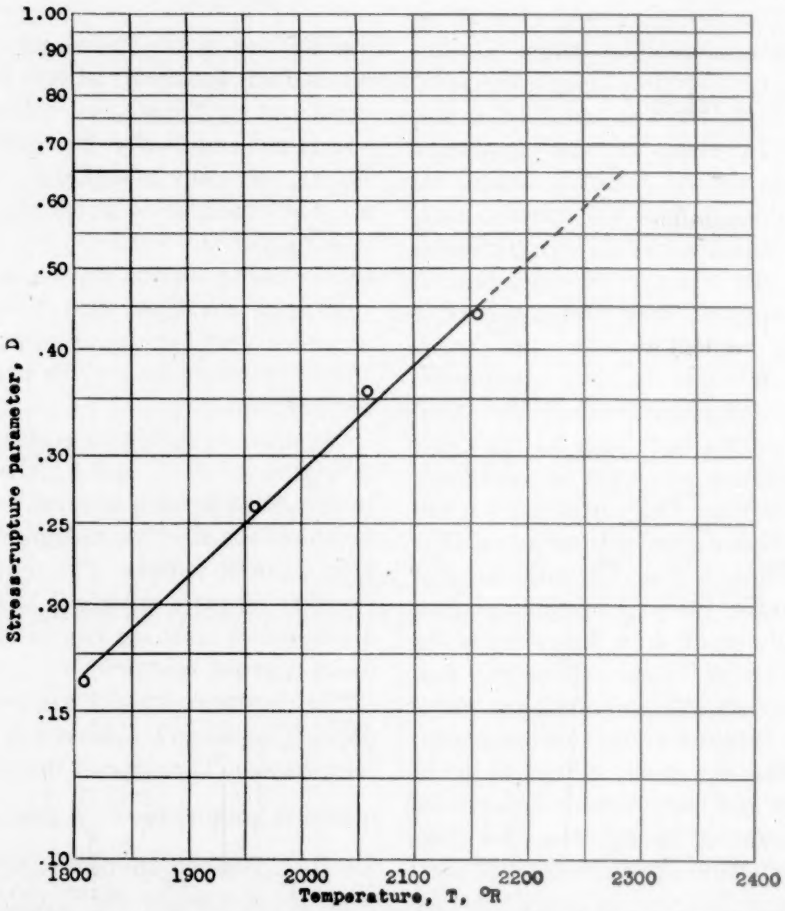

FIG 8—VARIATION OF LOG OF STRESS-RUPTURE PARAMETER D WITH TEMPERATURE T FOR FORGED S816.

The absolute slope of the 1350°F stress-rupture curve is

$$\frac{D}{T} = \frac{\log t_{r1} - \log t_{r2}}{\sigma_1 - \sigma_2} = \frac{3.00 - 2.00}{30{,}000 - 41{,}200} = 0.0000900$$

which then gives

$$D_{1350} = T \times 0.0000900 = 1810 \times 0.0000900 = 0.163$$

similarly,

$$D_{1500} = 0.264$$
$$D_{1600} = 0.350$$
$$D_{1700} = 0.435$$

The plot of log D against T is given in Fig 8. The slope of the straight line in Fig 8 is

$$F = \frac{\log 0.381 - \log 0.169}{2100 - 1810} = 1.218 \times 10^{-3}$$

The intercept of this straight line is

$$E = \log 0.381 - 1.218 \times 10^{-3} \times 2100 = -2.977$$

Equation 15 then gives for D at 1800°F

$$\log D = E + FT = -2.977 + 1.218 \times 2260 \times 10^{-3} = -0.220$$
$$D = 0.600$$

The intercept of the 1350°F stress-rupture curve in Fig 4 is

$$\log t_i = \log t_r + \frac{D}{T}\sigma = \log 1000 + \frac{0.163}{1810} \times 30{,}000$$
$$\log t_i = 5.70$$

Then

$$T \log t_i = 10{,}300$$

Similarly,

$$T \log t_i \ (1500) = 10{,}580$$
$$(1600) = 9320$$
$$(1700) = 8650$$

The plot of T log t_i against T is given in Fig 9. The slope of the straight line obtained is

$$B = \frac{10{,}420 - 9030}{1900 - 2100} = -6.950$$

The intercept is

$$A = 10{,}420 - (-6.95 \times 1900) = 23{,}630$$

Equation 14 was used, with the value of D at 1800°F and the values of A and B just determined, to obtain the stress-rupture curve for 1800°F that is shown plotted in Fig 4 as a dotted line. The experimental points are indicated by circles and give a measure of the accuracy that can be obtained using Eqs. 14 and 15 to predict stress-rupture data. It should be noted that the predicted values fall within the reproducibility of ±25 pct found by reference 7. This reproducibility figure was obtained for a duplicate series of stress-rupture tests of specimens taken from the same heat.

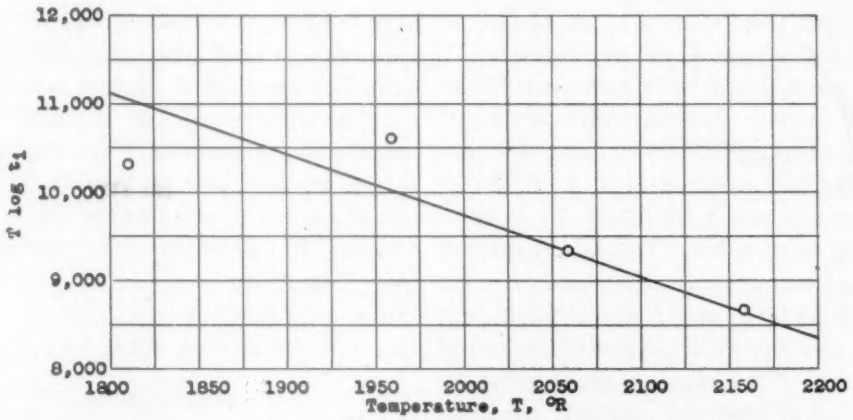

FIG 9—VARIATION OF T LOG t_i WITH TEMPERATURE T FOR FORGED S816.

The number of stress-rupture tests required at present can be materially reduced by using the method just described to predict data at new temperatures. Specifically, if it is desired to extend the stress-rupture data to higher temperatures, it is necessary according to present methods to obtain values of t_r for at least four different stresses at the higher temperature in order to be able to plot a curve of log t_r against log σ. If values of A, B, E, and F were computed for this alloy from the available data, only one test at the higher

temperature would be required to check whether the alloy structure was stable at this higher temperature. If the alloy structure was found to be stable—that is, the experimental value of t_r at the higher temperature checked within experimental error with the value predicted by Eqs. 14 and 15, the equations could be used for predicting the stress dependence of the rupture time at this higher temperature. Thus, about three fourths of the additional stress-rupture tests would be eliminated.

The metallurgist who performs stress-rupture tests in order to rate the heat-resisting properties of alloys can now make use of the four parameters A, B, E, and F as a means of rating the alloys. In order to have long rupture lives (high t_r) at constant stress and temperature, it is necessary that A and B be large and E and F small (see Eqs. 14 and 15). When A and B are larger and E and F are smaller simultaneously for one alloy than for another, the first alloy will have longer rupture life over the range of stress and temperature where the values of A, B, E, and F apply. Where the four parameters do not compare in this simple fashion, the stress-rupture ratings of various alloys will generally not be the same for different ranges of stress and temperature. These alloys therefore can be rated only with respect to their proposed use. For example, alloys for gas-turbine buckets can be rated on the basis of the design temperature and stress. Values of the structure parameters can then be used to obtain easily an order of merit rating at the set of conditions that correspond to the proposed use.

Summary

The equations of the theory of rate processes are applied to stress rupture and predict the experimental stress and temperature dependence of the time for rupture. It is concluded that, although this successful prediction for three alloys did not conclusively prove that stress rupture was a rate process, it did provide a basis for recommending that the rate-process stress-rupture equations obtained should be used to interpolate and extrapolate data for different temperatures and to reduce the number of stress-rupture tests.

It is indicated that stress may have an effect on the crystal structure by causing a phase change; also, it appears that the same rate-process mechanism is responsible for both transcrystalline and intercrystalline failure and that a correlation may exist between stress rupture and creep.

The recommendation is made that the method of presenting stress-rupture data on a semilog plot (logarithm of rupture time against stress), which has a basis in theory, be investigated for use instead of the present empirical method of presenting stress-rupture data on log-log plots of time for rupture against stress.

References

1. H. C. Cross and W. F. Simmons: Progress Report on Heat-Resisting Metals for Gas-Turbine Parts (N-102). OSRD No. 4717, Ser. No. M-477, NDRC, OSRD, War Metallurgy Committee, Feb. 20, 1945.
2. A. E. White, C. L. Clark and R. L. Wilson: The Rupture Strength of Steels at Elevated Temperatures. *Trans.* Amer. Soc. for Metals (1938) **26**, 52–69; discussion, 69–80.
3. A. E. White, C. L. Clark and R. L. Wilson: The Fracture of Carbon Steels at Elevated Temperatures. *Trans.* Amer. Soc. for Metals. (1937) **25**, 863–884; discussion, 885–888.
4. J. W. Freeman, F. B. Rote and A. E. White: High Temperature Characteristics of 17 Alloys at 1200° and 1350°F. NACA ACR No. 4C22, 1944.
5. S. Glasstone, K. J. Laidler and H. Eyring: The Theory of Rate Processes, 1–27, 153–201, 477–551. New York, 1941. McGraw-Hill Book Co.
6. A. S. Nowick and E. S. Machlin: Quantitative Treatment of the Creep of Metals by Dislocation and Rate-Process Theories. NACA TN No. 1039, 1946.
7. Anon: Statistical Analysis of Effect of Chemical Composition on Stress-Rupture Properties of a Group of Alloys Tested at M.I.T. AMP Rep. 122.1R, SRG Rep. 485, Columbia Univ., Statistical Res. Group, Appl. Math. Panel, NDRC, May 1945.
8. R. H. Harrington: The Role of Strain in Precipitation Reactions in Alloys. Age Hardening of Metals, Symposium on Precipitation Hardening, Twenty-First Annual Convention, Amer. Soc. for Metals, Chicago, Oct. 23–27, 1939, pp. 314–340; discussion, 341.

9. R. H. Thielemann and E. R. Parker: Fracture of Steels at Elevated Temperatures after Prolonged Loading. *Trans.* A.I.M.E. (1939) **135**, 559–575; discussion, 576–582.

curvature on their semi-log scale on Figs 4 and 5.

Upon examining the theory itself, it becomes

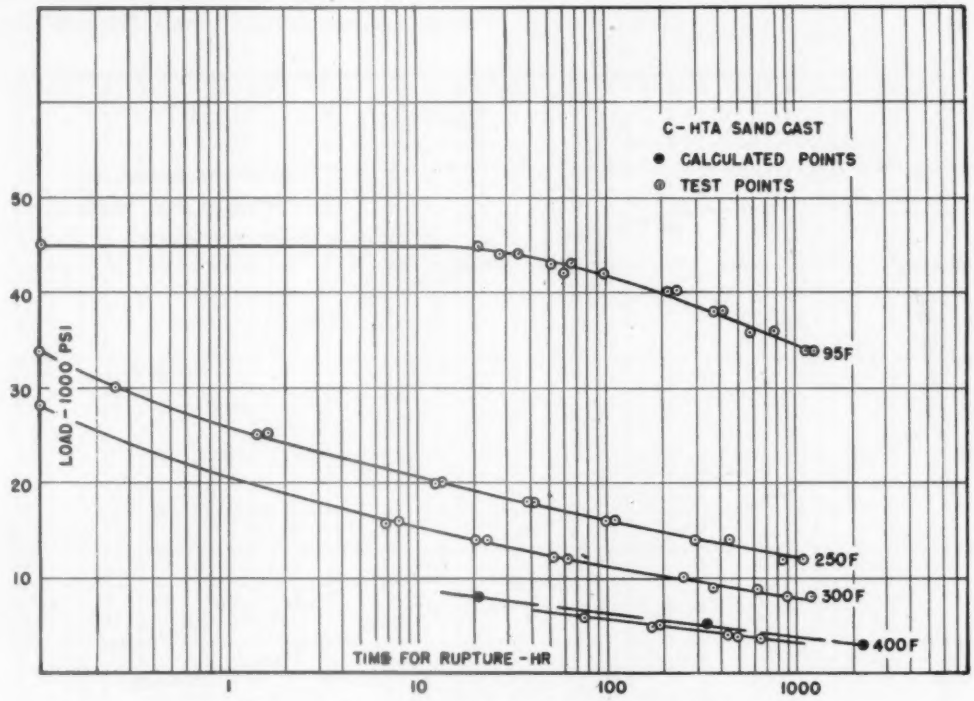

FIG 10—TEST RESULTS FOR A SAND CAST ALLOY.

DISCUSSION

(I. R. Kramer and H. J. French presiding)

E. F. PONCELET*—The authors have endeavored to establish a theory supporting their views that the relationship between applied stress and logarithm of duration required to obtain rupture is linear. Their views are based on stress-rupture data available in the literature for several alloys, none of which covers a range of durations of three full log-cycles.

The literature does, however, contain data covering ranges of durations 10,000 times more extended and covering seven log-cycles, for several glasses, ceramics and porcelains. These data show that the relationship between the applied stress and the logarithm of the duration is most decidedly non-linear, but that the relationship between the logarithms of the stress and of the duration is much closer to being so.† The authors' own plots show the characteristic evident that the authors have made untenable assumptions in order to arrive at their results. For instance, the authors' Eq 3 giving the net rate at which the rupture is assumed to proceed is obtained by subtracting a "reverse" rate from a "forward" rate, assuming tacitly that rupture is a reversible process. In this case, where the rupture is obtained by the propagation of a fracture across the specimen, the surface phenomena taking place simultaneously with the rupture, preclude the reversibility of even the "unit"-process itself.

Furthermore Eq 4 gives the duration of the stress required to obtain rupture as being inversely proportional to the rate. This statement is not true unless the rate is constant, and from Eq 5 it is apparent that the rate is not constant.

Again, Eq 5 gives the rate of the process as a function of the shear-stress σ. This cannot be true, as in the present case the process under consideration cannot be anything else than the propagation of a fracture across the specimen,

* Owens Illinois Glass Co., Toledo, Ohio.

† *Jnl. Appl. Phys.* March 1946.

and it is well known that fractures are caused solely by tensile stresses, not shear stresses.

The true rate of propagation of a fracture in terms of the variable tensile stress at the crack-tip is:

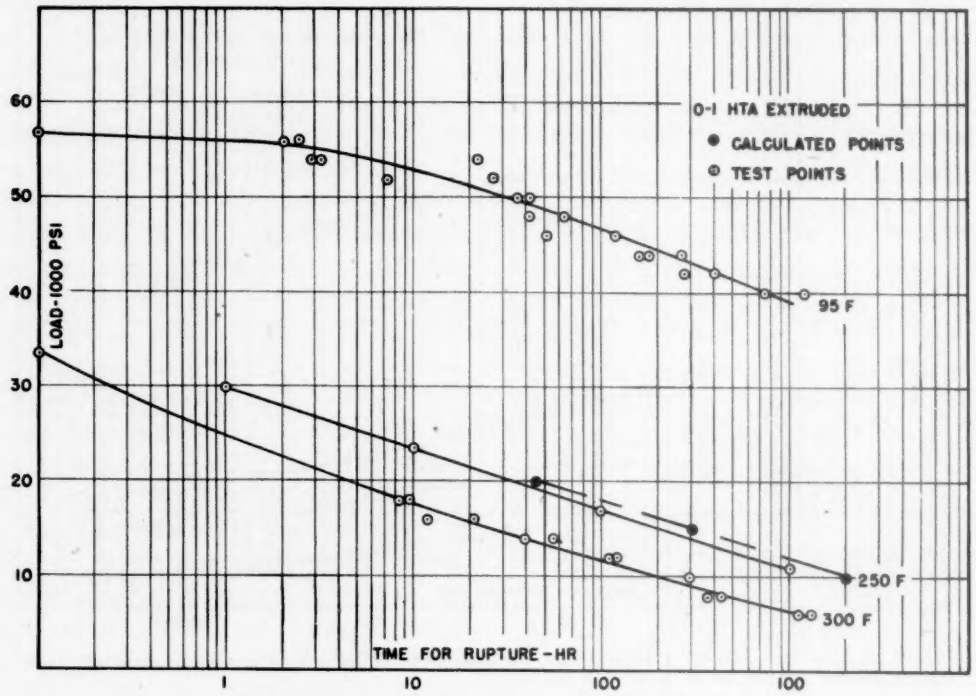

FIG 11—TEST RESULTS FOR AN EXTRUDED ALLOY.

$$r = C^{-E/KT}$$

in which E is a complicated function of the stress given in my paper on fractures.*

Since r is the rate of the phenomenon, that is the rate of propagation of the fracture depth which we may call a we have:

$$r = da/dt$$

The time required for the fracture to rupture the specimen is consequently:

$$t = \int dt = \int (1/r)da$$

The solution of this integral is too complicated to be given in a few minutes and shall be given in full in a later paper. Suffice it to say that the results agree very well with the experimental evidence.

As a conclusion I would suggest that extrapolation of results made with the authors' proposed method be used with very much caution.

W. LESZYNSKI*—Regarding the jump from single crystals to polycrystals, the rate theory operates within a single crystal, but the equations obtained this way are applied to polycrystals. This appears justified in the case of creep.

Do you consider it still justified in the case of rupture?

A. A. MOORE and J. C. MCDONALD†—The methods discussed in this article have been applied to experimental data on some magnesium-base alloys. The results were good.

Test results for a sand cast alloy, AZ92 (9 pct Al-2 pct Zn-Dowmetal C-HTA), at 95, 250 and 300°F were used to predict the experimental curve at 400°F. As shown in Fig 10, the agreement is good.

An extruded alloy, AZ80 (8.5 pct Al-0.5Zn-Dowmetal 0-1 HTA), was also studied. Test results at two temperatures only, 95 and 300°F,

* E. Poncelet: Fracture and Comminution of Brittle Solids. (1946) **169**, 37.

* American Electro Metal Corp., Yonkers, N. Y.

† The Dow Chemical Co., Midland, Mich.

were used to predict results at 250°F. As shown in Fig 11, the agreement here was also good.

The relatively straight line portions of the experimental curves between 100 and 1,000 hr were used in each case for determining parameters. Figs 12 and 13 are the work sheets for determination of the required quantities.

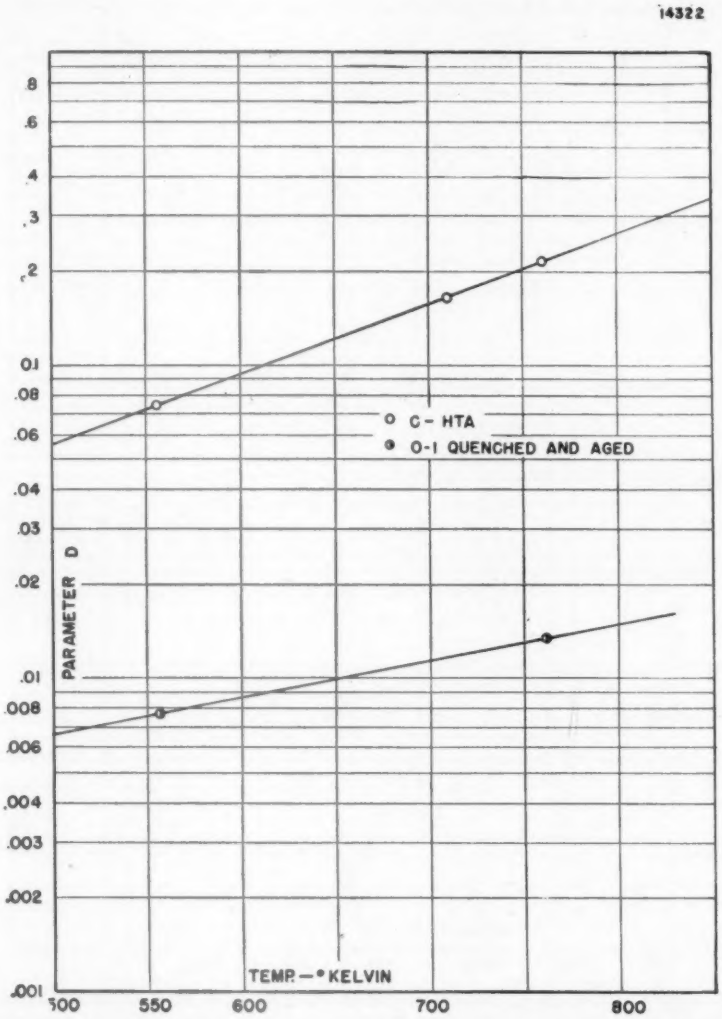

FIG 12—WORK SHEET INDICATING THE REQUIRED QUANTITIES FOR DETERMINING PARAMETERS.

H. S. AVERY*—The authors' conclusion that creep and stress-rupture behavior are related has been reached by many of those engaged in high temperature research. It seems obvious that the minimum or secondary stage creep rate is one of the factors that determine the final fracture time. However, there are several others as suggested by the list below: (1) Primary creep rate; (2) secondary creep rate; (3) third stage of creep, with complications from reduction in cross-sectional area and increasing unit stress; (4) ductility of the material, which in turn may be influenced by stress and the duration of the test; (5) selective oxidation; (6) form and distribution of carbides or intermetallic compounds; (7) precipitation of carbides or other compounds during the test; (these may superimpose contraction on the expected elongation from stress;) (8) phase changes, such as graphitization, replacement of ferrite by the sigma phase, etc; (9) grain size.

Because of the relation of creep to stress-rupture tests, which are actually creep tests continued to fracture, it is puzzling that the

* American Brake Shoe Co., Mahwah, N. J.

authors have not mentioned the work of several others who have applied mathematical treatment to creep data.[10–20]

Anyone who contemplates analyzing or extrapolating creep data, either by the method suggested in this paper or by other available techniques, should carefully read Gillett's pertinent remarks in his 1939 Howe Memorial lecture.[21]

The authors suggest that semi-log plotting be investigated for use. This has been the practice in some laboratories for years, but we cannot yet accept this relationship with assurance. At the American Brake Shoe Co. laboratory, the log-log plots are generally more satisfactory as shown in Fig 14, but some conditions are best served by the semi-log plot, as in the case where the growth of cast iron is superimposed on creep behavior. Several years ago, we reviewed a group of creep curves to determine trends on austenitic heat resistant alloys of the most common commercial types (26 pct Cr:12 pct Ni; 26 pct Cr:20 pct Ni; 16 pct Cr:35 pct Ni; 12 pct Cr:60 pct Ni; 21 pct Cr:9 pct Ni, and others.) These were plotted on log-log paper. The best curves drawn through the data points do not always show the same trends; a downward curvature suggests that the semi-log or hyperbolic sine plot would be more appropriate. Of 42 plots, 55 pct were concave downward, 19 pct were straight lines, and 26 pct were concave upward.

These proportions suggest the applicability of the semi-log method, though it should be

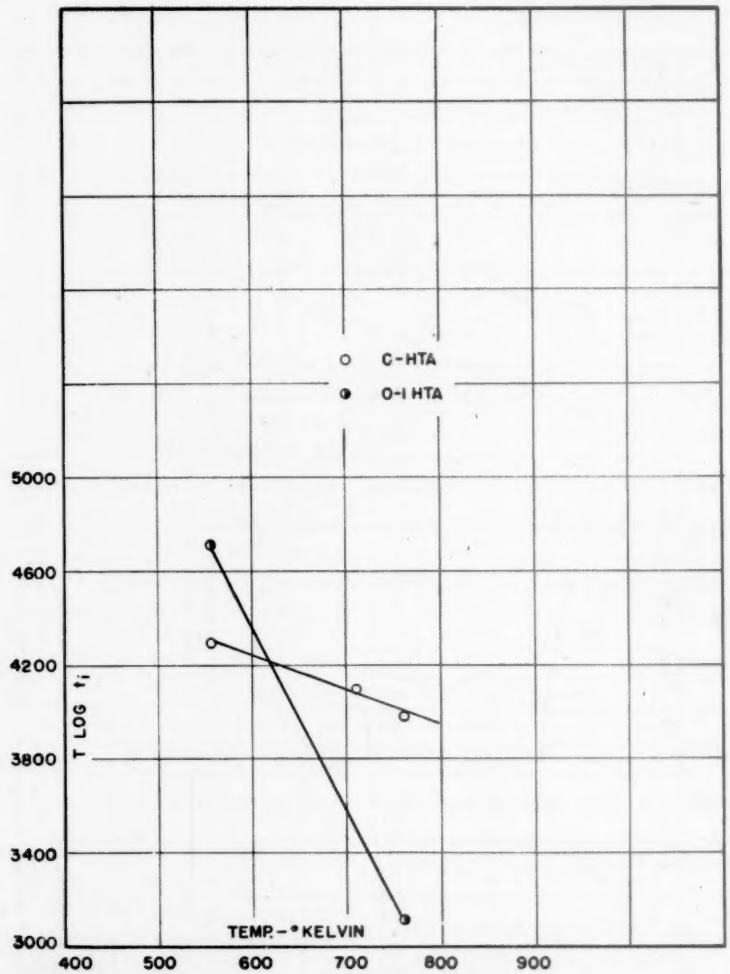

FIG 13—WORK SHEET INDICATING THE REQUIRED QUANTITIES FOR DETERMINING PARAMETERS.

noted that mere departure from the straight log-log line by downward curvature does not mean that the semi-log straight line is valid. However, closer inspection of the data indicated several disturbing factors. Unless very long tests were run, the minimum creep rate, which was the value in these plots was sometimes not attained at low stresses. This was not always apparent unless the time-elongation curves were carefully plotted on a magnified scale. If a rate in the primary stage is plotted because this status is not recognized, the log-log straight line breaks downward toward the low stress end.

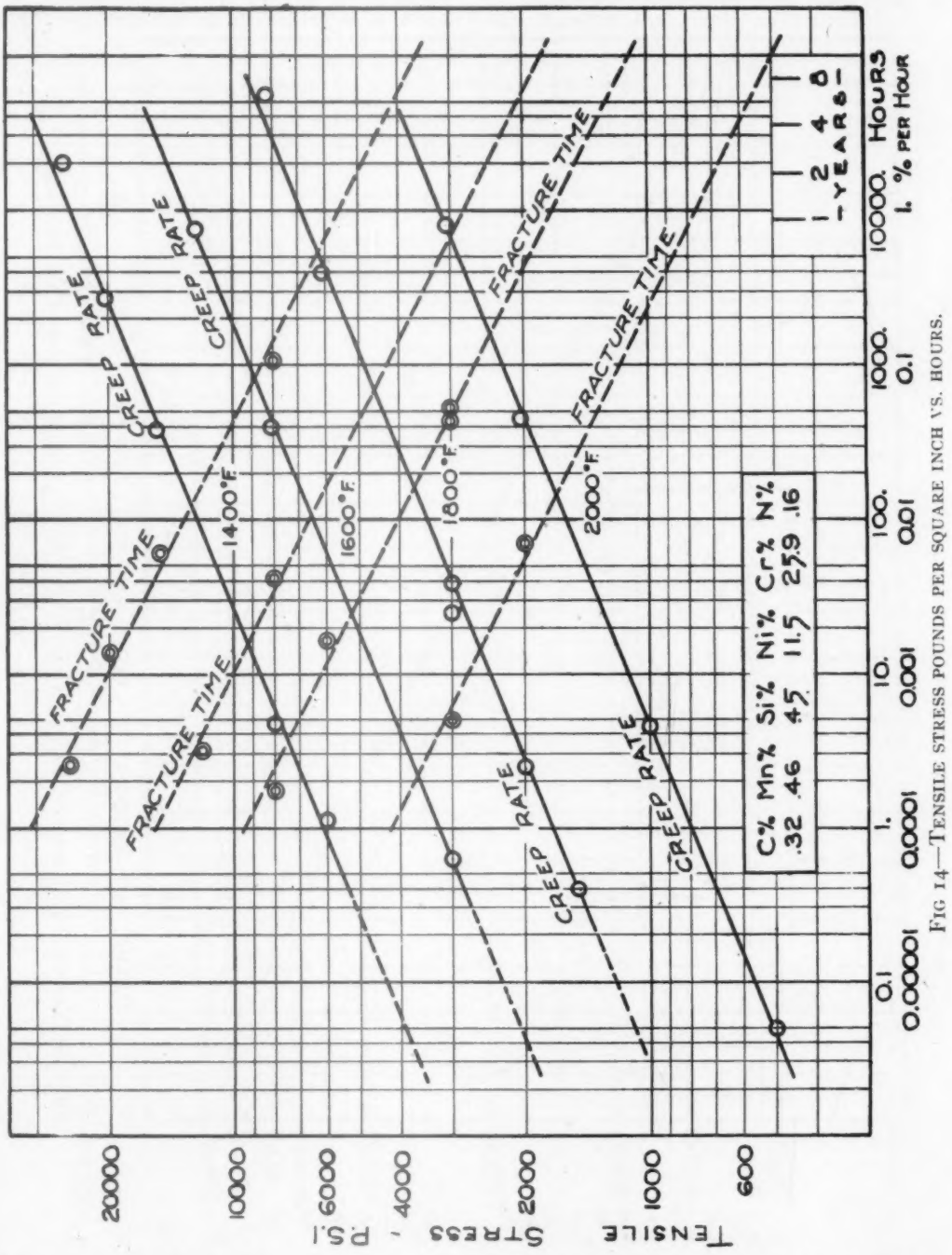

FIG 14—TENSILE STRESS POUNDS PER SQUARE INCH VS. HOURS.

Another discrepancy is introduced by the reduction of area in relatively ductile alloys. True stress just before stage three begins can be calculated from elongation (converted to reduction in area), providing there is no necking. Correction thus for an alloy that is relatively free from carbide precipitation effects, from intergranular oxidation, and from the erratic behavior associated with considerable carbide in the structure, suggests strongly that the log-log relationship is valid for such material, as in Fig 15. Unfortunately, the stronger materials complicated by these factors are commercially most interesting.

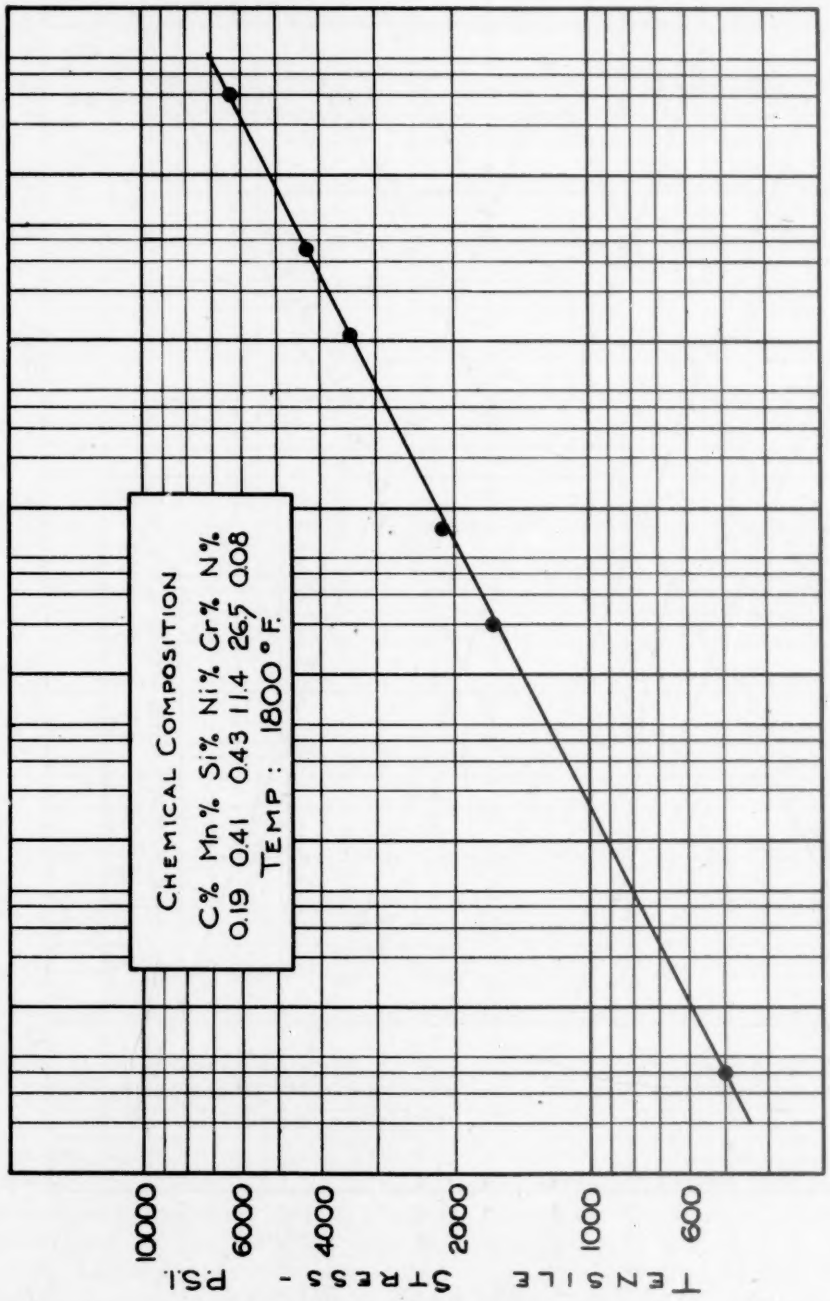

FIG 15—TENSILE STRESS POUNDS PER SQUARE INCH VS. MINIMUM CREEP RATE-PER CENT PER HOUR.

There is a serious lack of the experimental data necessary to clarify the stress-life and

stress-creep rate relationships. The evidence at best seldom covers more than about 3 log cycles, while the behavior for the next two is sought for engineering purposes. It is more practicable to obtain this for creep, as in Fig 15, than for fracture time, which would require over a year for one more cycle (10,000 hr) and nearly 12 yr for two more (100,000 hr), Fig 16.

The semi-log plot has the advantage of being conservative, as it suggests shorter life for a given stress than the log-log method. It also suggests that creep and fracture will occur at zero stress, which is unlikely. Some examples will illustrate the differences that may occur. Fig 17[23] is a log-log plot of a 16 pct Cr: 35 pct Ni alloy obtained in the American

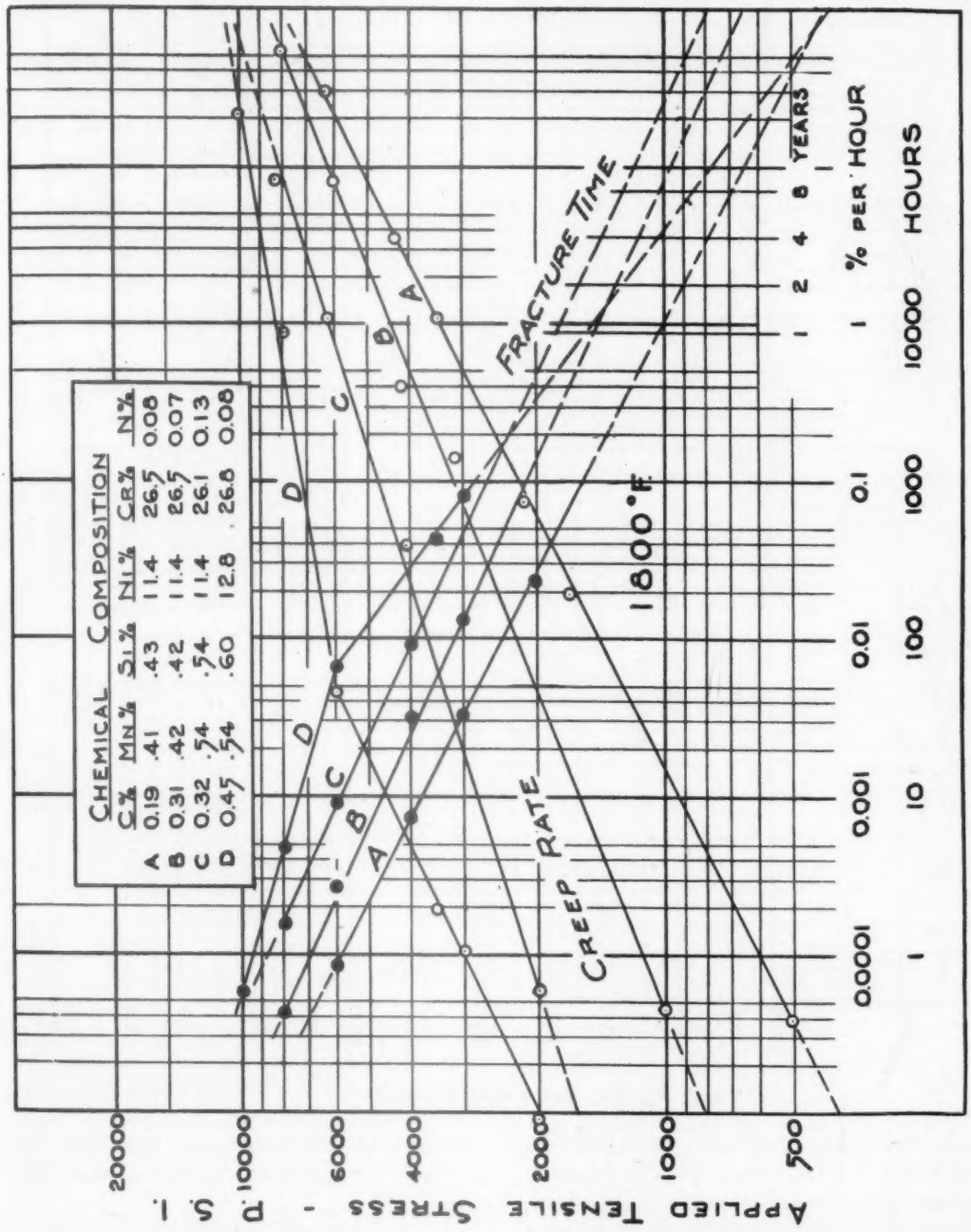

FIG 16—TENSILE STRESS POUNDS PER SQUARE INCH VS. FRACTURE TIME.

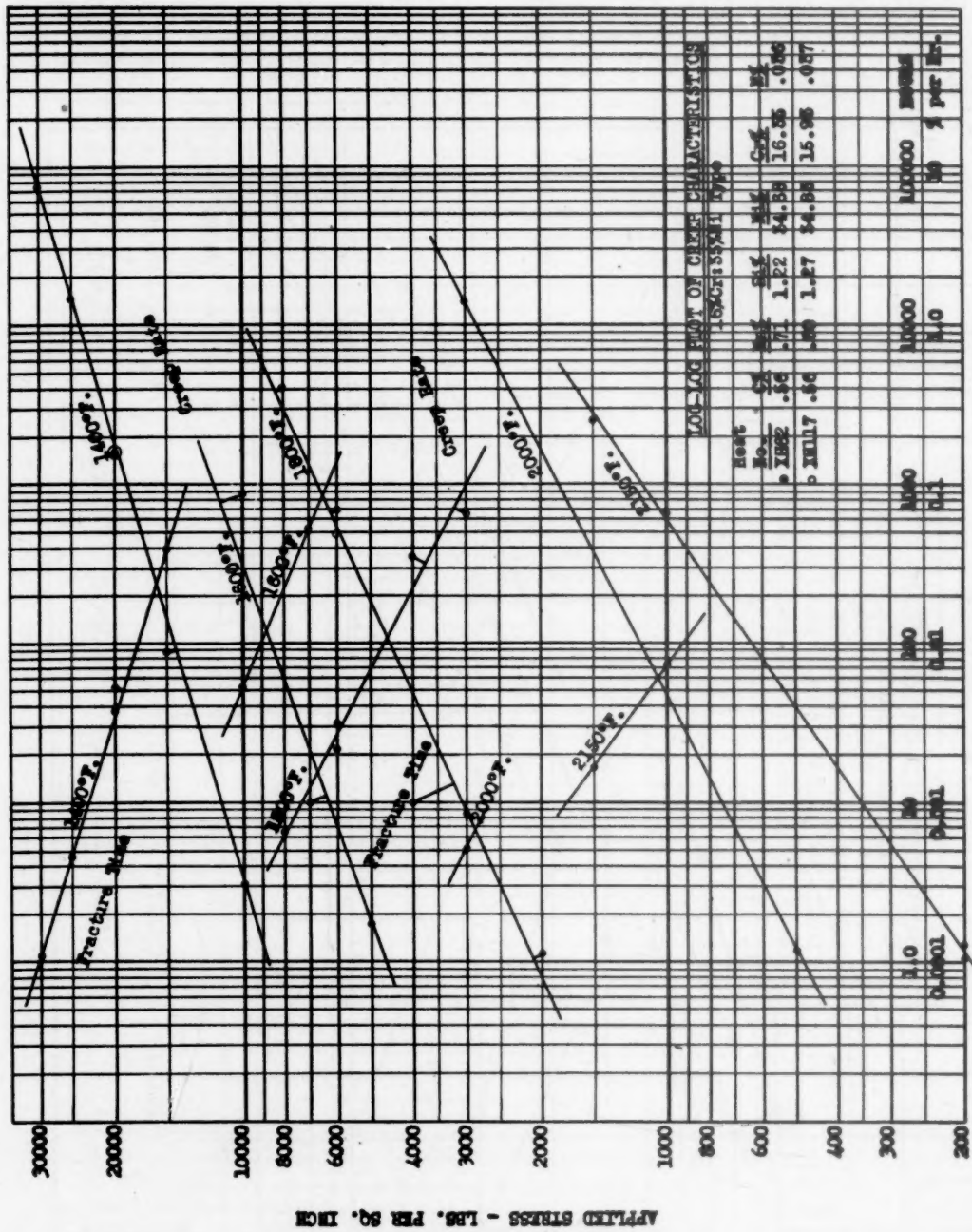

FIG 17—LOG-LOG PLOT OF A 16 PER CENT Cr:35 PER CENT Ni ALLOY.

Brake Shoe Co. laboratory. Note that the 1400°F and 2150°F creep rate and the 1400°F fracture plots agree well with the straight lines. The 1800°F fracture plot can be fitted to a straight line equally well on semi-log paper, extrapolating to about 1000 hr life at 2500 psi. A recent report from the Alloy Casting Institute research program on this type alloy includes a 2281 hr rupture time from 2500 psi at 1800°F that was not available when the chart was drawn.

The Alloy Casting Institute research has used semi-log plots for convenience as in Fig 18.[24] The lines from Fig 18 are plotted as curves on log-log paper in Fig 19, together with straight lines through the points for an indivi-

dual heat. The lines were drawn thus, from experience with this plotting convention, before the longest fracture time was available. It is perhaps more than coincidence that the fracture time line intersects the 5000 psi point at 3258 hr, disagreeing by about 1000 hr with the semilog extrapolation.

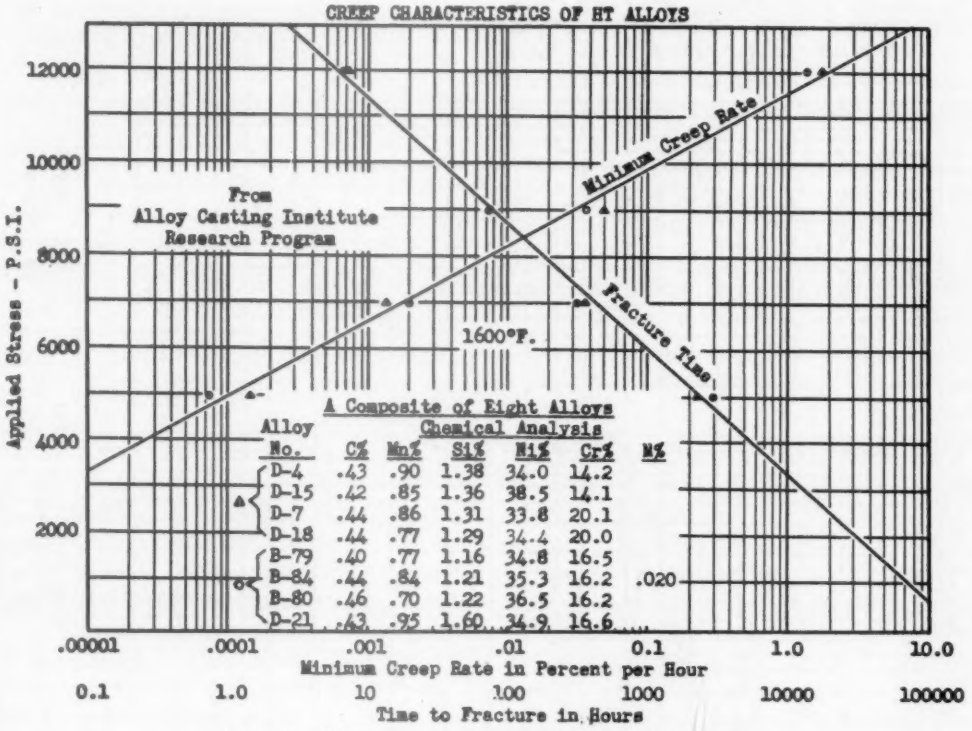
CREEP CHARACTERISTICS OF HT ALLOYS
Applied Stress - P.S.I.
12000
10000
8000
6000
4000
2000
From
Alloy Casting Institute
Research Program
Minimum Creep Rate
Fracture Time
1600°F.
A Composite of Eight Alloys
Alloy No. | Chemical Analysis C% Mn% Si% Ni% Cr% N%
D-4 .43 .90 1.38 34.0 14.2
D-15 .42 .85 1.36 38.5 14.1
D-7 .44 .86 1.31 33.8 20.1
D-18 .44 .77 1.29 34.4 20.0
B-79 .40 .77 1.16 34.8 16.5
B-84 .44 .84 1.21 35.3 16.2 .020
B-80 .46 .70 1.22 36.5 16.2
D-21 .43 .95 1.60 34.9 16.6
.00001 .0001 .001 .01 0.1 1.0 10.0
Minimum Creep Rate in Percent per Hour
0.1 1.0 10 100 1000 10000 100000
Time to Fracture in Hours

FIG 18—CREEP CHARACTERISTICS OF HT ALLOYS.

These examples are no more conclusive than those presented by the authors; the experimental errors involved may be masking the true relationship. However, they do indicate that a derived formula must be used very cautiously until its validity has been generally established.

I believe the authors have pointed out the dependence of fracture time on temperature as following about the same relationship. Does a plot of temperature versus, shall we say, fracture time for a 1000 hr, on semi-log paper conform to a straight line?

E. S. MACHLIN (author's reply)—No.

H. S. AVERY—On the same subject, if data like those of Fig 14, are plotted with stress on a log scale versus temperature on a linear scale, a straight line will usually connect them between 1400 and 1800°F.

The plots look something like this—straight to 1800°F and then breaking downward, indicating that something is occurring in the higher temperature ranges, Fig 20.

REFERENCES

10. Nadai, A. and McVetty, P. G.: Hyperbolic Sine Chart for Estimating Working Stresses of Alloys at Elevated Temperatures, Amer. Soc. Test. Materials *Trans.* (1943) **43**, 735–748.
11. McVetty, P. G.: Creep of Metals at Elevated Temperatures. The Hyperbolic Sine Relation Between Stress and Creep Rate, Amer. Soc. Mech. Eng. *Trans.* (October 1943).
12. McVetty, P. G.: Interpretation of Creep-test Data, Amer. Soc. Test. Materials *Trans.* (1943) **43**, 707–727.
13. Kanter, J. J. and Sticha, E. A.: Creep Rates from Tests of Short Duration, *Trans.* Amer. Soc. Metals (June 1940) 257–276.
14. Nadai, A.: The Influence of Time Upon Creep. The Hyperbolic Sine Creep Law. Stephen Timoshenko Sixtieth Anniversary Vol. (1938) 155–170, Macmillan.
15. Kanter, J. J.: The Problem of the Temperature Coefficient of Tensile Creep Rate. *Trans.* AIME (1938) **131**, 413.

16. Nadai, A.: On the Creep of Solids at Elevated Temperatures, *Jnl. Applied Physics*, **8**, No. 6 (June 1937), 418.
17. Robinson, E. L.: Effect of Temperature Variation on Creep Strength of Steel. *Trans.* Amer. Soc. Mech. Eng. (1938), Research Paper 60–65, 253–259.
18. Soderberg, C. R.: Plastic Flow and Creep in Polycrystalline Metals, Abst., *Jnl. App. Mech.* (Sept. 1938) **5**, A-13.
19. Marin, J.: Comparison of Methods Used in Comparing Creep Test Data, *Trans.* Amer. Soc. Test. Materials (1937) **37**, pt. 2, 258.
20. Kanter, J. J.: Interpretation and Use of Creep Results, *Trans.* Amer. Soc. Metals (1936) **24**, 870–912. Discussion F. H. Norton, 183–195; A. Nadai 916–917.

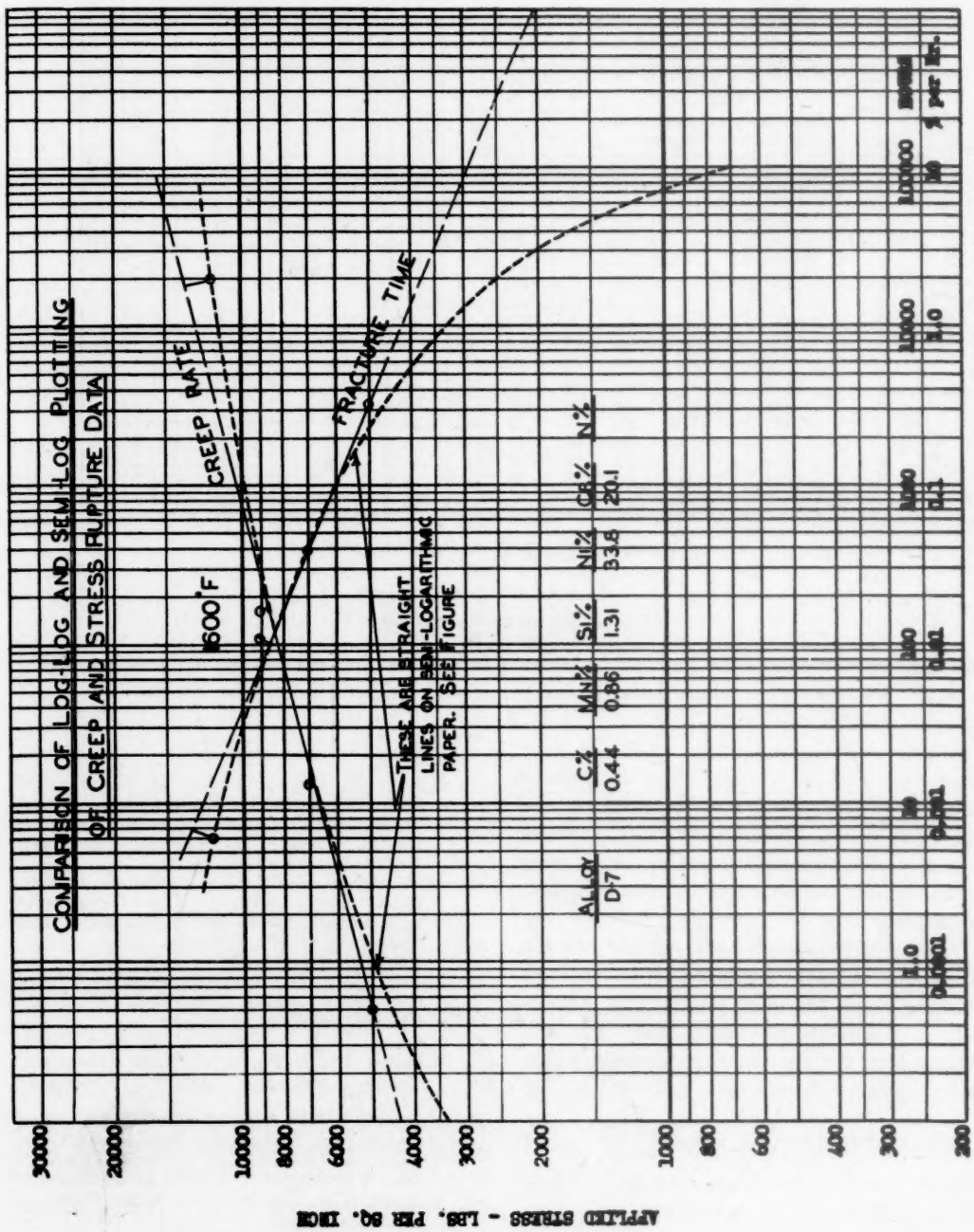

FIG 19—COMPARISON OF LOG-LOG AND SEMI-LOG PLOTTING OF CREEP AND STRESS RUPTURE DATA.

21. Gillett, H. W: Some Things We Don't Know About the Creep of Metals, *Trans.* AIME **135**, (1939) 49–51.
22. Avery, H. S., Cook E., Fellows, J. A.: Engineering Properties of Heat-resistant Alloys, *Trans.* (1943), AIME **150** 373–394.
23. Avery, H. S. and Matthews, N. A.: Cast Heat Resistant Alloys of the 16 pct Cr: 35 pct Ni Type, *Trans.* Amer. Soc. Metals (1947).
24. Avery, H. S.: Properties of 'HT' Alloys—A Summary. Alloy Casting Institute Bulletin No. 9 (October, 1946).

N. J. GRANT*—The field of high temperature metallurgy, especially with regard to the jet engine and gas turbine temperature ranges, is a very new field. A great many of the things we have learned about metallic behavior at low temperatures will have to be modified very severely in order to begin thinking about metallic behavior at high temperatures. We find ourselves concerned not only with elastic and plastic behavior but also with viscous and semi-viscous or semi-plastic modes of deformation. A review of the literature over the past fifteen years indicates that the use of the log log type of plot of rupture time versus stress or of stress versus minimum creep rate is favored by a large number of people in the field. We find an equally positive group who say the semi-log plot is best for the same data. A third group has been sponsoring the hyperbolic sine method for best explaining deformation at high temperatures.

Over the range of log cycles covered by the test data we find little reason to select any one in preference to the others. In most cases three or three and one-half log cycles constitute the total range of points. Actually we have found most data would not adequately permit a differentiation among these techniques. Good mathematical bases have been available in the selection of any of these three plot methods so that it is wrong to say that the use of the log log technique is any more empirical than is the use of the semi-log.

Since we have already gone through this same cycle of arguments in previous years, as the literature shows, it appears that the only real way to answer the questions regarding metallic behavior would be to get test data covering five or six log cycles in order to see which of the methods best fit the data.

One of the first criticisms of this paper should be based on the fact that the authors did not select very good rupture data to prove their theory. There was not sufficient attention paid to the reproducibility of tests or to the reproducibility of heats from which these many tests came.

In the second case, there was no consistency in selecting the curves to fit the points shown in the various plots.

In the third place, the use of this semi-log technique indicates that as higher test temperatures are used, the alloy deteriorates at a slower and slower rate, generally crossing the zero stress axis at some finite period of time, which as Mr. Avery pointed out, suggests failure under no stress. Certainly neither of these conclusions is warranted from experience in the field.

R. SMOLUCHOWSKI*—The authors point out that there is essentially only one mechanism of rupture. It seems to me we should take in account the possibility of having two different mechanisms operating, one on the grain boundary and the other within the grains. The existence of such two mechanisms should appear in different behavior of single crystals and polycrystalline material. I think it would be quite important to distinguish between transcrystalline and intergranular fractures and their relation to the theoretical formulae. Naturally the presence of more than one mechanism operating at the same time would also account for the nonlinearity of the various plots.

E. S. MACHLIN and A. S. NOWICK (authors' reply)—In reply to Mr. Avery, it should be noted that the authors do not state that the minimum or secondary stage creep rate is one of the factors that determine the final fracture time. They do state that a correlation between a steady-state creep rate parameter and a stress-rupture parameter may exist and they indicate that their belief that a correlation may exist is based on an agreement in the order of magnitudes of the free energy of activation for both processes. There are additional material parameters that determine the steady-state creep rate and time for rupture and no correlation has been discovered for these parameters. Thus, no correlation between

* Massachusetts Institute of Technology, Cambridge, Mass.

* Physicist, Carnegie Institute of Technology.

the steady-state creep rate and the time for rupture is expected and Mr. Avery's application of creep data interpretation to stress rupture data should be viewed in this light. No conclusion seems possible from the fracture

should make use of many data treated statistically for pure stable materials.

It would be interesting to know whether the data available to Mr. Avery obey the temperature dependence described in the authors'

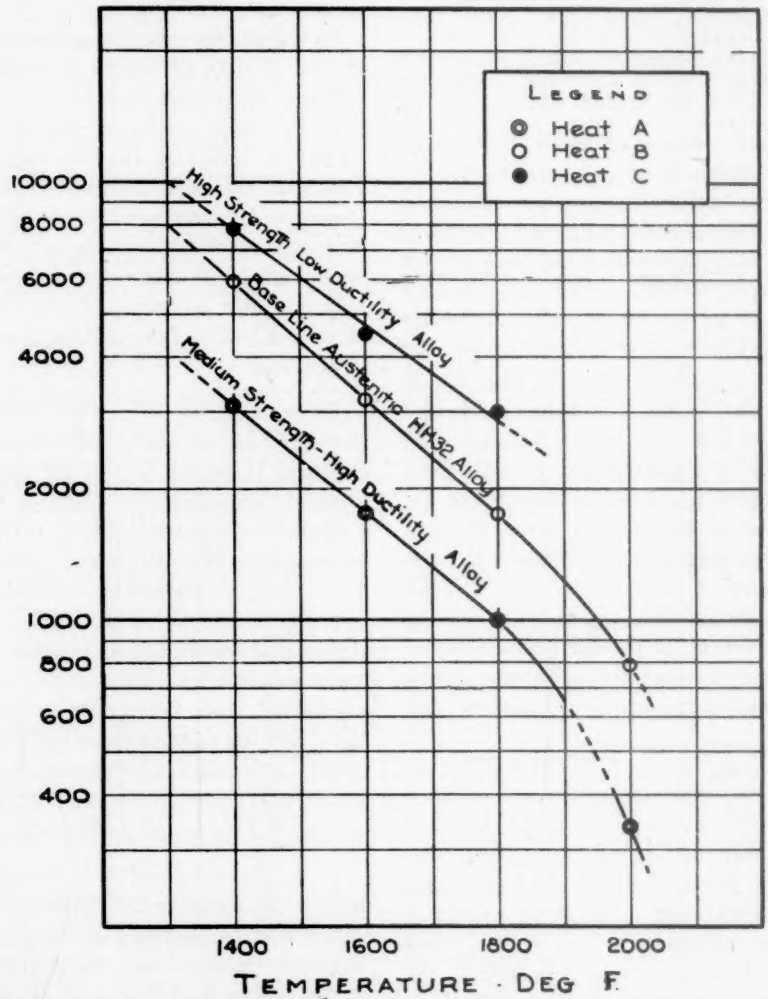

FIG 20—SEMI-LOG PLOT OF LIMITING CREEP STRESS VS. TEMPERATURE FOR THREE 26 PER CENT CR:12 PER CENT NI ALLOYS.

time data presented by Mr. Avery inasmuch as it seems that some of the data plot better on a semi-log basis whereas other data plot better on a log-log basis. It would seem that the data are insufficient for any conclusion in this respect. A scientific check of the theory the steady-state creep rate and the time for rupture is expected and Mr. Avery's application of creep data interpretation to stress rupture data should be viewed in this light. No conclusion seems possible from the fracture

paper. The latter check of the rate process equations for stress rupture is easier to make than a check of the stress dependence. In regard to Mr. Avery's comment that the semi-log equation predicts a finite life at zero stress, it should be noted that the semi-log equation is an approximation for high stresses. The equation that applies for all stresses as developed in the paper yields a hyperbolic sine term which predicts infinite time for fracture at zero stress.

It is interesting to note that Messrs. Moore and McDonald have found it possible to check the temperature dependence of the time for rupture for what seem to be structurally unstable materials. The authors wonder whether the reason for the good results may be explained on the basis that the materials become relatively stable after 100 hr at temperature.

Mr. Poncelet criticizes the authors' work on the basis of data obtained from glasses, ceramics, and porcelains. The authors wonder whether such an analogy is justified inasmuch as metals are crystalline and glass is vitreous, i.e., has an amorphous structure.

No assumption regarding thermodynamic reversibility is made except in using rate process theory to obtain the rate of the unit process. The assumption that is made there is that the initial reactants and activated complexes are always in equilibrium. Unless one has a physical model for the reactants and activated complexes it is impossible to judge the validity of the assumption except by subjecting the predictions of the theory to experimental check. It is entirely possible, for example, that the type of failure involved in a stress-rupture failure is a failure caused by shearing movements—we recommend the micrographs shown in reference 9 for visual evidence of such shearing-type failures. In this case it is quite possible to see that a crack can close under the action of shear stresses opposite to those which open the crack. (Cracks are closed under pressing or forging operations.) It is probable that such "reversibility" is not thermodynamic reversibility involving hysteresis effects, but this fact does not affect the assumptions of our paper.

In answer to the criticism of our derivation of the equation for the time for rupture, the following should be noted. Eq 4 is obtained as follows: $C = \int_0^{t_r} r_f \, dt$, where C is some critical number of unit processes required for failure. If r_f is independent of time t and, contrary to Mr. Poncelet's statement, if it is assumed, as we assume, that the parameters of the equation giving r_f (Eq 5) are independent of time, then

$$C = r_f \int_0^{t_r} dt = r_f t_r$$

or

$$t_r = \frac{C}{r_f}, \text{ our Eq 4.}$$

Inasmuch as we do not present a physical model for the failure process, the assumption that r_f is independent of time is as reasonable an assumption to start with as any other. Further, it has the advantage of simplicity. It is true that if it is shown that our predicted results are not in agreement with the data, then probably it is this assumption that is at fault. However, until it can be shown satisfactorily that the predicted results do not agree with the data, the assumption of time independence of r_f, and development of the rate process equations are satisfactory. As for vitreous materials, it may be true, as Mr. Poncelet suggests, that another assumption is required.

The parameter σ in Eq 5 is the applied tensile stress and not the shear stress, as Mr. Poncelet assumed. In any case, the process under discussion need not necessarily be the propagation of a crack. On the other hand, it may be, for example, the storing of internal strain energy over a period of time. Thus, Mr. Poncelot's comments regarding the use of shear stress instead of tensile stress are invalid.

In answer to Mr. Leszynski, the assumption that enabled us to treat polycrystals as well as single crystals is that the unit process, whatever it is, will occur at the fastest rate along a plane of maximum shear stress and that a sufficient number of crystals are favorably oriented for failure to occur.

In answer to Dr. Grant, the authors would have preferred better rupture data to test their theory. They searched the literature and sources such as the OSRD-Cross reports. Of the tremendous amount of data obtained, those presented in our paper were the most complete that could be used to check the theory. Unfortunately, Dr. Grant's data* could not be used because, as he showed, the stress-rupture properties of the materials he used were a function of time at temperature and stress. Ideally, data for "pure" materials (elements) are preferred as a check of the theory, but unfortunately such data were not available.

As regards the question raised about consistency in selecting curves to fit the points shown in the various plots, it should be noted that the data are too few in general to select lines by a least squares method. If three out of four points or four out of five points fell on

* *Trans.* Amer. Soc. Metals, **39**, 1947.

a straight line, the effect of the lone point was neglected if it was within the experimental-error distance from the line.

In answer to Dr. Grant's third comment, it should be obvious that no method of plotting *experimental* data can force the data to show trends that do not exist. Thus, if, as a measure of the rate of deterioration at given conditions we take the quantity $\left(\frac{d(t_r)}{d(\sigma)}\right)$ at those conditions, then examination will show the same trend in $\frac{d(t_r)}{d\sigma}$ with temperature on a log-log plot as on a semi-log plot. With respect to the statement about predicting a finite life for zero stress, as before it should be noted that the semi-log equation is an approximation for high stresses. The general equation derived in the text gives a hyperbolic sine dependence of time for rupture on stress which predicts infinite time for rupture at zero stress.

In answer to Dr. Smoluchowski, it is perfectly possible that two failure mechanisms are operating. However, as mentioned in our paper, one source showed data at one temperature such that failure changes from a transcrystalline mode to an intercrystalline mode as stress decreases. These data, when plotted, could be represented fairly well by one straight line which indicates that the parameters are the same for both types of failure. However, these data were not accurate enough to give assurance in this matter.

In general, it seems that well-controlled experiments will be required to check the stress dependence of the time for rupture. Already further checks of the temperature dependence of the time for rupture have been obtained by other investigators.*

It would seem, therefore, that the rate-process approach to stress rupture contains promise and should be subjected to scientific scrutiny.

---

* Personal communication. Dr. J. W. Freeman, University of Michigan.

Quantitative Metallography by Point-counting and Lineal Analysis*

By Robert T. Howard† and Morris Cohen,‡ Member AIME

(New York Meeting, March 1947)

It has long been realized among metallurgists that a fast, reliable method for the quantitative determination of the percentage of microconstituents in an alloy would be of great benefit in studies of equilibrium and transformation in the solid state. For example, Polushkin[1] has shown that the compositions of two coexisting phases in a binary system at a given temperature may be calculated very simply with the aid of two alloys lying in the two-phase field if the relative amounts of the two phases in each alloy can be determined. Recently, Grange and Stewart[2] have traced the course of the austenite-martensite reaction in a series of commercial steels by making visual estimates of the percentage of martensite formed as a function of cooling temperature. The correlation of mechanical properties with structure, a subject of wide-spread current interest, is likewise dependent upon quantitative microanalysis.[3] Yet, there are very few investigations described in the metallurgical literature, wherein methods of quantitative microscopy are employed. Usually, the relative amounts of the microconstituents are estimated in a qualitative or semiquantitative way.

The authors were faced with this problem some time ago in studying the kinetics of austenite decomposition. Several aspects of this research could not be treated satisfactorily by other quantitative tools, such as specific volume,[4] magnetic,[5] dilatometric,[6] electrical resistance[7] or x-ray measurements.[8] It became necessary to find an impersonal quantitative method that could be applied to microstructures.

Fortunately, it was noted that geologists and petrographers had coped with quantitative microscopy to a considerable degree in their attempts to evaluate the mineral contents of rocks. A number of excellent articles were found on this subject, and since they appear to be unknown generally to many metallurgists, the first part of the present paper is concerned with a review of the literature in some detail. With this survey as a background, the authors have adapted the so-called methods of point-counting and lineal analysis to metallography, as described in the second part of the paper. Austenite-martensite structures were selected for illustration not only because they are important in many ways, but because such fine intermixtures are notoriously difficult to estimate visually.

Literature Survey

Perhaps the earliest work on quantitative microscopic analysis goes back to Delesse[9] (1848) who proved mathemati-

---

* This paper is based on part of a thesis to be submitted by Robert T. Howard in fulfillment of the requirements for the degree of Doctor of Science in Metallurgy at the Massachusetts Institute of Technology. Manuscript received at the office of the Institute Jan. 25, 1947. Issued as T.P. 2215 in Metals Technology, August 1947.

† Republic Steel Corporation Fellow, Department of Metallurgy, Massachusetts Institute of Technology, Cambridge, Massachusetts.

‡ Professor of Physical Metallurgy, Massachusetts Institute of Technology, Cambridge, Massachusetts.

[1] References are at the end of the paper.

cally that in a uniform rock the volume proportions of the various minerals are equal to their areal proportions as viewed on a random section. Delesse measured the relative areas of minerals lying in a macroscopic section by cutting out segments of tin foil to represent the areas occupied by the various minerals. He then weighed the pieces of tin corresponding to a given mineral, and divided this by the total weight of tin corresponding to the entire structure.

Sorby[10] (1856) extended the areal method of analysis to microstructures by using a camera lucida for tracing on "an evenly thick piece of drawing paper" the outlines of minerals seen under a petrographic microscope. He weighed the whole sketch, and then cut the areas representing the various minerals and weighed them as Delesse did with tin foil for much coarser structures. Sollas[11] (1887) combined the two methods by cutting out areas of tin foil corresponding to a camera lucida tracing.

Julien[12] (1903) made similar determinations in a petrographic study, but attained greater precision by photographing the structure, and then cutting and weighing the paper segments of the micrographic print.

A few years earlier, Rosiwal[13] (1898) published his now classical paper on lineal analysis, in which he showed that the volume proportions of minerals in uniform rock are equal to the lineal proportions intercepted by the minerals on a random line passed through the structure. He not only demonstrated the applicability of lineal analysis to geometrically produced areas, but also found good agreement with the areal method of Delesse as applied to actual macroscopic sections. For microstudies, Rosiwal employed a micrometer ocular to measure the fraction of a line-traverse intersected by the minerals of each type. He stipulated that: (1) the length of the traverse must be at least 100 times the average diameter of the coarsest grain; (2) two traverses should not intersect the same grain; (3) structural characteristics determine the number of traverses necessary. Hirschwald[14] (1903) also used a micrometer ocular for lineal counting, but spaced his traverses at small equal intervals instead of observing Rosiwal's condition (2). Lincoln and Rietz[15] (1912) have since shown that condition (2) is not necessary.

A number of areal and lineal methods of measurement have been developed with a view to increasing precision and decreasing tedium. These later contributions are of particular interest to metallographers who realize the hopelessness of using cut-out or line-intercept procedures for finely dispersed accicular structures, like austenite-martensite.

Joly[16] (1903) traced the enlarged image of a microstructure (projected onto the ground glass of a camera) on graph paper, and estimated the proportions of the individual squares occupied by the various minerals. He then summed up the total area of each microconstituent in the polished section. Johannsen[17] (1919) made tracings of microconstituents with the aid of a camera lucida, and measured the areas with a regular planimeter.

The grid method for evaluating areas was advanced by Thomson[18] (1930) who counted the number of grid intersections falling on each constituent, instead of estimating fractional areas within the individual squares. This was done by viewing the structure through a microscope containing a ruled ocular plate in the eyepiece, or by projecting a grid and lantern slide of the structure on a screen or blackboard. Lightner and Herty[19] (1932) improved upon the point-counting procedure by photographically superimposing a grid on a print of the microstructure. This was achieved by exposing the printing paper first to the negative of the structure and then to the negative of a grid before

developing. Gardner[8] (1943) carried out point-counting by covering the micrographic prints with translucent graph paper. The method of Lightner and Herty was adopted for the present work.

Photometric methods for determining relative areas of dark and light constituents in a two-constituent structure have been proposed[20] and in fact used,[21,8] but they are fraught with uncertainties and are hardly suitable for routine work.

Methods of lineal analysis have also gone through several stages of improvement. Shand[22] (1916) developed a recording micrometer stage capable of yielding the cumulative length of particles of a given mineral intersected during the traversing of a section under a microscope. Wentworth[23] (1923) incorporated five micrometer heads on a single shaft to traverse the stage of a microscope. Each head was assigned to a given constituent, and was turned to move the stage while the corresponding constituent was under the ocular crosshair of the microscope. In this way, the cumulative traverse length occupied by each of five minerals could be read directly off the respective micrometer heads. Hunt[24] (1924) simplified the Wentworth stage, but the method remained tedious. Polushkin[1] (1925) appears to have been the first to apply lineal analysis to metallic structures. He mounted micrographs (up to 850×) on a movable platform, and used a recording tape to sum up the lengths of a given constituent intercepted during a traverse. In this arrangement, the tape was moved to carry an index from one boundary of a constituent particle to the other, and then the platform was adjusted to bring the next particle of the same constituent up to the index, after which the tape was moved again to sweep the second particle, etc. This process was then repeated for equally spaced traverses to cover the entire micrograph. Thus, the cumulative movement of the tape divided by the total traverse length gave the lineal, and therefore the volume fraction of the constituent being measured. Polushkin was able to determine the proportion (and calculate the composition) of eutectics and eutectoids in various alloys by this method of analysis.

All the above methods of lineal analysis are time-consuming and wearisome. Even though the line intercepts may be totalized by a suitable micrometer head or sliding tape, the stage must be carefully moved by hand, with myriad painstaking starts and stops at the boundaries of the constituents being measured. While precisions of the order of ±1 pct are possible if enough traverses are run to obtain proper sampling, eye strain and tedium become serious factors in the general applicability of these procedures. It remained for Hurlbut[25] (1939) to solve the problem with an electric semiautomatic counter, and this is the lineal method which has been adapted by the present authors for metallographic analysis. The polished specimen is moved under the ocular cross hair of a microscope on a mechanical stage driven by an accurate, fine-pitched screw. This screw is rotated by a motor and flexible shaft operating through a keyboard counting device (Fig 8). Each key, when depressed, activates the flexible shaft, thus causing the specimen to pass under the cross hair. Also, each key has associated with it a Veeder Root counter which tallies the number of revolutions while the key is depressed. Thus, with the keys assigned to the various constituents to be measured, the operator starts with constituent X, say austenite, under the ocular cross hair, and presses the X-key. This rotates the flexible shaft and moves the specimen along the mechanical stage, with counter X tallying the number of revolutions. When the austenite boundary reaches the cross hair, the operator releases the X-key which stops the specimen. Without looking

up from the microscope, he then depresses the key assigned to the constituent Y, say martensite, which starts the specimen moving again, but now the shaft revolutions are tallied on counter Y. When the opposite martensite boundary is reached, the Y-key is released, thus stopping the specimen again, and X-key is pressed once more if the adjoining constituent is austenite. Or the Z-key is pressed, if another constituent, like pearlite comes into the field. In this way, the whole specimen is traversed, and several traverses may be run for proper sampling. The number of revolutions shown by each counter, being proportional to the cumulated lineal intercepts of each constituent, is divided by the total number of revolutions to yield the volume fraction of each constituent. A separate counter, geared continuously to the flexible shaft irrespective of the key being pressed, provides the total number of revolutions. For convenience, the speed of the driving motor can be varied with a rheostat, and there are two reversing switches: one on the motor so that the counters may be turned back, and the other on the shaft so the traverse can be run in the opposite direction with the counters continuing their tallies. The back-lash error is eliminated by taking traverses in both directions.

A number of critical petrographic studies have been made to compare the areal and lineal methods of quantitative analysis. Thomson[18] (1930) has applied the Delesse, Rosiwal and grid methods to synthetic aggregates and actual structures, and has found agreement of all three techniques within a few percent. Larsen and Miller[26] (1935) showed good correlation between the lineal results of a modified Wentworth counter on minerals in a rock and subsequent heavy liquid classification of the minerals after being released by crushing. More recently, Postel and Lufkin[27] (1942) used lineal analysis to investigate the variation of thin sections cut from a large rock mass. And finally, Chayes[28] (1946) compared the Wentworth and Hurlbut counters in studying the statistical variability of mineral concentrations lying in one section and in several sections of granite. He concluded that the precision of the two methods was essentially the same, with the Wentworth stage giving somewhat better results for minor constituents. In both methods, the precision improved with the number of traverses. A standard error of ± 1 pct was readily obtained, but the Hurlbut counter had the important advantage of speed and ease of operation.

All methods of microscopic analysis lead to results on a volume basis rather than a weight basis. However, the conversion may be readily made[1] if the appropriate density values are available.

Experimental Results

Statistical Terminology

In order to present an impartial treatment of the precision of the quantitative measurements to be described, it is desirable to review some of the terminology used in elementary statistics.

If $x_1, x_2, x_3 \ldots x_n$ are n determinations of the percentage of a constituent, say austenite, then

$$\text{The } \textit{mean} = \bar{x} = \frac{\Sigma x}{n} \qquad [1]$$

$$\text{The } \textit{variance} = V_x = \frac{\Sigma(x - \bar{x})^2}{n - 1} \qquad [2]$$

The *standard deviation* =

$$s_x = \sqrt{V_x} = \sqrt{\frac{\Sigma(x - \bar{x})^2}{n - 1}} \qquad [3]$$

The *standard error* of the mean =

$$s_{\bar{x}} = \frac{s_x}{\sqrt{n}} = \sqrt{\frac{\Sigma(x - \bar{x})^2}{n(n - 1)}} \qquad [4]$$

The measure of precision to be used here is the standard error. According to statistical theory, there is a 65 pct probability that the mean $\bar{x}$ will fall between the limits $\bar{x} \pm s_{\bar{x}}$, and a 95 pct probability

that the mean will fall in the range $\bar{x} \pm 2s_{\bar{x}}$.

Chayes[28] has used Eq 4 to obtain the number of measurements required to yield a given standard error. For example, in microstructural determinations, if it is desired that $s_{\bar{x}}$ be no greater than ± 1 pct of the total structure, then

$$n_{65} = \left(\frac{s_x}{s_{\bar{x}}}\right)^2 = s_x^2 = V_x \qquad [5]$$

Stated more explicitly, n_{65} is the number of measurements necessary to provide a 65 pct probability that the error of the mean will not exceed ± 1 pct. It can also be shown that

$$n_{95} = 4\left(\frac{s_x}{s_{\bar{x}}}\right)^2 = 4s_x^2 = 4V_x \qquad [6]$$

where n_{95} is the number of measurements required to assure a 95 pct probability that the error of the mean will not exceed ± 1 pct.

The present paper is concerned with the comparative precision of visual estimation, point-counting and lineal analysis as applied to finely dispersed microstructures, with austenite-martensite mixtures being taken as a basis of discussion. To eliminate several confusing variables for the time being, the problem has been reduced to the following: having revealed an austenite-martensite structure by polishing and etching, what precision can be expected by the above methods in evaluating the relative areas (or volumes) occupied by the two constituents?

No attempt is made here to deal with the *accuracy* of the determinations, because the heat treatment and etching used to achieve good contrast between the constituents undoubtedly introduces additional variations over and beyond those involved in one's ability to measure what one sees in the microstructure. Only the latter problem is treated in this paper.

Visual Estimation

Three ¼-in. diam × ⅛ in.-thick discs of high carbon steel were prepared to contain approximately 15 pct, 50 pct, and 85 pct austenite with the remainder martensite. The treatments are unimportant here, except that the austenitizing temperature was high enough to dissolve substantially all the carbides, and the specimens were tempered at 275°C for 5 to 10 sec to darken the martensite. After considerable experimentation with etching reagents to achieve the maximum contrast between the dark martensite and light austenite, best results were obtained with 6 pct nital for the low austenite sample, 3 pct nital for the medium austenite and 1 pct nital for the high austenite. The structures were fine enough to require magnifications up to 1000×.

One representative micrograph of each specimen, as shown in Figs 1 to 3, was given to each of ten competent observers, with a request to estimate carefully the per cent of white constituent in the three pictures. This was not an attempt to determine the austenite contents of the specimens, but to test visual ability in evaluating relative areas of such irregular structures. Therefore, the problem of sampling was eliminated by furnishing the observers with prints, rather than with the specimens themselves.

The results of this preliminary survey are listed in Table 1. It will be noted that agreement among the observers was reasonably good, being best for the high austenite structure. The significance of these data will be discussed later in terms of point-counting measurements made on the very same micrographs. It may be pointed out, however, that the agreement here is much better than could be expected if the observations were based on direct microscopic examination rather than on macroscopic viewing of the

same micrographic prints. Even so, of the thirty observations listed in Table 1, only three were estimated more closely than the nearest 5 pct.

Point-counting

In the point-counting method of areal analysis, as used in this work, ten micrographs were taken across the diameter

FIG 1—1.1 PCT C–3.5 pct Ni STEEL QUENCHED IN LIQUID NITROGEN TO −190°C (−310°F), TEMPERED AT 275°C (525°F).
FIG 2—1.1 PCT C–3.5 PCT NI STEEL QUENCHED IN OIL TO 20°C (68°F), TEMPERED AT 275°C (525°F).
FIG 3—1.35 PCT C STEEL, QUENCHED IN WOOD'S METAL TO 80°C (175°F), TEMPERED AT 275°C (525°F).

FIGS 1–3—MICROGRAPHIC PRINTS OF AUSTENITE-MARTENSITE STRUCTURES SUBJECTED TO VISUAL ESTIMATION BY TEN INDEPENDENT OBSERVERS. NITAL ETCH. MAG. = 1000×. AUSTENITIZED AT 955°C (1750°F).

The precision-calculations given in Table 1, and in subsequent tables, are the same whether the percentages are computed for the austenite or martensite, because the sum of the two constituents must equal 100 pct.

of each of the three specimens which were described earlier. However, the edges of the specimens were avoided because the structures there might have been affected by possible decarburization. The pictures were all taken at 1000×

with an objective of 0.95 N.A. and printed through 10-mesh graph paper, as shown in Figures 4 to 6. This combination was found to be optimum for most austenite-martensite structures.

carefully prepared, there were obvious segregations. These segregations were desirable from the standpoint of the present paper because they must be coped with in any practical method of microanalysis.

4

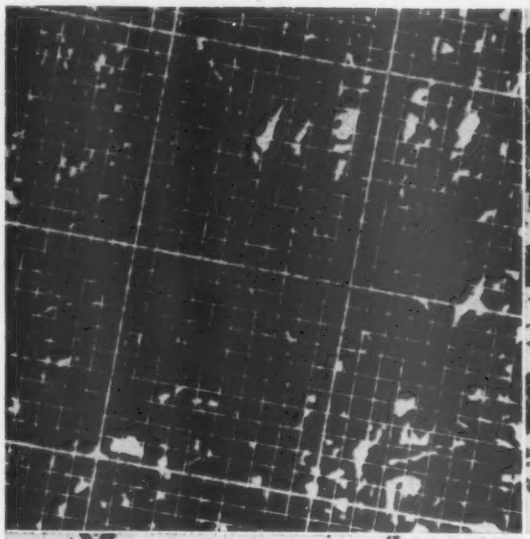

5

6

FIGS 4–6—MICROGRAPHIC PRINTS OF STRUCTURES SHOWN IN FIGURES 1–3, BUT WITH GRIDS SUPERIMPOSED IN RANDOM ORIENTATIONS. GRID SIZE = 10 LINES PER INCH.

In determining the relative areas occupied by the two constituents, there are two important aspects of the precision problem. One is the ability to obtain reproducible counts for a given micrograph, and the other is to take enough pictures so that the specimen can be adequately represented. Even though the steels were

To study the reproducibility factor, each of the three photomicrographs that were estimated visually in Table 1 were printed ten times with random orientations of the grid. The point-counting results are given in Table 2. As might be expected, the standard error is considerably less than for the visual estimates of the same

prints, but there is the same tendency for the standard error to become larger in the lower austenite cases. The mean values in Table 2 may be taken as being very close to the true amount of white constituent exhibited by the micrographs. The excellent correlation between point-counting and the x-ray method of Gardner[8] further testifies to the reliability of the point-counting procedure.

The relationship between the mean values determined visually (Table 1)

TABLE 1—*Visual Estimates by Ten Observers on Three Micrographs*

Observer No.	Low Austenite		Medium Austenite		High Austenite	
	Pct	$(x - \bar{x})^2$	Pct	$(x - \bar{x})^2$	Pct	$(x - \bar{x})^2$
1	15	1	55	25	90	1
2	10	16	60	0	93	4
3	15	1	60	0	90	1
4	30	256	70	100	90	1
5	10	16	60	0	90	1
6	15	1	65	25	95	16
7	15	1	55	25	95	16
8	15	1	50	100	85	36
9	7	49	50	100	90	1
19	6	64	70	100	90	1
Σ	134	406	595	475	908	78
Mean ($\bar{x}$)	14		60		91	
Variance (V_x)	45		53		9	
Standard Deviation (s_x)	±7		±7		±3	
Standard Error ($s_{\bar{x}}$)	±2		±2		±1	
No. observations for 65 pct probability of ±1 pct error (n_{65})	45		53		9	
No. observations for 95 pct probability of ±1 pct error (n_{95})	180		212		36	

TABLE 2—*Point-Counting Measurements Showing Reproducibility on Ten Prints of Each Micrograph*

Print No.	Low Austenite		Medium Austenite		High Austenite	
	Pct	$(x - \bar{x})^2$	Pct	$(x - \bar{x})^2$	Pct	$(x - x)^2$
1	14.0	2.0	55.4	5.3	83.9	0.8
2	14.7	0.5	52.4	0.5	80.1	8.4
3	16.6	1.4	52.9	0.0	82.8	0.0
4	15.1	0.1	53.0	0.0	82.8	0.0
5	12.2	10.2	53.3	0.0	84.1	1.2
6	14.6	0.6	53.1	0.0	83.5	0.3
7	16.6	1.4	51.1	4.0	83.6	0.4
8	16.9	2.3	52.3	0.6	82.4	0.4
9	14.9	0.3	52.7	0.2	82.2	0.6
10	18.7	10.9	54.7	2.6	84.8	3.2
Σ	154.3	29.7	530.9	13.2	830.2	15.3
Mean ($\bar{x}$)	15.4		53.1		83.0	
Variance (V_x)	3.3		1.5		1.7	
Standard Deviation (s_x)	±1.8		±1.2		±1.3	
Standard Error ($s_{\bar{x}}$)	±0.6		±0.4		±0.4	
No. Observations for 65 Pct Probability of ±1 Pct Error (n_{65})	3		2		2	
No. Observations for 95 Pct Probability of ±1 Pct Error (n_{95})	13		6		7	

and by point-counting (Table 2) on the same photomicrographs is shown in Fig 7. The dimensions of the rectangular blocks indicate the magnitude of the standard error in each case. Good agreement between the means was found only in the low austenite structure. In the other two cases, the visual estimates yielded means that were definitely too high—by amounts that were appreciably larger than the standard errors. This signified that, despite the fair agreement *among* the visual estimates for the two high austenite structures, the observers were more or less deluded by these structures, and tended to over-rate the amount of the white constituent. In the low austenite structure, this tendency was not apparent. In fact, small amounts of austenite might even be obscured if the etching were not sufficiently discriminating or if the resolving power of the microscope were not sufficiently high.

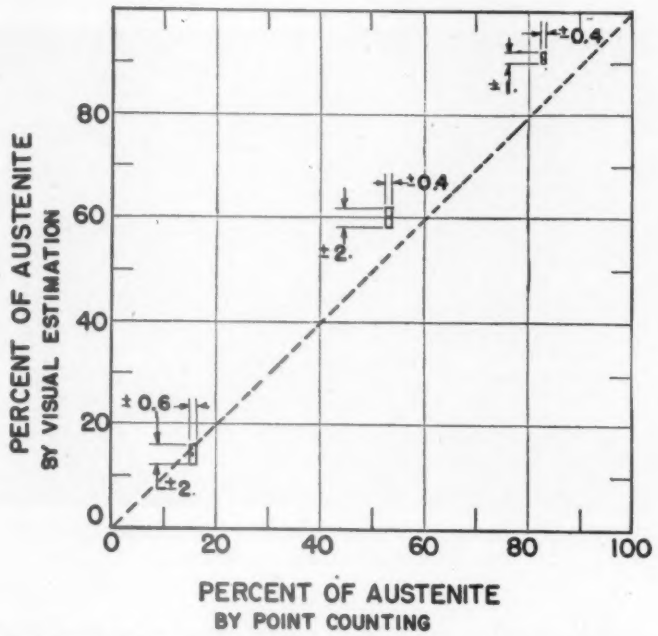

FIG 7—RELATIONSHIP BETWEEN THE MEAN OF TEN VISUAL ESTIMATES AND THE MEAN OF TEN POINT-COUNTING DETERMINATIONS ON EACH OF THREE MICROGRAPHS. DIMENSIONS OF RECTANGLES INDICATE STANDARD ERRORS.

After thus establishing the reproducibility of point-counting under the conditions at hand, this method of areal analysis was applied to each of the ten micrographs taken across the diameter of each of the three specimens. The results are listed in Table 3. It is seen that the standard error in each case was greater than that shown in Table 2. Hence, the variation from spot to spot in each specimen was larger than the reproducibility of point-counting measurements at any one spot. The difference must be attributed, at least in part, to segregations within the specimens, and these variations become the limiting factor in the precision of measurement rather than the point-counter's ability to evaluate any one micrograph.

Lineal Analysis

Despite the superiority of point-counting over visual estimation, it was evident that any method requiring photomicrography (1) was subject to uncertainties in the reproduction process, (2) necessitated many pictures to average out the

ever-present segregations (cf. Table 3), and (3) was quite tedious and time-consuming. Consequently, the lineal method of microanalysis was applied to the same order to have the specimen move slowly enough for observation at 1000×. Each number on the counter corresponded to 0.05 revolutions of the counter shaft or

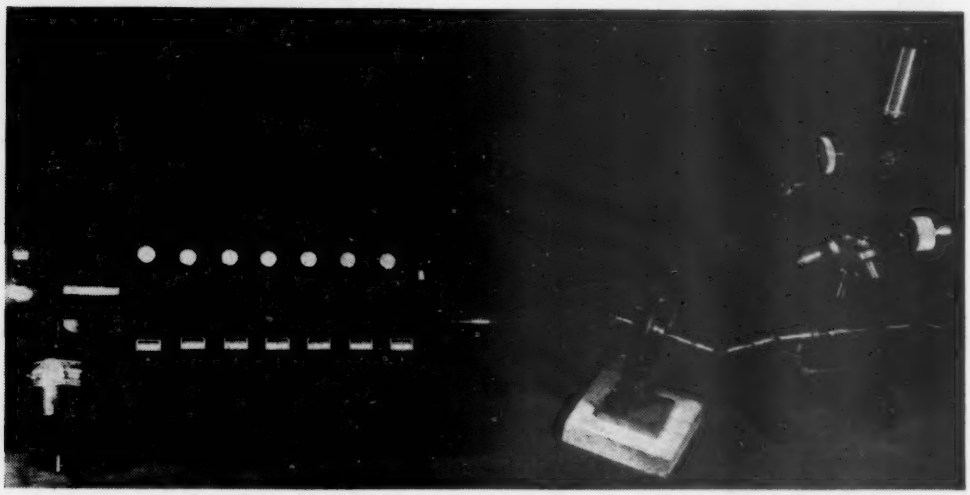

FIG 8—HURLBUT COUNTER ATTACHED TO STAGE OF MICROSCOPE THROUGH 100:1 REDUCING GEAR FOR LINEAL ANALYSIS AT 1000×.

three specimens, using the Hurlbut counter shown in Fig 8. It was necessary to interpose a 100:1 reducing gear between the counter and the microscope stage in 0.0005 revolutions of the screw driving the stage. This screw had a 32-pitch thread, which meant that each counter number registered a 0.000016 in. move-

TABLE 3—*Point-counting Measurements on Ten Micrographs of Each Specimen*

Micrograph No.	Low Austenite		Medium Austenite		High Austenite	
	Pct	$(x-\bar{x})^2$	Pct	$(x-\bar{x})^2$	Pct	$(x-\bar{x})^2$
1	20.1	10.9	55.7	4.8	78.3	19.4
2	21.2	19.4	61.0	56.3	85.1	5.8
3	22.2	29.2	55.5	4.0	84.7	4.0
4	18.7	3.6	49.9	13.0	80.9	3.2
5	15.3	2.3	54.7	1.4	81.6	1.2
6	15.4	2.0	51.5	4.0	71.8	118.8
7	6.9	98.0	51.3	4.8	86.5	14.4
8	13.7	9.6	54.4	0.8	84.8	4.4
9	20.5	13.7	46.7	46.2	86.7	16.0
10	13.8	9.0	54.0	0.3	86.6	15.2
Σ	167.8	197.7	534.7	135.6	827.0	202.4

Mean ($\bar{x}$)	16.8	53.5	82.7
Variance (V_x)	22.0	15.1	22.5
Standard Deviation (s_x)	±4.7	±3.9	±4.7
Standard Error ($s_{\bar{x}}$)	±1.5	±1.2	±1.5
No. Observations for 65 Pct Probability of ±1 Error (n_{65})	22	15	23
No. Observations for 95 Pct Probability of ±1 Pct Error (n_{95})	88	60	90

ment of the specimen. Each traverse ran about 12,000 numbers or 0.20 in., and took approximately 30 min.

The reproducibility of the lineal method was tested by running each specimen back and forth ten times on the same traverse and the calculated percentages of white constituent are listed in Table 4. Because of the large numbers registered on the counter, four digits are carried in Table 4, whereas only three digits were justified in Tables 2 and 3, and only two

TABLE 4—*Lineal Measurements Showing Reproducibility on Ten Runs Across a Single Traverse*

Run No.	Low Austenite		Medium Austenite		High Austenite	
	Pct	$(x - \bar{x})^2$	Pct	$(x - \bar{x})^2$	Pct	$(x - \bar{x})^2$
1	12.12	1.35	54.23	0.01	85.24	0.15
2	13.50	0.05	54.25	0.01	85.58	0.53
3	14.46	1.39	52.35	3.24	84.79	0.00
4	12.53	0.56	53.75	0.16	84.86	0.00
5	13.57	0.08	54.28	0.02	84.01	0.71
6	12.09	1.42	55.45	1.69	85.00	0.02
7	13.30	0.00	55.14	0.98	85.10	0.06
8	15.27	3.96	54.18	0.00	85.34	0.24
9	13.12	0.03	53.75	0.16	83.85	1.00
10	12.88	0.16			84.74	0.02
Σ	132.84	9.00	487.38	6.27	848.51	2.73
Mean ($\bar{x}$)	13.28		54.15		84.85	
Variance (V_x)	1.00		0.78		0.30	
Standard Deviation (s_x)	±1.00		±.88		±0.55	
Standard Error ($s_{\bar{x}}$)	±0.32		±0.28		±0.17	
No. Observations for 65 Pct Probability of ±1 Pct Error (n_{65})	1		1		1	
No. Observations for 95 Pct Probability of ±1 Pct Error (n_{95})	4		3		1	

TABLE 5—*Lineal Measurements on Ten Transverses Across Each Specimen*

Transverse No.	Low Austenite		Medium Austenite		High Austenite	
	Pct	$(x - \bar{x})^2$	Pct	$(x - \bar{x})^2$	Pct	$(x - \bar{x})^2$
1	16.10	0.24	52.25	8.07	85.11	1.04
2	15.91	0.09	57.82	7.45	85.22	1.28
3	17.91	5.29	55.11	0.00	85.34	1.56
4	15.71	0.01	57.00	3.65	83.18	0.83
5	15.10	0.26	51.21	15.05	83.90	0.04
6	15.52	0.01	53.67	2.02	84.03	0.00
7	15.66	0.00	58.07	8.88	82.73	1.85
8	14.39	1.49	54.60	0.24	83.71	0.14
9	16.49	0.77	55.81	0.52	85.15	1.12
10	13.28	5.43	55.32	0.05	82.54	2.40
Σ	156.07	13.59	550.86	45.93	840.91	10.26
Mean ($\bar{x}$)	15.61		55.09		84.09	
Variance (V_x)	1.51		5.10		1.14	
Standard Deviation (s_x)	±1.22		±2.26		±1.07	
Standard Error ($s_{\bar{x}}$)	±0.39		±0.71		±0.34	
No. Observations for 65 Pct Probability of ±1 Pct Error (n_{65})	2		5		1	
No. Observations for 95 Pct Probability of ±1 Pct Error (n_{95})	6		20		5	

digits in Table 1. The error of reproducibility for the lineal method (Table 4) was even less than that found for the point-counting technique (Table 2), and again there was the same trend toward greater precision in the higher austenite specimens.

Ten equally-spaced traverses were then run on each specimen, giving the results listed in Table 5. While the variation from traverse to traverse was somewhat greater than the reproducibility error shown in Table 4, the difference was much smaller than that found with the point-counting method. This superiority resulted from the fact that the ten separate traverses did a better job of averaging out the segregations than did the ten separate micrographs. In fact, from a comparison of the n_{65} and n_{95} values of Table 5 with those of Table 4, one can see just how many more micrographs would be needed than traverses to attain a standard error of ± 1 pct.

Within the standard errors of the point-counting and lineal techniques, the mean values of the two methods were in excellent agreement, as shown in Fig 9. The theoretical 45° line passes through the plotted rectangles whose dimensions correspond to the standard errors.

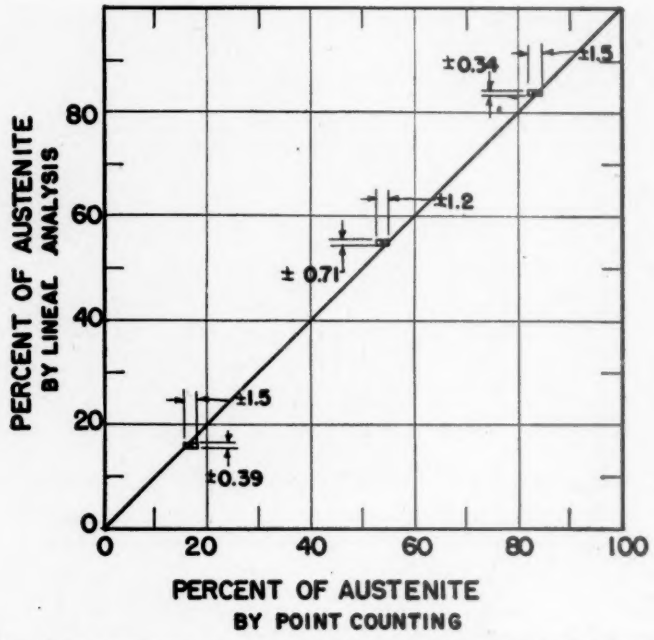

FIG 9—CORRELATION BETWEEN THE MEAN OF TEN DIFFERENT POINT-COUNTED MICROGRAPHS AND THE MEAN OF TEN DIFFERENT LINEAL TRAVERSES ON EACH OF THREE SPECIMENS. DIMENSIONS OF RECTANGLES INDICATE STANDARD ERRORS.

It may be said, then, that both methods of microanalysis are capable of yielding reliable answers, even when applied to complex structures of the austenite-martensite type, but the lineal procedure has the advantage of greater reproducibility and of better averaging for a given number of observations. Moreover, the Hurlbut counter makes the lineal method rapid and straight-forward. It avoids the necessity of picture-taking and permits the observor to scan larger areas than is feasible with a succession of high magnification micrographs. No detail is lost, as might be the case in picture-taking, and the observer can exercise better judgment in deciding the location of

constituent boundaries while looking at the structure "in the flesh" than he can when looking at a photograph thereof. Finally, the authors estimate that for the comparative data shown in Tables 3 and 5 the direct lineal analysis with the Hurlbut counter took approximately one-tenth the time required by the photographing and point-counting procedure.

Conclusions

1. A review of the literature has been presented on areal and lineal methods for measuring the relative amounts of micro-constituents. Of these, point-counting and the Hurlbut counter have been selected for comparative studies, using austenite-martensite structures for purposes of illustration

2. With the aid of impersonal statistical procedures, it has been demonstrated that both methods are reliable, whereas visual estimates may lead to erroneous results even though agreement among independent observers may be reasonably good.

3. Lineal analysis with the Hurlbut counter is superior to areal analysis by point-counting in the following respects:

a. Reproducibility
b. Averaging out segregations
c. Ease and speed of operation

Acknowledgments

The authors are indebted to the Republic Steel Corporation for a grant under which part of this research was conducted. Credit is also given to Mr. Donald Essman who carried out the point-counting work.

References

1. E. P. Polushkin: Determination of Structural Composition of Alloys by a Metallographic Planimeter. AIME *Trans.* (1925) **71**, 669.
2. R. A. Grange and H. M. Stewart: The Temperature Range of Martensite Formation. AIME *Metals Tech.* (June, 1946) T. P. 1996; *Trans.* (1946), **167**, 467.
3. A. H. Cottrell: Tensile Properties of Unstable Austenite and Its Low Temperature Decomposition Products. *Jnl Iron Steel Inst.* (1945) **151**.
4. S. G. Fletcher, and M. Cohen: The Effect of Carbon on the Tempering of Steel. A S M *Trans.* (1944) **32**, 333.
5. P. Gordon, M. Cohen, and R. S. Rose: The Effect of Quenching Bath Temperature on the Tempering of High Speed Steel. ASM *Trans.* (1944) **32**, 411.
6. P. Gordon, M. Cohen, and R. S. Rose: The Kinetics of Austenite Decomposition in High Speed Steel. ASM *Trans.* (1943) **31**, 161.
7. A. W. McReynolds: Electrical Observations of the Austenite-Martensite Transformation in Steel. *Jnl. App. Phys.* (1946) **17**, 823.
8. F. S. Gardner, M. Cohen, and D. P. Antia: Quantitative Determination of Austenite by X-Rays. AIME *Trans.* (1943) **154**, 306.
9. A. Delesse: Procede Mechanique Pour Determiner la Composition des Roches. *Annales des Mines* (1848) **13**, Fourth Series, 379.
10. H. C. Sorby: On Slaty Cleavage, as Exhibited in the Devonian Limestones of Devonshire. *Phil. Mag.* (1856) **11**, Fourth Series, 20.
11. W. J. Sollas: Contributions to the Knowledge of the Leinster Granites. *Trans.* Roy. Irish Acad. (1887–92) **29**, 471.
12. A. A. Julien: Genesis of the Amphibole Schists and Serpentines of Manhattan Island, New York. *Bull. Geol. Soc. Amer.* (Dec. 7, 1903) **14**, 466.
13. A. Rosiwal: Ueber Geometrische Gesteinsanalysen. Ein Einfacher Weg zur Ziffermaessigen Feststellung des Quantitaetsverhaeltnisses der Mineralbestandteile Gemengter Gesteine. Verhandlungen der K. K. Geologischen Reichsanstalt (1898) **5–6**, 143.
14. J. Hirschwald: Ueber ein Neues Mikroskopmodell und ein "Plainimeter Ocular" zur Geometrischen Gesteinanalysen. Centralblatt fuer Mineralogie und Paleontologie (1904), 626.
15. F. C. Lincoln and H. L. Rietz: The Determination of Relative Volumes of the Components of Rocks by Mensuration Methods. *Econ. Geol.* (1913) **8**, 120.
16. J. Joly: The Petrological Examination of Paving Sets. *Proc. Roy. Dublin Soc.* (1903–05) **10**, 62.
17. A. Johannsen: A Planimetric Method for the Determination of the Percentage Compositions of Rocks. *Jnl. Geol.* (1919) **27**, 276.
18. E. Thomson: Quantitative Microscopic Analysis. *Jnl. Geol.* (1930) **38**, 193.
19. M. W. Lightner and C. H. Herty, Jr.: The Traverse Impact Strength of Plain Carbon, Normalized Steels. Cooperative Bulletin 59 (1932). Carnegie Institute Tech. and Min. and Met. Advisory Boards.
20. H. S. Rawdon: Discussion of paper in reference (1).
21. E. R. Saunders and J. R. Kahles: A Study of Martensite Formation by a Photo-

metric Method. ASM *Trans.* (1942) **30,** 1139.
22. S. J. Shand: A Recording Micrometer for Geometric Rock Analysis. *Jnl. Geol.* (1916) **24,** 394.
23. C. K. Wentworth: An Improved Recording Micrometer for Rock Analysis. *Jnl. Geol.* (1923) **31,** 228.
24. W. F. Hunt: An Improved Wentworth Recording Micrometer. *Amer. Mineral.* (1924) **9,** 190.
25. C. Hurlbut: An Electric Counter for Thin Section Analysis. *Am. Jnl. Sci.* (1939) **237,** 253.
26. E. S. Larsen and F. S. Miller: The Rosiwal Method and the Modal Determination of Rocks. *Amer. Mineral.* (1935) **20,** 260.
27. S. W. Postel and H. M. Lufkin: Additional Data on the Delesse-Rosiwal Method. *Amer. Mineral.* (1942) **27,** 335.
28. F. Chayes: Linear Analysis of a Medium Grained Granite. *Amer. Mineral.* (1946) **31,** 261.

DISCUSSION

(*J. B. Austin presiding*)

J. B. AUSTIN*—Is it not true that these methods suffer from the basic handicap that one is looking at a polished specimen? As I understand it, one is comparing different methods of estimating the relative amount of each phase in a specimen as prepared by ordinary metallographic methods. Since such methods may not always reveal the true proportions of each structure, this still does not answer the question of what may actually be there.

*Research Lab., U.S. Steel Corp., Kearny, N.J.

R. T. HOWARD (author's reply)—That is correct.

J. B. AUSTIN—As I understand it, you are going to discuss the absolute calibration of these methods in a later paper.

R. T. HOWARD—That is correct. The issue pointed up by this paper is a matter of geometry rather than metallurgy. Metallographers are frequently handicapped in not having a convenient method for quantitatively estimating the proportions of constituents seen under the microscope. Obviously, unless the microstituents can be clearly revealed by polishing and etching, the methods described here cannot be applied properly. In this sense, metallographic art figures in the point-counting and lineal techniques. While some structures are too confused or finely dispersed to permit quantitative evaluation, there are nevertheless many cases in which the microstructures do clearly portray the relative amounts of the constituents. For example, little difficulty is experienced in using point-counting or lineal analysis for austenite-martensite (tempered) mixtures with 100 to 10 pct austenite, and good correlations with the X ray procedure of Gardner[8] have been obtained. However, when the austenite content is below about 8 pct, the etchant may not be sufficiently discriminating in delineating the austenitic areas, and this introduces an important case where metallographic methods are found wanting.

The Factorial Experiment in Engineering Research

By M. K. Barnett,* Junior Member AIME

(New York Meeting, March 1947)

Contents

	Page
A Practical Example in Experimental Design	428
Conventional Designs	428
Factorial Design	429
Expressions for Main Effects of Carbon, Manganese, and Phosphorus	429
Criteria for Judging Relative Merits of Designs	430
Precision of Conclusions	430
Comprehensiveness of Conclusions	431
Measurement of Interactions	431
Signs for Main Effects and Interactions	432
Advantages of Factorial Design	432
Two Additional Conventional Designs	433
Generalization of Factorial Design	433
Investigation of Subsidiary Factors	434
Determination of Mathematical Relation	435
Criticism of Factorial Design	436

Introduction

Engineering research consists, broadly speaking, in the investigation of the effect of the variations in a number of factors on some property of a product or characteristic of a process. The unambiguous description of the product or process requires that the property or characteristic be expressible in quantitative terms. For the purpose of practical control, it is likewise desirable that the independently variable factors governing the product or process be quantities, although this ideal goal is not always attained.

Maximum efficiency—i.e., the attainment of the maximum amount of reliable, useful information relating to the influence of the factors on the property of the product or characteristic of the process, for the least expense—is an important requirement for the satisfactory operation of a research organization. Obviously, a necessary condition for the attainment of maximum efficiency is an adequate knowledge of the specialized field in which the experimental research lies. While necessary, this condition is not sufficient. Proper attention must also be given to the general principles of experimental design together with the modern methods for the analysis and evaluation of experimental data.

The present discussion is confined to a single design, the so-called "factorial" design. This design is of special interest in that it attains its goal, maximum efficiency, by directly departing from the

Manuscript received at the office of the Institute Jan. 2, 1947. Issued as T.P. 2161 in Metals Technology, June 1947.

* Chemistry Department, University of Dayton, Dayton, Ohio. Formerly, Research Engineer, Battelle Memorial Institute, Columbus, Ohio.

time-honored practice of studying one factor or variable at a time, while holding all others constant.

Practical Example in Experimental Design

Suppose we wish to determine the influence of variations in carbon, manganese, and phosphorus contents on a certain property of cast iron. More specifically, suppose that we wish to determine the effect of raising the carbon from 3.00 to 3.50 pct, the effect of raising manganese from 0.30 to 0.60 pct, and the effect of raising phosphorus from 0.10 to 0.40 pct. The values of all other factors associated with the preparation and processing of the irons are assumed to be held relatively constant.

Let us ask ourselves, how may we design an experiment that will yield the maximum amount of information on the question at hand with the minimum expenditure of time and money; that is, the minimum number of tests? Suppose we put the question in a more specific form. Imagine that the allotment of funds for this particular experiment will suffice for the execution of only 24 tests. How should these 24 tests be utilized in order to furnish the maximum amount of information relevant to the effect of the specified variations in carbon, manganese, and phosphorus on the property?

Since there are three variable elements, each at two levels, there are eight possible compositions involving these different levels ($2 \times 2 \times 2 = 8$). To simplify the exposition, symbols are introduced for these compositions, which are given in Table 1. The letters c, m, and p denote carbon, manganese, and phosphorus, respectively. Whenever a composition contains the higher value of a particular element, the symbol for the element appears in the symbol for the composition; otherwise, it is omitted from the composition symbol. The symbol (1) denotes the composition in which all three elements are at their lower levels. Finally, the symbols of the first column of Table 1 are also used to denote the sums of the values of the specific property obtained from tests having these compositions. Thus, the symbol cp not only denotes the composition, 3.50 pct carbon, 0.30 pct manganese, 0.40 pct phosphorus, but also the sum of values of the specific property obtained from all tests having this composition.

Table 1—*Symbols for Compositions*

Composition Symbol	Composition, Pct		
	Carbon	Manganese	Phosphorus
(1)	3.00	0.30	0.10
c	3.50	0.30	0.10
m	3.00	0.60	0.10
p	3.00	0.30	0.40
cm	3.50	0.60	0.10
cp	3.50	0.30	0.40
mp	3.00	0.60	0.40
cmp	3.50	0.60	0.40

First Conventional Design

In designing the experiment in question, the research engineer might reason as follows: since 24 tests are available and three elements to be investigated, one third of the total, or eight tests, should be devoted to each element. Adopting some composition, say (1), as the standard or base composition, four tests would be made with carbon at the lower level and four with carbon at the higher level, manganese and phosphorus being maintained constant at the base level. The influence of carbon would then be determined by comparing the average value of the property obtained in four tests at the low-carbon level with the average of the four tests at the high-carbon level. The effect of manganese would be determined by the second series of eight experiments in which manganese was varied separately; and similarly for phosphorus. The layout of this design is represented

in Fig 1, where the 24 tests correspond to the 24 rectangles of the figure.

Second Conventional Design

Instead of employing a separate set of control tests for each element, a single set of control tests might be compared, in turn, with each set in which one element is varied at a time, the other two remaining at the low or control level. The experiment would thus consist of six control tests, six in which carbon was at the higher level, six in which manganese was at the higher level, and six in which phosphorus was at the higher level. The layout of the experiment is given in Fig 2.

(1)	c	(1)	m	(1)	p
(1)	c	(1)	m	(1)	p
(1)	c	(1)	m	(1)	p
(1)	c	(1)	m	(1)	p

FIG 1—FIRST CONVENTIONAL DESIGN.

(1)	(1)	(1)	(1)	(1)	(1)
c	c	c	c	c	c
m	m	m	m	m	m
p	p	p	p	p	p

FIG 2—SECOND CONVENTIONAL DESIGN.

(1)	c	(1)	c	(1)	c
m	p	m	p	m	p
cm	cp	cm	cp	cm	cp
mp	cmp	mp	cmp	mp	cmp

FIG 3—FACTORIAL DESIGN.

Factorial Design

Suppose that, instead of proceeding as in either of the conventional designs, we carry out tests on all of the eight possible combinations listed in Table 1. Since 24 tests are available, each composition may be tested in triplicate. Such an experiment, in which all possible composition combinations are represented, is said to be "factorially designed." The factorial design in the present case is illustrated in Fig 3.*

* For ease of comprehension the eight compositions of each replicate of the factorial design are represented in the same order on the diagram of Fig 3. In actual experimental work, for the sake of error control and measurement, the compositions should be randomized wherever possible. Thus, if the three replicates correspond to three different heats, the eight compositions should be poured in three different random orders from the three different heats.

EXPRESSIONS FOR MAIN EFFECTS OF CARBON, MANGANESE, AND PHOSPHORUS

In the First Conventional Design, the main effect of each element would be defined logically as the excess of the average value of the specific property measured for the four tests in which the element was maintained at its higher level over the average value of the specific property for the four corresponding control tests.

The expressions for the main effects of carbon, manganese, and phosphorus would then be $c/4 - (1)/4$, $m/4 - (1)/4$, and $p/4 - (1)/4$, respectively.

In the Second Conventional Design, the main effect of each element is defined as the excess of the average value of the specific property measured for the six tests in which the element was maintained at its higher level over the average value for the six control tests. The main effects of carbon, manganese, and phosphorus would be given by $c/6 - (1)/6$, $m/6 - (1)/6$, and $p/6 - (1)/6$, respectively.

Generalizing this definition for the Factorial Design, the main effect of each element is defined as the excess of the average value of the specific property measured for all compositions containing the element at its higher level over the average value for all compositions containing the element at its lower level. Thus, the main effects of carbon, manganese, and phosphorus, denoted by C, M, and P, respectively, are given by:

$$C = \frac{(c + cm + cp + cmp)}{12} - \frac{((1) + m + p + mp)}{12} \quad [1]$$

$$M = \frac{m + cm + mp + cmp)}{12} - \frac{((1) + c + p + cp)}{12} \quad [2]$$

$$P = \frac{(p + cp + mp + cmp)}{12} - \frac{((1) \times c + m + cm)}{12} \quad [3]$$

Since each composition is triplicated, each of the numerators in these expressions is the sum of 12 values, so that division by 12 gives the average. Note that the two averages entering into the expression for each main effect are strictly comparable, since for each composition entering into the one average there is a corresponding composition entering into the other, which differs from the first only in respect to the element whose main effect is being formulated. Thus, turning to the main effect of carbon, the two compositions of each of the following pairs are identical except for carbon content: c and (1), cm and m, cp and p, cmp and mp.

Criteria for Judging Relative Merits of Designs

Three criteria may be employed in judging the relative merits of the designs: (1) the precision or reliability of the conclusions; (2) the comprehensiveness or generality of the conclusions; and (3) the knowledge of interrelationships between the factors provided by the designs.

Precision of Conclusions

The precision of the comparison of two average values increases as the number of items entering into the averages increases; for common sense tells us that, as this number increases, there is less likelihood that an observed difference in the averages is accidental.

The Second Conventional Design determines the main effects of the three elements with greater precision than does the First Conventional Design, because, in the former, these effects are expressed as the differences in the average values of two groups of six items each, whereas in the latter they are expressed as the differences in the average values of two groups of only four items each. The Factorial Design determines these main effects with still greater precision, since each main effect is expressed as the difference in the average values of two groups of 12 items each. In fact, as a result of the symmetry of this design, all of the data enter into the expression for each main effect, so that each such effect is determined with the same precision that a conventional design would yield for the effect of one element if all 24 tests were devoted to the study of that element alone.*

* True, the precision of an average decreases as the scatter among the items entering into the average increases. Since the averages entering into the expressions for the main effects of the Factorial Design comprise dissimilar items while those employed in the main effects for the conventional designs include only absolute replicates, it might be supposed that the main effects of the Factorial Design, in spite of the greater number of measurements entering into them, might be determined with no more, or even less, precision than those of the conventional designs. However, in the statistical analysis of the Factorial Experiment, any variation in the observed effect of a factor, associated with the variation in the values of other factors, is segregated from the principal or main effect of the given factor (by a procedure called "the analysis of variance"), so that such variation does not affect the precision with which this main effect is determined.

To be reliable, a main effect must be significantly greater than the experimental error, so that the determination of the degree of reliability necessitates a comparison of the effect with the error. Therefore, a sensitive measure of reliability requires that the experimental error, as well as that of the effect, be measured with sufficient precision. In the factorial experiment in question, the discrepancies among the eight sets of triplicate measurements provide a pooled estimate of the experimental error of maximum precision. Pooling of the error is based on the assumption of a uniform distribution of error throughout all the tests—an assumption that is approximately realized provided suitable attention be given to the control and randomization of the accidental factors responsible for the error.

Comprehensiveness of Conclusions

A great disadvantage of the conventional designs is the restricted nature of their conclusions; that is, these conclusions hold only under the special set of "control" conditions. Thus, in our example, suppose that an experiment, laid out according to either the First or Second Conventional Design, showed that the specific property being measured decreased as the phosphorus content increased from 0.10 to 0.40 pct. This conclusion obviously would have been established only for the control conditions; i.e., while manganese was held at 0.30 pct and carbon at 3.00 pct. One immediately wonders, is this effect of phosphorus necessarily associated with the particular levels of manganese and carbon under which it was observed, or is it a general effect, which holds at other levels as well? Clearly, the conventional designs as they are outlined in Figs 1 and 2 provide no answer to this question, but merely point to the necessity of repeating the experiment with new choices of control conditions.

It is quite otherwise with the factorially designed experiment. From the formulas given for the main effects of carbon, manganese, and phosphorus, it is quite evident that these measure the effect of each element, not while the remaining two are held constant but while they are assuming, in turn, all possible combinations of values. Thus, the main effect of carbon can be analyzed as shown in Table 2.

TABLE 2—*Main Effect of Carbon*

CONDITION	CARBON EFFECT
Mn at high level, P at low level...	$(\frac{1}{2})(cm - m)$
Mn and P at high levels.....	$(\frac{1}{2})(cmp - mp)$
Mn and P at low levels.....	$(\frac{1}{2})(c - (1))$
Mn at low level, P at high level...	$(\frac{1}{2})(cp - p)$
Average or main effect of carbon:	$\frac{c + cm + cp + cmp - (1) - m - p - mp}{12}$

These main effects are thus over-all effects pertaining not to any special set of conditions but to the whole range of conditions embraced by the experiment. R. A. Fisher* has aptly described this feature of factorially designed experiments in the statement that such experiments provide a "wider basis of inductive inference."

Measurement of Interactions

Not only does the factorial experiment furnish conclusions respecting the main effects that are independent of any special conditions; it also provides a quantitative measure of the influence of changes in these conditions on the main effects. These influences are called "interactions" between the factors.

The interaction between two factors is logically measured by the influence that the change in level of one factor exerts on the effect of the other factor.

Turning to our example, the quantity

$$(cmp - mp) + (cm - m)$$

is a measure of the effect of carbon when manganese is at its higher level, while the quantity

$$(cp - p) + [(c - (1))]$$

is a measure of the effect of carbon when manganese is at its lower level. The excess of the first quantity over the second would be a measure of the influence, on the effect of carbon, of increasing the manganese content. Division by 12 is necessary to make the expression for the interaction comparable with those for the main effects. Denoting the interaction by CM, we have, after rearrangement of terms,

$$CM = \left[\frac{(cmp + cm + p + (1))}{12}\right] - \frac{(cp + mp + c + m)}{12} \quad [4]$$

The interactions between carbon and phosphorus (CP), and between manganese

* R. A. Fisher: The Design of Experiments. Edinburgh, 1937. Oliver and Boyd

and phosphorus (MP), are obtained in a similar manner and are given by:

$$CP = \left[\frac{(cmp + cp + m + (1))}{12}\right] - \frac{(cm + mp + c + p)}{12} \quad [5]$$

and

$$MP = \left[\frac{(cmp + mp + c + (1))}{12}\right] - \frac{(cm + cp + m + p)}{12} \quad [6]$$

There exists only one such interaction between any two factors. Thus, the effect of manganese, with carbon at its higher level, is measured by

$$(cmp - cp) + (cm - c)$$

and, with carbon at its lower value, by

$$(mp - p) + (m - (1))$$

The excess of the first quantity over the second becomes, after division by 12, the same as the expression 4 already given for CM. Therefore, the effect of manganese on the effect of carbon and the effect of carbon on the effect of manganese are two logically implicated, reciprocal effects, and are quantitatively identical.

When we are dealing with three elements or factors, as in the present case, there exists one so-called second-order interaction. In our example, for instance, this expresses the influence of phosphorus on the effect of manganese on the effect of carbon. Thus, the effect of manganese on the effect of carbon, when phosphorus is at its higher level, is measured by

$$(cmp - mp) - (cp - p)$$

and, when phosphorus is at its lower level, by

$$(cm - m) - (c - (1))$$

The excess of the first quantity over the second would be a measure of the influence of phosphorus on the effect of manganese on the effect of carbon. Denoting this interaction by CMP, we obtain, after division by 12 and rearrangement of terms,

$$CMP = \frac{cmp + p + m + c}{12} - \frac{mp + cp + cm + (1)}{12} \quad [7]$$

Since each interaction is expressed as the difference between the averages of 12 values, it is evident that the interactions are determined with the same precision as the main effects.

Signs for Main Effects and Interactions

Each of the main effects and interactions is formed from the same eight quantities; namely, (1), c, m, p, cm, mp, and cmp, denoting the sums of three values for the specific property being measured obtained from triplicate tests. The appropriate signs to be assigned these quantities, in order to obtain the desired main effect or interaction, are summarized in Table 3. After combining the eight quantities in the manner indicated in the table, division by 12 will then give the desired main effect or interaction.

TABLE 3—*Signs of Components for Main Effects and Interactions*

Effect	Sign of Component							
	cmp	cm	cp	mp	c	m	p	(1)
C	+	+	+	−	+	−	−	−
M	+	+	−	+	−	+	−	−
P	+	−	+	+	−	−	+	−
CM	+	+	−	−	−	−	+	+
CP	+	−	+	−	−	+	−	+
MP	+	−	−	+	+	−	−	+
CMP	+	−	−	−	+	+	+	−

ADVANTAGES OF FACTORIAL DESIGN

The following advantages are claimed for the factorial design over the conventional designs:

1. Greater precision is obtained without increasing the number of tests.

2. Conclusions are not limited by an arbitrary set of control conditions.

3. Interactions between the various factors are ascertained with the same precision as the main effects and without increasing the number of tests.

Two Additional Conventional Designs

Another very popular type of design is one in which replication is dispensed with or diminished in favor of assigning a variety of values or levels to each factor. Consideration of such designs has been delayed because they attempt to answer a different question than did the other three designs and are not strictly comparable with them.

Thus, in our example; the 24 tests might be allocated equally among the three elements as in the First Conventional Design, but, instead of assigning only two extreme values to each factor, eight different values, distributed in the interval embraced by the extreme values, might be assigned to each factor. Or, again, four different values might be distributed in the interval, thus permitting duplicate determinations. These two alternatives, here called the Third and Fourth Conventional Designs, are represented diagrammatically in Figs 4 and 5, respectively.

Any conclusion that may be drawn from the Third and Fourth Designs regarding the effect of a factor holds only for the special control conditions adopted for the other two factors. Further, those designs provide no information whatever about the interactions between the factors. In these respects, the Third and Fourth Conventional Designs are similar to the First and Second Conventional Designs.

In the Fourth Design, the effect of a factor, as measured by the difference in average values for the specific property being measured associated with any two levels of the factor, is even less precisely determined than it was in the First Conventional Design, since only two items now enter into each of these averages. The Third Design is not directly comparable with the other designs in respect to precision, since the precision of the former must derive from the consistency of a trend rather than from the behavior of replicates or parallels.

C Variable		Mn Variable		P Variable	
3.00	3.07	0.30	0.34	0.10	0.14
3.14	3.21	0.38	0.42	0.18	0.22
3.28	3.35	0.46	0.50	0.26	0.30
3.42	3.50	0.55	0.60	0.35	0.40
Mn = 0.30 P = 0.10		C = 3.00 P = 0.10		C = 3.00 Mn = 0.30	

FIG 4—THIRD CONVENTIONAL DESIGN.

C Variable		Mn Variable		P Variable	
3.00	3.00	0.30	0.30	0.10	0.10
3.17	3.17	0.40	0.40	0.20	0.20
3.34	3.34	0.50	0.50	0.30	0.30
3.50	3.50	0.60	0.60	0.40	0.40
Mn = 0.30 P = 0.10		C = 3.00 P = 0.10		C = 3.00 Mn = 0.30	

FIG 5—FOURTH CONVENTIONAL DESIGN.

Generalization of Factorial Design

The factorial design is applicable to many types of research problems. All that is required is that at least two independently controlled factors be involved, each capable of assuming at least two levels, and that the property or characteristic, whose dependence on the given factors is being examined be capable of quantitative expression. The factors themselves need not be quantities. Thus, "type of quenchant" might be a factor in a heat-treating experiment, and "oil" and "water" its two levels. Factors need not be all of the same kind: some may relate to composition, others to heat-treatment.

In practice, designs involving more than three factors at more than two levels may arise. To detect the presence of maximum or minimum effects with respect to a given factor, at least three levels are required. Not all the factors need have the same number of levels.

As the number of factors increases, the advantage in precision associated with the factorial design over the conventional designs also increases.

Table 4 illustrates a factorial design devoted to the study of the dependence of the property X of a series of steels on composition (8 levels), quenching treatment (4 levels), and pretreatment (2 levels). There are $8 \times 4 \times 2 = 64$ possible treatment combinations involving these three factors. The combinations were tested in duplicate, and the resulting 128 values comprise the body of the table.

TABLE 4—*Results of an* $8 \times 4 \times 2$ *Factorial Experiment Devoted to the Influence of Variations in Composition* (8 *Levels*), *Quenching Treatment* (4 *Levels*), *and Pretreatment* (2 *Levels*) *on the Property X**

(Each of the 64 composition-treatment combinations was duplicated. These duplicate values are reported as pairs in the table.)

Heat No.	Pre-treatment	Quenching Treatment				
		No. 1	No. 2	No. 3	No. 4	Average
10900						
	A	55, 56	28, 24	55, 47	12, 0	34.6
	B	29, 20	16, 8	6, 12	0, 0	11.4
	Av.	40.0	19.0	30.0	3.0	23.6
10901						
	A	11, 11	9, 10	0, 0	0, 0	5.1
	B	39, 26	5, 0	0, 2	0, 0	9.0
	Av.	21.7	6.0	0.5	0	7.1
10902						
	A	16, 20	12, 8	8, 24	0, 0	12.3
	B	29, 21	4, 2	0, 4	0, 0	7.5
	Av.	21.5	6.5	11.5	0	9.9
10903						
	A	34, 46	13, 14	9, 8	0, 13	17.1
	B	16, 23	10, 11	7, 3	12, 14	12.0
	Av.	29.7	12.0	6.7	9.7	14.6
10904						
	A	33, 31	63, 32	48, 82	0, 16	38.1
	B	37, 32	8, 13	11, 7	0, 2	13.8
	Av.	33.2	29.0	37.0	4.5	25.9
10905						
	A	73, 82	72, 84	45, 45	41, 40	60.3
	B	46, 56	59, 54	43, 27	25, 16	40.8
	Av.	64.2	67.2	40.0	30.5	51.1
10906						
	A	83, 72	35, 35[a]	14, 0	38, 60	42.1
	B	36, 32	41, 36	0, 0	14, 20	22.4
	Av.	55.7	36.7	3.5	33.0	32.3
10907						
	A	58, 58[a]	34, 26	9, 7	10, 2	25.5
	B	39, 49	29, 28	4, 4	11, 5	21.1
	Av.	51.0	29.2	6.0	7.0	23.3
Average, All Heats						
	A	46.2	31.2	25.7	15.1	29.4
	B	33.1	20.3	8.1	7.4	17.2
	Av.	39.7	25.7	16.9	11.0	23.3

[a] Filled in value.

* Reproduced by permission of Battelle Memorial Institute.

For the determination of the main effect of pretreatment, the data are divisible into two equal groups corresponding to the two types of pretreatment. The two groups are identical in all respects except pretreatment, so that the average values of X corresponding to them (29.4 and 17.2) are comparable and provide a measurement of the main effect of pretreatment. Similarily, division of the data into four equal groups, all identical except for quenching treatment, provides four averages (39.7, 25.7, 16.9, and 11.0) whose variation gives a measure of the main effect of quenching treatment. Finally, divison of the data into eight equal groups, all identical except for composition (heat number), provides eight averages (23.6, 7.1, 9.9, 14.6, 25.9, 51.1, 32.3, and 23.3) whose variation gives a measure of the main effect of composition.

As in the earlier example, there will be three first-order interactions, expressing the influence of quenching treatment on pretreatment, composition on pretreatment, and composition on quenching treatment, and one second-order interaction, expressing the influence of composition on the effect of pretreatment on the effect of quenching treatment. For example, the interaction between quenching treatment and pretreatment is expressed by the variation among the four differences: $46.2 - 33.1 = 13.1$, $31.2 - 20.3 = 10.9$, $25.7 - 8.1 = 17.6$, and $15.1 - 7.4 = 7.7$.

Subsidiary Factors

In every experimental investigation questions arise as to which of several

possible techniques are to be employed in the preparation and examination of the test material. In a melting experiment on cast metals, one may be confronted with the task of choosing the melting unit, the degree of superheat, the pouring temperature, the foundry sand, type of raw materials, the test bar pattern, or other factor. Such subsidiary factors, whose investigation is not the main object of the experiment, are always present as potential sources of variation.

If we adopt a rigid set of standard conditions corresponding to fixed values of the subsidiary factors, our experimental results are immediately open to the criticism that they have been established only for the narrow set of conditions achieved by standardization—a circumstance that may impose serious restrictions on the practical value of the research. If a sufficient number of replicates be available, the generality of the results may be greatly extended by incorporating the subsidiary factors along with the main factors in a single factorial design.

For illustration, suppose our problem is the determination of the effect of five different pig irons on the quality of the cast iron made from them. Assume the variability of the material and process requires, and the budget allows, eight heats with each pig iron. Should the heats be melted in the induction furnace or the gas-fired pot furnace? Should all of the silicon be added in the charge or a portion introduced as inoculant? If we make all heats in the induction furnace and add all of the silicon in the charge, the hereditary influence of the pig irons may not be the same as it would have been if some other combination of values had been chosen for those two subsidiary factors. However, if we incorporate the pig-iron iron factor along with subsidiary factors in a single $5 \times 2 \times 2$ factorial experiment, the generality of any conclusions respecting hereditary influences of the pig irons will be greatly extended, although there will still remain 20 pairs of duplicate heats for the estimation of the experimental error. The main effect of the pig-iron factor will be established with the same precision as though a single melting unit and method of silicon addition had been employed throughout; and, in addition, the effects of the subsidiary factors will be established with the same precision. Finally, any interrelationships between the pig-iron factor and the subsidiary factors will be thoroughly explored.

Determination of Mathematical Relation

Suppose that our problem, concerning the effect of variation of carbon, manganese, and phosphorus on a specific property of cast iron, had been the more formidable one of establishing a mathematical equation expressing the value of that property as a function of the three elements. Considerably more than 24 tests would be required to establish such a relation with any degree of precision. However, even with a large volume of data available, the problem still may present great difficulty because of doubt as to which form of relation to use. In this connection, the factorial design, by thoroughly exploring both main effects and interactions, can perform a useful service.

If we denote the specific property by I, the percentages of the three elements by c, m, and p, a function of x by $f(x)$, and a function of x and y, in which the variables are inseparable, by $f(x, y)$, the most general form of the equation relating I to c, m, and p, would be

$$I = f(c) + f(m) + f(p) + f(c, m) + f(c, p) + f(m, p) + f(c, m, p)$$

A factorial experiment, devoted to the effect of the three elements, should determine which of the terms in this general

expression need be retained; for the seven terms of the right-hand member clearly correspond to the three main effects, the three first-order interactions, and the single second-order interaction, which in the factorial design are investigated with equal precision. Thus, if all interactions are insignificantly small, all but the first three terms of the right-hand member may be dropped. The value of the property then becomes an additive function of the three elements, though it need not be linear. If certain interactions are significant, the terms corresponding to them must be retained. Thus, if the interaction between carbon and manganese is significant, the fourth term of the right-hand member must be retained, so that our final expression will contain a term, say, of the form kcm, where k is a constant. Having determined the general form of the relation, the task of evaluating the f functions by multiple correlation analysis will be greatly simplified.

Criticism of Factorial Design

By considering several criticisms of the factorial design, its proper function in experimental work may be better understood.

Excessive Generality

The factorial design is sometimes criticized on the basis that it establishes the main effects only for a widely varying set of conditions, whereas the effects under specialized conditions are of greater interest. Such a statement represents a misunderstanding of the proper function of the design rather than a valid criticism of it. In the first place, the design does measure the effects under special conditions. Thus, in our initial example of the design, the effect of carbon when manganese and phosphorus are held constant at their lower levels is given by $\frac{c - (1)}{3}$. However, such a specialized effect is determined only with greatly reduced precision. The fundamental answer to the criticism is that the design is suited only to cases where greater generality for the main effects and knowledge of the interactions are desired. To be sure, even when these conditions are not met, the factorial design will still provide greater precision for its main effects than any comparable designs. However, a high degree of precision does not enhance the value of an irrelevant conclusion.

Thus, in the initial example, it was tacitly assumed that the greater generality of the main effects and the knowledge of interactions provided by the design constituted a real advantage. If this had not been true, one of the conventional designs should have been employed—which particular conventional design would depend on the number of levels of particular interest and on the number of absolute replicates required to establish the conclusions.

Assumption of Linearity

One hears the criticism that two-level factorial experiments assume "linear" relations between the dependent variable and each factor. Such a criticism is erroneous since the question of the form of the relation is not even raised in such experiments. To determine the form of the relation, either the number of levels of the factor must be increased, thus increasing the number of tests required, or one of the conventional designs, involving three or more levels, must be employed at the expense of generality and the knowledge of interactions.

Excessive Number of Tests

A more valid criticism of the factorial design derives from the rapid increase in the number of tests required as the number of factors or levels increases. Thus, in a four-factor experiment, with two factors at three levels and two at

two levels, $3 \times 3 \times 2 \times 2 = 36$ treatment combinations would exist. To provide a measure of experimental error, tests should be at least duplicated, so that a minimum of 72 tests would be required.

To make the advantages of the factorial design practically attainable, economy must be practiced in choosing both factors and levels. As already noted, only factors whose interrelationships are of promising practical importance should be incorporated in the same design. If an investigation involves three melting-practice factors and three heat-treating factors, $2^6 = 64$ treatment combinations would result from the introduction of all six factors into the same design, each at two levels. However, if interactions between melting factors and heat-treating factors are of little interest, these factors should be segregated into two designs, thus reducing the number of treatment combinations to $2 \times 2^3 = 16$.

If maxima or minima are suspected, or if intermediate levels are of special interest for some other reason, one will naturally specify intermediate levels for some of the factors. Frequently, however, the principal reason for the inclusion of three or more levels of a factor rather than two is the feeling that the observed difference in results characterizing the upper and lower levels requires the supporting evidence of an intermediate result associated with an intermediate level before a "trend" can be established. The result obtained with the intermediate level has little significance in itself, but merely gives added weight to the observed difference associated with the two extreme levels. In factorial experiments, however, the difference between upper and lower levels is established with much greater precision, so the inclusion of the intermediate level as supporting evidence may be avoided.

The minimum number of tests required for a factorial experiment may sometimes be halved by employing one or more of the interactions as a measure of the error, thus avoiding the necessity for absolute replication. For example, in a two-level, five-factor experiment, the three third-order interactions, as well as the single fourth-order interaction, might be regarded as having no known practical significance; hence the variation associated with these interactions could be lumped together to provide a measure of experimental error, thus reducing the required number of tests from 64 to 32. In other cases, an interaction, even though its physical meaning be perfectly clear, nevertheless provides a logical measure of the experimental error whereby the significance of the main effects may be measured.*

Even though the ultimate intention be to investigate the factors at a variety of levels, whose incorporation into a single factorial design would entail a prohibitive number of tests, a two-level factorial experiment, embracing only the extreme levels of the factors, may be employed as the most economical means for conducting a preliminary exploratory survey of the principal features of the factors and their interactions. The results of such an experiment will not only give a reliable indication as to which factors merit further investigation by means of multilevel conventional designs but will provide a more logical basis for selection of the control conditions for such designs.

Excessive Heterogeneity

In order that a main effect or interaction of a factorial experiment may be reliable, the observed variation associated with it must be significantly greater than the variation assigned to experimental error. The larger number of treatment combinations required by the factorial experi-

* R. A. Fisher: *Op. cit.*, 219.

ment may be undesirable, not necessarily because of the prohibitive expense but because they require the extension of the experiment over a wider variety of experimental conditions, thereby increasing the variation associated with error and correspondingly decreasing the likelihood that the experiment will yield reliable main effects and interactions.

To illustrate this difficulty and its remedy, let us return to the earlier example, the $2 \times 2 \times 2$ factorial experiment, with three replicates, devoted to the study of the effect of variations in carbon, manganese and phosphorus on a specific property of cast iron. If, by means of ladle adjustments, all 24 test pieces could be poured from a single heat, preferably in random order, no difficulty would arise. The experiment could also be simply handled if as many as eight test pieces could be poured from one heat. Three heats would then be required, the eight tests of the same set of replicates being poured in random order from the same heat. Since the expressions for the main effects and interactions would involve only comparison of tests from the same heat, any difference among the heats, such as degree of superheat, gas content, and elementary composition, other than the three studied, would have no effect on the reliability of the results. In the analysis of the experiment, the variation due to such causes would be eliminated from the estimate of the experimental error.

A real difficulty arises, however, if we suppose that no more than four tests can be poured from one heat. Each set of replicates will then extend over two heats, and any inherent variation between the quality of the heats will increase the experimental error and decrease the reliability of the results.

This difficulty, and others like it, may be overcome by a device known as "confounding," but only at the expense of our knowledge of higher-order interactions. Thus, suppose that, instead of distributing the eight tests of each set of replicates at random over each pair of heats, we assign the compositions cmp, p, m, c to one of the heats, and the remaining ones, mp, cp, cm, (1), to the other. Eq 7 shows that the difference between the average property value, for the tests of the first heats of the three pairs and the average for the second heats of the three pairs is formally identical to the second-order interaction CMP. Actually, the procedure sacrifices our knowledge of this interaction, since any observed difference between the two averages may be the result of the difference in the quality of the heats. On the contrary, any variation among the heats will not reduce the reliability of the main effects and first-order interactions. For the expression for each of these is formed by combining a contrast of one pair of compositions with another pair from the same heat with a similar contrast in the other heat. Thus, the main effect of carbon is found by combining the contrast

$$(cmp + c) - (p + m)$$

involving only compositions from the first heat, with the contrast

$$(cp + cm) - [(mp + (1))]$$

involving only compositions from the second heat. Any variation due to the difference in quality of the heats may now be eliminated from the estimate of the error, with the result that the main effects and first-order interactions are determined with the same reliability that would have resulted from pouring all eight compositions from the same heat.

A New Method for Making Rapid and Accurate Estimates of Grain Size

By Frederick C. Hull,* Member AIME

(New York Meeting, March 1947)

The grain size of a metal or alloy is one of the most important factors determining its properties. In steels, for example, grain size affects hardenability, toughness and machinability; in brasses, grain size is related to hardness and deep-drawing quality. In the field of heat-resistant alloys, grain size has a marked effect on ductility, creep and endurance strength. In order to determine these effects, as well as to control the properties of materials, many accurate and rapid measurements of grain size must be made. This paper presents a new and improved method for the estimation of grain size.

Usual Methods of Evaluating Grain Size

A frequently used method of estimating grain size is that of comparing the image of a polished and etched specimen on the ground-glass screen of a metallographic microscope with standard grain-size charts. Several types of standards are available for use with different classes of microstructures.

Geometric Grids.—The Metals Handbook[1] has a series of hexagonal grids ranging in size from ASTM No. 1 to 8.

Idealized Grain Networks.—Idealized grain-boundary networks for ASTM grain sizes 1 to 8 are included in the American Society for Testing Materials Tentative Standard E19-39T.

Standard Micrographs.—The Metals Handbook and ASTM Tentative Standard E19-39T contain micrographs of hypoeutectoid and hypereutectoid steels ranging in grain size from No. 1 to 8.

The grain size of annealed brass (diameter of the average grain in millimeters) is obtained by comparison with 10 micrographs of varying grain size in ASTM Tentative Standard E2-39T.

A handicap to accurate evaluation of grain size by this method is the fact that it is difficult to compare photographs in a dimly lighted room with the image on the ground-glass screen, or, if the general illumination is increased so that the printed standards may be clearly seen, the contrast of the image of the unknown is decreased. It is easier to estimate grain size by comparing a micrograph of the unknown with the grain-size standards. However, photographing every specimen on which the grain size is desired is too costly in time and materials to be practicable.

For hardened steels, the Shepherd or Jernkontoret fracture grain-size standards are very accurate and useful, but this method obviously cannot be applied to ductile alloys such as brass, stainless steels and austenitic heat-resistant alloys.

Jeffries' method for grain-size measurements consists of counting the number

Manuscript received at the office of the Institute Jan. 2, 1947 Issued as T.P. 2160 in Metals Technology, June 1947.

* Research Metallurgist, Westinghouse Research Laboratories, East Pittsburgh, Pennsylvania.

[1] References are at the end of the paper.

of grains per unit area of the image on the ground-glass screen. The only objection to its use is the time required for counting a sufficiently large number of grains on

grain-boundary networks is that if the distribution of grain sizes is similar in unknown and standard, the operator can concentrate on matching the general

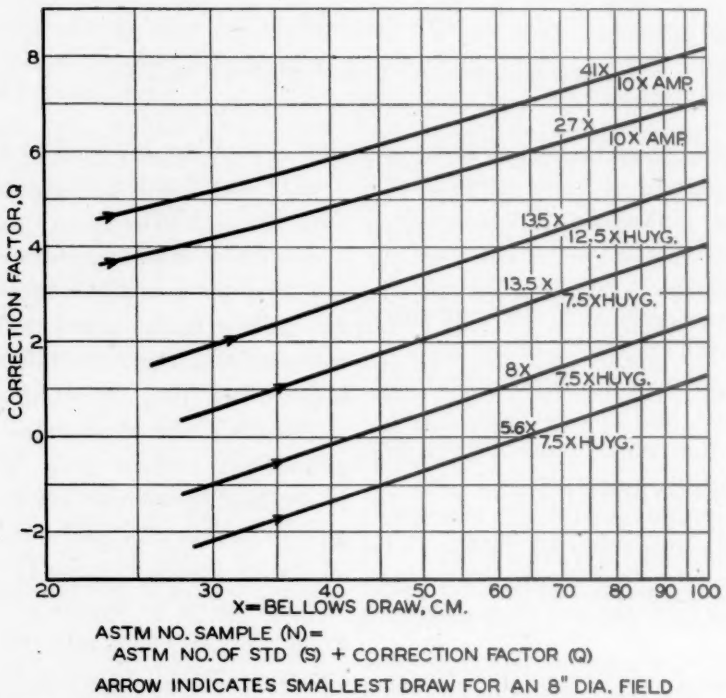

FIG 1—DETERMINATION OF ASTM GRAIN SIZE BY COMPARISON METHOD.

several areas to get an accurate evaluation of the grain size of the sample. This method is the theoretically correct way to determine the actual ASTM grain-size number of a given field of a specimen and was so used throughout this paper.

A grain-size micrometer eyepiece may be used with a microscope to estimate the grain size of a sample. A revolving disk with eight square grids of different sizes can be superimposed on the image of the specimen until the closest match is found. Estimates made with square or hexagonal grids as standards are usually coarser than the actual grain size because the observer misses the small grains in the unknown. The advantage of micrographs of actual materials or idealized appearance and does not have to compensate mentally for different percentages of small grains.

The tool-steel industry has adopted the intercept method of Snyder and Graff[2] for measuring and reporting grain size of high-speed steels. The number of grains intersected by a 5 in. line on an image of the specimen at 1000 diameter magnification is determined. Ten fields are examined, and the average number of intersections is reported as the grain-size number.

W. A. Johnson[3] has developed a method for determining the spatial grain size of metals that is suitable for special problems. From the frequency distribution of grain areas on the plane of polish,

the distribution of grain sizes in space is calculated. The average spatial grain size is then obtained by averaging on the basis of spatial grain-boundary area.

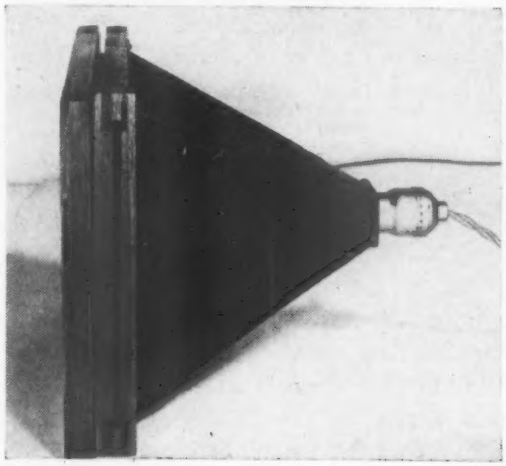

FIG 2—GRAIN-SIZE COMPARATOR FOLDED FOR STORAGE.
Slot in illuminator frame enables operator to select standard that matches unknown in general appearance.

The principal objection to the procedure is that one to two hours is required to classify the size of each of several hundred grains in one field of a single specimen. Even though the spatial grain count yields an accurate value for the field examined, since most materials exhibit considerable variation in grain size from area to area, this value may not necessarily be representative of the entire specimen. One grain count takes so much time that it is not generally feasible to evaluate more than one field on a specimen. Faster methods of estimation, however, permit several areas of the specimen to be evaluated with consequent gain in accuracy, as will be proved later.

THE COMPARISON METHOD

A new method for making rapid estimates of ASTM grain size has been devised that overcomes most of the limitations found in conventional methods. The method is based upon a comparison of the image of the sample on the ground-glass plate of a metallograph with a grain-size standard transparency illuminated

FIG 3—GRAIN-SIZE COMPARATOR IN USE.
Operator keeps image of unknown sharp with remote focusing screw as he adjusts bellows position until two images match.

by transmitted light.* This method differs from conventional comparison methods in the practice of choosing a suitable objective and eyepiece and varying the bellows extension until the image of the unknown has the same number of grains per unit area as the standard. When the observed bellows extension is referred to a curve for the particular optical system in use, Fig 1, a correction factor Q can be obtained which, when added to the ASTM grain size of the standard, yields the ASTM grain size of the unknown.†

The apparatus, illustrated in Figs 2 and 3, consists of a ground-glass plate‡ held in a frame that slides into the back of the camera in place of the plate holder or focusing screen. A light-weight illuminat-

* The use of a transparency is not new (see C. H. Davis.[4]).

† Other curves may be readily prepared, if desired, to yield results directly in terms of number of grains per square millimeter, diameter of the average grain in millimeters or grain intercepts on a 5-in. line at any magnification.

‡ The corners of the ground-glass plate should be cut off to permit free passage of air as the bellows are collapsed or extended.

ing unit is fastened to the frame, thereby providing simultaneous movement of the standard and the camera back. The two fields will therefore always be close together and the eyes may readily shift from one to the other in making a comparison without having to accommodate for a change in distance of the images. In addition to reducing the storage space, the hinged connection between the frame and the illuminating unit permits the angle of the standard screen to be adjusted so that the operator's line of sight is perpendicular to both images.

A slot is provided in the illuminating unit so that different standard transparencies may be substituted when desired. A ground glass is also inserted to diffuse the light from a 10-watt bulb. The more nearly the standard transparency matches the color and brightness of the image of the unknown, the more favorable are the conditions for making an accurate grain-size estimate. The intensity of the light can be varied by controlling the voltage with a variable transformer.

Fig 3 is a photograph of the grain-size comparator in use. The operator varies the bellows extension with one hand until the unknown matches the grain size of the standard. Minor adjustments in focus are required to keep the image sharp as the bellows are moved, but these can be made easily with the other hand.

Mathematical Analysis of the Comparison Method

The mathematical relationships that form the basis for the comparison method were derived from three fundamental expressions:

$$n = 2^{N-1} \qquad [1]$$

$$\frac{n}{n_M} = \left(\frac{M}{100}\right)^2 \qquad [2]$$

$$M = \frac{mx}{25.4} \qquad [3]$$

where n = number of grains per square inch of the unknown at 100 diam magnification.

N = ASTM grain-size number sought.

M = linear magnification.

m = product of objective magnification number and eyepiece power.

x = bellows extension, cm.

n_M = number of grains per square inch on ground-glass screen at magnification M.

Eq 1 defines the ASTM grain-size number N. Eq 2 states the well-known fact that the number of grains per square inch in the image varies inversely with the square of the magnification. Eq 3 states that the magnification of an image projected on the ground-glass screen is proportional to the bellows extension, the proportionality factor depending upon the objective and eyepiece selected.[5]

When an estimate is made by the comparison method, the bellows extension is varied until at a magnification M the image of the unknown has the same number of grains per square inch as the standard. At that point,

$$n_M = 2^{S-1} \qquad [4]$$

where S = the ASTM grain size of the standard. Now the number of grains per square inch that the sample would have at 100× can be obtained from Eq 2.

$$n = n_M \left(\frac{M}{100}\right)^2 = 2^{N-1}$$

Substituting for n_M from Eq 4,

$$2^{N-1} = 2^{S-1}\left(\frac{M}{100}\right)^2$$

$$2^{N-S} = \left(\frac{M}{100}\right)^2 \qquad [5]$$

Setting $N - S = Q$ yields [6]

$$2^Q = \left(\frac{M}{100}\right)^2 \text{ or} \qquad [7]$$

$$Q = 6.64 \log \left(\frac{M}{100}\right) \qquad [8]$$

Eq 8 can be placed in more convenient form for use with the comparison method by substituting for the magnification in terms of the bellows extension:

Then $$Q = 6.64 \log \frac{mx}{2540} \qquad [9]$$

$\frac{m}{2540}$ is a constant for any optical system so that Q versus bellows extension is a straight line on semilog paper.

The magnification of the Westinghouse Research Laboratories' Bausch and Lomb metallograph has been determined for several combinations of objectives, eyepieces and bellows extension. The magnification always varies linearly with bellows draw, but is not proportional to it in all cases. With the 10× negative amplifier eyepiece there is an appreciable negative intercept on the x axis. The magnification may then be accurately expressed by the equation,

$$M = \frac{m}{25.4}(x - b) \qquad [10]$$

where b = the intercept on the x axis in centimeters.

Calculated values of m and measured values of m and b for various optical systems are listed in Table 1. For accurate work on other metallographs, it is recommended that the magnifications of these instruments be determined and corrected values for m and b be established.

Substituting M from Eq 10 in Eq 8 yields,

$$Q = 6.64 \log \frac{m}{2540}(x - b) \qquad [11]$$

The correction factors Q for the Research Laboratories' metallograph for various optical systems are plotted in Fig 1. When b is zero, the lines are straight and parallel. The arrow on each curve represents the smallest bellows draw that will give an image 8 in. in diameter.

Accuracy of Estimation of Grain Size by Various Methods

Accuracy of Comparison Method

The comparison method was developed in order to facilitate the measurement of grain size in austenitic heat-resistant alloys, whose microstructures differed widely from any set of standards then available. As the work progressed, it became apparent that the method of estimating grain size could be applied advantageously to any type of alloy by selection of a suitable standard. Fig 4 shows three different microstructures that were selected for standards during preliminary investigation of the feasibility of estimating grain size by this method.

Table 1—*Calibration of Magnification of Westinghouse Research Laboratories' Bausch and Lomb Metallograph*

Objective	Eyepiece	m		b, Cm
		Calculated	Measured	
5.6 ×	7.5 × Huygenian	42.0	39.8	0
8 ×	7.5 × Huygenian	60.0	60.5	0
13.5 ×	7.5 × Huygenian	101.2	103.8	0
13.5 ×	12.5 × Huygenian	168.8	167.4	0
27 ×	10 × Negative amplifier	270	270	−10.1
41 ×	10 × Negative amplifier	410	407	− 7.3

The most favorable circumstance under which the comparison method was applied occurred when the standard and unknown had similar structures. This condition was obtained by comparing the standard with other fields on the same specimen from which the grain-size standard micrograph had been made. Three specimens were examined in this manner.

Fig 5 shows the frequency distribution

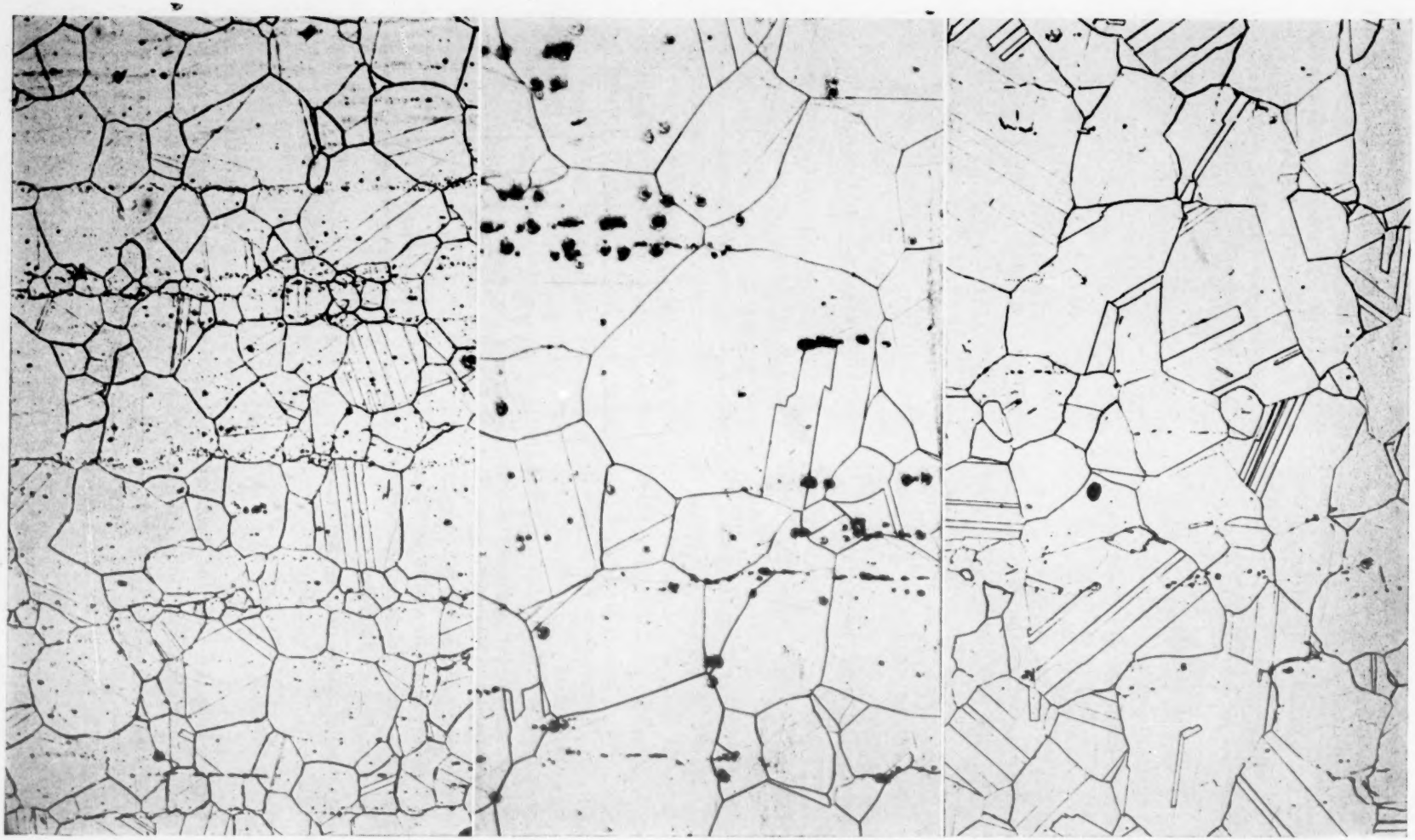

a W-I. ASTM 4.3 Spatial 4.1 ± 1.5 *b* W-II. ASTM 2.1 Spatial 1.9 ± 0.8 *c* W-III ASTM 3.2 Spatial 3.2 ± 1.3

FIG 4—TYPICAL GRAIN-SIZE COMPARISON STANDARDS FOR AUSTENITIC HEAT-RESISTANT ALLOYS. × 100.
Portions of fields of W-I, W-II and W-III standards. ASTM and spatial grain sizes indicated under figures.

curve* of errors in 54 measurements of grain size by three observers when comparing the W-II standard (Fig 4*b*) with six different fields on the same specimen been replotted in Fig 6 by the method described, to show that the errors in estimation obey the normal distribution law quite closely.

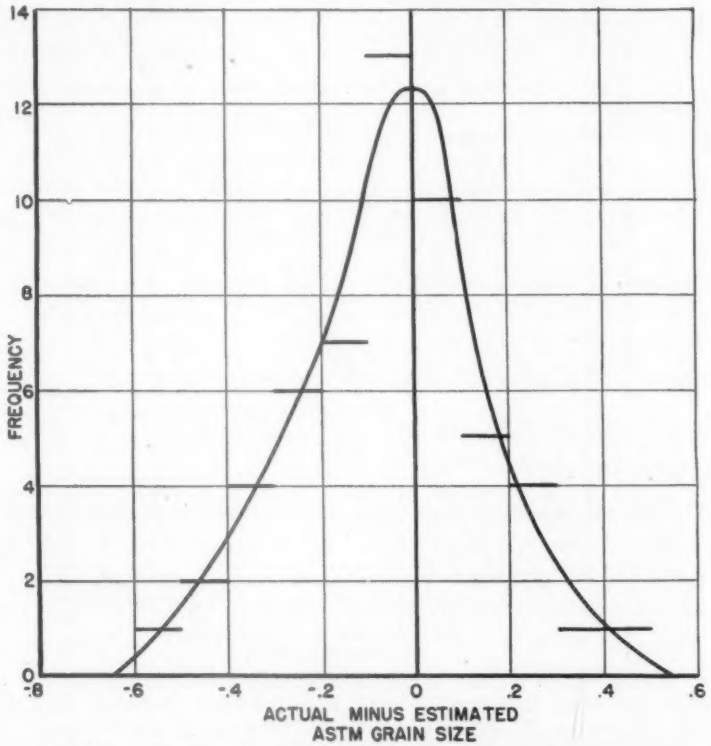

FIG 5—GRAIN-SIZE ESTIMATION BY COMPARISON METHOD.
Distribution of errors of 54 measurements by three observers. W-II standard and unknown. Probable error of one estimate was 0.14 grain-size number.

from which the W-II photograph was taken. The "actual grain size," in this and subsequent examples, was determined by calculation after the field examined had been photographed and the number of grains had been counted.

A convenient test of the normality of a series of errors can be carried out by plotting an ogive curve of the data on probability paper. In this type of curve the percentage of errors less than a given error are shown as a function of the errors. On probability paper, a straight line results if the data follow the normal distribution law. The data in Fig 5 have

One of the frequently used measures of precision of a series of observations is the probable error ($p.e._o$). This quantity has such a magnitude that from the standpoint of probability the true error in the observation on a *given* field due to accidental errors in observation is just as likely to be greater than this magnitude as it is to be less than this magnitude.* The probable error can be calculated from the average deviation ($a.d.$) for normal distribution of errors:

$$p.e._o = 0.845 a.d. = 0.845 \frac{\Sigma|d|}{J} \quad [12]$$

* For a discussion of theory of errors and precision of measurements, refer to T. K. Sherwood and C. E. Reed.[6]

* A later section of this paper will show how the probable error of an estimate on a random field can be calculated when the grain size in the specimen varies from field to field.

Portions of fields of W-I, W-II and W-III standards. ASTM and spatial grain sizes indicated under figures.

where $|d|$ equals the absolute values of the differences between the estimated and actual grain size and J equals the number of estimates.

the data of Fig 5 were separated into 18 measurements by each of three observers, it was found that the probable errors of one observation by the three

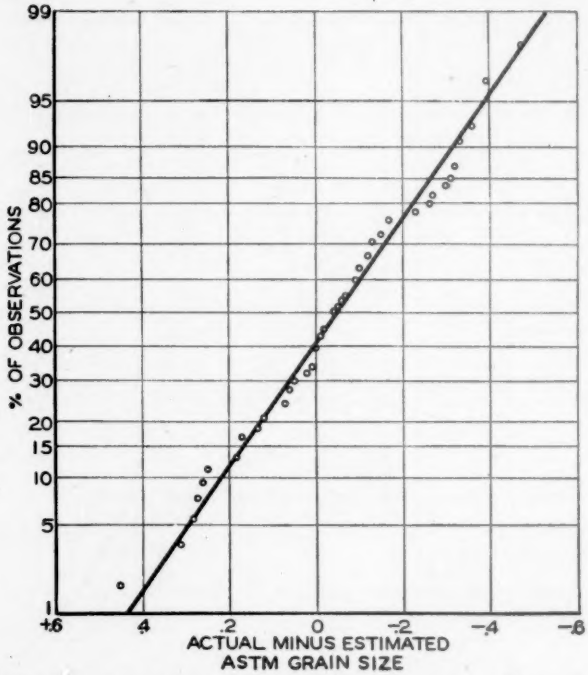

FIG 6—TEST OF THE NORMALITY OF THE DATA IN FIGURE 5.
Since the points fall close to a straight line when plotted on probability paper, it may be assumed that errors in estimation of grain size by the comparison method obey the normal distribution law.

Table 2 lists the probable errors that may be expected in single estimates of grain size by the comparison method under both favorable and unfavorable conditions. When matching or similar standards were used, the average probable error was 0.15 grain-size number. When

TABLE 2—*Estimation of ASTM Grain Size by Comparison Method*

Type of Structure Examined	Standard	Number of Estimates	Probable Error, *p.e.*
W-I	W-I	24	0.17
W-II	W-II	54	0.14
W-III	W-III	14	0.15
W-III	W-II	15	0.08
W-II	W-I[a]	8	0.43
W-III	W-I[a]	28	0.28

[a] Not a recommended standard for the type of structure examined.

individuals were 0.16, 0.13 and 0.15, respectively. The probable error of the mean of a group of J observations, however, taken from the same population is only,

$$P.E._{\text{Mean}} = \frac{p.e._o}{\sqrt{J}} \qquad [13]$$

Thus by taking three readings of the bellows extension for a field, the probable error of the estimate due to accidental observational errors can be reduced to less than one tenth grain-size number.

When standards are used that do not match the unknown, systematic errors are introduced in the comparison method that are similar to those encountered when grain sizes are estimated from geometric grids. To illustrate this point, the grain

size of one field of specimen W-III was estimated by comparison with the W-I standard photograph. In addition to the usual accidental errors, there was a systematic error of about 0.25 grain-size number. The W-I standard was likewise used to estimate the grain size on a field of the specimen from which the W-II standard originated. Since the standard had a higher percentage of fine grains, the observers again estimated too fine a grain size and the probable error was 0.34 grain-size number. Any time the grain-size distributions in sample and standard are widely different a larger probable error of the estimated grain size may be expected. For maximum accuracy in the application of the comparison method, it is therefore recommended that a standard be selected that approximates the appearance and grain-size distribution of the unknown. A relatively small number of standards would take care of a majority of microstructures encountered in the metallography laboratory. For special problems of an extended nature, it would be an easy matter to photograph one or more representative samples and prepare suitable standards.

Accuracy of Estimation of Grain Size by the ASTM Method E19-39T

The grain sizes of 12 micrographs taken of specimens W-I, II and III at several magnifications were estimated by 10 observers using the method outlined in the American Society for Testing Materials Tentative Standard E19-39T. The chart of idealized grains was used because it matched the appearance of the specimens more closely. Fig 7 shows that the frequency distribution of errors in estimation of grain size by this method does not obey the normal law very closely. The probable errors, calculated by Eq 12 in spite of the noted departure from normality, are listed in Table 3 for each of the three types of microstructures. The average probable error was 0.40 grain-size number. Under less favorable conditions, such as normally exist when an image of a specimen on a ground-glass screen is compared with printed charts, the error could be even greater.

TABLE 3—*Estimation of Grain Size According to ASTM Tentative Standard E19-39T*

Type of Structure Examined	Number of Estimates	Probable Error, $p.e._o$
W-I	10	0.30
W-II	70	0.40
W-III	40	0.42
	Weighted average $p.e._o$ = 0.40	

Accuracy of Estimation of Grain Size by Intercept Method

The intercept method described by Snyder and Graff for the determination of grain size is not necessarily limited to use with high-speed steels or to magnifications of 1000 diameters. As a matter of fact, for the sake of convenience in distinguishing and counting grains, the number of intersections on a 5-in. line should lie in the range 8 to 20; for grain sizes coarser or finer than this, the magnification of the image on the ground glass should be changed accordingly.

To evaluate the relative accuracies of the intercept and comparison methods, it was necessary to express the probable errors of both methods in terms of the same units, namely ASTM grain-size numbers. The conversion from one system to the other may be made by means of the following equation:

$$N = -3.9 + 6.64 \log \left(\frac{M}{100}\right) + 6.64 \log (y - 1) \quad [14]$$

where N is the ASTM grain-size number and y is the average number of grains touched by a 5-in. line at a magnification M.

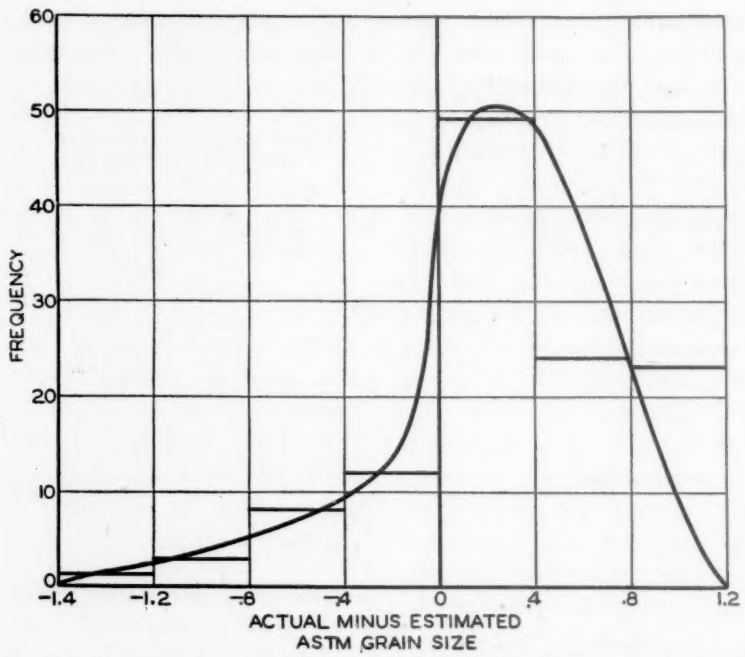

FIG 7—GRAIN-SIZE ESTIMATION ACCORDING TO ASTM TENTATIVE STANDARD E19–39T. Distribution of errors of 120 estimates on 12 micrographs by 10 observers. Schematic grain outlines were used as standards. Probable error of one estimate was 0.40 grain-size number.

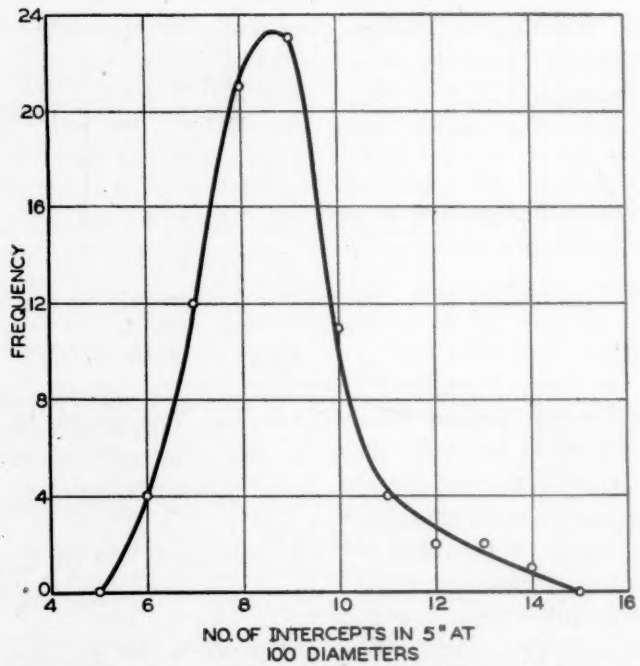

FIG 8—GRAIN-SIZE ESTIMATION BY INTERCEPT METHOD. Distribution of number of intercepts on 80 random lines drawn on a print of the W-II standard. Average number of grains intersected was 8.77. Probable error of one estimate was 1.02 intercepts, or 0.35 grain-size number.

Fig 8 is a frequency-distribution curve of numbers of intercepts on 80 random 5-in. lines drawn on a print of the W-II standard. The average number of intercepts in 5 in. was 8.77 grains. For one 5-in. line, the probable error was 1.02 in terms of number of intercepts, or 0.35 in terms of ASTM grain-size numbers (calculated from Eq 14). The probable errors of estimating grain size by the intercept method on 10 fields of three specimens are summarized in Table 4.

TABLE 4—*Estimation of Grain Size by Intercept Method*

Type of Structure	Specimen Field	ASTM Grain Size Count	Number of Lines	Average Number Grains Intersected by 5-in. Line	Probable Error in Terms of Number of Intercepts for One 5-in. Line	Probable Error in Terms of ASTM Grain Size Numbers, *p.e.*$_o$
W-I	Std.	4.12	67	18.5	2.05	0.32
W-II	Std.	2.06	80	8.77	1.02	0.35
	4	2.19	69	8.97	1.16	0.40
	5	2.00	70	8.49	1.45	0.51
	6	1.78	76	8.65	1.21	0.42
	7	1.90	73	8.52	1.15	0.40
	9	2.05	76	8.60	1.18	0.42
W-III	Std.	3.27	85	12.36	1.40	0.33
	1	3.84	71	14.56	1.42	0.28
	2	2.09	80	9.08	1.28	0.42
				Weighted average $p.e._o = 0.38$		

Accuracy by Evaluation of Grain Size by Jeffries' Method or by a Spatial Grain Count

It would normally be expected that a count of the number of grains in a given field by several observers should yield a constant result. In practice, however, it was found that small discrepancies occurred even after the most careful evaluations by competent observers. The sources of error appeared to be:

1. Slight differences in the location of lines drawn to limit the field counted.

TABLE 5—*Evaluation of ASTM Grain Size by Counts by Different Observers on 8 by 10-inch Prints of Standards*

Standard	ASTM Grain Size	Probable Error of Count on a Given Field (*p.e.*$_o$)
W-I	4.44	
	4.38	
	4.23	
	4.28	
	Average 4.33	0.076
W-II	2.00	
	2.10	
	2.20	
	2.07	
	2.02	
	1.99	
	2.04	
	Average 2.06	0.044
W-III	3.27	
	3.30	
	3.26	
	3.25	
	3.15	
	3.24	
	Average 3.24	0.032

2. Uncertainty as to whether some regions were twins or separate grains.

Table 5 lists counts on the three grain-size standards. The probable error of a count on a given field is 0.05 grain-size number.

Summary of Relative Accuracies of Various Methods of Evaluating Grain Size

Portions of Tables 2 to 5 have been summarized in Table 6 to show the relative accuracies and speeds of the various methods of estimating grain size.

TABLE 6—*Relative Speeds and Accuracies of Various Methods of Estimating Grain Size on a Known Field*

Method	Approximate Time for One Estimate, Min.	Probable Error of One Estimate in Grain-size Units, *p.e.*$_o$
ASTM, E19-39T.....	½	0.40
Intercepts in 5 in.....	½	0.38
Comparison.....	1	0.15
Jeffries.....	10–15	0.05
Spatial grain count.....	60–100	0.05

The first three methods may be classified as rapid and the fourth and fifth as slow. The comparison method has less than one half the probable error of the other rapid methods and thus requires only one fourth as many measurements for equivalent accuracy.

In addition to accidental errors in the method of measurement ($p.e._o$), an estimate on a random field may have an additional error caused by random variations in grain size throughout the specimen.* This actual variation in grain size from area to area, taken on groups of 150 to 250 grains, will be assumed to follow the normal law and will be designated the "probable deviation" ($p.d._s$), where the grain-size variation in the specimen is such that half the areas will be within $\pm p.d._s$ of the average grain size. The magnitude of $p.d._s$ will depend upon the size of the areas measured—the smaller the area, the greater the probable deviation.

The probable error of an estimate on a random field of a specimen by an approximate method of measurement can be calculated from the following equation:

$$p.e._{Est.} = \sqrt{(p.d._s)^2 + (p.e._o)^2} \qquad [15]$$

A quantitative evaluation of the effect of grain-size variation in the specimen on the accuracy of the estimate may be made from Table 7. One estimate by the approximate method is never as good as a count, but as the variation in the specimen approaches and exceeds the error due to the method of estimation (0.15 grain-size number), the two values become more nearly alike. If estimates by the comparison method are made on several fields of a typical specimen,† the average result is *more* accurate than a single grain count and can be obtained in a fraction of the time required for a count.*

TABLE 7—*Effect of Grain-size Variation in Specimen on Accuracy of Estimates of Grain Size on Random Fields*

Size Variation in Specimen, $p.d._s$	Probable Error of Estimate, $p.e._{Est}$			
	Grain Count on One Field	Comparison Method, Number of Fields Averaged		
		1	3	9
0.05	0.07	0.16	0.09	0.05
0.10	0.11	0.18	0.10	0.06
0.20	0.21	0.25	0.14	0.08
0.30	0.30	0.33	0.19	0.11
0.50	0.50	0.52	0.30	0.17

A measure of the grain-size variation throughout a specimen can be obtained when estimating grain size by the comparison method. From estimates made on about 10 fields, ($p.e._{Est.}$) can be determined, and since ($p.e._o$) equals about 0.15, ($p.d._s$) can be calculated from Eq 15. The probable deviation of the specimen, representing variation in average grain size from area to area for groups of several hundred grains, should not be confused with the deviation reported with a spatial grain count; for the latter is related to the distribution of sizes of individual grains in space, as calculated from one field of the specimen.

CONCLUSIONS

The comparison method of measuring ASTM grain size has the following advantages over conventional methods:

* Systematic variation in grain size from one part of a forging to another, for example, is not considered here.

† A specimen of moderately uniform grain size may have a $p.d._s$ value of 0.20.

* The question arises as to whether it is better to make several estimates on one field or to average the results of one estimate on several fields. The probable error of the average of J observations on one field is:

$$P.E._{Mean} = \sqrt{(p.d._s)^2 + \frac{(p.e._o)^2}{J}} \qquad [16]$$

whereas the probable error of the average of one estimate on J fields is always smaller as shown by

$$P.E._{Mean} = \sqrt{\frac{(p.d._s)^2 + (p.e._o)^2}{J}} \qquad [17]$$

1. An illuminated standard facilitates comparison with the image on the ground glass.

2. In the practice of the comparison method, the bellows draw is adjusted until the unknown has the same grain size as the standard. The grain size of the sample can then be read from a graph. In conventional methods, if the grain size lies between ASTM 4 and 5, for example, the observer must guess where the specimen belongs in this range. Because of the geometric nature of the grain-size numbering system, fractional estimates are difficult to make. It is much easier to judge when two images have identical grain sizes.

3. The method can be used for any type of material by selection of a suitable standard.

4. Grain-size determinations are not limited to the range No. 1 to 8. Any size can be measured by proper choice of objective and eyepiece to obtain a convenient magnification.

5. When a standard is used that has a grain-size distribution similar to the unknown, the comparison method has a probable error of a single estimate on a given field of only 0.15 ASTM grain-size number. Single estimates by the intercept method or by ASTM Tentative Standard E19-39T show twice as large probable errors, and thus require four times as many measurements for equivalent accuracy.

6. The comparison method is more rapid than actual counts of grains and is much more rapid than spatial grain counts.

7. The grain sizes in several fields can be readily averaged to take care of random variation in grain size throughout the specimen, thus yielding a more accurate estimate than a single precise count on a field than might not be representative.

8. Estimates by this method were equally good whether made by general laboratory personnel or by skilled metallographers.

References

1. Metals Handbook (1939) Amer. Soc. for Metals 755.
2. R. W. Snyder and H. F. Graff: *Metal Progress* (Apr. 1938) 377.
3. W. A. Johnson: *Metal Progress* (Jan. 1946) 87.
4. C. H. Davis: Grain Size Comparator. *Bull.* Amer. Soc. Test. Mat. (1941) No. 111, 45.
5. Research Metallographic Equipment and Accessories. Cat. No. 42-31-36, p. 17. Bausch and Lomb Optical Co., Rochester, N. Y.
6. T. K. Sherwood and C. E. Reed: Mathematics in Chemical Engineering, 344. New York, 1939. McGraw-Hill Book Co.

Transformation of Austenite in an Aluminum-chromium-molybdenum Steel

By R. A. Grange,* W. S. Holt* and E. T. Tkac*

(Atlantic City Meeting, November 1946)

Quantitative knowledge of the time element involved in austenite transformation in a particular steel provides a sound basis for understanding and planning heat-treatment. Such knowledge is conveniently obtained by measurement of austenite transformation as it occurs at each of a series of temperature levels. The results of these measurements usually are summarized in the form of the now familiar isothermal transformation diagram (I-T diagram, TTT diagram, or S-curve). Although a considerable number of such diagrams already have appeared in the literature, there remain many compositions of commercial importance for which no I-T diagram is available. The diagram for many such steels may be predicted from published data with sufficient accuracy for most practical purposes, but for others no satisfactory prediction can be made because the effect on austenite transformation of one or more of the important alloying elements present is not well enough known. Such a steel is Nitralloy, Type 135-Modified, which, containing about 1.25 per cent aluminum, differs from any whose I-T diagram has been published.

This paper presents results of a study of the isothermal transformation behavior of a sample from a commercial heat of this aluminum-chromium-molybdenum steel, together with pertinent supplementary data including the equilibrium transformation temperatures (Ae_3 and Ae_1), the temperature range of martensite formation, and the end-quench hardenability. These data are directly applicable to the heat-treatment of this type of steel and are of interest in revealing some of the fundamental effects of aluminum as an alloying element in steel.

Manuscript received at the office of the Institute July 9, 1946. Issued as T.P. 2109 in Metals Technology, December 1946.

* Research Laboratory, U. S. Steel Corporation, Kearny, N. J.

Material

All specimens were prepared from a 1¼-in. diam bar forged from a 5 by 5-in. billet from a commercial heat made in an electric arc furnace. The composition of the bar was; C, 0.41 per cent: Mn, 0.57: P, 0.016: S, 0.005: Si, 0.24: Ni, 0.17: Cr, 1.57: Mo, 0.36: Al, 1.26. The forged bar was normalized from 1750°F (955°C) and then tempered for one hour at 1200°F (650°C), this tempering treatment having been given to facilitate the machining of specimens.

Equilibrium Transformation Temperatures

In hypoeutectoid steel the minimum temperature at which austenite is completely stable, Ae_3, and the maximum temperature at which austenite is completely unstable, Ae_1, are of great significance in heat-treatment. Since these temperatures are dependent upon com-

position, it is of interest to measure them for this aluminum-chromium-molybdenum steel, thus gaining knowledge of the effect of aluminum; moreover, these temperatures determine the upper limits of the curves of the I-T diagram and consequently are necessary to its construction.

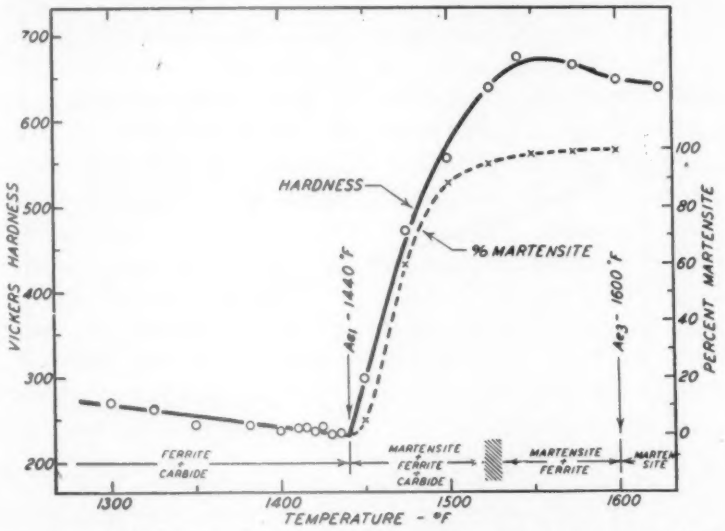

FIG. 1.—HARDNESS AND MICROSTRUCTURE OF SAMPLES USED FOR MEASURING Ae_1 AND Ae_3 OF TEST SPECIMENS.

To measure these temperatures, a number of small specimens were austenitized, quenched to martensite, and then reheated for 2 hr, each at a predetermined, closely controlled and carefully measured temperature; after this treatment, it was found that equilibrium had been sufficiently attained for all practical purposes.* The structure at temperature was "fixed" by brine-quenching to convert any austenite present to martensite which, after polishing and etching, was visible microscopically. The Vickers hardness of each specimen was measured, although in locating the Ae_1, and particularly the Ae_3, principal reliance was placed upon microscopic identification of the phases present.

Results are summarized graphically in Fig. 1, which shows the hardness and microstructure of this aluminum-bearing steel as thus equilibrated at any temperature slightly below, within, or slightly above the Ae_1-Ae_3 temperature range. Compared with those of most other types of low-alloy steel, the Ae_1 (1440°F) (780°C) and Ae_3 (1600°F) (870°C) shown are rather high Since in practice an austenitizing temperature well above 1600°F (870°C) is advisable to ensure complete austenitization, the use of 1700°F (925°C) as the austenitizing temperature, which is reported to be commonly used in practice, is justified by these results. Austenite in this steel remains completely stable above 1600°F (870°C), may partially transform to ferrite between 1600° (870°) and 1440°F (780°C), and is capable of transforming completely at a temperature below 1440°F (780°C). These equilibrium transformation temperatures, which were determined with a probable accuracy of ±5°F, apply to our particular sample, but those for material from other heats of

* Experience has shown that a 2-hr period is a reasonable compromise between a shorter time, which might not permit complete equilibrium, and a longer time, which entails difficulty in temperature control and in protecting the specimen from change in composition (oxidation, carburization, or decarburization).

the same steel undoubtedly would differ from these values by only a few degrees; the greatest variation would be expected in the Ae_3, which is influenced by carbon content as well as by segregation and composition otherwise.

It is of incidental interest to note that the hardness curve, Fig. 1, reaches a maximum some 50°F below Ae_3 and falls off slightly thereafter: this same behavior, which has been observed by us on other occasions, suggests that an austenite when not quite homogeneous (ferrite not completely in solution and carbon nonuniformly distributed) may sometimes be somewhat harder than when homogeneous.

Temperature Range of Martensite Formation

In this steel, as in all other carbon and low-alloy steels, austenite begins to transform to martensite on cooling to a certain temperature designated M_S: cooling below M_S increases the proportion of martensite until virtually all of the austenite has transformed to martensite. Although not an *isothermal* transformation, data for martensite formation may be represented on the I-T diagram and are, in fact, necessary to describe completely the process of austenite transformation: accordingly, martensite formation in this steel was studied by a rather involved metallographic technique, which has been described elsewhere.[1,2]

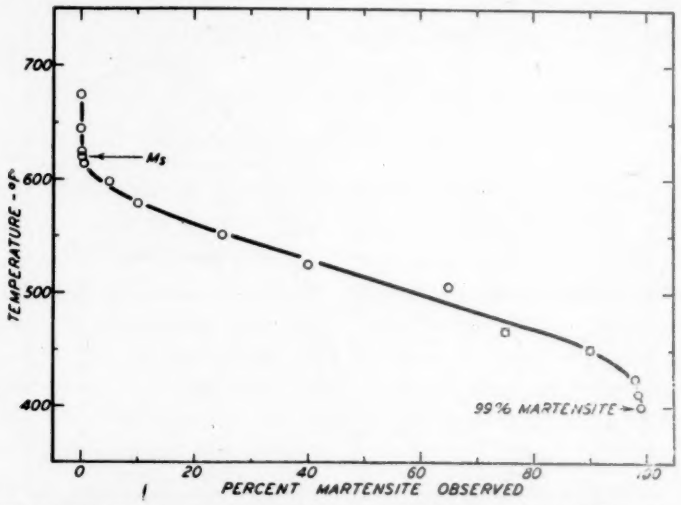

FIG. 2.—PROPORTION OF MARTENSITE OBSERVED IN SPECIMENS QUENCHED TO DIFFERENT TEMPERATURES.

Results of measurements of martensite formation are summarized in Fig 2, which shows the proportion of martensite formed on cooling to any temperature within the range 620° (325°C) to 400°F (205°C); they are also summarized in the I-T diagram (Fig 4). The M_S temperature was found to be 620°F (325°C). In order to determine the effect of the aluminum on M_S, it would be necessary to measure M_S for this same base composition without aluminum; although this has not been done, empirical formulas have been developed that permit calculation of M_S on the basis of chemical composition with a probable accuracy of about ±25°F. According to the revised formula proposed by Payson and Savage,[3,4] M_S for this composition without aluminum is 595°F (315°C), while that of Grange and Stewart[2] gives a calculated M_S of 560°F (295°C). Thus, depending upon which formula is

[1] References are at end of the paper.

used, one might deduce that 1.25 per cent Al either had substantially no definite effect on M_S* or raised it by about 60°F: the latter is in good agreement with the results of Zyuzin et al.[5] who found that each 1 per cent of aluminum raises M_S by 50°F. If aluminum does in fact raise M_S, this would constitute an advantage of aluminum steels, because higher M_S is believed to lessen the likelihood of quench cracking and possibly of thermal checking.

The shape of the curve in Fig 2 is similar to that for other steels;[2] however, the temperature range from M_S to virtual completion of martensite formation is somewhat greater in this steel than in most other low-alloy steels containing 0.4 per cent carbon, but more likely this is due to the relatively high chromium content than to aluminum.

Isothermal Transformation

The progress of isothermal transformation was measured dilatometrically† and by microscopic examination‡ of suitably heat-treated small specimens. The dilatometric method has the advantage that it is more convenient (at least when a dilatometer and necessary auxiliary equipment are already available) and yields results that are independent of the personal judgment required to interpret microstructure; on the other hand, it does not reveal the nature of the transformation product and is less precise in indicating the beginning and end of transformation. In this investigation, the dilatometric measurements, which were made first, served as a check and a guide to the heat-treatment of specimens for microscopic examination; the beginning and ending of transformation as shown in the I-T diagram, based, respectively, upon an estimated 0.1 and 99.9 per cent of transformation, were determined by the more precise microscopic observations rather than by dilatometric measurement.

Results of the dilatometric measurements are presented in Fig 3, which shows the length change with time in a bath at each temperature level studied. Each curve indicates an initial contraction while austenite was cooling to the bath temperature, followed by an expansion as it transformed at constant temperature. The increase in length caused by transformation at constant temperature is greater the lower the temperature; nevertheless, at each temperature level the proportion of total length change at any given time is approximately (but not necessarily exactly) equal to the proportion of austenite transformed. Thus, these dilatometric curves indicate the progress of transformation, as well as the approximate beginning and ending. The duration of the initial contraction shows that at most temperature levels about 20 sec was required for the specimen to reach constant temperature; this time includes that necessary to quench the $\frac{1}{16}$-in. thick specimen and to dissipate the heat added to the bath by the hot specimen and parts of the dilatometer that were immersed in the bath. Therefore, when expansion begins in less than 20 sec, the beginning time cannot be determined directly from these curves; when an abrupt minimum occurs in less than 20 sec, as at 500°F, transformation (martensite formation in this case) must have begun before the specimen had cooled to the bath temperature. Several arbitrary percentages of the total isothermal length change are indicated on the curves in

* Although direct subtraction indicates that according to the Payson and Savage formula aluminum caused a lowering in M_S of 25°F, this difference is too small to indicate a definite effect, since the probable accuracy of calculated values is no better than this.

† The dilatometric technique was similar in principle to that used by Davenport and Bain,[6] although a number of modifications were made in the apparatus to make it semi-automatic in operation.

‡ Measurement of isothermal transformation by the metallographic technique has been described elsewhere.[6,7]

Fig 3; despite certain limitations, these results are a reasonably accurate measure of the progress of isothermal transformation and useful in planning the heat-treatment of approximately 100 small specimens. The significance of the various lines and fields of the I-T diagram has been discussed elsewhere[8] and is too well known to

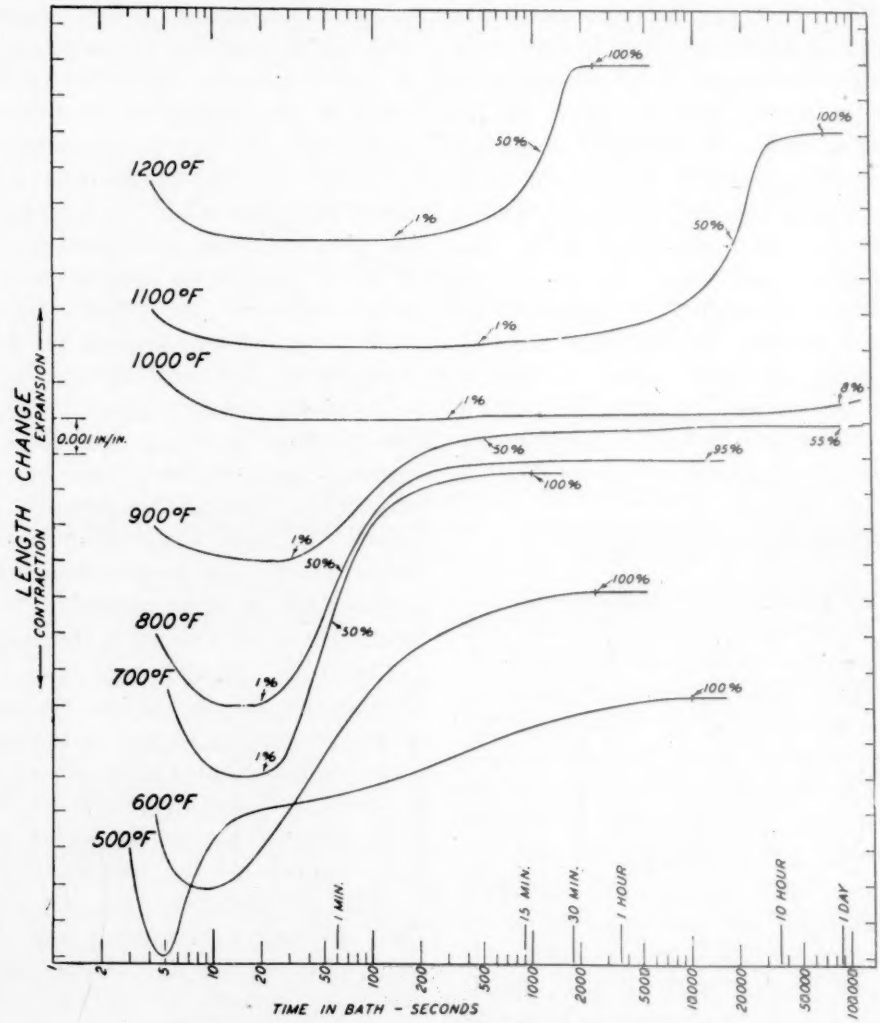

FIG. 3.—DILATOMETRIC TRANSFORMATION CURVES.
Alloy austenitized at 1700°F; grain size, 7–8.

of specimens for microscopic examination. The dilatometric measurements at 500°F (260°C) were especially helpful, since the progress of transformation at this level could not be satisfactorily estimated from the microstructure.

In constructing the I-T diagram (Fig 4), principal reliance was placed on the heat-treatment and microscopic examination require discussion here. The lower portion of the I-T diagram in Fig 4 includes the previously discussed data on martensite formation. Below M_S, transformation is never entirely isothermal because martensite formed continuously on cooling as indicated by arrows at a series of temperature levels in Fig 4; the portion of the austenite that did not transform to

martensite on cooling transforms at constant temperature to bainite, the time shown by the heavy dashed line below M_S being required for transformation of all austenite.

of "Zephiran Chloride"* was added to each 100 cc of standard picral. This modified picral appears to be a useful addition to etching reagents for steel, particularly alloy steels containing chromium.

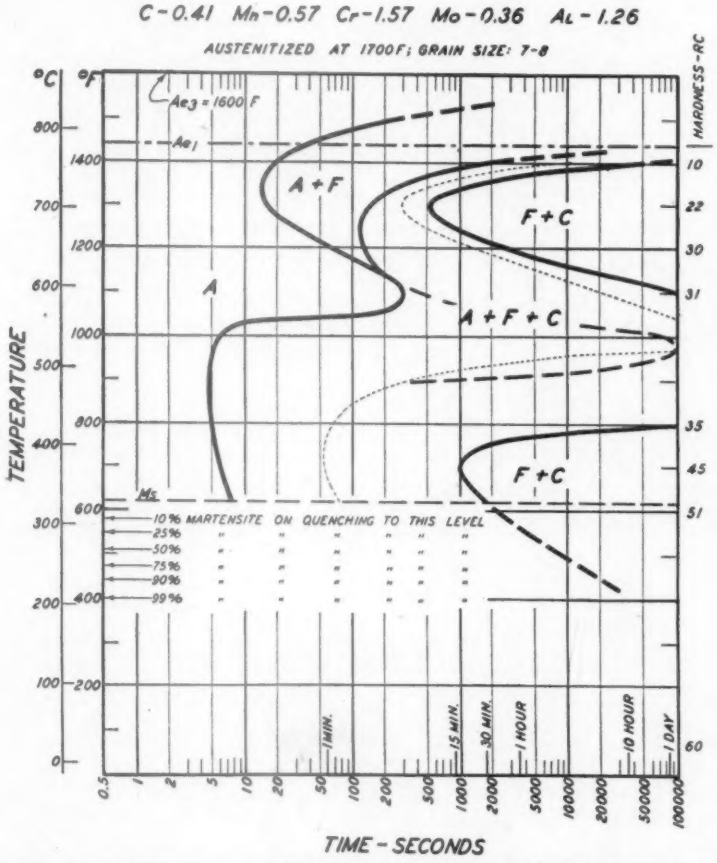

FIG. 4.—ISOTHERMAL TRANSFORMATION DIAGRAM WITH DATA ON MARTENSITE FORMATION ADDED. Transformation occurs entirely at constant temperature only above M_S.

The appearance of the isothermal transformation product at each temperature level is illustrated in Fig 5. These structures were etched in a modified picral reagent, not hitherto mentioned in the literature, which was used throughout this investigation. Standard picral (ethyl alcohol saturated with picric acid) did not etch this alloy in any reasonable time, presumably because of its chromium content; in order to accelerate the rate of etching and, at the same time, retain the advantages of a picral etch, 2 cc

The isothermal structures may be classified in three groups, as follows:

1. At 1100°F (595°C) and above, proeutectoid ferrite and pearlite.

2. Between about 1050°F (565°C) and 900°F (480°C), where transformation proceeded in two distinct stages, a first-stage product consisting of an acicular form of ferrite which may be, or at least was when

* "Zephiran Chloride" is an aqueous solution of benzalkonium chloride (high molecular alkyl-dimethyl-benzyl-ammonium chlorides) marketed by the Winthrop Chemical Company, Inc., New York, N.Y.

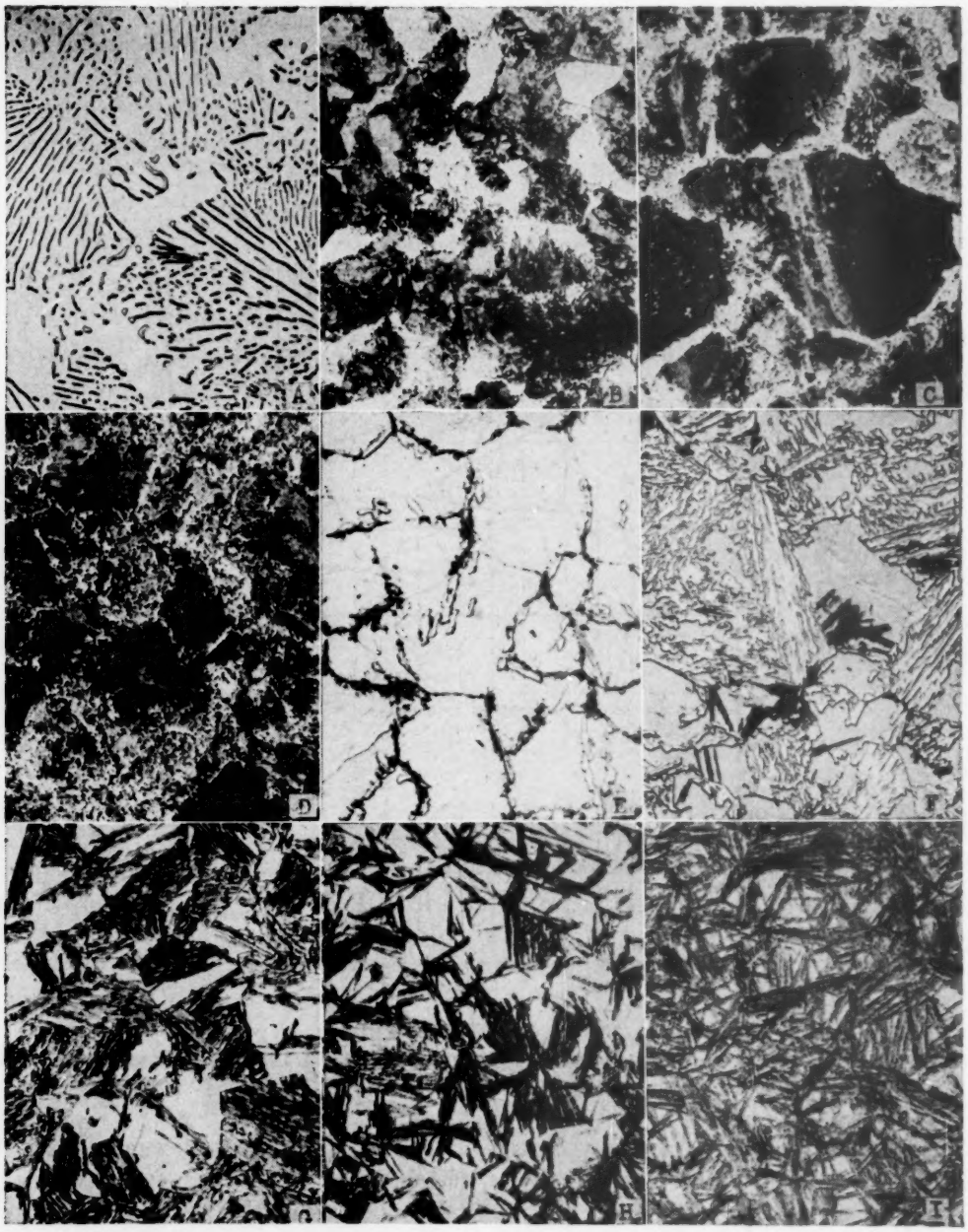

FIG. 5.—MICROSTRUCTURES RESULTING FROM ISOTHERMAL TRANSFORMATION OF NITRALLOY.

A. Complete trans. at 1400°F (21 hr)
B. Complete trans. at 1300°F (10 min)
C. Complete trans. at 1200°F (50 min)
D. Complete trans. at 1100°F (24 hr)
E. Partial trans. at 1000°F (4 days)
F. Partial trans. at 900°F (4 days)
G. Partial trans. at 800°F (1 min)
H. Partial trans. at 700°F (1 min)
I. Partial trans. at 600°F (2 min)

Etched in modified picral.
Original magnification 1000; reduced about ⅓ in reproduction.

first formed, supersaturated with carbon and therefore different from proeutectoid ferrite formed at higher temperatures, and a second-stage product which appears to be a very fine, dark-etching aggregate.

3. At 800°F (425°C) and below, bainite that is finer and more acicular the lower the temperature of transformation.

In Fig 5, the first group of structures is illustrated (*A*, *B*, *C* and *D*) by completely transformed specimens; the other two groups are illustrated by only partial transformation in order to illustrate better the character of each of these products. At 600°F (315°C), which is slightly below M_S, the structure contains bainite and some tempered martensite (formed on cooling to 600°F and then slightly tempered during the isothermal treatment); the latter appears in Fig 5*I* as darker broad needles as distinguished from the somewhat lighter needles, both in a matrix of light-etching quenched martensite, which represents austenite not transformed in 2 min at 600°F (315°C).

The structure formed at 900°F (480°C) and at 1000°F (540°C) (Figs 5*E* and *F*) are of special interest, since they are noticeably different from those observed in most other types of low-alloy steel; the two-stage reaction in this temperature range, however, is common to many types of low-alloy steel. In order to illustrate these interesting structures to best advantage, specimens were austenitized at 2100°F (1150°C) (to coarsen austenite grains and thus enlarge the units of the structure) and then transformed for each of a series of times at 900°F (480°C). Typical structures during transformation of this series are illustrated in Fig 6. The product of the first stage in the reaction, which proceeds very rapidly relative to the second stage, resembles acicular ferrite and might be regarded as a form of ordinary proeutectoid ferrite were it not for the fact that the proeutectoid ferrite formed at higher temperatures (even as high as Ae_1) always constituted a much smaller proportion of the total transformation product and decreased in amount with lower temperature until it had virtually disappeared at 1100°F (595°C) (Fig 5*D*). In many other low-alloy steels, a somewhat similar "flood" of ferrite-rich constituent forms in the first stage of transformation at about 900°F, but in most of them small spheroids of carbide are visible from the start in the "ferrite" needles. This has been called the "*X*" constituent by Davenport.[7] The steel shown in Fig 6*a* contains only a small amount of acicular "ferrite"; that in *b* and *c* contains about 50 per cent of this constituent, and both figures represent the same specimen, which was held at 900°F (480°C) for a time just short of the beginning of the second stage of transformation. Micrograph *b*, like *a* and *d*, represents the structure as etched in the modified picral reagent; micrograph *c*, the same specimen as *b*, etched electrolytically in alkaline sodium picrate* for the purpose of revealing carbides, which are blackened by this etch, at least when sufficiently large to be microscopically visible. Since there is no evidence of carbides in this structure, it is concluded that the "ferrite" probably is supersaturated with carbon, or at least that the carbide has not been precipitated so as to be microscopically visible, as happens in most other low-alloy steels. Fig 6*d* represents a sample held at 900°F (480°C) until the second stage in the transformation was well advanced, and illustrates the dark-etching second-stage product. Although definite proof is lacking, there is reason to believe that this second-stage product is much richer in carbon than acicular "ferrite," which formed in the first stage. Any specimen held at constant temperature in the range 900°F (480°C) to 1100°F (595°C) for a time greater

* Reagent No. 22, Metals Handbook, 1939. 724. Amer. Soc. for Metals.

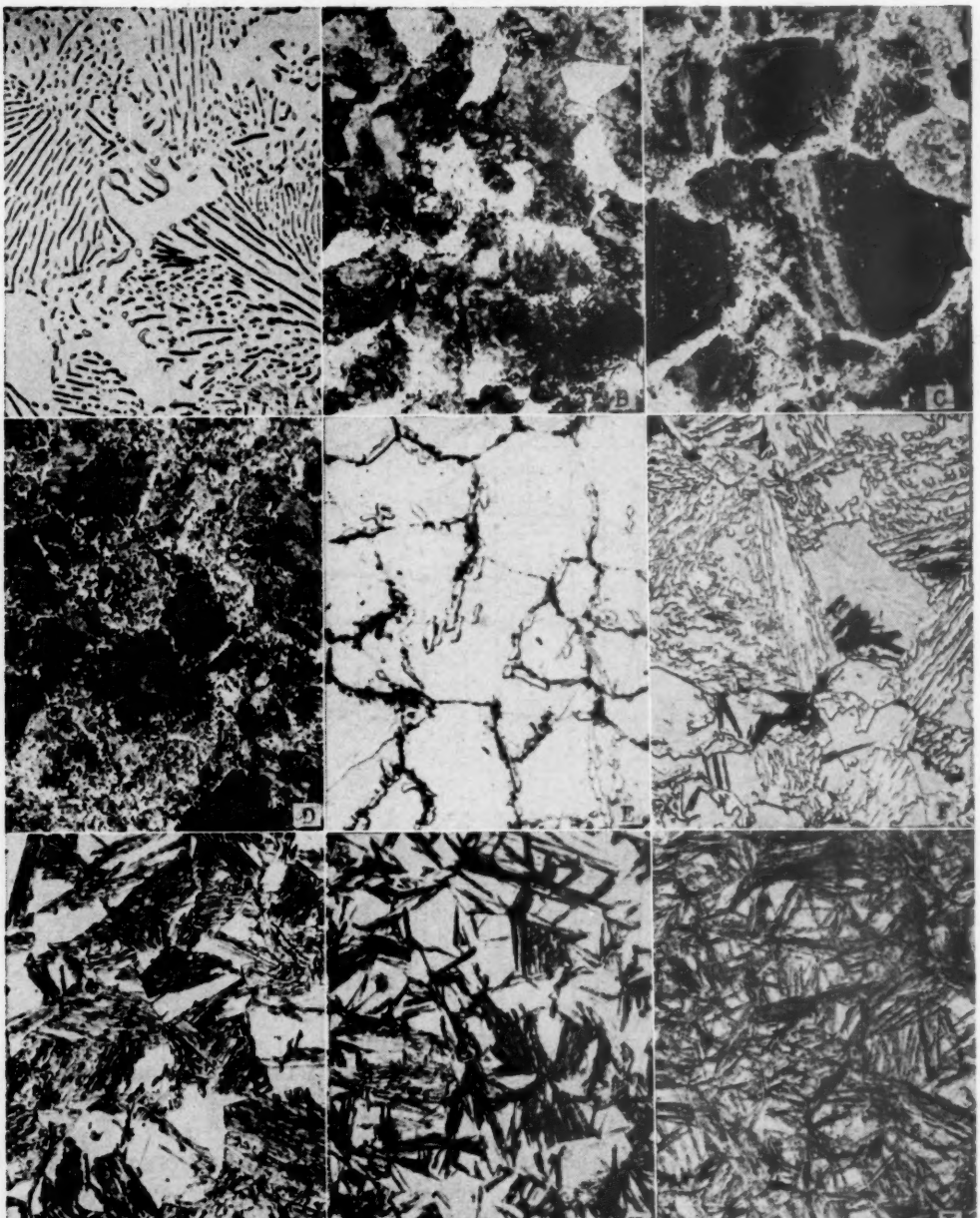

FIG. 5.—MICROSTRUCTURES RESULTING FROM ISOTHERMAL TRANSFORMATION OF NITRALLOY.

A. Complete trans. at 1400°F (21 hr)
B. Complete trans. at 1300°F (10 min)
C. Complete trans. at 1200°F (50 min)
D. Complete trans. at 1100°F (24 hr)
E. Partial trans. at 1000°F (4 days)
F. Partial trans. at 900°F (4 days)
G. Partial trans. at 800°F (1 min)
H. Partial trans. at 700°F (1 min)
I. Partial trans. at 600°F (2 min)

Etched in modified picral.
Original magnification 1000; reduced about ⅓ in reproduction.

first formed, supersaturated with carbon and therefore different from proeutectoid ferrite formed at higher temperatures, and a second-stage product which appears to be a very fine, dark-etching aggregate.

3. At 800°F (425°C) and below, bainite that is finer and more acicular the lower the temperature of transformation.

In Fig 5, the first group of structures is illustrated (*A*, *B*, *C* and *D*) by completely transformed specimens; the other two groups are illustrated by only partial transformation in order to illustrate better the character of each of these products. At 600°F (315°C), which is slightly below M_S, the structure contains bainite and some tempered martensite (formed on cooling to 600°F and then slightly tempered during the isothermal treatment); the latter appears in Fig 5*I* as darker broad needles as distinguished from the somewhat lighter needles, both in a matrix of light-etching quenched martensite, which represents austenite not transformed in 2 min at 600°F (315°C).

The structure formed at 900°F (480°C) and at 1000°F (540°C) (Figs 5*E* and *F*) are of special interest, since they are noticeably different from those observed in most other types of low-alloy steel; the two-stage reaction in this temperature range, however, is common to many types of low-alloy steel. In order to illustrate these interesting structures to best advantage, specimens were austenitized at 2100°F (1150°C) (to coarsen austenite grains and thus enlarge the units of the structure) and then transformed for each of a series of times at 900°F (480°C). Typical structures during transformation of this series are illustrated in Fig 6. The product of the first stage in the reaction, which proceeds very rapidly relative to the second stage, resembles acicular ferrite and might be regarded as a form of ordinary proeutectoid ferrite were it not for the fact that the proeutectoid ferrite formed at higher temperatures (even as high as Ae_1) always constituted a much smaller proportion of the total transformation product and decreased in amount with lower temperature until it had virtually disappeared at 1100°F (595°C) (Fig 5*D*). In many other low-alloy steels, a somewhat similar "flood" of ferrite-rich constituent forms in the first stage of transformation at about 900°F, but in most of them small spheroids of carbide are visible from the start in the "ferrite" needles. This has been called the "*X*" constituent by Davenport.[7] The steel shown in Fig 6*a* contains only a small amount of acicular "ferrite"; that in *b* and *c* contains about 50 per cent of this constituent, and both figures represent the same specimen, which was held at 900°F (480°C) for a time just short of the beginning of the second stage of transformation. Micrograph *b*, like *a* and *d*, represents the structure as etched in the modified picral reagent; micrograph *c*, the same specimen as *b*, etched electrolytically in alkaline sodium picrate* for the purpose of revealing carbides, which are blackened by this etch, at least when sufficiently large to be microscopically visible. Since there is no evidence of carbides in this structure, it is concluded that the "ferrite" probably is supersaturated with carbon, or at least that the carbide has not been precipitated so as to be microscopically visible, as happens in most other low-alloy steels. Fig 6*d* represents a sample held at 900°F (480°C) until the second stage in the transformation was well advanced, and illustrates the dark-etching second-stage product. Although definite proof is lacking, there is reason to believe that this second-stage product is much richer in carbon than acicular "ferrite," which formed in the first stage. Any specimen held at constant temperature in the range 900°F (480°C) to 1100°F (595°C) for a time greater

* Reagent No. 22, Metals Handbook, 1939. 724. Amer. Soc. for Metals.

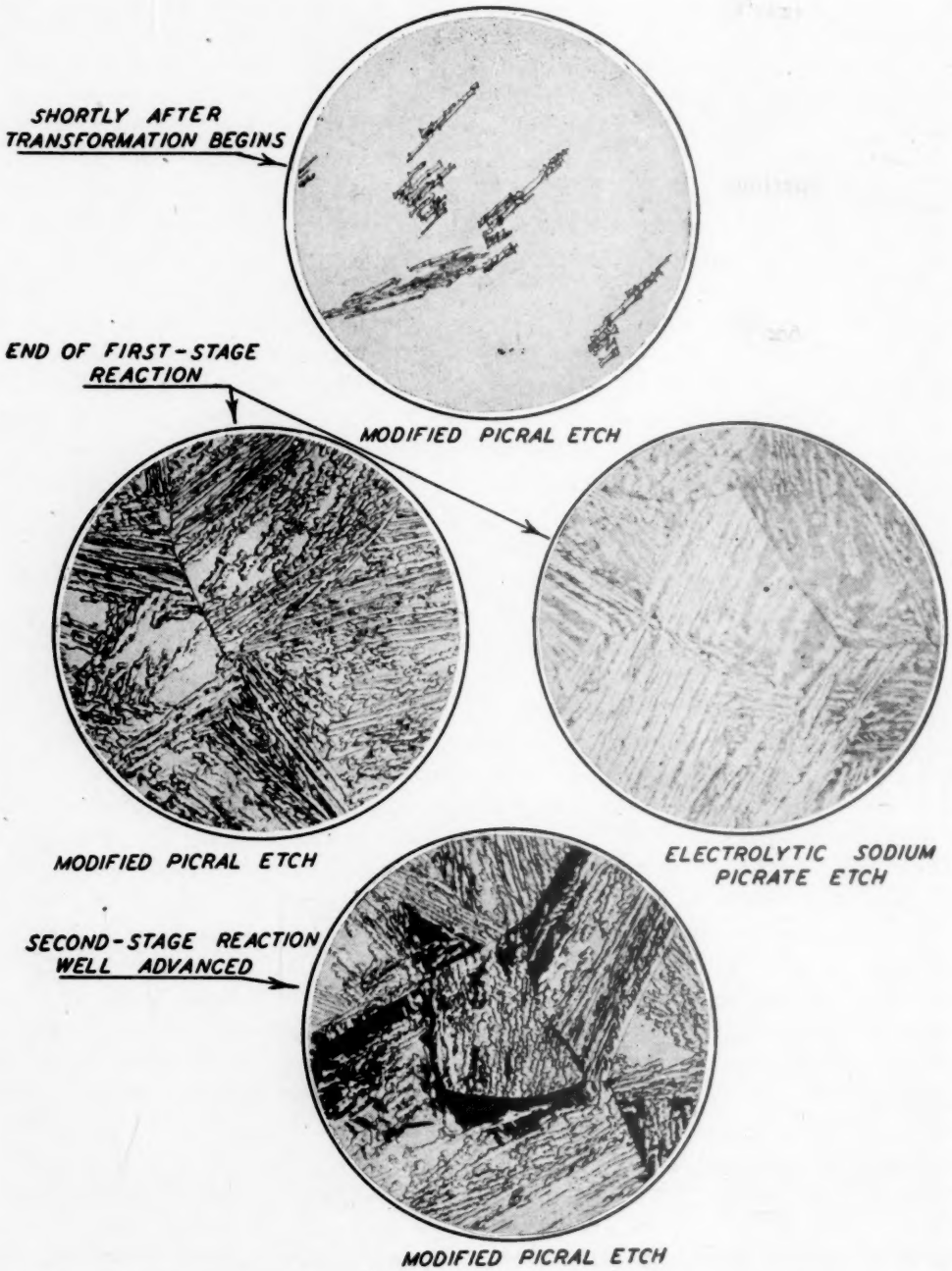

FIG. 6.—STRUCTURE OF SPECIMENS AUSTENITIZED AT 2100°F AND TRANSFORMED AT 900°F. Etched in modified picral.
Original magnification 1000; reduced about ⅓ in reproduction.

than indicated by the heavy dashed line in the I-T diagram (Fig 4) will contain some of this dark-etching aggregate; it will, however, rarely be observed in conventionally heat-treated steel of this composition, since such a very long time is required to form it.

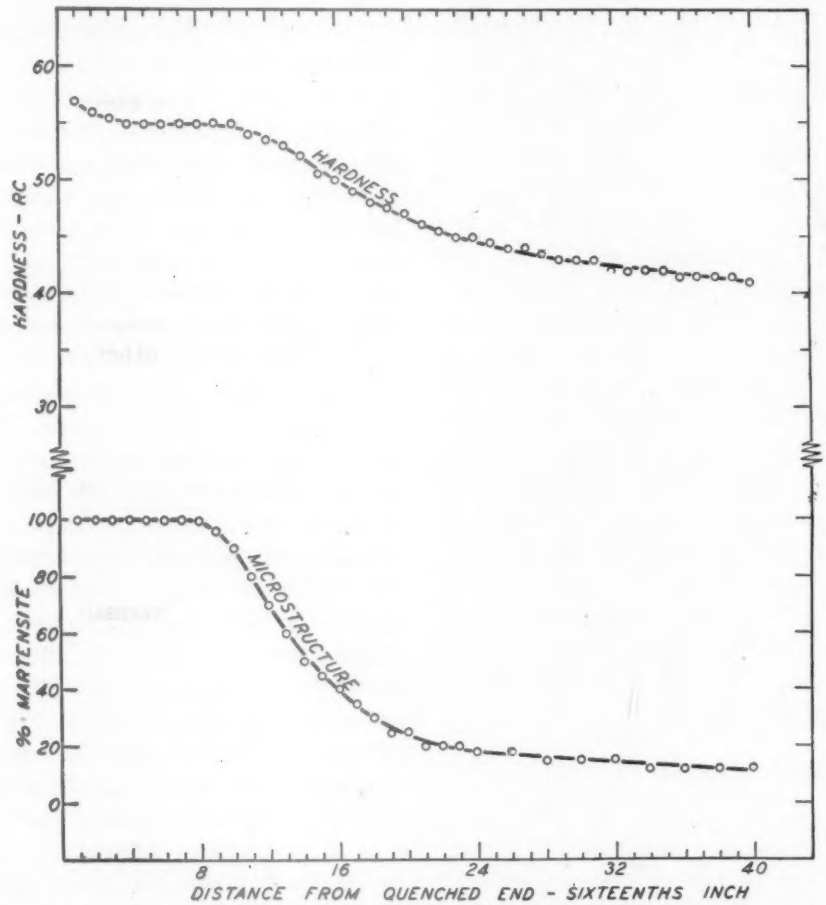

FIG. 7.—HARDNESS AND MICROSTRUCTURE OF END-QUENCH HARDENABILITY BAR.
C, 0.41 per cent; Mn, 0.57; Cr, 1.57; Mo, 0.36; Al, 1.26. Austenitized at 1700°F; grain size, 7–8.

END-QUENCH HARDENABILITY

Although the I-T diagram is fundamentally an indicator of hardenability, it is not so easily interpreted as the result of the more conventional end-quench hardenability test. It is of interest, therefore, as the final phase of this investigation of austenite transformation, to measure hardenability by an end-quench test made in accordance with ASTM specification. The hardenability bar, like other specimens of this investigation, was austenitized at 1700°F (925°C), and the austenite grain size was 7–8. Hardness measurements along the end-quenched bar are plotted in the usual way in Fig 7 (top curve). After hardness measurements were completed, one of the flat faces was polished and etched, and the structure was examined at each hardness impression. The lower curve of Fig 7 shows percentage martensite, estimated from the microstructure, plotted against distance from the quenched end of the bar.

As shown in Fig 7, this steel is fully martensitic to a distance of ½ in. from

the quenched end; thereafter, the hardness decreased as the structure contained less and less martensite, but even at the air-cooled end some martensite was present. The nonmartensitic transformation product at all locations in the bar was acicular, and mostly acicular "ferrite" and upper bainite. No proeutectoid ferrite or pearlite was observed anywhere in the bar, which indicates that in this steel, as in many other low-alloy steels, transformation of austenite to ferrite or pearlite begins less rapidly than transformation to those acicular products that form below about 1000°F (540°C). The interpretation of the microstructure in the end-quenched bar was greatly facilitated by our previous examination of isothermally transformed specimens; the same sort of constituents occurred in either case, although they were considerably more difficult to unscramble in the structure of the end-quenched bar. Thus, the general conclusions as to the hardenability and microstructure that might be drawn from the I-T diagram were confirmed by an actual hardenability test.

Discussion of Results

Aluminum is present in this alloy primarily to improve nitriding properties, but it is rarely used as an alloying element* in other commercial grades of low-alloy steel; consequently, very little is known at present of the effect of aluminum on austenite transformation. The results of this investigation permit us to draw certain limited conclusions as to the effect of aluminum through their comparison with corresponding data for chromium-molybdenum steels without aluminum. It would be desirable to have data for a steel of precisely the same composition but with no aluminum; but none is available, and it will be necessary to compare results with those for commercial grades of chromium-molybdenum steel, most of which contain somewhat less chromium and molybdenum than the alloy studied herein.

The Ae_1 and Ae_3 temperatures of this aluminum-bearing composition are high as compared with other aluminum-free low-alloy steels, and it is apparent that these equilibrium transformation temperatures are raised by aluminum. In fact, 1.25 per cent Al appears to have raised Ae_1 by about 50°F and Ae_3 by about 150°F. The relatively high Ae_1-Ae_3 temperature range necessitates a higher austenitizing temperature than is required for most other types of low-alloy steel of comparable carbon content. The associated high temperature of the minimum in the ending curve of the I-T diagram makes it necessary to select a relatively high transformation temperature in isothermal annealing; obviously, annealing should permit transformation in the range 1250° to 1350°F (675° to 730°C) to avoid the much longer time required for complete transformation at other temperature levels in the pearlite region.

Whereas most alloying elements lower the M_S temperature, the results suggest that it is raised by aluminum, although, as previously noted, the magnitude of this effect of aluminum is uncertain from results of this investigation because M_S for the same base composition without aluminum is not known precisely.

This steel is moderately deep-hardening compared with low-alloy steels in general, as is evident from the end-quench hardenability results (Fig 7), as well as from inspection of the I-T diagram (Fig 4). The end-quench hardenability curve lies about in the middle of the "hardenability band"* for SAE 4140 steel, and this may

* A small amount of aluminum is added as a deoxidizer to a great many steels, but when used in this way aluminum is not considered an alloying element.

* Tentative Hardenability Bands: Contributions to the Metallurgy of Steel No. 11, Soc. Automotive Engrs. and Amer. Iron and Steel Inst., July 1944.

be interpreted as evidence that aluminum contributed little, if anything, toward increased hardenability, and might even be construed as an indication that aluminum decreases hardenability.

The I-T diagram for this steel resembles in shape that of certain other low-alloy steels (SAE 4340 and 4150, for example). The temperature at which transformation is completed in the shortest time is 1300°F (705°C), and there is a "bay" in the vicinity of 1100°F (595°C). Between 1100°F and 800°F (425°C), a very long time is required for complete transformation of austenite. As in many other types of low-alloy steel, transformation in the range 900°F (480°C) to 1100°F (595°C) occurs in two distinct stages, the first proceeding quite rapidly so as to produce a "knee," and the second proceeding so slowly that weeks are required for complete transformation in this region. These features are about what would be expected for this base composition in the absence of aluminum, and thus aluminum seems to have had no very great effect upon the shape of the I-T diagram. It does seem likely, however, that aluminum has somewhat increased the amount of proeutectoid ferrite and also enlarged the $A + F$ field of the I-T diagram.

The sequence of microstructures as the transformation temperature is lowered follows the usual trend, as does the hardness of these structures. Except possibly for a little more proeutectoid ferrite, the microstructures above 1100°F (595°C) are similar to those observed in chromium-molybdenum steels without aluminum. It appears, however, that aluminum has altered the appearance of the structures formed below 1000°F (540°C). As illustrated in Fig 6, at 900°F (480°C) (and in this vicinity) the structure is characterized by a large volume of what appears to be acicular ferrite with no evidence of carbide, at least when examined microscopically in the usual way. Experience indicates that in this same composition without aluminum the structure formed at a corresponding temperature level would be similar except that the "ferrite" needles would contain dark-etching particles of carbide (the *X* constituent described by Davenport[7]); it appears, therefore, that aluminum has prevented the formation of carbides in the "ferrite" needles, possibly by making it relatively difficult for carbon to diffuse and precipitate. Although various theories have been advanced to explain the mode of formation of this intermediate transformation product, its true nature remains in doubt; in any event, it seems that aluminum has considerably altered its microscopic appearance. The bainite formed at 800°F (425°C), 700°F (370°C) and 600°F (315°C) was also slightly different in microscopic appearance from that observed in aluminum-free, chromium-molybdenum steels. Again, there seems to have been a certain reluctance for carbide to precipitate in clear-cut, microscopically distinct particles.

In general, aluminum belongs to the group of alloying elements that have less tendency to form carbide than iron and its effect on austenite transformation is more like that of the elements silicon, copper and cobalt than like manganese, chromium, molybdenum or vanadium.

Summary

The isothermal transformation diagram (Fig 4) for a chromium-molybdenum-aluminum steel (Nitralloy Type 135 modified) resembles in shape that of certain other low-alloy steels; SAE 4340, for example. Two minima occur in the isothermal beginning line, one at 1300°F (705°C) and the other at about 900°F (480°C), the latter being the more significant in respect to full hardening and the former of interest in annealing.

Although corresponding data for precisely the same composition as this steel

but without aluminum were not available for comparison, it is possible to draw the following conclusions as to the probable qualitative effect of 1.25 per cent aluminum in the aluminum-bearing steel investigated:

1. The Ae_1 and Ae_3 temperatures were raised.
2. The temperature range of martensite formation (M_S) probably was raised.
3. The time required for austenite to transform (hardenability) was not appreciably affected, and, if anything, seemed to be decreased rather than increased.
4. The volume of proeutectoid ferrite was somewhat increased.
5. The microscopic appearance of intermediate and low-temperature isothermal transformation products, particularly the first-stage product at 900°F (480°C) to 1000°F (540°C), was somewhat altered.

Acknowledgments

The authors are indebted to Carnegie-Illinois Steel Corporation for supplying the material and to associates at United States Steel Corporation Research Laboratory for advice and criticism.

References

1. A. B. Greninger and A. R. Troiano: Kinetics of the Austenite to Martensite Transformation in Steel. *Trans.* Amer. Soc. for Metals (1940) **28**, 537–574.
2. R. A. Grange and H. M. Stewart: The Temperature Range of Martensite Formation. *Metals Tech.*, A.I.M.E. (June 1946—*T.P. No.* 1996); *Trans.* AIME **167**, 467.
3. P. Payson and C. H. Savage: Martensite Reactions in Alloy Steels. *Trans.* Amer. Soc. for Metals (1944) **33**, 261–280.
4. A. E. Nehrenberg: Discussion of Ref. 2. *Metals Tech.*, A.I.M.E. (Sept. 1946).
5. V. Zyuzin, V. Sadovski and S. Baranchuk: Influence of Alloy Elements on Position of Martensite Point. *Metallurg* (1939) **14**, 75–80.
6. E. S. Davenport and E. C. Bain: Transformation of Austenite at Constant Subcritical Temperature. *Trans.* A.I.M.E. (1930) **90**, 117–154.
7. E. S. Davenport: Isothermal Transformation in Steels. *Trans.*, Amer. Soc. for Metals (1939) **27**, 837–886.
8. Atlas of Isothermal Transformation Diagrams. United States Steel Corporation, 1943.

DISCUSSION

(R. K. Kulp presiding)

N. C. Fick*—I want to ask Mr. Grange to say a few more words about the etching properties of this steel and the new reagent he has used. Will this reagent bring out carbides that are not shown by a picral etch? Does the presence of aluminum affect the etching quality?

R. G. Grange, W. S. Holt and E. T. Tkac (authors' reply)—In our experience, the "modified picral" described in the paper etches much more rapidly than ordinary picral, but is similar in behavior otherwise. For grades of steel that etch slowly in ordinary picral, the use of the modified picral reagent may be a distinct advantage, since inconveniently long etching times are not necessary. Thus far, we have not observed that the modified picral would reveal carbides or other details in microstructure not revealed by a sufficiently long etch in ordinary picral. However, there are some commercial low-alloy steels—our Al-Cr-Mo steel among them—which are not appreciably etched by ordinary picral in any reasonable time, if at all; such compositions usually contain considerable chromium, and it is for etching such steels that the modified picral etchant is especially recommended. The 1.25 pct aluminum in our Al-Cr-Mo steel may possibly have caused it to etch in ordinary picral more slowly than the same composition without aluminum, but, since no such direct comparison was made, we cannot be certain of this. In any event, the presence of aluminum did not appear to affect the "quality" of the etch.

J. V. Emmons†—I have a remark to make which is not in the least critical of the paper by Mr. Grange and his co-authors, but merely has to do with the state of our nomenclature on the decomposition products of austenite. For example—and I think Mr. Grange has presented some very good examples—in one of the micrographs, an unetched micro-constituent that appeared white on the micro-

* Battelle Memorial Institute, Columbus, Ohio.
† Chief Metallurgist, Cleveland Twist Drill Co., Cleveland, Ohio.

graph is called martensite. In another of the micrographs, a very coarse, dark-etching needle structure is also martensite. And in the same micrograph, very fine, faintly etching needles, which appear to be intermediate between the unetched martensite and the dark-etched martensite, have a new name of their own, bainite.

I wonder whether we could not have a little elucidation of the way in which one can distinguish between martensite that does not etch at all, martensite that is in very coarse needle, and bainite, which is perhaps in very small needles.

R. A. GRANGE—Like many of us, Mr. Emmons appears to be somewhat dissatisfied with present nomenclature for the decomposition products of austenite. For plain carbon steels, it seems adequate, but one is sometimes uncertain as to how to classify some of the microstructures encountered in alloy steels. From time to time, new names have been coined, but since they have not been generally accepted, their use leads to some confusion. A rational system of nomenclature including all variations in microstructure observed in alloy steels would seem to be contingent upon more complete knowledge of the transformation "mechanism" than is currently available.

Faced with the inadequacy of the present system of nomenclature in conveying a clear impression of the microstructures observed in our Al-Cr-Mo steel, it was necessary to resort to photomicrographs to tell the story. Although better than words, a photomicrograph is much less satisfactory than actual observation of a particular microstructure in the microscope, in which case different etches, vertical versus oblique illumination, examination of many different fields, and other such variations in the conditions of examination help the observer to interpret the structure. Moreover, when a micrograph is made, there is some loss in detail in the negative, in the print, and finally, in the reproduction of the print, whether a projection slide or a printed reproduction.

Our general approach in representing the microstructures resulting from isothermal transformation of austenite in the Al-Cr-Mo steel was to disregard the precise appearance of the martensite, which in these cases is of interest only insofar as it reveals the proportion of austenite not yet transformed after a particular holding period. The character of bainite could be shown to best advantage when the steel was only about half, rather than completely, transformed; since we were interested in the appearance of the bainite and not the martensite, the etching time chosen was optimum for revealing the bainitic structure, this being too short to darken martensite and thus leaving it white as in Fig 5, micrographs *G*, *H*, and *I*. At 1000°F and 900°F, months would be required for complete transformation; since we did not carry our measurements beyond two weeks, the micrographs representing these two levels (Figs 5*E* and 5*F*) are necessarily partially transformed. Their microstructure is comprised of acicular ferrite and a dark-etching aggregate in a matrix of martensite. In order to distinguish acicular ferrite from martensite, it was necessary to etch so that martensite would photograph darker than the white ferrite needles; in so doing, the aggregate constituent was unavoidably somewhat overetched. Obviously, the precise appearance of the martensites in Fig 5 is due to variation in etching technique designed to reveal the isothermal transformation products to best advantage, and has no significance with respect to the character of martensite itself.

MEMBER—Is it possible for the authors to explain the acicular structure of this unusual ferrite constituent?

R. A. GRANGE—The acicular ferrite comprising the first-stage transformation product formed at about this temperature range in many other grades of low-alloy steel. Several theories have been proposed to explain its formation; all assume that it differs in composition from the proeutectoid ferrite formed in hypoeutectoid steel at high temperature. The most recent theory has been proposed in a contemporary paper by Professor Hultgren, who may care to comment at this time.

A. HULTGREN*—Mr. Grange told us that there was no darkening of the ferrite with

* K. Tekniska Högskolan, Stockholm, Sweden.

time. I am not surprised. I have not been able to detect any darkening either.

This acicular ferrite has been shown and discussed so many times that it should not be new. Why is it acicular, the question was. I think that any phase that is precipitated at a fairly low temperature, under conditions that do not admit of too much diffusion, is apt to be limited in size, at least one way, therefore you would expect it to be acicular.

Then Mr. Grange referred to a suggestion of mine, that in alloy steels there may be a special kind of ferrite formed without diffusion of the alloy element. Only carbon is assumed to diffuse during the transformation. I see no objection to that interpretation in the evidence presented by Mr. Grange.

M. JACOBSON*—On page 457 of the paper, mention is made of the use of the quatenary ammonium compound Zephiran Chloride in "—a modified picral reagent not hitherto mentioned in the literature." Lest it be construed that this constituted the first use of the Zephiran reagent as an etchant, attention is called to the following excerpt from the 1946 ASM paper, "A Metallographic Etchant to Reveal Temper Brittleness in Steel" by Cohen, Hurlich and Jacobson: "Aside from its use in the investigation of the microstructural characteristics of the temper brittle phenomenon, the advantage obtained by adding a small quantity of Zephiran Chloride to picral or to picric acid-ether solution used for ordinary metallographic purposes was immediately recognized."

Information describing the use of Zephiran Chloride in a metallographic etchant was originally furnished the U.S. Steel Research Laboratory by Watertown Arsenal in 1944.

R. A. GRANGE—Mr. Jacobson correctly and pertinently points out that "Zephiran Chloride" was first used as one of the ingredients in a special etchant developed for the purpose of revealing susceptibility of steel to temper brittleness by Messrs. Cohen, Hurlich and Jacobson at Watertown Arsenal. This "temper-brittleness etch," which is made by mixing picric acid, ether, Zephiran Chloride and water, was described to us in the letter referred to by Mr. Jacobson. At the time we were much concerned with trying to etch satisfactorily the transformation structures in our Al-Cr-Mo steel; since this letter was marked "Restricted" by Government censors, and not declassified, as far as we knew, when our paper was written, we did not feel free to refer to it.

The ability of Zephiran Chloride to accelerate the rate of etching of the ether reagent suggested to us that it might have a similar accelerating effect in ordinary picral, which by itself, etches steel containing more than 1 pct of chromium much too slowly for convenient use. Accordingly, we spent considerable effort in trying various mixtures of Zephiran Chloride and picral and in making certain that the resulting modified picral reagents were revealing the true structure; the 2 pct Zephiran Chloride-98 pct picral combination was, as has been mentioned in the text, found to be about the best proportion. As this work was done and our paper printed before the contemporary paper by Messrs. Cohen, Hurlich and Jacobsen was available to us, we did not know that they were aware of the advantages of Zephiran Chloride in etchants other than the ether solution they used for a temper-brittleness etchant. In any event, they seem to have largely, if not entirely, overlooked what we believe to be the principal advantage of adding Zephiran Chloride to picral; namely, to provide a superior etchant for steels containing an appreciable percentage of chromium.

* Chemical Engineer, Watertown Arsenal Laboratory, Watertown, Massachusetts.

The Effect of Cobalt on the Rate of Nucleation and the Rate of Growth of Pearlite

By Malcolm F. Hawkes,* Junior Member, and Robert F. Mehl,† Member AIME
(New York Meeting, March 1947)

The rate of isothermal transformation of austenite to pearlite depends upon the rate of nucleation, N, and the rate of growth, G, of pearlite in austenite.[1,2] Values of N are given in terms of the number of nuclei forming in unit time per unit grain boundary area of unreacted austenite; values of G are given in terms of the linear rate of radial growth. Variations in the isothermal rate with temperature result from variation of N and G with temperature. Depth of hardening of a steel depends fundamentally upon values of N and G; changes in carbon and alloy content effect changes in N and G and thus affect depth of hardening. Quantitative studies are available on N and G for the formation of pearlite in plain carbon eutectoid steels.[3]

Systematic studies in this field are necessary if the phenomena are to be well enough known to furnish a proper basis for full rationalization and for theory. Accordingly, the studies are continuing, both with respect to the effect of alloying elements upon the values of N and G in the formation of pearlite and to the values of N and G for the formation of ferrite in hypoeutectoid steels.

The present paper is the first relating to the effect of alloying elements upon the values of N and G for pearlite. It offers special interest since cobalt is known to have an anomalous effect upon the rate of formation of pearlite, accelerating it, whereas all other elements retard it.[4] It will be shown that cobalt increases both N and G for pearlite and that this effect is inherent in the Fe-Co-C system and not dependent upon factors relating to austenite heterogeneity nor upon any recognizable adventitious factor. Inasmuch as the rate of diffusion of carbon in austenite and the interlamellar spacing of pearlite are variables related to G and possibly to N (in a manner not yet certain), measurements of the effect of cobalt upon them are also reported here. In the course of the work, measurements were made on the effect of cobalt upon the martensite temperature and these are given.

COBALT AS AN ALLOYING ELEMENT IN STEEL

Properties of Cobalt

Cobalt resembles iron more closely than does any other chemical element. Its atomic number is 27, hence it is the element immediately following iron in the periodic system. The two differ in atomic structure only in the fact that cobalt contains seven electrons instead of six in the third, or transition, level of the third shell. The next shell, which is the

---

This paper represents part of a thesis submitted by Malcolm F. Hawkes to the Graduate Committee of the Carnegie Institute of Technology in partial fulfillment of the requirements for the degree of Doctor of Science.

Manuscript received at the office of the Institute January 13, 1947. Issued as T.P. 2211 in Metals Technology, August 1947.

* Assistant Professor, Department of Metallurgical Engineering; Staff Member, Metals Research Laboratory, Carnegie Institute of Technology, Pittsburgh, Penna.

† Director, Metals Research Laboratory, and Professor, Department of Metallurgical Engineering, Carnegie Institute of Technology, Pittsburgh, Penna.

[1] The references are on page 492

outer or valence shell, contains two electrons in both cases, so the general chemical and physical properties of the two elements are similar. Cobalt exists in two allotropic

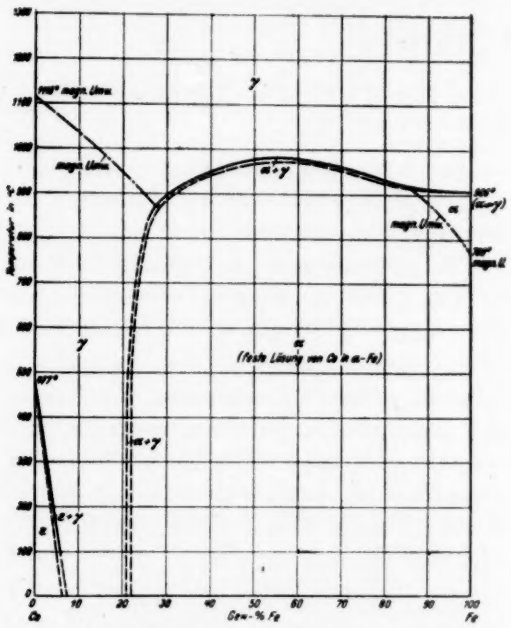

FIG 1—IRON-COBALT BINARY DIAGRAM.[6]

forms; the hexagonal close-packed arrangement is stable below about 450°C, and the face-centered cubic form is stable above that temperature. The latter phase is readily retained at room temperature by rapid cooling or by the presence of impurities such as hydrogen.

BINARY EQUILIBRIA

The face-centered cubic cobalt atom is only slightly smaller than the face-centered cubic gamma iron atom,[5] hence it is not surprising that a complete series of solid solutions is formed in the alloys of the two metals. This is shown in the iron-cobalt binary phase diagram which is illustrated in Fig 1. Three studies[7,8,9] related to iron-cobalt equilibria have been made since Fig 1 was published. They add nothing new except evidence for a superlattice at 50 pct cobalt and evidence for a somewhat wider alpha plus gamma field in the region of 80 pct cobalt.

Fig 1 shows that cobalt is an unique alloying element with respect to iron, for, although a large percentage stabilizes the gamma iron structure, moderate

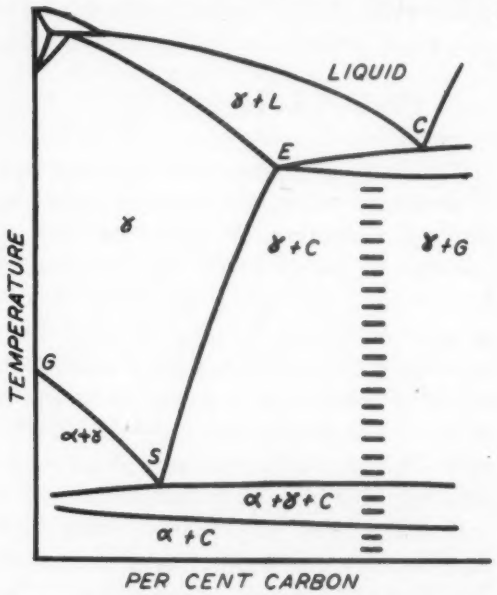

FIG 2—SCHEMATIC VERTICAL SECTION THROUGH FE-CO-C DIAGRAM. TO BE USED WITH TABLE 1.

amounts affect the A_3 temperature only very slightly. All other alloying elements raise or lower A_3 markedly.

TERNARY EQUILIBRIA OF IRON, COBALT, AND CARBON

The behavior of the binary alloys previously discussed would lead one to expect that cobalt would exert less effect than other alloying elements on iron-iron carbide equilibria. This was confirmed in an investigation of the ternary system by Vogel and Sundermann.[10] Over the entire range of cobalt contents studied no fundamental change was found in the shape of vertical sections through the ternary phase diagram parallel to the iron-carbon side, and but little change in the transformation temperatures. This is shown by means of a schematic vertical section of this type (see Fig 2) to be used in conjunction with Table 1. This table gives the temperatures and carbon concentrations of the important

points on the diagram as a function of cobalt content.

Cobalt increases the tendency of high carbon alloys to graphitize; this is shown by the position of the narrow shaded range in Fig 2 and Table 1. At carbon concentrations above this range, all the carbon in slowly cooled samples was precipitated as graphite; within the range, whose limits were not accurately determined, both carbide and graphite were found. This behavior is not surprising in view of the fact that cobalt is not known to form any stable carbides. It forms a simple binary eutectic system with graphite.[6]

TABLE 1—*Temperatures, in Degrees Centigrade, and Carbon Concentrations, in Per Cent, at Important Points in Fig 2.* (FE–CO–C–DIAGRAM)

Pct Cobalt	E	G	S	C	≣
2	1.7 C 1115°	900°	.9 C 715°	4.3 C 1130°	3.6 C
3.3	1.3 C 1100°	900°	.7 C 725°	4.2 C 1110°	3 C
10	1.4 C 1100°	910°	.7 C 770°	4.2 C 1115°	2.3 C
30	1.5 C 1120°	950°	.7 C 820°	3.9 C 1120°	Graphite at all carbon contents
50	1.2 C 1170°	970°	.7 C 850°	3.7 C 1190°	
70	1.2 C 1170°	880°	.6 C 720°	3.3 C 1190°	

THE EFFECT OF COBALT UPON HARDENABILITY

In 1927, Allison[11] made a comparative study of the effects of nickel and cobalt in steel. His principal conclusions were that cobalt promotes graphitization, raises the A_3 and A_1 temperatures, has little or no effect on the eutectoid carbon concentration, and has little effect on the hysteresis of the critical changes. He was apparently very close to the concept of the decrease of hardenability by cobalt, for he states: "A most important difference . . . , however, is that in the case of nickel a large temperature lag occurs between the critical points on heating and cooling, which in the case of cobalt is totally absent. The depression of the change point due to nickel is the chief cause of the nickel self-hardening steels . . . their occurrence in the cobalt steels is naturally precluded."

In the same year Scherer[12] observed that cobalt additions to carbon steels prevented them from hardening throughout, but he did not amplify.

It remained for Houdremont and Schrader[13] to make the first careful study of the effect of cobalt on the hardenability of steel. They found a ten-fold increase in the critical cooling velocity of a series of 0.90 pct carbon steels in which the cobalt content increased from 0 to 7 pct. The effect was also shown directly by quenching cylinders 30 mm in diameter in water. When the quenching temperature was 840°C (1544°F), the plain carbon steel hardened to a depth of 6 mm, while the 7 pct cobalt steel hardened to a depth of only 1 mm.

Esser, Eilender, and Majert[14] included cobalt in a study of the effect of a series of alloying elements on the critical cooling velocity of medium and high carbon steels. They confirmed the results of Houdremont and Schrader and likewise merely ascribe them to the fact that cobalt austenite has a greater velocity of reaction to pearlite than does unalloyed austenite.

The two studies just reported serve to illustrate the rather surprising fact that, although the German literature is a rich source of quantitative data on reaction rates in alloy steels, it offers little on the problem of the mechanism by which alloying elements exert their effect.

Davenport[4] determined S-curves for 0.95 pct carbon steels containing 0, 1, and 2 pct cobalt respectively. Typical data from his results are given in Fig 4. They confirm the effect shown by the German investigators.

EXPERIMENTAL RESULTS

Steels Used

Manufacture and Composition

The chemical compositions of the steels used in this investigation may be found in Table 2; in addition, essential features of the processing are given. Steels X, Y, and Z used in the early work were kindly supplied by Mr. E. S. Davenport; they are from the same stock used in his studies previously mentioned. They were in the form of $\frac{1}{10}$-in. thick hot rolled strip which had been produced as follows: from one heat of plain carbon open hearth steel, three slugs 4-in. in diam by 9-in. long were cast. These slugs were remelted separately in an induction furnace, the required cobalt and carbon were added, and the individual heats were each poured into steel molds $\frac{1}{4}$ in. by 6 in. in cross-section. These ingots were then hot rolled to $\frac{1}{10}$-in. strips. The three heats are silicon-killed and contain no aluminum.

Steels 1 to 5 inclusive were made at the Westinghouse Electric and Manufacturing Co., East Pittsburgh, Penna. with the cooperation of Dr. W. H. Brandt. In a magnesia crucible 150 lb of Armco iron and "washed metal" (Armco iron "saturated" with graphite) were melted in a 250 lb induction furnace. Ferro-manganese and ferro-silicon were added after the melt down; then a 26 lb ingot (Steel 1) was cast in a steel mold approximately 2 and $\frac{1}{2}$ in. square by 12 in. deep fitted with a refractory hot-top. Sufficient cobalt was then added to the furnace for Steel 2, the estimated silicon, manganese, and carbon losses were corrected by additions, and Steel 2 was poured. This process was repeated until the five steels were produced with an average of 12 min. elapsing between casts. No aluminum was used in this series. The ingots were hot forged to a $1\frac{1}{4}$ in. diam or less.

Table 2—*Steels Used in the Investigation*

Designation	C	Mn	Si	S	P	Co	Remarks
X	0.95	0.45	0.19	0.027	0.084		Cobalt additions made to open hearth steel when remelted in small laboratory induction furnace. Hot rolled. Si-killed.
Y	0.95	0.48	0.25	0.024	0.038	0.95	
Z	0.98	0.49	0.24	0.024	0.041	1.98	
1	0.76	0.42	0.26	0.026	0.006		150 lb induction furnace heat of Armco iron and graphite. Cobalt additions between casts of 25 lb ingots. Hot forged. Si-killed
2	0.71					1.95	
3	0.71	0.43	0.29			4.2	
4	0.68					7.4	
5	0.68					11.2	
E	0.64					7.5	1½ lb vacuum-melted induction furnace heats. Hot forged.
F	0.03					7.5	
J	1.4					7.9	
SS	0.11	0.09				4	Induction furnace heat.
8	0.73	0.62					Al-skilled, hot-rolled commercial steel.
10	1.08			0.22			
9	0.15	1.00					Cold-rolled commercial steels.
11	0.14						
T	1.13	0.25	0.35	0.014	0.014	5.0	30 lb induction furnace heats. Forged to 1 in. rounds
U	0.09	0.25	0.22	0.013	0.013	5.0	
P	0.99	0.03	.02 N (est.)				1½ lb vacuum melted induction furnace heats.
Q	0.88	0.10	No N				
R	0.92	0.10	No N			2 (est.)	Hot forged.
S	0.89	0.06	No N			4 (est.)	

Homogeneity

It is known that austenite heterogeneity accelerates the formation of pearlite and that, in plain carbon steels, this effect lies wholly in the effect of heterogeneity in increasing the rate of nucleation, N; the rate of growth G is unaffected.[3] A similar effect upon N may be expected in alloy steels; moreover, in this case, G may also be affected; quantitative data are not yet available on this point. It is at least

conceivable that the unusual effect of cobalt upon the isothermal rate might be the result of special heterogeneity factors associated with cobalt, operating to increase that rate. For this reason, extensive homogenization treatments were performed. The stock for all specimens of steels 1 to 5 used in the investigation was given a preliminary anneal of 10 hr at 1175°C. Except where otherwise noted, stock for all specimens of steels X, Y, and Z was annealed 13 hr at 1100°C.

In addition, homogenized samples of steels 3 and 4 were studied by the method developed by Roberts and Mehl[15] to establish an austenitizing treatment for the subsequent experimental work which would insure homogeneity. The method is based upon the fact, derived theoretically and confirmed experimentally, that a plot of the austenite grain size against the logarithm of the time to form 50 pct pearlite near A_{e1} from completely homogeneous austenite is a straight line of fixed slope for all steels. Continued austenitizing of a steel causes an increase in the half-reaction time resulting from both increasing austenite grain size and increasing homogeneity. When, upon continued austenitizing, the plot of austenite grain size against the logarithm of half-reaction time begins to parallel the theoretical straight line, then the austenite is homogeneous insofar as any determinable effect upon its rate of isothermal transformation is concerned.

The results on Steels 3 and 4 are shown in Fig 3. The curves for Steel 3 clearly indicate that 10 min. at 884°C insures homogeneity. The curves for Steel 4 are somewhat more doubtful but suggest that 10 min. at 920°C approaches the condition for homogeneity. Austenitizing treatments producing the same grain size in all steels of the series were desired, hence a somewhat higher temperature, where homogeneity seems certain, could be used for Steel 4. This analysis was not applied to the other steels of the series, but a rational austenitizing schedule was selected based on the fact that, from Fig 3, it would appear that an austenitizing

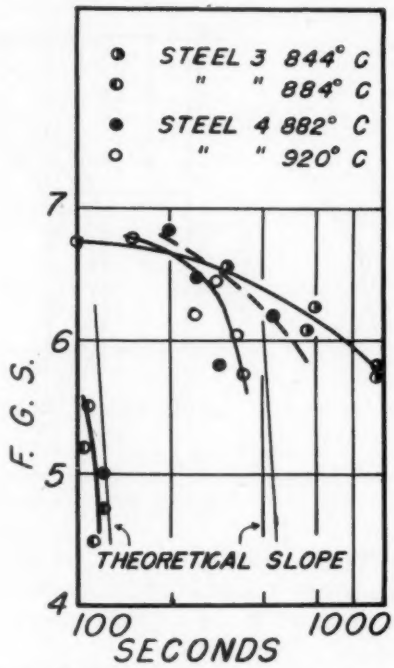

FIG 3—HOMOGENEITY OF STEELS 3 AND 4. FRACTURE GRAIN SIZE VERSUS TIME FOR HALF REACTION TO COARSE PEARLITE.

treatment producing a grain size of 5½ would also produce homogeneous austenite. The austenitizing treatments selected for later transformation studies are shown by the starred entries in Table 3. For Steels X, Y, and Z the treatment was 5 min. at 870°C as had been used by Davenport[4] in determining the S-curves of these steels.

Grain Size

The austenite grain size of Steels X, Y, and Z after 5 min. at 870°C was A.S.T.M. 4-5 as determined by fracture and microscopic methods. Previously homogenized specimens showed the same grain size as as-rolled specimens.

The austenite grain size of homogenized specimens of steels 1 to 5, held 10 min. at various austenitizing temperatures, was

determined by the fracture method. The results, shown in Table 3, indicate that a higher temperature is required to obtain a specified grain size as the cobalt content is increased to high values. The effect is slight, however, and is probably the result of the increase in the critical temperatures by cobalt.

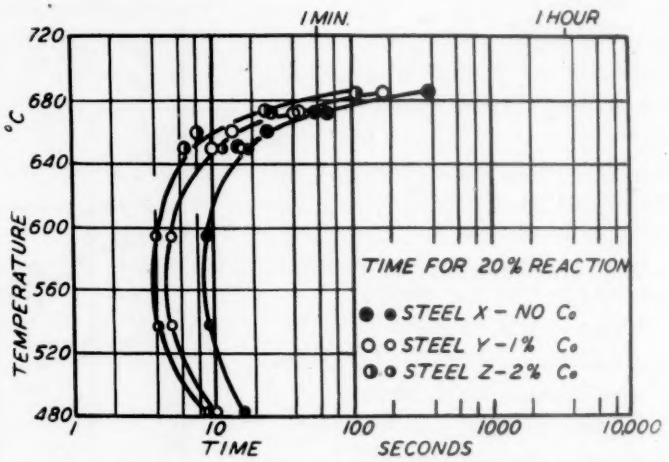

FIG 4—TIME FOR 20 PERCENT TRANSFORMATION IN STEELS X, Y, AND Z. SMALL SYMBOLS DAVENPORT'S RESULTS;[4] LARGE SYMBOLS THIS INVESTIGATION.

S-Curves

The first experiments consisted of extending the range of S-curves which had been prepared previously for Steels X, Y, and Z at the U. S. Steel Research Laboratory. The original isothermal reaction curves were obtained and to them were added runs at several higher temperatures. From these data, Fig 4 was constructed showing the time for 20 pct reaction. These S-curves depict more accurately the effect of cobalt than do the ordinary type showing beginning (0.5 pct) of transformation because of scatter in the data for these fast reacting steels at small amounts of transformation. The U. S. Steel results are confirmed essentially, and the effect of cobalt in increasing the rate of reaction to pearlite is clearly shown.

S-curves were also prepared for Steels 1 to 4 using the austenitizing treatments indicated previously in Table 3 to insure homogeneity. The results are shown in Figs 5 and 6 with the beginning and ending curves plotted separately for easy comparison. Once again, cobalt is shown to increase the rate of isothermal transformation of austenite at sub-critical temperatures. This effect is demonstrated for the entire temperature range from just below the eutectoid temperature to just above the temperature of the martensite transformation. Transformations in this range are shown to be similar to those in plain carbon steels in that no additional "knees" or "bays" in the S-curve are produced by the addition of

TABLE 3—*Austenite Grain Size of Steels 1–5 Held 10 Minutes at Various Temperatures. (Temperatures Used in Subsequent Studies Denoted By**)

Temperature Deg C	A.S.T.M. Grain Size Number				
	Steel 1 (No Co)	Steel 2 (2 Pct Co)	Steel 3 (4 Pct Co)	Steel 4 (7 Pct Co)	Steel 5 (11 Pct Co)
800	5¾	5¾			
840	5¼*	5½*	6¼		
880	4½	4½	5½*	6	6¾
920			5½	6	6¼
960				5½*	5¾*

cobalt. No constituents other than those also formed in plain carbon steels were observed in the cobalt steels.

rate of isothermal reaction of austenite to pearlite but not by means of an indirect effect on grain size or homogeneity, for

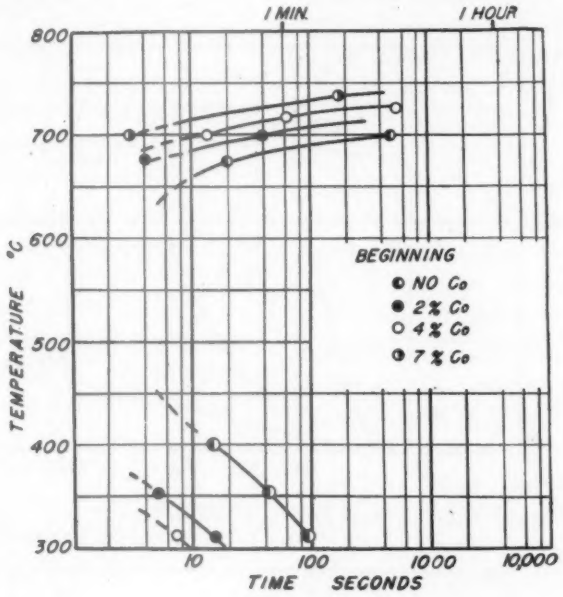

FIG 5

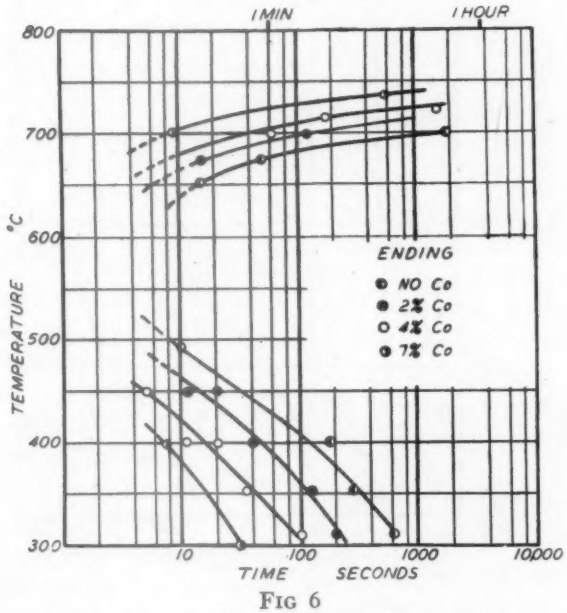

FIG 6

FIGS 5 AND 6—S-CURVES FOR STEELS 1 TO 4.

RATES OF NUCLEATION

Isothermal Studies

In the previous section, it was shown that the addition of cobalt increases the

all steels had the same grain size and all were homogeneous. The mechanism involved thus differs from those demonstrated for aluminum, vanadium, or any other elements which have heretofore

been reported to decrease hardenability. The search for an explanation would be simplified if it could be demonstrated that the effect of cobalt were predominantly upon one of the variables, rate of nucleation or rate of growth, to the exclusion of the other. For this purpose, studies on these two variables were made early in the investigation.

Rates of nucleation of pearlite were measured on Steels X, Y, and Z at two different temperatures using the Scheil "method of successive subtractions" which is described at length by Hull and Méhl.[16,3] This method is very tedious but is the only one which yields an absolute value for N if that quantity varies with time; Hull, Colton and Mehl[3] have shown that

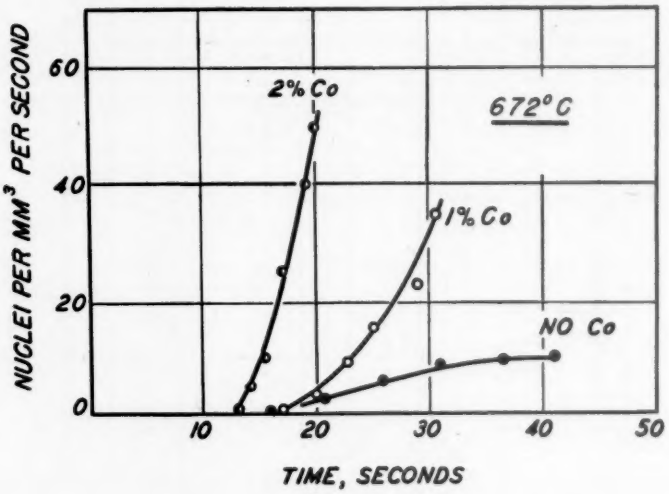

FIG 7

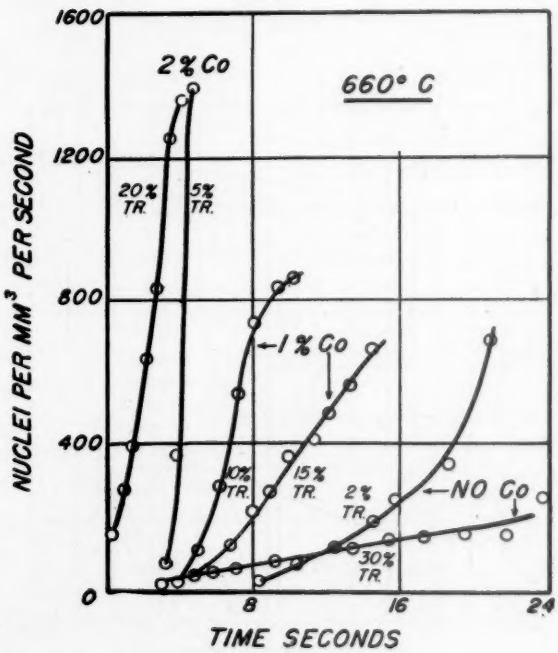

FIG 8

FIGS 7 AND 8—RATES OF NUCLEATION OF COBALT STEELS. VALUES ARE A FEW PER CENT LOW AT THE LONGER TIMES BECAUSE OF PARTIAL TRANSFORMATION.

it always does in the case of the formation of pearlite. A determination can be made on one partially reacted specimen, but, in all cases except one, two specimens at different degrees of transformation were used for a check. At 672°C, the results agreed quite well, and a single curve can be drawn through the two sets of points for any one steel. This is shown in Fig 7 where the number of nuclei formed per cubic millimeter of volume (uncorrected for partial transformation) per second is plotted as a function of time.

The results at 660°C are a little less precise because of the rapid rate of transformation, and the agreement between the two specimens is not so good. Hence, in plotting the results in Fig 8, separate curves were drawn for each specimen. Both figures show clearly, however, that cobalt increases the rate of nucleation markedly.

It is also seen that as the reaction progresses, N increases at a faster rate with respect to time as the cobalt content is increased. This same effect was observed by Hull, Colton and Mehl[3] on a series of specimens of 1.02 pct carbon steel austenitized for shorter and shorter times to produce faster and faster rates of nucleation. This seems normal, for it will probably be shown eventually that N vs. time curves for all steels start at zero and have the same shape.

Fig 7 suggests that there is an incubation period preceding nucleation, but this can be accounted for on the same basis[3] used to explain a similar feature on rate of growth curves; namely, when rates of nucleation are low, the number of nuclei formed in the first few seconds is extremely small. Hence, when making the experimental count, there is an extremely small probability of intersecting a nodule, the nucleus for which started at zero time. The apparent incubation period decreases with increasing rate of nucleation which is in accord with the above explanation.

Method of Determining Relative Rates of Nucleation at the "Knee" of the S-Curve

The data on Steels X, Y, and Z show that cobalt increases the rate of nucleation of pearlite at temperatures well above the "knee" of the S-curve. However, it is the rate of transformation *at* the "knee," where that rate is at a maximum, that determines hardenability. Hence it is proper to ask whether cobalt has the same effect on the rate of nucleation on cooling past the "knee" as it does during isothermal transformation at higher temperatures. No method for direct measurement of N, where transformation rate is as fast as it is at the "knee" in these steels, is available. A method was devised, however, which shows, when steels with increased transformation rates are studied, whether the increase is the result principally of N, of G, or whether the relative effect stays the same as both increase. The principle used follows.

A specimen can be gradient-quenched in such a way that, over a considerable area to be examined under the microscope, austenite will transform partially to fine pearlite at the "knee" of the S-curve, then cease reacting, and finally transform to completion in the martensite temperature range. The area can be chosen with regard to symmetry of the specimen so that the amount of transformation to fine pearlite will be constant over the area. If several such areas are examined, where the degree of transformation to fine pearlite is small enough so that impingement has not occurred, a plot can be made of number of nodules vs. per cent transformation. If such plots are made for two different steels to be compared, the results, in the general case, will be as shown in the upper two curves, $f(N)$, in Fig 9.

If now Steel A is known to transform more rapidly than Steel B, it can safely be said that whatever causes this difference does so by increasing N more effectively than G (keeping in mind that N appears

to the first power and G to the third power in the transformation equation).[2] This will necessarily be reflected in similar curves where maximum nodule radius

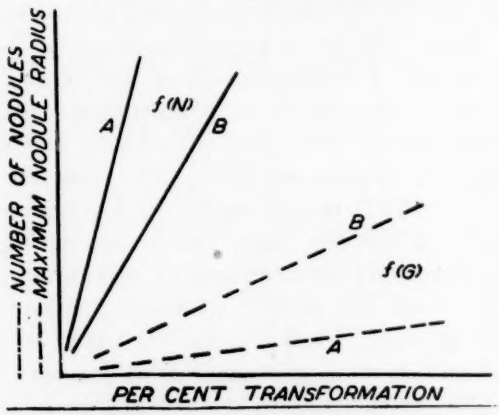

FIG 9—POSSIBLE RELATIONSHIPS BETWEEN N AND G ON COOLING.

(a function of G) is plotted as a function of percentage transformation. This is shown in the lower two curves of Fig 9. At a given fraction transformed there obviously cannot be both more and larger pearlite nodules.

On the other hand, Fig 9 could represent the case where Steel B transforms more rapidly on cooling, in which case it would be the result of an effectively greater influence of some factor on G than on N.

If, from one steel to the next, both N and G were increased in effectively the same degree then the $f(N)$ curves would superimpose, and obviously the $f(G)$ curves would have to do likewise. Valuable comparative data may be obtained by this method even though numerical values of N, G or their ratio are precluded by the fact that all three vary with temperature and with time and that different cooling rates are required to get the same amount of transformation in two different steels.

To make this method practical, a means had to be devised whereby a sample could be quenched, then examined under the microscope at various sections each of which would show a nearly constant degree of transformation; these sections would be chosen to encompass the range from 0 to approximately 10 pct transformation where impingement becomes

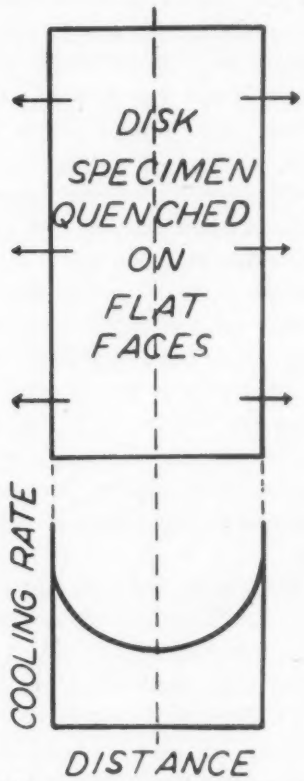

FIG 10—COOLING RATES IN DISK SPECIMEN QUENCHED ON FLAT FACES.

serious. An end-quenched bar, such as a Jominy specimen, suggests itself, but, on shallow-hardening steels of the type used in this thesis, the rate of change of structure with distance from the quenched end is too great in the gradient zone to allow accurate sampling. This difficulty was overcome by making use of the principles that structure is determined by cooling velocity and that the rate of change of cooling velocity with distance decreases to zero at the central plane in a disk specimen quenched on the two flat faces only. This is illustrated in Fig 10. Thus, for each steel, a thickness of disk can be selected such that the minimum useful amount of transformation (approximately

one pct) will be obtained at the center on a given quench. Even on shallow-hardening steels it will be found that, in a disk so quenched, the degree of transformation increases slowly enough with distance from the central plane to allow several different surfaces to be found and examined where the degree of transformation is nearly constant over the surface and is small enough that impingement has not occurred. Determinations of number of nodules, maximum nodule radius and percentage transformation on each of these surfaces then yield the data necessary for the curves needed.

Measurements of Rate of Nucleation at the "Knee" of the S-Curve

The method just described was applied in principle to Steels 2, 3, and 4, but experimental difficulties required some modifications. It was impossible to secure a constant degree of transformation across any one plane of polish, so, although the variation was over a range of only a few pct, it was considered more appropriate to rate each photograph of the surface separately and enter it as a point on the curve. Furthermore, only maximum nodule radius was measured; no accurate count on the number of nodules could be obtained because of the difficulty in distinguishing very tiny ones (which make up the largest portion) from inclusions and other imperfections and because of their tendency to form in "chains" along grain boundaries. The latter tendency makes measurements of maximum nodule radius less reliable also, but the effect is not serious, for independent nodules can always be found away from grain boundaries.

In view of the above objections, no great accuracy is claimed for the results; however, it is believed that they do show the true general trend. Although only maximum nodule radius was recorded, this is sufficient, as pointed out in the previous section, to determine whether cobalt influences chiefly N or G or effectively both to the same degree. That the latter case is essentially true is borne out by the results which are shown in Fig 11.

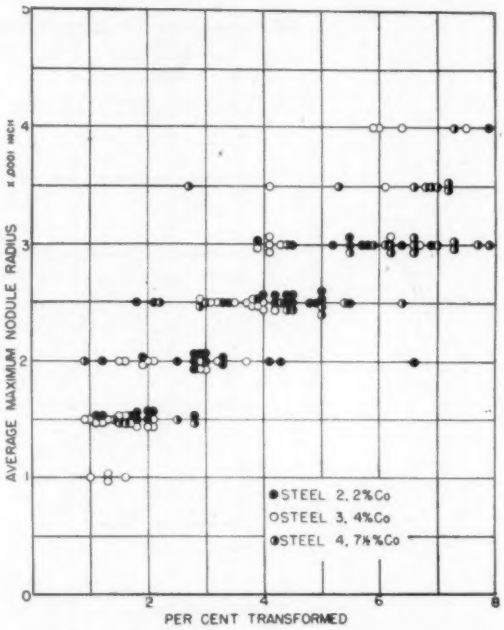

FIG 11—RESULTS OF STUDY ON EFFECT OF COBALT ON N AND G NEAR THE "KNEE" OF THE S-CURVE.

Each point represents an analysis of a 4½ by 5½ in. micrograph taken at 1000×. A fine grid of cross-sectional lines was printed on each micrograph so that nodule radius and percentage transformation could be measured quantitatively.

There is considerable scatter in the data, as would be expected, but within experimental error they show that the effect of cobalt is neither predominantly on N nor on G. Since it has been shown that cobalt increases the transformation rate, both must be increased in the same degree, effectively. From the Johnson-Mehl reaction rate expression,[2] this would mean that if the increase in G were by a factor of n, the increase in N would be by a factor of n^3.

RATES OF GROWTH

The rates of growth of pearlite in Steels X, Y, and Z were measured at two

different temperatures using the technique developed and fully described by Hull, Colton and Mehl in references [16] and [3]. This consists of examining partially reacted specimens in which nodule impingement has not yet occurred, and plotting maximum nodule radius against time of transformation. Apparently, the rate of growth is always constant throughout transformation[3], hence the slope of the resulting straight line is that rate. Such curves are shown in Figs 12 to 14; the first two of these figures show a fairly good check between as-rolled and homogenized specimens. Values of G for the two temperatures are given in Table 4. The data clearly show that cobalt increases the rate of growth of pearlite.

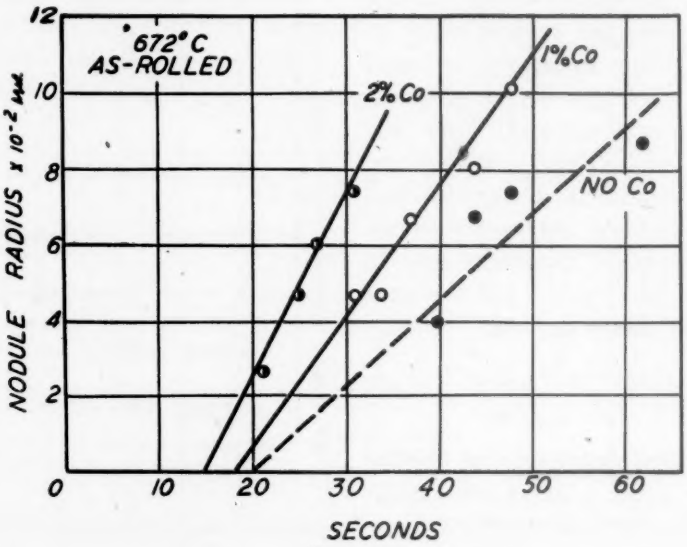

FIG 12

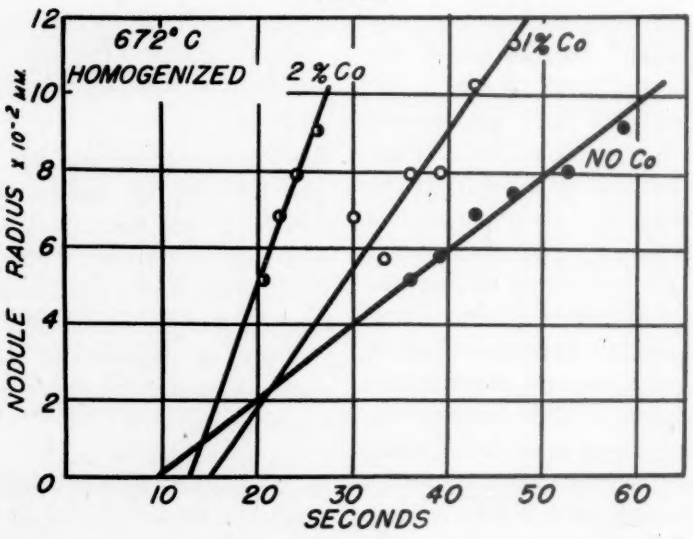

FIG 13

FIGS 12 AND 13—RATES OF GROWTH OF COBALT STEELS AT 672°C.

In comparing these data with those on N at the same reaction temperatures to ascertain whether or not cobalt acts preferentially on N or G, it must once

more be kept in mind that the effect on reaction rate of an n-fold increase in G is equivalent to an n^3-fold increase in N. Numerical comparisons are difficult because N cannot be measured as precisely as G. However, a comparison of Figs 7 and 8 with Table 4 indicates semi-quantitatively that these two variables are increased effectively to the same degree. Thus the dual effect of cobalt additions upon N and G for pearlite formation are demonstrated at temperatures near A_1 as well as at temperatures near the "knee" of the S-curve. The effect upon G at these lower temperatures was discussed in the previous section.

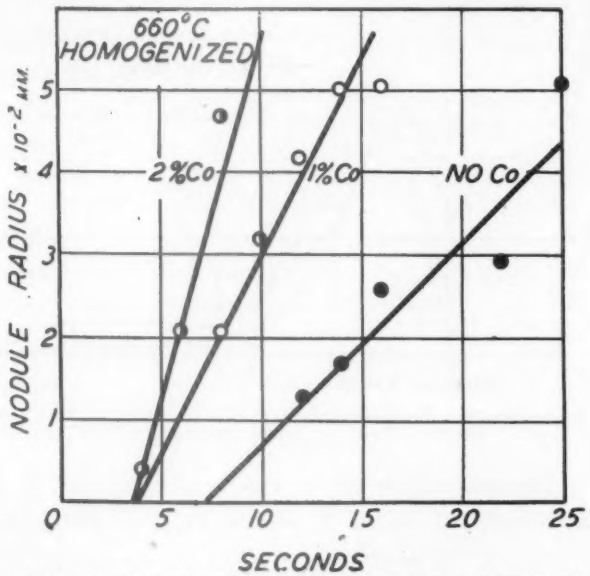

FIG 14—RATES OF GROWTH OF COBALT STEELS AT 660°C.

PEARLITE SPACING

Introduction

If the interlamellar spacing, S_o, of pearlite forming from austenite is varied by an alloying element, all other circumstances remaining the same, a variation in G would be expected, for varying S_o varies the concentration gradient for the diffusion process that promotes the segregation. In the present case, a decrease in S_o, resulting from cobalt, increasing the effective concentration gradient might be expected since cobalt has been shown to increase G. A change in pearlite spacing has been observed when alloying elements are added to steels.[17] Data follows on the effect of cobalt upon interlamellar spacing.

TABLE 4—*Rate of Growth of Pearlite at Various Temperatures*

CENTIMETERS PER SECOND × 10^{-4}

Temperature	"X" (No Co)	"Y" (1 pct Co)	"Z" (2 pct Co)
660°C Homogeneous	2.4	4.7	8.4
672°C Homogeneous	1.9	3.5	6.5
672°C As-Rolled	2.2	3.4	4.5

Measurements of Pearlite Spacing at High Transformation Temperature

Steels X (no Co), Y (1 pct Co), and Z (2 pct Co) were isothermally transformed at 700°C for the purpose of producing relatively coarse pearlite, the spacing of which can be measured with accuracy. They were in the form of small specimens,

about 1/16 in. thick, cut from homogenized stock; these specimens were austenitized 15 min. in vacuum at 1200°C to produce homogeneous austenite with little tendency to spheroidize on transforming. One specimen each of Steels Y and Z, both completely transformed to pearlite, were used in the study. However, in the case of Steel X, two specimens, one fully transformed, the other about 85 pct transformed were used; this was for the purpose of determining, in the same experiment, whether the constancy of spacing is maintained throughout transformation. Plane sections through each specimen were carefully prepared for metallographic observation of the relative areas occupied by small ranges of apparent spacing, according to the method fully described by Pellissier et al.[17] Qualitative evidence that cobalt decreases the interlamellar spacing of pearlite formed at 700°C was obtained at this point, for it was observed that only about one half of the lamellae could be resolved in the 2 pct cobalt steel, and that the 1 pct cobalt steel, though almost completely resolvable, contained more unresolved areas than did the steel with no cobalt. Results of the area measurements showed 1.8 pct unresolved pearlite in the 1 pct cobalt steel and an average of only 0.1 pct in the two specimens of steel without cobalt.

Detailed area measurements were not made on the 2 pct cobalt steel because of the large fraction of irresolvable areas; data on the other three specimens are presented in Fig 15. Each curve represents spacing measurements over the entire area of fifteen 5 × 7 in. micrographs taken at 2500 ×. The ordinate of each point on the curve gives the fraction of the total area of the micrograph exhibiting the spacing represented by the abscissa. Careful examination of the data at the first three stations along the abscissa shows a small but definite effect of cobalt in promoting a finer pearlite spacing. One might also infer that the completely transformed plain carbon steel contained finer pearlite, on the average, than the same steel partially transformed. The effect is believed to be within the experimental error, however, in view of the following calculations:

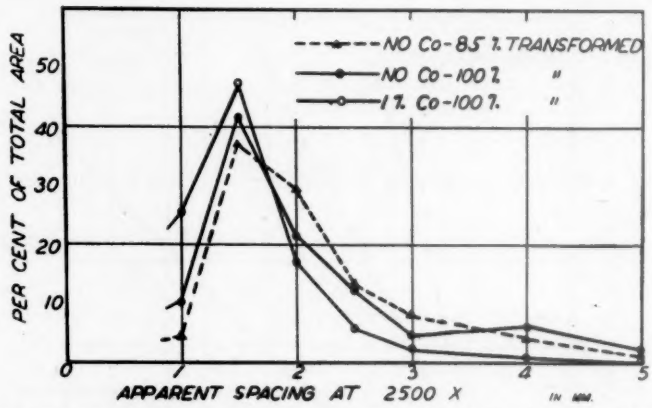

FIG 15—PEARLITE SPACING STUDIES ON COBALT STEELS. DISTRIBUTION OF APPARENT SPACINGS ON PLANE OF POLISH.

Values of the true pearlite spacing for the steels represented in Fig 15 were calculated by two methods developed in the research[17] previously cited.

Method No. 1 makes use of the relation:

$$f_s = \cos\left(\csc^{-1}\frac{S}{S_o}\right) \qquad [1]$$

where S = the apparent spacing measured on a plane of polish

f_S = the cumulative area (i.e., the fraction of the total area on the plane of polish exhibiting an apparent spacing equal to or less than S.)

S_o = the true pearlite spacing

From Fig 15, f_S and S are obtained, and thus equation [1] may be solved for S_o. Only intermediate values of f_S may be used with certainty, for small values are influenced in too great a proportion to the total value of f_S by small statistical variations of S_o, while slight errors in measuring the large values of f_S give large errors in $\frac{S}{S_o}$

Method No. 2 involves plotting f_S as a function of S for the experimental data, then sliding the theoretical curve of f_S vs. $\frac{S}{S_o}$ from equation [1] along the S axis until the best fit with the experimental curve is obtained. The intersection of the theoretical curve with the S axis is taken as S_o. This should give approximately the mean S_o if a statistical variation exists. Apparently such a variation is small in the present case for, as seen in Table 5, the two methods of calculation give the same result. There also it will be seen that the two specimens without cobalt have about the same spacing (S_o) within experimental error, while the 1 pct cobalt steel is 30 to 40 pct finer.

A rough determination of the true spacing of the 2 pct cobalt steel was also attempted. In spite of the fact that much of the pearlite was irresolvable, six micrographs had been taken for the record at the time the other steels were analyzed. These were later divided into areas exhibiting an apparent spacing of 1.0 mm or under at 2500 × and areas of 1.5 mm or larger spacing at 2500 ×. Into the former classification which gives the value for f_S at S = 1 mm (at 2500 ×), 61.6 pct of the areas fell. Thus from equation [1], the value 3.2×10^4 Å appearing in Table 5 for S_o for the 2 pct cobalt steel is obtained. This is only slightly lower than the value of 3.8×10^4 Å which is apparently the best value for the true spacing of the 1 pct cobalt steel; however it is felt that more accurate measurements at higher resolving power would prove the true spacing of the 2 pct cobalt steel to be considerably finer.

TABLE 5—*Pearlite Spacing of Cobalt Steels*

Method No. 1 From equation [1]

	Calculation at Apparent Spacing of (in Å)	True Pearlite Spacing (in A)
No Cobalt (85 pct Transformed)	6.0×10^3	5.6×10^3
	8.0×10^3	5.6×10^3
	10.0×10^3	5.2×10^3
No Cobalt (100 pct Transformed)	6.0×10^3	5.2×10^3
	8.0×10^3	5.6×10^3
	10.0×10^3	5.2×10^3
1 Pct Cobalt (100 pct Transformed)	4.0×10^3	4.0×10^3
	6.0×10^3	4.0×10^3
	8.0×10^3	3.6×10^3
2 Pct Cobalt (100 pct Transformed)	4.0×10^3	3.2×10^3

Method No. 2 Curve Fitting

	True Pearlite Spacing (in Å)
No Cobalt (85 pct Transformed)	5.6×10^3
No Cobalt (100 pct Transformed)	5.2×10^3
1 Pct Cobalt (100 pct Transformed)	3.6×10^3

Measurements of Pearlite Spacing at Temperatures Nearer the "Knee" of the S-Curve

From the standpoint of hardenability, the rate of formation of pearlite at temperatures near the "knee" of the S-curve is of much more significance than is the rate at higher temperatures. Therefore measurements of the effect of cobalt on the interlammelar spacing of pearlite formed near the knee were desired.

An electron microscope was available for the purpose of obtaining the high resolving power needed to measure the fine spacing of the cobalt steels. However, the very fast reaction rates, which cause

recalescence and prevent true isothermal transformation of any specimen of reasonable size, precluded experiments at temperatures actually as low as the "knee." A compromise temperature of 640°C was selected as reasonably safe. Specimens of steels 2, 3, and 4 were reacted at this temperature and photographed on the electron microscope.

Irregularities of the pearlite and variation of the spacing within colonies precluded the use of the outlining method used at the higher temperature. A method had to be developed, instead, involving a count of the intersections with lamellae of lines ruled across the photographs. From this count an average true spacing could be calculated.

Results of such measurements and calculations indicated no effect by cobalt. However, the fineness and irregularity of the pearlite and certain experimental difficulties introduced enough probable error to make these results of questionable significance. It seems probable that cobalt should continue to cause a decrease in pearlite spacing as the reaction temperature is decreased. However, when the transformation is rapid and the spacing is very fine, the effect may be too small to detect by present methods.

The Effect of Cobalt on the Coefficient of Diffusion of Carbon in Austenite

If the addition of an alloying element should cause an increase in the coefficient of diffusion of carbon in austenite but affect no other variable in the transformation process, it would increase the rate of reaction of austenite to pearlite, for the formation of pearlite obviously requires a segregation, that is, a diffusion, of carbon in austenite at the growing pearlite: austenite interface. Manganese, nickel,[18] and molybdenum[19] have been shown to affect this diffusion coefficient but slightly. However, evidence exists suggesting that cobalt may increase it. Houdremont and Schrader[20] claimed that the addition of cobalt increases the rates of carburization and decarburization of austenite. The latter effect was apparently confirmed in working with the two principal series of cobalt steels used in this investigation.

Harris,[21] on the other hand, attempts to explain differences in diffusion-penetration curves of alloy steels carburized under similar conditions on the basis of the effect of the alloying element on the surface equilibria involving carbon (in particular, the solubility of carbon in austenite at the temperature concerned). With several alloy steels, he was able to reproduce the experimental curves by using calculations based on the observed boundary carbon concentrations and on the diffusion coefficient for carbon in austenite. This diffusion coefficient was assumed to vary with temperature and carbon concentration according to the data of Wells and Mehl;[18] it was assumed to be independent of alloy concentration. Two high-nickel steels, however, showed a relatively low surface carbon concentration but deep penetration; i.e., the diffusion-penetration curve did not have the standard shape but was "flatter" suggesting a higher value of D. This is unlikely, however, in view of the negligible effect of nickel on D demonstrated by Wells and Mehl (loc. cit.).

The multiplicity of conflicting data of this type make it obvious that no inferences on the effect of alloying elements on the coefficient of diffusion of carbon in austenite should be drawn without making direct measurements. For this reason, measurements of this coefficient were made on various steels with and without cobalt using the technique perfected by Wells and Mehl (loc. cit.).

Measurements of Diffusion Coefficient for Carbon in Austenite Containing Cobalt

The first diffusion experiment was made on a couple consisting of steel F (.03 pct carbon and 7.5 pct cobalt) welded

to steel E (.64 pct carbon and 7.5 pct cobalt). The diffusion anneal was at 1056°C for 29 hr in an atmosphere of argon. Immediately following this run, a couple consisting of steel F (.03 pct carbon and 7.5 pct cobalt) welded to steel J (1.4 pct carbon and 7.9 pct cobalt) was annealed at 922°C for 40 hr in the same apparatus. Following the anneals, layers were removed for carbon analyses and diffusion penetration curves were plotted in the usual manner. Diffusion coefficients were obtained from the curves by the Matano[22,23] method and are shown in Table 6.

TABLE 6—*Diffusion Coefficients for Carbon in Cobalt Steels and in Plain Carbon Steels*

Temperature Deg C	Pct Cobalt	Diffusion Coefficient Cm^2 per Sec × 10^{-7}	Source
1056	7.5	5.3 at 0.3 wt pct C	This investigation
1056	None	5.7 at 0.3 wt pct C	Wells and Mehl[18]
922	7.7	1.4 at 0.7 wt pct C	This investigation
922	None	1.7 at 0.7 wt pct C	Wells and Mehl[18]

Table 6 also contains data, from the work of Wells and Mehl,[18] on the diffusion coefficient for carbon in plain carbon steels. A comparison of the results in the table indicates that if cobalt has any effect on the rate of diffusion of carbon in austenite, it is to produce a decrease in that rate. However, the agreement of the D values with and without the presence of cobalt is so close as to be within experimental error, and no such effect is to be accepted.

Soon after these results were obtained, Smoluchowski[24] reported that cobalt increases the diffusion coefficient for carbon in austenite. His results are shown in Fig 16. The experimental technique used for this work required unusual mathematical solutions for D values since only the low carbon half of the diffusion couple contained cobalt. By assuming negligible diffusion of cobalt, a modification of the Grube method permitting calculation of D values could be used. This required

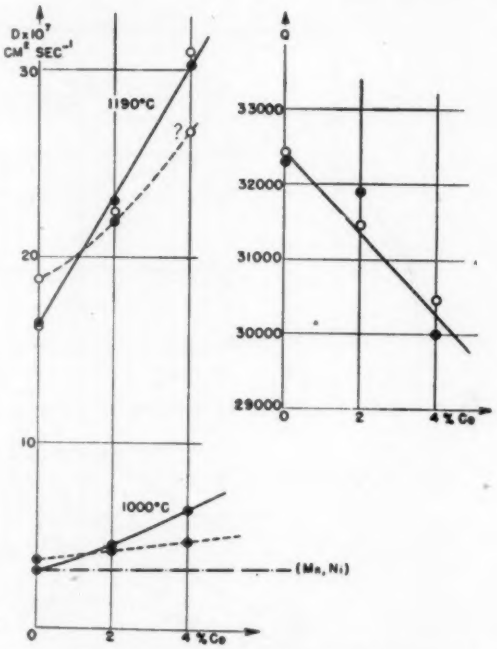

FIG 16—RESULTS OF SMOLUCHOWSKI ON THE EFFECT OF COBALT ON THE COEFFICIENT OF DIFFUSION OF CARBON IN AUSTENITE.[24]

knowledge of D values in the absence of cobalt that were obtained experimentally.

In view of Smoluchowski's results, further diffusion runs, again using the standard Wells and Mehl technique, were made in this laboratory. In this second set of experiments, couples with and without cobalt were annealed simultaneously in the same furnace to get an absolute basis for comparison. This was done at two different temperatures, thus providing four couples from which the usual diffusion-penetration curves could be obtained. D values were obtained from these curves by the Matano method and are given in Table 7. There it will be seen that there is but little difference between the results on the cobalt steels and the results on the plain carbon steels. If allowance is made for the difference in carbon content at which the calculations

were made, any possible effect of cobalt is entirely within the limits of experimental error. The effect of carbon concentration on D will be considered in succeeding paragraphs.

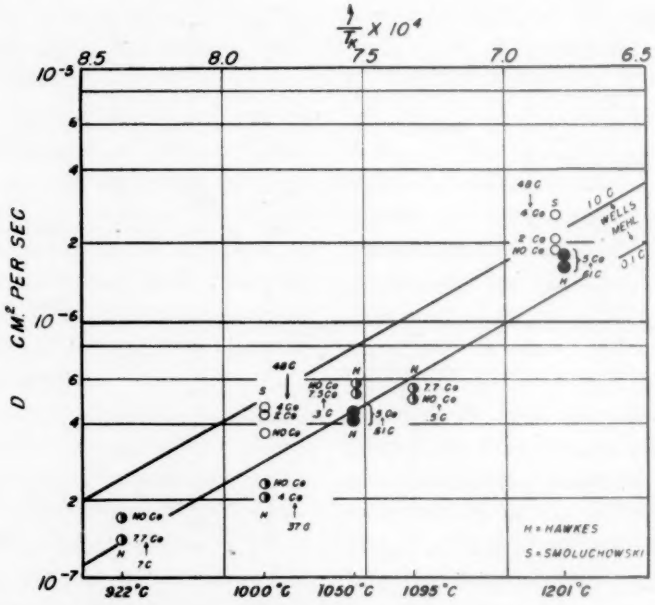

FIG 17—LOG D VERSUS $\frac{1}{T}$ FOR ALL DIFFUSION EXPERIMENTS MENTIONED IN TEXT.

The D values in Table 7 are somewhat lower than those of Wells and Mehl[18] on plain carbon steels because of some decarburization of the couples. However the couples to be compared were run simultaneously under identical conditions, so the relative D values should be reliable. Nevertheless, more fully trustworthy results were desired, so further experiments, described in the next paragraph, were undertaken.

Through the courtesy of Messrs. Parke and Ham, the improved facilities and technique[19] for diffusion experiments at the Climax Molybdenum Co. Research Laboratory were made available. Couples were prepared from cylindrical bars each having a polished, optically flat surface prepared on one end. The two members of each couple, slightly separated, were heated to the temperature of the diffusion anneal, then welded by forcing them together under pressure, then held for the desired time. This entire operation was carried out under high enough vacuum to prevent any detectable decarburization or oxidation. This technique gives a perfect weld, accurate alignment of the

TABLE 7—*Diffusion Coefficients for Carbon in Cobalt and in Plain Carbon Steels Annealed Simultaneously*

Couple No.	Temperature Deg C	Time Hours	Pct Cobalt	Diffusion Coefficient cm² per sec × 10⁻⁷
1 (a)	1000	38¼	4	2.1 at 0.4 wt pct C
2 (b)	1000	38¼	None	2.6 at 0.5 wt. pct C
3 (c)	1095	20	7.7	5.7 at 0.5 wt pct C
4 (d)	1095	20	None	4.9 at 0.4 wt pct C

(a) Steel No. 3 (.71 pct C and 4.2 pct Co) welded to Steel No. SS* (.11 pct C and 4 pct Co)
(b) Steel No. 10 (1.1 pct C and no Co) welded to Steel No. 11 (.14 pct C and no Co)
(c) Steel No. J (1.4 pct C and 7.9 pct Co) welded to Steel No. F (.03 pct C and 7.5 pct Co)
(d) Steel No. 1 (.76 pct C and no Co) welded to Steel No. 9 (.15 pct C and no Co)
* Steel No. SS was kindly supplied by Dr. Smoluchowski and was one of the steels used in his investigation.

couple, and allows precise measurement of the diffusion time. Couples consisting of Steel T (5 pct Co, 1.13 pct C) welded to Steel U (5 pct Co, 0.09 pct C) were given previously mentioned. It will be seen that the results at 1201°C closely check those of Wells and Mehl[18] for plain carbon steel at the same temperature. The results

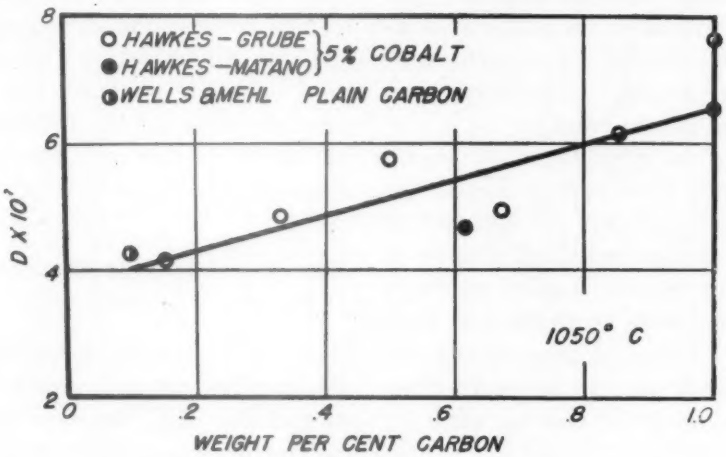

FIG 18

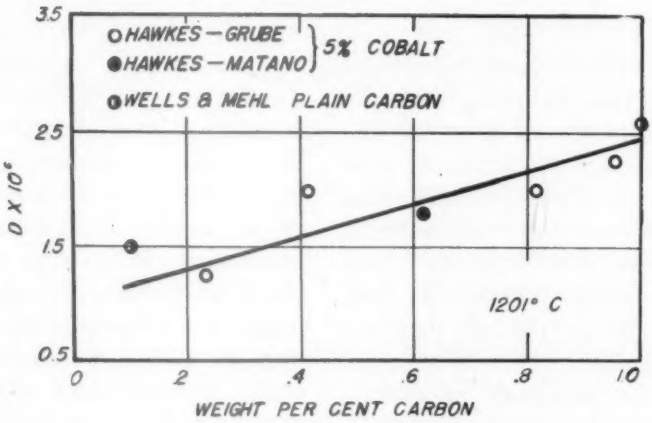

FIG 19

FIGS 18 AND 19—EFFECT OF CARBON CONCENTRATION OF COEFFICIENT OF DIFFUSION OF CARBON IN AUSTENITE.

diffusion anneals at 1050°C and at 1201°C. Duplicate couples were used in both runs, hence four diffusion-penetration curves were obtained.

Mean values for D for the duplicate couples (which checked to better than 10 pct in both cases) are shown as full circles in Fig 17; they were calculated in each case at the average carbon concentration (0.61 wt pct). For the sake of comparison, Fig 17 also contains the results of all other measurements of D at 1050°C are slightly lower than the values for plain carbon steels.

Effect of Carbon on the Diffusion Coefficient

In view of Smoluchowski's[24] surprising results showing a decrease in D with increasing carbon content, calculations of the effect of carbon were made using data from the experiments last described. Grube[23] solutions for D were calculated at various carbon concentrations and are plotted in Figs 18 and 19. This method

was used because of the difficulty of accurately measuring slopes at a distance from the interface for the Matano method and also for a check on the latter method. (Wells and Mehl[18] showed that but little error was introduced by the Grube assumption of D independent of concentration provided the actual dependency were small as in the case at hand.)

Contrary to the effect found by Smoluchowski,[24] D is seen to increase as the carbon content increases in these cobalt steels just as it does with an increase in carbon content in plain carbon steels. In fact, two points from the Wells and Mehl data are also plotted on these curves and the agreement is seen to be fairly good. The Matano result is also included for comparison.

Conclusions

All the experimental evidence obtained in this investigation indicates that the addition of cobalt has no effect on the coefficient of diffusion of carbon in austenite. Contrary to this is the only other experimental evidence on the subject, that of Smoluchowski[24] who finds that D_e is approximately doubled by the addition of 4 pct cobalt. The only explanation for this discrepancy that is apparent at present is the difference in experimental techniques; Smoluchowski used a couple containing cobalt only on one side of the interface and required a rather unusual mathematical solution to determine values for D.

However, assuming Smoluchowski's results are correct, it still appears that the effect shown is too small to explain the influence of cobalt on the pearlite reaction. Brandt[25] and Zener[26] have derived expressions for the rate of growth G of pearlite in terms of the coefficient of diffusion D of carbon showing G to increase linearly with D. Data presented in a previous section show that the addition of 2 pct cobalt more than doubles G in the neighborhood of 675°C. Smoluchowski, however, finds less than a two-fold effect on D with 4 pct cobalt at higher temperatures and lower carbon concentrations; furthermore, his data show the effect to decrease as the temperature decreases and as the carbon concentration increases. It is thus felt that we must look beyond the possible effect on the diffusion coefficient of carbon to find an explanation for the anomalous behavior of cobalt.

The Rate of Diffusion of Cobalt in Austenite

It has frequently been suggested that alloying elements may retard the formation of pearlite (i.e., increase hardenability) because of a postulated requirement that they diffuse during the reaction. For the opposite case, where an alloying element, such as cobalt, increases the rate of reaction, it is difficult to envision any mechanism in which the rate of diffusion of the alloying element could be used to explain the effect. Even though the cobalt atoms attain a "required" degree of partition more rapidly than the carbon atoms do, the rate of formation of pearlite should not be greater than that obtaining when cobalt is not present.

Nevertheless, data on the diffusion coefficient for cobalt in austenite seemed desirable, for such data are available for manganese,[27] nickel,[28] and molybdenum,[29] and an outstanding difference in the case of cobalt might furnish a clue regarding the mechanism of its effect. For instance, an abnormally high diffusion coefficient might indicate a "loosening" of the austenite lattice or weakening of the face-centered-cubic bond and a lower activation energy for atoms rearranging to form a body-centered cubic lattice.

Two diffusion experiments were carried out using couples consisting in both cases of steel 8 (0.73 pct C, no Co) and steel 5 (0.68 pct C, 11.2 pct Co). One couple

was given a diffusion anneal* of 404 hr at 1200°C and the other a diffusion anneal of 98 hr at 1316°C. Chemical analyses for cobalt on layers subsequently machined off parallel to the interface gave the data for diffusion-penetration curves. From these curves, *D*-values for the diffusion of cobalt in austenite were obtained by the Matano method. The results are plotted as two points on Fig 20 which also gives data on manganese,[27] nickel,[28] and molybdenum[29] for comparison. The carbon contents given with the cobalt *D*-values are slightly lower than those given previously for the steels used in the couples. Some decarburization occurred during the diffusion anneal, so an estimate of the average carbon content during the run was made. No claim for the temperature dependence of the *D*-value for cobalt is made since only two points are available, and the carbon concentration is not known precisely.

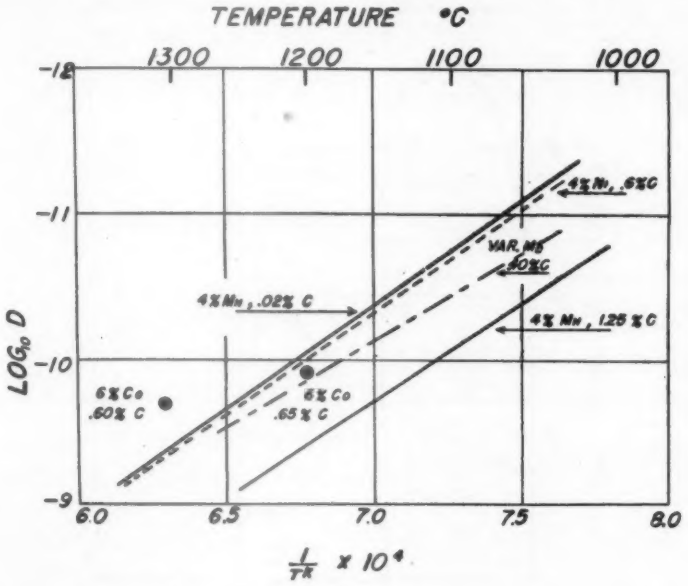

FIG 20—LOG D VERSUS $\frac{1}{T}$ FOR DIFFUSION OF ALLOYING ELEMENTS IN AUSTENITE.

Fig 20 shows clearly that cobalt is not abnormal with respect to its rate of diffusion in austenite; at any given temperature, its diffusion coefficient is of the same order of magnitude as those for manganese, nickel and molybdenum, all of which are orders of magnitude smaller than that for carbon.

The Effect of Nitrogen on the Rate of Transformation of Cobalt Steels

Speculation on the role of nitrogen in the transformation of austenite has existed since the introduction of steels treated with small amounts of boron or other special addition agents which often are strong nitride formers. Furthermore, although nitrogen may not be added intentionally, the addition of some elements, notably chromium, is known to increase the amount of nitrogen absorbed from the air in steel-making. It was considered of interest, therefore, to determine whether cobalt might not behave likewise and, if so, to determine whether the effect of cobalt on the rate of decomposition of

* The diffusion anneals were very kindly performed by Mr. John Ham of the Climax Molybdenum Company Research Laboratory.

austenite could be attributed to an indirect mechanism involving nitrogen.

The two principal series of steels used in the investigation were analyzed* for nitrogen; the results are shown in Fig 21. There it is seen that an increase in cobalt concentration causes a marked increase in the amount of nitrogen absorbed from the atmosphere. Experiments were then devised to ascertain the effect of, or eliminate, this difference in nitrogen content.

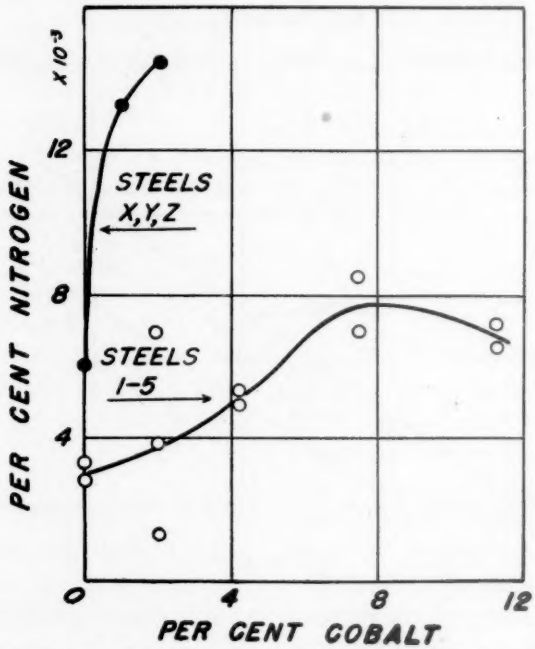

FIG 21—NITROGEN CONTENT OF TWO SERIES OF COBALT STEELS MADE UNDER ORDINARY ATMOSPHERE (AIR).

Attempts were made to prepare two heats of cobalt steel, of eutectoid carbon concentration, which would be alike in all respects except for a large difference in nitrogen content. The requirements on chemical composition were met by melting two similar charges under vacuum in a small laboratory induction furnace, then admitting dry nitrogen into the atmosphere above one of the melts, and finally allowing the two to freeze in the crucible. In two such pairs of heats, analyses showed one of the pair to contain no nitrogen and the other to contain approximately 0.025 pct. Large differences in austenite grain size, however, prevented comparing the two members of either pair of heats to isolate the effect of nitrogen upon hardenability. Regardless of the hot working or homogenization treatments used, the nitrogen bearing heats remained very fine grained (ASTM No. 7 to 8) up to temperatures approximating 1100°C, then coarsened abruptly to a large non-uniform grain size.

The problem was then approached in a different manner. A series of three steels, Q, R, S, alike except for cobalt content, were melted and allowed to freeze under vacuum. This provided a uniform grain size and negligible nitrogen content throughout the series, thus allowing the effect of cobalt on hardenability to be isolated. A plain carbon steel, P, made under

* The author is indebted to Dr. G. Derge of this laboratory for vacuum fusion determinations of the nitrogen content of steels used in this study.

nitrogen was prepared at the same time to determine whether the pronounced grain growth restraining influence of nitrogen would be obtained in the absence of cobalt. The results of grain size determinations from 875°C to 1175°C are shown in Table 8. There, the powerful effect of nitrogen is demonstrated in a plain carbon steel; the austenite grain size of steel P is kept fine at a temperature considerably higher than that at which an ordinary "fine-grained" aluminum killed steel would be expected to coarsen.

TABLE 8—*Composition and Austenite Grain Size of Steels for Nitrogen Study*

Steel	P	Q	R	S
Pct Nitrogen (estimated)	0.02	None	None	None
Pct Cobalt (estimated)	None	None	2	4
Pct Carbon	0.99	0.88	0.92	0.89
Pct Manganese	0.03	0.10	0.10	0.06
Fracture Grain Size after 10 min. in deg C				
875	7?	6	6½	6
925	8½	5½	6¼	6¼
975	8	4½	4¾	5½
1075	7½			
1175	5			

TABLE 9—*Effect of Cobalt on the Rate of Transformation of Austenite to Pearlite in the Absence of Nitrogen*

Steel	Q No Co	R 2 Pct Co	S 4 Pct Co
Time at 699°C in Seconds:			
0 (Brine Quench)			0
3			75
7		0	90
10	0	50	99
20	1	99	100
30	25		

Steels Q, R, and S were used to determine the effect of cobalt on the rate of formation of pearlite in steels which are in no way affected by nitrogen. For this purpose, $\frac{1}{16}$-in. thick specimens of each steel were austenitized 10 min. at 875°C, isothermally transformed at 699°C for various time intervals, and rated for percentage transformation to pearlite. The results, shown in Table 9, indicate that cobalt increases the reaction rate and does not depend upon nitrogen for its effect.

THE EFFECT OF COBALT ON THE MARTENSITE TEMPERATURE RANGE

No reasonable basis for a quantitative relationship between the hardenability of a steel and the temperature range over which martensite forms in that steel has ever been proposed, nor has such a relationship been established experimentally; nevertheless, most alloying elements in solution in austenite increase hardenability and most of them lower the M_s temperature.[30,31,32,33] Only cobalt[30,31] and aluminum[30] have been reported to raise it; in the latter case, it was not made clear whether the aluminum was entirely in solution in austenite or not.

TABLE 10—*Effect of Cobalt Additions on the Martensite Temperature Range*

Steel	Per Cent Martensite Formed			
	1 No Co	2 2 Pct Co	3 4 Pct Co	4 7 Pct Co
Temperature, deg C				
300		0	0–5	
270	0	10	10–50	
240	0-Trace	15–20	50–75	80–90

Fig 22, from Chiswick and Greninger[31] shows that cobalt additions raise the M_s temperature in 1.1 pct carbon steels. An attempt was made to obtain similar data at lower carbon contents by using steels 1 to 4 of this investigation; this was unsuccessful because of the rapid rate of transformation of austenite to bainite in the same temperature region. However, in Table 10, a confirmation of the effect of cobalt additions in raising the martensite temperature range is shown.

There the degree of transformation of austenite to martensite at three different temperature levels on cooling is shown to increase in each case as the cobalt content increases.

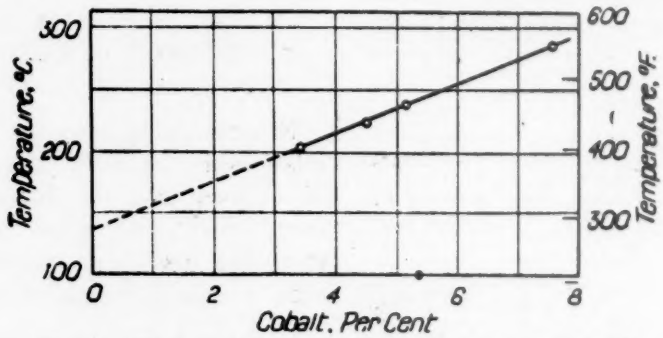

FIG 22—EFFECT OF COBALT ON THE M_s TEMPERATURE.[31]

REMARKS

It appears clear from the foregoing experimental evidence that cobalt increases both N and G and that this effect is intrinsic in the Fe-Co-C system. The effect exists when heterogeneity factors that affect N and G in alloy steels are absent; adventitious factors, such as a possible effect of nitrogen, appear absent. The effect of cobalt in increasing N and G must therefore be sought by considering those factors that are now believed to be fundamental in nucleation and growth processes, particularly as they apply to the pearlite reaction. Our knowledge of these factors is so primitive that our discussion can be little more than speculation.

First, as to the rate of growth, G: An increase in the rate of diffusion of carbon in austenite may be expected to increase G as pointed out early.[1] The data presented above would appear to rule out this possibility, but it must be pointed out that arguments on the effect of alloys upon the diffusion coefficient in this and other cases are not unambiguous. Diffusion coefficients are determined within normal austenite solid solution ranges, not exceeding one pct carbon, but the concentration differences at the pearlite: austenite interface that excite diffusion are related to the extrapolated austenite phase boundaries, and thus are presumably far greater than those employed in determining diffusion coefficients. For example, Brandt[25] believes these to be between 0.5 and 5.0 pct carbon for the formation of pearlite in simple carbon steels at 600°C. The values of the diffusion coefficient above one pct within this range have not been determined; it is at least conceivable that cobalt, at high percentages of carbon, may markedly increase the diffusion coefficient, and that the effect of cobalt on G lies in this circumstance.

An uncertainty also obtains with respect to the effect of cobalt upon the extrapolated concentration differences, for although Brandt adduces argument to show that this can be only a minor effect, it may none the less be at least a contributing factor here, for the effect of cobalt upon G is not great.

A decrease in the interlamellar spacing S_o, from whatever cause, should be accompanied by an increase in G. It was also pointed out early that G and S_o should, with other factors unchanged, be inversely proportional,[1] and subsequent more complete analyses[25,26] employ the same relationship. The data given above on S_o in cobalt steels, while not of high quality (for the difficulty in determining S_o with high accuracy is extraordinary)

show roughly that 1 pct cobalt decreases S_o by a factor of two to three. This same amount of cobalt increases G by the same factor. At this writing, with all of the uncertainties that attend the subject, it appears that this is the most likely explanation of the effect of cobalt on G. This argument, of course, only restates the problem (though with some progress): why should cobalt effect S_o? Zener's[26] excellent proposal that the interlamellar spacing is correlated with the amount of free energy that the austenite-pearlite reaction affords, with a greater free energy providing a smaller spacing, may be pertinent, but there appears to be no way to confirm it, for the free energy of the pearlite reaction is far too small to be measured with present means, and of course differences in this free energy occasioned by the presence of alloying elements are smaller yet.

The explanation of the effect of cobalt upon N is even less certain. Presumably any increase in the free energy of the pearlite reaction, furnishing additional energy to create the nucleus: austenite interface, would permit smaller stable nuclei to form and thus increase the rate of their formation.[34] If the argument given above were taken as proof that cobalt does increase the free energy of the reaction, then the increase in N exerted by cobalt might be assigned to this cause. This argument, unfortunately, is thin, for other factors might well be influential, for example, the effect of cobalt upon the specific interface energy itself.

The requirement of a knowledge of solid-solid interface energies imposed by formal nucleation and growth theory, constitutes a major difficulty in the present stage of development of this subject. There is no way at the moment to measure these energies, nor to approximate them with a degree of certainty that would afford a useful and discriminating result. In view of this general difficulty, and in view of the additional theoretical difficulties relating specifically to the eutectoid reaction as discussed above, it is probable that purely theoretical attack on this and allied problems will prove relatively difficult. It appears that progress will be afforded primarily by careful experimental measurements of N and G as affected by alloying elements, in the hope that such measurements will bring relationships to light that are now obscured by the complexities and inadequacies of theory.

CONCLUSIONS

The addition of cobalt increases the rate of decomposition of austenite at all temperatures between A_{e1} and $A_{r''}$. There is, however, no change in the shape of the S-curve or in the nature of the austenite decomposition products formed.

The influence of cobalt is not exerted by indirect means involving such factors as austenite grain size or the presence of second phases or inhomogeneities in austenite.

Cobalt has been shown to increase the amount of nitrogen absorbed from the air during the melting and casting of steels. However, this effect was shown to have no connection with the mechanism by which cobalt decreases hardenability, for this anomalous decrease was demonstrated in nitrogen-free cobalt steels.

Cobalt increases the rate of reaction of austenite to pearlite by increasing both rate of nucleation and rate of growth to effectively the same degree.

Cobalt decreases the interlamellar spacing of pearlite formed isothermally at a temperature slightly below A_{e1}.

In repeated experiments, no effect by cobalt on the coefficient of diffusion of carbon in austenite could be demonstrated. Other evidence exists to support the contention that cobalt increases this coefficient; the magnitude of the effect claimed,

however, appears to be too small to explain the influence of cobalt on hardenability.

The coefficient of diffusion of cobalt in austenite is of the order of magnitude to be expected in view of the values for nickel, manganese, and molybdenum.

Cobalt is the only element which has been shown to raise the temperature range over which martensite forms in homogeneous austenite.

REFERENCES

1. R. F. Mehl: The Physics of Hardenability in Hardenability of Alloy Steels, American Society for Metals, Cleveland, 1939.
2. W. A. Johnson and R. F. Mehl: *Trans.* AIME (1939) **135,** 416.
3. F. C. Hull, R. A. Colton, and R. F. Mehl: *Trans.* AIME (1942) **150,** 185.
4. E. Davenport: *Trans.* ASM (1939) **27,** 837.
5. W. Hume-Rothery: The Structure of Metals and Alloys, The Institute of Metals, London, 1939.
6. M. Hansen: Der Aufbau der Zweistofflegierungen, J. Springer, Berlin, 1936.
7. Andrew and Nicholson: First Report of the Alloy Steels Research Committee, The British Iron and Steel Institute, 1936, 93.
8. Rodgers and Maddocks: Second Report of the Alloy Steels Research Committee, The British Iron and Steel Institute, 1939, 167.
9. Ellis and Greiner: *Trans.* ASM (1941) **29,** 415.
10. Vogel and Sundermann: *Archiv Eisenhüttenwesen* (1932) **6,** 35.
11. F. Allison: *Trans.* AIME (1937) **75,** 234.
12. R. Scherer: *Archiv Eisenhüttenwesen* (1927) **1,** 325.
13. Houdremont and Schrader: *Archiv Eisenhüttenwesen* (1932) **5,** 523.
14. Esser, Eilender, and Majert: *Archiv Eisenhüttenwesen* (1933) **7,** 367.
15. G. A. Roberts and R. F. Mehl: *Trans.* AIME (1943) **154,** 318.
16. F. Hull: Reaction Kinetics of the Austenite to Pearlite Transformation, Doctorate Thesis, Carnegie Institute of Technology, 1941.
17. Pellissier, Hawkes, Johnson, and Mehl: *Trans.* ASM (1942) **30,** 1049.
18. C. Wells and R. F. Mehl: *Trans.* AIME (1940) **140,** 279.
19. Ham, Parke, and Herzig: *Trans.* ASM (1943) **31,** 877.
20. Houdremont and Schrader: Archiv. Eisenhüttenwesen (1932) **5,** 523.
21. F. Harris: *Metal Progress* (1943) **44,** 265.
22. C. Matano: *Japanese Journal of Physics* (1933) **8,** 109.
23. R. Mehl: *Trans.* AIME (1936) **122,** 11.
24. R. Smoluchowski: Phys. Rev. (1942) **62,** 539.
25. W. Brandt: *Trans.* AIME (1946) **167,** 405; *Metals Tech.* Dec. 1945—T.P. 1857.
26. C. Zener: *Metals Tech.* AIME Jan. 1946—T. P. (1925); *Trans.* (1946) **167,** 550.
27. C. Wells and R. F. Mehl: *Trans.* AIME (1941) **145,** 315.
28. C. Wells and R. F. Mehl: *Trans.* AIME (1941) **145,** 329.
29. J. Ham: *Trans.* ASM (1945) **35** 331.
30. Zyuzin, Sadovsky, and Baranchuk: Metallurg no. 10–11 (1939) 75.
31. Chiswick and Greninger: *Trans.* ASM (1944) **32,** 483.
32. Payson and Savage: *Trans.* ASM (1944) **33,** 261.
33. R. A. Grange and H. M. Stewart: *Metals Tech.* AIME June, 1946—T.P. (1996); *Trans.* (1946) **167,** 467.
34. R. F. Mehl and L. K. Jetter: The Mechanism of Precipitation from Solid Solution. The Theory of Age Hardening. ASM Symposium on Age Hardening, 1940.

Hot Deformation Structures, Veining and Red-shortness Cracks in Iron and Steel

By Axel Hultgren,* Member AIME, and B. Herrlander†

(Atlantic City Meeting, November 1946)

The original aim of the present investigation was to study the mechanism of cracking on hot-deforming red-short steels. During the microscopical examination of hot-deformed soft steels attention was directed to various patterns of so-called veining in the ferrite, as related to variations in the deformation procedure and the heat-treatment of the steels. Later, a hot-short steel of higher carbon content was also studied.

Historical

Storey[1] suggested in 1914 that veining developed during the gamma-alpha transformation from the growing together of several alpha nuclei within the same gamma grain.

Rawdon and Berglund[2] found that in soft steel, forged somewhat below A_3, the ferrite showed profuse veining, while usually there was very little veining after forging at very high temperatures. They emphasized the similarity between the pattern of veining formed by deformation about 600°C and that of slip lines formed by deformation at room temperature. They also suggested a relation between the gamma-alpha transformation and veining. They became convinced from etching and from the slip-line pattern in cold-deformed material, that the orientation within any ferrite grain showing veining was uniform. In recrystallized alpha grains veining was absent. Veining did not appear materially to affect the properties of ferrite. Independent of veining, continuous networks, attributed to pre-existing delta and gamma grain boundaries were sometimes found, the former only in cast steel. Those networks were usually connected with small inclusions.

Ammermann and Kornfeld[3] confirmed that recrystallized ferrite grains showed no veining. In soft steel annealed between A_1 and A_3 there was veining only in the ferrite grains formed during cooling. Electrolytic iron deformed at 880° was free from veining. Bannister and Jones[4] considered veining in ferrite to be a manifestation of microscopical and submicroscopical inclusions.

Northcott,[5,6] in studies on veining in steel and other metals and alloys, attributed veining to oxide inclusions. It could generally be removed by annealing in hydrogen, a suggestion earlier made by Rawdon and Berglund. Tritton (discussion in ref. 5) emphasized the importance of perfect polishing for bringing out veining by etching, and thought the veins or subboundaries were produced during the gamma-alpha transformation, when it was rapid, as a result of the volume change and contraction during cooling. Slight distortion would not allow projecting parts of a growing crystal to join up with atomic symmetry.

Hanemann and co-workers[7,8] showed that veining in ferrite consisted of ridges

Manuscript received at the office of the Institute July 23, 1946. Issued as T.P. 2106 in Metals Technology, December 1946.

* Professor of Metallography, K. Tekniska Högskolan, Valhallavägen, Stockholm, Sweden.
† K, Tekniska Högskolan.

[1] The references are at the end of the paper.

or rows of points in relief, within the grains. Such ridges of the "veining constituent" were also present in the grain boundaries. Heating of cold-worked ferrite produced

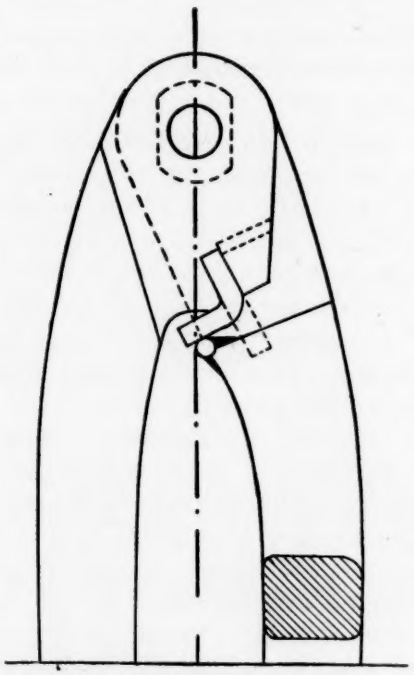

FIG. 1.—TONGS FOR HOT-DEFORMING ROD OF 5 MILLIMETERS DIAMETER.

the veining constituent in the slip lines that were previously etched as grooves. During the gamma-alpha transformation veining is formed as a result of different parts of the same alpha grain growing together and not having exactly the same orientation. The veining constituent is not colored by sodium picrate solution. Hanemann and his co-workers assume that the veining constituent is a ferrite boundary region of irregular atom arrangement characteristic of grain boundaries, the thickness of the region being increased by the presence of impurities.

From Laue diagrams of ferrite, Greninger[9] concluded that each grain had a macromosaic structure, with a scatter in orientation of 1° to 10°. He thought that macromosaic boundary lines accounted for some of the veining observed in ferrite.

Goss[10] found that subboundary structures, or veining, also indicated by asterism in Laue diagrams, were common in alpha iron. They were believed to result from strains produced either by the gamma-alpha transformation or by forces that cause recrystallization and subsequent grain growth.

Present Investigation

MATERIAL

The steels listed in Table 1 were investigated. They were all red-short.

TABLE 1.—*Composition of Steels Investigated*

Steel No.	Composition, Per Cent				
	C	Si	Mn	P	S
1	0.02	tr.	0.05	0.012	0.035
2	0.05	tr.	0.09	0.019	0.024
3	0.004	tr.	0.01	0.009	0.008
7	0.48	0.01	0.03	0.029	0.017

DEFORMATION AND HEAT-TREATMENT

Turned rods 5 mm in diameter by 25 mm were bent 90° over a radius of 5 mm, using a fixture in the form of a pair of tongs as shown in Fig 1. The front part of the fixture was preheated to the desired temperature by submerging it in a salt or lead bath, usually the former, or occasionally in a box furnace, the specimen was applied in its seat and the fixture replaced in the bath or furnace. After 3 to 5 min for heating the specimen, the bending was carried out by moving the handles together. Three different speeds of bending were used, corresponding to a bending time of approximately 0.5 sec (fast), 4 sec (medium) and 11 sec (slow). The bent or broken specimen was cooled in air or water.

Certain heat-treatments not connected with deformation, using different holding periods at high temperature or different rates of cooling, were carried out in a box furnace.

All soft steels, as received, contained veining. When it was desired to produce a material free from veining and coarse grained, the steel was stretched 3 to 5 per cent in a tensile-testing machine and then recrystallized at 870°C for 5 days, then cooled in air. The treatment was generally successful.

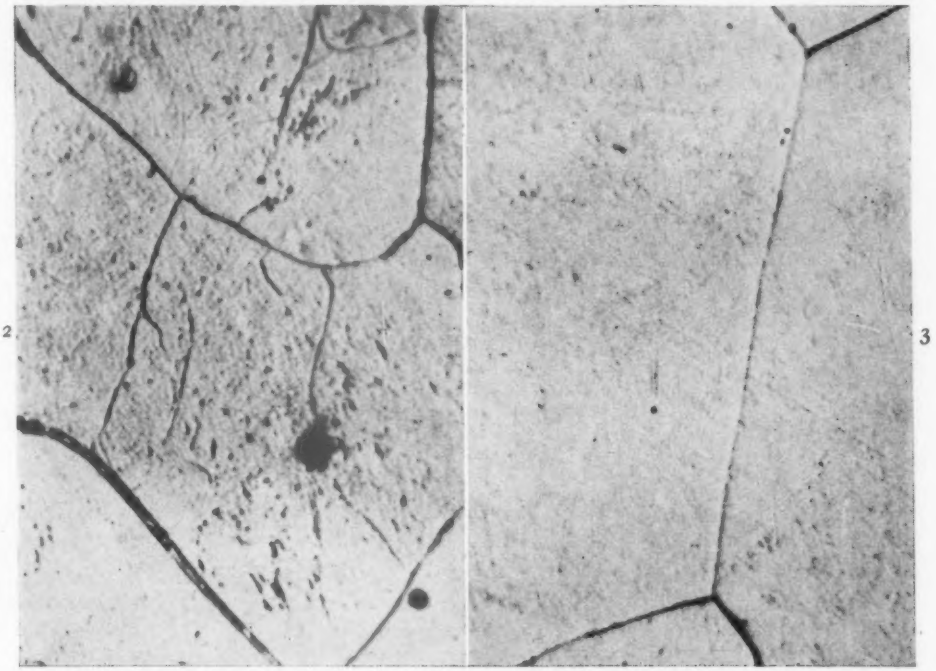

FIG. 2.—STEEL 1. SMALL SPECIMEN COOLED FROM 1000° TO 925°C WITH FURNACE THEN IN AIR. × 1200.

FIG. 3.—STEEL 1. SMALL SPECIMEN COOLED FROM 1000° TO 925°C WITH FURNACE, THEN AT RATE OF 5°C PER HOUR TO 846°C, THEN IN AIR. × 1200.

PREPARATION FOR MICROSCOPICAL EXAMINATION

Sections through the symmetry plane of the bent or broken rods, after being encased in Bakelite, were ground and electrolytically polished, with a Jacquet solution modified by v. Hámos,[11,12] containing perchloric acid (60 per cent) 19.4 per cent: anhydrous acetic acid (95 per cent), 59.7 per cent, and acetic acid (98–100 per cent), 20.9 per cent by volume. During electrolysis the specimen was rotating at 60 rpm and a stirrer at 400 rpm. Current density was about 0.09 amp per sq cm and time of polishing 7 to 9 minutes.

Electrolytic polishing was greatly superior, of course, to mechanical polishing for enabling fine details in the structure, such as veining, to be brought out clearly by etching, but was not suitable in studying the cracks, since they were enlarged in the process, losing detail. Etching was usually done in 4 per cent picric acid in alcohol. All micrographs showing veining were taken under oblique illumination from the left.

DEFINITION OF TERMS USED

To facilitate description, the following terms will be used:

Veining appearing as ridges; *positive* veining (Figs 2 and 12).

Veining appearing as grooves; *negative* veining (Fig 6, partly).

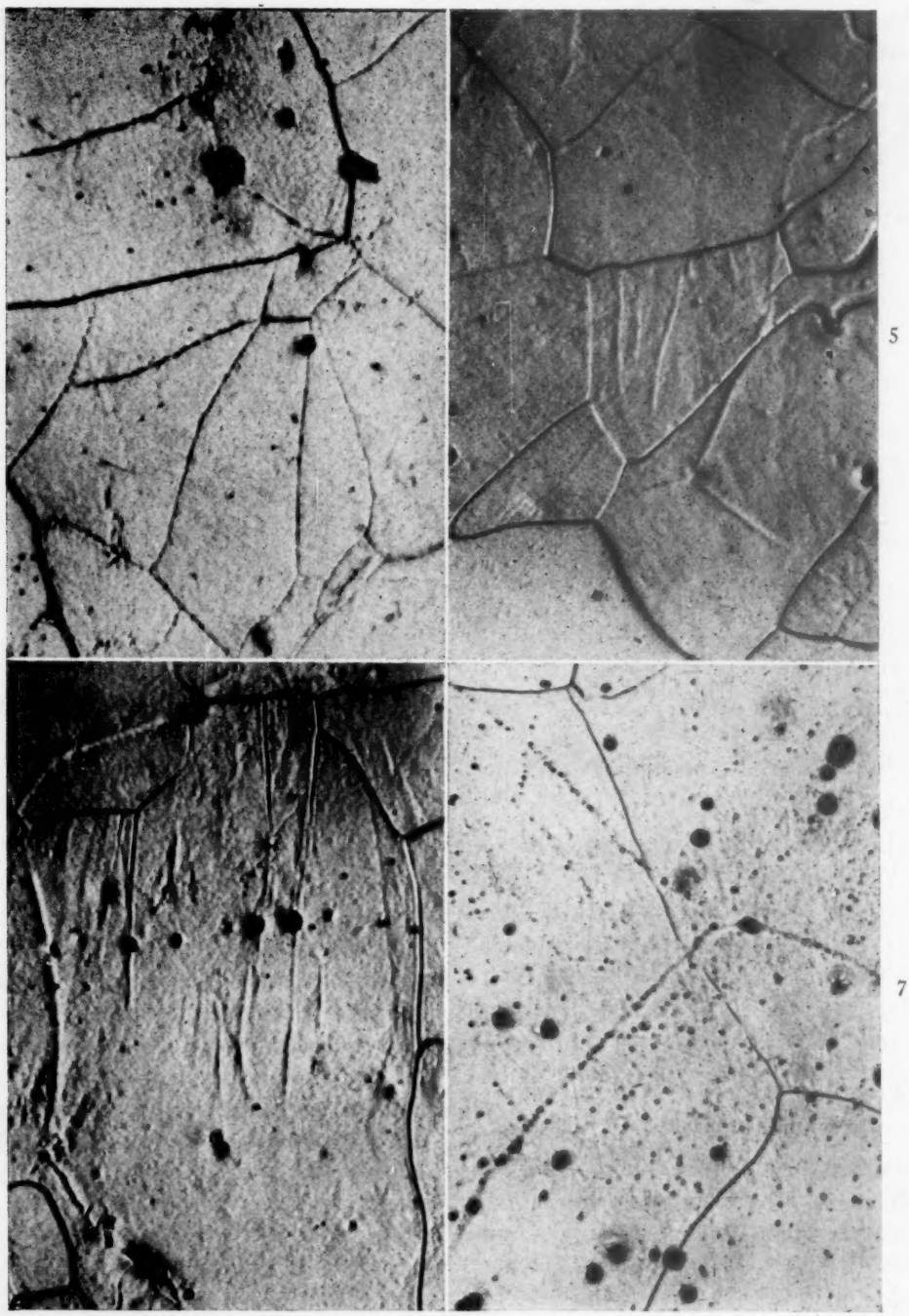

FIG. 4.—STEEL 1. SMALL SPECIMEN HEATED TO 925°, COOLED AT RATE OF 135°C PER HOUR. × 1200.
FIGS. 5 AND 6.—STEEL 1. SMALL SPECIMENS HEATED TO 925°, QUENCHED IN WATER. × 1200.
FIG. 7.—STEEL 1, RECRYSTALLIZED, COARSE GRAINED. SMALL SPECIMEN HEATED IN SALT BATH TO 850°, COOLED IN AIR. × 300.

Veining within the ferrite grains; *subboundary* veining (Fig 12).

Veining along the ferrite grain boundaries; *boundary* veining (Fig 3).

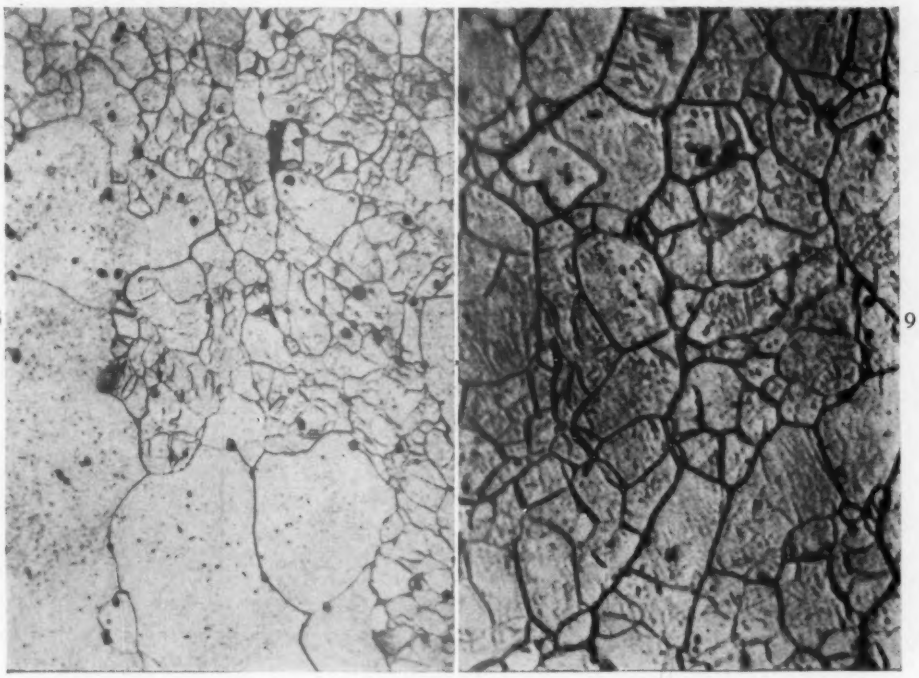

FIGS. 8 AND 9.—STEEL 1. DEFORMED SLOWLY AT 850°. COMPRESSED SIDE.
Fig. 8, × 300.
Fig. 9, × 1200.

Continuous network, probably indicating grain boundaries of pre-existing austenite; *gamma network* (Fig 19).

RESULTS

Soft Steel. Heating to a Temperature above Ac_3, Cooling at Different Rates

Three small specimens of steel 1 were heated to 1000°C, allowed to cool with the furnace to 925° and then cooled in different ways. One (Fig 2) was cooled in air, another (Fig 3) in the furnace at a rate of 5°C per hour to 846°C, then in air, and a third all the way to room temperature at the slow rate. The last two specimens showed the same structure. Veining is seen in Fig. 2 as narrow, discontinuous ridges, positive veining, within the ferrite grains and in the grain boundaries, in Fig 3 only in the boundaries. Similar experiments, using a slow cooling rate, were made with specimens of steel 2, which was fine grained, and steel 3, which was coarse grained. In steel 2 no subboundary veining was observed; in steel 3, even as slow a rate of cooling as 3°C per hour did not entirely prevent the formation of subboundary veining.

Another set of three small specimens of steel were heated to 925° and cooled in the following ways; one (Fig 4) was cooled in the furnace at a rate of 135°C per hour, one in air and the third (Figs 5 and 6) quenched in water. The furnace-cooled and air-cooled specimens showed positive subboundary veining, perhaps more continuous in the former. (In Fig 5 the center grain shows subboundary veining, but as grooves, negative veining.) In Fig 6 the large grain shows veins that are partly positive, partly negative. In

addition, a more or less continuous network of grooves is shown, believed to indicate the austenite grain boundaries existing at the moment of quenching,

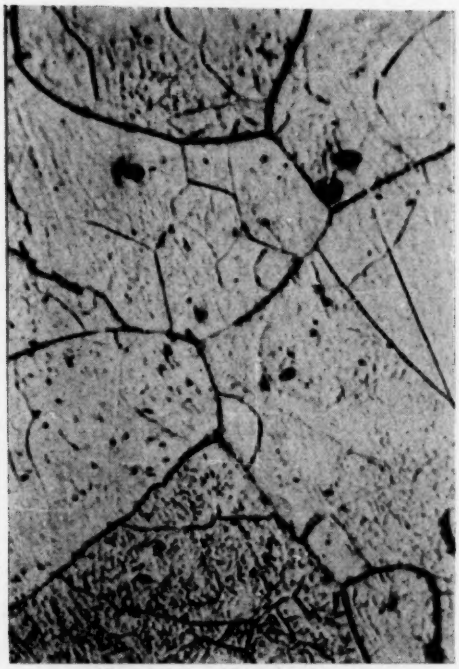

FIG. 10.—STEEL 1. DEFORMED SLOWLY AT 850°. CENTER × 1200.

the gamma network. Boundary veining was generally present after all rates of cooling.

Further attempts to fix the position of the austenite grain boundaries in the ferrite structure by quenching in water were at first unsuccessful—another type of structure was obtained showing ferrite units in Widmannstätten arrangement. On investigation, it was found that there is a certain rate of cooling that results in the gamma network being brought out by etching. After slower cooling, no trace of the gamma network is seen; after too rapid cooling, each austenite grain is subdivided into numerous ferrite areas of Widmannstätten arrangement. The suitable rate of cooling of small specimens for producing the gamma network was found to be obtained by quenching in water of 50° to 90°C (112° to 194°F). Examples of such structures are seen in Figs 18 to 23. Various periods of holding in the gamma state were tried, up to one hour. No difference in etching characteristics of the gamma network was found after such variations.

Soft Steel. Heating to a Temperature below Ac_3

A small specimen of steel 1, recrystallized as described, coarse grained and free from veining, was heated by plunging into a salt bath of 850°C, held 5 min and allowed to cool in air. The resultant structure contained negative subboundary and boundary veining, probably formed during cooling. In Fig 7 a branched network of small inclusions is visible, suggestive of old grain boundaries that migrated to their present position during heating. Since the old grain boundaries ought to be fairly stable after heating for 5 days at 870°C, it is suggested that the thermal stresses arising on heating in the salt bath have caused the boundary migration.

Soft Steel. Deformation at Temperatures below Ac_3

The following bending experiments were made on rods of steel 1 in a salt bath. After bending, the specimen was removed from the tongs and allowed to cool in air. When not otherwise stated, the steel before testing was in the normalized state.

After slow bending at 850°, the structure was as shown in Figs 8 to 10. Figs 8 and 9 were taken from the compressed side near the surface; Fig 10 from the center portion of the rod. Figs 8 and 9 show profuse positive veining, the old grain boundaries being unrecognizable. There are also dots and lines in relief within the subgrains (Fig 9). Partial recrystallization has set in during or after deformation (Fig 8). The recrystallized grains are interspersed with a fine rod-shaped precipitate. In Fig 10, representing a part less deformed, positive boundary and sub-

boundary veining are also well developed. Here the ferrite grain boundaries can be distinguished easily from the sub-boundaries. In comparison of Figs 9 and 10, it would appear that, on sufficient hot deformation, the ferrite grain boundaries are deformed to suit the subgrains.

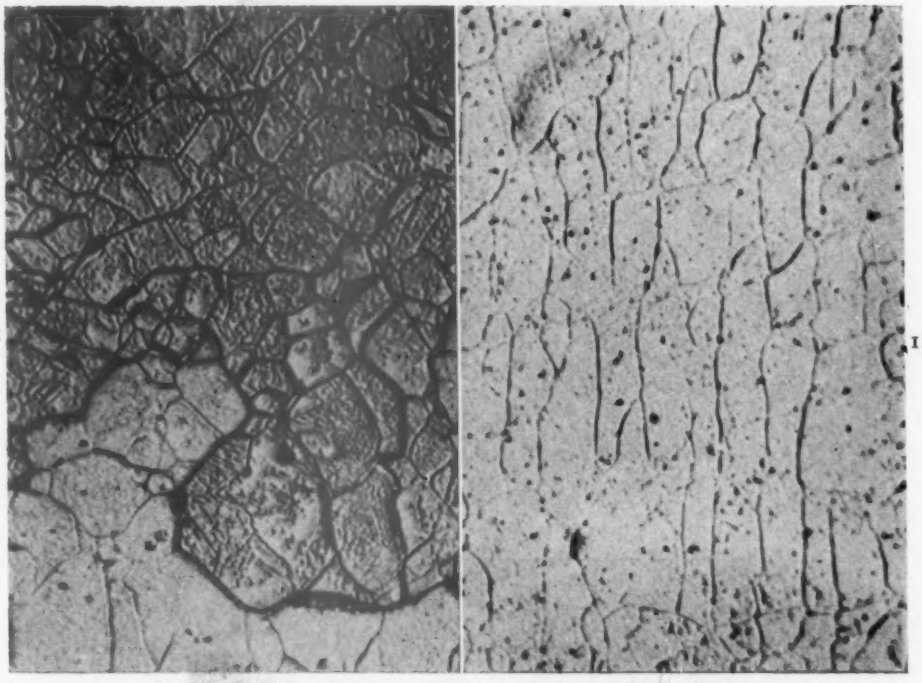

FIGS. 11 AND 12.—STEEL 1. DEFORMED AT MEDIUM RATE AT 850°. STRETCHED SIDE. × 1200.

Similar structures were obtained on deforming at a medium rate at 850°C (Fig 11, stretched side). Fig 12, from the same specimen, shows a portion of a grain having a network of veining ridges, where portions having one particular direction stand out in higher relief and probably are wider than other portions.

The results of rapid deformation at 850° are shown in Figs 13 and 14. Intercrystalline red-shortness cracks are evident in Fig 13. In comparison of Figs 8 and 9 with Figs 13 and 14, it is seen that, after rapid deformation, the subgrains are smaller and the veins have preferred directions, in certain grains approaching the regularity of slip lines produced on deformation at room temperature. Fig 14 shows that the grain boundaries, which are clearly visible, have locally changed their course to accommodate the sub-grains; also rows of small inclusions are situated at the grain boundaries. Fig 15 shows the structure of a recrystallized and coarse-grained specimen of steel 1, after the same deformation treatment, stretched side. The red-shortness crack and the grain boundary coincide only locally and there is no veining. Obviously, the ferrite has recrystallized after cracking, which probably followed the original grain boundary.

Deformation tests at 825° and 875°C gave results similar to those described. There was, however, a difference in the velocity of recrystallization, which increased with temperature and rate of deformation. The specimen deformed slowly at 825° showed only traces of recrystallization, whereas the specimen deformed rapidly at 875° was almost wholly re-

13

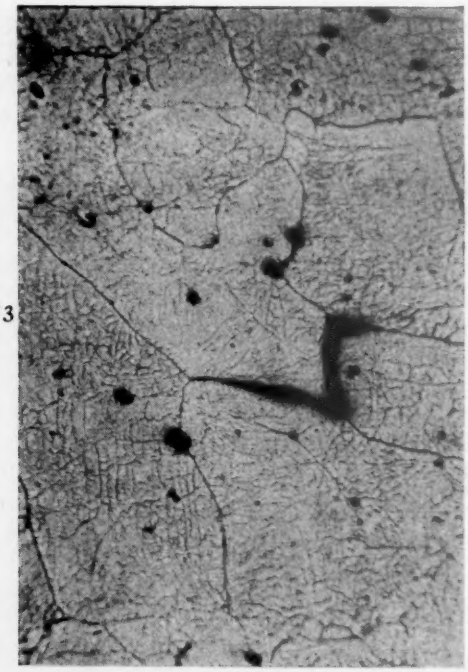

14

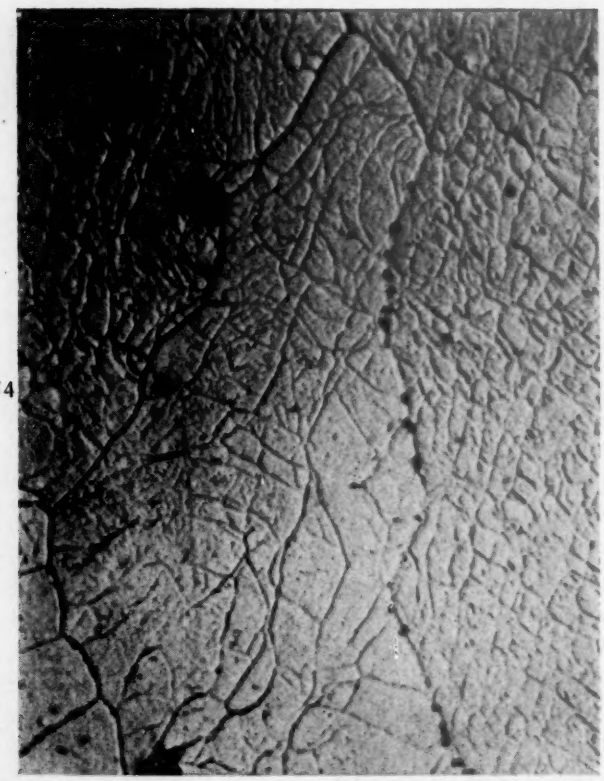

FIGS. 13 AND 14.—STEEL 1. DEFORMED RAPIDLY AT 850°. STRETCHED SIDE.
Fig. 13, × 300.
Fig. 14, × 1200.

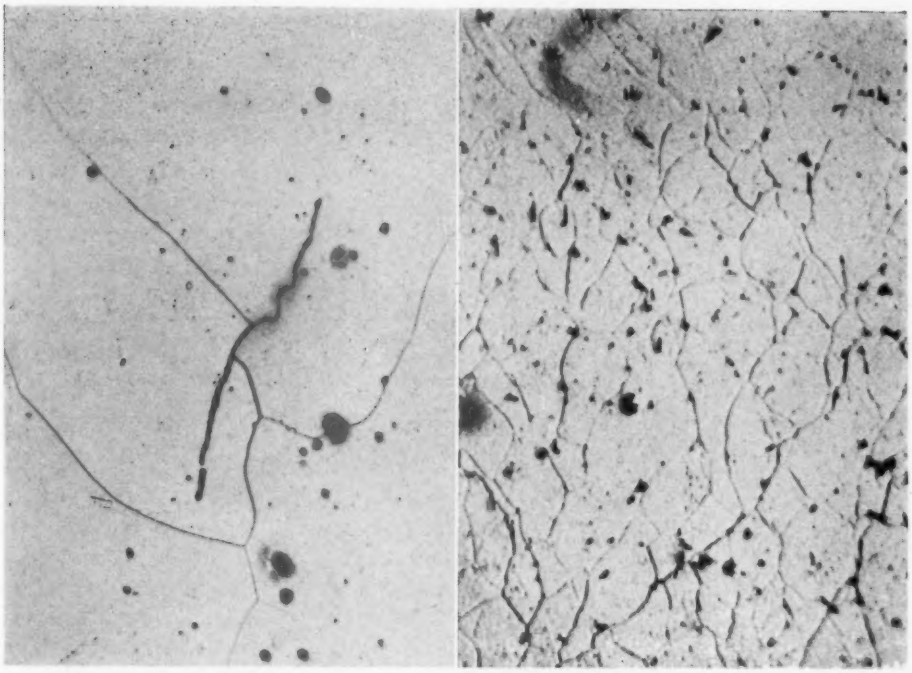

FIG. 15.—STEEL 1, RECRYSTALLIZED, COARSE GRAINED. DEFORMED AT RAPID RATE AT 850°. × 300
FIG. 16.—STEEL 1. DEFORMED AT MEDIUM RATE AT 850°. × 1200.

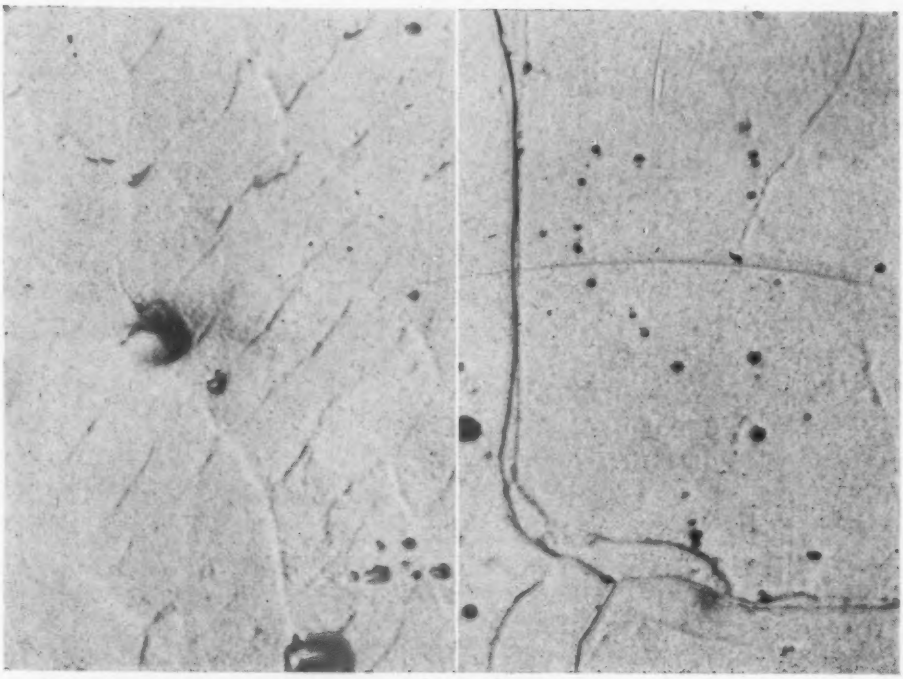

FIG. 17.—STEEL 3. RECRYSTALLIZED. DEFORMED RAPIDLY AT 825°, IMMEDIATELY QUENCHED IN COLD WATER. × 1200.
FIG. 18.—STEEL 3, QUENCHED IN WATER OF 65°C FROM 950°. × 1200.

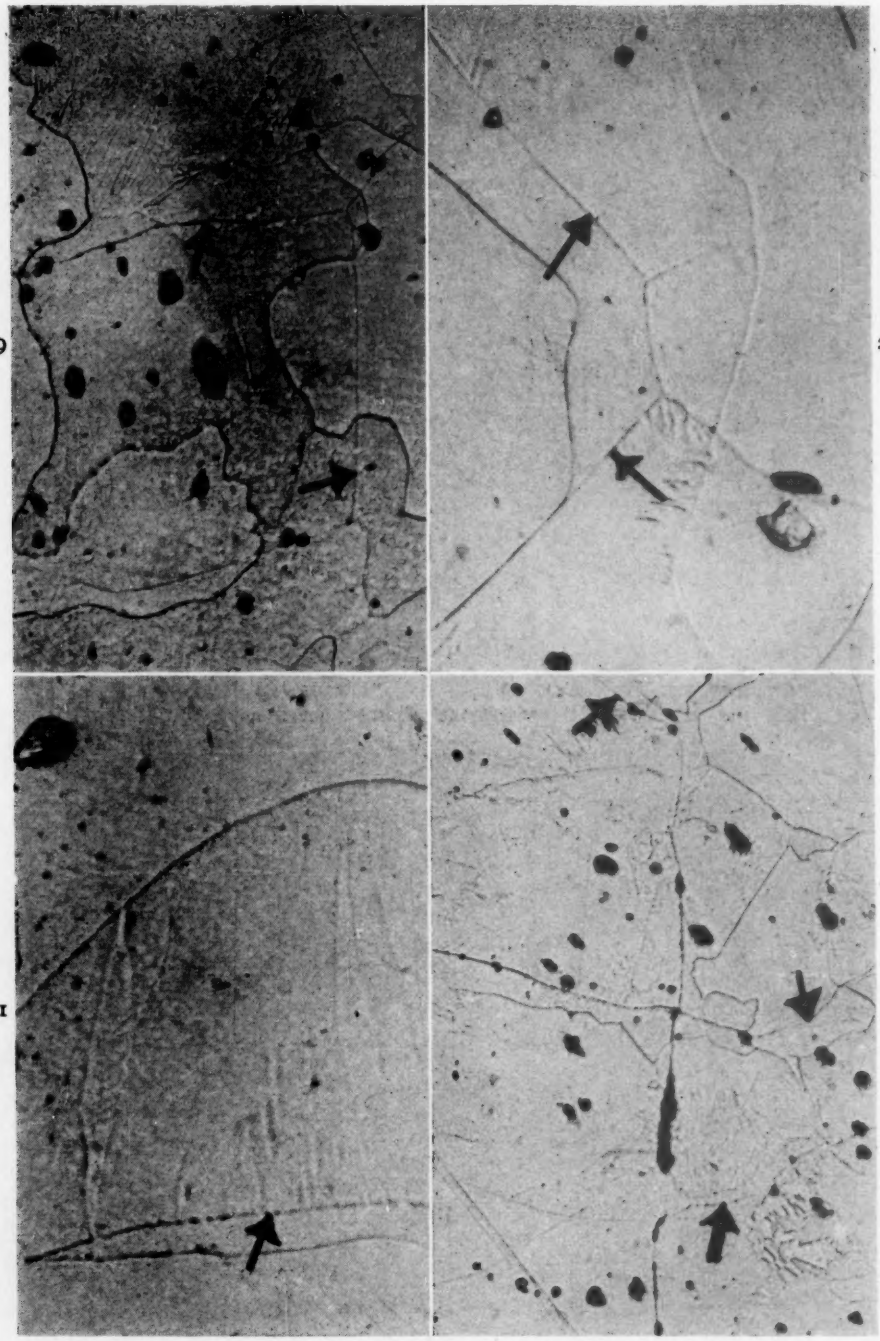

FIGS. 19–22.—STEEL 3, DEFORMED RAPIDLY AFTER 3 MINUTES AT 925°, QUENCHED IN WATER OF 50°C.
ARROWS INDICATE GAMMA NETWORK.
Fig. 19, × 300.
Fig. 20, × 1200.
Fig. 21, × 1200.
Fig. 22, × 1200.

crystallized. In some cases, recrystallization appeared to set in early during deformation, the recrystallized grains showing veining. Fig 16 shows what is believed to be one recrystallized grain, with veining and precipitated small rods or plates.

All veining observed in specimens deformed at temperatures of 825° to 875°C and air-cooled was positive. The specimen showed in Fig 7, which was heated to 850° and cooled in air, showed negative veining.

A specimen of steel 3, recrystallized, was deformed rapidly at 825° and immediately quenched in cold water. The structure obtained is shown in Fig 17. A set of parallel positive veins crosses another set of parallel negative veins.

Soft Steel. Deformation at Temperatures Above Ac_3

The method described of quenching in warm water from a temperature above Ac_3, was utilized to determine the relation between the ferrite structure and the austenite structure, from which it was formed, and to determine the relation between hot-shortness cracks and the austenite grain boundaries. It has been used for all specimens described in this section. Steel 3 was employed for these experiments.

Fig 18 shows the structure of a specimen heated to 950° and quenched as described. In this case the ferrite grain boundaries deviate only slightly from the gamma network. The latter, as always, appears as grooves. A few negative veins are present.

Fig 19 shows, at low magnification, the structure of a specimen held for 3 min at 925°C, deformed rapidly and quenched. The arrows indicate the gamma network. In this case the ferrite grain boundaries apparently have no relation to the gamma network. Figs 20 and 21 show, at high magnification, various details of the same structure. The deformation pattern discernible in the ferrite cannot be described as veining, rather as aggregations of twinlike units. The ends of such units generally coincide with a ferrite grain

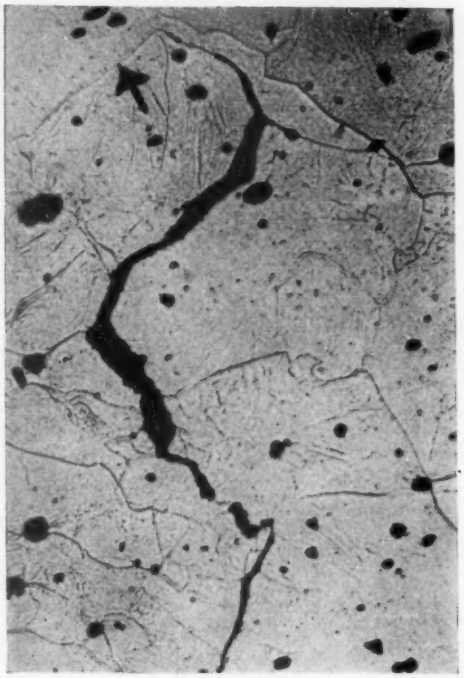

FIG. 23.—STEEL 3, DEFORMED RAPIDLY AFTER 5 MINUTES AT 950°, QUENCHED IN WATER OF 50°C. × 300.

boundary or, peculiarly enough, with a gamma network line.

Assuming that the gamma network lines represent some kind of irregularity in the ferrite lattice, inherited from the austenite grain boundaries, those lines may, like the actual grain boundaries of the ferrite, serve as barriers when the twinlike deformation units are formed, probably as a result of quenching stresses. On the other hand, there may have been deformation features in the austenite, not obliterated by recrystallization, which in some way may have been inherited by the ferrite. Fig 22, taken from the same specimen, shows fine red-shortness cracks coinciding with the gamma network.

Similar hot-shortness cracks that appear to follow the gamma network are

shown in Fig 23, taken from a specimen held 5 min at 950°C and quenched in warm water.

Generally, the soft steel showed more hot-shortness in the form of surface and internal cracks on rapid than on slow bending and was more prone to breaking when bent at 925° to 975° than at 825° to 875°C. However, the bending test as carried out in this investigation is too mild to detect anything but fairly pronounced red-shortness.

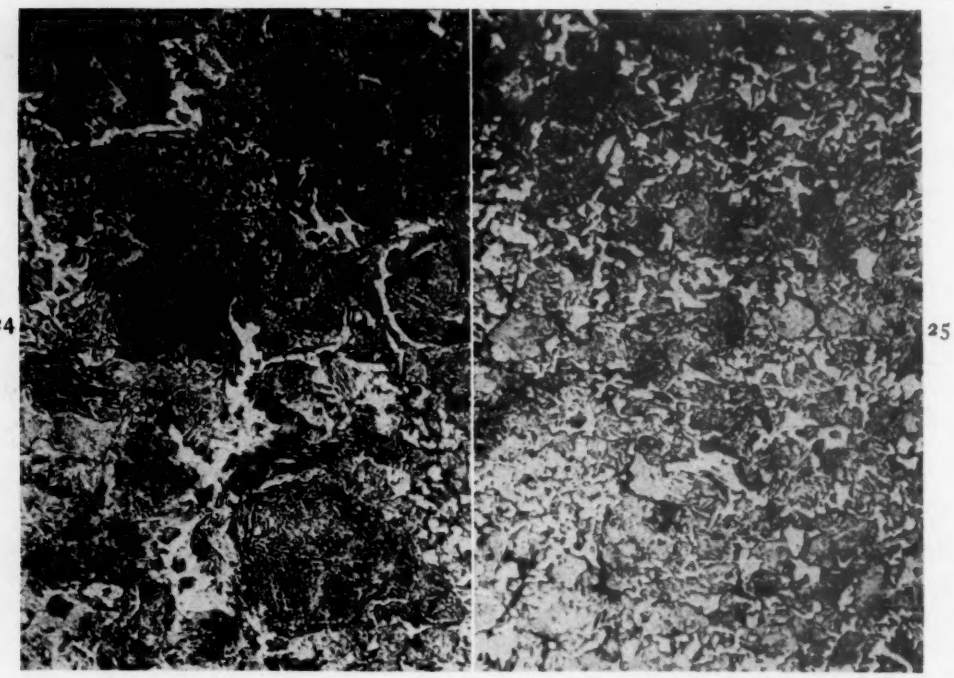

FIGS. 24 AND 25.—STEEL 7, DEFORMED SLOWLY AT 850°C (FIG. 24) AND 900°C (FIG. 25). × 300.

Medium Carbon Steel. Deformation at Temperatures above Ac_3

Bending tests were made at different rates at 850°, 900°, 950° and 975°C, with subsequent cooling in air. Hot-shortness cracks were obtained at all temperatures. Fig 24 shows the structure at low magnification after slow deformation at 850°, Fig 25 at 900° and Figs 26 and 27 at 975°. There are indications that the ferrite grains of Fig 25 do not outline the grain size of the undeformed austenite but either that of the deformed, or the deformed and finely recrystallized, austenite. This is also seen when comparison is made with Fig 24, where the ferrite network is coarser. In these two figures, some cracks appear to follow what may be assumed to have been austenite grain boundaries, while others do not. The same variations occur in the coarser structures of Figs 26 and 27. The main crack in Fig 27 appears to be transcrystalline.

Certain features of the pearlite structure of the deformed specimens deserve mentioning. Fig. 28 shows the structure of a specimen deformed slowly at 950°. Areas of pearlite are subdivided by lines of discontinuity into smaller units, showing the same general direction of the lamellae. This phenomenon will be discussed presently.

DISCUSSION OF RESULTS

The fact that, on increasing the rate of deformation, the veining or subboundary pattern of ferrite deformed at temperatures

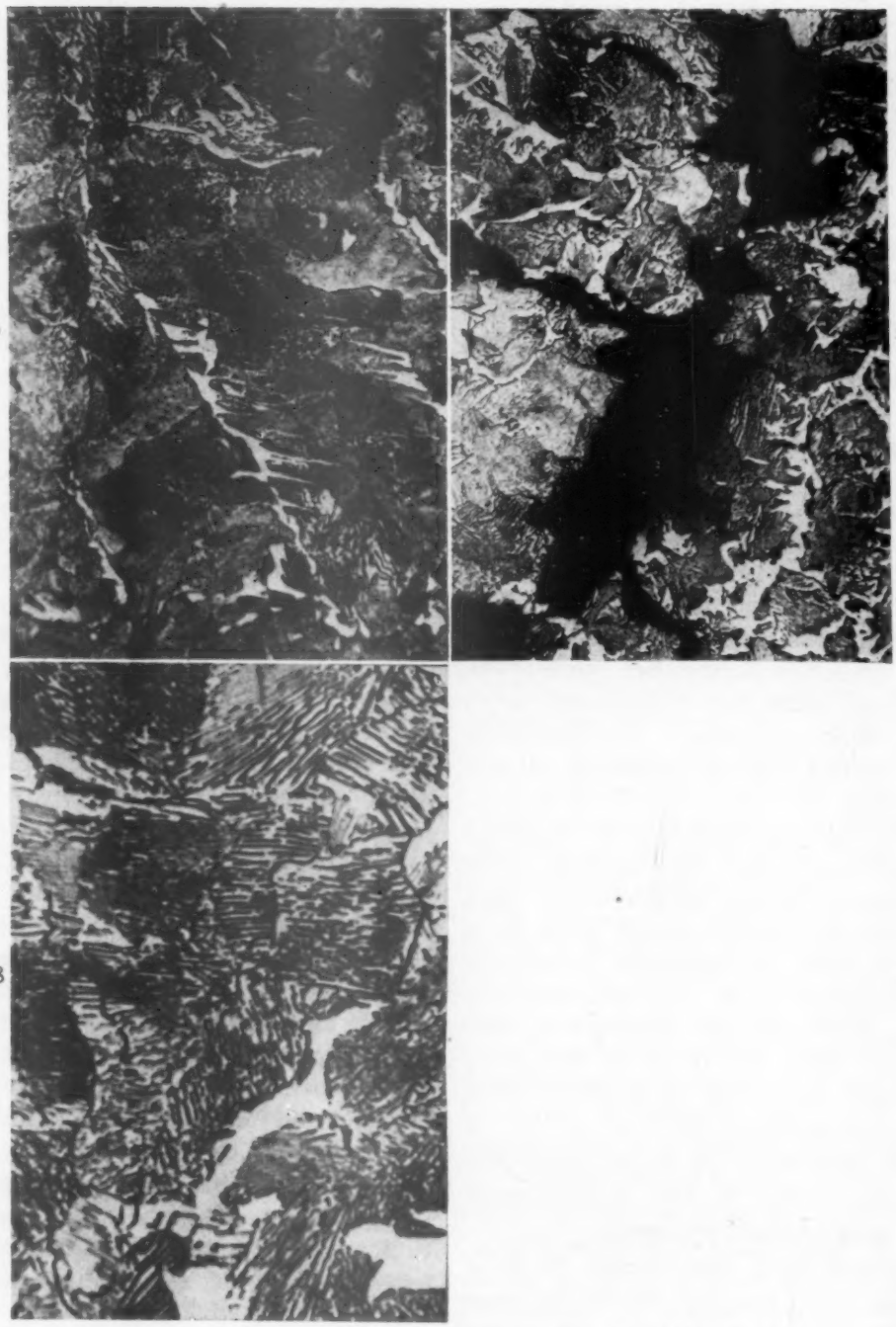

FIGS. 26–28.—STEEL 7. DEFORMED SLOWLY AT 975°C. × 300.

somewhat below A_3 becomes more finely meshed and more regular, in the sense of showing preferred directions indicates that it originates in plastic deformation. If so, there is probably a continuous series of subboundary structures between the irregular veining of ferrite slowly deformed just below A_3 and the intersecting sets of parallel slip lines of ferrite cold-deformed at room temperature and lower temperatures, as suggested by Rawdon and Berglund.[2]

It would be possible to visualize slip along irregular cylindrical surfaces which, in transverse or oblique section, would present a pattern similar to the usual veining network. Longitudinal sections would then appear as parallel lines. Judging from the parallelism of veins sometimes observed, this type of deformation probably occurs but, under the influence of the high temperature, probably other phenomena are associated with such a relative movement of the subgrains.

One such phenomenon is suggested by the observation that the ferrite grain boundaries, during deformation at high temperatures, move locally, in such a manner that the subgrains formed are accommodated (Fig 14), and with the effect, after sufficient deformation, particularly when this is slowly performed, that they cannot be distinguished from the subboundaries (Figs 8, 9, 11). A similar movement, or rather migration, probably occurs in the subboundaries while deformation is proceeding.

Another likely phenomenon is some rotation of the subgrains during deformation. This appears to be borne out by the X-ray results of Greninger[9] and by Goss.[10]

Hanemann showed that, after heating above 300°C, the veining constituent appeared in relief in slip lines of previously cold-deformed ferrite. The present investigation has shown veining that is partly negative in specimens quenched immediately after deformation at 825° and in specimens quenched from a temperature above A_3. This indicates that veins, like slip lines, are originally negative—i.e., appear as grooves on etching—but quickly become positive if subjected to the influence of a sufficiently high temperature. The different heights and widths of the positive veins of different directions in Fig 12 possibly suggest that a greater amount of slip produces more disturbance in the atom arrangement at the subboundaries and, in consequence, more of the veining constituent. The author offers no suggestion as to the nature of the veining constituent. A so-called "light phenomenon" of similar appearance has been observed by Mrs. Gayler during aging of aluminum-copper alloys.[13]

Veining, as pointed out by several investigators, may be produced when soft steel is cooled through the gamma-alpha transformation. It has been shown that, on such cooling, the number of veins formed can be considerably reduced, or veining altogether prevented, by very slow cooling. It is suggested that the stresses arising from the transformation may cause plastic deformation of ferrite already formed. Possibly the still untransformed austenite is deformed in a similar way. Whether that would affect the ferrite formed from it, and in what manner, is not known. The stresses are associated naturally with the change in specific volume on transformation and possibly with the accumulation of carbon in the portions of austenite adjoining the growing ferrite.

The gamma network, visible in the etched ferritic structure after quenching in warm water from a temperature above A_3, appears as grooves and indicates some kind of disturbance of the atomic arrangement, inherited by the ferrite from the austenite. The ferrite, in this case,

forms quickly. During the growth of a ferrite crystal across an austenite grain boundary there may not be sufficient time for the boundary atoms to assume the perfect lattice arrangement. There may also be an effect of difference in composition at the boundaries persisting after transformation, but the absence of any influence of prolonged holding at temperature would not appear to support that idea. It is believed that the gamma network and the delta network observed occasionally by Rawdon and Berglund both were gamma networks accentuated by precipitated inclusions. The so-called delta network was found only in cast steel and was very coarse meshed. The gamma grains would be coarse meshed in a cast steel. The suggestion that ferrite grains may inherit their boundaries from the parent austenite grains (Goss) is not borne out by the present work, except locally, on rare occasions (Figs 18 and 20).

Generally, there was no relation between the ferrite grain boundaries and the gamma network. This means, of course, if there is a regular relation between the crystal orientations of the ferrite nucleus and the mother austenite, as found by Mehl and co-workers,[14–16] that an austenite grain boundary is no barrier to the growth of a ferrite grain into an austenite grain where the orientation relationship is irregular.

A great deal of attention has been paid to inclusions connected with veining.[2–6] The results of the present investigation indicate that veining is essentially a deformation phenomenon. The veining constituent is a secondary phenomenon and so probably is the precipitation of inclusions at places of disturbance in the atomic lattice such as veins and grain boundaries (Figs 7 and 14).

Fig 7 shows an example of grain-boundary migration believed to be promoted by thermal stresses set up on heating in the salt bath.

In the 0.5 per cent carbon steel deformed at a temperature above A_3 and cooled in air, areas of lamellar pearlite were observed in the structure, having lines of discontinuity not unlike the veins of hot-deformed ferrite. The fact that the lamellar direction was uniform within such an area consisting of several subgrains argues against the thought that each subgrain grew from a separate nucleus. It is suggested that the lines of discontinuity represent surfaces where deformation has occurred similar to the process described for hot deformation of ferrite. Probably this deformation was produced in the austenite during the bending operation, and recrystallization did not follow. In hot-worked carbon steels such discontinuities in the lamellar pearlite structure are common. They may result from the hot-working operation or, possibly, from the transformation stresses in passing through Ar_1. Hull and Mehl[17] have demonstrated veining in the pearlitic ferrite. That phenomenon is believed to be due to deformation during the Ar_1 transformation just as veining in ferrite is produced during the Ar_3 transformation.

In soft steel hot-shortness cracks were found to follow the grain boundaries of ferrite, when they were formed below A_3, and of austenite, on deformation above A_3. In medium carbon steel, deformed above A_3, the cracks appeared sometimes to follow the austenite grain boundaries sometimes to pass through the grains.

All steels examined were hot short from deficiency of manganese in relation to the sulphur content. No connection was found between the paths of cracks and existing inclusions. It seems that sulphur not rendered harmless by an appropriate amount of manganese causes weakness in the grain boundaries of both ferrite and austenite.

This harmful sulphur may be present in solid solution or as a submicroscopic precipitate of sulphide.

Summary

Specimens of low and medium carbon, red-short steel have been subjected to deformation at temperatures somewhat below and above Ac_3 and the structures obtained have been studied in the microscope. The results indicate that:

1. Veining (or subboundaries) in ferrite is a result of plastic deformation at high temperatures, corresponding to slip lines at lower temperatures.

2. The veining pattern of ferrite varies with temperature and rate of deformation; becoming finer and more regular, the quicker the deformation.

3. Deformation of ferrite may be superseded by recrystallization, in which case veining is obliterated.

4. Veining in ferrite when formed during the gamma-alpha transformation is a special case, where deformation results from stresses set up during transformation. After very slow cooling through Ar_3 veining may be absent.

5. If the steel is quickly cooled immediately after deformation at a high temperature below A_3, the veins formed during deformation wholly or largely etch as grooves—negative veining—but if the steel is kept for some time at the high temperature, or less quickly cooled, all veins appear as narrow ridges—positive veining. The nature of this veining constituent has not been determined.

6. Veining being essentially a deformation phenomenon, the association between veining and inclusions probably is a secondary one, inclusions preferably being precipitated at places of disturbance in the atomic lattice such as grain boundaries and veins.

7. Small specimens of soft steel quenched in warm water from a temperature above A_3 display a grooved continuous network where the austenite grain boundaries were before quenching—the gamma network.

8. The ferrite grain boundaries in such steel so treated generally run independently of the pre-existing austenite grain boundaries.

9. In medium carbon steel deformed above A_3 and cooled in air, discontinuity lines may appear in the structure of certain areas of lamellar pearlite, the lamella direction of the pearlite being generally the same on both sides of such a line.

10. The lines described probably are caused by deformation of the austenite, much in the same way as veining is formed by deformation of ferrite, the discontinuities in the austenite affecting the growth of the pearlite.

11. In soft steel hot-shortness cracks probably are always formed along the grain boundaries of ferrite below A_3 and of austenite above A_3.

12. In medium carbon steel hot-shortness cracks formed above A_3 sometimes follow the grain boundaries of austenite: sometimes do not.

13. There seems to be no connection between the paths of hot-shortness cracks and inclusions in the steel.

Acknowledgments

The present investigation was started at the instigation of the research organization of Jernkontoret (Swedish Ironmasters Association) and has been supported by its Research Council. The investigation was supervised by a committee including the late Mr. G. Phragmén, Messrs. G. Malmberg, L. Morsing, G. Thalén and the senior author. The authors wish to express their gratitude for the committee's valuable advice.

In the preliminary stages of the investigation, the senior author was assisted by Messrs. E. Holmblad and S. Gulda, to whom his thanks are also due.

References

1. Storey: *Trans.* Amer. Electrochem. Soc. (1914) **25**, 489.

2. Rawdon and Berglund: Nat. Bur. Stds. *Sci. Rept.* 571, 649.
3. Ammerman and Kornfeld: *Archiv Eisenhuttenwesen* (1929–30) **3**, 307.
4. Bannister and Jones: *Jnl.* Iron and Steel Inst. (1931) **123**, 395.
5. Northcott: *Jnl.* Iron and Steel Inst. (1932) **126**, 267.
6. Northcott: *Jnl.* Inst. Metals (1936) **59**, 225.
7. Hanemann, Schrader und Tangerding: *Archiv Eisenhuttenwesen* (1932–33) **6**, 567.
8. Hanemann and Schrader: Atlas Metallographicus, Fig. 566–591, Berlin, 1927.
9. Greninger: *Trans.* A.I.M.E. (1936) **120**, 293.
10. Goss: *Trans.* A.I.M.E. (1941) **145**, 272.
11. v. Hámos: *Nature* (1935) **135**, 1076.
12. v. Hámos: *Jernk. Ann.* (1942) **126**, 568.
13. Gayler: *Jnl.* Inst. Metals (1946) **72**, 243.
14. Mehl, Barrett and Smith: *Trans.* A.I.M.E. (1933) **105**, 215.
15. Mehl and Smith: *Trans.* A.I.M.E. (1934) **113**, 203.
16. Smith and Mehl: *Trans.* A.I.M.E. (1942) **150**, 211.
17. Hull and Mehl: *Trans.* Amer. Soc. for Metals (1942) **30**, 381.

Austenite Grain Size in Cast Steels

By Malcolm F. Hawkes,* Junior Member AIME

(New York Meeting, March 1947)

Austenite grain size has long been recognized by metallurgists as an important property of steels because of its influence on toughness, hardenability, machinability and creep strength. Much research has been carried out on wrought steels to develop methods for disclosing austenite grain size, and to provide knowledge of the grain-size characteristics of steels produced and heat-treated in various ways.

Much less work in these fields has been done on steel castings; partly because, owing to the variable and complex microstructures of cast steels, it is frequently very difficult to obtain results that are not questionable. The object of this investigation, therefore, was to establish, for a wide variety of carbon and alloy cast steels, suitable methods for disclosing austenite grain size and some knowledge of the grain-size variations to be expected.

The steel foundryman is interested in austenite grain size at two different stages in the manufacture of his products; one is just after the steel is cast, and the other is after any reheating operation carried out above the critical temperature range. In both, it must always be kept in mind that the grain size being sought is actually a previous austenite grain size, and that the austenite no longer exists once the steel has cooled to room temperature. The problem of the investigator is always to use evidence obtained from the structure at room temperature to deduce this previous austenite grain size, which was established the last time the steel existed at a temperature above the critical range.

Since most steel castings today are at least annealed or normalized, the measurement of austenite grain size established by heat-treatment will be considered first. More than 50 commercially produced cast steels representing a wide variety of compositions and melting practices were used in the study. For each steel, grain-size determinations were made after each of three widely varying heat-treating schedules namely, one hour at 1550°F, one hour at 1700°F, and six hours at 1700°F. The list of steels and results obtained on them will be found in the appendix. (See page 530.) A discussion of the knowledge gained on the applicability of various test methods and on grain-size characteristics of cast steels in general follows.

MEASUREMENT OF AUSTENITE GRAIN SIZE ESTABLISHED BY HEAT TREATMENT

Methods Suitable for Determining Austenite Grain Size after Heat-treatment at Ordinary Temperatures and Times

It was desired, as one of the results of this investigation, to be able to recommend to steel foundries a method, or methods, of disclosing grain size best suited to accurate

Manuscript received at the office of the Institute Dec. 16, 1946. Issued as T.P. 2170 in Metals Technology, June 1947.

This article sets forth the results of research conducted by the Carnegie Institute of Technology and supported by the Steel Founders' Society of America. Copyright, 1946, by the Steel Founders' Society of America.

* Assistant Professor, Department of Metallurgical Engineering, Carnegie Institute of Technology, Pittsburgh, Pennsylvania

routine testing of a wide variety of steels. Methods involving complicated or delicate apparatus, or requiring excessive time, were therefore not considered. The following list of recognized methods contains all those deemed adaptable to the foundry laboratory; all were used on every steel for all three heat-treating schedules:

1. Fracture.
2. "Oxidation."
3. "Normalizing."
4. Gradient Quench.
5. Martensitic Etch.

Each of these methods will be discussed in detail in a subsequent paragraph. The McQuaid-Ehn test, which also was used on all steels, is a high-temperature test only, and is discussed in a separate section.

Of these methods, the first involves visual comparison of a fractured specimen with a set of fracture standards for steel. The remaining four involve polishing and etching a microsection, and comparing the structure with those in the ASTM standard charts[1] for rating austenite grain size under the microscope. In this investigation, all such work was done using actual micrographs of the samples for comparison. The fracture and the ASTM microscopic standards use the same numerical scale in the range of cast-steel grain sizes; namely, in units of one number from about No. 1 for very coarse grains to No. 8 for very fine grains. Separate observations by at least two observers on all specimens rarely showed a difference of more than one grain-size number; as will be shown, better precision than this is not warranted.

It was considered important, in checking one method against another, to devise a way to eliminate any variables in the steel composition and in the heat-treatment. This was done in all cases by performing the five tests on a single specimen, the dimensions of which are shown in Fig 1. This specimen was given the desired time-temperature heat-treating schedule in a tubular laboratory resistance furnace having a uniform temperature zone longer than the specimen. To satisfy the conditions for all five tests, it was then gradient-quenched in water as shown in Fig 1, so that the rapidly cooled end transformed throughout to 100 pct martensite (except in the very low-carbon steels) while the other end transformed slowly to pearlite and ferrite (except in the deepest hardening steel). Slow cooling at the top end was ensured by having the tongs at a temperature of approximately 1800°F before quenching. Further details on the methods and results are discussed under separate headings in the following pages.

[1] References are at the end of the paper.

The Fracture Method

The fracture test for austenite grain size was developed[2] for use on high-carbon tool steels, which usually are fine-grained, and is eminently suited for that purpose. Its use has been extended to a wide range of medium carbon steels, but little has been published on its suitability in that field.

This test is the simplest and most rapid of all those studied. A small specimen that has been heated according to the desired schedule is merely rapidly quenched to martensite, fractured, and compared visually, or with the aid of a magnifying glass, with a set of fracture grain-size standards.* It is usually assumed that the only precaution necessary is that the steel have enough hardenability and that the specimen be quenched fast enough to form 100 pct martensite throughout or that if the steel be shallow hardening, only that part of the fracture lying in the fully hardened surface be considered in the rating. This is because other structures such as pearlite and ferrite undergo permanent deformation before fracture and the fracture appearance varies with the degree of deformation.

* Those in use in America are the Shepherd Fracture Grain Size Standards obtainable from the Thermist Co., Phillipsburg, N. J.

In the present work it was attempted to quench in such a way that all specimens would harden completely to some distance above the notch illustrated in Fig 1. Fracturing through the notch then gave a small section that could be rated and preserved, and left the remainder of the specimen for rating by other grain-size methods.

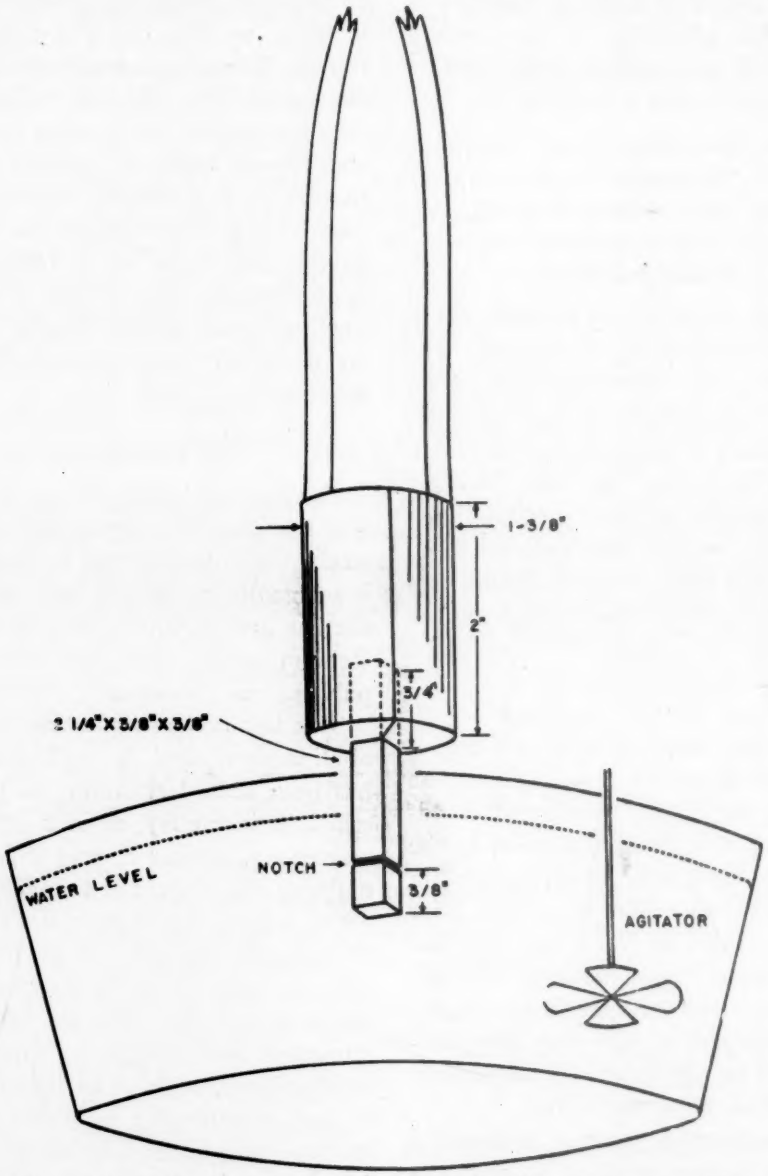

FIG 1—AUSTENITE GRAIN-SIZE TEST SPECIMEN AND METHOD OF COOLING.

Results on the many steels showed that, in the first place, the fracture method failed to work at all in about one third of the cases studied. Occasionally this was because very low hardenability in the steel caused a structure containing softer constituents as well as martensite, but much more often it was because the specimens exhibited a ductile fracture even though they were 100 pct martensite. This is evidenced by bending before fracture, and can be checked by matching the pieces after

fracture. Such ductility is not unusual in low-carbon martensite, and extends to higher carbon contents (such as 0.30 or 0.40 pct) as the alloy content of steels is increased. No definite limiting carbon content for the test could be established even in plain carbon steels, however, and this is not surprising in view of the further variability to be described in the next paragraph.

In addition, it was observed that even when apparently no ductile fracture occurred, the fracture rating did not check the ratings established by agreement among the microscopic methods. There were two reasons for this failure. In the first place, as will be discussed later, most cast steels exhibit a range of grain sizes. This sometimes extends uniformly over a band of three or four grain-size numbers; at other times it occurs as a definite proportion of coarse grains and a definite proportion of very much finer grains, both groups representing only one or two grain-size numbers. The latter is the familiar "duplex grain size" rated, for example, as 75 pct Nos. 7 to 8, 25 pct Nos. 3 to 4. Fractures will yield a qualitative indication of pronounced "duplex grain size" to the trained observer, because the appearance will show some similarity to both a coarse-grained and a fine-grained fracture in the standard set if viewed with a magnifying glass. On the other hand, mild "duplexing" or a broad range of grain sizes usually will be rated as a single number by the fracture test, thus leaving important information undisclosed.

A second reason that fracture ratings may be erroneous is more elusive in nature, and may occur even when the grain size is uniform. In these cases, it is found that, although the fracture apparently has been brittle and a rating has been made, actually the fracture does not have the exact appearance of those in the standards. Instead, it is somewhat duller and has an appearance approaching to a greater or lesser degree that of the so-called "fibrous" fractures of ductile steel. The cause of this was not established, but the evidence suggests strongly that the phenomena recently reported by Grossmann[3] are involved. Grossmann maintains that in some hardened steels martensite fractures intergranularly (through paths that formerly were austenite grain boundaries) and in other cases it fractures transgranularly. The former mechanism apparently always occurs in high-carbon tool steels and results in the bright faceted appearance of the fracture standards. The latter cases appear to be met with (at least through part of the fracture) about half the time in the ordinary range of cast steels.

Results give no indication that conditions for reliability of the test can be specified except to say that chances for success are better with higher carbon steels. The best statement that can be made is: "disregard fracture grain-size results unless the fracture was brittle and its appearance was exactly like that of the fracture standards."

The fracture test has its place, however, because occasionally all other methods fail, and because occasionally a grain-size determination is needed but no miscroscope is available. A rough check on whether the steel is coarse or fine can be made, providing the fracture is brittle, and this does no require even a set of fracture standards.

The "Oxidation" Method

The oxidation method and those described on the following pages are alike in that they produce a structure in which, after suitable etching, the location of former austenite grains can be seen under the microscope. Comparison of micrographs taken at 100 diameters with the ASTM standard charts then gives an accurate rating. These methods differ only in the microstructure produced, the way of producing it, and the method of etching it to bring out the former austenite grains.

The so-called oxidation method is thoroughly discussed in papers by Tobin and

Kenyon[4] and by Day and co-workers.[5,6] There it can be seen that these authorities are not in agreement on the reliability of the method.

The method is easy to carry out on the specimen illustrated in Fig 1, so it was used on all tests. First, all specimens were polished on No 2/0 metallographic emery paper along one side before they were heated. Heating was done in an atmosphere of still air inside a 1½-in. i.d. silica tube with closed ends. The essential process occurring during heating in this slightly oxidizing atmosphere is decarburization, which proceeds at a faster rate at austenite grain boundaries than within the grains. This grain-boundary decarburization near the surface is so nearly complete that, on the subsequent quench, ferrite is formed at the boundaries even though the remainder of the structure at the quenched end is martensite. The former austenite grain boundaries can then be outlined strikingly with a special etchant, consisting of 15 pct HCl, balance ethyl alcohol, which turns the ferrite boundaries black, but leaves the martensite white.

An advantage of the oxidation method is that it rarely, if ever, fails to give good outlining of grains and a structure that is easy to rate. A big disadvantage is that, apparently, one can never be sure that the grain size observed on the decarburized surface is the same as it is throughout the remainder of the specimen. In about half the tests run, this method checked with the other more reliable microscopic methods; in the balance, it gave a rating from one to two grain-size numbers too fine. This is illustrated in Figs 2 *a* to *c*.

When the method fails to show up the coarser grains (e.g., gives a rating of No. 7 or 8 when the other methods agree on 5 to 8) it is undoubtedly in error. Possible reasons for this, such as grain-growth restraint at the surface because of oxidation of aluminum or alloying elements, are discussed in the references cited previously.

On the other hand, when the oxidation method indicates that some grains apparently are too fine (e.g., gives a rating of 6 to 9 when the other methods agree on 6 to 7) it may or may not be in error, for the other methods are not always sensitive to very fine grains. For instance, the mode of distribution of the constituents used to outline grain boundaries may obliterate small grains before large grains are outlined sufficiently for rating. The ferrite envelopes obtained in the oxidation specimens are always thin enough to outline grains as fine as No. 10, although such grains are not necessarily representative of the structure throughout the specimen.

Many variables, such as composition of the steel, oxidizing power of the furnace atmosphere and time of heating, were studied, but no rules could be established to determine when the method would be reliable. It was observed, however, that ratings should be made at the deepest point below the surface where grains are still completely outlined. Grain sizes observed close to the scale layer were frequently one or two numbers finer than those observed deeper in the steel. This tendency can be seen in Fig 2*a*, which shows a section cut at a slight angle to the surface and extending from the scale through the area of outlined grains.

In summary, it may be said that the oxidation method probably should not be used unless all other methods fail. There it can be used at least to distinguish between coarse-grained and fine-grained specimens, except in borderline cases.

The "Normalizing" Method

It is well known that most slowly cooled plain carbon wrought steels with carbon contents between about 0.25 and 0.7 pct exhibit a microstructure consisting of pearlite plus a more or less continuous network of ferrite, which precipitated at previous austenite grain boundaries. Similar structures are obtained in steels with

greater than 0.80 pct carbon except that iron carbide outlines the grains. Frequently this is the simplest basis for a determination of grain size, since the commercial processes of annealing, normalizing, or even casting, often produce the necessary structure.

To be able to apply this method to steels of the widest possible range of carbon contents, it is necessary to have control over the cooling rates when the specimens are being tested in the laboratory.

In this investigation, such control of cooling rates was obtained automatically by use of the method illustrated in Fig 1. Cooling rates are very slow at the end of the specimen held in tongs previously heated to 1800°F, and increase gradually toward the water-quenched end. At some intermediate position, the best structure for rating grain size by ferrite outlining should be found.

This normalizing method gives the true austenite grain size when it works, but there are several reasons why, with cast steels, it usually fails to produce a structure in which former austenite grains are outlined. The first reason is that factors such as low carbon content, presence of alloying elements, and fast cooling rate tend to promote an evenly distributed, needle-like (Widmanstätten) ferrite pattern in the microstructure rather than a grain-boundary pattern. At cooling rates just slow enough to prevent martensite formation, such a pattern usually is formed. Furthermore, as slower and slower cooling is used to avoid the pattern, an excessive amount of ferrite is produced, and its distribution usually is merely random or on a dendritic pattern rather than in grain boundaries. The complete transition from a needlelike to a random distribution is shown in Figs 3*a* to *c*. The structure in Fig 3*b* might be

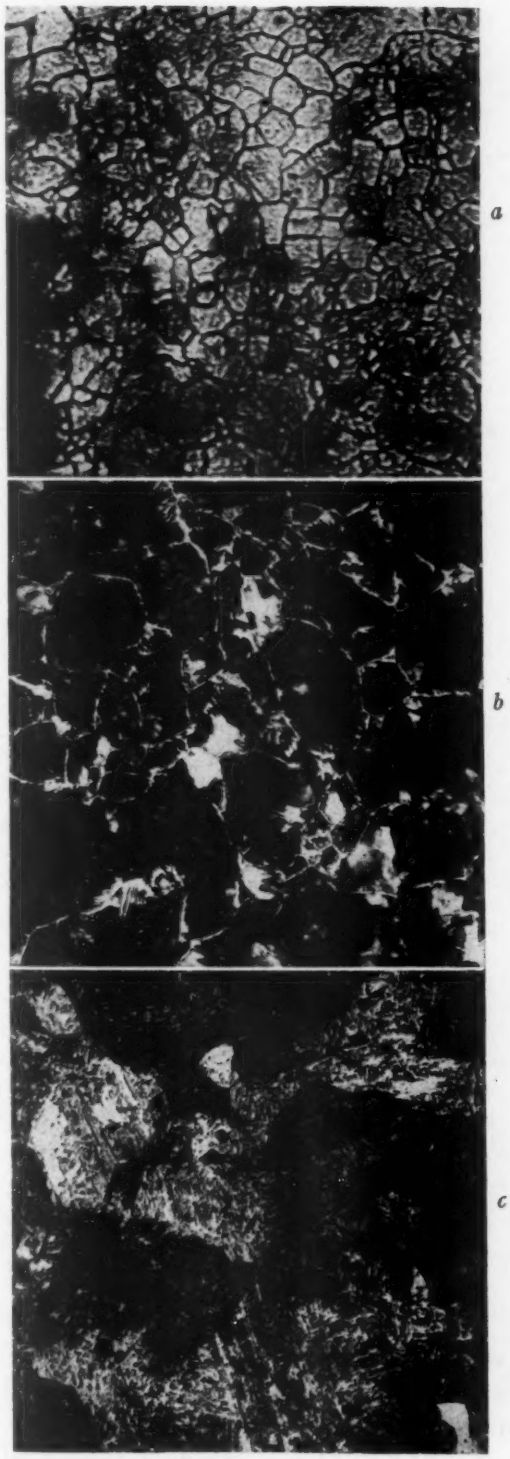

FIG 2—OXIDATION, NORMALIZING AND MARTENSITIC ETCH METHODS FOR GRAIN SIZE USED ON SAME SAMPLE. × 100.

Oxidation gives too fine an outline. 0.42 pct C, 0.95 pct Mn, silicon-killed cast steel. Heated one hour at 1700°F.

a. HCl-alcohol etch.
b. Nital etch.
c. Picral-HCl etch.

mistaken for a grain-boundary outline, but experience shows it to be a pattern caused by dendritic segregation, as will be discussed in a succeeding paragraph. Fig 3*d* shows a different steel, in which the microstructure developed a pronounced dendritic pattern (rather than a random pattern) on cooling at a rate slow enough to prevent the Widmanstätten pattern.

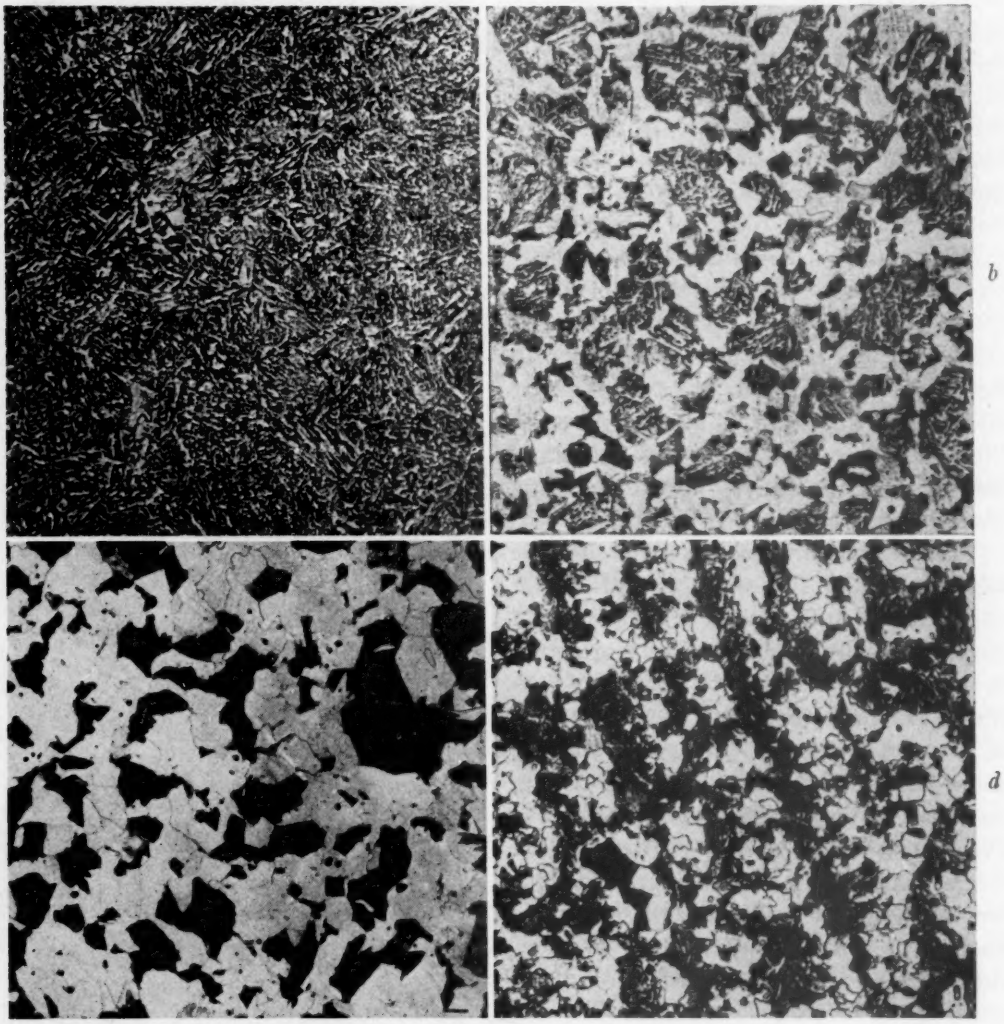

FIG 3—EFFECT OF COOLING RATE UPON MODE OF DISTRIBUTION OF FERRITE AND PEARLITE. × 100. NITAL ETCH.

a. NE 8620 cast steel, silicon-killed, normalized from 1550°F.
b. Same except cooled somewhat more slowly.
c. Same except furnace-cooled.
d. 0.36 pct C, 1.2 pct Ni, 0.34 pct Mo steel, silicon-killed, furnace-cooled.

With steels containing more than 0.40 pct carbon there appears to be a better probability for success with this method, though a statistical study would have to be made to prove the point. On the other hand, increasing alloy content decreases the chances for success, because it increases both the tendency for a needle-like pattern to be developed at relatively fast cooling rates and a dendritic pattern at slow cooling rates.

Results of this study also indicate that at least two types of structure occur com-

monly upon normalizing that can be mistaken for grain-boundary ferrite outlining, and thus lead to erroneous results. The first of these is illustrated in Fig 4. It is a dendritic pattern* in a structure lying midway in the transition series from Widmanstätten to random ferrite. The true grain size was established using the next two methods to be discussed, and was found to be considerably finer than the apparent one in Fig 4. This pitfall can be avoided by subjecting any specimen showing a large proportion of Widmanstätten ferrite in the normalized microstructure to slower cooling and then re-examining it.

Another deceiving structure is illustrated in Fig 5*a*. At first glance this micrograph appears to show complete grain-boundary outlining by ferrite. Actually, the ferrite is distributed in a random pattern as shown in Fig 5*b*, which is taken from the same field of view but photographed at 500 diameters. Fortunately, this pattern is deceiving only with fine grain sizes, and the over-all fineness of the pattern is itself influenced by previous austenite grain size. Therefore, although a structure such as that in Fig 5*a* usually will be rated too fine, the error is not great. However, if one is to be precise, doubtful cases should be examined at magnifications of 500.

In summary, it may be said that the normalizing method usually works on plain-carbon cast steels but fails to work on most alloy cast steels. It is easy to run in conjunction with other tests, and gives correct results when it does work. Some familiarity with normalized structures in general is required, however, if misinterpretation of misleading structures is to be avoided.

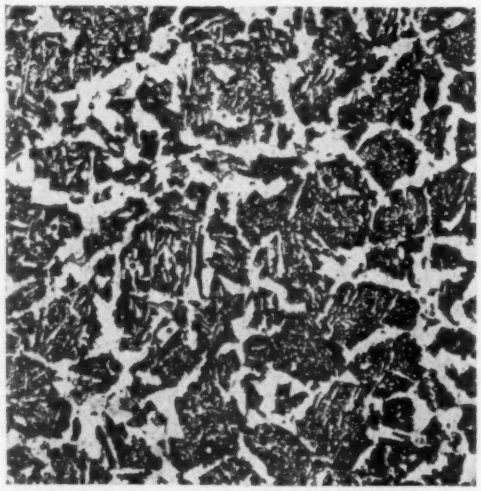

FIG 4—DENDRITIC FERRITE PATTERN EASILY CONFUSED WITH TRUE GRAIN-BOUNDARY FERRITE OUTLINE. × 100. NITAL ETCH.
NE 8620 cast steel, silicon-killed, normalized from 1550°F.

The Gradient Quench Method

It is well known that if a medium-carbon, plain-carbon steel is cooled at a rate slightly less than its critical cooling velocity, its structure will contain small amounts of dark-etching nodular fine pearlite formed at about 1100°F, and a large amount of light-etching martensite formed at lower temperatures. The nodules of fine pearlite usually are found in the regions that were austenite grain boundaries at the heat-treating temperature, because usually the rate of nucleation of austenite to fine pearlite is faster at the grain boundaries than within the grains. Thus, if such a steel is cooled at just the right rate, the pearlite nodules should outline each former austenite grain sufficiently for a measurement of size, and yet not encroach into the grain centers enough to

* Such structures are readily recognized when many steels have been examined after cooling at rates just too slow to form a 100 pct Widmanstätten pattern. The few patches of chunky ferrite may be arranged in an obvious dendritic pattern (which is often true when very slow cooling gives a dendritic pattern) or, as in Fig 4, in a pseudo-grain-boundary pattern (which is often true when slow cooling gives a random pattern), or even in an apparently random pattern. Actually all these patterns must be the result of dendritic segregation; if the steel were not segregated, the transition from Widmanstätten ferrite plus pearlite to random ferrite plus pearlite would take place at the same cooling rate regardless of position within the specimen.

give a misleading size effect or to obliterate small grains.

The optimum cooling rate for this purpose cannot readily be predicted for any steel, so the gradient quench method employs a range of rates within which the desired rate should be found. In this investigation, this was accomplished, as illustrated in Fig 1 and described in the previous section. The optimum zone for rating grain size is found much nearer the quenched end than is the zone used for the normalizing method. After the specimen had cooled to room temperature, it was examined along a surface ground parallel to the longitudinal axis, and the grain size was estimated by comparison with the ASTM standards at the optimum position; i.e., where the optimum cooling rate obtained. An example of a suitable structure for such a determination is shown in Fig 6.

This method, like the normalizing method, is successful a fair portion of the time on plain carbon cast steels and will, in addition, work on eutectoid steels where no ferrite can be precipitated. Like the normalizing method, however, it fails most of the time on alloy cast steels. There are two principal reasons for this.

The first reason is that with many alloy steels, especially those containing chromium or molybdenum, the microconstituent appearing with martensite at cooling rates just slower than the "critical cooling velocity" is not grain-boundary nodular pearlite—it is one of several possible needle-like, light-etching constituents bearing such names as lower bainite, acicular ferrite, X-constituent. Fig 7 is an example of such a structure. These constituents usually are distributed randomly, rarely outlining former austenite grains, and frequently they are difficult to distinguish from low-carbon martensite.

The second reason why the gradient quench method usually fails on alloy cast steels is illustrated in Fig 8. Over only a small portion of the area of the micrograph does nodular fine pearlite outline former austenite grain boundaries. In the remainder of the area, it is distributed in a dendritic pattern established by segregation of alloying elements during freezing of the casting, or it is not present at all

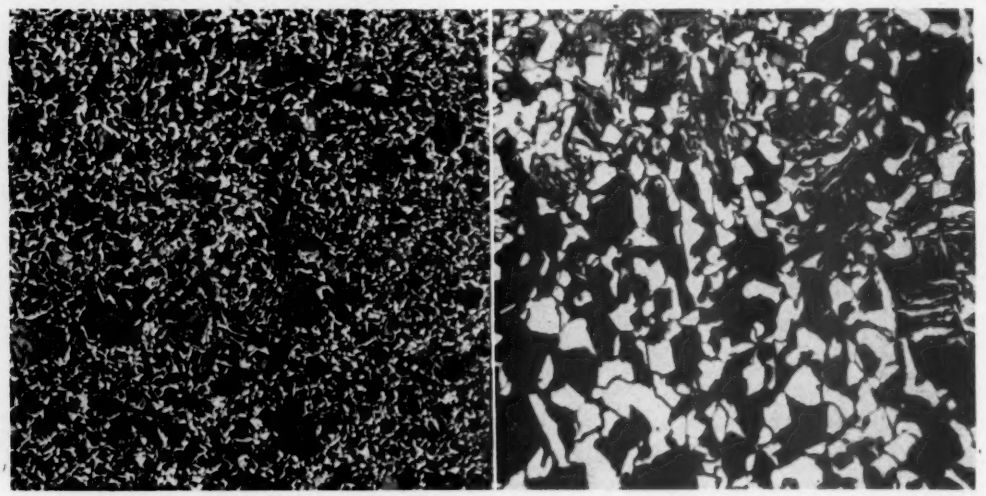

a *b*

FIG 5—RANDOM FERRITE PATTERN EASILY CONFUSED WITH TRUE GRAIN-BOUNDARY FERRITE OUTLINE.
NE 1330 cast steel deoxidized with ferrotitanium. Normalized from 1550°F.
a. × 100, nital etch.
b. × 500, nital etch.

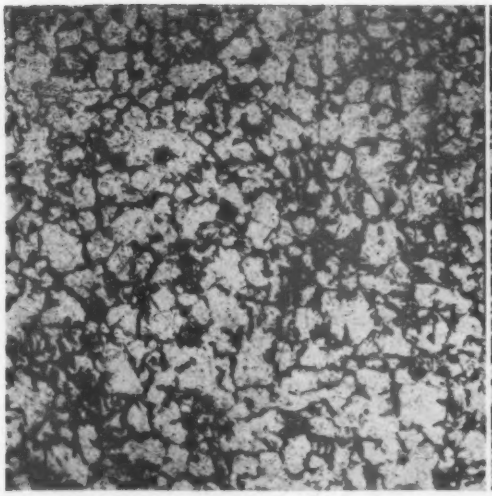

Fig 6.

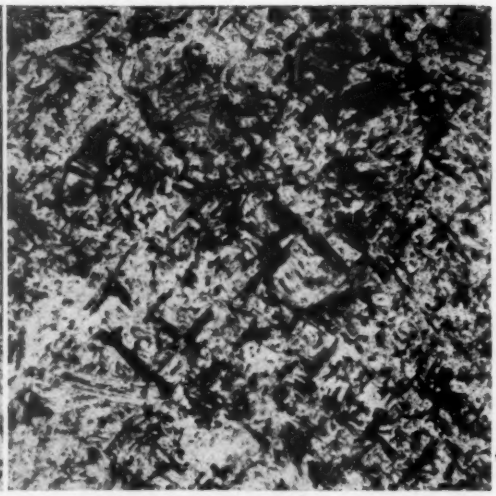

Fig 7.

Fig 6—Austenite grain size revealed by gradient quench method. × 100. Nital etch
0.20 pct C cast steel, silicon-killed. Heated one hour at 1550°F.
Fig 7—Gradient quench method fails because bainite and acicular ferrite form instead of nodular fine pearlite. × 100. Nital etch.
NE 9430 cast steel, silicon-killed, heated one hour at 1700°F.

because the hardenability at the particular location was sufficient to cause the formation of 100 pct martensite.

It should not be assumed that the grain size in the areas not outlined is the same as in the areas that are. Grain size frequently may be shown to vary over a segregated structure. Furthermore, the segregate patterns often are much sharper than that shown in Fig 8; in many such instances there is no grain outlining at all.

In summary, it may be said that, like normalizing, the gradient quench method fails to give results on most alloy cast steels, but it is easy to run in conjunction with the other tests and gives correct results when it does work. Like all the other tests, it may be the only one that works on a particular steel and, as such, and as a check upon the others, it has value.

The Martensitic Etch Method

The martensite etch method is a test method too commonly overlooked by metallographers. It was developed by Vilella[7] to make possible the determination of the previous austenite grain size in quenched and tempered steel, but it should have wide application for grain-size rating in general, for reasons to be shown.

The test is a very simple one to perform

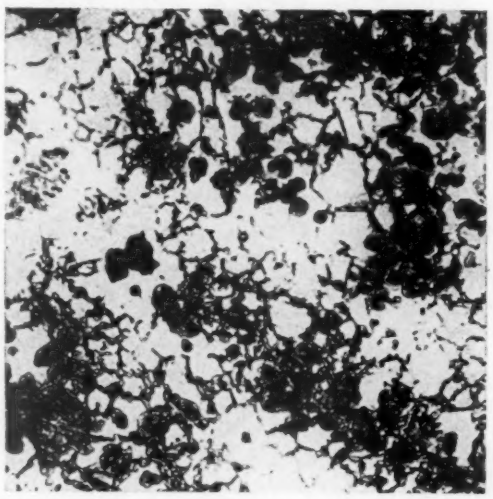

Fig 8—Partial failure of gradient quench method because of dendritic segregation. × 100. Nital etch.
0.42 pct C, 1 pct Mn cast steel, silicon-killed, heated one hour at 1550°F.

in conjunction with those already discussed, because it requires merely that the specimen to be rated must be quenched to

martensite after the heating cycle under investigation is completed. Thus, with the specimen used in this investigation, a section on either side of the notch, ground below the surface, is suitable. The key operation in the test is etching the carefully polished section in a solution of 1 gram of picric acid and 5 cc of concentrated HCl in ethyl alcohol. The structure developed by this reagent will usually be easier to rate if the martensite is tempered for half an hour at about 600°F before etching.

This test differs from the previous microscopic tests in that no second phase is present in the microstructure to show the position of former austenite grain boundaries. Instead, use is made of the circumstance that each former austenite grain had a definite crystalline orientation differing from that of its neighbors, and that the orientation of the martensite formed on the quench is fixed by the orientation of the austenite grains from which it comes. The rate of chemical attack by the special etching solution varies greatly with the orientation of the martensite, thus producing a typical "grain contrast etch."

A structure suitable for grain-size determination can thus be developed a great majority of the time in both carbon and alloy cast steels, and over the entire range of grain sizes encountered. This is illustrated in Figs 9 and 10 for fine grain size and coarse grain size, respectively. In both cases, another method was also successful, enabling a check on the martensitic etch method. The agreement is excellent, and this is always true when clear-cut ratings are obtained by the methods involved. Furthermore, whereas neither the normalizing nor the gradient quench methods were successful in more than one fourth of the tests made, the martensitic method was successful more than three fourths of the time. During the latter part of the work, as experience was gained, this figure was greatly exceeded. With a little practice, no foundry laboratory should have difficulty getting the method to work nearly every time.

Figs 11 and 12 are two of many examples of structures suitable for rating where the

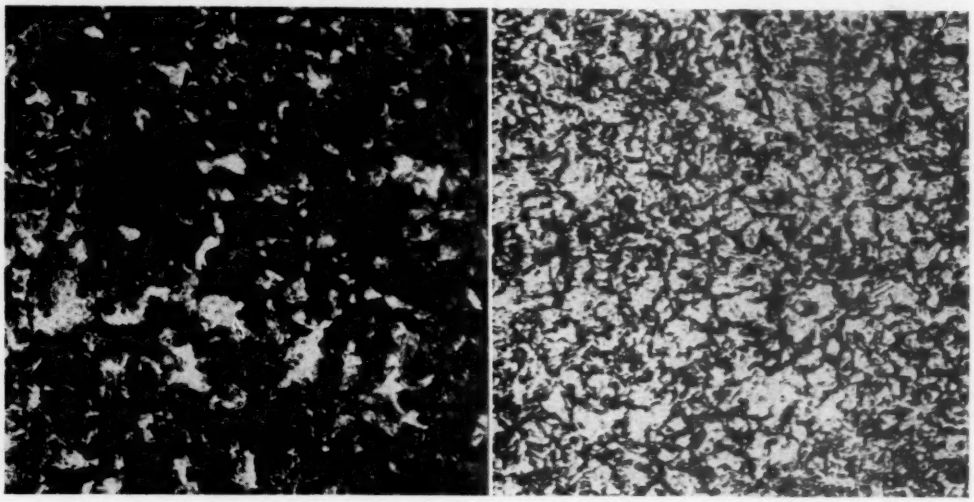

a *b*

FIG 9—AUSTENITE GRAIN SIZE IN 0.30 PER CENT CARBON CAST STEEL DEOXIDIZED WITH ALUMINUM AND TITANIUM.
Heated one hour at 1550°F.
a. Martensitic etch method. × 100. Picral-HCl etch.
b. Gradient quench method. × 100. Nital etch.

only reliable method that worked was the martensitic etch method. This was true for more than half the number of steels studied, which represented a wide variety impossible to rate by other reliable methods.

It is obvious from these illustrations that the hydrochloric acid-picric acid reagent

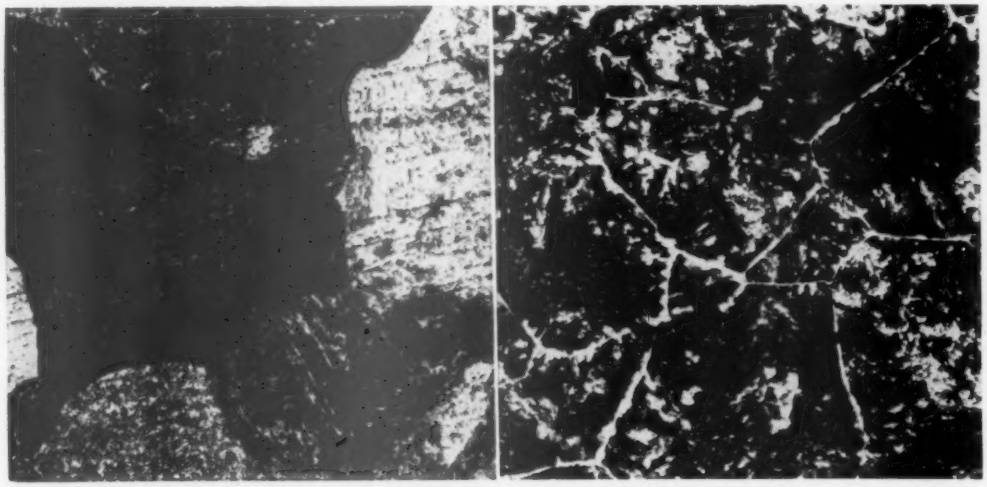

a *b*

FIG 10—AUSTENITE GRAIN SIZE IN NE 8620 CAST STEEL, SILICON-KILLED, HEATED SIX HOURS AT 1700°F.
a. Martensitic etch method. × 100. Picral-HCl etch.
b. McQuaid-Ehn method. × 100. Nital etch.

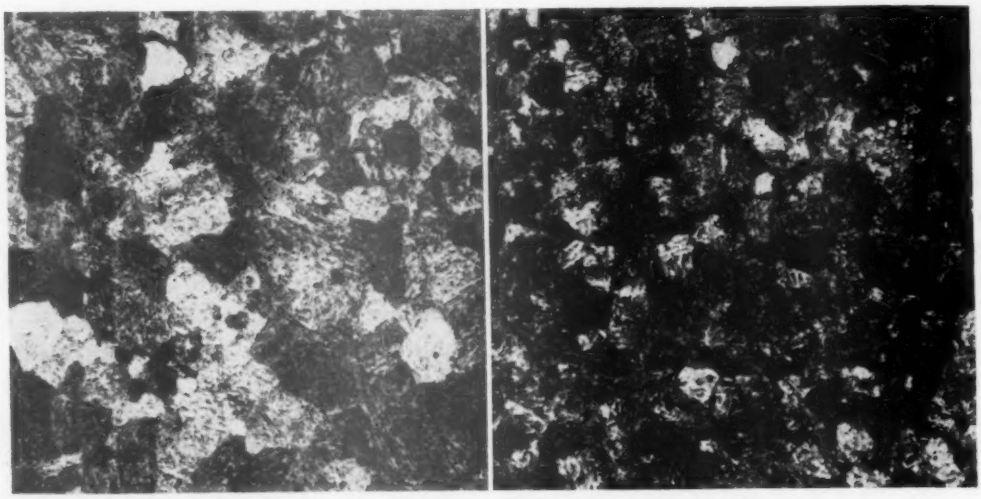

FIG 11. FIG 12.

FIG 11—AUSTENITE GRAIN SIZE IN NE 8640 CAST STEEL. SILICON-KILLED, HEATED ONE HOUR AT 1700°F. × 100. PICRAL-HCl ETCH.
FIG 12—AUSTENITE GRAIN SIZE IN NE 9530 CAST STEEL, DEOXIDIZED WITH Ca-Mn-Si, HEATED ONE HOUR AT 1550°F. × 100. PICRAL-HCl ETCH.

of alloy compositions, heat-treatments, and grain sizes. The deep-hardening Mn-Cr-Ni-Mo steel of Fig 12 is typical of the type prone to be badly segregated, transformed to a variety of intermediate products, and produces a grain-contrast etch, not a grain-boundary etch. Hence, it is usually impossible to determine the exact location of the complete boundary to every grain. This is not a great disadvantage when

one remembers that the other more common methods frequently are found, on close observation, to obliterate certain boundaries and to fail to delineate others.

polishing and etching will reveal a suitable structure.

In summary, it may be said that the martensitic etch method is very successful,

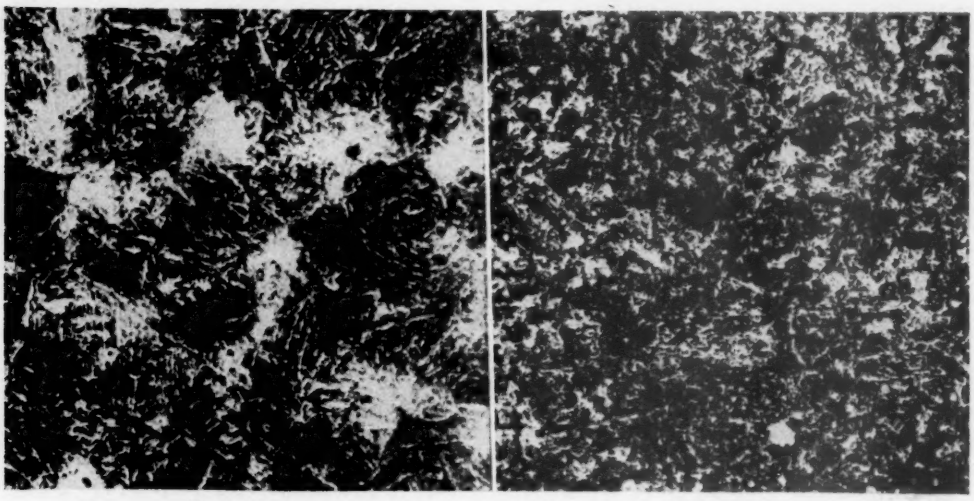

FIG 13. FIG 14.

FIG 13—MARTENSITIC ETCH METHOD FAILS BECAUSE OF EXTREME DENDRITIC SEGREGATION. × 100 PICRAL-HCl ETCH.
0.46 pct C, 0.7 pct Cr, 1.4 pct Ni, 0.3 pct Mo cast steel, silicon-killed, heated six hours at 1700°F.

FIG 14—MARTENSITIC ETCH FAILS TO REVEAL GRAIN SIZE. × 100. PICRAL-HCl ETCH.
NE 1330 cast steel, deoxidized with titanium, heated one hour at 1500°F.

With a little practice, the average laboratory worker can learn to rate grain size on *good* martensitic etch micrographs as accurately as he does on the more common types. There is great advantage in a method that gives the results of Figs 11 and 12 for steels on which no other accurate method works at all.

Occasionally even the martensitic etch fails or gives a structure that is not clear cut throughout. This is sometimes the result of extreme dendritic segregation, as illustrated in Fig 13, where the dendritic pattern might be mistaken for grain contrast at first glance. More often, however, when failures do occur with the martensitic method, they are merely because the etch fails to yield enough grain contrast (Fig 14). The cause for this has not been determined, but frequently repeated re-

reliable, and simple enough to warrant its regular use in the steel-foundry laboratory to make routine grain-size determinations on a variety of carbon and alloy cast steels heat-treated according to various schedules. It is by far the most satisfactory test studied for general work on cast steels.

THE MCQUAID-EHN TEST

The McQuaid-Ehn test is the oldest and probably the most familiar of all the methods for obtaining a quantitative measurement of an austenite grain size. It was developed[8] for the very special purpose of determining to what size the austenite grains in the surface layer of a low-carbon steel grow during case carburizing by a long-time, high-temperature

treatment in a carburizing atmosphere. The test is admirably suited for this purpose; however, frequently, without caution, it has been used on higher carbon steels never intended to be carburized or to be heat-treated at temperatures as high as are necessary for carrying out the test. The results frequently have been applied inadvisedly.

The standard test requires carburizing of the specimen 8 hr at 1700°F, then slow-cooling it to allow iron carbide to precipitate in the austenite grain boundaries on cooling. A lower temperature, such as would be used for hardening a medium carbon steel, is not suitable for producing a carbide network, but shorter times frequently are used to speed production and to approach more nearly ordinary heat-treatments. Less than 6 hr, however, is seldom enough to outline grains; this is a disadvantage because appreciable grain growth can occur between one and six hours.

Another criticism leveled at the indiscriminate use of the McQuaid-Ehn test is that the great increase in carbon content at the region where the grain-size measurement is to be made may alter the normal grain-growth behavior; in other words, case and core may have different grain sizes, and it is really the core grain size that is representative of the steel.

The various limitations of the McQuaid-Ehn test for the general run of grain-size work have long been recognized,[9] but it continues to be used extensively, probably through force of habit and because grain outlining is easily obtained, for actually the test is more troublesome and time-consuming than any of those previously described. Because of its popularity, the test was used on all steels studied in this investigation. Six hours at 1700°F in a natural gas atmosphere was found to be sufficient to give grain outlining following furnace cooling. Companion specimens taken from adjacent positions in the castings and heated side by side in the furnace were gradient-quenched so that the McQuaid-Ehn grain size could be checked by all the other methods (except, of course, the oxidation method).

The majority of the steels studied were appreciably coarser after 6 hr at 1700°F than after one hour at the same or a lower temperature. For example, a 0.32 pct C, 2 pct Ni steel, gradually coarsened from ASTM No. 5 to 8 or less to No. 1 to 3 through the three treatments. Occasionally steels that did not coarsen at 1700°F in one hour did so in 6 hr at that temperature; an example is a 0.30 pct C, 1.7 pct Mn, 0.45 pct Mo steel that coarsened from ASTM 6 to 8 to 1 to 3 in the extra 5 hours.

In the cases just cited, the McQuaid-Ehn test gives true results, which, however, are not very significant; in fact, they are likely to be misleading in view of the probable heat-treatment of the steels involved.

In a few cases, the McQuaid-Ehn method was found to produce austenite grains appreciably larger than those found below the surface layers of the same specimens. An example is illustrated in Figs 15*a* to *d*, in which all micrographs are of samples of a 0.30 pct carbon steel heated 6 hr at 1700°F. As specified previously, *a*, *b*, and *c* are from a sample cut adjacent to the sample used for photo *d*. It is interesting to note that this steel was treated with ferrotitanium and that the same effect apparently was observed in another so treated. Many more data would have to be secured, however, to infer the influence of titanium.

In summary, it may be said that the McQuaid-Ehn test nearly always works, and usually gives a true rating of the austenite grain size developed at the particular temperature and time of the test; however, these results are usually of significance only for low-carbon steels to be carburized. This

is because medium carbon steels are frequently fine grained at their proper heat-treateng temperature, but coarse grained at the McQuaid-Ehn temperature.

to cast steels. Thus, as a casting cools austenite forms at or slightly below the freezing point. This is at a very high temperature, so the grain size of that aus-

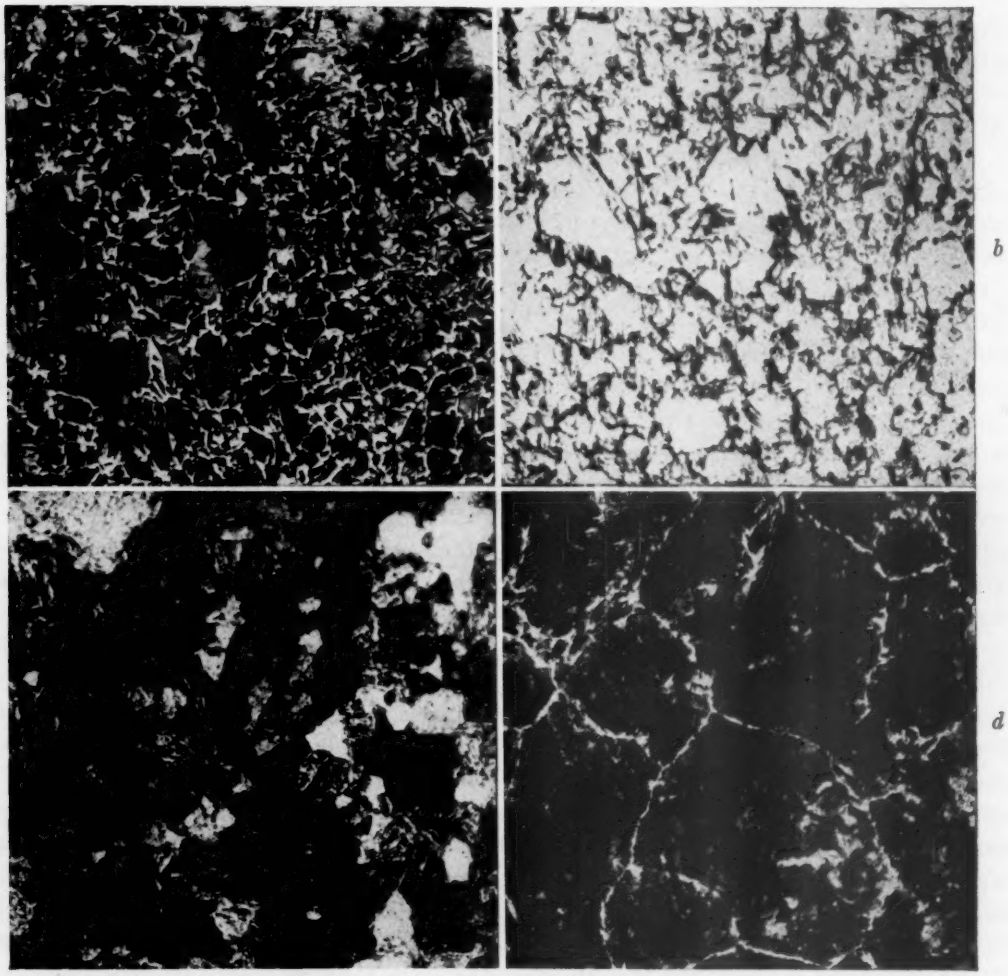

FIG 15—AUSTENITE GRAIN SIZE OF 0.30 PER CENT CARBON STEEL DEOXIDIZED WITH ALUMINUM AND FERROTITANIUM. HEATED SIX HOURS AT 1700°F. × 100.
a. Normalizing method. Nital etch.
b. Gradient quench method. Nital etch.
c. Martensitic etch method. Picral-HCl etch.
d. McQuaid-Ehn method. Nital etch.

GRAIN-SIZE CHARACTERISTICS OF CAST STEELS

General

From the results of studies made during this investigation, it can be concluded that most of the knowledge relating to austenite grain size in wrought steels can be applied

tenite is very large. On subsequent cooling, apparently no change in the size of the austenite grains occurs; with the ordinary carbon and alloy steels, the austenite completely decomposes as it cools through the critical range. If a suitable microstructure results, etching with the proper reagent enables one to deduce the size of the

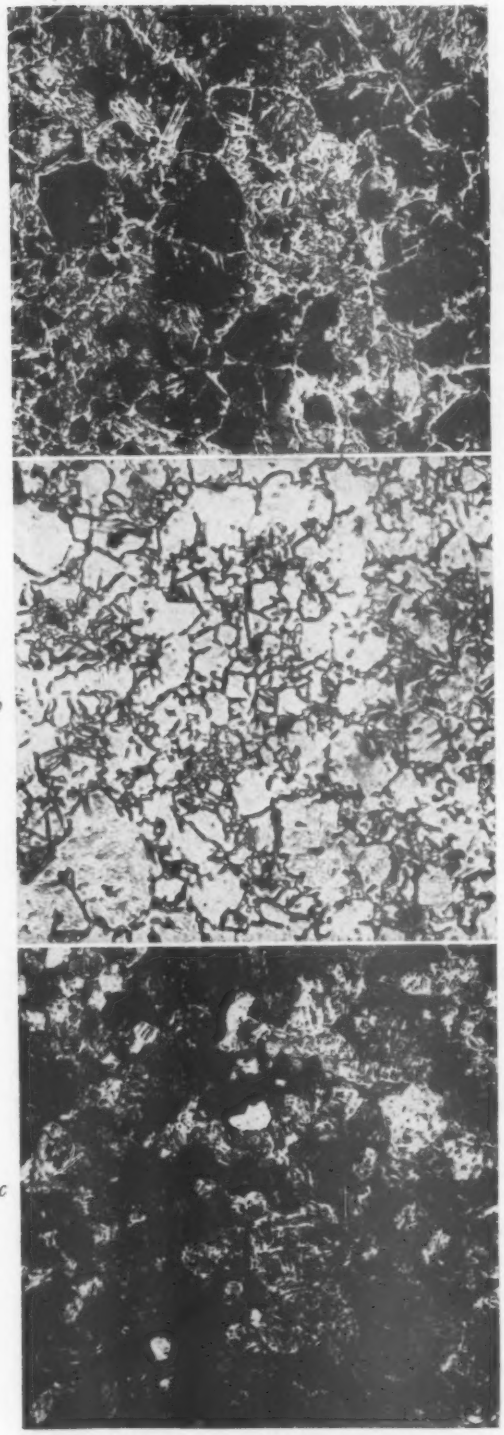

FIG 16—WIDE RANGE OF GRAIN SIZES EXISTING IN SILICON-KILLED, NE 1330 CAST STEEL HEATED ONE HOUR AT 1550°F. × 100.
a. Normalizing method. Nital etch.
b. Gradient quench method. Nital etch.
c. Martensitic etch method. Picral-HCl etch.

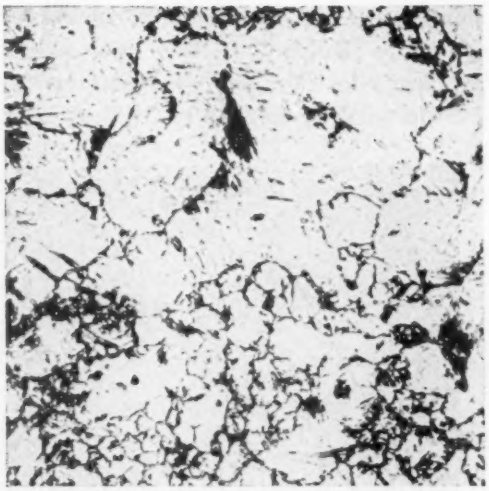

FIG 17—DUPLEX GRAIN SIZE IN ALUMINUM-KILLED, NE 1330 CAST STEEL, HEATED SIX HOURS AT 1700°F. GRADIENT QUENCH METHOD. × 100. NITAL ETCH.

austenite grains before this decomposition occurred. Results of such studies are reported in a later section.

Fortunately, when a steel casting is reheated for the first time, a new set of austenite grains is formed on passing through the critical range. These grains are quite small when they first form, but they grow as the temperature and time increase. In a given heat of steel, the temperature to which a sample is heated is the principal factor governing the size attained by the new austenite grains; the previous as-cast austenite grain size apparently has only a minor effect at the most, as indicated by the data of the next section.

The variation, from heat to heat, in the grain size of several steels given the same heating schedule results chiefly from differences in deoxidation practice. Thus, steels treated with aluminum, titanium, vanadium, or other strong deoxidizers tend to suffer less grain growth as heat-treating temperatures and times are increased. Many of these fully killed steels undergo almost no grain growth (e.g., remain about ASTM 7 to 8) until their so-called coarsening temperature is reached. Above this temperature (e.g., 1700°F), they usually begin to

coarsen rapidly, though not necessarily uniformly throughout the microsection; this leads to "duplex" grain-size ratings. Further increase in time or temperature of heat-treatment usually will fully coarsen these steels (e.g., they reach grain size No. 3 or larger throughout).

Silicon-killed or other mildly deoxidized steels, on the other hand, are usually considered to coarsen gradually throughout any temperature range in which they are normally heat-treated. Silicon-killed *cast* steels, however, are sometimes quite resistant to grain growth, as will be illustrated in a later paragraph.

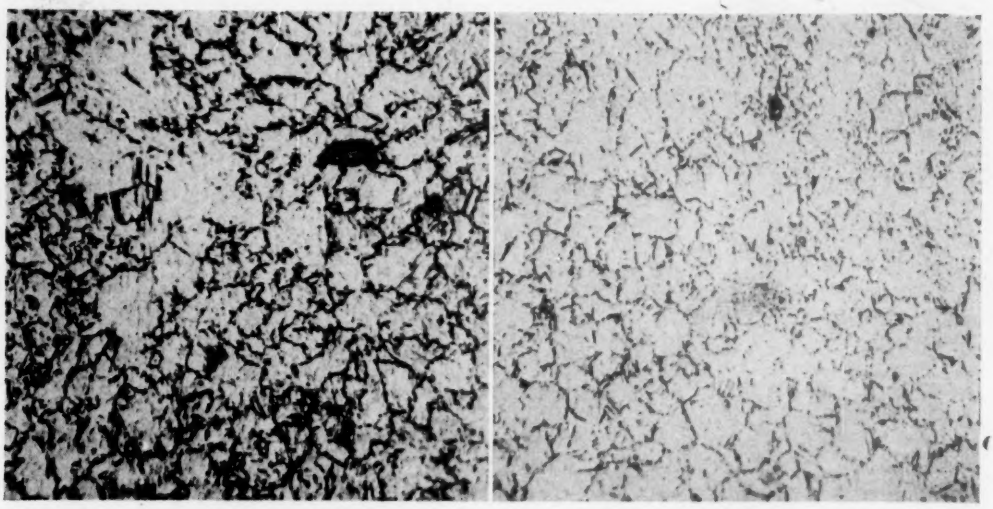

a *b*

FIG 18—0.34 PER CENT C, 1.3 PER CENT Mn, ALUMINUM-KILLED, CAST STEEL RESISTANT TO GRAIN GROWTH. GRADIENT QUENCH METHOD. × 200. NITAL ETCH.
a. Heated one hour at 1550°F.
b. Heated six hours at 1700°F.

GRAIN-SIZE CHARACTERISTICS OF CAST STEELS STUDIED IN THIS INVESTIGATION

A complete summary of the austenite grain sizes of a wide variety of carbon and alloy cast steels after each of three different heating schedules is given in the Appendix (see note on page 530). Some conclusions resulting from the investigation and illustrated in the appendix will be discussed in the following paragraphs.

First, no single ASTM grain-size number usually is suitable for expressing the grain size of a cast steel. There exists more commonly a range of grain sizes including three or four numbers on the scale. This is illustrated in Figs 16*a*, *b*, and *c*. It is not to be confused with the true duplex grain size common in aluminum-killed steels that have been heated just into the coarsening-temperature range. The latter is illustrated in Fig 17 and refers to the special case of fine-grained steels that have been heated to relatively high temperatures where pronounced coarsening begins in various separated areas.

In finer grained specimens, a smaller spread usually is reported (e.g., 7 to 8 rather than 3 to 6). Whether this is truly representative of the steels, or merely indicates that grains finer than No. 8 are easily obliterated and overlooked, is open to question. It is not unlikely, however, that the finer grained steels, which usually are fully killed, have a more uniform grain size.

In any event, after rating a wide variety of steels, one is quite likely to come to the

conclusion that rating with a precision of one grain-size number or better is meaningless, and that (except for tool steels) the ASTM grain-size scale would be just as useful in industrial work and less bothersome if it contained only the odd or the even numbers.

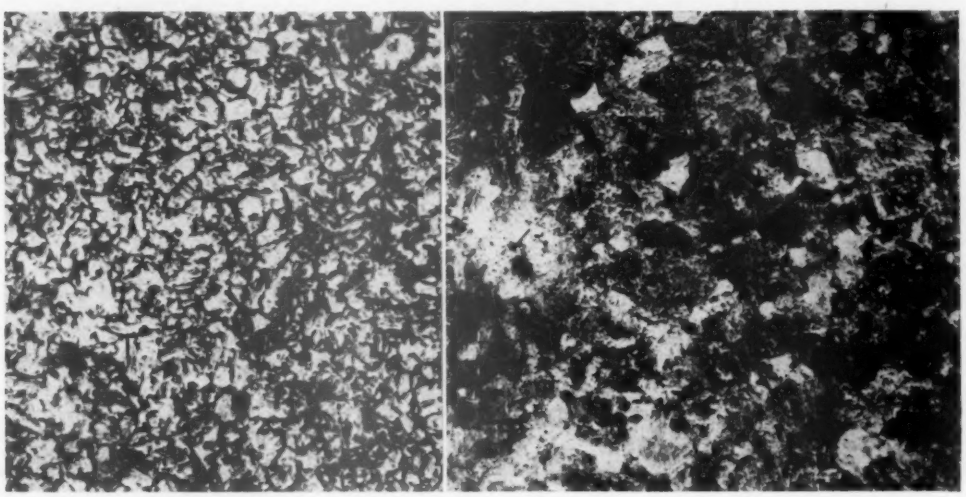

a *b*

FIG 19—FINE-GRAINED, SILICON-KILLED, 0.26 PER CENT CARBON CAST STEEL TO WHICH TITANIUM-BORON AND CALCIUM-SILICON ADDITIONS WERE MADE. HEATED SIX HOURS AT 1700°F. × 100.
a. Gradient quench method. Nital etch.
b. Martensitic etch method. HCl-picral etch.

The aforementioned range of grain sizes is also found in many wrought steels. The reason why metallurgists working with wrought steels are less conscious of this range of grain sizes is that most automotive and tool steels (on which the majority of grain-size rating is done) are made according to so-called "fine-grain practice" (e.g., are carefully controlled throughout melting, then aluminum-killed). On the other hand, many alloy cast steels are silicon-killed.

Continuing this comparison of cast and wrought steels, it should be pointed out that cast steels can be made just as resistant to grain growth as wrought steels. An excellent illustration is shown in Figs 18 *a* and *b* where a micrograph at 200 diameters is needed to properly rate an aluminum-killed 0.34 pct C, 1.3 pct Mn cast steel. This steel did not coarsen appreciably even in 6 hr at 1700°F.

Furthermore, even silicon-killed cast steels can be fine grained, and frequently they are finer than one expects a silicon-killed *wrought* steel to be. Probably this is a result of the large silicon additions and frequent use of special addition agents common in the steel-castings industry. This can be illustrated by a 0.26 pct carbon cast steel reported by the manufacturer to be silicon-killed and coarse grained. This steel had been treated with 4 lb per ton of titanium-boron and 2 lb per ton of calcium-silicon. After 6 hr at 1700°F, it was still rather fine grained, as can be seen from Figs 19 *a* and *b*.

In the Appendix, many examples can be found of steels fine grained at 1550°F, which contained no other deoxidizer than silicon. To be sure, they usually coarsen at higher temperatures, where aluminum-killed steels might not, but it must be remembered that most of these steels are quenched from about 1550°F; their grain size at 1700°F is not very significant.

AUSTENITE GRAIN SIZE OF STEELS IN THE AS-CAST STATE

As discussed in a previous section, austenite grains form at a very high temperature during or shortly after the freezing of a steel casting; in size, they are of the order of magnitude of 10 times as large as the very coarse-grained ASTM No. 1 standard.

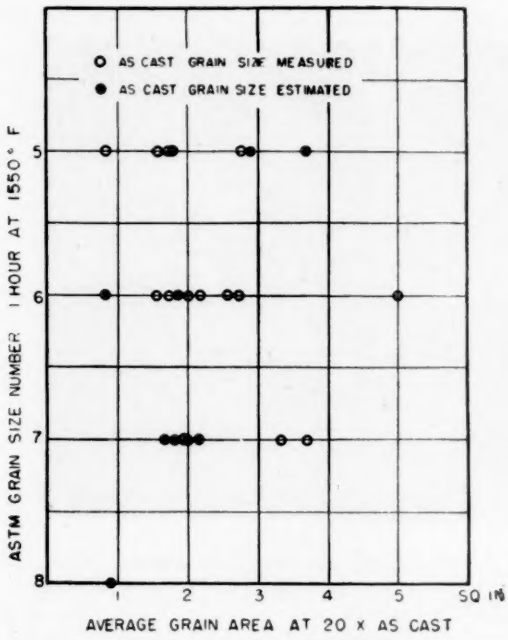

FIG 20—RELATIONSHIP BETWEEN AS-CAST AUSTENITE GRAIN SIZE AND AUSTENITE GRAIN SIZE AFTER HEAT-TREATMENT FOR SEVERAL CARBON AND ALLOY CAST STEELS.

It is of obvious interest to be able to measure this grain size, which existed during cooling in the mold, but it also poses a problem in that the possible techniques are limited. The method used cannot involve a reheating operation above about 1350°F, for a new and much smaller set of grains would thus be formed; instead, one is essentially limited to examining the as-cast microstructure and attempting to deduce the former austenite grain size from the pattern assumed by the decomposition products existing at room temperature. These products usually are ferrite and pearlite, and they are distributed according to a wide variety of patterns from steel to steel. Only occasionally does ferrite outline the former austenite grain boundaries in the manner made use of in the normalizing method for grain size. Probably special etching reagents or techniques can be developed to locate grains in the other cases but for the purpose of this investigation only the ferrite outlining was used.

Several steels had as-cast structures in which every individual grain could be identified by a ferrite outline. The total number of such grains over a large area was counted, using specimens set up under a 20× microprojector. The average grain area at 20 diameters could thus be calculated and used as a measure of the as-cast grain size of the steel under investigation. Such values are plotted against grain size developed in the corresponding steels on reheating for one hour at 1550°F; these are the open circles in Fig 20. Although more evidence, covering a wider range of grain sizes on reheating, is desirable (and is being accumulated) there appears to be no correlation. A few other steels whose structures were partially outlined were included in the analysis by estimating their as-cast grain sizes from comparison with the first set of steels. These are represented by the filled circles in Fig 20.

To illustrate more graphically that a very coarse as-cast grain structure does not necessarily prevent grain refining by a single heat-treatment, one of the coarsest as-cast structures was photographed at a representative point (Fig 21*a*); the grain size after reheating one hour at 1550°F was relatively fine (Fig 21*b*).

CONCLUSIONS

1. For general work involving measurement of austenite grain size in carbon and alloy cast steels, five methods may con-

veniently be used simultaneously. Of these:

a. The fracture and the "oxidation" methods are likely to give incorrect results, and are of use principally where all other methods fail.

b. The "normalizing" and the gradient quench methods usually work on plain carbon steels, but fail to work most of the time on alloy cast steels. They give correct results when they do work.

c. The martensitic etch method works most of the time and gives correct results. Its use as a routine foundry laboratory test is recommended.

2. The McQuaid-Ehn test is restricted to studies of austenite grain size developed during long-time high-temperature treatments. The results are not indicative of the grain size of the steel at lower temperatures, and at times are not even indicative of the true grain size at the temperature of the test (because of the effect of carburization upon grain size).

3. Most cast steels exhibit a range of gain sizes (e.g., 3 to 4 ASTM grain-size numbers) after any heat-treatment. The range is smaller in the finer grained aluminum-killed steels. Similar ranges are found in wrought steels, but this fact is not well recognized because most grain-size work on wrought steels is done on the aluminum-killed types.

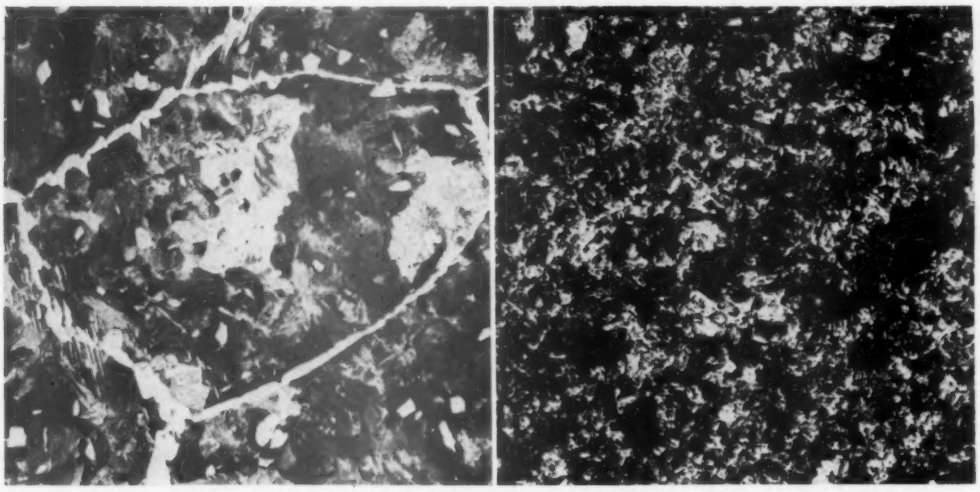

a *b*

FIG 21—NE 8630, SILICON-KILLED CAST STEEL, COARSE-GRAINED AS-CAST, FINE-GRAINED AFTER HEAT-TREATMENT.

a. As-cast. × 25. Nital etch.
b. Heated one hour at 1550°F. Martensitic etch method. × 100. Picral-HCl etch.

4. Fine-grained structure and resistance to grain growth can be secured as readily in cast steels as in wrought SAE steels.

5. Silicon-killed cast steels can be made fine grained at their proper heat-treating temperatures. Furthermore, they can be made resistant to grain growth at higher temperatures by the use of special addition agents.

6. Although the austenite grain size of as-cast steels without subsequent heat-treatment is very large, this as-cast grain size appears to have little influence on the grain size of the steel after subsequent heat-treatments.

ACKNOWLEDGMENT

The author wishes to thank the Steel Founders' Society of America for the support that made this investigation possible. The friendly cooperation of its Technical Research Committee, its Research Director, Mr. Charles W. Briggs, and many of its member foundries and their metallurgists, is deeply appreciated. Credit for much careful metallographic work and the development of several techniques are due Mr. Donald Wilson and Mr. Eugene Hughes.

REFERENCES

1. A. S. T. M. Standards, pt. I, Metals (1945).
2. R. Arpi: *Metallurgia* (1931) **11**, 123.
   B. Shepherd: *Trans.* Amer. Soc. for Metals (1934) **22**, 979.
3. M. Grossmann: *Metals Tech.*, A.I.M.E. (April 1946—T.P. 2020); *Trans.* A.I.M.E. (1946) **166**.
4. Tobin and Kenyon: *Trans.* Amer. Soc. for, Metals (1938) **26**, 133.
5. Austin and Day: *Ibid.* (1940) **28**, 354.
6. Miller and Day: *Ibid.* (1942) **30**, 541.
7. J. Vilella: Metallographic Technique for Steel, 38, 1938.
8. McQuaid and Ehn: *Trans.* A.I.M.E. (1922) **67**, 341.
9. Schempp and Shapiro: *Ibid.* (1937) **125** 411.

APPENDIX

An Appendix consisting of five tables giving a complete summary of austenite grain sizes of a variety of carbon and alloy cast steels after heating, has been deposited with the American Documentation Institute. To obtain them, write to the American Documentation Institute, 1719 N St., N. W., Washington 6, D. C., asking for Document No. 2382 and enclosing 50 cents for microfilm (images 1 in. high on standard 35-mm motion-picture film) or 50 cents for photocopies (6 by 8 in.) readable without optical aid.

DISCUSSION

(*J. H. Frye presiding*)

J. H. FRYE—There are two questions I would like to ask Dr. Hawkes about gradient quench method. He says that this method does not work very well with alloy steel. In general, how high must the alloy content be before trouble is encountered? To what extent is this difficulty encountered in wrought steels?

A. M. WHITE*—In addition to the methods of detecting grain size which have been so excellently presented by the author, I believe that mention should be made also of an etching reagent which was discussed in the paper by Cohen, Hurlich and Jacobson at the recent meeting of the American Society for Metals.† It was shown that their reagent, essentially a picral reagent containing a wetting agent, will, when properly used, reveal grain boundaries, but only in steels which are temper brittle. In these days of cast alloy steels the necessity for the steel to have been embrittled by tempering is not as great a restriction on the method as it may seem at first.

It might also be mentioned that temper brittle specimens etched for long periods of time in dilute picral will, upon light repolishing, also show grain boundaries.

C. H. DESCH‡—Have experiments been made with aqueous solutions of picric acid? We have found that such a solution will develop grain boundaries. A drop of nitric, or sometimes hydrochloric acid is added, and the grain boundaries are well developed. I have found that such boundary etching will sometimes reveal instances of temper-brittleness.

M. F. HAWKES (author's reply)—There is no minimum alloy content below which the gradient quench method for grain size will not fail because of dendritic segregation. Some plain carbon steels have enough dendritic segregation to cause failure; conversely a steel with 2 or 3 pct of alloying elements which can nevertheless be rated, is found occasionally.

I have not had enough experience to answer the question regarding wrought steels. However, I am sure that in some high alloy heats, intermediate transformation products form in bands and do not outline grain boundaries.

I have not experimented with the picric acid reagents mentioned.

---

* Physics Division, American Cyanamid Co., Stamford, Conn.

† J. B. Cohen, A. Hurlich and M. Jacobson: A Metallographic Etchant to Reveal Temper Brittleness in Steel, Amer., Soc. Metals preprint No. 17, 1946.

‡ Iron and Steel Institute of Great Britain, London, England.

The Diffusion Rates for Carbon in Austenite

By F. E. Harris*

(New York Meeting, March 1947)

It has been said that carbon is "ubiquitous" with reference to iron alloys. Certainly at temperatures where carbon and iron form the solid solution, austenite, it may be readily added to, or removed from, steel surfaces. Differences in concentration potential are the sole requirements for carbon flow.

To measure the rate of carbon flow, a proportionality factor, D, is arbitrarily expressed in units of $(\text{length})^2 \times (\text{time})^{-1}$. If the term used for carbon concentration is weight pct C, as is customary, then a factor must be found, changing this term to one of weight per unit volume when the diffusion coefficient, D, is used in flow formulae.

The determination of D values for carbon is complicated since D varies with the concentration itself. The Matano method has often been employed for systems involving a variant D. This method expresses an evaluation of unsteady flow whereby D is given a relationship with the numerical value of C-X slopes. The author contends that this solution is incorrect, except when D is invariant.

The primary purpose of this paper is to support this contention. Here diffusion is controlled under two conditions of flow. The first part deals with the steady state; the second part considers unsteady flow under definite restrictions. Beginning with the fundamental concept, the development is continued until equations for C-X curves are obtained. The solution is then subjected to experimental data.

It is realized that a great amount of reliable data is required for a rigorous proof. No such research is claimed. Instead an attempt is made to set forth the physical significance of the diffusion mechanism, and particularly to express the factors which influence the flow of carbon in austenite. Of equal significance is the implication that gaseous media may be employed with reasonable accuracy in making these determinations.

The Steady State Diffusion of Carbon in Austenite

The fundamental experiment defining diffusion in solid metals may be readily performed for carbon in gamma iron.[1] For this experiment a thin plate of medium carbon steel is chosen. The surfaces of this plate may be taken as two parallel planes which may be considered infinite for points well in the center of the planes. These two planes are held at different concentrations of carbon at a constant temperature. This temperature, 1700°F for example, is one where the single phase, carbon in solution with gamma iron, exists. When these conditions are held for a sufficient time the concentration of carbon of the different points of the solid settles down towards its steady state value. At points well removed from the ends, the concentration will remain the same along planes parallel to the surfaces of the plate.

Manuscript received at the office of the Institute Oct. 21, 1946. Issued as T.P. 2216 in Metals Technology, August 1947.

* Furnace Engineer, Buick Motor Division, Flint, Michigan.

[1] References are at the end of the paper.

Under these experimental conditions, the weight of carbon which flows through a given surface area in a given time may be readily expressed in terms of the surface concentrations and the thickness of the plate. Thus we may write:

$$\text{Pounds of carbon per square inch per hour} = .0028\, D_1 \frac{C_1 - C_o}{L} \quad [1]$$

where C_1 = pct C at the higher concentration
C_o = pct C at the lower concentration
L = thickness of plate in inches
D_1 = proportionality factor in inches^2 per hr

When the range of concentration is small (i.e. as C_o approaches C_1) the factor D_1 approaches the diffusion coefficient, D.

It has been well established that the diffusivity of carbon is not constant for a given temperature. Rather, the diffusion coefficient, D, varies with carbon concentration. The assumption that D is a linear function of the concentration should make a close approximation to the actual state. This we may express:

$$D = D_o[1 + K(\text{pct Carbon})] \quad [2]$$

Here D_o is constant for a given temperature.

It will be our purpose to derive the value of K, in Eq 2, by a steady state experiment. This we may do, if the assumption that D varies in a linear manner with concentration be the correct one. We shall begin by deriving certain expressions for steady state gradients. From these equations, the experimental data may be analyzed.

Steady State Equations

The general solution for flow in the steady state may be derived from Eqs 1 and 2. It will be helpful to standardize the units involved in the equations.

Four relative terms are employed. The first deals with the relative carbon concentration for which the symbol C_r is chosen. The unit of thickness, L, in Eq 1, is represented by X, while relative values of the diffusion coefficient will be termed D_r. To these three symbols are added a ratio term R whose significance will be derived from Eq 2.

Let us begin with the thin plate, bounded at the surfaces with planes of concentration, C_1 and C_o. As before, C_1 represents the higher concentration of carbon and C_o the lower, with the flow from higher to lower concentration. We now develop a standard for the C-X plot. Arbitrarily, C_1 is represented by a C_r value of unity, while C_o is represented by a C_r value of zero. Values of C_r are thus obtained:

$$C_r = \frac{C - C_o}{C_1 - C_o} \quad [3]$$

All concentration values on the right are expressed in percentage of carbon.

The abscissa scale for the C-X plot is chosen arbitrarily. Thus for the plane representing the higher concentration, we choose an X value of zero, while for the bounding plane of the lower concentration X is taken as unity. In terms of the relative concentration, C_r, we may bound the thin plate:

$$C_r = 1 \text{ at } X = 0$$
$$C_r = 0 \text{ at } X = 1$$

Since we are assuming D to be a linear function of concentration, the relative D value for $C_r = 0.5$ may be taken as unity. From this scale we may express D_r in terms of D_{C_1}/D_{C_o} which is the ratio of the diffusion rates for the surface concentrations. This ratio is given the symbol R.

Fig 1 shows a plot of C_r versus D_r. Let D_r at $C_r = 0$ be $\frac{2}{R+1}$. Then D_r at $C_r = 1$ becomes $\frac{2}{R+1} + 2\left(1 - \frac{2}{R+1}\right)$ which sim-

plifies to $\frac{2R}{R+1}$. But $\frac{2R}{R+1} \Big/ \frac{2}{R+1} = R$. Hence we may write:

$$D_r = \frac{2}{R+1} + 2\frac{R-1}{R+1} C_r \qquad [4]$$

We are now ready to derive expressions for the C-X graphs. From Eq 1 we find that the expression $\frac{C_1 - C_o}{L}$ is proportional to $\frac{1}{D}$. But $\frac{C_1 - C_o}{L}$ is the slope of the curve, or

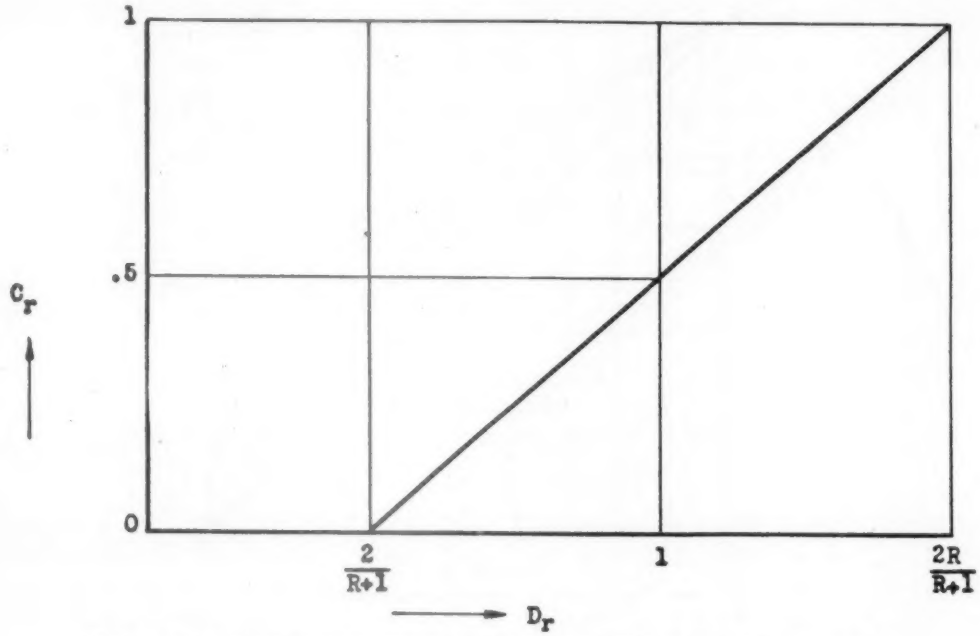

FIG 1—C_r VERSUS D_r IN TERMS OF R. (IN THE FIGURE AS DRAWN R = 3.58.)

which expresses the relative diffusion rate in terms of R and C_r. From Eq 2 we may express R in terms of the actual boundary concentrations. We may write:

$$D_{C_1} = D_o(1 + K.C_1)$$
$$D_{C_o} = D_o(1 + K.C_o)$$

Hence $$R = \frac{1 + K.C_1}{1 + K.C_o} \qquad [5]$$

Now K, which we are to find, will have but one value. R will thus depend upon the bounding concentrations C_1 and C_o. From Eq 5 it will be seen that as C_o approaches C_1, R approaches a value of one. Let us supply a value for K and assume values for C_1 and C_o. Here we are anticipating our experimental data.

Let $K = 2.15$, $C_1 = 1.38$ and $C_o = .05$

Then $R = \frac{1 + 2.15(1.38)}{1 + 2.15(0.05)} = 3.58$

$\frac{dc}{dx}$. Omitting the r subscripts we may write

$$\frac{dc}{dx} \alpha\ 1/D$$

But $D = \frac{2}{R+1} + 2\frac{R-1}{R+1} C$, from Eq 4. Thus we may write the differential equation for the C-X curve

$$\frac{dc}{dx} = \frac{K}{\frac{2}{R+1} + 2\frac{R-1}{R+1} C}$$

This equation is subject to the boundary conditions, $C = 1$ at $X = 0$ and $C = 0$ at $X = 1$. Collecting terms,

$$\frac{2}{R+1} dc + 2\frac{R-1}{R+1} C\, dc = dx.$$

The solution thus becomes

$$\frac{R-1}{R+1} C^2 + \frac{2}{R+1} C = 1 - X \qquad [6]$$

From Eq 6 we may solve for the area enclosed by the curve and the C-X coordinates. This we write

$$A = \frac{2R + 1}{3R + 3} \qquad [7]$$

medium capable of maintaining the higher carbon concentration at both surfaces for a sufficient time to insure that the plate reaches this concentration. A second plate is subjected tc a medium which

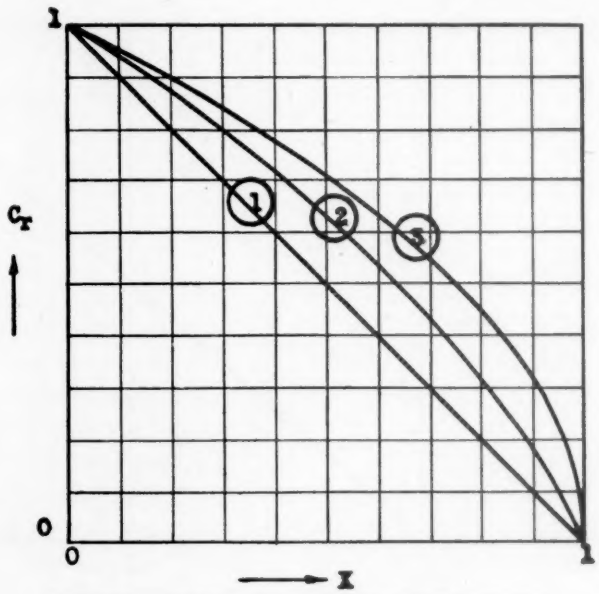

Mark	R	Equation	Area under Curve
1	1	$C = 1 - X$	0.500
2	3.58	$0.563C^2 + 0.437C = 1 - X$	0.594
3	∞	$C^2 = 1 - X$	0.666

FIG 2—C-X CURVES AND TABULATION.

Fig 2 shows the C-X curves for $R = 1$, 3.58, and ∞, when D varies linearly with C.

The area under the curve is directly related to the average concentration of the entire section normal to the bounding surfaces. From Fig 2, for example, the area under the straight line representing $R = 1$ will equal the area where $C_r = 0.5$ for the entire thickness, X. Thus Fig 3 represents the average C_r values for $R = 1$, 3.57 and ∞.

It is evident that the area under the curve is equal numerically to the average C_r value for the plate thickness.

The steady state experiment employs three thin plates. One is exposed to a medium capable of maintaining the higher carbon concentration at both surfaces for a sufficient time to insure that the plate reaches this concentration. A second plate is subjected tc a medium which will maintain the lower concentration, until this plate reaches the lower concentration throughout. The third plate is subjected to the first medium on one side and the second medium on the other side. Each plate is then analyzed for carbon using a sample uniformly milled from the plate cross section, normal to the surfaces and away from the plate edges. The first plate gives C_1 for plate three; the second determines C_o; the plate three concentration determines the area, since

$$C_r = \text{area} = \frac{C - C_o}{C_1 - C_o}$$ where C is pct C average of plate three. From the area, we determine R, Eq 7. Since R, C_1 and C_0

are now known, the value of K is found from Eq 5. This determination of K is the purpose of the experiment.

The Steady State Experiment

We have outlined the principles defining diffusion in the solid state. It now remains to apply a physical interpretation of the means by which we may best perform the experiment. The discussion may be divided in two parts, as follows:

1. An analysis of the gaseous media by which the high and low carbon concentrations may be consistently maintained on the test plate surfaces.

2. A description of the apparatus employed.

We begin with the gaseous media. It is evident from the iron carbon diagram that the solution of carbon in gamma iron, termed austenite, may range in concentration from zero carbon to approximately 1.35 pct C at 1700°F. Carbon diffuses at quite a rapid rate at this temperature, and since the possible range of carbon concentrations is satisfactory, we choose this temperature for the experiment.

The steady state flow of carbon through the plate demands that carbon be supplied at a constant rate to one surface, while it is being removed from the opposite surface at the same rate. This means that the first gaseous phase must be carburizing to a high concentration; the second phase is to be decarburizing to a low concentration of carbon.

The identical carrier gas is used for both phases by supplying suitable additions. This gas contains 20 pct carbon monoxide and 80 pct nitrogen. With this

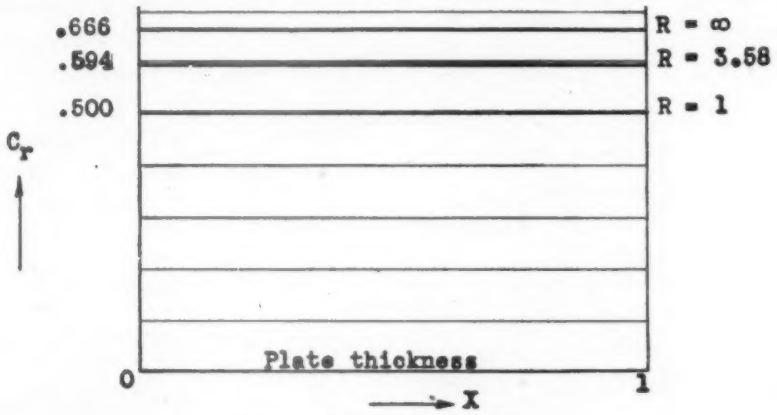

FIG 3—AVERAGE C_r VALUES.

CO content, 0.1 pct CO_2 is in equilibrium with saturated austenite at 1700°F; for 0.05 pct C, the CO_2 percentage is approximately 1.5 pct for equilibrium (no carbon flow). Thus we must enrich the carrier gas for supplying carbon at the saturated austenite level; for decarburization at 4 pct saturated austenite, the CO_2 content of the carrier gas must be in excess of 2 pct.

These additions are natural gas for carburization, and water vapor for decarburization. The presence of methane and absence of CO_2 in the effluent gases assures a sufficient carbon supply for the first condition. Saturating the carrier gas with water vapor establishes 2.5 pct CO_2 in the effluent; this analysis insures a sufficient capacity for abstracting carbon at a low carbon level.

A pit type carburizing furnace with a 20 in. diam × 36 in. deep work chamber is employed in the test. A fixture carrying the three test pieces is designed to hang from the test piece opening in the furnace cover. This fixture is shown in Fig 4.

An open wrought iron pipe, 2 in. diam × 18 in. long is copper plated on the outside surface. One test piece, *A*, is tack welded to the inside surface. The second plate *B*, approximately 2 in. diam, is welded across the open end of the pipe; plate *C* is hung beneath. These three plates are cut from a single sheet, SAE 1065 and 0.060 in.-thick. The top of the 2 in. pipe is then enclosed by welding a plate carrying a ¼-in. pipe. This pipe extends above the 2 in. section approximately 20 in. From the top a long piece of 3/16 in. copper tubing extends well into the 2-in. pipe. This tubing, carrying the water saturated carrier gas is brazed securely to the upper end of the ¼ in wrought iron pipe, there being sufficient clearance to allow the effluent gases an easy passage. Provisions are made for gas sampling.

Some 16 in. above the 2 in. section, a heavy plate fitting the test piece opening, is welded to the ¼ in. pipe. Through this plate provision is made for venting to the atmosphere the carburizing gas from the work chamber proper, and also for gas sampling. Thus with a container inserted within a container, plate *A* is subjected on both sides to the decarburizing gas, while plate *B* is exposed to decarburization on one side, and carburizing gases on the reverse. Plate *C* is exposed to the carburizing gas on either surface.

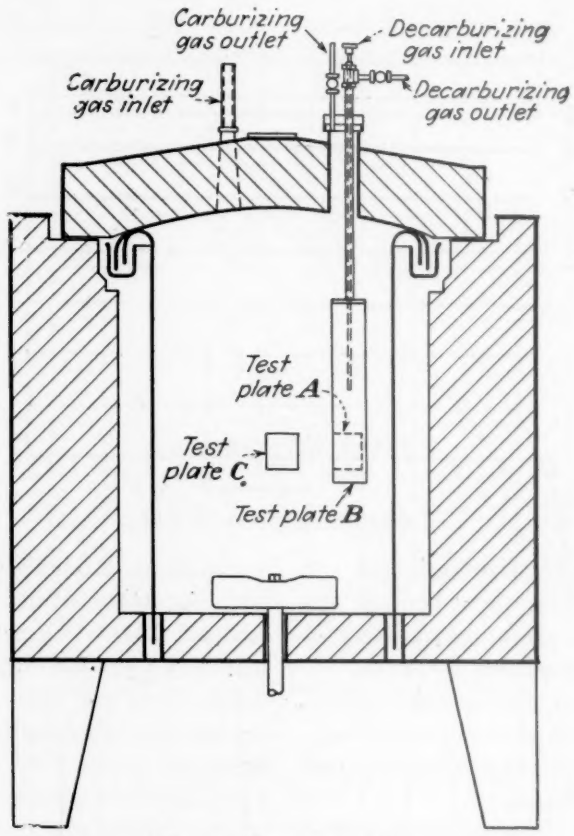

FIG 4—TEST ASSEMBLY.

The carburizing work chamber is thoroughly conditioned at 1700°F, and the cold fixture purged with gas before the fixture is inserted through the furnace cover opening. The carrier gas, saturated with water at 100°F is supplied to the auxiliary

container at the rate of 3 cu ft per hour. Flow to the retort proper is 60 cu ft of carrier gas plus 4 cu ft of natural gas per hour.

The elapsed time at 1700°F is 24 hrs. It will be noted that the duration of the test is not important, save that sufficient time be allowed to insure equilibrium conditions of carbon flow.

Much of the test data has already been given. *A* analyzes 0.05 pct C, *B* is 0.84 pct C while *C* averages 1.38 pct C. Taking the surface concentrations of plate *B* as 1.38 and 0.05, we have

$$C_r \text{ for } 0.84 \text{ pct } C = \frac{0.84 - 0.05}{1.38 - 0.05} = 0.594$$

$$\text{From Eq 6 } \frac{2R + 1}{3R + 3} = .594 \text{ and } R = 3.58$$

$$\text{But } R = \frac{1 + K(1.38)}{1 + K(0.05)} \text{ and } K = 2.15$$

We may call K the concentration coefficient, since it determines the dependency of the diffusion coefficient with concentration. If D is varying linearly with concentration we may write from our test

$$D = D_o[1 + 2.15 \text{ (pct } C)] \qquad [8]$$

for the diffusion of carbon in austenite. The concentration coefficient derived by Wells and Mehl,[2] from unsteady state experiments is 0.9. From a carburizing experiment, Harris and Groves[3] report a value of 2.7 for K.

The micrographs of Fig 5 verify, in a measure, the conclusions drawn from the test.

Diffusion for Defined Conditions of Unsteady Flow

The flow of solute through a unit area may be expressed for steady flow:

$$\frac{Q}{t} = D\frac{dc}{dx} \qquad [9]$$

where Q is the mass of solute per unit area. For the unsteady state, where the amount varies with time, we may write a similar expression.

$$\frac{\partial Q}{\partial t} = D\frac{\partial C}{\partial x} \qquad [10]$$

For variable flow, we may also write[4]

$$Q = \int C\,dx \qquad [11]$$

from which is derived

$$\frac{\partial Q}{\partial x} = C \qquad [12]$$

If D is nonvariant, a new expression is obtained.

$$\frac{\partial Q}{\partial x \partial t} = D\frac{\partial^2 C}{\partial x^2} \quad \text{(differentiating Eq 10 with respect to } X\text{)}$$

$$\frac{\partial Q}{\partial x \partial t} = \frac{\partial C}{\partial t} \quad \text{(differentiating Eq 12 with respect to } t\text{)}$$

or

$$\frac{\partial C}{\partial t} = D\frac{\partial^2 C}{\partial x^2} \qquad [13]$$

In a similar manner for D variant, the relationship becomes

$$\frac{\partial C}{\partial t} = \frac{\partial}{\partial x}\left(D\frac{\partial C}{\partial x}\right)$$

We shall attempt to obtain values for D at a single temperature, 1700°F, for the diffusion of carbon in austenite. For this we are to employ definite boundary conditions for unsteady flow. These conditions are to be analyzed with respect to Eqs 13 and 14. The development of the solution may be arranged in three steps:

1. Boundary conditions and the general solution.
2. The empirical solution of experimental data.
3. Data, and comments.

A General Solution

In the steady state experiment, a concentration representing the saturated value for austenite is maintained on one

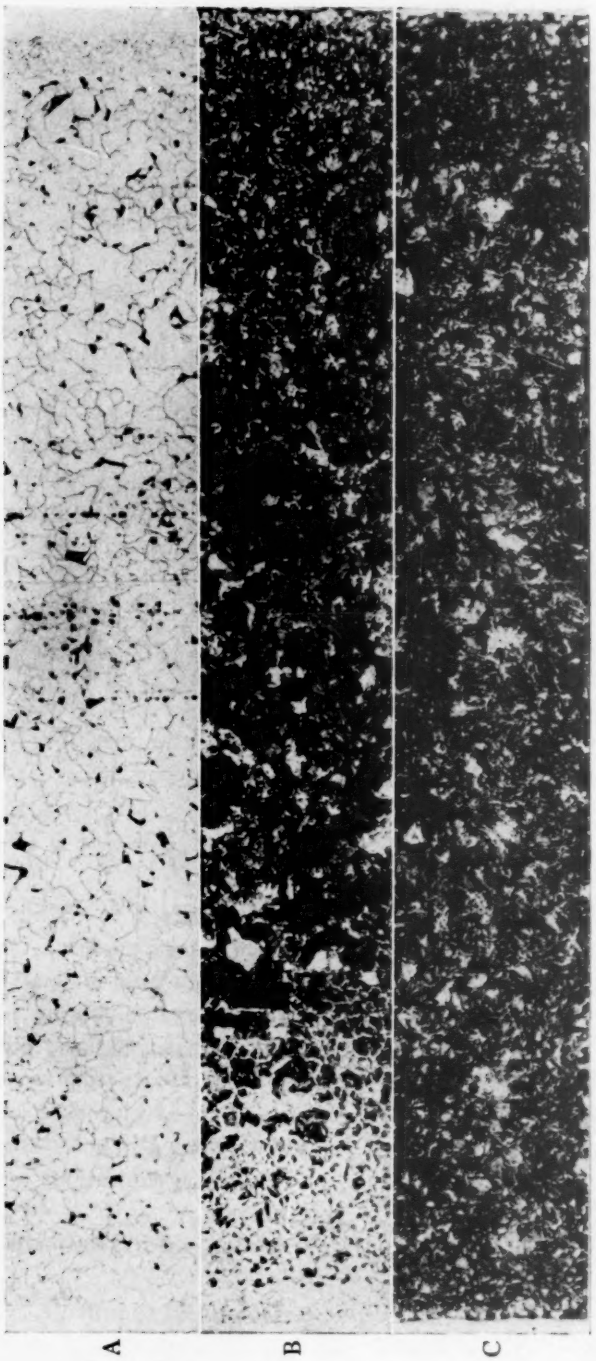

FIG 5—MICROGRAPHS OF TEST PLATES. ALL PLATES AT 1700° FAHRENHEIT 24 HOURS. (NITAL ETCH, X—100.)
Test Plate A—Average pct C = 0.05. Either end subjected to decarburizing medium.
Test Plate B—Average pct C = 0.84. Left end subjected to decarburizing medium. Right end subjected to carburizing medium.
Test Plate C—Average pct C = 1.38. Either end subjected to carburizing medium.

surface of the plate. On the opposite surface, a concentration not exceeding 0.05 wt pct carbon is held. Carbon is transported at a steady rate through various levels of concentration, ranging from the saturated solution to the dilute solution. The flow of carbon is steady, and the concentrations at all points along a line normal to the surfaces remain constant with time.

The unsteady state will be illustrated by two distinct experiments. These experiments differ in the direction of flow of carbon in relation to the plate surfaces.

In the first unsteady state experiment carbon is added to a homogeneous low carbon plate. A surface concentration, represented by the saturated value for austenite at 1700°F, is maintained on the plate surfaces for the elapsed time of the experiment. A definite time limit is imposed by the thickness of the plate specimen, such that at some point on a line normal to the surfaces, the original or core carbon is not changed. Under these experimental conditions, the rate at which carbon is added to the specimen is continually changing. Two points of concentration remain constant with time. The highest concentration is found at the surface and remains constant at all times; similarly at some point inward from the surface, the initial or lowest concentration of the specimen remains at its original value throughout the elapsed time of the experiment. In relation to the surface, this first experiment may be described as one where definite boundary values are applied for the flow of carbon inward *from* the plate surface.

In the second experiment, the boundary values are reversed. Thus the experimental plate becomes one of a high and homogeneous carbon concentration. This concentration may be that of saturated austenite at 1700°F, or of some lesser concentration. The surface concentration is maintained at a low and constant value, which will be 0.05 wt pct carbon or lower. This experiment describes, under definite boundary values, the flow of carbon outward to the plate surface. This carbon flow, as for the first experiment, is unsteady, i.e., it is constantly changing with time.

A mathematical solution for the *C-X* plots is available for both experiments for a non-variant D, as expressed in Eq 13.

$$\frac{\partial C}{\partial t} = D\frac{\partial^2 C}{\partial x^2}$$

For experiment 1 we may write

$$1 - C_r = \frac{2}{\sqrt{\pi}}\int_0^{\frac{x}{\sqrt{4Dt}}} e^{-y^2}dy$$

while for the second experiment,

$$C_r = \frac{2}{\sqrt{\pi}}\int_0^{\frac{x}{\sqrt{4Dt}}} e^{-y^2}dy$$

Values for the expression at the right of equality signs are fully tabulated in tables of the probability function, or ϕ tables, for various values of X. Since the X of the ϕ table is $\frac{X}{\sqrt{4Dt}}$ for our solution, we may express the two experiments in terms of these tables:

$$C_r = 1 - \phi\left(\frac{x}{\sqrt{4Dt}}\right) \quad \text{for flow from the surface (carburizing)} \qquad [15]$$

$$C_r = \phi\left(\frac{x}{\sqrt{4Dt}}\right) \quad \text{for flow to the surface (decarburizing)} \qquad [16]$$

If, for the flow of carbon in austenite, D were independent of concentration, then the *C-X* gradients from our experiments would conform to Eq 15 and 16. Since D is a function of concentration, we require a solution of Eq 14.

$$\frac{\partial C}{\partial t} = \frac{\partial}{\partial x}\left(D\frac{\partial C}{\partial x}\right)$$

The solution about to be derived compares the experimental gradients with those of the independent D of Eqs 15 and 16. This D we choose to call D_1. Referring to Eq 11

$$Q = \int C dx$$

The total amount of carbon added through a unit area of the outside surface of the specimen may be represented by the area between the curve and the coordinates. For Eq 15 draw the C-X curve, with its particular coordinates. The area, representing Q, now becomes

$$\int_0^\infty C_r \, dx = \frac{1}{\sqrt{\pi}}$$

Let us choose the units for D_1 as (inches)^2 per hour. Arbitrarily, Q will be represented for the carburizing experiment by the term "added carbon," where the quantity added is in pounds of carbon for 10 ft^2 of surface area. This figure is readily obtained from concentration cuts by multiplying (pct C − pct C initial) by four times the width of the cut in inches.

We may also express, from our experimental data, the range of concentration (pct C max. − pct C min.) by the term "carbon spread."

$$\left(\frac{\text{Added Carbon}}{\text{Carbon Spread}}\right)^2 \Big/ 20.4T = D_1 \quad [17]$$

where T = time in hours.

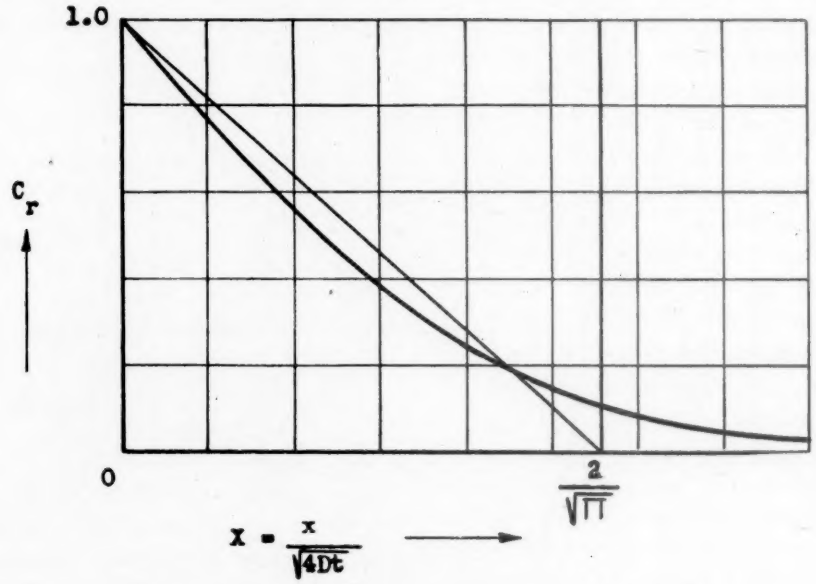

FIG 6—PLOT FOR THE EQUATION $C_r = 1 - \phi\left(\frac{x}{\sqrt{4DT}}\right)$.

D_1 may now be defined in terms of experimental data. Simply stated, it represents the single valued coefficient which would cause the same flow of carbon through the outside surface actually found when D varies with concentration. D_1 then must represent the value for some concentration between C_1 (the maximum pct C) and C_0 (the minimum pct C). The general solution will define that point of concentration where D_1 equals D_0.

It should be noted, in Eq 17, that the term "carbon spread" which is expressed as a difference of concentrations, involving percentages, is modified by a constant such that the D unit becomes (inches)^2 per hour. Similarly (in Eq 17), it must be

realized that $\frac{Q}{C_r}$ is also a significant term $\left(\text{here termed } \frac{\text{added carbon}}{\text{carbon spread}}\right)$. Referring to part one Eq 9, from which all other equations are derived, it will be noted that D is a function of the solute flow per unit concentration difference. Now Q is represented by the total area under the gradient, when flow is considered through the outside surface. We shall now deal with areas through which the carbon flows, other than the outside surface. In a linear diagram these areas are represented by straight lines perpendicular to the X axis just as the outside surface is represented by the C_r ordinate at $x = 0$. These "planes" are of constant concentration; the concentration is represented by the value of the C_r ordinate at the intersection of the C-X curve. The Q value for any such plane (or rather for unit area of the plane) is now represented by the area to the right of that line, between the C-X curve, the line itself and the X axis. Thus

$$Qc_r = \int_{x=x}^{x=\infty} C dx$$

This area shall be designated as A. In a similar fashion, $\frac{Q}{C_r}$ becomes $\frac{A}{C_r}$. This expression will be used throughout the solution, expressing C_r (limits 0 to 1) by the simple C.

To develop an orderly analysis, it is essential to standardize the scale of the C-X curves and to define the terms by which the curve properties are interpreted. Since the test data may be readily expressed in terms of D_1 (Eq 17), the distance scale or abscissa may be expressed using this term. The area under the C-X curve for D_1 is $\frac{1}{\sqrt{\pi}}$ where $C = \frac{\text{Pct } C\text{-}C_0}{C_1\text{-}C_0}$, and $X = \frac{x}{\sqrt{4D_1T}}$. This figure, $\frac{1}{\sqrt{\pi}}$, is rather awkward for expressing added solute values. Arbitrarily, the scale of the abscissa may be changed such that the area under the curve equals one-half. Thus $\frac{x}{\sqrt{4D_1T}} \cdot \sqrt{\pi} \cdot \frac{1}{2} = x \frac{\sqrt{\pi}}{\sqrt{16D_1T}}$ and the coordinate representations become

$$C = \frac{\text{Pct } C\text{-}C_0}{C_1\text{-}C_o} \qquad [18]$$

$$X = x \frac{\sqrt{\pi}}{\sqrt{16D_1T}} \qquad [19]$$

A straight line connecting the points on the coordinates, $X = 0$, $C = 1$ and $X = 1$, $C = 0$ will include an area of one-half, and the added solute scale is now determined. As before, C_0 is the pct C for the minimum concentration, and C_1 is the pct C representing the maximum; these concentrations "bound" the C-X curves. The lower case x is expressed in inches, and represents the penetration with reference to the outside surface; T is expressed in hours, and D_1 has the units (inches)^2 per hour.

From these coordinates, terms are given to the C-X curves. Thus it will be convenient to call the curve for D_1 the D_1 gradient. In contrast, since D varies with concentration, the actual bounded concentration-penetration curves are termed D_c gradients. The slope of these standardized curves for any particular plane whose concentration value is expressed by C becomes $\frac{dC}{dX}$. As given before, the area under the curve to the right of the particular C ordinate, which represents a plane of the concentration C whose "slope" is $\frac{dC}{dX}$, will be represented by A for the D_c gradient and by A_1 for the D_1 gradient. The scale is chosen such that for $C = 1$ (where $X = 0$), A (or A_1) has a value of unity.

Values for X, $\frac{dC}{dX}$, and A for D_1 gradient may be readily obtained from tables of probability integral functions.[5] For example X becomes $\frac{\sqrt{\pi}}{2} x$, where x is the table

value, and slopes in the table when multiplied by $\frac{2}{\sqrt{\pi}}$ are converted to $\frac{dC}{dX}$.

The general interpretation for the solution of D_c values is given in the Appendix. It will be convenient, however, to define the D_1 point of concentration for a given D_c gradient. This representation is shown graphically in Fig 7.

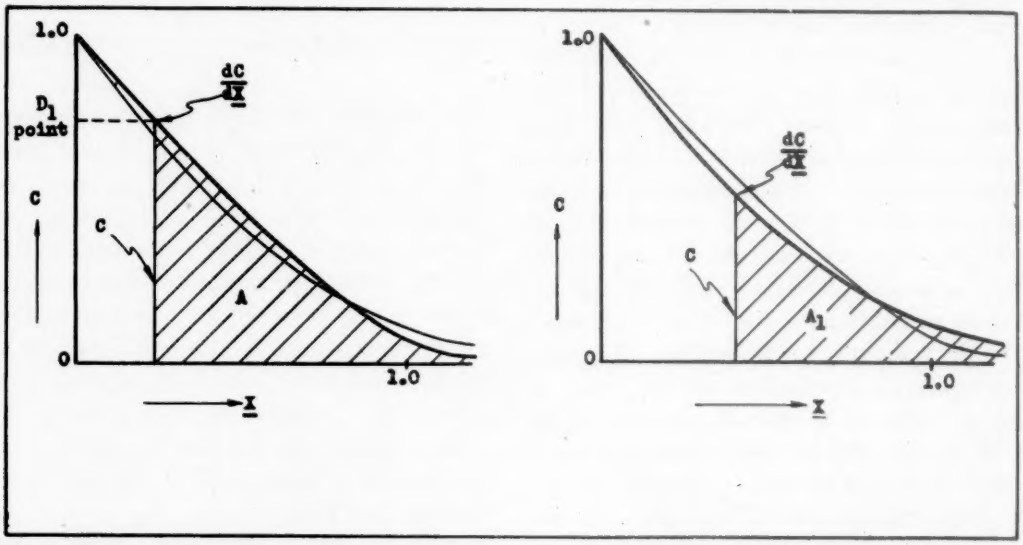

FIG 7a,b—GRAPHS ILLUSTRATING THE INTERPRETATION OF THE D_1 POINT OF CONCENTRATION FOR A D_c CURVE.

The C value for the D_c gradient whose D_c value equals D_1 is required for this solution. This value of C is defined when, for a common $\frac{dC}{dX}$ value for both the D_c and D_1 gradients, the value of $\frac{A}{C}$ is identical with $\frac{A_1}{C}$.

The general solution for D_c is given

$$\frac{Dc}{D_1} = \left(\frac{A}{C} \Big/ \frac{A_1}{C}\right)^{\frac{2}{3}}_{\frac{dC}{dX}} \qquad [20]$$

The subscript $\frac{dC}{dX}$ is added to show that the A/C and A_1/C values must be derived for the same value of $\frac{dC}{dX}$ for the D_c and the D_1 gradient. Using this equation, an empirical solution is derived from data obtained from both carburizing and decarburizing experiments.

An Empirical Solution for Gradients

If D is a linear function of concentration, it seems likely that a group of C-X equations may be derived whose $\frac{A}{C}$ values also vary in a linear manner with concentration. To conform to our standard coordinates, the area beneath the gradient as enclosed by the C-X ordinates must equal 0.5. Such a family of equations where A, $\frac{dA}{dC}$, slope, $\frac{A}{C}$ and X are all functions of C are tabulated in Table 1.

Note that these curves, numbered from 0 to 10, vary the $\frac{A}{C}$ value progressively from 1 to C, where for intermediate values $\frac{A}{C}$ is expressed as a linear function of concentration. At this point a general equation may be written for this family:

$$X = a(1\text{-}C) - \frac{1\text{-}a}{2} \log_e C$$

Before an attempt is made to apply

equations of this type to experimental data, it will be interesting to derive graphs approximating Eqs 15 and 16 which are repeated:

$$C = 1 - \phi\left(x\sqrt{\frac{\pi}{16D_1T}}\right) \quad \text{for flow } \textit{from} \text{ the surface}$$

$$C = \phi\left(x\sqrt{\frac{\pi}{16D_1T}}\right) \quad \text{for flow } \textit{to} \text{ the surface}$$

These two equations may be described in our terms by making R (Eq 5) equal to unity for both. The approximate curve for C-X as derived from the ϕ table (Eq 15) is:

$$X = 0.5(1\text{-}C) - 0.25 \log_e C \qquad [21]$$

A comparison is made in Fig 8, where the curve is drawn from the ϕ table data, while the circles indicate values from Eq 21.

Equation 21 may be said to represent the theoretical curve where $R = 1$ for flow from the surface, under the conditions outlined for unsteady flow, for the first experiment. This may well be called the D_1 curve (for D independent of concentration).

In a similar manner, an expression for $R = 1$ may be derived where the flow is *to* the surface.

$$X = 0.5C - 0.25 \log_e (1\text{-}C) \qquad [22]$$

In terms of the general equation, we may expect a solution for $R > 1$, flow *from* surface, when a values are *greater* than 0.5. These equations will follow the form of Eq 21. For flow *to* the surface, the equations for $R > 1$ will follow Eq 22, with a values lower than 0.5.

We shall now attempt an empirical solution for carbon gradients, properly bounded, based on Eq 20 which is repeated:

$$\left(\frac{A}{C} \Big/ \frac{A_1}{C}\right)^{3/5} = D_r$$

Here $\frac{A_1}{C}$ values are obtained from the ϕ table, and values of $\left(1 \Big/ \frac{A_1}{C}\right)^{3/5}$ are plotted against the slope or $\frac{dC}{dX}$ values. These

TABLE 1—*Tabulation for* $\frac{A}{C}$ *as a Function of* C

Curve No.	A	$\frac{dA}{dC}$	Slope, $\frac{dC}{dx}$	$\frac{A}{C}$	Equation
0	C	1	$2C$	1	$X = -0.5 \text{ Log}_e C$
1	$0.9C + 0.1C^2$	$0.9 + 0.2C$	$\frac{2C}{0.9 + 0.2C}$	$0.9 + 0.1C$	$X = 0.1(1\text{-}C) - 0.45 \text{ Log}_e C$
2	$0.8C + 0.2C^2$	$0.8 + 0.4C$	$\frac{C}{0.4 + 0.2C}$	$0.8 + 0.2C$	$X = 0.2(1\text{-}C) - 0.4 \text{ Log}_e C$
3	$0.7C + 0.3C^2$	$0.7 + 0.6C$	$\frac{2C}{0.7 + 0.6C}$	$0.7 + 0.3C$	$X = 0.3(1\text{-}C) - 0.35 \text{ Log}_e C$
4	$0.6C + 0.4C^2$	$0.6 + 0.8C$	$\frac{C}{0.3 + 0.4C}$	$0.6 + 0.4C$	$X = 0.4(1\text{-}C) - 0.30 \text{ Log}_e C$
5	$0.5C + 0.5C^2$	$0.5 + 1.0C$	$\frac{2C}{0.5 + C}$	$0.5 + 0.5C$	$X = 0.5(1\text{-}C) - 0.25 \text{ Log}_e C$
6	$0.4C + 0.6C^2$	$0.4 + 1.2C$	$\frac{C}{0.2 + 0.6C}$	$0.4 + 0.6C$	$X = 0.6(1\text{-}C) - 0.20 \text{ Log}_e C$
7	$0.3C + 0.7C^2$	$0.3 + 1.4C$	$\frac{2C}{0.3 + 1.4C}$	$0.3 + 0.7C$	$X = 0.7(1\text{-}C) - 0.15 \text{ Log}_e C$
8	$0.2C + 0.8C^2$	$0.2 + 1.6C$	$\frac{C}{0.1 + 0.8C}$	$0.2 + 0.8C$	$X = 0.8(1\text{-}C) - 0.10 \text{ Log}_e C$
9	$0.1C + 0.9C^2$	$0.1 + 1.8C$	$\frac{2C}{0.1 + 1.8C}$	$0.1 + 0.9C$	$X = 0.9(1\text{-}C) - 0.05 \text{ Log}_e C$
10	C^2	$2C$	1	C	$X = 1\text{-}C$

points are shown and tabulated in Fig 9. In an arbitrary manner, a straight line is drawn and $\left(1 \Big/ \frac{A_1}{C}\right)^{\frac{3}{5}}$ is designated by the term [1.85 − 0.635 slope)]. It must be noted that this line is but a rough approximation, and that the line is extrapolated where no data is available from the ϕ tables $\left(\text{i.e., for the higher values of } \frac{dC}{dX}\right)$. Hence an empirical solution for D_r may be written:

$$D_r = \left(\frac{A}{C}\right)^{\frac{3}{5}} [1.85 - 0.635 \text{ (slope)}] \quad [23]$$

Applying Eq 23 to Eq 21 the tabulation is shown in Table 2. Also included in this table are the comparisons of C-X values for the equation with ϕ values, and values for $-\log_e C$.

It will be noted that the D_1 curve is analyzed in a fair manner by Eq 23. The value of D for this equation should of course be unity for all values of C. From Eq 23 the D values approximate unity for all except the lower values of $\frac{dC}{dX}$.

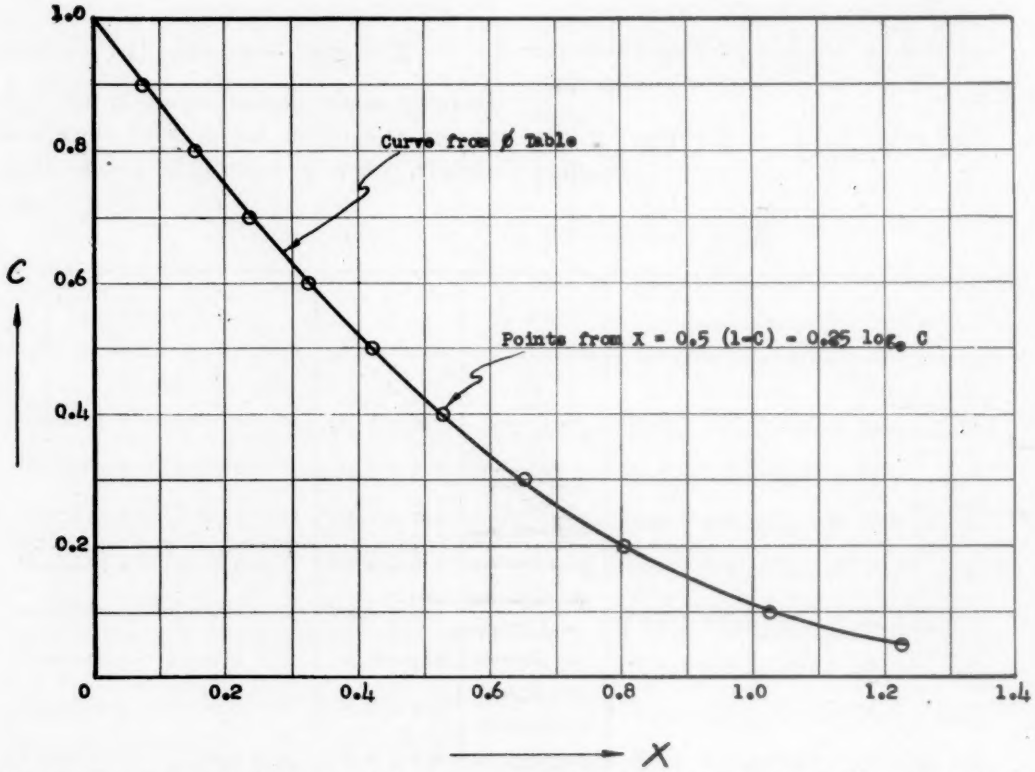

FIG 8—COMPARISON OF CURVE FROM ϕ VALVES WITH THE PLOTS OF $X = 0.5(1 - C) - 0.25 \text{ LOG}_e \text{ C}$.

Eqs 21, 22 and 23 will now be applied to two experimental runs. The first represents a carburizing experiment, the second a decarburizing test. Both of these gradients have been reported in previous publications, and the boundary values well proven. The data used is changed in one particular, only. In the decarburizing experiment, the surface concentration is taken as 0.05 pct to conform with the data obtained in the steady state.

Data and Comments

A standard carbon concentration test bar is carburized for 8 hr at 1700°F. The initial carbon is 0.20 pct C and the surface concentration, presumably held constant for eight hours at temperature,

is 1.34 pct C. The equation for this gradient is:

$$X = 0.9(1 - C) - 0.05 \log_e C$$

which is plotted, in Fig 10, where the circles represent the experimental data.

TABLE 2—*Application of Equation 23 to Equation 21 and Comparisons of C-X Values, R = 1*

$X = 0.5(1\text{-}C) - 0.25 \log_e C$

1-C	$\frac{A}{C}$	$\left(\frac{A}{C}\right)^{2/3}$	Slope	1.85 − 0.635 × Slope	D_r
0.0	1.00	1.0000	1.3330	1.000	1.000
0.1	0.95	0.9664	1.2750	1.041	1.000
0.2	0.90	0.9381	1.2300	1.070	1.000
0.3	0.85	0.8973	1.1660	1.110	0.996
0.4	0.80	0.8618	1.0900	1.158	0.998
0.5	0.75	0.8255	1.0000	1.215	1.000
0.6	0.70	0.7884	0.8888	1.286	1.010
0.7	0.65	0.7503	0.7500	1.374	1.030
0.8	0.60	0.7114	0.5714	1.487	1.050
0.9	0.55	0.6712	0.3333	1.638	1.090

C	− Log$_e$ C
1.00	0.0000
0.95	0.0513
0.90	0.1054
0.85	0.1625
0.80	0.2231
0.75	0.2877
0.70	0.3567
0.65	0.4308
0.60	0.5108
0.55	0.5978
0.50	0.6931
0.45	0.7985
0.40	0.9163
0.35	1.0498
0.30	1.2040
0.25	1.3863
0.20	1.6094
0.15	1.8971
0.10	2.3026
0.05	3.0000

C	X	ϕ Table
1.00	0.000000	0.00000
0.90	0.076350	0.07897
0.80	0.155775	0.15881
0.70	0.239175	0.24149
0.60	0.327700	0.32870
0.50	0.425775	0.42273
0.40	0.529750	0.52748
0.30	0.651000	0.64451
0.20	0.802350	0.80310
0.10	1.025650	1.03157
0.05	1.225000	1.22831

A complete tabulation of data and D_r values is contained in Table 3.

We proceed to analyze the data, beginning with Eq 17 which is repeated:

$$D_1 = \left(\frac{\text{Added Carbon}}{\text{Carbon Spread}}\right)^2 / 20.4T$$

where the added carbon value is 0.1624, the carbon spread becomes 1.34 − 20 or 1.14 and t is 8 hr then:

$$D = \text{(in.)}^2 \text{ per hour} = 124 \times (10)^{-6}$$

The a value in the general equation is 0.9. If we are to define the D_1 point as the concentration for experimental data where $D_1 = D_e$ it will be useful to determine D_1 points in terms of a. Since we have the equation for the D_1 curve, the C values where $\frac{A}{C} = \frac{A_1}{C}$ at equal slopes may be solved. This equation becomes, (for $a > 0.5$),

$$C \text{ (for } D_1 \text{ point)} = 0.666 + 0.084a \quad [24]$$

where $a < 0.5$ (flow to the surface or decarburizing) the equation becomes:

$$C \text{ (for } D \text{ point)} = 0.333 - 0.084a \quad [25]$$

From Eq 24, C (by which we mean C_r) becomes; 0.666 + 0.0756 or 0.74. But

$$C_r = 0.74 = \frac{\text{Pct } C\text{-}20}{1.34\text{-}20}$$

or

$$C_r = 1.04 \text{ pct } C$$

while

$$D \text{ for } 1.04 \text{ pct } C = 124 \times (10)^{-6}$$

We now turn to D_r values. From Table 3, the D_r values from which the straight line is drawn in Fig 5 are:

$$D_r, \text{ pct } C = 0.20, \text{ is } 0.440$$
$$D_r, \text{ pct } C = 1.34, \text{ is } 1.195$$

then

$$R = \frac{1.195}{0.440} = 2.71$$

and K (the concentration coefficient) may be obtained:

$$2.71 = \frac{1 + K(1.34)}{1 + K(0.20)}$$

and $K = 2.15$ as in the steady state experiment. Let us write for the diffusion of carbon in austenite at 1700°F.

$$(10)^6 \times D = 39(1 + 2.15 \cdot \text{pct } C) \quad [26]$$

solving for pct $C = 1.04$ we obtain

$$39(1 + 2.15 \cdot 1.04) = 125,$$

TABLE 3—1020 *Bar Carburized Eight Hours at* 1700° *Fahrenheit Surface Carbon* 1.34 *Pct, C,* $R = 2.7$

Cut	Pct C	Pct C-20	Added Carbon	Added Carbon, Pct	Added Carbon, Pct / 200	C_r	X
0.005	1.30	1.10	0.02200	13.257	0.06773	0.9649	0.0351
0.010	1.20	1.00	0.02000	12.315	0.06158	0.8772	0.1052
0.015	1.13	0.93	0.01860	11.453	0.05726	0.8158	0.1754
0.020	1.05	0.85	0.01700	10.467	0.05234	0.7456	0.2456
0.030	0.94	0.74	0.02960	18.226	0.09113	0.6491	0.3509
0.040	0.76	0.56	0.02240	13.793	0.06897	0.4912	0.4913
0.050	0.60	0.40	0.01600	9.852	0.04926	0.3508	0.6317
0.060	0.43	0.23	0.00920	5.665	0.02833	0.2017	0.7721
0.070	0.32	0.12	0.00480	2.955	0.01478	0.1052	0.9125
0.080	0.25	0.05	0.00200	1.231	0.00616	0.0439	1.0529
0.090	0.22	0.02	0.00080	0.493	0.00247	0.0175	1.1933
0.100	0.20	0.00	0.00000				
			0.16240	99.997	0.50000		

$$X = 0.9\,(1 - C) - 0.05\,\mathrm{Log}_e C$$

C	$\frac{A}{C}$	$\left(\frac{A}{C}\right)^{2/3}$	Slope	$1.85 - 0.635 \times$ Slope	D_r
1.0	1.00	1.0000	1.0530	1.181	1.1810 (1.195)
0.9	0.91	0.9390	1.0460	1.186	1.1140 (1.120)
0.8	0.82	0.8747	1.0390	1.190	1.0410 (1.040)
0.7	0.73	0.8107	1.0290	1.198	0.9712 (0.970)
0.6	0.64	0.7426	1.0160	1.205	0.8948 (0.890)
0.5	0.55	0.6712	1.0000	1.215	0.8155 (0.820)
0.4	0.46	0.5959	0.9756	1.230	0.7330 (0.740)
0.3	0.37	0.5154	0.9375	1.225	0.6314 (0.660)
0.2	0.28	0.4280	0.8695	1.298	0.5555 (0.590)
0.1	0.19	0.3305	0.7142	1.396	0.4614 (0.510)
					(0.440)

C	X	C	X
1.00	0.000000	0.45	0.534925
0.95	0.047515	0.40	0.585815
0.90	0.095270	0.35	0.637490
0.85	0.143125	0.30	0.690200
0.80	0.191155	0.25	0.744315
0.75	0.239385	0.20	0.800470
0.70	0.287835	0.15	0.859855
0.65	0.336540	0.10	0.925130
0.60	0.385540	0.05	1.005000
0.55	0.434890		
0.50	0.484655		

as compared with 124 from our data. In a similar manner, an analysis of the data is made for a 1.24 pct C bar decarburized for 8 hr at 1700°F. The data conform rather closely to an a value of zero for the general equation, (as Fig 11 and Table 4).

$$X = -0.5 \log_e C$$

The D_1 point is at $C_r = 0.333$, Eq 25, which represents a pct C of 0.45 since

$$0.333 = \frac{\text{pct } C - 0.05}{1.24 - 0.05}$$

but

$$D_1 = \left(\frac{0.1354}{1.19}\right)^2 / 163.2 \text{ or } 73 \times (10)^{-6}$$

also

$$R = \frac{1.85}{0.58} = 3.2$$

while

$$3.3 = \frac{1 = K(1.24)}{1 = K(0.5)}, \text{ or } K \doteq 2.15 \text{ as before}$$

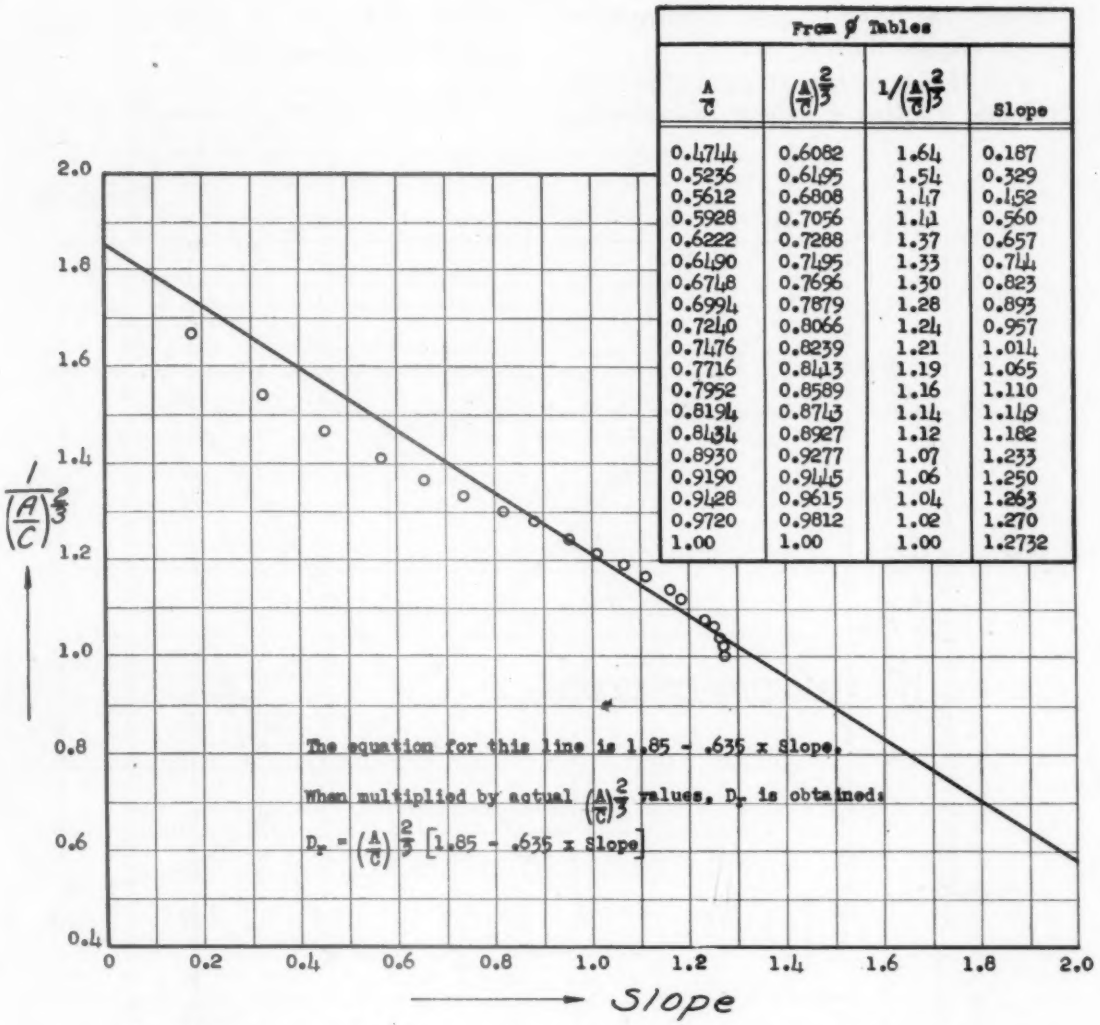

FIG 9—PLOT ILLUSTRATING THE DERIVATION OF AN EMPIRICAL SOLUTION FOR D_r.

Substituting in Eq 26

$$(10)^6 \times D = 39[1 + 2.15(0.45)]$$

or

D at 0.45 pct C $= 77 \times (10)^{-6}$, compared with $73 \times (10)^{-6}$ from data.

From this analysis, Eq 26 seems quite satisfactory. Thus we may say for 1700°F that D_0 is approximately $39 \times (10)^{-6}$ and that K is close to a value of 2.15.

Other values of R may be solved for the flow of carbon in either direction. From these data, Fig 12 is obtained. Here the equation for the curve may be written for any bounding concentrations, since R may be approximated from Eq 26.

APPENDIX

Unidirectional Solute Flow for the Semi-Infinite Solid

The flow of solute may be expressed for planes of constant concentration, these planes being parallel to the outside surface of the solid and being normal to the direction of solute flow. The flow is to planes of lower concentration and all solute found in these lower concentration planes above the initial or core concentration has passed

through the plane of given concentration in the elapsed time, T.

For the bounded gradient, the flow through a plane of given concentration

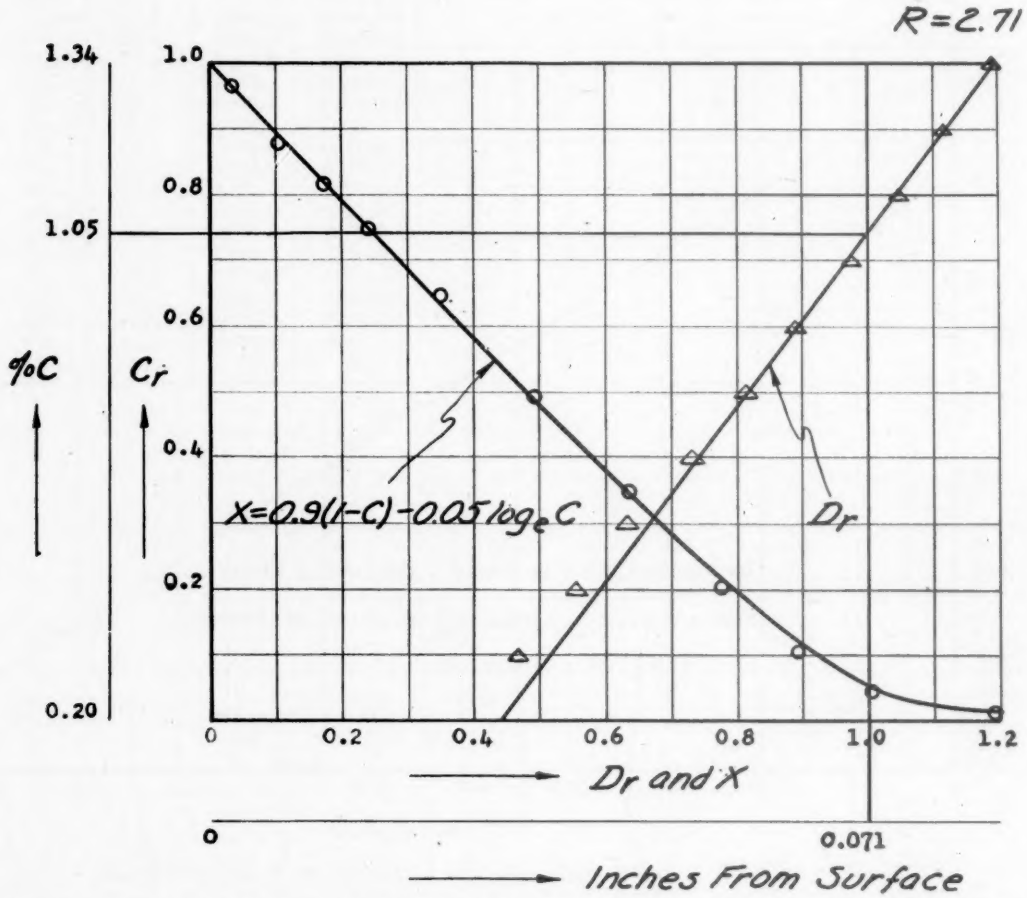

FIG 10—0.20 PERCENT CARBON BAR CARBURIZED EIGHT HOURS AT 1700 DEGREES FAHRENHEIT SURFACE CARBON 1.34 PERCENT CARBON.

may be written

$$\text{Added Solute} = K \cdot \text{Solute Spread} \cdot \sqrt{T} \qquad [27]$$

where the term, solute spread is given by the weight per cent of solute for the given plane minus the initial weight per cent (or core concentration) at $T = 0$. The added solute may be arbitrarily expressed for a unit of plane area. Thus for carbon flow, if the unit area be taken as 10 sq ft and the C-X plot be made on weight per cent C — inches, then

$$10 \text{ ft}^2 = 1440 \text{ in}^2 \quad 1440 \cdot \Delta x = \text{in.}^3$$

$$\text{lb } C = 0.28 \cdot 1440 \cdot \Delta x \cdot \frac{\text{pct } C\text{-}C_0}{100} = 4 \cdot \Delta x \cdot \text{pct } C\text{-}C_0$$

or the added carbon in pounds per 10 sq ft of plane area equals four times the area under the significant portion of the C-X plot, the ordinate representing pct C above the core concentration, C_0, and the abscissa scale being in inches.

The instantaneous rate of flow at a given elapsed time, t, through the plane of

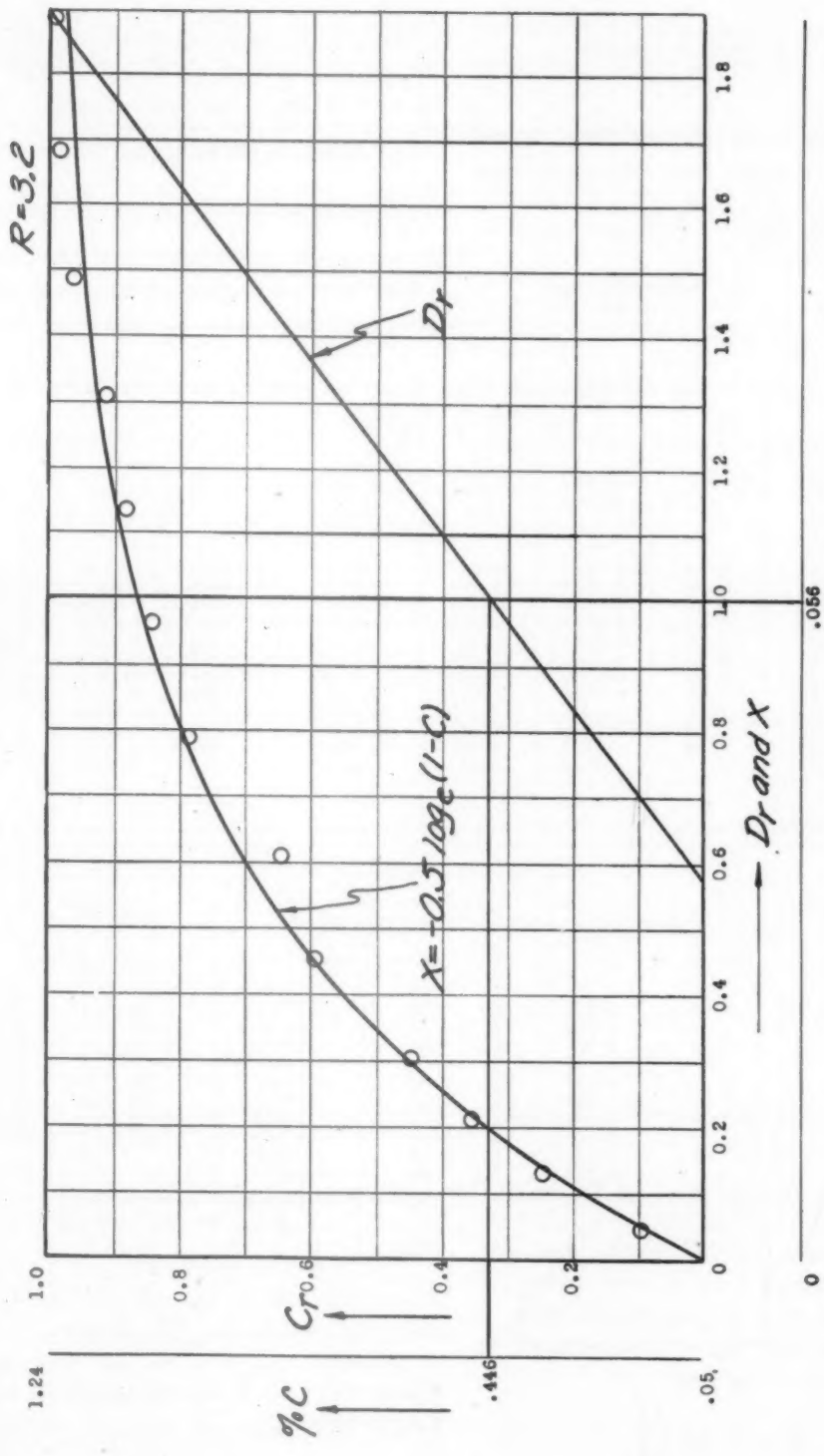

FIG 11—1.24 PERCENT CARBON BAR DECARBURIZED EIGHT HOURS AT 1700 DEGREES FAHRENHEIT. SURFACE CARBON 0.05 PERCENT CARBON.

concentration, C, is derived directly from Eq 27.

$$\frac{dQ}{dT} = \frac{K \cdot \text{Solute Spread}}{2\sqrt{T}} \qquad [28]$$

Also for the total elapsed time, t, the average rate of solute flow may be written

$$\frac{Q}{T} = \frac{K \cdot \text{Solute Spread} \cdot \sqrt{T}}{T} = \frac{K \cdot \text{Solute Spread}}{\sqrt{T}} \qquad [29]$$

instantaneous rate is directly proportional to the average rate, the rate of change of concentration with distance as obtained by gradient slopes on the C-X plot may be used in Eq 30 for evaluating D.

In dimensional analysis, the term $\frac{A}{C}$ may be used to represent $\frac{Q}{T}$, since the comparative expression is the added solute per unit concentration difference. The arbitrary scale for the C-X plot is

TABLE 4—1.24 *Pct C Bar Decarburized Eight Hours at 1700° Fahrenheit Surface Carbon* 0.05 Pct C, $R = 3.2$

Cut	Pct C	Pct $C - 0.05$	Added Carbon	Added Carbon, Pct	Added Carbon, Pct / 200	$1 - C_r$	C_r	X
0.005	0.16	0.11	0.0216	15.952	0.07976	0.9076	0.0924	0.04394
0.010	0.34	0.29	0.0180	13.293	0.06647	0.7563	0.2437	0.13182
0.015	0.47	0.42	0.0154	11.373	0.05687	0.6471	0.3529	0.21970
0.020	0.58	0.53	0.0132	9.748	0.04874	0.5547	0.4453	0.30758
0.030	0.71	0.66	0.0212	15.656	0.07828	0.4454	0.5546	0.43939
0.040	0.84	0.79	0.0160	11.816	0.05908	0.3521	0.6479	0.61514
0.050	0.98	0.93	0.0104	7.880	0.03840	0.2185	0.7815	0.79089
0.060	1.05	1.00	0.0076	5.613	0.02807	0.1597	0.8403	0.96664
0.070	1.10	1.05	0.0056	4.136	0.02068	0.1177	0.8823	1.14240
0.080	1.14	1.09	0.0040	2.954	0.01377	0.0841	0.9159	1.31810
0.090	1.20	1.15	0.0016	1.182	0.00591	0.0345	0.9655	1.49390
1.000	1.22	1.17	0.0008	0.591	0.00296	0.0169	0.9831	1.66960
			0.1354					

$X = -0.5 \text{ Log}_e (1\text{-}C)$

C	Slope	$D_r = \frac{1.85 - 0.635}{X \text{ Slope}}$	C	X	C	X
0.0	2.0	0.580	0.00	0.00000	0.55	0.39925
0.1	1.8	0.707	0.05	0.02565	0.60	0.45815
0.2	1.6	0.834	0.10	0.05270	0.65	0.52490
0.3	1.4	0.961	0.15	0.08125	0.70	0.60200
0.4	1.2	1.088	0.20	0.11155	0.75	0.69315
0.5	1.0	1.215	0.25	0.14385	0.80	0.80470
0.6	0.8	1.342	0.30	0.17835	0.85	0.94855
0.7	0.6	1.469	0.35	0.21540	0.90	1.15130
0.8	0.4	1.596	0.40	0.25540	0.95	1.50000
0.9	0.2	1.723	0.45	0.29890		
1.0		1.850	0.50	0.34655		

The average rate of solute flow for any given elapsed time is thus twice the instantaneous rate of flow at the time, t. The average rate may be expressed in terms of steady state flow

$$\frac{Q}{T} = -SD\frac{dc}{dx} \qquad [30]$$

where S is the plane area. Since the

taken

$$C = \frac{\text{pct } C\text{-}C_0}{C_1\text{-}C_0} \qquad [31]$$

where $C_1 - C_0$ is the total solute spread for the plot

$$X = x\sqrt{\frac{\pi}{16D_1T}} \qquad [32]$$

where x is the distance from the outside or bounding surface surface. D_1 is the invariant coefficient which will transport an identical added solute through the outside surface to that of the actual test case. For the coordinates chosen the area under both the D_c and D_1 gradients is equal to one-half. With the aid of the probability integral functions, the added solute for any $\frac{dC}{dX}$ value may be derived in terms of D_1. Thus the amount of carbon transferred through the outside surface in an elapsed time, t, is correlated with D_1

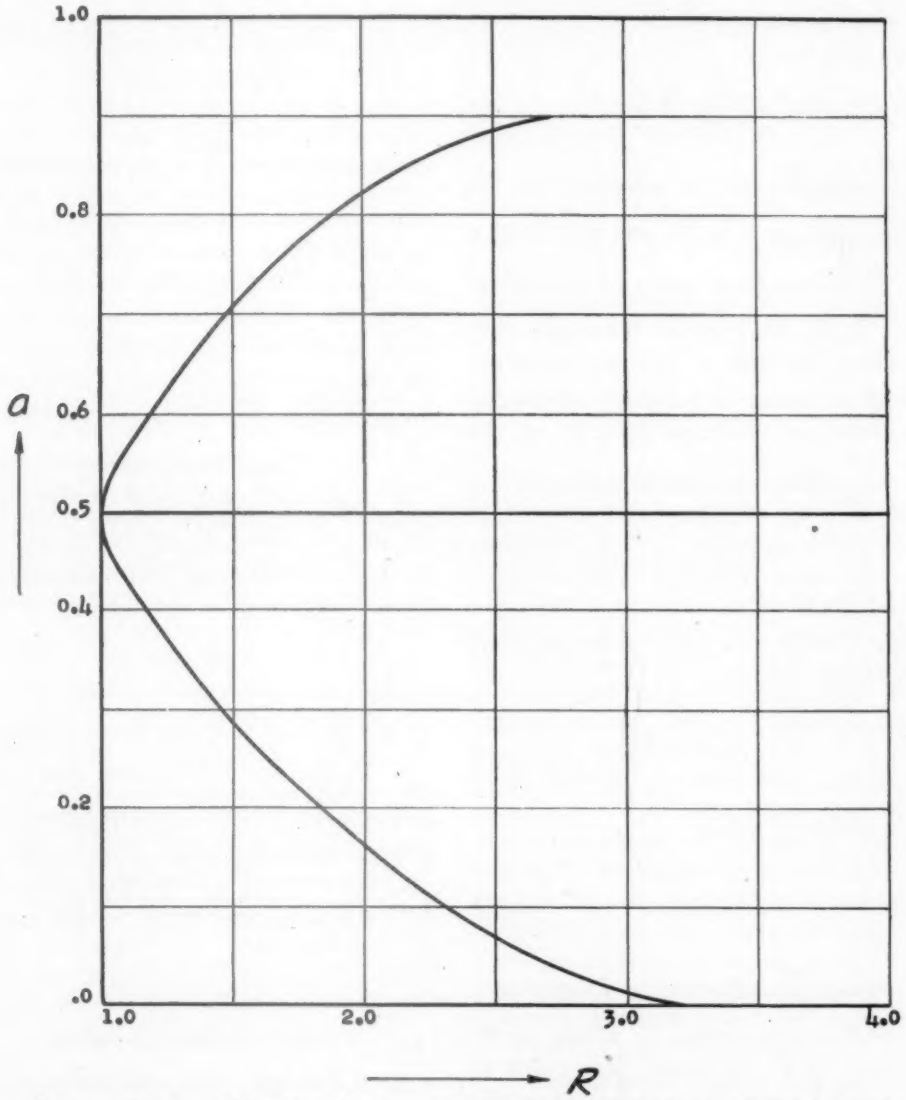

FIG 12—PLOT OF R VERSUS A FOR CARBURIZING AND DECARBURIZING EQUATIONS.

$$\frac{\text{Added Carbon}}{\text{Carbon Spread}} \cdot \sqrt{\frac{\pi}{16 D_1 T}} = 4 \cdot \frac{1}{2} \quad [33]$$

or

$$D_1 = \left(\frac{\text{Added Carbon}}{\text{Carbon Spread}}\right)^2 \Big/ \frac{64T}{\pi}$$

If x is given in inches and t is in hours, D_1 is given in inches^2 per hour.

In analyzing the solute flow through a plane of given concentration, attention must be paid to the added solute scale. For the chosen abscissa scale,

$$X = \frac{x}{\sqrt{D_1}} \sqrt{\frac{\pi}{16T}}$$

the $\frac{dC}{dX}$ values must be correlated to the distance dimension, x. For example, take a given $\frac{dC}{dX}$ value, for a plane of concentration, C, on the D_1 gradient. The scale of X is constant for both C-X plots. Thus the value of x, which determines the added solute scale, is modified directly by the term $\frac{1}{\sqrt{D_1}}$. Thus the flow formula,

$$\frac{A_1}{C} \alpha D_1,$$

must be corrected to obtain relative added solute values. Hence

$$\frac{A_1}{C} \Big/ \sqrt{D_1} \alpha D_1$$

or for a given $\frac{dC}{dX}$ value

$$\frac{A_1}{C} \alpha D_1^{3/2} \qquad [34]$$

For the same $\frac{dC}{dX}$ value on the D_c gradient, a plane of concentration, C, whose coefficient value is D_c, is found. This plane of concentration must be analyzed from the distance coordinate $X = \frac{x'}{\sqrt{D_c}} \sqrt{\frac{\pi}{16T}}$. Here the added solute is modified by the factor $1/\sqrt{D_c}$, and for this same $\frac{dC}{dX}$ value on the D_c gradient,

$$\frac{A}{C} \Big/ \sqrt{D_c} \alpha D_c \text{ or } \frac{A}{C} \alpha D_c^{3/2} \qquad [35]$$

The value for D_1 is known; the values of $\frac{A_1}{C}$ and $\frac{A}{C}$ are obtained from their respective C-X plots. Thus D_c may be found, since

$$\frac{D_c}{D_1} = \left(\frac{A/C}{A_1/C}\right)^{\frac{2}{3}}_{\frac{dC}{dX}} \qquad [36]$$

The subscript $\frac{dC}{dX}$ is added to emphasize the necessary condition that the analysis be made for a common slope on the two gradients. X for a given gradient may be expressed directly on an actual length scale, and thus the demand that slopes be expressed as the rate of change of concentration with distance is fulfilled.

ACKNOWLEDGMENT

I wish to thank Mr. E. E. Thum, Editor of *Metal Progress*, for continued interest, helpful suggestions, and criticisms concerning carburizing evaluations.

REFERENCES

1. H. S. Carslaw: Theory of Heat Conduction Dover Publication, 1945.
2. C. Wells and R. Mehl: Rate of Diffusion of Carbon in Austenite in Plain Carbon in Nickel and in Manganese Steels. *Trans.* AIME (1940), **140**, 279.
3. F. Harris and W. Groves: Formulation of Carburizing. *Metal Progress*, 1944.
4. H. Reddick and F. Miller: Mathematics for Engineers, Wiley and Sons, 1944.
5. Tables of the Probability Functions, Federal Works Agency, Works Project Administration, 1941.

DISCUSSION

(*H. J. French presiding*)

H. J. FRENCH*—Can you elaborate a little on this relative rate of diffusion between austenite and ferrite, bearing in mind that there is ordinarily a difference in temperature involved.

F. E. HARRIS (author's reply)—The relative rates of diffusion of carbon as between ferrite and austenite may be compared at temperatures where both phases may exist. For the

* International Nickel Co., Inc., New York City.

ferrite phase, the greatest concentration gradient possible is very small since the range of carbon concentrations may not exceed about 0.03 pct C. At 1400°F, for example, more carbon can be transferred, by decarburization, through a ferrite boundary layer than may be added for the same time and temperature by carburization, where the flow is in the austenite phase. The diffusion coefficient for carbon in ferrite must be many times as large as that for carbon in austenite, since the concentration gradient for flow in austenite is many times greater than that for ferrite, under the conditions of the experiments.

L. S. DARKEN*—In the first part of this paper the author has developped a somewhat novel and certainly interesting way of determining diffusivity from steady state measurements. In the past the diffusivity of non-gaseous elements in metals has usually been determined by non-steady state methods. A comparison of the present results with those of the comprehensive investigation of Wells and Mehl[2] at 1700°F (1200°K) is shown in the following tabulation of diffusivities in cm^2 per sec.

Per Cent C	Steady State Method—Harris	Diffusion Weld Method—Wells and Mehl
0	0.7×10^{-7}	1.05×10^{-7}
0.7	1.75	1.68
1.0	2.2	1.95

The agreement in the center of the range covered is excellent but Harris finds a much greater variation with composition. The manner of calculation used by Harris may be given more explicitly as follows:

From the definition of diffusivity, the rate of transport of carbon across any plane of unit area parallel to the surfaces is $-D\frac{dC}{dx}$. At steady state this rate is the same for all planes and hence may be set equal to a constant $-A$.

$$D\frac{dC}{dx} = A \text{ or } D\,dC = A\,dx.$$

If it is assumed that $D = D_0(1 + KC)$ then

$$(1 + KC)\,dC = \frac{A}{D_0}\,dx.$$

Integrating from one face to the other $x = 0$, $C = Co$ to $x = X$, $C = C_1$

$$(C_1 - C_0) + \tfrac{1}{2}K(C_1^2 - C_0^2) = AX/D_0$$

The total carbon in a section of unit area and thickness X is clearly

$$\int_0^x C\,dx = \frac{D_0}{A}\int_{C_0}^{C_1} C(1 + KC)\,dC$$

and C_m the average value of C in this section is this integral divided by X

$$C_m = \frac{\tfrac{1}{2}(C_1^2 - C_0^2) + \tfrac{1}{3}K(C_1^3 - C_0^3)}{(C_1 - C_0) + \tfrac{1}{2}K(C_1^2 - C_0^2)}$$

Solving this expression for K

$$K = \frac{C_m - \tfrac{1}{2}(C_1 + C_0)}{\tfrac{1}{3}(C_1^2 + C_0C_1 + C_0^2) - \tfrac{1}{2}C_m(C_1 + C_0)}$$

Inserting the values $C_1 = 1.38$, $Co = 0.05$, $C_m = 0.84$, it is found that the concentration coefficient, $K = 2.15$ as given in the paper.

Unfortunately the author cites only a single experimental result so that the precision is very difficult to estimate. If the average carbon content of the diaphragm were 0.82 pct C (instead of 0.84) then K would be found to be 1.44 (instead of 2.15). Also it is quite possible that the compositions at the boundaries of the diaphragm at steady state were not identical with those of the test pieces equilibrated with the same atmospheres. The calculated value of K is sensitive to these boundary conditions; for example if the carbon content at the outgoing surface were 0.10 pct instead of 0.05, then K would be calculated to be 1.64 (instead of 2.15). The assumption that the diffusivity is linear with carbon content introduces another source of possible error; present evidence indicates that the diffusivity usually rises more rapidly with concentration at higher concentration than at lower. All these uncertainties could be eliminated by a sectional analysis of the diaphragm to obtain the composition-distance relationship; in fact this method seems more promising for precise data than the diffusion weld method—or than any other non-steady state method. It is certainly to be hoped that the author will continue this investigation after the excellent start he has made.

* Research Laboratory, U. S. Steel Corp., Kearny, N. J.

The second part of the paper, dealing with the composition-distance relationship during carburization and decarburization, presents a semi-empirical method of obtaining the diffusivity from such data. In my opinion such an empirical solution is dangerous to use as it may lead to serious errors. In the present case it seems altogether unnecessary, as an exact method of handling such data is already available and well known as the Boltzmann or Matano method. To illustrate the dangers inherent in an empirical method, it is seen that the points in Fig 5 may quite adequately be represented empirically as falling on a straight line over the range from $C_r = 0.2$ to 1.0; setting $\frac{\partial^2 C}{\partial x^2} = 0$ it may readily be shown that the diffusivity varies linearly with the square of $C_1 - C$ (C_1 being the surface concentration); this conclusion is obviously quite at odds with that deduced by the author using another empirical representation.

F. E. HARRIS—Dr. Darken's remarks are very welcome. It is quite true that the steady state experiment should be repeated by a sectional analysis of the diaphragm to confirm the concentration-distance relationships. It is gratifying that he recognizes this method as having possibilities in accurately determining the dependency of diffusion coefficients on concentration.

For the non-steady flow, there is no dearth of data concerning the rates at which carbon may be added in carburization, or removed in decarburization. The difference in these rates for the two operations had led to this development of a "D_1 point" concept to correlate these data in terms of D_c.

The author must disagree with the use of the derivation known as the Matano or Boltzmann method as a solution for D_c. It is hoped that the following dissertation may aid in clarifying this contention.

THE SOLUTION FOR D_c

The functional dependence of C upon X may be expressed, for discussion purposes, in parametric form: $C = f_1 D$ $X = f_2 D$. The general equation for linear diffusion may then be written:

$$\frac{\partial C}{\partial t} = \frac{\partial}{\partial f_2 D}\left(D \frac{\partial C}{\partial f_2 D}\right)$$

A particular solution is desired for this equation when C is a function of $\frac{X}{\sqrt{T}}$. Following the Matano derivation, a factor may be chosen to replace X and T in the general equation. This factor, Z, must also include D, if areas under the C-Z curve are to be used in solving for D. In other words, these areas must be independent of D itself. Such a factor is $Z = \frac{X}{\sqrt{DT}}$.

General solution in D_1	$\frac{\partial c}{\partial t} - D_1 \frac{\partial^2 c}{\partial x^2} = 0$
Particular solution, $Z = \frac{X}{\sqrt{D_1 T}}$	$\frac{1}{2} z \frac{dc}{dz} - \frac{d^2 c}{dz^2} = 0$
Multiply by dz, making C the independent variable	$\frac{1}{2} z dc - d\left(\frac{dc}{dz}\right) = 0$
Integrate	$\frac{1}{2}\int_{c_0}^{c} z\, dc - \frac{dc}{dz} = 0$
Simplify	$D_1 \frac{dc}{dx} = -\frac{1}{2t}\int_{c_0}^{c} X\, dc$

Since X is expressed in units of length, D must be single-valued; that is, D must be independent of C and X. Such a transformation is illustrated in the preceding table.

The transformation factor is dimensionless, since $Z = X/\sqrt{DT} = L/\sqrt{L^2/T \cdot T} = L/L$. This is a necessary condition, if the equation is to remain true, regardless of the magnitude of the fundamental units. The Matano Derivation is not a solution for D_c in the general diffusion equation,

$$\frac{\partial C}{\partial t} = \frac{\partial}{\partial x}\left(D_c \frac{\partial C}{\partial x}\right).$$

It is an exact solution only for D_1, where D_1 is independent of C and X.

The C-Z curves of the test may be used to illustrate this contention. These curves are plotted with Z as an arbitrary parameter, where $Z = X\sqrt{\frac{\pi}{16DT}}$ X may be given in any unit of length, and T in any unit of time.

Z may be made equal to X by making $DT = \frac{\pi}{16}$. Where a solution is possible an equation is then obtained:

$$\frac{\pi}{8D}\left(\frac{\partial c}{\partial T}\right)_{z=x} = Z\frac{dC}{dZ}$$

$Z\frac{dC}{dZ}$ may be plotted for the carburizing and

C-Z Curves	Equations	$Z\frac{dc}{dz}$ Interpretation	Curve
Carb. D_e	$Z = 0.9(1 - C) - 0.05 \text{ Log}_e C$	Equals $\frac{\pi}{8D}\left(\frac{\partial c}{\partial t}\right)_{z=x}$ at D_1 point only	*A*
Carb. D_1	$Z = 0.5(1 - C) - .25 \text{ Log}_e C$	Equals $\frac{\pi}{8D}\left(\frac{\partial c}{\partial t}\right)_{z=x}$	*B*
Decarb. D_e	$Z = -0.5 \text{ Log}_e C$ $Z = -0.5 \text{ Log}_e C$	Equals $\frac{\pi}{8D}\left(\frac{\partial c}{\partial t}\right)_{z=x}$ at D_1 point only	*E*
Decarb. D_1	$Z = 0.5C - .25 \text{ Log}_e C$	Equals $\frac{\pi}{8D}\left(\frac{\partial c}{\partial t}\right)_{z=x}$	*F*

decarburizing curves, the plot being given against *C*. *C* is the only variable having *D* values in common to all curves.

A and *E* may not be interpreted in terms of $\frac{\partial c}{\partial t}$ because if *T* is constant, *Z* is not equal to *x* since *D* varies with *C*. Since $D_e = D_1$ at the D_1 point of concentration, the equation in $\frac{\partial c}{\partial t}$ is correct at this *C* value. Since D_1 is single valued, the transformation is correct for *B* and *F*.

Fig 13 gives the plots for $Z\frac{dc}{dz}$ vs. *C* for the four curves. The D_1 points of concentration are shown on the plot, both as derived in the text, and as given by the Matano derivation. The inadequacy of the Matano derivation as a solution for D_e is apparent

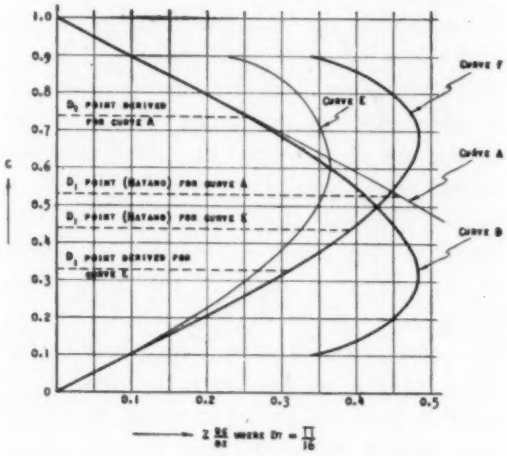

FIG 13—$Z\frac{dc}{dz}$ VS. *C* FOR FOUR CURVES.

Equation *A*			*C*	Equations *B* and *F*			*C*	Equation *E*		
Z	$\frac{dc}{dz}$	$Z\frac{dc}{dz}$		*Z*	$\frac{dc}{dz}$	$Z\frac{dc}{dz}$		*Z*	$\frac{dc}{dz}$	$Z\frac{dc}{dz}$
0.0000	1.053	0.0000	1.0	0.0000	1.273	0.0000	0.0	0.0000	2.000	0.0000
0.0953	1.046	0.0996	0.9	0.0787	1.262	0.0994	0.1	0.0527	1.800	0.0949
0.1911	1.039	0.1986	0.8	0.1588	1.233	0.1957	0.2	0.1115	1.600	0.1789
0.2873	1.029	0.2961	0.7	0.2415	1.182	0.2854	0.3	0.1783	1.400	0.2496
0.3855	1.016	0.3917	0.6	0.3286	1.110	0.3647	0.4	0.2554	1.200	0.3065
0.4846	1.000	0.4846	0.5	0.4227	1.014	0.4287	0.5	0.3465	1.000	0.3465
0.5852	0.976	0.5709	0.4	0.5274	0.893	0.4712	0.6	0.4581	0.800	0.3665
0.6902	0.938	0.6471	0.3	0.6495	0.744	0.4833	0.7	0.6020	0.600	0.3612
0.8005	0.870	0.6960	0.2	0.8031	0.560	0.4498	0.8	0.8047	0.400	0.3219
0.9251	0.714	0.6607	0.1	1.0310	0.329	0.3393	0.9	1.1510	0.200	0.2301

From P. I. Tables

For additional discussion, see page 658.

Controlled Atmospheres from City Gas for the Heat-treatment of Steels

By Ivor Jenkins,* Member AIME

(New York Meeting, March 1947)

Processes employing controlled atmospheres in the heat-treatment of metals and alloys are now well established on an industrial scale, and the general principles involved and the advantages to be gained in the use of the technique have received considerable publicity over a period of years. During this time the greatest emphasis has been on the establishment of the process in industry, the main effort being devoted to development work on various types of atmospheres, their useful fields of application and the design of suitable heat-treatment furnaces in which they are to be used. The various types of controlled atmospheres are fairly well standardized, but there still remains a considerable field for the investigation of related problems, in connection with both the gas-generating equipment and the surface chemistry of the heat-treatment of metals, especially in complex controlled atmospheres. This paper describes certain investigations of this nature that were carried out in England up to 1939.

The development of processes employing controlled atmospheres has been associated to a very large extent with the heat-treatment of steels, both because of the major importance of steel in industry and the many diverse and difficult problems of surface chemistry involved when steels of such a wide range of composition are heated in the presence of active gases. Controlled atmospheres such as dissociated and burnt ammonia or charcoal gas are used in the heat-treatment of low-carbon and high-carbon steels, but from certain points of view a suitable atmosphere generated by the partial combustion of city gas is to be preferred.

Both the ammonia derivatives are comparatively expensive, and even if the burnt ammonia is regenerated, thereby reducing operating costs, the capital expenditure of the gas plant may make it prohibitive for the smaller type of furnace installation. Charcoal-gas generators are not without their operating difficulties, especially those associated with the quality of the charcoal, clinker formation and the removal of carbon dust from the generated gas. City gas has the advantage of being comparatively cheap and "on tap" in most if not all industrial centers.

The use of raw city gas as a protective atmosphere in the heat-treatment of steels has been described,[1] but it presents certain difficulties because of its complex composition and its explosive nature when mixed with air. These factors, together with the tendency toward sooting at elevated temperatures, arising mainly from the hydrocarbon gases present, all militate against its use as a protective atmosphere in industrial furnaces. The following analysis, based on the analyses of city gas in different localities in Great Britain, indicates the wide limits existing

Manuscript received at the office of the Institute Nov. 27, 1945; revised July 24, 1946. Issued as T.P. 2121 in Metals Technology, January 1947.

* Research Metallurgist, General Electric Co., Ltd., Wembley, England.

[1] References are at the end of the paper.

in the concentrations of the various constituents:

Constituent	Per Cent
Carbon dioxide	2.0– 5.6
Carbon monoxide	6.1–16.6
Methane	15.0–27.5
Hydrogen	39.2–57.8
Oxygen	0.5– 1.5
Unsaturated hydrocarbons	1.7– 3.5
Nitrogen	6.5–13.5

Processes[2,3] have been developed using flue gases from gas-fired muffle furnaces, sometimes enriched with the raw fuel gas, in order to prevent oxidation and other undesirable gas-metal reactions during heat-treatment, but whereas the technique has met with some success in the nonferrous field, control over the composition of the final atmosphere does not appear to be adequate for the heat-treatment of steels.

It is, however, practicable and much more economical to burn city gas with a volume of air less than that required for complete combustion; and with a suitable design of combustion chamber, it is possible to ensure that the burnt products are not only nonexplosive but still retain some of the original reducing gases, such as carbon monoxide and hydrogen, while being free from oxygen and, if necessary, hydrocarbon gases. The combustion products will also contain, as generated, carbon dioxide, water vapor, nitrogen and sulphurous gases, the latter originating from the organic sulphur compounds present in the raw gas.

The bright annealing of low-carbon steel in such a complex atmosphere involves a careful consideration of the physical chemistry of gas-metal reactions in order to ensure that at no stage during the heat-treatment will oxidation of the iron take place. Furthermore, it is necessary to consider the catalytic activity of the iron for certain reactions between gases, and the effect of such activity upon the final surface condition of the heat-treated steel. With high-carbon steels there is the added complication of the reactivity of the carbon with the furnace atmosphere and the need for maintaining the surface carbon content of the steel if the required properties are to be fully developed.

Irrespective of what further processing the burnt city gas atmosphere may receive after it has been generated and before it finally enters the furnace chamber, it is most important, therefore, that the factors influencing the composition of the generated gas should be fully appreciated. This paper discusses the design of the gas-generating equipment and describes an experimental investigation of the factors influencing the composition of the generated gas, and of certain problems arising from the use of the atmosphere for the heat-treatment of low-carbon and high-carbon steels.

Theoretical Considerations

GAS GENERATION

When city gas is burned with air the main combustion reactions are the following:

$$H_2 + \tfrac{1}{2}O_2 = H_2O + 57.5\ K\ \text{cal} \quad [1]$$
$$CO + \tfrac{1}{2}O_2 = CO_2 + 67.7\ K\ \text{cal} \quad [2]$$
$$CH_4 + \tfrac{3}{2}O_2 = CO + 2H_2O + 143.1\ K\ \text{cal} \quad [3]$$
$$CH_4 + 2O_2 = CO_2 + 2H_2O + 210.8\ K\ \text{cal} \quad [4]$$
$$C_nH_m + O_2 = CO_2 + H_2O. \quad [5]$$

Complete combustion requires a volume of air approximately four to five times that of the raw gas, depending on the composition of the latter, but for the bright heat-treatment of steel, partial combustion only is required, the combustion products retaining certain percentages of reducing gases, which are insufficient, however, to give rise to explosion risks in the heat-treatment furnace.

For bright heat-treatment work it is essential that the generated gas should not contain any free oxygen. Thus, for example, less than 0.1 pct of free oxygen

in an otherwise reducing atmosphere is sufficient to give rise to pronounced roughening of a mild-steel surface on annealing, owing to alternate oxidation and reduction. If the steel is cooled in a flow of such an atmosphere, an oxidized surface is obtained, since iron oxides that form above 150°C are not readily reduced below 300°C (Fig 1).

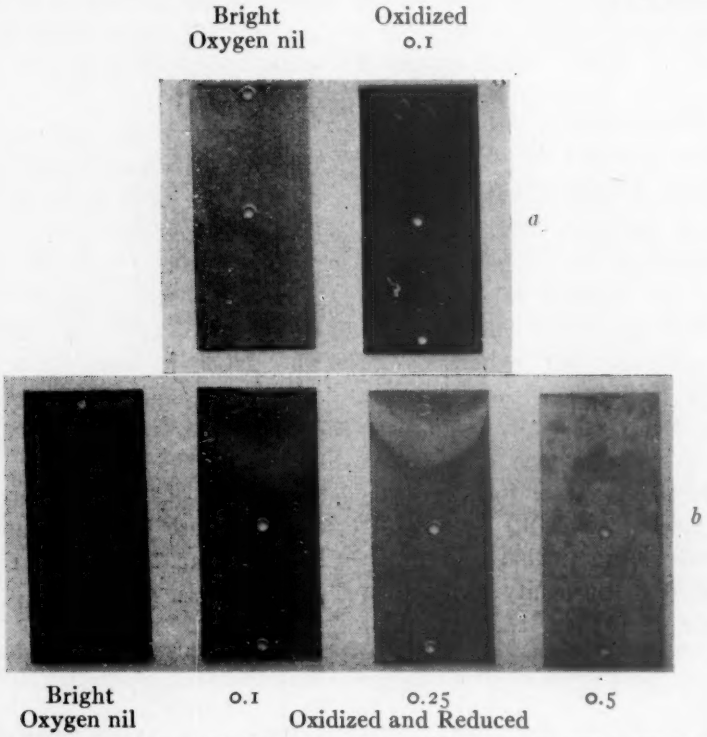

FIG 1—BRIGHT ANNEALING OF LOW-CARBON STEEL. EFFECT OF FREE OXYGEN IN FURNACE ATMOSPHERE.

Specimens treated for 10 minutes at 700°C before cooling. Basic Furnace Atmosphere: 4.0 pct CO_2; 9.7 CO; 15.2 H_2; 71.1 N_2.

a. Cooled in flow of gas.

b. Cooled under positive pressure of gas.

Percentage of oxygen in atmosphere is noted above or below each specimen.

Unsaturated hydrocarbons present in raw city gas are unstable at temperatures above approximately 500°C, and dissociate in the combustion chamber of the generator with the deposition of soot or coke to an extent dependent, among other factors, upon the temperature and the amount of oxygen introduced for combustion. It is important that unsaturated hydrocarbons should not be present in the final products of combustion, as they give rise to sooting, both of the steel charge and of the interior of the furnace. The latter may result in short circuits in electric furnaces, and disintegration of refractory furnace linings. High percentages of methane in the burnt city gas may give rise to similar trouble, although in this instance it is possible to ensure chemical stability of the hydrocarbon by maintaining a hydrogen concentration at, or in excess of, the equilibrium value relative to that of the methane.

Apart from the primary combustion reactions, however, various side reactions may take place in the generator between the active constituents of the partially burnt gas, to an extent determined by their relative concentrations and the tem-

perature. The reactions that may take place include:

$$CO_2 + H_2 \rightleftarrows CO + H_2O - 10.2\ K \text{ cal} \quad [6]$$
$$CO_2 + C \rightleftarrows 2CO - 41.3\ K \text{ cal} \quad [7]$$
$$H_2O + C \rightleftarrows CO + H_2 - 31.1\ K \text{ cal} \quad [8]$$
$$CH_4 \rightleftarrows C + 2H_2 - 19.1\ K \text{ cal} \quad [9]$$
$$H_2O + CH_4 \rightleftarrows CO + 3H_2 - 50.2\ K \text{ cal} \quad [10]$$
$$CO_2 + CH_4 \rightleftarrows 2CO + 2H_2 - 60.4\ K \text{ cal} \quad [11]$$

The variation with temperature of the equilibrium constants for these reactions, from the data of Austin and Day,[4] are given in Table 1.

TABLE 1.—*Equilibrium Constants for Inter-gas Reactions*[a]

Temperature, Deg C	K_6 $\frac{P_{CO_2} \cdot P_{H_2}}{P_{CO} \cdot P_{H_2O}}$	K_7 $\frac{P^2CO}{P_{CO_2}}$	K_8 $\frac{P_{CO} \cdot P_{H_2}}{P_{H_2O}}$	K_9 $\frac{P^2H_2}{P_{CH_4}}$	K_{10} $\frac{P_{CO} \cdot P^3H_2}{P_{H_2O} \cdot P_{CH_4}}$	K_{11} $\frac{P^2CO \cdot P^2H_2}{P_{CO_2} \cdot P_{CH_4}}$
400	12.3	9×10^{-5}	1.11×10^{-2}	5.66×10^{-2}	6.26×10^{-5}	5.09×10^{-6}
500	4.88	4.7×10^{-3}	2.3×10^{-2}	0.422	9.68×10^{-3}	1.98×10^{-3}
600	2.55	0.096	0.245	2.09	0.512	0.201
700	1.56	1.06	1.65	7.16	11.8	7.59
800	1.05	7.48	7.85	20.1	157.9	150.3
900	0.765	37.76	28.9	48.3	1,394	1,824
1000	0.589	146.5	86.3	102.4	8,837	1.50×10^4
1100	0.474	463.4	219.7	192.0	4.22×10^4	8.90×10^4
1200	0.395	1,244	487.4	335.0	1.63×10^5	4.13×10^5
1300	0.339	2,951	1,005	547.0	5.47×10^5	1.62×10^6

Reactions:
$CO + H_2O \rightleftarrows CO_2 + H_2$ [6]
$C + CO_2 \rightleftarrows 2CO$ [7]
$C + H_2O \rightleftarrows CO + H_2$ [8]
$CH_4 \rightleftarrows C + 2H_2$ [9]
$H_2O + CH_4 \rightleftarrows CO + 3H_2$ [10]
$CO_2 + CH_4 \rightleftarrows 2CO + 2H_2$ [11]

[a] From Austin and Day.[4]

With increasing temperature the reactions will tend to proceed from left to right, but in a complex mixture of the gases, all the reactions are interdepenednt, and this will influence the extent to which any one of the reactions will proceed to equilibrium. Thus, in a city gas burner the final composition of the products of combustion, from a given ratio of air to gas, is determined by the temperature of the combustion chamber, the time for which the gases are in the chamber and the possible catalytic effect upon the inter-gas reactions of any materials in the combustion chamber.

The extent to which the reactions proceed in the generator determines to what extent they may be promoted in the heat-treatment furnace by the metal charge, either catalytically or by direct reaction. This is of especial importance in the heat-treatment of steel, not only from the point of view of possible oxidation of the iron but also because of the catalytic activity of iron toward most inter-gas reactions and the effect upon the carbon content due to direct reaction with carburizing or decarburizing gases.

OXIDATION OF IRON

Iron reacts with carbon dioxide and water vapor according to the following reactions:

$$Fe + CO_2 \rightleftarrows FeO + CO$$
$$\text{Equilibrium constant } \frac{P_{CO_2}}{P_{CO}} \quad [12]$$
$$Fe + H_2O \rightleftarrows FeO + H_2$$
$$\text{Equilibrium constant } \frac{P_{H_2O}}{P_{H_2}} \quad [13]$$

Both of these reactions have been discussed frequently and very fully in previous publications.[4,5] Suffice it to say that the reactions are reversible at all temperatures above approximately 300°C, and in accordance with the laws of physical chemistry, for any one reaction the con-

centration ratios shown must equal a certain constant, the value for which varies with temperature, if the reaction is to be in equilibrium (Table 2). The equilibrium conditions are essentially independent of the carbon content of the iron, although iron activity does change slightly with carbon concentration.[11]

Excess of hydrogen or carbon monoxide, with respect to these equations, will promote the reduction of iron oxide, and this is the basis of industrial processes for the scale-reduction of hot-rolled steel strip. For the bright annealing or normalizing of steel in partially burnt city gas, the combustion of the raw gas is controlled so that the concentrations of carbon monoxide and hydrogen are on the reducing side of equilibrium at the maximum heat-treating temperature. The equilibrium concentration of water vapor with respect to hydrogen, however, decreases with decreasing temperature and precautions must be taken to prevent oxidation during cooling. In continuous furnaces the rate of cooling of the steel is usually sufficiently rapid to prevent oxidation, but in batch-type furnaces cooling under a pressure, rather than in a flow of gas, is advisable. Drying the controlled atmosphere may be insufficient to prevent oxidation during cooling in a flow of gas because of the possible formation of water vapor in the annealing chamber by side reactions.

TABLE 2.—*Equilibrium Constants for Gas-metal Reactions*[a]

Temperature, Deg C	K_{12}	K_{13}
	$\frac{P_{CO}}{P_{CO_2}}$	$\frac{P_{H_2}}{P_{H_2O}}$
400	0.74	9.12
500	0.96	4.68
600	1.17	2.99
700	1.53	2.38
800	1.90	2.00
900	2.24	1.72
1000	2.57	1.51
1100	2.88	1.37
1200	3.21	1.26
1300	3.49	1.18

Reactions:

$Fe + CO_2 \rightleftarrows FeO + CO$ [12]

$Fe + H_2O \rightleftarrows FeO + H_2$ [13]

[a] From Austin and Day.[4]

CARBURIZING-DECARBURIZING REACTIONS

The main reactions involving carbon may be listed as follows:

$$C + CO_2 \rightleftarrows 2CO \qquad \text{Equilibrium constant } \frac{P^2_{CO}}{P_C \cdot P_{CO_2}} \qquad [7]$$

$$C + H_2O \rightleftarrows CO + H_2 \qquad \text{Equilibrium constant } \frac{P_{CO} \cdot P_{H_2}}{P_C \cdot P_{H_2O}} \qquad [8]$$

$$C + 2H_2 \rightleftarrows CH_4 \qquad \text{Equilibrium constant } \frac{P_{CH_4}}{P_C \cdot P^2_{H_2}} \qquad [9]$$

In the equilibrium ratios listed above, the factor P_C represents the activity of the carbon and is dependent upon the form in which the carbon exists. Thus, for equilibrium with respect to graphite, the activity is taken as unity; for iron carbide the value is slightly greater than unity. In other words, graphite is stable with respect to cementite, at least within the temperature range 650° to 1100°C.[6,7] The data given in Table 1 for the reactions 7 to 9 are with respect to graphite. For steels which, at any temperature, are not saturated with carbon, the activity function P_C varies from zero to that for iron carbide, depending upon the concentration of carbon in solution in the iron, and, in turn, the composition of the atmosphere in equilibrium with the steel is determined by the carbon content. This is illustrated for reactions 7 and 9 in the diagrams in Fig 2, from a paper by Austin and Day.[4] The lower the carbon content of the steel, the lower must be the concentrations of carburizing gases relative to the decarburants for equilibrium. Further, the carburizing-decarburizing reactions are confined to the surface

of the steel and involve solely the carbon in solution, any free cementite that is present having no effect other than that of solution in the iron to replace any carbon removed at the surface. Since the solubility of carbon in iron is a function of the temperature, the susceptibility of a steel to changes in carbon content due to surface reactions increases with temperature, and control over the composition of the furnace atmosphere becomes much more critical.

Reported investigations on the decarburization of carbon steels by pure hydrogen are not concordant,[8,9] but from the work of Austin[10] and the author's own experiments there appears to be little doubt that the gas is decarburizing to carbon steels above 800°C, as the micrographs in Fig 3 show. For work below this temperature and for comparatively short times of treatment, pure hydrogen or hydrogen-nitrogen atmospheres are acceptable for industrial practice, provided that the purity of the atmosphere is maintained in the furnace chamber. Water vapor, however, increases considerably the decarburizing power of otherwise pure hydrogen (Fig 4) and Austin[10] has reported on the marked decarburization of hypereutectoid steels in wet hydrogen at temperatures as low as 700°C. From this point of view, small concentrations of carbon dioxide can be equally dangerous. The cleanliness of the heat-treatment container for use with pure hydrogen is most important, in that adsorbed films of decarburizing gases and direct reduction of the oxidized surface of the container can give rise to decarburizing conditions (Fig 4).

In order to counter decarburizing reactions that may be promoted in the furnace chamber, it is advisable to use a controlled atmosphere containing one or more carburizing gases such as methane or carbon monoxide. Synthetic atmospheres of this type have been very thoroughly studied by Slowter and Gonser,[12] and similar investigations on atmospheres

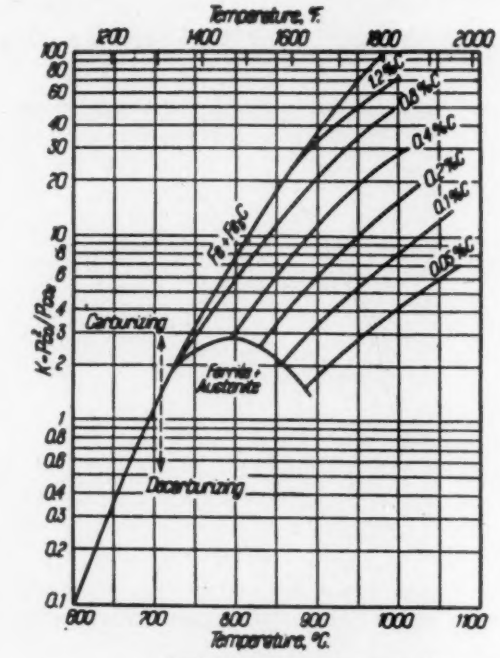

Equilibrium Constant for the Reaction $Fe_3C + CO_2 = 3Fe + 2CO$, as a Function of Temperature and Carbon Content.

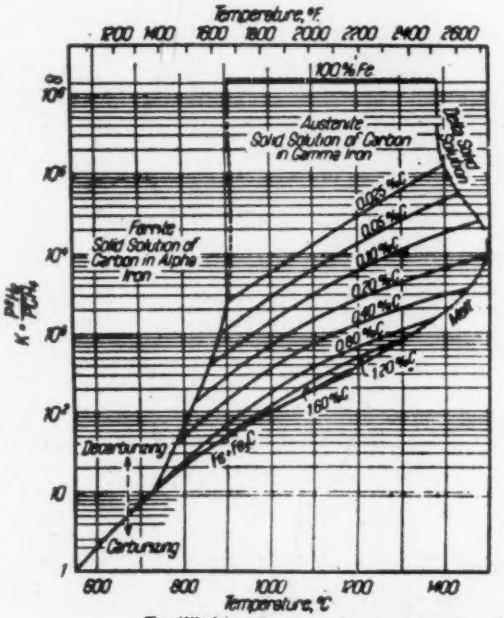

Equilibrium Constant for the Reaction $3Fe + CH_4 = Fe_3C + 2H_2$, as a Function of Temperature and Carbon Content.

FIG 2—EQUILIBRIUM CONSTANTS AS FUNCTIONS OF TEMPERATURE AND CARBON CONTENT (*Austin and Day*).

derived from charcoal and from hydrocarbon gases have been described.[13,14] Partially burnt city gas is a complex mixture of both carburizing and decarburizing action of carbon dioxide according to reaction 7. Similarly, if the carbon dioxide content is reduced to a sufficiently low level, carburization by carbon monoxide

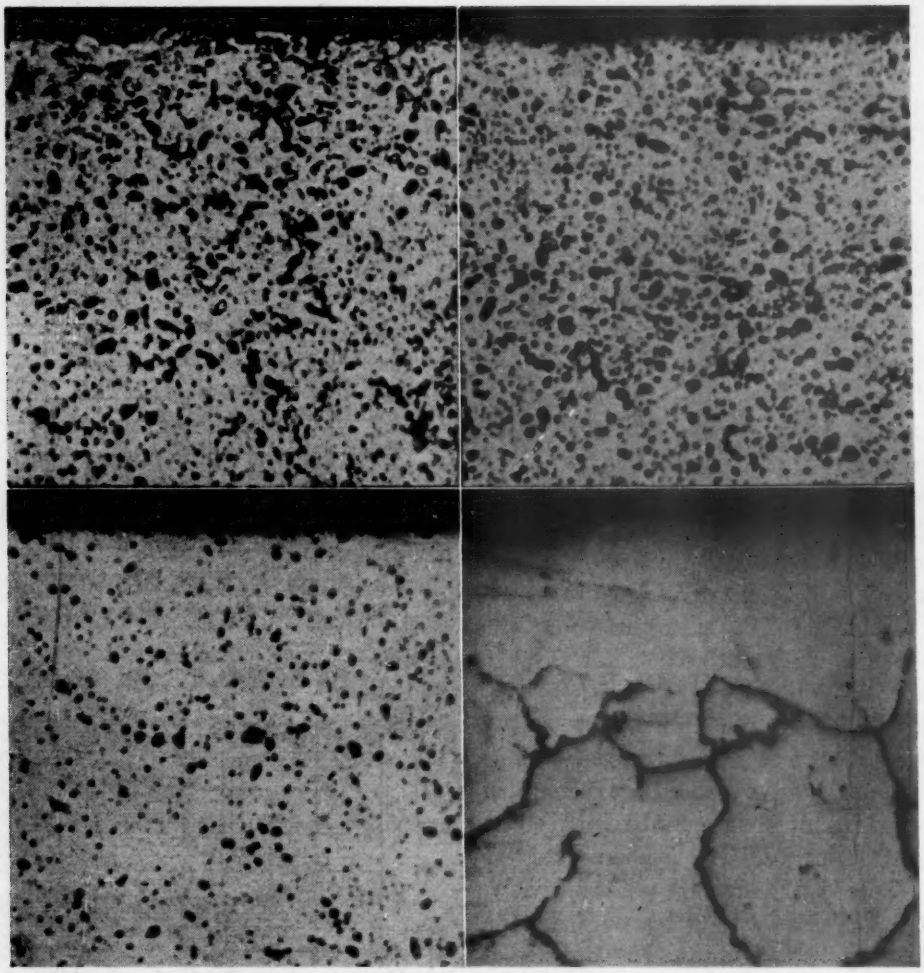

FIG 3—DECARBURIZATION OF 1.2 PER CENT CARBON STEEL IN PURE HYDROGEN (HYDROGEN MAINTAINED BRIGHT A CHROMIUM TEST PIECE). × 500, PICRATE ETCH.

a. As received.
b. 700°C for 5 hours. No change.
c. 800°C for 5 hours. Slight surface decarburization.
d. 900°C for 5 hours. Showing hypereutectoid cementite as a grain-boundary network, not extending to the surface.

gases, diluted with nitrogen. Water vapor can be efficiently removed by commercial drying agents to a very low dew point, and thereby carburization of the iron is promoted by reaction 8, although this may be countered by the decarburizing is promoted, which, in turn, can be neutralized by water vapor. Thus, by the complete removal of one of the active decarburizing gases and the control over the concentration of the other with respect to the carbon monoxide and

0.98 pct carbon steel annealed at 750°C 1 hr in quartz tube

0.5 pct carbon steel annealed at 760°C 2 hr in heat-resisting pot

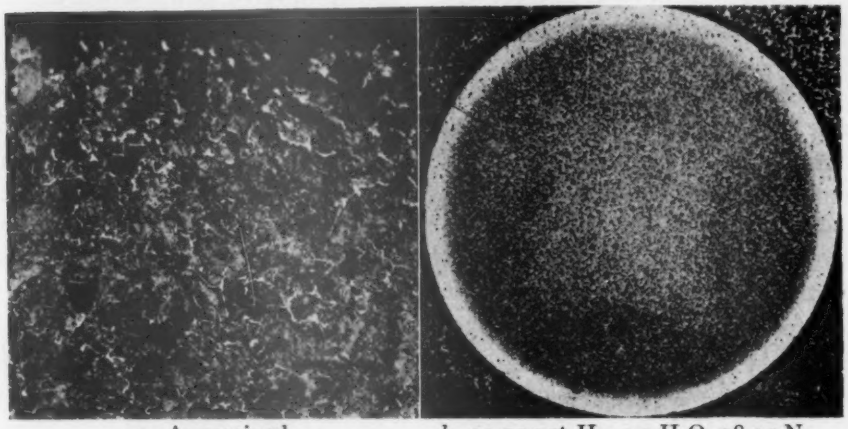

a. As received.

b. 19.75 pct H_2, 2.3 H_2O, 78.95 N_2.

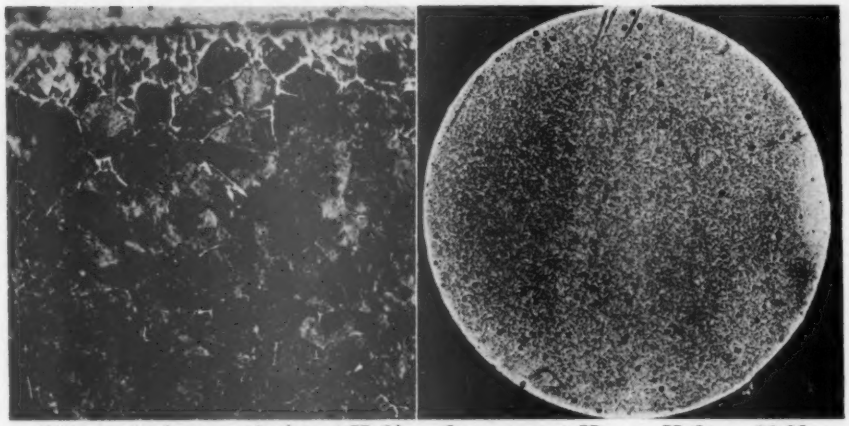

c. Wet cracked ammonia (2 pct H_2O).

d. 20.12 pct H_2, 0.0 H_2O, 79.88 N_2.

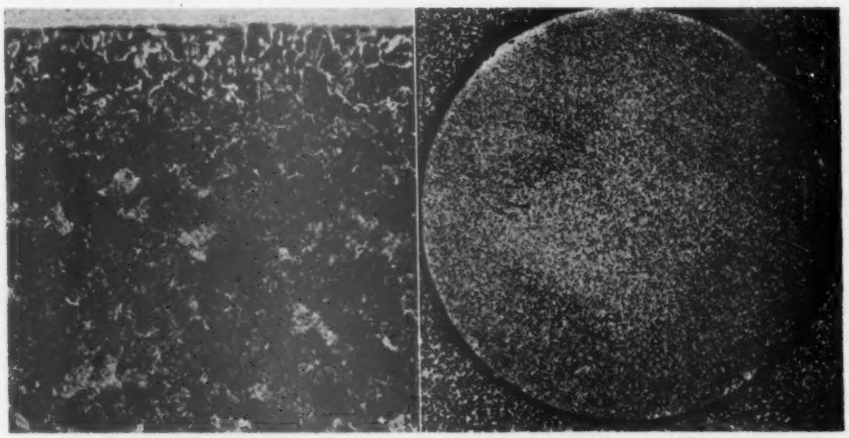

e. Dry cracked ammonia.

f. 20.12 pct H_2, 0.0 H_2O, 79.88 N_2. Annealing container preheated at 900°C in dry hydrogen.

× 100 × 10

FIG 4—DECARBURIZATION OF CARBON STEELS ETCHED IN 2 PER CENT NITAL.

hydrogen contents, an atmosphere could be generated that would be in equilibrium with a carbon steel at any particular temperature.

The question of carburization of low-carbon steel during annealing or normalizing in partly burnt city gas is not a serious problem. In fact, the composition of the the atmosphere normally used is decarburizing to steels of less than about 0.1 pct carbon at all temperatures above 750°C, but even so, the over-all effect is very small.

INTER-GAS REACTIONS

Of the reactions that may take place between the constituent gases of partly burnt city gas on heating, two in particular are of some importance—the so-called "producer-gas" and "water-gas" reactions—since both are catalyzed by a steel surface.

Producer-gas reaction:

$$CO_2 + C \rightleftarrows 2CO \qquad [7]$$

Water-gas reaction:

$$CO_2 + H_2 \rightleftarrows CO + H_2O \qquad [6]$$

In reaction 7 the carbon is solid carbon.

During the annealing of steel in a burnt fuel gas, if the active gases are not in equilibrium with one another, especially at the annealing temperature, as well as being on the reducing side with respect to iron, roughening of the steel surface will occur. Marshall[15] appears to have been the first and only investigator of this phenomenon, and concluded that the roughening is due to the catalytic activity of the iron in promoting reactions in the gas phase. The producer-gas and water-gas reactions were considered to be the primary reactions involved. The investigation was confined to annealing temperatures near to 650°C and indicated the severity of the roughening of the steel surface over a wide range of atmosphere compositions on either side of equilibrium for the two reactions. The atmospheres used by Marshall differ in general composition from those generated in Great Britain by the partial combustion of city gas, while the annealing temperatures used in the steel strip and steel sheet industries may be of the order of 700°C or more. Gas etching has been studied therefore with particular reference to burnt city gas atmospheres and annealing and normalizing temperatures typical of those used in Great Britain.

Generation of Partially Burnt City Gas

DESIGN OF GAS GENERATOR

Descriptions of various types of generators for producing controlled atmospheres by the combustion of city gas or similar hydrocarbon-containing gases have been published,[16,17] but details of the construction of these units have not been very fully described.

A generator or burner, of which a typical arrangement is shown in Fig 5, embodies the following essential features:

1. The accurate control of the volume of air and city gas supplied for the combustion, and consequently of the air-gas ratio employed.
2. A combustion chamber designed to maintain its temperature within the desired limits.
3. Cooling towers and condensers for removing the excess of water vapor formed during the combustion process.

Supply of Air and City Gas

The method employed for close control of the volumes and the ratio of air and city gas supplied for combustion normally depends upon the rated capacity of the generator. For comparatively small units, delivering up to 350 cu ft per hour of the burnt gas, the air and gas mixture may be fed to the combustion chamber by means of a small rotary blower. Most types are fitted with automatic lubricating devices and a loaded relief valve, which

operates in an emergency and permits the circulation of the air-gas mixture inside the blower. The rates of flow of the air and gas to the suction side of the blower are indicated on suitable orifice-type flowmeters, the rates of flow being controlled by needle valves set in the respective mains. The thorough mixing obtained in the blower avoids the necessity for a separate mixing vessel.

For generators of larger capacity, automatic gas-and-air-mixing apparatus may be used, in which the filtered air and city gas supplies, at atmospheric pressure, are drawn into a positive rotary sliding-vane compressor through a proportioning

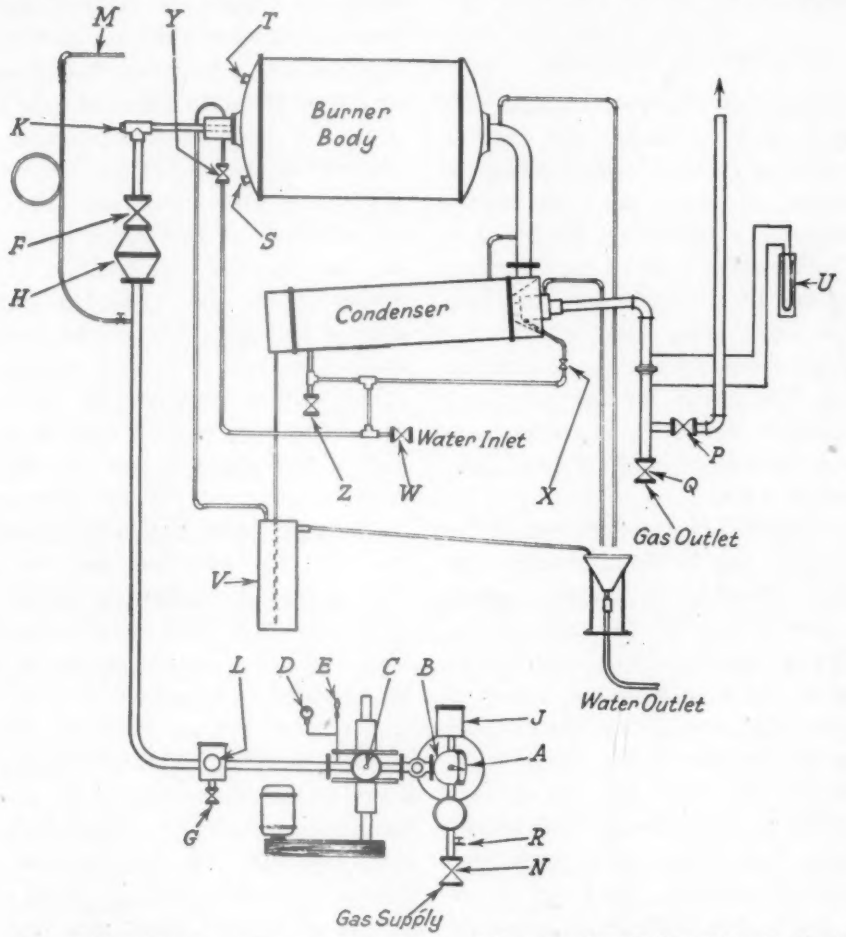

FIG 5—GENERATOR FOR BURNT CITY GAS. (*Courtesy The G.E.C. Ltd., England*)

A. Air-gas mixing control.
B. Automatic gas-air mixer.
C. Rotary compressor.
D. Pressure gauge 0-100 in., W.G.
E. Gas pilot flame.
F. Air-gas throttle valve.
G. Drain, oil trap.
H. Flame trap.
J. Air filter.
K. Burner sight glass.
L. Flame trap safety disk.
M. Gas poker.
N. Coal-gas supply valve.
P. Waste pipe valve (starting up).
Q. Isolating valve.
R. Air purge cock.
S. Sealing cap, igniter hole.
T. Starting-up vent.
U. Flowmeter.
V. Condenser sealing tank.
W. Water-inlet control valve—main.
X. Water-inlet control valve to condenser head.
Y. Water-inlet control valve to burner nozzle.
Z. Condenser drain valve.

valve that is operated by suction or back pressure created by the compressor. The combustion ratio is regulated by adjustment of the respective inlet ports at the valve.

Combustion Chamber

The combustion chamber consists of a brick-lined steel container, the internal dimensions of which are determined by the rated output of burnt gas. Combustion takes place at a nozzle or jet fitted in one of the insulated ends of the chamber, and two additional holes are provided, one for a sight glass and one for the insertion of a gas poker during the starting-up period. The outlet for the burnt gas at the opposite end of the chamber leads to cooling condensers and, if necessary, a purification train.

In all controlled-atmosphere generators of this type in use in Great Britain, the combustion chamber is heated solely by the combustion of the mixture of air and city gas from which the atmosphere is generated. There is, therefore, always a temperature gradient from the burner jet along the length of the chamber to the outlet for the burnt gas, the zone of maximum temperature being a few inches away from the source of combustion. During normal working, the input of air and city gas to the chamber is adjusted so that the zone of maximum temperature falls within a certain recommended range.

The design of the burner jet is of some importance, since the mixture for combustion should be supplied from it at a pressure and a line velocity more than sufficient to offset the rate of flame propagation. This will prevent "burning back" without at the same time promoting excessive back pressure or a concentrated flame, which leads to incomplete combustion of the oxygen and hydrocarbons in the mixture. A water-cooled nozzle reduces the danger, associated with the noncooled type, of an increase in the rate of flame propagation due to preheating of the air-gas mixture, and is to be preferred.

There are many burners for city gas using an empty or "nonpacked" combustion chamber that are giving satisfactory service in industry, usually operating at temperatures in excess of 1000°C. These units rely upon the completeness of combustion at the burner jet and contact of the burnt gases with the hot lining of the chamber to produce a burnt mixture of the required composition. In some generators of this type the burner jet gives a turbulent flow of the burnt gases around the wall of the hot chamber, while others utilize catalysts in the form of metal turnings, located near the discharge end of the chamber, for the removal of some sulphur and of the last traces of free oxygen from the burnt gases. Alternatively, the chamber may be packed with refractory material, about ½ to ¾-in. diameter, which provides hot surfaces over which the burnt gases pass and attain the required composition. A more ordered construction is one in which the combustion chamber is bricked up to within a few inches of the burner jet and of the burnt-gas outlet. This brickwork, which may or may not be continuous, has definite passages, usually molded holes, for the stream of burnt gas. Here again the hot refractory surfaces are relied upon to promote reactions between the gases and to remove the last traces of free oxygen and hydrocarbon gases.

A further development of this type of construction is the use of porous refractory for the internal brickwork, which is impregnated with metal catalysts for the promotion of gas reactions. The catalyst is prepared by soaking the porous bricks in a solution of a metal salt which is readily dissociated by heating, leaving behind the metallic oxide, which is reduced in pure hydrogen. In this way the bricks become impregnated with highly dis-

persed metal particles, which at temperature serve as active spots for inter-gas reactions. Metal catalysts used in this way include iron, nickel and copper

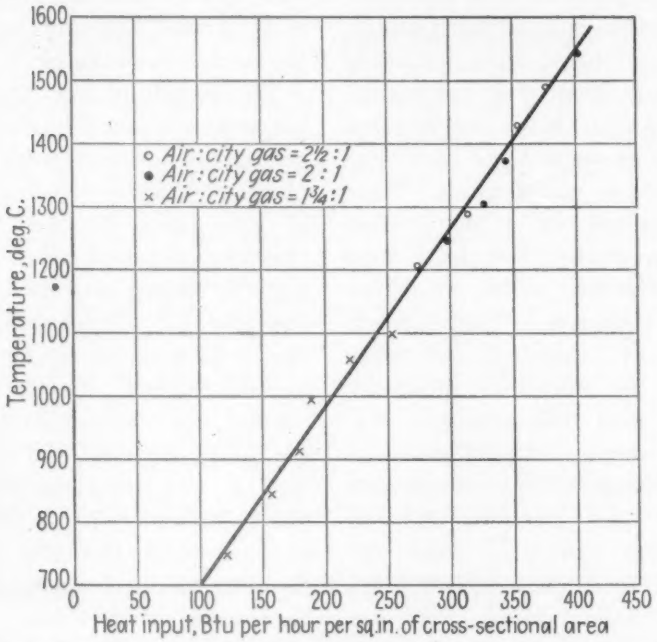

FIG 6—RELATIONSHIP BETWEEN HEAT INPUT AND MAXIMUM TEMPERATURE OF A GENERATOR FOR BURNT CITY GAS.

Dry Analysis of City Gas, Volume Per Cent

Carbon dioxide	2.8	Hydrogen	45.5
Illuminants	2.4	Methane	22.5
Oxygen	0.8	Nitrogen	13.5
Carbon monoxide	13.3	Calorific value	500 Btu per cu ft

with or without additions of rare earth oxides such as ceria and thoria. Copper is the catalyst usually employed for the removal of the final trace of free oxygen, and suitably impregnated bricks can be placed in the zone of the combustion chamber that operates between 600° and 800°C. Nickel and iron catalysts are more usually employed to promote inter-gas reactions among the main reactive constituents of the combustion products. The use of metal catalysts in the combustion chamber of a generator for burnt city gas, however, has a very limited application, mainly because of the very short effective life of the catalyst under continuous service conditions. Sulphur compounds in the combustion products poison the active points fairly rapidly, and with high gas velocities the loosely held metallic particles may be dislodged and carried away out of the combustion chamber. Metal catalysts, however, give a much longer and more satisfactory performance if used in an externally heated chamber through which the cooled, and preferably desulphurized, burnt gas is circulated.

The recommended maximum operating temperature for a burnt-fuel-gas generator is within the range 1100° to 1250°C, and it is possible to maintain this temperature condition for different fuel gases and combustion ratios, either by controlling the input of the air-gas mixture or by selecting a combustion chamber of suitable cross section. The latter would set a serious limitation on the standardization of gas-burner design, but fortunately the rated output of a generator is not critical

and covers a range sufficient to ensure that whatever the local conditions the maximum temperature of the combustion chamber falls within the aforementioned range. From this point of view the cross-sectional area of the chamber is important.

To obtain an approximate indication of the cross-sectional area of a combustion chamber for a particular application, data such as are shown in Fig 6 have been found to provide a useful guide. These data were obtained on a combustion chamber 9 in. square by 18 in. long, filled with ¼ in. refractory cubes to within 4 in. of the burner jet. Temperature measurements were taken ¼ in. below the surface of the refractory filling by four chromel-alumel thermocouples enclosed in silica sheaths, spaced at equal intervals along the diagonal of the section of the chamber. The total heat input to the chamber was calculated from the combustion ratio used, on the assumption that total combustion of the city gas required five volumes of air per volume of gas. Furthermore, the heat value plotted was obtained from the heat of total combustion at room temperature using oxygen, whereas the temperature readings were obtained for combustion with air. For comparative purposes, however, it is considered that the data shown in Fig 6 form a very useful basis of design.

Thus, for example, a generator is to be designed to burn 250 cu ft per hour of city gas (calorific value 500 Btu per cu ft) with 625 cu ft per hour of air (combustion ratio 2½:1). Assuming a ratio of 5:1 for complete combustion, the heat of combustion for this example is:

$$\frac{2.5}{5} \times 250 \times 500 = 62{,}500 \text{ Btu}$$

For a maximum generator temperature of 1200°C, it will be seen from Fig 6 that the equivalent heat input is 275 Btu per hr per sq in. and the required cross-sectional area of the combustion chamber is approximately 227 square inches.

Data such as these can be applied only when the combustion chamber under consideration has the same general design and thermal efficiency as that on which the data were obtained.

The length of the combustion is also important, in that if it is too short oxidation of the hydrocarbon gases may be incomplete, and sooting may occur in parts of the plant beyond the combustion chamber, especially between the latter and the cooling towers where temperature and metallic surface conditions promote the breakdown of the hydrocarbons. The over-all internal dimensions of the combustion chamber, making allowances for any filling material, should be planned so that at the maximum output from the plant (measured at normal temperature and pressure) the free volume of the chamber would be changed not more than once every 5 to 6 sec. In general the length of the packed-type of combustion chamber is less than that with no filling, since in the former type more intimate mixing of the combustion products inside the chamber is obtained, and a greater surface of hot refractory is available to promote the necessary reactions.

Cooling Towers

The cooling towers may be of the contact or the surface type, but the latter usually are preferred because of the danger of free oxygen being introduced into the burnt gases from direct contact with the cooling water. The surface cooler is of simple construction, comprising a series of thin-walled steel tubes contained in a cylindrical steel shell, the hot gases passing through the tubes counterflow to the cooling water on the outside. Steel tubes are used because of the presence of sulphurous gases in the combustion products. Provision is made for the automatic drainage of the condensate through an open

water seal on the cooler. Efficient cooling is necessary to prevent further condensation in pipe lines leading from the gas-generating equipment, and water spray carried over with the cooled gases is removed in towers packed with earthenware rings.

COMPOSITION OF BURNT CITY GAS

On any one installation, the factors that control the composition of the burnt city gas are the air-gas ratio used and the total flow of the mixture delivered to the combustion chamber. The latter factor will influence the operating temperature of the generator and the time that the burnt gases are in the combustion chamber.

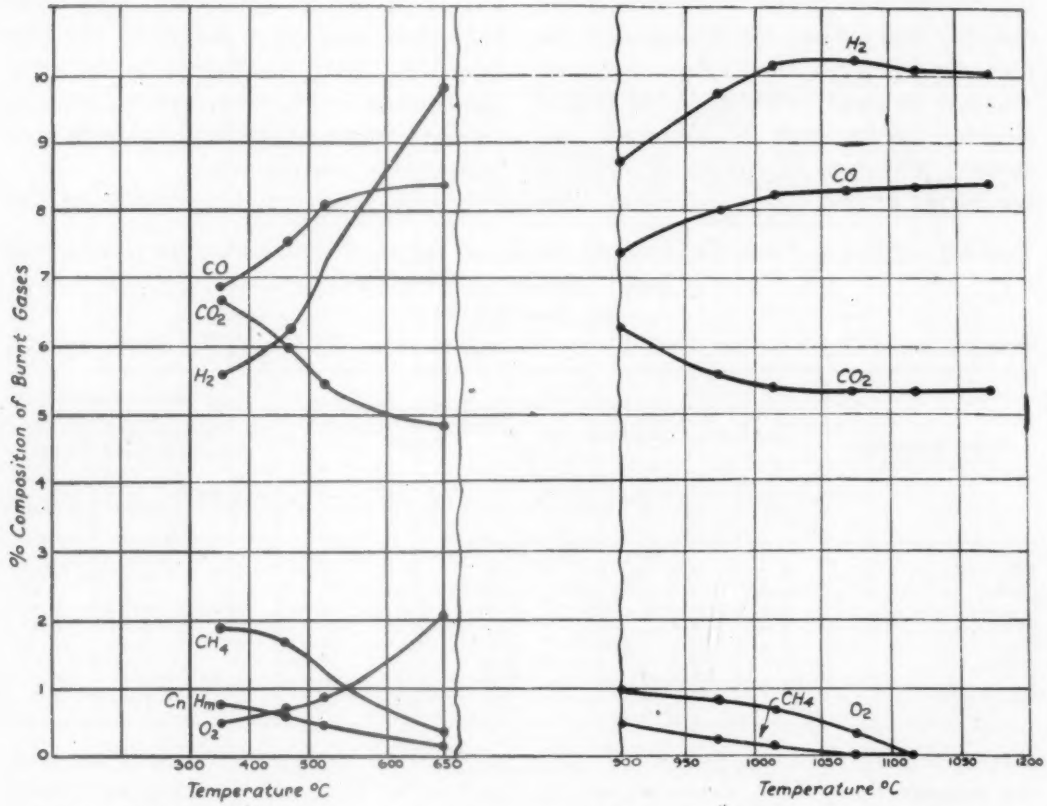

FIG 7—EFFECT OF MAXIMUM BURNER TEMPERATURE ON COMPOSITION OF BURNT CITY GAS (AIR: GAS = 3:1).

SAFETY DEVICES

A city-gas burner usually is fitted with safety devices to compensate for any failure of gas or electrical supplies. These devices include, for example, a flame trap in the air-gas supply line to the combustion chamber to protect the blower and other parts against a strike-back of the flame from the burner nozzle. Various magnetic valves are also available to close the mixture supply main if the blower fails because of an electrical shutdown, and pilot lights or alarm bells may be used to indicate the "seizing-up" of the blower.

EFFECT OF GENERATOR TEMPERATURE

Tour[18] has described the variation of the composition of burnt city gas with the temperature of the generator and with the ratio of air to city gas. Marshall[15] has supplied similar data on the effect of the air-gas ratio, but, unfortunately, like most other workers, he does not specify the generator temperature, so that the information loses some of its significance. The variation in composition

of the burnt gases with changes in the maximum temperature of a controlled-atmosphere unit of the packed type is shown in Fig 7. The combustion chamber in this instance was filled with refractory, and the flow of burnt gas was maintained approximately constant at 10 fpm (NTP); i.e., one volume change of the combustion chamber every 6 sec. As the temperature rose, the hydrogen and carbon monoxide contents increased while those of carbon dioxide, oxygen and hydrocarbons decreased. The lack of continuity between the curves at the higher and lower temperatures is in the main associated with the comparatively high concentration of free oxygen in the gas produced below 650°C.

Unsaturated hydrocarbons are unstable above 800°C. and pyrolyze into methane and hydrogen. The reaction is not chiefly a surface effect but takes place through the body of the gas, so that the removal of these hydrocarbons in any type of city-gas burner is not difficult, provided the operating temperature is above 700°C. However, even at 800°C, especially with combustion ratios of air to gas below 2:1, complete combustion of the unsaturated hydrocarbons may not be obtained and thermal decomposition, with heavy sooting, will occur. This will give rise to pressure difficulties and some soot may be carried over with the burnt gases into the cooling towers and the furnace. Operating temperatures as low as 800°C are not recommended, and a combustion ratio less than 2:1 may approach so near to the lower limit of inflammability of the particular air-gas mixture being used that there may be a danger of the heat generated being insufficient to maintain the combustion; i.e. the reaction between air and city gas may cease to be exothermic and become endothermic.

As the maximum temperature of the combustion chamber increases, the composition of the burnt gas changes because of the alteration in equilibria for the various inter-gas reactions and the increased velocity with which these reactions tend toward equilibrium. In the same way, combustion rates increase, with the result that the free oxygen in the burnt gases is more readily consumed and complete combustion of the total oxygen available is the more readily achieved. The presence of hot surfaces, either of refractory or metallic materials, on which these reactions may proceed, has a marked influence on the degree of equilibrium obtained. The decomposition of methane is mainly a surface phenomenon promoted by increasing temperature, and the gas

TABLE 3.—*Effect of Nickel Catalyst and Maximum Burner Temperature upon Composition of Burnt City Gas Cooled to* 20°C

Air: City Gas, 2.5:1

Composition of City Gas: 2.0 pct CO_2; 13.3 CO; 45.5 H_2; 22.5 CH_4; 2.4 C_nH_m; 0.8 O_2; 13.5 N_2

Gases Analyzed (Volume Pct)	No Refractory in Combustion Chamber			Combustion Chamber Filled with Alundum Bricks			Combustion Chamber Filled with Alundum Bricks Impregnated with Finely Divided Nickel		
	900°C	950°C	985°C	900°C	955°C	1000°C	905°C	960°C	1000°C
CO_2	5.7	5.6	5.2	5.8	5.6	5.45	5.9	5.7	5.5
C_nH_m	0.0	0.0	0.0	0.0	0.0	0.0	0.0	0.0	0.0
O_2	2.4	2.7	3.2	0.8	0.7	0.55	0.85	0.6	0.5
CO	7.8	8.1	8.4	7.9	8.1	8.7	8.6	8.8	9.0
H_2	9.4	9.7	10.1	9.9	10.2	10.3	10.3	10.5	11.0
CH_4	1.3	1.3	1.2	0.5	0.32	0.20	0.1	0.0	0.0
N_2	69.4	68.8	68.1	73.3	73.38	73.0	73.05	73.1	73.1
H_2O (vapor)	2.3	2.3	2.3	2.3	2.3	2.3	2.3	2.3	2.3

is more readily removed in packed than in empty combustion chambers (Table 3). The higher the generator temperature, the more complete is the removal, but too high a temperature is not recommended, especially at low combustion ratios of the order of 2:1, because of the formation of a hard coke resulting from methane decomposition. Continued deposition of the coke may give rise to excessive back pressures and stoppages inside the combustion chamber, especially if it is of the packed type. For normal operation, the temperature of the combustion chamber should be limited to the range of 1100° to 1250°C, which will ensure continued satisfactory operation.

Apart from the maximum temperature of the generator, the temperature along the length of the combustion chamber is of some importance. The reactions involving the combustion of the last traces of oxygen and methane require both time and a suitable high temperature, even in the presence of metal catalysts, to proceed to completion. The temperature gradient should be as small as possible and the combustion chamber must be designed accordingly to ensure that these conditions are obtained. The variation

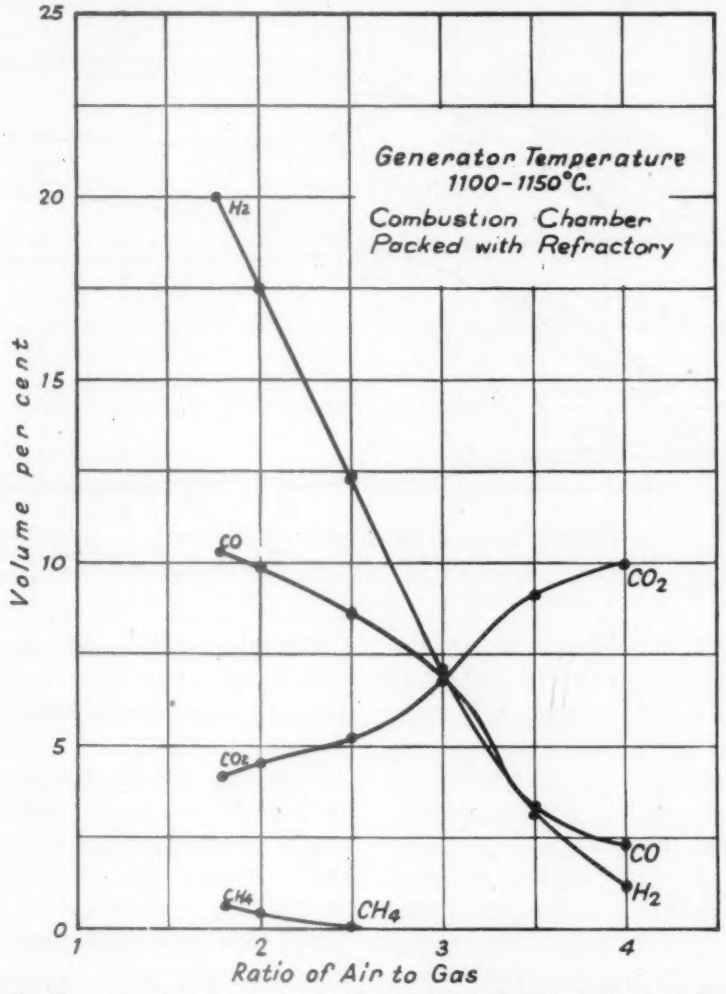

FIG 8—EFFECT OF COMBUSTION RATIO ON COMPOSITION OF BURNT CITY GAS.

in the calorific value of city gas in different localities gives rise to added difficulties in this connection. If the mixture of air and fuel gas is supplied to the combustion chamber at intervals along its length, the flexibility of the unit, both with respect to variation in output, combustion ratio, and the composition of the raw gas, is very much increased. The volume of the air-gas mixture supplied at any point is limited to that necessary to maintain that part of the combustion chamber within the specified temperature limits. Supply points are brought into service when necessary, starting with that farthest away from the burnt-gas outlet from the combustion chamber. Tour[18] has suggested a design incorporating the use of external heating by electricity, oil or gas in order to provide the required temperature in depth in the combustion chamber. This would seem to be an advance toward absolute control of the composition of the controlled atmosphere generated.

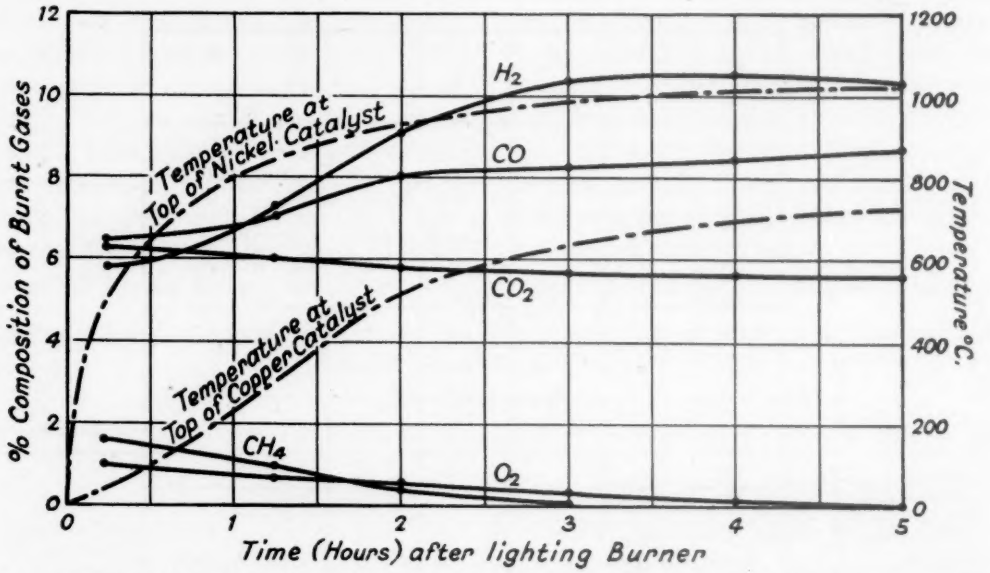

FIG 9—EFFECT OF BURNER TEMPERATURE ON COMPOSITION OF BURNT CITY GAS (AIR:GAS = 3:1). Nickel and copper catalysts in burner chamber.

EFFECT OF RATIO OF AIR TO CITY GAS

The variation in composition of the burnt city gas with different air-gas combustion ratios, at a maximum generator temperature of 1150°C, is shown in Fig 8. With the city gas used, no free hydrocarbons of any kind are detected by ordinary analytical methods above a combustion ratio of 2½:1. Free oxygen is entirely absent at combustion ratios above 1¾:1.

With city gas or coke-oven gas, it is not possible to operate a city-gas burner below an air-gas ratio of approximately 1¾:1. Richer gas mixtures than this are virtually noncombustible because they do not generate sufficient heat to maintain the temperature of the combustion chamber, and the reactions between the air and the city gas are predominantly endothermic in nature. Plants have been developed for the treatment of such mixtures over special catalysts maintained at temperature by a suitable furnace, the resulting atmosphere being used primarily in the heat-treatment of high-carbon steels. As far as the city-gas burner is concerned, however, the lower limit of the air-gas combustion ratio that is recommended is about 2:1.

Effect of Metal Catalysts

The part played by metal catalysts in promoting inter-gas reactions is shown in Fig 9, which gives the analysis of the burnt gases during the heating-up stage of a standard generator. In this particular unit the combustion chamber was packed with small refractory bricks, those nearest the burner jet and at the maximum temperature of the chamber being impregnated with nickel. Farther along the chamber was a copper-impregnated refractory zone, which at steady temperature conditions operated between 600° and 800°C. Comparison of Figs 7 and 9 indicates the influence of the catalysts upon the composition of the products of the combustion, especially at the lower temperatures.

Effect of Composition of City Gas

Table 4 gives the composition of controlled atmospheres that may be obtained from various city gases commercially available in different parts of Great Britain. For a given combustion ratio and generator temperature the variation in composition of the burnt gases is quite considerable, but the important point is that the active gases should be present in certain ratios determined by the particular application. However, the dependence of the composition of city gas upon the source of supply makes it difficult to forecast the composition of the burnt gases, even under standard conditions of ratios of air to city gas and of generator temperature.

PROCESSING PARTIALLY BURNT CITY GAS

Partially burnt city-gas, as generated, has a number of applications, including the bright annealing of low-carbon steel. In certain cases, however, it is necessary to remove one or more of the constituent gases which would promote undesirable reactions in the heat-treating furnace. Thus desulphurization (e.g., by activated carbon) is necessary if the atmosphere is to be used for the bright annealing of copper and of nickel alloys and when the furnace chamber has exposed electric resistors. Dry gas can be readily obtained by the use of commercial desiccants such as activated alumina or silica gel, and carbon dioxide can be removed completely by absorption in organic solvents, which are regenerated after use.[19,20] Alternatively, treatment of the burnt gas over charcoal at approximately 1000°C. results in the reduction of both the carbon dioxide and the water vapor to very low concentrations, according to reactions 7 and 8. Complete removal of these decarburizing gases, however, may not be desirable, and a simple means of reducing the concentration of carbon dioxide may be preferred.

Table 4.—*Composition of Controlled Atmospheres Obtainable from City Gas*
Generator Temperature, 1100° to 1200°C
Combustion Chamber Packed with Refractory

Composition of City Gas for Combustion, Pct						Air-City-gas Ratio	Composition of Cooled Burnt Gases, Pct			
CO_2	CO	H_2	CH_4	C_nH_m	O_2		CO_2	CO	H_2	CH_4
2.0	13.3	45.4	22.5	2.4	0.8	2:1	4.5	9.8	14.9	0.2
						2½:1	5.3	8.4	11.75	0.0
5.2	12.0	45.0	22.9	2.4	0.7	2¼:1	7.2	8.2	10.23	0.0
2.0	6.1	57.8	25.0	2.1	0.5	2½:1	4.5	8.9	15.7	0.3
4.8	6.0	46.2	23.8	2.0	0.5	2¼:1	6.7	8.6	12.5	0.2
5.6	16.5	48.5	20.0	2.1	0.5	2:1	7.0	8.2	9.8	0.0
2.0	7.5	49.5	27.5	3.5	0.5	2¼:1	5.8	8.6	11.9	0.2

Tour[21] has described the effect of reheating upon the composition of burnt fuel gas and the following describes a similar technique which has been developed in Great Britain.

The analyses of burnt city gas quoted in the foregoing do not include water vapor, the products of combustion usually being cooled to about room temperature in the condensers and the water-vapor content reduced to saturation at that temperature; i.e., about 2.5 to 3.0 pct water vapor. In the combustion chamber, however, the water-vapor concentration may be fairly high, and in propane combustion, for example, Tour[18] has calculated that the concentration may be as much as 18 pct. The hot gases in the combustion chamber approach a general state of equilibrium at the temperature of the chamber, and the removal of part of the water vapor by cooling and condensation upsets this equilibrium. Thus, if the cooled burnt city gas is reheated to a high temperature in the presence of hot refractory or metal catalysts, reactions among the constituent gases take place with the production of more water vapor, and, as Table 5 shows, the composition of the cooled burnt gas changes. The process may be repeated, water vapor being condensed after every reheating, until the dew point of the hot gases is below the temperature of the cooling water in the condenser (Table 6). The decrease in the volume of the carbon dioxide and of the hydrogen after reheating is very nearly equal to the volume increase of the carbon monoxide and water vapor (Tables 5 and 6) so that the main reaction taking place during reheating is the water-gas reaction:

$$CO_2 + H_2 \rightleftarrows CO + H_2O - 10.2\,Kcal \quad [6]$$

This principle has been proposed for use in the heat-treatment of medium and high-carbon steels.[22] In this way an atmosphere containing less than 1 pct of carbon dioxide and more than 20 pct of carbon monoxide can be produced and controlled to meet the conditions called for in the heat-treating furnace.

TABLE 5.—*Change in Composition of Burnt City Gas on Reheating*

Catalyst	Temperature, Deg C	Composition of Burnt Gases after Reheating, Pct				
		CO_2	CO	H_2	CH_4	H_2O
Refractory...	800	4.25	9.76	13.9	0.2	2.30
Iron.....		4.00	9.80	13.52	0.2	2.45
Nickel.....		3.78	10.20	13.20	0.15	2.87
Refractory...	900	4.05	9.80	13.82	0.2	2.51
Iron.....		3.45	10.70	12.95	0.15	3.10
Nickel.....		2.89	11.15	12.65	0.15	3.53
Refractory...	950	3.95	9.60	13.70	0.20	2.48
Iron.....		3.00	10.95	12.75	0.00	3.57
Nickel.....		2.20	11.75	11.75	0.00	4.16
Refractory...	1000	3.90	9.78	13.70	0.10	2.54
Iron.....		2.45	12.05	11.85	0.00	3.95
Nickel.....		1.76	12.35	11.57	0.00	4.58
Burnt city gas before reheating.....		4.35	9.75	13.91	0.05	2.3

TABLE 6.—*Change in Composition of Burnt City Gas on Repeated Reheating Over a Nickel Catalyst and Cooling to Water-vapor Saturation of 2.3 Per Cent*

Temperature, Deg C	Number of Reheats	Composition of Treated Gases, Vol Pct				
		CO_2	CO	H_2	CH_4	H_2O (Before Condensing)
800	1	3.70	10.35	13.05	0.18	2.88
	2	3.28	10.83	12.68	0.15	2.80
	3	2.90	11.15	12.30	0.10	2.68
900	1	2.95	11.10	12.70	0.12	3.44
	2	1.90	12.25	11.78	0.05	3.31
	3	1.35	12.78	11.25	0.05	2.79
1000	1	1.60	12.55	11.42	0.0	4.81
	2	0.86	13.40	10.65	0.0	3.05
	3	0.42	13.85	9.15	0.0	2.75

Bright Annealing of Low-carbon Steel

GAS ETCHING

The gas etching of low-carbon steel strip during annealing and normalizing in a controlled atmosphere of partially

burnt city gas has been investigated. The atmospheres used were typical of those employed on an industrial scale for the bright annealing of low-carbon steel and were generated in a city-gas burner of the "packed" type, similar to that already described. In all the experiments, the atmosphere used was that supplied at room temperature from the generator, except for the dried atmospheres, which were treated in a commercial drier over activated alumina.

Experimental Procedure

Specimens of a 0.15 pct carbon steel strip, measuring 2 by ⅞ by 0.036 in., were freely suspended in a quartz tube of 1¼ in. diameter, the central 10 in. of which was heated by a vertical-tube electric furnace thermostatically controlled to within ±3°C of the required temperature. The quartz tube extended on either side of the furnace by about 7 in. and was fitted at both ends with rubber stoppers, the lower carrying a gas-inlet tube of quartz and the upper a similar tube as a vent. The steel specimen was suspended through the gas vent on a fine wire of nickel-chromium alloy and the test temperature was indicated by means of a fine-wire chromel-alumel thermocouple attached to the specimen, which in every test was cleaned in acetone and dried in ether. Before test the specimen was suspended in the lower, unheated, portion of the quartz tube and the latter well purged with a high flow of the test atmosphere. The flow of the latter was then fixed at 50 liters per hour and the specimen was drawn quickly up into the furnace zone, where it was held for the necessary time at the required temperature and then lowered into the unheated zone and cooled under a positive pressure (i.e., no flow) of gas. The surfaces of specimens treated in this way were examined under the microscope.

Results

Series A

The preliminary experiments were carried out on bright cold-rolled steel strip at 700°, 800° and 900°C, the time at temperature in all cases being 5 hr. The compositions of the atmospheres used and micrographs of the treated surfaces are shown in Fig 10. The specimens at 700° and 800°C showed grain-boundary etching, slight pitting and a general roughening of the surface, especially at the higher temperature.

In both of these experiments, the carbon dioxide and water-vapor concentrations in the atmospheres used were on the reducing side of equilibrium at the test temperatures, but in the 900°C experiment, the atmosphere was oxidizing and produced a silver-gray surface, identified by X-ray analysis as ferrous oxide.

Table 7.—*Gas Etching of 0.15 Per Cent Carbon Steel in Various Burnt City Gas Atmospheres*

Temperature of Test, Deg C	Heat-treating Atmosphere, Volume Pct	Ratio $\frac{P^2CO}{PCO_2}$		Ratio $\frac{PCO \cdot PH_2O}{PCO_2 \cdot PH_2}$	
		In Ingoing Gas	At Equilibrium, with Graphite	In Ingoing Gas	At Equilibrium, Theoretical
700°C	2.5 CO_2; 14.8 CO; 28.2 H_2; 2.3 H_2O; 52.2 N_2	0.88	1.06	0.48	0.64
800°C	4.7 CO_2; 9.4 CO; 12.9 H_2; 2.3 H_2O; 70.7 N_2	0.19	7.48	0.355	0.95
900°C	6.0 CO_2; 7.3 CO; 9.8 H_2; 2.3 H_2O; 74.6 N_2	0.09	37.76	0.28	1.31

With regard to inter-gas reactions, however, and in particular the "water-gas" reaction 6 and the "producer-gas" reaction 7, the atmosphere used at 700°C, while almost satisfying equilibrium conditions for reaction 7 with respect to

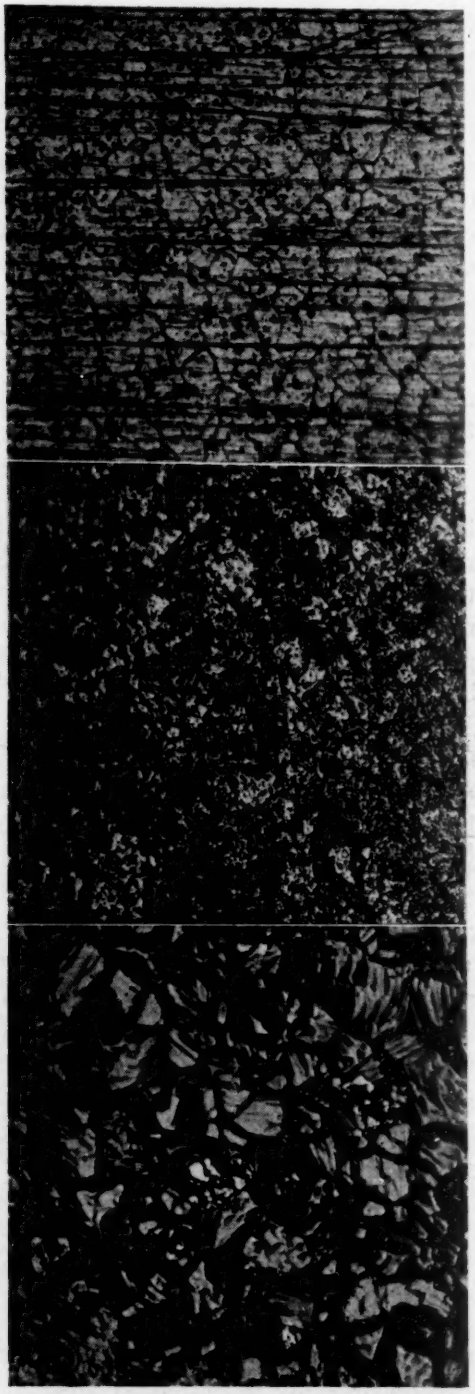

FIG 10—SURFACES OF 0.15 PER CENT CARBON STEEL AFTER ANNEALING FOR 5 HOURS IN BURNT CITY GAS ANALYZING AS SHOWN BELOW. × 200.

a. 700°C; 2.5 pct CO_2, 14.8 CO, 28.2 H_2, 2.3 H_2O.

b. 800°C; 4.7 pct CO_2, 9.4 CO, 12.9 H_2, 2.3 H_2O.

c. 900°C; 6.0 pct CO_2, 7.3 CO; 9.8 H_2, 2.3 H_2O.

graphite, was far removed from equilibrium with respect to reaction 6 (Table 7) and the etching obtained is attributed to the catalytic activity of the iron in promoting this reaction:

$$CO_2 + H_2 \rightleftarrows CO + H_2O \quad [6]$$
$$CO_2 + C \rightleftarrows 2CO \quad [7]$$

At 800°C, the atmosphere was unbalanced with respect to both reactions, and with the increased activity due to the higher temperature of test, the etching obtained was even more pronounced.

Series B

Further experiments were carried out on samples of cold-rolled steel strip containing 0.15 pct carbon, which were polished before test with 200-mesh magnesia on wet selvet cloth, followed by degreasing with acetone and drying in ether. The time of heating at the test temperatures of 720°, 820° and 920°C was up to one hour maximum, this being more representative of commercial practice. Details of the atmospheres used, and equilibrium data for the main reactions are given in Table 8, and Fig 11 shows micrographs of some of the steel surfaces after treatment. Reflectivity measurements were made on these surfaces, a freshly polished surface being taken as the standard of 100 pct reflectivity. The average results are given in Table 9.

In general the initial etching rate appeared to be slow, but increased considerably once the etching had commenced, and a period of one hour under the various test conditions was sufficient in all cases to destroy the original polished surface. At any one temperature the extent of etching increased with the degree of combustion of the city gas. However, in all the atmospheres used, and at every test temperature, the relative concentrations of carbon monoxide and carbon dioxide with respect to equilibrium with graphite (reaction 7) were on the high-dioxide side, and it is improbable that this reaction in itself accounted for

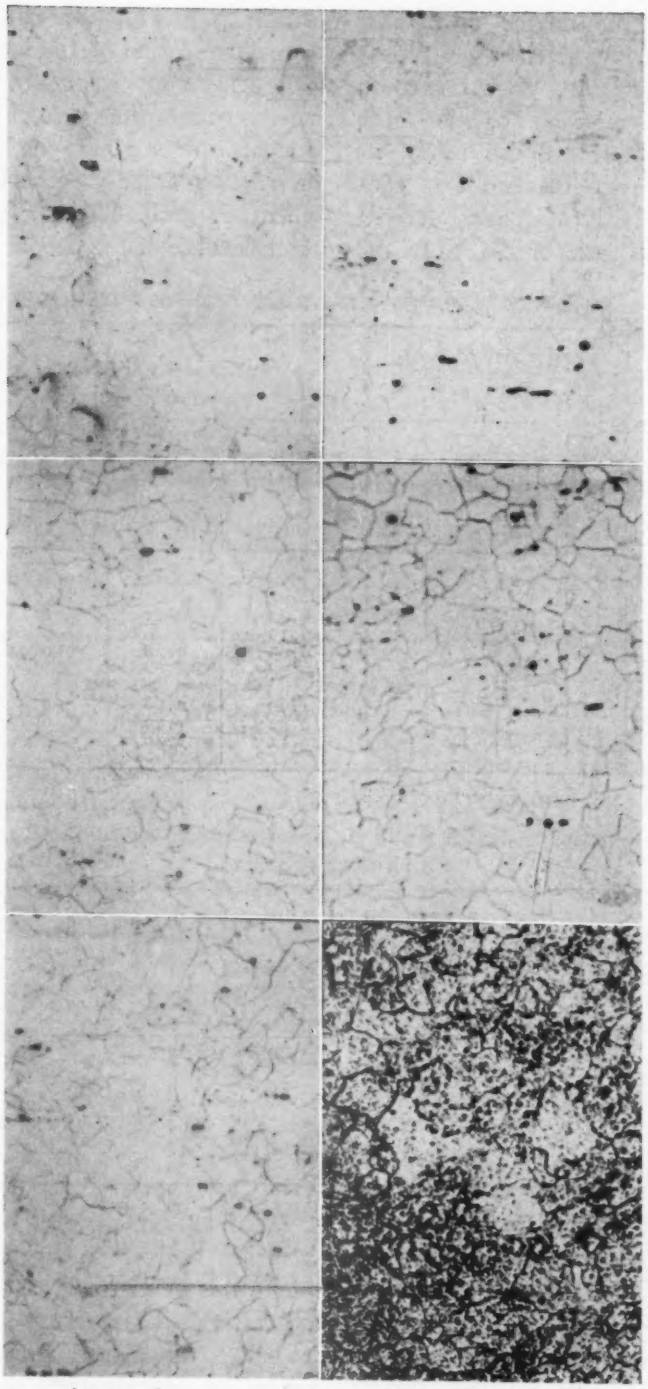

FIG 11—GAS ETCHING OF 0.15 PER CENT CARBON STEEL SURFACES ANNEALED IN BURNT CITY GAS. × 200.

the variation in the degree of etching obtained in the various atmospheres at any one temperature. With regard to the "water-gas" reaction 6, the only test in which equilibrium conditions for this reaction were approached was that at 720°C with the atmosphere derived from a combustion ratio of 1¾:1. In the latter test, etching was comparatively light, but the further experiments at the same temperature in the more completely burnt atmospheres resulted in appreciable etching and pitting after only 15 min at the test temperature. The results indicated that at temperatures of 720°C or less, provided that the $P_{CO} \cdot P_{H_2O}/P_{CO_2} \cdot P_{H_2}$ ratio approximates to equilibrium conditions at the heat-treating temperature, the P^2_{CO}/P_{CO_2} ratio can be varied within quite wide limits on the excess carbon dioxide side of the equilibrium value before any marked etching of a low-carbon steel surface will occur. At the higher temperature studied, the rate of etching increases markedly, especially at 920°C, when the grain boundaries become indistinct because of the deepness of the etch.

TABLE 8.—*Atmospheres Used for Gas-etching Experiments, Series B and C*

Nature of Production of Annealing Atmosphere	Composition of Heat-treating Atmosphere, Vol Pct				Ratios of Constituents in Ingoing Gas			
	CO_2	CO	H_2	H_2O	Producer-gas Reaction, $\frac{P^2CO}{P_{CO_2}}$	Water-gas Reaction, $\frac{P_{CO} \cdot P_{H_2O}}{P_{CO_2} \cdot P_{H_2}}$	$FeO + H_2 = Fe + H_2O$, $\frac{P_{H_2O}}{P_{H_2}}$	$FeO + CO = Fe + CO_2$, $\frac{P_{CO_2}}{P_{CO}}$
Air to city gas combustion ratio:								
1¾:1	3.5	10.7	17.0	2.3	0.33	0.42	0.13	0.32
2:1	4.7	9.4	12.9	2.3	0.19	0.36	0.18	0.50
2¾:1	6.0	7.3	9.8	2.3	0.09	0.28	0.24	0.82
Theoretical equilibrium ratio:								
At 720°C					1.62	0.68	0.44	0.65
At 820°C					10.52	1.00	0.52	0.54
At 920°C					50.11	1.40	0.61	0.44

TABLE 9.—*Etching of Polished Mild-steel Surfaces in Burnt City Gas Atmospheres*
Reflectivity Measurements, Series B and C, Polished Untreated Specimen, 100 Per Cent Reflectivity Factor

Reflectivity, Pct of Untreated Specimen	Temperature of Treatment, Deg C	Time at Temperature, Min	Atmosphere: CO_2 3.5 Pct; CO 10.7; H_2 17.0; H_2O 2.3; N_2 66.5	Atmosphere: CO_2 4.7 Pct; CO 9.4; H_2 12.9; H_2O 2.3; N_2 70.7	Atmosphere: CO_2 6.0 Pct; CO 7.3; H_2 9.8; H_2O 2.3; N_2 74.6	Atmosphere: Dry CO_2 4.8 Pct; CO 9.7; H_2 13.2; H_2O Nil; N_2 72.3
	720	5	96	94	87	96
	720	15	90	86	80	80
	820	5	87	76	66	67
	820	15	80	70	56	59
	920	5	74	64	49	48
	920	15	66	57	36	43

With an air–city-gas combustion ratio of 2¾:1 the carbon dioxide in the atmosphere was in excess of its equilibrium concentration with respect to iron (reaction 12) at all temperatures above 720°C, yet oxidation was observed only in the specimens heated at 920°C for periods of time greater than 5 min. The absence of oxidation at the lower temperatures was due to the counteracting effect of the hydrogen present, in excess of the water vapor in the

atmosphere. This may be readily calculated as follows:

In the reaction tube, the main reaction whereby the composition of the atmosphere proceeds to equilibrium is the "water-gas" reaction 6. In the atmosphere derived from a combustion ratio of 2¾:1, the ratio of the reactants for this reaction is

$$\frac{P_{CO} \cdot P_{H_2O}}{P_{CO_2} \cdot P_{H_2}} = 0.28$$

This value is lower than the equilibrium constants for the reaction at the various temperatures, and the reaction proceeds with the formation of more carbon monoxide and water vapor, in equal proportions.

ing ratios in the calculated atmospheres listed above, especially at 920°C., and it is probable that at this temperature secondary reactions would be sufficient to throw the atmosphere over onto the oxidizing side with respect to iron. The initial rate of oxidation appeared to be slow, but increased with the etching of the steel surface, giving a smooth, gray-matte surface oxide, very compact and adherent. The controlled oxidation of mild steel in this way may have interesting practical applications.

Series C

There appears to be some difference of opinion, especially among practical

TABLE 10.—*Equilibrium Conditions in Calculated Furnace Atmospheres, with Respect to Reactions Oxidizing to Iron*

Temperature, Deg C	Furnace Atmosphere as Calculated at Equilibrium, Pct				$Fe + CO_2 \rightleftharpoons FeO + CO$, $\frac{P_{CO_2}}{P_{CO}}$		$Fe + H_2O \rightleftharpoons FeO + H_2$, $\frac{P_{H_2O}}{P_{H_2}}$	
	CO_2	CO	H_2	H_2O	In Furnace	For Equilibrium	In Furnace	For Equilibrium
720	4.8	8.5	8.6	3.5	0.58	0.65	0.40	0.44
820	4.4	8.9	8.2	3.9	0.50	0.54	0.49	0.52
920	3.8	9.5	7.6	4.5	0.40	0.44	0.59	0.61

Assuming that equilibrium conditions are attained at the various test temperatures, and that the volume increase in the carbon monoxide and in the water-vapor concentration is x per cent in both cases, we have

$$\text{At } 720°C \quad \frac{(7.3 + x)(2.3 + x)}{(6.0 - x)(9.8 - x)} = K_{720} = 0.68$$

By solution, $x = 1.2$ pct approx.
Similarly at 820°C $x = 1.6$ pct approx.
at 920°C $x = 2.2$ pct approx.

Thus, the furnace atmospheres at the three test temperatures would be

720°C.....4.8 pct CO_2; 8.5 CO; 8.6 H_2; 3.5 H_2O
820°C.....4.4 pct CO_2; 8.9 CO; 8.2 H_2; 3.9 H_2O
920°C.....3.8 pct CO_2; 9.5 CO; 7.6 H_2; 4.5 H_2O

The equilibrium constants (Table 10) for the oxidizing reactions 12 and 13 are very nearly identical with the correspond-

men, as to the effect of water vapor on gas etching, although the work of Marshall[15] definitely showed that water vapor must be present in burnt fuel gas if etching is to be prevented. This view has been confirmed to some extent in the present work by a series of experiments on low-carbon steel, conducted under conditions similar to those just described, the atmosphere being burnt city gas derived from a combustion ratio of 2:1 and dried over activated alumina. The results obtained after tests at 720°, 820° and 920°C for 5 and 15 min are shown in Fig 12 and Table 9. There was no very marked increase in the etching compared with the wet gas, at temperatures up to 820°C, but at 920°C the surface roughening was considerably greater. The results suggested that the velocity of the water-gas

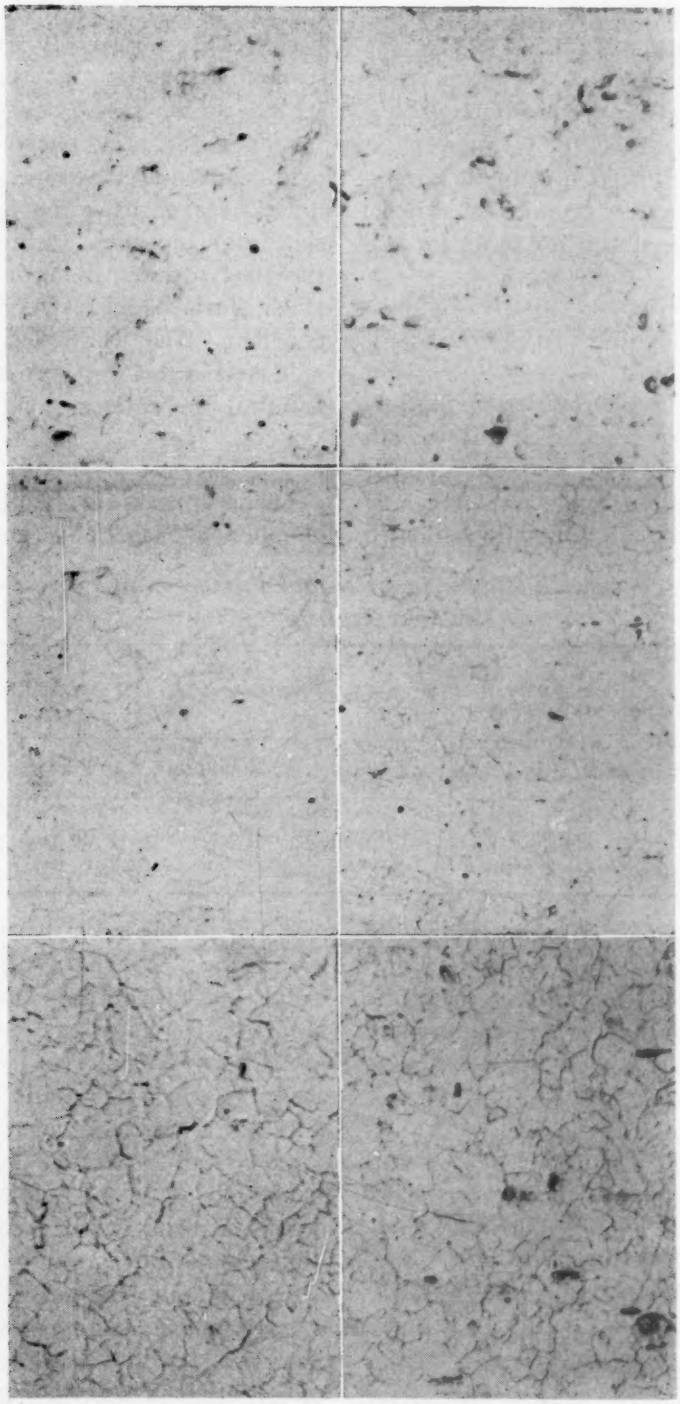

Atmosphere: 4.7 pct CO_2, 9.4 CO, 12.9 H_2, 2.3 H_2O, 70.7 N_2 4.8 pct CO_2, 9.7 CO, 13.2 H_2, 0.0 H_2O, 72.3 N_2

FIG 12—GAS ETCHING OF 0.15 PER CENTCARBON STEEL SURFACES IN WET AND DRY BURNT CITY GAS. × 200.

reaction (and also the time of treatment) is an important factor in the degree of etching obtained, being comparatively slow below approximately 820°C. This

700°C while for normalizing the atmosphere derived from a 1¾:1 combustion ratio is preferred. The experimental results indicate that both atmospheres can

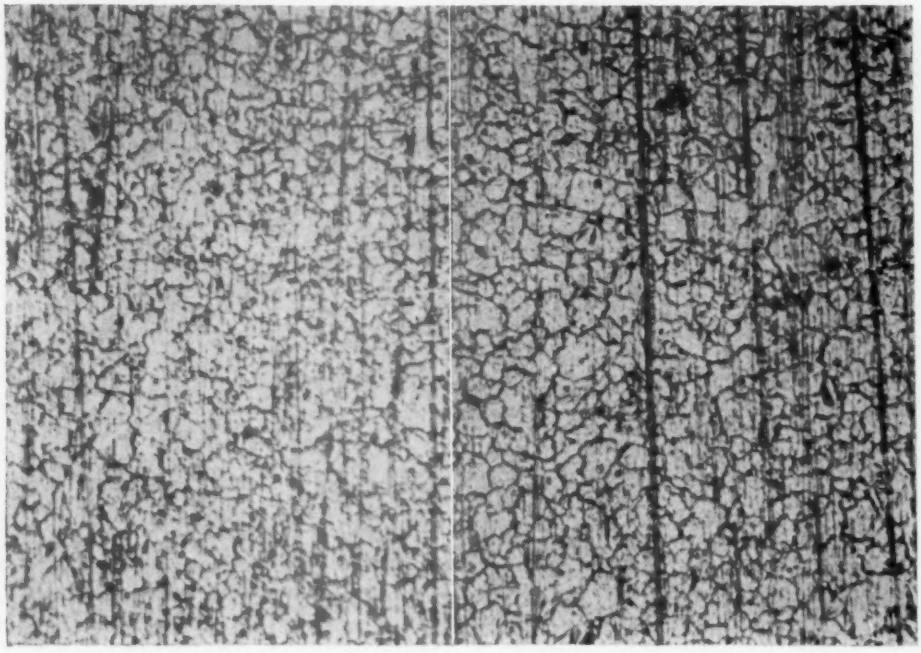

a 2½ hours at 950°C

b 5 hours at 950°C

FIG 13—ETCHED SURFACES OF 0.15 PER CENT CARBON STEEL AFTER CARBURIZATION IN CARBON MONOXIDE. × 100.

may well have a considerable bearing on the selection of a controlled atmosphere for the bright heat-treatment of low-carbon steel.

DISCUSSION OF RESULTS

The etching observed in these experiments was less severe than that reported by Marshall,[15] but the difference in the results can be attributed probably to differences in conditions of the steel surfaces prior to test and to the duration of the etching process.

The atmospheres used in the experiments described are typical of those used in Great Britain for the heat-treatment of low-carbon steel, that generated from a combustion ratio of 2:1 being used for bright annealing at temperatures up to

give rise to appreciable surface roughening of low-carbon steel even after short times of treatment at the corresponding annealing and normalizing temperatures. Further, while the rate of etching at 720°C is dependent upon the composition of the atmosphere, it is possible to work within fairly wide limits of composition without attaining excessive roughening. With increasing temperature, however, the etching rate increases rapidly and these limits are considerably reduced.

The function of the steel in promoting the various gas reactions to equilibrium may not be solely catalytic, but it may supply an additional element such as carbon or oxygen, which enters into the reactions at the steel surface and assists in the establishment of true gaseous

equilibrium. Thus carburizing and decarburizing reactions both roughen a steel surface and give rise initially to pronounced grain-boundary etching (Figs 13 and 14) and a general roughening of the crystal surfaces. Below 700°C, however, the rates of carburizing-decarburizing reactions are very slow, and probably do not account for the heavy etching obtained, for example, at 650°C (Fig 15). However, even at this temperature the extent of the roughening appears to increase with the carbon content of the steel, probably because of the increased chemical activity associated with steels of increasing carbon content. Deoxidation reactions probably contribute to the etching of the almost carbon-free iron, as shown in Fig 15, and in this connection it is interesting to note that a very broken surface may be obtained on rimming-steel sheets annealed in gas-fired furnaces (Fig 16). The effect is most pronounced in the rim portion of the sheet when annealing is done in single sheets rather than in a pack.

The nature of the gas-etching process appears to be determined both by the composition of the steel and the temperature of treatment. It is considered that below the Ac_1 point, the main factor is the catalytic activity of the iron in promoting inter-gas reactions, and the indications are that the water-gas reaction contributes mainly to the effect. In this case the process is purely one of adsorption, possibly involving surface migration of metal-gas complexes. The etching may be accentuated by direct surface reactions, as, for example, the removal of elements such as oxygen in solution in the iron. Above the Ac_1 point, it is suggested that surface roughening is almost entirely associated with surface reactions involving the transference of a constituent either into or from solution in the iron, and in

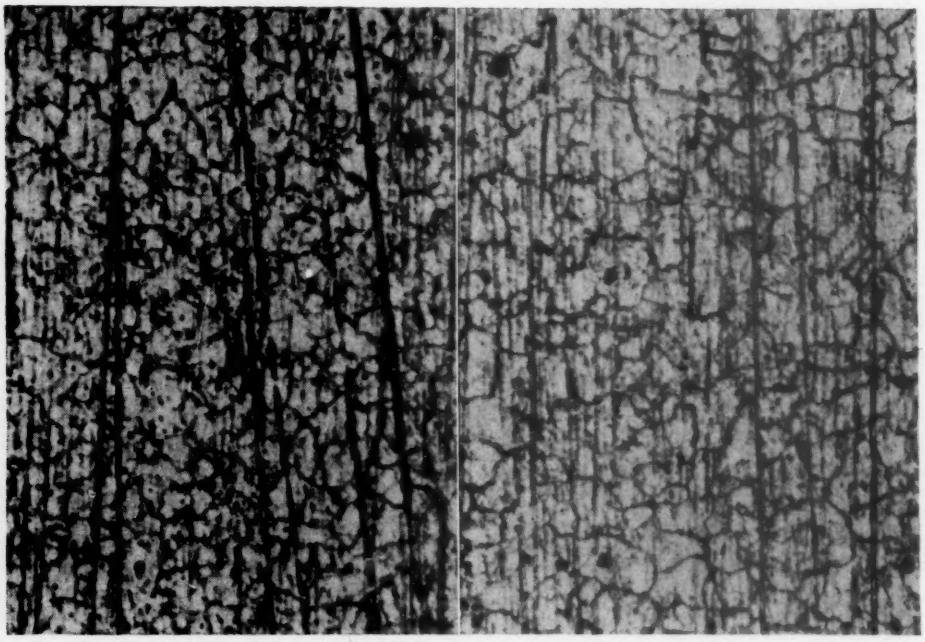

a 0.4 pct carbon steel

b 0.98 pct carbon steel

FIG 14—ETCHED SURFACES OF CARBON STEELS AFTER DECARBURIZATION IN WET HYDROGEN AT 900°C. × 200.

FIG 15—SURFACE ETCHING OF VARIOUS CARBON STEELS. × 200.

After annealing at 650°C for 5 hours in burnt city gas analyzing:
4.7 pct CO_2, 9.4 CO, 12.9 H_2, 2.3 H_2O, 70.7 N_2.
a. Swedish iron.
b. 0.20 pct carbon steel.
c. 0.4 pct carbon steel.

this respect carburizing-decarburizing reactions probably predominate.

PRACTICAL CONSIDERATIONS

In the heat-treatment of low-carbon steel strip in coils in batch furnaces, it is

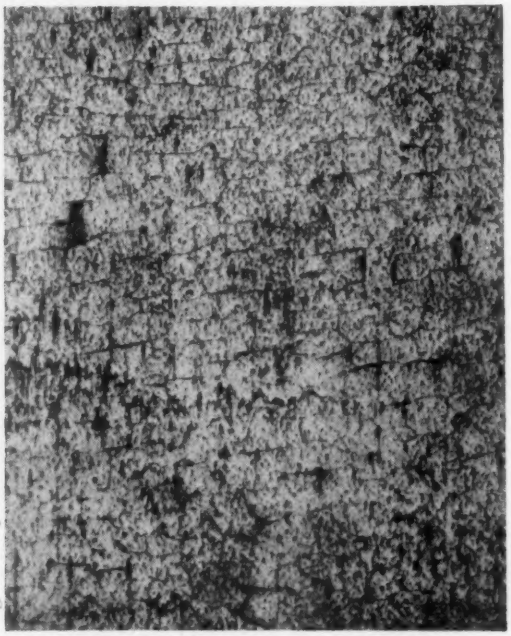

FIG 16—"EGG-SHELL" PATTERN ON RIMMING-STEEL SHEET ANNEALED IN OPEN GAS-FIRED FURNACE.

mainly the outside turn of every coil that comes into direct contact with the controlled atmosphere, and is subjected to the effect of nonequilibrium conditions in the atmosphere. Any gas penetrating between the coil turns will, in all probability, attain equilibrium before it has gone very far, and any surface etching will be concentrated at the outer edges of the coiled strip. From many points of view, the uniformity of surface finish of a heat-treated metal is of greater importance than the degree of brightness obtained. It is therefore most important that in batch annealing such effects as gas etching should be minimized, either by using an atmosphere that is in equilibrium at the annealing temperature with respect to the etching reactions who—rich

is not always practicable—preventing penetration of the atmosphere into the charge of steel.

The continuous bright heat-treatment of a steel strip, sheet or wire presents no difficulty from the point of view of surface finish, since the whole of the surface of the material is exposed to the controlled atmosphere.

It has been suggested that a gas-etched surface may be particularly suitable for subsequent coating processes such as tinning, enameling, etc. Large-scale bright-annealing experiments on cold-rolled black plate with this object in view have indicated that uniformity of results can be obtained only if the sheets are annealed singly, as in continuous furnaces. Even so, however, bright-annealed surfaces are not readily coated with tin, probably because of the presence of invisible oxide films, and in this respect the more active gas-etched surfaces may be even more difficult to tin without a preliminary light acid dip.

DECOMPOSITION OF CARBON MONOXIDE IN ATMOSPHERES USED FOR BRIGHT HEAT-TREATMENT OF LOW-CARBON STEEL

When pure carbon monoxide is heated it tends to decompose into carbon dioxide and free carbon, according to reaction 7.

$$2CO \rightleftarrows CO_2 + C + 41.3\ K\ \text{cal} \quad [7]$$

The rate of breakdown, however, is comparatively slow, unless the reaction is promoted by a catalytic surface, and in this respect, both nickel and iron are very active catalysts.[23] The solid carbon thus produced can either remain unchanged or be absorbed by the metal catalyst, and, in iron or steel, provided that the temperature is suitable, surface carburization is obtained. Below the Ac_1 point, however, the solubility of carbon in alpha iron is very small; if decomposition of carbon monoxide takes place the free carbon cannot be absorbed to any great extent by the iron and except for the possible formation of a surface film of iron carbide, will remain as soot. Below 750°C the equilibrium concentration of carbon monoxide relative to graphite and carbon dioxide falls off very rapidly (Table 2), so that decreasing temperature favors the decomposition reaction.

During the heat-treatment of low-carbon steel in partially burnt city gas, which may contain up to 12 pct of carbon monoxide, the steel, during both heating and cooling, passes through a range of temperature, usually below 600°C, in which the carbon monoxide is much in excess of its equilibrium concentration relative to graphite and carbon dioxide. Conditions exist therefore which favor sooting of the steel—obviously an effect of some importance in a bright heat-treatment process. An investigation of the "producer-gas" reaction with respect to the annealing of low-carbon steel has been carried out.

EXPERIMENTAL

The experimental work has covered conditions obtaining in both batch and continuous-furnace annealing, in so far as the rates of cooling of the steel in both types of furnaces are very different.

Series A

Specimens of polished 0.15 pct carbon-steel strip measuring 2 by ⅞ by 0.036 in. were heated in a static atmosphere of burnt city gas in a 1¼-in. transparent quartz tube, the central 10 in. of which was enclosed in an electric resistance furnace. The temperature of the specimen was measured by means of a fine chromel-alumel thermocouple attached to it and was thermostatically controlled to within ±3°C of the required test temperature, which, in this series of experiments, covered the range 250° to 700°C. When the specimen was at temperature, partially

burnt city gas was passed through the quartz tube for 30 min at a flow of 25 liters per hour, following which the gas outlet from the tube was closed and the

The partially burnt gas was first dried by means of activated alumina to a dew point of approximately −60°C, and then passed through a series of bubbling

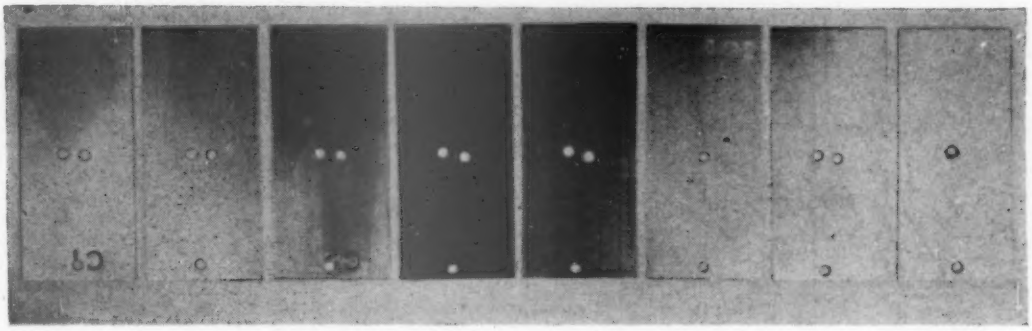

FIG 17—EFFECT OF HEATING 0.15 PER CENT CARBON STEEL IN FLOW OF BURNT CITY GAS. Gas flow maintained only at particular temperature, for 30 minutes. Composition of Atmosphere: CO_2, 4.7 pct; CO, 9.4; H_2, 12.9; H_2O, 2.3; N_2, 70.7.

specimens quickly cooled by withdrawal of the tube from the furnace. In order to remove any oxide films that might have been produced during test, all specimens were given a final reheat in dry hydrogen at 600°C for 15 min and quickly cooled in the gas. Photographs of the surfaces of the treated specimens are shown in Fig 17.

The deposition of carbon, as indicated by the blackening of the leading edge of the specimen, commenced at 600°C., and was still present at 250°C. The most critical range for the decomposition was between 350° and 450°C, although since the ratio P^2_{CO}/P_{CO_2} in the atmosphere used corresponded to equilibrium for the "producer-gas" reaction at 620°C, the sooting obtained at 600°C indicated the critical nature of equilibrium conditions for the reaction in the presence of iron at this temperature.

In view of the known activity of water vapor in promoting catalytic processes, a further series of experiments was carried out in an atmosphere of composition similar to that given above, but with a controlled concentration of water vapor.

bottles containing a solution of sulphuric acid of known strength, maintained at 25°C in a thermostatically controlled water bath. Vapor-pressure data for the various acid solutions used were taken from International Critical Tables and were cross-checked gravimetrically by absorption of the water vapor in phosphorus pentoxide. The steel specimen for test was cleaned on emery, degreased, dried, and weighed and then heated to 720°C in the quartz tube in a static atmosphere of the test gas. After holding at temperature for 5 min, the test gas was passed through the tube at 25 liters per hour, while the specimen was cooled at approximately 5°C per minute down to 250°C by slowly withdrawing the quartz tube from the furnace. All specimens were given a treatment in dry hydrogen at 600°C for 15 min before the final weighing.

The results, shown in Fig 18, indicated that small amounts of water vapor of about 0.005 pct reduce considerably the amount of soot formation, although the perfectly dry atmosphere gave rise to heavier sooting. In no case was sooting completely suppressed. Subsequent ex-

periments with dry charcoal gas, containing solely the oxides of carbon and nitrogen, and a maximum hydrogen content of 0.5 pct, showed that the sheet or strip-annealing furnaces. The following factors, and their effects upon the decomposition of carbon monoxide, were studied:

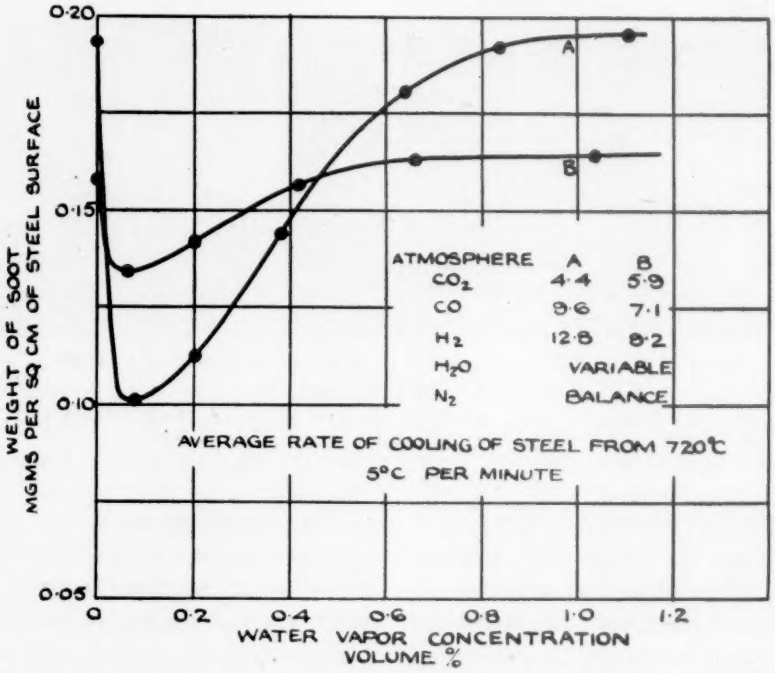

FIG 18—EFFECT OF WATER-VAPOR CONTENT OF FURNACE ATMOSPHERE ON SOOTING OF BRIGHT MILD STEEL COOLED IN A FLOW OF BURNT CITY GAS.

elimination of hydrogen and water vapor, either individually or collectively, does not prevent the decomposition of carbon monoxide on steel in the presence of carbon dioxide. Pure carbon monoxide, on the other hand, especially at high gas rates, does not decompose on iron at temperatures up to at least 650°C. The promotion of sooting in the presence of carbon dioxide may be associated with activation of the iron surface by adsorption or other surface reactions, while traces of water vapor retard the decomposition of the carbon monoxide, possibly by preferred adsorption on the active iron surface.

Series B

A further series of experiments was carried out under conditions that approached those met in continuous single-

1. The composition of the annealing atmosphere. Three atmospheres were used, derived from combustion ratios of air and city gas of 1¾:1; 2:1; and 2¾:1. Their analyses are given in Table 9.
2. The rate of gas flow over the specimen.
3. The rate of cooling of the specimen.

The experimental furnace and the nature of the specimens treated were as described for series A. Experiments with cold-rolled 0.15 pct carbon steel strip were carried out at 720°C, the time of heating at temperature in all cases being 15 min. The rates of gas flow employed were based upon data from a continuous furnace using a protective atmosphere of burnt ammonia. The three rates of flow employed were 39, 54 and 62 liters per hour (equivalent to 2.6, 3.6 and 4.2 ft per min, respectively) the furnace tube being 1¼-in. internal diameter. The rate

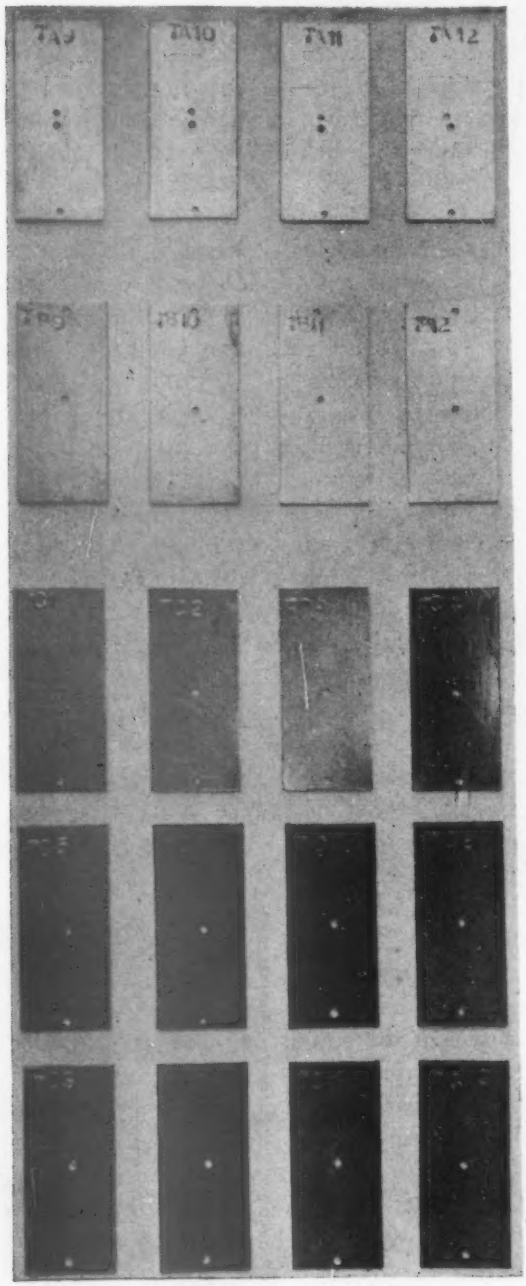

FIG 19—CARBON DEPOSITION ON 0.15 PER CENT CARBON STEEL COOLED IN FLOW OF BURNT CITY GAS.

of cooling was controlled by the rate of withdrawal of the specimen from the hot zone to the cooler zones of the quartz tube, this being effected by wire attachment to one end the of specimen. Four rates of cooling were investigated, the time taken to cool over the active carbon deposition range of 500° to 250°C being 1¼, 2, 6¾ and 23½ min, respectively.

The results, illustrated in Fig 19, show that within the range of gas compositions studied carbon deposition occurred only with the atmosphere derived from the highest combustion ratio of air: city gas of 2¾:1. In the latter case, marked sooting was produced even with the quickest rate of cooling, this being very pronounced at the higher gas flows. It was anticipated that the greatest degree of sooting would be obtained in an atmosphere with the highest P^2_{CO}/P_{CO_2} ratio; i.e., with a combustion ratio of air-city gas of 1¾:1. That this was not obtained is due to the slow rate of the decomposition reaction on a comparatively inactive steel surface. The mild-steel specimens used were typical of those resulting from cold-rolling, and such surfaces do not appear to have a very great catalytic effect on the producer-gas reaction during treatments of comparatively short duration. However, annealing at 720°C in an atmosphere derived from a combustion ratio of 2¾:1 gives rise to surface etching, as has been previously illustrated. This was sufficient to speed up the rate of decomposition of the carbon monoxide in the burnt city gas during cooling. The etching produced in the other annealing atmospheres used, however, was insufficient to promote the breakdown within the range of gas flows and rates of cooling studied.

Since the producer-gas reaction, especially at the lower temperatures, must be catalyzed in order to proceed to any marked extent, the activity of the catalytic surface has naturally a great effect upon the progress of the dissociation. In this respect an ordinary cold-rolled surface probably is one of the least active states. Any rust marks on the steel surface, however, are reduced at the annealing temperature to black iron particles of a fairly adherent nature, having marked chemical activity. Irrespective of the composition of the atmosphere, rate of cooling and gas flow, carbon deposition invariably occurred around such particles when present on specimens treated under the test conditions described. As shown in Fig 20, the deposition is local, the nonrusted areas remaining free from soot.

Sintering of the iron particles by using a higher temperature of heat-treatment reduced their activity. Thus, for example, a matte surface resulting from the scale reduction of hot-rolled mild steel in burnt city gas at 950°C was found to be comparatively inactive. Variations in the composition of the furnace atmosphere, the rate of flow, and the rate of cooling of the specimens were identical to those employed in the experiments on the cold-rolled steel. Carbon deposition was observed only when the time of cooling over the range from 500° to 250°C exceeded 5 min and was independent of both gas composition and gas flow.

Practical Considerations

During the heating of a charge of steel in a batch furnace and in a burnt city gas atmosphere typical of that used for bright annealing or bright normalizing, carbon deposition will tend to occur up to at least 600°C. In general, the rate of heating of steel charges through this range of temperature is comparatively rapid, and in any case the annealing atmosphere usually is polluted by vaporized rolling lubricants and air entrapped in the charge. Under such conditions the decomposition of carbon monoxide in the original burnt city gas is likely to be slight. Thus the most suitable atmosphere is one that is high in carbon dioxide while retaining

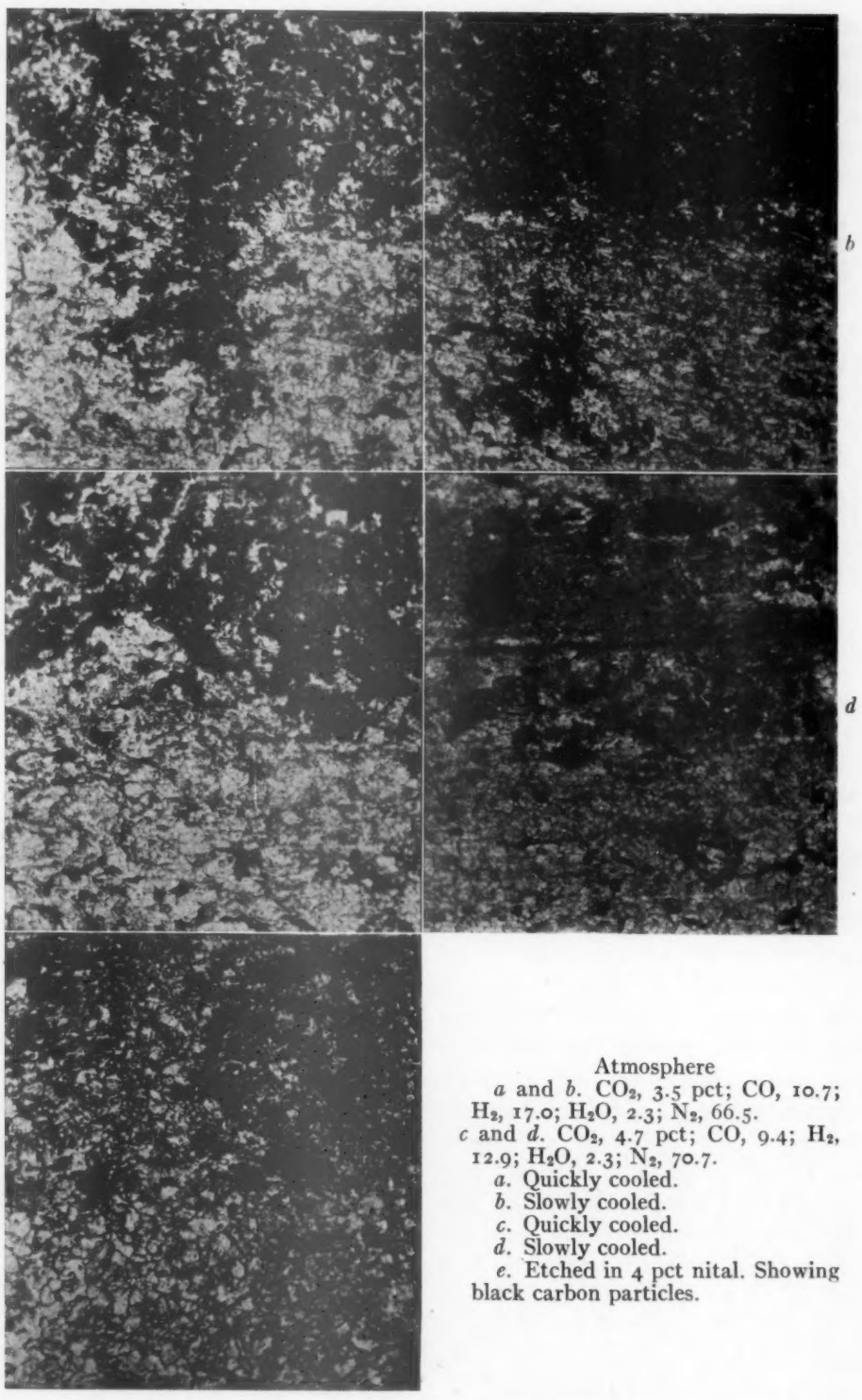

Atmosphere
a and *b*. CO_2, 3.5 pct; CO, 10.7; H_2, 17.0; H_2O, 2.3; N_2, 66.5.
c and *d*. CO_2, 4.7 pct; CO, 9.4; H_2, 12.9; H_2O, 2.3; N_2, 70.7.
a. Quickly cooled.
b. Slowly cooled.
c. Quickly cooled.
d. Slowly cooled.
e. Etched in 4 pct nital. Showing black carbon particles.

FIG 20—PROMOTION OF SOOTING BY REDUCED IRON OXIDE OR RUST. × 100.
Steel cooled from 720°C in flow of burnt city gas.

nonoxidizing conditions to the steel at the heat-treating temperature.

During cooling of the charge, carbon deposition will again occur if a flow of gas is maintained through the container, and on a commercial scale this has been found to be quite appreciable even in an atmosphere containing less than 5 pct of carbon monoxide. Sooting of the work can be overcome, either by completely sealing the heat-treating container and cooling under conditions that approach to vacuum cooling, or by sealing only the outlet of the container and maintaining a positive pressure of burnt city gas on the inlet side. In the latter case the carbon deposition resulting from the gas left in the container is negligible. This method is to be preferred in practice, since the rate of cooling of the charge is increased by heat conduction and convection via the controlled atmosphere.

In continuous furnaces the prevention of gas etching is most important, but even so it is advisable to cool the metal as quickly as is practicable through the critical temperature range for the decomposition of carbon monoxide, if sooting of the work is to be prevented. In addition to the work being treated, the interior parts of continuous furnaces, particularly those located permanently in the cooling zone, may be subject to sooting. The water-cooled walls of the cooling zone remain unaffected, since the temperatures of the jacketed surfaces are too low to permit the reaction to proceed, but in many cases the mechanical devices for conveying the material through the furnaces are permanently in the cooling zone—rollers, etc.—and here sooting may, in time, give rise to difficulties. The catalytic activity of such surfaces, however, is unlikely to be very great, and the rate of build-up of soot is slow. In severe cases the soot must be removed periodically by cleaning or by burning with hot air. It is often recommended that the velocity of the gas through the cooling zone should be as high as is economically possible

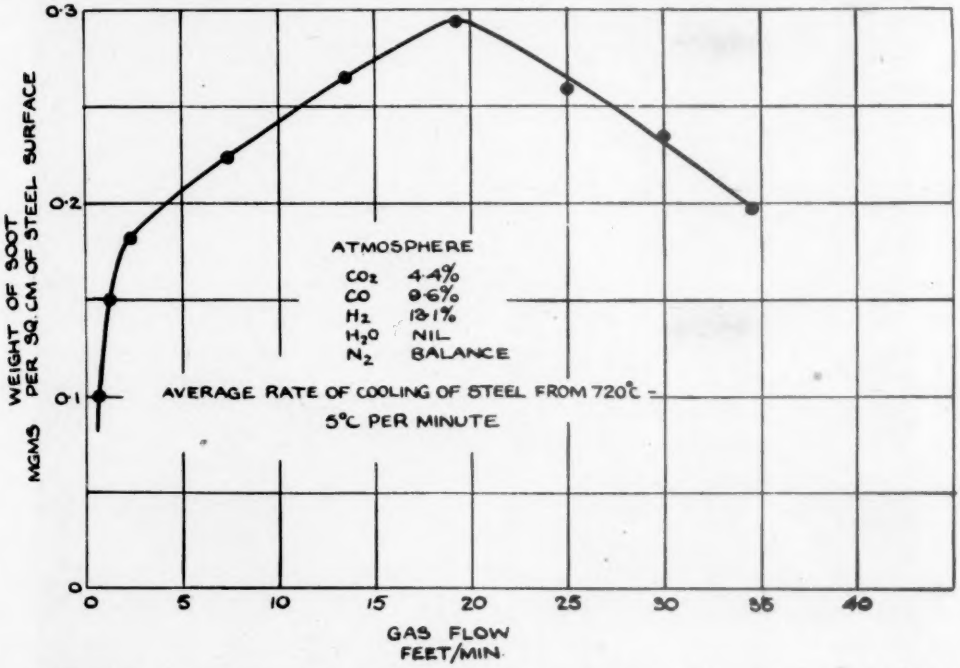

FIG 21—EFFECT OF RATE OF FLOW OF GAS OVER STEEL SURFACE ON SOOTING OF BRIGHT MILD STEEL COOLED IN BURNT CITY GAS.

in order to reduce the extent of the carbon deposition. Experiments carried out in the same furnace as those in Series B, with increasingly high gas rates, showed that the maximum gas flow necessary to effect any appreciable reduction in sooting during comparatively slow cooling is very high indeed and quite an uneconomical proposition (Fig 21).

EFFECT OF LUBRICANTS ON BRIGHT HEAT-TREATMENT OF LOW-CARBON STEEL

Lubricants on the charge can have an important influence on the bright annealing of steel, particularly in batch-type furnaces. In such furnaces there is a tendency for oil that is vaporized during heating to crack, both on the outer and usually hotter portions of the charge and also in pockets in the charge that are not effectively swept by the controlled atmosphere. In order to avoid or minimize this effect, it is advisable to have a high flow or surge of gas during the initial stages of the heating cycle, so that oil vapors are swept out of the annealing container before they have an opportunity to crack. Mineral and rape oils normally give little trouble in this respect, but complex soluble oils crack more readily, leaving behind carbon deposits that are comparatively inactive, although there is some evidence to suggest that staining of the steel is less in atmospheres containing carbon dioxide, presumably due to interaction to form the monoxide according to reaction 7.

Soap-drawn steel wire presents similar difficulties during bath annealing, although even on continuous annealing the best bright annealing is obtained if the wire is subjected to a scouring action,—as in a lead bath, for example—in addition to being protected by a controlled atmosphere. In batch annealing, a slow rate of heating, up to 450° or 500°C, which ensures a good purge of the annealing container while the soap vapors are slowly forming, effects a considerable improvement. A "clean batch anneal" can be obtained by heating the wire in a current of air up to approximately 500° to 550°C. The soap vapors are burned and the products of combustion carried out of the container, whereas the steel itself is lightly oxidized. At 550°C the air is replaced by a controlled atmosphere and the annealing is completed in the normal way, the iron oxide being reduced and a clean matte surface obtained.[24] Steel articles for bright heat-treatment should be treated as soon as possible after the last working operation, as exposure to air results in the oxidation of the oil film on the material, which on heating leads to adherent, carbonaceous residues.

REDUCTION OF SCALE ON HOT-ROLLED STEEL

The descaling of hot-rolled steel strip in a controlled atmosphere of regenerated burnt ammonia is practiced to a limited extent in Great Britain. The treatment usually is combined with normalizing and is carried out in continuous furnaces of the roller-hearth type at temperatures up to 950°C. There are certain economic advantages in the use of partially burnt city gas for this purpose, and an investigation has been made of the comparative descaling properties of the two types of atmospheres.

Experimental

Two types of steel were used for the investigation; namely, 16-gauge hot-rolled strip, 0.15 pct carbon, and 13-gauge hot-rolled strip, 0.4 pct carbon. Specimens for test measuring 2 by ⅞ in. were cut from the strip with a hand guillotine, care being taken to avoid the flaking of the scale along the sheared edges.

The apparatus used for descaling was identical to that described for the gas-etching experiments, the procedure being

TABLE 11.—*Descaling of 16-gauge Hot-rolled Mild-steel Strip in Burnt City Gas Atmospheres*

Specimens 2 inches long by 7/8 inches wide. Heated at 950°C, for varying times. Average weight of samples 16.75 grams

Depth of scale (from cracked ammonia test), 0.485 thousandths of an inch

Data	Atmosphere (Air-gas Ratio 1¾:1): CO_2 3.5 pct; CO 10.7; H_2 17; H_2O 2.3; N_2 66.5					Atmosphere (Air-gas Ratio 2:1): CO_2 4.9 pct; CO 9.4; H_2 12.3; H_2O 2.3; N_2 71.1					Atmosphere (Air-gas Ratio 2½:1): CO_2 6.3 pct; CO 7.0; H_2 9.3; H_2O 2.3; N_2 75.1				
	2 Min	5 Min	10 Min	15 Min	20 Min	2 Min	5 Min	10 Min	15 Min	20 Min	2 Min	5 Min	10 Min	15 Min	20 Min
Loss in weight, grams	0.0304	0.0403	0.0400	0.0401	0.0401	0.0289	0.0404	0.0406	0.0403	0.0401	0.0254	0.0363	0.0400	0.0402	0.0401
Loss in original weights, pct	0.186	0.240	0.238	0.241	0.240	0.170	0.240	0.242	0.240	0.243	0.153	0.220	0.243	0.243	0.240
Equivalent oxide, pct	0.62	0.80	0.795	0.805	0.80	0.565	0.80	0.81	0.80	0.81	0.515	0.735	0.810	0.810	0.800
Equivalent weight of scale per 100 sq in. of surface, grams	2.9	4.1	3.8	3.9	3.9	2.75	4.2	4.4	4.1	3.9	2.40	3.45	3.80	4.00	3.90
Equivalent depth of scale in thousandths of an inch (density of scale = 5.1 grams per cc)	0.35	0.495	0.485	0.490	0.490	0.33	0.505	0.53	0.495	0.490	0.290	0.415	0.485	0.485	0.490
Appearance of treated samples	Not completely reduced; surface oxide	Clean matte; completely reduced				completely reduced; surface oxide	Clean matte; completely reduced				Not quite reduced	Clean matte; completely reduced			

TABLE 12.—*Descaling of 13-gauge Hot-rolled 0.4 Per Cen Carbon Steel Strip in Burnt City Gas Atmospheres*
Specimens 2 inches long by ⅞ inches wide. Heated at 950°C for varying times. Average weight of samples, 20.5 grams
Depth of scale (from cracked ammonia test), 0.3 thousandths of an inch

Data	Atmosphere (Air-gas Ratio 1¾:1): CO_2 3.5 pct; CO 10.7; H_2 17.0; H_2O 2.3; N_2 66.5					Atmosphere (Air-gas Ratio 2:1): CO_2 4.9 pct; CO 9.4; H_2 12.3; H_2O 2.3; N_2 71.1					Atmosphere (Air-gas Ratio 2½:1): CO_2 6.3 pct; CO 7.0; H_2 9.3 H_2O 2.3; N_2 75.1				
	2 Min	5 Min	10 Min	15 Min	20 Min	2 Min	5 Min	10 Min	15 Min	20 Min	2 Min	5 Min	10 Min	15 Min	20 Min
Loss in weight, grams	0.0266	0.0254	0.0260	0.0264	0.0262	0.0227	0.0255	0.0260	0.0258	0.0261	0.0198	0.0218	0.0260	0.0258	0.0260
Loss in original weight, pct	0.130	0.126	0.128	0.131	0.130	0.110	0.129	0.129	0.132	0.130	0.098	0.106	0.131	0.130	0.132
Equivalent oxide, pct	0.435	0.420	0.426	0.437	0.435	0.366	0.430	0.430	0.440	0.435	0.325	0.354	0.437	0.435	0.440
Equivalent weight of scale per 100 sq in. of surface, grams	2.55	2.45	2.50	2.53	2.51	2.17	2.46	2.50	2.48	2.51	1.90	2.08	2.50	2.48	2.50
Equivalent depth of scale in thousandths of an inch (density of scale = 5.1 grams per cc)	0.310	0.29	0.30	0.305	0.302	0.262	0.296	0.30	0.30	0.302	0.230	0.250	0.30	0.30	0.30
Appearance of treated samples	Bright; completely reduced					Not completely reduced; surface oxide	Bright; completely reduced				Not completely reduced; surface oxide	Not completely reduced; surface oxide	Bright; completely reduced		

very similar. The specimen for test, after degreasing and weighing, was heated up to 950°C in a static test atmosphere, and when at temperature a flow of the atmosphere was maintained for the necessary time. The specimen was then lowered quickly into the unheated portion of the furnace tube, cooled under a positive pressure of gas, and weighed. Experiments were carried out with burnt city gas mixtures of three different compositions, and these, together with the results, are given in Tables 11 and 12. During descaling the gas flow was 50 liters per hour, equivalent to a linear flow of 3.4 fpm. Standards of complete reduction were obtained by treating samples of both steels at 950°C in cracked ammonia, to constant weight.

Results

Complete reduction of the scale on both steels was obtained in all the atmospheres used, the minimum times necessary for complete reduction at 950°C being approximately 3½, 5 and 8 min for the atmospheres derived from air–city-gas combustion ratios of 1¾:1, 2:1 and 2½:1 respectively. Burnt ammonia, on the other hand, gave complete reduction of the scale in just under 2½ min, and produced a silver-matte finish which was bright in comparison with the dull matte surface of the burnt city-gas products. The descaling experiments were repeated using dry burnt city gas, otherwise of the same compositions as given in Tables 11 and 12, but there was no marked decrease in the time for total reduction as compared with the wet gas.

To obtain a rate of oxide reduction comparable with that in burnt ammonia, it is necessary to use a dry burnt city gas having a combined carbon monoxide and hydrogen concentration of nearly 30 pct. This brings the composition near to that which would be explosive when mixed with air.

Table 2 shows that the equilibrium ratios of P_{CO}/P_{CO_2} and P_{H_2}/P_{H_2O} with respect to oxidation of iron are 2.41 and 1.61 respectively at 950°C. Of the atmospheres used in the descaling experiments, only that derived from a combustion ratio of 1¾:1 had a concentration of carbon dioxide below that for equilibrium with respect to reaction 12 at 950°C.

$$Fe + CO_2 = FeO + CO \qquad [12]$$

The water-vapor content of the atmosphere was 2.3 pct, the equivalent equilibrium concentration of hydrogen at 950°C with respect to reaction 13 being 3.7 pct.

$$Fe + H_2O \rightleftarrows FeO + H_2 \qquad [13]$$

Thus the excess of hydrogen available for reduction at 950°C was 17.0 pct − 3.7 pct = 13.3 pct, and the atmosphere from this point of view can be considered as comparable to an 85 pct nitrogen, 15 pct hydrogen mixture. In actual fact, however, it was found that the latter atmosphere possessed a far greater reducing power than the richest of the burnt-city-gas mixtures used, and it is considered that this was associated with a reduction of the hydrogen content in the furnace by reaction with carbon dioxide according to reaction 6:

$$CO_2 + H_2 \rightleftarrows CO + H_2O \qquad [6]$$

The equilibrium constant for this reaction at 950°C is 0.67, while the ratio $\frac{P_{H_2} \cdot P_{CO_2}}{P_{H_2O} \cdot P_{CO}}$ for the richest burnt-city-gas mixture was 2.4; i.e., reaction 6 would tend to go from left to right. While an equivalent volume of carbon monoxide is formed, the latter gas does not appear to be so strong a reducing agent as hydrogen, at least at normalizing temperatures. It is also possible that the concentration of carbon monoxide may become sufficiently high to promote carburization of the iron, and this has been observed on Swedish iron, heated at 950°C in atmospheres similar to the above.

Bright Annealing of High-carbon Steel

An investigation has been made of the annealing of medium and high-carbon steels in atmospheres generated by the partial combustion of city gas, with the object of establishing conditions that will ensure a clean and bright product, free from decarburization. The basic atmospheres used in all the experimental work were generated in a city-gas burner of the "packed" type, similar to that already described.

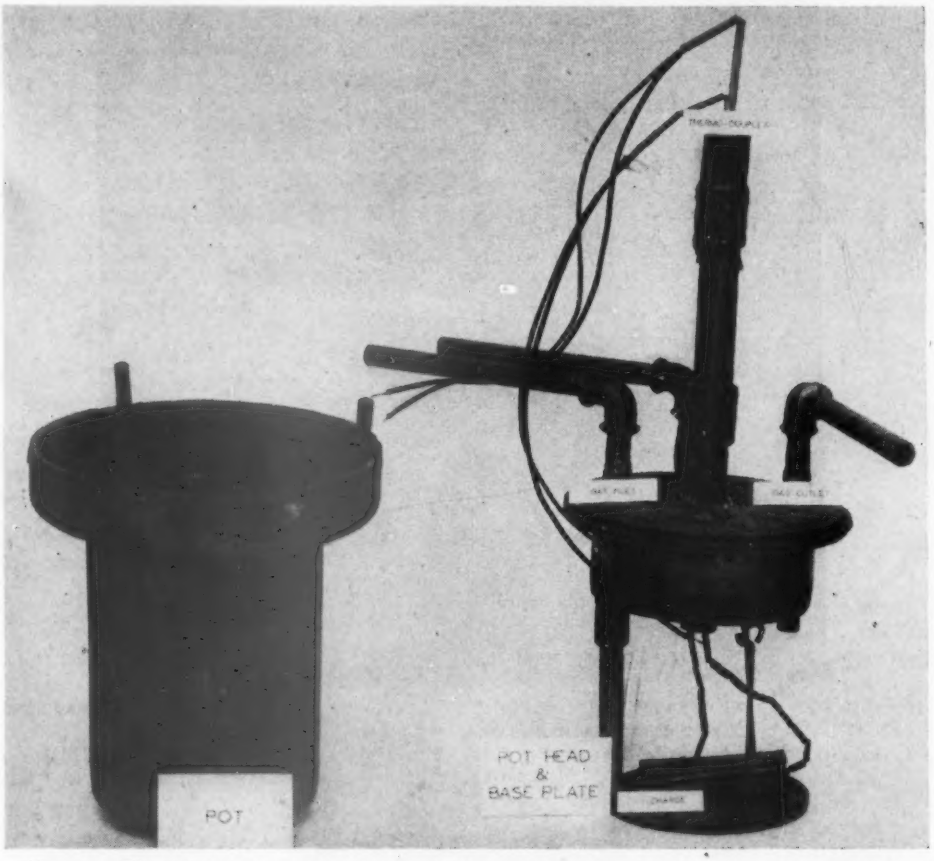

FIG 22—VERTICAL CYLINDRICAL POT AND INTERIOR FOR ANNEALING EXPERIMENTS.

BURNT CITY GAS CONTAINING CARBON DIOXIDE

EXPERIMENTAL

Samples of steel of composition A, shown in Table 13, in the form of soap-drawn wire $\frac{3}{16}$ in. in diameter by 4 in. long were treated in bundles of twenty. The annealing was carried out in a small, vertical cylindrical furnace and heat-resisting pot (Fig 22), the latter having a deep, insulated head and a loading space of 6-in. diameter by 6 in. deep. A typical charge of wire specimens is shown assembled on the base plate.

TABLE 13.—*Composition of Carbon Steels Used in the Experiments*

Number	Carbon	Silicon	Manganese	Sulphur	Phosphorus
A	0.50	0.11	0.70	0.032	0.033
B	0.40	0.17	0.55	0.018	0.018
C	0.68	0.16	0.40	0.014	0.019
D	0.98	0.23	0.32	0.011	0.014

The controlled atmosphere was fed into the pot via an inlet pipe passing through

the head and extending to the base of the pot, while the gases discharged through a vent in the top of the pot. Chromel-alumel thermocouples, sealed into the head, could be attached to the charge of steel. The furnace was heated electrically and was thermostatically controlled to within ± 3°C.

After the steel samples had been charged and the cover bolted down, the pot was purged with the test atmosphere, transferred to the hot furnace, and heated up in 2 hr to the annealing temperature. Throughout the heating up and the holding period, which also was for 2 hr, the test atmosphere was passed through the pot at a rate equivalent to six volume changes of the pot per hour, but cooling was done under a pressure of gas, by closing the gas vent in the pot head.

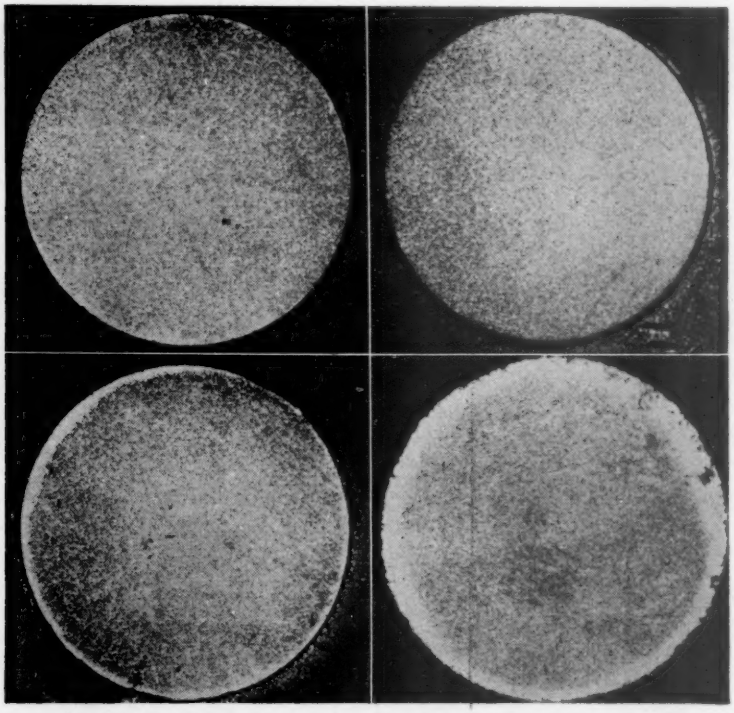

FIG 23—EFFECT OF TEMPERATURE ON DECARBURIZATION OF 0.5 PER CENT CARBON STEEL IN BURNT CITY GAS. × 20. ETCHED IN 2 PER CENT NITAL.
Composition of Gas: 4.6 pct CO_2, 9.6 CO, 14.8 H_2, 2.3 H_2O, 0.2 CH_4, 68.5 N_2.
a. As received.
b. 600°C 3 hours.
c. 700°C 3 hours.
d. 750°C 3 hours.

Most of the steel samples before annealing were slightly decarburized but in view of the fact that data on the effect of the treatment upon the surface finish of the soap-drawn wire, as well as upon its carbon content, were required, the decarburized skin was not removed before test.

Burnt City Gas as Generated

The initial experiments covered the temperature range 650° to 750°C, the composition of the burnt city gas used being typical of that normally recommended for the bright annealing of low-carbon steel. Micrographs of the results obtained, together with the composition of the atmosphere, are given in Fig 23. Up to 680°C, decarburization was negligible,

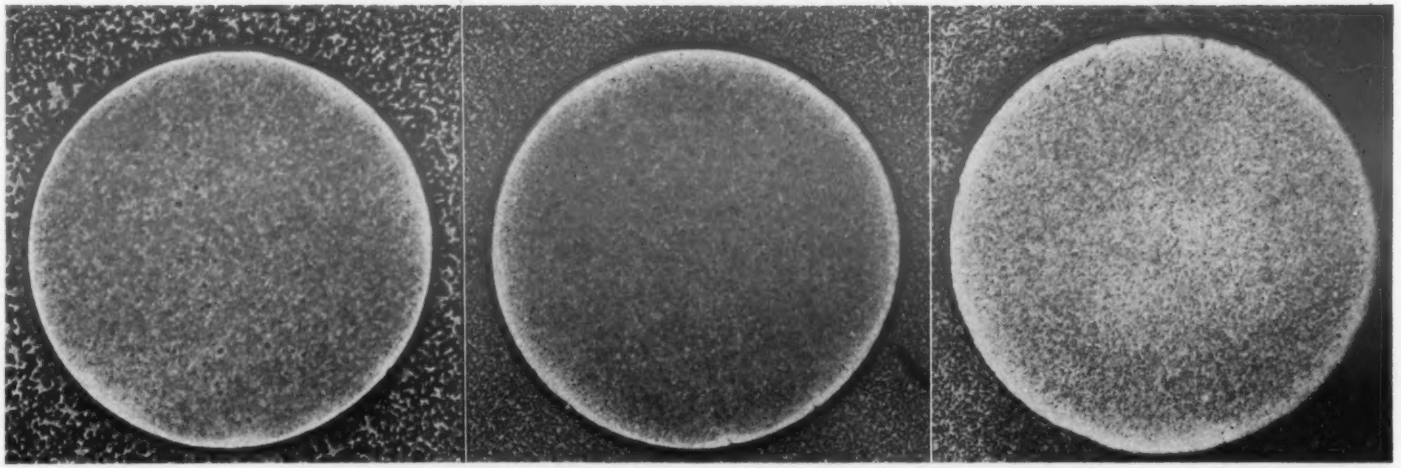

a. Wet; 10 liters per hour. Exit gas: 3.65 pct CO_2, 10.95 CO, 13.5 H_2, 0.0 CH_4.

b. Wet; 70 liters per hour. Exit gas: 4.40 pct CO_2, 9.85 CO, 13.61 H_2, 0.0 CH_4.

c. Dry; 10 liters per hour. Exit gas: 3.18 pct CO_2, 11.00 CO, 13.16 H_2, 0.0 CH_4.

FIG 24—SPECIMENS OF 0.50 PER CENT CARBON STEEL ANNEALED 2 HOURS AT 760°C IN PARTIALLY BURNT CITY GAS. × 10. ETCHED IN 2 PER CENT NITAL.
Gas Analysis: 4.6 pct CO_2, 9.6 CO, 14.8 H_2, 2. 3 H_2O, 0.2 CH_4, 68.5 N_2.

but at 700°C it was appreciable and at 750°C it was excessive.

Subsequent experiments were carried out at 760°C, which is just above the Ac_1 point for the 0.5 pct carbon steel, and Fig 24 shows the considerable decarburization obtained after treatment in burnt city gas at this temperature. The decrease in the concentration of carbon dioxide, as shown by the composition of the atmosphere leaving the pot, gives some further indication of the extent of the decarburization. Additional tests were carried out at a gas rate equivalent to 40 volume changes of the container per hour, but although the composition of the discharged atmosphere did not show such a marked decrease in the carbon dioxide content as was obtained at the lower gas rate (Fig 24) this was offset by the increased volume of gas coming into contact with the steel. Even so there was a slight, but noticeable, decrease in the degree of decarburization obtained (Fig 24).

In all of these tests, the treated wire had a very light film of carbon, which could be readily brushed away, leaving a bright steel surface.

Dry Burnt City Gas

The atmosphere used in the initial experiments contained approximately 2.3 pct of water vapor. A similar series of experiments was carried but with the burnt city gas dried to a dew point of about −60°C by activated alumina. To reduce the possibility of contamination of the dried atmosphere the annealing pot was baked at 1000°C in especially purified hydrogen, and the line carrying the burnt city gas from the alumina drier to the pot was of clean metal tubing. The results, as shown in Fig 24, indicated a reduction in the degree of decarburization, as compared with that in the wet gas, although the concentration of the carbon dioxide in the discharged gases was also less. This latter effect probably is due to reaction of the carbon dioxide with hydrogen to form water vapor according to reaction 6:

$$CO_2 + H_2 \rightleftarrows CO + H_2O \qquad [6]$$

Reheated Burnt City Gas

The foregoing experiments indicated that under the conditions of test both the carbon dioxide and the water vapor were active decarburizing agents, and that drying the burnt city gas was in itself insufficient to suppress decarburization. As indicated earlier in the paper, the carbon dioxide content of partially burnt city gas can be appreciably reduced by reheating the cooled gas in the presence of a catalyst at a temperature of 1000° to 1200°C. A further series of experiments therefore was carried out using a burnt city gas generated from an air–city-gas ratio of 2:1, which was cooled to room temperature and then reheated to 1200°C in a silica tube packed with crushed refractory. The treated gas was cooled quickly to room temperature and the water-vapor content thereby reduced to about 2.5 pct. The annealing results obtained with this atmosphere, together with the gas composition, are given in Fig 25.

The degree of decarburization obtained was comparable to that obtained with the dry burnt city gas just described. With a higher gas rate, there was some further decrease in the extent of decarburization, but this was very small (Fig 25).

The carbon dioxide content of the gases discharged from the pot showed an increase above that of the ingoing atmosphere, this being much more marked in the test with a low gas rate. It is interesting to note that the ratio of the increase in carbon dioxide concentration for the two gas rates—i.e., 2.0:0.3—was very nearly equal to the inverse ratio of the respective gas rates used; i.e., 10:70. In other words, the total volume of

carbon dioxide formed was approximately the same in the two experiments.

The treated samples from both tests were clean and free from surface deposits, but somewhat etched.

described previously. Micrographs of the steel annealed in the gas, at the low and high gas rates, together with the composition of the annealing atmosphere, are given in Fig 25. Decarburization was

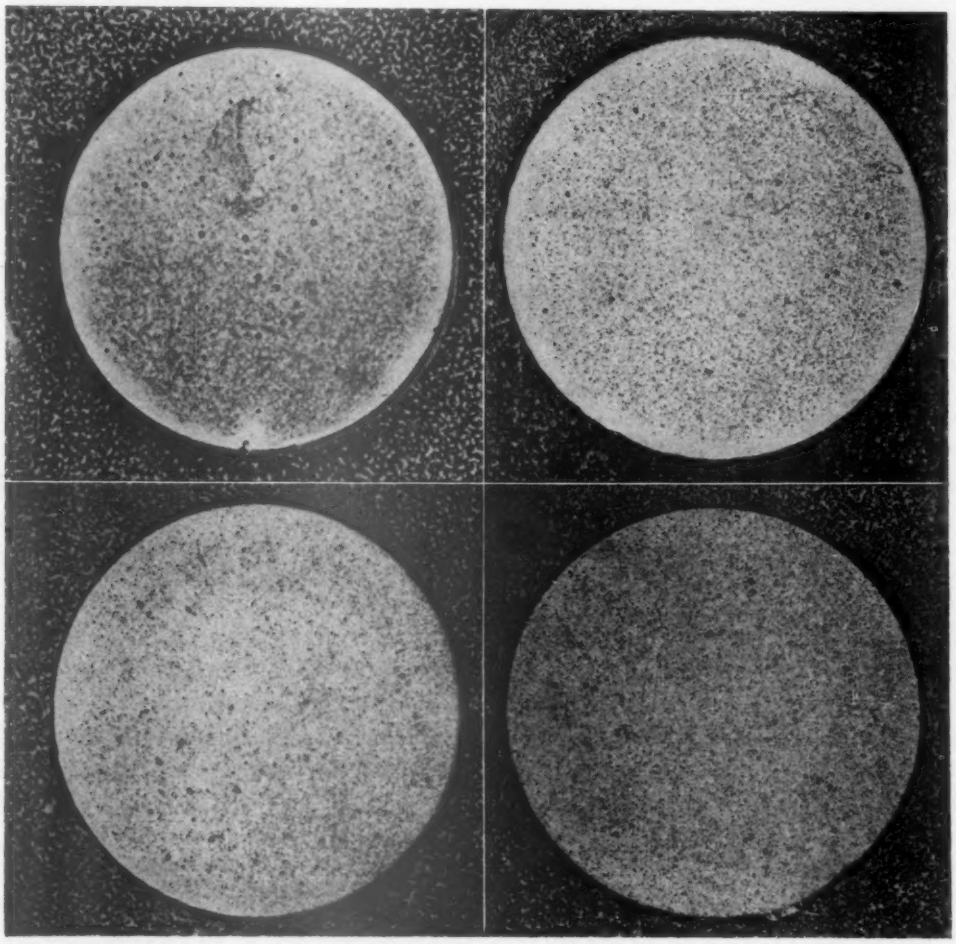

FIG 25—SPECIMENS OF 0.5 PER CENT CARBON STEEL ANNEALED 2 HOURS AT 760°C IN REHEATED BURNT CITY GAS. × 10. ETCHED IN 2 PER CENT NITAL.

Gas Analysis: 1.4 pct CO_2, 13.1 CO, 12.2 H_2, 0.1 CH_4, 2.3 H_2O, 70.9 N_2.

a. Wet; 10 liters per hour.
Exit gas: 3.4 pct CO_2, 11.7 CO, 11.2 H_2, 0.0 CH_4.

b. Wet; 70 liters per hour.
Exit gas: 1.7 pct CO_2, 12.5 CO, 12.1 H_2, 0.0 CH_4.

c. Dry; 10 liters per hour.
Exit gas: 2.0 pct CO_2, 12.0 CO, 11.7 H_2, 0.0 CH_4.

d. Dry; 70 liters per hour.
Exit gas: 1.4 pct CO_2, 13.2 CO, 11.9 H_2, 0.0 CH_4.

Burnt City Gas, Reheated and Dried

A final series of experiments was conducted, using the reheated burnt city gas as described, and drying over activated alumina. Precautions were taken to maintain the dryness of the atmosphere, as completely suppressed and in certain specimens there was evidence of slight surface carburization, especially in those treated in a high gas flow. This was supported by the order of the increase in the carbon dioxide content of the spent furnace

gases relative to the decrease in carbon monoxide, in the experiment with a low gas rate, and by the fact that the specimens so treated had a light film of soot, which could be brushed off easily, leaving the wire with a dull, etched surface.

Discussion of Results

The experiments have shown that partially burnt city gas as generated is suitable for the annealing of medium and high-carbon steels only at temperatures below approximately 680°C, when the solubility of carbon in iron is so small and the rate of decarburizing so slow that decarburization is negligible. At higher temperatures, however, even short-time treatments result in excessive decarburization, and it is necessary to reduce considerably the concentrations of the active decarburizing gases, carbon dioxide and water vapor. The removal of only one of these gases, while effecting some improvement, is insufficient to prevent decarburization of a 0.5 pct carbon steel at 760°C, but complete suppression of the reaction can be obtained in a dry atmosphere in which the ratio of carbon monoxide to carbon dioxide is greater than 9:1.

As previously pointed out, the lowest combustion ratio of air to city gas recommended for use on a city-gas burner is 2:1, this yielding a partially burnt gas containing about 10 pct carbon monoxide and 4 pct carbon dioxide. It is not possible, therefore, to produce in a generator of this type an atmosphere sufficiently low in carbon dioxide to be suitable for the annealing of carbon steels above the Ac_1 point. Reheating of the burnt gas over a catalyst, however, will reduce the carbon dioxide concentration to a sufficiently low level, and when dried the atmosphere is slightly carburizing at 760°C to a

Table 14.—*Composition of Test Atmospheres Equilibrated at* 760°C *with Respect to Reaction* $CO_2 + H_2 \rightleftarrows CO + H_2O$

Atmosphere	Composition of Gas Entering Furnace, Pct						Composition of Gas Equilibrated at 760°C, Pct						Ratio $\frac{P^2CO}{P_{CO_2}}$ in Equilibrated Gas
	CO_2	CO	H_2	CH_4	H_2O	N_2	CO_2	CO	H_2	CH_4	H_2O	N_2	
Burnt city gas as generated...	4.6	9.6	14.8	0.2	2.3	68.5	3.2	11.0	13.4	0.2	3.7	68.5	0.38
Dry burnt city gas.....	4.9	10.1	15.3	0.2	0.0	69.5	2.8	12.2	13.2	0.2	2.1	69.5	0.52
Reheated burnt city gas.....	1.4	13.1	12.2	0.1	2.3	70.9	1.9	12.6	12.7	0.1	1.8	70.9	0.89
Burnt city gas reheated and dried.....	1.6	13.7	12.8	0.1	0.0	71.8	1.0	14.3	12.2	0.1	0.6	71.8	2.05

Equilibrium ratio $\frac{P^2CO}{P_{CO_2}}$ for a 0.5 pct carbon steel at 760°C = 1.8 (after Becker[25]).

0.5 pct carbon steel, which may be an advantage in the recovery of any decarburized skin on the steel.

If the compositions of the various atmospheres used in the foregoing tests are equilibrated with respect to the water-gas reaction 6, the ratio of P^2_{CO}/P_{CO_2} in the calculated atmosphere will indicate the decarburizing properties of the ingoing furnace atmosphere (Table 14). According to Becker,[25] the equilibrium ratio of P^2_{CO}/P_{CO_2} for a 0.5 pct carbon steel at 760°C is approximately 1.8 for an undiluted mixture of carbon monoxide and carbon dioxide. According to Table 14, the reheated and dried burnt city gas would be slightly carburizing and the remaining atmospheres would be decarburizing, as was found to be true.

The tendency for a decrease in decarburization with increasing gas rate is not perfectly clear, but it is possible that this may be associated with the low tem-

perature attained by the atmosphere during its rapid circulation through the annealing pot while the steel itself was maintained by radiation at or near to the annealing temperature.

From the point of view of surface finish, the best results were obtained with the undried, reheated burnt city gas. Drying this gas promoted sooting as well as carburization and it would appear that in order to prevent decarburization and to retain a bright, clean surface, the composition of this type of atmosphere must be controlled within very critical limits.

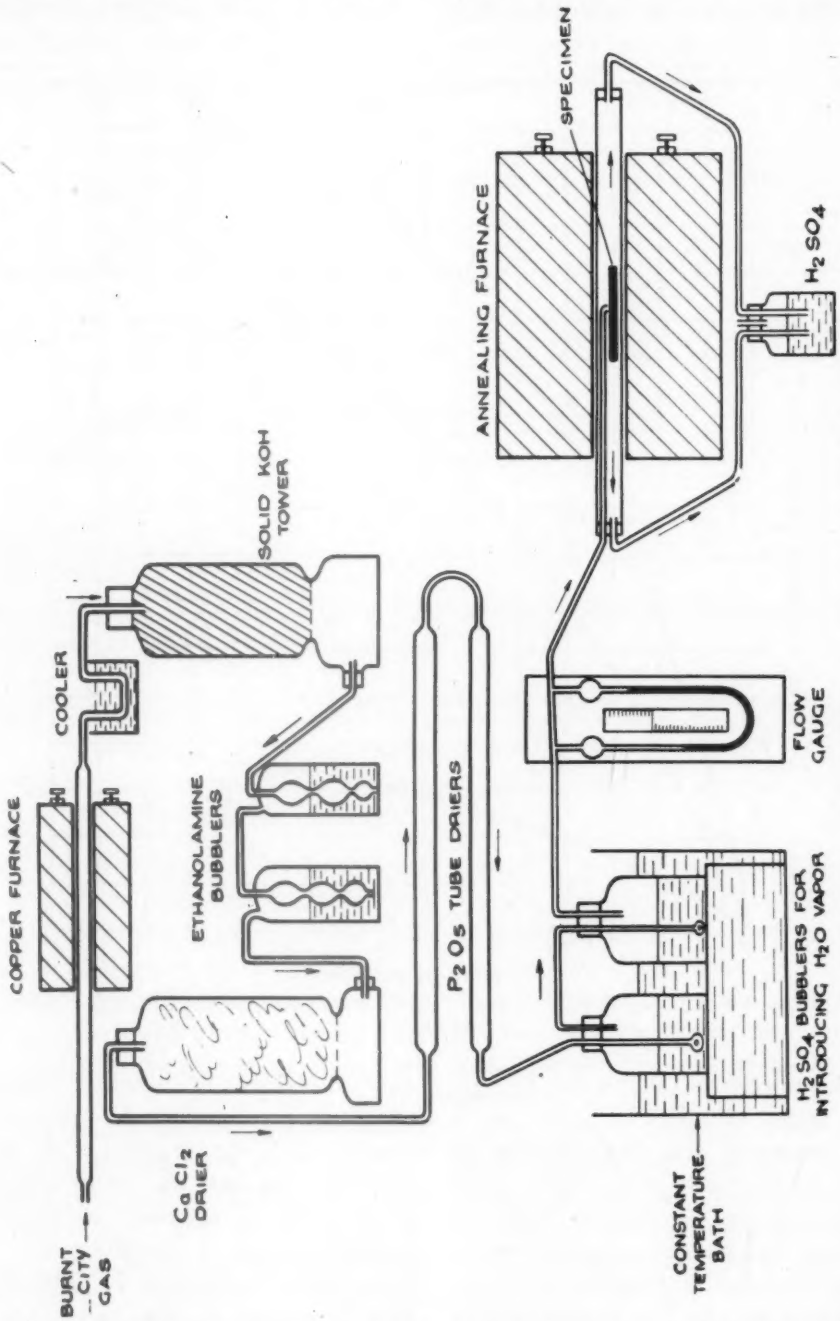

FIG 26—APPARATUS FOR DECARBURIZATION TESTS.

BURNT CITY GAS FREE FROM CARBON DIOXIDE

Experimental

All of the experiments included in this part of the investigation were carried out in the apparatus shown in Fig 26. Partially burnt city gas, supplied by a standard generator, was first fed through a furnace tube packed with copper swarf and maintained at 700°C, in order to convert any free oxygen to water vapor or carbon dioxide by reaction with the reducing gases present. The carbon dioxide and sulphurous gases were then completely absorbed by passing the atmosphere over solid caustic potash and through a solution of monoethanolamine, and the processed mixture finally was dried over calcium chloride and phosphorus pentoxide. Water vapor in controlled concentrations was reintroduced into the dried atmosphere by passing the latter through sulphuric acid solutions of known strength as described earlier in the paper. When experiments were carried out with the perfectly dry gas, the latter, after treatment over phosphorus pentoxide, was passed through a liquid-air trap before being fed to the furnace. In order to reduce the possibility of the pickup of water vapor by the dry gas, rubber connections were reduced to a minimum.

The heat-treating furnace contained three tubes of fused silica, ¾-in. inside

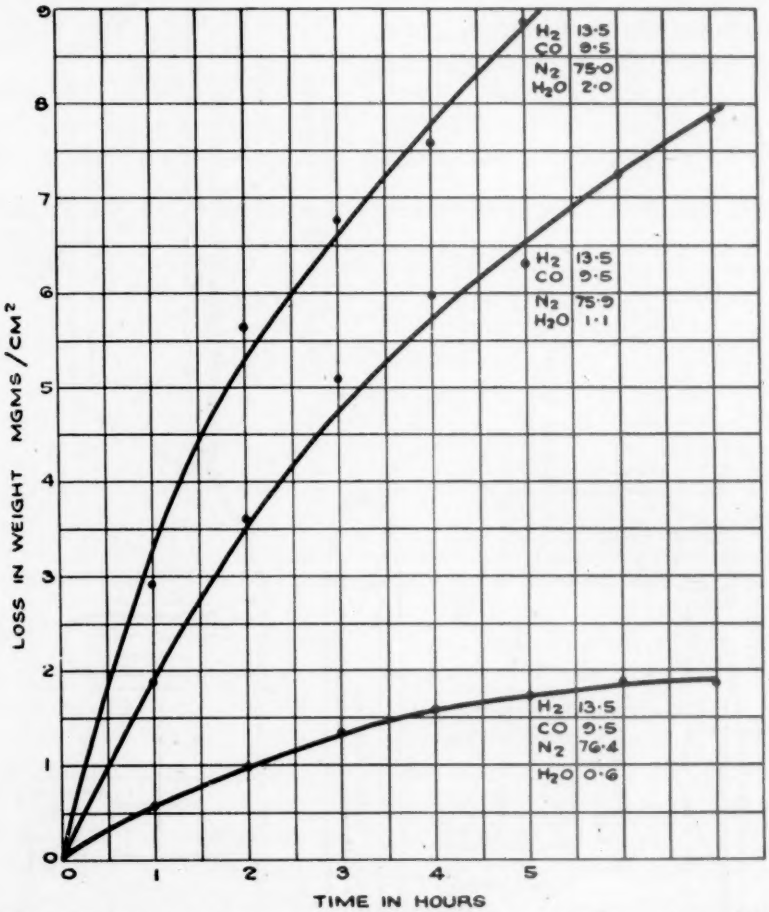

FIG 27—DECARBURIZATION OF 0.98 PER CENT CARBON STEEL AT 780°C IN H_2-CO-H_2O-N_2 ATMOSPHERES.

diameter, and was thermostatically controlled. The test atmosphere was brought in at the middle of each tube, directly above the center of the steel specimen, and was controlled to flow at equal rates to the ends of the tube, which were sealed with bubbling bottles filled with sulphuric acid. In all the experiments the gas flow employed was 10 liters per hour and cooling of the specimen was always carried out under a positive pressure and not a flow of gas.

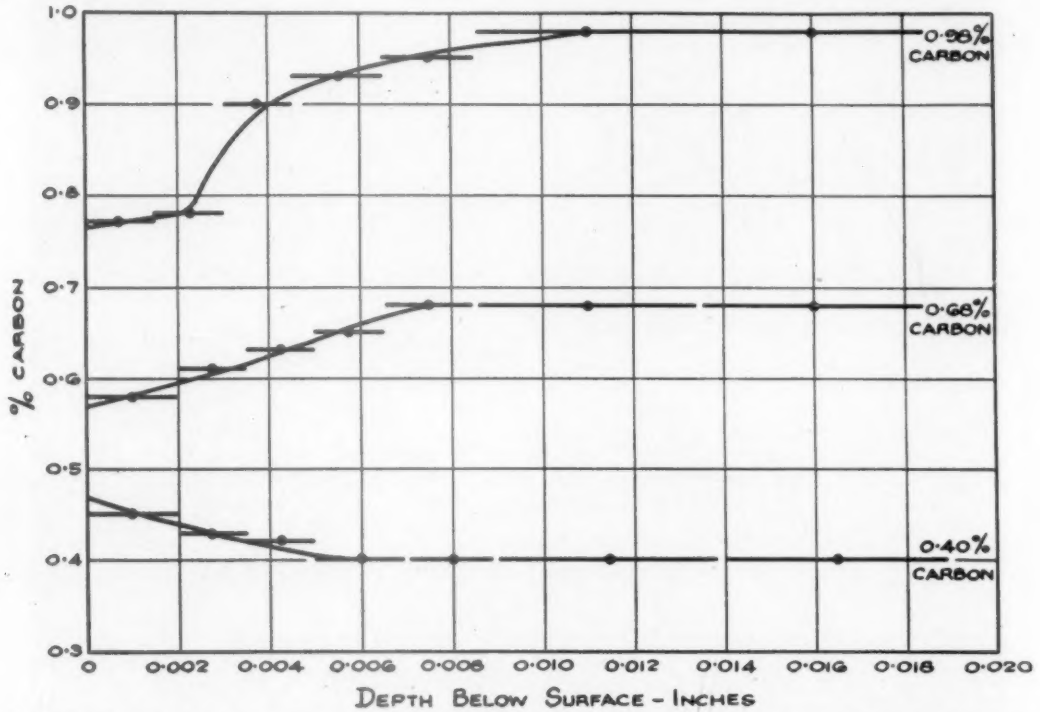

FIG 28—CARBON CONTENT VS. DEPTH FOR CARBON STEELS ANNEALED AT 750°C ONE HOUR IN ATMOSPHERE OF 9.8 PER CENT CO, 13.8 H_2, 0.75 H_2O, 75.65 N_2.

The three steels used in the experiments contained approximately 0.4 pct, 0.68 pct and 0.98 pct of carbon. Details of their compositions B, C and D are given in Table 13. Specimens for test, measuring 150 mm long by 12 mm in diameter, were turned down from ⅝-in. diameter rolled bar, any decarburization resulting from earlier processes being thereby removed. The specimens were machined to a very smooth, bright finish and before test were cleaned in acetone, dried in ether and weighed. When accurate machining was to be carried out on the annealed specimens, provision was made for the turning of the bars between centers. During test the specimen was supported centrally in the furnace tube on a silica support, which gave only point contacts with the surface of the specimen. The gradient along any specimen at the maximum temperature of treatment was never greater than ±3°C.

The results obtained were considered from the point of view of the change in carbon content and of the finish of the surface of the steel. The factors studied were the carbon content of the steel, the composition of the furnace atmosphere and the time and temperature of treatment. Experiments were carried out at temperatures of 710°, 750°, 780°, 800° and 830°C on each of the three steels. In the majority of the tests the carbon

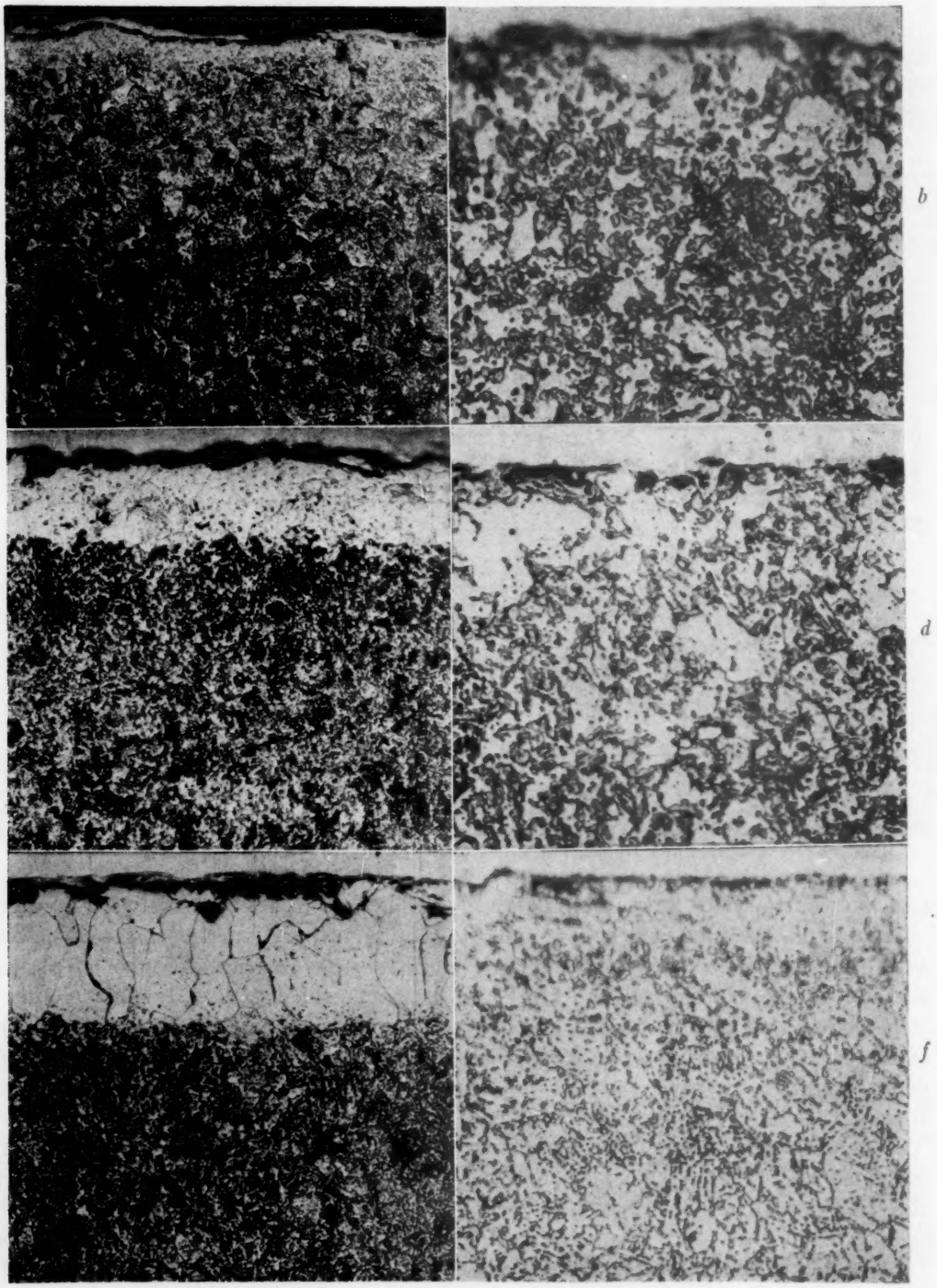

× 100.
0.98 pct carbon

× 500.
0.40 pct carbon

FIG 29—CARBON STEELS ANNEALED AT 710°C FOR 5 HOURS IN BURNT CITY GAS FREE FROM CO_2. ETCHED IN 2 PER CENT NITAL.

Effect of water-vapor content on decarburization.

Gas Analysis: CO, 9.6 pct; H_2, 13.6; plus:
a and *b*, 0.83 H_2O; *c* and *d*, 1.75 H_2O; *e* and *f*, 2.74 H_2O; remainder N_2.

Loss: *a*, 0.17 mg per sq cm — *b*, 0.07 mg per sq mm
c, 0.63 mg per sq cm — *d*, 0.26 mg per sq mm
e, 0.91 mg per sq cm — *f*, 0.32 mg per sq mm

monoxide and hydrogen contents of the furnace atmosphere were maintained as constant as possible at 9.6 and 13.75 pct, respectively, the water-vapor content being varied. Decarburization or otherwise was determined by change in weight measurements and by metallographic examination, and some of the results obtained are shown in Figs 29 to 32. Typical loss in weight-time curves are shown in Fig 27. For tests at 750°C carbon analyses were made on samples turned off the treated bars at various depths below the surface. Curves for carbon content vs depth typical of that shown in Fig 28 were thereby obtained. Details of the results obtained from all the experiments are given in Table 15.

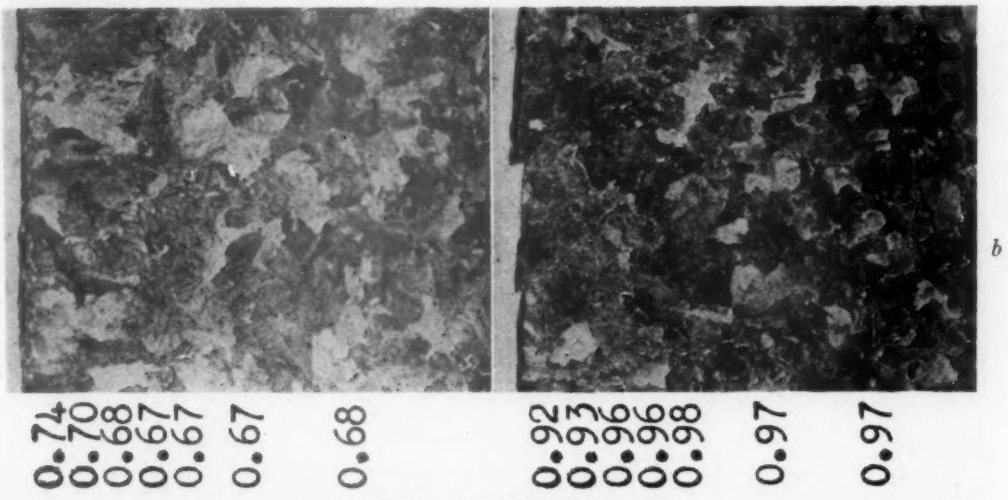

FIG 30—EFFECT OF WATER VAPOR ON DECARBURIZATION OF CARBON STEELS ANNEALED AT 750°C FOR 5 HOURS IN A BASIC ATMOSPHERE OF 9.8 PER CENT CO, 13.8 H_2, 76.4 N_2. × 100. ETCHED IN 2 PER CENT NITAL.

a and *c*, 0.68 pct carbon steel *b* and *d*, 0.98 pct carbon steel

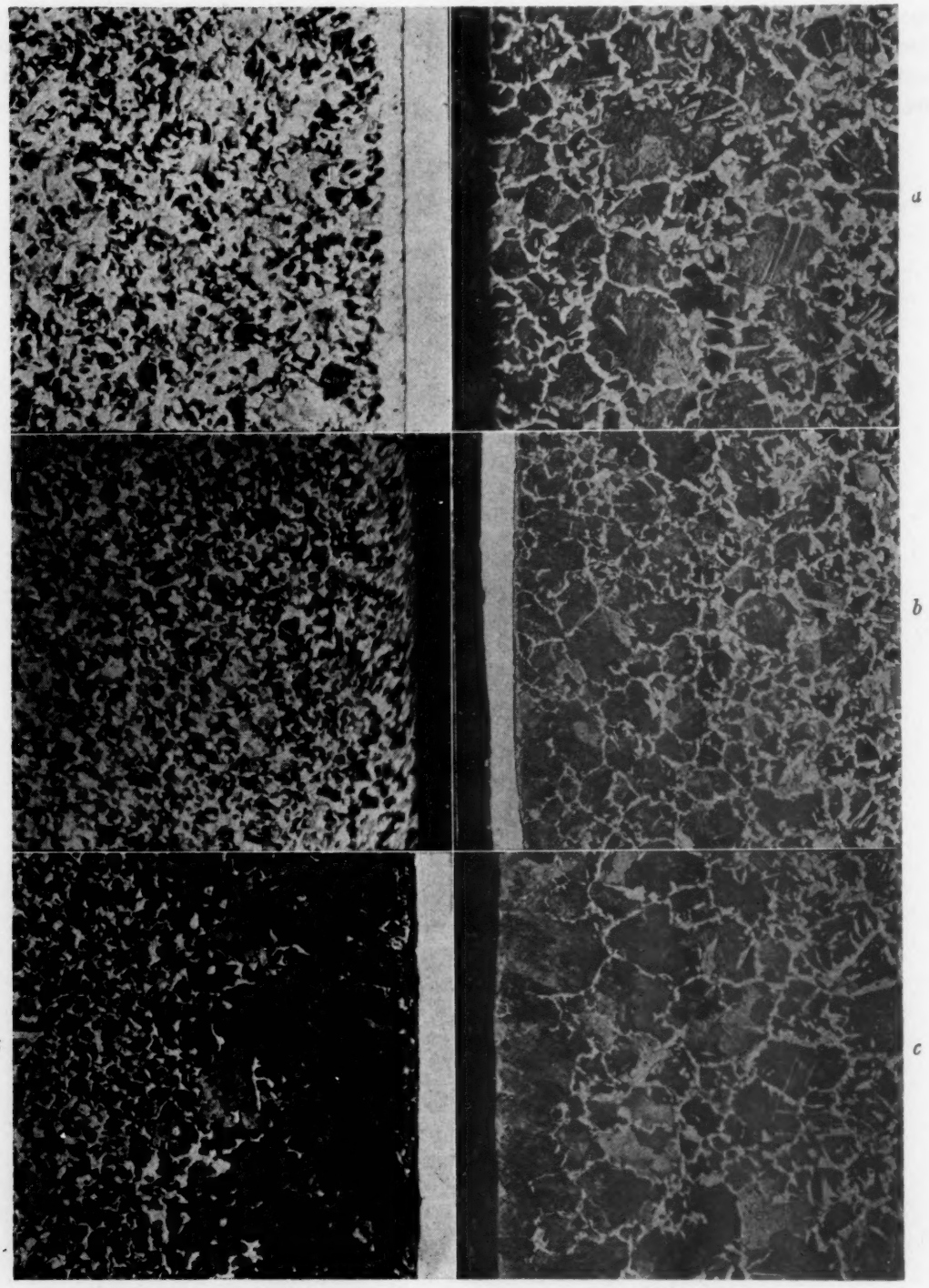

Fig 31, 780°C × 200. Fig 32, 830°C × 100.

FIGS 31 AND 32—SPECIMENS OF 0.4 PER CENT CARBON STEEL HEATED FOR 5 HOURS IN BURNT CITY GAS FREE FROM CO_2. ETCHED IN 2 PER CENT NITAL.

Ingoing gas, Fig 31:

a. CO, 10.2 per cent; H_2, 15.2; H_2O, 0.75.
b. CO, 10.2 per cent; H_2, 15.2; H_2O, 0.54.
c. CO, 10.2 per cent; H_2, 15.2; H_2O, 0.15.

Ingoing gas, Fig 32:

a. CO, 9.6 per cent; H_2, 13.6; H_2O, 0.34.
b. CO, 9.6 per cent; H_2, 13.6; H_2O, 0.26.
c. CO, 9.6 per cent; H_2, 13.6; H_2O, 0.15.

Discussion of Results

Bramley and co-workers[26] have reported on the effect of hydrogen in promoting the rate of carburization of iron in carbon monoxide-hydrogen atmospheres, and the present investigation has shown that the carburizing properties of such atmospheres persist down to temperatures as low as 750°C (Fig 30).

The results obtained have shown that the carburizing properties can be neutralized by a controlled concentration of water vapor, thus establishing an equilibrium condition between the active gases in the controlled atmosphere and the carbon content of the steel, according to reaction 8:

$$C + H_2O \rightleftarrows CO + H_2 \quad [8]$$

With an atmosphere of fixed carbon monoxide and hydrogen contents, the equilibrium concentration of water vapor

TABLE 15.—*Heat-treatment of Carbon Steels in Burnt City Gas, Free from* CO_2

Carbon in Steel as Received, Pct	Temperature of Treatment, Deg C	Time at Temperature, Hr	Heat-treating Atmosphere, Pct				Change in Weight, Mg per Sq Cm	Surface Carbon Content (Analyzed), Pct	Steel Surface	
			CO	H_2	H_2O	N_2			Metallographic Examination	Appearance after Treatment
0.40	710	5	9.6	13.6	2.74	74.06	−0.32		Decarburized	Clean and bright
			9.6	13.6	1.75	75.05	−0.26		Decarburized	Lightly sooted
			9.6	13.6	0.83	75.97	−0.07		Slightly decarburized	Thin adherent deposit of carbon
0.98	710	5	9.5	13.5	2.74	74.26	−0.91		Decarburized	Clean and bright
			9.5	13.5	1.75	75.25	−0.63		Decarburized	Bright except for carbon deposit nearest gas inlet
			9.5	13.5	0.83	76.17	−0.17		Slightly decarburized	Lightly sooted
0.40	750	1	9.9	13.8	0.11	76.19	+0.59	0.62	Carburized	Thin surface film of carbon
			9.9	13.8	0.21	76.09	+0.43	0.52	Carburized	Thin surface film of carbon
			9.9	13.8	0.39	75.91	+0.31	0.48	Carburized	Thin surface film of carbon
			9.9	13.8	0.75	75.55	+0.06	0.45	Slightly carburized	Thin surface film of carbon
0.68	750	1	9.8	13.8	0.11	76.29	+0.31	0.93	Carburized	Thin surface film of carbon
			9.8	13.8	0.21	76.19	+0.21	0.83	Carburized	Thin surface film of carbon
			9.8	13.8	0.39	76.01	+0.07	0.75	Slightly carburized	Thin surface film of carbon
			9.8	13.8	0.75	75.65	−0.08	0.59	Slightly decarburized	Clean and bright
0.98	750	1	9.8	13.8	0.11	76.29	+0.23	1.27	Carburized	Thin surface film of carbon
			9.8	13.8	0.21	76.19	+0.09	1.16	Carburized	Thin surface film of carbon
			9.8	13.8	0.39	76.01	+0.03	0.98	No change	Bright except for carbon deposit near gas inlet
			9.8	13.8	0.75	75.65	−0.26	0.77	Decarburized	Clean and bright
0.40	780	5	10.2	15.2	0.75	73.85			Slightly decarburized	Clean and bright
			10.2	15.2	0.54	74.06			Slightly carburized	Very light sooting
			10.2	15.2	0.40	74.20			Carburized	Thin surface film of carbon
			10.2	15.2	0.15	74.45			Carburized	Thin surface film of carbon
0.98	780	5	9.6	13.6	0.60	76.20			Decarburized	Clean and bright
			9.6	13.6	0.40	76.40			Slightly decarburized	Bright except for carbon deposit near gas inlet
			9.6	13.6	0.15	76.65			Slightly carburized	Thin surface film of carbon
0.40	800	1	9.9	13.8	0.21	76.09	+0.30		Carburized	Thin surface film of carbon
			9.9	13.8	0.25	76.05	+0.22		Carburized	Thin surface film of carbon
0.68	800	1	9.9	13.8	0.21	76.09	+0.04		Slightly carburized	Light carbon deposit, mainly near gas inlet
			9.9	13.8	0.25	76.05	0.0		No change	Clean and bright
0.98	800	1	9.9	13.8	0.21	76.09	0.0		No change	Light carbon deposit, mainly near gas inlet
			9.9	13.8	0.25	76.05	−0.17		Decarburized	Clean and bright
0.40	830	5	9.6	13.6	0.34	76.46	+0.03		Slightly carburized	Clean and bright
			9.6	13.6	0.26	76.54	+0.11		Carburized	Thin surface film of carbon
			9.6	13.6	0.15	76.65	+0.39		Carburized	Surface film of carbon
0.98	830	5	10.2	15.2	0.34	74.26	−0.46		Decarburized	Clean and bright
			10.2	15.2	0.26	74.34	−0.21		Decarburized	Clean and bright
			10.2	15.2	0.15	74.45	0.0		No change	Clean and bright

decreased with both the carbon content of the steel and the temperature of treatment, and becomes increasingly critical at temperatures above approximately 750°C. Thus, for example, a decrease of 0.60 pct in the water-vapor content can convert an atmosphere that is decarburizing for a 0.4 pct carbon steel at 780°C into one that is strongly carburizing (Fig 31). At 830°C only a small variation (less than 0.1 pct) in the water-vapor content outside its equilibrium concentration is required to have a very marked effect upon the carbon content of the steel surface (Fig 32). Further, having fixed the carbon monoxide and hydrogen concentrations by a selected combustion ratio on the burnt-city-gas generator, it is necessary to ensure that these concentrations shall be maintained, otherwise the equilibrium concentration of the water vapor will change accordingly.

At temperatures below 800°C, sooting of the steel was obtained where the atmosphere used was either neutral or carburizing and, in certain cases, even when the steel showed surface decarburization after treatment. The soot thus deposited, on X-ray examination, proved to be the so-called "amorphous" carbon, as distinct from the high-temperature graphitic form. The relative stabilities of cementite and of graphite have been the subject of much investigation and discussion, but the comparatively recent work of Wells and Mehl[6,7] has definitely established that iron carbide is unstable relative to graphite and iron saturated with graphite at temperatures above 650°C. The present work and the experimental conditions obtaining do not permit of any definite conclusions, but it would be of interest to establish whether cementite is also unstable with respect to the "amorphous" carbon described above.

The bright annealing of high-carbon steel below 800°C in the type of atmosphere used in the present investigation, therefore, is attained only at the expense of some decarburization. However, it has been found that if the combined partial pressures of the carbon monoxide and hydrogen are decreased, there is an apparent slight increase in the value of the equilibrium constant with respect to a given carbon steel for the reaction 8 (Table 16):

$$C + H_2O \rightleftarrows CO + H_2 \qquad [8]$$

Bramley and Turner[26] have reported that the effect of hydrogen in promoting carburization by carbon monoxide reaches a maximum when the volume ratio of hydrogen to carbon monoxide is approximately 2:1. In the atmospheres detailed in Table 16, this ratio decreases from 1.54:1 to 0.98:1, with a corresponding decrease in the degree of carburization.

The effect of hydrogen in promoting carburization by carbon monoxide is associated probably with side reactions

TABLE 16.—*Heat-treatment of* 0.98 *Per Cent Carbon Steel at* 750°C *for One Hour in* CO_2—H_2—H_2O—N_2 *Atmospheres*

Effect of P_{H_2}/P_{CO} Ratio on Decarburization

Ingoing Gas			Equilibrated Gas				Equilibrated Gas		Change in Weight of Steel, Mg per Sq Cm	Condition of Steel after Test
CO	H_2	H_2O	CO_2	CO	H_2	H_2O	$\frac{P_{CO} \cdot P_{H_2}}{P_{H_2O}}$	$\frac{P_{H_2}}{P_{CO}}$		
10.2	15.2	0.45	0.20	10.00	15.40	0.25	6.2	1.54	+0.04	No change
9.8	13.8	0.39	0.18	9.62	13.98	0.21	6.4	1.46	+0.03	No change
7.6	8.8	0.21	0.11	7.49	8.91	0.10	6.7	1.19	−0.06	Slightly decarburized
5.8	5.6	0.10	0.055	5.745	5.655	0.045	7.2	0.98	−0.21	Decarburized

in the adsorbed film on the surface of the steel:

$$H_2 + CO_2 \rightleftarrows H_2O + CO \quad [6]$$
$$2CO \rightleftarrows CO_2 + C \quad [7]$$

trations of part or all of the reactants. The apparent variation in the value of the equilibrium constant for reaction 8 with the ratio of hydrogen to carbon monoxide

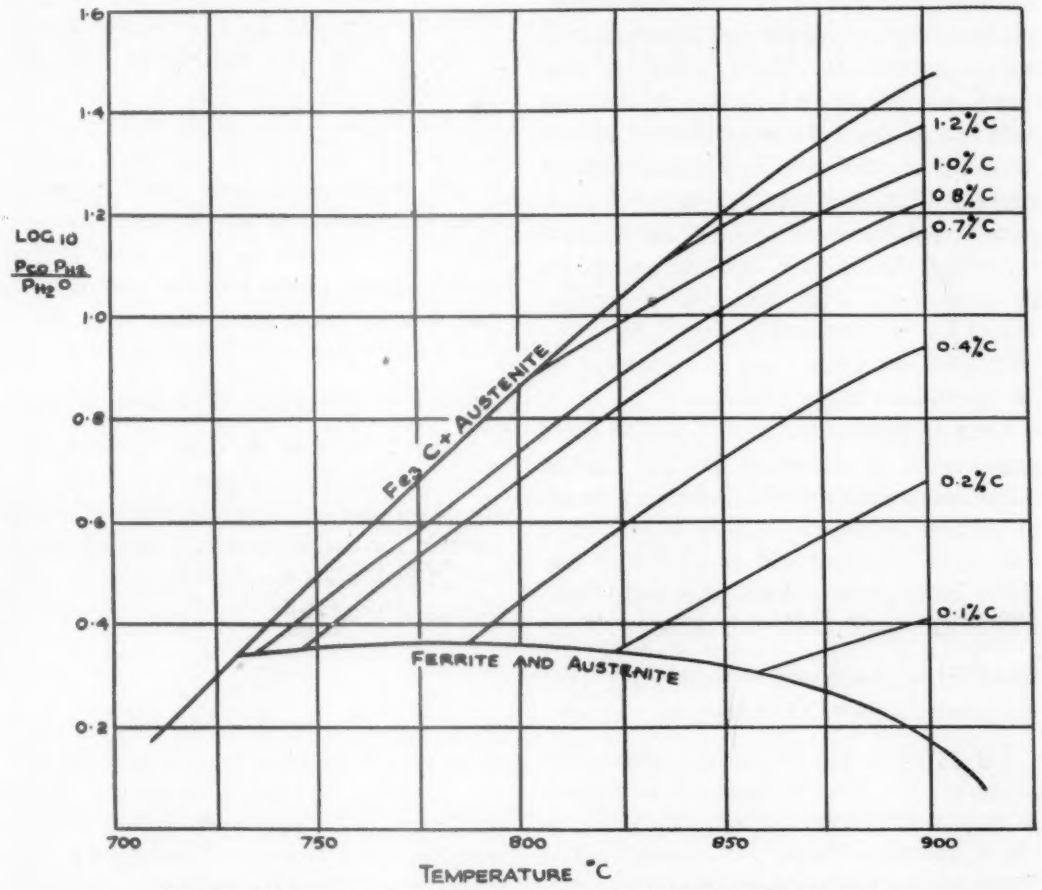

FIG 33—EQUILIBRIUM FOR SYSTEM C (IN IRON) + $H_2O \leftrightarrows CO + H_2$.
Calculated values from data for reactions C (in iron) + $CO_2 \leftrightarrows 2CO$ (*Becker*[25]), $CO + H_2O \leftrightarrows CO + H_2$ (*Austin and Day*[4]).
Data for 1.0 per cent C and 0.7 per cent C obtained by extrapolation.

The symbol "C" in reaction 7 refers to carbon in iron. The carbon dioxide formed from reaction 7 tends to "blanket" the steel surface against further carburization by the carbon monoxide. The hydrogen, however, being strongly adsorbed, promotes the removal of the carbon dioxide according to reaction 6 and thus maintains the carburizing reaction.

It is impossible in any system, however, that the equilibrium constant of the whole at any one temperature can vary appreciably according to the concen- probably is associated with the slowing down of the reaction velocity, and it would seem that the speed of the forward carburizing reaction is proportional to the product $(P_{CO}) \times (P^2_{H2})$. Hence, in atmospheres in which no water vapor is present, the maximum rate of carburization will be attained in one in which the ratio of hydrogen to carbon monoxide is 2:1. At ratios different from this optimum value, the velocity of reaction to equilibrium is slowed down, so that for short-term treatments an apparent variation

in the value of the equilibrium constant of the system may be obtained.

Reaction velocities in gas-metal systems, especially those associated with the heat-treatment of metals in controlled atmospheres, do not appear to have received sufficient attention. An equilibrium constant for a reaction serves as a very valuable guide to the assessment of correct atmosphere conditions in a heat-treatment process. From the practical point of view, however, data on the permissible latitude on either side of true equilibrium, which is associated with reaction velocities, would be most valuable, especially when correlated with the time of treatment at any particular temperature.

Decarburization at 710°C can be quite appreciable, as shown in Fig 29. On the other hand, atmospheres containing excess of carbon monoxide and hydrogen, gave rise to sooting but not to carburization, since in the steels used the alpha iron was already saturated with carbon.

Equilibrium for System C (in iron) + $H_2O \rightleftarrows CO + H_2$

Fig 33 gives the theoretical equilibrium diagram for the system with respect to steels of various carbon contents, in the temperature range 700° to 900°C. The diagram has been constructed from the known data for the following reactions:

$$CO + H_2O \rightleftarrows CO_2 + H_2 \qquad K_6$$

$$\text{C (in iron)} + CO_2 \rightleftarrows 2CO \qquad K_7$$

$$\text{C (in iron)} + H_2O \rightleftarrows CO + H_2 \qquad \frac{K_7}{K_8} = K_6 \cdot K_7$$

From the experimental results detailed in Table 15, atmosphere compositions can be selected which, for any test temperature and carbon steel, were found to be nondecarburizing and at the same time gave the minimum degree of carburization of the atmospheres used. The selected compositions are listed in Table 17 and have been equilibrated with respect to the water-gas reaction 6 at the particular test temperature. The table also gives the corresponding equilibrium ratios of

$$\frac{P_{CO} \cdot P_{H_2}}{P_{H_2O}}$$

for the particular test conditions as derived from Fig 33. The experimental results are in good agreement with the theoretical data (Table 17), except for the results at 710°C. With regard to the latter, most of the steel specimens treated at the temperature were sooted, arising from the breakdown of carbon monoxide, which would result in an increase in the decarburizing power of the atmosphere and a loss in its potential carburizing power due to the deposition of carbon.

Control of Atmosphere for Industrial Use

The investigation has shown that burnt city-gas mixtures, processed for the removal of carbon dioxide, can be made suitable for the annealing of carbon steels with freedom from decarburization, by control of the ratio

$$\frac{P_{CO} \cdot P_{H_2}}{P_{H_2O}}$$

Control of Ratio.—The following methods of control of the ratio suggest themselves:

1. Drying of the atmosphere to a fixed dew point and varying the carbon monoxide and hydrogen contents by control of the original air–city-gas combustion ratio.

2. Constant carbon monoxide and hydrogen concentrations, and variation of the dew point by controlled refrigeration.

3. Constant carbon monoxide and hydrogen concentrations and complete drying of the bulk of the gas over activated alumina, by-passing sufficient of the undried gas to give a water-vapor content in the final mixture, necessary for equilibrium.

In view of the foregoing investigation, method 1 is not practicable, since a

variation in the combustion ratio will affect both the carbon monoxide and hydrogen contents, and control would be thereby complicated. Further, as already shown, the reaction velocities are dependent upon the ratio of carbon monoxide to hydrogen in the atmosphere, and some knowledge of the equilibrium tolerances for different carbon monoxide-hydrogen ratios would be necessary for satisfactory operation. Controlled refrigeration to a dew point less than 0°C introduces difficulties associated with refrigerator design and performance, which have not, as yet, been satisfactorily overcome. Method 3 however, does not present any great difficulty in control, provided that the water-vapor content of the undried atmosphere is reasonably constant. Normally, the carbon dioxide in the atmosphere is removed by absorption, in which case the dew point of the purified gas is determined by the vapor pressure, or, in other words, the temperature of the absorbent, which, in a closed circuit involving absorption and regeneration, is reasonably well stabilized.

TABLE 17.—*Experimental Results in Relation to Equilibrium for the System* C (in iron) $+ H_2O \rightleftarrows CO + H_2$

Carbon in Steel, Pct	Temperature-Deg C	Ingoing Gas			Equilibrated Gas				$\frac{P_{CO} \cdot P_{H_2}}{P_{H_2O}}$		Condition of Treated Steel
		CO	H_2	H_2O	CO_2	CO	H_2	H_2O	In Equilibrated Gas	For Equilibrium	
0.4	710	9.6	13.6	0.83	0.43	9.17	14.03	0.40	3.2	1.87	Slightly decarburized
	750	9.9	13.8	0.75	0.35	9.55	14.25	0.40	3.4	2.27	Slightly carburized
	780	10.2	15.2	0.54	0.24	9.96	15.44	0.30	5.1	2.3	Slightly carburized
	800	9.9	13.8	0.25	0.08	9.82	13.88	0.18	7.6	2.9	Carburized
	830	9.6	13.6	0.34	0.14	9.46	13.74	0.20	6.5	4.17	Slightly carburized
0.68	750	9.8	13.8	0.39	0.18	9.62	13.98	0.21	6.4	2.6	Slightly carburized
	800	9.9	13.8	0.25	0.10	9.80	13.9	0.15	9.1	5.01	No change
0.98	710	9.5	13.5	0.83	0.41	9.09	13.91	0.42	3.0	1.86	Slightly decarburized
	750	9.8	13.8	0.39	0.21	9.59	14.01	0.18	7.5	3.65	No change
	780	9.6	13.6	0.4	0.18	9.42	13.78	0.22	5.8	5.89	Slightly decarburized
	800	9.9	13.8	0.21	0.06	9.84	13.86	0.15	9.1	8.13	No change
	830	10.2	15.2	0.15	0.01	10.19	15.21	0.14	11.1	11.16	No change

Conclusions

1. City gas itself is unsuitable as an atmosphere for the annealing of steels, but by controlled combustion with air the hydrocarbons can be almost completely eliminated and the reducing gases controlled over fairly wide limits of concentration. The main factors influencing the composition of the generated gas are the composition of the raw gas, the combustion ratio, the temperature attained in the generator, and the use of catalysts in the combustion chamber.

2. A low air-gas combustion ratio and a low burner temperature promote sooting in the combustion chamber, and free oxygen and unsaturated hydrocarbons may be retained in the generated gas. On the other hand an excessively high temperature promotes the premature cracking of the hydrocarbons, with the formation of a hard coke, which gives rise to excessive back pressure and stoppages. The recommended lower limit of combustion ratio is 1.75:1 and maximum generator temperature, 1100° to 1250°C. Metal catalysts in the combustion chamber promote inter-gas reactions but have a short, effective life and are better employed in subsequent processing of the cooled and desulphurised burnt gas.

3. The design of the combustion chamber is important and should be such that the recommended temperature conditions are

obtained within the rated capacity of the generator. A minimum contact time of 5 sec between the gases and the combustion chamber is recommended.

4. The decarburizing power of partially burnt city gas can be reduced appreciably by reheating the cooled gas in contact with a suitable catalyst whereby the following reaction is promoted:

$$CO_2 + H_2 \rightleftarrows CO + H_2O$$

The water vapor thus produced can be partly or wholly removed by combustion and/or drying and the process repeated with a continued reduction in the carbon dioxide concentration.

5. The etching of low-carbon steel in partially burnt city gas increases rapidly with rising temperature, with the degree of combustion of the raw gas and with the carbon content of the steel. Below approximately 700°C the primary reaction responsible for the etching is the "water-gas" reaction:

$$CO_2 + H_2 \rightleftarrows CO + H_2O$$

The extent of the etching is increased if there is present in the steel an element capable of reaction at the surface with any of the surrounding gases. Below 725°C, this latter effect is probably very small, but above the critical temperature it is considered to be the major factor contributing to surface etching.

6. Iron is an active catalyst for the "producer-gas" reaction ($2CO = CO_2 + C$) and when cooled in partially burnt city gas such as is used for bright annealing, sooting is obtained at temperatures as low as 250°C. The extent of the sooting is determined primarily by the rate of cooling and by the activity of the iron or steel surface. In the latter connection a cold-rolled surface is the least active, a reduced oxide surface slightly more so, and a gas-etched surface very active. Similarly, reduced rust provides active centers of unsintered iron particles around which sooting takes place. Slow cooling under a flow of gas, as in batch furnaces for example, leads to sooting, but in continuous furnaces the rate of cooling is sufficiently great to prevent the effect, provided that gas etching of the metal surface has not taken place to any appreciable degree.

The decomposition of carbon monoxide appears to be promoted in the presence of carbon dioxide. Water vapor has a similar effect, although the perfectly dry gas gives rise to greater sooting than one with about 0.005 pct of water vapor. High gas flows do not reduce appreciably the amount of sooting.

7. Rolling lubricants may give rise to surface staining due to the dissociation of the heavy oil vapors during annealing. There should be the minimum delay between working and annealing in order to prevent oxidation of the oil on standing in air, since this tends to give gummy deposits. Soap-drawn wire can be clean annealed if a very slow rate of heating is employed. Alternatively the wire can be preoxidized in air up to about 550°C to burn off the soap, followed by completion of the anneal in burnt city gas, which gives a clean, matte surface finish.

8. Burnt city gas does not descale hot-rolled strip as rapidly as a burnt ammonia atmosphere of the composition normally used for this purpose, excepting the atmospheres so rich in hydrogen and carbon monoxide as to be explosive and toxic.

9. Partially burnt city gas is suitable, as generated, for the bright annealing of medium and high-carbon steels only at temperatures below approximately 680°C. At higher temperatures the concentrations of carbon dioxide and water vapor lead to excessive decarburization. The complete removal of both of these gases leaves an atmosphere that is carburizing to carbon steels at temperatures above approximately 750°C. The carburizing power,

however, can be neutralized by a controlled concentration of either of the decarburizing gases. Thus, controlled low concentrations of carbon dioxide can be obtained by reheating the generated gas, cooling and drying as in the manner already described. Alternatively, if carbon dioxide is completely removed, the dew point of the gas can be suitably controlled; as, for example, by the controlled mixing of the undried and the dried gas.

10. In either of the modified burnt city gas atmospheres it does not appear to be possible to bright anneal, without decarburization, below 800°C, since a nondecarburized surface is obtained only with some sooting. The soot produced is the so-called "amorphous" carbon and it is possible that equilibrium conditions with respect to this form of carbon differ from those for graphitic carbon.

11. Hydrogen in the burnt city gas increases the carburizing power of the carbon monoxide, possibly by promoting the removal of adsorbed films of carbon dioxide, but as the ratio of carbon monoxide to hydrogen decreases, the effect is less pronounced.

12. With increasing temperature the equilibrium concentration of the decarburizing gas becomes increasingly critical and only a very small variation near to the equilibrium point is required to cause a change in the surface carbon content of the steel. It is advisable to take adequate precautions to prevent the pickup of decarburizing gases by the atmosphere either en route to the furnace or inside the heat-treating chamber.

References

1. F. Heathcoat: *Fuel* (1934) **12**(2), 36–44.
2. J. A. Dow: Discussion in Carburizing Symposium. *Trans.* Amer. Soc. for Metals (1937) 115–116, 310.
3. H. W. Smith: *Wire and Wire Products*, 14(11), 643–645, 655; *Metal Ind.* (London) (1939) **55**, 550–552.
4. J. B. Austin and M. J. Day: Controlled Atmospheres. Amer. Soc. for Metals.
5. J. Chipman and S. Marshall: *Jnl.* Amer. Chem. Soc. (1940) **62**, 299.
6. R. F. Mehl and C. Wells: *Trans.* A.I.M.E. (1937) **125**, 429.
7. C. Wells: *Trans.* Amer. Soc. for Metals (1938) **26**, 289.
8. W. Herwig: *Stahl und Eisen* (1931) **33**, 1721.
9. W. P. Sykes: *Trans.* Amer. Soc. Steel Treat. (1927) **12**, 737.
10. C. R. Austin: *Trans.* Amer. Soc. Steel Treat. (1934) **22**, 31.
11. V. F. Körber and W. Oelsen: *Archiv Eisenhüttenwesen* (1931) **5**, 569.
12. E. E. Slowter and B. W. Gonser: *Metals and Alloys* (1937) **8**, 159–168, 195–205; (1938) **9**, 33–39, 59–62.
13. E. E. Slowter and B. W. Gonser: *Metal Progress* (1941) **39**, 560–566, 628.
14. A. Johansson, R. Von Seth and N. Elfstrom: *Jernkontorets Ann.* (1932) **116**, 565.
15. A. L. Marshall: *Trans.* Amer. Soc. for Metals (1934) **22**, 605–625.
16. U. Schwedler: *Metalltechnik* (1938) **17**(38), 1006.
17. A. G. Hotchkiss: Symposium on Furnace Atmospheres for Metallurgical Processes. Amer. Chem. Soc. Div. of Gas and Fuel Chemistry, 1940.
18. S. Tour: Amer. Soc. for Metals Preprint No. 6 (Oct. 1940).
19. J. W. Mason and B. F. Dodge: *Trans.* Amer. Inst. Chem. Eng. (1936) (**331**), 27–48.
20. P. R. Bottoms: *Chem. and Met. Eng.* (1931) **38**, 465.
21. S. Tour: *Trans.* Amer. Soc. for Metals (1940) **29**, 710.
22. I. Jenkins and S. V. Williams: Brit. Pat. 481283.
23. F. R. Schenk: Physical Chemistry of Metals. New York, 1919. John Wiley and Sons.
24. I. Jenkins and S. V. Williams: Brit. Pat. No. 539556.
25. M. L. Becker: *Jnl.* Iron and Steel Inst (1930) **121**, 337.
26. A. Bramley and G. Turner: Iron and Steel Inst. Carnegie Schol. Mem. (1922) **57**, 23–66.

DISCUSSION

(H. S. Avery presiding)

C. E. Peck*—Mr. Jenkins has presented a very complete survey of this subject and has supplemented it with his own tests and operating experience. Such data are of great value in published form.

The tests which were run using city gas with carbon dioxide scrubbed out show the importance of limiting the water vapor content to very low values if decarburization is to be prevented. In tests shown in Fig 27, water vapor was too high to prevent decarburization.

* Westinghouse Electric Corporation, Meadville, Pa.

Experiences in United States using any type of fuel gas source including city gases have shown that it is possible to bright anneal high carbon steel (1 pct and higher) for long cycles in critical range and not lose any carbon from surface using a gas of composition approximately as follows: CO 3 pct, H_2 4 pct, H_2O 0.01 pct or less, and balance N_2. In other words all CO_2 and H_2O are completely removed from the gas. A gas of this composition is quite inert and yet has no decarburizating tendency because of the very low water vapor content and presence of some CO but not enough CO to cause etching or sooting as steel is slowly cooled down after annealing.

In connection with bright hardening high carbon content steels without decarburization, equipment has been successfully developed and applied to thoroughly react very rich mixtures of air and *city gas* heated in prience of a catalyst to produce a gas containng no CO_2 and dewpoints of the order of 0°F. This is done much more easily with high hydrocarbon gases such as natural gas, propane, and butane, than it is with city gas which contains very much smaller amounts of hydrocarbons.

However, through a means of depositing and controlling formation of free carbon in catalyst bed produced directly from the gas, it is possible to react city gases to a nondecarburizing composition even though they contain appreciable CO_2 to start with. This development allows direct use of city gas for bright hardening whereas previously it was not practical to do this.

S. Tour*—The paper is interesting, not only because it is timely, but because it presents new and useful information and points the way for further work. Mr. Jenkins is to be congratulated for having been able to pack so much worth while information into one paper and to have put it in such clear and understandable form.

Mr. Jenkins makes references to two papers presented by me to the American Society for Metals in 1940; one concerns water vapor and the other atmosphere generators. In the intervening six years practically every manufacturer in this country of furnace atmosphere generators has applied some of the principles outlined in those two papers to the design and construction of their equipment.

The suggestion by Mr. Jenkins that the temperature along the length of the combustion chamber might be maintained more uniformly by supplying the mixture of air and gas at intervals along its length is worthy of most serious consideration by the equipment builders. When using the richer mixes, some difficulties may be encountered in maintaining the combustion reaction at the multiple individual burners. Placing catalyst-carrying refractory material near the burners is of some assistance in this matter but introduces difficulties resulting from overheating when leaner mixtures or larger volumes are used. It does not seem feasible to construct the combustion chambers so that the distance from burner tip to refractory may be varied and so adjusted for mixture ratios and volumes.

The writer's suggestion of 1940 that external heating be used to provide the required temperature in depth in the combustion chamber is widely used in this country. Unfortunately, most of the constructions in use do not provide for zonal control of heat input and, therefore, of temperature. The result is that there is a tendency to overheat near the burner with lean mixtures and underheat with the richer mixes. When the heat input is subject to zonal control, it is possible to operate any one given generator over a large range of mixes and over a wide range of volumes and still maintain an accurate control over the product of the generator.

There is another possible method of control which might be superimposed upon the zonal heat control and permit of using the same generator with such lean mixes as those approaching perfect combustion. This method involves the use of water spray atomized or injected as steam with the gas-air mixture being fed to the burners. The introduction of water in this fashion with lean mixtures overcomes the troubles resulting from intensive heat developed near the burners. With the richer mixes, it provides water for the water-gas reaction to produce more of the desired hydrogen and carbon monoxide. The writer is currently experimenting in this field and hopes to be able to supply more information in the future.

Mr. Jenkins does well to call attention to the problem and the mechanism of soot deposition during heating or cooling through the lower

---

* Sam. Tour and Co., New York City.

temperature ranges. He ascribes it to the decomposition of carbon monoxide to form carbon dioxide and free carbon. His conclusions with respect to the effect of water vapor on this reaction are somewhat disconcerting. He does not seem to have carried his experiments to the point of trying water vapor percentages high enough to involve the water-gas reaction. This reaction is in common use in the synthetic ammonia manufacturing field where, at 800°F in the presence of a suitable catalyst, CO is converted almost wholly to CO_2 without the deposition of free carbon. Iron and iron oxide seem to be catalysts for this reaction as well as for the producer gas reaction to which Mr. Jenkins has confined himself. Some of the atmosphere generators now used in industry have combustion chambers producing relatively high CO with low CO_2, but followed by oxygen eliminators and desulphurizers operating at 500 to 1000°F in which the water-gas reaction converts some of the CO to CO_2. The net result is the same as if the combustion chamber were operating at a lower temperature. The product is higher in CO_2 than is necessary or desirable.

The information given by Mr. Jenkins on the carburizing and decarburizing reactions in gas mixtures free of carbon dioxide might well be studied in the light of the very worth while paper presented by E. G. deCoriolis, O. E. Cullen and Jack Huebler.* Total elimination of carbon dioxide requires absorption towers and special equipment. Generators with heated combustion chambers produce atmospheres high in carbon monoxide and sufficiently low in carbon dioxide that with suitable low water vapor content they can be used for carburizing of steel. Water vapor removal is much simpler and easier than carbon dioxide removal from the products of a generator.

H. S. Avery†—We gather, from the final portion of Mr. Jenkins' paper, that he would recommend for industrial use a burned city gas that has about a two-to-one hydrogen-to-carbon monoxide ratio, and that he would remove the carbon dioxide from this by reheating over a catalyst. Then he would supply a small controlled amount of water vapor to get the balance he wishes for the steel to be treated from by-passing some of the undried gas and adding to the dried mixture. Is that correct—especially the hydrogen-carbon monoxide concentrations involved?

S. Tour—I am afraid that that is slightly extrapolating his recommendations. His limit is primarily a limit of a gas-air mixture, using city gas, which will maintain combustion in an unheated generator, which therefore sets his limit to that ratio which will not give much more hydrogen-carbon monoxide than the two-to-one of which he speaks.

His recommendation, therefore, refers to the ability of a generator to function without external heating. He does not have a catalytic method of removing carbon dioxide. It must be removed in absorption towers, as with the Gerbitol process that we have in this country—caustic soda or any other method of straight out-and-out absorption in an absorption tower to remove carbon dioxide.

H. S. Avery—Some of his curves had a balance of 13.5 pct hydrogen as against 9.5 pct carbon monoxide. Is that the one that he would consider about optimum?

S. Tour—As I tried to say, that is not optimum. That is almost the limit that can be obtained with that type of generator. In this country, in the heated generators using city gas, it is possible to obtain from 15 to 20 pct carbon monoxide and 30 to 40 pct hydrogen. Using natural gas in this country it is standard practice now to produce about 40 pct hydrogen, 20 pct carbon monoxide, and less than 1 pct carbon dioxide. It is impossible to do that in the type of generator which does not get heat from the outside, because the combustion reaction will not maintain itself.

J. Huebler*—The article covers the manufacture of partially burned city gas. The resultant gas, with or without additional processing, is discussed relative to its use in various heat-treating operations.

Two serious objections to the use of partially burned city gas as an atmosphere for bright annealing low-carbon steels are pointed out. One of the objections is the sooting tendency of the gas at moderate temperatures. The other objection is the phenomenon of etching. Dry-

* Carbon Concentration Control. Amer. Soc Metals, Nov. 1946

† American Brake Shoe and Foundry Co., Mahwah, N. J.

* Research Engineer, Surface Combustion Corp., Toledo, O.

ing the gas and/or removing the CO_2 do not remove the objections. It should be pointed out that removing the CO, CO_2, and H_2O will cure the difficulties. This may be accomplished in many ways. One is to burn the city gas with a slight air deficiency and then remove the CO_2 and H_2O leaving a gas of 96 pct N_2, 2 pct CO, and 2 pct H_2. This gas will not soot or etch, but it must be used in a tight furnace. Another atmosphere may be generated from partially burned city gas by passing the combustion products through a catalyst at about 800°F, causing the water gas shift to occur. When this gas is dried and the CO_2 removed, its composition can be 89 pct N_2, 10 pct H_2, and 1 pct CO. This gas will not soot or etch and also has a high reducing capacity. Either of these two atmospheres has the added advantage of being completely non-explosive and non-toxic while partially burned city gas is both explosive and toxic. The author tends to minimize the dangers involved in using his gas.

In the section on carbon control the author adapts his atmosphere to his needs in a clever manner and following the necessary basic principles. It seems, however, that the processing of the gas is rather more involved than necessary. City gas may be catalytically cracked to directly yield an atmosphere suitable for carbon control. It has been shown recently that when the CO and H_2 contents of the atmosphere are substantially constant, carbon control is strictly a function of dew point control. Cracking city gas with air over a catalyst gives the constant CO and H_2 values. Control of the air-gas ratio yields the desired dew point and hence the desired carbon control. The same precautions against explosion must be observed with the cracked gas as with the author's gas. In some localities it may be necessary to remove the sulfur from the raw gas but this should be less difficult than the stripping, drying, and mixing required in the author's method.

S. TOUR—Mr. Huebler's discussion is in line with my remarks—based on the fact that in this country we have so much natural gas that we tend to go over to the use of natural gas or to propane. In England, unfortunately, they must get along with what they call town's (city) gas, which is made from a rather low grade of coal as compared to our city gas. Incidentally, it is a high sulphur type of coal with which they have difficulties.

If this discussion were to include heated combustion chamber generators, it would be in an entirely different field from that of the simple generator to which Mr. Jenkins refers, where we simply take the richest mixtures it is possible to take, mix them together and try to make them burn in a combustion chamber.

The field of atmosphere generation is so wide and involves so many variables and so many simultaneous reactions, it is difficult to study the field from any one reaction.

An attempt has been made this past year by DeCoriolis to add up the reaction constants of five or six simultaneous reactions and arrive at a composite constant for all of the reactions at once. It seems to me that that is somewhat dangerous ground.

I. JENKINS (author's reply)—It is a pleasure to record my thanks to Mr. Tour for having undertaken, at comparatively short notice, the presentation of the paper in my absence.

The primary object of most of the work described in the paper was to examine the fundamentals of certain gas-metal reactions, to determine the factors influencing the course of such reactions, and to consider the application of a burnt city gas atmosphere to the heat-treatment of low and high carbon steels. It is unfortunate that much of the discussion has centered around the merits of atmosphere, alternative to that used in the present work. There is little comment on the more fundamental aspects that were presented for discussion and that are applicable to any atmosphere generated from city gas or a hydrocarbon, whether of the exothermic or the endothermic type.

In Great Britain the endothermic type of atmosphere, generated from rich city gas-air mixtures, is by no means uncommon, and is used for carbon and alloy steel hardening, carbon restoration, and as a carrier-gas in gas carbonizing. Its main disadvantages are associated with variability in the composition of the raw city gas, and its explosive and toxic nature, the latter being an aspect which has received much attention in all controlled atmosphere work.

Mr. Huebler's comments appear to be a little inconsistent. While criticizing the atmosphere used in the present work because of its toxicity

and explosive tendency, he does not hesitate to recommend an endothermic gas, much higher in hydrogen and carbon monoxide for the heat-treatment of carbon steels. Furthermore, while the processing of the burnt city gas, suggested in the paper for carbon control, is considered involved, Mr. Huebler puts forward an equally involved processing schedule for an atmosphere for low carbon steel annealing.

On the question of toxicity it should be borne in mind that any atmosphere containing carbon monoxide is toxic, the only difference between the atmosphere containing 2 pct of the gas, referred to by both Mr. Peck and Mr. Huebler, and that used in the present work, is one of degree. The effect on a man who has to work on an inadequately vented furnace for some hours a day is little different, whether he inhales only 2 pct or 10 pct of carbon monoxide. The answer here lies, not with the type of atmosphere used, but in furnace design and ventilation.

Mr. Huebler does well to qualify his remarks regarding the atmosphere containing only 2 pct hydrogen and 2 pct carbon monoxide, that it must be used in a tight furnace. Perhaps we should go further and say that neither must it be contaminated with gases from any other source, such as furnace parts and the steel charge itself. Since both of these latter are rather unpredictable factors, it is a matter of speculation as to whether such an atmosphere has a sufficient "factor of safety," with regard to oxidation, etching and sooting.

Mr. Tour's remarks on the mechanism of soot deposition are interesting, especially with regard to the effect of water vapor at concentrations higher than those used in the present work. The experimental investigation of this problem was confined to use of atmospheres typical of those used in Great Britain for the bright annealing of low carbon steel and would not, therefore, have come into the range of water vapor contents to which Mr. Tour refers.

I wish to thank those who have taken part in the discussion on this paper. The field of controlled atmospheres and gas-metal reactions is very wide and there will probably be, for some time yet, considerable speculation as to the merits or otherwise of a certain type of atmosphere for a particular application. There is much work still to be done on the fundamentals of gas-metal reaction, and in particular, on reaction velocities, and discussions of this kind serve a most valuable purpose if they stimulate such work. Furnace engineers also have the responsibility of improving furnace design to ensure the accuracy of atmosphere control within the furnace, without which the full advantage of any fundamental research work cannot be obtained. Finally there is the education of the practical man, to whom this field is even now still comparatively new and often made to appear far more involved than it should be.

SYMPOSIA

Some Questions on Interrelated Processes Going on in the Blast Furnace

By B. M. Larsen,* Member AIME

In spite of the great amount of operating experience and of studies directed toward elucidation of the interrelation of the several processes going on in the blast furnace, the present picture of its operation is based largely on indirect evidence and on speculation. The reason for this unsatisfactory situation is the extreme difficulty of making direct observations and significant measurements while the furnace is operating, and of translating laboratory experience to the conditions obtaining in the smelting process. Yet there are questions that can be investigated with some promise of a definitive answer; and it is the purpose of the present paper to set forth some of these questions, as a basis for discussion, which may, it is hoped, lead to active work on some of them.

In order to provide a starting point for this discussion, some views held tentatively by the writer are outlined, along with a certain amount of evidence gathered from operating records and interpreted on the basis of the ideas expressed. These opinions may prove not to be pertinent, and may well not be in accord with the opinions of others; they have been included to encourage others to do likewise and on purpose to provoke informal discussion. In this way it should be possible to transcend the limitations of formal papers; to bring forth suggestions of new hypotheses or new methods of investigation; and to promote better understanding between investigators and operators in this difficult field. The statements made express the present views of one physical chemist who is not too familiar with all the difficulties of maintaining these enormous reaction vessels in reasonably smooth and economical operation; who, however, is persuaded that some of these difficulties would be less formidable if surer knowledge of the several interrelated and concurrent processes were available and made use of. For these difficulties arise largely, it is believed, from variation in conditions which the operator must meet as best he can, and should lessen as these conditions can be brought under control so that they are either made substantially constant or the variations are neutralized by compensating methods.

Presented at the Blast Furnace, Coke Oven and Raw Materials Conference, April 1947. Manuscript received at the office of the Institute Nov. 6, 1946. Issued as T.P. 2132 in Metals Technology, February 1947 and printed in Blast Furnace Proceedings (1947).

*Research Laboratory, U. S. Steel Corporation, Kearny, New Jersey.

A. Variation in Burden and in Mixing of Charge

To the scientific investigator, who aims to control the conditions of experiment and to limit the number of variable factors, the most perplexing aspect of the blast-furnace process is that nothing seems to remain constant for long. Variations of burden seem to be unnecessarily frequent; and, even if the charge were constant from hour to hour, its constituents usually are not mixed as intimately as they might well be. It is understandable that separate layers of coke and of ore, also separate layers according to size, promote permeability and the

more uniform gas-solid contact so necessary to smooth operation. But would regularity not be further promoted by more intimate mixing of ore and flux, in accordance with experience on other industrial chemical processes? Prepared ores or sinters could have all necessary lime or dolomite intimately incorporated; natural ores could be mixed with the necessary flux before charging, instead of being dumped in separately. One might even consider using two continuous bucket conveyors, feeding alternate layers of coke and of ore fractions, the latter already carrying the flux it requires.

This matter is complicated by present lack of exact knowledge of the sequence of processes by which the final slag is formed. Does an early, low-melting liquid disintegrate the lumps of partly reduced ore and start to form slag before the iron melts? Or do slag formation, melting and carburization of iron all occur together just above the tuyere zone? Does an early basic slag, containing all the lime or magnesia charged, form somewhere in the bosh? Or does a substantial amount of flux remain free to combine later with the coke ash set free in the combustion zone? The uncertainty on such points suggests that investigations of ore reduction should be extended to higher temperatures so as to cover the formation of liquid slag and molten iron as well as the reactions between liquid slag and solid carbon.

A related question is how much of the apparently inherent irregularity of smelting rate and of slag composition is related to the manner of slag formation. Can ore and flux remain poorly mixed in the first slag-forming zone so that, for example, the early slag is too acid on one side of the furnace but too basic on the other, or viscous and late in forming in one place but fluid and early in another? Such differences over the furnace cross section in the slag-forming zone could occur, yet leave little evidence in the final slag in a single runoff; if they do occur, they might affect smelting rate and metal composition. While making statistical studies of sulphur removal in relation to composition of slag and of metal, as measured in a single cast or as averaged over a 24-hr period, the writer has often noticed that even with slags of substantially identical average composition there were substantial differences in distribution ratio of sulphur between slag and metal, a fact that is hard to understand on any rational physicochemical basis unless the samples analyzed were not representative of the coexisting phases. Variation of temperature in the hearth zone may be a factor, but this may be subsidiary to some nonuniformity over the cross section of the zone in which slag largely forms, or in the slag-forming process. The early slag usually is thought of as relatively basic, since it does not yet contain the coke ash; and as richer in MnO and FeO than the final slag; yet this is little more than speculation. However this may be, an interesting question is whether this slag is a rather viscous liquid or is admixed with solid portions; another, whether more intimate mixture of ore and flux would improve uniformity of the slag and smoothness of operation. The proposal to introduce part of the flux as powder through the tuyere, if carried out systematically, might throw some light on these points, particularly if this is supplemented by appropriate laboratory work.

The precise reasons for making frequent changes in burden are not always clear to the man seeking to understand how best to control the operation of the furnace. The frequency curves in Fig 1 show the fractional deviation of the percentage of lime and of magnesia in 24-hr aggregate samples of slag from the mean of each over a 9-months period. The lime comes almost entirely from the ore, the magnesia from added dolomite, and furnace control was better than average; yet apparently

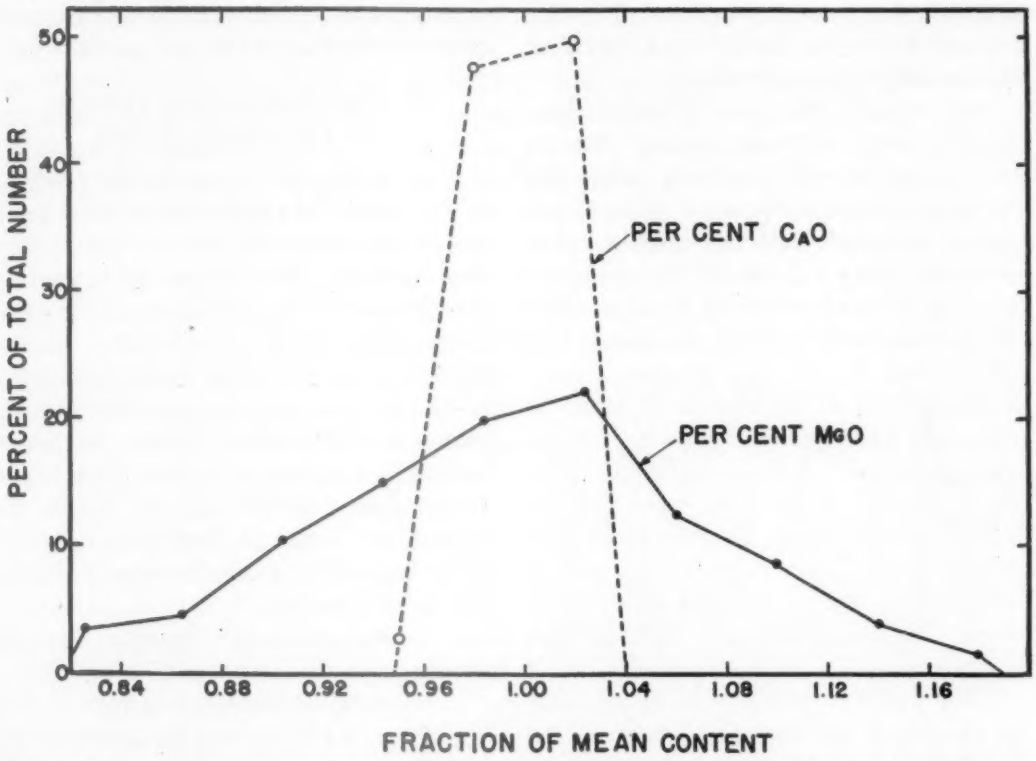

FIG 1—FREQUENCY CURVES SHOWING FRACTIONAL DEVIATION OF PERCENTAGE OF LIME AND MAGNESIA IN 24-HOUR AGGREGATE SAMPLES OF SLAG FROM MEANS OVER 9-MONTHS PERIOD.

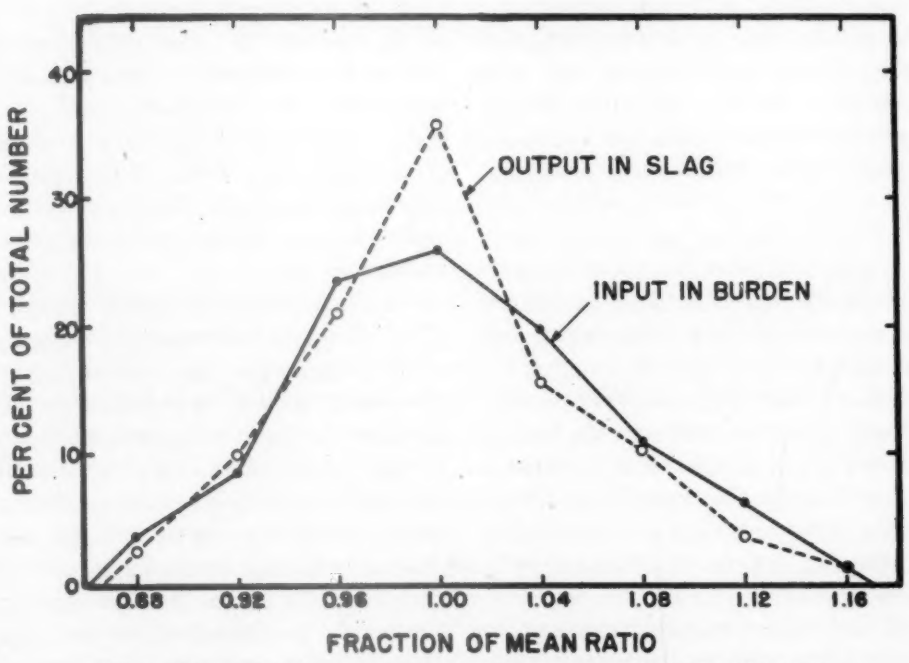

FIG 2—DEVIATIONS FROM MEAN IN WEIGHT RATIO OF LIME TO SILICA.

intentional relative changes in magnesia content were more than twice as great as the variation of lime content.

The frequency curves in Fig 2 summarize some data on another furnace over a few selected periods in which the type and composition of ore charged was almost constant, and the coke-ore ratio was unusually uniform. The numbers entering into the curves are 24-hr averages of the CaO/SiO_2 ratio in the charge (full curve) and in the slag (broken curve). The similarity of the two curves would be expected; their spread tends to confirm the assumption that considerable variations of slag composition were brought about by apparently intentional changes in the charge, even during those periods when other factors were reasonably constant. The use of frequent shifts of blast temperature and volume as a measure of control are not difficult to understand, as they exert an immediate effect on the conditions prevailing in the furnace. But changes in charge can produce little appreciable effect until several hours have elapsed, and tend to upset regularity of operation unless they are compensated at the proper time by other changes. An explanation by operators of the basis, and of their reason, for these frequent changes in relative amount of the several materials charged would be welcome.

Questions

The considerations outlined in the foregoing pages raise the following specific questions:

1. What is the approximate sequence of processes in slag formation as the material descends through the furnace? Is variation in this sequence, or in degree of uniformity over the cross section of the furnace, a substantial source of irregularity of operation?

2. Would more uniform intimate mixing of ore and flux improve regularity?

3. To what extent is frequent change of burden a necessary means of control?

B. Variation in the Process of Reduction of Ore

Change in the temperature gradient down through the shaft, which, as pointed out in the preceding section, may affect the regularity of operation by modifying the process of slag formation, may itself be brought about by variation in the sequence of the other processes going on in the shaft, and in turn modify this sequence still further. To clarify the picture we list the main processes that might affect temperature distribution, in what we believe to be the approximate order of their beginning, as the burden descends through the furnace:

1. Expelling water brought in the burden.

2. Heating the burden.

3. Expelling CO_2 from limestone (dolomite, iron carbonate).

4. Reducing solid FeO by CO—so-called indirect reduction.

5. Reaction of CO_2 with coke to form CO—so-called solution loss.

6. Melting of slag and iron—minimum temperature not less than 2200°F(?).

7. Reducing remaining FeO in liquid slag by carbon—so-called direct reduction.

8. Reducing P_2O_5, SiO_2 and MnO (mainly in liquid slag?) by carbon to phosphorus, silicon and manganese dissolved in iron.

9. Dissociating all water carried in by the blast into hydrogen and oxygen.

Setting aside for the moment the important factor of variation in effective contact between solid or liquid and gas, which would affect efficiency of both heat transfer and gaseous reduction, these nine items appear to be the essential factors affecting vertical temperature distribution. Of these, the last four proceed only in the high-temperature zone, at lower levels approaching the tuyeres.

No. 9 undoubtedly affects the supply of high-temperature heat available near the tuyeres; its elimination from the too-large number of variables would be desirable. However, operations with dry blast or with a blast temperature compensated for moisture variation have shown that the main sources of variability still remain; so we eliminate it for the purposes of this discussion. No. 6 is essentially a constant factor with a given burden; and this is substantially true also of No. 8, for any appreciable variation of heat absorption due to variable content of silicon and manganese in iron is presumably a result and not a cause of variability. Would No. 7, the presumed direct reduction of FeO dissolved in the early slag as it flows over the hot coke thus be left as the only source of significant variation in heat absorption at or below the zone of initial formation of liquid slag?

Of Nos. 1 to 5, which occur at the lower temperature higher in the shaft, the first three presumably should be nearly constant with respect to heat requirement for a given burden. Indirect or gaseous reduction by CO (No. 4) apparently is a slightly exothermic reaction. Variation in its rate of approach to completion, however, would permit formation of a variable amount of CO_2 in lower zones hot enough to permit the solution-loss reaction (No. 5) to occur; this would also be true of carbonate dissociation (No. 3). Thus, would item No. 5, the solution of carbon by reaction of CO_2 at coke surfaces where the temperature is above about 1650°–1700°F appear to be the only large factor *directly* affecting the amount of heat absorption in the shaft above the zone of early slag formation?

Indirect reduction of FeO by CO (item 4) has the advantages of absorbing none of the heat supply in the shaft and of permitting all the carbon to reach the tuyeres to be burned to generate the necessary heat. In the unlikely event that all iron is reduced completely before reaching any zone at a temperature above 1650° to 1700°F, the main items causing variable heat absorption (Nos. 5 and 7) would be suppressed. Its disadvantages, however, are: (1) that it is not very efficient as measured by amount of iron reduced per pound of coke, and (2) that it cannot utilize excess high-temperature heat available lower in the shaft.

Gaseous reduction by the reaction:

$$FeO + CO \rightarrow Fe + CO_2 \qquad [1]$$

can reduce an estimated maximum of about 1.5 lb Fe per pound coke; this reaction, if all the iron were produced in this way, and if it went to equilibrium, could give an estimated minimum coke requirement of 1350 to 1400 lb per net ton of iron produced. Direct reduction by carbon, in accordance with the reaction

$$FeO + C \rightarrow CO + Fe \qquad [2]$$

can yield 4.2 lb Fe per pound coke and still leave CO available for reaction 1, to give a total of about 5.0 to 5.2 lb reduced iron per pound coke and a possible minimum of about 470 lb coke per net ton iron produced. Such a yield could be approached only in the electric shaft furnace, with its independent source of high-temperature heat. With respect to the ordinary blast-furnace process in which heat is supplied by combustion of carbon, the difference between reactions 1 and 2 is in the heat requirement. Reaction 1 evolves a small amount of heat; reaction 2 not only absorbs about 4200 Btu per pound coke consumed but also prevents this pound of coke from reaching the tuyeres, where it could be burned to CO with evolution of about 3800 Btu.

If reaction 2 can occur in the bosh zones by reaction between FeO in early liquid slag and coke, it can, in theory, save coke as well as make use of excess high-temperature heat supplied in a controlled

manner by higher blast temperature or by oxygen enrichment of the blast. There is little direct evidence with respect to such a reaction. Can a fairly large volume of FeO remain to enter the slag that forms first? Is the reaction rate high, and is it affected by slag viscosity; that is, by the thickness of the liquid slag layers flowing over the hot coke? Is it not true, moreover, that this is the only process that could absorb any large excess of high-temperature heat made available by very high blast temperature or by oxygen enrichment?

Combination of reaction 1 and the solution-loss reaction

$$CO_2 + C \rightarrow 2CO \qquad [3]$$

is chemically equivalent to reaction 2; so that to the extent that it is not related to lowered and variable efficiency of the reduction reactions below 1800°F, and that extra heat is available between 1800°F and the temperature at which initial slag forms (?) to compensate for its heat absorption, such carbon solution would also seem to lead to lowering of coke consumption. Conversely, if the time rate of either reaction 2 or reaction 3 is variable, may this variability not be the main source of irregularity in furnace working? Variation in gas-solid contact, or in total cross-sectional area of gas flow, and its uniformity through the burden, undoubtedly are important as one, perhaps the main, group of fundamental variables leading to irregularity: the question is that of the mechanism of the resultant variability lower in the furnace.

Questions

4. Is variable solution loss of carbon the essential variable directly affecting heat consumption in zones above that of initial slag formation?

5. Can an appreciable proportion of unreduced FeO reach the early slag-forming zone, there to dissolve in liquid slag and react directly with solid carbon? Is it possible to get direct evidence on the extent, if any, of this reaction, its rate and dependence on slag viscosity?

6. Is variability in time-rate of this direct reduction the main cause of temperature variation in the slag-forming and final smelting zones? Could such variability lead to hanging and serious irregularity in furnace working?

C. Limitations on Increasing the Temperature or Oxygen Content of the Blast

If empirical operating results are taken at their face value, it appears that different limiting or optimum blast temperatures exist for different furnaces or different burdens. Certain furnaces operating on lean, wet burden are reported to work badly when the average preheat temperature is above 800° to 900°F. Others, operating on Mesabi ore, seem to run most smoothly with a blast temperature around 1000° to 1100°F, with less regular behavior and in certain cases a somewhat higher coke consumption on higher average blast temperatures; yet still others using similar soft ore have made good use of blast temperatures up to 1300° to 1400°F. One case is reported of furnaces working on a burden, probably made up mainly of coarse and prepared ores, using a blast temperature of 1500° to 1600°F to good advantage with low coke rate and high production. Another group, using a very rich, prepared burden, utilizes an average 1400°F blast with extremely low coke consumption.

There seems to be no clear explanation of these differences. Inconclusive indications tend to connect limitations on maximum effective blast temperature with: (1) low top-gas temperature, (2) fine or crumbly ore, and (3) high moisture content of the burden. In the few cases in which the blast temperature is 1400°F or higher, there is a trend toward burdens of low

moisture content and physical factors generally favoring uniform gas-solid contact. Offhand, it would seem that higher blast temperature would give either an enlarged zone of liquid slag and of conditions permitting reaction between liquid slag and solid coke, or an increased smelting rate with but little increase in hearth temperature. Operating results indicate that very high blast temperature tends to yield iron lower in silicon, to increase production rate, with only slightly higher slag and iron temperatures.

It seems highly probable that some condition enters the hearth and bosh zone which favors absorption of the extra high-temperature heat supplied by the blast. About the only factor that could do this would seem to be an increased amount of direct reduction of FeO dissolved in the early liquid slag according to reaction 2. It is not difficult to believe that if top gas temperature is down around 250°F, an increase in blast temperature could not be accompanied by decreased consumption of coke; any decrease in volume of gases resulting from less coke or increased direct reduction by either reaction 2 or reaction 3 would leave an insufficient amount of shaft heat to dry and preheat the burden and to burn the carbonate fluxes; this would in turn lead to an increased temperature gradient in the material approaching the smelting zone, with a possible resultant instability. More puzzling, however, are the indications of irregularity of operation on higher blast temperature even with the same, or slightly higher, amount of coke in the burden. The following are possible factors in this:

1. That somehow melting and flow of the initial slag become irregular, because slag must form more rapidly or a steeper temperature gradient.

2. That temperature in hearth and bosh zone becomes irregular because there is more possibility of greater absolute variation in the rate of reactions—hence in amount of heat absorbed—and in the levels at which they occur.

It is reasonable that this variation in heat absorption (No. 2) could affect slag formation (No. 1), and that a greater excess of coke in the burden might be needed to take care of the extremes of the swings. On the other hand, if slag *can form and flow* at a greater *but regular rate*, either high blast temperature or oxygen enrichment should result in smaller coke rate and higher production; for oxygen enrichment is in many respects completely analogous to higher blast temperature. In certain German pilot tests with enriched blast, it was found that as oxygen in the blast exceeded a certain point in the range 25 to 28 pct, the furnace began to work irregularly, a result apparently similar to that sometimes observed with higher blast temperature.

As to the fundamental cause of these irregularities, it is probable, as mentioned above, that it is to be sought in the group of factors that affect uniformity of gas-solid contact and of gaseous reduction in the shaft. This group includes: (1) fineness, caking tendency, degree of crumbling under load, and extent of size segregation of the ore and (2) size and resistance to shattering and abrasion of the coke. Anything that tends to impede uniform gas flow through the burden tends to cause a greater average, but less regular, amount of unreduced ore to descend to higher temperature zones, and consequently solution loss and direct reduction would increase in amount and become more irregular.

Is it possible, however, that total amount of moisture in the burden is also a factor? Many operators consider this to be unimportant, but there is some evidence, admittedly inconclusive, to indicate that a decrease in water charged with the burden may make it feasible to utilize higher hearth temperature with less consumption of coke and greater produc-

tion rate. Many furnaces are burdened with 500 to 600 lb, or even more, water for each ton of coke used. Even though the supply of heat in the shaft is adequate to vaporize all water and still leave the top gases hot enough (250° to 300°F, or higher), may not the large total heat of evaporation affect the temperature gradient in lower zones of the shaft?

Oxygen enrichment offers the possibility of a much greater rate of supply of high-temperature heat in lower zones of the furnace. Presumably, effective use of this excess hearth heat requires a larger proportion of direct reduction; but the problem of achieving regularity in this greater rate of slag formation and of direct reduction would perhaps be even more essential than it is in present practice.

With present lack of precise knowledge of the higher temperature processes in the blast furnace, a brief survey such as this can hardly present a clear picture; but it may serve in some degree as a background for the following questions:

Questions

7. How seriously can we regard operating reports of "bad furnace behavior" when blast temperature exceeds a certain level, these levels being widely different for different furnaces or operations? Are these differences inherent, or could higher blast temperature be utilized by readjustment of operation or furnace design?

8. Is it reasonable to assume that, in a furnace producing the same iron but utilizing an increase in hearth heat produced by oxygen enrichment, moisture removal, or higher blast temperature, there must be a greater proportion of direct reduction to absorb most of this increased supply of high-temperature heat? Could more detailed heat balances, broken down with respect to the heat requirements of separate zones in the furnace, be used to predict more specifically how increased hearth heat correlates with amount of direct reduction and with related changes. By lowering the shaft heat requirements, could one then produce the over-all heat needed with lower coke consumption?

9. If an increase in direct reduction results automatically when more heat is supplied to the hearth zone, is it the irregularity in time rate of this direct reduction, and the consequent irregularity in heat absorption and temperature in the slag-forming zones, that causes the furnace to work irregularly and prevents effective utilization of an increase in "high-temperature heat"? Variability in rate of melting and flow of slag could then be merely a subsidiary result of these temperature swings; or is this variability partly independent?

10. Conversely, may we assume that, insofar as increased hearth heat is accompanied by more direct reduction *yet without appreciable fluctuation of its time rate* and by substantially regular rate of slag formation, it should be feasible to correspondingly lower consumption of coke and to increase production rate by use of conditioned blast, higher blast temperature, or oxygen enrichment?

11. Even though we admit that uniform gas flow and intimate gas-solid contact are indispensable for regularity of operation, should we not also consider the possibility that: (*a*) more uniform and intimate mixing of ore and flux, and (*b*) keeping to a minimum the amount of water in the burden, may be of comparable importance to both steadiness in operation and effective utilization of excess hearth heat?

D. Coke Quality

The blast-furnace man is sometimes blamed, perhaps unjustly, for using "poor coke quality" as a universal alibi for all unexplainable difficulties in operation; it seems unquestionable, nevertheless, that in many instances this is an important item of the problem. Yet, to a physical

chemist not too conversant with blast-furnace and cokemaking problems, the endless controversy about coke quality begins to take on the aspect of a night-

burden. These are the important things, at least. It is admittedly better to have coke low in sulphur and ash content, this being an easily understood and separate

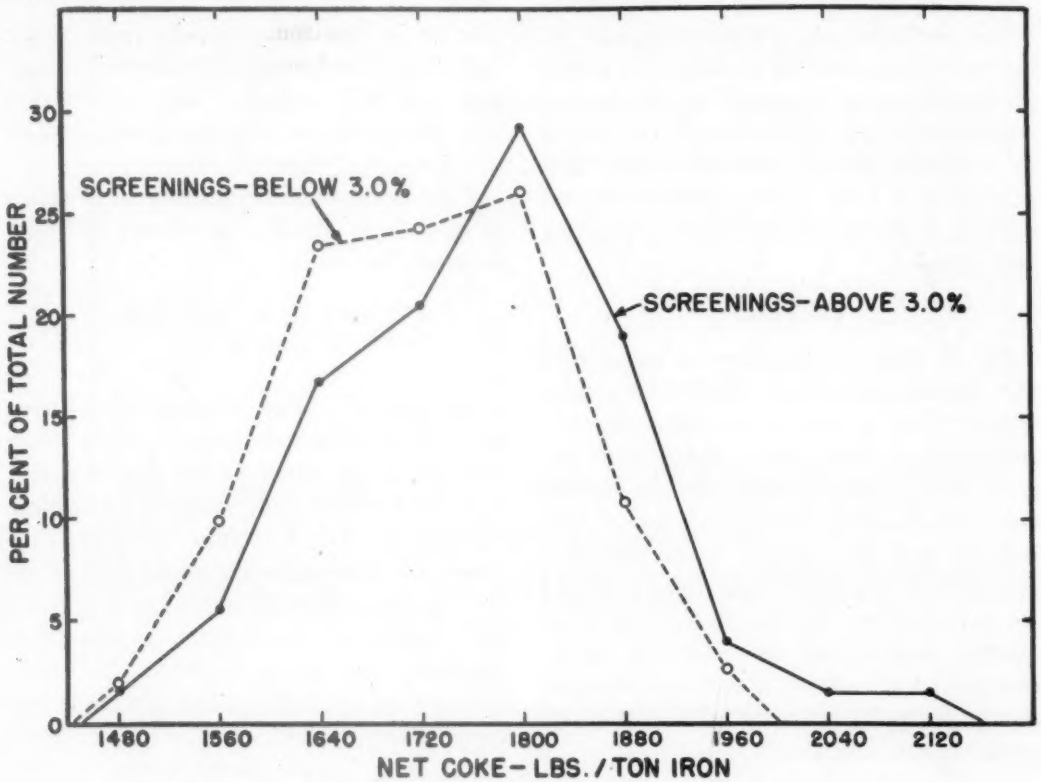

FIG 3—RANGE OF SCREENINGS, 1.5 TO 75 PER CENT OF GROSS COKE.

mare; and he wonders whether the matter may not have been confused by introducing variables that are mostly only minor or even insignificant. We may safely assume that coke has both chemical and physical functions in the smelting process. Its chemical function is to burn with air to supply both heat and reducing gas, but there is much evidence to indicate that almost any kind of carbon, from charcoal to highly graphitic coke, burns at a satisfactory speed at the high temperature levels of the tuyere zone in a modern blast furnace. Its physical function is to remain as hard lumps in spite of abrasion and crushing as it descends through the furnace, and thus to promote maintenance of easy, uniform gas flow through the

aspect of the matter. It may be of some importance that the coke have a low reactivity to CO_2 in the solution-loss temperature range above 1750° to 1800°F, but hard, tough coke with desirable physical properties will usually have low reactivity. May it be that the various "fuel indexes" that have been concocted have unnecessarily complicated the coke problem, and that good coke is nothing more or less than coke with maximum resistance to cracking, crushing and abrasion?

The frequency curves of Fig 3 are derived from monthly averages of net coke charged per ton iron for several furnaces in a period when the coke supply was quite variable in physical properties,

and the amount of screenings of fine coke discarded at the furnace varied from about 1.5 to 7.5 pct, or 30 to 150 lb per ton of gross coke arriving at the screens feeding the skips at the furnace. Since many other variables are almost certainly involved in this monthly average, the degree of correlation with amount of breakage is considered good. This example is merely an indication of the possibility that coke quality is at least largely, perhaps almost entirely, a matter of resistance to crushing and abrasion.

Questions

12. Is there a tendency to exaggerate the importance of an ill-defined "coke quality" as a source of blast furnace irregularity? Have we perhaps unnecessarily complicated the problem of suitable coke for the blast furnace by use of fuel indexes that give weight to factors that are really of negligible importance? Should we not consider the possibility that coke quality, aside from the admitted desirability of low content of ash and sulphur, can be gauged simply by its resistance to crushing and abrasion?

E. Elimination of Sulphur in the Blast Furnace

The frequency curves in Fig 4 are based on about 1200 iron analyses from as many separate casts from one furnace over a 9-months period, with corresponding values of the moisture content of the blast in the period before each cast. It seems probable that the indicated correlation between higher moisture in the blast and lower sulphur in iron may be direct, since we have not been able to relate them secondarily through some other variable, and since the indirect effect of water dissociation in lowering hearth-zone temperature would tend in the opposite direction (this aspect has been largely eliminated in Fig 4 by taking casts in which the silicon is nearly constant). Presumably water vapor reacts immediately with coke to form CO and H_2, the hydrogen then acting either as a carrier or catalytic agent to promote the transfer of sulphur from metal to slag, or to remove sulphur directly in the gases. There seem to be very few data on sulphur content of top gas, but most sulphur balances indicate that nearly all the sulphur is being carried out in slag and iron.

Fig 5 is based on a similarly large group of data from which were chosen all those in which the ratio

$$\frac{\text{Mols CaO} + \text{Mols MgO}}{\text{Mols SiO}_2}$$

in the slag lay within a narrow range near the most frequent value. From this selected main group with substantially constant basicity ratio, we compare sulphur content in iron for those subgroups in which the corresponding MgO content of the slag was high (about 6 to 8 pct) or low (about 3 to 5 pct). Apparently, therefore, from Fig 5, equivalent substitution of CaO by MgO within this range has increased the tendency to eliminate sulphur from the iron; this seems somewhat surprising, since MgO usually has been considered as a less effective desulphurizer. It happens that slag viscosity is in general lowered by MgO in this range; may it be that with less viscous slags there is a better contact between liquid slag and metal and consequently more rapid reaction? Or at temperatures high enough to make the slags equally fluid, would those with less MgO be better for elimination of sulphur? Reasonably complete and accurate data on the equilibria in sulphur distribution for the commercial range of compositions of both slag and iron should help to resolve these uncertainties.

Questions

13. Is there other evidence of an appreciable effect of hydrogen on elimination of

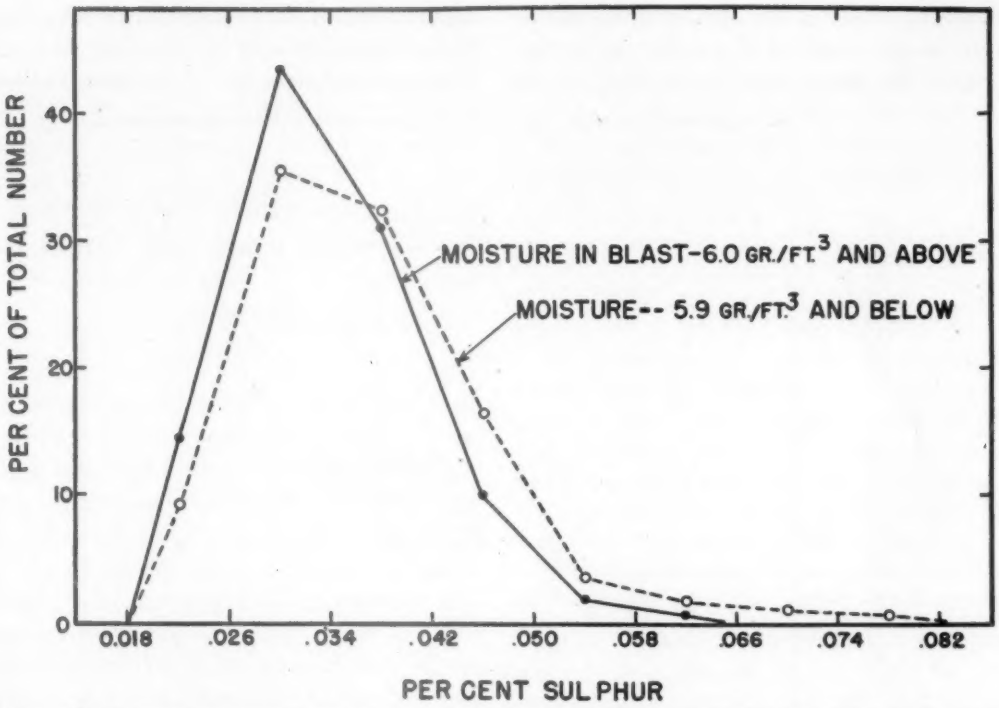

FIG 4—FREQUENCY CURVES FROM IRON CASTS OVER 9-MONTHS PERIOD WITH SILICON RESTRICTED TO WITHIN 0.15 PER CENT FROM MEAN VALUE.

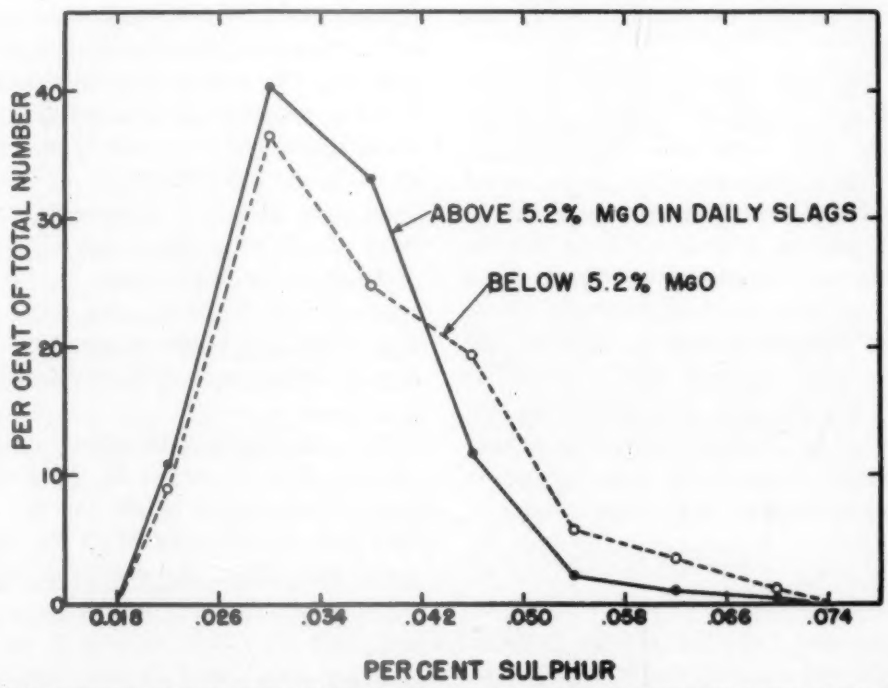

FIG 5—FREQUENCY CURVES FROM IRON CASTS OVER 9-MONTHS PERIOD WITH MOL RATIO $CaO + MgO/SiO_2$ WITHIN 1.57 TO 1.64.

sulphur? If so, is it a catalytic or carrier action or a removal of sulphur in the gas phase? Are there any direct data on the

factor, which largely controls the final temperature of slag and metal, and is a "critical temperature" level above which

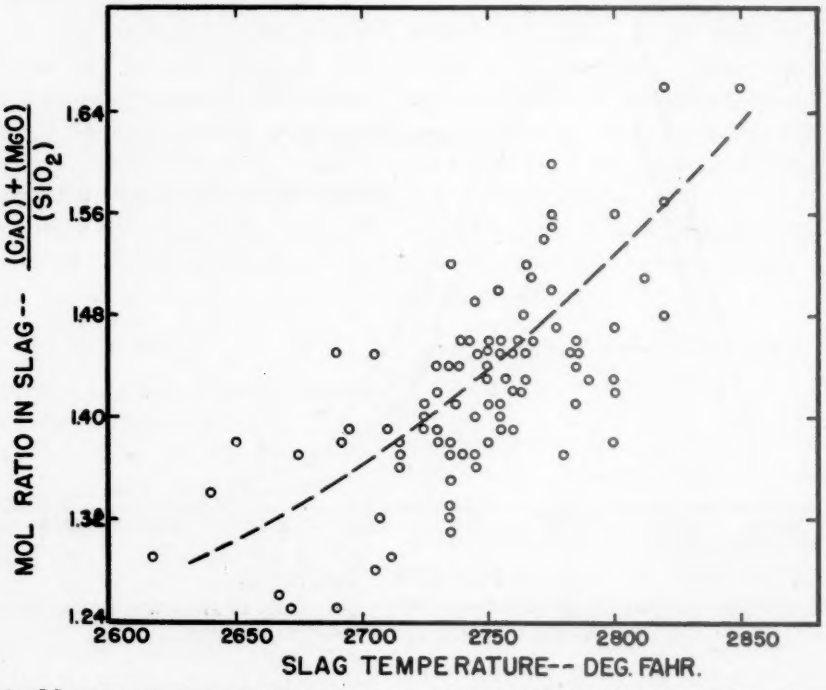

FIG 6—MEASURED SLAG TEMPERATURES VS. CORRESPONDING MOLAL BASICITY RATIOS.

range of sulphur content of blast-furnace top gas?

14. Although definite statistical correlations can be traced between slag composition and sulphur-distribution ratio, erratic differences are often encountered. So little is known about true equilibrium in this system that we are unable to estimate the relative importance of reaction rate and of equilibrium as affected by composition, or whether oxygen pressure is a significant or a constant and unimportant factor. For example, could slag viscosity, as affected by its MgO content, be a dominant factor through its effect on rate of transfer of sulphur from metal to slag?

F. CRITICAL TEMPERATURE THEORY OF PROCESS

About 1905, J. E. Johnson, Jr., proposed that the free-running temperature of the (early or bosh?) slag is a fundamental

all heat useful for the hearth-zone processes of melting and final reduction must be supplied. This theory is not only reasonable in many respects but also explains general variations in efficiency and coke consumption. On the other hand, do we really yet know how closely it represents the true state of affairs in the furnace, or clearly understand its mechanism? In the years ensuing since Johnson's proposal, has any real effort been made to correlate it with furnace behavior or with physicochemical principles?

We still know little about the composition and properties of the first slag, formed presumably before the last of the FeO and much of the MnO has been reduced and before the coke ash has been taken into solution. How uniform is this slag over the cross section of the slag-forming zone? And is the free-running temperature of this slag an important regu-

lating factor? What of the steepness of temperature gradient below this zone, the relative amount of FeO still to be reduced by direct reaction with coke, and the effect of these conditions on extent of silicon reduction?

In Fig 6 we have plotted some measured slag temperatures against the corresponding molal basicity ratio

$$\frac{\text{Mols CaO} + \text{Mols MgO}}{\text{Mols SiO}_2}$$

for a number of slags all so low in MgO that the ordinates are close to the molal CaO/SiO_2 ratio. It is tempting to regard this correlation (even though it is probably directly related to operating adjustments in the burden) as a relation between basicity and free-running temperature and the automatic controlling effect of that temperature. From the data of McCaffery, the corresponding viscosity variations over this range of slag composition seem too small to account for this relation; however, these are final slag compositions, and if we knew the composition and viscosity-temperature relations of the corresponding *early* slags we might find a more marked and consistent relationship of which this plot is only a pale reflection?

Questions

15. Are there any new data, or methods of further investigation, by which to elaborate or clarify the significance of Johnson's "critical" or "free-running" temperature theory? Are the properties of the early slag, and the uniformity of these properties over the furnace cross section, the all-important regulating factors in the over-all process?

Conclusion

The fact that it is much easier to ask such questions than to answer them will no doubt occur to the reader. Even though he may think that some of these questions are poorly expressed or even somewhat foolish or inconsequential, we hope that he will not be deterred from contributing his own questions or from discussing any of these in which he may be interested, either from the standpoint of possible future studies and methods of attack or of clarifying them by submitting data and practical observations on operating furnaces.

DISCUSSION*

(D. P. Cromwell presiding)

D. P. Cromwell†—I think Mr. Larsen has opened up a field of discussion on which we are going to have some pros and cons developed this afternoon. Some of the operators will not like some of the ideas and will offer constructive criticism. But, I think it will bring out the argument that most of us like to hear.

We have some prepared discussions and I shall call on Professor Joseph to present his discussion.

T. L. Joseph‡—Mr. Larsen's paper was written to provoke discussion. As this meeting progresses, I think we will find that he has accomplished his purpose. Conditions have not returned to normal but they have improved in some respects so that it is opportune to take a fresh look at some of the controversial features of furnace practice. The quality of raw materials seems to be deteriorating thus requiring more expensive coke. If we are to maintain the prewar level of efficiency with somewhat poorer raw materials, some improvements in practice must be made.

The various questions which Mr. Larsen has raised will be discussed by several speakers and I do not want to encroach upon their remarks. I would, however, like to make some general observations based upon the premise that aside from the quality of raw materials, problems of efficiency and control of product are very closely related to gas distribution, heat transfer, improper and irregular preparation of the charge in the shaft and resultant variable conditions of temperature in the hearth. Important phases of the process, such as ore reduction, calcination, reduction of silicon and desulphurization are based upon chemical reactions, but I think we have been inclined

* Reprinted from *Proc.* Blast Furnace, Coke Oven and Raw Materials Conference, 1947.

† Youngstown Sheet and Tube Co., Youngstown, O.

‡ Professor of Metallurgy, Minnesota School of Mines, Minneapolis, Minn.

to overlook the problem of heating large quantities of raw materials up to temperature levels at which these various reactions will first begin and then proceed at satisfactory rates. The heat required to sustain the reactions is small, but it is difficult to heat the charge uniformly so that chemical changes will occur uniformly in various parts of the furnace and at the same rate from hour to hour.

In other words the physical process of heating the stock by the rapidly rising current of hot gases from the tuyeres is very important. Uniform heating is, however, very difficult, in fact impossible, with the physical character of raw materials and the large volume of gas involved.

With this general perspective of the process in mind, I shall consider briefly one or two of the questions raised by Mr. Larsen. For example, he asks whether mixing the ore and flux and perhaps some modification in charging to prevent segregation, would assure more uniform proportions of bases and acids all around the furnace at the fusion zone.

I believe differences in the loss of ore as dust from one side of the furnace to the other rather than improper proportioning of ore and flux around the furnace at the stock line is the principal cause for any variations in the ratio of bases to acids at the fusion zone. Crushing the stone to permit mixing would reduce the differential in the loss of ore and flux as dust but it is questionable whether such a procedure can be justified.

Variations in Temperature

Setting aside the effect of gas distribution, he asks whether variations in the amount of physical and chemical change in the shaft are responsible for temperature variations at the fusion zone and below. Variations in the amount of smelting work of both a physical and chemical nature are so closely related to gas flow problems that it is questionable in my mind whether we can separate them.

Consider first temperature differences from one side of the furnace to the other. On the skip side the furnace is hotter all the way from the stockline to the furnace bottom. The question is by what sequence of changes did it get that way. The peripheral distribution of the stock is fairly uniform. In other words just as much burden and smelting work is imposed on the hot side as on the cold side. However, the temperature is affected not alone by the heat capacity of the stock but by the amount of gas and in turn the heat carried to various parts of the charge. If we could maintain uniform gas flow such a condition of widely differing temperature gradient could be eliminated, but it is impossible to prevent occasional variations in peripheral gas flow.

Once such a condition is established, it is aggravated by more solution loss on the cold side that receives less gas. This means that the sequence of chemical and physical changes, which take place according to temperature and not furnace location, will be completed lower in the furnace on the cold side. Correction requires first of all a restoration of uniform peripheral gas flow.

Consider another case that may be more nearly in line with the condition Mr. Larsen had in mind. Assume that normal radial temperature differences exist but the vertical temperature gradient is the same from one side of the furnace to the other. With no apparent change in raw materials the furnace gets colder all around at the fusion zone and in the hearth. Here again, some change in gas distribution which may effect heat transfer is the most likely cause of the change. But once the stock as a whole is not so well prepared in the shaft, more solution loss is likely to occur in the bosh and hearth with the final result that we are not only liberating less heat but using it less efficiently.

Variations in Charge

Let us take the third case where there is an actual change in raw materials. The ore may be denser, coaser, and more difficult to reduce. Larger pieces of limestone may be slower to calcine. Gas distribution is normal. It is conceivable that such a change in raw materials would carry reduction and calcination to lower levels in the furnace, increase solution loss and reduce the amount of heat liberated. With the same pattern of gas distribution, heat utilization would be about constant but less heat would be available.

By and large, most of the irregularities begin with faulty gas distribution more likely caused by changes in the physical properties of the coke that occupies two thirds of the furnace volume. We are forced to reach high linear gas velocities under present demands for tonnage. These high velocities start channeling in the upper part of

the stock and set up temperature differences that extend downward to the hearth. If we want equal heating we must carry equal amounts of heat to various parts of the stock with equal gas flow.

D. P. CROMWELL—Thank you, Professor Joseph. Mr. Carl Hogberg has some remarks on this same subject.

C. G. HOGBERG*—Mr. Larsen is to be complimented for his efforts in stimulating a renewed interest in the theoretical aspects of the iron blast-furnace process. The number and complexity of the questions he has raised are ample evidence of our general lack of knowledge of details concerning the sequence and relative importance of each of the reactions and factors involved in the production of iron within the furnace.

One of the most important phases of the process is the formation of slag. It is also the phase concerning which we have the least knowledge, particularly with reference to its early stages. Our remarks will be confined to the problem of slag control, with emphasis upon the effect of changes in analysis of the early slag upon furnace operation.

SLAG CONTROL

In a paper[1] presented before this group in 1942, attention was called to the fact that two distinctly different types of slag are made in the blast furnace: (1) the final slag drawn from the furnace hearth, and (2) the bosh slag, which differs from the final slag in that it is not diluted by the highly siliceous oxides of coke ash released as the coke burns at the tuyeres; the bosh slag is, therefore, highly basic, and as such possesses characteristics of high viscosity and higher melting temperature associated with basic slags. Fig 7 is a reproduction of the portion of the ternary diagram of the mineralogical system $CaO.Al_2O_3.SiO_2$ in which lie slags of the type associated with the operation of the coke-fired iron blast furnace. On this diagram are plotted points representing the composition of bosh slag under conditions when the flux requirement is changed by the conventional charging method in providing for a change in analysis of coke ash from 7 to 13 pct. These points, represented by A' to G', inclusive, lie in an area of melting temperatures ranging from 1900°C to 1980°C (3450°F to 3595°F). Moreover, the slags in this area are extremely viscous. Under normal operation, analysis of the final slags also varies widely under conditions of varying ash in coke; the theoretical melting temperatures range from 1425°C to 1625°C (2595°F to 2955°F) as shown by points *a* to *g*, inclusive, under the assumed conditions of no adjustment in flux burden to compensate for changes in the analysis of ash in coke. This wide range of final slag analyses, and its accompanying range in desulphurizing power, is no doubt a major cause of poor iron quality control brought about by unforeseen changes in analysis of coke ash.

It is proposed that a high degree of control of final slag analysis could be attained if part of the normal flux requirement were introduced through the tuyeres rather than with the regular burden components at the furnace top. By variation in the amount of flux so introduced, this would enable achievement of an almost immediate change in final slag analysis within a wide range of analyses, and would eliminate the necessity of waiting from 7 to 10 hr for a conventional change in flux burden to finally produce its effect in the furnace hearth after its travel from the furnace top.

INTRODUCTION OF FLUX THROUGH TUYERES

But more important, the reduction of lime in the normal charge as a corollary to flux introduction through tuyeres would yield a pronounced decrease in the melting temperature of the primary or bosh slag and, as a result, would provide a helpful decrease in viscosity. This is indicated by point *Y* on Fig 7, which denotes a melting temperature of only 1780°C (3235°F) for the bosh slag obtained when blowing 20 pct of the flux requirement through the tuyeres. The free-running character of such a bosh slag would, we believe, promote in this critical zone of the furnace a degree of smoothness of operation impossible of attainment with conventional means. As the result of easier gas penetration, it offers the possibility of successful operation with high blast temperatures when using Mesabi ores. In addition, the recog-

* Assistant to Chairman Blast Furnace Committee, U. S. Steel Corp. of Delaware, Pittsburgh, Pa.

[1] C. G. Hogberg: Slag Control by Introduction of Flux through Blast Furnace Tuyeres. AIME, *Proceedings* of the Blast Furnace and Raw Materials Committee (1942) 2.

Pct Coke Ash	Stone Burden Adjusted for Ash in Coke	Stone Burden Not Adjusted for Ash in Coke
	Final Slag	
7	A	a
8	—	b
9	—	c
10	—	d
11	—	e
12	—	f
13	G	g
	Bosh Slag	
7	A′	c′
8	B′	c′
9	C′	c′
10	D′	c′
11	E′	c′
12	F′	c′
13	G′	c′

X and Y denote bosh slags at flux injection rates of 15 and 20 pct, respectively.

Isotherms are in degrees centigrade.

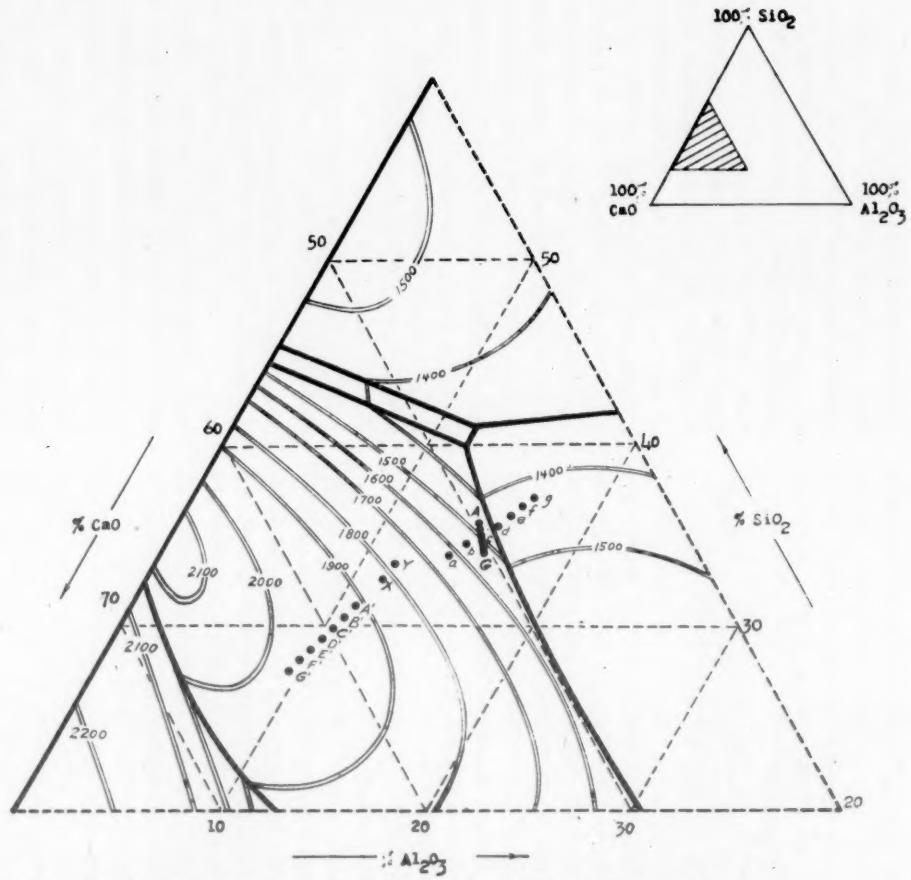

FIG 7—EFFECT OF VARIATION IN COKE ASH ON COMPOSITION AND MELTING POINT OF FINAL AND BOSH SLAGS.

nized advantages of relatively lean slags in providing for operation with "clean" walls are indicated. These benefits are all in addition to the obvious merits of immediate control of final slag composition.

It is recognized that the system $CaO.Al_2O_3.SiO_2$ is not wholly applicable in a discussion of bosh slags, since it does not comprehend the inclusion of calcium ferrites and iron silicates known to be present in such slags. Although not much is known of the effect of iron oxides on blast-furnace bosh slags within the range in which we are interested, it has been established[2] that increased basicity in slags containing iron oxides has relatively the same effect on melting point and viscosity as increased basicity in slags free from iron oxides.

At the time the proposal of flux introduction through tuyeres was first advanced to this group, Dr. T. L. Joseph pointed out the possibility that introduction of relatively cold flux into the hearth might decrease the hearth temperature to the detriment of the operation. But with the use of calcined limestone, ground to a powder to obtain rapid transfer of heat from the hot blast, we believe no serious difficulties will arise in chilling. If they do, the introduction of only a small quantity of oxygen would probably eliminate them quickly; and this suggests a further and possibly a more practical approach to the application of oxygen enrichment on blast furnaces producing basic hot metal.

Much of the speculation and uncertainty in connection with the inner working of the blast furnace arises from our lack of intimate knowledge of the character and relative disposition of raw materials at lower elevations in the furnace. It is true that we have fairly adequate information on the radial and peripheral flow of gases within the stock column, particularly in the upper area, but almost nothing is known of the physical and chemical character of raw materials in the zone extending from near the top of the bosh to the tuyeres—the "critical" region where all of the slag is formed and most of the ore reduction is known to occur. In this connection, an investigation[3] conducted on an iron foundry cupola in Great Britain is of considerable interest. A normally operating cupola was quickly quenched with water within a 40-min. period, and the charge carefully sampled and photographed as it was removed "piecemeal" from the top downward. The results, which are covered in detail in the published report, will prove interesting to students of the blast-furnace process as well as those concerned with cupola operation. It has occurred to us that a similar investigation conducted on an iron blast furnace would yield the type of evidence required to provide unqualified answers to many of the questions propounded by Mr. Larsen. Unless this or a similar study is made, we must be content to be confined to the relatively narrow limits imposed by present theory in our knowledge of the blast-furnace process.

D. P. Cromwell—I am sure that is one other phase to the well-known sampling of materials that develops knowledge that we hope to get in the future. We would like now to hear from Dr. John Chipman, who has information for us on this subject.

Cooperation Needed to Find Answers

J. Chipman*—It is evident that Mr. Larsen has devoted a great deal of thought and study to the formulation of these fourteen questions. They are timely and stimulating, and in seeking their answers we are sure to come out with a better understanding of the blast-furnace process. I believe that the mechanism for finding the answers to questions of this sort will involve the cooperation of operating men with experimental and theoretical researchers. Meetings of this kind can go far toward promoting this essential cooperation.

The metallurgist or physical chemist familiar with the more clearcut problems of laboratory research must ask some very simple and elementary questions and obtain unequivocal answers before he can contribute much to the discussion of these erudite questions on complex interrelated processes. How, for example, does a furnace operator know when a change in burden is necessary or desirable? What are the symptoms of furnace behavior that demand the

[2] I. D. Balon. Viscosity of Blast Furnace Slags. *Stal.* (1946) **6**, 344–353. (Chemical Abstracts, May 10, 1947 **41**, 9).

[3] N. E. Rambush and G. B. Taylor. Iron-foundry Cupola Operation—Investigating the Behavior of Charge Material. *Jnl.* Iron and Steel Inst. (Oct. 1945).

* Dept. of Metallurgy, Massachusetts Institute of Technology, Cambridge, Mass.

change? How do you know when furnace conditions demand an increase in blast temperature and what kind of trouble results if the blast is too cold or too hot? These are mere simplifications of some of Mr. Larsen's questions. They are oversimplified to emphasize the fact that some of us who would like to contribute something to an understanding of the process have only a very slight knowledge of practical operating problems.

Some of Mr. Larsen's questions point to the need for laboratory research along several lines. His questions 1 and 5 point to the incompleteness of our knowledge of the rates and mechanisms of the chemical reactions of ore reduction, especially at higher temperatures. The seriousness of this lack was demonstrated several years ago when operation under pressure was first proposed; it was not possible to predict on theoretica' grounds whether this would accelerate the reduction of ore.

Even in the chemical behavior of slags, when much experimental work of high quality has been carried out, we are unable to distinguish the difference between equilibrium and rate effects in desulphurization. Laboratory research in this field has simply not covered the ground thoroughly enough to provide a basis for answering question 14.

Data Needed on Processes

Research on processes occurring in the furnace itself is also needed. The metallurgical literature of recent years is totally lacking in data on the actual occurrences inside the shaft. In order to form a mental picture of what is going on inside the stock column we must go back to the 1920s and 1930s and read the classic reports by a research team in the Bureau of Mines. The investigators of that time set out to learn what was actually going on inside the shaft and we have been dependent on their reports ever since. These pioneer researches were admittedly incomplete. The development and application of methods of sampling gases and stock in the shaft and of measuring gas and stock temperatures and velocities was a major achievement. Most of our real information on conditions inside the furnace dates back to these investigations. Yet to see how incomplete they were we need point out only one of the questions that was by-passed, namely that of uniformity within a given plane of the furnace. All of the charts representing the results of their study were drawn symmetrically on the assumption that the opposite side of the furnace was behaving the same as the side at which the test holes were located. One of the major needs of the day is a resumption and extension of the work so auspiciously begun 25 years ago with proper emphasis, as Larsen points out, upon a study of the effects of nonuniformity in the stock column on overall furnace performance. A concerted and well-directed research program along these lines with all the modern aids to research such as electronics, supersonics, radioactive tracers, and new analytical techniques would surely yield results of the highest importance to the blast-furnace industry.

D. P. Cromwell—Thank you, Mr. Chipman. We will now call upon Mr. L. M. Fulton.

L. M. Fulton*—Mr. Larsen's brief, yet comprehensive, paper presents a challenge to everyone who has arrived at the conclusion that solution of blast-furnace problems is, above every other steel-plant problem, a task for the fullest cooperative effort. Experimental methods are costly and uncertain, and statistical methods require data to be provided over as wide a range as possible.

This contribution to the discussion is intended to offer only those general principles which are common knowledge, along with opinions derived from the experiences of the contributor and his associates with furnaces using high-silica, high-phosphorus ore and weak high-sulphur coke, making only open-hearth iron.

A chemist who becomes a blast-furnace operator formulates theories prodigiously and, more often than not, drops them precipitously, but eventually he hammers out a working hypothesis which is more or less satisfactory to himself. The working hypothesis upon which this contribution to the discussion mainly rests and proceeds is simply the well established heat transfer theory. No one formula is able to explain blast-furnace behavior, but no set of formulas can begin to explain it, unless it includes this basic theory.

---

* Assistant General Superintendent, Dominion Steel Corp., Nova Scotia, Canada.

Heat Transfer

Heat is transferred from the gas to the stock at a rate proportional to the temperature difference, or

$$q = K(T_g - T_s)$$

where q is the heat transferred
T_g is the gas temperature
T_s is the stock temperature
and K is the heat transfer coefficient.

One salient point may be dealt with easily and quickly. Since at the tuyeres T_g is the hearth gas temperature and T_s is the temperature of the coke which approximates the free-running temperature of the slag, Johnson's "critical temperature" theory is a first approximation to a solution of this equation. However, the approximation covers a limited range, as Johnson himself recognized. Nevertheless, the "critical temperature" theory provides a good working hypothesis, even though there is much adjusting to be done to make it work.

When the blast temperature is increased, or the blast is dried, or oxygen is added, the gas temperature in the tuyere zone is increased, the rate of heat transfer is accelerated in the lower zone of the furnace, and more work is done there. However, in the upper zone the rate of heat transfer and the time allowed for it may be decreased. As a consequence the upper zone may not do as much work as before the increase in tuyere zone temperature. At any rate, the ratio between work done above and work done below some definite level is disturbed. If the furnace previously had heat to spare in the upper zone no irregularity will develop.

However, if previously the work done in the upper zone was just enough to prepare the stock for the lower zone, now the upper zone will be unable to match the increased rate of work in the lower zone, and irregularity will develop. One particular form of irregularity will be examined.

In the shaft of a furnace reduction of oxides and the calcination of carbonates are the predominant reactions. Besides this the stock as it descends gets gradually hotter and requires more room as it expands. At some level formation of slag begins and the expansion of the stock gives way to contraction. The bosh is designed to accommodate contraction, just as the shaft is designed for expansion.

An increase in tuyere zone temperature may so accelerate bosh melting as to outrun shaft preparatory work. Stock will reach the point where the furnace design requires contraction without being hot enough to contract. The stage is thereupon set for hanging, slipping and blowing through.

On the recommendation of engineering and operating departments, one blast furnace was provided with stoves, gas-washing equipment and burners, that would allow the use of a straight line blast temperature of 1400°F. Previously it had been difficult to maintain 1100°F.

Hanging and Slipping

With the new equipment and high blast heat, hanging, slipping and blowing through became the order of the day. The operators, being loath to admit that they could not use the new and expensive equipment they had asked for, tried all the tricks of the trade that they had ever heard of, all the suggestions that expert consultants could give, and finally were compelled to resort to consideration of the fundamental blast furnace function, the transfer of heat from gas to stock, and its implications.

Ultimately, the problem was solved by tempering the tuyere zone temperature by the use of steam, admitted at the cold blast inlet to the stoves. Thus, they were able to run a straight line temperature of 1400°F with a tuyere zone temperature equivalent to that formerly obtained with 1100°F blast temperature.

The solution of the problem of bad behavior in this case was developed from the assumption that the shaft could not prepare stock for all the work the bosh was doing. At the next relining more shaft working space was provided by putting in a thinner lining above the mantle. Results showed that this was a step in the right direction but did not go far enough. It is planned on next relining to reduce the height of the bosh in an attempt to restore the balance between shaft and bosh.

Answers to some of Mr. Larsen's questions are implied in the foregoing. More explicit attention is given each of them to some extent in what follows.

Slag Formation

Question 1—The approximate sequence of slag formation is determined by the melting points

of the slags which may be formed from the materials charged. At any given temperature no slag with a higher melting point can be formed, so that the earliest slag is probably a ferrous silicate. As the temperature increases the slag will pick up other constituents.

The first silicate slag formed will run ahead of the lime with which it was charged. It will appropriate lime from charges as it travels downward to hotter zones. The final slag is, therefore, not a product of any one charge but of several, perhaps many charges.

In the tuyere zone only coke remains solid. Above that is a layer of coke containing undigested lime, so that slag and metal are finally filtered through a bed of lime and coke.

This brief statement of the sequence of slag formation is, of course, over-simplified. Many variables, new and old, require consideration.

The operator, observing a change in slag or metal, begins to guess whether it is a temporary disorder which will clear up without a burden change, or whether it is permanent and must have a burden change. Generally he attempts to make a change of a nature and extent which, if wrong, he can control by heat or blast volume adjustment. Guessing correctly or straddling successfully more often than not are effective factors in blast furnace operation.

Nonuniformity of the sequence of slag formation, either vertically or horizontally, can be a substantial source of irregularity.

Mixing of Charge

Question 2—Experience as an analyst making crucible fusions is a great teacher of the value of uniform and intimate mixing of materials that are to form a melt. Undoubtedly, such mixing would improve furnace regularity. However, two factors which do not enter into laboratory fusions have to be considered in mixing blast furnace materials.

As the stock leaves the bell it encounters an upward current of gas that tends to segregate the sizes. To avoid this segregation each material should be uniformly sized, and if more than one material is dropped from the bell at once, each material should be of a size that would give it the same velocity as the others, according to Stokes' Law of falling bodies.

The other factor is the angle of repose which is different for the charge materials, even though each is sized so as to give the same velocity when falling. Correction of this would require the coke, ore and flux to be passed through a concrete mixer.

Question 3—Frequent changes of burden should only be necessary when the qualities of the materials, such as size or analysis, change frequently.

Question 4—Many calculations of solution loss have shown remarkably small variations with uniform materials. If it does occur, variation in solution loss must proportionately affect heat consumption in zones above the initial slag-forming levels.

Question 5—A cold furnace makes a final slag that is high in FeO. This would indicate that FeO can exist in appreciable amounts, well below the initial slag-forming zone.

It is possible, but by no means easy, to get other evidence by withdrawal of core samples at different levels.

Question 6—All the evidence available indicates that reduction phenomena in present day practice are of very minor importance. Up to the present, at least, blast furnace practice is almost wholly a matter of preparing materials and supplying heat in the proper places and at the proper times to form a slag which will remove all possible undesirable elements from the iron.

Question 7—Reports of "bad furnace behavior" must be considered seriously. An operator need not add a single word to a simple recital of the facts to make the story sufficiently startling. However, "readjustment of operation or furnace design" usually is the ultimate remedy.

Higher Hearth Heat

Question 8—Higher hearth heat increases the work done in the hearth. Probably, since direct reduction undoubtedly is part of the work done in the hearth the amount of direct reduction is also increased.

More detailed heat balances for separate zones could determine whether or not increased hearth heat correlates with direct reduction. Evidence accumulates to indicate that increased hearth heat results in higher solution loss but without any indication that this higher solution loss is undesirable. In almost every instance the higher solution loss following upon

increased hearth heat has been attended by lower coke consumption.

Question 9—No evidence has been uncovered that would lead to any other conclusion than that irregular or unbalanced heat transfer is always the cause of irregular furnace performance. However, nothing points very seriously to variations in direct reduction as a cause, but only as an attendant circumstance.

Question 10—Without appreciable fluctuation of the time rate of an increased direct reduction, and with substantially regular rate of slag formation, at the regular levels, lower coke consumption and a high production rate will result from the use of conditioned blast, higher blast temperature or oxygen enrichment.

Question 11—Uniform gas flow and intimate gas-solid contact are dependent, to a considerable if not great extent, on uniform and intimate mixing of ore and flux, and all are indispensible to regularity of operation.

The use of water has been limited to what is required periodically for washing off the bell and hopper. Keeping water in the burden to a minimum is considered important in conserving shaft heat and, indirectly, hearth heat.

Question 12—Uniformity, low ash and sulphur, with high resistance to crushing and abrasion are the only qualities so far determined to be essential to good blast furnace coke. However, only those who are responsible, both for making the coke and for operating the blast furnaces, need refrain from blaming the coke for furnace misbehaviors that are difficult to explain.

Sulphur in Pig

Question 13—With a furnace using from 3 to as high as 12 grains of moisture per cubic foot, no correlation was clearly evident between blast moisture and sulphur in the iron. The slight indication was that the sulphur varied directly with the blast moisture.

During this period several attempts were made to determine what form of sulphur passed off in the gas. No sulphur at all was found in dust-free gas.

Question 14—An extensive trial of dolomite as part of the flux disclosed that MgO lowered the viscosity of the slag, but that pound for pound it was not so effective as CaO in removing sulphur.

Question 15—Johnson's theory has already been mentioned as a corollary of the general heat transfer equation. The properties of the early slag and the final slag are of great importance to fuel economy, those that require the lowest final temperature to produce good iron being the most economical. However, slags which require quite high temperatures can be used with surprising ease, if the furnace is designed for them, and adequate means of increasing hearth temperature quickly is kept in reserve.

This contribution to the discussion is based on data secured with furnaces using raw materials far down on the scale of suitability. It may be that detailed data from such an operation is of interest to some whose materials promise sooner or later to run down the scale. It has been considered enough now to present only the conclusions; but, to the interested, the fullest available details will be furnished, as part of the program of cooperation, which Mr. Larsen's excellent paper encourages and invites.

D. P. Cromwell—Mr. Fulton, I am sure we appreciate your analysis of Mr. Larsen's paper. The Committee has seen fit to divide Mr. Larsen's paper into separate portions, and discuss each separate portion in such a way as to try and get Mr. Larsen and ourselves some of the answers. At this time, Mr. T. W. Plante, will discuss the variations in burden and in mixing of charge.

Variations in Burden and in Mixing of Charge

T. W. Plante*—Mr. Larsen has advanced questions which have puzzled blast-furnace operators for years, particularly since the time of Lowthian Bell, when blast furnacing was first recognized as being of a more or less scientific nature. If definite answers could be supplied for the majority of the questions, they, together with a few of the simple facts we know, would furnish a rather comprehensive and solid working basis. The blast furnace has reached its present status only as the result of operating trials and experiments. The operator is constantly theorizing as to what goes on inside of the blast furnace, but most of us are reluctant to put thoughts into words, lest we be forced to

* Superintendent Blast Furnaces, Jones and Laughlin Steel Corp., Cleveland, Ohio.

back them up with proof. Too little is known about the inner workings, and research in actual practice reveals a wide range of conditions. The author mentions the extreme difficulty of making direct observations and measurements while the furnace is operating, and of translating laboratory experience to the conditions obtaining in the smelting process. We ask that this be remembered when we try to advance answers to a few of his questions.

Slag Formation

The author *first* questions what is the approximate sequence of processes in slag formation as the material descends through the furnace and is variation in this sequence, or in degree of uniformity over the cross section of the furnace, a substantial source of irregularity of operation?

To answer this we must immediately take refuge in theory, supplementing it with a small amount of general knowledge. All raw materials contribute their quota of slag components. As the materials descend the stack it is reasonable to suppose that the slag-forming components become available at different heights in the furnace, and it is probable that the same component may become available at different levels as a result of faster travel of certain portions of the stock column. We also know that much of the silica entering the slag is not available until the coke containing it is consumed at the tuyeres. Therefore it may be assumed that slag formed higher in the furnace is preponderantly basic. We can always find accumulations of chemically unsatisfied lime above the tuyeres when cleaning stock out of a furnace, and no doubt this condition exists during operation. We know that a highly basic slag tends towards high viscosity; also that slight changes in analyses in the high basic ranges have marked effect on viscosity. It is reasonable to believe that viscosity in turn has a marked effect on gas flow. Irregular gas flow, whatever the source, can readily upset a furnace.

Let us assume, then, a smooth-working furnace with conditions balanced in the upper portion to overcome the excess lime necessary to satisfy the silica released by the coke at the tuyeres. The slag being flushed or tapped from the hearth is satisfactory to the operator, that is, it is "good" slag for that particular furnace, and is a strong indication that good iron will be produced. The furnace then goes "off." There is a strong probability that the chemical balance has been upset, because of an unknown change in analyses, which in turn changes the viscosity with the consequent disruption of gas flow, and a "sick" furnace may result. If the change is only minor, a change of wind or heat may correct the condition; if not, then other measures must be taken.

When a furnace is operating on high ash coke, necessitating a highly basic slag in the upper portions, the furnace can go "off" more readily. Could this be caused by the more marked swings in viscosity of slag above the tuyeres? Following the theory advanced, this could well be possible.

We would answer the question in the affirmative, that is, that variation in sequence, or in degree of uniformity over the cross-section of the furnace, can be a substantial source of irregularity of operation.

Mixing of Ore and Flux

The author asks a *second question*, would more uniform intimate mixing of ore and flux improve regularity?

This cannot be answered by an unequivocal yes or no. Normal operation is to weigh and charge the ore and flux separately onto the big bell. With this procedure the tendency is to distribute the flux more evenly over the stock column. Mixing the usual size flux with a much smaller sized ore prior to placing on the big bell might tend to a greater proportion of the flux being segregated towards the center of the furnace when the charge is dumped. At various times we have placed the materials on the big bell so that there is a mixing tendency when the charge is dumped into the furnace. A distinct change in furnace operation results, but it is one which is not too favorable; on our furnaces a sharp increase in flue dust production accompanies such mixing. On rare occasions, a few charges of so-called mixed filling are helpful, but attempts to make this a standard fill have never been successful in our operations. While the filling discussed is not identical with uniform initmate mixing of ore and flux, the approximation is close enough to enable us to form a negative opinion on the question.

Change of Burden

The *third question* is to what extent is frequent change of burden a necessary means of control?

Controls for furnace operation are few indeed. The ratio of burden to fuel and the method of charging are perhaps the only items over which the operator has jurisdiction prior to the actual reduction process. Once the materials have been committed to their 9 to 12 hr passage through the furnace, control is confined to the amount and temperature of the wind blown, with the effectiveness of these controls often definitely limited.

We believe the author's statement to the effect that "considerable variations of slag composition were brought about by apparently intentional changes in the charge, even during those periods when other factors were reasonably constant" should be qualified. There was probably some logical reason for making the change, even though the ordinary operating records did not indicate such reason. It is true that changes are sometimes made to offset some anticipated swing which does not occur; but the operator should not delay until the effects of such a swing are evidenced later in the operation. He should always work "ahead of the furnace."

Operators make as few changes as possible. When a furnace is functioning smoothly and at what appears to be the optimum production of metal within the desired analyses, the tendency is to "let well enough alone." With such a condition, trial changes might be attempted for constant improvement, but such changes are processed a little at a time, with the operator ever-ready to retreat to safer ground. When a furnace starts to misbehave, changes are more prevalent, marked by increased vigilance to discover any possible error in mechanical operation which may have entered the picture.

Changes may be divided into two categories. First, there are those made to compensate for some known or foreseen change in the raw materials, or to produce iron of different analyses, as for instance when making various kinds of merchant iron. With an intimate knowledge of the individual furnace the operator can make these changes with no distress to the furnace. Second, there are the changes made to rectify some operating irregularity. At times these changes may be numerous and it may be said that practically all are made necessary because of variations in the raw materials. Too often the operator is unaware of such irregularities until the furnace is in trouble. Usually the minimum unit for which an ore analyses is furnished is a 7000 to 14000 ton cargo of ore. Time after time it has been demonstrated that the average analyses does not reflect the sometimes very wide swings of that same cargo. Blast furnaces cannot operate on averages; swings in analyses are measured from cast to cast, or even from ladle to ladle in the same cast. Variations in ore analyses can be compensated for only in the burdening of the furnace, even though this regulation be exercised somewhat late. Control over the ore would be much more effective if applied prior to the blast furnace.

With respect to fuel, the furnace man is again operating under difficulties. At many plants the coke is charged into the furnaces before any change in the analyses is available. Variations in analyses can be compensated for only by changing the burden or flux ratios, and again this control may be somewhat late. The rapid deterioration of coking coal quality during the past few years has contributed to the need for more changes at many of the plants. Here, too, control would be more effective if applied at a point far ahead of the blast furnaces.

Briefly the question can be answered by another question, i.e.—how often do the analyses of the raw materials change?

In general, we believe the time has not yet arrived when we can ask for direct answers to blast furnace questions. Perhaps it would be more logical to expend study on the means or methods for obtaining reliable answers. During recent years we have entered what might be termed the age of radiation. Perhaps some research scientist may some day show us how to investigate the inside of a blast furnace by analyses of its radiations.

Variation in Process of Reduction of Ore

D. P. Cromwell—Thank you, Mr. Plante. The next part of the subdivision will be discussed by Mr. George Steudel on variation in the process of reduction of ore.

G. E. STEUDEL*—Mr. Larsen's paper for the purpose of stimulating discussion, with the possibility of arriving at some constructive investigational work, was read with keen interest and approval. There is no question that work of this nature has been badly neglected. Since McCaffery's studies on slags and the Bureau of Mines' investigations within the furnace stack in the twenties, very little experimental or investigational work on actual furnace operation has been done in the United States. This, no doubt, was largely caused by the depression which hit the steel industry in the thirties, followed by all-out production to meet the emergencies caused by the recent World War II.

As my assignment is to answer the questions on variations in the process of reduction of ore, I consider it opportune to first discuss, briefly, a few factors which have a decided bearing on these variations.

Beneficiation of Coal and Ore

Today, the blast furnace operator is confronted with problems that differ from those of 25 years ago. He has a furnace over twice as large; and, as the Bureau of Mines' investigations indicate, the larger we build circular furnaces, the more inefficient the unit becomes. This is true unless the combustion zone at the tuyeres can be made to cover a greater cross-sectional area of the hearth and the material distribution from the big bell be improved to meet the larger furnace conditions. Ores have gradually become finer and more siliceous. To improve this condition, it will be necessary to beneficiate the ores in order to reduce slag volumes and eliminate excessive flue dust. Because of the poorer coals available, coke has decidely deteriorated in the last six years, both physically and chemically. Many plants will have to resort to washing and bedding of coal, not only for sulphur removal, but also to obtain a more uniform product for cokemaking purposes. Only through a well-planned over-all investigation will we be able to determine the extent of these improvements to justify their installation or adoption.

The sequence of this investigational work should be as follows: first, to improve the coke; second, to beneficiate the ore; and last, to experiment with the furnace to obtain its maximum efficiency.

Mr. Larsen asks, in *Question* 4, "Is variable solution loss of carbon the essential variable directly affecting heat consumption in the zones above that of initial slag formation?"

There is no question that variable solution loss of carbon is one of the main variables affecting heat consumption in this locality of the furnace. Solution loss, within certain limits, is not necessarily detrimental to good furnace practice. Its variability, however, is harmful. It may be of interest to refer here, to Mr. S. P. Kinney's paper, "The Blast Furnace Stack Column," and his summary of a comparison between a 700-ton furnace in the Chicago District and a 300-ton furnace in the Birmingham District. In both of these furnaces, four planes in the stack above the mantle were investigated. These planes, with respect to each furnace, were approximately in comparable positions.

Differences in Blast Furnaces

Mr. Kinney states: "1. Results of gas analyses at the various planes of the two furnaces indicate higher CO-CO_2 ratios in the northern than in the southern furnace.

"2. Of the reduction of iron oxide in the southern furnace, 80.5 pct occurred above the plane, 19¼ feet above the tuyeres, and 19.5 pct was carried on below this plane in the hearth and bosh. In the northern furnace, it was found that only 24.4 pct of the reduction was being carried on in the shaft above the plane 24 ft above the tuyeres, and 75.6 pct was taking place below this plane in the hearth and bosh.

"3. The decrease of oxygen in the stack gases of the northern furnace indicates reoxidation of partly reduced iron oxides, probably by CO_2 produced from the calcination of limestone.

"4. Coke used in the southern furnace was lower in fixed carbon but higher in sulphur, yet a greater portion remained on 2 and 1½ in. screens in tumbler tests. Smaller and more friable coke was used in the northern furnace; 87 pct of the carbon charged as coke was burned before the tuyeres of the southern furnace, whereas only 73.7 pct was burned in the northern

* Division Superintendent Blast Furnaces, Carnegie-Illinois Steel Corp., South Works, Chicago, Ill.

furnace. The smaller and more friable coke probably promoted loss of solution in the northern furnace."

Before discussing the details of this summary, it might be well to state that the southern furnace had a 14 ft 6 in. hearth diam and 84 ft height from the centerline of tapping hole to deck ring. Its production rate was 2.20 net tons per sq ft hearth area, it had a slag volume of 1595 lb per net ton of iron; and a carbon rate of 1884 lb per net ton. The northern furnace had a 19 ft 3 in. hearth diam and a 90 ft height from tapping hole to deck ring. Its production rate averaged, over the period of the test, 2.70 tons per sq ft hearth area; it had a slag volume of about 891 lb per ton, and a carbon rate of 1492 lb per ton of iron. The difference in the material, both physically and chemically, used in these furnaces, prohibits a comparative analysis of their productions, yet it is extremely interesting to note the wide differences of the gas composition in the stack.

The southern furnace follows more closely Gruner's theory for an ideal furnace with a higher indirect reduction in the stack and, likewise, a higher percentage of carbon burned at the tuyeres. If we compensated for the difference in slag volume by the usual method of assuming that it requires 33 lb of coke to melt a 100 lb of slag, it can readily be calculated that the northern furnace, with a low indirect reduction in the stack, was far more efficient.

Mr. Kinney believed that calcination of limestone takes place at points higher up in the northern furnace than in the southern furnace, and the increased rate of driving the northern furnace caused a greater amount of direct reduction to take place in the hearth. He also states that the smaller and more friable coke promoted a higher solution loss in the northern furnace. Both of these statements—on the rate of driving and physical quality of coke—have been generally accepted as factual by the furnace operators.

As the northern furnace was the only furnace of appreciable size on which so complete and comprehensive an investigation was made of gases in the stack, it may be of further interest to determine the amount of carbon that was lost in solution and deposition. The amount of carbon lost to the iron and flue dust was approximately 105 lb per ton of iron. As the carbon rate per ton of iron was 1492 lb and 73.7 pct of this amount was burned at the tuyeres, the total carbon accounted for was 1099.6 plus 105 equals 1204.6 lb per ton of iron. The difference, 1492 less 1204.6 equals 287.4 lb of carbon per ton of iron which represents the solution and deposition loss.

Again Mr. Larsen asks in Question 5 "Can an appreciable proportion of unreduced FeO reach an early slag-forming zone, there to dissolve in liquid slag and react directly with solid carbon? Is it possible to get direct evidence on the extent, if any, of this reaction, its rate, and dependence on slag viscosity?"

Unreduced FeO

As discussed under Question 4, the amount of unreduced FeO that can reach an early slag-forming zone may vary from 15 to 75 pct. The furnace operator has no means of determining this. Occasionally, varying percentages of FeO pass the tuyeres and may be found in the slag and, infrequently, in the iron. We have no evidence as to its extent, other than what can be detected through the tuyeres and by noting the appearance of the slag and of the iron at cast. There is no direct evidence as to its rate. Slags with an appreciable amount of FeO are generally gummy and cold. Slags containing as high as 35 pct FeO have been reported.

In *Question* 6 Mr. Larsen asks, "Is variability in time-rate of this direct reduction the main cause of temperature variation in slag-forming and final smelting zones? Can such variability lead to hanging and serious irregularity in furnace working?"

Since we have no direct evidence of the extent or time-rate of this reaction, it is difficult to estimate its effect; however, it is reasonable to assume that changes in the time-rate or extent would naturally result in temperature variations in the slag-forming and final smelting zones of the furnace. It is these temperature variations that effect changes in slag viscosities, which, in turn, frequently contribute to hanging and furnace irregularities. The causes for all these variations in direct and indirect reduction, solution loss, reoxidation and carbon deposition are many. Some are the result of poor furnace practice, others may be attributed to furnace design or faulty equipment; but the major causes generally are in the materials that the operator is requested to use.

Blast Temperature

D. P. Cromwell—Thank you, Mr. Steudel. The next portion of the breakdown on this paper of Mr. Larsen's will be handled by Mr. William Bennett on the limitations on increasing the temperature or oxygen content of the blast.

W. Bennett*—The introduction of the hot blast by Neilson in 1828 led, as we all know, to immediate advances of considerable extent in fuel economy and production. The first temperatures used were, of course, quite moderate as compared to those with which most of us are familiar nowadays. As stove equipment was improved and increasingly higher blast heats became available, it became the disappointing experience of many operators to find that there appeared to be a limit to the amount of heat a given furnace would take and that this limit varied widely among the various furnaces. Even today we find some furnaces working irregularly if attempts are made to carry blast heats higher than 900°F while others run fairly regularly on a heat of 1400°F or more. Experiments with the use of oxygen enriched blast in Germany and Russia disclosed a similar difficulty when the oxygen in the blast was increased over 26 pct. Workers with a third form of blast conditioning, dehydration, report irregularities in furnace working under certain conditions, when the moisture level of the blast drops to 2 grains per cu ft or less. Apparently, there is some relationship between all three of these phenomena.

I shall attempt to discuss the subject from the standpoint of an operator and to present some new thoughts, some new versions of old thoughts, and a question or two of our own concerning this puzzling subject.

In looking over the matter of utilization of hot blast temperatures, we find, as Larsen has mentioned, some furnaces operating on hard, lean ores are unable to use blast heats in excess of 800–900°F, others on soft Mesabi ore working with a maximum of 1000–1100°F blast temperatures and still others on similar soft ores utilizing heat of 1300–1400°F. Again we find some furnaces, operating on prepared burdens with low coke rate and high production, utilizing blast heats as high as 1500–1600°F while other furnaces operating on rich ore burdens with very low coke rates using 1400°F maximum heat. What is the explanation of these differences? Is there a simple answer? We believe so.

Let us examine the matter on a simple basis. Why does the charge in a furnace in blast cease to settle at times? The generally accepted explanation is that the sum of the support offered by the blast, the friction of the walls and the viscosity of the plastic zone equal the weight of the charge and, therefore, the stock cannot move. The viscosity of the materials in the plastic zone depends on their chemical and physical composition and the heat quantities to which they are subjected. The wall friction varies with the physical nature of the stock and the cleanliness of the wall. Lastly, the support offered by the blast depends on the volume of the blast products, their viscosity and temperature and the free path available at this temperature through the stock.

It is the relationship between the amount of free path offered through stock and the volume of gases to be forced through it that we believe to be the controlling factor in most furnace irregularities connected with blast temperature or oxygen enrichment.

Some writers speak of hanging up of the charge as being related, among other things, to the compression of the combustion zone (Korevaar's theory of heat compression). We do not believe so, as it is difficult to postulate the hanging of the charge at or just above the tuyere level. At any rate, it is not commonly observed in practice. It would seem that that part of the problem of furnace irregularity which concerns stock movement is no simpler or more complicated then as stated above. It may well be that limitations of the use of higher blast heats in this connection are related directly to the free path offered the blast products up through the different levels of the stock in combination with their temperature at these successive levels. Whether or not we can utilize higher blast heats in this regard will depend on whether the added heat in the hotter blast can be absorbed in the hearth and bosh (through increased direct reduction of FeO, SiO_2, or other compounds) or merely raise the temperature of the blast products. This would increase their velocity and viscosity and possibly further affect the effective free path through the charge by driving the fusion

* Carnegie Illinois Steel Corp., Chicago, Ill.

zone higher and into a smaller cross section of the furnace.

In support of this reasoning, we offer the oft-observed result that when the blast heat is "pulled" as little as 50°F on a hanging furnace, the furnace is frequently observed to almost instantly break in pressure and slip on this small heat change. The one logical conclusion for such action would appear to be that the volume of blast products has been decreased sufficiently by the heat change to bring it in proper balance with the available free path for more normal working. It is difficult to see how any other factor than actual blast volume could effect such a rapid change. Most certainly cinder melted by an expanding heat zone (Korevaar's theory) would not effect this change in such time. While we do not deny that time rate of slag melting, viscosity of slag and variability in rate of slag formation are important factors in the limitation of the use of higher blast heats, we believe that they are indirect factors, i.e., they affect the area of available free path for the blast products through the change and it appears that we should recognize them as such.

It has been commonly observed that, other things being equal, lean slags permit the utilization of higher heats than do limey slags. Why? We believe it is because leaner slags melt and run down out of the way more readily than limey slags, thus leaving more free path for the blast products.

Furnaces with high rates of direct reduction, such as ferromanganese furnaces, can utilize maximum blast heat. We believe the reason for this is that when extra heat is added to the hearth of such a furnace in the form of a higher blast heat, the temperature of the hearth and the blast products is not raised appreciably because the extra heat goes to promote more high temperature reactions. There is also a large free path present in this practice as compared to standard basic iron caused by the large amount of coke in the burden.

Furnaces on standard basic iron, using soft Mesabi ore, may or may not utilize high blast heats, depending on the extent to which direct reduction is involved. Such furnaces are normally blown with maximum wind and if they operate with a low coke rate and low direct reduction, there is not such hope of utilizing high blast heats for the following reasons: (1) at maximum wind rate, there is no excess free path area; (2) on soft ores and low coke rate operation, voids in the charge are apt to be already at a minimum. Further reduction in the coke rate may result in too tight a burden, necessitating a "pull" of wind and heat to correct; (3) where there is only a small amount of direct reduction in the hearth, additions to the blast heat can only result in raising the temperature of the blast products and thus of the stock, and in driving the fusion zone into a higher part of the furnace. In support of this argument, we should like to mention an experience involving a 23 ft 6 in. hearth furnace working on soft Mesabi ore and washed coke, utilizing temperatures of around 1500°F continuously for several months. In August, 1937, this furnace produced at the rate of 975 tons of iron per day at a net coke rate of 1761 lb per ton, with a blast heat of 1489°F and a top temperature of 395°F. The following month, the furnace produced at the rate of 966 tons of iron per day at a net coke rate of 1794 lb per ton with an average blast heat of 1509°F and a top temperature of 416°F. The average top gas ratio CO/CO_2 during this time was 2.00 to 1.00. The furnace ran smoothly in this operation and took the heat well. We believe the reason for this was that the furnace was being filled with a charge meant for a smaller furnace and there was a great deal of direct reduction going on in the hearth as evidenced by the high top gas ratio CO/CO_2 and the higher than normal top temperature. This large amount of direct reduction permitted the absorption of large amounts of heat brought in by the high temperature hot blast and thus prevented over heating of the blast products with consequent dislocation of the fusion zone. So much for irregularity caused by unbalance between the available free path and the volume of ascending furnace gases.

Channeling of Gases

Another cause of furnace irregularity, which Larsen mentions but does not appear to emphasize sufficiently, at least from an operator's point of view, is the influence on furnace action of channelling of the gases in the stock column, as a result of dirty or irregularly eroded walls, segregated stock, faulty bell action, etc. The shifting of the gases from one side of the stack to the other in certain furnaces is an ever

present problem for the operator. The more efficient the furnace is, that is, the lower its coke rate, the more harmful the results of such irregular flow of gases. While it is not denied that variability in slag forming rates may and doubtless does initiate many furnace irregularities, we are inclined to feel that more often shifting gas flow is itself the initiator of these irregularities in slag forming rates.

Higher Blast Temperature

Every operator of basic iron furnaces knows well the difficulties of trying to advantageously carry higher blast heat on such furnaces. It is our thought that the answer to the problem for each plant will very likely be different but we feel that higher blast heats than those now used can be carried. Whether the resulting operation would be economical is outside the scope of this paper.

In order to utilize higher blast heat we probably would do the following: (1) Induce more direct reduction in the hearth; (2) Provide greater free path for the furnace gases through the stock by: (*a*) Use of sized material; (b) Use of leaner slags or at least more easily melted slags; (c) Change of furnace design; (d) Use of strong coke; (e) Use of beneficiated material such as sinter.

There are certain other limitations on the use of higher heats which we have not yet mentioned. In those furnaces operating with low coke rates and low top temperatures, and which show a capacity for carrying higher blast heats, probably caused by a relatively high rate of direct reduction, further gain in efficiency through use of higher blast heats to replace coke would not be permissible because of the low top heat, unless water was being used on the burden, which same could be reduced or eliminated. When the top temperature gets below about 230°F there is danger of caking the downcomers and dustcatchers with wet dust.

High hot blast heats would not be permissible on furnaces running on such a low coke rate that further reduction in this rate would not provide sufficient CO gas to carry out a proper amount of indirect reduction in the stock.

Burdens of high moisture content coupled with moderately low top temperatures would impose a limitation on the use of higher blast heats, the same as a real low top temperature would.

Larsen states that operating results indicate that very high blast temperature tends to yield iron lower in silicon, to increase production with only slightly higher slag and iron temperatures. We would say this is only an apparent effect. Blast heat is constantly being used as a heat stabilizer in the furnace by the operator and naturally when the furnace is cooling off and the silicon is low, the highest heats are carried.

Larsen makes a good point, we believe, when he indicates that a steep temperature gradient in the slag fusion zone makes it more imperative that we have fewer variations in slag melting rates or greater furnace instability will result. We feel that this situation would be aggravated in operation with oxygen enriched blast.

We do not believe that total moisture in the charge will affect the temperature gradient in the lower zones of the shaft as any increase in temperature in this zone would very likely have to be compensated for by blast heat "pulls" where maximum heat was already being carried.

We do not believe that an increase in direct reduction results automatically when more heat is supplied to the hearth zone, but think this apparent action is merely the result of the fact that where there is a sizable amount of direct reduction in the hearth, higher blast heats are generally carried. If, as stated by Larsen, "Insofar as increased hearth heat is accompanied by more direct reduction yet without appreciable fluctuation of its time-rate and by substantially regular rate of slag formation," it should be possible to lower consumption of coke correspondingly and to increase production rate by use of conditioned blast and higher blast temperature, provided there is sufficient coke to take care of the chemical requirements of the process (CO gas) and there is an excess of heat in the stack. The same can be accomplished, we believe, by use of oxygen enrichment provided there was previously an excess of heat in the stack.

Oxygen-enriched Blast

We have talked almost exclusively on the limitations of increasing the hot blast temperature. The use of oxygen enriched blast is, in many respects, almost identical in its effects

to the use of heated blast air. Both increase the temperature of the available heat in the hearth without much altering the quantity of heat in the hearth.

A notable point to mention in connection with oxygen enrichment is the fact that for the same amount of carbon burned at the tuyeres, the oxygen enriched blast actually brings in less heat to the hearth than the air blast when both are preheated to the same temperature. This brings out one of the first limitations in the use of oxygen enriched blast. If we are after fuel economy, as one of the returns to be gained in its use, we will likely be disappointed when we attempt to apply it to those highly efficient and modern furnaces producing standard basic iron, and working on lake ores with low top temperatures. The reason for this is that the lower rate of heat input with higher oxygen blast and the fact that direct reduction tends to increase with its use, both work to lower the top temperature and, if this temperature is already dangerously low, we cannot further lower it without running into trouble.

On the other hand, furnaces operating on high top heats and large excesses of stack heat, coupled with deficiencies of hearth heat, offer the largest promise of substantial reductions in coke rate with the use of oxygen. We can expect to run into difficulty with increasing oxygen contents of blast where there is no large demand for hearth heat, the same as we experience in the use of higher blast heats. Oxygen enrichment to 26–27 pct on German furnaces operating on burdens comparable to ours have run into irregularities, which have only been eliminated by "pulls" of blast heat, wind volume or oxygen content. This seems to be a condition quite similar to that we encounter with high blast heats, as higher oxygen contents were not reported as giving particular difficulties when applied on ferromanganese furnaces.

It is possible that the difficulties experienced so far with oxygen enrichment to 30 pct could be largely eliminated through changes in the design of the furnace such as lowering and steepening the bosh and making changes in the composition of the "early" slag. Another possibility is the injection of heating gases in the stack.

When the coke rate is already low, top temperature low and the burden very rich, only a small increase in oxygen content of blast could be made before instability caused by increased direct reduction would appear.

There is another possible limitation in that the lumpiness of ore and stone might become singularly important with the steeper temperature gradient in the fusion zones of the furnaces unless compensations could be made by increase in blast heat or coke rate.

Conclusion

The factors which, alone or in combination with others, appear to limit the use of higher blast temperatures are; low top temperature, low rate of direct reduction in the hearth, high furnace efficiency as reflected in a low coke rate in conjunction with use of fine materials, and, possibly, improper furnace design (for use of higher heats).

Some factors which limit the amount of oxygen enrichment are; heat leaving hearth must equal shaft requirement, top heat must be maintained at a minimum of 230°F, retarded slag formation causing irregular working, lumpy material (ore and stone) giving wide fluctuations in amount of direct reduction and low coke rate furnaces.

At the present time, however, perhaps the main limitation on the use of oxygen is still the financial consideration. Oxygen gas of 90 pct purity has been promised at $4.00 per ton which might make its use in certain blast furnace practices attractive but there are those in the industry who consider this estimate as optimistic. A plant building in Brownsville, Texas, may furnish the answer.

Quality of Coke

D. P. Cromwell—Mr. Plimpton will now comment on coke quality.

T. F. Plimpton*—It is easy to understand how "the endless controversy about coke quality begins to take on the aspect of a nightmare" to Mr. Larsen. But I do not believe that his nightmare is so acute as the one a blast furnace operator suffers when he encounters really bad coke.

---

*Superintendent Blast Furnaces, Inland Steel Co., East Chicago, Ind.

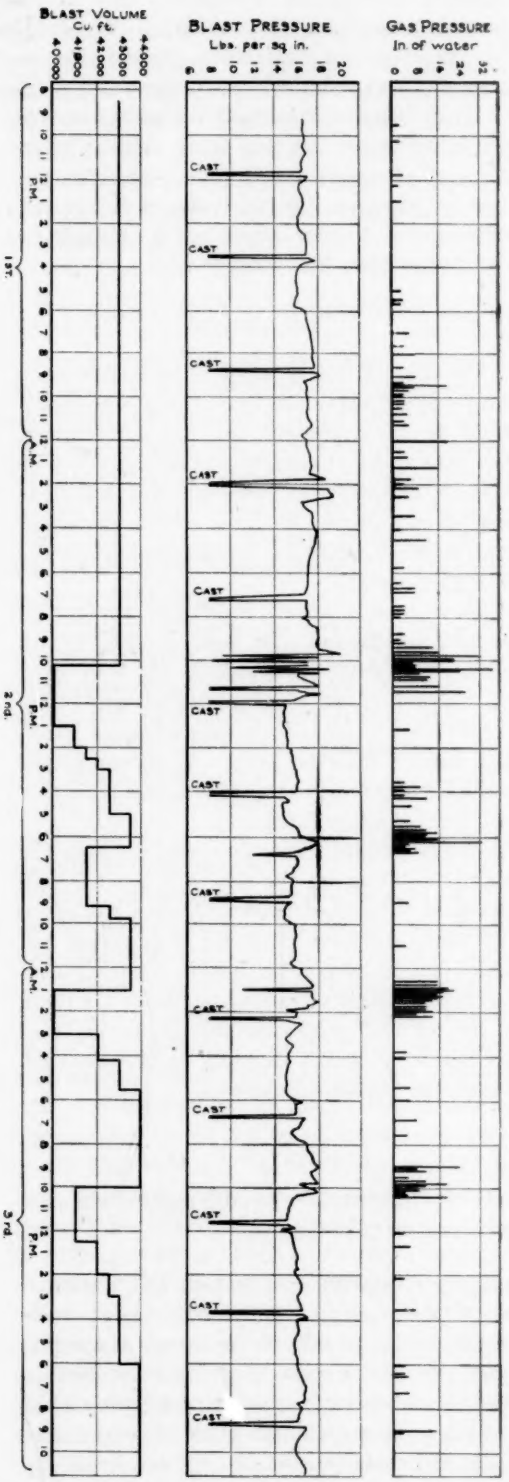

FIG 8—OPERATING DATA FOR NO. 3 FURNACE DEC. 1935.

There are many reasons for bad blast furnace operation and poor coke is one of them. With good coke it is possible to have poor blast furnace operation, but with poor coke, it is not only impossible to have good operation but it is also quite likely that the operator will have a rough time of it.

As Mr. Larsen suggests, we may have complicated the problem of coke quality unnecessarily, although we must guard against oversimplification. We believe his point about reactivity is well stated. It has never seemed to us that within the range of variables ordinarily encountered that the reactivity of coke is significant. It also appears that in combining various properties of coke into an index of quality we run the risk of masking certain effects.

The fact that the resistance of coke to crushing and abrasion is the really important consideration is well supported by the author's data. Second only in importance to this, however, is the matter of uniformity.

In considering uniformity, I should like to point out that it is impossible to get a sample of coke for any test purpose that will adequately represent what the blast furnace has been using for a 24 hr period. We may take from one to a half dozen samples of 50 lb each to represent a thousand tons that the furnace has used.

It may well be that half a dozen tests represent an average of the thousand tons, but that does not reflect what the operation of the furnace might be because the furnace is interested in each layer of coke charges, not the average. Fig 8 does not apply directly but does illustrate this point. At one time we were attempting to use the coke which was screened out of the flue dust at the sintering plant. These were mostly large pieces which were present in the flue dust from a hanging furnace. The coke was screened twice to make it as clean as possible. One skip load of this coke was charged in the furnace at the start of each 8-hr turn. There were about 240 skip loads of material going into the furnace in each 8-hr turn so it represented less than ½ of 1 pct. You will note on the figure that shortly after the start of each 8-hr turn the furnace would start to hang and slip for a period of about ½ hr. This continued for several turns when we noticed what was happening and discontinued the use of the

rescreened coke; immediately the trouble stopped. We tried it again several days later and it repeated itself.

This property of uniformity of coke is most important. We may have two days of blast furnace operation in which the coke was identical except that one bad oven was pushed and went into one furnace. That would cause great difficulty and might result in a 10 pct reduction in tonnage produced. However, if that one oven, which might represent 1/10 of 1 pct of the coke charged into the furnace, was not sampled, the physical test would never have demonstrated the difference and the coke for the two days would have been identical. None of our present methods of testing coke can measure this variation and until we are able to get such a measurement we will never be able to correlate accurately. The obvious solution is to go back to the source. If every charge of coal going into every oven is identical, and if segregation in the oven is kept at a minimum, if the ovens are all coked at the same temperature for the same length of time and given the same treatment before delivery to the furnace, then the coke should be the same. If this standard can be maintained day after day, then we can have more faith in the data we accumulate and in our conclusions in applying those data to blast furnace operation.

Sulphur

D. P. Cromwell—Thank you, Mr. Plimpton. One of the other difficult problems of the blast furnace operator is sulphur. Mr. Paul Nichols will now discuss that feature of Mr. Larsen's paper.

P. R. Nichols*—Blast furnace operators are indebted to Mr. Larsen for his presentation of this paper. Perhaps most of us have been rather busy these last few years attempting to achieve maximum operation of our facilities and have failed to give some of the theoretical phases of the process the attention and thought which they deserve. An operator's life has not been an easy one and he in general appreciates the helpful stimulation of the research fraternity. Much work remains to be done on the problem of sulphur elimination, a problem which is very pressing on some operators today and one which will become of increasing and real concern to all operators in the years just ahead. Accordingly, we should welcome assistance from all quarters in developing more effective and more economical means of eliminating sulphur from the blast furnace product.

Mr. Larsen, in Fig 4, presents a picture which appears to be conclusive evidence of the value of increased blast moisture in lowering iron sulphur. It would seem that those operators having facilities for blowing at controlled low levels of moisture could give definite and conclusive evidence on this problem. There are numerous plants where steam addition to the blast is a common practice. However, in discussing this subject with advocates of both high and low moisture they report no evidence of a correlation such as is shown in Fig 4 of Mr. Larsen's paper. At the same time they point out that the difference in sulphur content shown by the two lines in Fig 4 is rather small and might not come to light without careful checking and study of the operation. If, as is suggested, there is some relationship, perhaps those operators having facilities for operating at controlled moisture levels could rather simply determine its existence. Whether hydrogen librated in the hearth from blast moisture is responsible for increasing the ratio of slag sulphur to iron sulphur is not readily determined. However, if such is the case hydrogen must be a very effective catalyst since it can be shown that when blowing air containing 9 grains of hydrogen there is but two thousandths (0.002) of the total weight of blast as hydrogen. With a modern dry blast installation lower moisture levels could be utilized which would reduce the weight of hydrogen available to a point where its effect would be negligible. Careful control and observation under such conditions should establish the answer, at least in part, to Mr. Larsen's Question 13.

It might not be amiss to suggest, as a prophecy, that the growing technique in the use of radioactive tracers may eventually throw considerable light on the problem here presented, not only as regards sulphur elimination, but upon some of the other questions Mr. Larsen has asked earlier in his paper.

Another confusing factor in this picture is the conflicting effect of lower hearth temperature that results from the dissociation reaction. Many of our foremost investigators in the past have stressed the important role

* Assistant Superintendent Blast Furnaces, Wisconsin Steel Works, South Chicago, Ill.

of slag temperature in its desulphurizing ability. Higher blast moisture resulting in more hearth heat absorbed and consequently lower slag temperature should tend to make the slag less able to remove sulphur. Under these circumstances, if such small amounts of hydrogen can have the result intimated then it must be an exceedingly active catalyst in a reaction which is not clearly understood.

As to the range of sulphur content in dust free top gas the average blast furnace operator has little or no information. There are formidable difficulties in accurately determining this quantity, and, furthermore, he would probably reply that sulphur balances generally account for all but about 2 pct of the sulphur charged (the 98 pct being in slag, iron and flue dust), so that for the present at least he is not too much concerned with the gaseous removal of sulphur. Of much more immediate importance to practical sulphur elimination, as this problem confronts the average operator, is the subject raised by Mr. Larsen in Question 14. Slag viscosity as affected by its magnesia content is probably a factor in determining the rate of transfer of sulphur from metal to slag. Fig 5 illustrates a generally accepted conclusion that magnesia when held at about the 6 pct level is effective in promoting desulphurization. In actual experience with slags containing up to 20 pct magnesia it has been demonstrated that this tendency is not maintained, in spite of a decrease in viscosity. Perhaps the answer to Question 14 can be accurately established when we have more reliable information on the dual role of viscosity, i.e., low viscosity on the one hand promoting desulphurization by permitting greater contact area between slag and metal while on the other we require a viscosity high enough to retard the descent of the iron globules so as to provide a greater time interval for the desulphurization reaction. It is understood that in each case the chemical composition must be such as to promote transfer of sulphur from iron to slag.

Slag Viscosity

The optimum magnesia content then is one which results in a viscosity tending to fulfill these requirements both mechanically and chemically. From the data portrayed in Fig 5 it is apparent that the optimum value for that particular operation is above 5.2 pct magnesia.

While not specifically mentioned by Mr. Larsen, the influence of the other principal slag constituents, alumina, lime, and silica, cannot be disregarded in discussing the function of magnesia. In this connection I would point out that it is sometimes to advantage to increase magnesia beyond its optimum desulphurizing range. Particularly is this true where wide variations in raw materials have developed a badly working furnace. The higher magnesia then removing the slag chemistry from a region of critical temperature-viscosity relationships to an area where relatively wide swings in composition still remain within the phase boundary.

While much has been learned regarding the functions of the various slag components and of temperature there still exists a need, as Mr. Larsen points out, for reliable data on sulphur distribution for the commercial range of compositions of slag and iron.

Different combinations of raw materials as experienced at different plants tend to indicate that the most advantageous slag composition at one plant may not be quite as efficient in another. And in such considerations of slag composition and desulphurizing power we must also include other interrelated factors which bear on the end result—the most economical production of pig iron. It is theoretically possible to demonstrate fuel economy and production gains while operating a furnace on low slag volume with the slag sulphur quite high and iron sulphur acceptable, yet it is unlikely that two operators will find the optimum conditions to be the same. In meeting the problem of sulphur elimination there are at hand several choices of procedure that may furnish the answer under various raw material situations.

Coal Blending

Coal washing and blending to insure uniformity of analysis in both washed and unwashed coals have demonstrated effectiveness at several plants, and several very encouraging reports have been published within the past year. More uniform materials with secondary regard to the level at which uniformity is achieved is the goal of most operators. They are aware of the economies which can be realized

when they do not have to burden for peak conditions. Blending of coals to eliminate peaks in ash and sulphur content is an integral part of our sulphur elimination problem.

The field of desulphurization external to the blast furnace continues to receive considerable study. Changing techniques and desulphurizing mediums may point the way in many operations to the most economical means of solving this problem.

In some quarters it has been found advisable to increase manganese content to achieve a lower sulphur product. Where this procedure can be followed it may be possible to improve the overall economy of both blast furnace and open hearth operations.

It has been a long held opinion of many operators that the field of economical sulphur removal has not been fully covered until a thorough trial had demonstrated what can be accomplished by the introduction with the blast of that portion of the flux required to combine with the coke ash. It would seem that this type of operation which would enable the furnace to work on a lean bosh slag would yield economies in smooth operation and lower coke rate which cannot long remain overlooked.

Finally it is perhaps elementary to point out that, inasmuch as about 90 pct of all sulphur charged enters the furnace through the coke, the reduction of coke rates offers a good approach to the problem of sulphur elimination.

Reaction of Ore Particles

J. J. Howard*—After over forty years of operation, the blast furnace still appeals to me as a remarkable piece of equipment. Year after year I have attended meetings and listened to the excuses of operators for poor results from a furnace. I have heard many men state that "the furnace got sick," but my reply has always been that no furnace could get sick, the operator had to make it get sick, and he should find out what he had done that caused the interruption in operation.

Mr. Larsen has made a modest approach to the problem, but he evidently knows as much about furnace reactions as many men who are running blast furnaces at this time. He has touched on some fundamental and very interesting points in blast furnace operation, and it would take a long paper to attempt an answer to all the questions that he asks because they cover such a broad field.

In the first place, it helps to appreciate that solids can hardly be made to react with each other, and he certainly touched on a vital point (p. 622) when he takes notice of the fact that the smaller the particle size, the more intimate the contact, and consequently the most rapid reaction. Too much stress has been placed on the fact that CO will reduce iron in iron ore. This reaction however, is of no use to the blast furnace man unless he is able to agglomerate the iron so reduced, which means it has to go into the liquid phase and to do this, the temperature has to be above 2200°F. Basically, the trouble with the so-called sponge process is that while the iron can be reduced at comparatively low temperatures, when attempt is made to put this iron into economic shape, the difficulty arises.

Concerning Mr. Larsen's first question, there really is no operating slag in the blast furnace until the final stage in the region where the ash from the coke is picked up and joins the lime and gangue from the ore.

To start with, a furnaceman should at least know the melting points of the ores he is using, since complete reduction can be made only after the liquid phase is reached. A few years ago I had the literature examined, and was astounded to find practically nothing regarding the melting points of the different ores used in blast furnaces. Many operators criticize certain ores as being "refractory" when in reality they were simply hard physically. One of the softest ores in the Lake Region has a melting point of close to 2900°F which really, as far as temperature is concerned, puts it in the class of commercial refractories. Consider an iron ore with 64 pct iron, 2.23 silica, 1.27 alumina, with less than 0.3 of 1 pct bases present. After all of the iron is reduced out of this ore, there is a mixture containing about 64 pct silica 36 pct alumina, and if this is checked on the phase diagram, it will be found to melt at a temperature away above any ordinary temperature in the blast furnace.

Refractory Gangue

This gangue material from the ore, after the iron and manganese are reduced, is, I believe,

*Vice President, E. J. Lavino and Co., Philadelphia, Pa.

the basic *cause of all blast furnace scaffolds and most irregularities*. It should be of interest to every blast furnace operator to take the ores used in his plant, and check what the melting points of the gangue would be after the removal of the iron and manganese. This gangue has to move down in the furnace until it picks up the lime, but oddly enough when that occurs, there is almost twice as much lime added to the gangue as is needed to make a fusible slag. This occurs because the limestone is calculated to take care also of the ash in the coke that is picked up only as the coke is consumed. If these reactions could be synchronized, it would be most advantageous for the blast furnace man. Mr. Larsen was however, bordering on the answer when he suggested that prepared ores and sinters should have the necessary fluxing material intimately incorporated. We have an existing example of such material in the Alabama ore—which is practically self-fluxing and which melts at a temperature below 2300°F. With only 34 pct of metallic iron in the ore, these Alabama furnaces have produced very large tonnages of pig iron, even with coke that is not comparable with most of the northern cokes.

When the big blast furnaces in the Pittsburgh district were operated at the turn of the century with 74° angle in the bosh, it was almost impossible to find a furnace that would not slip. In fact there were a few very serious disasters following heavy slips on blast furnaces.

When furnaces slip the first thing blamed is the coke, but I could not agree with any such criticism. There should be some intensive research, however, into producing coke that would burn fast at the tuyeres and second, resist the action of CO_2 in the upper part of the furnace.

In the summer of 1945, I presented a short paper before the Eastern States Blast Furnace and Coke Oven Association in Pittsburgh, and indicated that where fine ores or flue dust have to be sintered or nodulized, there should be sufficient lime added to flux the gangue. This would also lower the melting point making a strong sinter and reducing the cost of replacing grate bars. It would also tend to lower the loss of coke incurred by the liberation of the CO_2 produced by burning the limestone. We have tested certain cokes and found that CO_2 will attack them at as low as 1200°F and that at 1900°F they will develop CO very rapidly, which means a definite loss of coke.

A blast furnace can make pig iron only as fast as it can burn coke, for coke is about the only thing in a blast furnace that will not melt. High blast temperatures have been blamed for many difficulties, but the higher the blast temperature, the higher the flame temperature in the front of the tuyeres, with a resultant faster combustion of coke. All of the efforts to use oxygen in a blast furnace were intended to increase the combustion of the coke.

Coke Problems in Blast-furnace Operation

K. Neustaetter*—I believe Mr. Larsen's paper is an exceptionally good one. I say this not because Mr. Larsen has expressed any revolutionary ideas, or because he has solved any tough problem, but rather because his paper is stimulating and because it forces one to do some thinking of one's own. The questions that Mr. Larsen propounds are those that confront all operators and students of the process. His scholarly comments will help to guide future study.

Mr. Larsen as a scientist is baffled about some of the things the operators do, just as many operators have no conception about the work of the scientist. I do not want to call this a misunderstanding. Where there is not sufficient contact there can be neither understanding nor misunderstanding. This lack of contact is not on the higher level. Works managers and superintendents are familiar with both theory and practice, but the research worker and the general foreman most of the time live in different worlds. Greater familiarity with each other on the level facing the daily routine is needed and a deliberate effort should be made to bring this about.

Mr. Larsen questions whether all the changes made by the operators are really necessary; the operator believes they are. There is no agreement on how to make even the most frequent of all changes, namely the change of the ore to coke ratio in case the furnace is too hot or too cold. Some operators insist that the charging of extra coke is the answer, a practice which is vigorously condemned by others who prefer increasing and decreasing the ore charge.

* Blast Furnace Engineer, Inland Steel Co., East Chicago, Ind.

This is a question that could easily be resolved by a cooperative effort between operator and scientist. Experimental runs could be arranged with a minimum of cost, and much knowledge could be gained by an intelligent evaluation of existing records.

My studies during recent years on gas flow and coke consumption in the blast furnace enable me to make some remarks about sections C and D of Mr. Larsen's paper.

J. B. Austin proved in his paper "Efficiency of Blast Furnace Process" that for our common grades of pig iron the coke consumption is determined by the carbon requirement necessary for reduction purposes rather than by the carbon requirements necessary for heat. It appears to me that in some cases the coke requirement for mechanical purposes exceeds the requirement for both of the other two purposes. Furnaces operating on Mesabi ore are very sensitive toward changes of ore and coke size and toward the mechanical strength of the coke. When operating on "full" wind, furnaces are close to the edge all the time. A small amount of undersize coke forces a wind cut, while a relatively small amount of screened ore permits additional wind. The same is true for varying strength of the coke. The standard tumbler stability seems to measure this strength best, though it is not 100 pct satisfactory. Higher blast heat has the same effect as an increase in the wind blown, namely, to increase the volume of gas which has to pass through the stock. Varying size of ore and coke and other local peculiarities will naturally cause different upper limits for blast heat and volume for different plants. This reasoning explains the phenomenon Mr. Larsen noticed of higher coke rates and higher blast heats at the same time.

Incidentally, if the authors of technical papers describing furnace operation under varying conditions would state whether the amount of wind blown was all the wind the furnace would take or whether the wind rate was determined by other factors, it would be of great help to a person studying these problems.

In his twelfth question Mr. Larsen asks whether the importance of an ill defined "coke quality" as a source of blast furnace irregularity might not be exaggerated and might be replaced by the coke's simple resistance against crushing and abrasion. Our answer to this would be an affirmative one, and for an example we could cite our practice during the war years. From 1940 to late in 1943 top production was maintained in spite of many difficulties in operating conditions and many coke changes. In 1943, however, many new coals were introduced and there was a decided decrease in coke strength together with a marked increase in coke ash. These changes caused a pronounced falling off in the average wind that the furnaces could handle and a consequent decrease in production.

M. B. Bever*—In recent decades steelmaking has been studied by a rapidly growing number of investigators but the fundamental aspects of pig iron production have attracted only scant attention. As a result, current knowledge of the physical chemistry of steelmaking is far ahead of our understanding of the blast furnace process. The paper under discussion encourages the hope that this lag of blast furnace theory may not be permanent.

The questions raised in this paper illustrate the complex nature of blast furnace problems most of which depend simultaneously on several variables: heat transfer, chemical equilibria, the partition between direct and indirect reduction, catalytic effects and reaction rates as well as a number of mechanical operating factors. Complex industrial problems commonly cannot be solved unless they are broken down into constituent problems of a fundamental nature. For this reason it will probably not be possible to answer some of the questions asked in this paper without experimental work much of which will be of a laboratory nature.

This paper employs very effectively the statistical evaluation of plant data. In some of the frequency distribution plots, Figs 3 to 5, the data should perhaps be divided into more than two ranges. The question may also be raised as to whether in general line of regression plots (as used in Fig 6) are not preferable to frequency distribution curves.

The dissociation of all moisture in the blast into hydrogen and oxygen is mentioned in B 9. Even at the high temperatures in the tuyere zone water does not dissociate to any extent but reacts with coke as discussed in Section E. The heat effect of this reaction agrees with that assumed in Section B.

* Dept. of Metallurgy, Massachusetts Institute of Technology, Cambridge, Mass.

At times in every field of inquiry the formulation of fundamental questions is the most important contribution that can be made. The present paper unquestionably constitutes such a contribution to the theory of the blast furnace process

Author's Reply

B. M. Larsen—On behalf of the AIME Committee on the Physical Chemistry of Steelmaking, the writer wishes to thank all the contributors for such stimulating discussion as well as for their charity toward the raising of more or less unanswerable questions by the author. Regardless of the wisdom, or lack of such, in the choice of these questions, the discussion as a whole makes a basis for a future program of studies on the metallurgy of the blast-furnace process, and the elaboration of such a program would seem the next logical step. Before attempting to outline such a program in a very tentative form, a few comments on some points in the discussion may be justifiable, even though the obvious need is for more data, more measurement rather than more talk and speculation.

Gas Flow

There appears to be general agreement on the importance of gas flow distribution and heat transfer in the shaft zone, but many details in the process still require clarification. Some of these are, for example, (1) the quantitative effect of lowering the moisture content of the burden on the temperature-time period for indirect reduction (by CO) and on the irregularity caused by a possible too-steep temperature gradient approaching the initial slag-forming zone; (2) the degree of self-correction of non-uniformity resulting from the fact that the gas stream is both the heating and the reducing agent so that rate of heating, rate of reduction, and rate of flow of solids could perhaps automatically compensate for variable rates of gas flow; (3) the reactions of CO_2

$$CO_2 + Fe \rightleftharpoons FeO + CO,$$

or

$$CO_2 + C \rightleftharpoons 2CO;$$

near limestone surfaces in the calcination zone by these, and probably other details of the shaft processes need clarification. This clarification may be brought about by (a) more direct measurement and sampling in operating furnaces; (b) calculations of such things as separate heat balances for the shaft zone; and (c) correlated laboratory experiments.

Tuyere Lime

Experimental trials on the introduction of powdered lime into the tuyeres is apparently long overdue, and this suggestion by Mr. Hogberg deserves very serious consideration. It has a probable practical aspect, but is also of importance to our subject here since it should give us additional clues about the process of slag formation. The interesting point was brought out that with present trends toward higher-ash coke, the difference between initial and final slag composition tends to increase.

Burden Changes

Considerable light has been cast on the logic or burden changes, but there is perhaps room for much more complete explanations of this problem. However, the great importance of variable ore and coke and the inadequacy of both control and sampling methods is well illustrated. There is a fair degree of agreement with the concept of ash plus S contents together with resistance to breakage as the all-important qualities in blast furnace coke, but Mr. Plimpton also emphasizes the overriding importance of *uniformity*. As coal washing and mixing improves, the next immediate problem is that of much improved control of coking conditions in each individual coke oven and/or testing methods to segregate inferior coke batches.

Slag Formation

There is general agreement about our relative ignorance on the details of slag formation. There is a strong probability that the solution of lime progresses gradually down through the melting zone. Still largely a matter of speculation, however, are the problems relating to the details of initial formation of a eutectic mixture (perhaps FeO, MnO and SiO_2 with some CaO), the disintegration of the reduced ore lumps, and the stage in the process at which liquid iron is formed, etc. It is generally believed that there is some direct reduction between coke carbon and FeO dissolved in early slag liquid, but as to its amount, rate, effect on variability, and relation of its increase to

increased carbon solution loss at higher levels we apparently have little information. There is evident skepticism about the importance of the effect of the heat absorption in this reaction on furnace swings and irregularity. However, if this direct carbon reduction is very appreciable in amount, its heat absorption can in theory affect slag formation and high temperature smelting reactions, so that this probably should remain an open question until we learn more about these processes.

Information Needed

Largely because of our present limited understanding of these higher temperature changes and reactions, and despite many significant points brought out in this discussion, there is apparently a need for much more information to clarify our understanding of hanging, slipping and irregularity and their relationship to increased hearth heat supply by hotter blast or oxygen enrichment.

We wish to extend special thanks to Mr. Fulton of Dominion Iron and Steel of Canada for his stimulating discussion, along with the hope that he or his associates will find time to prepare a paper summarizing the raw material conditions and blast furnace operating results in his plant.

Both Mr. Fulton and Mr. Bennett offer very plausible and reasonable explanations of the effect of increased blast temperature on the tendency toward hanging and irregular furnace action. But if one tries to extend the reasoning into details of mechanism or of fundamental cause and effect for either of those explanations, or to compare them with each other, one soon encounters the insufficiency of our background of data on the slag-forming zone.

There is much evident agreement in this discussion on (1) the need for more direct observation in the blast furnace plus correlated experiment and calculation; and (2) the feeling that this is the time for a resurgence of activity in this field such as was carried on by the Bureau of Mines and others in the 1920's and has been relatively neglected in the war and depression years. Because of the combination of great size and complexity and difficulty of measurement in the process, the problem has need for a cooperative research program. As a mere beginning toward a tentative outline of such a program, we offer the following suggestions:

1. Further measurements of temperatures and velocities etc. and especially sampling of solids inside the furnace such as was carried on by Kinney and others about 20 years ago.

2. Cooling of an operation unit under conditions such as to give the minimum of change in the materials present while in operation; careful digging out and study of such furnace by visual observations coupled with chemical and microscopic studies of both stock and refractory surface layers or adherent material.

3. Experiments on powdered flux or other material introduced into the tuyeres with such coordinate measurement as will help to interpret the effects in terms of mechanism of slag formation and of bosh zone reactions.

4. Experiments with furnace design changes such as further steepening of bosh angles and lining of bosh and hearth walls with carbon or other material such as would permit the nearly complete elimination of cooling water in the refractory lining, etc.; perhaps first started with a small commercial or an experimental furnace.

5. Extensive laboratory studies on reduction and slag-forming reactions with gases and carbon in the higher temperature range of 2000–2800°F. Slag-metal equilibrium studies such as S-distribution on the actual blast furnace composition ranges.

6. Data and calculations leading to heat balances of separate zones in the furnace. Measurement and/or calculations on gas flow resistance or pressure drop effects of temperature change in the higher temperature range.

7. The various commercial experiments made on oxygen enrichment, high-pressure operation, ore beneficiation, etc. to be implemented with such scientific control and measurement as to help in making their results throw most light on the general problem of the physical chemistry of the blast furnace.

The financial and manpower implications of such a broad program are such as to demand the cooperation of much of the industry as well as a few university, industrial and governmental laboratories, and perhaps the cooperation or leadership of the U.S. Bureau of Mines. But we should perhaps also face the fact that the magnitude of the problem almost demands a reasonably broad cooperative program if we are to hope for reasonably rapid progress in understanding the blast-furnace process.

Discussion on Diffusion Rates for Carbon in Austenite

(This volume, pp. 531–552)

C. E. BIRCHENALL*—The steady-state method employed here by Mr. Harris for determining the rate of diffusion of carbon through an austenite plate is an experiment very well worth while. The value of future experiments of this type would be greatly enhanced by analyzing sections taken from the plate perpendicular to the direction of flow of carbon. Since the system is in a steady state, the quantity of carbon flowing through any cross section in a unit of time P is identical throughout the sample. In order to obtain D at each point on the penetration curve, one need only measure the slope $\frac{dc}{dx}$ of the penetration curve at the point and the total rate of flow of carbon through the sample. *At each point* the quantities are related by the first Fick equation

$$P = -D\frac{dc}{dx} \qquad [1]$$

The extreme complexity of Mr. Harris's mathematical treatment of the diffusion of carbon in austenite raises the question of whether a simpler method is not more desirable, and the dubious nature of the assumptions stated in his equations 1 and 2, from which the treatment derives, raises the question of whether another method might not be more valid even though the numerical agreement with existing data may not be as good as can be obtained by the arbitrary selection of correction factors.

In regard to the author's Eq 1, the experimental data[6] show that the rate of diffusion for two cases with the same $C_1 - C_0$, L being held constant, will be greater for that case in which C_1 and C_0 are greater. D_1, irrespective of how it is defined, cannot be a constant in Harris' Eq 1, but must depend on the magnitudes of C_1 and C_0, becoming greater as C_1 and C_0 increase.

Reference to the experimental data will also show that $D(c)$ is not a linear function of concentration as assumed in Harris' Eq 2. However, $D(c)$ has been shown to satisfy the relation

$$D_1 = \frac{D(c)}{\left(\gamma_1 + C_1\frac{d\gamma_1}{dc_1}\right)} \qquad [2]$$

up to 1 pct carbon, where D_1 is now a constant, γ_1 is the activity coefficient for carbon in austenite and C_1 is its concentration.

Wells and Mehl[6] have shown that nearly identical results are obtained in the case of the diffusion of carbon in austenite whether the Grube analysis or a Matano type method is used. This is a consequence of the fact that the areas on the penetration curves between the following: the gas-metal interface, the distance corresponding to the concentration for which the calculation is made, the C_0 axis, and the penetration curve, will be nearly the same for a curve obeying the Grube assumptions and the experimental curve. Therefore, in order to recalculate a carburization penetration curve within the combined limits of error of the three sets of determinations—(*a*) the diffusion coefficients,[6] (*b*) the carburizing rates[8] and (*c*) the activities of carbon in austenite[9] (additional error is introduced by the necessity for interpolating both activity and diffusion data and possibly by extending Eq 2 into a range for which it is not yet empirically established)—it is sufficient to replace D in the Grube solution for the semi-infinite solid by $D(c)$. The solution is then

$$\frac{\Delta C}{\Delta C_0} = 1 - \phi(y)dy \qquad [3]$$

where

$$y = \frac{x}{2\left[D_1\left(\gamma_1 + C_1\frac{d\gamma_1}{dc_1}\right)t\right]^{1/2}}$$

ΔC_0 is the difference between the base carbon concentration and the surface concentration, ΔC is the difference between the concentration at distance x from the surface and the base carbon content of the original sample, t is the time and $\phi(y)dy$ is the Gauss error integral. By fixing t and choosing successive values of $\frac{\Delta C}{\Delta C_0}$, one may evaluate x point by point.

Let us first compare a solution of this equation with the master curve given by Harris[8] for the following arbitrarily chosen set of conditions: surface concentration, 1.5 pct carbon (the saturation value according to Smith[9]); bulk of sample carbon free; temperature, 1000°C; time, 10^5 sec; $D_1 = 0.258 \times 10^{-7}\frac{cm^2}{sec}$.[7]

* Metals Research Lab., Carnegie Institute of Technology, Pittsburgh, Pa

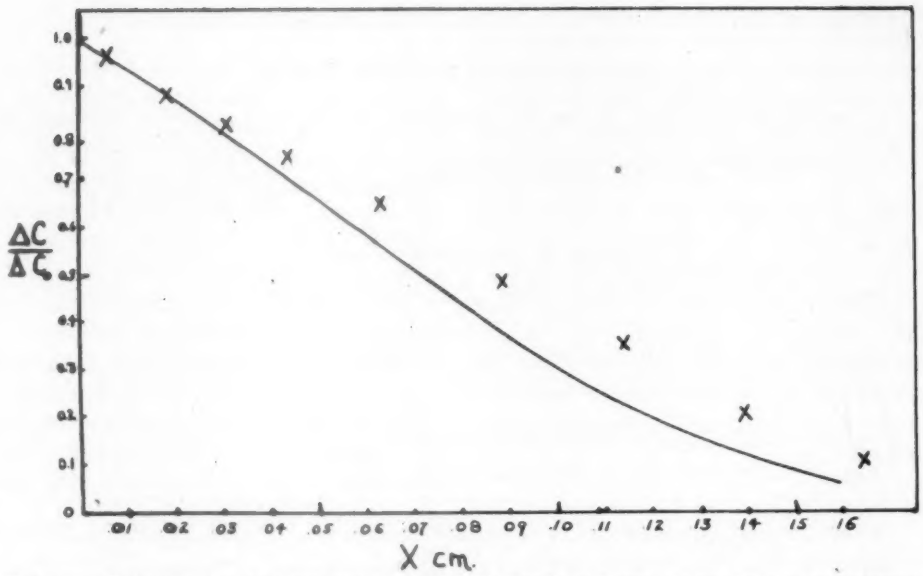

FIG 13—COMPARISON OF EQUATION 3 WITH HARRIS'S MASTER CURVE FOR CARBURIZING. The solid lines are calculated from equation 3. The crosses are from the Harris data.

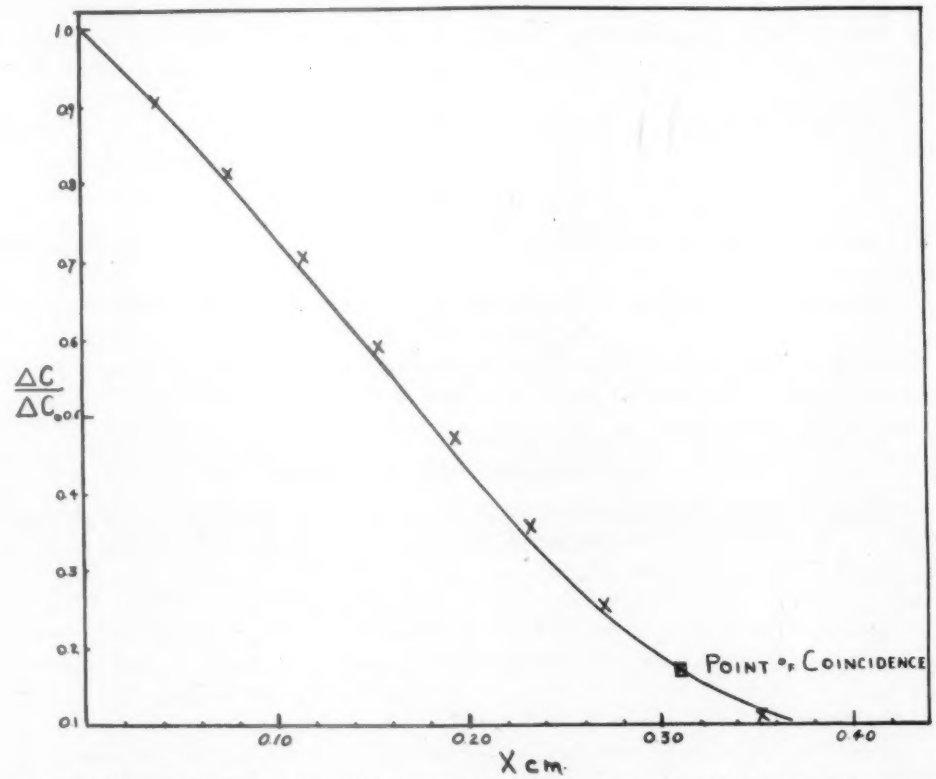

FIG 14—COMPARISON OF EQUATION 3 WITH HARRIS'S 8-HOUR 927°C CARBURIZING RUN. The solid lines are calculated from equation 3. The crosses are from the Harris data.

It is necessary to choose a point of coincidence in addition to the surface concentration. This has been indicated in Fig 13, where the results of the solution are compared with the experimental master curve. Eq 3 is observed to yield a curve of the same shape as the experimental curve.

For direct comparison with a carburization run, let us choose Mr. Harris's 927°C, 8-hr treatment with a saturated austenite surface. These data are plotted in Fig 14 for comparison with the theoretical curve. In view of the approximations involved and the possible errors in the several sets of experimental data, the agreement must be considered quite satisfactory.

References

6. C. Wells and R. F. Mehl: *Trans.* AIME (1940) **140,** 279.
7. C. E. Birchenall and R. F. Mehl: AIME *Tech. Pub.* 2168 (1947).
8. F. E. Harris: *Metal Progress* (1943) **44,** 265; (1944) **45,** 1111.
9. R. P. Smith: *Jnl.* Amer. Chem. Soc. (1946) **68,** 1163.

F. E. Harris—Dr. Birchenall presents a valid criticism when he mentions the complexity of the treatment, for there is no questioning the relative simplicity of the Matano or Boltzmann method in analyzing concentration-depth curves. However, when this method is applied to flow in opposite directions with reference to the outside surface, the inadequacy of the Matano method becomes readily apparent. Certainly diffusion coefficients must be independent of the direction of solute flow.

The simplicity of Eq 2 in his discussion cannot be denied. Here again the interpretation of the general diffusion equation upon which this derivation is based (namely, from the assumption that C is a function of $\frac{x}{\sqrt{t}}$ only) must surely be questioned. Since an attack on diffusion problems from a thermodynamic basis, as Dr. Birchenall suggests, is highly desirable, a thorough study of such derivations would be welcomed.

Institute of Metals Division, Volume 171 Transactions AIME, 1947

Institute of Metals Division Lectures

PAGE

The Separation of Gases from Molten Metals. By ALBERT J. PHILLIPS. (*Metals Tech.*, June 1947, T.P. 2208) 17

Electrons, Atoms, Metals and Alloys. By WILLIAM HUME-ROTHERY. (*Metals Tech.*, April 1947, T.P. 2130) 47

Copper and Copper Alloys

Twin Relationships in Annealed Copper Strip. By P. COHEUR and C. S. BARRETT. (*Metals Tech.*, Dec. 1946, T.P. 2104. 63

The Alpha Solid Solution Area of the Copper-manganese-aluminum System. By R. S. DEAN, J. R. LONG, T. R. GRAHAM, A. H. ROBERSON and C. E. ARMANTROUT. (*Metals Tech.*, Oct. 1946, T.P. 2099.) 70

Copper-manganese-aluminum Alloys—Properties of Wrought Alpha Solid Solution Alloys. By R. S. DEAN, J. R. LONG and T. R. GRAHAM. (*Metals Tech.*, Feb. 1947, T.P. 2142.) With discussion. 89

Copper-manganese-zinc Alloys—Physical Properties of Wrought Copper-rich Alloys. By R. S. DEAN, J. R. LONG and T. R. GRAHAM. (*Metals Tech.*, April 1947, T.P. 2183.) With discussion. 105

Solubility of Carbon in Molten Copper-manganese and Copper-nickel Alloys. By JOHN R. ANDERSON and MICHAEL B. BEVER. (*Metals Tech.*, April 1947, T.P. 2151.) With discussion. 119

Zinc Diffusion in Alpha Brass. By A. D. SMIGELSKAS and E. O. KIRKENDALL. (*Metals Tech.*, Oct. 1946, T.P. 2071.) With discussion 130

Thermodynamic Activities and Diffusion in Metallic Solid Solutions. By C. ERNEST BIRCHENALL and ROBERT F. MEHL. (*Metals Tech.*, June 1947, T.P. 2168.) With discussion 143

Interaction and Structure in Copper-zinc Alloys. By C. ERNEST BIRCHENALL. (*Metals Tech.*, June 1947, T.P. 2169.) With discussion. 166

Aluminum and Aluminum Alloys

German Practice in Refining Secondary Aluminum. By JAMES T. KEMP. (*Metals Tech.*, April 1947, T.P. 2143.) With discussion 176

Precipitation in Age-hardened Aluminum Alloys. By A. H. GEISLER and F. KELLER. (*Metals Tech.*, Oct. 1946, T.P. 2108.) With discussion. 192

Stress Rupture and Creep Tests on Aluminum-alloy Sheet at Elevated Temperatures. By A. E. FLANIGAN, L. F. TEDSEN and J. E. DORN. (*Metals Tech.*, Sept. 1946, T.P. 2033.) With discussion. 213

Magnesium and Magnesium Alloys

Twinning in Polycrystalline Magnesium. By C. S. BARRETT and C. T. HALLER, JR. (*Metals Tech.*, Dec. 1946, T.P. 2103.) With discussion 246

Hydrogen in Magnesium Alloys. By R. S. BUSK and E. G. BOBALEK. (*Metals Tech.*, Oct. 1946, T.P. 2105.) With discussion. 261

A Process of Augmenting Cold-drawability of the Magnesium +1.5 Per Cent Manganese Alloy. By LOUIS A. CARAPELLA and WILLIAM E. SHAW. (*Metals Tech.*, April 1947, T.P. 2149.) With discussion. 277

Some Effects of Zirconium on Extrusion Properties of Magnesium-base Alloys Containing Zinc. By J. P. DOAN and G. ANSEL. (*Metals Tech.*, Dec. 1946, T.P. 2107.) With discussion. 286

Miscellaneous Metals and Alloys

PAGE

An Electron Diffraction Study of Oxide Films Formed on Iron, Cobalt, Nickel, Chromium and Copper at High Temperatures. By E. A. GULBRANSEN and J. W. HICKMAN. (*Metals Tech.*, Oct. 1946, T.P. 2068.) With discussion 306

An Electron Diffraction Study of Oxide Films Formed on Alloys of Iron, Cobalt, Nickel and Chromium at High Temperatures. By J. W. HICKMAN and E. A. GULBRANSEN. (*Metals Tech.*, Oct. 1946, T.P. 2069.) With discussion 344

An Electron Diffraction Study of Oxide Films Formed on Molybdenum, Tungsten, and Alloys of Molybdenum, Tungsten and Nickel. By J. W. HICKMAN and E. A. GULBRANSEN. (*Metals Tech.*, April, 1947, T.P. 2144.) With discussion 371

The Constitution of the Bismuth-indium System. By OTTO H. HENRY and EDWARD L. BADWICK. (*Metals Tech.*, April 1947, T.P. 2159.) With discussion 389

The Crystal Structure of AuBe. By B. D. CULLITY. (*Metals Tech.*, April 1947, T.P. 2152) 396

Solubility of Hydrogen in Electrolytic Manganese and Transition Points in Electrolytic Manganese. By E. V. POTTER and H. C. LUKENS. (*Metals Tech.*, Sept. 1946, T.P. 2032.) With discussion 401

The Melting of Molybdenum in the Vacuum Arc. By ROBERT M. PARKE and JOHN L. HAM. (*Metals Tech.*, Sept. 1946, T.P. 2052.) With discussion 416

Spot Welding of Titanium. By R. S. DEAN, J. R. LONG, E. T. HAYES and D. C. ROOT. (*Metals Tech.*, Oct. 1946, T.P. 2102.) 431

Powder Metallurgy

Plastic Deformation in Metal-powder Compacts. By ROBERT KAMM, MORRIS STEINBERG and JOHN WULFF. (*Metals Tech.*, Feb. 1947, T.P. 2133.) With discussion. . 439

Some Factors Affecting Particle Size of Hydrogen-reduced Tungsten Powder. By BERNARD KOPELMAN. (*Metals Tech.*, Oct. 1946, T.P. 2100.) 457

Iron-graphite Powder Compacts. By ALEXANDER SQUIRE. (*Metals Tech.*, April 1947, T.P. 2164) With discussion. 473

Density Relationships of Iron-powder Compacts. By ALEXANDER SQUIRE. (*Metals Tech.*, April 1947, T.P. 2165) With discussion. 485

Introduction to Seminar—Review of Literature on Pressing of Metal Powders. By RICHARD PAUL SEELIG. (*Metals Tech.*, Aug. 1947, T.P. 2236.) With discussion. . 506

Symposium: Effect of Multiaxial Stresses on Metals

The Mechanical Equation of State. By JOHN H. HOLLOMON. (*Metals Tech.*, Sept. 1946, T.P. 2034.) With discussion. 535

A Statistical Theory of Fracture. By J. C. FISHER and J. H. HOLLOMON. (*Metals Tech.*, Aug. 1947, T.P. 2218) 546

Some Problems in Unstable Plastic Flow under Biaxial Tension. By W. T. LANKFORD and EDWARD SAIBEL. (*Metals Tech.*, Aug. 1947, T.P. 2238.) 562

The Plastic Flow of Aluminum Alloy Sheet Under Combined Loads. By W. T. LANKFORD, J. R. LOW and M. GENSAMER. (*Metals Tech.*, Aug. 1947, T.P. 2237) . 574

Comparison of Various Structural Alloy Steels by Means of the Static Notch-bar Tensile Test. By G. SACHS, L. J. EBERT and W. F. BROWN, JR. (*Metals Tech.*, Dec. 1946, T.P. 2110) 605

Work-hardening and Rupture in Metals. By LLOYD R. JACKSON. (*Metals Tech.*, Oct. 1946, T.P. 2072.) With discussion. 622

A Thermodynamic Theory of the Fracture of Metals. By EDWARD SAIBEL (*Metals Tech.*, Feb. 1947, T.P. 2131) With discussion 639

INDEX

(NOTE: In this index the names of authors of papers and discussions and of men referred to are printed in SMALL CAPITALS, and the titles of papers in *italics*.)

A

ABORN, R. H.: *Discussion on Boron in Certain Alloy Steels*, 302
ADAMS, J. Q.: *Discussion on Production of Low-sulphur Sponge Iron*, 87
Alloy: austenite-martensite structures: quantitative determination of percentage of microconstituents by point-counting and lineal analysis, 413
microconstituents: quantitative determination by point-counting and lineal analysis, 413
Alloys: heat-resisting: deformation: methods of explaining, 409
stress rupture as a rate process: application, 389, 399, 410
equations: practical application, 395
theory, 386
stress rupture: relation to creep, 395, 401, 409
Alloy steel. *See* Steel.
Austenite. *See* Steel.
AUSTIN, J. B.: *Discussion on Quantitative Metallography by Point-counting and Lineal Analysis*, 426
AVERY, H. S.: *Discussion: on Anomalous Changes in Tensile Properties of Quenched Iron-cobalt Alloys*, 385
on Controlled Atmospheres from City Gas for the Heat-treatment of Steels, 615
on Izod Impact Strength of Heat-treated Alloy Steel, 318
on Stress Rupture of Heat-resisting Alloys as a Rate Process, 401

B

BACH, J. H.: *Discussion on Anomalous Changes in Tensile Properties of Quenched Iron-cobalt Alloys*, 385
BARNETT, M. K.: *The Factorial Experiment in Engineering Research*, 427
BENNETT, W.: *Discussion on Interrelated Processes Going on in the Blast Furnace*, 645
Bessemer process: mechanism, 24
BEVER, M. B.: *Discussion on Interrelated Processes Going on in the Blast Furnace*, 655
BIRCHENALL, C. E.: *Discussion on Diffusion Rates for Carbon in Austenite*, 658
Blast-furnace process: iron: (see also Ironmaking):
carbon deposition: effect of pressure: laboratory study, 46, 65
mechanism, 23
Blast-furnace process: iron: questions re interrelated and concurrent processes: beneficiation of coal and ore, 644
burden variation, 621, 641, 642, 656
charge, mixing, 621, 634, 635, 640, 641, 642, 653, 656
coke quality, 628, 636, 649, 654
cooperation needed to find answers, 637
critical temperature, 632, 641
data needed on process, 638, 654
difference in furnaces: effect, 644
hearth heat, 640
heat transfer, 639, 656
heating charge uniformly 633, 639
oxygen content of blast: limitations on increasing, 626, 645, 648
reduction of ore, 624, 643, 645
refractory gangue, 653
slag control, 635
slag formation: sequence, 640, 642, 656
sulphur elimination, 630, 641, 651
temperature of blast: limitations on increasing, 625, 634, 645
reduction of iron oxides: effect of ore size, 69
interfering processes, 69
rate: laboratory study, 46
silica: effect on production, 18
sintering charge: value, 16
vanadium-rich slags: preparation, 71, 75
recovery of vanadium, 72
BOGROW, A., MAREK, L. F. and KING, G. W.: *Experimental Laboratory Study on Effect of Pressure on Carbon Deposition and Rate of Reduction of Iron Oxides in the Blast-furnace Process*, 46; *discussion*, 69
BOLOTSKY, M.: *Discussion on Boron in Certain Alloy Steels*, 302
Boron: effect in alloy steels: deoxidation important, 298, 302
hardness, 273, 281
notched-bar toughness, 289
recovery of boron, 276
replacement of molybdenum, 295
temper brittleness, 292, 302
BROWER, T. E. and LARSEN, B. M.: *Oxygen in Liquid Open-hearth Steel—Effect of Special Additions, Stirring Methods and Tapping*, 164; *discussion*, 174
Oxygen Content during the Refining Period, 137; *discussion*, 151
BUEHL, R. C., SHOUB, E. P. and RIOTT, J. P.: *Production of Low-sulphur Sponge Iron*, 76; *discussion*, 85

C

Carbon: diffusion in austenite. *See* Steel.
deposition. *See* Blast-furnace Process.
Cast iron: variable elements: determining influence by factorial design, 428
Cast steel: austenite grain size: characteristics, 524
methods for determining: fracture, 511
gradient quench, 517, 530
martensitic etch, 519
McQuaid-Ehn, 522
metallographic etchant, 530
normalizing, 514
oxidation, 513
picric acid solution, 530
CHANG, LO CHING and DERGE, G.: *An Electrochemical Study of the Properties of Molten Slags of the system* $CaO\text{-}SiO_2$ *and* $CaO\text{-}Al_2O_3\text{-}SiO_2$, 90; *discussion*, 116
CHIPMAN, J.: *Discussion on Interrelated Processes Going on in the Blast Furnace*, 637
on Oxygen in Liquid Open-hearth Steel, 175
Cobalt: as alloying element in steel: diffusion in austenite, 486
effect on diffusion coefficient of carbon in austenite, 482
effect on hardenability, 469
effect on rate of nucleation and rate of growth of pearlite, 467, 473, 477
effect on temperature range of martensite, 489
equilibria: binary, 468
equilibria: ternary, 468
properties, 467
transformation rate: effect of nitrogen, 487
COHEN, M. and HOWARD, R. T.: *Quantitative Metallography by Point-counting and Lineal Analysis*, 413; *discussion*, 426
COMSTOCK, G. F.: *Discussion on Calculation of Tensile Strength and Yield Point from the Chemical Composition and Cooling Rate*, 271
CRAFTS, W.: *Discussion on Boron in Certain Alloy Steels*, 301
CRAFTS, W. and LAMONT, J. L.: *Effect of Alloys in Steel on Resistance to Tempering*, 222; *discussion*, 242
Izod Impact Strength of Heat-treated Alloy Steel, 303; *discussion*, 317
CRANE, E. V.: *Discussion on Effect of Prior Tensile Strain on Fracture*, 371
Creep in metals: relation to stress rupture, 395, 401, 409

D

DAPOGNY, M. L.: *Discussion on Mechanism of Carbon-oxygen Reaction in Steelmaking*, 191
DARKEN, L. S.: *Discussion on Diffusion Rates for Carbon in Austenite*, 553
DARKEN, L. S.: *Discussion: on Electrochemical Study of Properties of Molten Slags*, 116
on Mechanism of Carbon-oxygen Reaction in Steelmaking, 190
DERGE, G.: *Discussion: on Oxygen in Liquid Open-hearth Steel*, 174
DERGE, G. and CHANG, LO CHING: *An Electrochemical Study of the Properties of Molten Slags of the System* $CaO\text{-}SiO_2$ *and* $CaO\text{-}Al_2O_3\text{-}SiO_2$, 90; *discussion*, 116
DERGE, G. and URBAN, S. F.: *Oxygen in Basic Electric-furnace Baths*, 196; *discussion*, 210
DESCH, C. H.: *Discussion on Austenite Grain Size in Cast Steels*, 530
DE SY, A.: *Discussion on Oxygen in Liquid Open-hearth Steel*, 156
DEVRIES, G.: *Discussion on Izod Impact Strength of Heat-treated Alloy Steel*, 320
Dolomite: sulphur-control agent in production of sponge iron, 76, 88
Duplex process of steel-making: mechanism, 25

E

Education: training of engineers: rates of payment, 219
training of metallurgical engineers in the steel industry, 212
cooperation of college and industry, 218
Electric-furnace practice: three-phase system and principal reactions, 177
Electric-furnace process: basic: oxygen in bath: behavior, 196
sulphur in bath: behavior, 206
mechanism, 25
Electrochemical study of properties of molten slags of systems $CaOSiO_2$ and $CaO\text{-}Al_2O_3\text{-}SiO_2$: reversible cell measurements, 90
EMMONS, J. V.: *Discussion on Transformation of Austenite in an Al-Cr-Mo Steel*, 464
EPSTEIN, S.: *Discussion on Boron in Certain Alloy Steels*, 302
Etching reagents: modified picral: composition, 457
efficiency, 464, 466

F

Factorial design: advantages, 432
criteria for judging relative merits of designs, 430
definition, 427
determination of mathematical relation, 435
function in experimental work, 436
practical experiment with metals, 428
FICK, N. C.: *Discussion on Transformation of Austenite in an Al-Cr-Mo Steel*, 464
FISCHER, R. P.: *German Iron Ores Yield Vanadium*, 71; *discussion*, 75
Fracture of metals: chart of work-hardening characteristics, 372, 373
effect of prior tensile strain, 363
plastic vs. brittle: definition,
rupture and fracture not interchangeable terms, 370, 372
theory: thermodynamic, 363
FRENCH, H. J.: *Discussion on Diffusion Rates for Carbon in Austenite*, 552
FRYE, J. H.: *Discussion on Austenite Grain Size in Cast Steels*, 530

FULTON, L. M.: *Discussion on Interrelated Processes Going on in the Blast Furnace*, 638
Furnace bottoms: basic open-hearth: crystalline constituents: identification in etched polished sections, 121

G

Gas: city: use in heat-treatment of steel, 556
GEIL, G. W., MCADAMS, D. J., JR. and MEBS, R. W.: *Influence of Plastic Deformation, Combined Stresses, and Low Temperatures on the Breaking Stress of Ferritic Steels*, 323
GORSUCH, P. D., KRAMER, I. R. and NEWHOUSE, D. L.: *Calculation of Tensile Strength and Yield Point from the Chemical Composition and Cooling Rate*, 244; *discussion*, 271
GRAHAM, H. W.: *Factors Which Determine Iron and Steel Making Processes*, 15
Discussion on Production of Low-sulphur Sponge Iron, 85, 86, 87
Grain size in metals: estimating: methods: accuracy, 443
comparison: advantages over older methods, 441, 443
mathematical analysis, 442
geometric grids, 439
idealized grain networks, 439
standard micrographs, 439
GRANGE, R. A., HOLT, W. S. and TKAC, E. T.: *Transformation of Austenite in an Aluminum-chromium-molybdenum Steel*, 452; *discussion*, 464
GRANT, N. J.: *Discussion on Stress Rupture of Heat-resisting Alloys as a Rate Process*, 409

H

HARRIS, F. E.: *The Diffusion Rates for Carbon in Austenite*, 531; *discussion*, 552, 660
HAWKES, M. F.: *Austenite Grain Size in Cast Steels*, 510; *discussion*, 530
HAWKES, M. F. and MEHL, R. F.: *The Effect of Cobalt on the Rate of Nucleation and the Rate of Growth of Pearlite*, 467
Heat-treatment: of steels: processes employing controlled atmospheres from city gas, 556
HERRLANDER, B. and HULTGREN, A.: *Hot Deformation Structure, Veining and Red-shortness Cracks in Iron and Steel*, 493
High-temperature metallurgy. *See* Metals or Alloys.
Hiperco: iron-cobalt alloy, 374
HODGE, J. M.: *Discussion on Izod Impact Strength of Heat-treated Alloy Steel*, 317
HOGBERG, C. G.: *Discussion on Interrelated Processes Going on in the Blast Furnace*, 635
HOLLOMAN, J. H.: *Discussion on Effect of Alloys in Steel on Resistance to Tempering*, 242
HOLT, W. S., GRANGE, R. A. and TKAC, E. T.: *Transformation of Austenite in an Aluminum-chromium-molybdenum Steel*, 452; *discussion*, 464
HOWARD, J. J.: *Discussion on Interrelated Processes Going on in the Blast Furnace*, 653
HOWARD, R. T. and COHEN, M.: *Quantitative Metallography by Point-counting and Lineal Analysis*, 413; *discussion*, 426
HUEBLER, J.: *Discussion on Controlled Atmospheres from City Gas for the Heat-treatment of Steels*, 615
HULL, F. C.: *A New Method for Making Rapid and Accurate Estimates of Grain Size*, 439
HULTGREN, A.: *Discussion on Transformation of Austenite in an Al-Cr-Mo Steel*, 465
HULTGREN, A. and HERRLANDER, B.: *Hot Deformation Structures, Veining and Red-shortness Cracks in Iron and Steel*, 493

I

Iron: hot-shortness cracks. *See* Steel.
Iron: ingot, breaking stress: influence of combined stresses, 323, 334
influence of notch angle, 341
influence of plastic deformation, 323, 326
variation with temperature, 341
technical cohesive strength at room temperature: influence of plastic deformation, 339
sponge. *See* Sponge Iron.
veining. *See* Steel.
Iron-cobalt alloys: Hiperco, 374
soft (35 pct Co): tensile properties: anomalous changes, 374
Iron ore: Geneva: composition: mineralogical and chemical, 29
reduction rate: apparatus for study, 29
laboratory study with hydrogen, 27
reduction: rate: laboratory study, 46
reduction in blast furnace: heat penetration important, 31, 41, 43
time related to porosity, 27, 41
Ironmaking (*see also* Blast Furnace):
effect of manganese, 18
effect of oxygen, 19
effect of sulphur, 18
pressure: normal, 21
processes: determining factors, 15
direct: difficulties of solid phase, 20
mechanism, 23
rate of speed, 22
raw materials: fine ore: sintering: value, 16
reasons for molten phase, 19
silica content of ore: effect on blast-furnace production, 18
titanium undesirable, 18

J

JACOBSON, M.: *Discussion on Transformation of Austenite in an* Al-Cr-Mo *Steel*, 466
JENKINS, IVOR: *Controlled Atmospheres from City Gas for the Heat-treatment of Steels*, 556; *discussion*, 613

JOHNSON, B. L.: *Discussion: on Anomalous Changes in Tensile Properties of Quenched Iron-cobalt Alloys*, 385
on Izod Impact Strength of Heat-treated Alloy Steel, 318
JOHNSTON, T. L.: *Discussion on Production of Low-sulphur Sponge Iron*, 87
JOSEPH, T. L.: *Discussion on Interrelated Processes Going on in the Blast Furnace*, 633
on Rate of Reduction of Geneva Iron Ore, 43

K

KING, G. W., MAREK, L. F. and BOGROW, A.: *Experimental Laboratory Study on Effect of Pressure on Carbon Deposition and Rate of Reduction of Iron Oxides in the Blast-furnace Process*, 46; *discussion*, 69
KRAMER, I. R.: *Discussion on Izod Impact Strength of Heat-treated Alloy Steel*, 320
KRAMER, I. R., GORSUCH, P. D. and NEWHOUSE, D. L.: *Calculation of Tensile Strength and Yield Point from the Chemical Composition and Cooling Rate*, 244; *discussion*, 271

L

LAMONT, J. L. and CRAFTS, W.: *Effect of Alloys in Steel on Resistance to Tempering*, 222; *discussion*, 242
The Izod Impact Strength of Heat-treated Alloy Steel, 303; *discussion*, 317
LARSEN, B. M.: *Some Questions on Interrelated Processes Going on in the Blast Furnace*, 621; *discussion*, 633
Discussion: on Effect of Pressure on Carbon Deposition, 69
on Identification of CaO-MgO Orthosilicate Crystals, 135
on Mechanism of Carbon-oxygen Reaction in Steelmaking, 191
on Oxygen in Basic Electric-furnace Baths, 210
on Rate of Reduction of Geneva Iron Ore, 43
LARSEN, B. M. and BROWER, T. E.: *Oxygen in Liquid Open-hearth Steel—Effect of Special Additions, Stirring Methods and Tapping*, 164; *discussion*, 174
Oxygen in Liquid Open-hearth Steel—Oxygen Content during the Refining Period, 137; *discussion*, 151
LESZYNSKI, W.: *Discussion on Stress Rupture of Heat-resisting Alloys as a Rate Process*, 400
LEWIS, J. R.: *Rate of Reduction of Geneva Iron Ore*, 27; *discussion*, 44
Lineal analysis. *See* Alloy.

M

MACHLIN, E. S. and NOWICK, A. S.: *Stress Rupture of Heat-resisting Alloys as a Rate Process*, 386; *discussion*, 399
MACKENZIE, I. M. and URIE, T.: *Discussion on Mechanism of Carbon-oxygen Reaction in Steelmaking*, 189
MACKENZIE, I. M. and URIE, T., *Discussion on Oxygen in Liquid Open-hearth Steel*, 155
Manganese: effect in iron and steel making, 18
MAREK, L. F., BOGROW, A. and KING, G. W.: *Experimental Laboratory Study on Effect of Pressure on Carbon Deposition and Rate of Reduction of Iron Oxides in the Blast-furnace Process*, 46; *discussion*, 69
Martensite. *See* Steel.
MARTIN, A. E.: *Discussion on Electrochemical Study of Properties of Molten Slags*, 117
MCADAM, D. J. JR.: *Discussion on Effect of Prior Tensile Strain on Fracture*, 371
MCADAM, D. J. JR., GEIL, G. W. and MEBS, R. W.: *Influence of Plastic Deformation, Combined Stresses, and Low Temperatures on the Breaking Stress of Ferritic Steels*, 323
MCDONALD, J. C. and MOORE, A. A.: *Discussion on Stress Rupture of Heat-resisting Alloys as a Rate Process*, 400
MEBS, R. W., MCADAM, D. J. JR. and GEIL, G. W.: *Influence of Plastic Deformation, Combined Stresses, and Low Temperatures on the Breaking Stress of Ferritic Steels*, 323
MEHL, R. F. and HAWKES, M. F.: *The Effect of Cobalt on the Rate of Nucleation and the Rate of Growth of Pearlite*, 467
Merwinite: identification in etched polished sections of basic open-hearth slags and furnace bottoms, 121
Metallurgical engineers: demand for trained personnel, 220
training in the steel industry, 212
rates of payment, 219
Metals: behavior at high temperatures: methods of explaining, 409
MILLER, O. O.: *Discussion on Boron in Certain Alloy Steels*, 302
MOORE, A. A. and MCDONALD, J. C.: *Discussion on Stress Rupture of Heat-resisting Alloys as a Rate Process*, 400
Multiaxial stress: effect on metals: symposium, Vol. 171

N

NEUSTAETTER, K.: *Discussion on Interrelated Processes Going on in the Blast Furnace*, 654
NEWHOUSE, D. L., KRAMER, I. R. and GORSUCH, P. D.: *Calculation of Tensile Strength and Yield Point from the Chemical Composition and Cooling Rate*, 244; *discussion*, 271
NICHOLS, P. R.: *Discussion on Interrelated Processes Going on in the Blast Furnace*, 651
Notch hardness test: influence of angle. *See* Iron and Steel.
NOWICK, A. S. and MACHLIN, E. S.: *Stress Rupture of Heat-resisting Alloys as a Rate Process*, 386; *discussion*, 399

O

Open-hearth process: mechanism, 23
Oxygen: effect in iron and steel making, 19
in electric furnace process. *See* Electric.
in liquid open-hearth steel. *See* Steel.

P

Pearlite. *See* Steel.
PECK, C. E.: *Discussion on Controlled Atmospheres from City Gas for the Heat-treatment of Steels*, 613
Perrin process: mechanism, 24
PHILBROOK, W. O.: *Discussion: on Oxygen in Liquid Open-hearth Steel*, 153
on Rate of Reduction of Geneva Iron Ore, 41
Phosphorus: effect in steelmaking, 17
PLANTE, T. W.: *Discussion on Interrelated Processes Going on in the Blast Furnace*, 641
Plastic deformation: influence on breaking stress. *See* Iron and Steel.
PLIMPTON, T. F.: *Discussion on Interrelated Processes Going on in the Blast Furnace*, 649
Point-counting. *See* Alloy.
PONCELET, E. F.: *Discussion: on Effect of Prior Tensile Strain on Fracture*, 370
on Stress Rupture of Heat-resisting Alloys as a Rate Process, 399

Q

Quantitative microscopy: adaptation to determination of microconstituents in a metal alloy, 413
literature survey, 413

R

Rate processes: theory, 386
Red-short cracks. *See* Steel.
Reduction of iron ore. *See* Iron Ore.
Research: engineering: factorial design. *See* Factorial.
RIOTT, J. P., SHOUB, E. P. and BUEHL, R. C.: *Production of Low-sulphur Sponge Iron*, 76; *discussion*, 85
ROSENTHAL, P. C. and UDY, M. C.: *Boron in Certain Alloy Steels*, 273; *discussion*, 301

S

SAIBEL, E.: *Effect of Prior Tensile Strain on Fracture*, 363; *discussion*, 370
Sampling: steel for oxygen content, 175
SHOUB, E. P., BUEHL, R. C. and RIOTT, J. P.: *Production of Low-sulphur Sponge Iron*, 76; *discussion*, 85
Silica: effect on blast-furnace production, 18
SIMS, C. E.: *The Mechanism of the Carbon-oxygen Reaction in Steelmaking*, 176; *discussion*, 189
Discussion: on Oxygen in Basic Electric-furnace Baths, 210
on Oxygen in Liquid Open-hearth Steel, 151, 174
Sintering: value in blast-furnace process, 16
SISCO, F. T.: *Discussion on German Iron Ores Yield Vanadium*, 71
Slag: basic open-hearth: crystalline constituents: identification in etched polished sections, 121
merwinite: identification in etched polished sections, 121
Slag: basic open-hearth: systems CaO-SiO_2 and CaO-Al_2O_3-SiO_2: molten: properties: electrochemical study: reversible cell measurements, 90
SMITH, E. C.: *Discussion on Production of Low-sulphur Sponge Iron*, 87
SNOW, R. B.: *Identification of* CaO-MgO *Orthosilicate Crystals, Including Merwinite* ($3CaO$-MgO-$2SiO_2$) *through the Use of Etched Polished Sections*, 121; *discussion*, 135
SOSMAN, R. B.: *Discussion on Identification of CaO-MgO Orthosilicate Crystals*, 135
on Mechanism of Carbon-oxygen Reaction in Steelmaking, 191
Sponge iron: low-sulphur: production: dolomite as sulphur-control agent, 76, 85
rotary-kiln method, 76
production: rotary-kiln method, 76
sagger method, 85
Swedish: Höganas process: desulphurization of product, 85
purity, 86
STANLEY, J. K.: *Anomalous Changes in Tensile Properties of Quenched Iron-cobalt* (35 *Pct* Co) *Alloys*, 374; *discussion*, 385
Steel: alloy: effect of boron. *See* Boron.
heat-treated: Izod impact strength: cast steels, 318
Izod impact strength: longitudinal room-temperature tests of commercial bars: prediction, 303
significance in selection of steel, 308, 318
alloys: stress rupture as a rate process. *See* Alloys.
aluminum-chromium-molybdenum: austenite: isothermal transformation: measurements, 452, 455
effects of aluminum: revealed by isothermal transformation behavior, 452
end-quench hardenability: indicated by isothermal transformation behavior, 461
martensite formation: temperature range, 454
austenite: carbon diffusion coefficient: effect of cobalt, 482
carbon diffusion in. *See* carbon below
cobalt diffusion in: rate, 486
transformation in Al-Cr-Mo steel, 452
austenite-martensite structures: quantitative determination of percentage of microconstituents by point-counting and lineal analysis, 413
carbon: diffusion in austenite: factors that influence flow, 531
mechanism: physical significance, 531
steady state: equations, 532, 656
steady state: experiment, 531, 535, 553, 656
unidirectional flow of solute for semi-infinite solid: equations, 547
unsteady flow: equations, 539
unsteady flow: experiment, 537, 554
diffusion between ferrite and austenite: rate, 552

Steel: cast. *See* Cast Steel.
cobalt: pearlite nucleation and growth, 467
transformation rate: effect of nitrogen, 487
ferritic: breaking stress: influence of combined stresses, 323, 334
influence of notch angle, 341
influence of plastic deformation, 323, 326
variation with temperature, 341
technical cohesive strength at room temperature: influence of plastic deformation, 339
hardness: changes caused by tempering, 222
and tensile strength in tempered condition: prediction, 222
heat-resisting. *See* Alloys.
heat-treatment: processes employing controlled atmospheres from city gas, 556
martensite: temperature range: effect of cobalt, 489
open-hearth: liquid: oxygen content: during refining period, 137
effect of special additions, stirring methods and tapping, 164
sampling technique, 175
slag. *See* Slag.
pearlite: rate of isothermal transformation from austenite: growth: effect of cobalt, 467, 477
nucleation: effect of cobalt, 467, 473
red-short: cracks: paths, 504
veining: patterns, 497 et seq
result of hot deformation, 493
resistance to tempering: effect of alloys, 222
tensile strength and yield point: calculating from chemical composition, 244
correlation with cooling rate, 244
veining: forms, 495
literature, 493, 506
Steelmaking: carbon-oxygen reaction: bubble formation, 182, 190
chemical equilibrium: nature, 179
mechanism, 176, 181
electric furnace, 177
effect of manganese, 18
effect of oxygen, 19
phosphorus: permissible amount, 17
processes: acid and basic, 17
determining factors, 15
direct: difficulties of solid phase, 20
essentials, 16
mechanism, 23
rate of speed, 22
raw materials: fine ore: sintering: value, 16
reasons for molten phase, 19
STEUDEL, G. E.: *Discussion on Interrelated Processes Going on in the Blast Furnace*, 643
STOTT, C. T.: *Discussion on Oxygen in Liquid Open-hearth Steel*, 151
Stresses: multiaxial: effect on metals, Vol. 171
Sulphur: effect in iron and steelmaking, 18
Symposium: Effect of Multiaxial Stresses on Metals, Vol. 171

T

Talbor process: mechanism, 24
Temperature: influence on breaking stress. *See* Iron and Steel.
TENENBAUM, M.: *Discussion on Effect of Pressure on Carbon Deposition*, 69
on Mechanism of Carbon-oxygen Reaction in Steelmaking, 191
on Oxygen in Liquid Open-hearth Steel, 152
TIGERSCHIÖLD, M.: *Discussion on German Iron Ores Yield Vanadium*, 71
on Production of Low-sulphur Sponge Iron, 85, 86, 87
Titanium: undesirable in ironmaking, 18
TKAC, E. T., HOLT, W. S. and GRANGE, R. A.: *Transformation of Austenite in an Aluminum-chromium-molybdenum Steel*, 452; *discussion*, 464
TOUR, S.: *Discussion on Controlled Atmospheres from City Gas for the Heat-treatment of Steels*, 614, 615, 616

U

UDY, M. C. and ROSENTHAL, P. C.: *Boron in Certain Alloy Steels*, 273; *discussion*, 301
URBAN, S. F. and DERGE, G.: *Oxygen in Basic Electric-furnace Baths*, 196; *discussion*, 210
URIE, T. and MACKENZIE, I. M.: *Discussion on Mechanism of Carbon-oxygen Reaction in Steelmaking*, 189
on Oxygen in Liquid Open-hearth Steel, 155

V

Vanadium: recovery: from German iron ores, 71
Veining in steel. *See* Steel.

W

WELLS, C.: *Discussion on Izod Impact Strength of Heat-treated Alloy Steel*, 319
WHITE, A. M.: *Discussion on Austenite Grain Size in Cast Steels*, 530
WINKLER, T. B.: *Discussion on Oxygen in Basic Electric-furnace Baths*, 210
WRIGHT, E. C.: *Training of Metallurgical Engineers in the Steel Industry*, 212

Z

ZADRA, J. R.: *Discussion on Boron in Certain Alloy Steels*, 301
Zephiran chloride: composition, 457
uses, 464, 466